

24th International QUENCH Workshop

13-15 November 2018
Karlsruhe Institute of Technology
Karlsruhe, Germany

Editor: Martin Steinbrück

DOI: 10.5445/IR/1000088229

AGENDA

24th International QUENCH Workshop*

Karlsruhe Institute of Technology, Campus North, H.-von-Helmholtz-Platz 1, 76344 Egg.-Leopoldshafen, Germany
13-15 November 2018

Meeting Location: Fortbildungszentrum für Technik und Umwelt (FTU), Auditorium (Aula)

Tuesday, 13 Nov 2018

9:00	Welcome	W. Tromm/M. Steinbrück, KIT
	INTERNATIONAL PROGRAMS (Chair: M. Steinbrück, KIT)	
9:20	IAEA Activities in the Area of Nuclear Power Reactor Fuel Engineering	M.S. Veshchunov, IAEA
9:40	CoreSOAR project on update of the Core Degradation State-of-the-Art Report: Summary and Conclusions	T. Haste, IRSN
10:10	An Update on the SAREF/ Pre-ADES projects	D. Bottomley, JAEA
10:30	**Coffee break (Group Photo)**	
	QUENCH PROGRAM I (Chair: M. Veshchunov)	
11:00	Update of the QUENCH program	M. Steinbrück, KIT
11:30	First Results of the QUENCH-18 Post-Test Benchmark in the Frame of the NUGENIA QUESA Project	T. Hollands, GRS
12:00	Interpretative analysis of QUENCH-18 using SCDAPSim/Mod3.5/psi	J. Birchley, consultant
12:35	Post-Test Modelling of the Concurrent Steam-Air Experiment QUENCH-ALISA Using SOCRAT Code	A. Vasiliev, IBRAE
13:00	**Lunch**	
	QUENCH PROGRAM II (Chair: T. Haste, IRSN)	
14:00	Post-test calculation results of QUENCH-18 experiment using different RELAP/SCDAPSIM Mod3.5 code versions and different Zr oxidation correlations	T. Kaliatka, LEI
14:20	First results of the bundle test QUENCH-19 with FeCrAl claddings	J. Stuckert, KIT
14:50	Pre- and Post-Test Simulations of the ATF Experiment QUENCH-19 with AC2	T. Hollands, GRS
15:20	**Coffee break**	
15:50	Status and first results of the BWR control blade degradation test under steam-starved conditions	A. Pshenichnikov, JAEA

Wednesday, 14 Nov 2018

	MODELLING AND CODE APPLICATION I (Chair: C. Allison, ISS)	
~~9:00~~	~~Uncertainty Analysis of QUENCH-06 Experiment Using RELAP-SCDAPSIM~~	~~A. Ali, EAEA~~
9:20	Comparative analysis of simulation results for the bundle tests QUENCH-07 and QUENCH-09 conducted with the Severe Accident Analysis Code ASTEC V2.1	J.M. Peschel, RUB
9:40	Uncertainty and Sensitivity Analysis by means of ASTEC/URANIE platform of the QUENCH-08 Experiment	F. Gabrielli, KIT
10:00	Validation of ASTEC2.1 using VVER QUENCH-12 Experiment	A.K. Mercan, KIT
10:20	**Coffee break**	
	MODELLING AND CODE APPLICATION II (Chair: J. Birchley, consultant)	
10:50	Numerical simulation of QUENCH-15 experiment with SOCRAT/V1 code	M. Philippov, IBRAE
11:10	RELAP/SCDAPSIM Code Re-Assessment - Integrated Uncertainty Analysis of CORA-13 and other Selected CORA PWR Experiments	S. Asmaa, Alexandria Uni
11:30	Integrated Uncertainty analysis of selected CORA BWR experiments	R. Mustafa, JAEC
11:50	RELAP5 MOD3.4 with IUA LOFT L3-7 Experiment	B. Kedzierska, TU Warsaw
12:10	PSI-KIT Nitriding Model with Validation Calculations	B. Jäckel, PSI
12:30	**Lunch**	
	EXPERIMENTS (Chair: L. Ott, ORNL)	
13:30	Behavior of nitrogen with oxidized zirconium - Findings and Remaining Questions	S. Park, ACT
13:50	Effect of flow rate on the oxidation behavior of zirconium cladding under oxygen and air at 1000°C	G. Kim, HGU
14:10	High Temperature Oxidation of Sponge-based E110 Cladding Alloy in Air	P. Vrbka, CTU
14:25	Recent activities for analyses of PWR cladding during LOCA condition	H. Wu, HUST
15:00-21:00	**Visit of Speyer Cathedral and invited dinner**	

Thursday, 15 Nov 2018

	EXPERIMENTS cont. (Chair: J. Stuckert, KIT)	
9:00	Overview of R&D Progress on Cladding Behavior under LOCA condition in CIAE	X. He, CIAE
9:20	The CODEX-AIT-3 integral air ingress experiment	N. Ver, MTA

	<u>ATF CLADDING MATERIALS</u> (Chair: M. Grosse, KIT))	
9:50	An overview of high-temperature oxidation behavior of various ATF cladding candidates in steam	C. Tang, KIT
10:20	Overview of recent CEA-Framatome-EDF results obtained o Cr-coated M5 cladding tested upon LOCA conditions	J.-C. Brachet, CEA
10:50	**Coffee break**	
11:20	Experimental behavior of Cr-coated claddings	J. Krejci, UJP
11:40	Zirconium alloy coatings with Si based compounds – INCT experiments	B. Sartowska, INCT
12:00	Silicon concentration changes in Zry-2 coated with Zr-Si and ZrSi2-Cr during the autoclave oxidation tests	A. Krześniak, INCT
12:20	High Temperature Interaction of SiC with Zircaloy-4	M. Große, KIT
12:50	**Closure of the Workshop**	M. Steinbrück, KIT
13:00	**Lunch**	
14:00	**CoreSOAR Progress Meeting (only for project partners)**	T. Haste, IRSN

**** In Cooperation with the International Atomic Energy Agency (IAEA)***


Karlsruhe Institute of Technology
IAEA
24th
International QUENCH Workshop
Karlsruhe Institute of Technology, Germany
13-15 November 2018
In cooperation with
the International
Atomic Energy Agency
Internet
SSID: KA-WLAN





Karlsruhe Institute of Technology

Welcome Address:
24th QUENCH Workshop at KIT

Outlook Programme NUSAFE at KIT and HGF

Th. Walter Tromm, Programme Nuclear Waste Management, Safety and Radiation Research







Nuclear Waste Management, Safety and Radiation Research

Participating Helmholtz - Centres

Forschungszentrum Jülich GmbH (FZJ)

Helmholtz – Zentrum Dresden – Rossendorf (HZDR)

Karlsruher Institut für Technologie (KIT)







Statements from Mid-term evaluation 2018:

- The research in all three centers yielded outstanding outcome over POF III
- The work is well recognised at international level
- The research facilities constitute a particular strength

7th German Energy Research Programme (1/2): Reactor Safety Research:

Nuclear phase-out until 2022 in Germany- but on an international level, nuclear energy has a long-term perspective. Political guidelines emphasize importance of nuclear competence in Germany beyond 2022

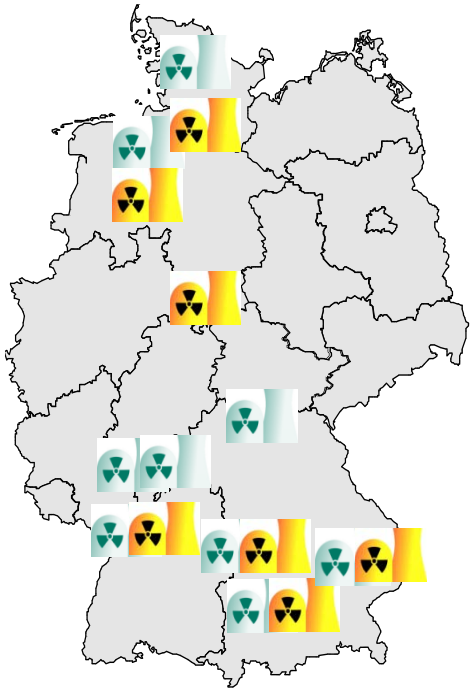
- Preservation of the necessary national expertise also for the **participation in national and international committees** remains absolutely necessary.
- Including **sufficient personnel resources**
- It is in Germany's long-term safety interest to be able to monitor developments in neighbouring countries with regard to **existing and planned plants** from a technical point of view.



Federal Ministry for Economic Affairs and Energy

7th German Energy Research Programme (2/2): Reactor Safety Research:

- Make technical and scientific contributions for the safety of the remaining operation of German NPPs
- Ensure safety competence for the assessment and further development of the safety of nuclear installations abroad including new reactor concepts which are under development internationally
- Use methods and tools of reactor safety research for the investigation of selected questions on the disposal of radioactive waste, in particular in connection with extended interim storage (e.g. long-term behaviour of irradiated fuel elements and radioactive waste)
- Include alternative disposal strategies as well as disposal strategies pursued abroad

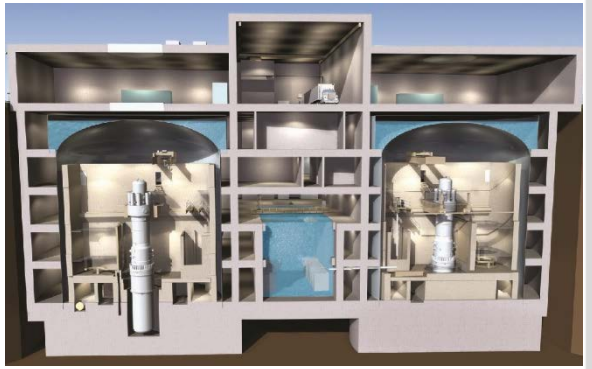


- Make a substantial contribution to the establishment, further development and maintenance of scientific and technical competence and the promotion of young scientists in the field of nuclear safety research.

Strategy for Reactor Safety

- Covering key aspects regarding safety of nuclear reactors today in Germany and beyond 2022 abroad
- Ensure expertise and maintain competencies:
  - to access and contribute to the developments in nuclear safety technology
  - to cooperate with key international partners
  - participation in international expert groups
- **Synergies of scientific expertise with research fields of non-nuclear programs**



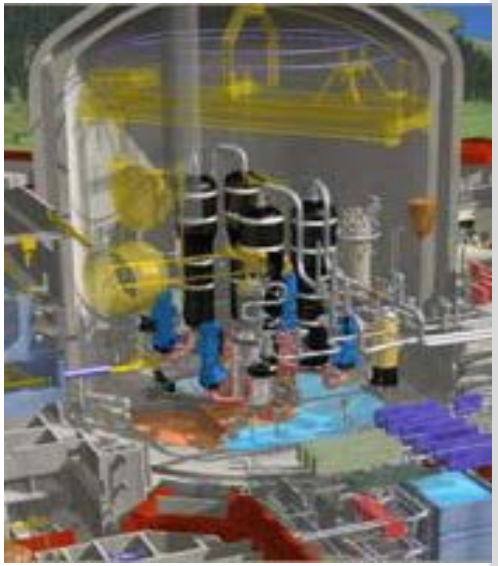




Important Aspects of the Program NUSAFE

Reactor Safety

- Safety assessment of nuclear power plants including innovative designs (LWR, SMR, Gen-IV, ASTRID, MYRRHA) and their transmutation capabilities within European projects
- Improvement of severe accident integral codes to support Severe Accident Management Guidelines, including experimental investigations
- Multi-criteria decision analysis (MCDA) and agent based modeling (ABM) to better understand decision making under high uncertainties for all emergency situations
- Synergies of scientific expertise with other research fields, e.g. waste management, or non-nuclear programs, e.g.: Liquid metal for concentrating solar power or hydrogen safety



EPR



Training workshop on SAMG-D at the IAEA

Networking and cooperations

NUSAFE Collaborations in Germany

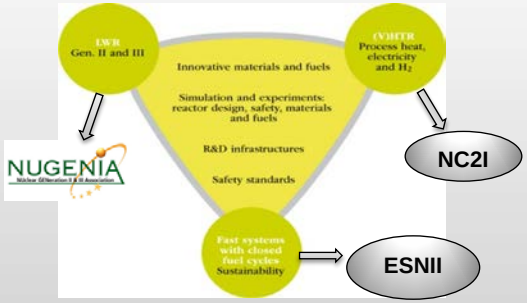
- Alliance for Competence in Nuclear Technology (KVKT) with universities, authorities and industry

Cooperations 2016

- Scientific cooperations: **61**
- Industry contracts: **22**
- Co-ordinated research programmes: **21**

European collaborations

SNETP
Sustainable Nuclear Energy Technology Platform



EERA European Energy Research Alliance

NERIS

enen

Bilateral cooperations

research and industry

(national & international)

IRSN

cea

PAUL SCHERRER INSTITUT PSI

VTT

framatome

SCK·CEN

JAEA

KAERI

Advisory boards / Committees

- Reactor Safety Commission
- Nuclear Waste Management Commission

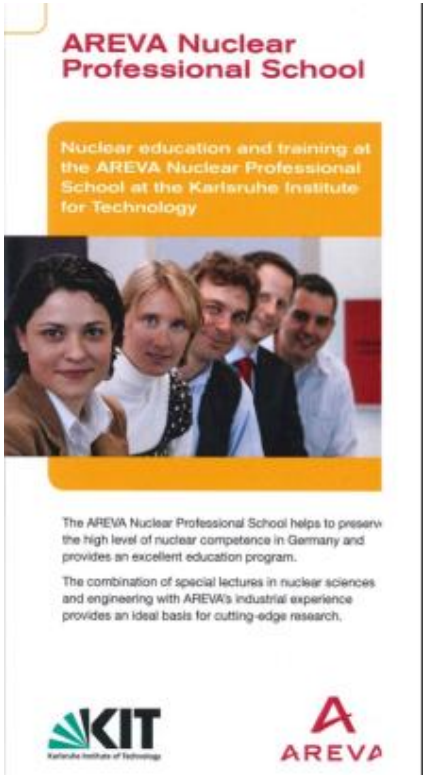
International Atomic Energy Agency IAEA

NEA Nuclear Energy Agency

Education & Training

	2016
Nuclear technology lectures	26
PhD students	37
Various funding sources	

- Cooperation within ENEN (European Nuclear Education Network):
  - ANNETTE
  - ENEN+
- Frederic Joliot Otto Hahn Summer School (together with CEA)
- AREVA Nuclear Professional School sponsored by Framatome



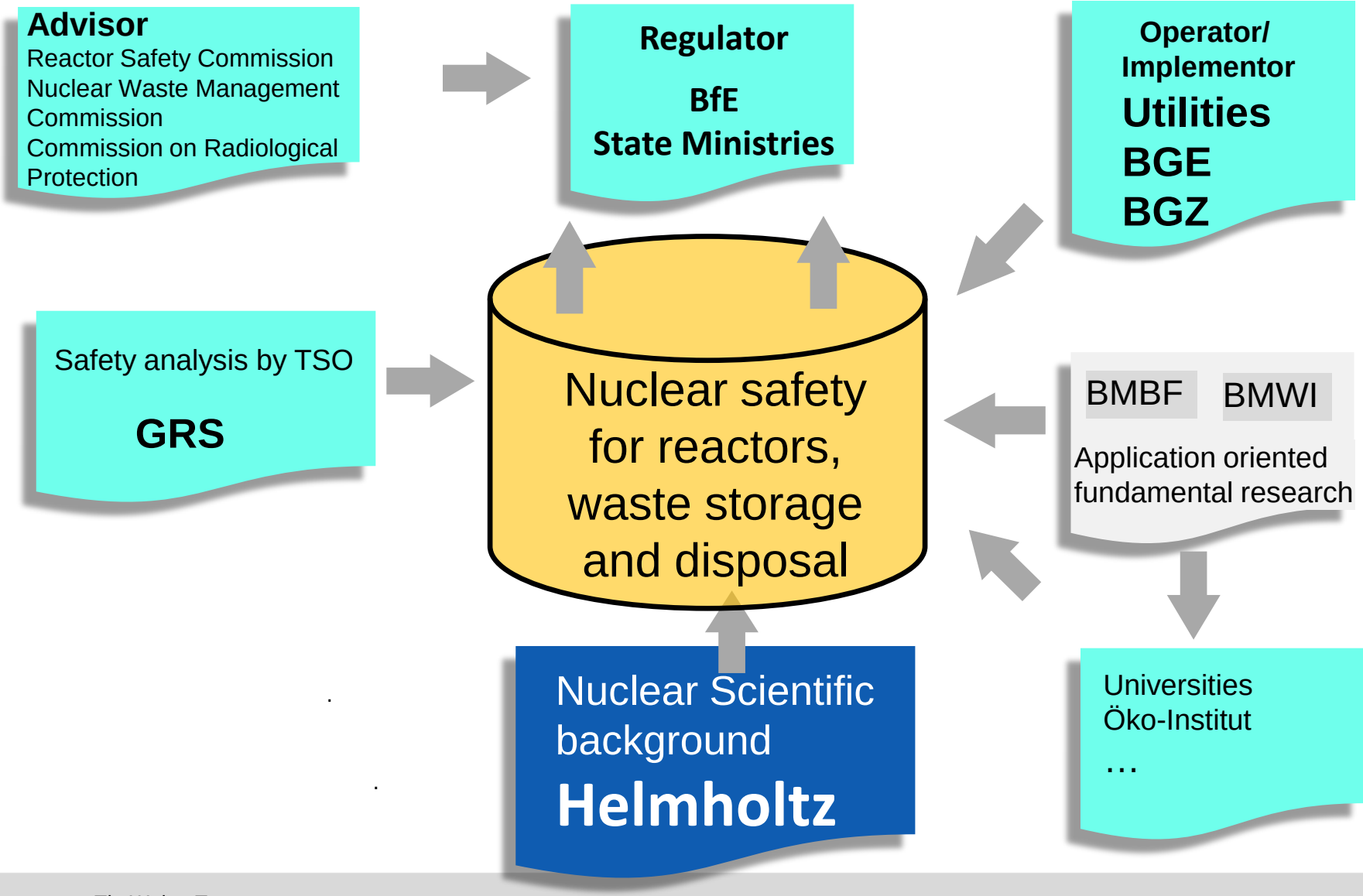

FJOH-Summer School

Our Mission

KIT reactor safety research as an integral part of Helmholtz research

- Contributions to immediate and long-term impact on reactor safety
- International cutting-edge research by multidisciplinarity and innovation with a long-term perspective – beyond 2022
- Enhancement of cooperation with important international players
- Ensure competencies for continuing tasks in nuclear technology for research, industry and authorities

Nuclear Safety Organisations in Germany



Thank you for your attention



Th. Walter Tromm
Karlsruhe Institute of Technology
Programme Nuclear Safety Research

walter.tromm@kit.edu

IAEA activities in the area of Nuclear Power Reactor Fuel Engineering

M.S. Veshchunov

Nuclear Fuel Cycle and Materials Section, Division of Nuclear Fuel Cycle and Waste Technology, Department of Nuclear Energy, International Atomic Energy Agency

Vienna International Centre, PO Box 100, 1400 Vienna, Austria

Abstract

The main IAEA program implementation tools in the area of fuel engineering are Coordinated Research Projects (CRP), Technical Meetings (TM), Expert Reviews, and Databases. Since 2011 a special attention is being paid to projects related to the IAEA Nuclear Safety Action Plan initiated after Fukushima accident, that include Coordinated Research Projects “Fuel Modelling in Accident Conditions” (CRP FUMAC) and “Analysis of Options and Experimental Examination of Fuels for Water-Cooled Reactors with Increased Accident Tolerance” (CRP ACTOF). This report provides update on organization and implementation practices of these activities, and summarizes their major outputs.


KIT
Karlsruher Institut für Technologie

IAEA
International Atomic Energy Agency

IAEA Activities in the Area of Nuclear Power Reactor Fuel Engineering

M. Veshchunov

Technical Lead (Fuel Engineering)

Nuclear Fuel Cycle and Materials Section

Division of Nuclear Fuel Cycle and Waste Technology

Department of Nuclear Energy

IAEA, Vienna, Austria

m.veshchunov@iaea.org

24th International QUENCH Workshop
Karlsruhe Institute of Technology, Germany
13-15 November 2018

Outline

- **Who are we?**
  - IAEA statute and structure
- **Who are our customers/partners?**
  - Developed and developing countries
- **How can we meet their needs?**
  - Sub-Programme 1.2.2: NP Reactor Fuel and Fuel Cycle Facilities
- **What are our deliverables?**
  - CRPs, TMs, Publications, Data Bases, …

IAEA: Statute and objectives

Established in 1957

170 Member States

~ 2,560 multidisciplinary professional and support staff from more than 100 countries



ATOMS FOR PEACE AND DEVELOPMENT

The Agency shall seek to accelerate and enlarge the contribution of atomic energy to peace, health and prosperity throughout the world.

IAEA: Main areas of work





Safeguards and Verification | Safety and Security | Science and Technology

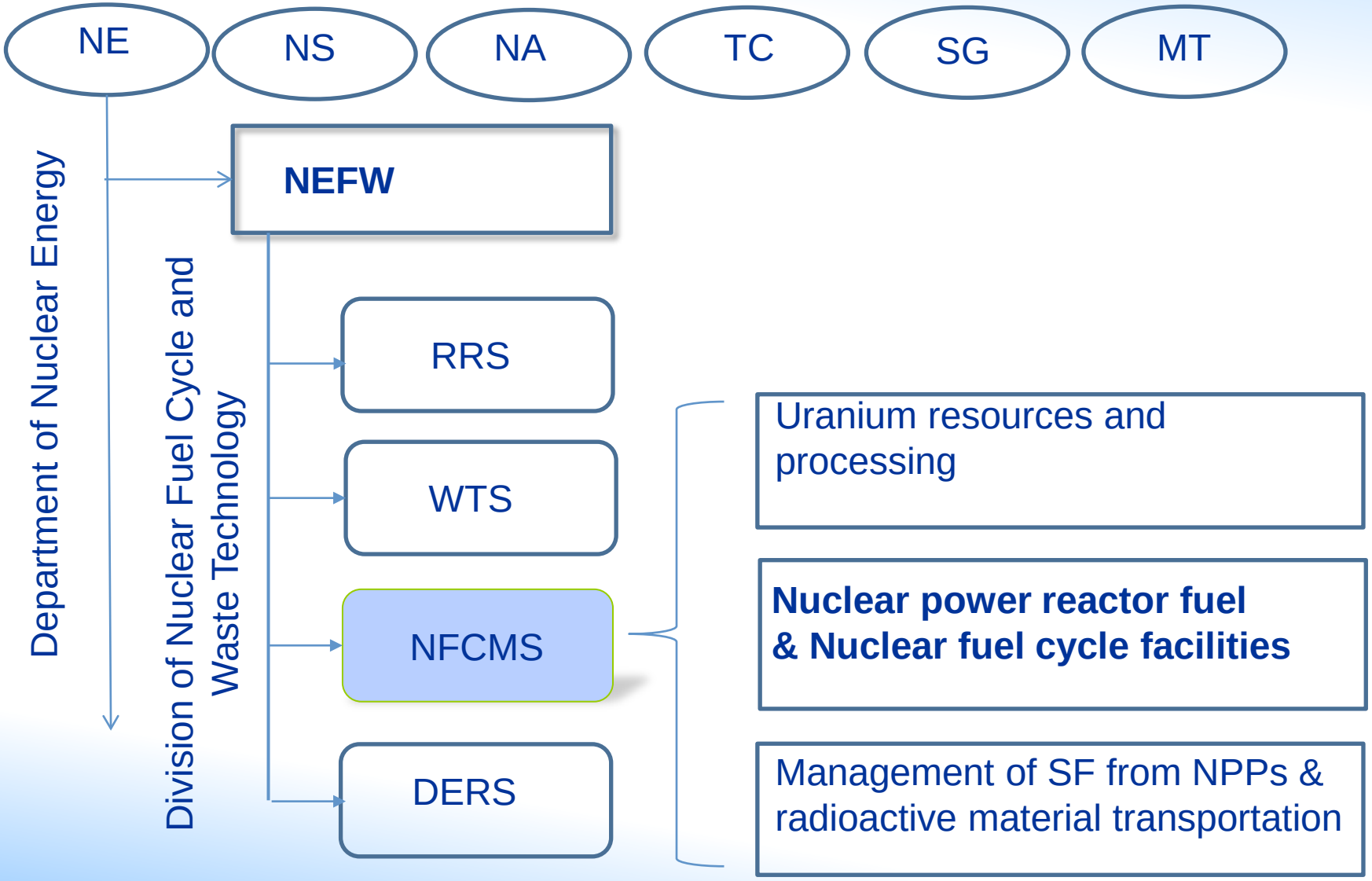
Gather Best Practices, Support Scientific Development
Publications, Coordinated Research Projects

Peace

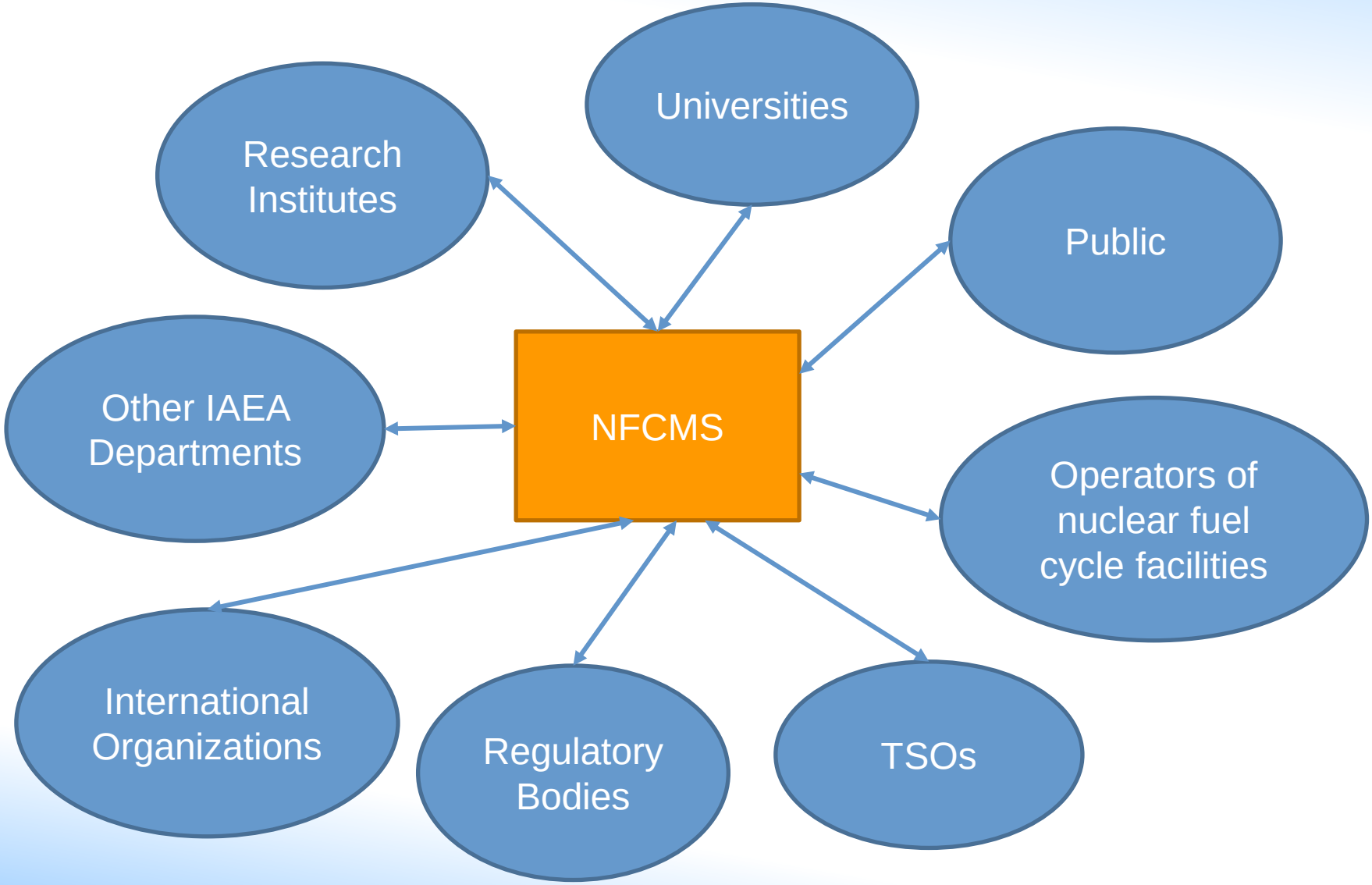
Development

Disseminate Information and Support Programmes
Networks, Peer Reviews, Technical Cooperation Projects

Who are we?


NE
NS
NA
TC
SG
MT
Department of Nuclear Energy
Division of Nuclear Fuel Cycle and Waste Technology
NEFW
RRS
WTS
NFCMS
DERS
Uranium resources and processing
Nuclear power reactor fuel & Nuclear fuel cycle facilities
Management of SF from NPPs & radioactive material transportation

Who are our customers/partners?



IAEA Sub-programme 1.2.2: Nuclear Power Reactor Fuel

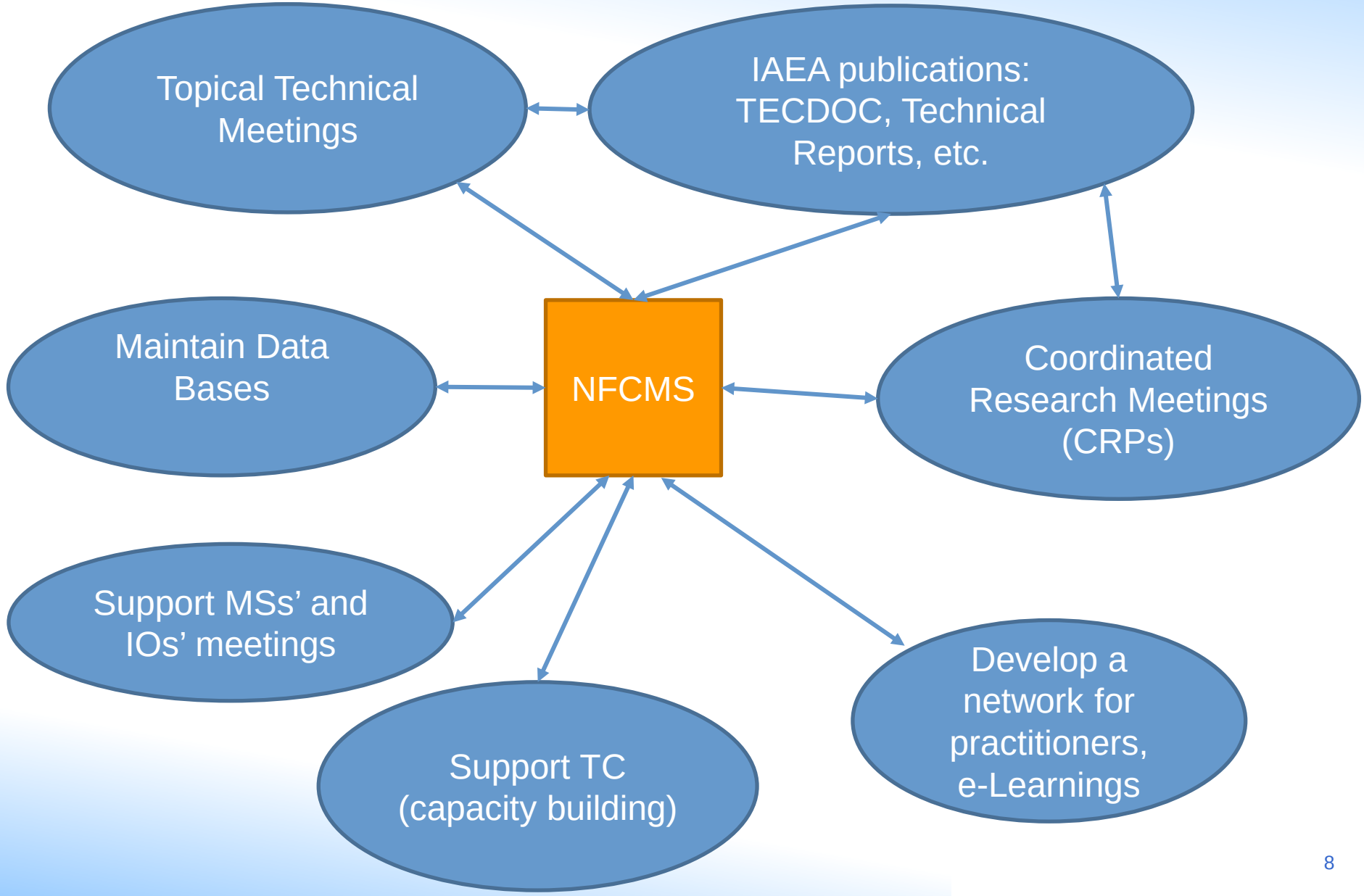
Objectives

- Support MS to understand and address factors affecting the design, fabrication and in-pile behaviour of currently operating and innovative nuclear fuels and materials for power reactors
- Support MS to technically implement IAEA Safety Standards when operating or upgrading existing nuclear fuel cycle facilities, and to understand and address factors affecting the ageing of these facilities.

Advised by TWG FPT

- The Technical Working Group on Fuel Performance and Technology (TWGFPT) is a group of recognized experts from MSs to provide advice and support programme implementation, reflecting a global network of excellence and expertise in the area of nuclear power reactor fuel engineering (25 Members)

What are our deliverables?



Coordinated Research Projects (CRPs)

- CRPs are a mechanism for organizing international research work within the IAEA programme of work
- A CRP theme is scoped in consultation with experts, and authorized by the IAEA for proposals of work from Member States
- Typically ~4 years, organized around 3 research coordination meetings (RCMs)
- A very good opportunity to work with many groups around the world
- CRP direction is largely defined in the first RCM by the CRP participants
- Finalized as an IAEA TECDOC
- Results are available, free of charge, to scientists, engineers and other users from all Member States

CRP on Analysis of Options and Experimental Examination of Fuels with Increased Accident Tolerance (ACTOF)

- **Status**
  - IAEA CRP T12030 (2014-2018)
  - Regular Budget (Project 1.2.2.003: AP Support Related to Nuclear Power Reactor Fuel)
  - RCM-1: on 2-4 November 2015 in Vienna
  - RCM-2: on 20-22 June 2017 in Vienna
  - RCM-3: *planned* on 26-29 November 2018 in Vienna
- **Participants** (17 organizations from 13 MSs)

  Argentina (CNEA), Brazil (USP), China (CNPRI, CIAE, NPIC), Finland (VTT), Germany (KIT), India (BARC), Italy (NINE), Korea (KAERI), Poland (INCT), Russian Federation (VNIINM, IBRAE), United States (Westinghouse, Batelle), Czech Republic (ChTU), JAEA (Japan) [*joined at RCM-2*]
- **Observers**

  OECD-NEA, EPRI (USA), US NRC, GRS (Germany) - *active*

ACTOF Joint Actions

- Round Robin Tests of ATF claddings
  - Provide Zr alloy substrate for coating (Westinghouse)
  - Preparation and pre-characterization of coated cladding materials (INCT, KAERI, KIT, CTU, VTT)
  - Autoclave tests and post-test characterization (INCT, TU, VTT)
  - High temperature steam tests and post-test characterization (KIT, TU, VTT)
- Benchmark exercise on FeCrAl-UO_2
  - Provide modelling input, normal operation case specification (UO_2-FeCrAl) and LOCA case specification, output format for FeCrAl (INL)
  - Perform benchmark calculation using different codes; include BISON (INL), FRAPCON (USP), BACO (CNEA), TRANSURANUS (NINE), FEMAXI-7 (Waseda University)
- Severe Accident benchmark exercise (QUENCH-19)
  - Provide results of severe accident testing, including separate single rod test and QUENCH-19 (FeCrAl) test (KIT)
  - Benchmark calculation for QUENCH-19 (FeCrAl) test using SOCRAT code (IBRAE) and ATHLET-CD (GRS)

Coordinated Research Projects (CRPs)

Coordinated Research Projects (CRPs)	14	15	16	17	18	19	20	21	22	23
Fuel modelling in accident conditions (FUMAC)										
Reliability of high power, extended burnup and advanced PHWR fuels										
Analysis of options and experimental examination of fuels for water-cooled reactors with increased accident tolerance (ACTOF)										
Accelerator simulation and theoretical modelling of radiation effects (SMoRE-2)										
Fuel Materials for Fast Reactors (embedded meeting in FR-17, June 2017; CM in 2018; RCM-1 in 2019)										
Testing, Modelling and Simulations for ATF (ACTOF-2)										

Technical Meetings

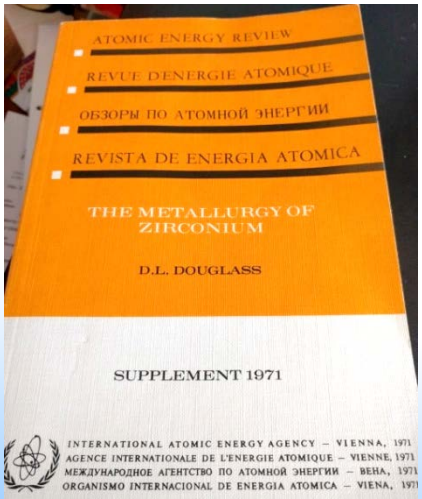
Technical Meetings	Hosts	18	19	20	21	
TM-2 on Beyond 5% enrichment limit for LWR: perspectives and problems (TM-1 in 2015)	Moscow (Russia)					
TM on Nuclear Fuel Cycle Facilities (Information System and Ageing Issues)	Vienna					
TM on Progress on Pellet Cladding Interaction and Stress Corrosion Cracking: Experimentation, Modelling and Methodologies Applied to Support the Flexible Operation of Nuclear Power Plants	Aix-en-Provence (France)					
TM on Modelling of Fuel Behaviour in Design Basis Accidents and Design Extension Conditions	Shenzhen (China)					
TM on the Control and Monitoring of Coolant Chemistry and Related Issues on Fuel Reliability in Pressurized Heavy Water Reactors	Toronto (Canada)					
TM on Advances in post-irradiation examination techniques for power-reactor and innovative fuels						
TM on Advanced (including MOX) fuel design, fabrication and operation in Water cooled Reactors						
TM on Control and Monitoring of Coolant Chemistry and Related Issues on Fuel Reliability in PHWRs						
TM on Small Modular Reactors (SMRs) Fuel design, fabrication and operation						

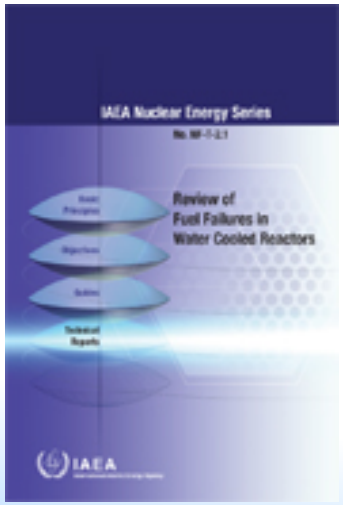
In-Cooperation Support of International Conferences

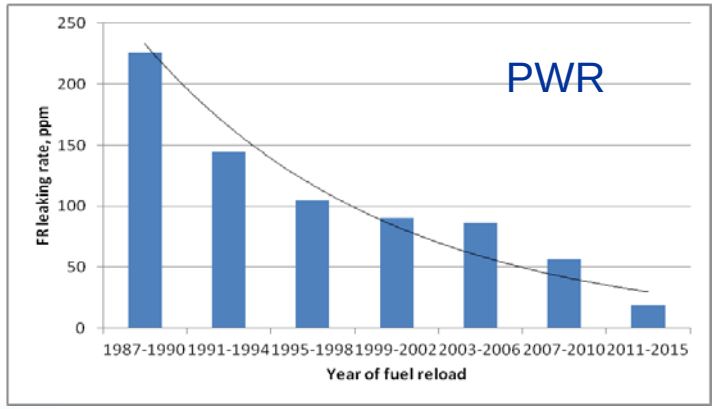
- NuMat International Conference
- Water Reactor Fuel Performance Meeting and Top Fuel Conference
- International Conference on WWER Fuel: Performance, Modelling and Experimental Support (Bulgaria)
- International Conference on CANDU Fuel (Canada)
- HOTLAB International Conference (Belgium)
- International QUENCH Workshop (Germany)
- International Conference on Characterization and Quality Control of Nuclear Fuels (CQCNF) (India)
- ……

Notable Publications under Preparation

- Book on The Nuclear Metallurgy of Zirconium
  - a comprehensive book, covers all aspects of Zr
  - updates the earlier published IAEA Zr book (by D. Douglass, 1971)
  - 3 Volumes, 9 Chapters
  - Contributions from 14 authors (Chief Editor C.E. Coleman)
  - 1500 pages (A4 size), 1074 figures
- NE Series Report on Review of Fuel Failures in Water Cooled Reactors in 2006-2015
  - updates the earlier published IAEA Fuel Failure Reviews







Database systems

- 3 database systems (NFCIS, PIE Facilities Database, MADB) and 1 simulation tool (NFCSS)
- Individual databases were initially developed in electronic form in 1980's
- Web based system with public access since 2001
- On IAEA NUCLEUS platform since 2012/13



https://infcis.iaea.org/Default.asp

IAEA
International Atomic Energy Agency

Thank you!

CoreSOAR project on update of the Core Degradation State-of-the-Art Report: Summary and Conclusions

Tim Haste, Marc Barrachin, Florian Fichot, Georges Repetto (Institut de Radioprotection et Sûreté Nucléaire (IRSN), Cadarache, France); Christophe Journeau, Romain Le Tellier, Frédéric Payot, Pascal Piluso, Yves Pontillon (Commissariat à l'Energie Atomique et aux Energies Alternatives (CEA), Cadarache, France); Christine Guéneau (CEA, Saclay, France); Alix Le Belguet (EDF R&D, PERICLES, Paliseau, France); Zoltán Hózer (Centre for Energy Research, Hungarian Academy of Sciences (ETA MK), Budapest, Hungary); David Bottomley (JAEA, ex- EC/JRC Karlsruhe, Germany); Thorsten Hollands, Henrique Austregsilo (Gesellschaft für Anlagen- und Reaktorsicherheit (GRS) Ggmbh, Garching, Germany; Gabor L. Horvath (NUBIKI Nuclear Safety Research Institute, Ltd., Budapest, Hungary); Alexei Miassoedov, Martin Steinbrück, Juri Stuckert (Karlsruhe Institute of Technology, Germany); Sevostian Bechta (KTH Royal Institute of Technology, Stockholm, Sweden), Terttaliisa Lind (Paul Scherrer Institute (PSI), Switzerland); Jon Birchley (Consultant, ex-PSI); Michael Buck, Georg Pohlner (University of Stuttgart, Germany)

ABSTRACT

In 1991 OECD/CSNI published the first State-of-the-Art Report on In-Vessel Core Degradation, updated to 1995 under the EC 3rd Framework programme, covering phenomena, experiments, material data, main modelling codes, code assessments, identification of modelling needs, and conclusions including the needs for further research. This knowledge was fundamental to safety issues such as in-vessel melt retention of the core, recovery of the core by water reflood, hydrogen generation and fission product release.

However in the last 20 years, there has been much progress in understanding, with major experimental series finished, e.g. the integral Phébus FP tests, while others have many tests completed, e.g. the QUENCH series on reflooding degraded rod bundles, PRELUDE/PEARL on debris bed quench, and LIVE on melt pool behaviour in the lower head, similarly regarding integral codes, e.g. MELCOR and MAAP (USA) and ASTEC (Europe), which encapsulate current knowledge quantitatively. After two EC-funded projects on the SARNET network of excellence, continued in the NUGENIA association, it is timely to take stock of the knowledge gained in the experimental and modelling areas.

The CoreSOAR project, in NUGENIA/SARNET, draws together the experience of 11 European partners to update the state of the art in core degradation, to finish by the end of 2018. Integral experiments, separate-effects data, modelling codes and code validation have been reviewed, so the final stages of the report have focussed on summarising the experimental results, reviewing the status of severe accident modelling codes and their assessment, drawing overall conclusions, and identifying needs for further research. This presentation indicates the results of these final steps in the project. The final report is a reference point for ongoing and future research programmes in NUGENIA, in other EC research projects such as in Horizon2020 (e.g. IVMR), and for projects in OECD/CSNI (e.g. PreADES and TCOFF).

Presentation at the 24nd International QUENCH Workshop, Karlsruhe Institute of Technology, 13-15 November 2018.


ologie
KIT

CoreSOAR Core Degradation SOAR Update: Summary and Conclusions

24th International QUENCH Workshop

Karlsruhe Institute of Technology, Germany

13th - 15th November 2018

T. Haste, M. Barrachin, F. Fichot, G. Repetto (IRSN); A. Miassoedov, M. Steinbrück, J. Stuckert (KIT); M. Buck, G. Pohlner (IKE); S. Bechta (KTH); A. Le Belguet, M. Torkhani (EDF); Th. Hollands, H. Austregesilo (GRS); Ch. Guéneau, Ch. Journeau, **R**. Le Tellier, F. Payot, P. Piluso, Y. Pontillon (CEA); T. Lind (PSI); J. Birchley (Consultant, formerly PSI); Z. Hózer (MTA EK); G.L. Horvath (NUBIKI); P.D.W. Bottomley (JAEA, formerly JRC/ITU)

OUTLINE

- Introduction
- Motivation, Scope and Method
- Partners
- Status
- Experimental database
- Severe accident computer modelling codes
- Summary

INTRODUCTION

- The CoreSOAR in-kind project to update the in-vessel core degradation SOAR of OECD/CSNI of 1991 and updated in the EC 3rd framework programme to June 1995 received ExCom approval in May 2014, and technical work started in June 2016;
- The scope of the work was agreed amongst the 11 European partners, with a view to complete the final report by the end of 2018, with publication of a summary in the open literature and the editing of a NUGENIA position;
- Material covered includes small-scale and integral tests, the main modelling codes in use in Europe, summary of main phenomena, and identification of current research needs;
  - The scope has been extended from previous reports to include CANDU-specific matters, VVER-specific matters, BWR-specific matters (particularly in view of Fukushima), and the important industry severe accident analysis code MAAP;
  - It is coordinated with other European projects such as H2020 IVMR (in-vessel melt retention);and OECD projects such as BSAF (based on Fukushima);
- Papers/presentations were given in NENE2016 and NENE2017, with a status report in ERMSAR2017, and a final presentation planned for ERMSAR2019.

MOTIVATION and SCOPE (1/2)

- OECD/CSNI published the first State-of-the-Art Report on In-Vessel Core Degradation, NEA/CSNI/R(91)12, in 1991, updated to June 1995 under the EC 3rd FWP, EUR 16695 EN;
- These reports covered phenomena, small- and large-scale experimental programmes, material data, modelling codes, code assessments, identification of modelling needs, and conclusions/ recommendations including needs for further research;
- Such knowledge is relevant to such safety issues as in-vessel retention of the core, recovery of the core by water reflood, hydrogen generation and fission product release;

MOTIVATION and SCOPE (2/2)

- In the following ~25 years, there has been much progress in understanding, with major experimental programmes finished (e.g. Phébus FP) or well under way (e.g. QUENCH, LIVE), similarly regarding modelling codes (e.g. MAAP, MELCOR (USA), ASTEC (Europe), ATHLET-CD (Germany)) that quantitatively encapsulate current knowledge;

- Material covered includes small-scale and integral tests, the main modelling codes in use in Europe, summary of main phenomena, and identification of current research needs;

  - The scope has been extended from previous reports to include CANDU-specific matters, VVER-specific matters, BWR-specific matters (particularly in view of Fukushima), and the important industry severe accident analysis code MAAP;

  - It is coordinated with other European projects such as H2020 IVMR (in-vessel melt retention);and OECD projects such as BASF (based on Fukushima);

METHOD

- Taking EUR 16695 EN as a starting point, the state-of-the art is reviewed taking account of published material, and the conclusions of EC/SARNET and previous EC framework programmes regarding research priorities and the need for further work;
- Advantage is also taken of the CSNI in-vessel code validation matrix report NEA/CSNI/R(2000)21, CSNI International Standard Problems, code benchmarks performed under the aegis of EC/SARNET, and the Crosswalk code comparison exercises (MAAP/MELCOR/ASTEC) based on Fukushima;
- Experiments are ordered by phenomena covered rather than by the physical scale of the facility;
- A tabular approach is adopted for separate-effects tests, so that their main features can be more easily compared;
- The revised report was prepared over ~2.5 years, end Dec. 2018, with new material covered in full, and previously reported material summarised and referenced so that a complete, up-to-date picture of the field can be readily obtained;

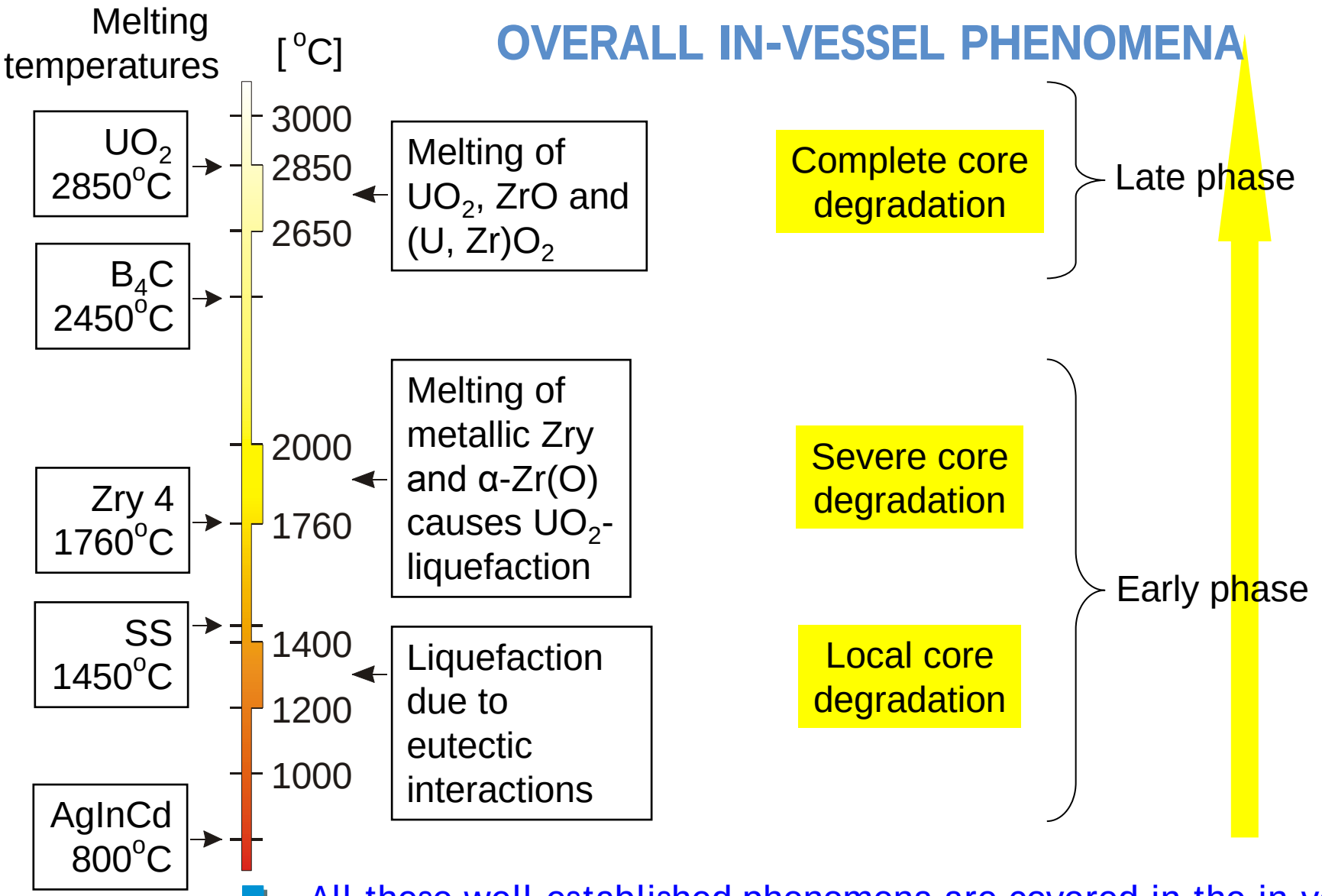
PARTNERS

- These eleven European partners took part, with main responsibilities as indicated:
  - IRSN France, lead: Phébus FP, BECARRE, PRELUDE/PEARL, air oxidation, ASTEC and ICARE/CATHARE codes etc., CANDU-specific matters;
  - KIT Germany: QUENCH, LIVE, small-scale materials interaction tests, air oxidation and quench tests, ISTC;
  - IKE Stuttgart Germany: IKE small-scale experiments and modelling (DEBRIS, MEWA etc.), KESS code (now incorporated into ATHLET-CD);
  - KTH Sweden: ISTC, KTH melt pool tests and modelling;
  - GRS Germany: ATHLET-CD, summary of research priorities;
  - EdF France: MAAP-PWR;
  - CEA France: CEA experiments: core degradation aspects of VERCORS and VERDON, KROTOS, BALI, etc.;
  - MTA EK Hungary (was AEKI): VVER-1000 specific matters, MTA EK/AEKI experiments such as CODEX;
  - NUBIKI Hungary: VVER-440 matters, MAAP-VVER;
  - JRC Karlsruhe Germany (was ITU): EU, late phase matters, PIE, ISTC;
  - PSI Switzerland: USNRC codes MELCOR, and SCDAP/RELAP5, with its extension SCDAPSIM by ISS.

STATUS

- ExCom granted a NUGENIA label in May 2014, the approval was transmitted in July 2014. A consortium agreement was agreed by all the partners in mid-2016;
  - Planning meeting held at Karlsruhe in Nov. 2014, with the kind agreement of KIT, in association with the 20th QUENCH Workshop, the schedule was agreed, along with the scope, method, partition of the work, and a detailed contents list with recommended lengths of the chapters;
  - A workspace was organised under NUGENIA/ECCP under 'in-kind' projects, in which current versions of the final report are maintained, with a planning spreadsheet and agendas/minutes of project meetings;
  - Technical work started in June 2016, with final report due end Dec. 2018. Progress meetings were coordinated with QUENCH workshops, IVMR project meetings, ERMSAR meetings etc., as far as is possible. The last one (5th) was held in Tenerife on 18th April coordinated with SARNET/TA2 meetings, while the concluding meeting is scheduled after this QUENCH workshop;
  - The final report is due to appear by the end of this year;
  - Papers included in the Nuclear Energy in New Europe (NENE) conferences in Sept. 2016 and 2017, on small-scale experiments and on code status respectively, and an overall status report for ERMSAR2017, Warsaw, May 2017. A concluding paper and presentation are being prepared for ERMSAR2019, Prague, March 2019 along with an open literature paper.

OVERALL IN-VESSEL PHENOMENA



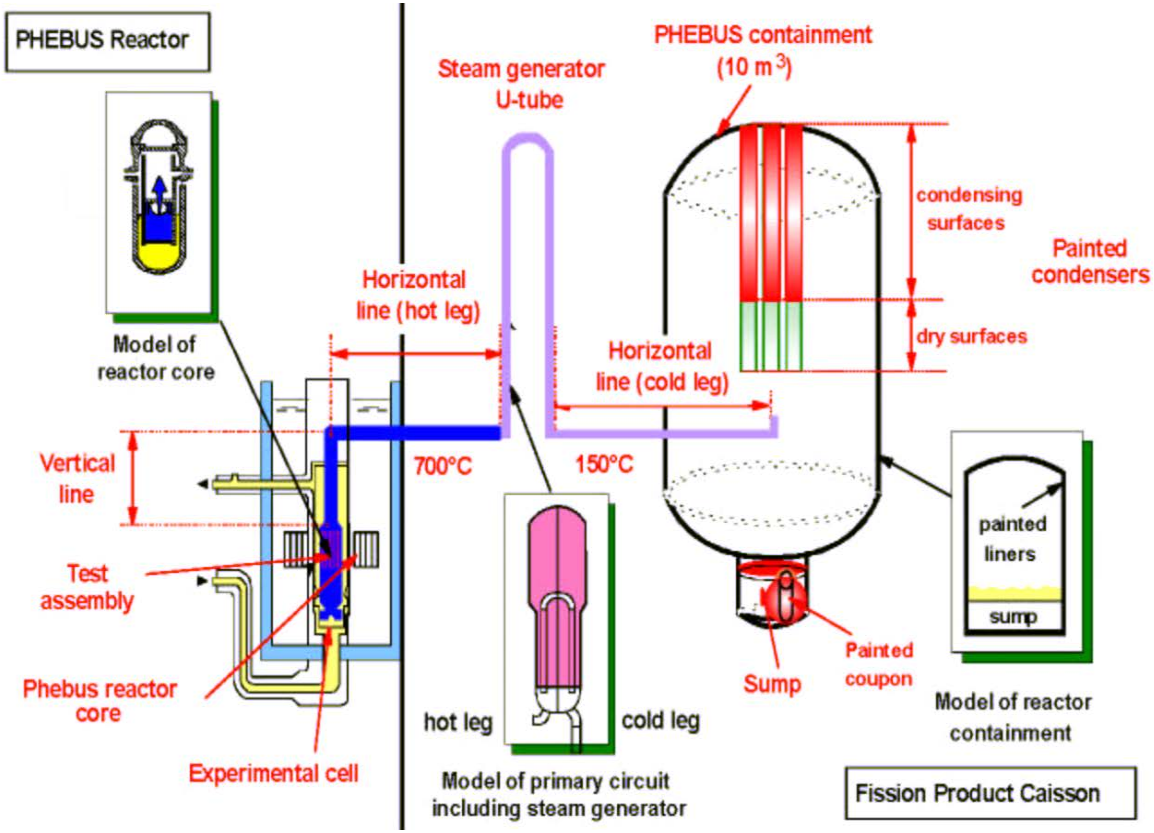
All these well-established phenomena are covered in the in-vessel core degradation SOAR update final report SARNET-CoreSOAR-D3.

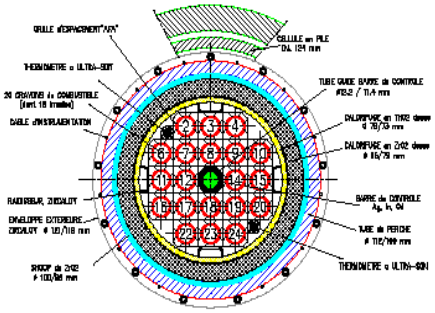
EXPERIMENTAL DATABASE

- Integral tests;
  - Nuclear-heated Phébus FP bundle experiments at IRSN, data on core degradation and fission product release as well as data on circuit transport and containment behaviour;
  - Electrically-heated QUENCH bundle experiments at KIT, reflood of degraded cores in mainly rod-like geometry;
- Separate-effects tests:
  - Many tests on material interactions including air oxidation of Zr-based alloys - ISTP/MOZART programme (IRSN), oxidation of B_4C absorber materials and relocated mixtures with steam - ISTP/BECARRE programme (IRSN), similar oxidation studies in steam and air and investigation of B_4C and Ag/In/Cd control rod failure mechanisms (KIT), dissolution of fuel by Zr-based cladding with relocation of the resulting mixtures;
  - HEVA-VERCORS & VERDON FP release/relocation data for irradiated PWR fuel (CEA):
  - Debris bed quench is studied in small-scale facilities such as PRELUDE and PEARL (IRSN), DEBRIS (IKE), COOLOCE and STYX (VTT), POMECO (RIT) and SILFIDE (EDF);
  - Lower head - the LIVE programme at KIT studies melt pool behaviour in the reactor pressure vessel and assesses melt retention concepts using simulant materials, while the KROTOS programme of CEA studies molten-fuel coolant interaction in-vessel as well as ex-vessel;

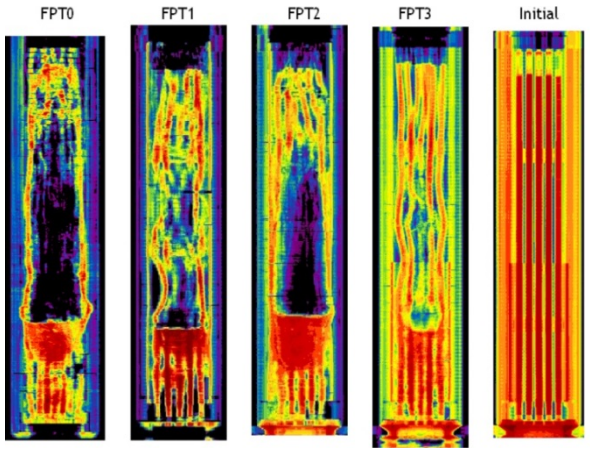
PHEBUS FP Overview

- Phébus FP facility for in-reactor integral experiments investigated fuel rod degradation and the behaviour of fission products released via the primary coolant circuit into the containment building
- Main core degradation parameters varied over 4 bundle tests: coolant (steam-rich or steam-poor), control rod (AIC or B_4C) and the final bundle power), irradiated/trace-irradiated fuel; 1 debris bed test also performed.





Bundle X-section



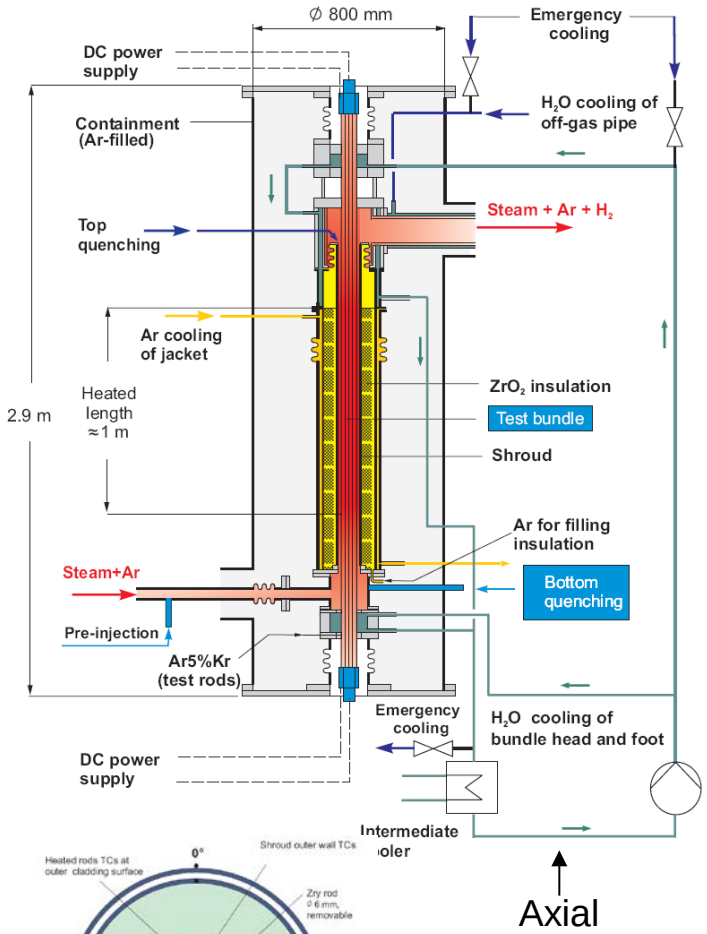
Scale: 1:5000

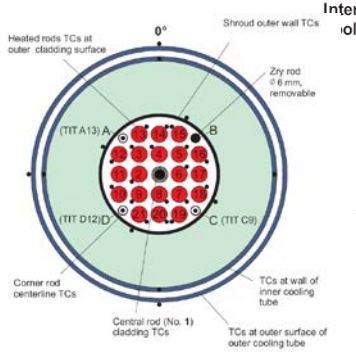
[IRSN, Ann. Nucl. En. Phébus FP special issue 62, 2013]

PHEBUS FP CONCLUSIONS – CORE DEGRADATION

- A vast amount of information was obtained on core degradation phenomena from the initial stages through to the formation of a melt pool in the rodded region;
- Concerning control rod effects, B_4C has more effect than Ag/In/Cd, in promoting degradation, and also contributes to hydrogen production, consistent with CORA and QUENCH;
- A steam-poor period leads to slower, more progressive degradation;
- Irradiated fuel degrades more quickly than unirradiated fuel - the experiments also yielded detailed data on melt composition;
- The transition to rod-like to melt pool geometry may be expressed simply in modelling codes by a temperature criterion, 2500±200 K, consistent with the results of the separate-effects ISTP/VERCORS experimental programme conducted by CEA;
- These conclusions are supported by other integral and separate-effects tests.

QUENCH Overview





QUENCH bundle X-sections

Radial

[KIT, Nucl.. Tech. 147(2) 2004, pp. 202-215]

- To explicitly investigate the effect of reflood on bundle degradation, the QUENCH program was initiated in Karlsruhe in 1996 and is still on-going;
- This comprises bundle experiments as well as complementary separate-effects tests.
- So far, 19 integral bundle QUENCH tests with 21-31 electrically-heated fuel rod simulators of 2.5 m length using zirconia as fuel substitute have been conducted;
- The temperature histories were achieved through successive power ramps;
- The effects of pre-oxidation, temperature at reflood initiation, flooding rate, of neutron absorber materials (B_4C, AIC), air ingress, and of the type of cladding alloy were investigated;
- The QUENCH-Debris test investigated the formation and coolability of a debris bed in the core.

QUENCH-16 (air ingress/reflood); middle part of bundle after dismounting of ZrO_2 insulation (deleted together with shroud parts) showing severe degradation



[KIT, Prog. Nucl. En., 71, pp. 134-141].

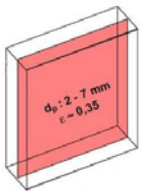
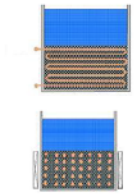
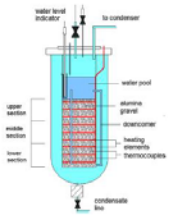
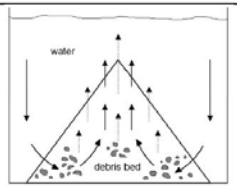
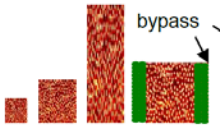
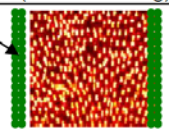
QUENCH CONCLUSIONS

- Reflood behaviour of degraded cores in mainly rod-like geometry was studied in QUENCH, following the earlier CORA series, leading to improved experimental understanding of the phenomena involved, with corresponding model improvements made and in progress;
  - A nuclear reactor core is coolable as long as the core is still basically intact and no or only local melt formation has already taken place;
  - Model improvements made with the help of separate-effects tests;
- Research priorities were identified in the SARNET EU Network of Excellence, completed in 2013, taking into account the QUENCH results;
- Main uncertainties for degradation now concern cooling of debris beds, experiments and model development continue; e.g. tests QUENCH-DEBRIS (KIT) completed, PRELUDE/PEARL (IRSN) underway, others at IKE Stuttgart etc.;

[GRS et al, Ann. Nucl. En. 74 (2014) 4-11]

SMALL-SCALE REFLOOD EXPERIMENTS

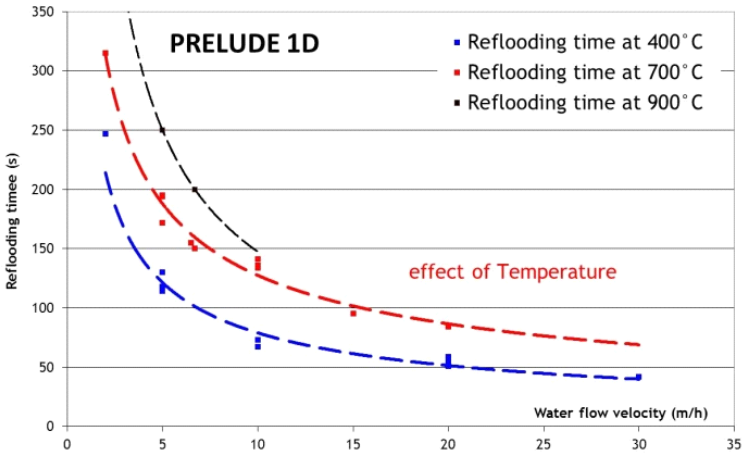
- Reflooding of debris beds is a priority safety issue in NUGENIA/SARNET;
- Many small-scale tests have been and are being performed to improve knowledge in this area, leading to a reduction of modelling uncertainties.

Experiments Parameters	SILFIDE EDF (2000)	POMECO RIT	STYX VTT	COOLOCE VTT	DEBRIS IKE	PRELUDE-IRSN (2009-2013)	PEARL IRSN (> 2015)
Reflooding	Only dry out	Top flooding and dry out	Effect of lateral and top flooding	Top flooding and dry out	Bottom and Top flooding, dry out	Bottom flooding	Bottom and Top flooding
Temperature (K)	Up to 473	Up to 775				Up to 1200	Up to 1300
Pressure (MPa)	0.1	0.1	0,11 up to 0,7 MPa	0,11 up to 0,7 MPa	0.1 to 0.5 MPa	0,1 MPa	0.1 to 1MPa (10bar)
Subcooling (K)	0 - 5	80			80	293 K (room temp.)	0 to 50
Water inlet velocity ($m^3/h/m^2$)	0	Gravity driven with downcomer			1 to 36	2, 5, 10, 20	2 to 50
Heating process	Induction	Internal heaters	Internal heaters	Internal heaters (up 70 kW)	Induction	Induction Power maintained during quench (40 to 200W/kg)	Induction Power maintained during quench (100 to 300W/kg)
Geometry Debris mass					 37 kg	 1 2 3 4 bypass 5kg 24kg 57kg 58kg	 500 kg
Diameter/height	500.600.100mm Parallepipedic geometry	Ø350/450mm	Ø300/600mm	Ø 500 mm/ 270 mm conical shape (17,5 l)	Ø125/640mm Ø150/640mm	1 : Ø110/100mm 2 : Ø180/200mm 3 : Ø180/500mm 4 : Ø290/250mm	Ø540/500mm
Particle diameter (mm)	2 to 7.2	0.2 to 1	Irregular particles (0,25 to 10 mm) Average Ø 3.46 mm	zirconia/silica particles 0.82–1.13 mm	3 to 6 + mixtures and irregular shape	Stainless steel 1, 2, 3 4 + mixtures + non homogeneous size	Stainless steel spherical part. Ø2, 3 and 4 mm

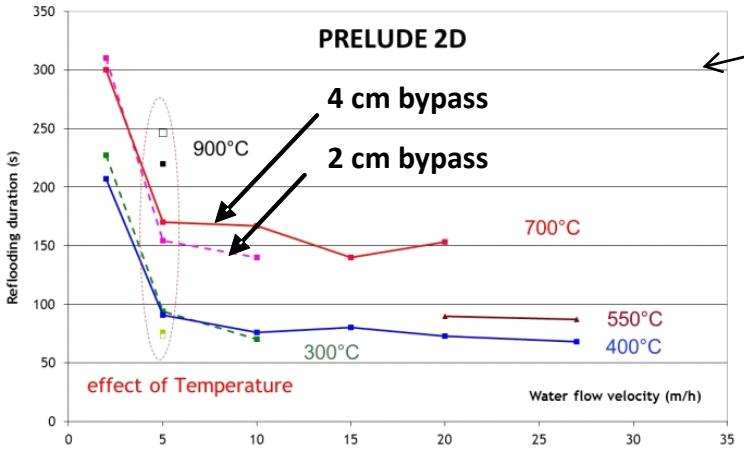
©2011/2018 IRSN, G. Repetto et al., adapted from NURETH-14, paper 216, and private communication, 2018.

DEBRIS BED COOLING EXPERIMENTS – PRELUDE/PEARL

- Debris bed coolability is important regarding stopping or at least slowing down severe accident evolution; a major concern of safety studies is to evaluate the consequences of water reflooding of a severely damaged reactor core, where a large part of the core has collapsed and formed a debris bed;
- The already extensive knowledge base is being extended by the PRELUDE experiments conducted by IRSN, supported by EDF and the EU in the frame of SARNET, to validate codes such as ASTEC;
  - These tests at atmospheric pressure involving different particle bed sizes (Ø170 and Ø290 mm), and debris bed heights (200 to 250 mm) gave very useful information on debris bed cooling, for example the dependence of reflooding time and steam production on the initial temperature of the debris bed, and on the reflood flow rate - interpretation of these data continues, while tests at a larger scale continue in the PEARL programme.



Tests without bypass



Tests with bypass

Duration of reflooding in the PRELUDE tests as a function of water flow velocity

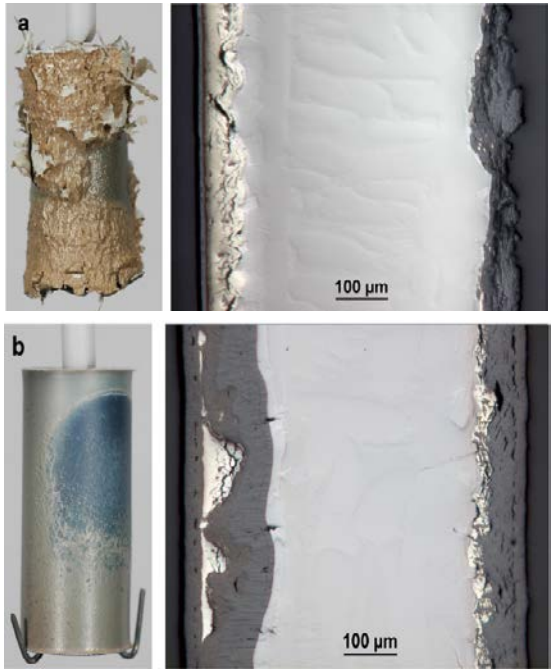
[IRSN, NURETH-14, Toronto, Sept. 2011, NURETH-15, Pisa, May 2013, Nucl. Eng. Des. 264 (2013), pp. 176-186]

SMALL-SCALE MATERIAL INTERACTION EXPERIMENTS - IRSN

- IRSN supplemented the Phébus FP experiments by separate-effects tests to understand better the phenomena observed, and to serve as a basis for model development and improvement;

- The EU-funded International Source Term Program (ISTP) included small-scale tests on air oxidation of Zr-based cladding (MOZART series) and on B_4C interactions (BECARRE series) at IRSN Cadarache;

  - Experiments included those *on oxidation kinetics of B_4C/SS liquid mixtures* in Ar/steam up to 1527°C, those on degradation of B4C control rod segments up to ~2000°C, those on *degradation of Zircaloy-4 and M5™ cladding tubes in air* in isothermal conditions at 600°C to 1200°C (in an 'as-received' bare state, or after steam pre-oxidation at 500°C to simulate in-reactor waterside corrosion), and those *investigating the specific effect of nitrogen on oxidation of Zircaloy-4 and M5™* claddings (samples pre-oxidised at 500°C in O_2, with different pre-oxidation modes, inducing significant variation in the pre-oxide microstructures).



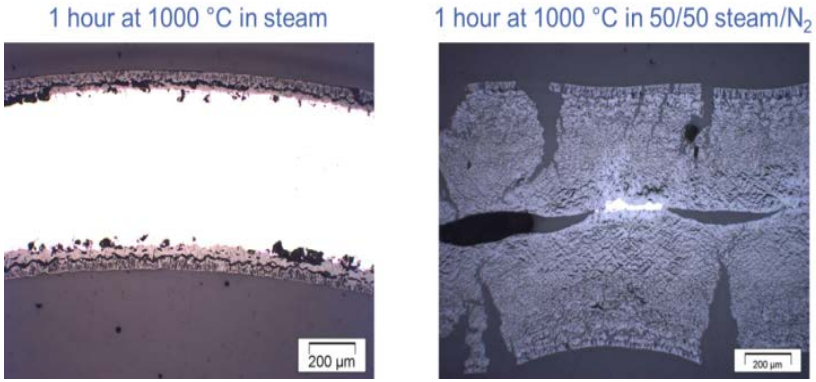
Zircaloy-4 pre-oxidised 20 days in O_2 at 500°C, nitrided 25 min in N_2 at 1100°C, then oxidised in air: (a) 26 min at 700°C; (b) 10 min at 1100°C

[IRSN, J. Nucl. Mat. 441, 2013, 84-95]

SMALL-SCALE MATERIAL INTERACTION EXPERIMENTS - KIT

- KIT performed many small-scale tests on clad oxidation including H_2 behaviour and control rod (CR) material interactions at high temperatures;
- CR failure mechanisms have been studied, different for boron carbide (B_4C) and Ag-In-Cd (AIC) CRs, although failure temperatures are similar, 1250-1450°C;

  - For AIC control rods, eutectic interactions between SS & the Zry guide tubes cause CR failure & release of the AIC components, first Cd in sudden bursts, then In & Ag – contact between the SS and Zry is believed to be due to rod bending;
  - B_4C melts at around 2450°C, but eutectic interactions with SS cause rapid liquefaction of the SS cladding above 1250°C;
  - Oxidation kinetics of B_4C-SS-Zry absorber melts are very high compared with the pure solid materials, oxidation of Zry and B_4C is highly exothermic, all give H_2 ;
  - Absorber melts aggressively attack adjacent fuel elements - Zry liquefied by absorber materials starts dissolution of the UO_2 >1000 K below the UO_2 m.p., accelerating core degradation;
  - Oxidation of current Zr alloys has been measured in various atmospheres at 600-1600°C;
  - Parabolic correlations apply > 1050°C, below that breakaway oxidation can occur with rapid H_2 uptake by underlying metal, approx. linear kinetics;
  - N_2 accelerates oxidation especially from 800 to 1400°C, through the formation ZrN at the metal/oxide interface, which oxidises rapidly owing to the formation of very porous, non-protective oxide scales.

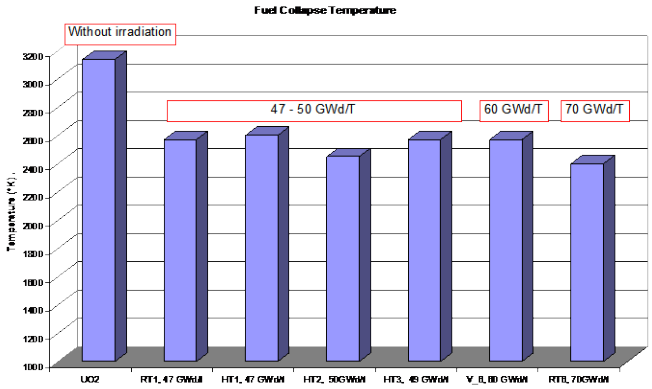


Influence of nitrogen on the oxidation of Zry-4, 1 hr at 1000°C

[KIT, ICAPP-2016, San Francisco, CA, USA, 2016]

SMALL-SCALE MATERIAL INTERACTION EXPERIMENTS - CEA

- Specific technical facilities, set up in shielded hot cells at CEA Centres, have been developed around the HEVA-VERCORS & VERDON programmes;
- These programmes are more specifically devoted to the FPs released from PWR fuel samples during conditions representative of severe accidents, up to loss of fuel integrity;
- Systematic fuel collapse detected at 2400-2600 K whatever the burn up from 47 GWd/t – 70 GWd/t, thus there is no great effect of high burn up;
  - Whatever the atmospheric conditions, the temperature at which the fuel loses its integrity is systematically inferior to both the melting point of unirradiated UO_2 and the solidus temperature of the ZrO_2-UO_2 eutectic;
  - The fuel collapse temperature decreases in oxidizing conditions, in reducing conditions for HT1 and HT3 and oxidizing conditions for HT2, the fuel collapse temperatures are ~2500 K for HT1 and HT3, ~2300 K for HT2.



	HT1 (~47 GWd/t)	HT2 (~47 GWd/t)	HT3 (~47 GWd/t)
T (K)	~2500	~2300	~2500
Atm	reducing	oxidizing	reducing

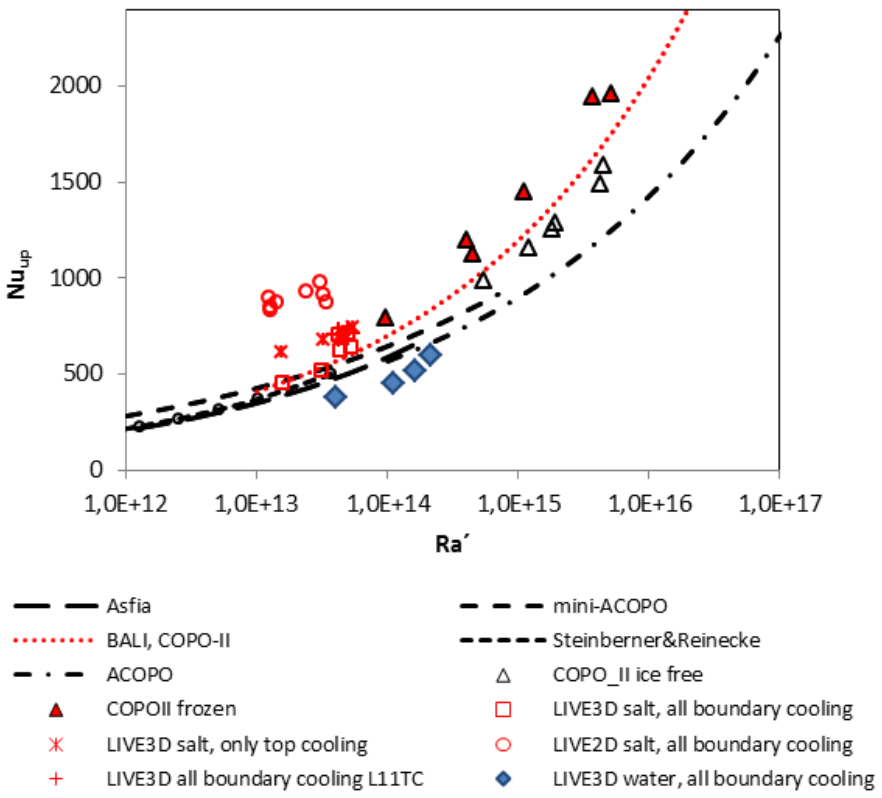
Fuel collapse temperatures in VERCORS compared with the melting point of non-irradiated UO_2 , 3142 K)

[CEA, Nucl. Tech. 108, 1994, 33-35; Nucl. Eng. Des. 208, 2011, 109-203; Ann. Nucl. En. 101, 2017, 109-117]

EXPERIMENTS ON PHENOMENA IN THE LOWER HEAD - LIVE

- The main objective of the LIVE programme at Karlsruhe Institute of Technology (KIT) is to study melt pool behaviour in the reactor pressure vessel and assess different melt retention concepts, carried out in 2D and 3D facilities with electric power used to simulate decay heat;

  - Tests were performed with water and with non-eutectic melts such as simulant fluids to study the heat flux distribution when the melt pool is covered by water from the top;
  - Melting of debris in the reactor lower plenum after relocation of liquid melt in a large-scale hemispherical geometry was also studied, e.g. the main part of the LIVE-3D facility is a 1:5 scaled semi-spherical lower head of a typical PWR;
  - Transient and local thermal loads on the RPV wall under different melt relocation scenarios were examined and the steady-state pool behaviour of both homogenous pool and two-layer pool configurations were investigated;
  - Data such as the temperature of crust and boundary layers were obtained for analysis/modelling of the characteristics of corium pools with crust formation.

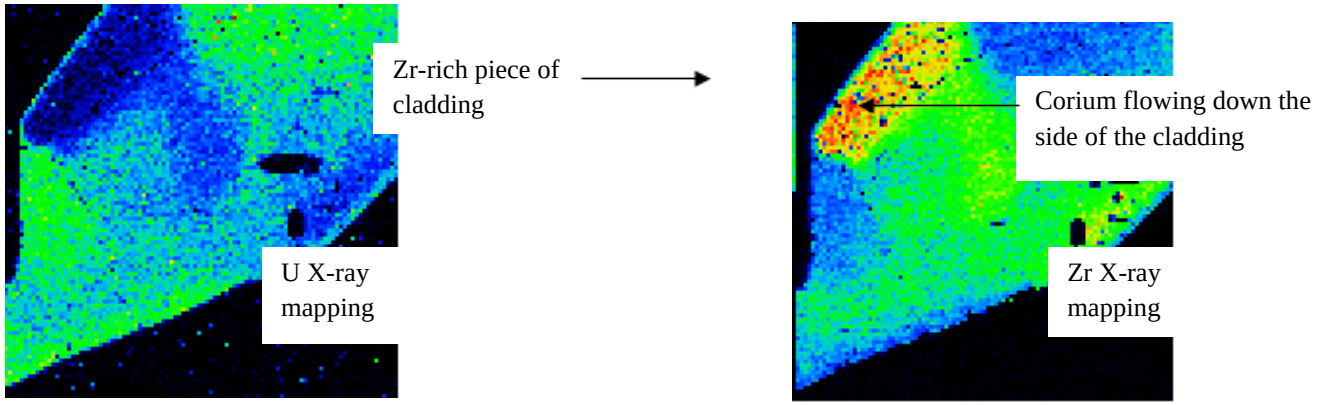


Upward heat transfer in 2D and 3D LIVE experiments compared with previous predictions and data

[KIT, ICONE17, Brussels, Belgium, 2009 and ICONE24, Charlotte, NC, USA, 2016]

DETAILED MICROSTRUCTURAL STUDIES – Melt composition

- Considerable work on the detailed structure of corium has been performed, following earlier analysis of samples from TMI-2, aiming to identify the main phases and thereby the principal reactions contributing to the degradation, hence elucidating the mechanisms and temperatures at which the degradation occurs;
  - Often the structures undergo further phase changes on cooling and so knowledge of both the high and low temperature structures is needed to follow the complete series of reactions and transitions that occurred;
- For example, extensive studies were carried out on the bundle final states of the Phébus FP tests, an example is given of the melted bundle and corium pool generated during FPT1 that included an Ag/In/Cd control rod, with degradation in a steam-rich atmosphere;

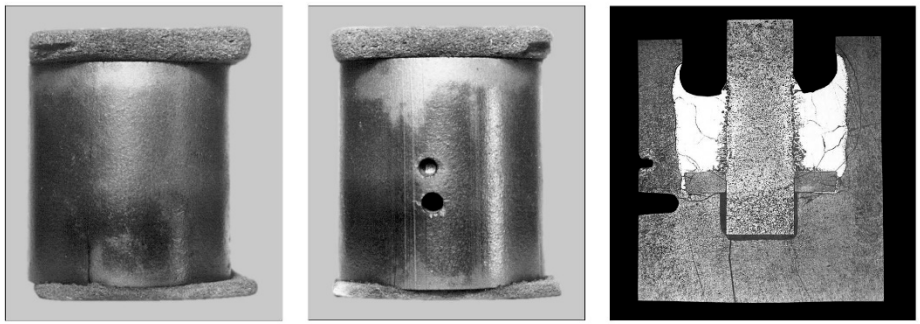


Upper part of the Phébus FPT1 bundle at 607mm axial elevation, showing a small piece of irradiated cladding with molten corium flowing down the side

- Detailed examinations of such samples gives important data on the melt compositions all over the bundle and helps understand the mechanisms involved.

DETAILED MICROSTRUCTURAL STUDIES – Competitive reactions and irradiation effects

- In the EU 5th Framework Programme COLOSS project separate-effects tests helped to understand better kinetics of the key reactions UO_2–ZrO_2 and Zr, at KIT, RIAR Dimitrovgrad, ETA-MK and JRC Karlsruhe;
- The RIAR work was a series of simple crucible tests at 2000-2200°C, the most advanced used crucibles of UO_2 with Zr metal placed inside it with a rod of ZrO_2 inserted in the middle of the Zr metal;
  - These showed reactions between Zr and ZrO_2 - the Zr metal dissolves and oxidises using oxygen from the ZrO_2, it similarly attacks the UO_2 to dissolve and also chemically react with the fuel;
- JRC tests showed that irradiated fuel dissolves more quickly than non-irradiated fuel, as the presence of numerous cracks in the irradiated fuel and the formation of large fission gas pores create a surface area for attack by the melt and generally improves the melt-fuel contact, consistent with results from the in-reactor Phébus FP integral experiments, where both trace-irradiated fuel and fuel irradiated to 23 to 32 GWD/tU were used.



RIAR Test 2 on simultaneous dissolution of UO_2 and ZrO_2 (2200°C, 200s)

[IRSN et al., Nucl. Eng. Des. 235, 2005, 178-198]

SEVERE ACCIDENT COMPUTER MODELLING CODES (1/3)

- The original SOAR and its EU update provided details of computer codes used in Europe for predicting in-vessel core degradation - these codes provide the quantitative link between the state of knowledge (as interpreted from small-scale experiments) and reactor safety assessments;
  - These were ATHLET-CD (GRS), development and use continues; ICARE/CATHARE (IRSN), superseded by ASTEC (EU led by IRSN); KESS (Uni. Stuttgart), incorporated into ATHLET-CD; SCDAP/RELAP5 (USNRC/Idaho NL) now continuing as the private code SCDAPSIM (ISS); ESTER (EU), no longer supported; and MELCOR (USNRC/Sandia NL), development and use continues;
- The main codes treated in the CoreSOAR final report are ASTEC, ATHLET-CD, MELCOR, SCDAP/RELAP5 + SCDAPSIM and also the fast-running industry code MAAP (EPRI/FAI);

SEVERE ACCIDENT COMPUTER MODELLING CODES (2/3)

- The codes are continually updated to reflect current knowledge - this process is favoured by benchmarks regularly organised e.g. by OECD/NEA and under SARNET (Phébus FPT1 for core degradation under steam-rich conditions, with fission product release; QUENCH-11 for boil-off/reflood; QUENCH-10/QUENCH-16 for air oxidation/reflood; LIVE-L6 for melt pool behaviour in the lower head; and an exercise based on TMI-2 conditions;

- In parallel, the major codes have been modified to deal with more reactor designs and situations for which they were initially designed;

SEVERE ACCIDENT COMPUTER MODELLING CODES (3/3)

- Most of the codes can now deal with spent fuel pool simulations, thanks to the addition of air oxidation models and adaptations of the thermal hydraulic models;
  - The range of reactors that can be treated by each code is now large;
    - ASTEC, originally made for Western PWRs has been extended to deal with VVERs, PHWRs and BWRs. ATHLET-CD has seen similar extensions (except for PHWR), while MAAP, which has a less flexible software structure, has been extended to deal with VVERs of different types, as well as BWR and PHWR (CANDU), with a different code version for each basic reactor design;
- This is a clear indication of the maturity of severe accident codes, even though some improvements are and will be necessary for them to be to be more accurate and reliable;
- Very recently, renewed interest in the in-vessel retention issue has led the developers of the major codes to improve their description of phenomena occurring in the lower plenum;
  - This effort will continue, in particular during the European IVMR project (until 2019).

RESEARCH NEEDS (1/2)

- Research priorities were organised under the SARNET first phase of the 6th EU FWP, published in 2008, to help to ensure that severe accident research work was efficient and well-focused, optimising resource use, avoiding duplication and ensuring that important gaps in knowledge were not omitted;
  - research was devoted to core coolability during reflood and debris quenching, the effect of air ingress into the vessel and its effect on increasing clad oxidation and fission product release (especially Ru), hydrogen generation during reflood and melt relocation in-vessel, corium coolability in the lower head, i.e. corium pool behaviour and its thermal loading on the vessel, possibly leading to failure;
  - over the years, these have been progressively refined, taking into account increasing knowledge, and covering all important severe accident phenomena, conclusions being published in 2014 at the end of the then current phase of SARNET;

RESEARCH NEEDS (2/2)

- Since then, a specific effort has been devoted to the ASTEC code in the 7th Euratom FWP CESAM project, 2018, including benchmarking against other codes, giving an up-to-date list of priorities to inform ASTEC development:
  - for in-vessel core degradation, research for the V2.1 version was devoted to modelling *reflooding severely damaged cores*;
  - includes a new model for reflood of porous media (debris bed) representative of the late degradation phase;
  - other topics include corium behaviour in the lower head after its slumping from the core: upwards radiative exchanges between this relocated corium and the core support plate bottom face, up to its melting or collapse; new functionality in the original core magma oxidation model to simulate the oxidation of a corium pool once formed in the lower head;
  - also new features to address better *in-vessel melt retention strategies* (behaviour of corium layers and crust in the lower head, etc.).

CONCLUSIONS

- The technical work on CoreSOAR is essentially complete, regarding review and experiments, material data and severe accident computer codes;
- It remains to finalise the conclusions and agree the research priorities (final project meeting immediately after this QUENCH Workshop);
- The project is on schedule to complete by the due date, end December 2018, with the issue of the Final Report;
- Publications are to include at least one open literature paper, and a final presentation at ERMSAR2019 at Prague in March 2019;
- The partners would like to thank the NUGENIA/SARNET management teams for their support over the duration of this 2½ year project.

Thank you for your attention!

An Update on the SAREF/ Pre-ADES project (Preparatory Study on Analysis of Fuel Debris)

T. Washiya & D. Bottomley, Japan Atomic Energy Agency, Collaborative laboratory for Advanced Decommissioning (JAEA-CLADS Laboratory), Iwaki, Japan

ABSTRACT

The Pre-ADES (Preparatory Study on Analysis of Fuel Debris) project was one of two Near-Term Projects proposed by the CSNI Senior Expert Group on Safety Research Opportunities Post-Fukushima (SAREF) recommended to address safety knowledge gaps and to support decommissioning of Fukushima Dai-ichi reactor units. The second project proposed was Examinations inside RBs and CVs and water sampling (ARC-F), which will be complementary to Pre-ADES and is also proceeding.

This project is being supported by the Japanese government and JAEA through the OECD-NEA-CSNI. it is a three-year project running to mid-2020 and has 7 countries and the European Commission, JRC participating. Its overall objective is to gather data and information together to enable an optimal extraction of samples, a good analysis and maximum use of this information to assist the decommissioning operations and understand the conditions and causes of the severe accident.

It is divided into 3 main tasks:

1) Collection of information for improving knowledge and methodologies for fuel debris characterization in support of fuel debris sampling.
2) Identification of the required fuel debris analysis for the Fukushima Daiichi decommissioning and for an improved knowledge-base and understanding of severe accidents.
3) To prepare a future international R&D framework on fuel debris analysis, where an overseas expertise and facilities could be pooled.

The presentation will describe the progress in the first two tasks and give some examples before indicating the time schedule for this project and its integration with other current international projects relevant to Fukushima Dai-ichi.



An Update on the SAREF/ Pre-ADES project

Preparatory Study on Analysis of Fuel Debris

T. Washiya & D. Bottomley*

Japan Atomic Energy Agency

CLADS

***presenter**

Outline

- Background
- Outline of each Tasks in PreADES
  - Task 1 Study on fuel debris characterization
  - Task 2 Needs identification and major issues for future fuel debris analysis
  - Task 3 Future international R&D framework using fuel debris sampling from Fukushima Daiichi.
- Topics of 2rd meeting (July 4-6, @Tokyo)
  - Task 2.1 Group discussion; “Criticality control in degraded cores”
- Project Schedule
  - Next meeting (Jan 25-29, @Paris)

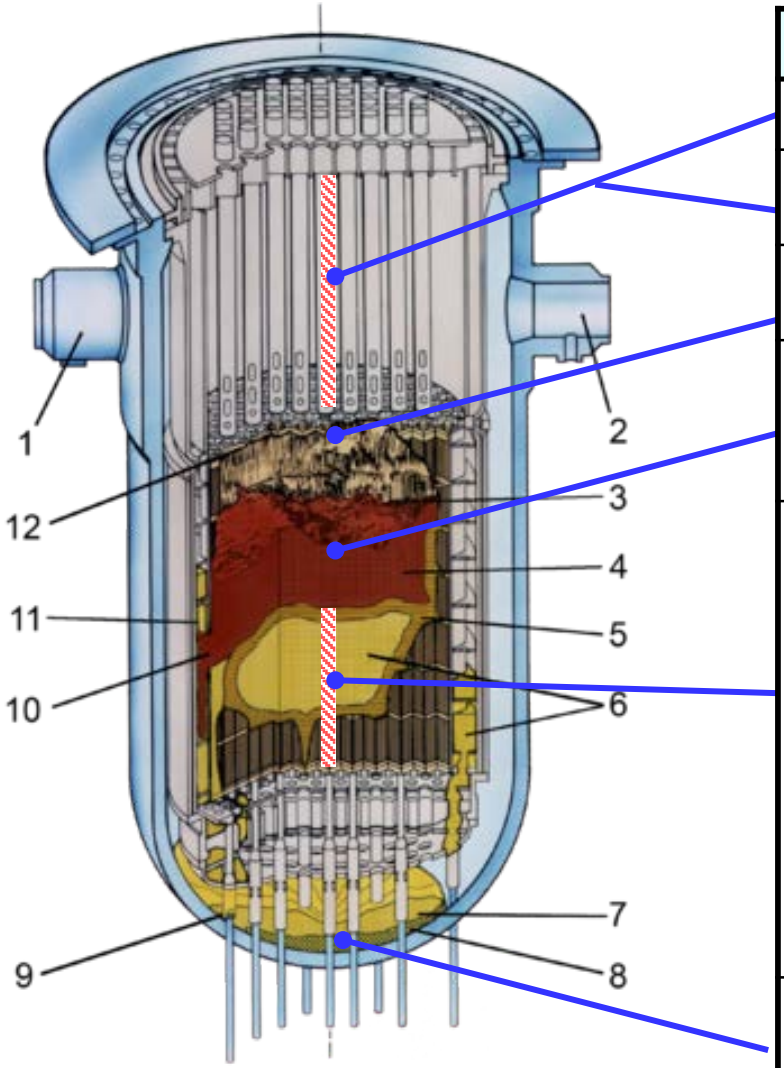
Background

- In February 2017, the CSNI **Senior Expert Group on Safety Research Opportunities Post-Fukushima (SAREF)** recommended two **Near-Term Projects** in its report to address safety knowledge gaps and to support timely decommissioning.
  - **Preparatory study on actual fuel debris analysis (PreADES)**
  - Examinations inside RBs and CVs and water sampling (ARC-F)
- **Objectives:**
  - **To collect information for improving knowledge and methodologies** for **fuel debris characterization** that will support future fuel debris sampling at the Fukushima Daiichi Units 1–3.
  - **To identify the needs for fuel debris analysis** that will **contribute to decommissioning** of the Fukushima Daiichi plant and deepen the **knowledge-base of severe accidents**.
  - **To prepare a future international R&D framework** on fuel debris analysis.

Project Participation and MB/PRG

- **7 countries and 15 organizations** joined the PreADES project
  - Canada(CNL), France(CEA, IRSN, EDF), Japan(JAEA, NRA, CRIEPI), Korea(KAERI, KINS), Sweden(SSM), Switzerland(PSI), United States(NRC DOE EPRI) and the EC/JRC (JRC-Karlsruhe)
- Elected chair/vice-chair for MB/PRG
  - Management board (MB):
    - MB Chair: Mr. Richard Lee, NRC
    - MB Vice-Chair: Mr. Didier Jacquemain, IRSN
  - Program Review Group (PRG)
    - PRG Chair: Mr. Jin Ho Song, KAERI
    - PRG Vice-Chair: Mr. Tadahiro Washiya, JAEA
  - Project manager: Mr. Akira Nakayoshi, JAEA

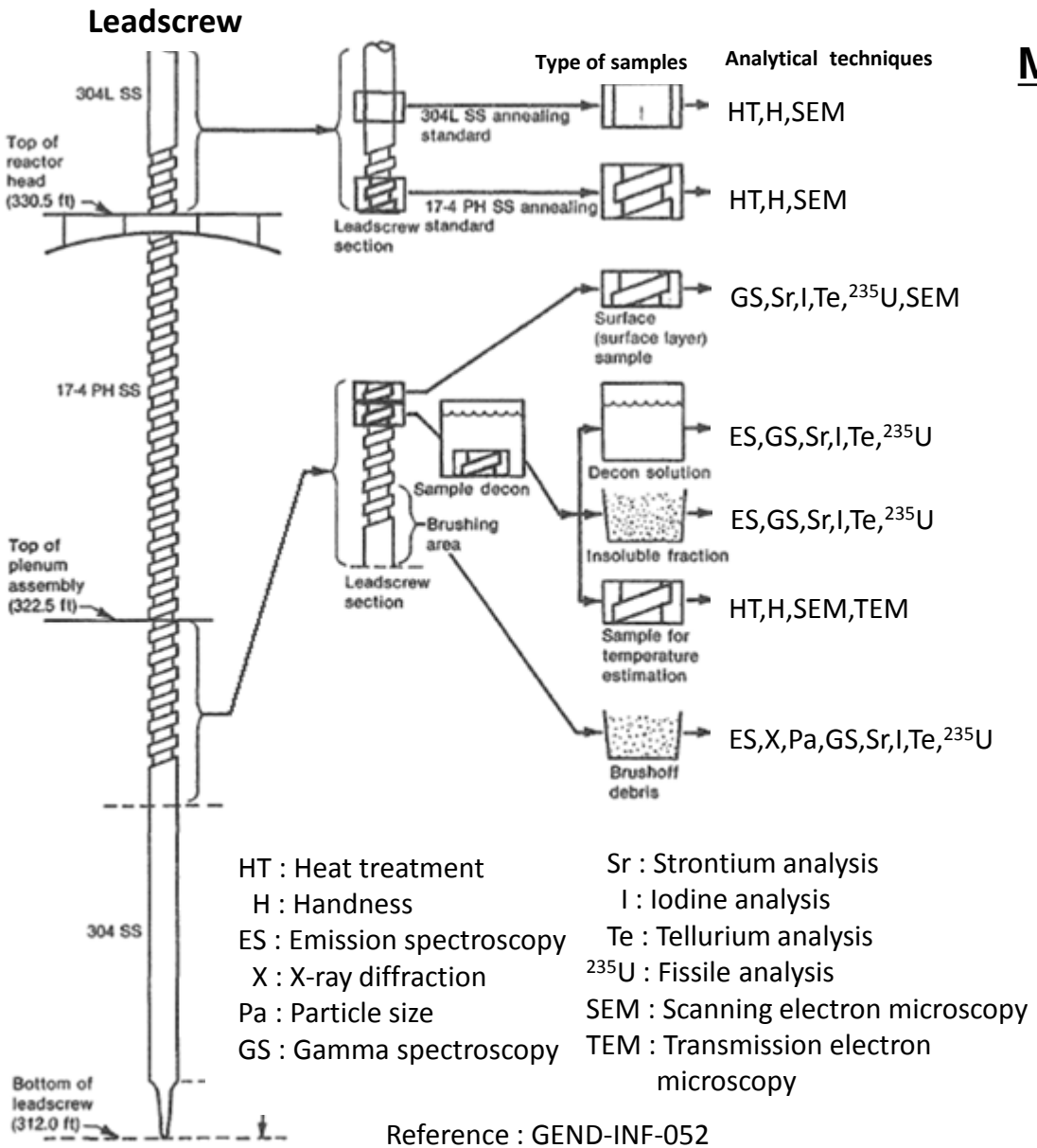
Information from damaged reactor samples



Sample	Temperature Analysis
Control Rod	393-982 ℃
Upper support pillar	510-732 ℃
Internal component	1227-1477 ℃ (stainless steel, inconel)
Upper Debris Layer	> 2537℃ : $(U,Zr)O_2$ (Av. < 1727℃) (2827℃: Partially melted)
Core boring Sample	[Upper Crust] > 2537℃: Melted $(U,Zr)O_2$
	[Remelted Layer] > 2537℃: Melted $(U,Zr)O_2$
	[Lower Crust] 1127-1727 ℃: Melted Structural Material and Control Rod
	[Stubbed Fuel] < 647℃: No Crystallization of Cladding Material
Lower Debris Layer	> 2537℃: Melted $(U,Zr)O_2$ (2827℃: Partially change of UO_2)

Reference : Nuclear Technology Vol.87 1989

Examination of TMI-2 Leadscrew



HT : Heat treatment
H : Handness
ES : Emission spectroscopy
X : X-ray diffraction
Pa : Particle size
GS : Gamma spectroscopy
Sr : Strontium analysis
I : Iodine analysis
Te : Tellurium analysis
^{235}U : Fissile analysis
SEM : Scanning electron microscopy
TEM : Transmission electron microscopy

Reference : GEND-INF-052

Major outcome from Leadscrew Analysis

- Local peak temperatures was estimated
- Nature of the core component was determined
- Deposition of UO_2 and Zr was observed to greater extent in area near the core.
- Radionuclide concentrations (axial gradient) was observed; the highest concentration is near the top of the plenum assembly.
- Chemical composition and gradients were confirmed for the surface radionuclide concentrations in the plenum assembly.

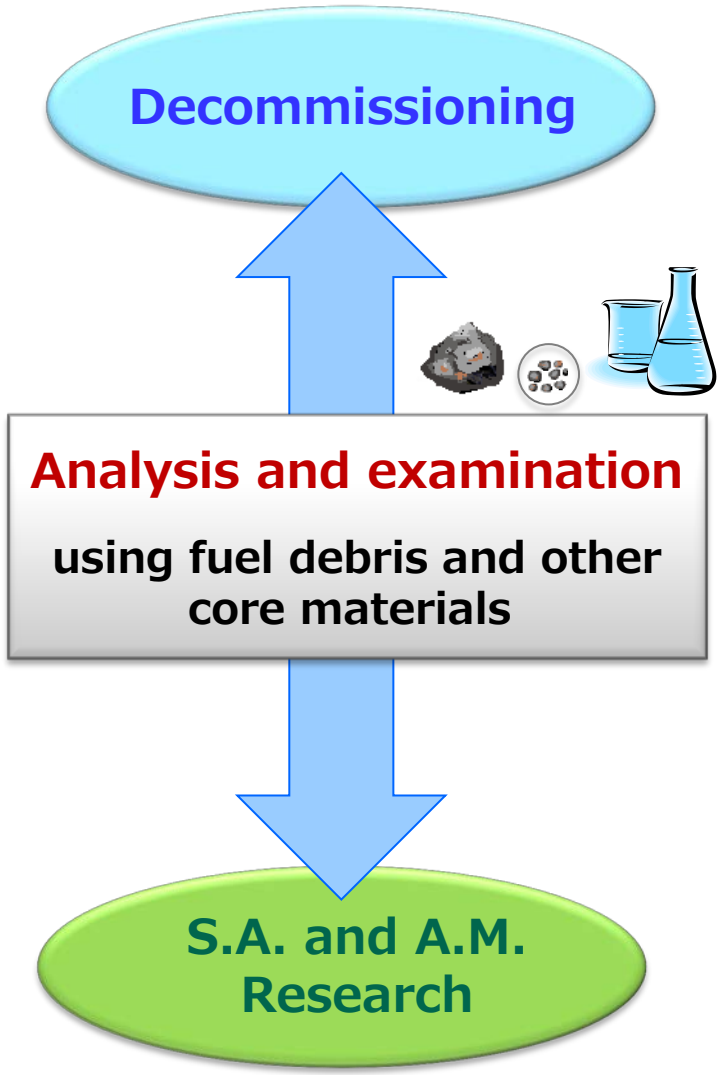
Contribution of analytical results

◆ Contribution to decommissioning

- **To understanding the damaged state inside the reactors;** quantity, shape, composition, etc.
- **To understanding the contamination;** radiation, nuclides, chemical form, etc.
- **To understanding the safety;** criticality, hydrogen, corrosion, etc.
- **To examining the defueling;** criticality, tools, method, etc.
- **To storing and storage**
- **To treatment and disposal**

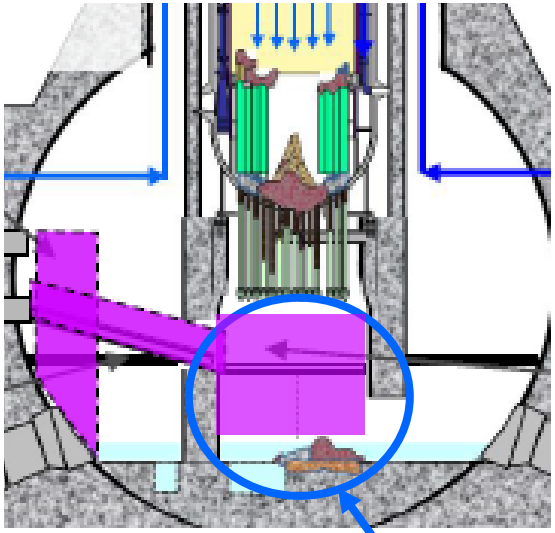
◆ Contribution to SA and AM*

- **To investigating the accident progression;** in/ex-vessel phenomena, containment failure, fission product behavior, and source term, etc.
- **To investigating the system reliability;** coolability , containment, corrosion and erosion, etc.



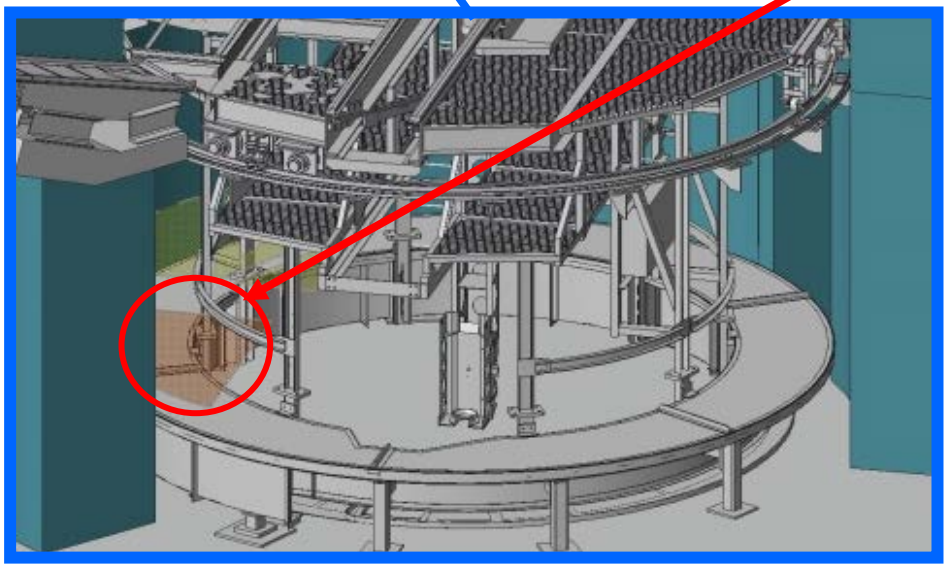
*Accident Management

Unit 2 investigation: Pedestal Floor



Pedestal floor and wall Fuel debris? and a fuel assembly handle







Unit 2 PCV investigation in the pedestal floor

Outline of each Tasks in PreADES

- **Task 1:** Joint study on fuel debris characterization
  - Discuss about fuel debris conditions location in the 1F unit 1-3 (Ref. from BSAF-2 , 1F , TMI-2, CheNPP, SA studies etc.)
  - Discuss about debris properties in the location

    Properties : Micro and Macro-scopic viewpoints
- **Task 2:** Needs identification and issues discussion for future fuel debris analysis
  - Discuss needs for analysis from Criticality, Confinement Cooling function, Radiation exposure, etc.
  - Discuss major issues for sampling; Analysis methods, Facility functions, Transportation, Accounting, etc.
- **Task 3:** Planning a future international R&D framework using actual fuel debris from Fukushima Daiichi.

How to progress with Task 1

Task 1 Joint study on fuel debris expected properties and characterization

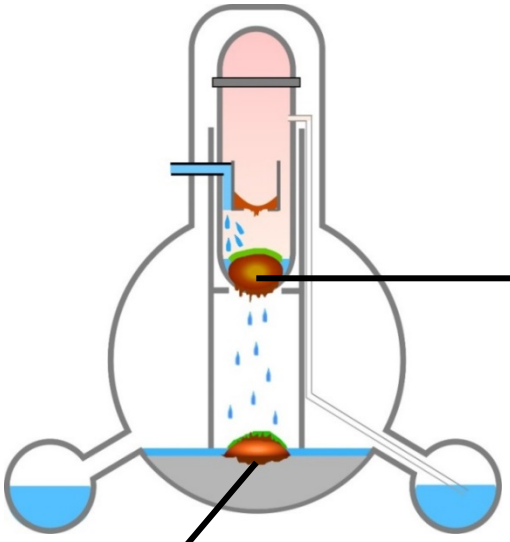
Task 1-1: Estimate fuel debris properties

- Discuss about fuel debris conditions location in the 1F unit 1-3
  - ✓ BSAF-2
  - ✓ IRID study
  - ✓ 1F inspection
  - ✓ TMI-2, CheNPP, etc.
  - ✓ SA study etc.
- Discuss about debris properties in the location
  - ✓ Characteristic table (Macro-scopic properties table)
  - ✓ Characteristic table (Micro-scopic properties table)

Task 1-2: Sharing of knowledge base on fuel debris characteristics

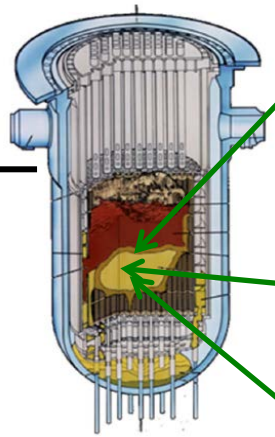
- ✓ How to characterize debris information
- ✓ Sharing knowledge from each country

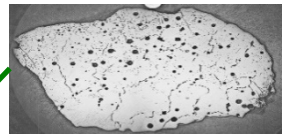
Estimated debris properties for 1F



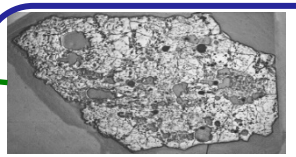
Typical perspective view of 1F reactor

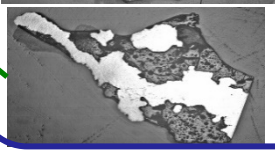
In-vessel : Solidified molten core





Upper/lower crust :
・Massive debris generated by cooling molten fuel & solid debris relatively quickly.
・$(U,Zr)O_2$-Cubic, etc

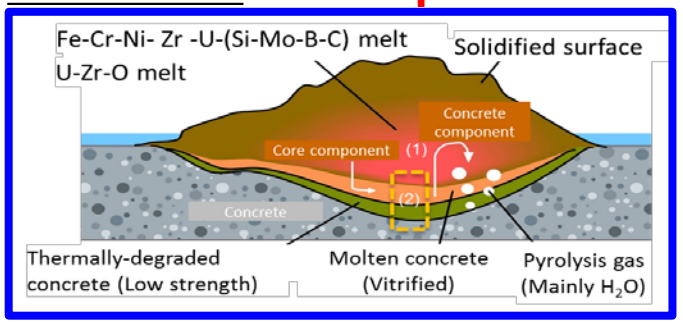


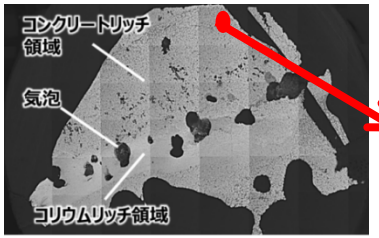


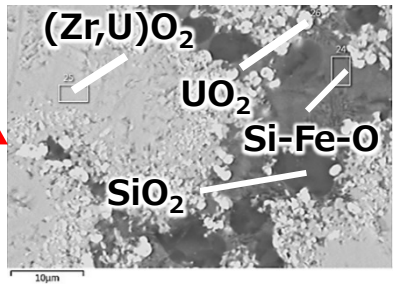
Solidified pool:
Massive debris generated by cooling molten fuel slowly.
・$(U,Zr)O_2$-Tetragonal/monoclinic
・SUS-Zry alloy fused pieces, etc

Estimated results using actual fuel debris of TMI-2 accident

Ex-vessel : MCCI products







MCCI products
・$(Zr,U)O_2$-Cubic/Tetragonal
・$(Zr,U)SiO_4$
・SiO_2, etc.

Example : VW-U1 sample (Upper crust)

Estimated results using previous VULCANO-MCCI samples (JAEA-CEA collaboration)

ro table)

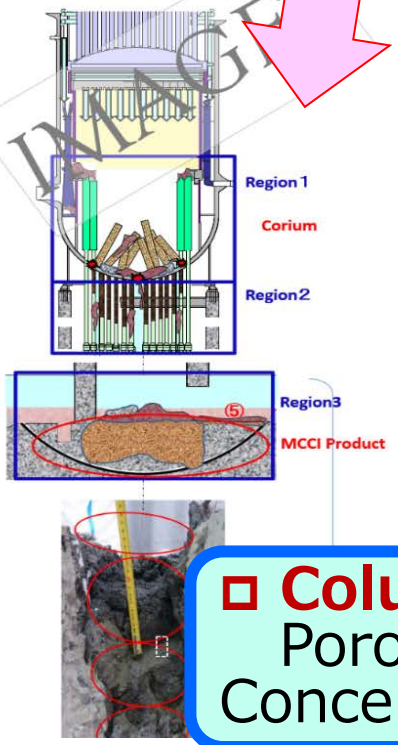
e rectors

s in each location

ate debris properties

- Region
- Image/appearance
- SEM
- Remark

Region	Image of appearance	SEM	Remark	Composition	Size	Porosity (%)	Bulk density (g/cm³)	Moisture (wt%)
	((Similar to debris in RPV))							
	VBS-U 4 -Samples close to 1 F condition from corium composition (ZrO_2 / UO_2 ratio) and concrete composition (Si… -MCCI test using oxide molten corium and metals -As in 1F, siliceous concrete was used for the test, and the test time is approximately 2h 50 min.							
	・Crust - MCCI product b		Porosities of several millimeters can be confirmed.	$(U,Zr)O_2$ ZrO_2 SiO_2 Cr_2O_3 Fe_3O_4 Fe		…arent porosity : 22.26	6.15	5.0
	・Molten corium pool -MCCI product a		Density is not uniform. The surface is rough and the color is uniform.	$(U,Zr)O_2$ ZrO_2 SiO_2 Cr_2O_3 Fe_3O_4 Fe ($ZrSiO_4$)		…arent porosity : 9.91	4.66	5.0
	・Metal - MCCI product d		No pores	$(U,Zr)O_2$ ZrO_2 SiO_2 Cr_2O_3		…ent porosity : 5.72		



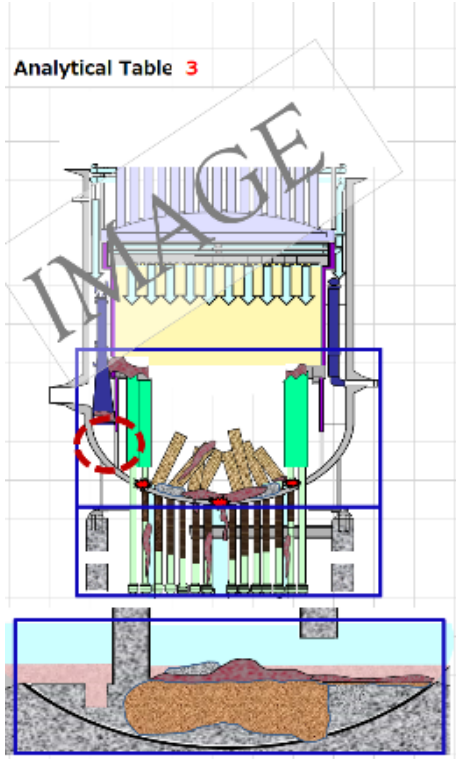
- **Columns is estimated as follows,**
  Porosity, Density, Moisture, G value (shear modulus), Concentrations …

-Characteristic table- (micro table)

☐ Estimate debris' location in the rectors

Density (g/cm^3)	Vickers Hardness (GPa)	Elastic Modulus (GPa)	Fracture Toughness ($MPa\ m^{1/2}$)	Thermal Conductivity (W/mK)	Specific Heat (J/g K)	Melting Point (°C)	Behaviour at high temperature	Stability

- Discussing methodologies to estimate debris properties



Characteristic Table micro

Categories / Material / Phases	Density (g/cm^3)	Vickers Hardness (GPa)	Elastic Modulus (GPa)	Fracture Toughness ($MPa\ m^{1/2}$)	Thermal Conductivity (W/mK)	Specific Heat (J/g K)	Melting Point (°C)	Behaviour at high	Stability
Oxide									
UO_2	11.0	5.9	193	0 - 1.5	10	0.28	2850		oxidised under oxygen existing, and it causes volume
ZrO_2-C	6.1	15	200	0 - 10	1 - 3	0.61	2700		
$(U,Zr)O_2$-C	6.1 - 11.0	5.9 - 11	200	0 - 3.0	1 - 3	0.28 - 0.61	2500 - 2850		
$(U,Zr)SiO_4$	4.6 - 8.3	11	166	0 - 1.2	6.1	0.45 - 0.82	2500		
Metallic									
U									
Zry-2									There are explosion cases of Zr fires
α-Zr(O)									
SUS/Fe									
Fe2(Zr,U)									
Others									
B4C									
ZrB2									

How to progress with Task 2

Task 2 Identifying needs and major issues for future fuel debris sampling, retrieval, and analyses

Task 2-1: Needs for fuel debris analysis

Discuss points ;

- ✓ Criticality Control
- ✓ Confinement
- ✓ Cooling function
- ✓ Radiation expsure

Task 2-2: Study on safety major issues related to future debris sampling, retrieval, analysis , transport, treatment, storage and disposal

Task 2-3: Experimental/analytical techniques and demands in hot-testing facilities

PCV inspection at 1F

◆ Current inspection;

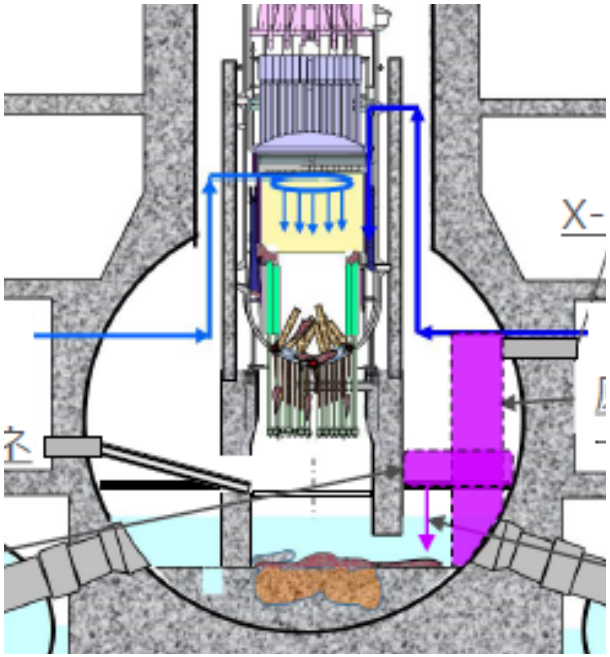
- Unit 1: outside pedestal
- U
- U

pedestal

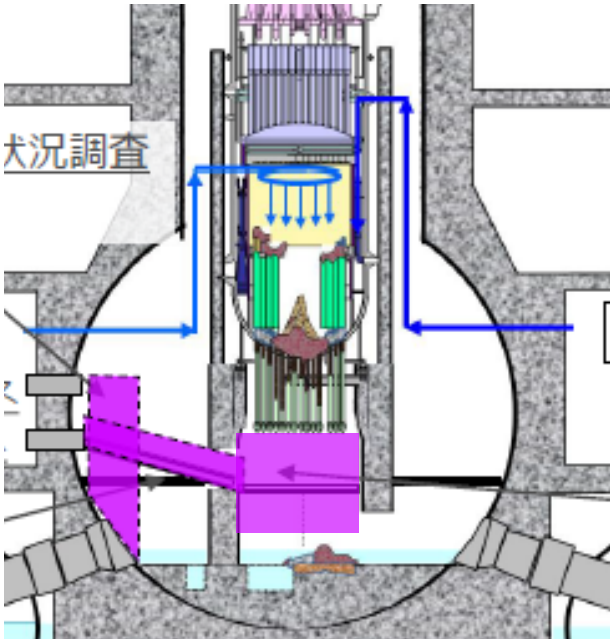
◆ Purpose of PCV inspection is to confirm inside reactor condition as follows;

- Debris location and its condition, etc.

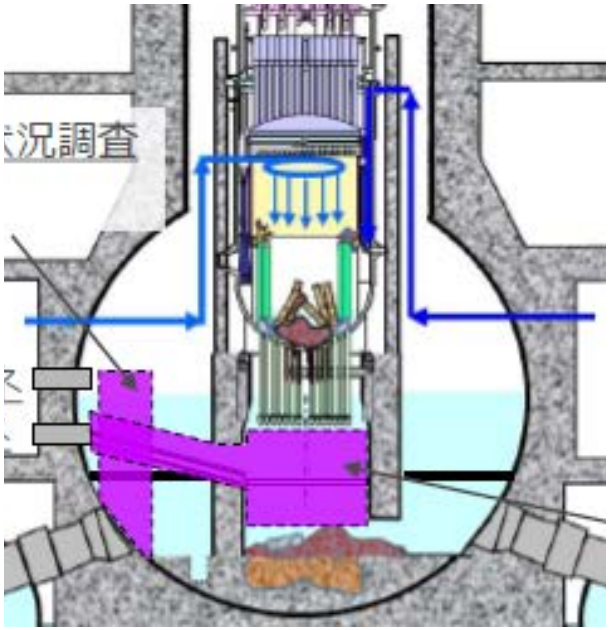
Sampling approach and Analysis method is discussion-based prioritization.



Unit 1

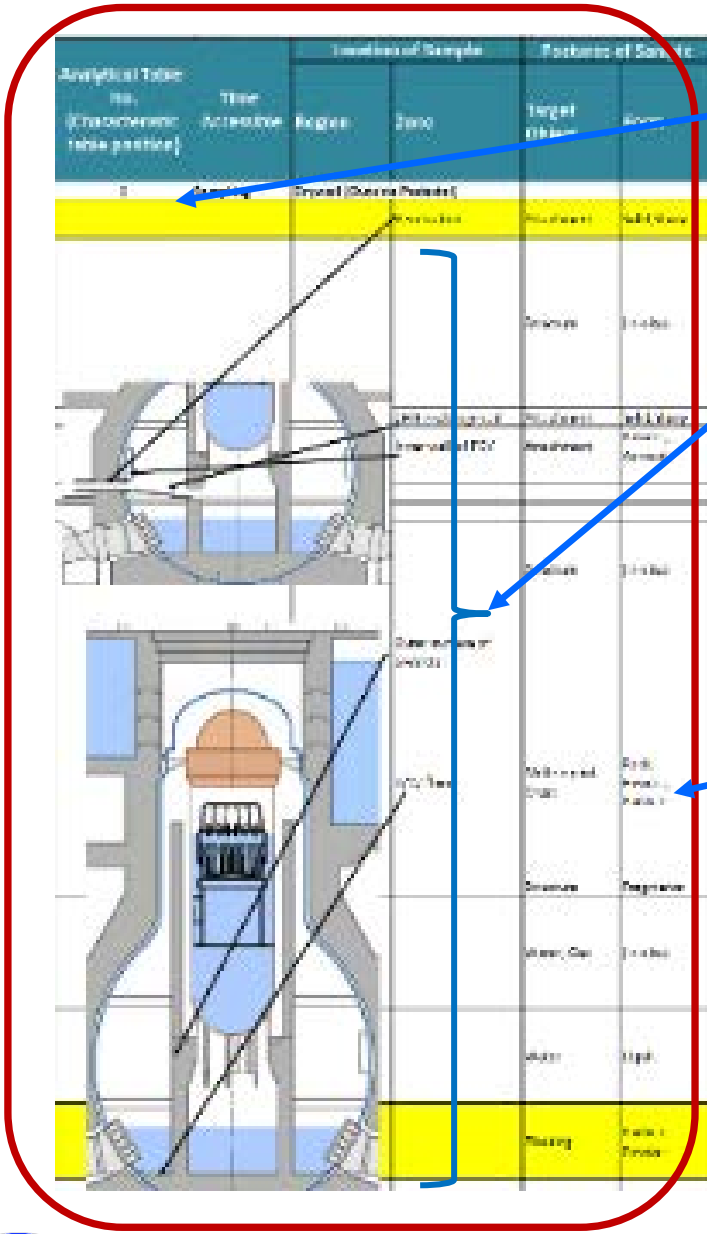


Unit 2



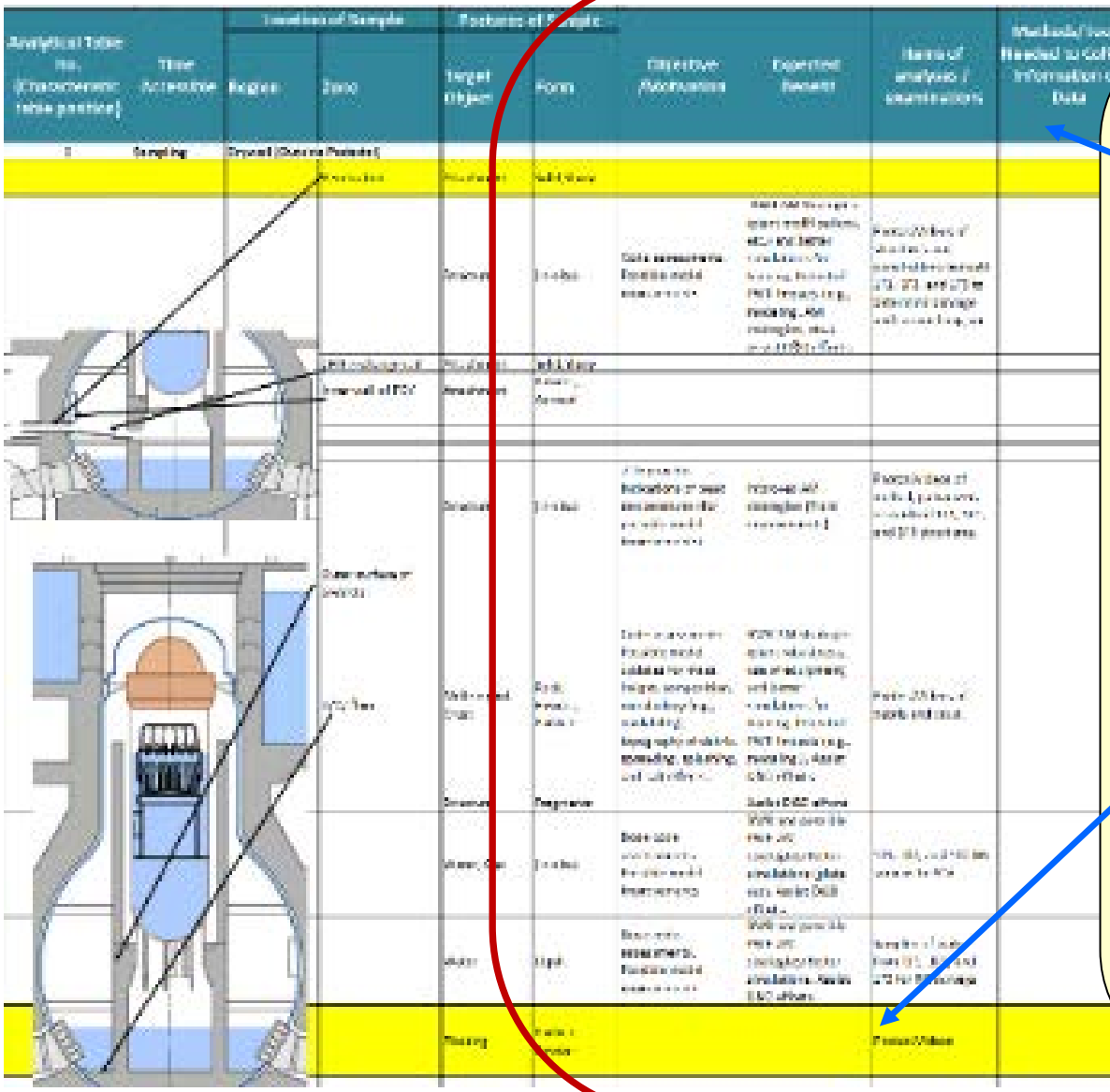
Unit 3

Task 2-1 : Analytical table of fuel debris



- **Match with Characteristic table's items**
- **Time accessible**
  assumed sampling times in each location
- **Location of sample**
- **Features of sample**
  Target, Object, Form(Shape)

Task 2-1 : Analytical table of fuel debris



- **Objective/Benefit**
- **Items of analyses**
- **Methods/Tools needed to collect information or data**
- **Collection date**
  Date of actual sampling

* **Yellow markers are actual samples (solid) already taken from 1F**

* **If lines are completed (e.g. sediment , attachment), discuss the priority of each line**

Debris retrieval and inspection

- Fuel debris to be retrieved 'step-by-step'

  (Side-Entry system is one possible candidate)

  - In early stage, amount of removed debris is small and will gradually increase in amount with improved methods.
  - Accumulate knowledge on fuel debris and make retrieval schedule (should be flexible).
  - Side entry method for debris retrieval is the most feasible method currently

- Policy of 1F PCV inspection

  - PCV inspection carried out to obtain information in the reactor; that is mostly concentrated on understanding of inside conditions
  - The analytical information will be fed back to decommissioning work to minimize risk for debris retrieval, storage, etc.
    - Estimating debris location, current conditions in the reactors

      ⇒ Planning of debris retrieval, Safety consideration, etc.

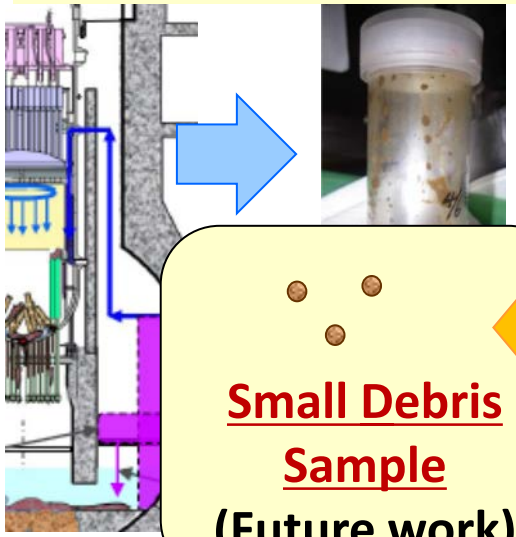
How to contribute to the future sampling

Feedback of debris analysis results

- Discussed how to feedback analysis data to debris removal; as example of 1F Unit-1 sediment analysis data, in this discussion various aspects of re-criticality was pointed out.

Sample (ex.Sediment)

Task 2-1 Discussion



Small Debris Sample (Future work)

Analysis items

- Pu contents
- Boron contents
- Porosity
- Chemical form

Discuss on
- Analysis Items
- Analysis Methods

etc.

- SEM-EDX, XRD
- ICP-MS, etc.

Expected benefit

- Sub-criticality assessment
- Sediment generation

Key words to Discuss
- **Criticality control**
- **Confinement**
- **Cooling function**
- **Radiation exposure**

Feedback

- Criticality Safety control
- Sediment recovery and anagement
- ediment eneration henomena nalysis

- Prioritization of items needs to carried out, but should be flexible.

Group Discussion : Criticality Control

2nd Meeting, July 2018

Object: From viewpoints of the criticality control (CC) in degraded cores, discuss material properties of fuel debris in analysis tables.

How to progress with the work

2nd Meeting, July 2018

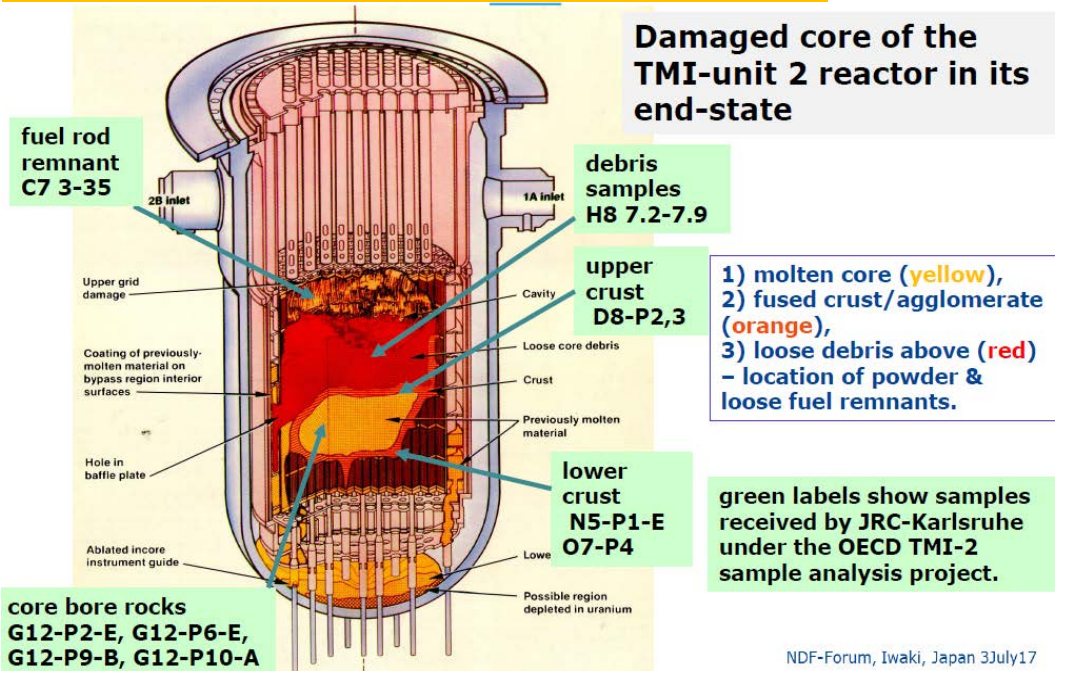
- Sharing the fundamental issues on CC and discuss 1F.
  - Agreement on objectives, role, & how to progress CCG
  - Review of basic issues of CC
  - CC in 1F decommissioning & List Material Properties relevant to CC
  - Discussion on prioritization
- Collecting other scenarios concerning CC.
- List essential material properties for CC
- Considering adequate measurement techniques of the material properties.
- Prioritization (both CC & material analysis issues)
- Summary of PIE items

◆ Discuss future international R&D framework using fuel debris sample from Fukushima Daiichi.

Discussion item (TBD);

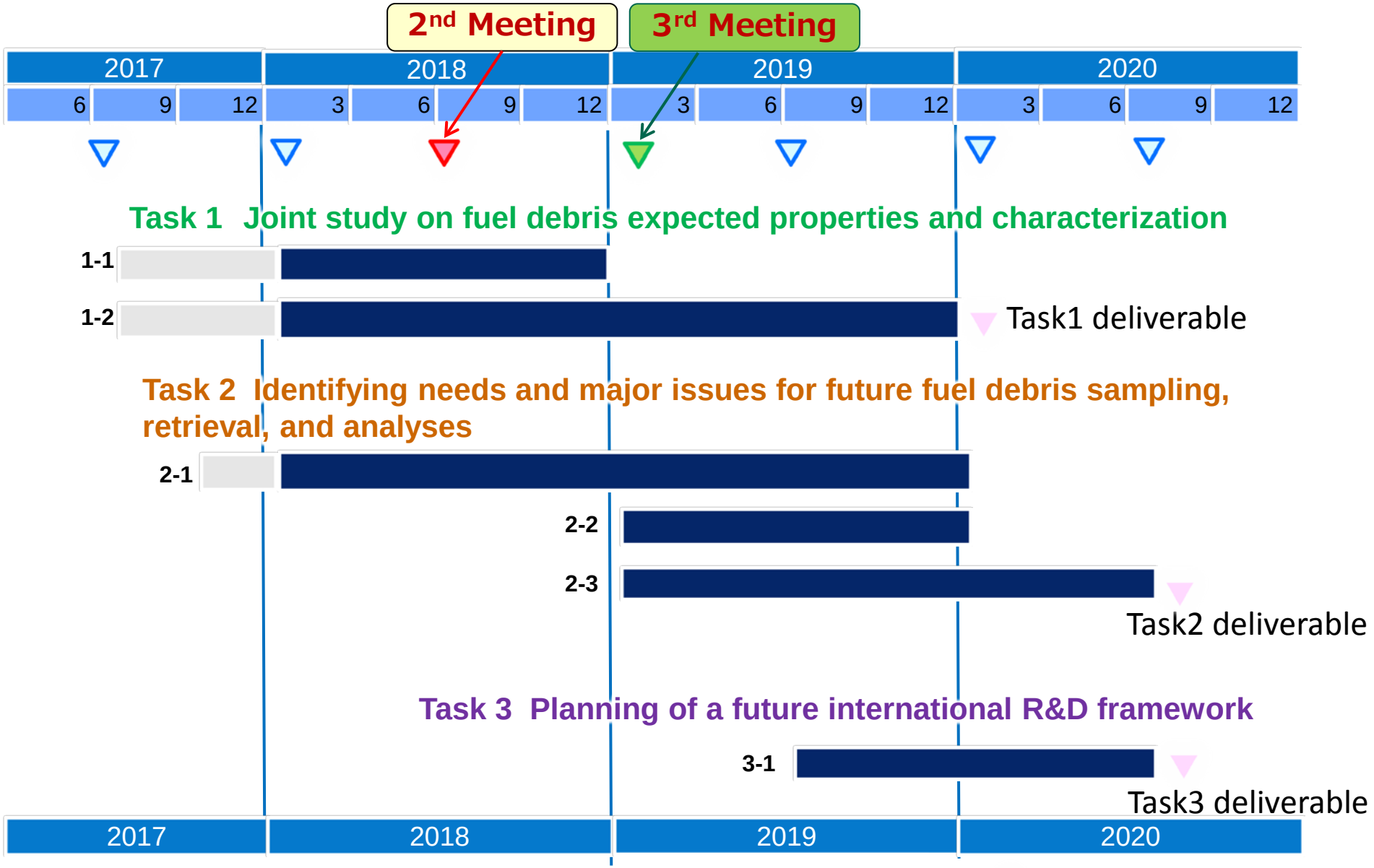
- Purpose
- Analysis method
- Precision of analysis
- Sample location
- Organization, Implementation,
- Leading institute
- International Framework
- etc.

OECD TMI-2 Sample Analysis Project



- ✓ What was corium composition
- ✓ What temperature was reached
- ✓ What condition (O_2 potential H_2) prevailed
- ⇒ Hence what degradations were likely.

PreADES schedule

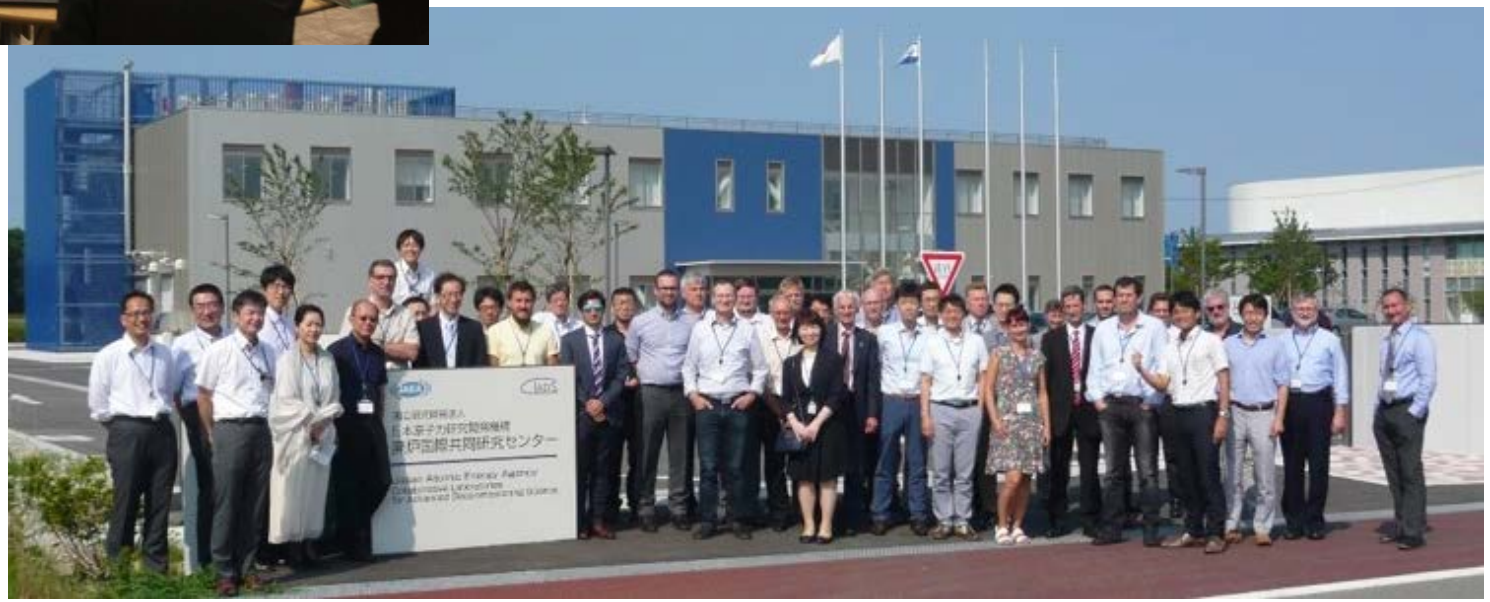


Summary of 2nd meeting

- 2nd meeting was successful carried out and identified contributions from each Participating Organizations (PO).
- Valuable and important contributions for each task from participating organizations are proposed.
- Coordination among Pre-ADES, BSAF, TCOFF, WGAMA and ARC-F is important and should be properly implemented.
- Next meeting : 25-29 January 2019, OECD, Paris, in association with ARC-F, TCOFF and BSAF meetings.

Thank you for your attention !





24. International QUENCH Workshop, 13-15 Nov 2018, KIT, Karlsruhe, Germany

Update of the QUENCH program

Martin Steinbrück, Juri Stuckert, Mirco Große et al.

The main objective of the QUENCH program at KIT is the investigation of the hydrogen source term and materials interactions during LOCA and the early phase of severe accidents including reflood. Bundle experiments as well as separate-effects tests are conducted to provide data for the development of models and the validation of severe fuel damage code systems.

The QUENCH bundle facility is a unique out-of-pile bundle facility with electrically heated fuel rod simulators and extensive instrumentation. So far, 19 experiments with various severe accident (SA) scenarios as well as a series of seven DBA LOCA experiments were conducted. The QUENCH-LOCA series was completed in 2016. One of the main results is the definition of the conditions for secondary hydriding around the burst position and its influence on the mechanical properties of the cladding rods.

The last SA test QUENCH-19 was the worldwide first large-scale bundle test with ATF cladding. It was conducted with FeCrAl cladding in cooperation with ORNL, USA. First very promising results were presented by Stuckert.

Separate-effects tests during 2018 were focused on the high-temperature behavior of various ATF cladding candidates. Many of these experiments were done in the framework of the EC ILTROVATORE and IAEA ACTOF programs.

QUENCH bundle tests are part of the validation matrices of most SFD code systems which was also reflected during the session “Modelling and code validation”.

Finally, the status of reporting and publishing as well as the numerous national and international cooperations were briefly described and acknowledged.


KIT
Karlsruher Institut für Technologie

Karlsruhe Institute of Technology

Institute for Applied Materials

Update of the QUENCH Program

M. Steinbrück, J. Stuckert, M. Große et al.

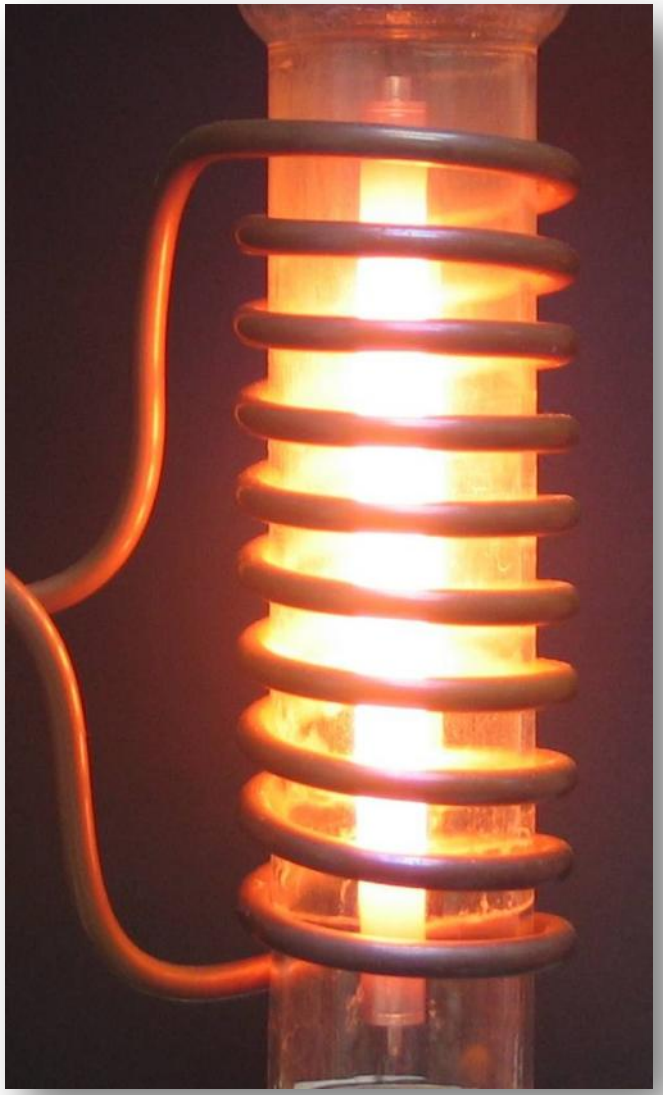
24th International QUENCH Workshop, Karlsruhe, 13-15 November 2018

Institute for Applied Materials, Programme NUSAFE



Outlook

- Motivation
- Bundle experiments
- Separate-effects tests
- ATF activities
- Modelling / Code validation
- Future planning



Motivation

- Reflood is a prime accident management measure to terminate a nuclear accident
- Reflood may cause temperature excursion connected with increased hydrogen and FP release (severe accidents) and embrittlement of cladding and secondary hydriding (LOCA)
- Coolability of a degraded core is a matter of high priority (Fukushima)
- QUENCH experiments (bundle+SET) provide data for development of models and validation of SFD code systems

QUENCH Programme

Investigation of hydrogen source term and materials interactions during LOCA and early phase of severe accidents including reflood



Separate-effects tests

Modelling → CODES → Application

Validation



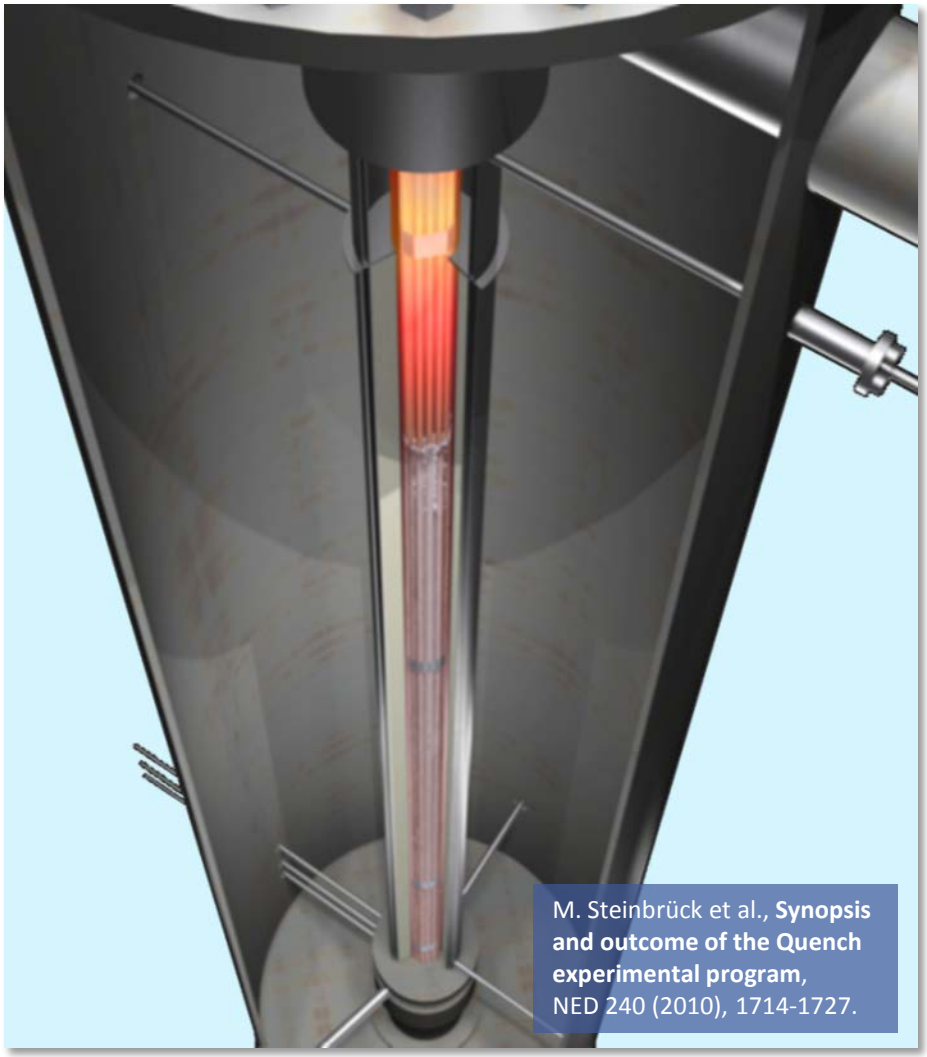
Bundle experiments



PWR fuel element

QUENCH facility

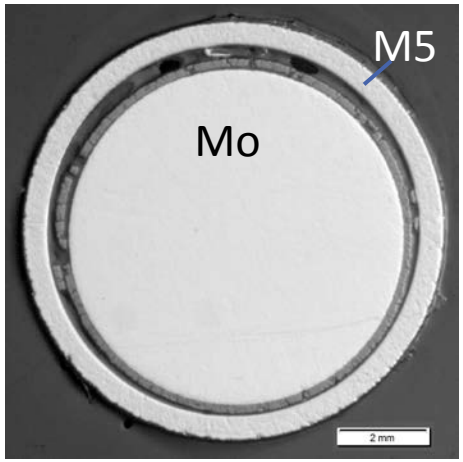
- Unique out-of-pile bundle facility to investigate reflood of an overheated reactor core
- 21-31 electrically heated fuel rod simulators; T up to >2000°C
- Extensive instrumentation for T, p, flow rates, level, etc. + MS
- So far, 19 experiments on SA performed (1996-today)
  - Influence of pre-oxidation, initial temperature, flooding rate
  - B_4C, Ag-In-Cd control rods
  - Air ingress; debris formation
  - Advanced cladding alloys
- 7 DBA LOCA experiments with separately pressurized fuel rods



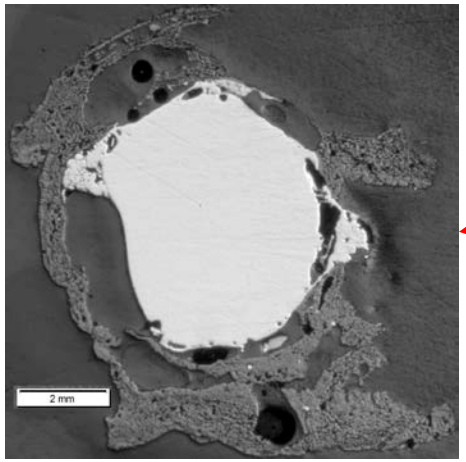
M. Steinbrück et al., **Synopsis and outcome of the Quench experimental program**, NED 240 (2010), 1714-1727.

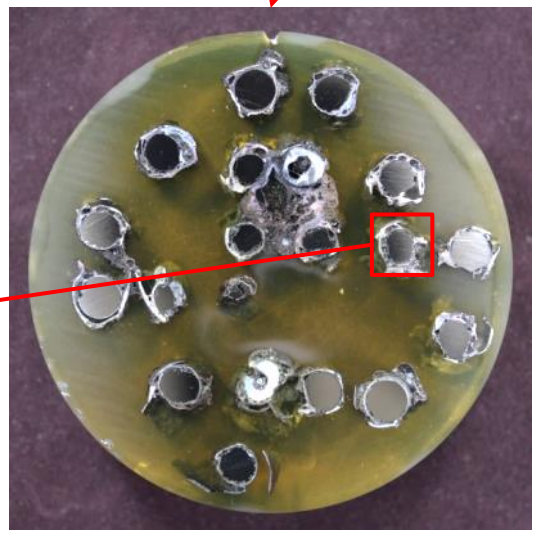
QUENCH-18

- Successfully conducted in Sept 2017
- In the framework of the EC-China ALISA project
- With M5® cladding, two pressurized rods, two Ag-In-Cd absorber rods, and air ingress
- Strongly degraded bundle
- PTE of the main bundle part still pending
- Issue with MS measurements of O_2 concentration in presence of H_2O



Intact rod at 1450 mm





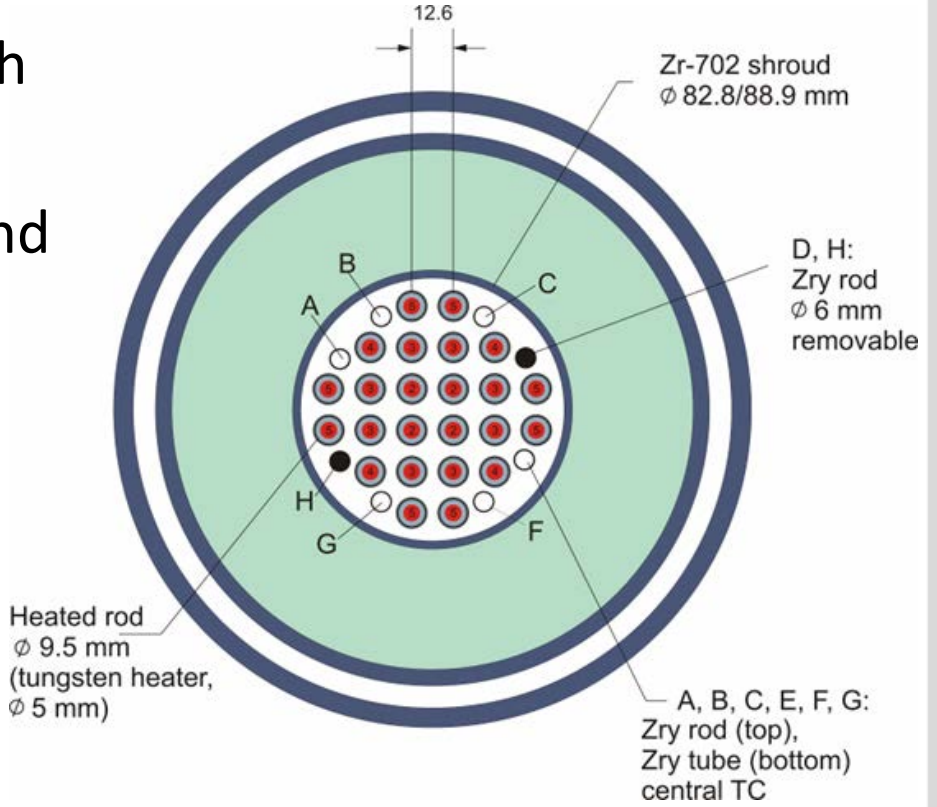
Strongly degraded bundle at 1250 mm





QUENCH-19

- Worldwide first bundle test with ATF cladding
- With FeCrAl cladding, shroud and spacer grids
- In cooperation with ORNL
- Scenario similar to QUENCH-15 (same bundle geometry, same electrical power input)
- Conducted on 29th August 2018

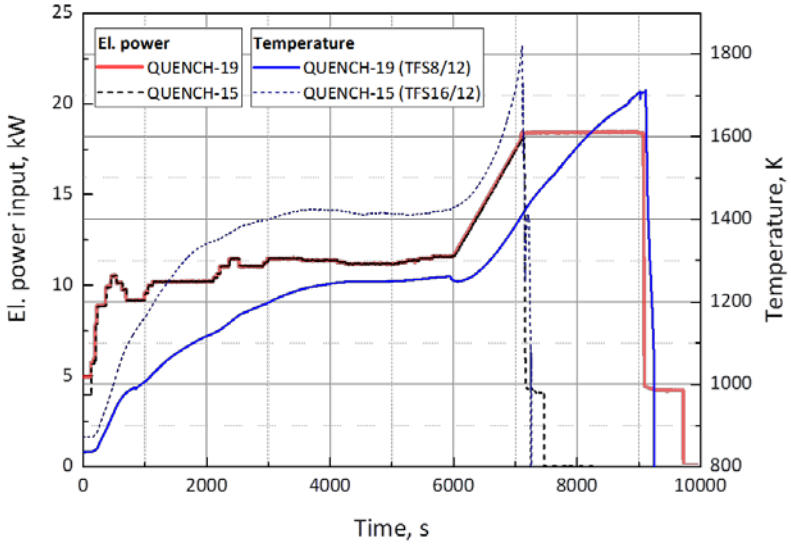


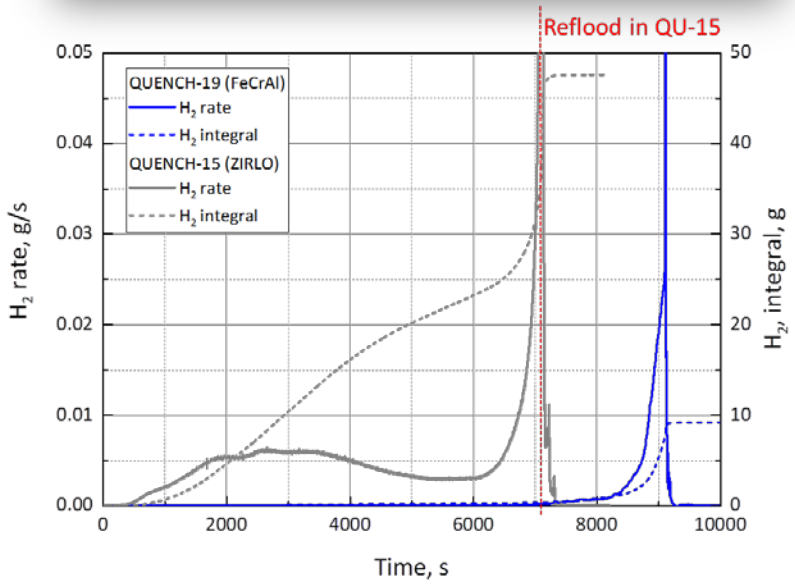


QUENCH-19

- 100x less hydrogen released up to quenching time of Q-15
- Melting temperature of FeCrAl locally reached
- Significant gain of coping time with FeCrAl compared to Zr alloy





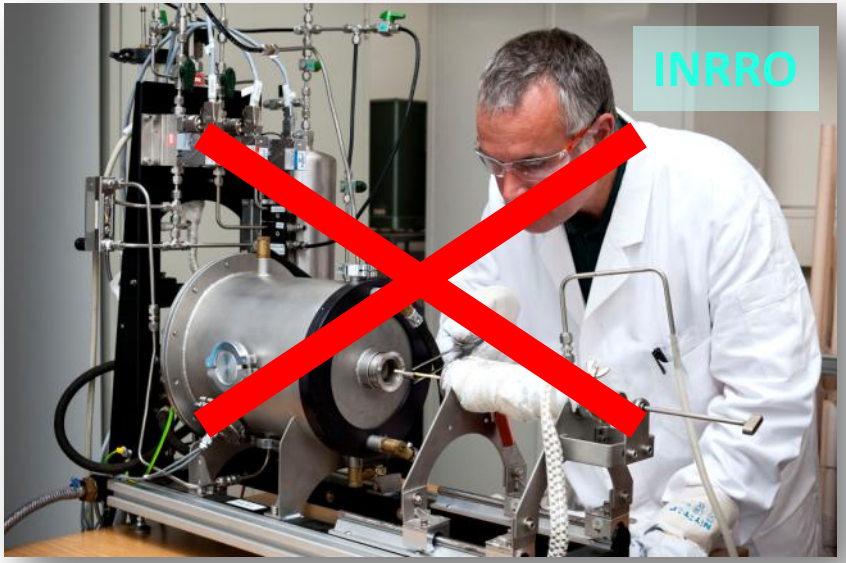


Separate-effects tests in 2018

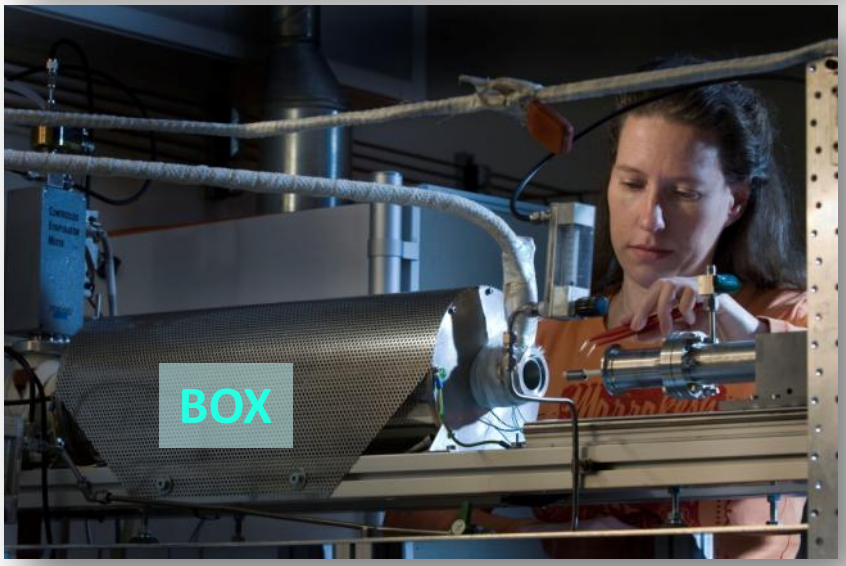
- Experiments on high-temperature oxidation of silicon carbide ceramic-matrix-composites in various atmospheres for different applications
- Optimization of Cr_2AlC MAX phase coatings on Zry
- Autoclave tests with MAX phase coatings at Westinghouse, USA
- High-temperature oxidation of various ATF cladding materials (Fe alloys, MAX phases, coated Zr alloys…) in the framework of international cooperations
- Interaction between SiC and Zry

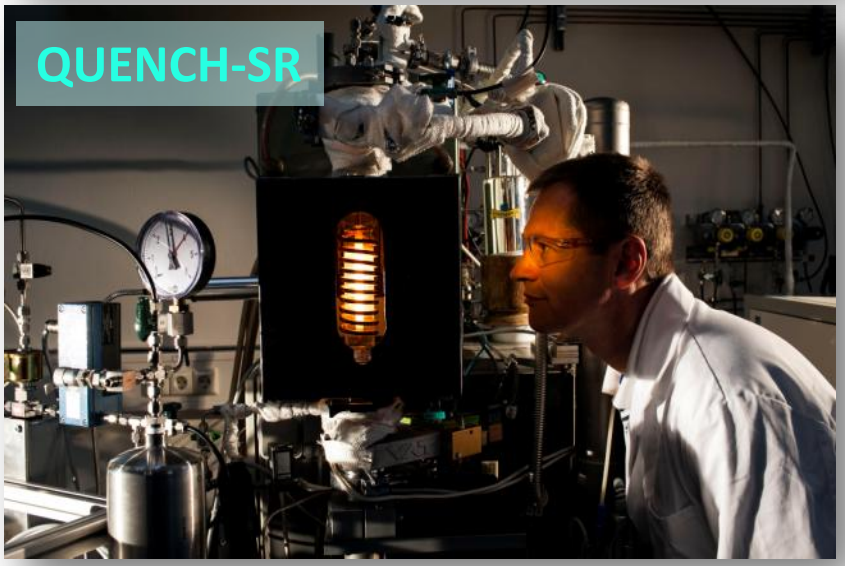
- CODEX-AIT3 at MTA Budapest proposed by KIT (SAFEST)

QUENCH Separate-effects tests: Main setups

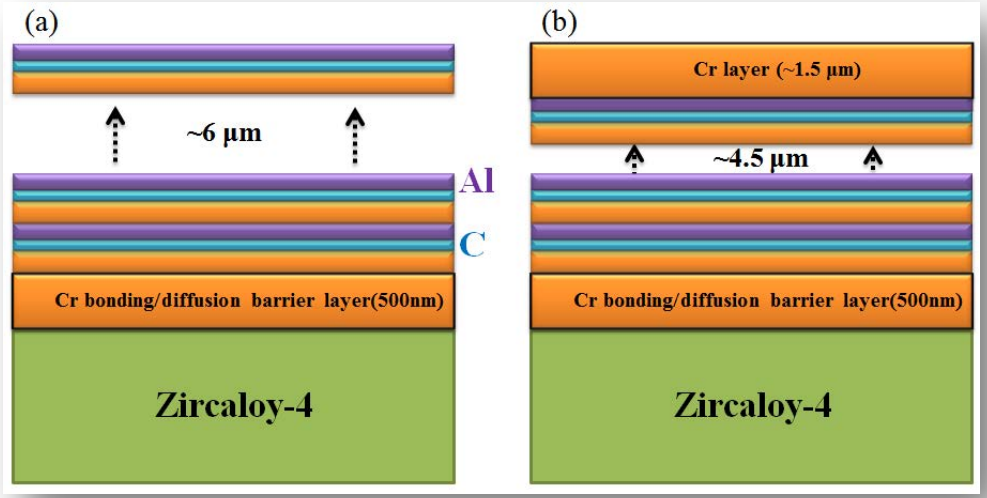




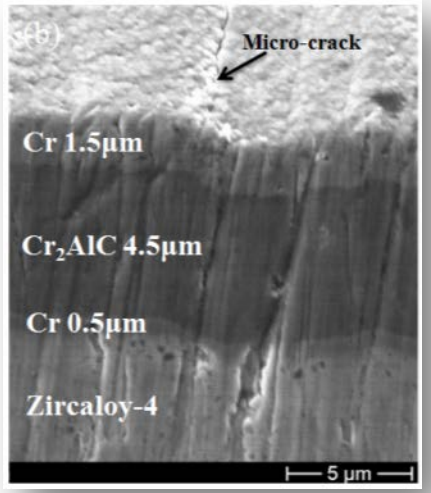




Cr_2AlC MAX phase coating on Zry-4

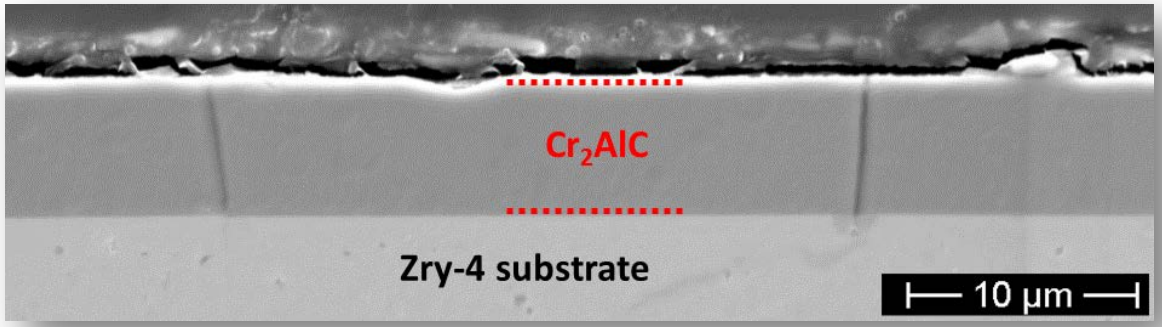


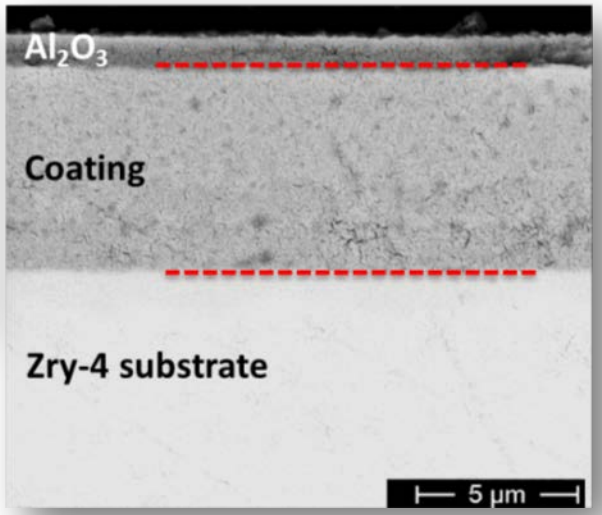
Annealing



Magnetron sputtered Cr/C/Al nano layers

Pure MAX phase

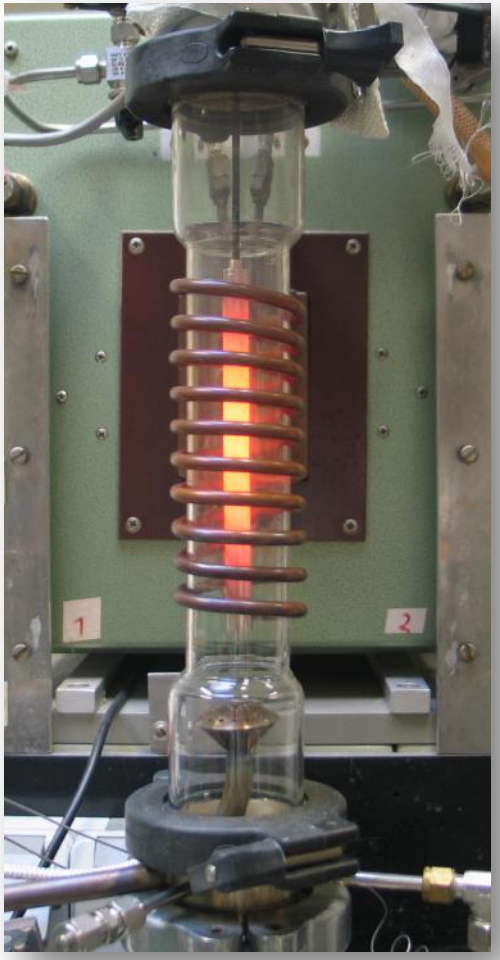




- Excellent behavior of coatings during autoclave tests (↑) and HT oxidation in steam up to 1200°C (→)

HT oxidation in steam of SiC_f-SiC cladding

- QUENCH-SR rig with inductive heating of graphite as susceptor
- Two samples
- Four experiments
  - Transient test with target temperature 2200°C (sample 1)
  - Three subsequent isothermal tests at 1600, 1700, and 1750°C terminated by quenching with water (sample 2)

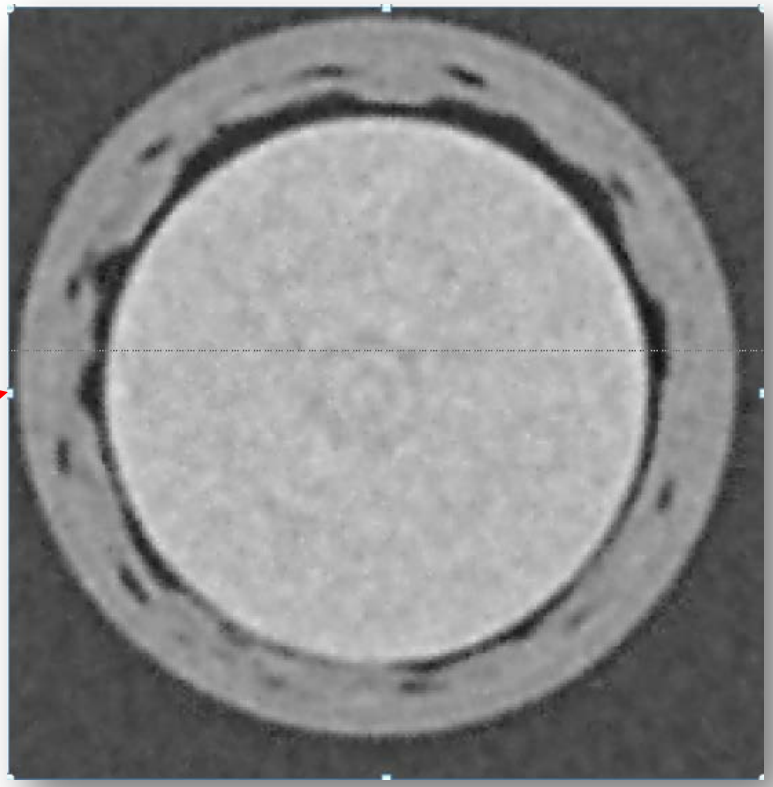


QUENCH-SR with inductive heating

SiC_f-SiC samples

- Provided by General Atomics
- Leak tight with welded end plugs and filled with graphite

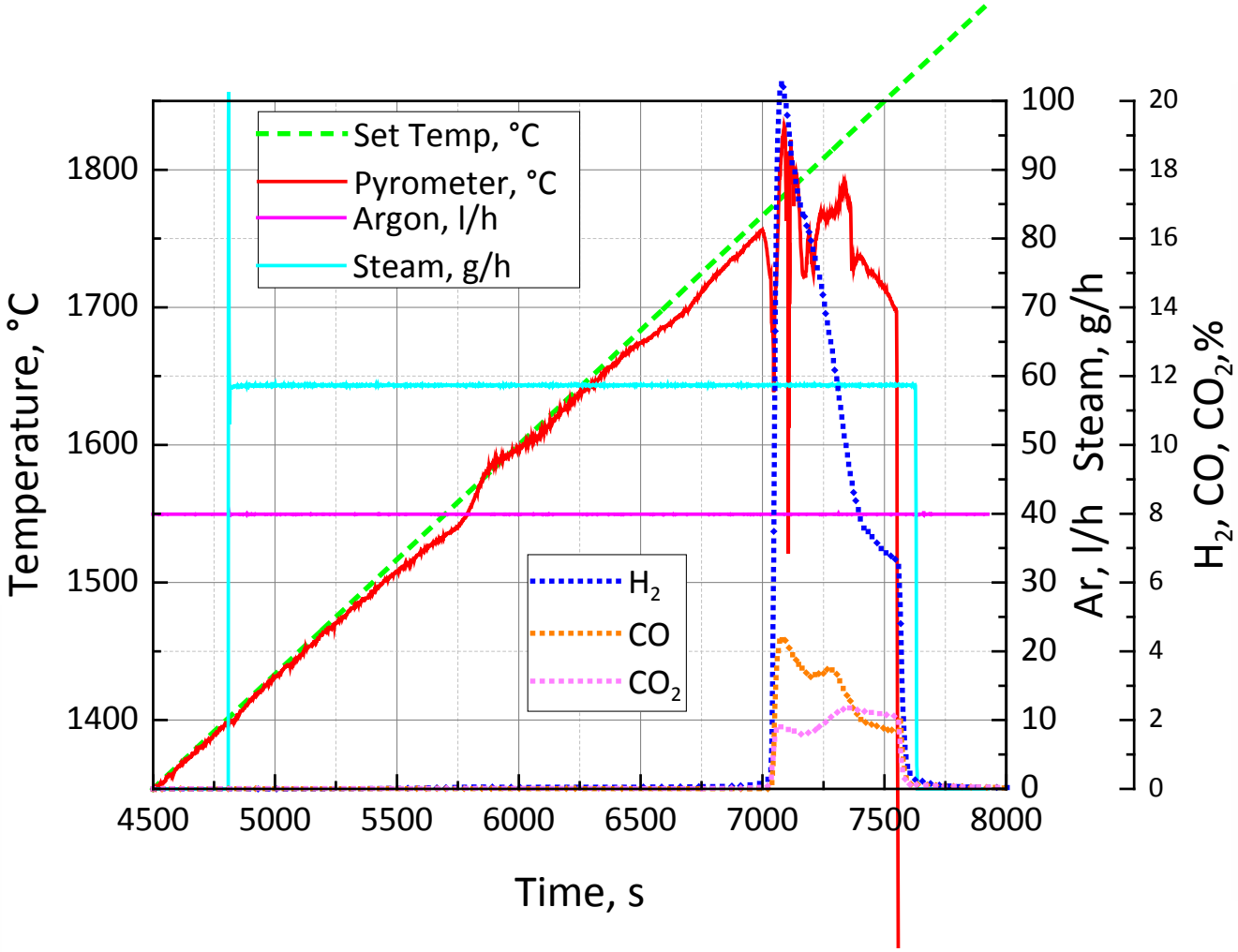


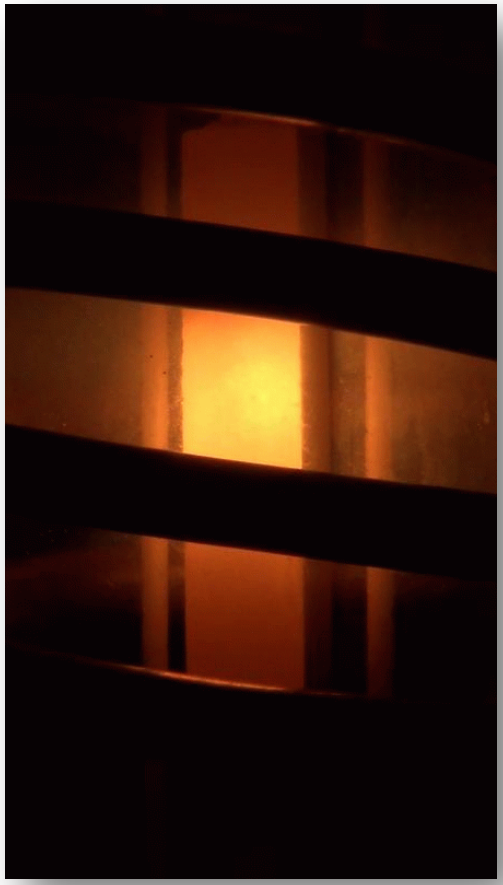


Neutron tomography of as-received sample



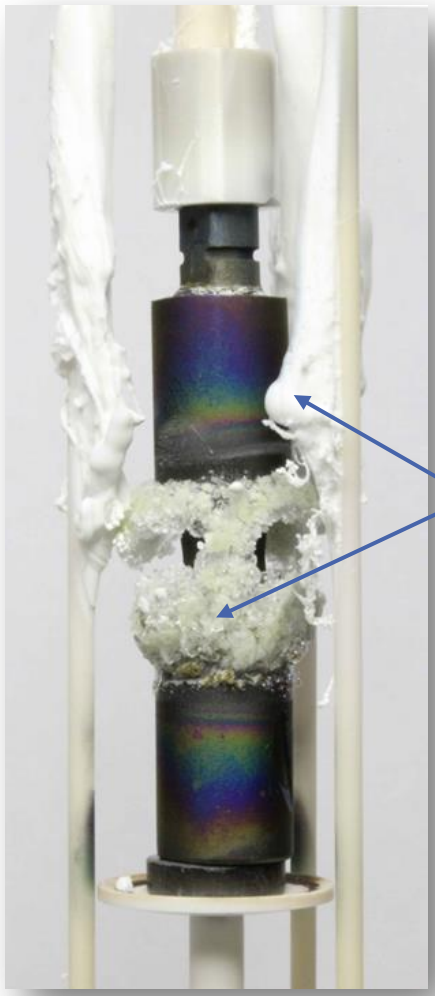
Transient test: Conduct and MS results





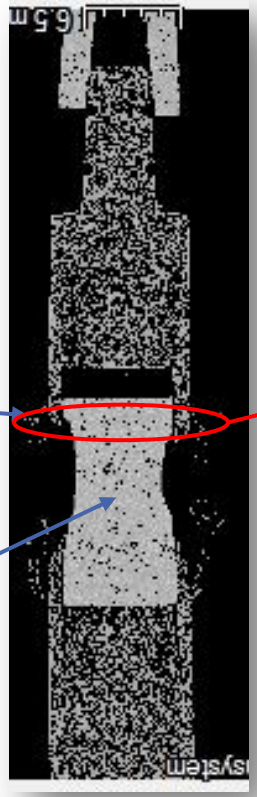
- Bubble formation, strong gas release, SiO_x volatilization above ~1750°C

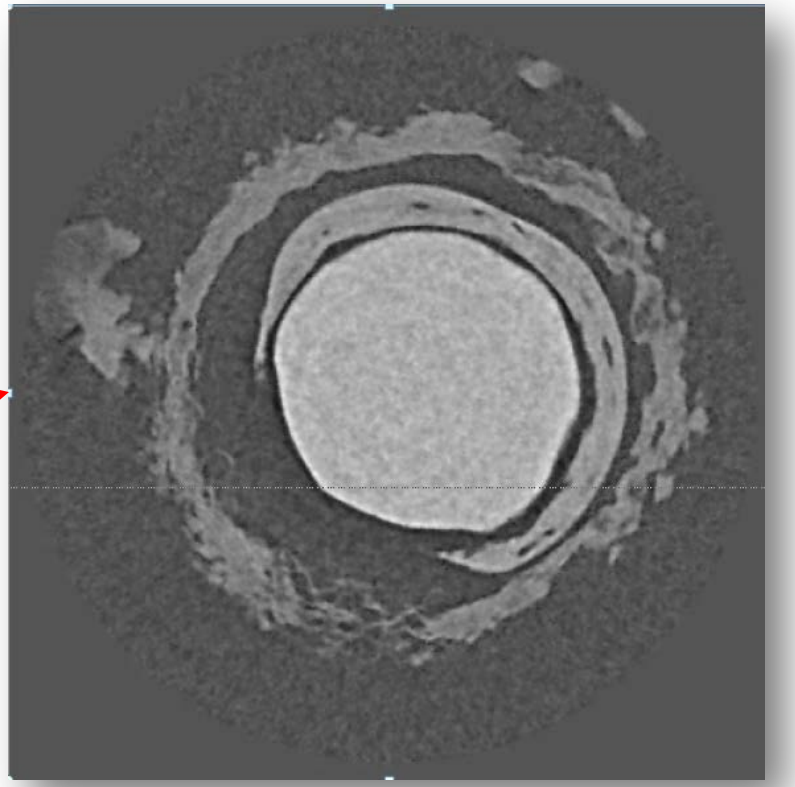
Transient test: Post-test appearance



SiO_x

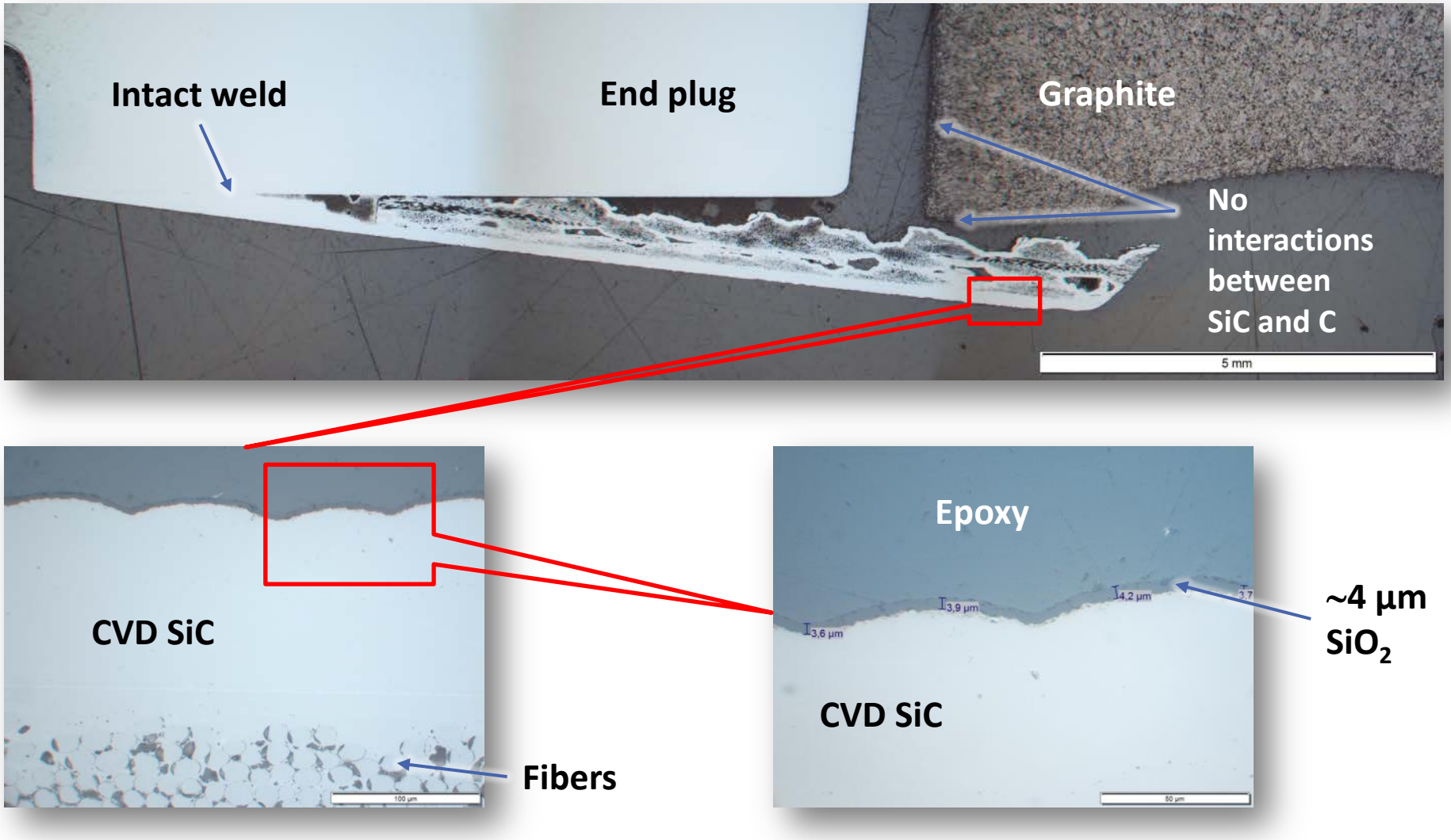
Graphite





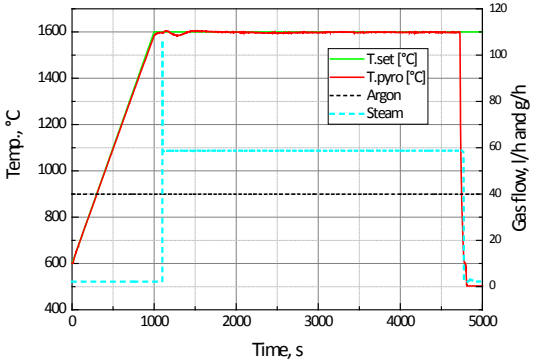
Neutron tomography after transient test

Transient test: Micrographs of longitudinal cross section

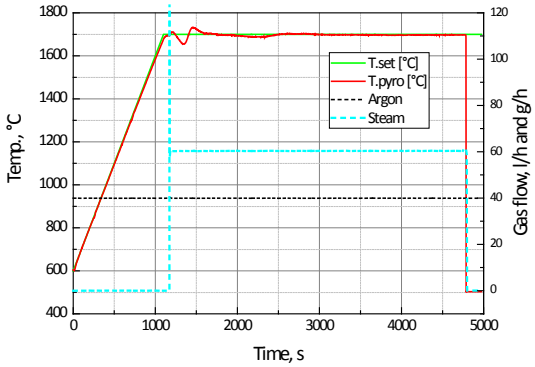


Isothermal tests: conduct and post-test appearance

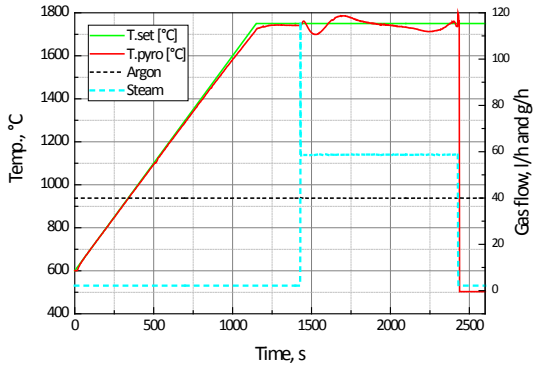
1 h @ 1600°C

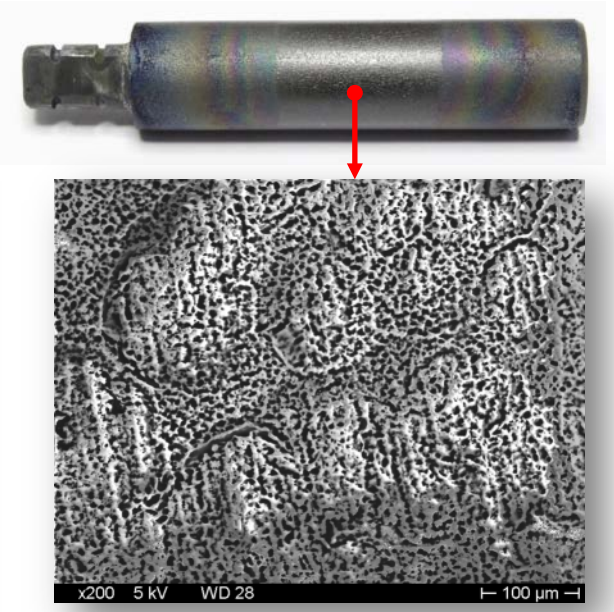


1 h @ 1700°C



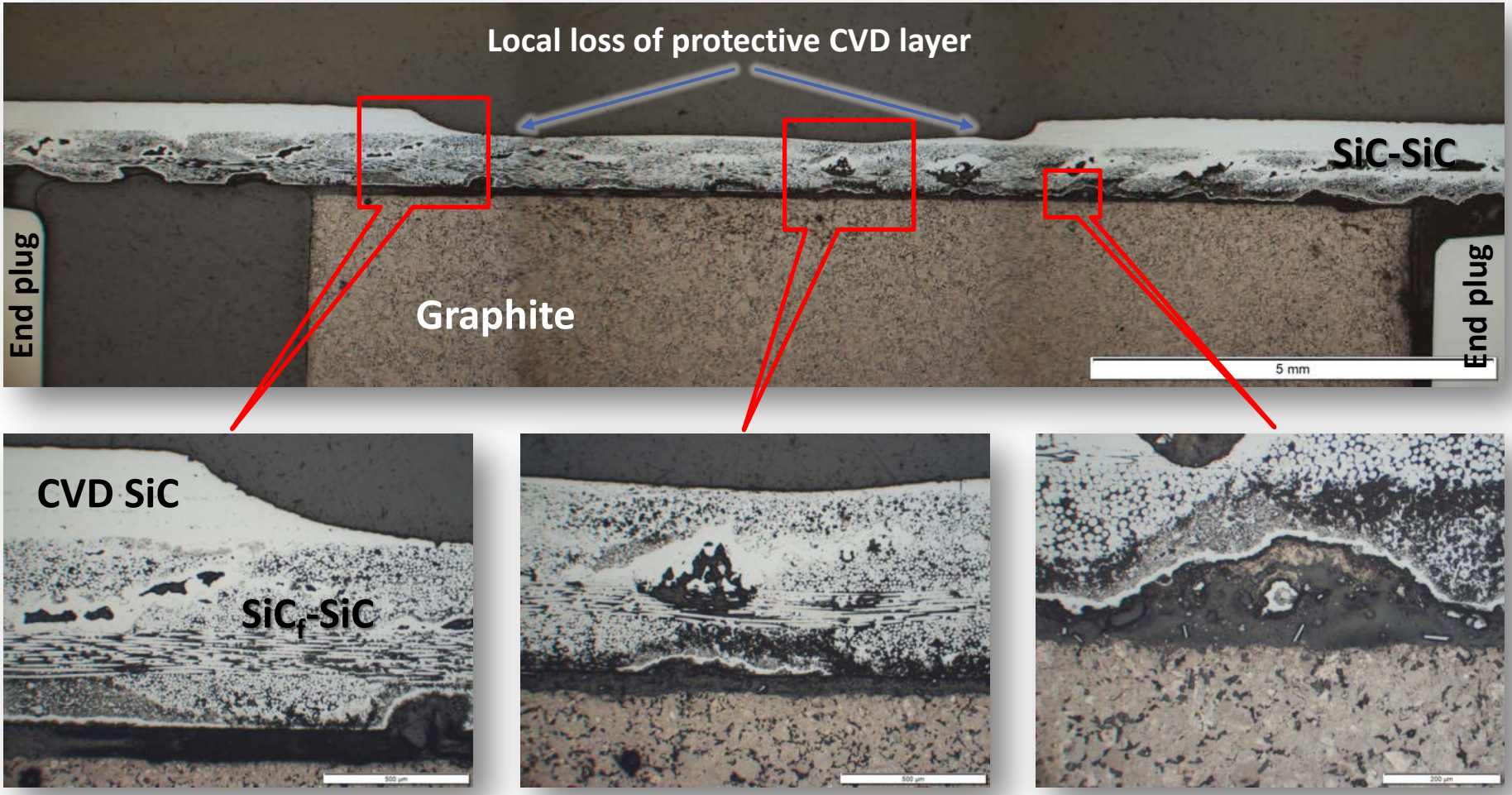
16 min @ 1750°C



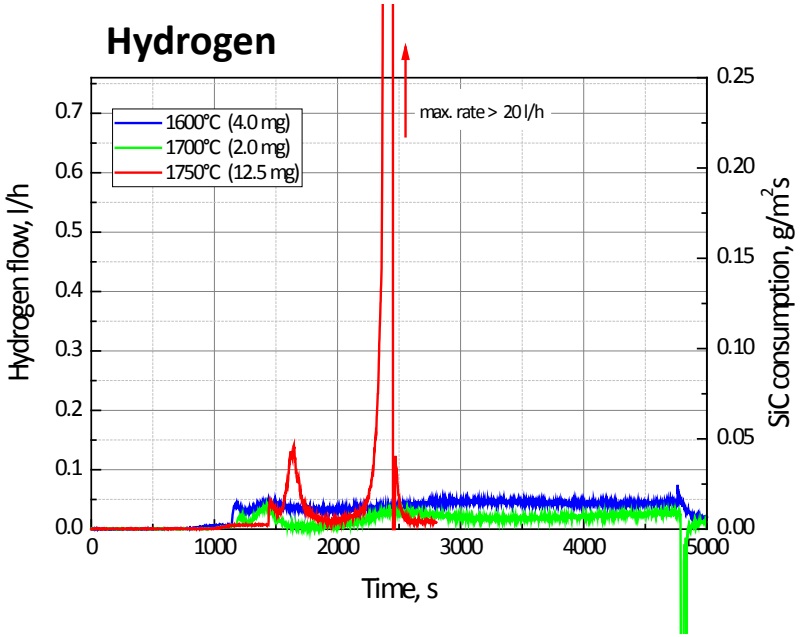


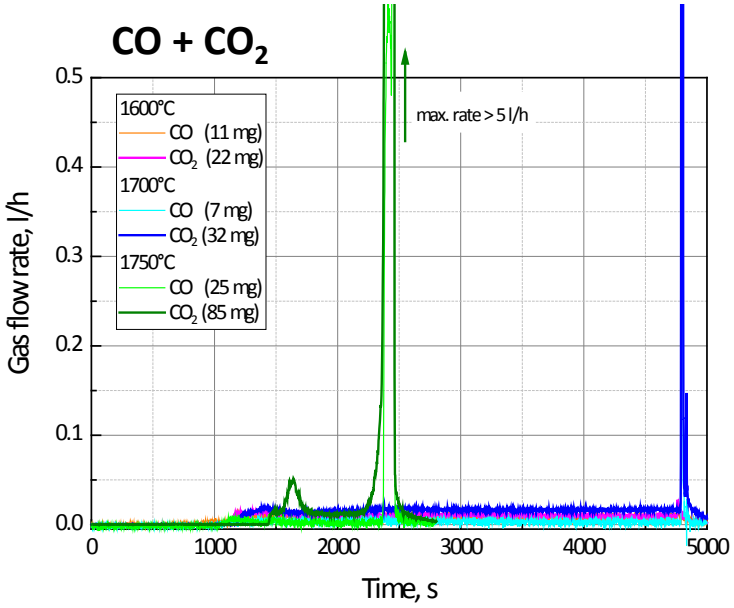
- SEM/EDX: all surfaces are covered with SiO_2

Isothermal tests: Micrographs of longitudinal cross section



Isothermal tests: Gas release





- Very limited oxidation of the SiC_f-SiC cladding at 1600 and 1700°C
- Local failure of the sample after 16 min at 1750°C resulting in strong gas release
- Failure mechanism not yet identified

QUENCH activities for Accident Tolerant Fuel Claddings

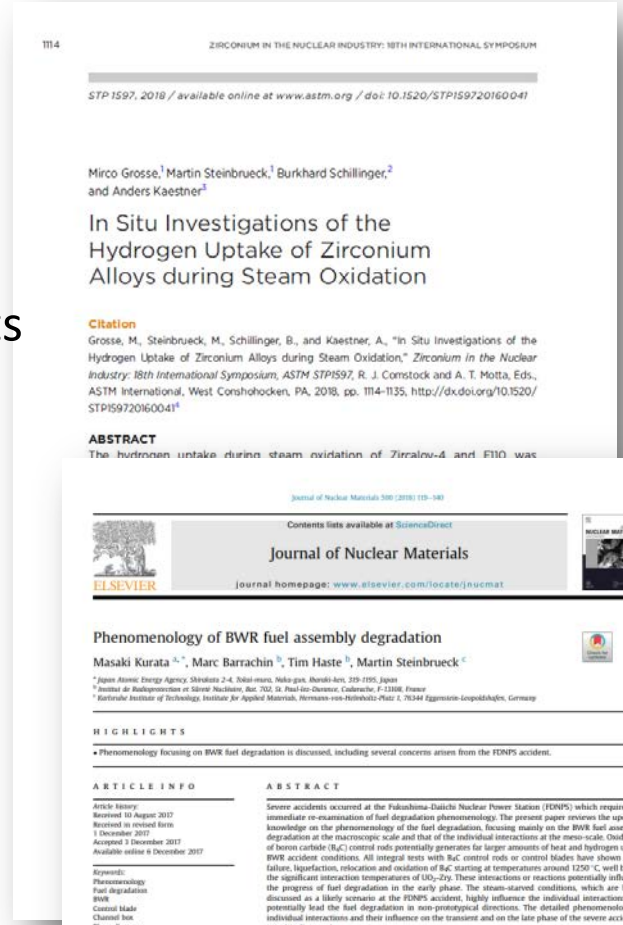
- PhD thesis
  - Development of high-temperature resistant coatings for zirconium alloy cladding tubes
- Participation in the OECD-NEA Expert Group on Accident Tolerant Fuels for LWRs (EGATFL, final meeting 01/2018, follow-up program under discussion) as well as in the new TOPATF initiative
- Participation in the IAEA CRP on Accident Tolerant Fuel Concepts for Light Water Reactors (ACTOF)
- WP leader (coolant-cladding-fuel interaction) in the EC project IL TROVATORE in the framework of HORIZON2020
- Partner in the CARAT project lead by Westinghouse, USA

Modelling and code validation

- QUENCH bundle tests are part of validation matrices of most SFD code systems
- Pre-test calculations for QUENCH-18/-19/-20 by various organisations
- Post-test calculations for QUENCH-18 in the framework of the NUGENIA QUESA project by GRS, PSI, IBRAE, LEI, EdF and of QUENCH-19 by GRS
- QUENCH data were used in the frame of IAEA FUMAC project
- RELAP5/SCDAPSIM analyses of various QUENCH tests
- Separate-effects test data on air oxidation of Zr alloys are used by PSI, RUB, EdF, ISS and others for model development

Reporting

- QUENCH-LOCA: KIT Scientific Reports available online
- LOCA summary paper planned for ASTM Symp. Zr in Nucl. Ind. 2019
- Papers, book chapters and conference contributions (>15 Scopus references)
- Plenary talk at NUMAT 2018



1114 ZIRCONIUM IN THE NUCLEAR INDUSTRY: 18TH INTERNATIONAL SYMPOSIUM

STP1597, 2018 / available online at www.astm.org / doi: 10.1520/STP159720160041

Mirco Grosse,[1] Martin Steinbrueck,[1] Burkhard Schillinger,[2] and Anders Kaestner[3]

In Situ Investigations of the Hydrogen Uptake of Zirconium Alloys during Steam Oxidation

Citation

Grosse, M., Steinbrueck, M., Schillinger, B., and Kaestner, A., "In Situ Investigations of the Hydrogen Uptake of Zirconium Alloys during Steam Oxidation," *Zirconium in the Nuclear Industry: 18th International Symposium, ASTM STP1597*, R. J. Comstock and A. T. Motta, Eds., ASTM International, West Conshohocken, PA, 2018, pp. 1114–1135, http://dx.doi.org/10.1520/STP159720160041

ABSTRACT

The hydrogen uptake during steam oxidation of Zircaloy-4 and E110 was



Journal of Nuclear Materials 500 (2018) 115–140

Contents lists available at ScienceDirect

Journal of Nuclear Materials

journal homepage: www.elsevier.com/locate/jnucmat

Phenomenology of BWR fuel assembly degradation

Masaki Kurata [a, *], Marc Barrachin [b], Tim Haste [b], Martin Steinbrueck [c]

[a] Japan Atomic Energy Agency, Shirakata 2-4, Tokai-mura, Naka-gun, Ibaraki-ken, 319-1195, Japan
[b] Institut de Radioprotection et Sûreté Nucléaire, Bat. 702, St. Paul-lez-Durance, Cadarache, F-13108, France
[c] Karlsruhe Institute of Technology, Institute for Applied Materials, Hermann-von-Helmholtz-Platz 1, 76344 Eggenstein-Leopoldshafen, Germany

HIGHLIGHTS

• Phenomenology focusing on BWR fuel degradation is discussed, including several concerns arisen from the FDNPS accident.

ARTICLE INFO

Article history:
Received 10 August 2017
Received in revised form
1 December 2017
Accepted 3 December 2017
Available online 6 December 2017

Keywords:
Phenomenology
Fuel degradation
BWR
Control blade
Channel box
Phase diagram
U-Zr-O system
UO_2-Zry system
B_4C-Stainless steel system
B_4C/SS-Zry system
Eutectic interaction model
Hydrogen uptake in Zry
B_4C oxidation
Fukushima-daiichi nuclear power plant accident

ABSTRACT

Severe accidents occurred at the Fukushima-Daiichi Nuclear Power Station (FDNPS) which required an immediate re-examination of fuel degradation phenomenology. The present paper reviews the updated knowledge on the phenomenology of the fuel degradation, focusing mainly on the BWR fuel assembly degradation at the macroscopic scale and that of the individual interactions at the meso-scale. Oxidation of boron carbide (B_4C) control rods potentially generates far larger amounts of heat and hydrogen under BWR accident conditions. All integral tests with B_4C control rods or control blades have shown early failure, liquefaction, relocation and oxidation of B_4C starting at temperatures around 1250 °C, well below the significant interaction temperatures of UO_2–Zry. These interactions or reactions potentially influence the progress of fuel degradation in the early phase. The steam-starved conditions, which are being discussed as a likely scenario at the FDNPS accident, highly influence the individual interactions and potentially lead the fuel degradation in non-prototypical directions. The detailed phenomenology of individual interactions and their influence on the transient and on the late phase of the severe accidents are also discussed.

© 2017 Elsevier B.V. All rights reserved.

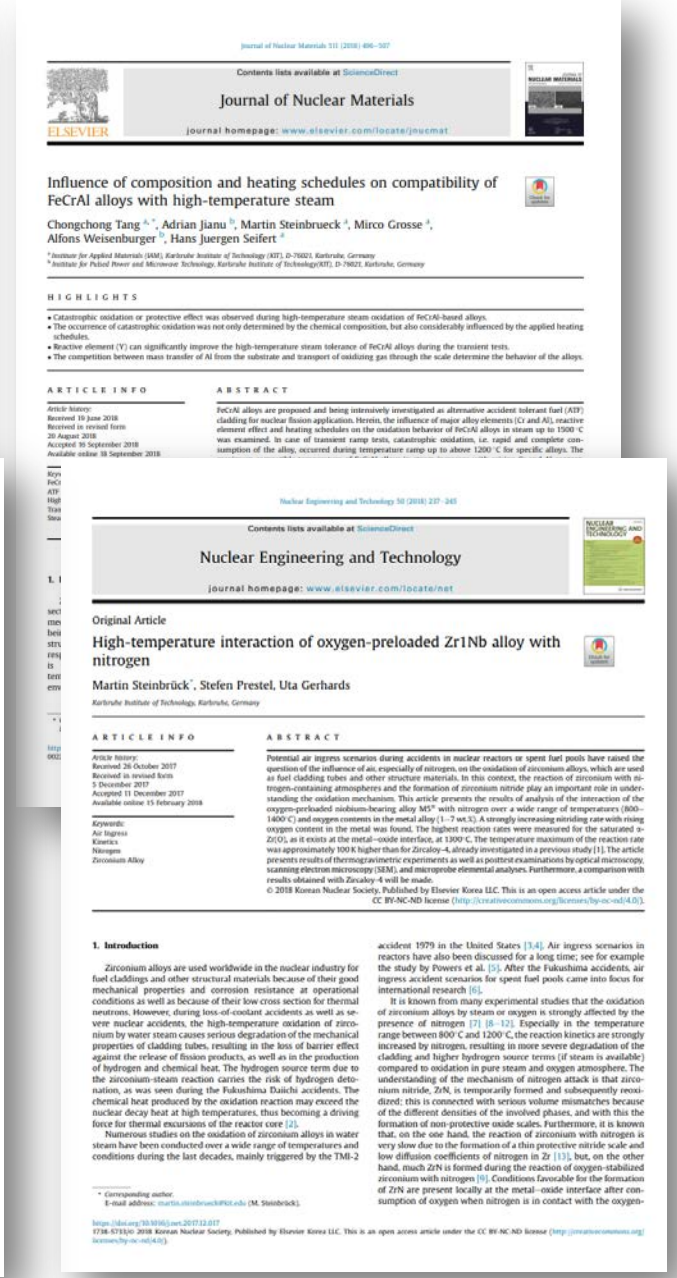
Contents

1. Introduction 120
2. Integral tests with B_4C control blade 121
2.1. US and Canadian tests 121
2.2. CORA BWR tests 121
2.3. Control blade degradation test in JAEA 122
2.4. Potential effect of B_4C in the FDNPS accident 122
3. Integral tests with B_4C absorber rods 125

Abbreviations: FDNPS, Fukushima-Daiichi Nuclear Power Station; SA, Severe Accident; BWR, Boiling Water Reactor; PWR, Pressurized Water Reactor.

* Corresponding author.
E-mail address: kurata.masaki@jaea.go.jp (M. Kurata).

https://doi.org/10.1016/j.jnucmat.2017.12.004
0022-3115/© 2017 Elsevier B.V. All rights reserved.



Journal of Nuclear Materials 511 (2018) 496–507

Contents lists available at ScienceDirect

Journal of Nuclear Materials

journal homepage: www.elsevier.com/locate/jnucmat

Influence of composition and heating schedules on compatibility of FeCrAl alloys with high-temperature steam

Chongchong Tang [a, *], Adrian Jianu [b], Martin Steinbrueck [a], Mirco Grosse [a], Alfons Weisenburger [b], Hans Juergen Seifert [a]

[a] Institute for Applied Materials (IAM), Karlsruhe Institute of Technology (KIT), D-76021, Karlsruhe, Germany
[b] Institute for Pulsed Power and Microwave Technology, Karlsruhe Institute of Technology(KIT), D-76021, Karlsruhe, Germany

HIGHLIGHTS

- Catastrophic oxidation or protective effect was observed during high-temperature steam oxidation of FeCrAl-based alloys.
- The occurrence of catastrophic oxidation was not only determined by the chemical composition, but also considerably influenced by the applied heating schedules.
- Reactive element (Y) can significantly improve the high-temperature steam tolerance of FeCrAl alloys during the transient tests.
- The competition between mass transfer of Al from the substrate and transport of oxidizing gas through the scale determine the behavior of the alloys.

ARTICLE INFO

Article history:
Received 19 June 2018
Received in revised form
20 August 2018
Accepted 19 September 2018
Available online 18 September 2018

ABSTRACT

FeCrAl alloys are proposed and being intensively investigated as alternative accident tolerant fuel (ATF) cladding for nuclear fission application. Herein, the influence of major alloy elements (Cr and Al), reactive element effect and heating schedules on the oxidation behavior of FeCrAl alloys in steam up to 1500 °C was examined. In case of transient ramp tests, catastrophic oxidation, i.e. rapid and complete consumption of the alloy, occurred during temperature ramp up to above 1200 °C for specific alloys. The

Nuclear Engineering and Technology 50 (2018) 237–245

Contents lists available at ScienceDirect

Nuclear Engineering and Technology

journal homepage: www.elsevier.com/locate/net

Original Article

High-temperature interaction of oxygen-preloaded Zr1Nb alloy with nitrogen

Martin Steinbrück*, Stefen Prestel, Uta Gerhards

Karlsruhe Institute of Technology, Karlsruhe, Germany

ARTICLE INFO

Article history:
Received 26 October 2017
Received in revised form
5 December 2017
Accepted 11 December 2017
Available online 15 February 2018

Keywords:
Air ingress
Kinetics
Nitrogen
Zirconium Alloy

ABSTRACT

Potential air ingress scenarios during accidents in nuclear reactors or spent fuel pools have raised the questions of the influence of air, especially of nitrogen, on the oxidation of zirconium alloys, which are used as fuel cladding tubes and other structure materials. In this context, the reaction of zirconium with nitrogen-containing atmospheres and the formation of zirconium nitride play an important role in understanding the oxidation mechanisms. This article presents the results of analysis of the interaction of the oxygen-preloaded niobium-bearing alloy M5® with nitrogen over a wide range of temperatures (800–1400 °C) and oxygen contents in the metal alloy (1–7 wt.%). A strongly increasing nitriding rate with rising oxygen content in the metal was found. The highest reaction rates were measured for the saturated α-Zr(O), as it exists at the metal–oxide interface, at 1300 °C. The temperature maximum of the reaction rate was approximately 100 K higher than for Zircaloy-4, already investigated in a previous study [1]. The article presents results of thermogravimetric experiments as well as posttest examinations by optical microscopy, scanning electron microscopy (SEM), and microprobe elemental analyses. Furthermore, a comparison with results obtained with Zircaloy-4 will be made.

© 2018 Korean Nuclear Society, Published by Elsevier Korea LLC. This is an open access article under the CC BY-NC-ND license (http://creativecommons.org/licenses/by-nc-nd/4.0/).

1. Introduction

Zirconium alloys are used worldwide in the nuclear industry for fuel claddings and other structural materials because of their good mechanical properties and corrosion resistance at operational conditions as well as because of their low cross section for thermal neutrons. However, during loss-of-coolant accidents as well as severe nuclear accidents, the high-temperature oxidation of zirconium by water steam causes serious degradation of the mechanical properties of cladding tubes, resulting in the loss of barrier effect against the release of fission products, as well as in the production of hydrogen and chemical heat. The hydrogen source term due to the zirconium-steam reaction carries the risk of hydrogen detonation, as was seen during the Fukushima Daiichi accidents. The chemical heat produced by the oxidation reaction may exceed the nuclear decay heat at high temperatures, thus becoming a driving force for thermal excursions of the reactor core [2].

Numerous studies on the oxidation of zirconium alloys in water steam have been conducted over a wide range of temperatures and conditions during the last decades, mainly triggered by the TMI-2 accident 1979 in the United States [3,4]. Air ingress scenarios in reactors have also been discussed for a long time; see for example the study by Powers et al. [5]. After the Fukushima accidents, air ingress accident scenarios for spent fuel pools came into focus for international research [6].

It is known from many experimental studies that the oxidation of zirconium alloys by steam or oxygen is strongly affected by the presence of nitrogen [7] [8–12]. Especially in the temperature range between 800 °C and 1200 °C, the reaction kinetics are strongly increased by nitrogen, resulting in more severe degradation of the cladding and higher hydrogen source terms (if steam is available) compared to oxidation in pure steam and oxygen atmosphere. The understanding of the mechanism of nitrogen attack is that zirconium nitride, ZrN, is temporarily formed and subsequently reoxidized; this is connected with serious volume mismatches because of the different densities of the involved phases, and with this the formation of non-protective oxide scales. Furthermore, it is known that, on the one hand, the reaction of zirconium with nitrogen is very slow due to the formation of a thin protective nitride scale and low diffusion coefficients of nitrogen in Zr [13], but, on the other hand, much ZrN is formed during the reaction of oxygen-stabilized zirconium with nitrogen [9]. Conditions favorable for the formation of ZrN are present locally at the metal–oxide interface after consumption of oxygen when nitrogen is in contact with the oxygen-

* Corresponding author.
E-mail address: martin.steinbrueck@kit.edu (M. Steinbrück).

https://doi.org/10.1016/j.net.2017.12.017
1738-5733/© 2018 Korean Nuclear Society, Published by Elsevier Korea LLC.

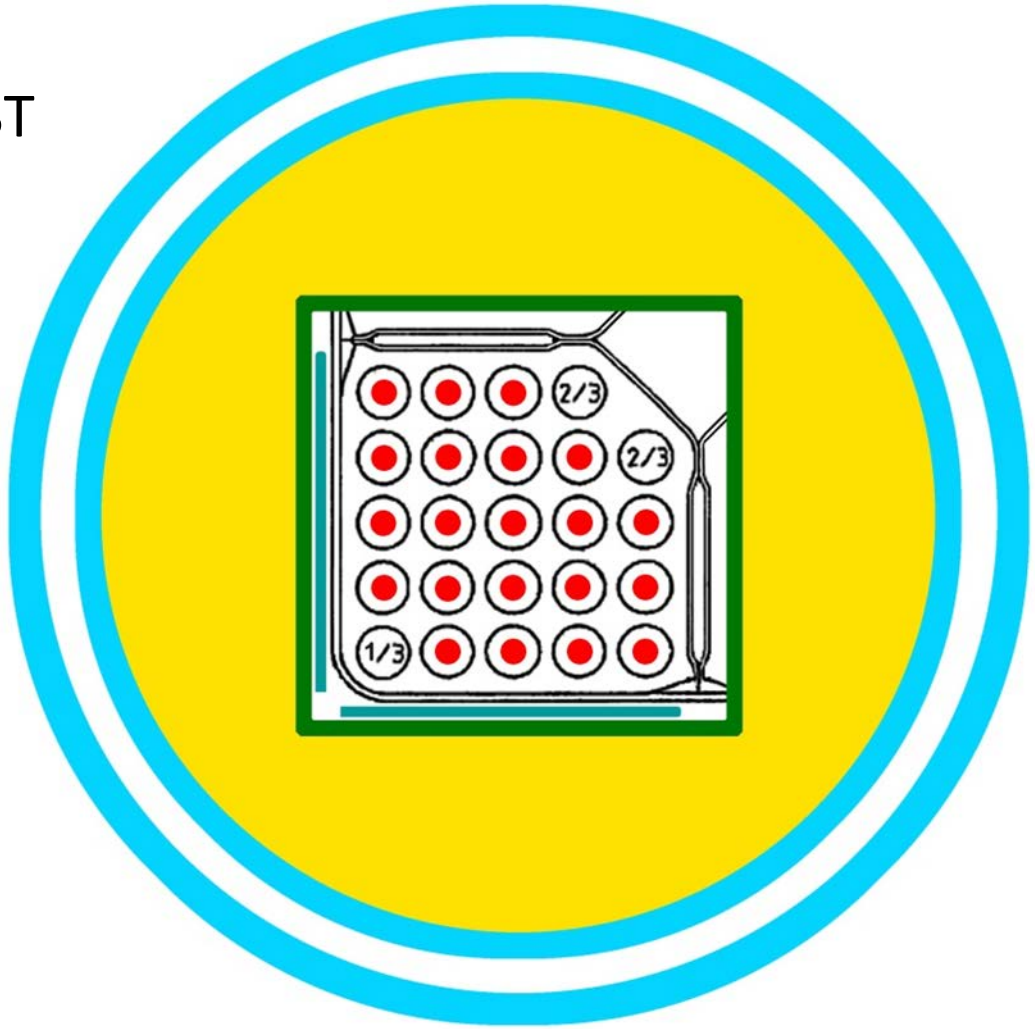
This is an open access article under the CC BY-NC-ND license (http://creativecommons.org/licenses/by-nc-nd/4.0/).

Outlook 2019-2020

- BWR bundle test with in the framework of the EC SAFEST program beginning 2019
- Post-test examinations of QUENCH-18/-19/-20
- Discussion with various international partners on further bundle tests with ATF claddings
- SETs on various further topics with the focus on ATF cladding high temperature oxidation
- Activities on safety of long-term dry intermediate storage

BWR bundle test QUENCH-20

- Planned to be conducted beginning 2019 in the framework of the EC SAFEST program
- Proposed by Swedish regulatory body and supported by Westinghouse
- Square bundle cross section
- Including boron carbide absorber blades and water channels



Co-operations

Programs

- NUGENIA
- HORIZON 2020
- IAEA
- OECD-NEA

Bilateral

- PSI
- MTA EK
- IRSN, CEA, EdF
- RUB-LEE, IKE
- JRC
- GRS
- Westinghouse
- USNRC
- KONICOF
- NECSA, BAM, HMI
- NRA, JAEA
- ISS
- ORNL
- Various Chinese Organizations

Acknowledgements

- Helmholtz Association for funding program NUSAFE at KIT
- Program NUSAFE and IAM institute's management for broad support of our activities
- IAEA for financial support of four participants

- And last but not least the QUENCH team:
  J. Glaser, M. Heck, J. Laier, J. Moch, H. Muscher, U. Peters, U. Stegmaier, C. Tang, P. v. Appeldorn, M. Walter

Karlsruhe Institute of Technology

Institute for Applied Materials

Update of the QUENCH Program

M. Steinbrück, J. Stuckert, M. Große et al.

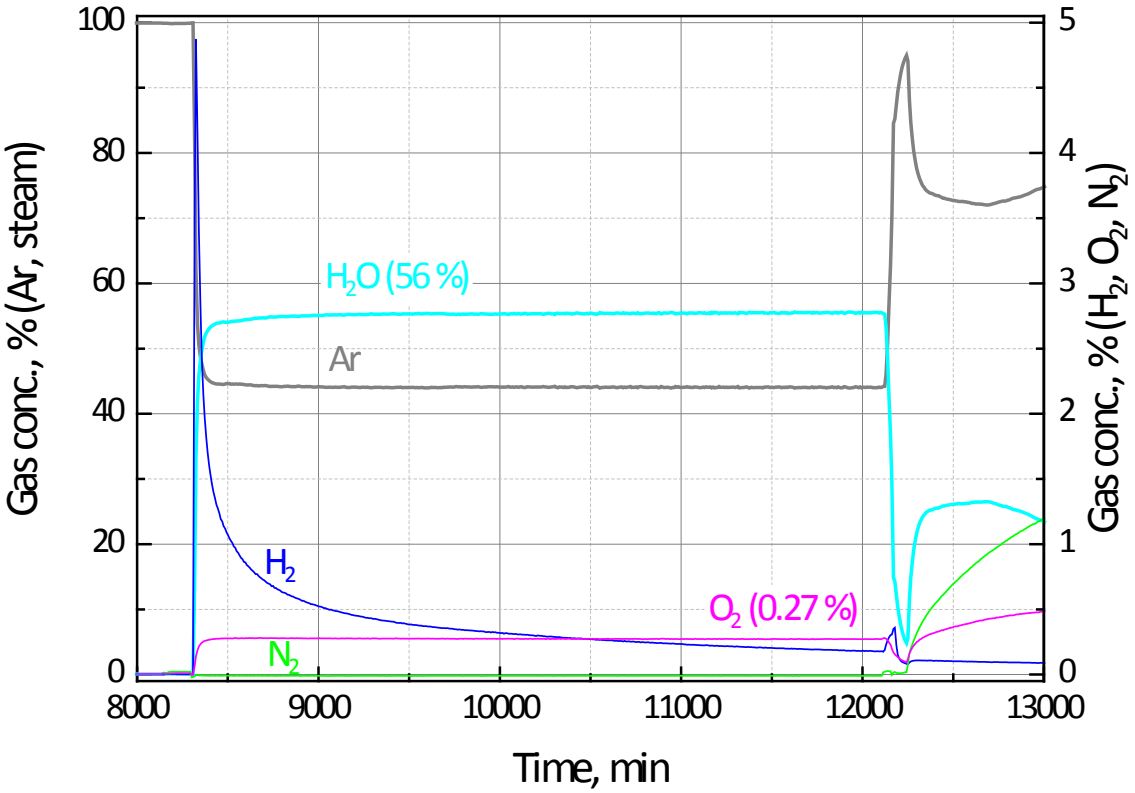
24th International QUENCH Workshop, Karlsruhe, 13-15 November 2018

Institute for Applied Materials, Programme NUSAFE



MS issue with O_2 signal in presence of steam

- Since July 2017 after change of filaments
- Small artificial O_2 signal (<1%) in presence of steam without any correlation to other signals (N_2, H_2)



Example:
Zry-4 oxidation in steam
at 1200°C

First Results of the QUENCH-18 Post-Test Benchmark in the Frame of the NUGENIA QUESA Project

Thorsten Hollands
Gesellschaft für Anlagen- und Reaktorsicherheit (GRS) gGmbH, Germany

Abstract

During a severe accident in an NPP, air ingress into the vessel will lead to a mixed atmosphere inside the core region that is mainly composed of steam and air. As air is a highly oxidizing this can lead to an enhanced core oxidation and degradation affecting the release of Fission Products (FP). Therefore, the understanding of the phenomena governing cladding oxidation by air is a pre-requisite for realistic source term predictions. Based on the ALISA calls for proposal, the idea was to define a counterpart of QUENCH-16, but with a mixture of air and steam instead of pure air in order to be more representative of a reactor case. QUENCH-18 was performed at KIT in 2017 as this counterpart test in the frame of the ALISA project considering a steam/air phase with the aim to achieve oxygen and steam starvation for nitride formation. The experiment was supported by pre- and post-test simulations in the frame of the NUGENIA QUESA project.

The post-test analyses are performed in the frame of a benchmark organized by GRS with contribution by three participants using three codes (ATHLET-CD of AC^2, SOCRAT, RELAP/SCDAPSIM). The chosen model options for the simulations are comparable for steam oxidation but differ for the air ingress phenomena, especially for nitride formation which is explicitly simulated in ATHLET-CD and SOCRAT, and indirectly by an accelerated oxidation in RELAP/SCDAPSIM. In general, all simulations show that the qualitative behaviour of the measured test conduct can be predicted. For the first phases (pre-oxidation and intermediate cooldown) the results are quite close to each other, but afterwards in the air/steam phase and the subsequent reflooding the calculated temperatures are spread for the different calculations. During the air/steam phase all codes predict oxygen and steam starvation in close agreement to the experiment, which allows nitride formation calculated by ATHLET-CD and SOCRAT. After oxygen starvation steam oxidation and nitride formation is calculated in parallel as it can be observed in single effect tests at KIT. The predicted hydrogen generation is during the whole test underestimated by SOCRAT, while ATHLET-CD and RELAP/SCDAPSIM are in good agreement to the measured H_2 generation until reflooding. Afterwards, both codes also underpredict the experimental value, but this value needs further investigations to asses which component contributes to the total generation, because not all components are modelled in the simulations. The final evaluation of the simulation results will be done after the final experimental investigations are finished.



First Results of the QUENCH-18 Post-Test Benchmark in the Frame of the NUGENIA QUESA Project

Thorsten Hollands

Gesellschaft für Anlagen- und Reaktorsicherheit (GRS) gGmbH, Germany

24th International QUENCH Workshop

Karlsruhe Institute of Technology

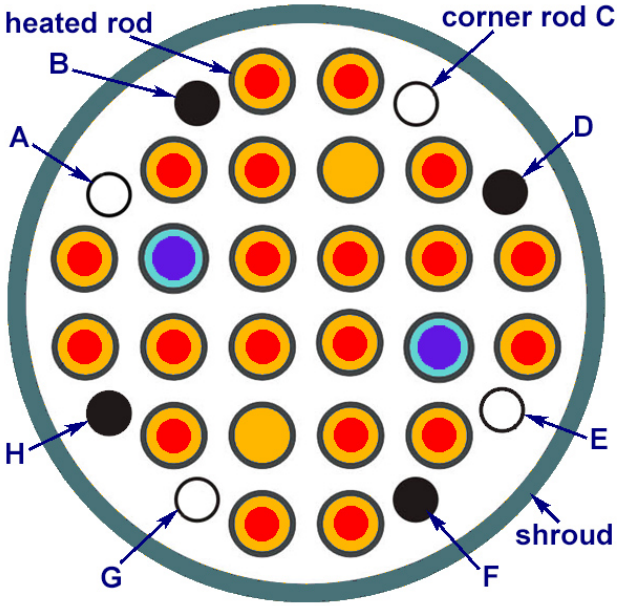
13. – 15. November 2018

Content

- QUENCH facility
- QUENCH-18: Scopes and transient
- Participants and codes
- Model options of applied severe accident codes
- Results of post-test simulations
- Main findings

QUENCH-18 test

Component	No.	Material properties	Outer diameter (mm)	Inner diameter (mm)
Rod Cladding	22	M5®	9.50	8.36
SIC Absorber Rod	2	Ag 80%, In 15%, Cd 5% density: 10.17 g/cm³	7.65	
Absorber Cladding	2	Stainless Steel	9.68	7.72
Absorber Guide Tube	2	M5®	12.45	11.25
Corner Rod	8	Zry-4	6.00	
Shroud	1	Zry	89.00	83.00

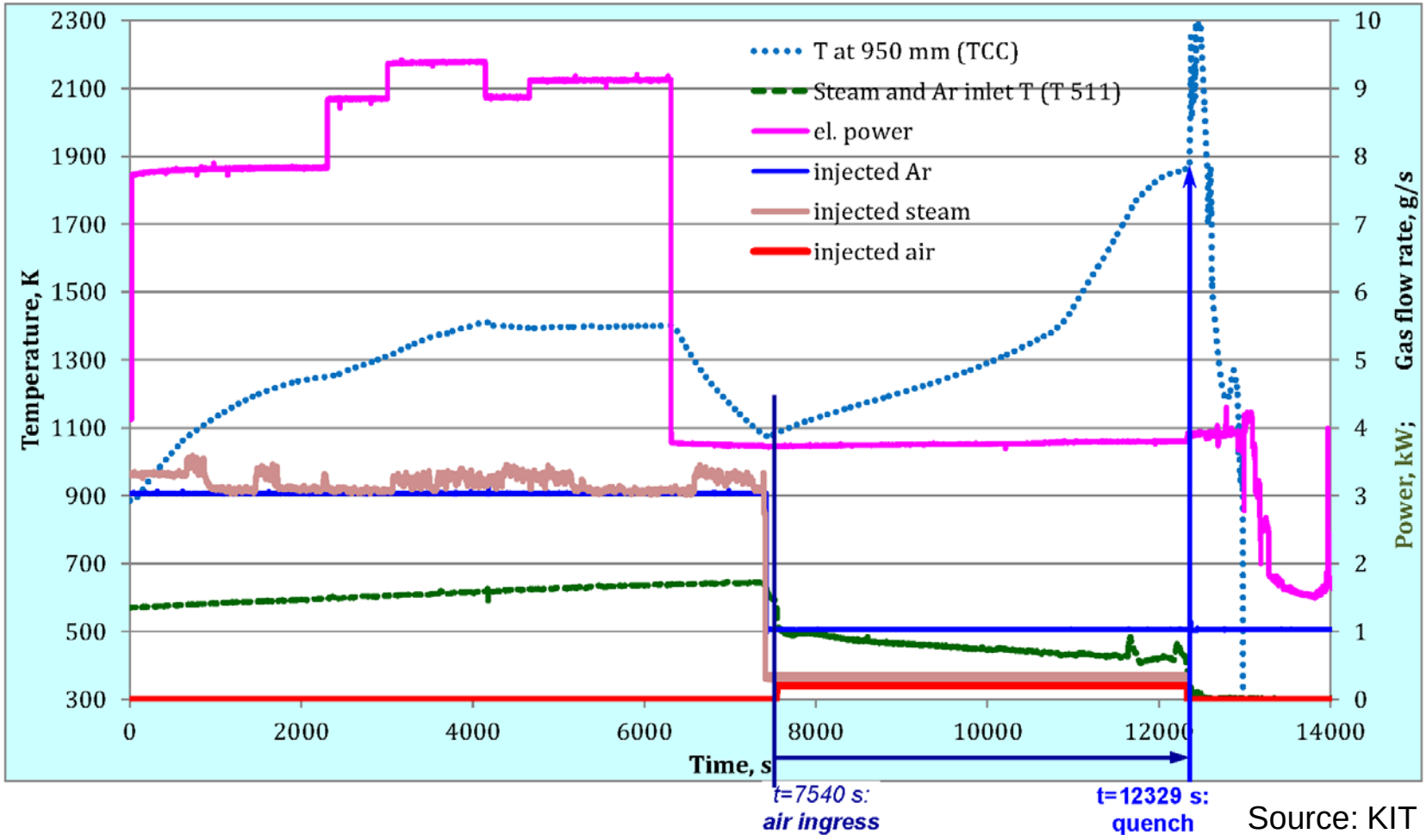


Source: KIT

QUENCH-18 – Scopes and transient

- Scope of the test:
  - First integral test on oxidation with air/steam mixture
  - Starvation of oxygen and/or steam (global or local) is very important, because data concerning nitride formation are expected
- Test transient:
  - Pre-oxidation
  - Intermediate cooldown
  - Air/steam ingress
  - Quenching

QUENCH-18 – Transient



Source: KIT

Current Participants and Codes for the Post-Test Benchmark (status August 2018)

- Participants:
  - GRS ATHLET-CD as part of AC^2
  - EDF MAAP5
  - Jon Birchley SCDAPSim
  - LEI RELAP/SCDAPSim
  - IBRAE SOCRAT

Modelling with Severe Accident codes
- Model options -

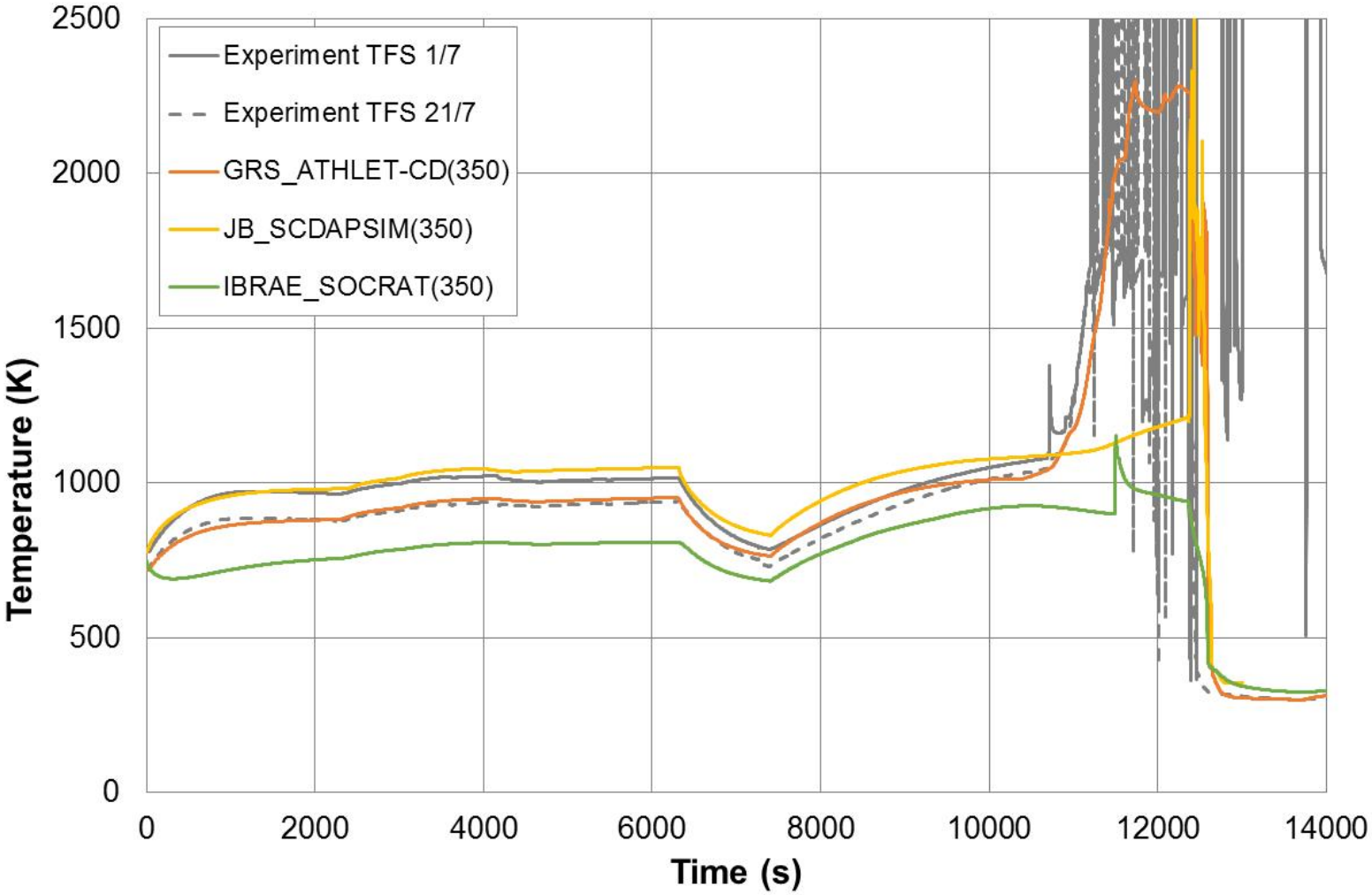
Code Version	ATHLET-CD 31a	SCDAPSim/3.5da/psi	SOCRAT v2
Electrical resistance (mOhm/rod)	3.5	3.6	4.0
Steam Oxidation Correlation	Cathcart - Prater/Courtright	Leistikow-Schanz/ Prater-Courtright	Cathcart-Pawel & Leistikov-Schanz / Prater/Courtright & Leistikov-Aly
Air Oxidation (or Oxygen) Correlation	NUREG2 (T<1180K) and NUREG1 (T>1450K) with interpolation inbetween	Utsuega-Hofmann/Urbanic Heidrick; FM reduction factor for low concentration	Oxygen diffusion enhancement factor depending on ZrN molar fraction. Pure oxygen is treated as vapour except chemical heat.
Nitriding Correlation	Hollands	No nitriding. Birchley model for accelerated oxidation	Empirical model depending on nitrogen content in gas mixture.
SIC degradation /release	release model not used	Candling of molten SIC when cladding and guide tube liquefied	no
Cladding failure criterion	max. strain 38 %	MATPRO ballooning burst	On temperature (T) if ZrO2 layer thickness (d) less than prescribed value.
SIC failure criterion	1523 K	MATPRO Fe-Zr liquefaction	1450 K
Possibility of nitrides reoxidation	reoxidation not modelled – consideration of porosity	no	no

Results of post-test simulations
- Main events -

		ATHLET-CD	SCDAPSim	SOCRAT
Total H_2 generation (g)	end of preoxidation	10.5	12.3	5.2
	end of reflood	151.0	202.7	33.0
Maximum T (K)	end of pre-ox (before cooldown)	1382	1416	1267
	end of intermediate cooldown	1038	1071	942
	during reflood	(3000)	3069	2584
Time (s)	of Tmax at the end of air phase	12329	12329	12336
	of Tmax during reflood	12410	12434	12304
	of final QUENCH	13450	12988	15372
	onset of complete O_2 consumption	10400	10836	10570
Lowest elevation	O_2 was complete consumed (mm)	150	650	850
	at time (s)	12300	11374	10570
Lowest elevation	control rod failure (mm)	50	450	950
	at time (s)	12225	11450	10452

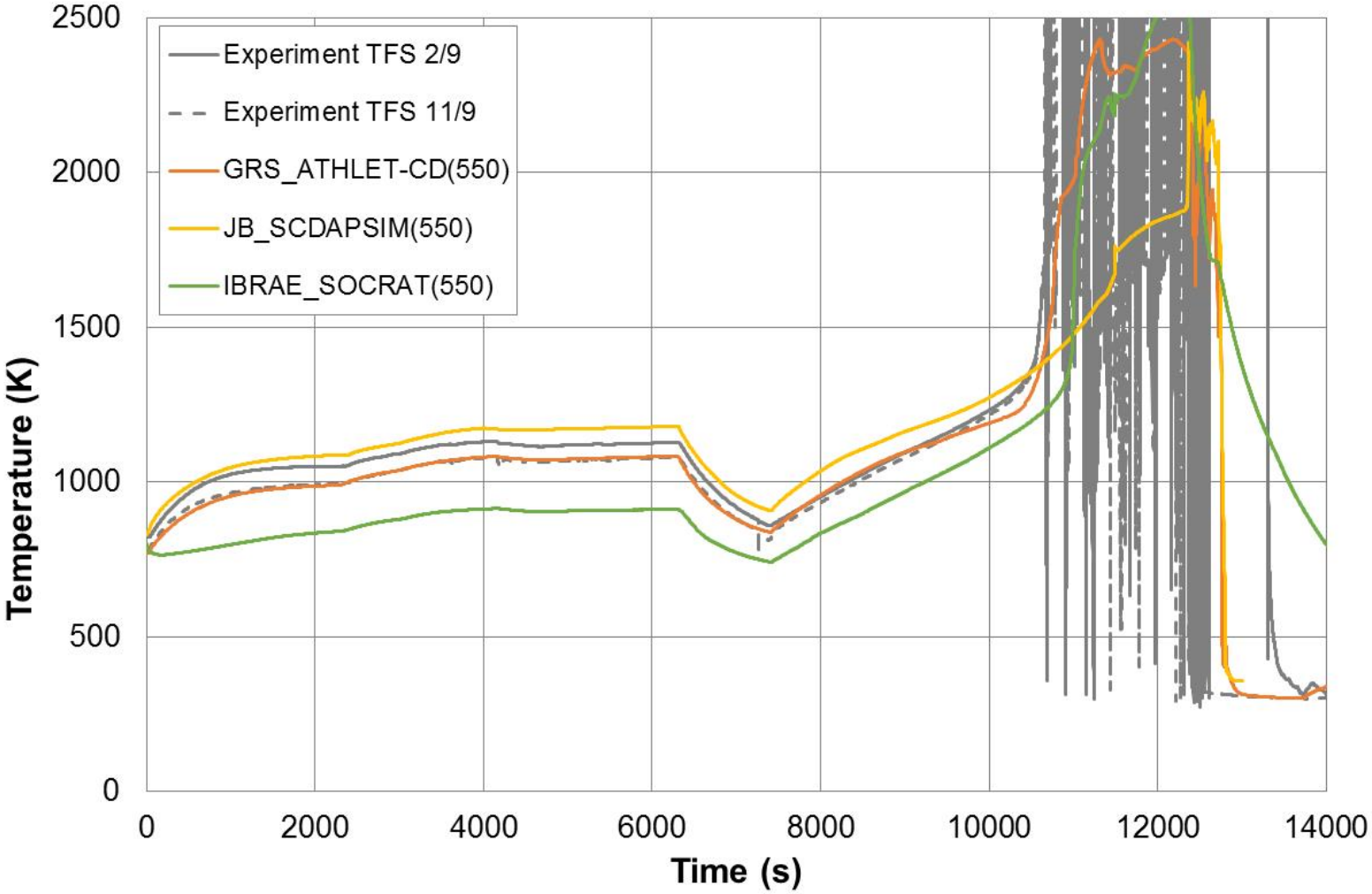
Results of post-test simulations
- Temperatures (I) -

- Temperatures at 350 mm



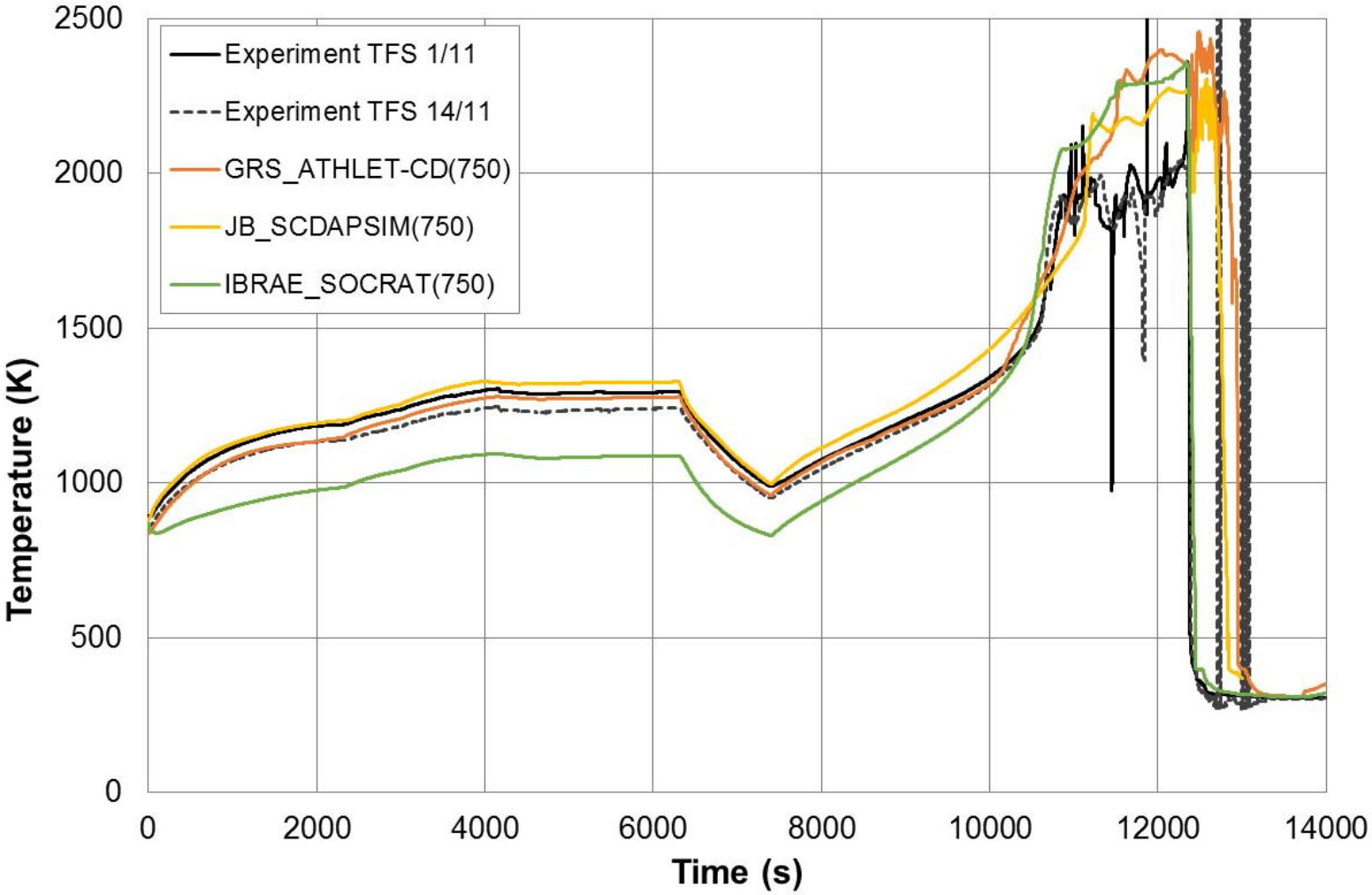
Results of post-test simulations
- Temperatures (II) -

- Temperatures at 550 mm



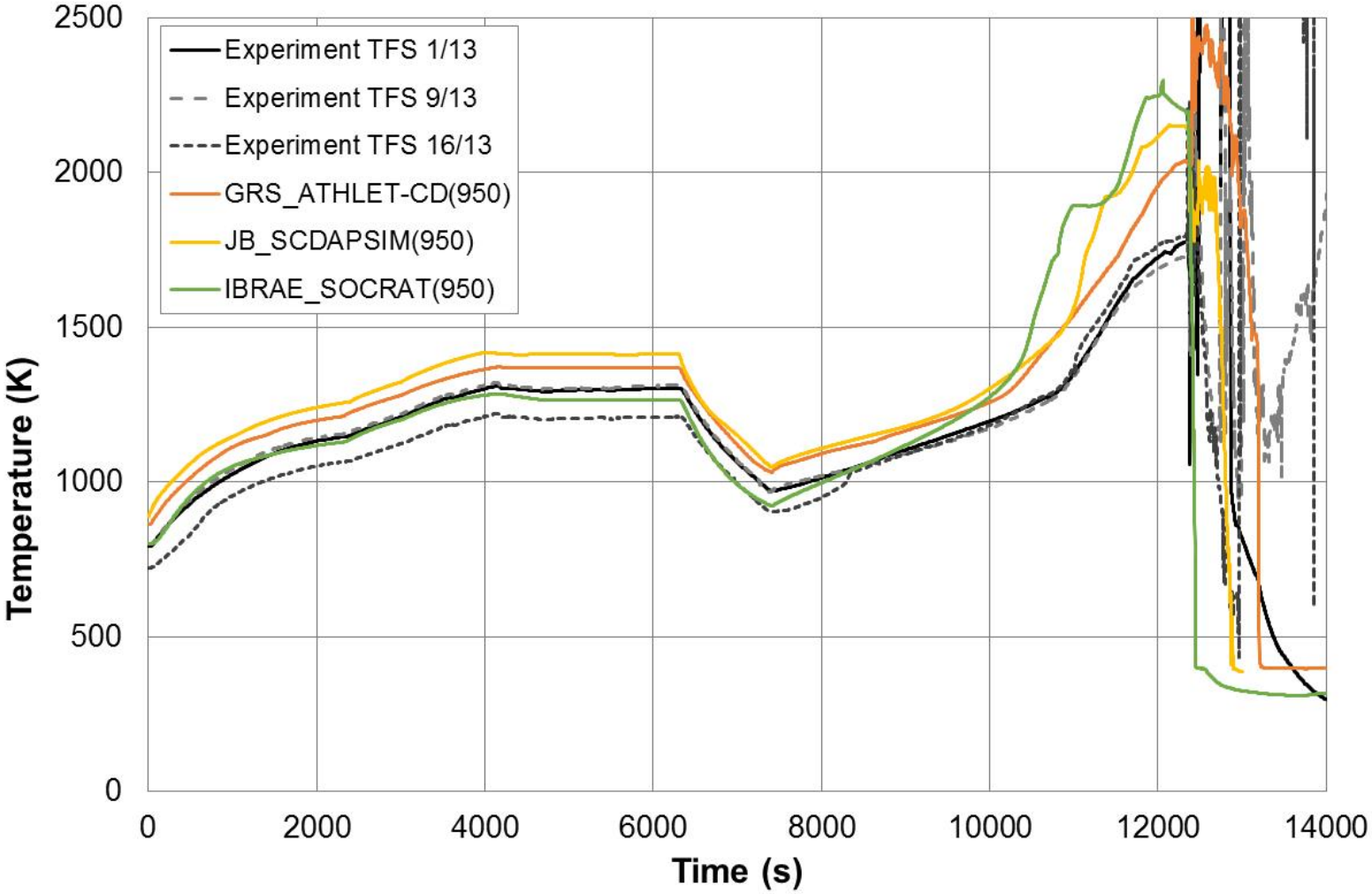
Results of post-test simulations
- Temperatures (III) -

- Temperatures at 750 mm



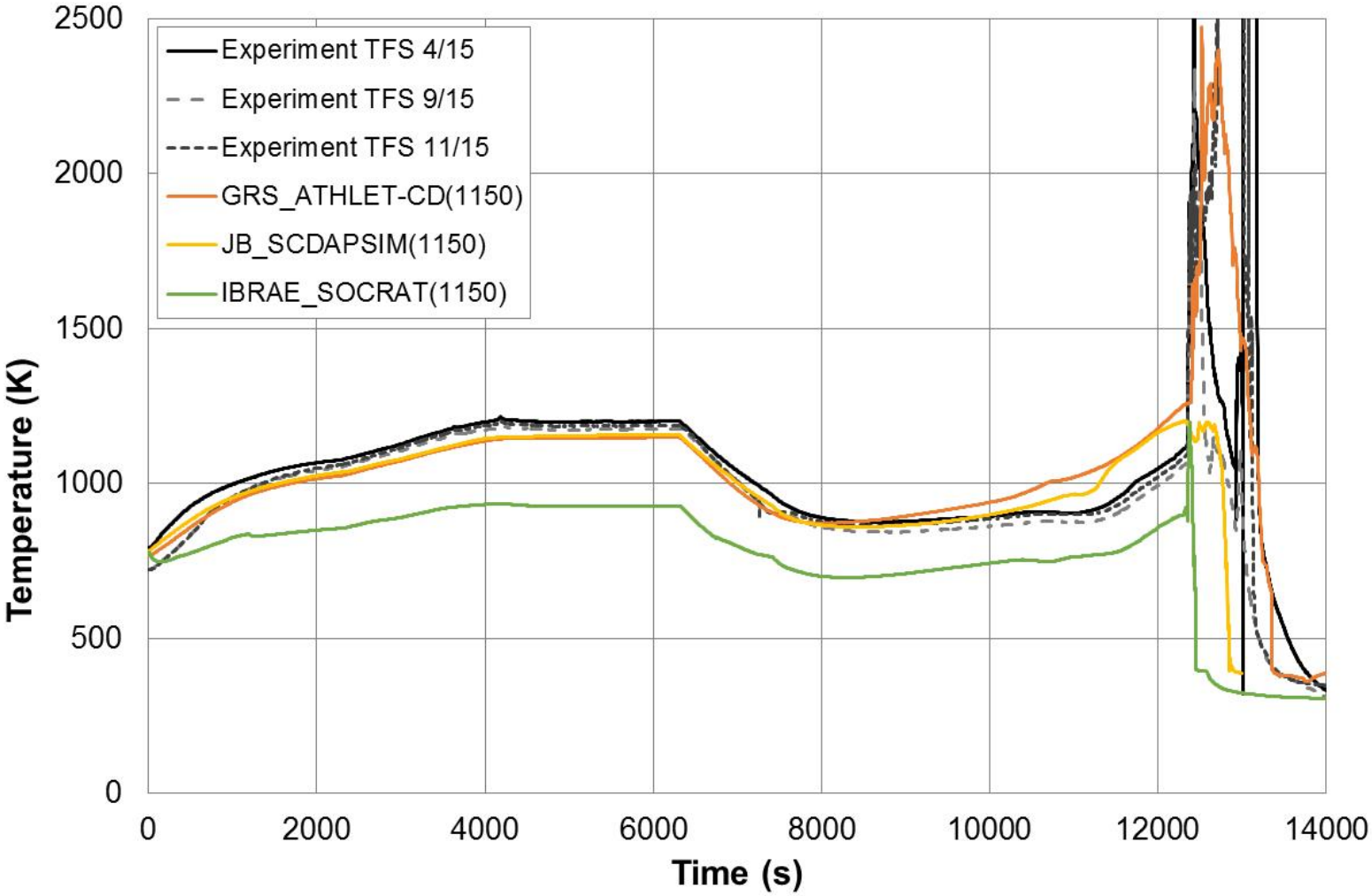
Results of post-test simulations
- Temperatures (IV) -

- Temperatures at 950 mm

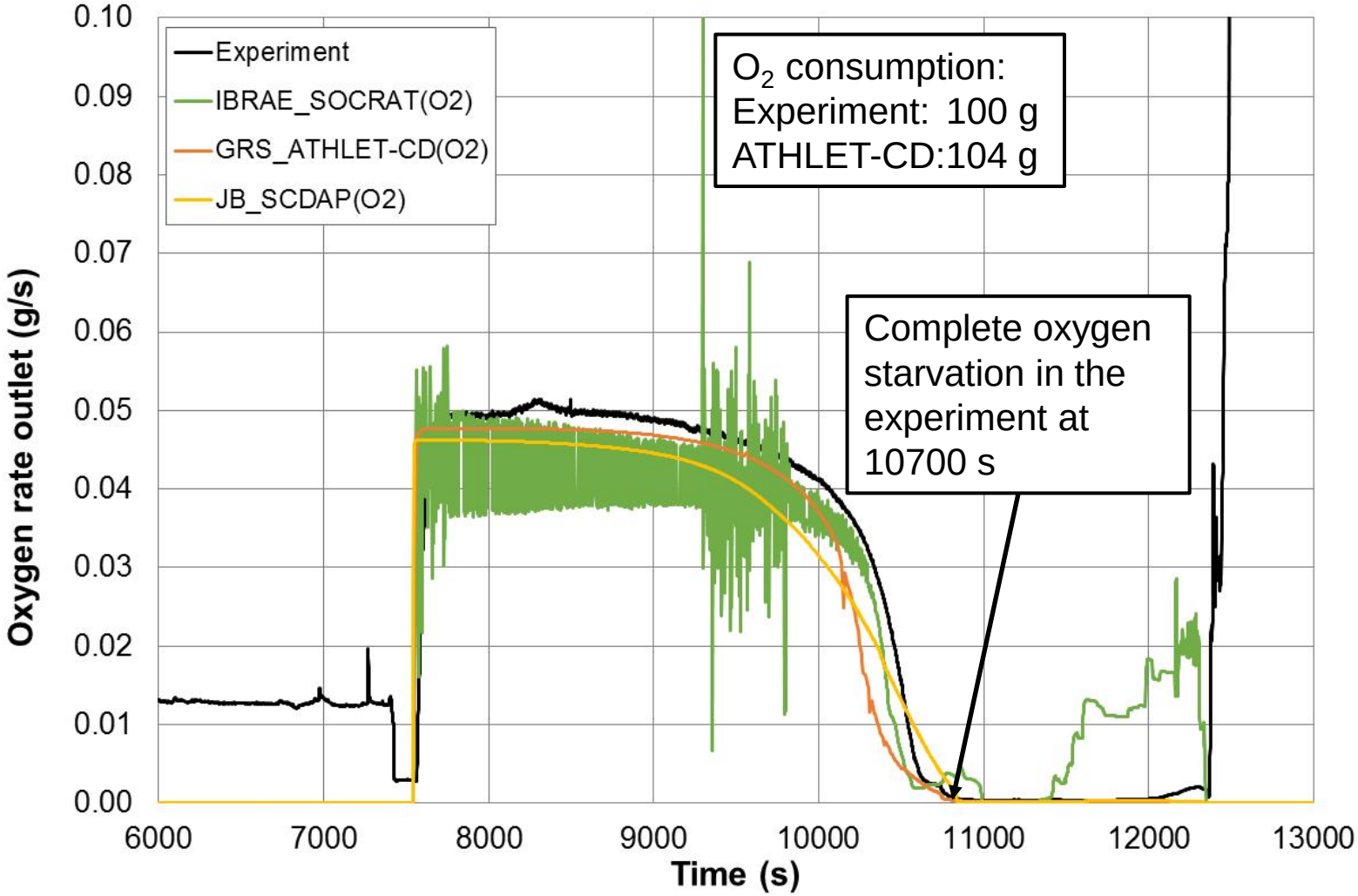


Results of post-test simulations
- Temperatures (V) -

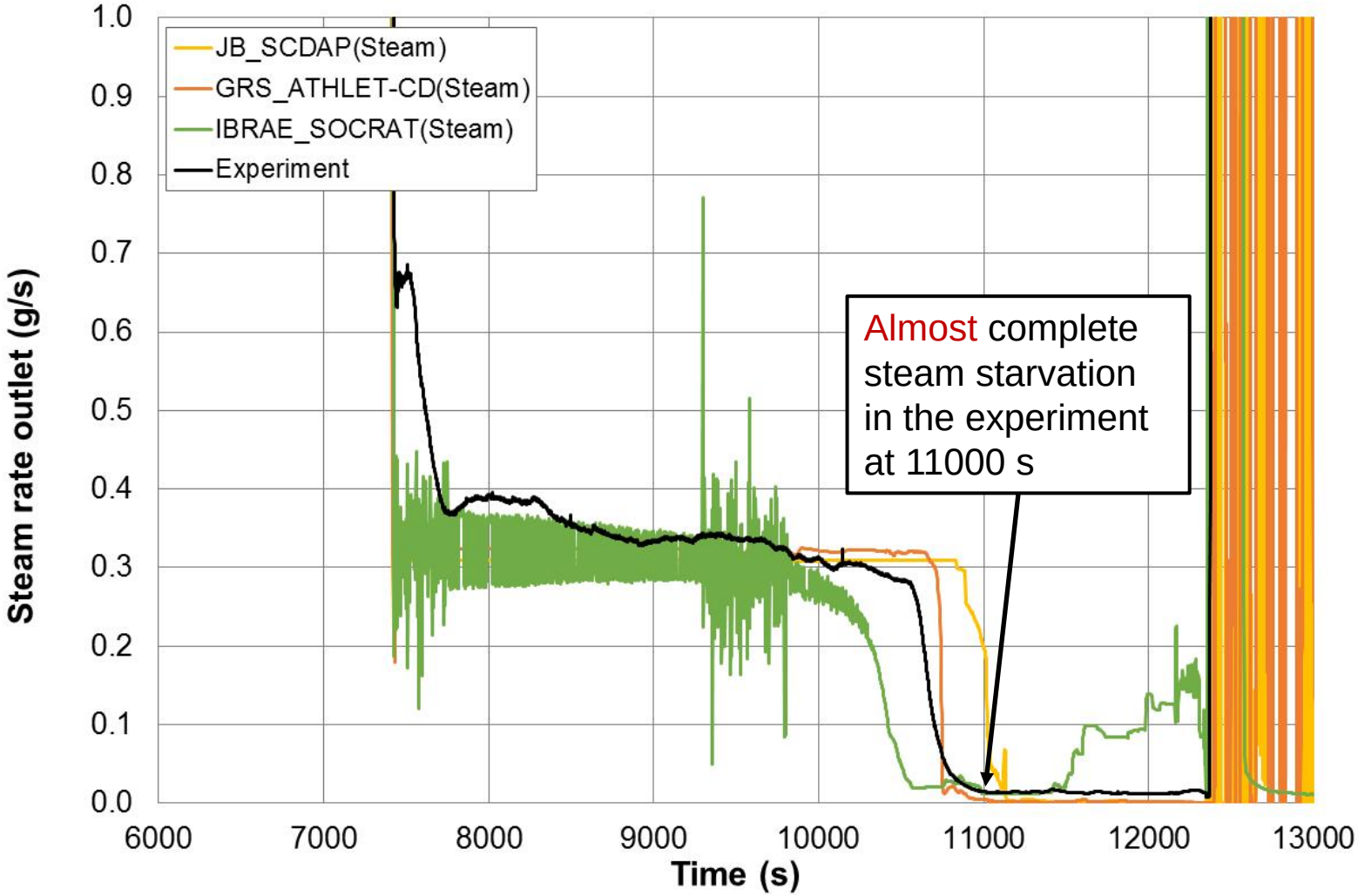
- Temperatures at 1150 mm



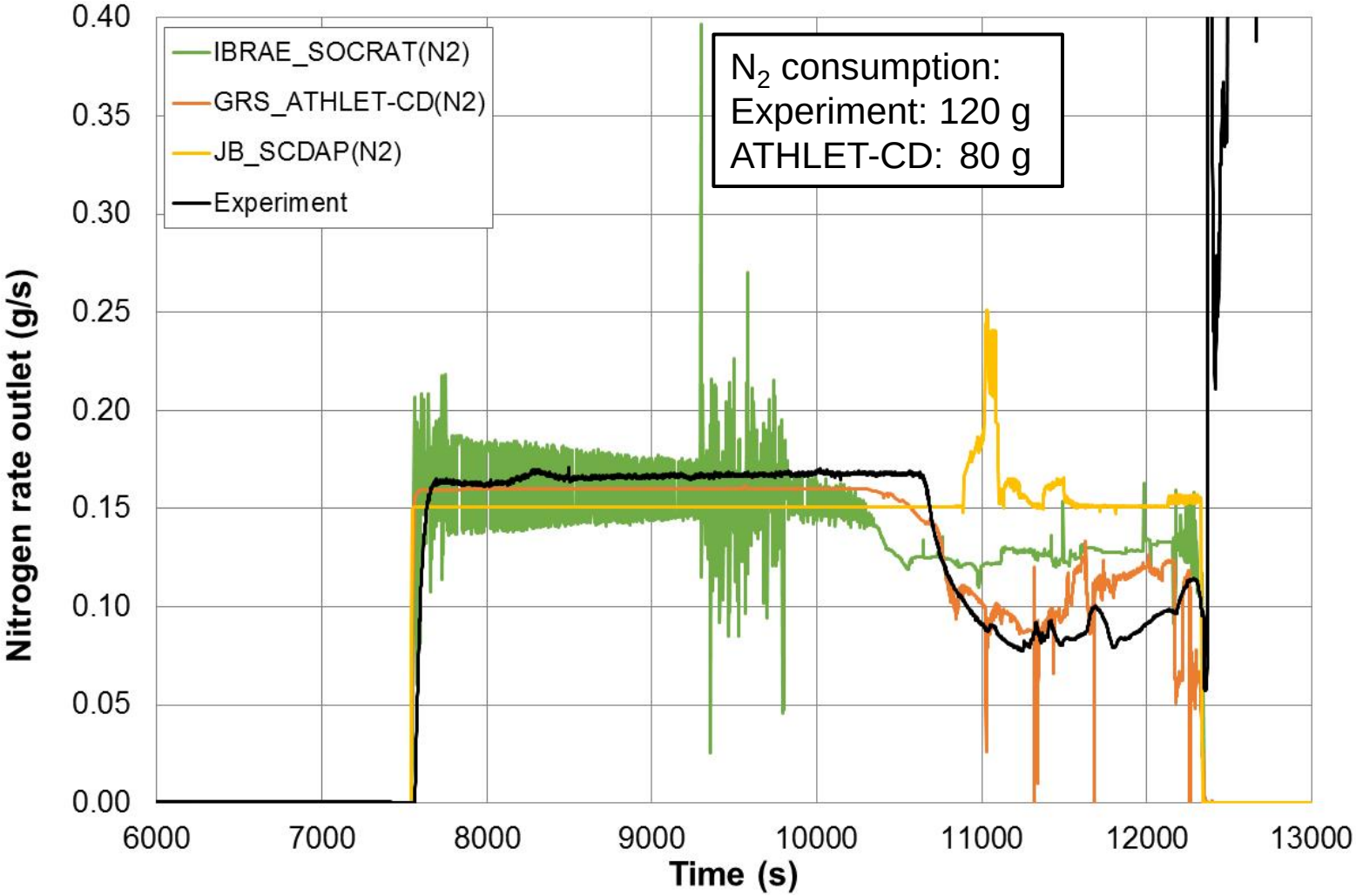
Results of post-test simulations
- Oxygen flow rate at outlet -



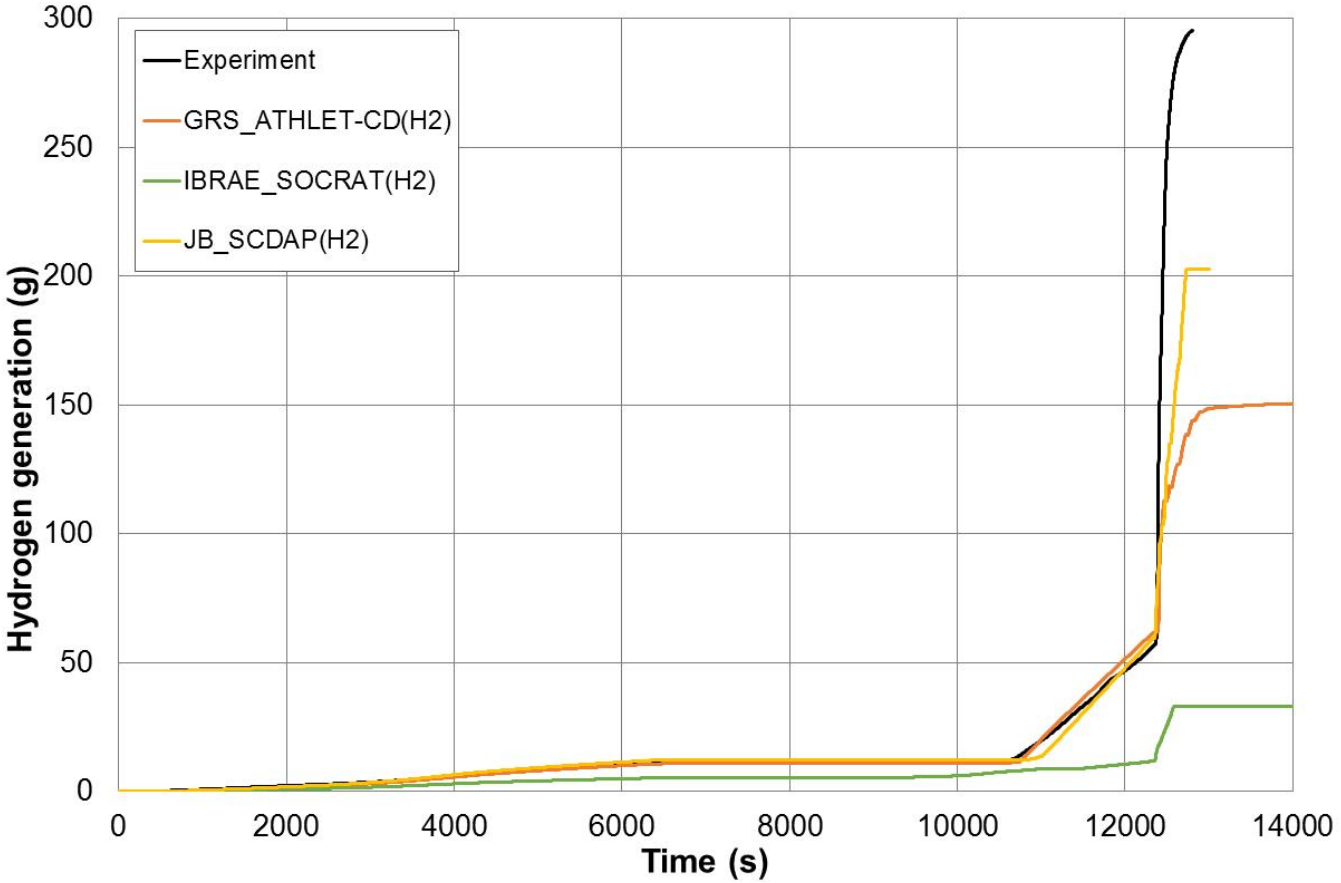
Results of post-test simulations
- Steam flow rate at outlet -



Results of post-test simulations
- Nitrogen flow rate at outlet -



Results of post-test simulations
- Hydrogen Generation -



		Experiment	ATHLET-CD	SCDAPSim	SOCRAT
Total H_2 generation (g)	end of pre-oxidation	11.5	10.5	12.3	5.2
	end of reflood		151.0	202.7	33.0

Main findings

- In general, all three codes predict the experimental behaviour
- Oxygen and steam starvation is calculated in all simulations
- Lowest elevation of O_2 starvation is much lower for ATHLET-CD (150 mm) compared to SCDAPSim (650 mm) and SOCRAT (850 mm)
- Steam and nitrogen consumption in parallel calculated by ATHLET-CD and SOCRAT
- No dedicated nitrogen consumption model for SCDAPSim
- The hydrogen generation or release during quenching is underestimated by all codes
  - Final experimental quantification for each component is necessary to evaluate the simulation results
- The post-test benchmark will be continued, additional simulations with other codes

Preliminary Interpretation of QUENCH-18 using SCDAPSim/mod3.5/da

Jon Birchley

A preliminary analysis of QUENCH-18 is performed with SCDAPSim/mod3.5/da which contains the PSI-developed model for oxidation in the presence of nitrogen. The simulation follows on from pre-test calculations using the same code and input model. The starting point for the post-test calculations differs from the pre-test only in respect of using the actual boundary conditions.

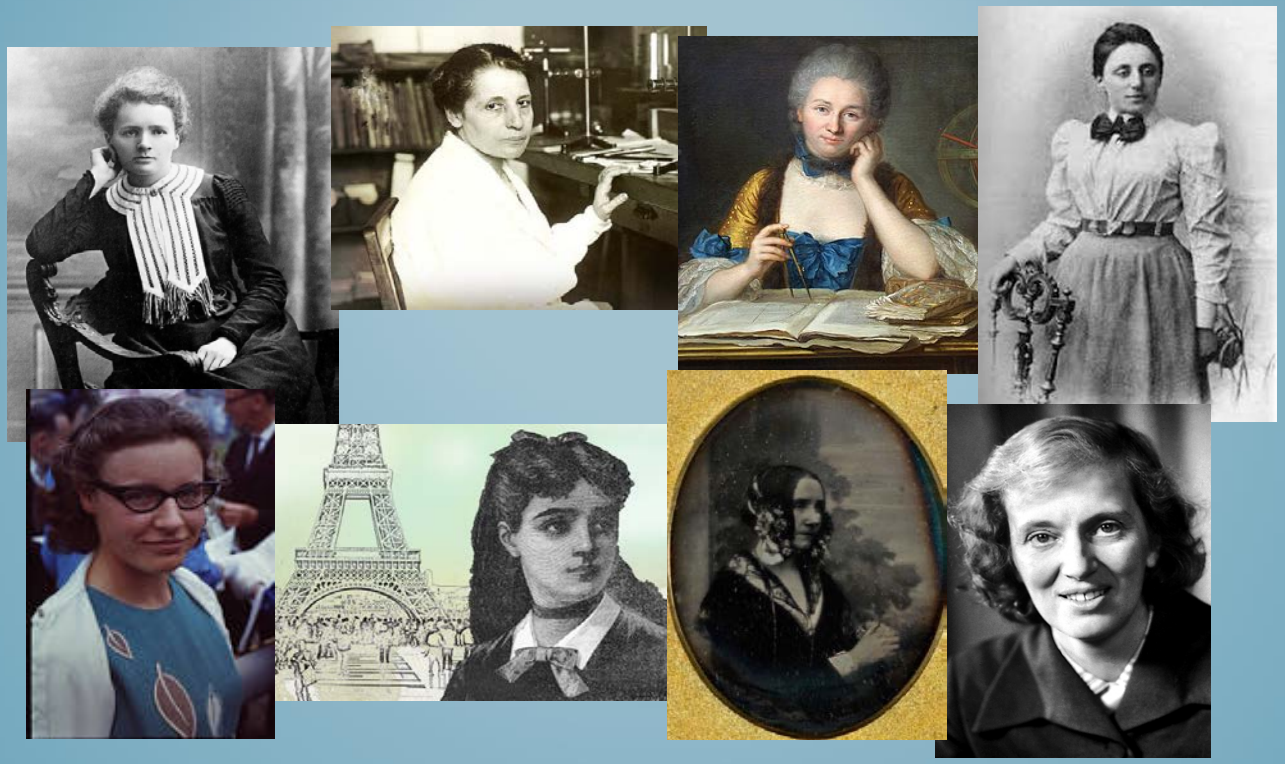
Comparisons with experiment enable several aspects of the experiment to be studied. Alternative treatments of air oxidation investigate the effects of low oxygen concentration on its consumption rate, and demonstrate the influence of nitrogen both when present and continuing afterwards. Sensitivity to the steam oxidation correlation was also examined.

Concerning degradation, alternative assumptions on failure of the oxide crust indicate how the exposure of relocated metallic melt can enhance the oxidation excursion during reflood. Some modelling and knowledge limitations are identified, particularly regarding oxidation in steam-air mixtures, the roles of nitrogen and zirconium nitride as chemically active species.

Several observed features of the experiment are as yet unresolved. Simulations suggest that a breach in the shroud hindered the reflood progression. The bundle state at reflood initiation is also currently unknown to the present author, but it may well have already been damaged by then, with further impact on the refilling and quench progression. Interpretation is therefore provisional, pending more information on the facility state.


KIT

“Science is not a set of rules to tell us how machines work. Science is about uncovering the reality behind appearances.”



Interpretative Analysis of QUENCH-18 using SCDAPSim/3.5/psi



24th International QUENCH Workshop
Karlsruhe Institute of Technology
November, 2018

Jonathan Birchley (Consultant)

Outline

- Code and input models
  - evolution of models
  - air oxidation model
  - metallic melt release/oxidation
  - cases simulated
- Analysis of pre-oxidation
  - effect of steam oxidation models
- Simulation of air ingress phase
  - effect of N2-accelerated oxidation models
- Analysis of reflood
  - effect of oxidation models
  - effect of bundle assumptions
- Conclusions

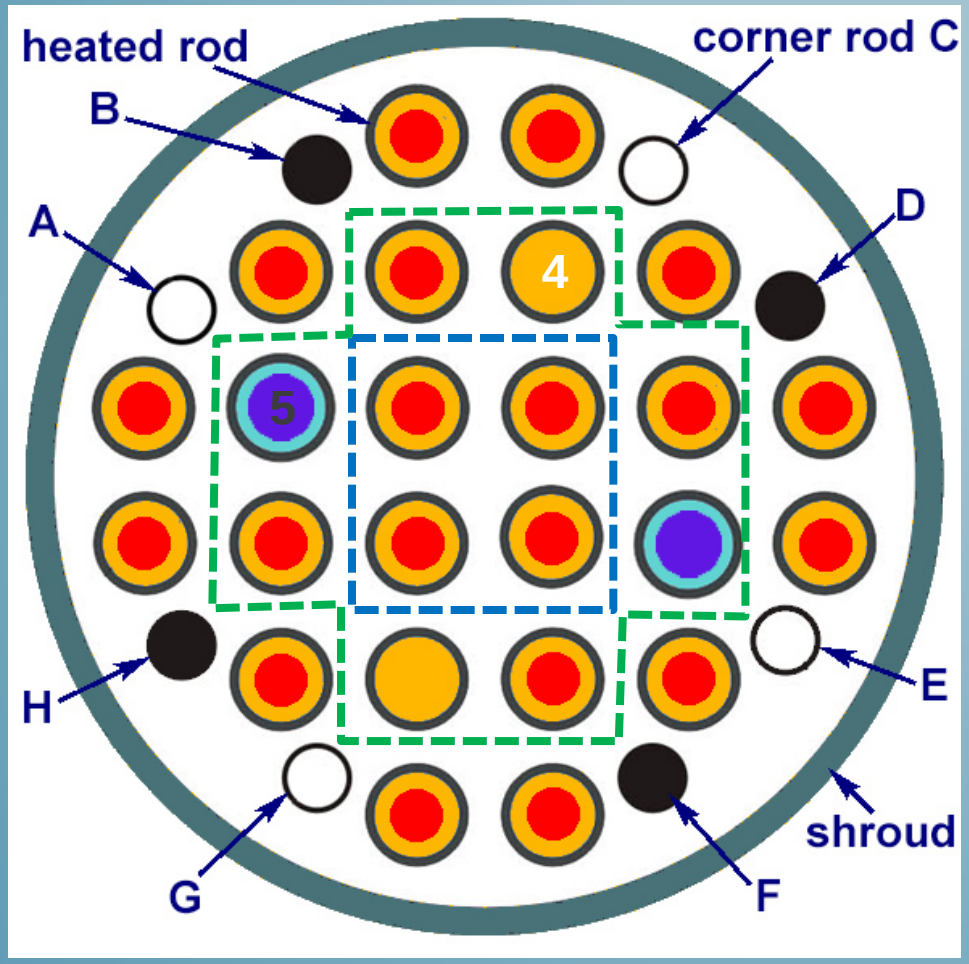
Code and input models

- Evolution of code and QUENCH-air model
- PSI oxidation model
- Effect of low [O2] on oxidation rate
- Oxidation in steam+O2 mixture
- Melt oxidation
- Cases simulated

Code and input model evolution

- SCDAPSim/mod3.5/da/psi
  - air oxidation model developed/assessed by PSI, implemented by ISS (L. Siefkin)
  - O2 consumed before steam, N2 acceleration
  - special version with reduced kinetics at low [O2] (…./da/psi/lfm)
- Input based on QUENCH-10/-16 benchmark model
  - inclusion of SIC absorber and unheated pressurised rods
  - adapted for QUENCH-15 layout (4sim, 4sim + 2pres + 2SIC, 12sim)
  - used in pre-test planning and pre-benchmark ….
  - …. and starting model post-test with experimental boundary conditions
  - default steam oxidation kinetics (Cathcart-Pawel/Urbanic-Heidrick)
  - PSI default air oxidation kinetics (Uetsuka-Hoffman-Birchley)
- Modified models (base case and variants)
  - boundary conditions adjusted for reflood in light of events
  - alternative oxidation kinetics, suppression of metallic melt relocation

Bundle configuration / SCDAP components



Zone 1

1: Central heater rods (4)

Zone 2

2: Inner ring heater rods (4)

4: Unheated rods (2)

6: SIC rods (2)

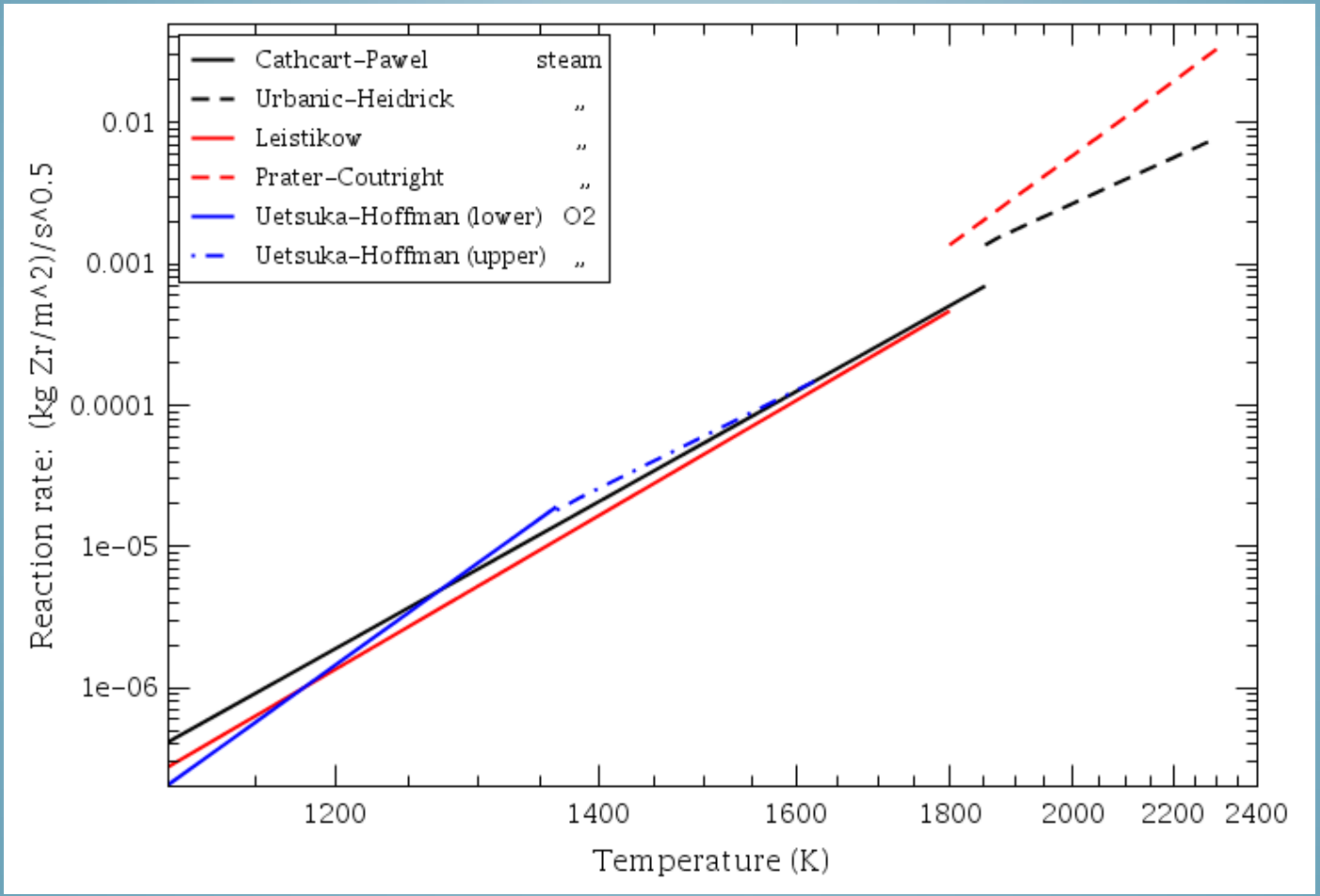
Zone 3

3: Outer ring heater rods (12)

5: Corner rods (8)

7: Shroud (1)

Steam and oxygen kinetics



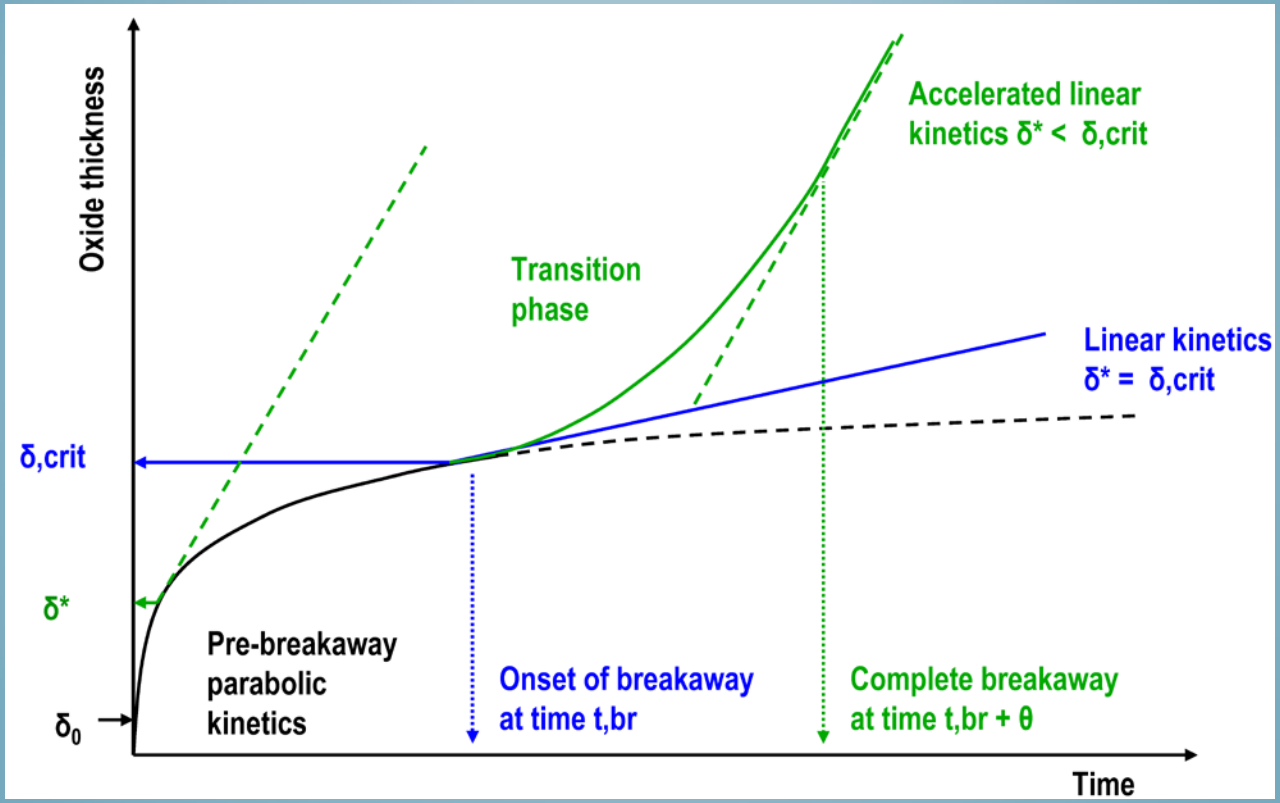
Parabolic correlations for steam and oxygen used in analysis

Moderate different between correlations below 1800 K

Minor difference between CP and Ls

Large difference between UH and PC

PSI oxidation model: transition to linear kinetics



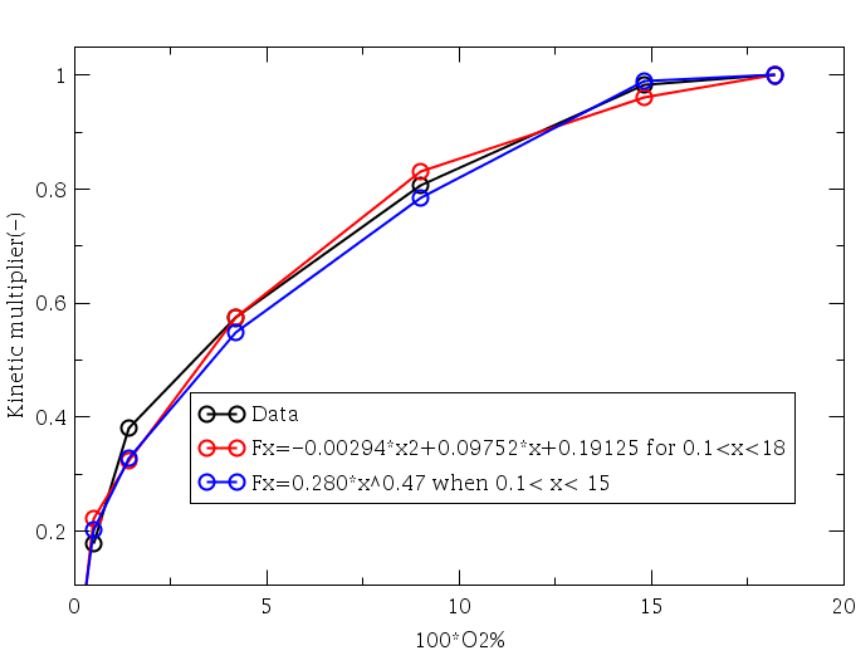
Model for breakaway oxidation in steam and acceleration due to N2

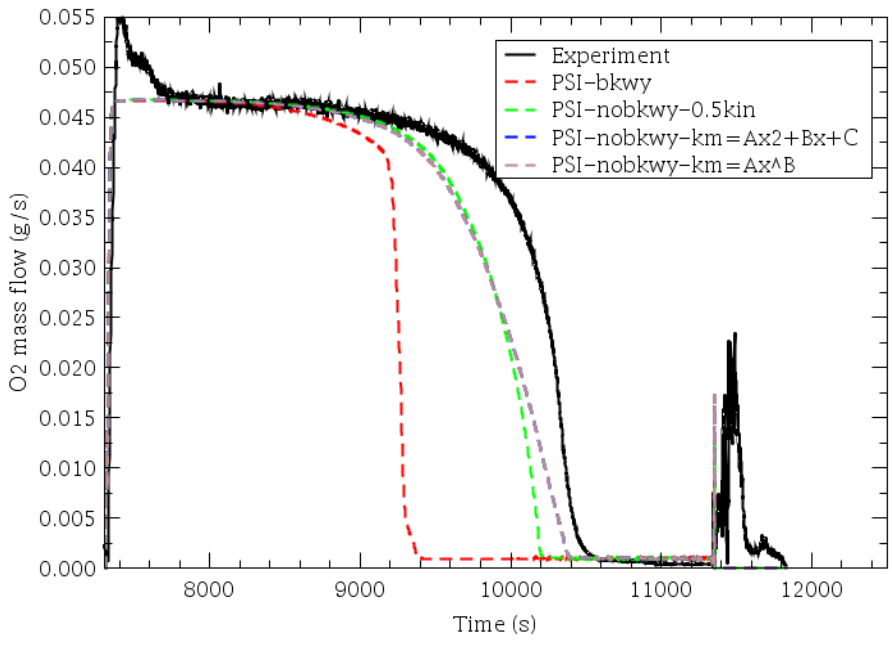
N2-acceleration treated macroscopically like breakaway

Even low [N2] can strongly enhance the kinetics.

The model treats N2 only as a catalyst, which is inapplicable when significant nitriding occurs.

Effect of low [O_2] on oxidation rate: SE + QUENCH-16





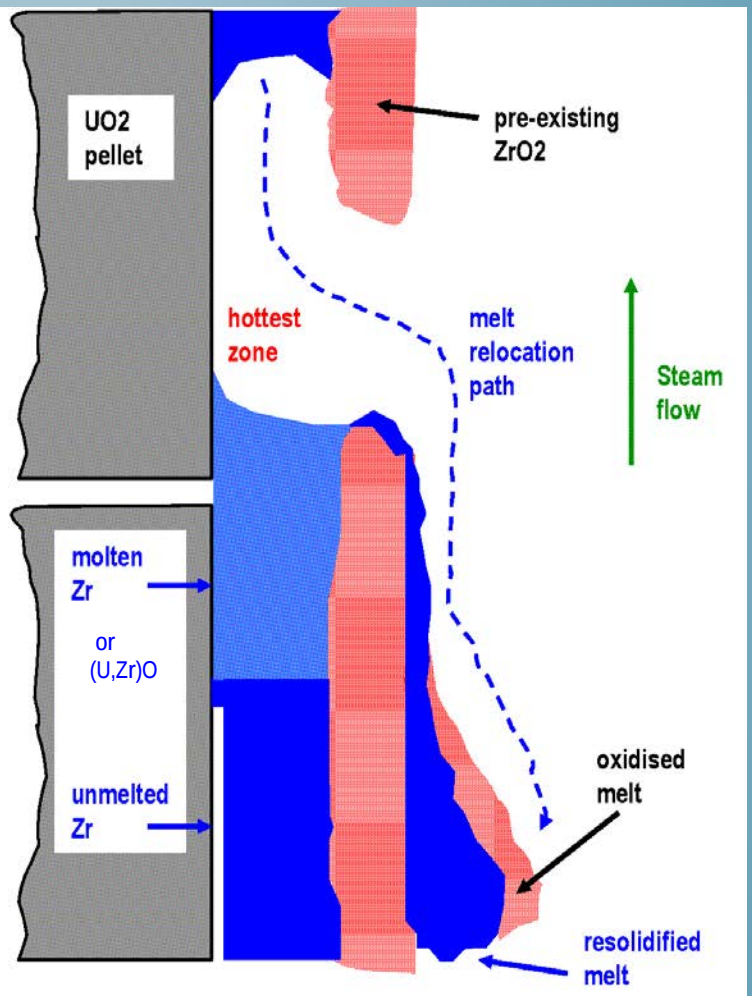
Oxidation experiments with Air+Ar mixtures demonstrate slower kinetics as the air concentration is reduced

An empirical fit to the data was used in a trial version of the PSI air oxidation model implemented in SCDAPSim/m35

Used in a comparison with Q-16 air phase

Melt oxidation

- Molten cladding may be held in place by an undamaged oxide layer
- If the layer is broken or eroded the molten metal breaks out and "candles" downward, typically resolidifying
- There would not at first be an oxide layer to limit the oxidation
- The process can repeat
- Modelling is difficult
  - model for intact cladding may be applied
  - or no modelling at all
  - **in short term** enhanced rate parabolic model using estimated area of exposed surface, with repeated breakout and reforming
  - **in longer term** oxygen diffusion from surface into bulk of unoxidised metallic



Codes typically use a criterion for failure of the oxide scale
MELCOR and recent versions of SCDAP attempt to represent the oxidation

SCDAP adopts a surface renewal principle where the oxide layer repeatedly forms and breaks

Cases simulated

1. *SCDAPSim/mod3.5/da/psi (CP/UH correlation; oxide breach at 2200 K, reduced injection + Ar flow due to shroud breach)*
2. *As (1) but breakaway and N2 accelerated kinetics switched off*
3. *SCDAPSim/mod3.5/da/psi/lfm (as (1) but kinetics reduced at low [O2])*
4. *As (3) but Ls/PC steam correlation instead of CP/UH (Benchmark)*

5. *As (3) but no effect of shroud breach*
6. *As (3) but oxide breach at 2600 K to suppress melt relocation*
7. *As (3) but postulated steam inflow during reflood*
8. *As (4) but postulated steam inflow during reflood*

Data

Results displayed in groups over three phases

1, 4 data:	*pre-oxidation*	*) steam oxidation*
1, 2, 3, 4 data:	*air/steam, reflood*	*) air/steam oxidation*
5, 6, 7, 8 data:	*reflood*	

Analysis of pre-oxidation

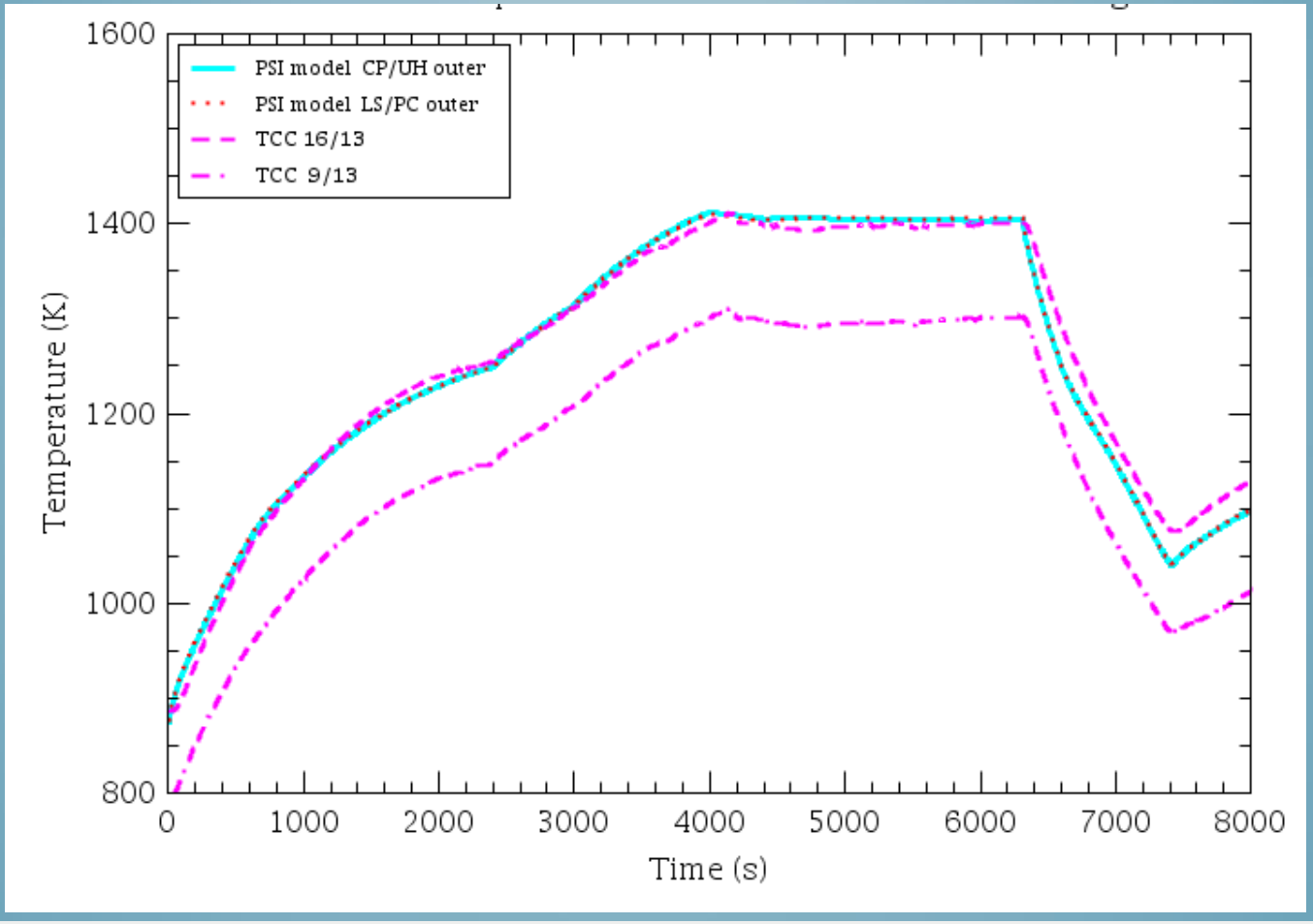
- Cases and signature variables
- Effect of oxidation models

Cases and signature values

- Two distinct simulations
  - nominal case using same options as in pre-test
    - only difference is boundary conditions
    - same external resistance (3.6 mΩ/rod)
    - CPl/UH steam oxidation model (default)
    - Ls/PC correlation for steam oxidation

- Look at two signature variables
  - rod centreline temperature at 950 mm
    - limited bundle temperature data through reflood
  - hydrogen generated

Pre-oxidation: centreline temperature at 950mm



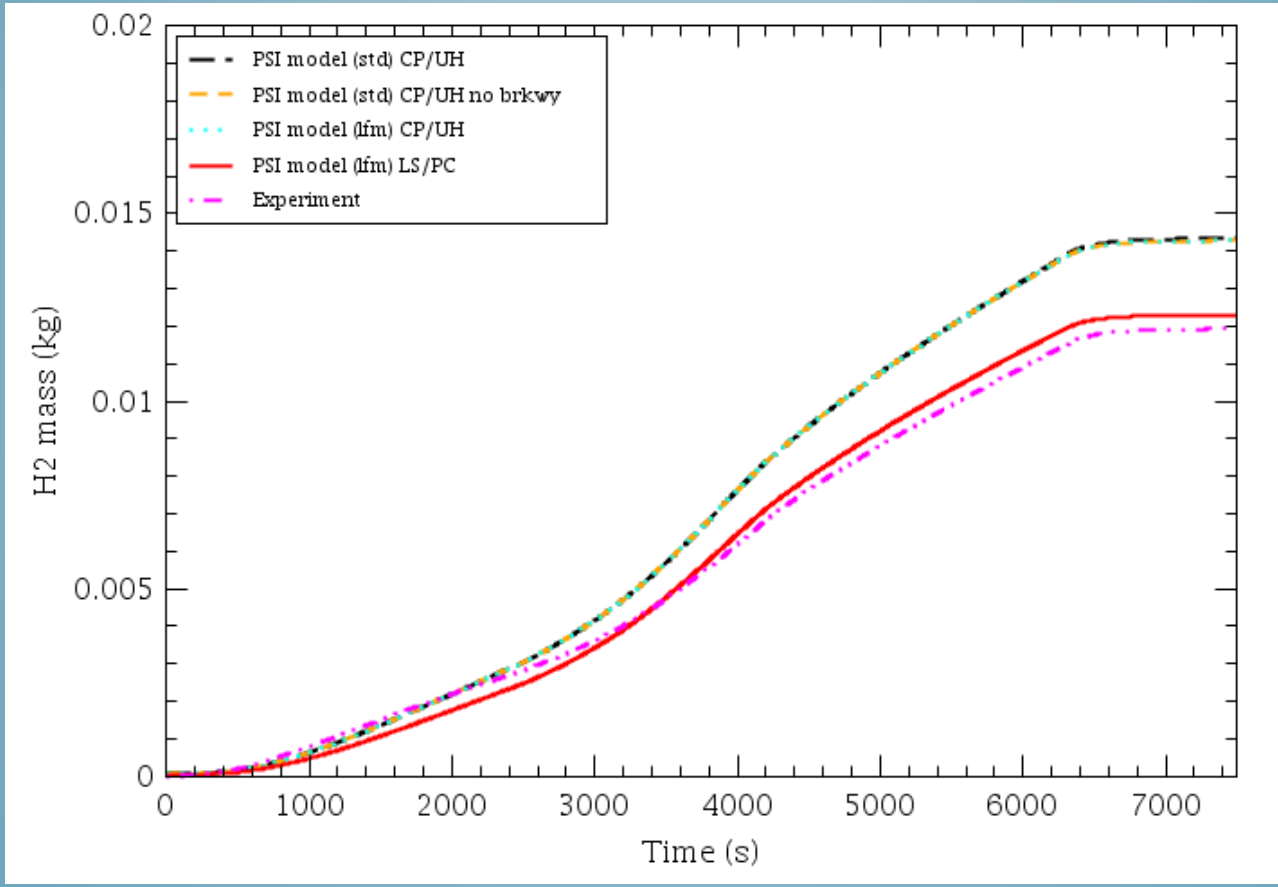
950 mm elevation as “marker cell”

Faithful replication of temporal trends

No noticeable difference between CP and Leistikow

Surprising difference between (equivalent) rods 9, 16

Pre-oxidation: hydrogen generated



Faithful replication of temporal trend

Confirmation that all CP/UH cases are the same with 3 different air models

Leistikow gives improved agreement – reflects better temperature dependence of kinetics?

Analysis of air/steam phase

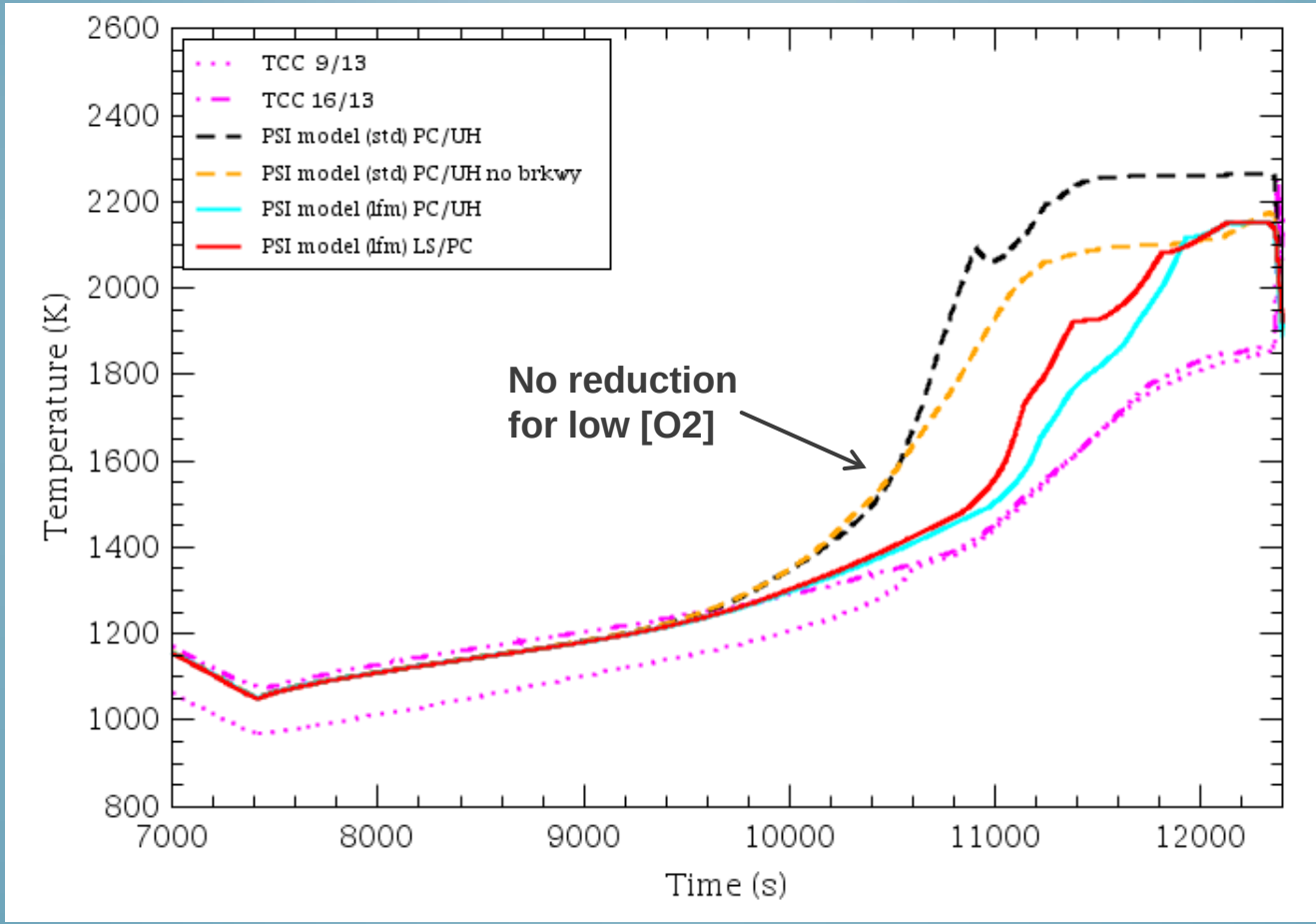
- Cases and signature variables
- Effect of oxidation models
- Effect of steam+O2 mixture
- Summary of pre-reflood

Cases and signature variables

- Four calculations, same as for pre-oxidation
  - default steam oxidation (CP/UH) with 3 different treatments of air oxidation
    - "standard" PSI model for air with N2-acceleration on
    - "standard" PSI model for air N2-acceleration turned off
    - "modified" PSI model: reduced kinetics at low [O2], N2-acceleration on
  - "Ls/PC correlation for steam oxidation
    - "modified" PSI model N2-acceleration on, reduced kinetics at low [O2]

- Look at signature variables
  - rod centreline temperature at 950 mm
  - H2 generated
  - O2 and steam consumption

Air phase: centreline temperature at 950mm

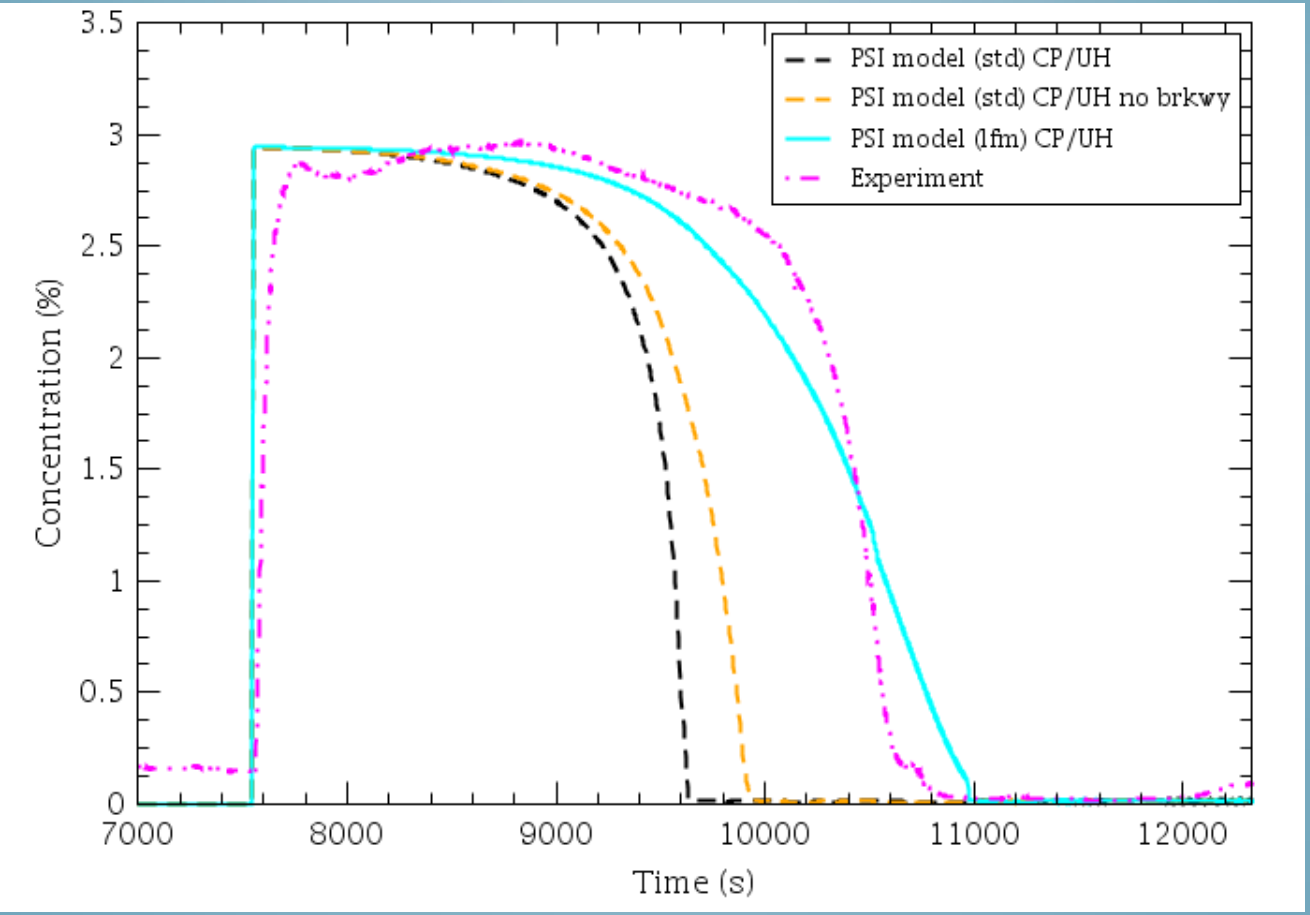


Early agreement but escalation overestimated in all cases

Smaller escalation without N2-acceleration or with reduction at low [O2]

Difference between experimental inner/outer rings disappears

Air phase: O2 concentration at bundle exit

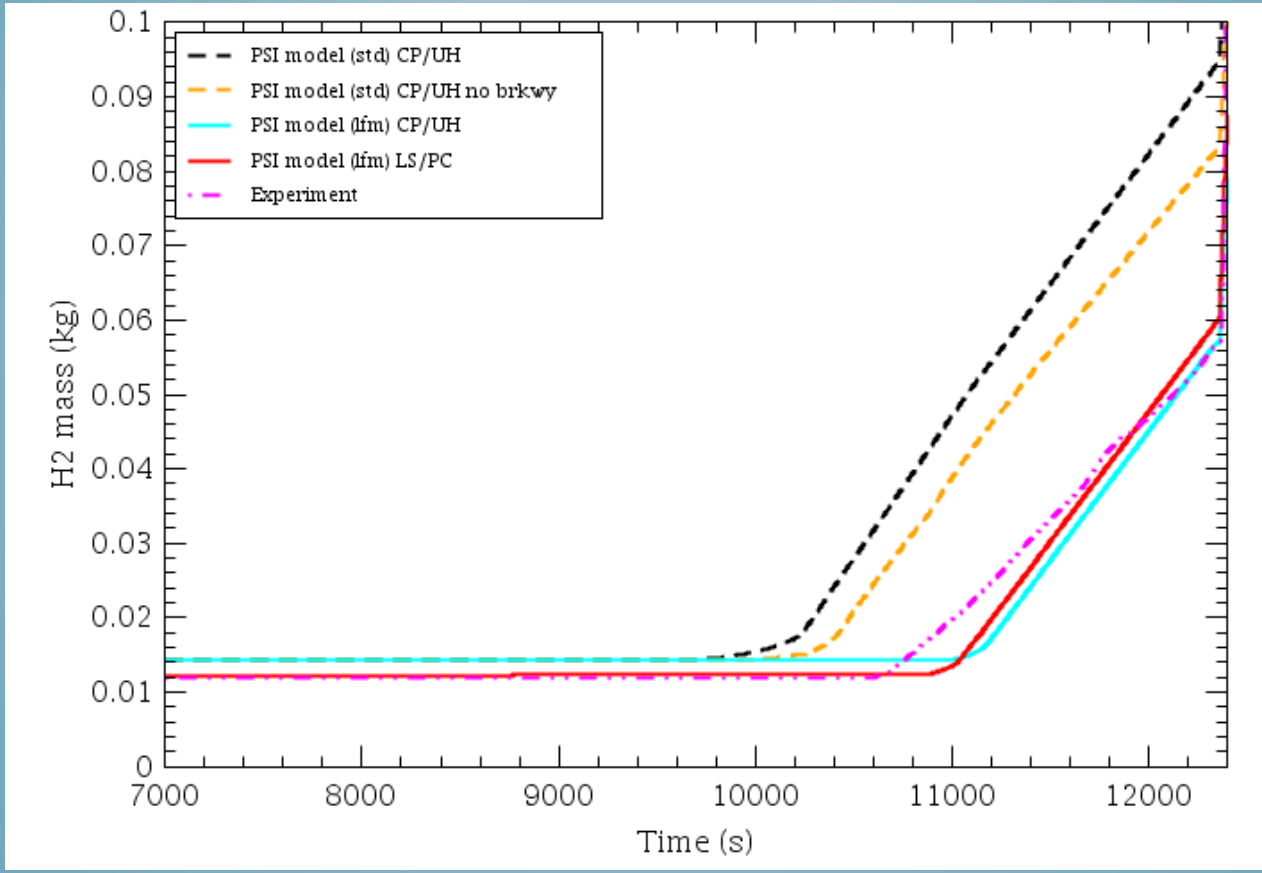


O2 consumption rate overestimated by PSI/std but slightly underestimate by PSI/lfm

Reduction factor for low [O2] night be incorrect for air+steam

Rapid O2 consumption coincides with onset of escalation, both data and simulations

Air phase: hydrogen generated



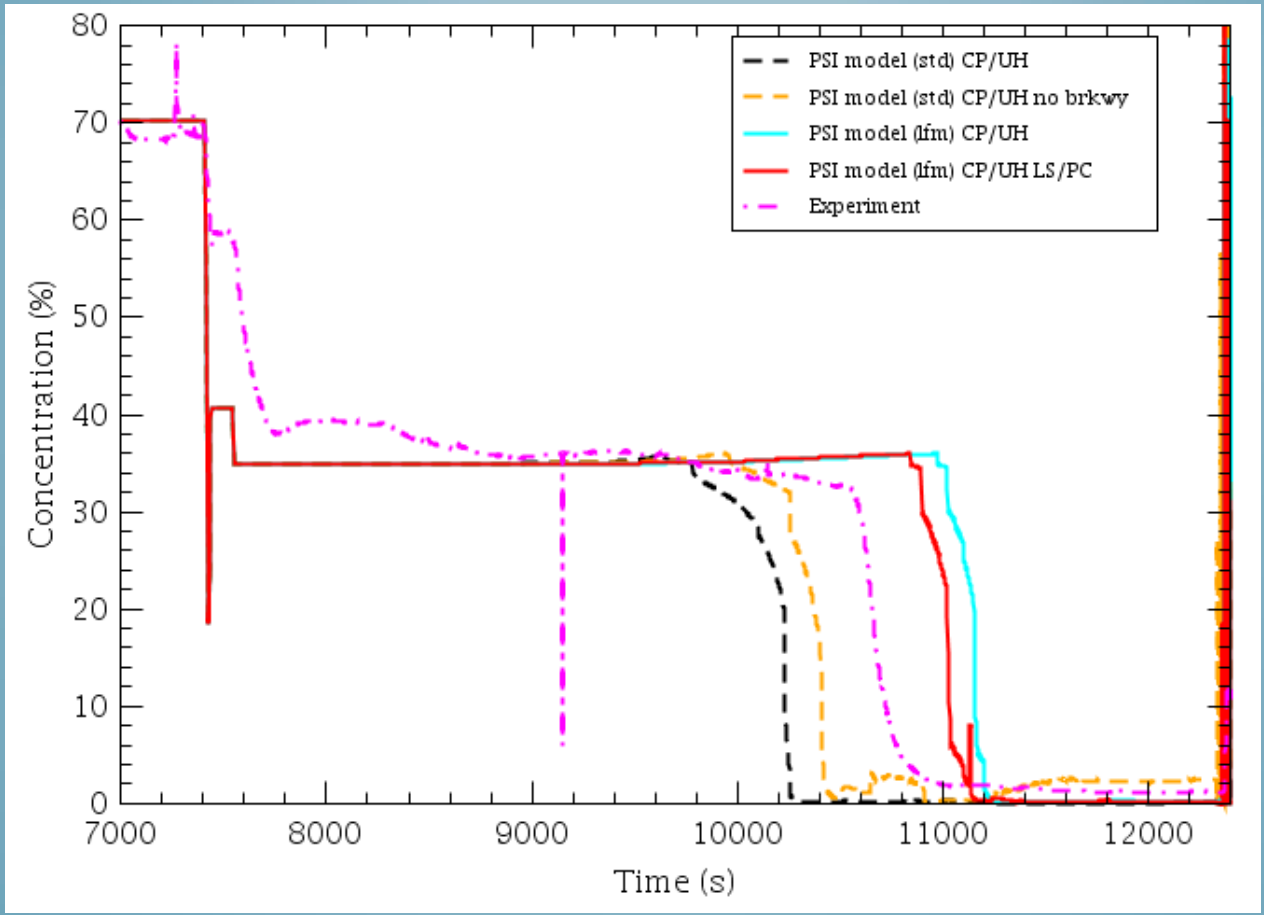
After O2 consumed, rapid transition to total steam consumption

Experiment shows H2 less than should be from total steam consumption

Minor effect of N2 acceleration on timing

PSI/lfm+L/PC gives good agreement for H2 pre-reflood: regard as Best Estimate case

Air phase: steam concentration at bundle exit



Slow steam consumption experiment before O2 fully consumed

Increases when all O2 consumed

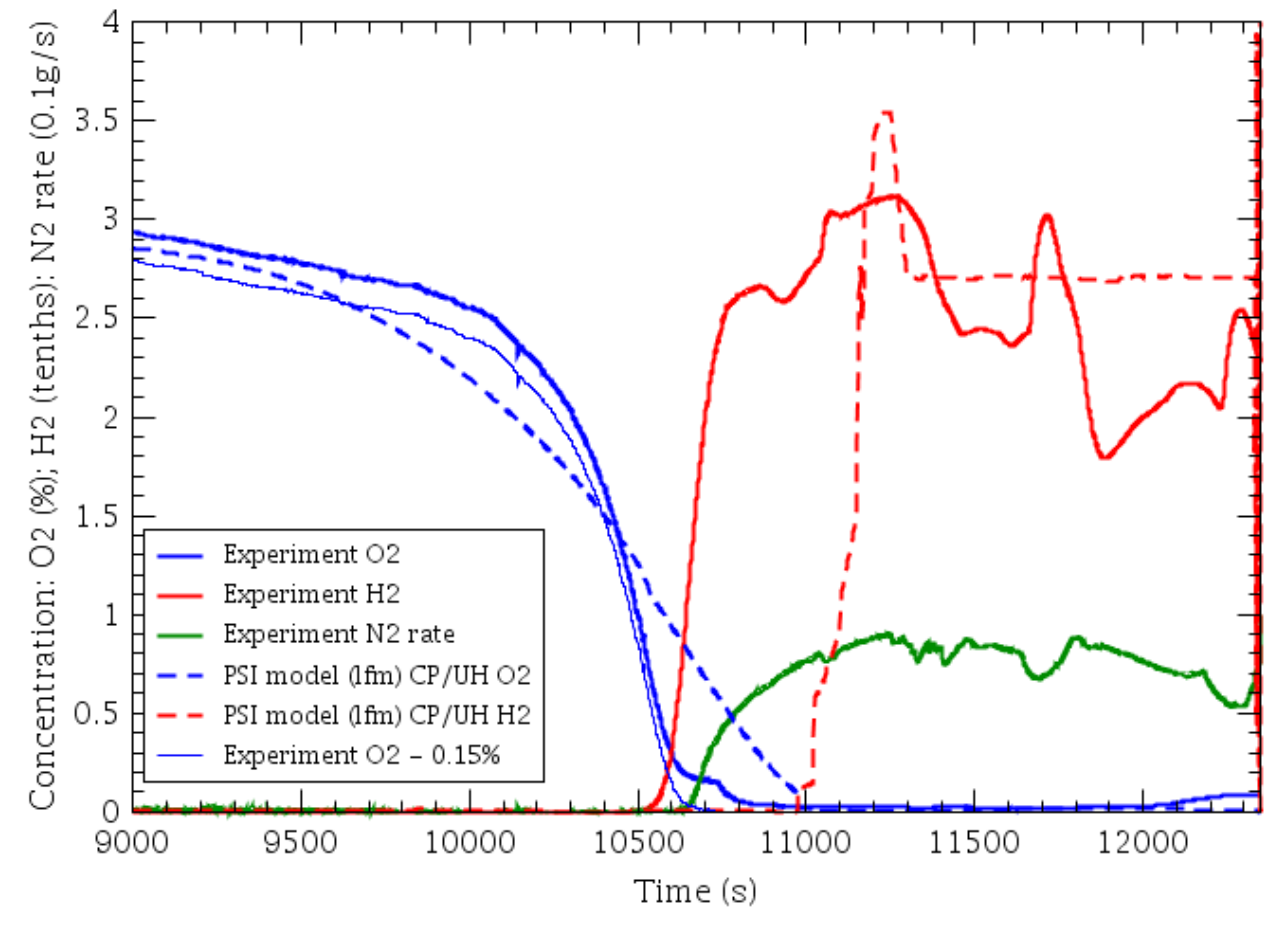
Model assumes steam consumption only when O2 fully consumed

Impact of steam+O2 on oxidation

- In presence of O2, H2 production is not observed in SE tests
  - model assumes no oxidation by steam if O2 present
  - can be justified on basis that H2 and O2 would recombine
  - rates of both oxidation and recombination limited by gas diffusion at low [O_2]
  - empirically derived reduction applied in special version SDCAPSim/3.5psi/lfm
  - even if correct for air+Ar mixtures, it may underestimate rate for steam+air
  - in Q-18 air phase, inlet [O2] and [H2O] are ca. 0.025 and 0.34 respectively
- Model does not consider simultaneous reactions
  - $Zr + 2H_2O \rightarrow ZrO_2 + 2H_2$
  - $Zr + O_2 \rightarrow ZrO_2$
  - $2H_2 + O_2 \rightarrow 2H_2O$

  possibly underestimates O2 consumption rate if steam present

Air phase: overlap in O2 and H2 at exit



Observed overlap between O2 consumption and H2 release not simulated

Conjecture: O2 consumed and H2 produced but not in same place at same time

H2/O2 recombination probably incomplete during early stage of H2 production

N2 consumption reaches ca. 50%; begins just after onset of H2 release

Summary of pre-reflood analysis SKIP?

- Improvement for H2 during pre-oxidation with Ls over CP
  - does not imply Ls is necessarily an improvement
- Difficult to compare in air/steam phase as oxidation was steam-limited
- Early O2 starvation both with/without N2-acceleration, hence a longer steam oxidation time and overestimated pre-reflood H2
  - reduction for low [O2] gave delayed onset of steam consumption
- H2/O2 mixture at exit was not captured
  - would need to represent radial concentration profile
- H2 production inconsistent with inlet steam during air/steam
  - possibly some of the H2 was uptaken in the cladding
  - fortuitous agreement for total H2 production at reflood initiation

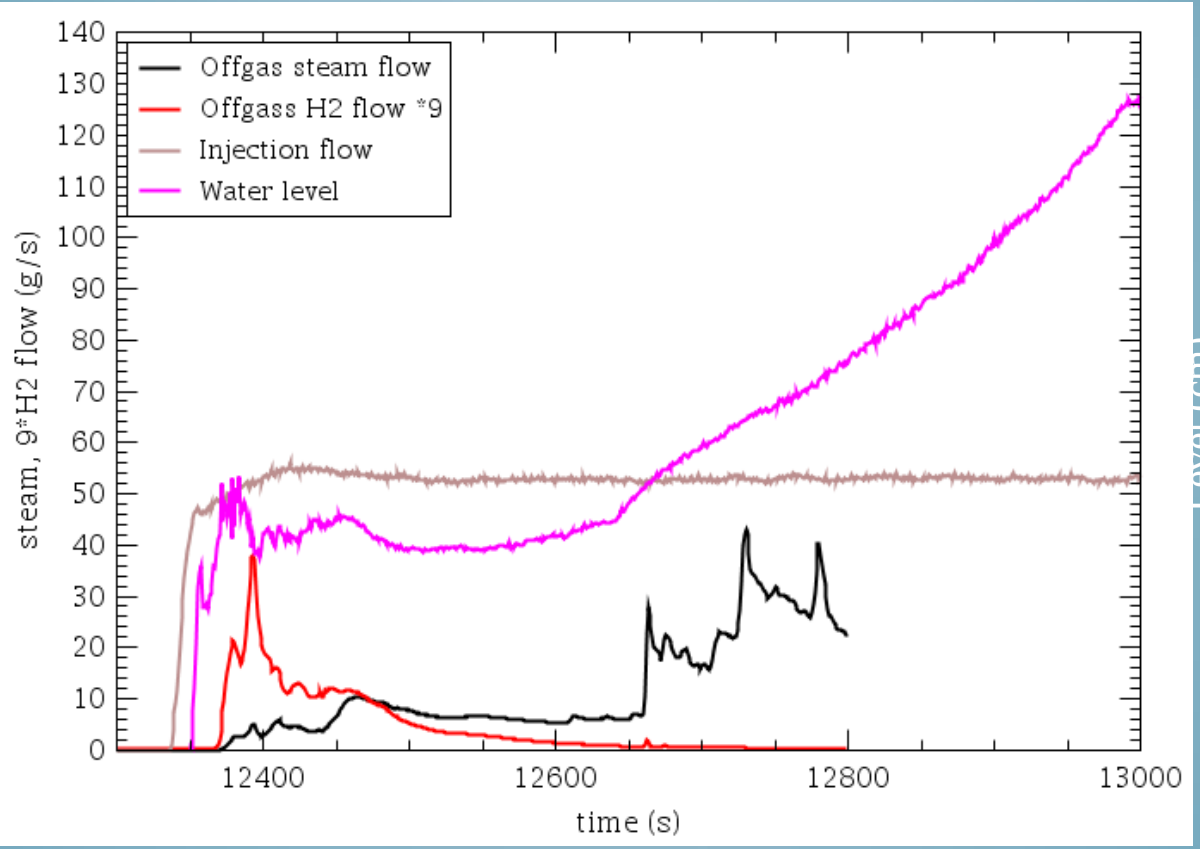
Analysis of reflood

- Cases and signatures variables
- Observed reflood signatures
- Effect of oxidation models
- Effect of alternative bundle assumptions
- Summary of reflood

Cases and signature variables

- We consider effect of the above oxidation modelling ….
- …. and also factors specific to reflooding
  - metallic melt breakout from oxide shell
  - flow of water into and Ar out of shroud breach
  - reasons for rapid early large H2 generation
- We look at signature variables
  - rod temperature at 950 mm
  - hydrogen generated
  - refilling of bundle
  - quench progression

Observed reflood signatures



Level stays at 400-500 mm from 12400 to 12650 s

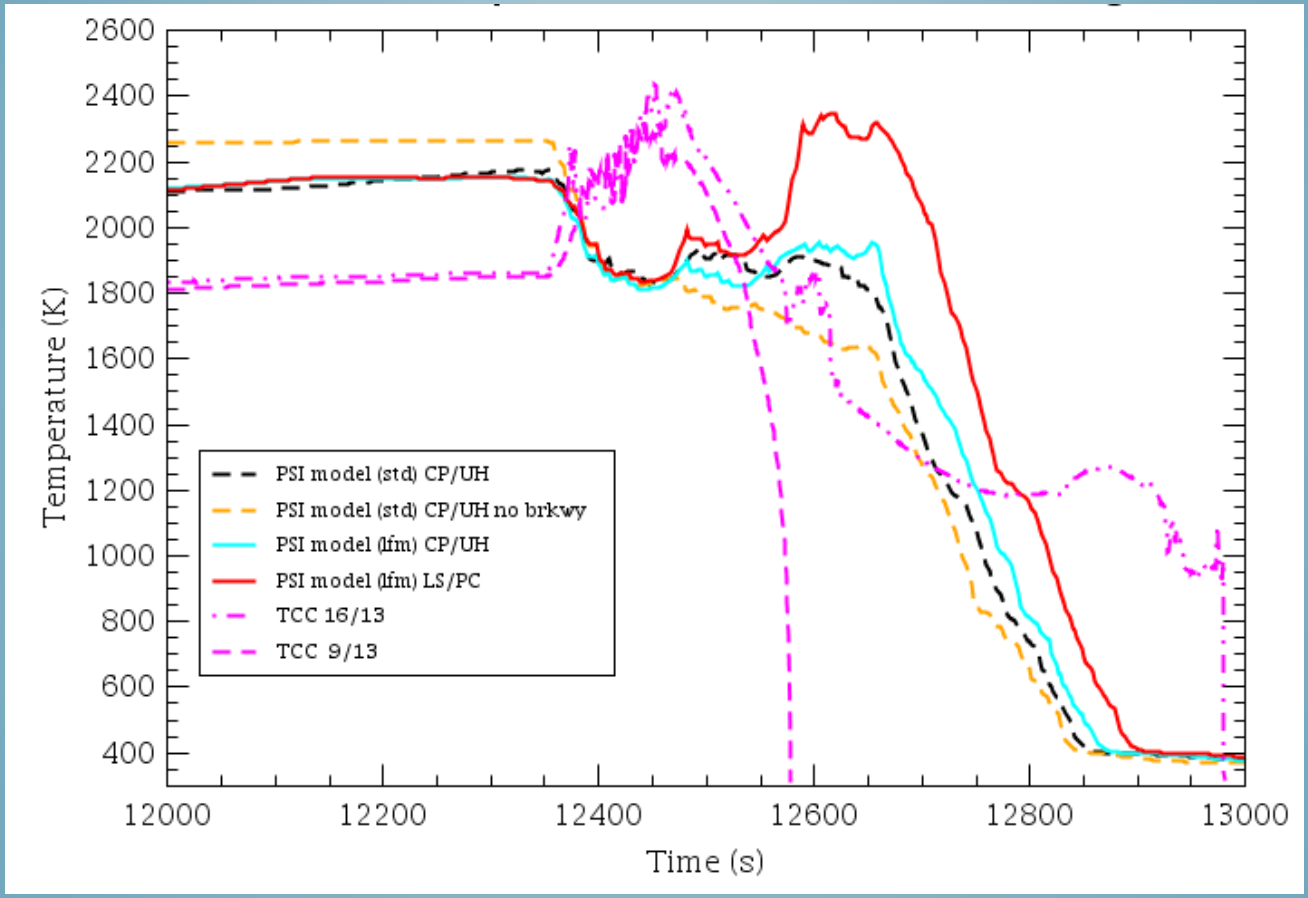
Offgas steam and H2 flows equivalent to ca. 12 g/s water

Suggests 40 g/s average for 250 s lost via breach at about this level

Measured Ar flow from behind shroud 0.5 to 1.0 g/s

Modified boundary conditions accordingly for revised base case

Reflood temperature at 950 mm: oxidation models



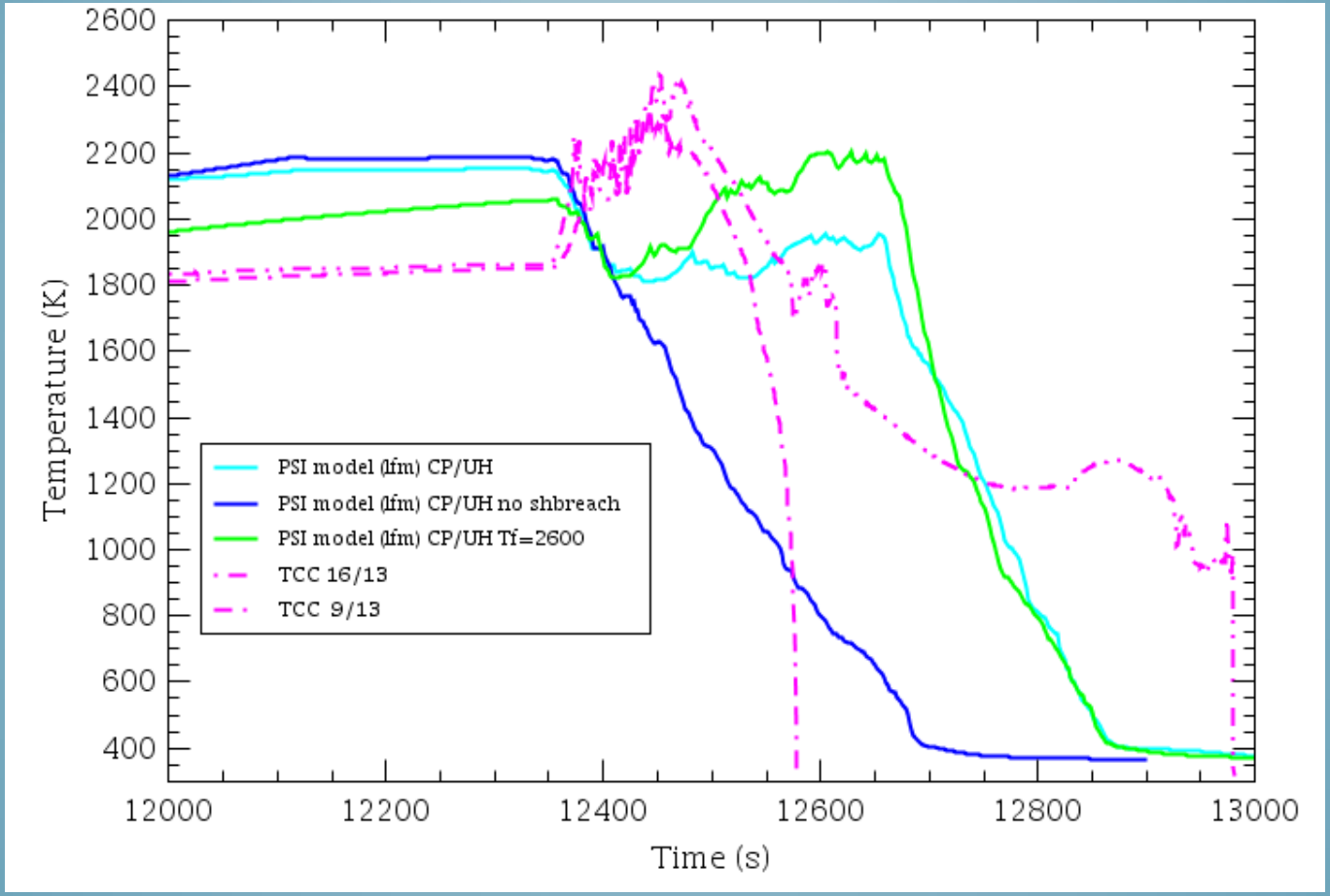
Temperature overestimated at reflood initiation

All cases show initial cooling, opposite to experiment

Case with L/PC correlation shows excursion, though later than observed

All cases show earlier final quench than in experiment

Reflood temperature at 950 mm : bundle assumptions

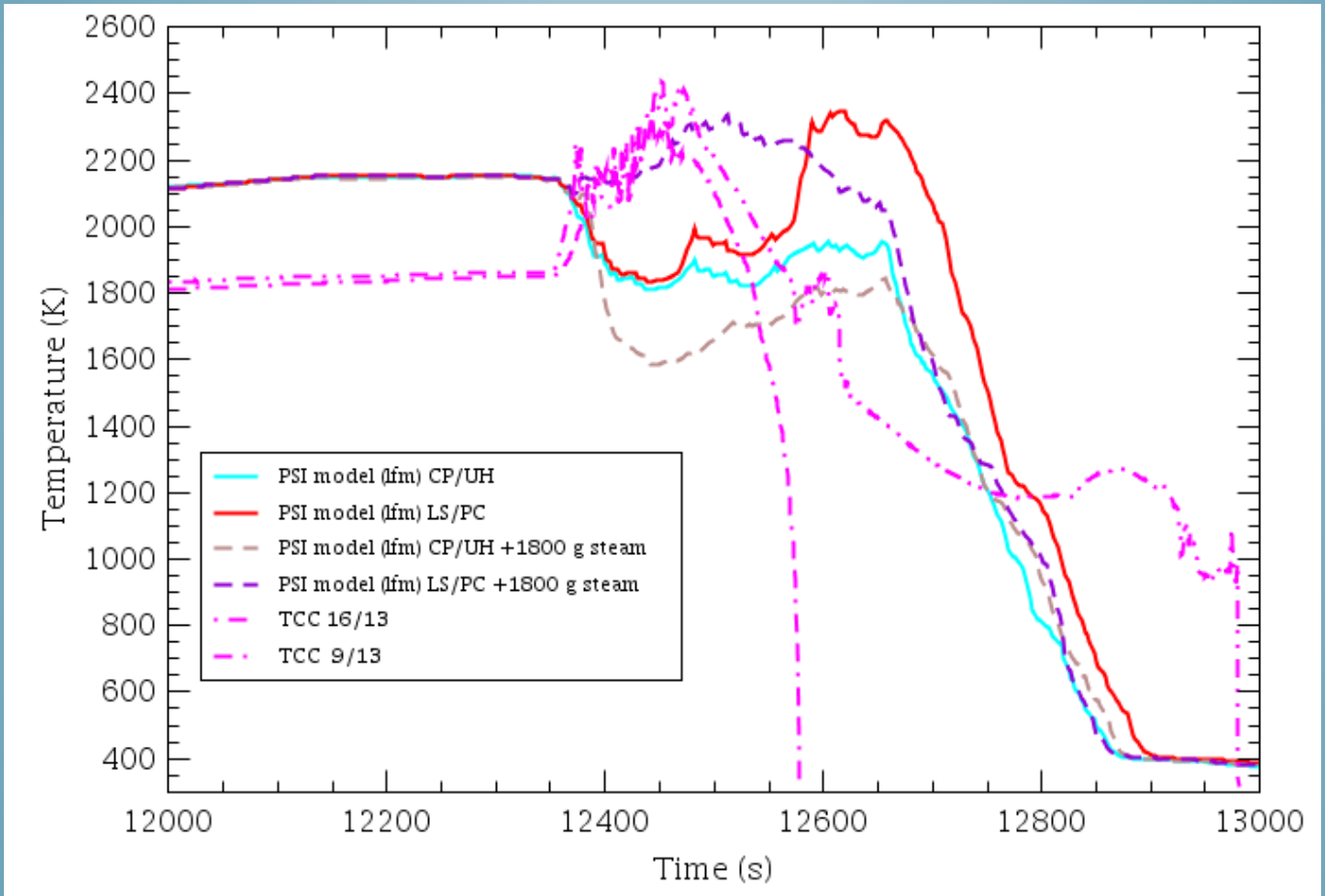


Cooling and early quench with nominal injection

Other cases show similar heating/cooling trends and quench time

Added steam case is attempt to understand observed initial excursion

Reflood temperature at 950 mm : +steam and ox.orr.

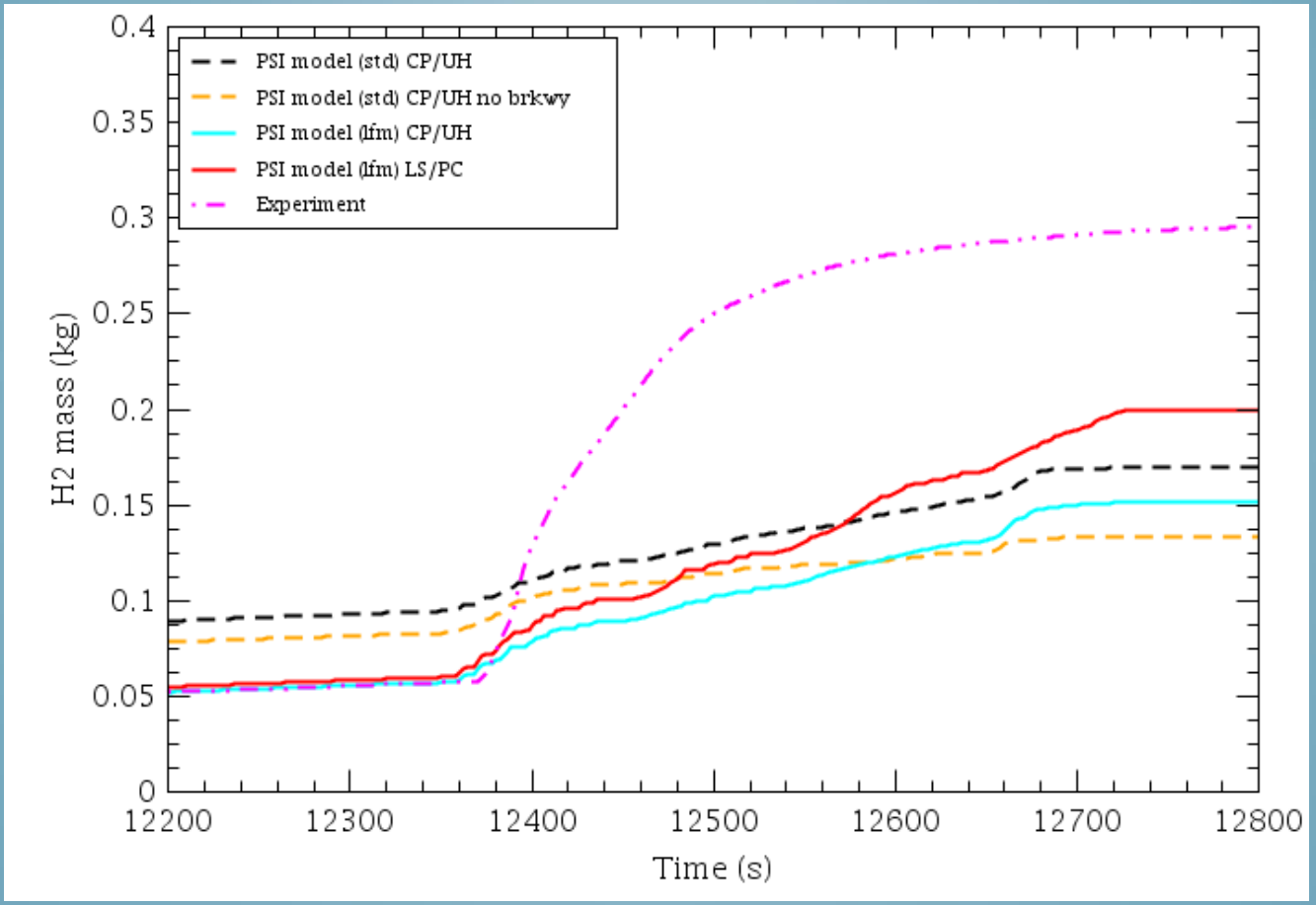


Cases with added steam aim to understand observed initial excursion

Early excursion captured by L/PC and added steam

Similar quench time in all cases despite different previous thermal transient

Reflood H2 generation: oxidation models



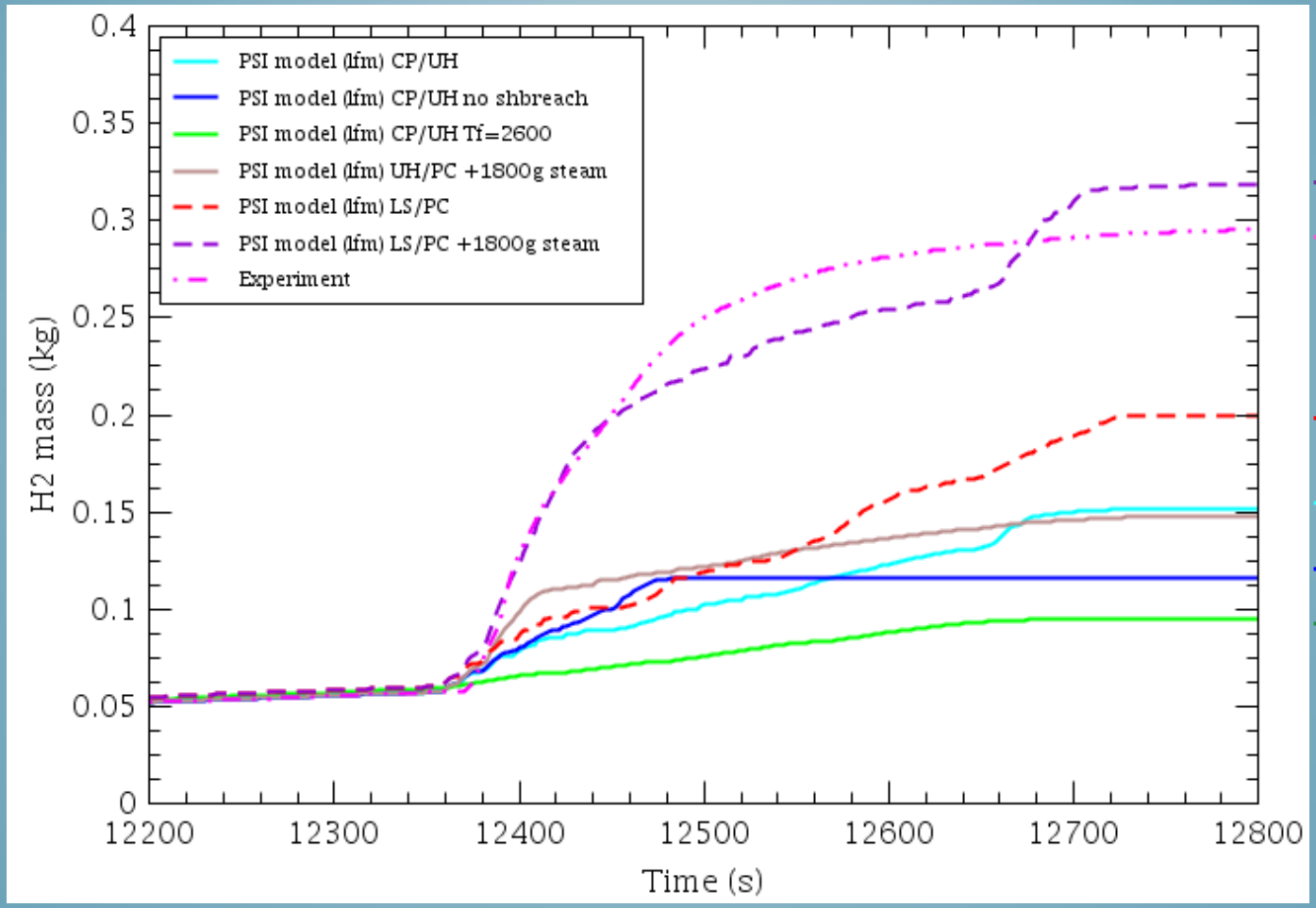
All cases underestimate H2 and not capture initial rapid excursion

N2-acceleration during air phase promotes reflood oxidation (+75 vs. +51)

L/PC leads to more oxidation than CP/UH (+140 vs. +75)

More prior oxidation reduces H2 during reflood

Reflood H2 generation: bundle assumptions



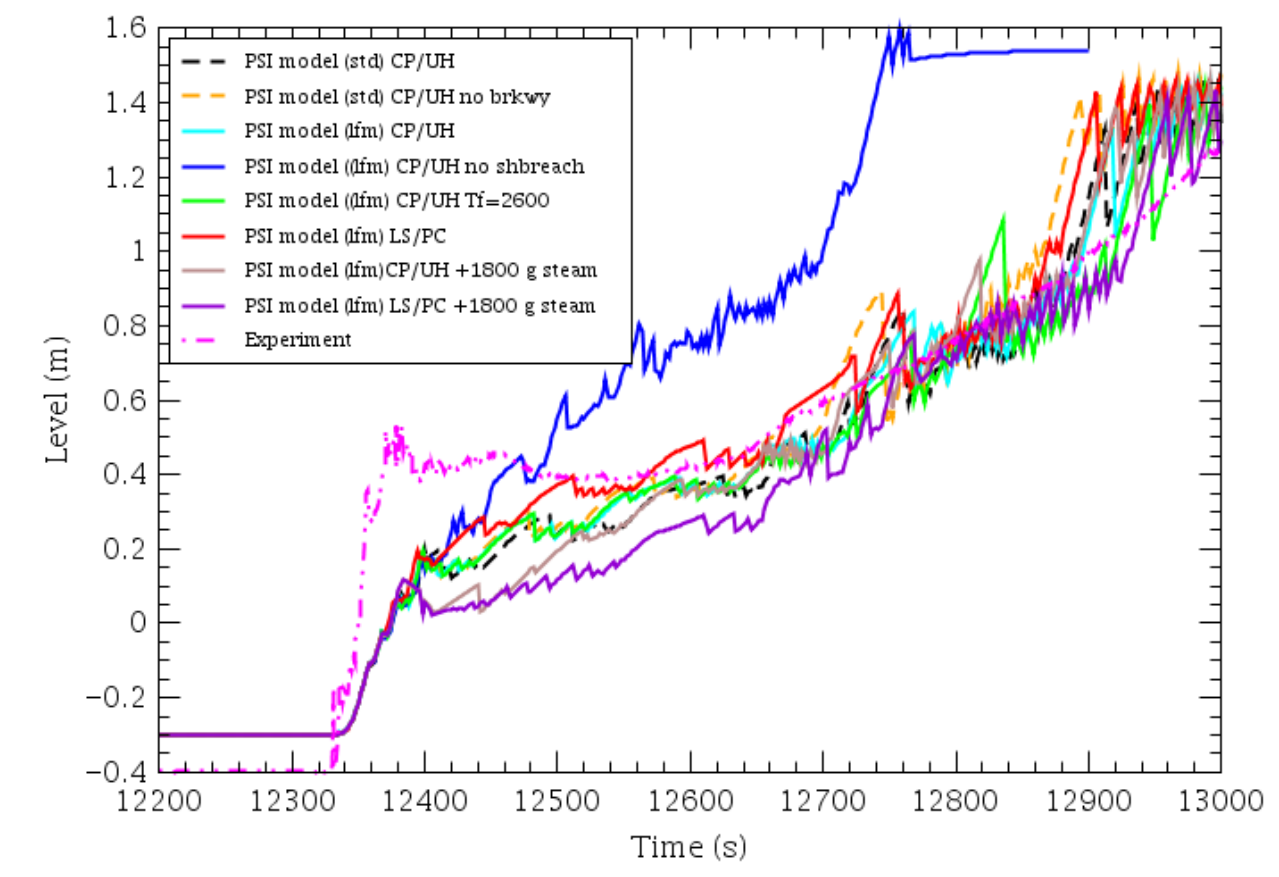
Added steam + L/PC gives (fortuitous?) good agreement (+269 vs. +239)

Added steam + CP/UH gives similar total H2 (+92 vs. +96)

Suppression of oxide failure results in lowest oxidation (+36)

Short oxidation, less H2 with nominal boundary conditions (+59 vs. 96)

Water level in bundle



Rapid early rise in experiment not captured

Case without adjusted injection to simulate breach calculates early refill

Other cases similar and in fair agreement with experiment after initial increase

Calculated refilling is very jerky compared with experiment

Summary of reflood analysis SKIP?

- Rapid early filling to ca. 500 mm not captured in any simulation
  - due to major relocation and blockage and/or large dynamic Δp?
- Major early oxidation – ca. 150 g in 75 s
  - implies significant sustained steam flow of at least 18 g/s
  - would seem to be result of water contact with hot material
- Bundle refill stalled for ca. 250 s
  - analyses consistent with shroud breach outflow of ca. 10 kg water
- Experimental final quench delayed after bundle refilled
  - not captured in simulations
  - channels blocked by relocated hot material?
- Wide range of oxidation scenarios
  - surprising synergies and sensitivities in reflood simulations
- Release of N2 from ZrN oxidation
  - moderate contribution to H2 generation (max. ca. 40 g)
  - insufficient to explain discrepancy but may have promoted excursion

Conclusions

- Conclusions for phenomenology
- Conclusions for modelling

Conclusions for phenomenology

- Simultaneous steam/O2 consumption but not necessarily in same location
  - simultaneous H2+O2 in offgas due to incomplete recombination?
- Nitriding not observed while O2 present
- Reoxidation of nitride contributes modestly to H2 generation during reflood
  - may promote faster oxidation of metallic during reflood
- Discrepancy between inlet-outlet steam and H2 release
  - H2 takeup in cladding due to effect of N2 on oxide?
- Impact of bundle disruption
  - spillage reduced effective injection from 2 g/s/rod to 0.5 g/s/rod
  - oxidation of released relocated metallic
    - ➔ Stb = m,inj (h,steam – h,water) / (Q,elec + Q,oxid) ≤ 1
  - blockages may have delayed final quench
- Elements of reflood remain difficult to explain
  - large early H2 generation, rapid early refill; upper level excursion
  - interpretation hindered by uncertain initial state of test section
  - some N2 release does not correspond to H2 release

Conclusions for modelling

- Leistikow/Prater-Courtright correlation works well for QUENCH-18
  - good alternative to Cathcart-Pawel/Urbanic-Heidrick
- Steam+air mixture is more realistic than steam followed by air
  - need for further data and model development
  - models should take account of past as well as current gas environment
- Present simulations compromised by lack of nitriding model
- Degradation strongly enhances subsequent oxidation
  - oxidant starvation and N2 may both weaken oxide scale
  - important to model oxidation of released metallic
  - effect of N2 on oxidation continues after end of air ingress
- Reflood simulation shows large steam and oxidation spikes
  - progressive quench through node preferred to entire node quench at once
- Surprising synergies and sensitivities in reflood simulations
  - need to be considered when performing and interpreting simulations

Acknowledgments

- I wish to thank KIT Karlsruher Institut für Technologie for funding my participation
- …. the team for technical exchange
- .... Leticia Fernandez Moguel (PSI)



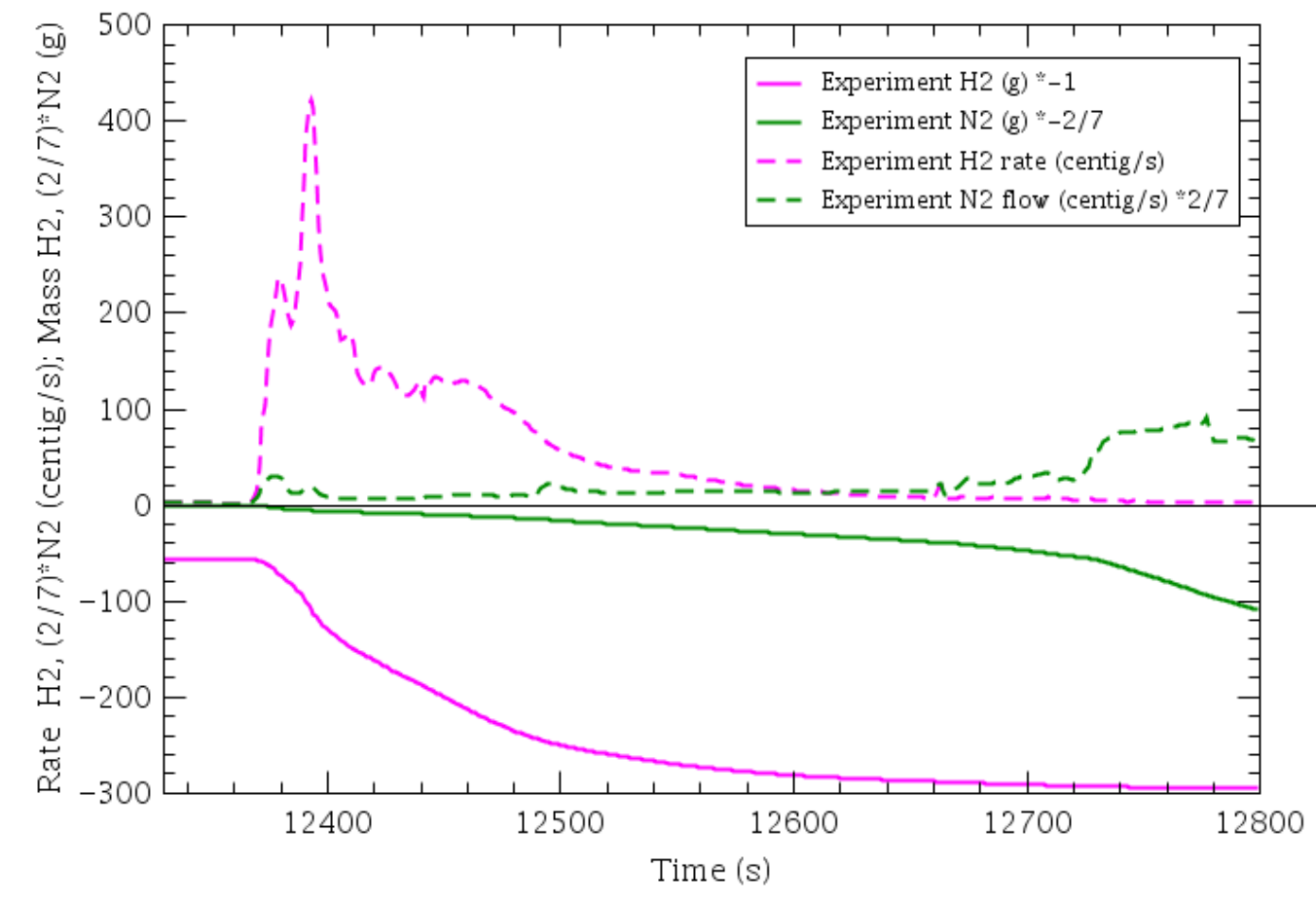
…. and Larry Siefkin (ISS)



for their work with the PSI air oxidation model

Thank you for your attention

H2 and N2 release during reflood



Significant release of N2 during reflood

Reaction $2ZrN + 4H_2O \rightarrow 2ZrO_2 + 4H_2 + N_2$

Not all of the N2 corresponds to H2 (max. ca. 40g)

Post-Test Modelling of the Concurrent Steam-Air Experiment QUENCH-ALISA Using SOCRAT Code

Alexander Vasiliev
Nuclear Safety institute (IBRAE)
B.Tulskaya 52
115191, Moscow, Russia
vasil@ibrae.ac.ru

ABSTRACT

The thermal hydraulic and SFD (Severe Fuel Damage) best estimate computer modelling code SOCRAT/V3 has been used for the post-test calculation of QUENCH-ALISA (QUENCH-18) experiment.

The QUENCH-ALISA test conditions simulated a representative scenario of LOCA (Loss of Coolant Accident) nuclear power plant accident sequence in which the overheated core would be reflooded from the bottom by ECCS (Emergency Core Cooling System). The QUENCH-ALISA experiment included the following phases: first heat-up phase, pre-oxidation phase, slow cool-down phase (preparatory to steam/air ingress), the steam/air ingress phase and bottom water flooding phase. The important feature of QUENCH-ALISA test was the concurrent steam/air ingress phase during which the steam and air together were supplied to the working section of experimental installation.

The QUENCH-ALISA steam-air ingress and aerosole release test was successfully conducted at the KIT, Karlsruhe, Germany, on September 27, 2017. The primary objective of this test was to investigate the oxidation of M5 cladding in the steam/air mixture following a limited pre-oxidation in the steam and to achieve a long period of oxygen and steam starvation to promote the interaction with the nitrogen. Unexpectedly high cladding oxidation rate was detected during flooding phase which resulted in huge hydrogen production in QUENCH-ALISA. It was due to zirconium nitride formation in a cladding which induced a diffusion transparency of zirconium dioxide layer.

The calculated results obtained for phases before steam/air ingress phase are in a reasonable agreement with experimental data which justifies the adequacy of thermal hydraulic modelling capabilities of SOCRAT code. However, the SOCRAT drastically underestimated the hydrogen generation and integral production at steam/air ingress. This is due to very complicated physical and chemical phenomena that have arisen at steam/air ingress phase in the QUENCH-ALISA. The hypothesis of equal priority for oxygen and steam oxidation of Zr postulated in the SOCRAT code is occurred to be erroneous and will be fixed in the future.

As a result of implementation of “transparent” ZrO_2 layer model into SOCRAT, the sharp hydrogen generation rise is calculated, as it was observed in test QUENCH-ALISA. The “transparent” ZrO_2 layer occurrence is connected with formation of nitrides in α-Zr layer at oxygen and steam starvation phase, the “transparency” is modelled by enhancement of oxygen diffusion coefficient.

The SOCRAT predicts well the time of oxygen starvation and underpredicts the time of steam starvation which is connected with equal priority approach for O_2 and H_2O oxidation in the SOCRAT.



Post-Test Modelling of the Concurrent Steam-Air Experiment QUENCH-ALISA Using SOCRAT Code

Alexander Vasiliev

Nuclear Safety Institute of Russian Academy of Sciences (IBRAE),
B.Tulskaya 52, 115191 Moscow, Russia

Content of Presentation

1. Introduction

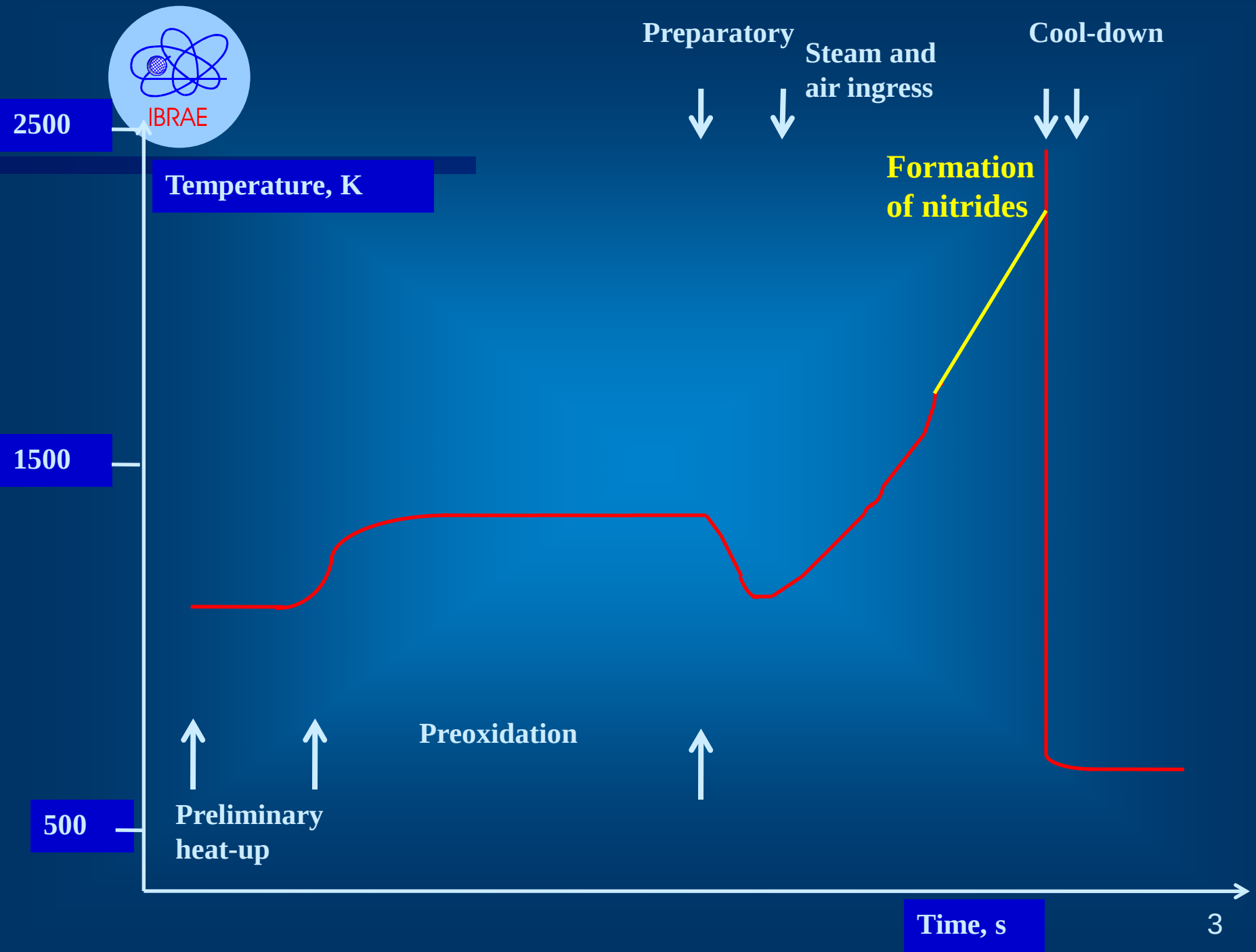
2. SOCRAT Post-Test Results for QUENCH-ALISA

The brilliant test embracing plenty of colourful distinctive physical and chemical phenomena

3. Steam-Air Ingress Phase Analysis

4. Integral Hydrogen Production in Test and in Code

5. Conclusions Made on the Basis of Post-Test Results


IBRAE
2500
1500
500
Temperature, K
Preparatory
Steam and
air ingress
Cool-down
Formation
of nitrides
Preoxidation
Preliminary
heat-up
Time, s

Priority of Probable Reactions. Thermodynamic Potential Change

$Zr+O_2=ZrO_2$	$\Delta\Phi\cong$-800 kJ/mole Zr
$Zr+2H_2O=ZrO_2+2H_2$	$\Delta\Phi\cong$-480 kJ/mole Zr
$Zr+0.5N_2=ZrN$	$\Delta\Phi\cong$-220 kJ/mole Zr

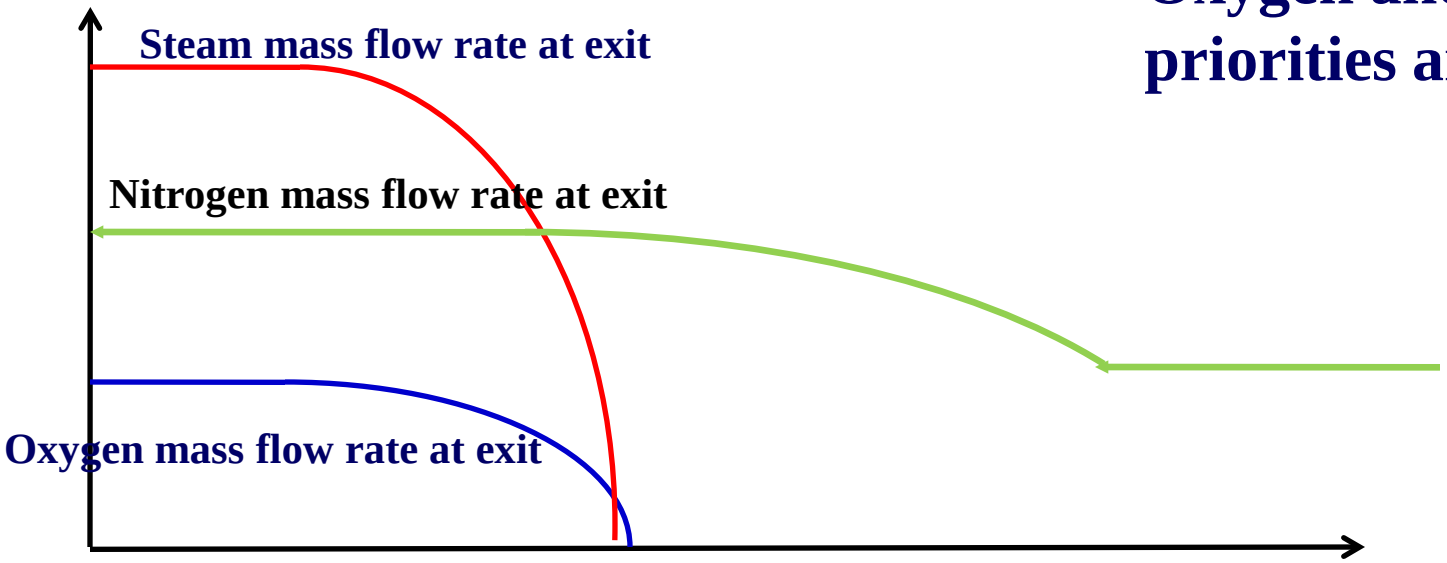
From thermodynamic considerations first reaction should be $Zr+O_2=ZrO_2$

Second reaction should be $Zr+2H_2O=ZrO_2+2H_2$

Third reaction should be $Zr+0.5N_2=ZrN$

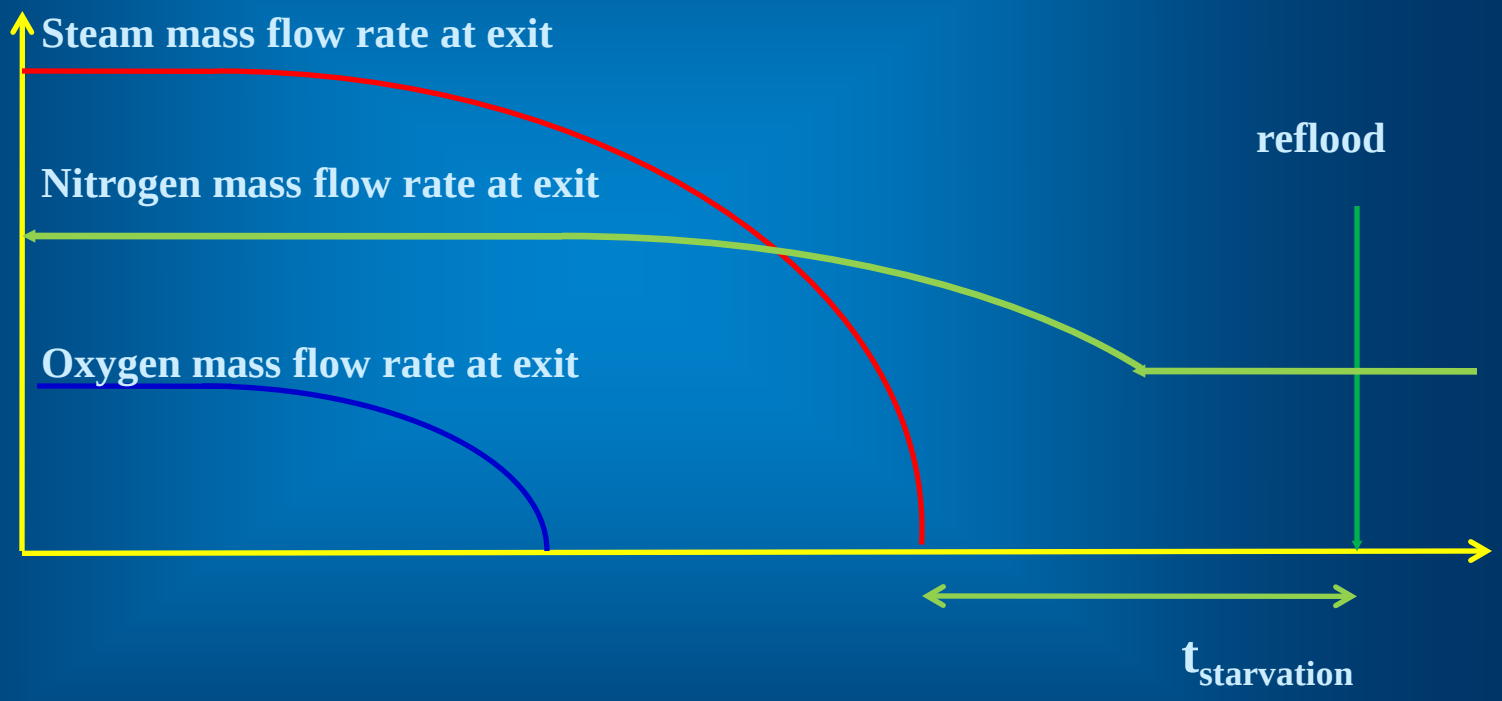
The post-test results including the oxygen and steam starvation and the nitrogen consumption have elucidated this matter.

Oxygen and Steam Together, Nitrogen Last



Oxygen and steam priorities are equal!

Oxygen First, Steam Second, NitrogenThird



O_2 and H_2O mass flow rates at exit in dependence of time

Characteristic Values of Parameters

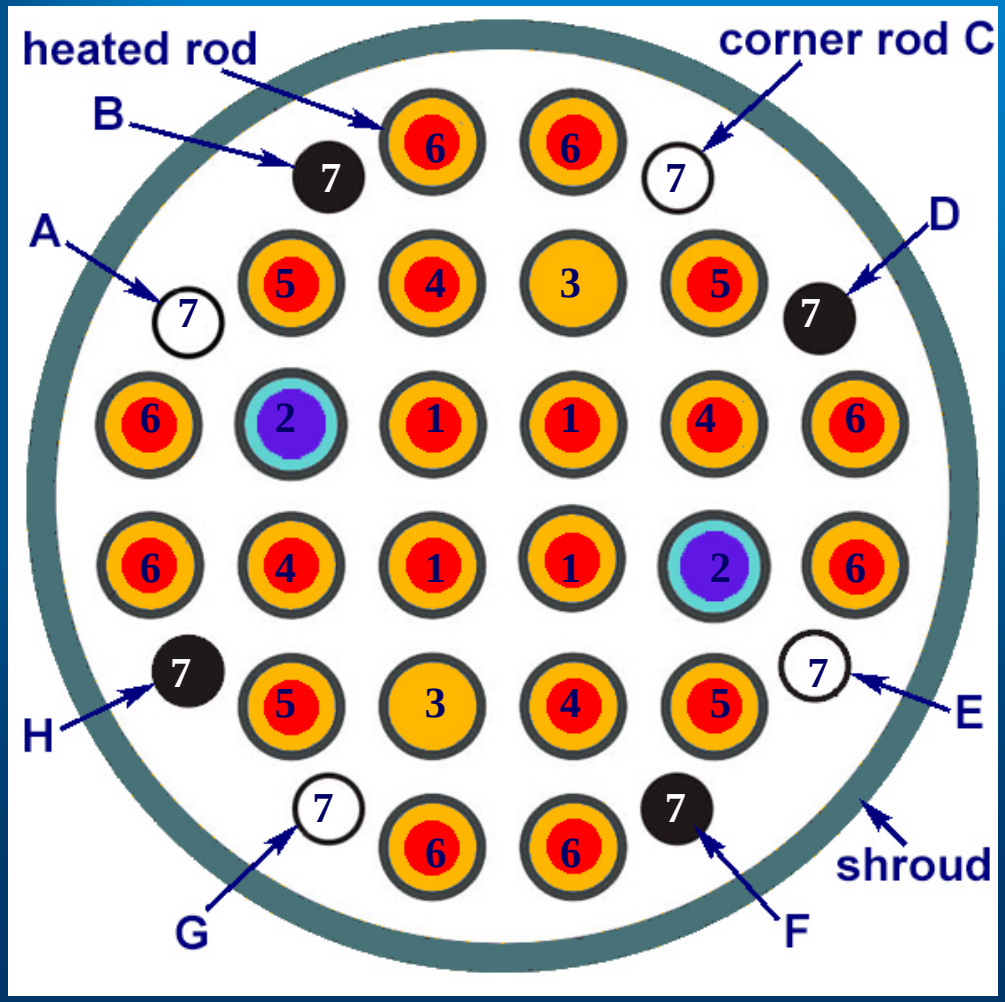
Variable	QUENCH-10	PARAMETER-SF4	QUENCH-16	QUENCH-ALISA
$A_{mixture}$, g/s	3.95	2.5	1.222	1.55
Δt, s	50	320	860	1340
δ_{ZrO2}, μm	510	120	140	100÷150

$A_{mixture}$ – gas mixture mass flow rate at air ingress phase

Δt - duration of starvation phase

δ_{ZrO2} - thickness of ZrO_2 layer before beginning of starvation

Radial Radiative Groups
ALISA Bundle



1 – four heated rods in the centre

2 – two control rods

3 – two unheated rods

4 – four heated rods in big square 4×4 (not in the corner)

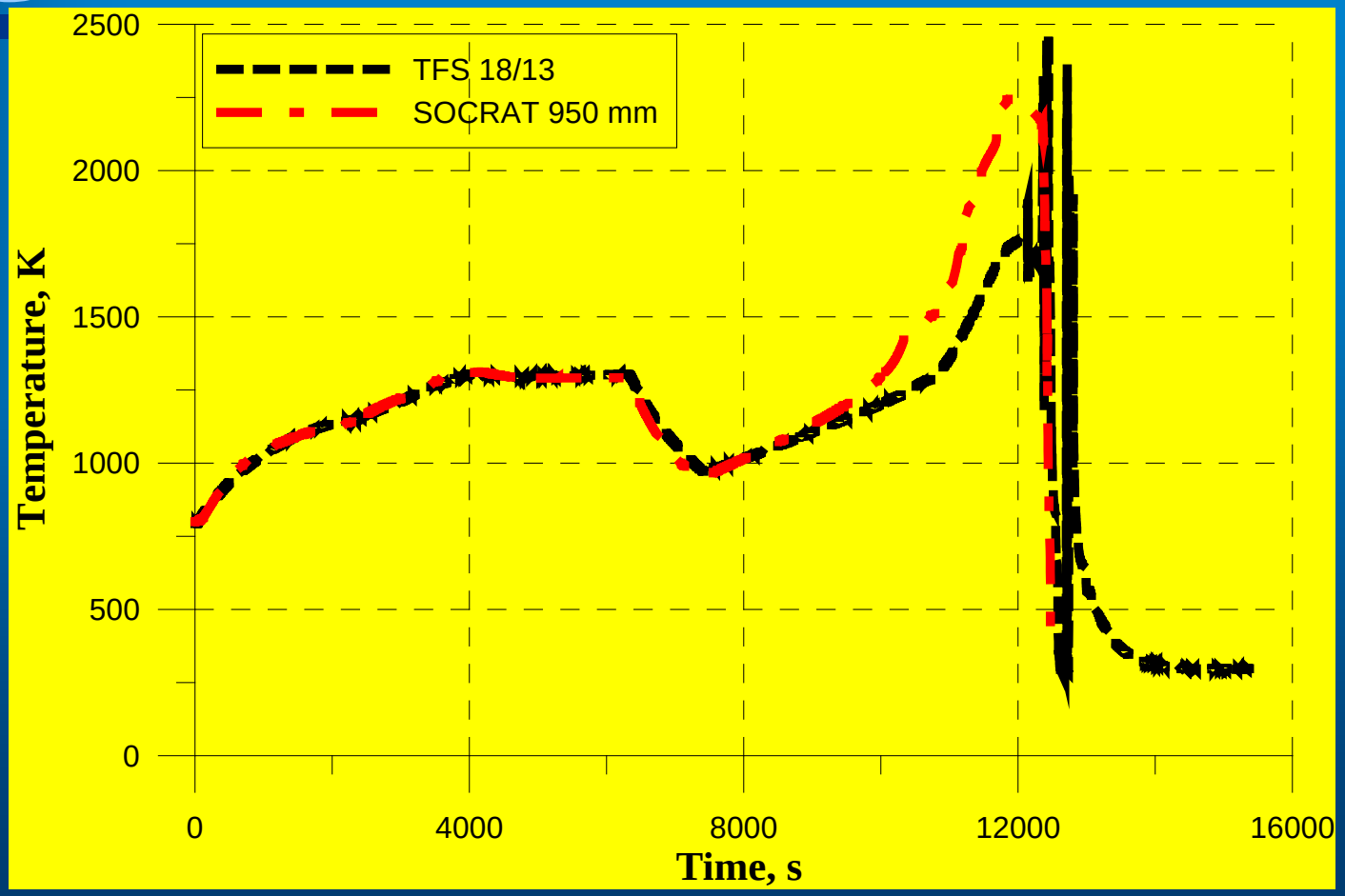
5 – four heated rods in the corner of big square 4×4

6 – eight periphery heated rods

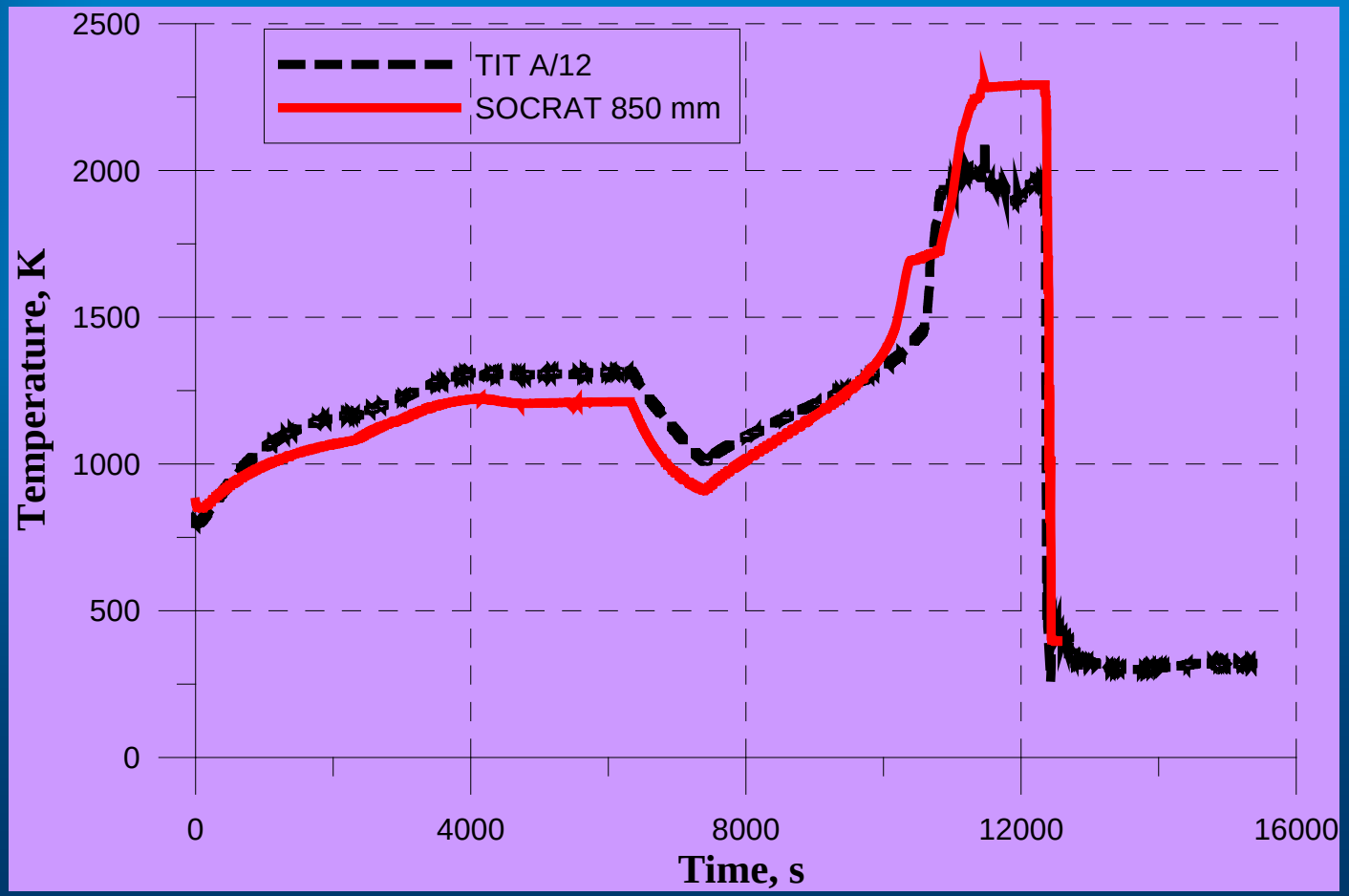
7 – eight corner rods

8 – inner surface of the shroud

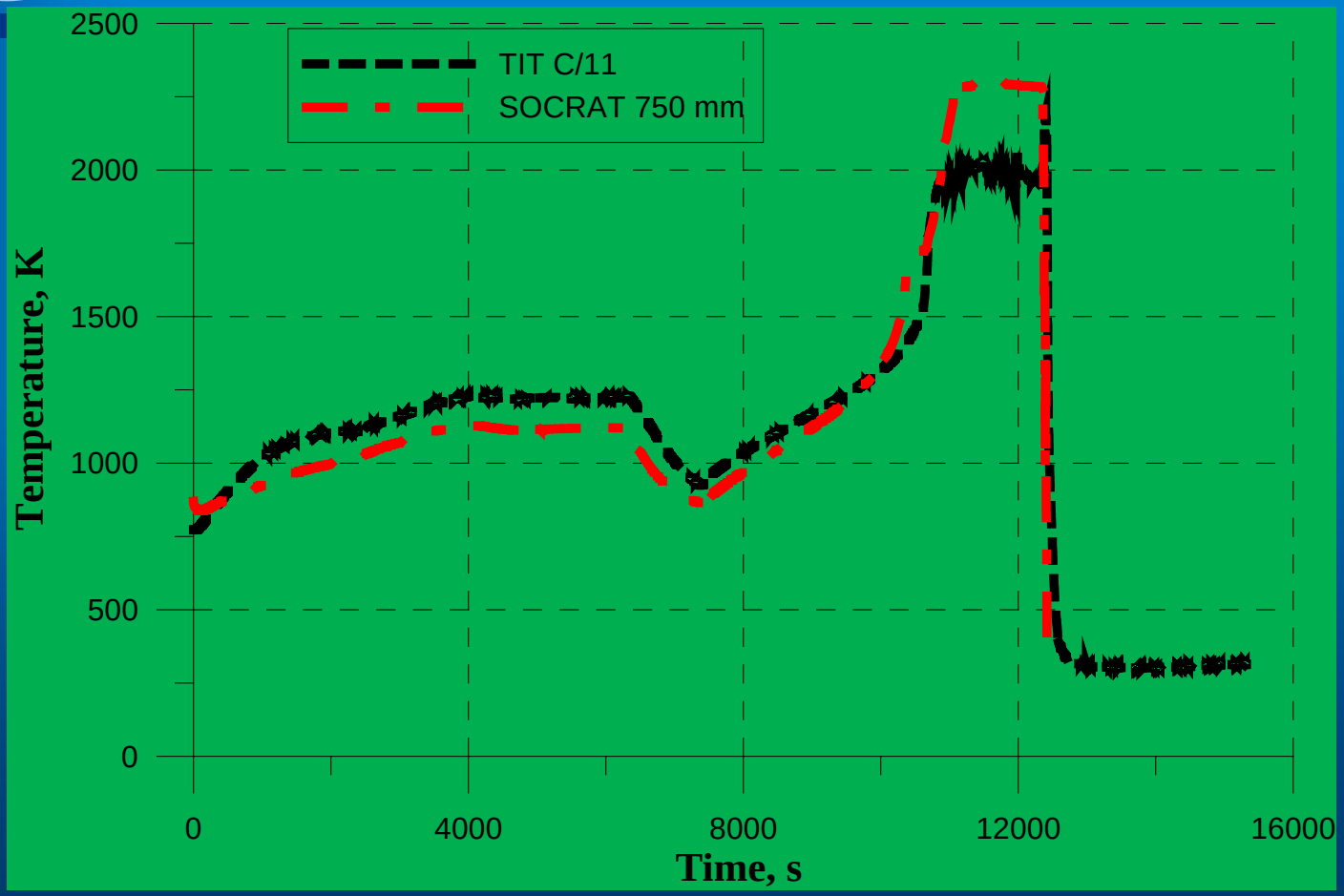
Temperature at level 950 mm



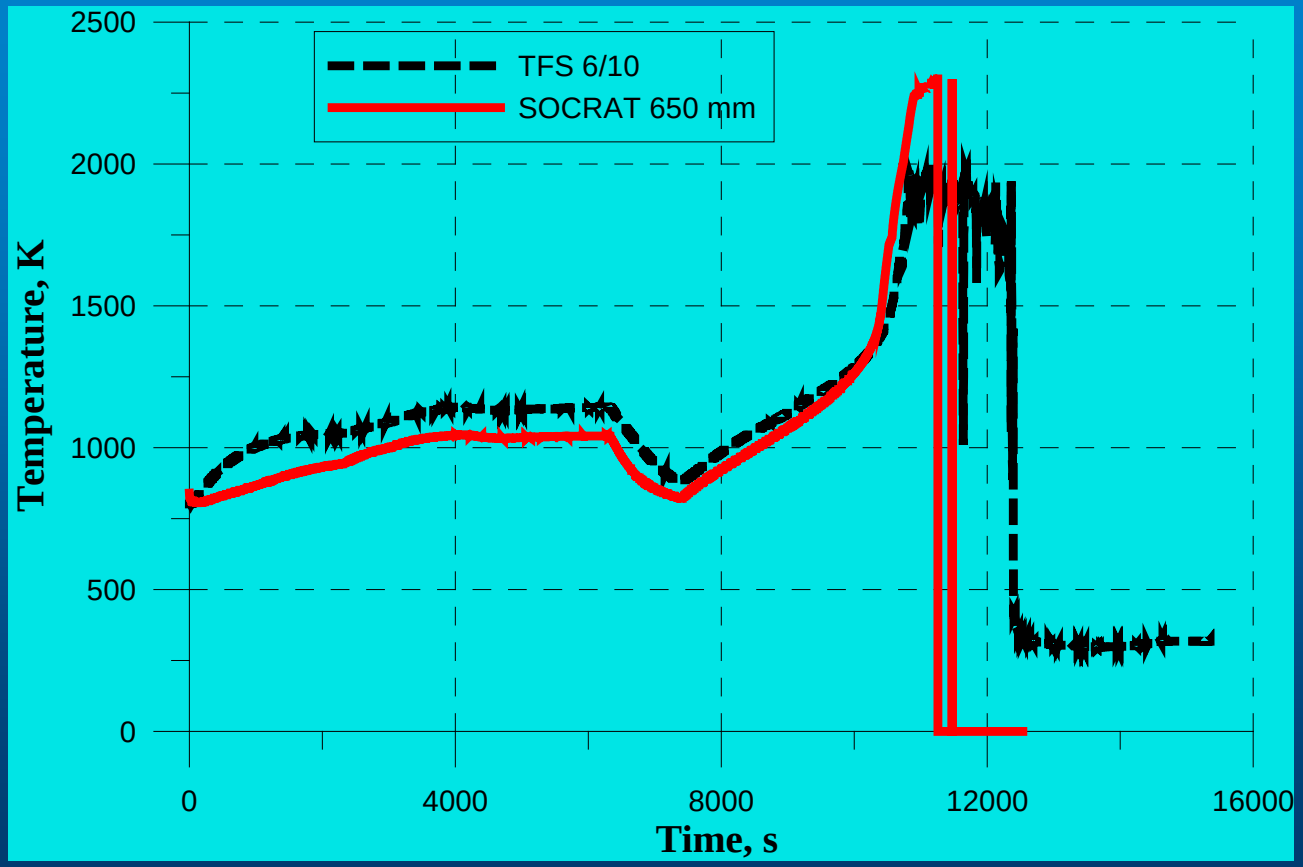
Temperature at level 850 mm



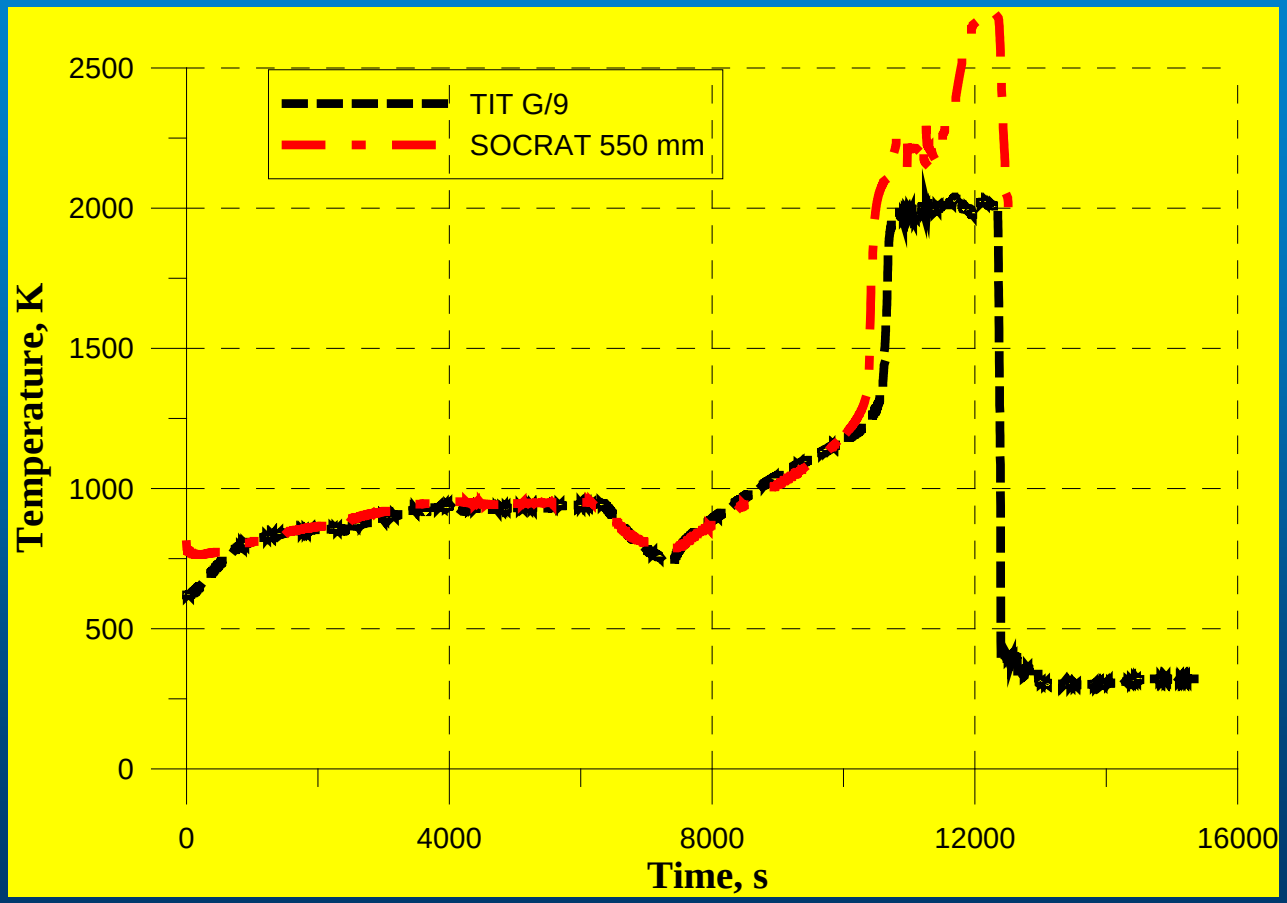
Temperature at level 750 mm



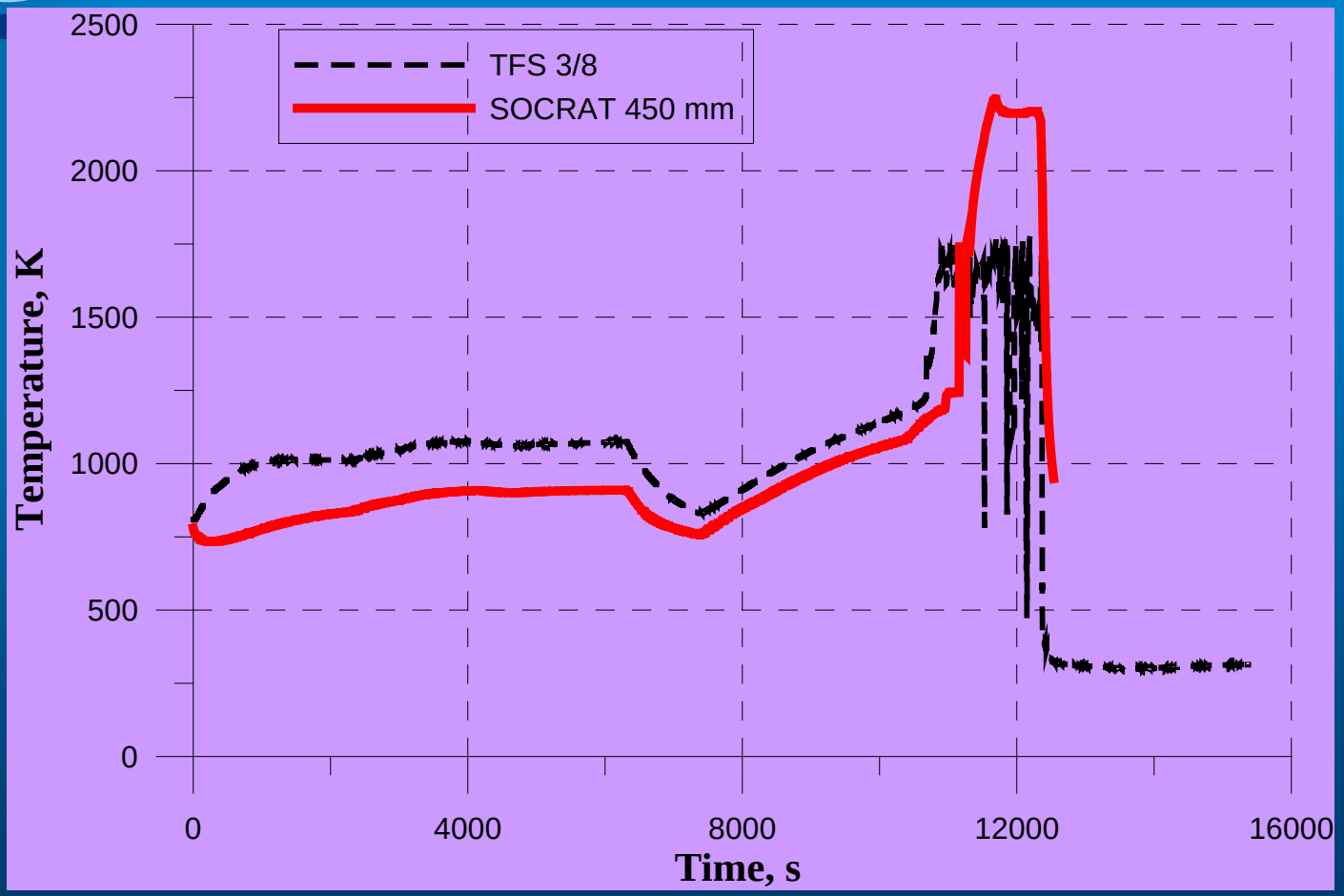
Temperature at level 650 mm



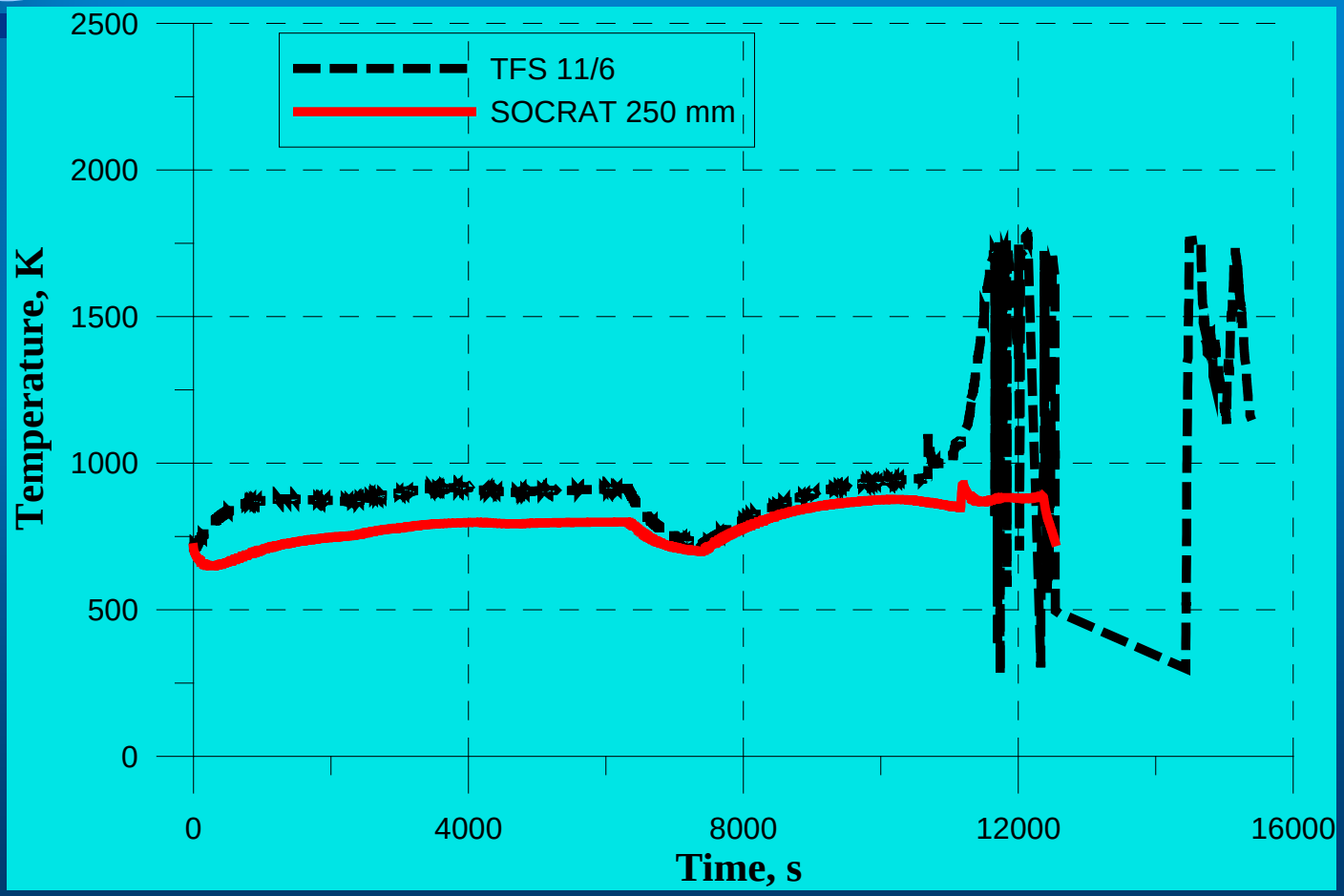
Temperature at level 550 mm



Temperature at level 450 mm



Temperature at level 250 mm

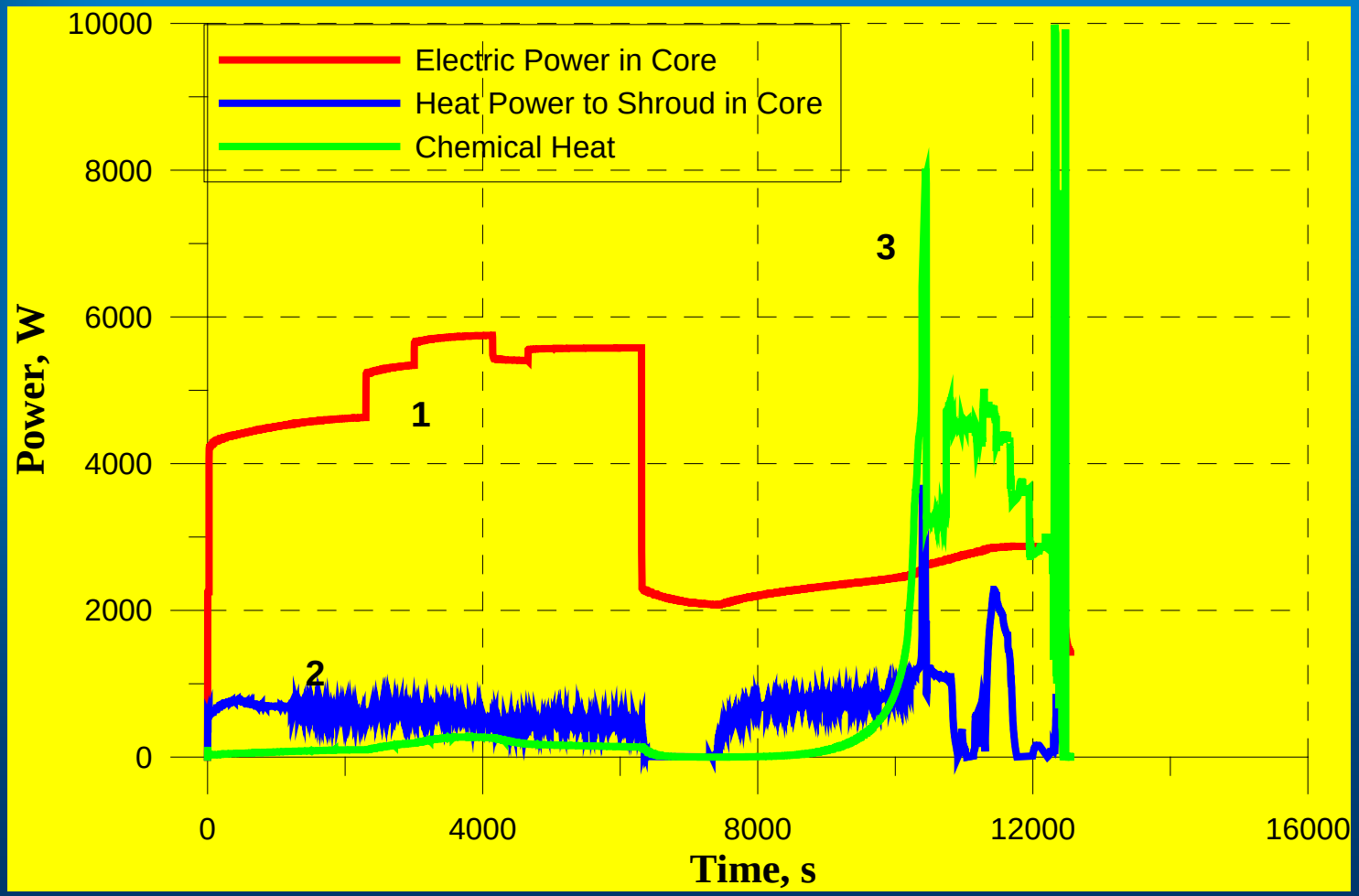


Overestimation of Temperature at Steam-Air Phase by SOCRAT

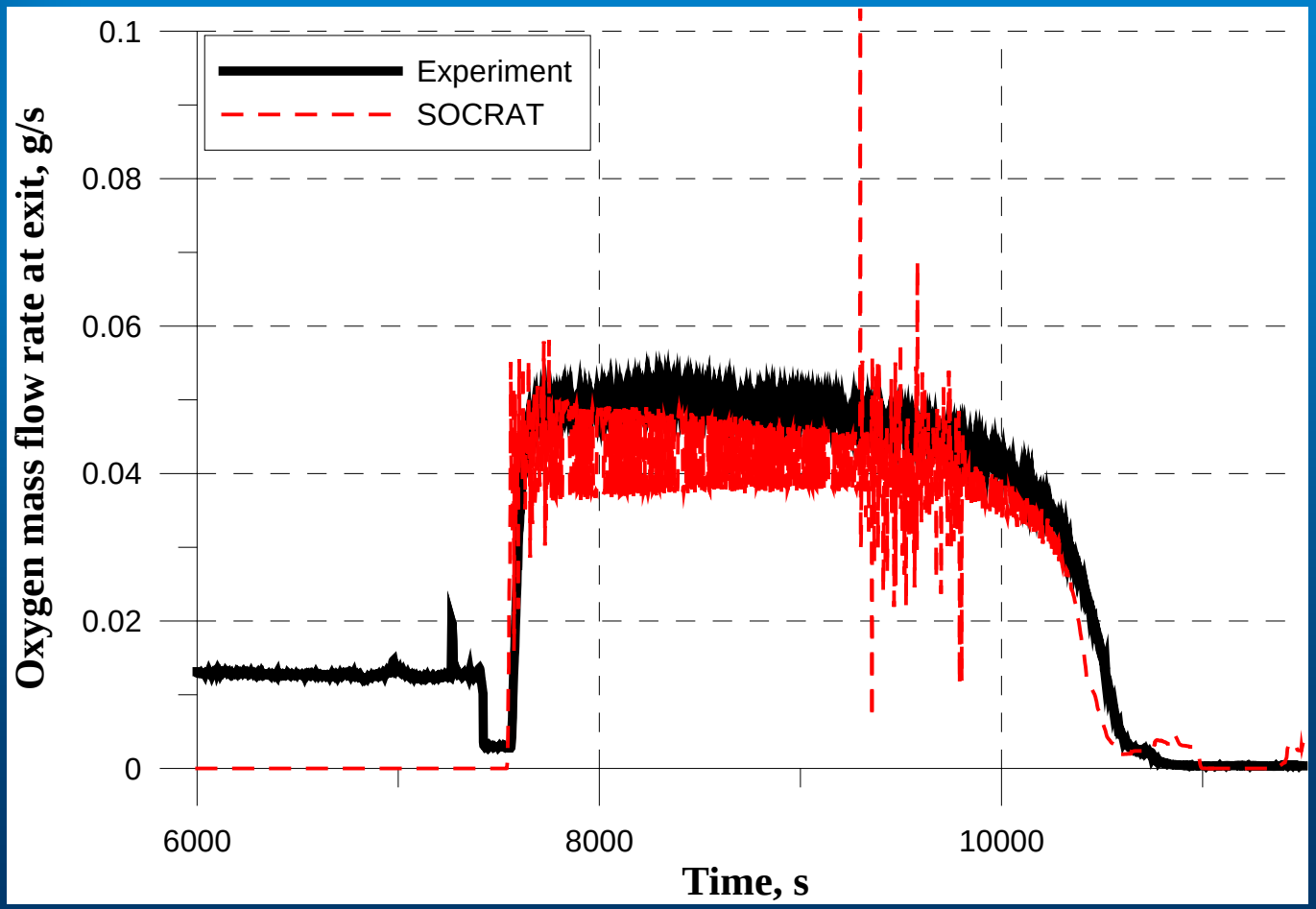
For a majority of elevations the calculated temperatures are overestimated compared to experimental data for steam-air ingress phase.

The reason is not adequate consideration of steam mass flow and correspondingly of convective heat transfer.

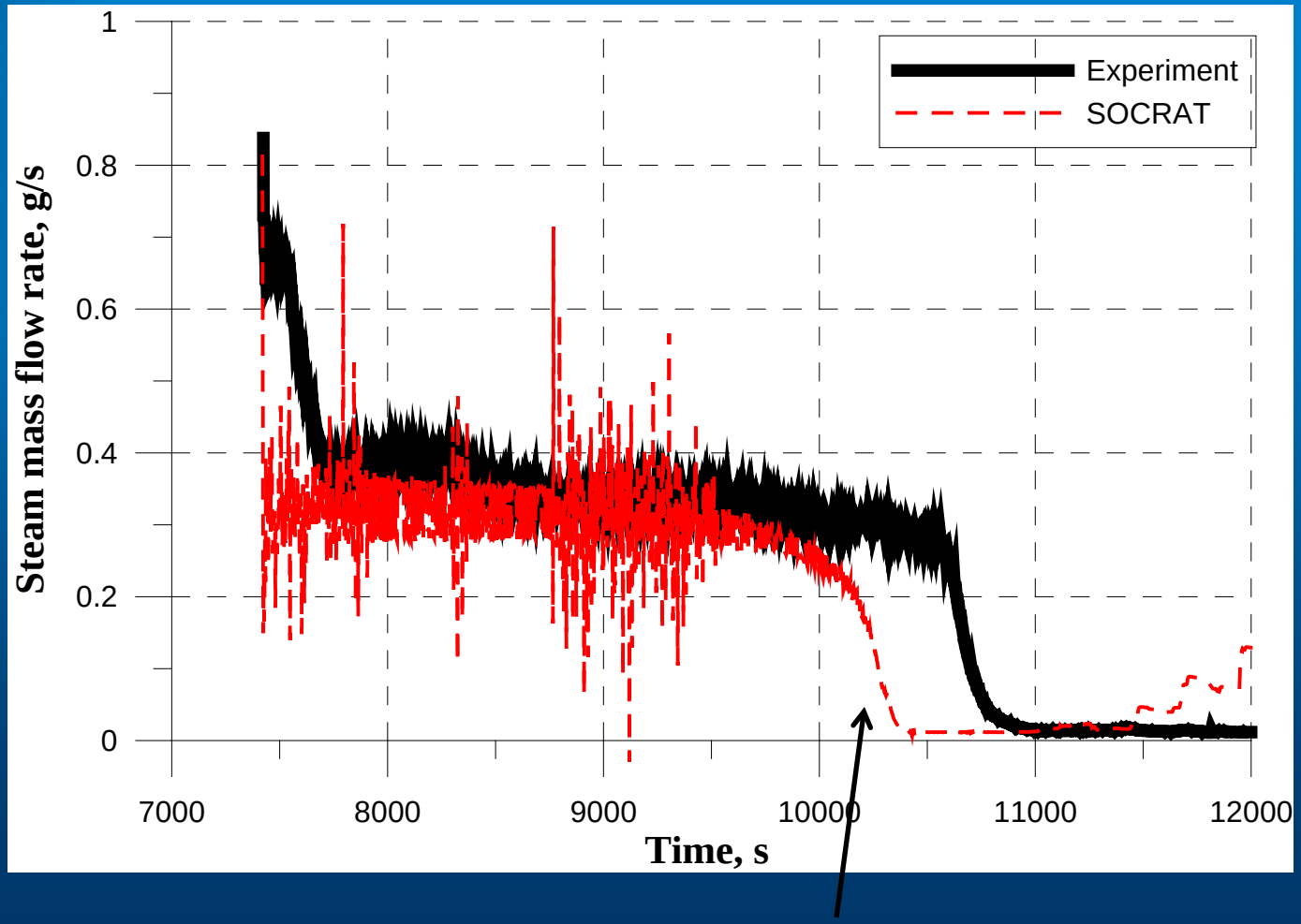
Calculated Heat Balance in QUENCH-ALISA



Steam-Air Ingress Phase: Oxygen Exit Mass Flow Rate

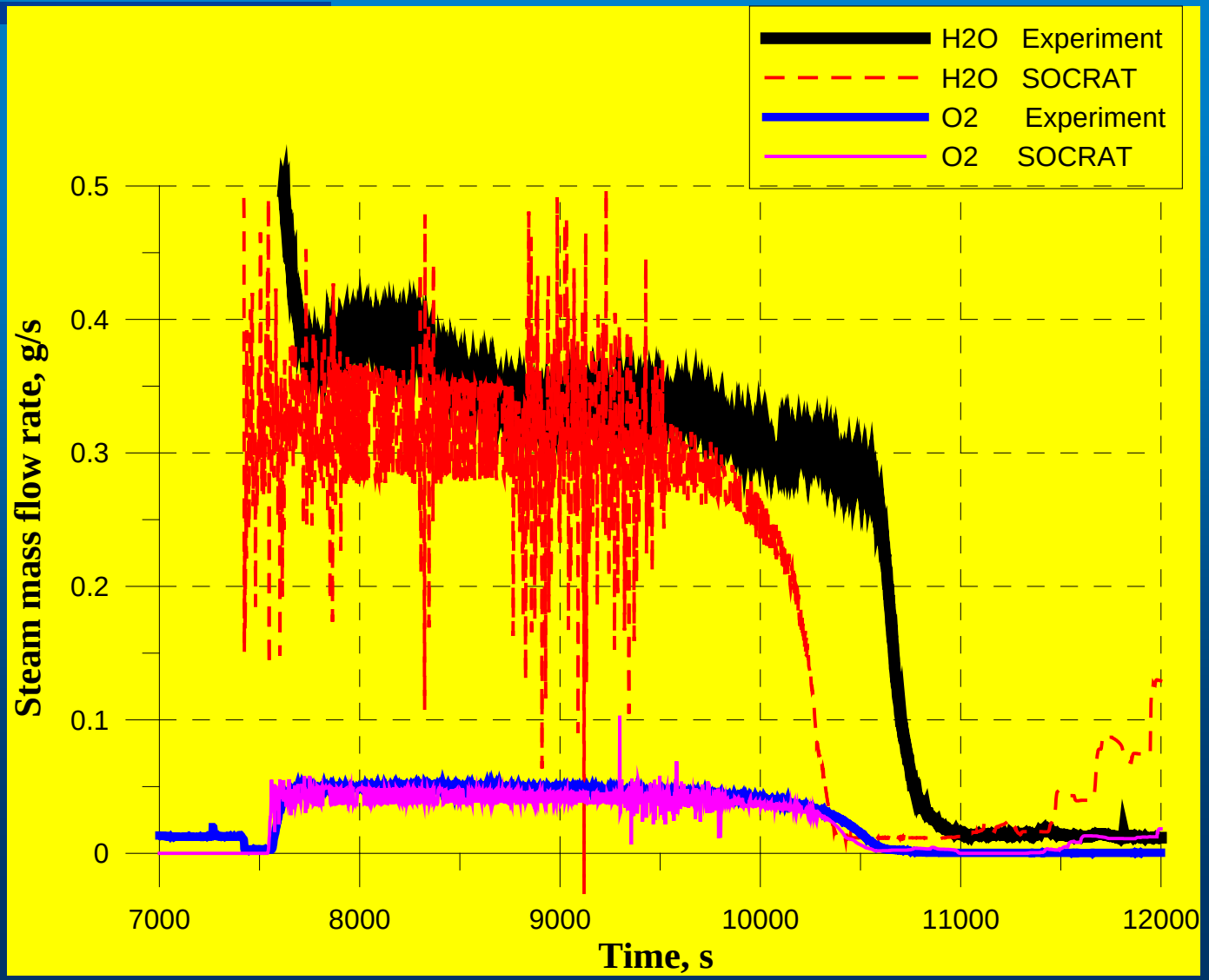


Steam-Air Ingress Phase: Steam Exit Mass Flow Rate

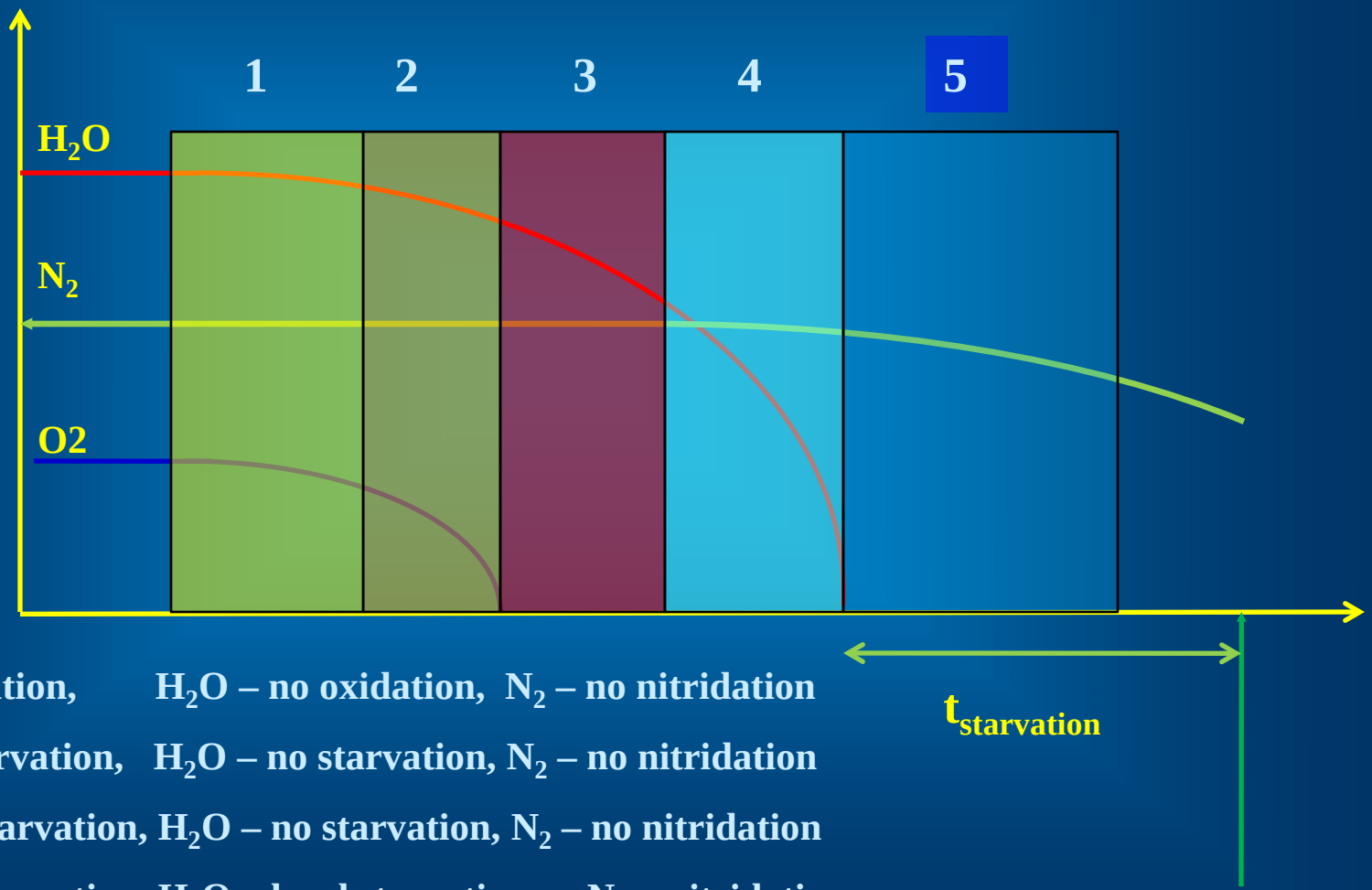


Due to equal priority approach for oxygen and steam oxidation, the steam starvation time is underestimated in SOCRAT !

Steam-Air Ingress Phase: Oxygen and Steam Mass Flow Rates



Oxygen First, Steam Second, NitrogenThird



1: O_2 – no starvation, H_2O – no oxidation, N_2 – no nitridation

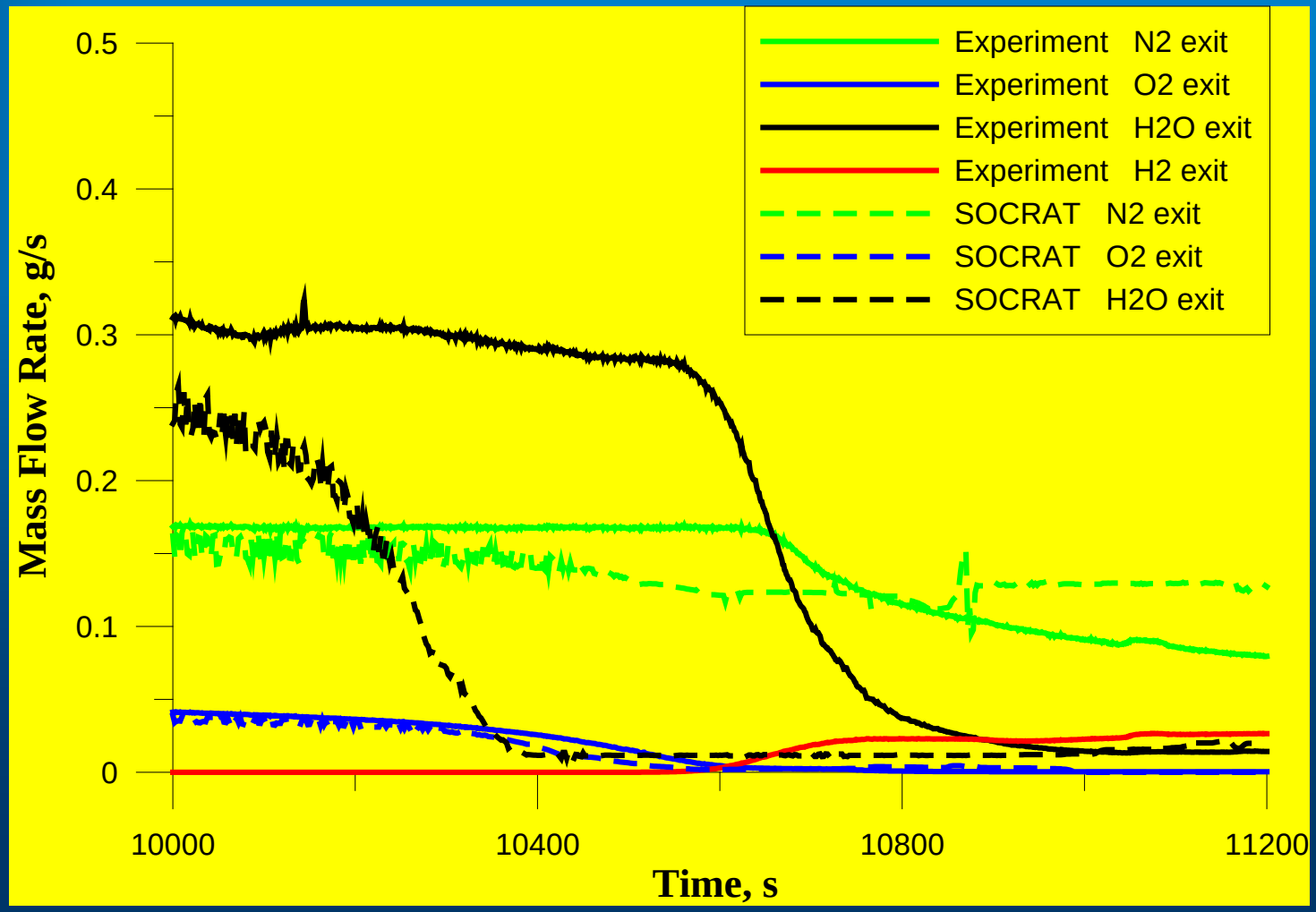
2: O_2 – local starvation, H_2O – no starvation, N_2 – no nitridation

3: O_2 – global starvation, H_2O – no starvation, N_2 – no nitridation

4: O_2 – global starvation, H_2O – local starvation, N_2 – nitridation

5: O_2 – global starvation, H_2O – global starvation , N_2 – nitridation

Steam-Air Ingress Phase: Gases' Mass Flow Rates at Exit



Underestimation of Steam Global Starvation Time at Steam-Air Phase by SOCRAT

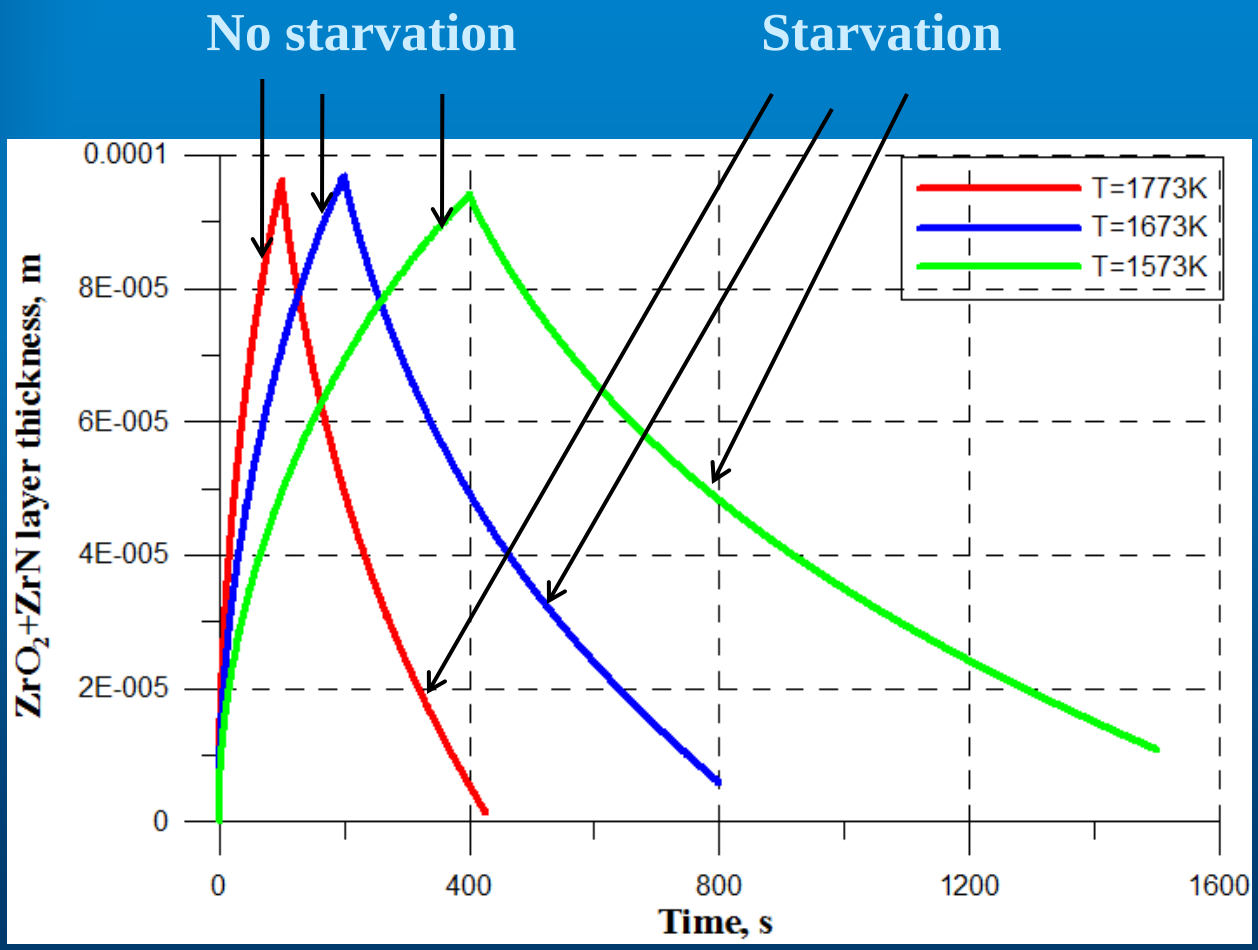
Point of steam global starvation is drastically underestimated by code (10,400s instead of 11,000s).

The reason is not adequate consideration of steam mass flow (equal priority for steam and oxygen oxidation).

As a first approximation changing of priority will fix situation.

But detailed calculation of local starvation conditions is necessary (including influence of diffusion in gas mixture) for adequate calculation.

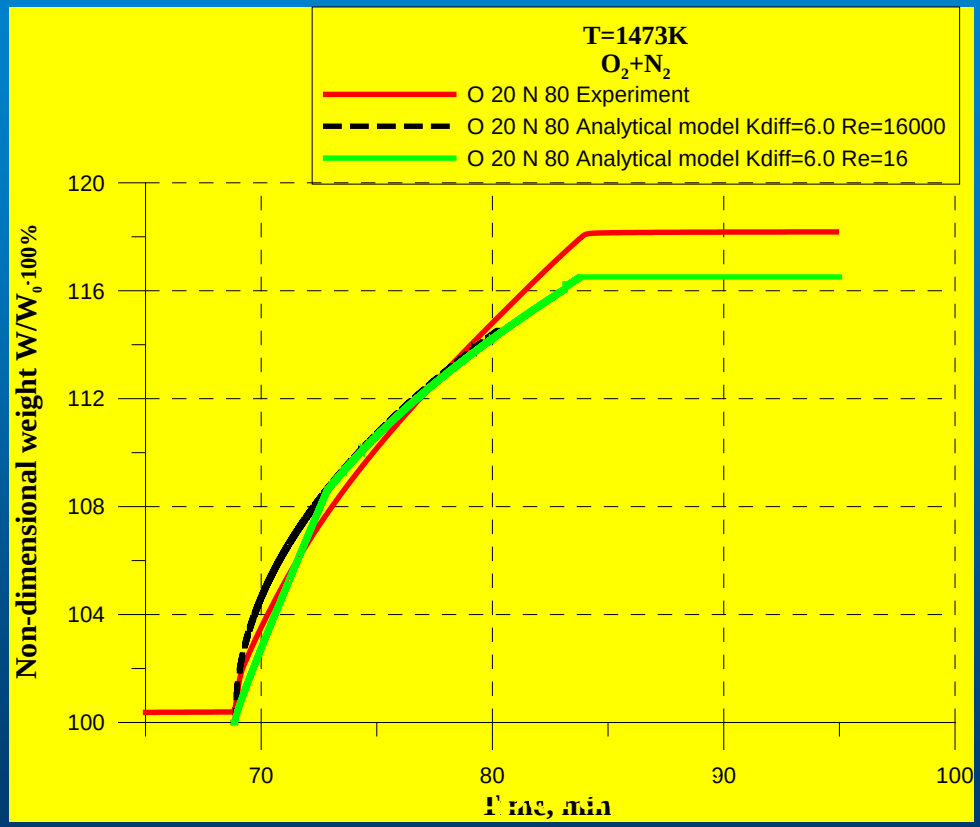
Dynamics of Oxide Layer during Oxygen or Steam Starvation



Characteristic times for ZrO_2 layer dissapepearance are:

1573K – 500s
1673K – 250s
1773K – 150s

Enhanced Oxygen Diffusion Coefficient K_{diff} Can Predict Adequate Oxidation Rate



K_{diff}=6

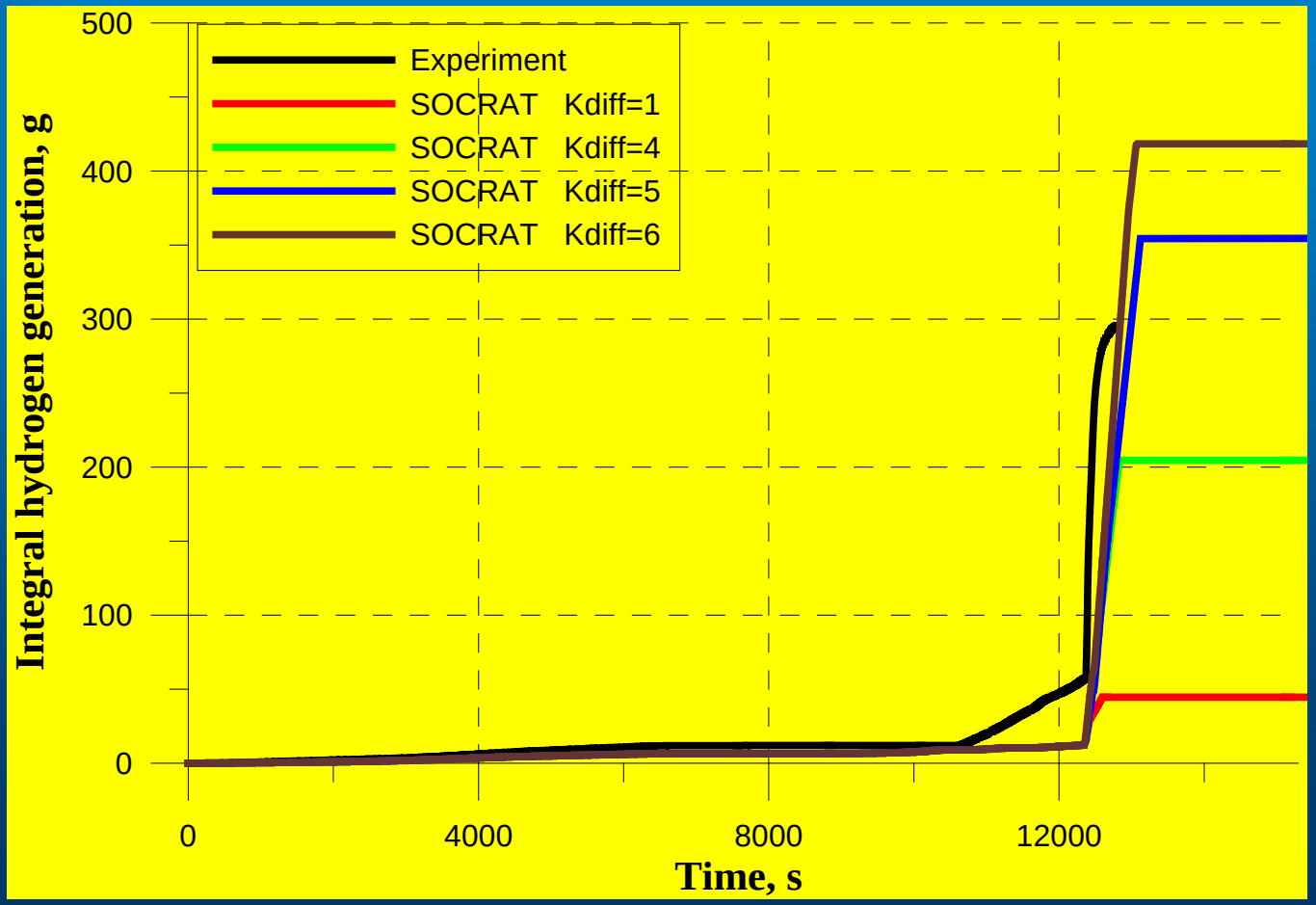
High-temperature oxidation of Zircaloy-4 in steam-nitrogen mixtures.
M. Steinbrück*, F. Oliveira da Silva, H.J. Seifert
NuMat2014: The Nuclear Materials Conference, 27-30 October 2014, Clearwater Beach, Florida, USA.

Summary of High Temperature Oxidation. Influence of Nitrogen Concentration on Kdiff – Enhancement Coefficient for O and N Diffusion

T=1473K

Mixture composition	K_{diff}
O 100% N 0%	1
O 90% N 10%	5
O 80% N 20%	6
O 70% N 30%	7
O 60% N 40%	8
O 50% N 50%	9
O 40% N 60%	5
O 30% N 70%	3

Integral Hydrogen Production



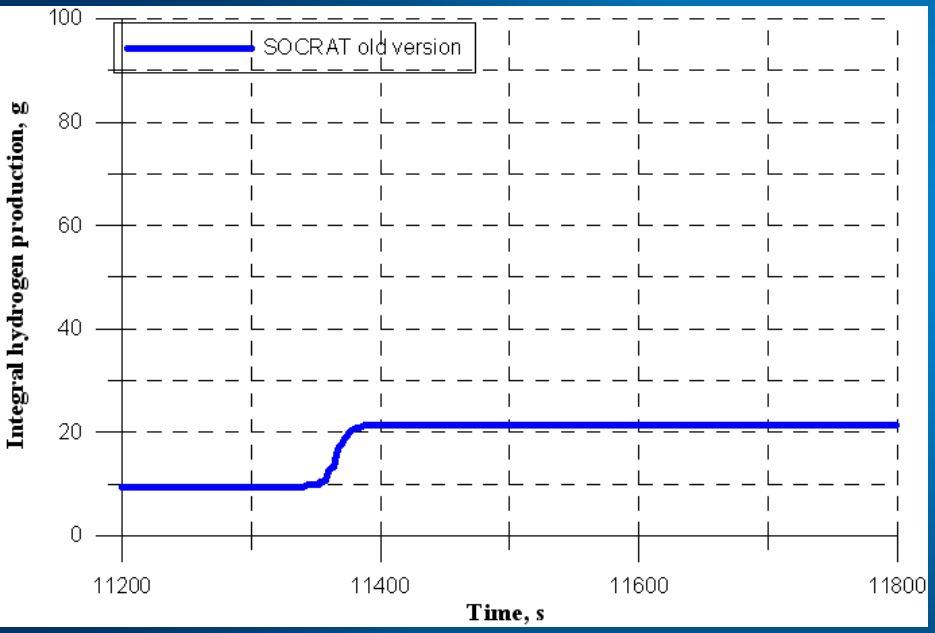
Underestimation of Hydrogen Release at Steam-Air Phase by SOCRAT

Hydrogen generation due to Zr oxidation by steam at steam-air ingress phase is drastically underestimated by code.

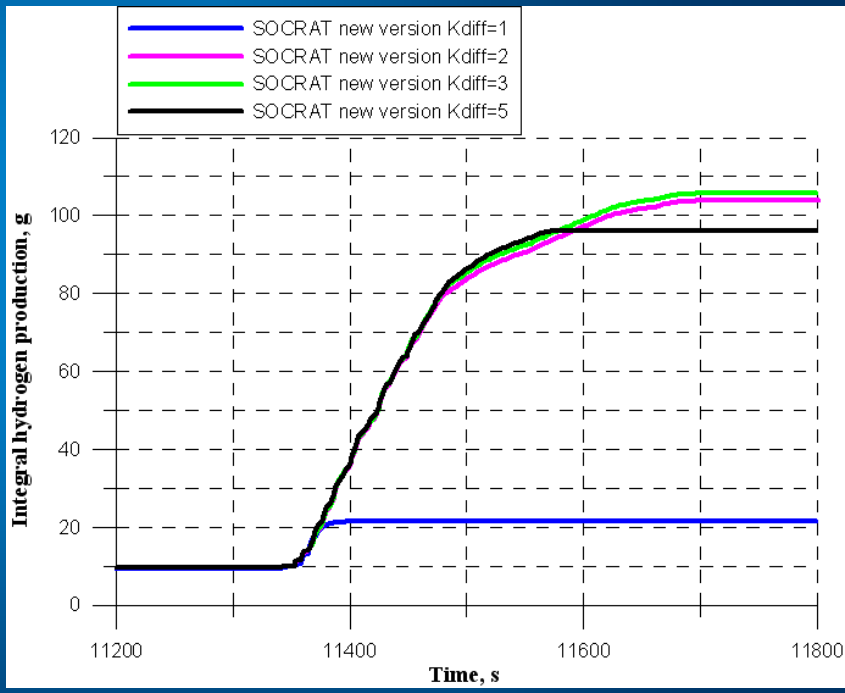
The reason is not adequate consideration of steam mass flow and correspondingly of hydrogen generation.

Retrospective View. QUENCH-16: Calculated Integral Hydrogen Mass Production during Reflood

Ordinary diffusivity in ZrO_2 layer

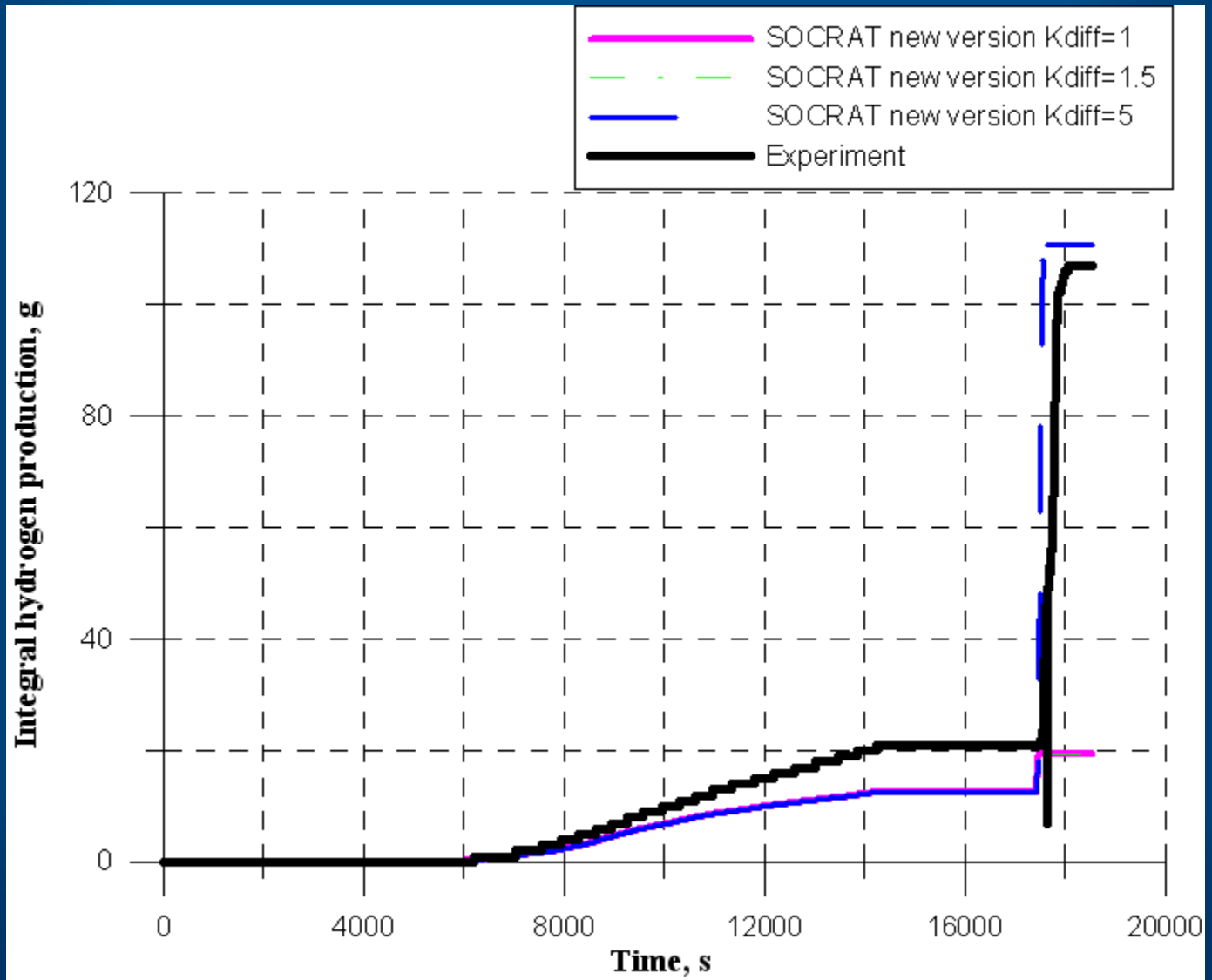


Enhanced diffusivity in ZrO2 layer

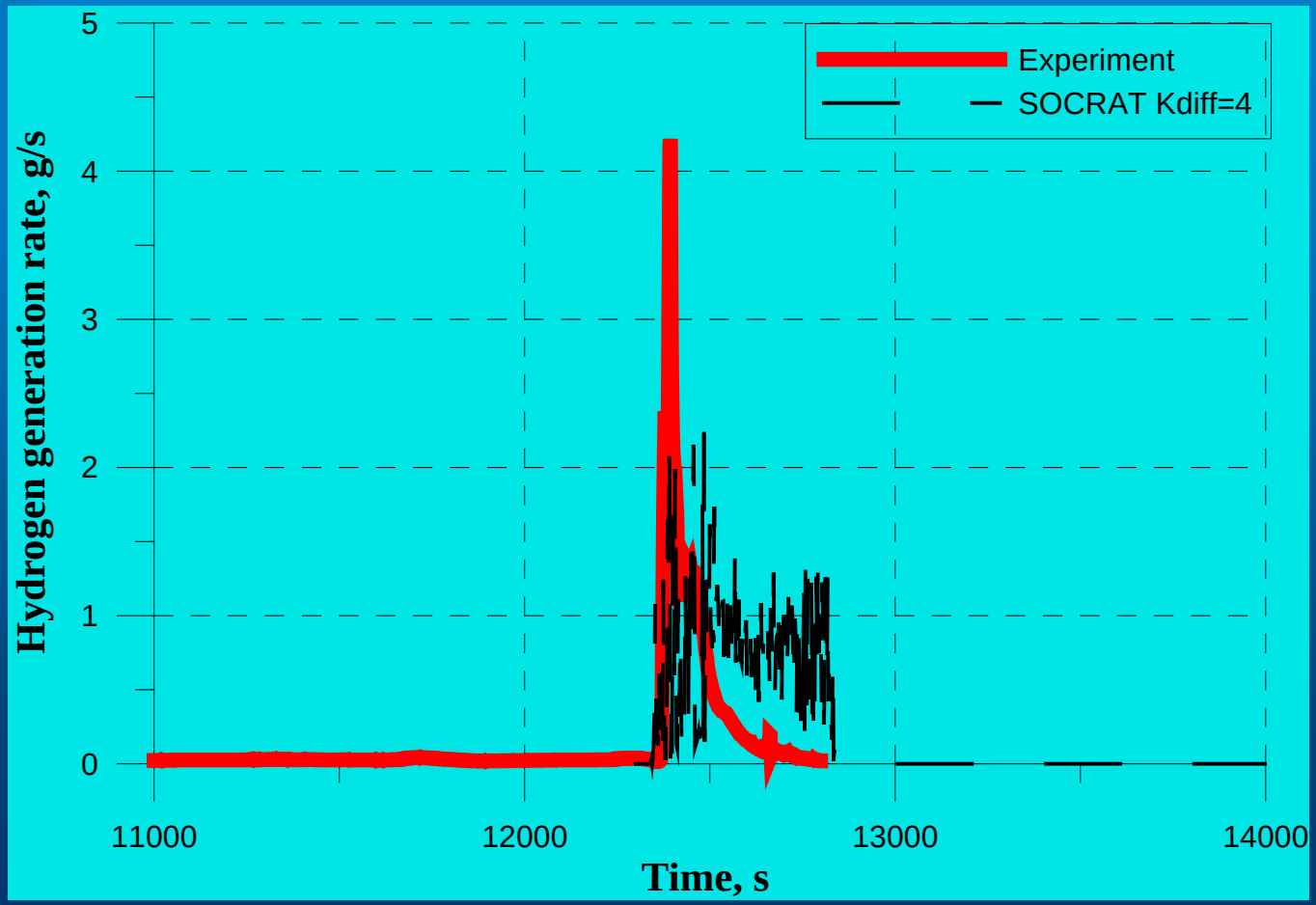


It seems that a huge hydrogen spike is observed in a case of nitrides existence when a maximal temperature before reflood is more than 1600-1700K in contrary to a case of nitrides absence when temperature should be more than 1900K

Retrospective View. PARAMETER-SF4 Hydrogen Production



QUENCH-ALISA
Hydrogen Release Rate



Hydrogen generation rate drops more steeply in experiment compared to calculation!

Summary

Is the end of the rainbow just another lonely place?

The QUENCH-ALISA demonstrated exclusively special interesting bundle behaviour during steam-air ingress phase and reflood. Main findings include:

1. **The reaction of oxygen with Zr has highest priority. If there is oxygen and no local starvation then available steam and nitrogen do not participate.**

2. **The reaction of steam with Zr has second priority and the reaction of nitrogen with Zr has lowest priority in the case of absence of local starvation ;**

3. **Fault of SOCRAT – O_2 and H_2O reactions with Zr have the same priority that is they go simultaneously. Things to do – to change a priority and recalculate;**

4. **A huge amount of hydrogen was produced during the test and it can be modelled by enhanced oxygen diffusion coefficient (or change of parabolic constant) ;**

The QUENCH-ALISA results help us in more deep understanding of very complicated mechanisms accompanying Zr oxidation in H_2O-O_2-N_2 gas mixtures.

Post-test calculation results of QUENCH-18 experiment using different RELAP/SCDAPSIM Mod3.5 code versions and different Zr oxidation correlations

Tadas Kaliatka, Lithuanian Energy Institute, Breslaujos str. 3, LT-44403 Kaunas, Lithuania

ABSTRACT

Experiment QUENCH-18 on air ingress and aerosol release was successfully conducted at KIT on 27 September 2017. The primary aims were to examine the oxidation of M5® claddings in air/steam mixture following a limited pre-oxidation in steam, and to achieve a long period of oxygen and steam starvations to promote interaction with the nitrogen. In general this test consists of three stages: (1) pre-oxidation in steam, (2) period of air ingress, and (3) reflood. QUENCH-18 have big similarities to the earlier air ingress experiments QUENCH-10 and QUENCH-16, however, these two tests were performed without steam flow during the air ingress stage.

For the analysis of the QUENCH-18 experiment the RELAP/SCDAPSIM code was used. This code is the semi-mechanistic lumped parameter code for transient analysis of a reactor core and coolant system. The latest code concept is Mod3.5. This code concept implies several new zirconium oxidation correlations in steam and air ambient implemented by Innovative Systems Software (code maintenance group) and Paul Scherrer Institute. However, this code concept is not fixed and available only for the participants of SCDAP Development and Training Program. For this reason it is available different versions of RELAP/SCDAPSIM Mod3.5 code. For the analysis of the QUENCH-18 two RELAP/SCDAPSIM Mod3.5 code version are used: 1) [dg] and 2) [dp]. QUENCH-18 experiment modelling results received using different code versions were compared with experimental data. Calculation results showed significant differences, this difference must be discussed with the code developers. Additionally, the influence of the different zirconium oxidation correlations to the maximal bundle temperature and hydrogen generation were investigated.


TOSHIBA

LITHUANIAN ENERGY INSTITUTE
http://www.lei.lt

NATIONAL OPEN ACCESS SCIENTIFIC CENTRE FOR FUTURE ENERGY TECHNOLOGIES

OPEN R & D LITHUANIA

Post-test calculation results of QUENCH experiments using different RELAP/SCDAPSIM Mod3.5 code versions

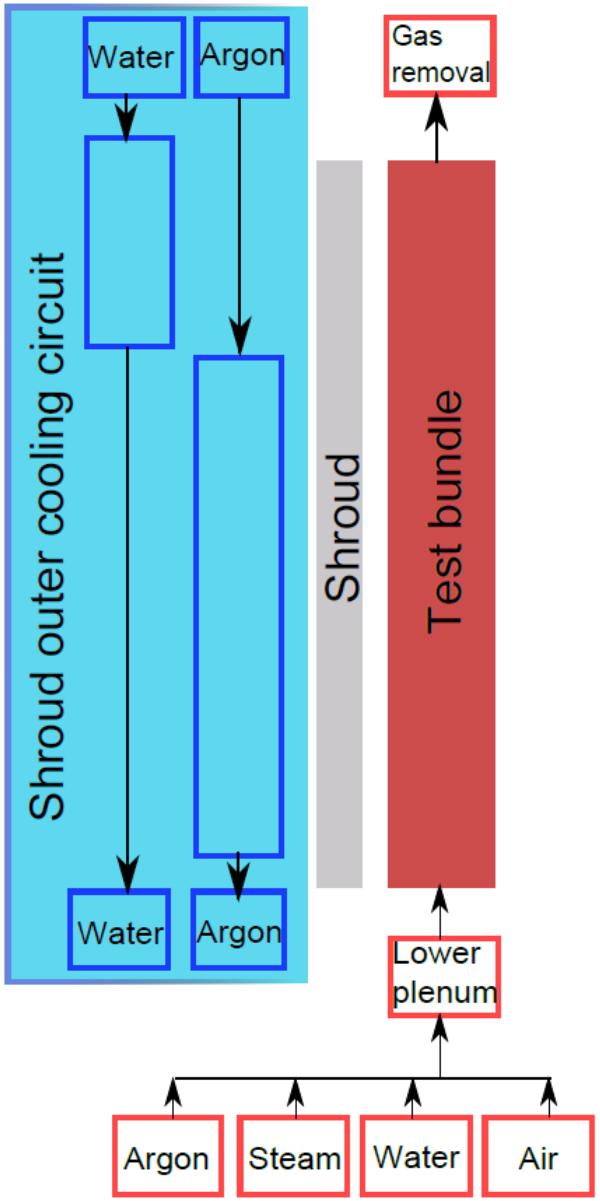
Tadas Kaliatka

Outline

- Modelling and results of QUENCH-10
  - Comparison of results of different code versions
- Modelling and results of QUENCH-18
  - Influence of different code versions
  - Influence of different calculations of heat transfer due to radiation
  - Influence of different oxidation models

QUENCH-10

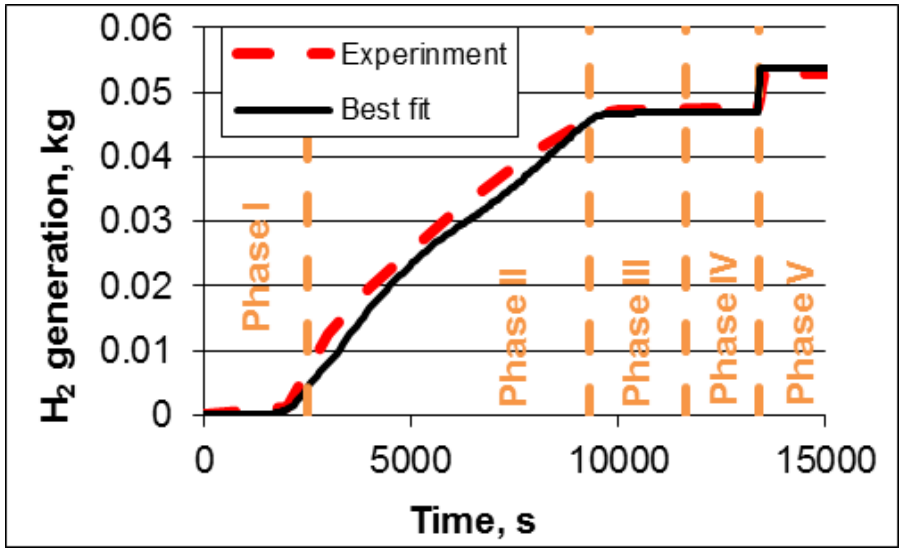
RELAP/SCDAPSIM model of the QUENCH test



- RELAP module (thermal hydraulics):
  - All Elements

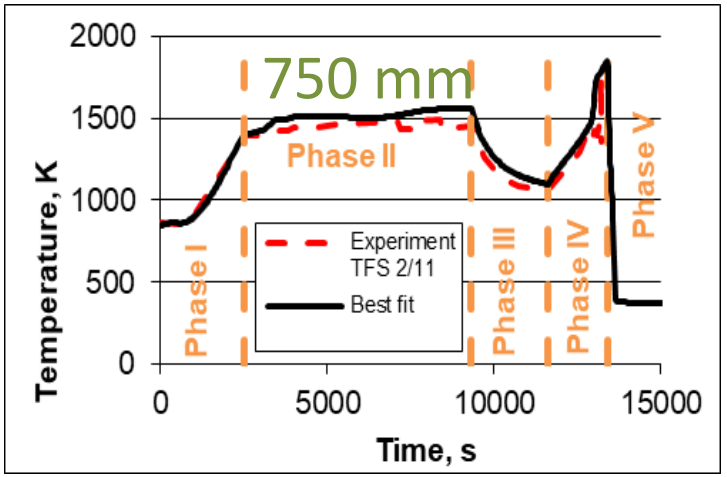
- SCDAP module (behaviour of the core and vessel structures):
  - component 1 - one central rod (not heated), modelled as a "fuel" element is composed of ZrO_2 pellets in the centre, a gas-filled gap and cladding of Zircaloy;
  - component 2 - 8 heated rods (around the central rod) which simulates heated fuel rods, modelled using "Cora" component which is composed of tungsten heating elements in the centre, ZrO_2 pellets, gas-filled gap and cladding of Zircaloy;
  - component 3 - 12 heated rods, modelled using "Cora" component;
  - component 4 - the four rods in the corners, modelled as "fuel" component;
  - component 5 – shroud of the bundle, modelled as "shroud" component, which consists of the inner Zircaloy layer, an insulating layer of ZrO_2 and Inconel layer (using properties of stainless steel).

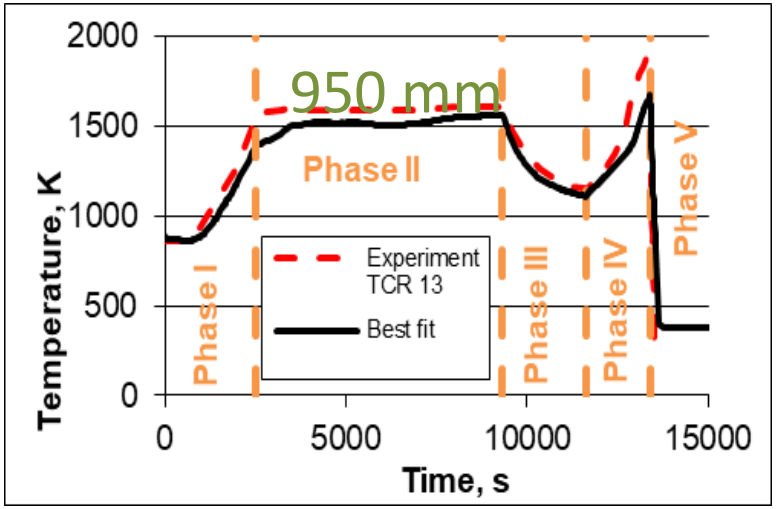
QUENCH-10 test



RELAP/SCDAPSIM Mod3.5 [dp]

Calculation results using Cathcart-Pawel/Urbanic-Heidrick and MOZART oxidation models and **3.8 mOhm** resistance of sliding contacts are presented





QUENCH-10 test

RELAP/SCDAPSIM Mod3.5 [dp]

Nuclear Engineering and Design 337 (2018) 341–350

Contents lists available at ScienceDirect

Nuclear Engineering and Design

journal homepage: www.elsevier.com/locate/nucengdes

Modelling of severe accidents in spent fuel pools, analysis of the heat-up of the fuel assemblies in the steam and air environment

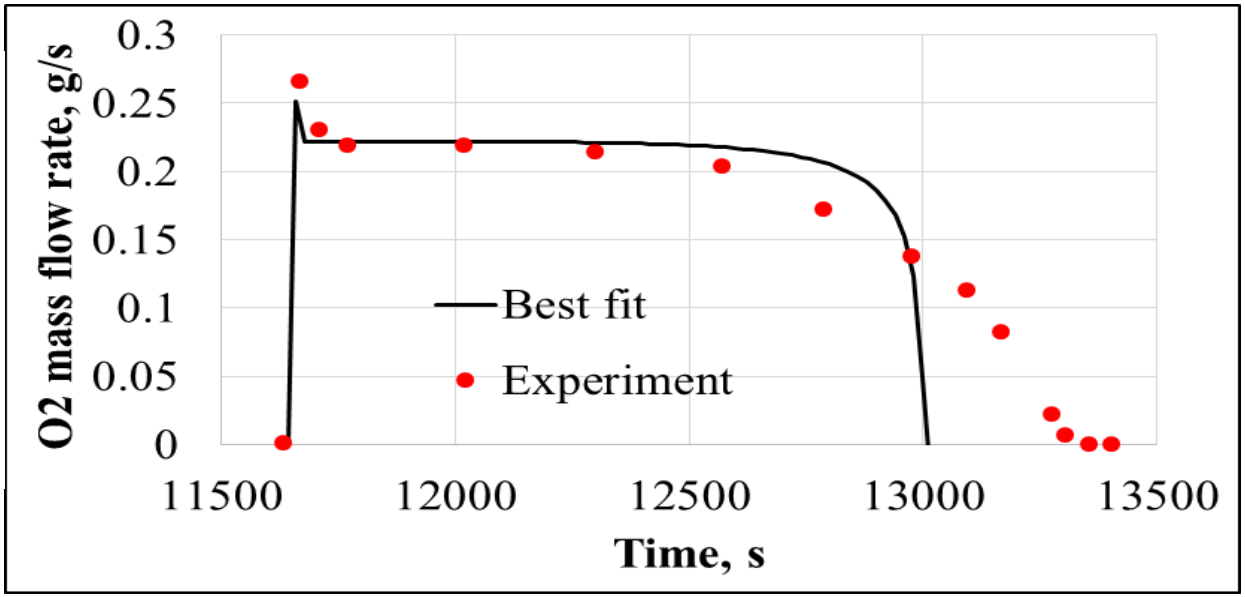
Tadas Kaliatka[a,*], Algirdas Kaliatka[a], Judy K. Hohorst[b], Chris M. Allison[b]

[a] Lithuanian Energy Institute, Breslaujos Str. 3, LT-44403 Kaunas, Lithuania
[b] Innovative Systems Software, 3585 Briar Creek, Ammon Idaho 83406, USA

ARTICLE INFO

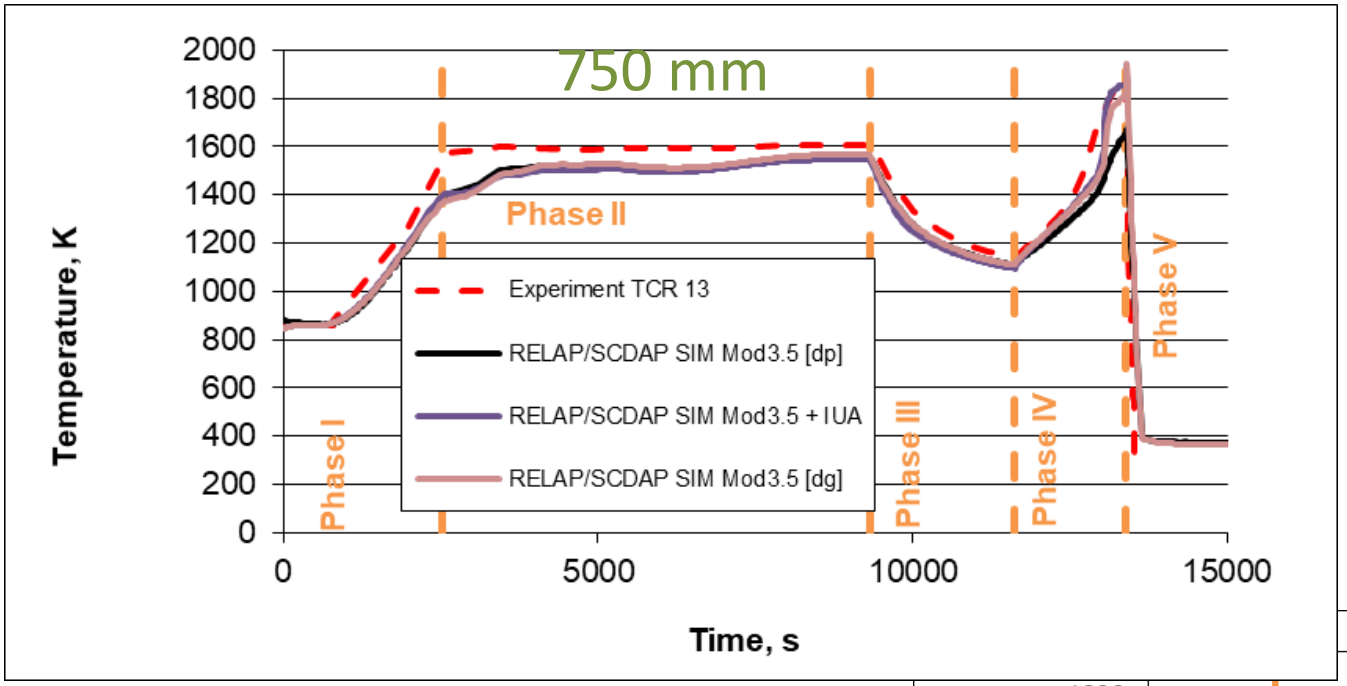
Keywords:
QUENCH-10

https://doi.org/10.1016/j.nucengdes.2018.07.016



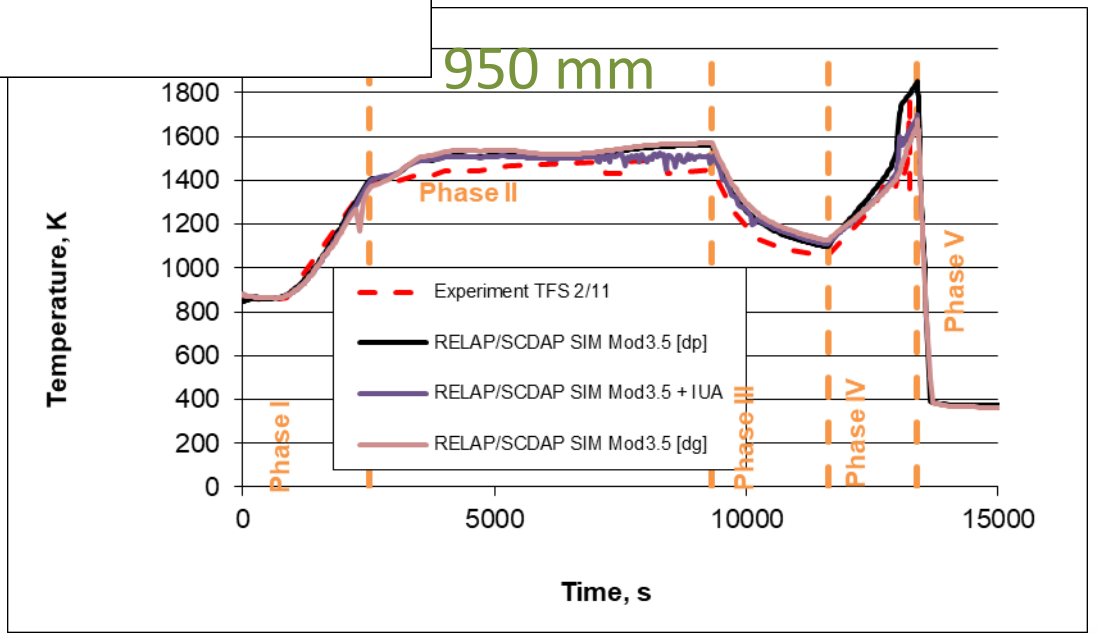
Conclusion: The PSI developed oxidation model using the Cathcart-Pawel/Urbanic-Heidrick and MOZART oxidation correlations reasonably reflects the experimental data and sufficiently replicates the measured data of QUENCH-10 test.

Comparison of different versions

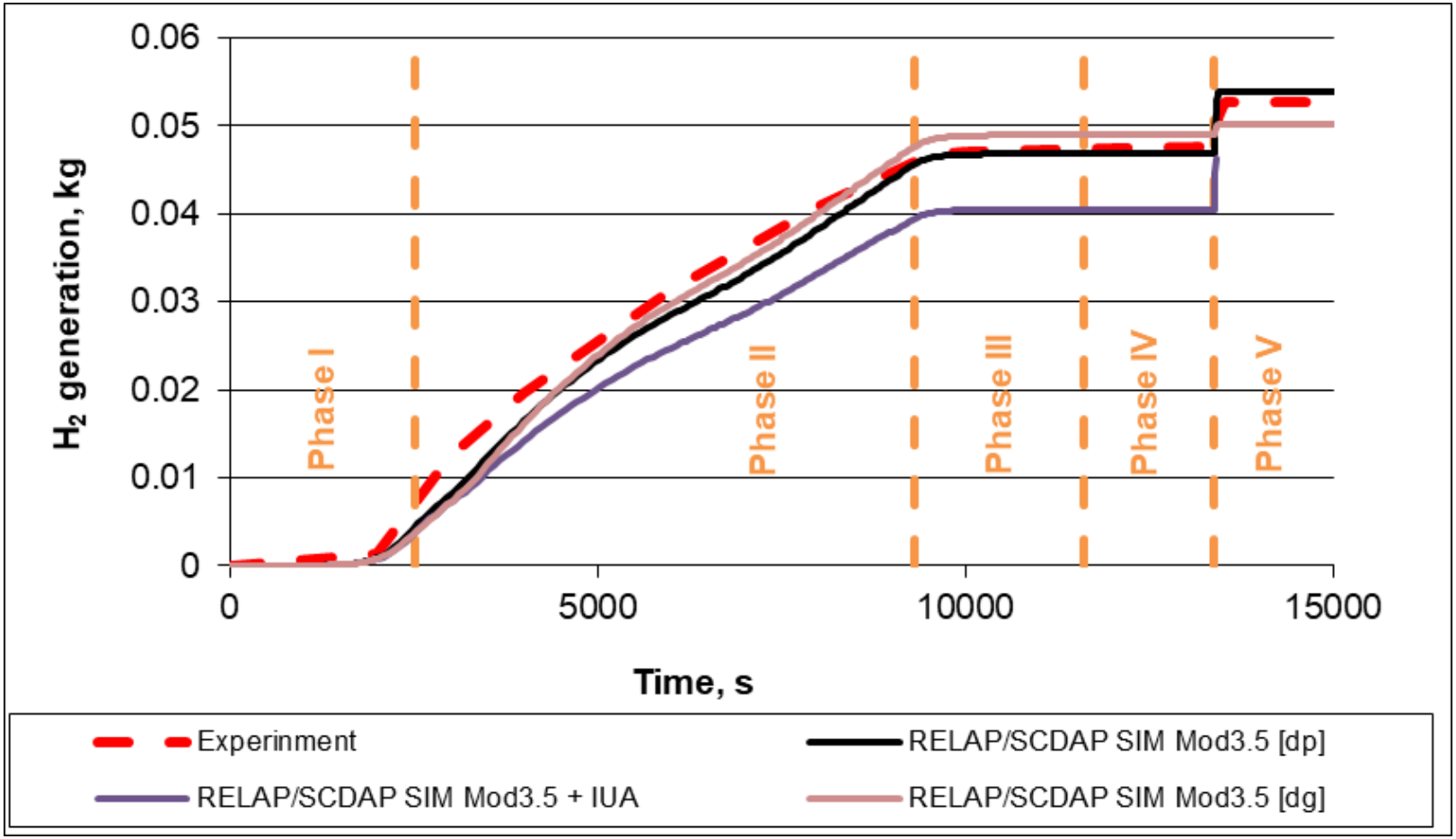


The same input deck was used for the calculations using different code versions

Calculations using *RELAP/SCDAP SIM Mod3.5 + IUA* was terminated due to failure at the quenching phase

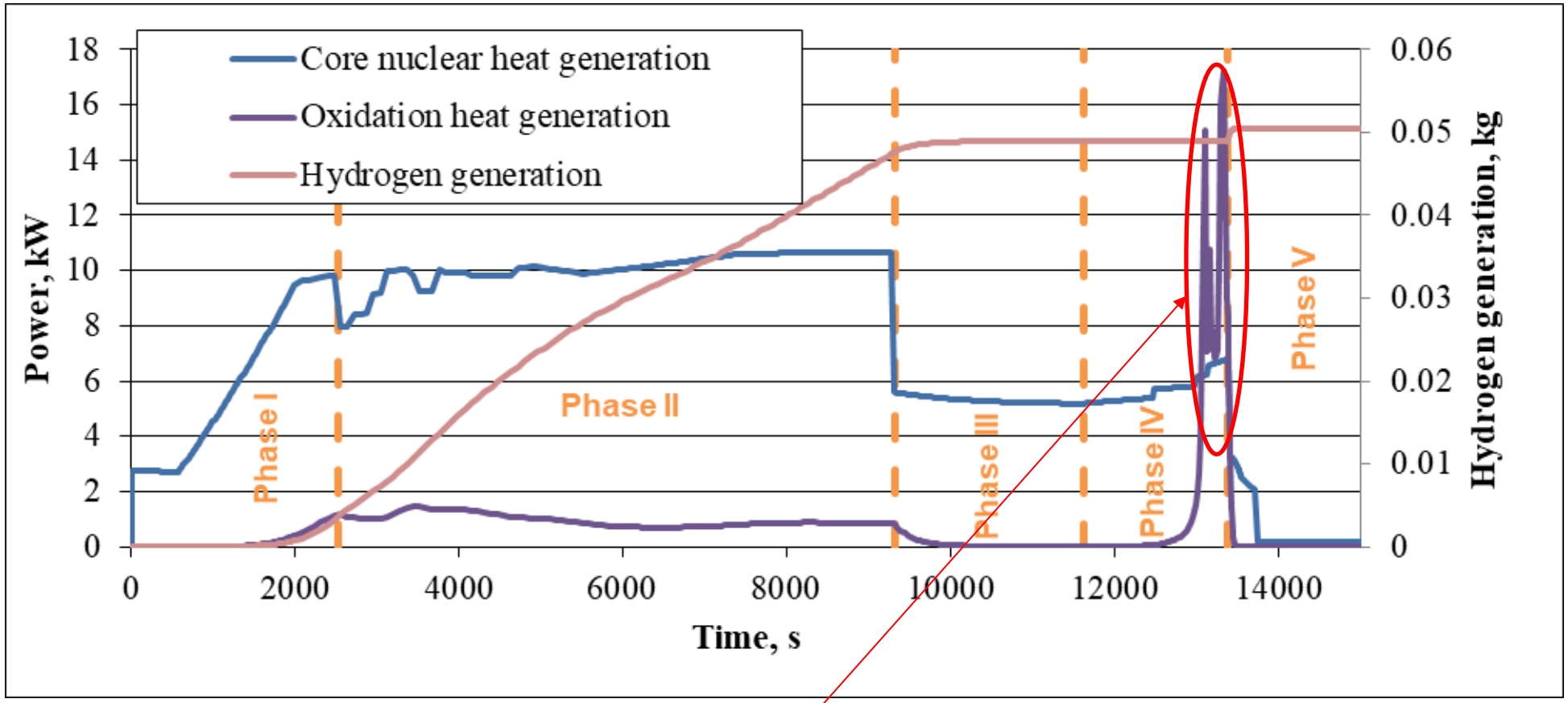


Comparison of different versions



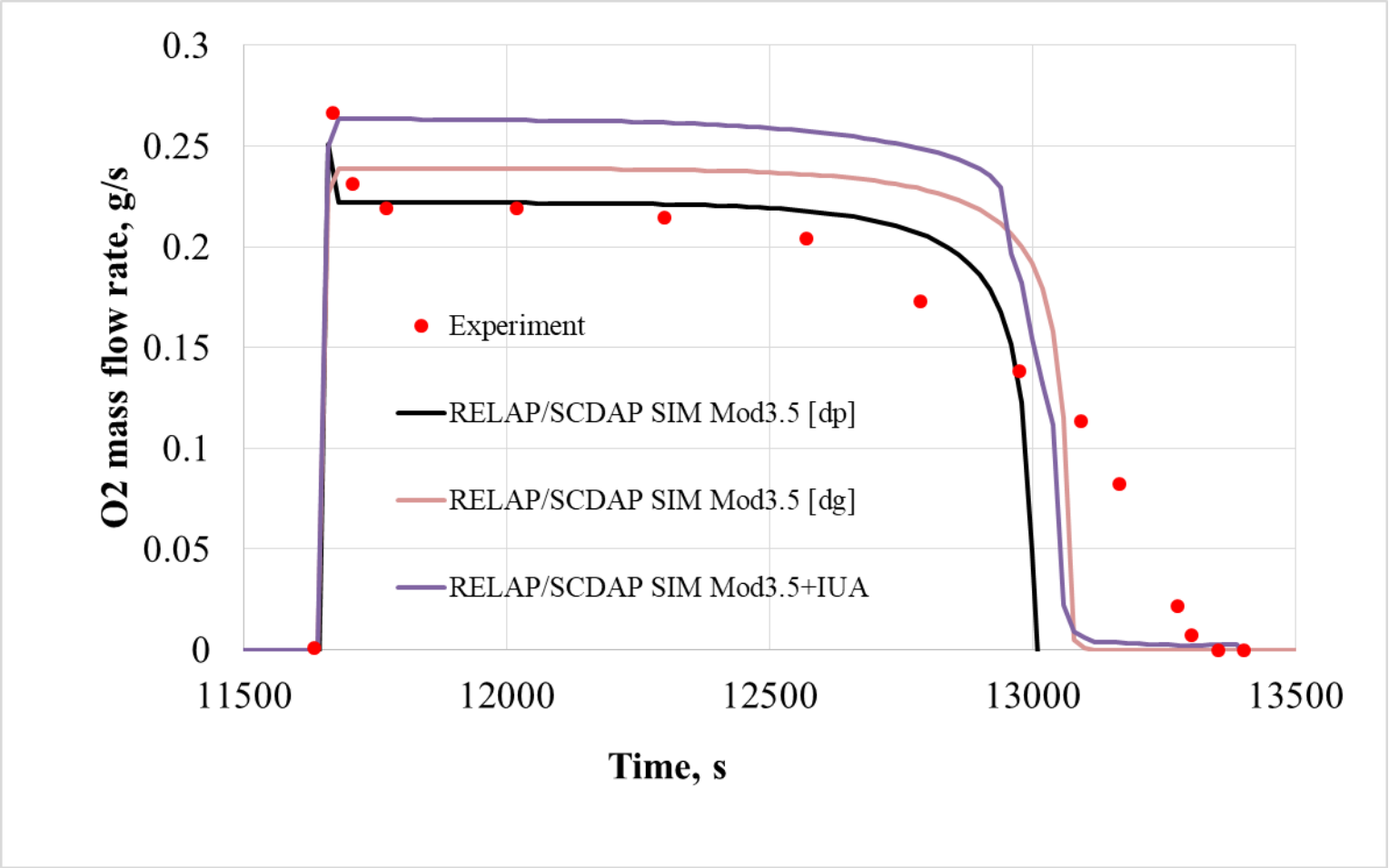
Despite the similarities of the calculated temperatures – the hydrogen generation were received different.

RELAP/SCDAPSIM Mod3.5 [dg]



The calculated amount of the hydrogen generation do not correlates to the amount of the power generated due to oxidation

Comparison of different versions



Significant calculation differences were observed also in the oxygen flow rate during air ingress phase.

ALISA/QUENCH-18

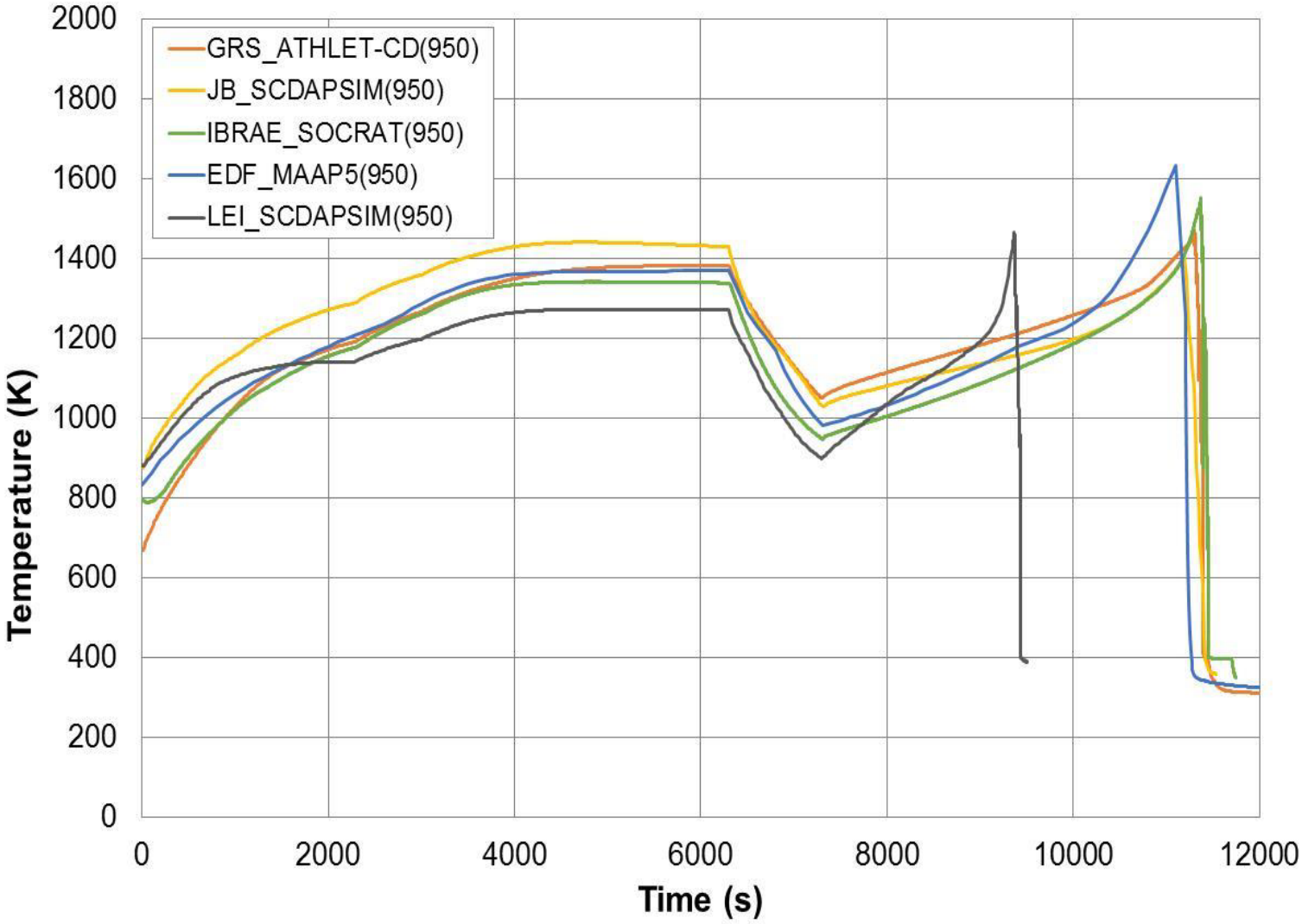
Air together with steam injected after pre-oxidation phase

Pre-test calculations

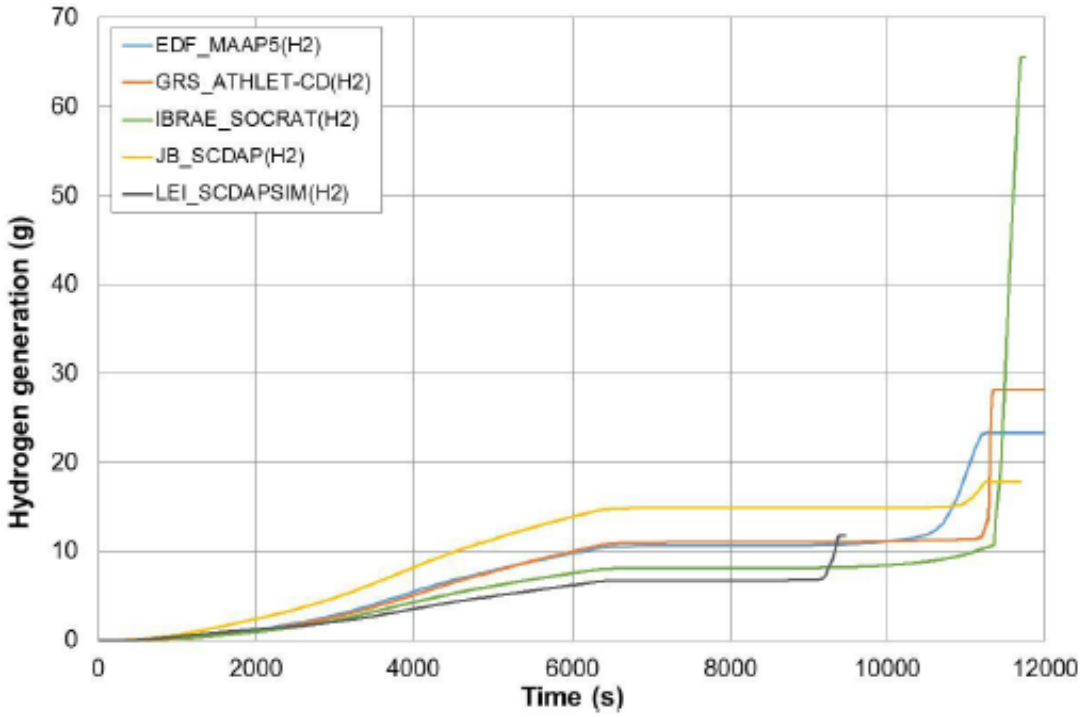
Participants:

- GRS ATHLET-CD
- EDF MAAP5
- Jon Birchley SCDAPSim/35/psi/lfm
- LEI RELAP/SCDAPSIM/MOD3.5[dp]
- IBRAE SOCRAT

Temperatures at 950 mm

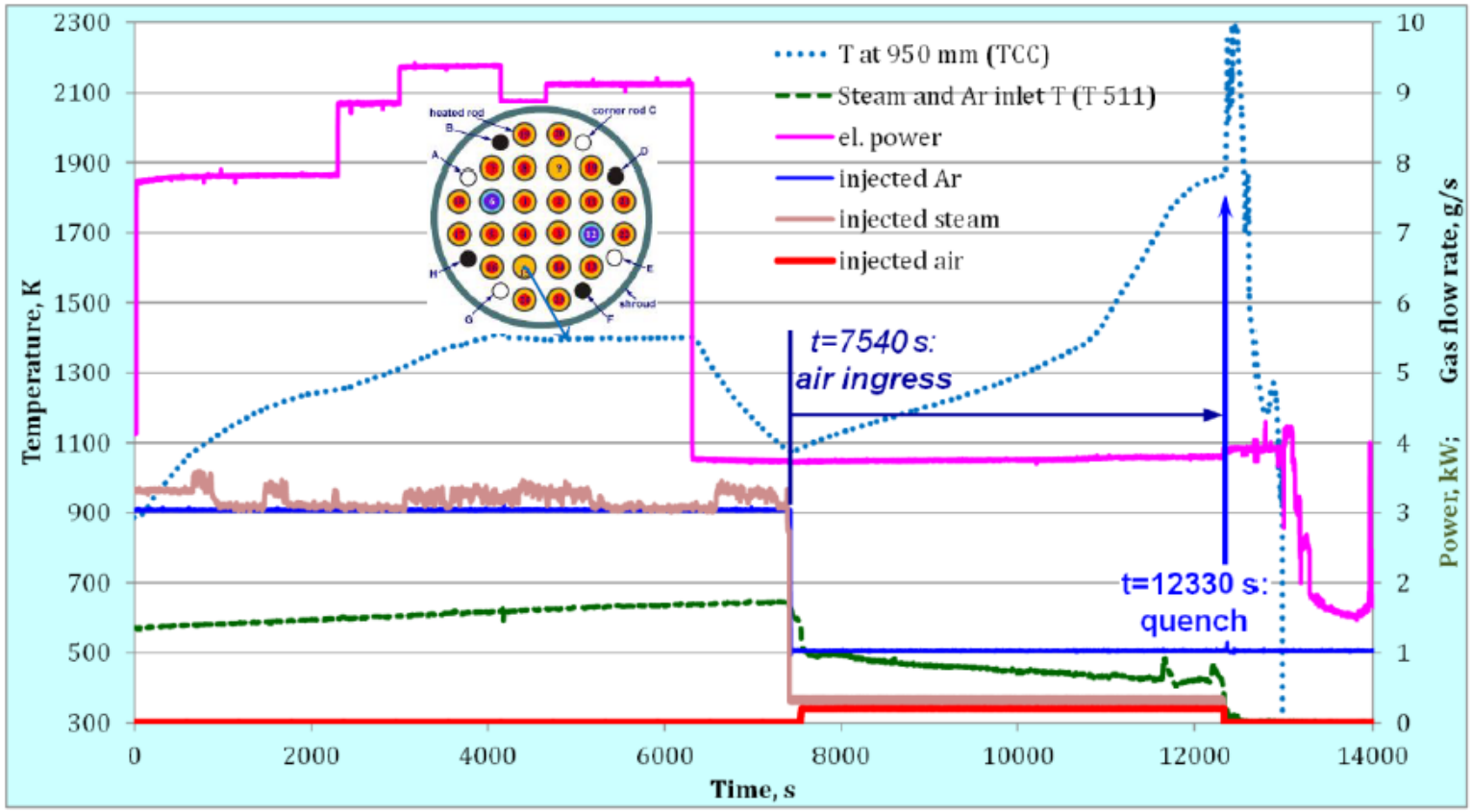


Hydrogen Generation

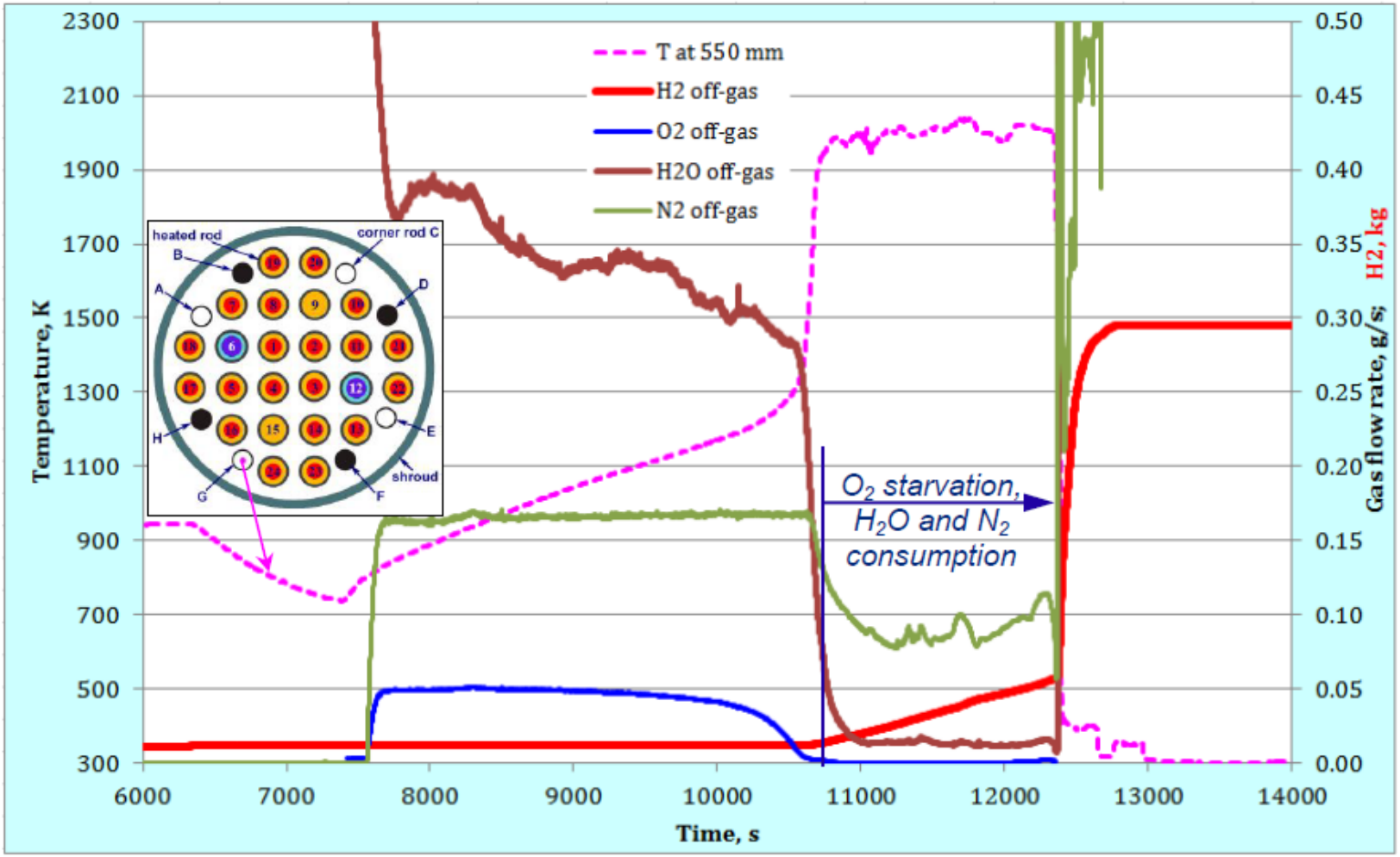


		ATHLET-CD	MAAP5	SCDAPSim (JB)	RELAP/ SCDAPSIM (LEI)	SOCRAT
Total H_2 generation (g)	end of pre-oxidation	11.0 g	10.7 g	14.9 g	6.8 g	8.1 g
	end of reflood	28.2 g	23.5 g	17.9 g	11.8 g	65.5 g

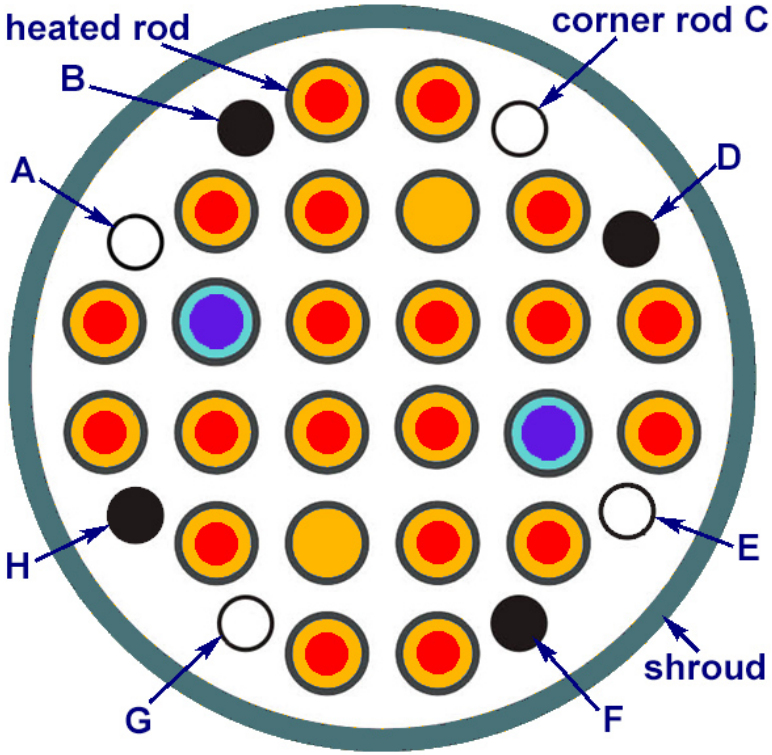
Post-test

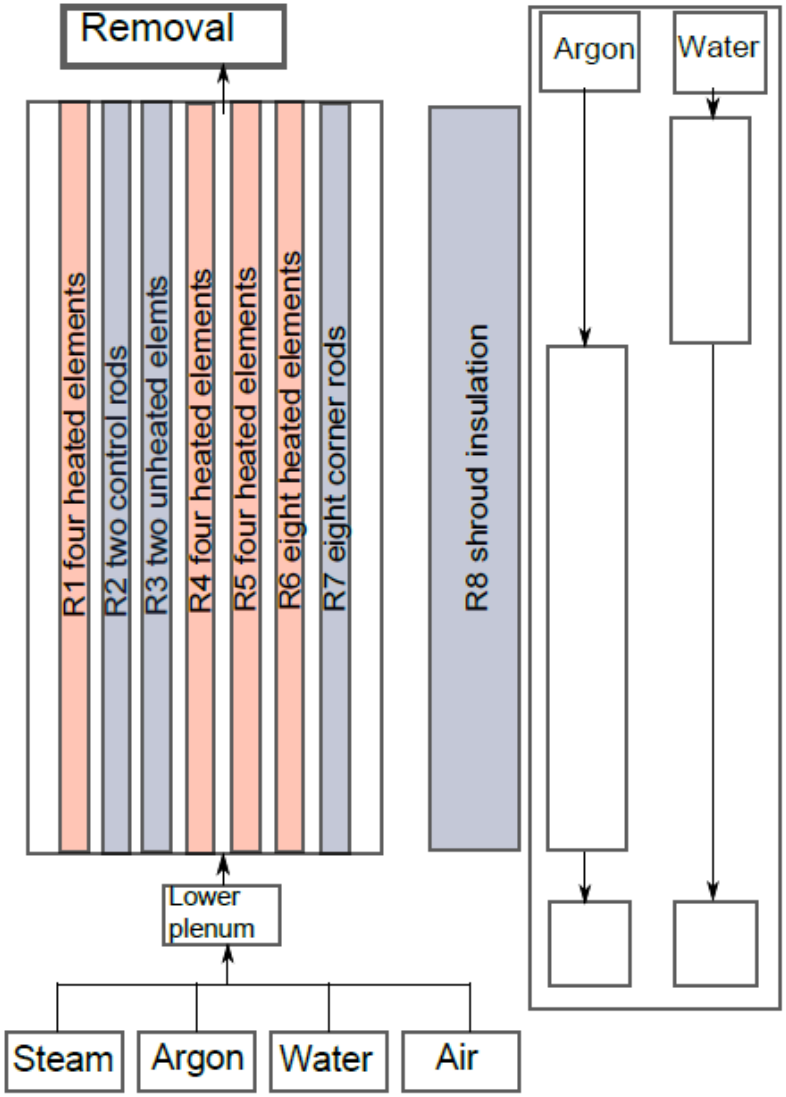

T at 950 mm (TCC)
Steam and Ar inlet T (T 511)
el. power
injected Ar
injected steam
injected air
t=7540 s:
air ingress
t=12330 s:
quench
heated rod
corner rod C
shroud
Temperature, K
Power, kW; Gas flow rate, g/s
Time, s
2300
2100
1900
1700
1500
1300
1100
900
700
500
300
10
9
8
7
6
5
4
3
2
1
0
0
2000
4000
6000
8000
10000
12000
14000

Post-test


T at 550 mm
H2 off-gas
O2 off-gas
H2O off-gas
N2 off-gas
heated rod
corner rod C
shroud
A
B
D
E
F
G
H
O2 starvation, H2O and N2 consumption
Temperature, K
Gas flow rate, g/s; H2, kg
Time, s
2300
2100
1900
1700
1500
1300
1100
900
700
500
300
0.50
0.45
0.40
0.35
0.30
0.25
0.20
0.15
0.10
0.05
0.00
6000
7000
8000
9000
10000
11000
12000
13000
14000

Post-test calculations



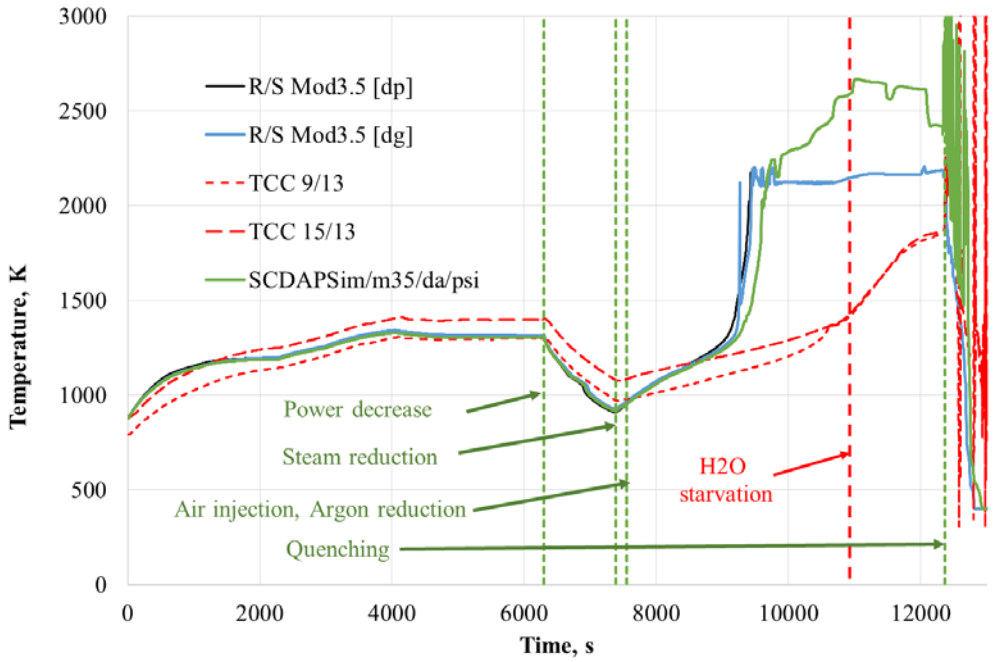


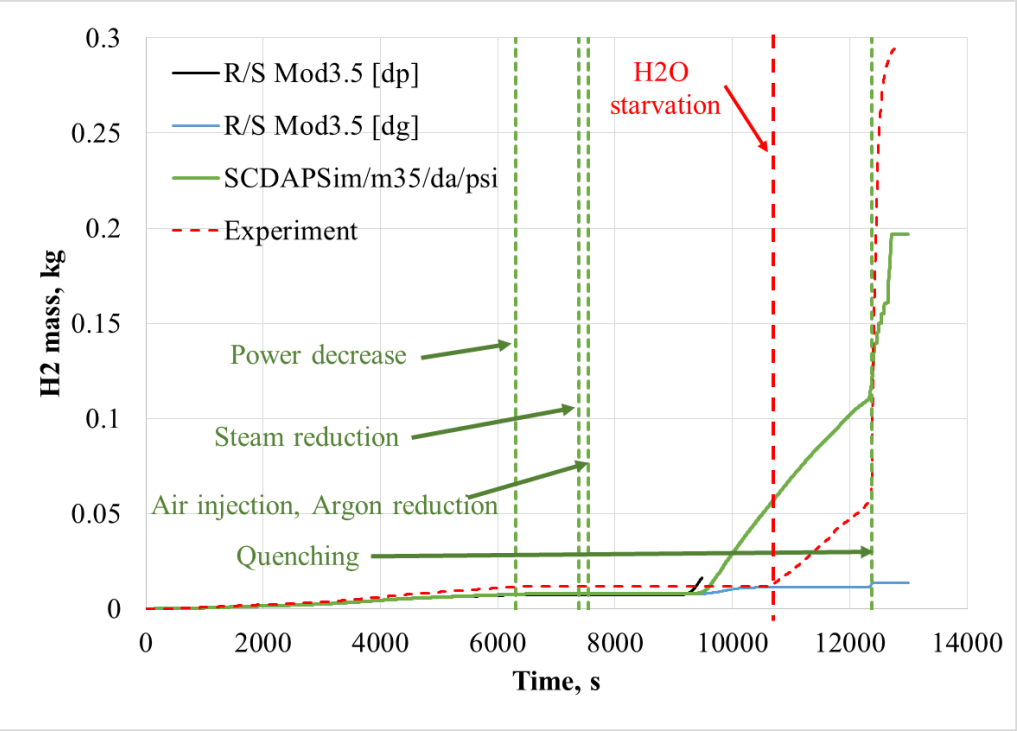
Reflood injection reduced from 52 g/s to 12 g/s for a period of 250 s starting 70 s after reflood initiation during which the observed water level remained roughly constant.



Influence of different code versions

Post-test calculations Influence of different code versions

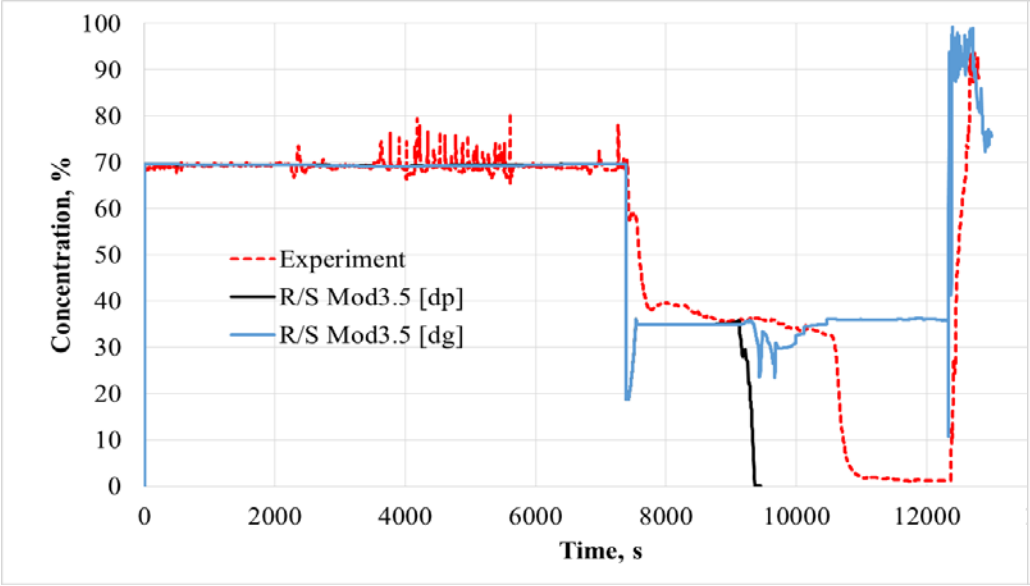




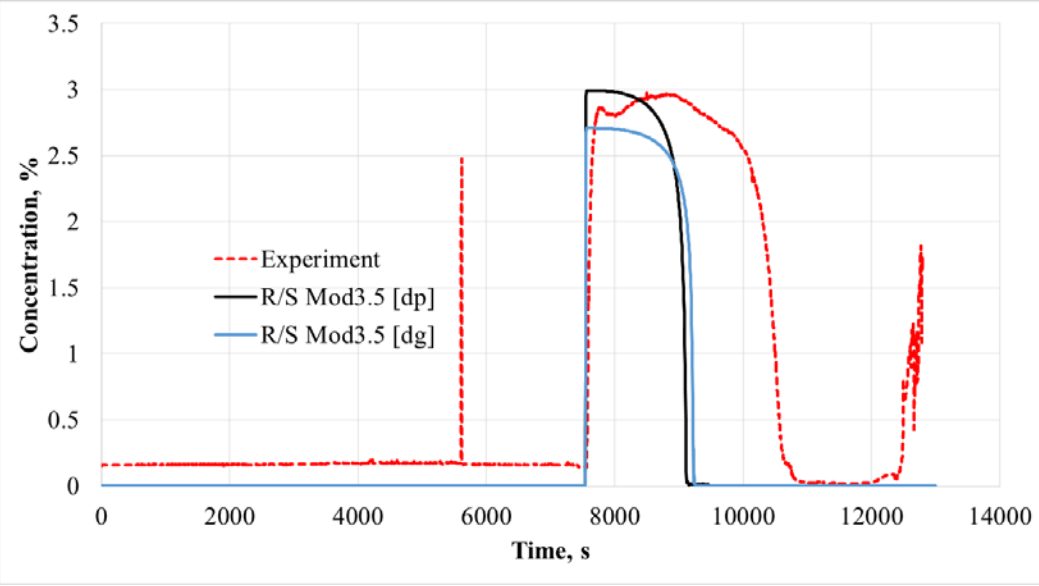
- **R/S Mod3.5 + IUA** was terminated by failure at the first second of the calculation.
- **R/S Mod3.5 [dp]** calculations were terminated by failure approx.. in the middle of the air injection phase, when steam consumption and O2 starvation were observed.
- **R/S Mod3.5 [dg]** calculations results were also strange for H2 generation and steam consumption.
- **SCDAPSim/m35/da/psi** calculations made by J. Birchley using my input deck and his program version.

The calculation results observed using **SCDAPSim/m35/da/psi** were closest to the experimental data

Influence of different code versions



H2O consumption

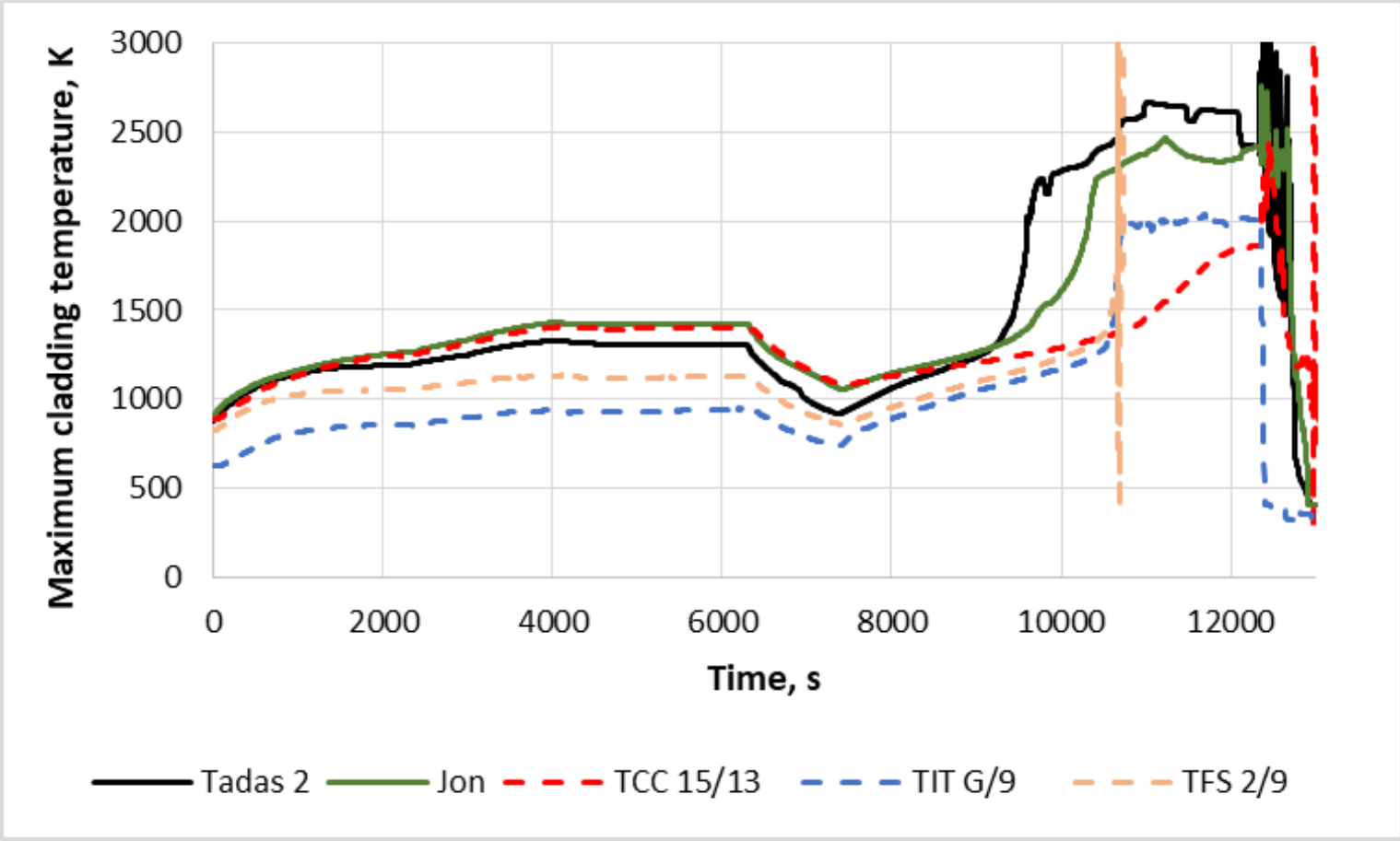


O2 starvation

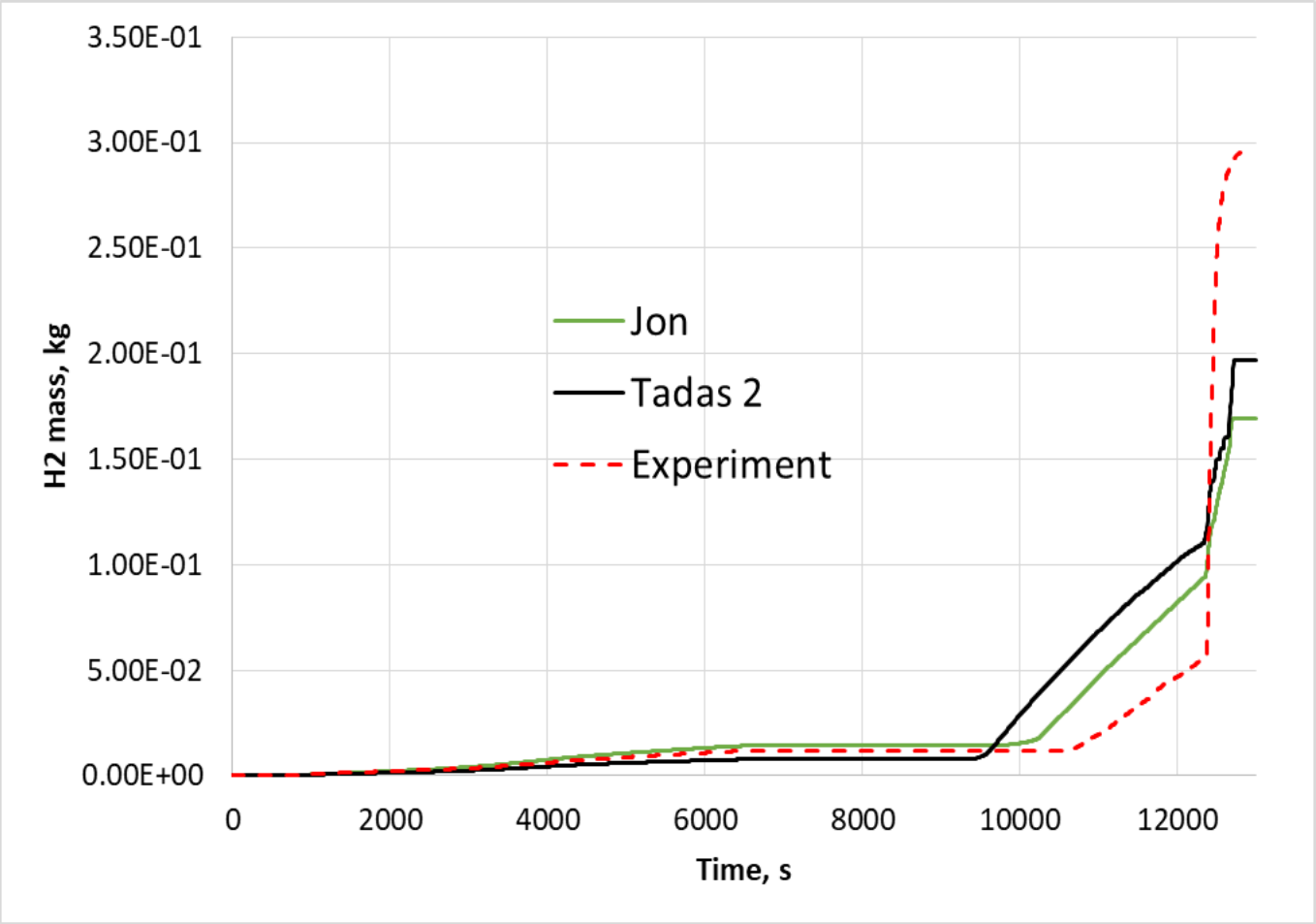
- **R/S Mod3.5 [dp]** calculations were terminated some seconds when steam consumption and O2 starvation were observed.
- **R/S Mod3.5 [dg]** calculations results again is strange for H2O consumption.

SCDAPSim/m35/da/psi

- Calculation was provided using the same code version but using different input models (provided by J. Birchley and me) of QUENCH-18 test.
- Calculations have been provided using code version SCDAPSim/m35/da/psi by J. Birchley.



SCDAPSim/m35/da/psi



The input models were different by several aspects: different oxidation correlations used, slightly different initial parameter and conditions, different nodalization, etc. Calculation results is not in good agreement, however the trend is similar and results are logical.

Both input models have not good agreement with experimental data, but with some “tuning” it would be possible to get better agreement.

Influence of different calculations of heat transfer due to radiation

Influence of different calculation of the heat transfer due to radiation

- Specified radiation view factors and path lengths

```
49110000  bundle
49111000    1      2      3      4      5      6      7      8
49111001  .3397 .1483 .1143 .2285 .1173 .0316 .0000 .0203     ** v
49111002  .2264 .0000 .0272 .2128 .1306 .2264 .0804 .0962
49111003  .2285 .0356 .0000 .2127 .1270 .2285 .0786 .0891
49111004  .2285 .1394 .1064 .0316 .1270 .2285 .0786 .0600
49111005  .1173 .0855 .0635 .1270 .0000 .2044 .1573 .2450
49111006  .0158 .0742 .0571 .1143 .1022 .1270 .0786 .4308
49111007  .0000 .0417 .0311 .0623 .1245 .1245 .0541 .5618
49111008  .0093 .0289 .0204 .0274 .1122 .3945 .3249 .0824
*
*            1      2      3      4      5      6      7      8
49111101  0.0000 0.0126 0.0126 0.0126 0.0252 0.0252 0.0252 0.0378
49111102  0.0126 0.0378 0.0378 0.0126 0.0126 0.0126 0.0126 0.0252
49111103  0.0126 0.0378 0.0378 0.0126 0.0126 0.0126 0.0252 0.0252
49111104  0.0126 0.0252 0.0126 0.0252 0.0126 0.0126 0.0126 0.0252
49111105  0.0252 0.0126 0.0189 0.0126 0.0378 0.0252 0.0126 0.0126
49111106  0.0252 0.0189 0.0189 0.0126 0.0126 0.0378 0.0126 0.0126
49111107  0.0252 0.0189 0.0189 0.0252 0.0126 0.0126 0.0252 0.0126
49111108  0.0378 0.0252 0.0252 0.0252 0.0189 0.0126 0.0126 0.0000
```

View factors were calculated by A.D. Vasiliev

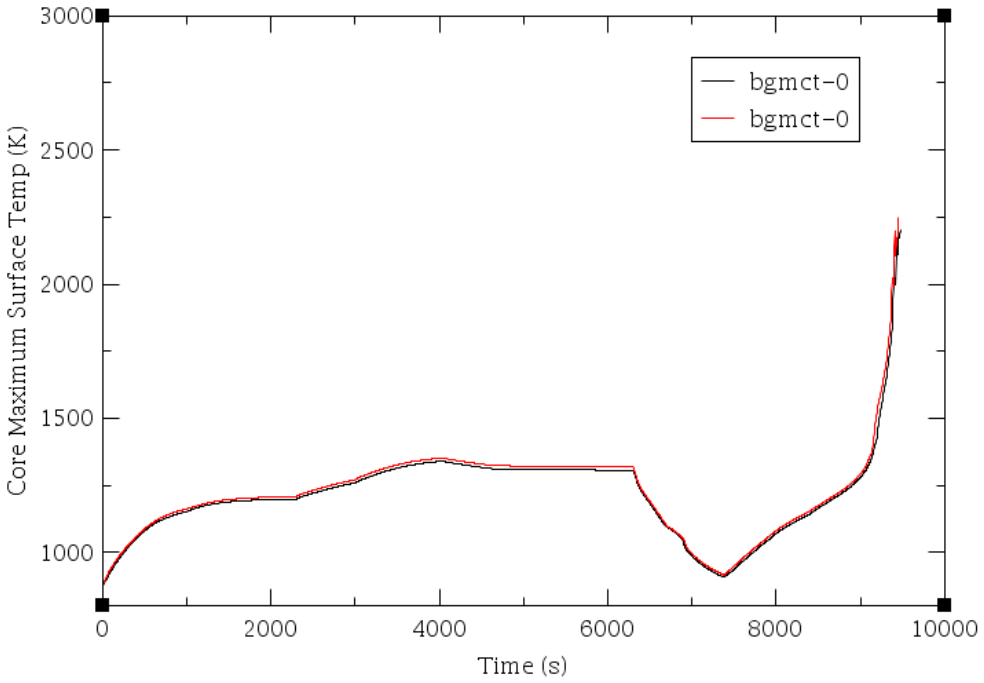
- View factors and path lengths automatically generated

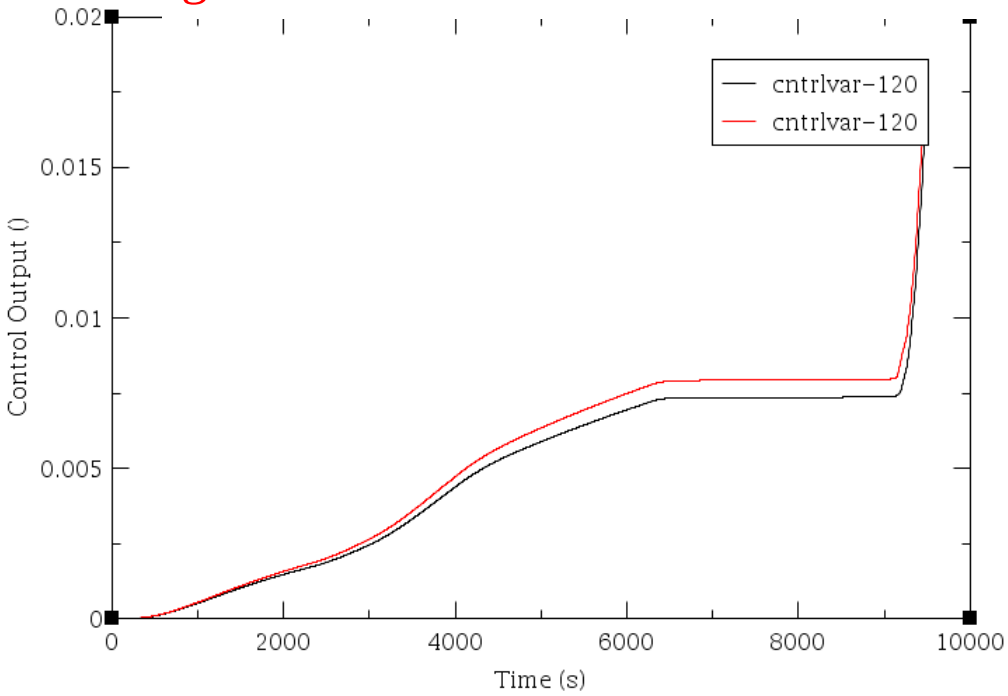
```
* radiation heat transfer input
49010000  bundle
49012000  0.0126 8
49012001  0, 7, 6, 6, 7, 0
49012002  7, 2, 4, 3, 5, 7
49012003  6, 5, 1, 1, 4, 6
49012004  6, 4, 1, 1, 5, 6
49012005  7, 5, 3, 4, 2, 7
49012006  0, 7, 6, 6, 7, 0
```

Influence of different calculation of the heat transfer due to radiation

- R/S Mod3.5[dp]
- View factors and path lengths:
  - **Generated automatically**
  - **Specified**

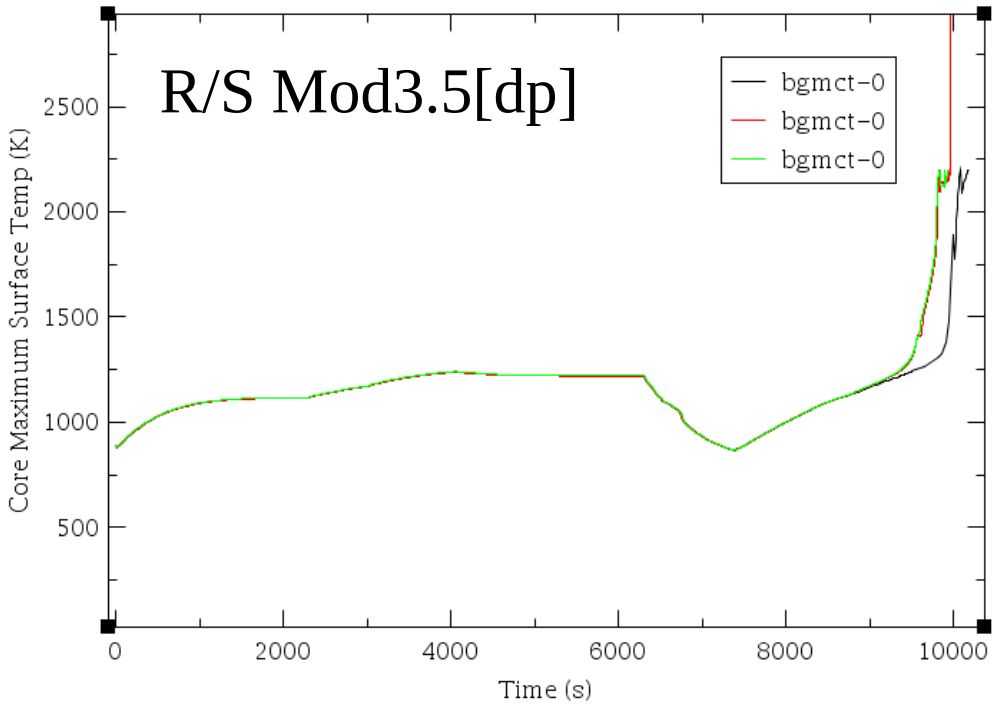
Influence of different calculations of heat transfer due to radiation showed very small temperature changes, however this temperature changes are very significant to the hydrogen generation.

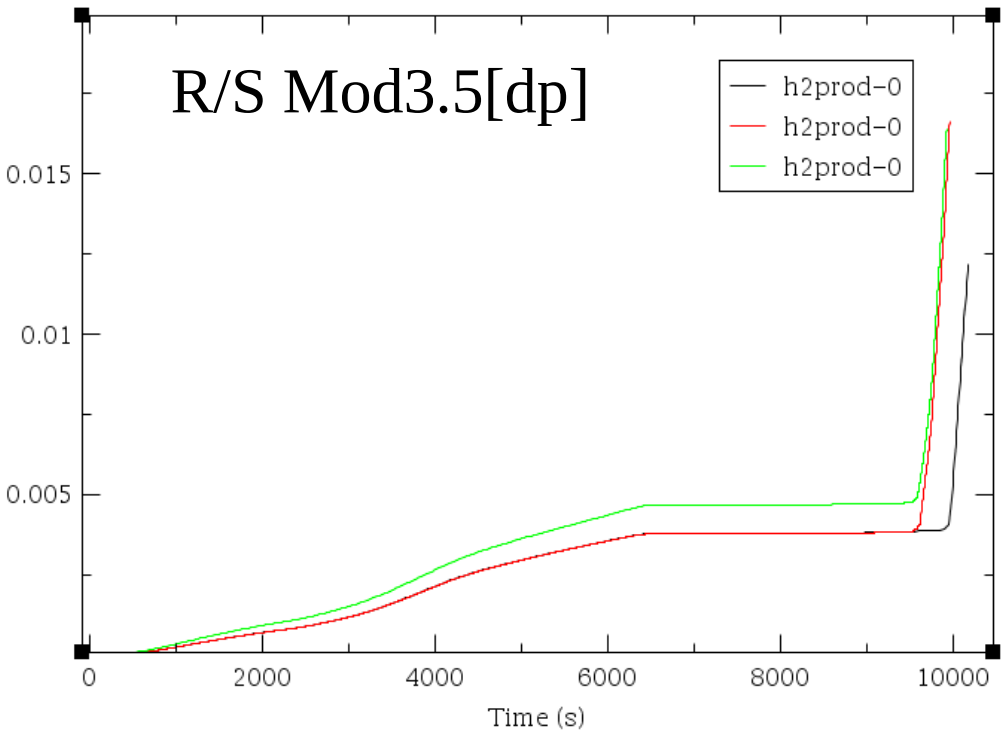




Influence of different oxidation models

Influence of different oxidation models





- Calculation results - Leistikov-Schanz/Prater-Courtwright and MOZART oxidation models (Recommendations after QUENCH-10 calculation)
- Calculation results - Leistikov-Schanz/Prater-Courtwright and Hofmann-Birchley oxidation models (Recommended by Gerhard Schanz of KIT)
- Calculation results - Cathcart-Pawel/Urbanic-Heidrick and Hofmann-Birchley oxidation models (Default option in R/S)

Conclusions

- The latest RELAP/SCDAPSIM code concept is Mod3.5. This code concept implies several new zirconium oxidation correlations in steam and air ambient implemented by Innovative Systems Software (code maintenance group) and Paul Scherrer Institute. However, this code concept is not fixed and available only for the participants of SCDAP Development and Training Program. For this reason it is available different versions of RELAP/SCDAPSIM Mod3.5 code.
- For the analysis of the QUENCH-10 three RELAP/SCDAPSIM Mod3.5 code version are used:

    1) [dg]
    2) [dp]
    3) Mod3.5+IUA.

Conclusions

- QUENCH-10 experiment modelling results received using different code versions were compared with experimental data. Calculation results showed significant differences.
  - **RELAP/SCDAPSIM Mod3.5 [dg]** version showed strange results. The biggest discrepancy is in the end of the phase IV, where the calculated amount of the hydrogen generation do not correlates to the amount of the power generated due to oxidation.
  - **Unfortunately the RELAP/SCDAPSIM Mod3.5 + IUA** code version was terminated due to failure at the quenching phase. The generated amount of hydrogen is significant lower using this program code, while calculated temperatures is very similar especially in the first 3 phases.
  - **RELAP/SCDAPSIM Mod3.5 [dp]** version showed best agreement with experimental data.

Conclusions

- QUENCH-18 experiment modelling results received using different code versions were compared with post test data.
  - All calculation results using different code versions showed significant differences with experimental data. The calculation results observed using **SCDAPSim/m35/da/psi** were closest to the experimental data.
  - Influence of different calculations of heat transfer due to radiation showed very small temperature changes, however this temperature changes are very significant to the hydrogen generation.
  - Different oxidation models were compared. Chosen oxidation correlation have significant influence in the temperature and hydrogen generation.

Conclusions

- RELAP/SCDAPSIM Mod3.5 [dg] version is not suitable for the calculation of the QUENCH-18 test. RELAP/SCDAPSIM Mod3.5 + IUA version did not started calculation. However, SCDAPSim/m35/da/psi version were closest to the experimental data and results are logical. Similar results during peroxidation and power decrease phases showed RELAP/SCDAPSIM Mod3.5 [dp] version using Leistikov-Schanz/Prater-Courtwright and Hofmann-Birchley oxidation models when radiation view factors and path lengths were specified according A.D. Vasiliev.

LITHUANIAN ENERGY INSTITUTE
http://www.lei.lt

NATIONAL OPEN ACCESS SCIENTIFIC CENTRE FOR FUTURE ENERGY TECHNOLOGIES

OPEN R & D LITHUANIA

Thank you for the attention

Tadas Kaliatka

Tadas.Kaliatka@lei.lt

First results of the bundle test QUENCH-19 with FeCrAl claddings.

J. Stuckert, M. Große, J. Laier, J. Moch, U. Peters, U. Stegmaier, M. Steinbrück (KIT), K. Terrani (ORNL)

The QUENCH-19 bundle experiment with FeCrAl(Y) claddings and 4 FeCrAl(Y) spacer grids as well as 8 KANTHAL APM corner rods and KANTHAL APM shroud was conducted at KIT on 29th August 2018. This was performed in cooperation with the Oakridge National Laboratory (ORNL).

The test objective was the comparison of FeCrAl(Y) and ZIRLO™ claddings under similar electrical power and gas flow conditions. In common with the previous QUENCH-15 experiment, the bundle was heated by a series of stepwise increases of electrical power from room temperature to a maximum of ≈600 °C in an atmosphere of flowing argon (3.45 g/s) and superheated steam (3.6 g/s). The bundle was stabilised at this temperature, the electrical power being ≈4 kW. During this time the operation of the various systems was checked.

In a first transient, the electrical power was controlled with the same electrical power history as the QUENCH-15 test. As a result, the bundle was heated to peak cladding temperature of about 1000 °C reached at about 4000 s. It showed a slowed bundle heating than for the QUENCH-15 bundle (1200 °C reached at about 3000 s). In this test phase about 0.3 g of hydrogen were produced (QUENCH-15: 23.3 g).

In the following phase, the power was increased continuously to 18.12 kW (corresponds to maximal power of the QUENCH-15 test). After reaching of this value the power was kept constant during about 2000 s. At the end of this phase the maximal peak cladding temperature of T_{pct}≈1500 °C was reached. Much lower heating rate in comparison to QUENCH-15 was measured. Exceeding T_{pct}≈1400 °C sharp increase of hydrogen release rate was observed.

Then reflood was initiated at ≈9100 s, connected with switching the argon injection to the top of the bundle, first rapidly filling the lower plenum of the test section with 4 kg of water, and continuing by injecting ≈48 g/s of water. The electrical power was reduced to 4.1 kW during the reflood.

A temperature excursion was not observed. The temperatures at all elevations decrease immediately after water injection. The total hydrogen release during the whole test was 9.2 g compared to 47.6 g in the QUENCH-15 test with much shorter high electrical power phase.

The videoscope observation of the bundle at the positions of the withdrawn corner rods showed the damage of several claddings at the bundle elevations between 850 and 1000 mm. The claddings were failed either due to interaction with melted thermocouples (mostly) or by spalling of small annular cladding parts.



Karlsruhe Institute of Technology

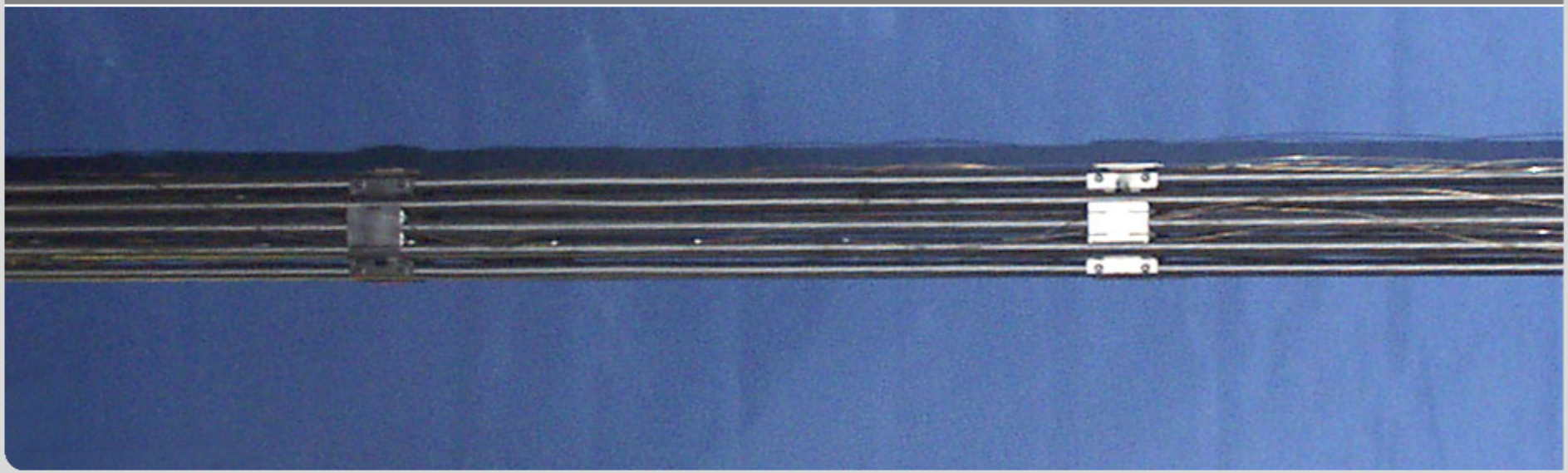
Institute for Applied Materials

First results of the bundle test QUENCH-19 with FeCrAl claddings

J. Stuckert, M. Große, J. Laier, J. Moch, U. Peters, U. Stegmaier, M. Steinbrück (KIT),
K. Terrani (ORNL)

QWS-24, Karlsruhe 2018

Institute for Applied Materials; Program NUSAFE



Chemical compositions and oxidation in steam of FeCrAl alloys

Material	Fe	Cr	Al	Y	Si	Mn	C	comment
Conventional Kanthal APM	Balance	22	5.8	-	0.7	0.4	0.08	used for shroud and corner rods in QUENCH-19
FeCrAl(Y) alloy B136Y3 (ORNL)	**Balance**	**13***	**6.2**	**0.03**			**0.01**	used for **claddings** of heated rods in QUENCH-19

*reduced in comparison to Kanthal to decrease the hardening under irradiation

$$\Delta m/S = K_m\sqrt{t}$$

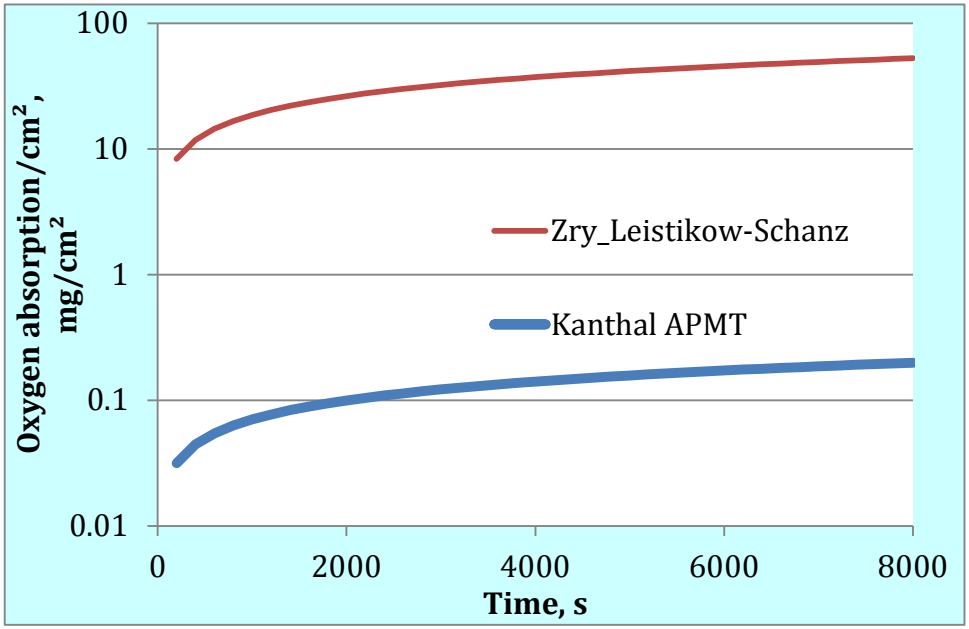
$$K_m(T) = K_0 \exp(-\frac{E_0}{RT})$$

Material	E_0 (J/mol)	K_0 ($g/cm^2s^{0.5}$)
Zry-4*	87144	0.724
APMT**	172000	2.8

Oxidation kinetics in steam

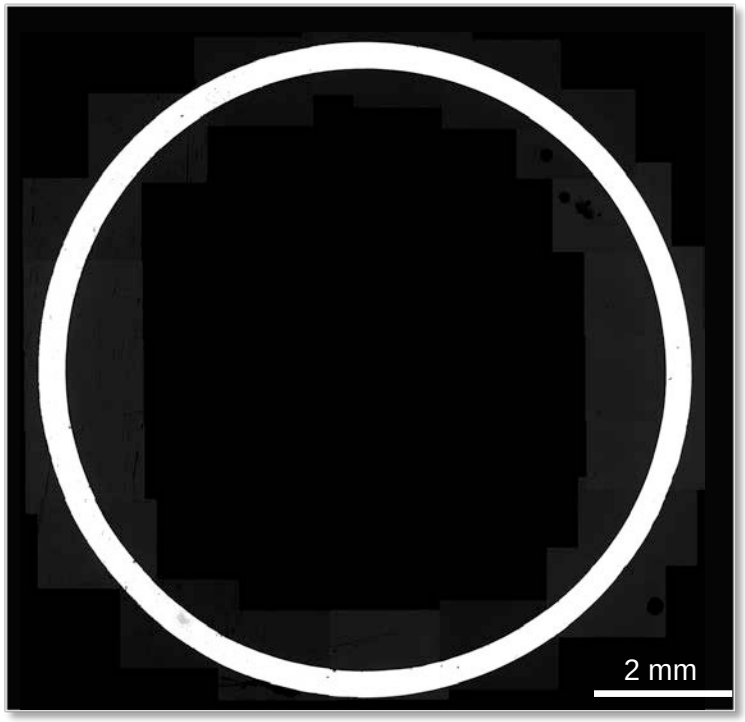
*G. Schanz, FZKA 6827,
https://publikationen.bibliothek.kit.edu/270054544/3814367

**K. Field et al., ORNL/SPR-2018/905,
https://info.ornl.gov/sites/publications/Files/Pub114121.pdf



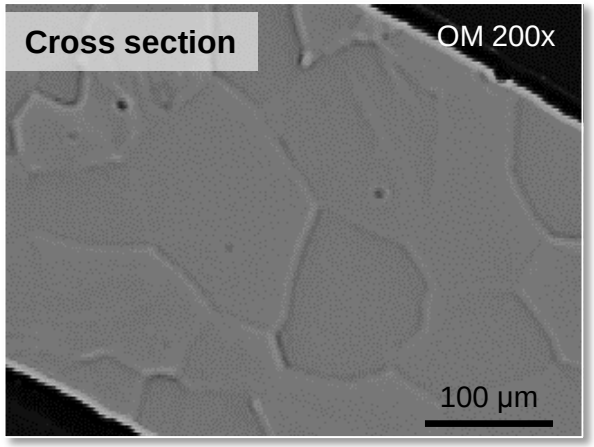
Oxidation in steam at 1200 °C in comparison with Zry-4

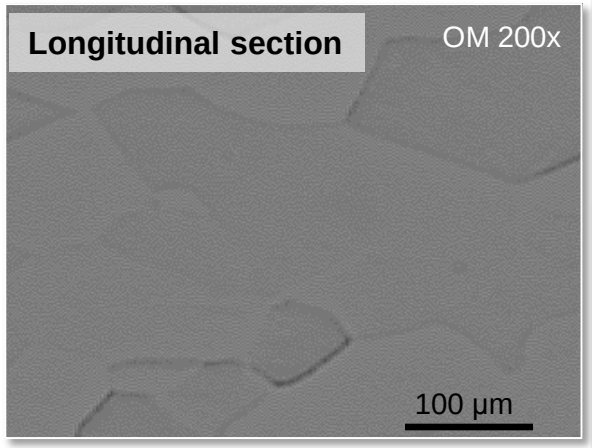
Cladding tubes B136Y3 (by Century Tubes Inc./ORNL)



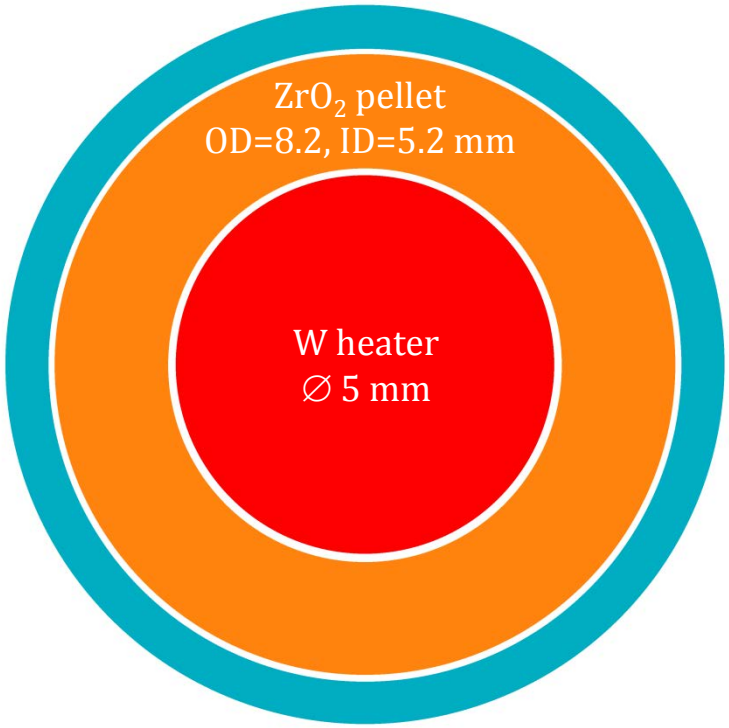
- Made by **cold-drawing**
- OD: 9.52 mm
- WT: 382 µm ± 12 µm
- Grain size: ~80-100 µm

Hardness: 254 ± 7 HV

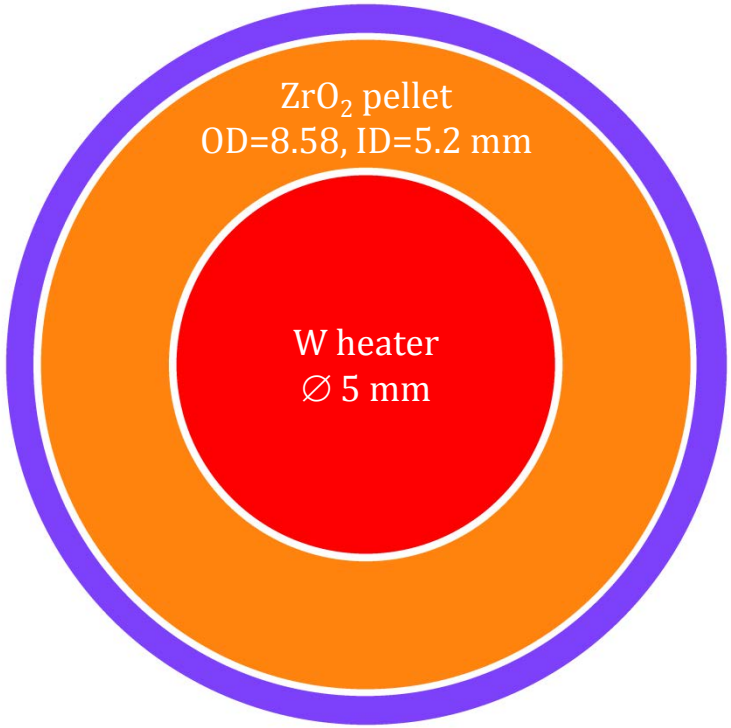




Cross sections of fuel rod simulators (in comparison to reference test QUENCH-15 with ZIRLO claddings)



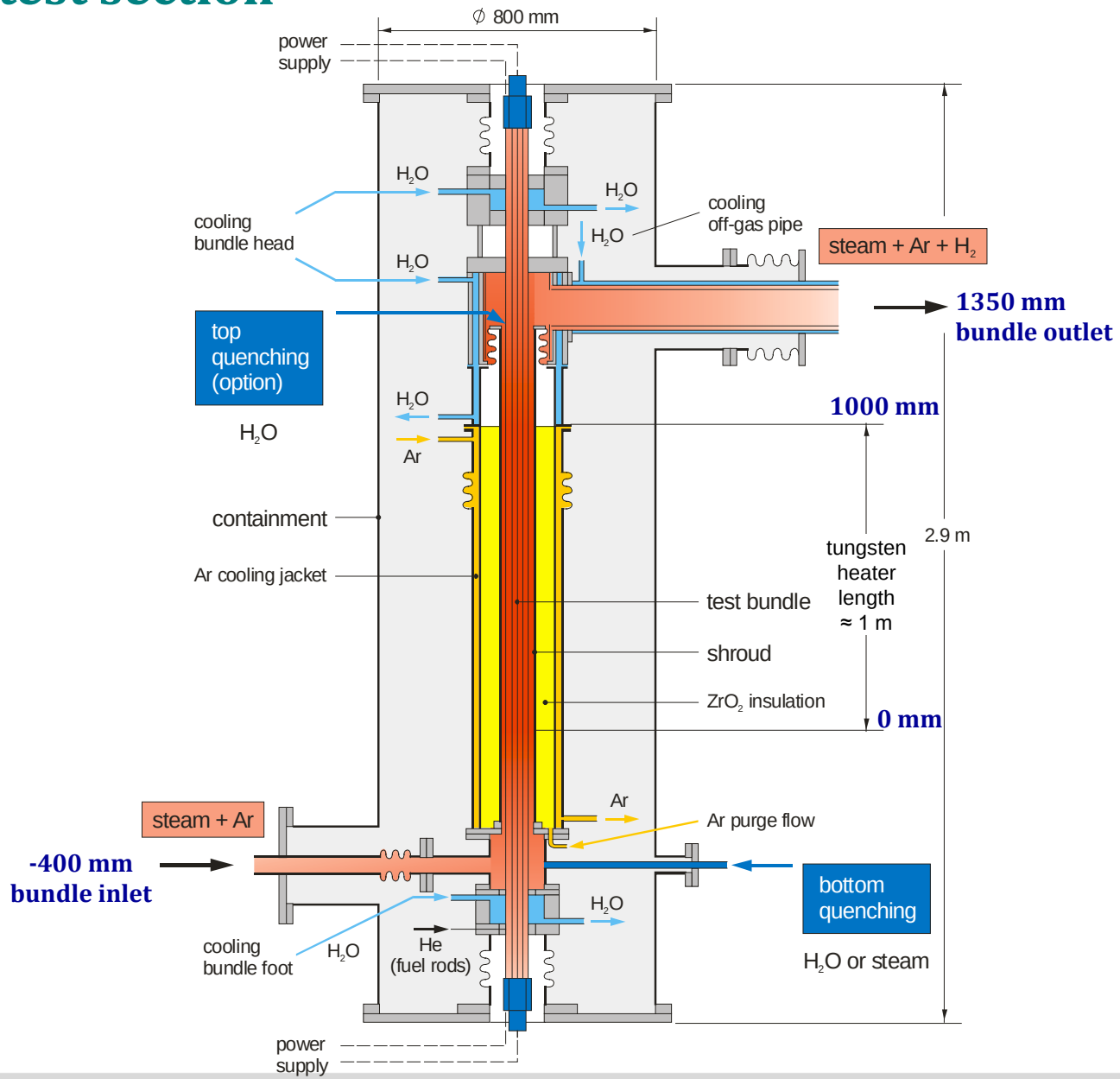
QUENCH-15 (**ZIRLO** cladding with OD=9.5 mm, **WT=572 µm**)



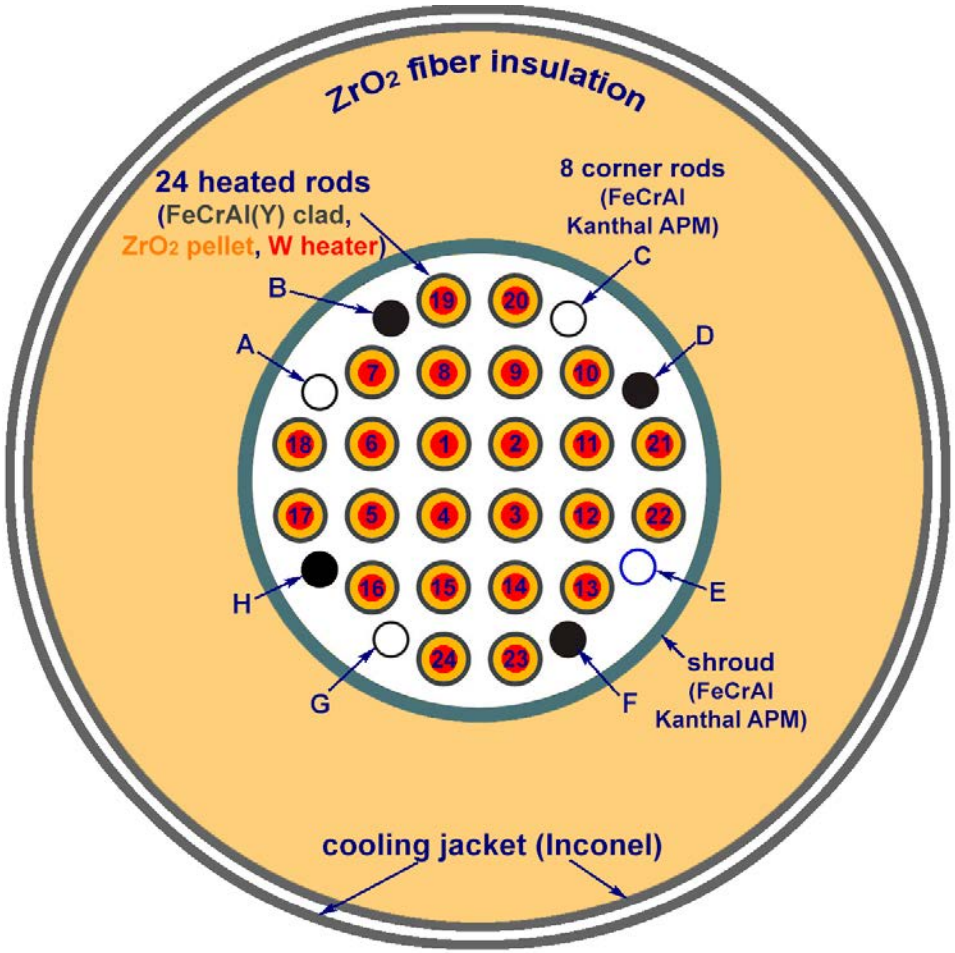
QUENCH-19 (**FeCrAl(Y)** cladding with OD=9.52 mm, **WT=381 µm**)

	heat capacity	heat conductivity	thermal expansion	melting point
FeCrAl (Kanthal)	≈ 460 J/(kg·K)	≈ 11 W/(m·K)	$14 \cdot 10^{-6}$ /K	≈ 1790 K
ZIRLO	≈ 270 J/(kg·K)	≈ 23 W/(m·K)	$5.7 \cdot 10^{-6}$ /K	≈ 2030 K

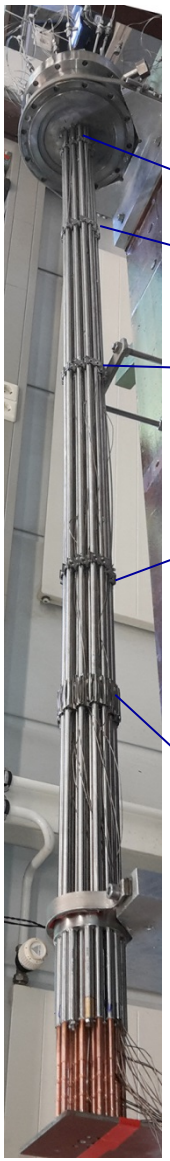
QUENCH test section



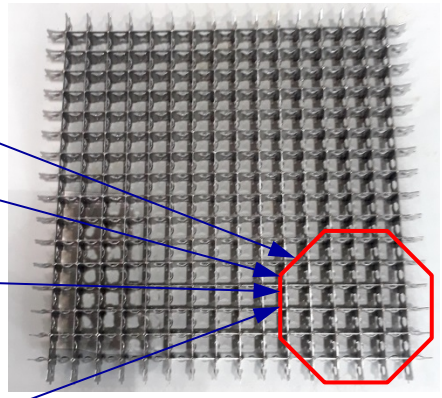
Composition of test bundle QUENCH-19



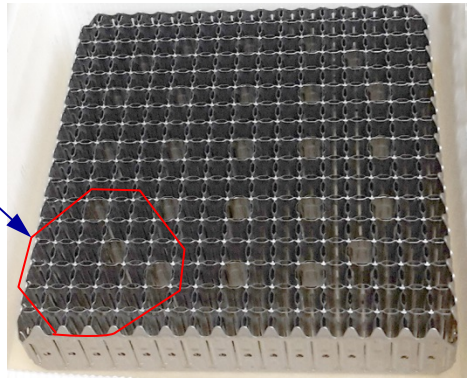
cross section
(arrangement the same as for QUENCH-15)



test bundle (length 2m)

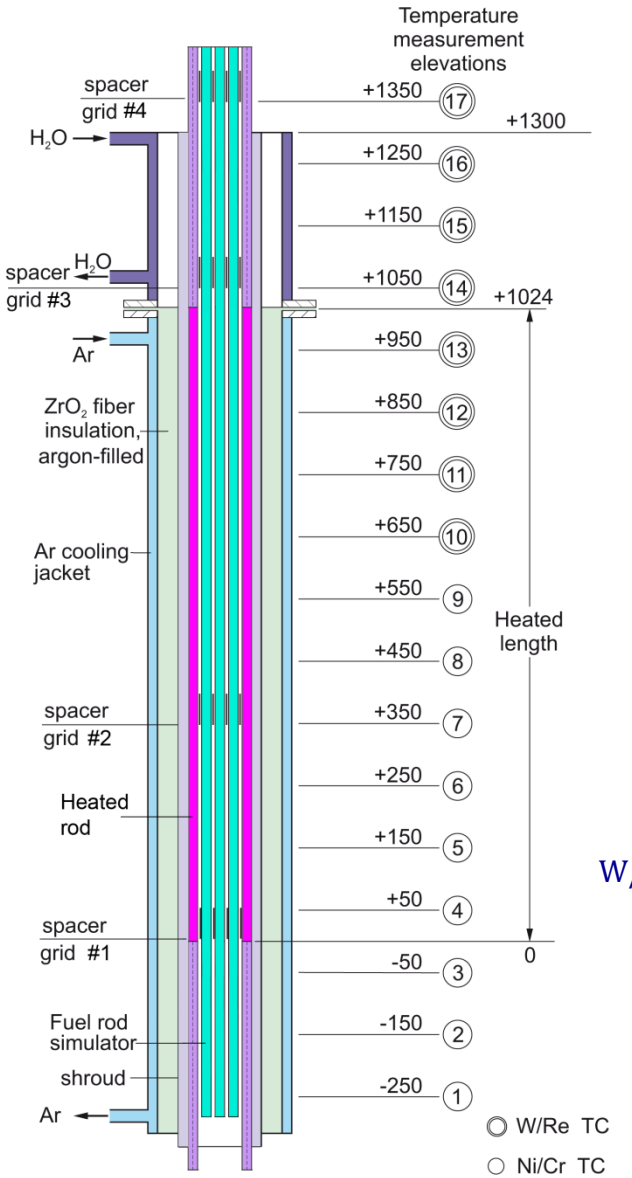


ORNL FeCrAl(Y) **spacer grids**:
height 22 mm,
sheet thickness 0.5 mm



AREVA Inconel **spacer grid**:
height 45 mm,
sheet thickness 0.5 mm

QUENCH-19 bundle instrumentation (thermocouples at cladding surface)



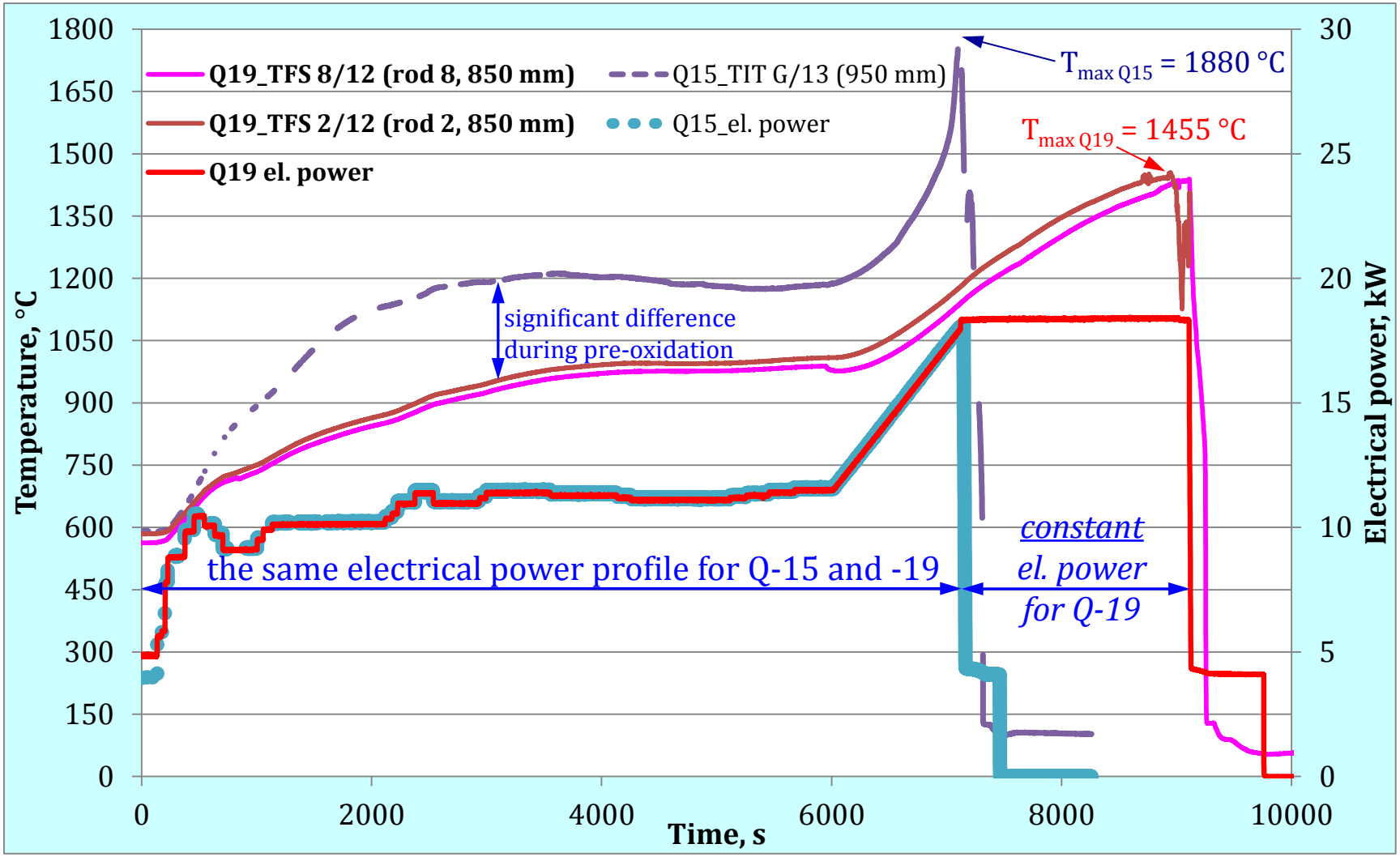


TFS 12/15
W/Re TC sheathed by steel
at 1150 mm, rod #12

TFS 14/14
W/Re TC sheathed by steel
at 1050 mm, rod #14

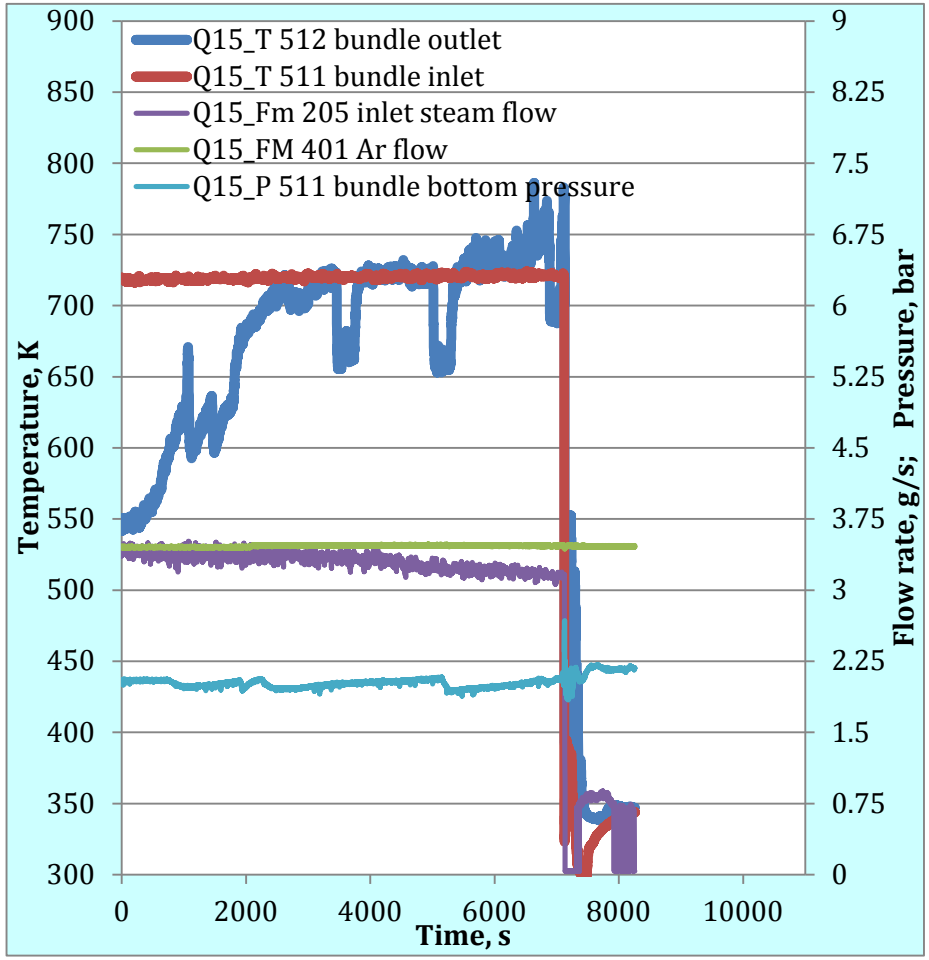
TFS 15/13
W/Re TC sheathed by steel
at 950 mm, rod #15

Test performance: comparison of QUENCH-15 (ZIRLO) and -19 (FeCrAl)

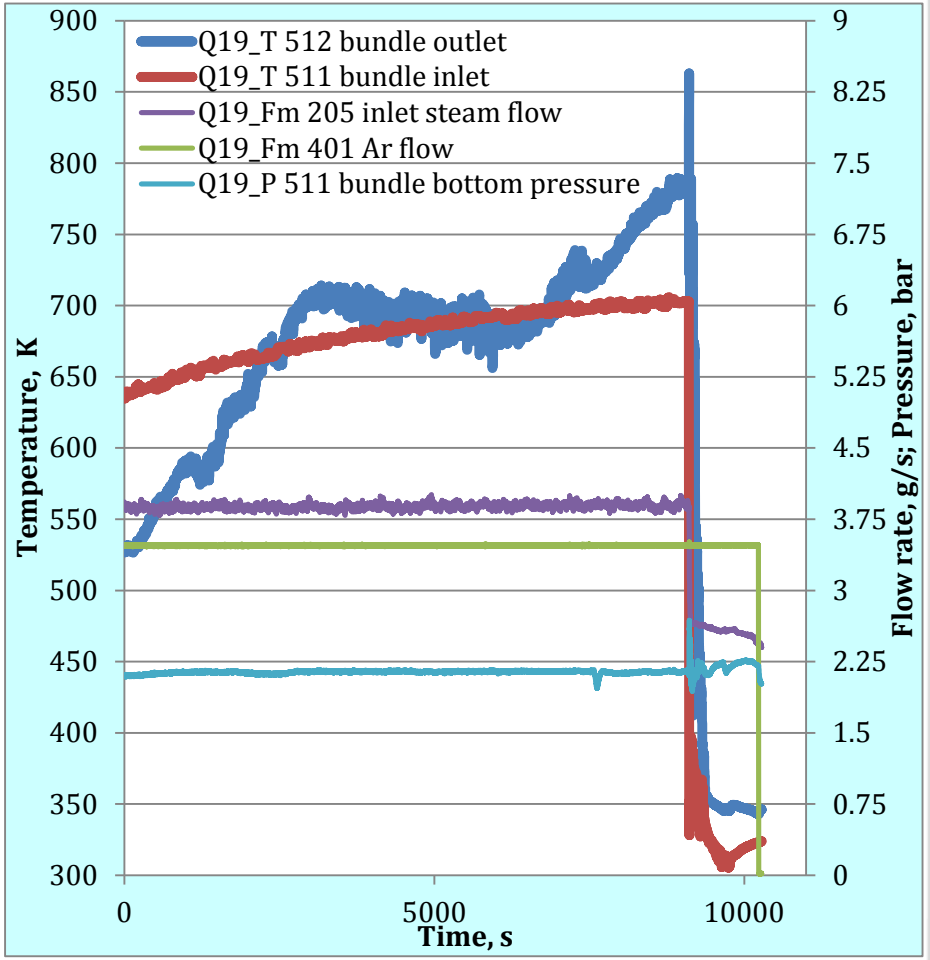


Energy release during Q15 pre-oxidation (i.e. until 6000 s): **electrical E_e = 63.7 MJ** **chemical E_{ch} = 3.5 MJ** $\Rightarrow E_{ch} \ll E_e$

Parameters of gas atmosphere at bundle inlet and outlet

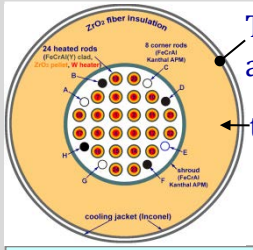


QUENCH-15:
inlet gas (steam + Ar) $T_g \approx 720$ K;
steam flow rate $3.2 < F_s < 3.4$ g/s;
Ar flow rate $F_{Ar} = 3.5$ g/s



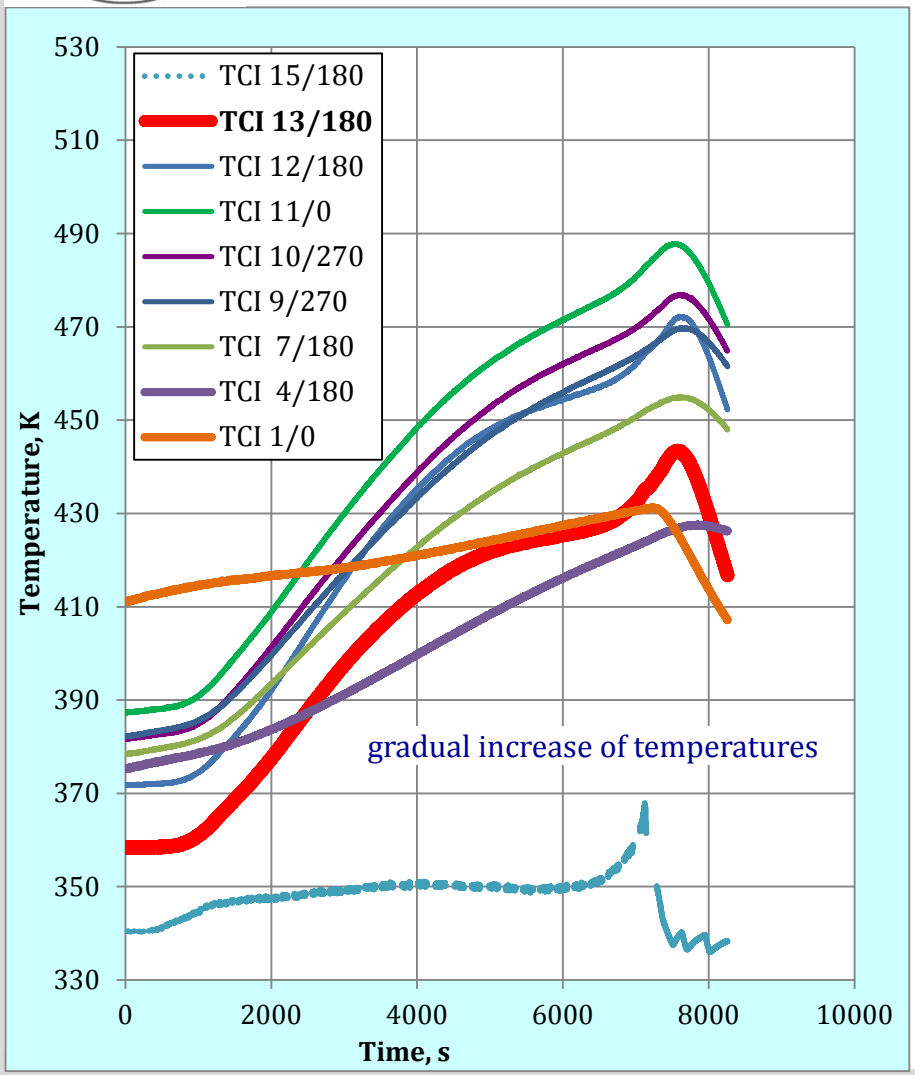
QUENCH-19:
inlet gas (steam + Ar) $640 < T_g < 700$ K;
steam flow rate $F_s \approx 3.8$ g/s;
Ar flow rate $F_{Ar} = 3.5$ g/s

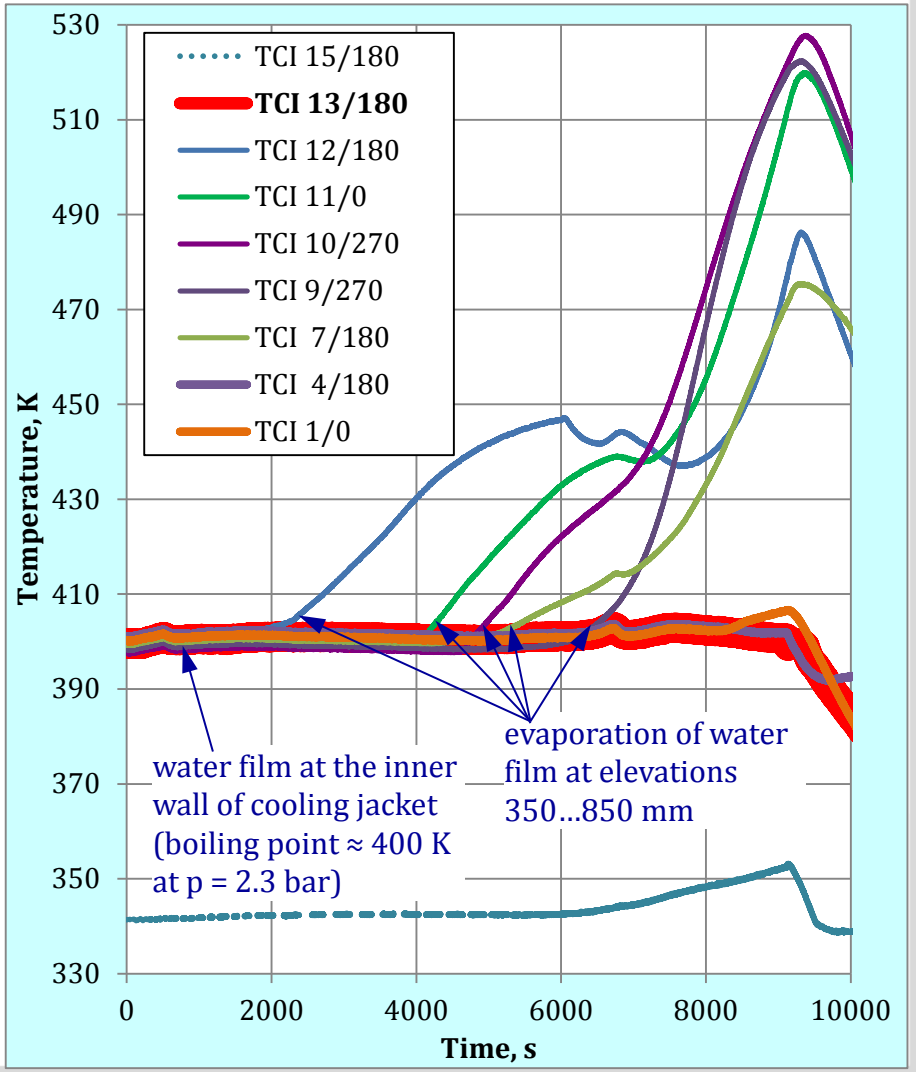
(Q15 ≈ Q19)
similar inlet and outlet



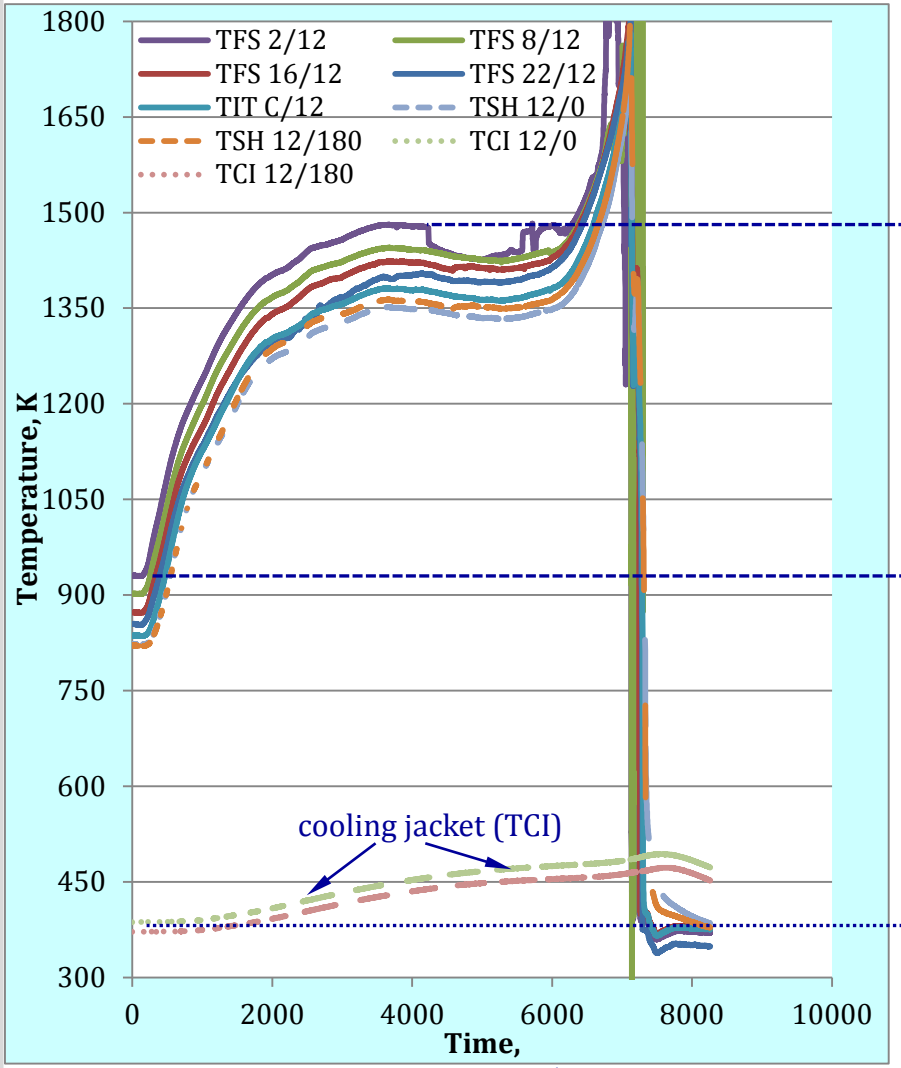
Boundary conditions (temperatures behind heat insulation)

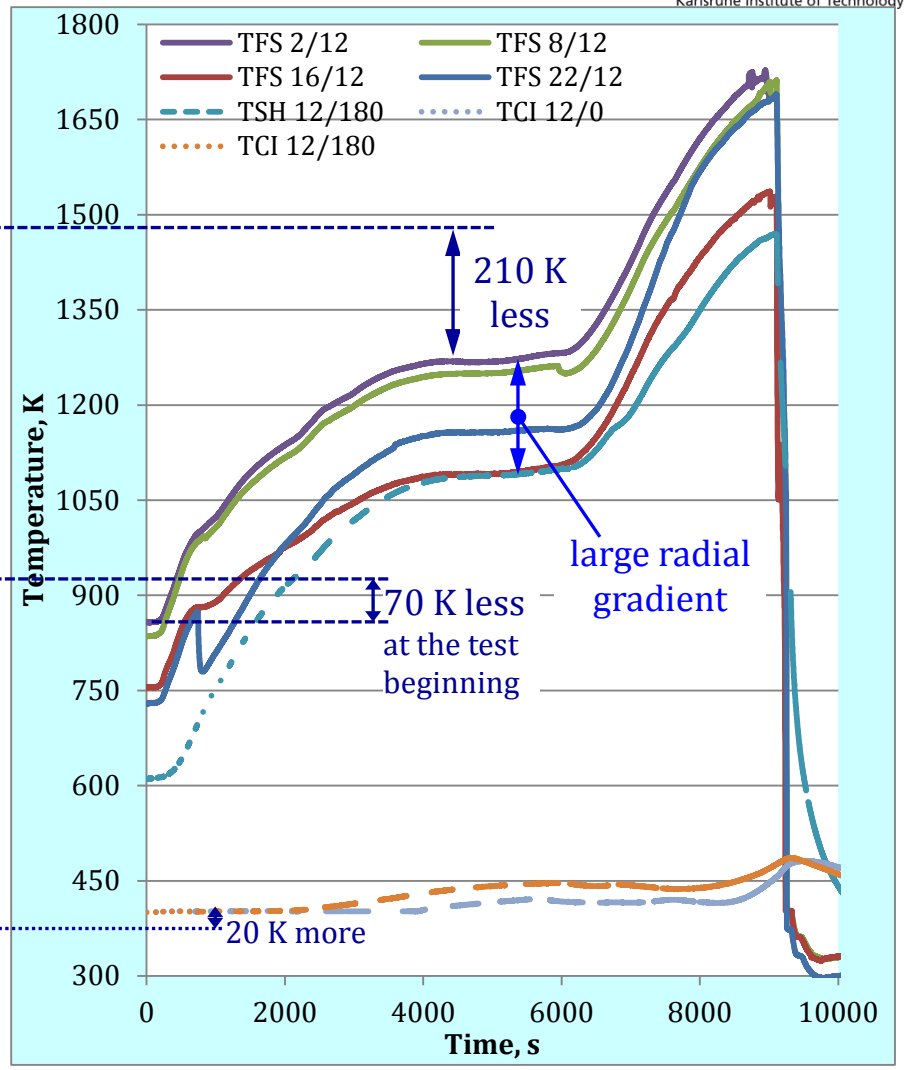
(Q15 ≠ Q19)
porous heat insulation filled with dry Ar in Q15 and **with humid Ar in Q19** (leakage of steam into insulation)





Readings of thermocouples at 850 mm (hottest elevation for QUENCH-19)



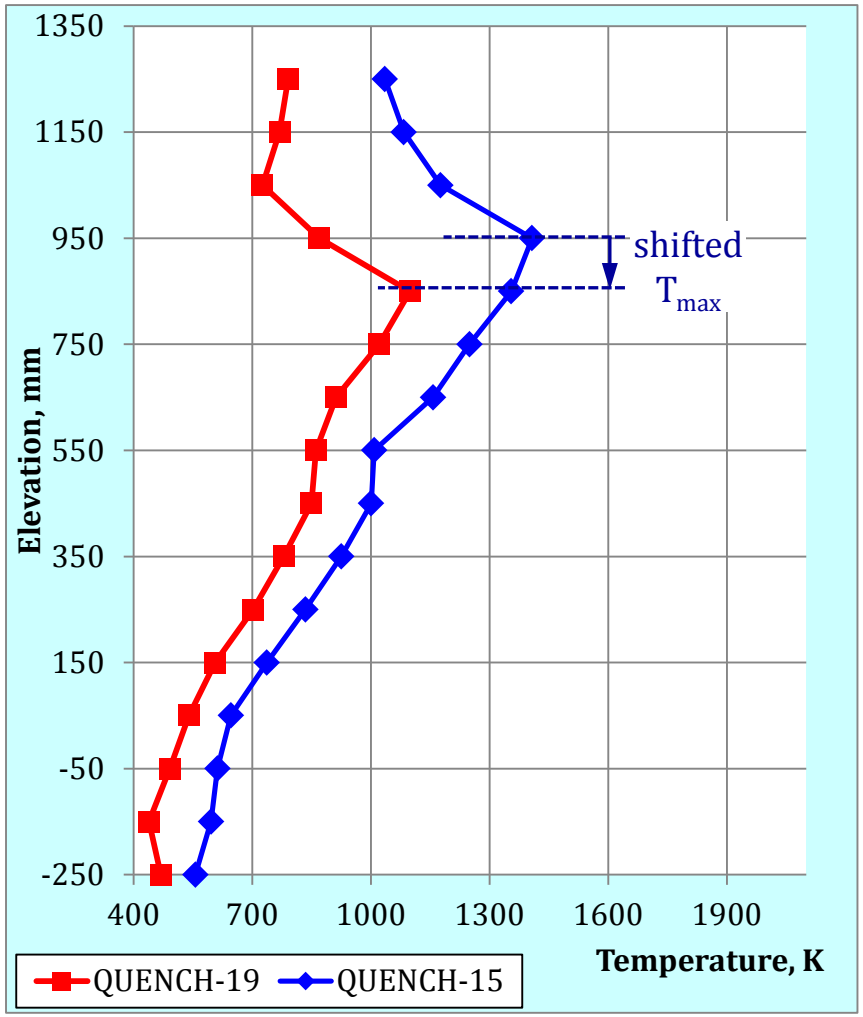


QUENCH-15: strong T escalation during transient

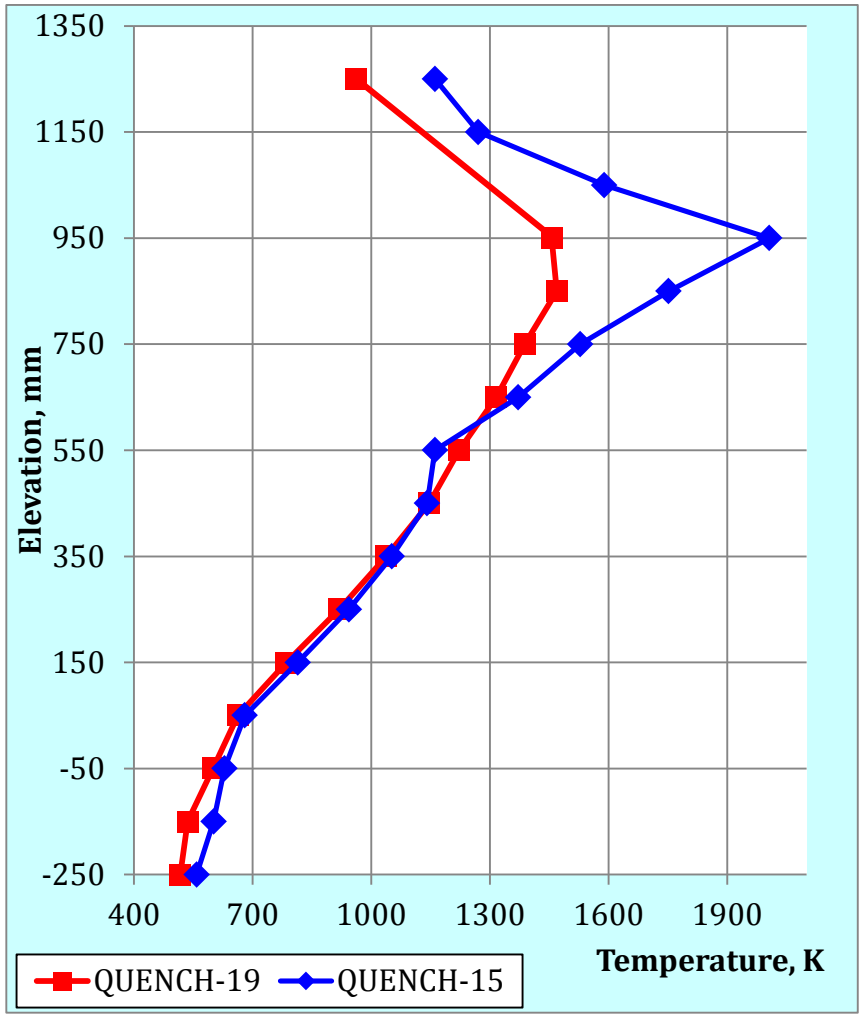
QUENCH-19: 1) **no temperature escalation during extended transition**;

2) special features of test (the reason is not yet clarified): a) lower temperatures ; b) larger radial ∇T.

Axial temperature profiles at shroud

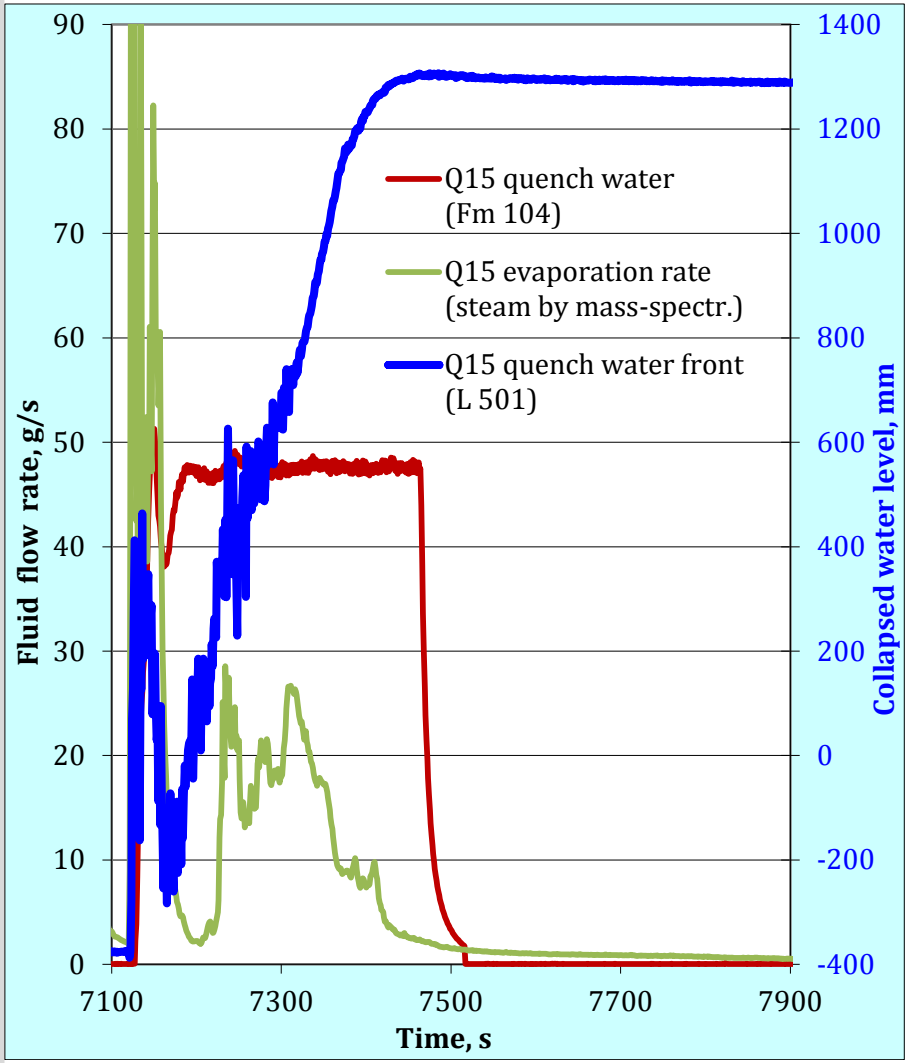


at the beginning of transient

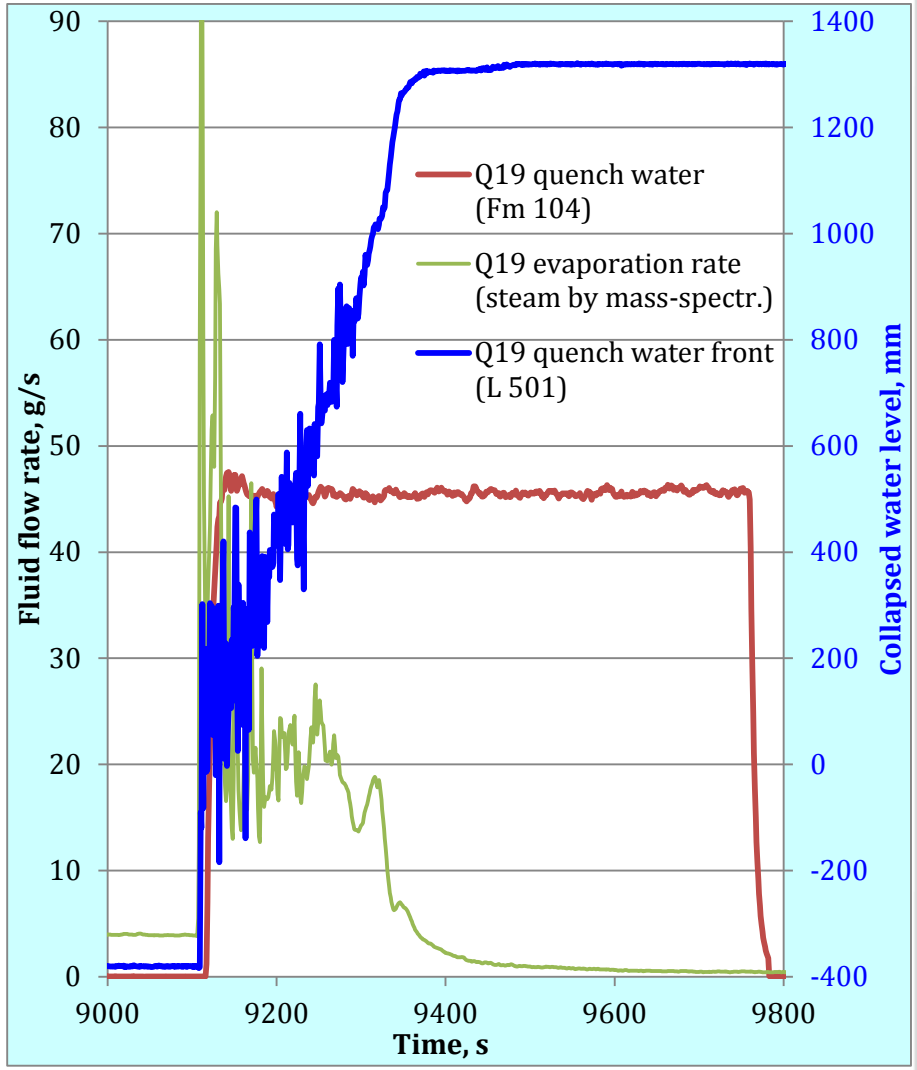


at the onset of reflood

Quench stage: evaporation of injected water, collapsed water front progress

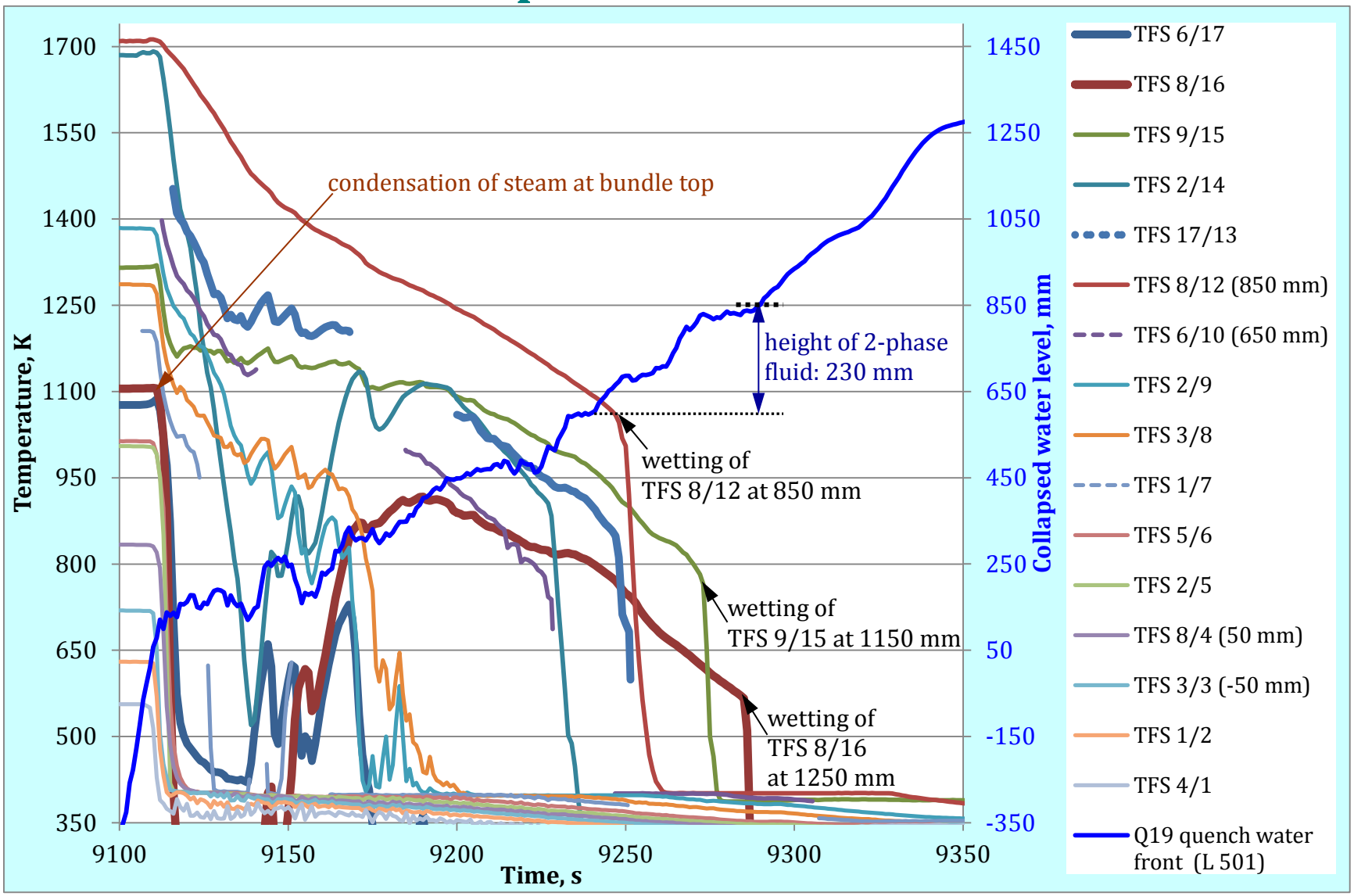


QUENCH-15: water rise duration 330 s

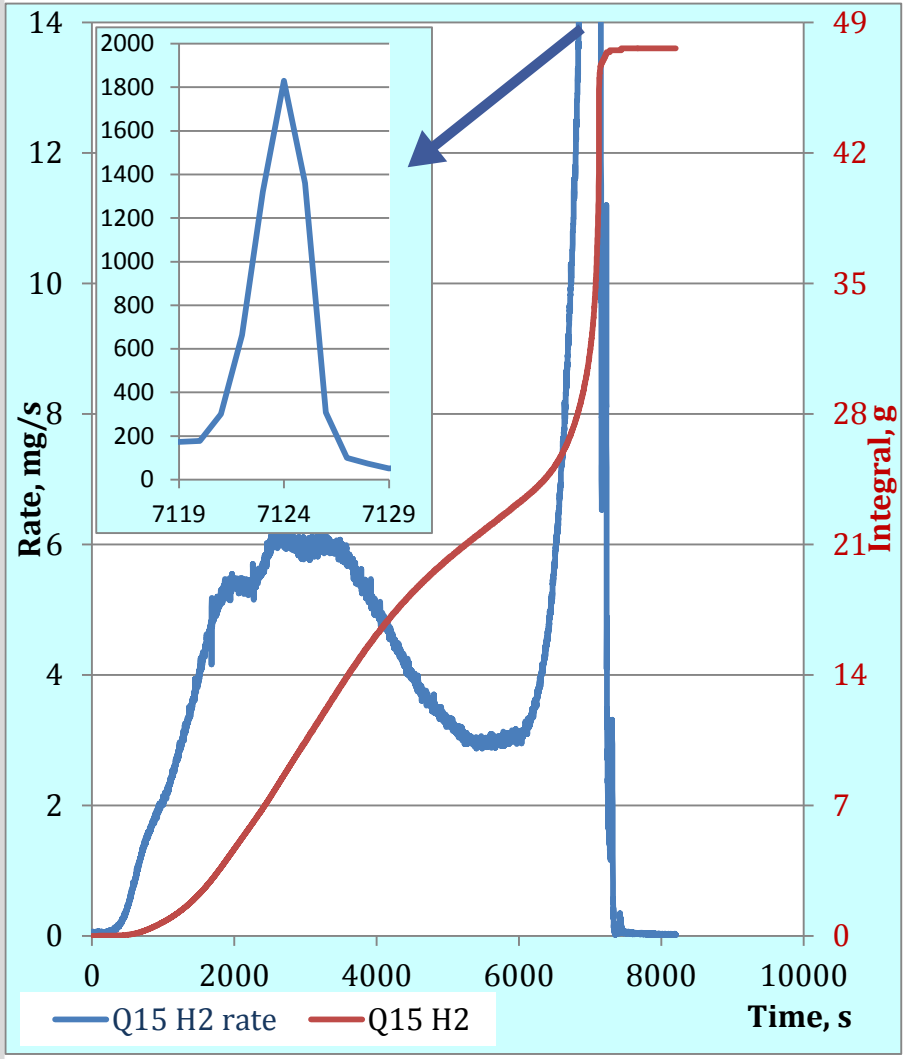


QUENCH-19: water rise duration 270 s

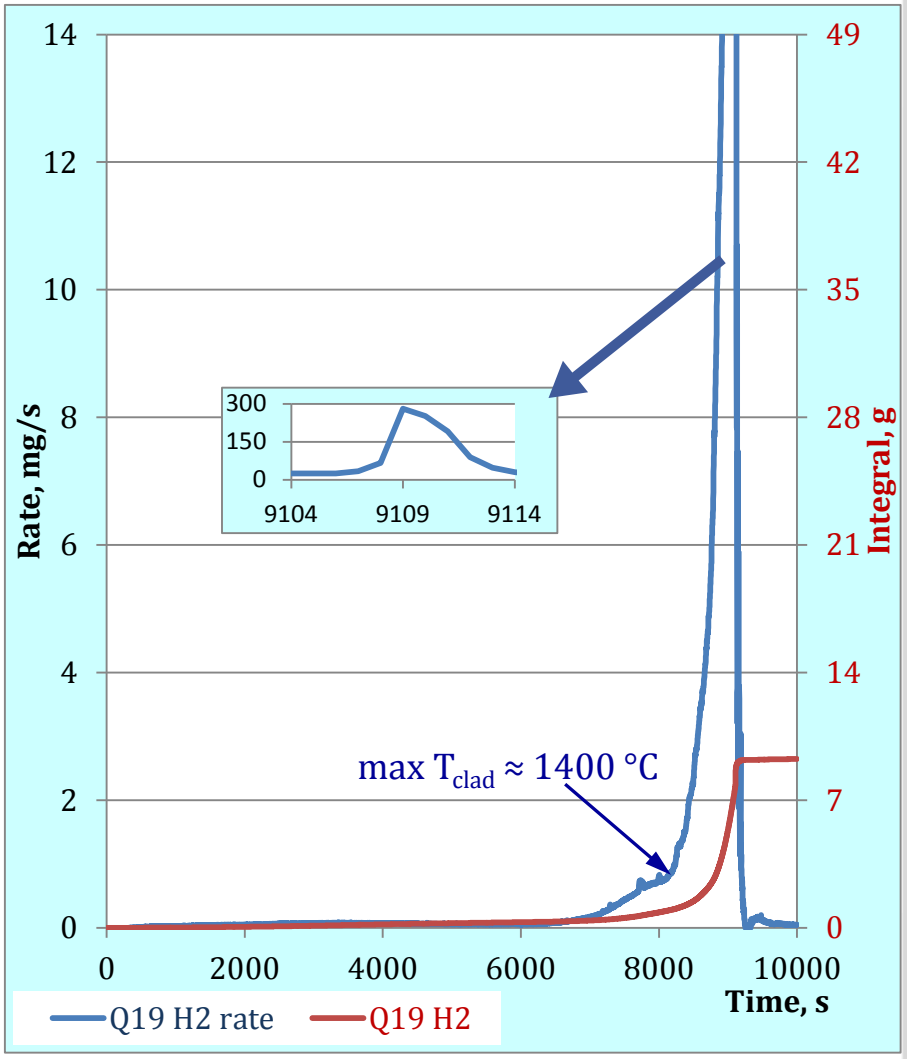
QUENCH-19: wetting of thermocouples by two-phase fluid



Hydrogen release

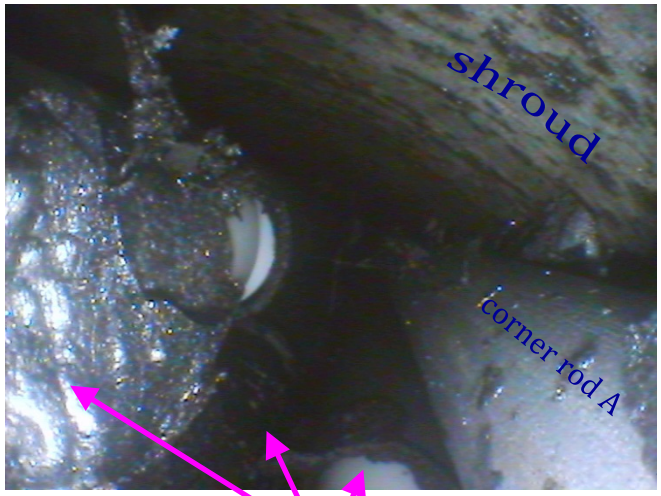


QUENCH-15: max rate 1830 mg/s; totally 47.6 g H_2

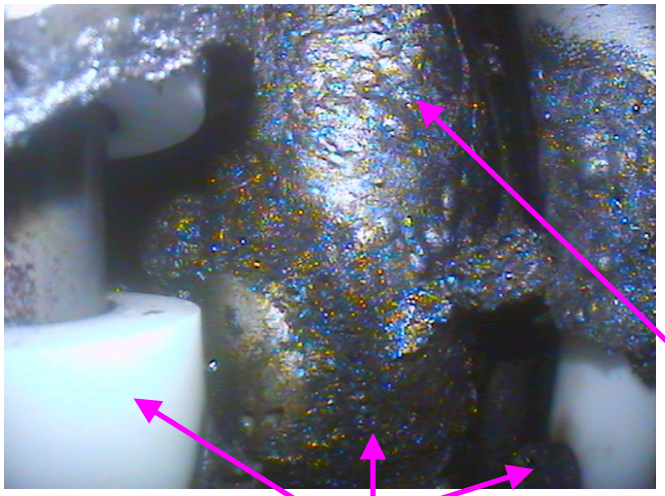


QUENCH-19: max rate 280 mg/s; totally 9.2 g H_2

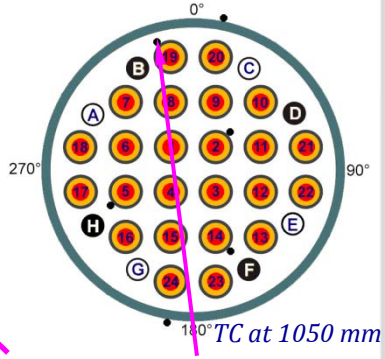
QUENCH-19: videoscope observations of damaged (partly melted) claddings at upper part of heated zone



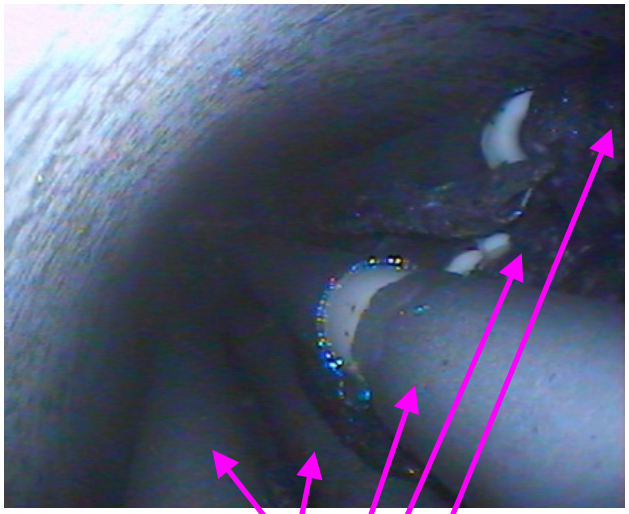
rods 19, 8, 7
(front look at 1000 mm)



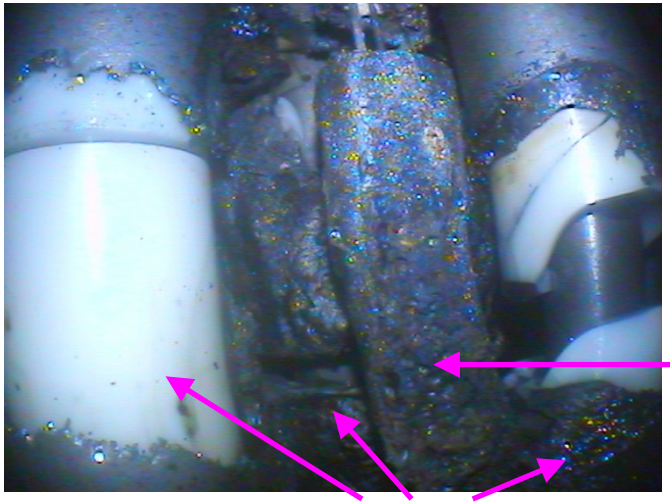
rods 19, 8, 7
(side look at 1000 mm)



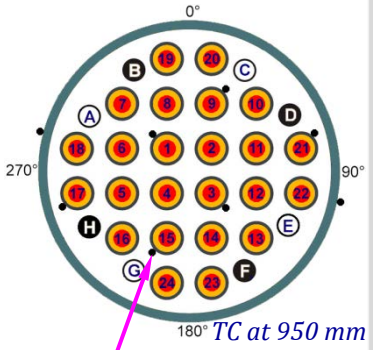
melt from TFS 19/14



rods 5, 17, 16, 15, 24
(front look at 950 mm)



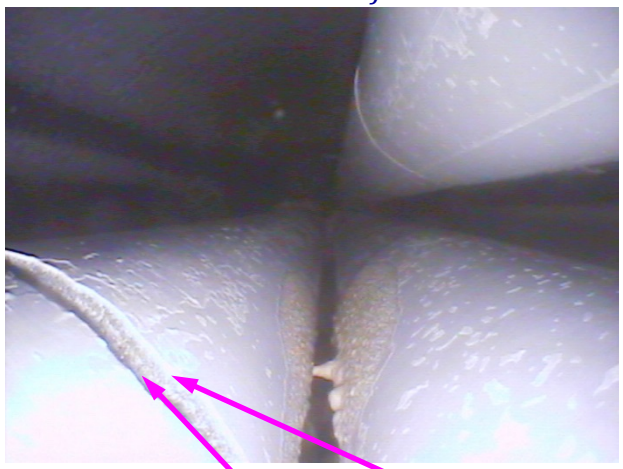
rods 16, 15, 24
(side look at 950 mm)



TFS 15/13

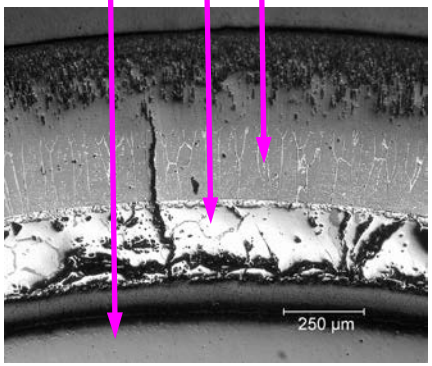
Videoscope observations of claddings at hottest positions of bundles QUENCH-15 (ZIRLO) and -19 (FeCrAl)

***Q15**: circumferential cladding cracks at hottest elevation of 950 mm*



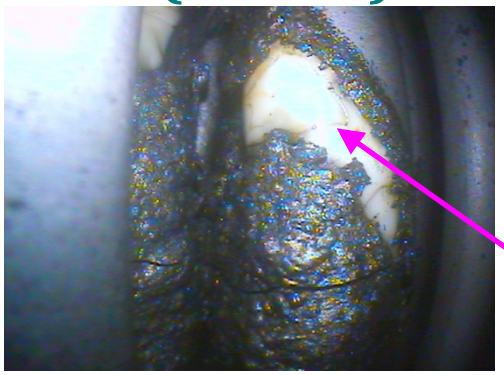
thick oxide

partially molten metal captured between pellet and oxide



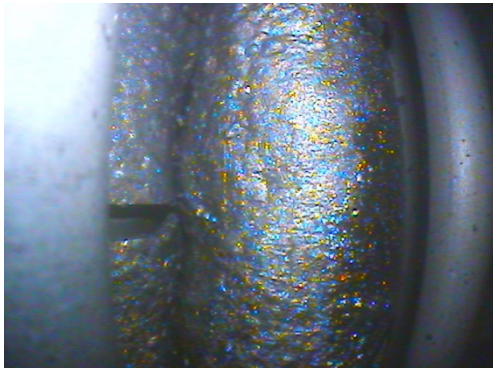


molten claddings of rods 13 and 12
(**Q19** front look at 1000 mm)

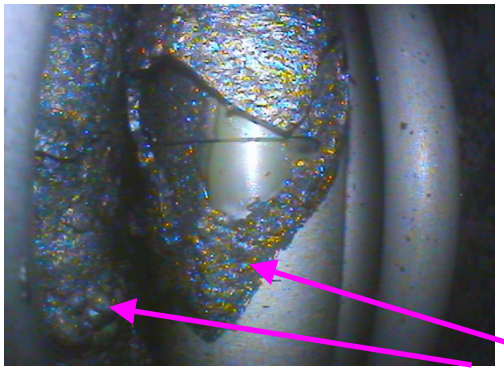


900 mm

pellet



850 mm



800 mm

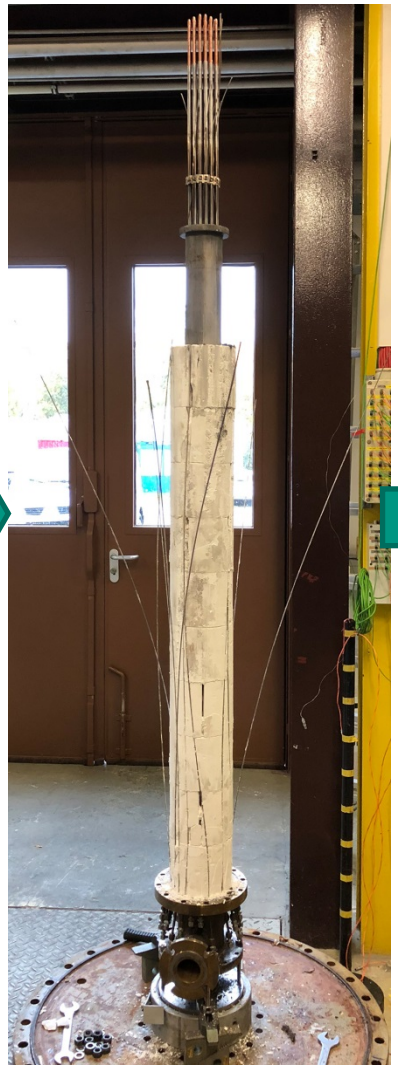
Q19 side look: molten claddings of rods 14 and 13

QUENCH-19 bundle extracting



Bundle inside cooling jacket

jacket removed



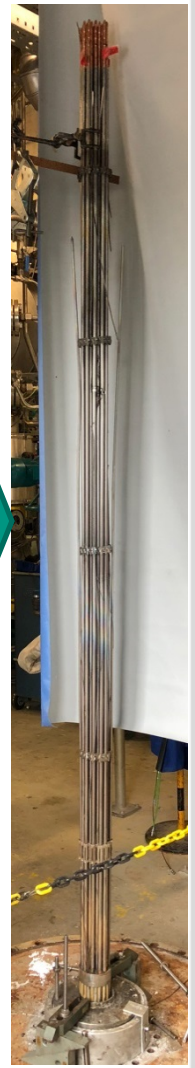
Bundle surrounded by porous ZrO_2 heat insulation

insulation removed



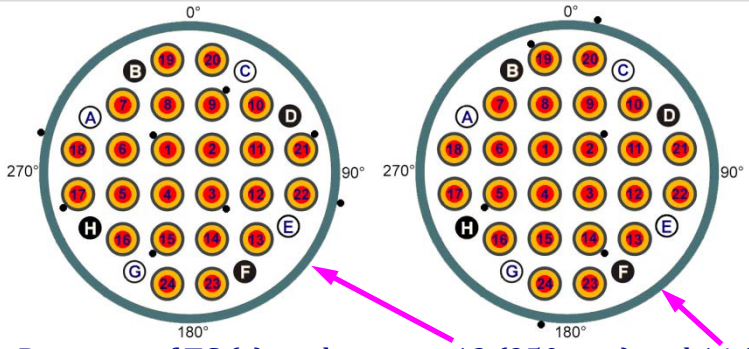
Bundle surrounded by FeCrAl shroud (KANTHAL APM)

shroud removed



Bundle

QUENCH-19 bundle at elevations between 900 and 1100 mm: cladding damages by molten thermocouple steel (AISI 304) sheaths

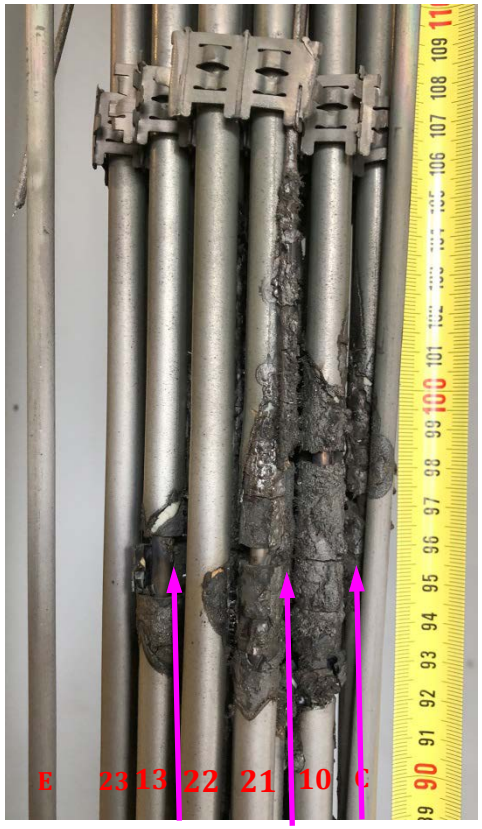


Positions of TC (•) at elevations 13 (950 mm) and 14 (1050 mm)

- the melting range of 304 steel is 1400…1450°C
- the melting range of FeCrAl alloys is 1500…1520°C



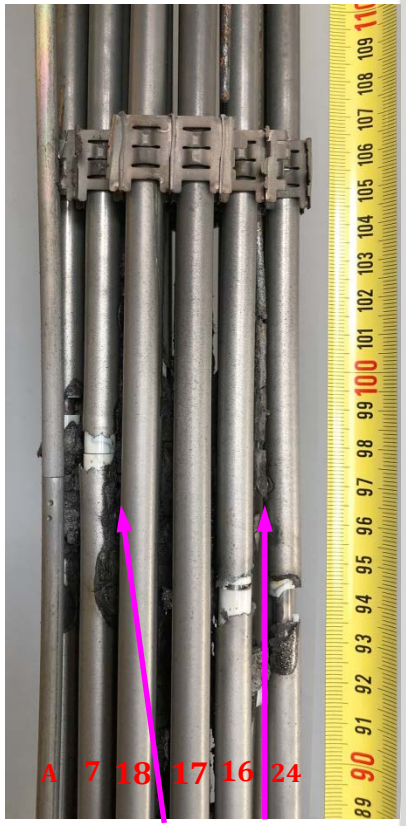
0°: TFS 9/13 and 19/14



90°: TFS 3/13, 21/13, 9/13



180°: TFS 15/13 and 14/14



270°: TFS 1/13, 15/13

Summary

- The QUENCH-19 test with bundle containing 24 heated rods with FeCrAl(Y) cladding and 4 FeCrAl(Y) spacer grids as well as 8 KANTHAL APM corner rods and KANTHAL APM shroud was performed at KIT on August 29, 2018 with similar electrical power history as reference test QUENCH-15 (ZIRLO^{TM} claddings).
- Four test stages of QUENCH-19:

  1) pre-oxidation during about 6000 s (similar to QUENCH-15),

  2) transient during about 1130 s (similar to QUENCH-15),

  3) extended period with constant electrical power of 18.32 kW during 1970 s (to extend the temperature increase stage),

  4) test termination by water flooding with rate of 48 g/s (similar to QUENCH-15).
- The peak cladding temperatures during the pre-oxidation stage were about 200 K lower in comparison to QUENCH-15. The radial temperature gradient was noticeable larger in comparison to QUENCH-15. The reason of these test differences are not yet completely clarified.

Summary (cont.)

- Much lower heating rate in comparison to QUENCH-15 was measured. A temperature of about 1150°C was reached at the time point as a local melting of QUENCH-15 claddings occurred. No temperature escalation was observed during the extended transient. Maximum cladding temperature measured before reflood was about 1460 °C.
- The coping time was about 3200 s (≈ 1200 s for QUENCH-15).
- Sharp increase of hydrogen release rate was observed about 800 s before reflood. Probable trigger of this event could be the melting of steel thermocouple claddings. The maximum hydrogen release rate reached before reflood was 280 mg/s (1830 mg/s for QUENCH-15). Total hydrogen production 9.2 g (47.6 g for QUENCH-15).
- Many claddings were damaged at elevations between 850 and 1000 mm: 1) by interaction with melted thermocouples or 2) parts of claddings were spalled (probably due to thermal expansion followed by quench shrinkage).

Acknowledgment

The QUENCH-19 experiment was supported by the KIT program NUSAFE and partly sponsored by ORNL. The cladding materials and thermocouples were provided by ORNL. IKET/KIT colleagues were involved into bundle dismounting.

The authors would like to thank all colleagues involved in the pre-test calculations (GRS, ORNL, PSI).

Thank you for your attention

http://www.iam.kit.edu/awp/666.php
http://quench.forschung.kit.edu/

Pre- and Post-Test Simulations of the ATF Experiment QUENCH-19 with AC²

Thorsten Hollands, Christa Bals
Gesellschaft für Anlagen- und Reaktorsicherheit (GRS) gGmbH, Germany

Abstract

In 2018 the QUENCH-19 bundle experiment was performed at KIT to investigate the ATF cladding material FeCrAl under severe accident conditions. ATF claddings are one option under investigation to reduce the thermal impact by oxidation as well as to enlarge the time margins for accident management measures. On the other hand the melting temperature of e.g. FeCrAl is lower compared to Zry and the neutron absorption is higher.

To support the test QUENCH-19 pre- and post-test analyses were performed at GRS by application of the module ATHLET-CD as part of the code system AC². Due to a lack of information on material properties and oxidation behaviour of FeCrAl cladding for the pre-test simulations assumptions were necessary. To predict the range of the possible bundle behaviour two scenarios were investigated using the same boundary conditions like in QUENCH-15 with Zirlo claddings: One without oxidation and another with oxidation by application of the strongest Zry oxidation (Cathcart / Prater-Courtright) under consideration of ZrO_2 properties instead of FeCrAl oxides. The results show a plausible behaviour of the temperature evolution with maximum temperatures below the melting point of FeCrAl (no oxidation: 1350 °C, with oxidation: 1475 °C) and no escalation during quenching, not like in QUENCH-15 where temperatures above 2000 °C occurred. For the post-test simulations an oxidation correlation for KANTHAL APMT was available and also a second approach derived from an OECD/NEA report. Both approaches were implemented in ATHLET-CD. Compared to Zry oxidation both approaches are orders of magnitude lower and are only valid for one special composition, while different materials were used in the experiment. Additionally, it was assumed that due to the bundle heat-up conditions only Al_2O_3 was formed by oxidation and no other oxides. The results of the post-test simulations show that ATHLET-CD is able to predict the thermal behaviour of the experiment in good agreement to the measured values, especially along the heated length. Compared to the observed radial temperature profile of up to 200-300 °C in the experiment ATHLET-CD calculates only a maximum of app. 50 °C. The maximum temperature was measured at 850 mm, while it is calculated at 950 mm with an underestimation of app. 50 °C. Both oxidation approaches for FeCrAl strongly underestimate the measured H_2 generation of app. 9 g. For a detailed evaluation of the calculated hydrogen generation the post-test examination of the bundle is necessary to know which components contribute to the total value. Nevertheless, the oxidation modelling for FeCrAl will be improved.


TOSHIBA

Pre- and Post-Test Simulations of the ATF Experiment QUENCH-19 with AC²

Thorsten Hollands, Christa Bals

Gesellschaft für Anlagen- und Reaktorsicherheit (GRS) gGmbH, Germany

24th International QUENCH Workshop

Karlsruhe Institute of Technology

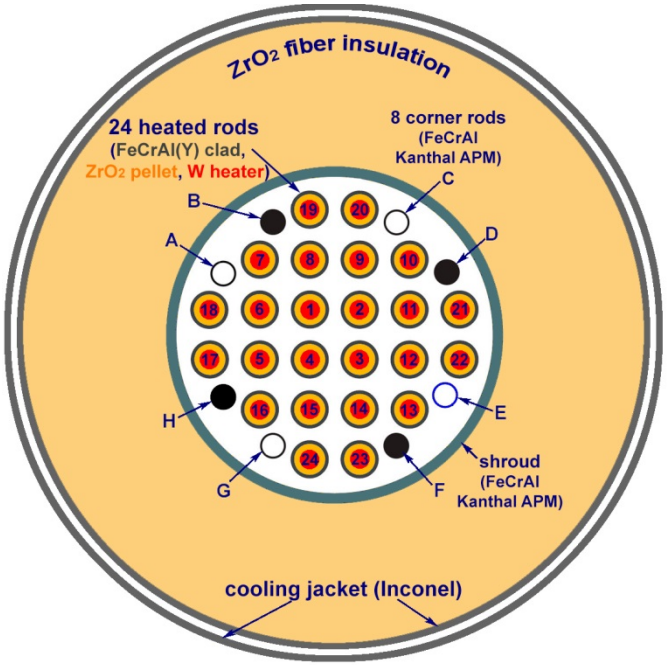
13. – 15. November 2018

Outline

- QUENCH-19 Bundle Configuration an Test Objectives
- Pre-Test Simulations
  - Assumptions and Model Options
  - Results
  - Main Findings
- Post-Test Simulations
  - Assumptions and Model Improvement
  - FeCrAl Oxidation Model
  - Results
  - Conclusions

QUENCH-19 Bundle Configuration an Test Objectives

- QUENCH bundle experiment with FeCrAl claddings to investigate the cladding material behaviour under severe accident conditions
- Scenario similar to QUENCH-15
  (same bundle geometry, same electrical power input)
- In cooperation with ORNL
- Bundle configuration made of different FeCrAl compositions:
  - 24 heated rods with tungsten heater and ZrO_2 pellet
  - 8 corner rods
  - 5 grid spacer
  - Shroud



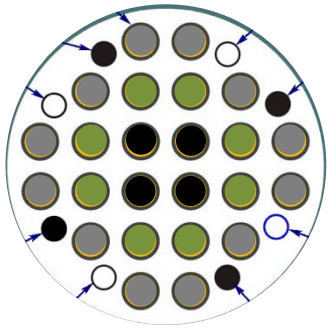
Source: KIT

Pre-Test Simulations

Pre-Test Simulation
– Assumptions and Model Options (I) –

- Standard ATHLET-CD input deck for QUENCH tests
- Original QUENCH-15 scenario without any changes
- Bundle design implemented as given by KIT
- The fluid channel through the core is divided into two sub channels:
  - BUNDLE representing 90 % of the core are and is connected to the RODs
  - BYPASS representing 10 % of the core area and allows bypass flow if the core is blocked
- The bundle is divided into three groups:

		Rods
• ROD1:	4 central rods	1, 2, 3, 4
• ROD2:	8 rods (intermediate ring)	5, 6, 8, 9, 11, 12, 14, 15
• ROD3:	12 rods (outermost ring)	7, 10, 13, 16, 17, 18, 19, 20, 21, 22, 23, 24

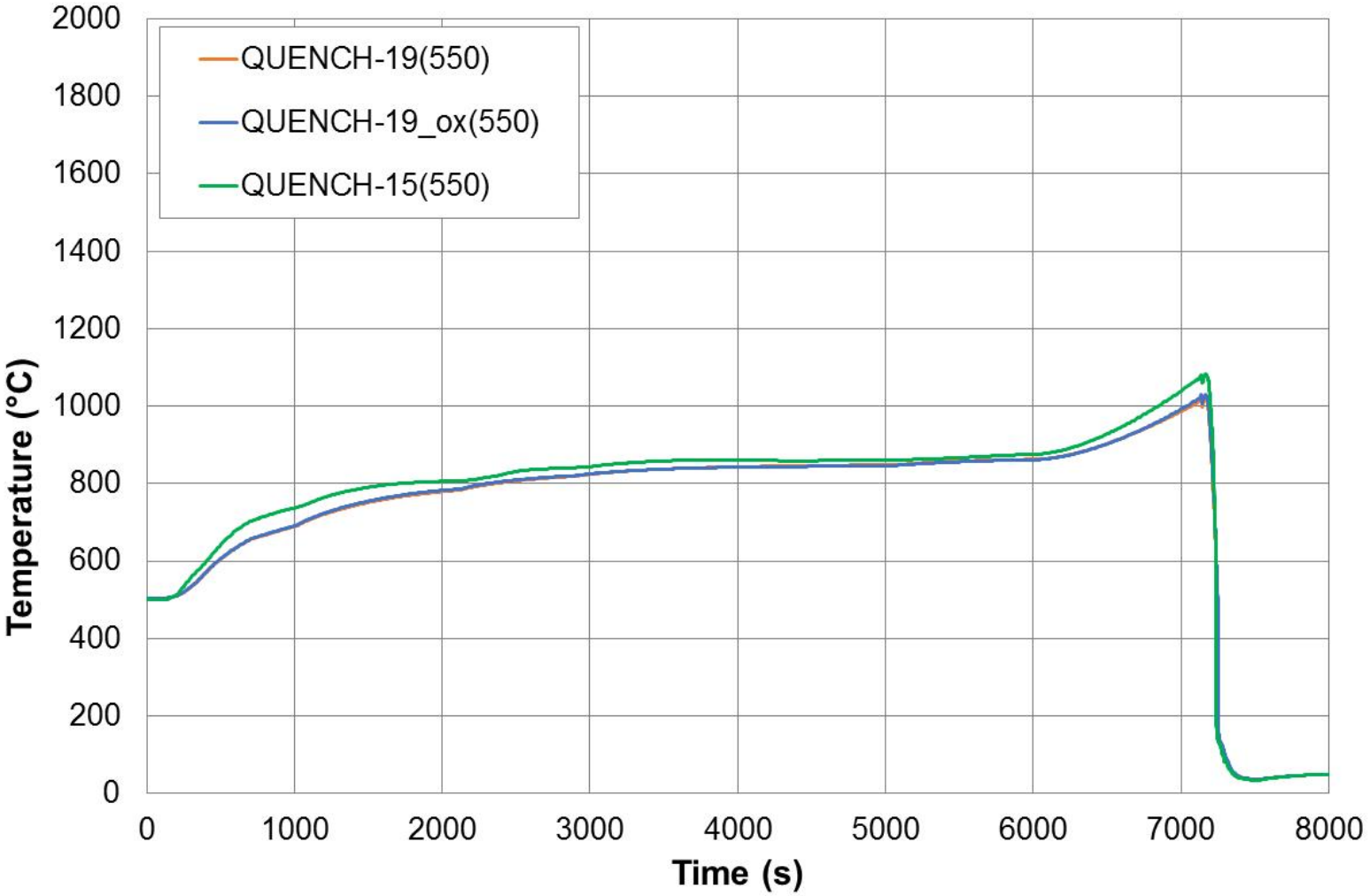


Pre-Test Simulations
– Assumptions and Model Options (II) –

- FeCrAl properties instead of Zry4 properties
- No oxidation considered for the base case, because FeCrAl oxidation rate should be about 1/1000 of Zry oxidation
- Oxidation scenario investigated:
  - Oxidation of rods, corner rods, shroud and spacer grids considered
  - Zry oxidation model (Cathcart / Prater-Courtright)
  - No FeCrAl oxide properties used/available => ZrO_2 properties for cases with oxidation
- Results of the Pre-Test Simulations are given for ROD2

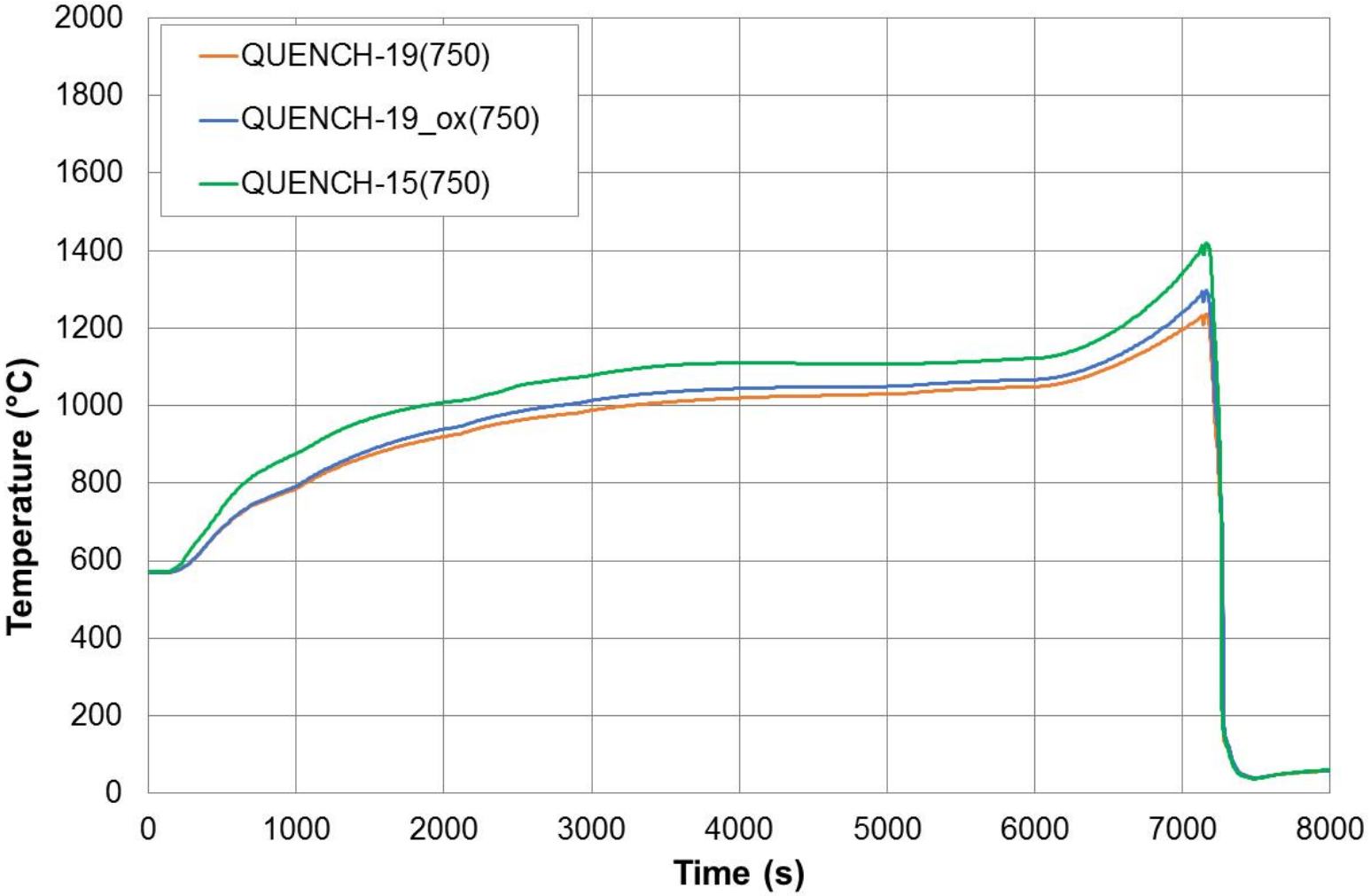
Pre-Test Simulations
– Results (I) –

- Temperatures at 550 mm



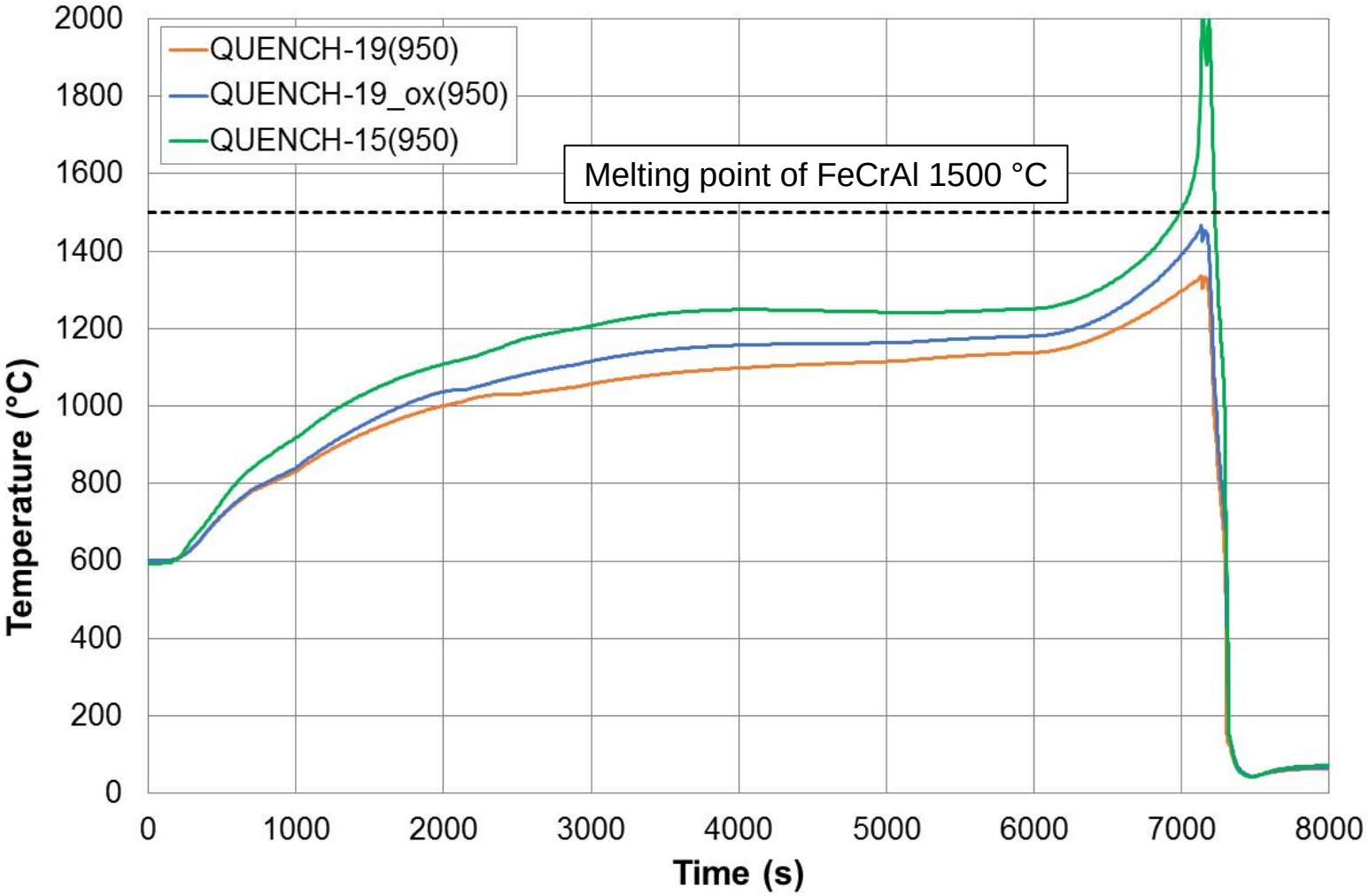
Pre-Test Simulations
– Results (II) –

- Temperatures at 750 mm



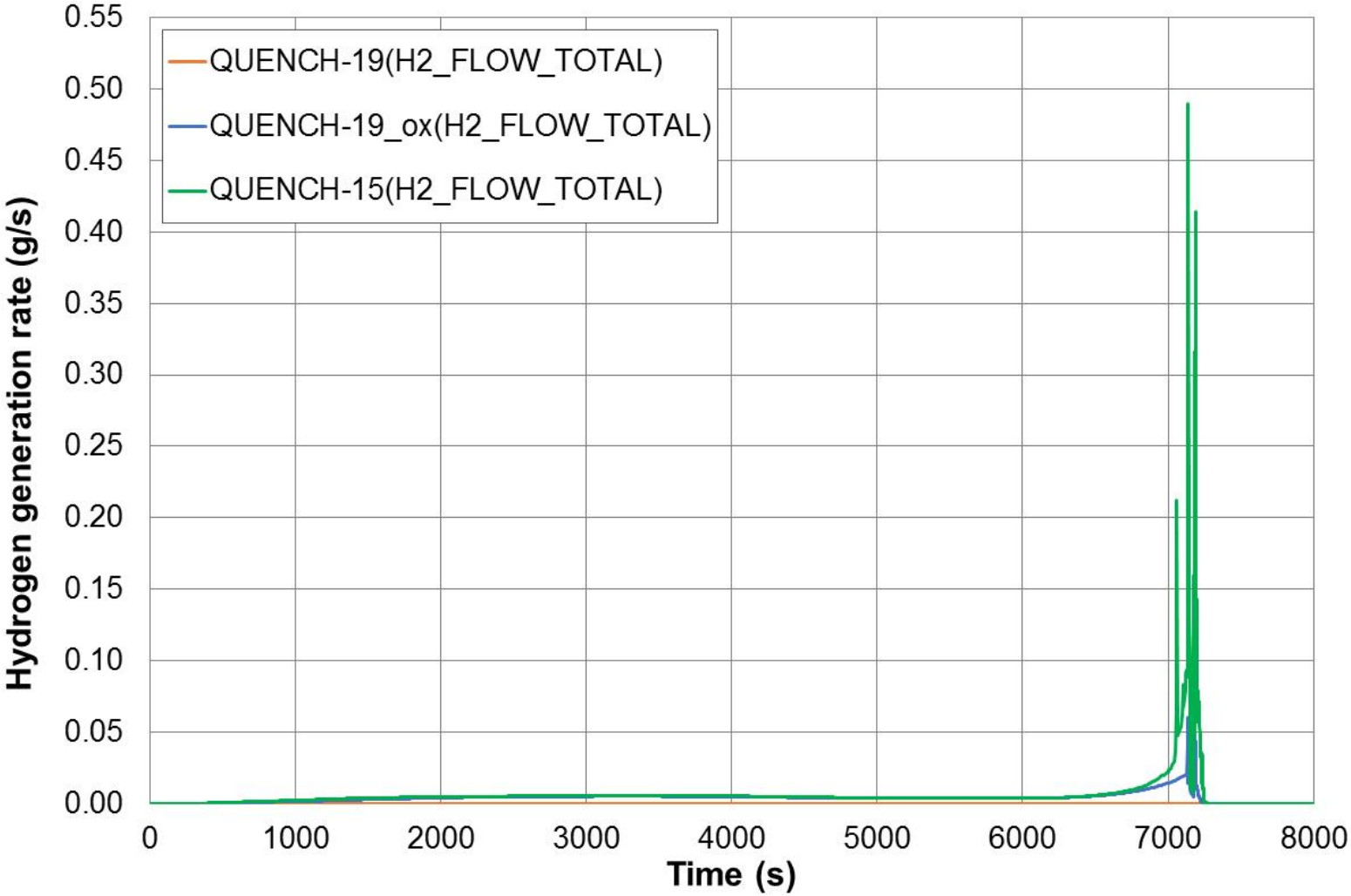
Pre-Test Simulations
– Results (III) –

- Temperatures at 950 mm



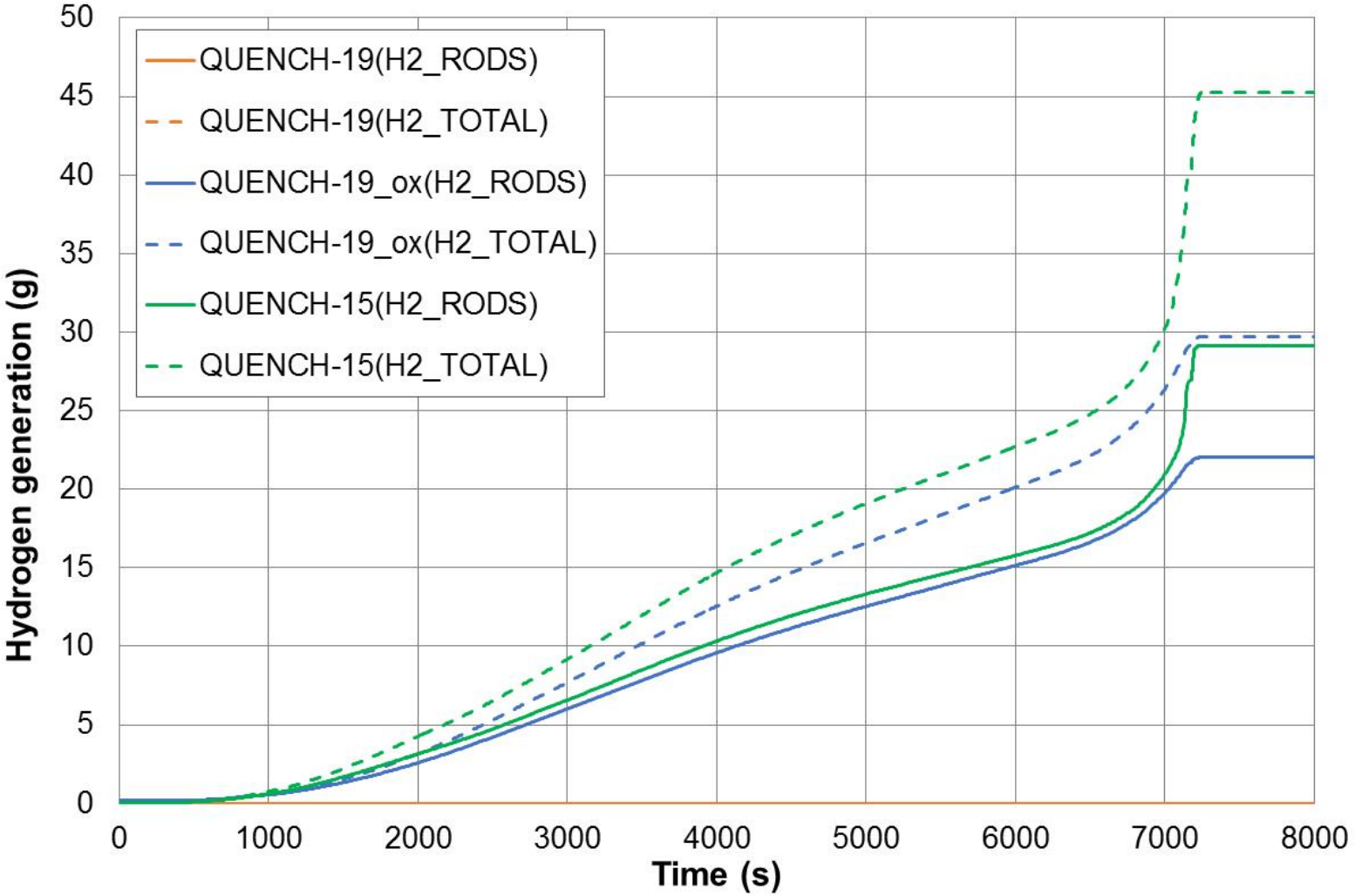
Pre-Test Simulations
– Results (IV) –

- Hydrogen Generation Rate



Pre-Test Simulations
– Results (V) –

- Hydrogen Generation



Pre-Test Simulations
– Main Findings –

- ATHLET-CD is capable to simulate the foreseen scenario of QUENCH-ATF with the necessary assumptions
- Maximum test temperature (no increase/escalation during quenching):
  - No oxidation: 1350 °C, before quenching
  - With oxidation: 1475 °C, before quenching
- Nearly no radial temperature profile
- Shroud temperatures are below the outermost rod temperatures
- H_2 generation occurs if “full” Zry4 oxidation is applied, but does not lead to a temperature escalation, just a slight increase
- Due to the fact that FeCrAl oxidation should be much lower than Zry oxidation the temperatures should be lower than in the assumed oxidation case

Post-Test Simulations

Post-Test Simulation
– Assumptions and Model Improvement –

- Standard ATHLET-CD input deck for QUENCH tests
- Basic assumptions for Bundle and Rods are the same as for pre-test simulations
- Boundary conditions in input deck as given by data file
- External electrical resistance of 5.0 mOhm was used
- Oxidation model for cladding material, corner rods, spacer grids and shroud was implemented as given by KIT for FeCrAl
- FeCrAl / Al_2O_3 properties instead of Zry / ZrO_2 properties (no temperature dependency considered)

Material Property	FeCrAl	Al_2O_3
Density	7.1 ·10³ kg/m³	3.9 ·10³ kg/m³
Thermal conductivity	11 (323 K) → 35 (1673 K)	35 W/mK
Specific Heat	460 (293 K) → 800 (1673 K)	880 J/kg K

Post-Test Simulation
– FeCrAl Oxidation Model (I) –

- Chemical reaction
  - Assumption: only oxidation of Al

    $Fe_xCr_yAl_z + z/2 \cdot 3\ H_2O \rightarrow Fe_xCr_yAl_{2z}O_{3z} + z/2 \cdot 3\ H_2 + z \cdot \Delta h$

    $\Delta h = 9.3 \cdot 10^5$ J/mol

    ⟹ production of hydrogen and heat release
  - Assumption of molar mass of FeCrAl

    $M_{FeCrAl} = 99.8 \cdot 10^{-3}$ kg/mol → $\Delta h = 9.32 \cdot 10^6$ J/kg$_{FeCrAl}$
  - Resulting Oxide Al_2O_3

    $M_{Al2O3} = 102.0 \cdot 10^{-3}$ kg/mol

Post-Test Simulation
– FeCrAl Oxidation Model (II) –

- Oxidation rate
  - Parabolic law derived from the analytical solution of the diffusion equation as used for the oxidation of Zr

$dW^2 = K\,dt$

$dW/dt = K / 2W$

W: m_{O2} /A [kg/m²]

K: reaction rate [kg²/m⁴s]

t: time [s]

  - Reaction rate K is defined by an Arrhenius formulation:

$K = A\ e^{-B/(R\,T)}\ g(p_s)$

R = 8.314 J/mol K (gas constant)

A = 3.1 kg²/m⁴s } given by KIT

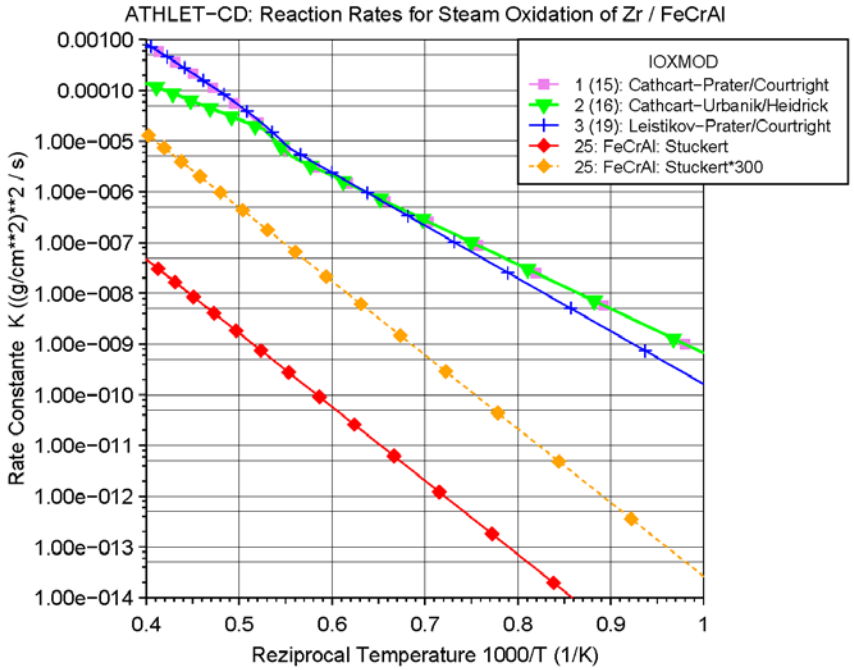
B = 2.78519 · 10⁵ J/mol } for one composition

T: cladding temperature [K]

$g(p_s)$: reduction factor to consider steam starvation

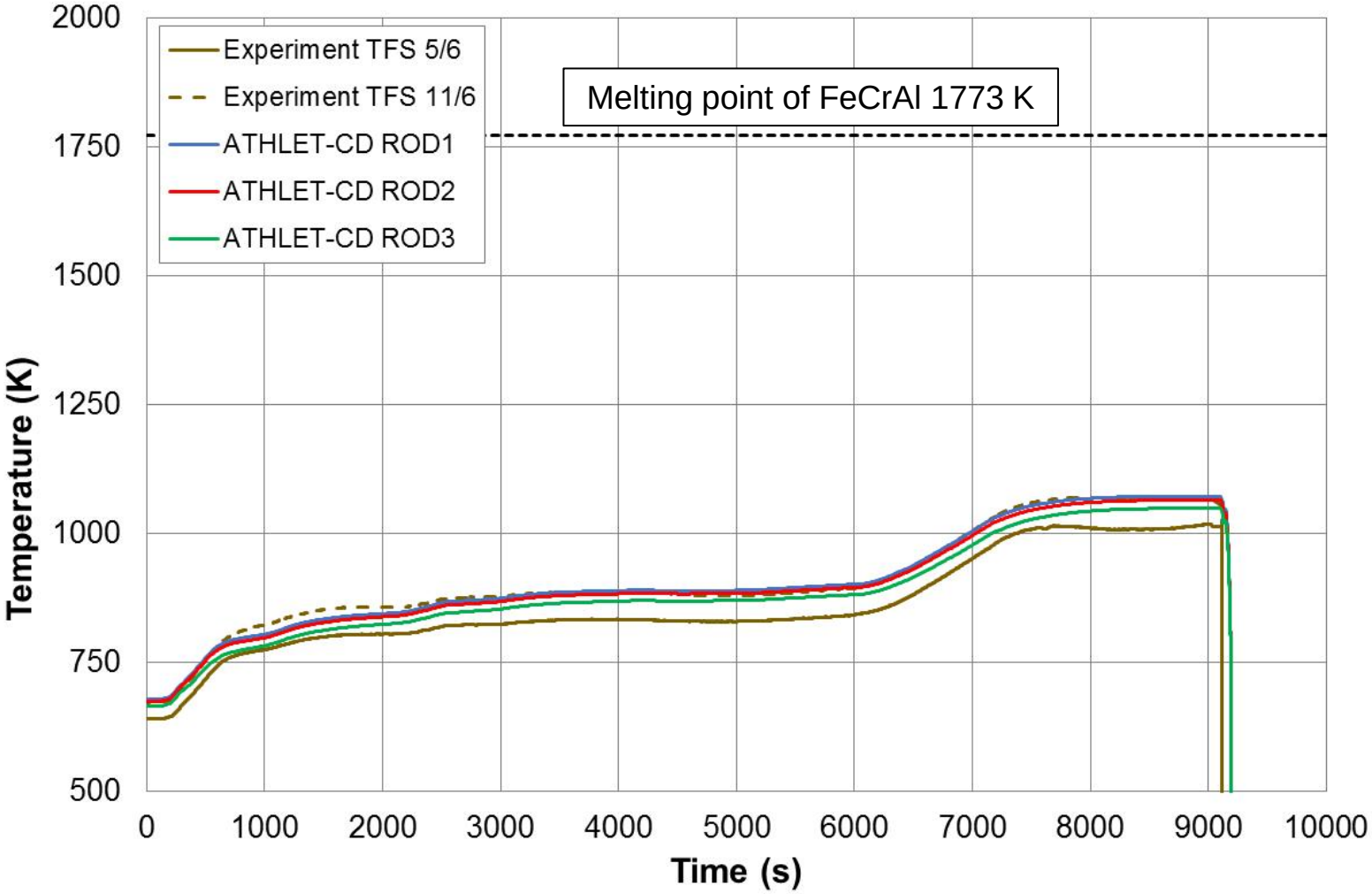
Post-Test Simulation
– FeCrAl Oxidation Model (III) –

- Reaction rate of FeCrAl versus Zry4
- Model 25 is based on a publication by Pint et al. (JNM 440) for KANTHAL APMT (69Fe+21.6Cr+4.9Al) and provided by KIT
- Model 25 multiplied by 300 is derived from the ”State-of-the-Art Report on Light Water Reactor Accident-Tolerant Fuels“ of the OECD/NEA (NEA No. 7317)



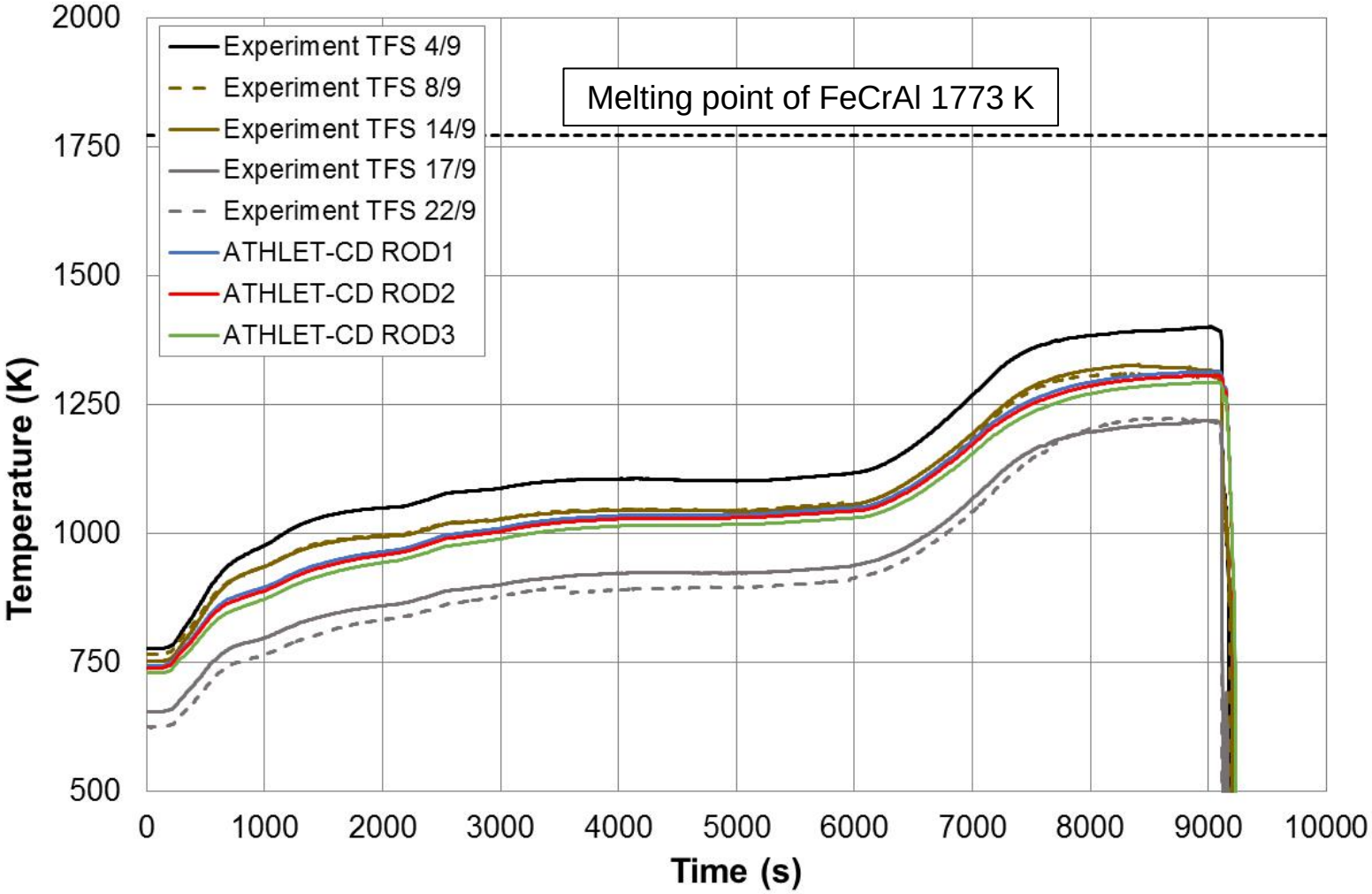
Post-Test Simulation
– Results (I) –

- Temperatures at 250 mm



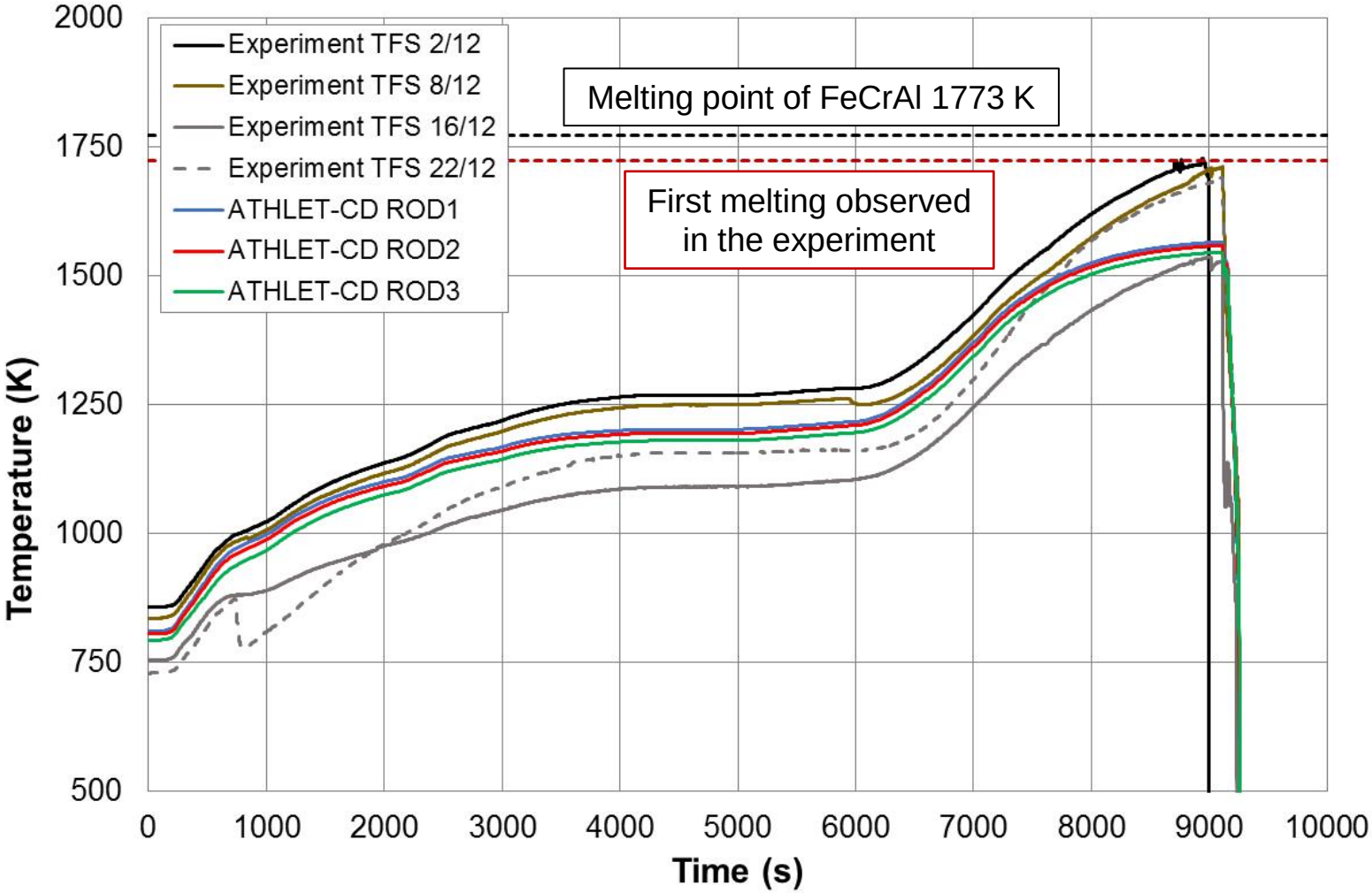
Post-Test Simulation
– Results (II) –

- Temperatures at 550 mm



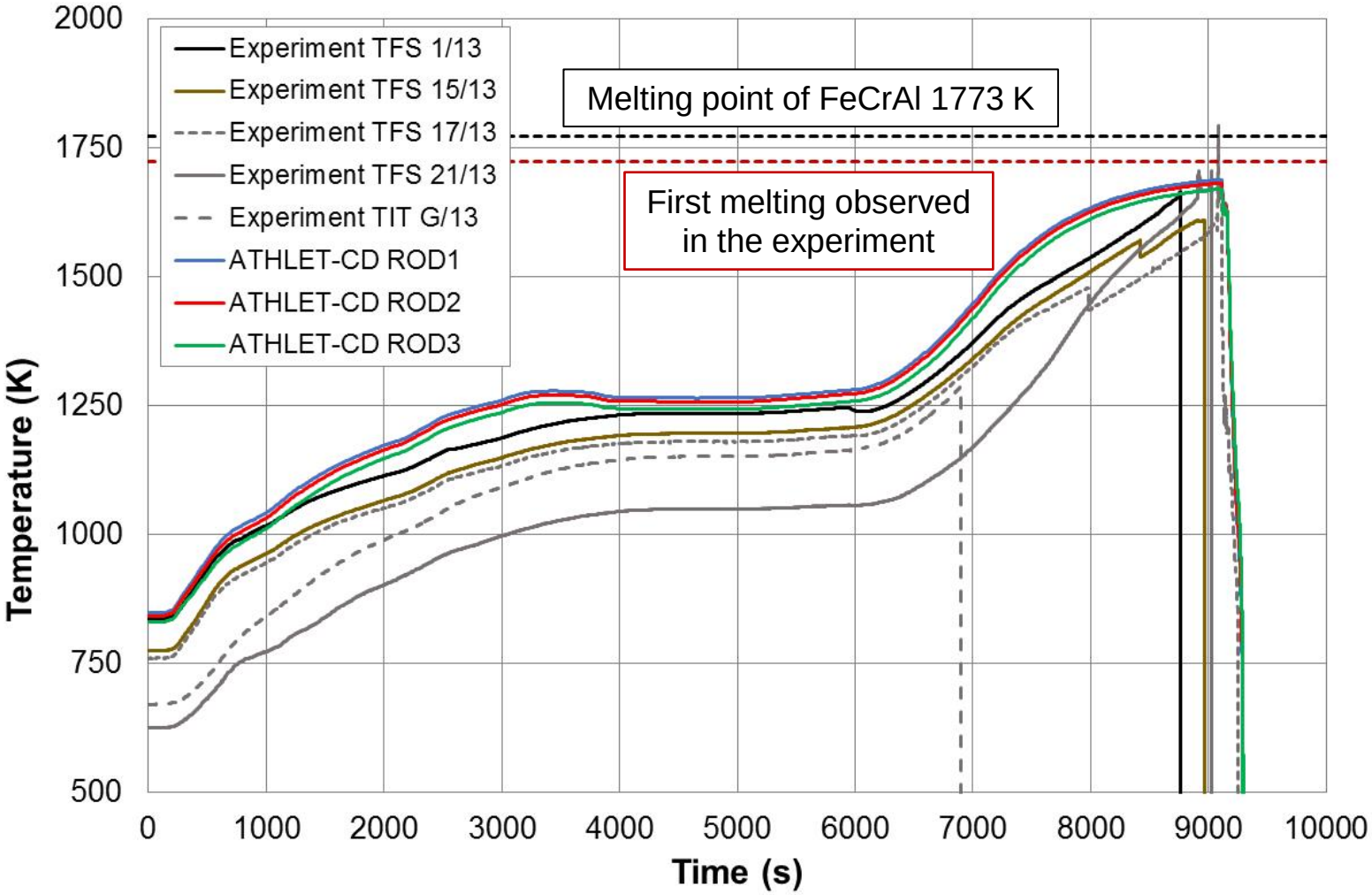
Post-Test Simulation
– Results (III) –

- Temperatures at 850 mm



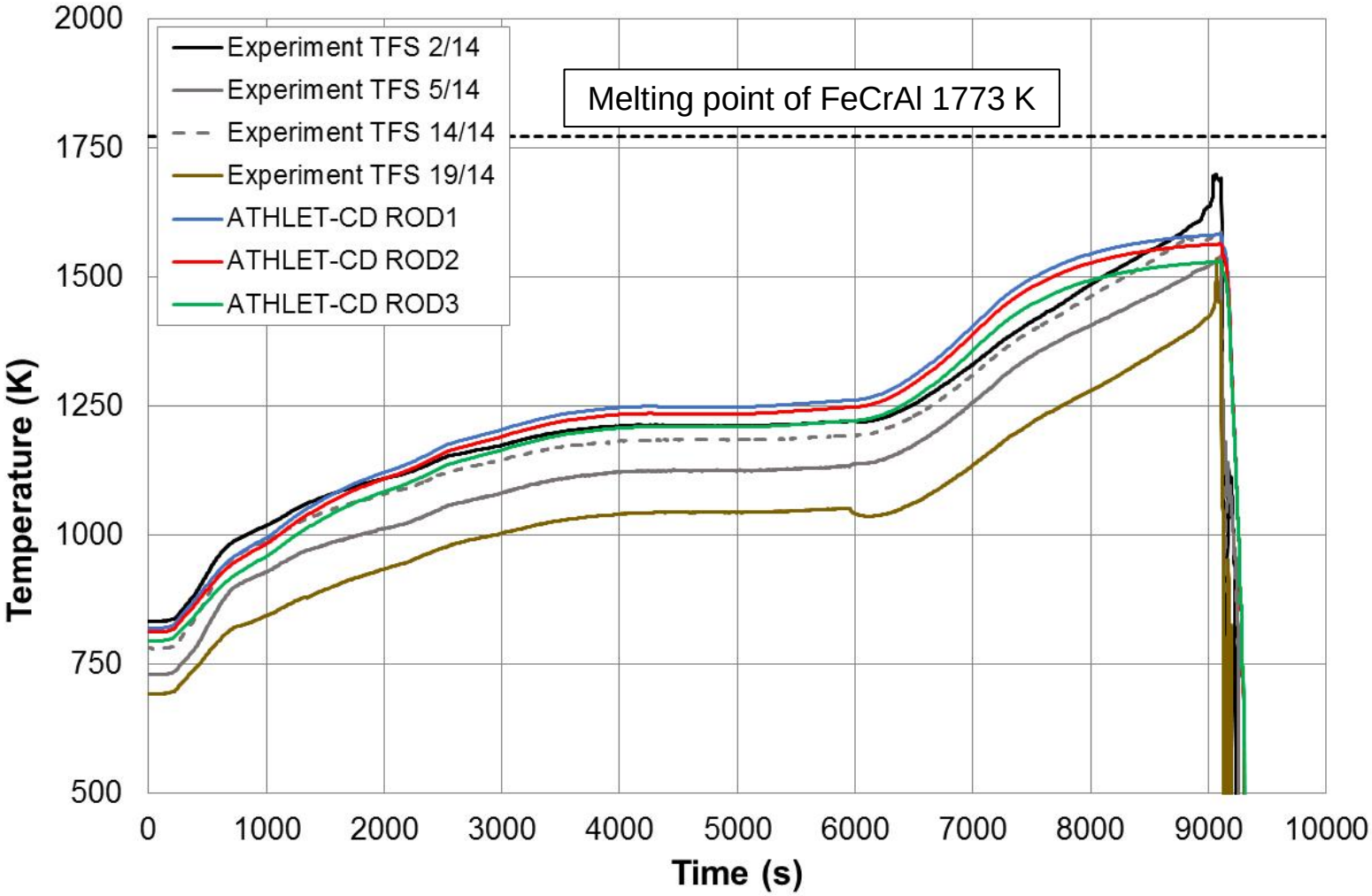
Post-Test Simulation
– Results (IV) –

- Temperatures at 950 mm



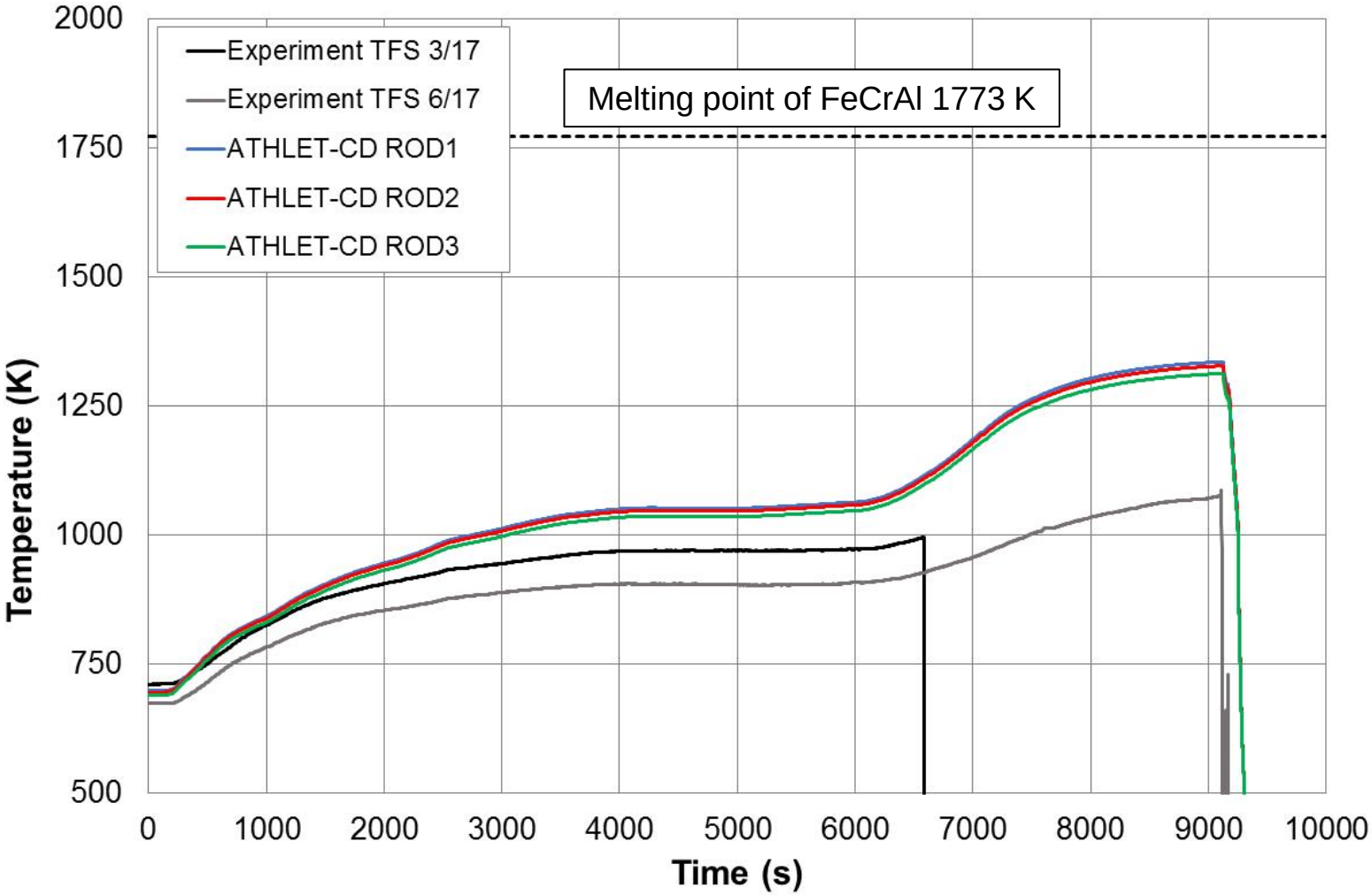
Post-Test Simulation
– Results (V) –

- Temperatures at 1050 mm



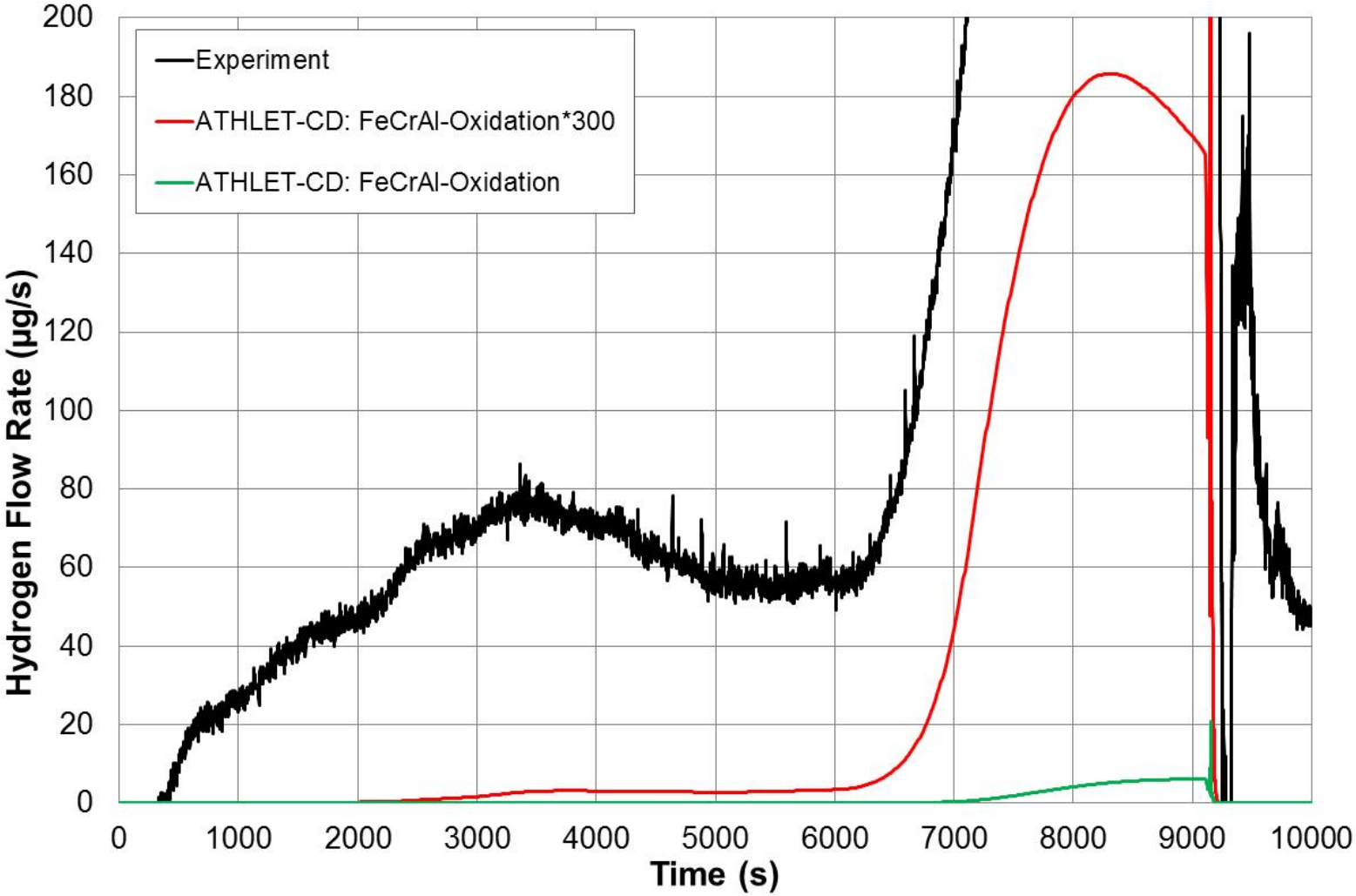
Post-Test Simulation
– Results (VI) –

- Temperatures at 1350 mm



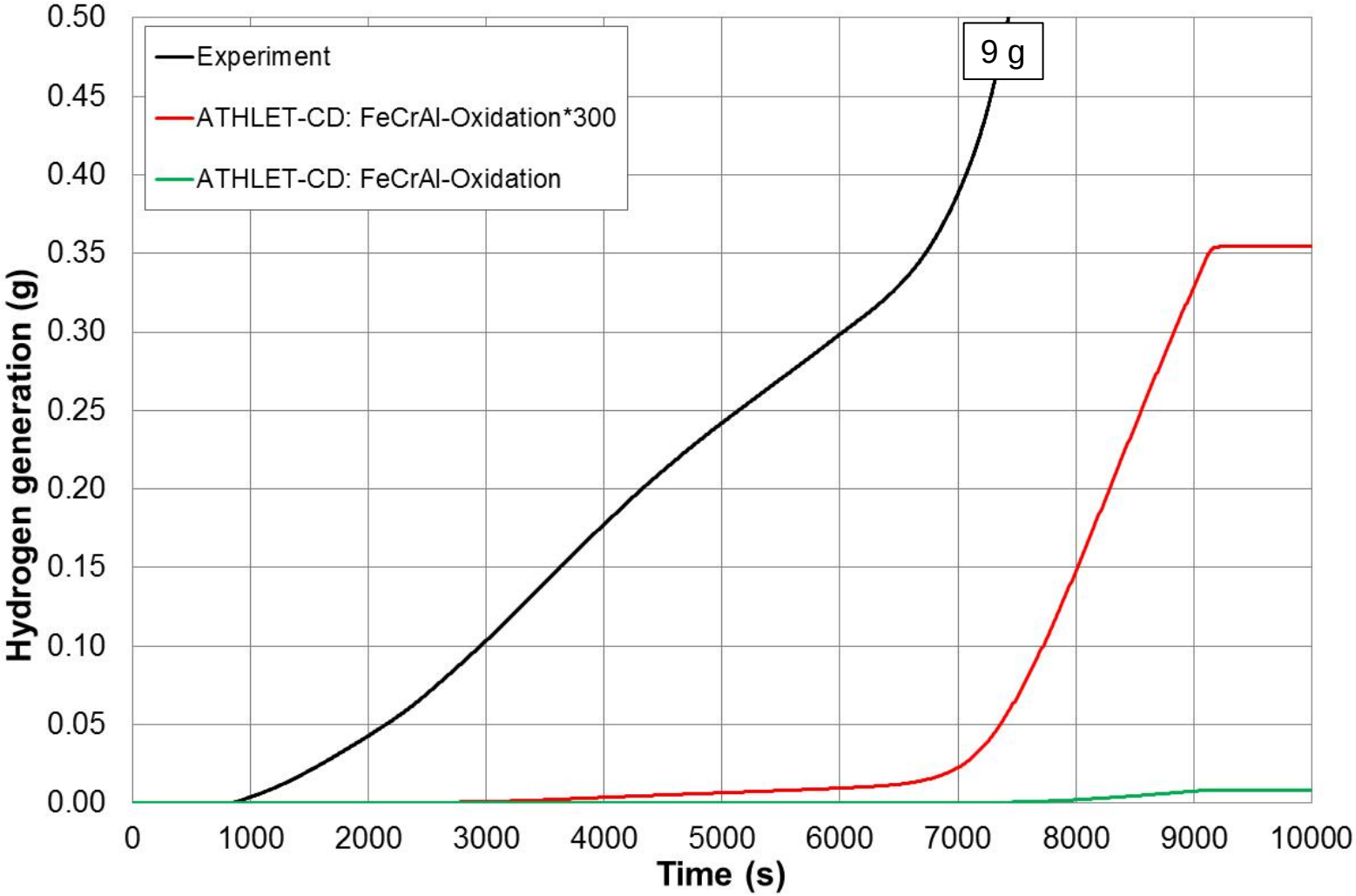
Post-Test Simulation
– Results (VII) –

- Hydrogen Generation Rate



Post-Test Simulation
– Results (VIII) –

- Hydrogen Generation



Post-Test Simulation
– Conclusions (I) –

- The oxidation model given by KIT for one dedicated FeCrAl composition was implemented in ATHLET-CD
- ATHLET-CD simulated the QUENCH-19 test with the given boundary conditions and the given oxidation behaviour
- No temperature escalation is calculated as shown in the test
  - Maximum temperature in the test: 1730 K at 850 mm elevation
  - Maximum temperature in the simulation: 1685 K at 950 mm elevation
- No further temperature increase during quenching in agreement with the test
- Good agreement of temperatures within heated length, but overestimation of temperatures above heated length

Post-Test Simulation
– Conclusions –

- The radial temperature profile is lower than in the test and can also not be captured by implementing the capacity of the wet insulation as observed in the experiment
- H_2 generation is much lower than measured (0.008 g simulated – 9 g measured) with the given correlation for one FeCrAl composition and derived from an OECD report and the assumption of only Al_2O_3 as resulting oxide
  - The oxidation model for FeCrAl cladding has to be further developed for ATHLET-CD based on the current very simple modelling
- Furthermore, the observed beginning of melting which may lead to accelerated oxidation is not modelled and could be one additional point for model improvement

Status and first results of the BWR control blade degradation test under steam-starved conditions

Anton P. Pshenichnikov, Saishun Yamazaki, Yuji Nagae, Masaki Kurata

Collaborative Laboratories for Advanced Decommissioning Science (CLADS), Japan Atomic Energy Agency (JAEA)

790-1 Motooka Ohtsuka, Tomioka, Futaba district, Fukushima prefecture, 979-1151, Japan.

Abstract

Big advances in understanding of BWR accident progression have been made in the past at SNL and KfK and recently in JAEA regarding Fukushima Daiichi accident. However, there are still many uncertainties around 1F Unit 2, where accident was likely to develop under special conditions, including the phase of steam starvation. New experimental information is necessary because materials behaviour and ability of protective oxide films to survive under specific conditions is very hard to predict. In particular, control blade degradation happens first and under steam-starved conditions can totally change the degradation from BWR-drainage to TMI-like scenario. This result in debris with different properties and in first case it has an impact on the RPV failure mode. Another important concern is boron interaction with surrounding stainless steel and Zr changing materials compositions and properties. The important lack of knowledge has therefore been identified and then the proper test scenario maximally close to the real 1F Unit 2 accident scenario was proposed.

A large-scale control blade degradation test facility introduced to QUENCH audience in the year 2017 has been used to conduct the Mock-up Assembly Degradation test (CLADS-MADE-01). In situ video of the experiment and mass-spectrometric analysis of the output gases (H_2, CO, CO_2) were carried out during tests. Initial heating rate for the experiment was around 0.4 K/s. Steam flow rate was increased stepwise 20, 30, 40 g/min during transient heating to simulate oxidation during boil-away. After reaching 1475 °C in the hottest point the steam was switched off to create steam-starved conditions for 45 minutes. The temperature in the furnace at the moment had smooth axial gradient 420 °C/m. Temperature was stabilised at 1475 °C as we wanted to investigate the beginning phase of an accident. Finally, the assembly was cooled down by natural heat losses in Ar.

Previous data using the same equipment has been collected in JAEA for BWR high-temperature degradation in pure Ar and in steam environment. The results showed difference in reaction between molten control rod and channel box. But the mock-up assemblies were not prototypically oxidised. Oxidation during transient heating was not enough to prevent channel box melt-through. Therefore, prototypic oxidation is necessary to approach real accident conditions. The impact of pre-oxidation, steam flow rate and temperature definitely has some critical point where the transition between two scenarios: BWR-drainage scenario and TMI-like pool formation becomes impossible at the beginning phase of severe accident.

The results of the present study were found to be in accord with the data from SNL, KfK and JAEA previous tests and complement them providing useful information on degradation of the assembly under specific accident conditions close to 1F Unit 2 including steam starvation phase. In particular, problem of heterogeneous core degradation, boron behaviour, control blade liquefaction and melt relocation were analysed. Melt relocation features: onset, progress, candling, blockage formation and its subsequent melting was directly observed in situ using video cameras. It was established, that the control blade melt was stratified into Fe and Cr enriched layers and saturated with boron. Chromium rich layer which obviously had higher melting point helped control blade claddings to survive and prevented relocation and oxidation of B_4C and formation of boron aerosols during the test. Post-test investigation is underway.

This study is performed in “Advanced Multi-scale Modeling and Experimental Tests on Fuel Degradation in Severe Accident Conditions” supported by Ministry of Economy, Trade and Industry, Japan (METI).


TOSHIBA

Status and first results of the BWR control blade degradation test under steam-starved conditions

A. P. Pshenichnikov, S. Yamazaki, Y. Nagae, M. Kurata

Presentation at 24th QUENCH workshop

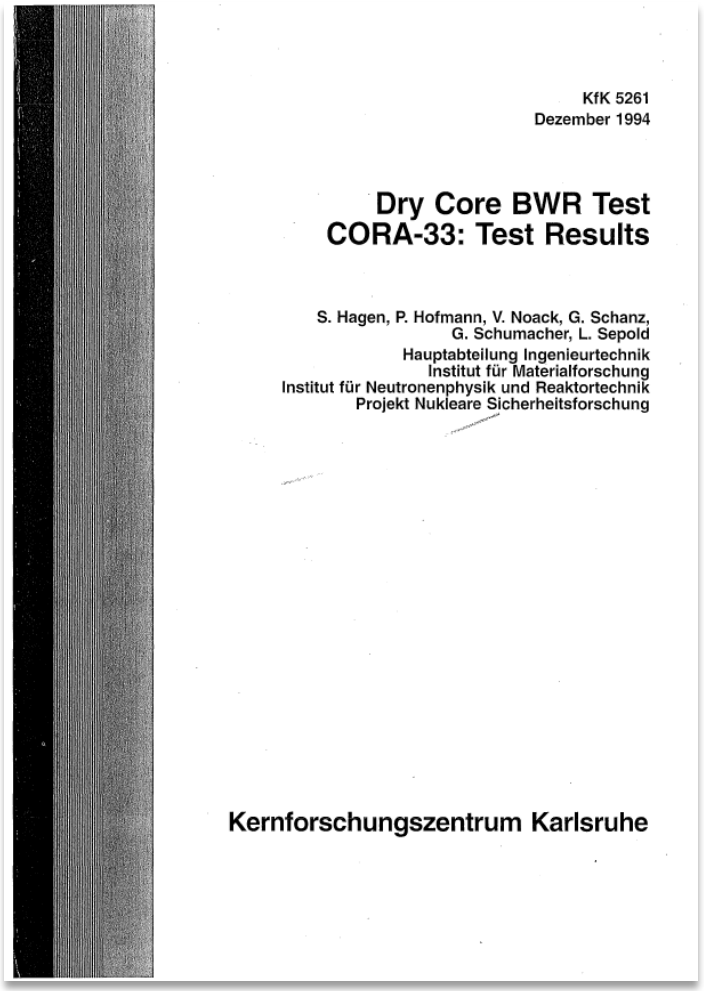
Collaborative Laboratories for Advanced Decommissioning Science



Part 1
Introduction

Background

First concerns were in DE and US 1988-1994



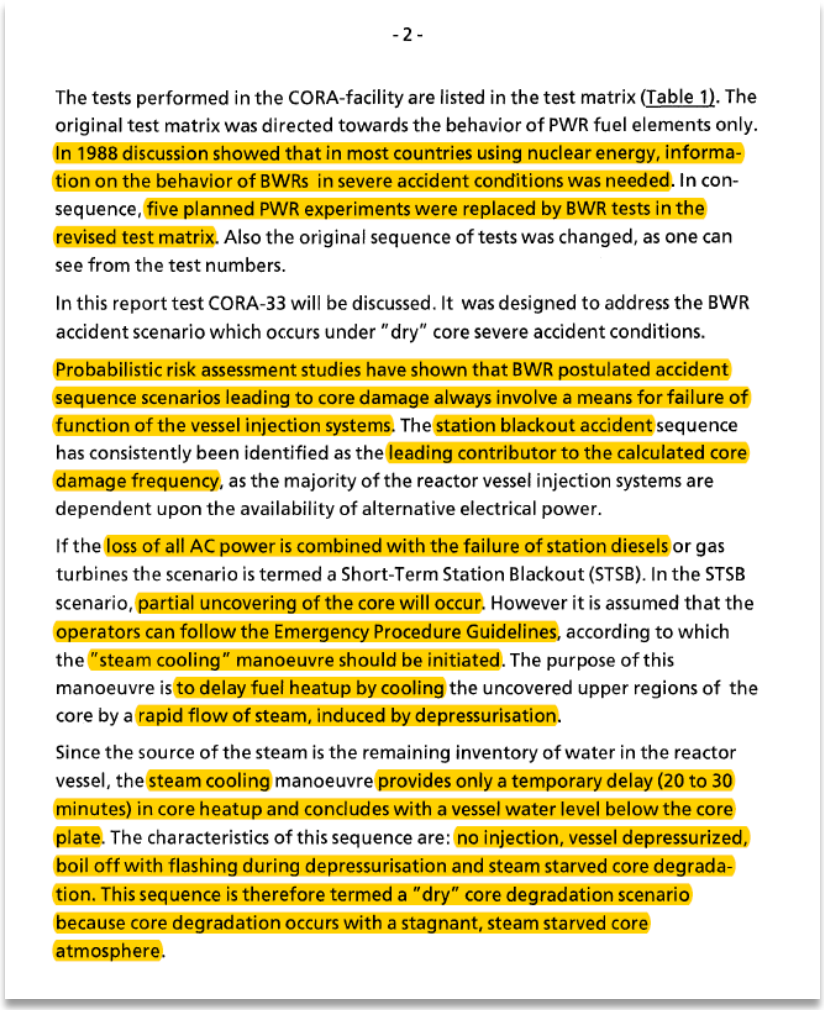
KfK 5261
Dezember 1994

Dry Core BWR Test CORA-33: Test Results

S. Hagen, P. Hofmann, V. Noack, G. Schanz, G. Schumacher, L. Sepold
Hauptabteilung Ingenieurtechnik
Institut für Materialforschung
Institut für Neutronenphysik und Reaktortechnik
Projekt Nukleare Sicherheitsforschung

Kernforschungszentrum Karlsruhe

Page 2



The tests performed in the CORA-facility are listed in the test matrix (Table 1). The original test matrix was directed towards the behavior of PWR fuel elements only. In 1988 discussion showed that in most countries using nuclear energy, information on the behavior of BWRs in severe accident conditions was needed. In consequence, five planned PWR experiments were replaced by BWR tests in the revised test matrix. Also the original sequence of tests was changed, as one can see from the test numbers.

In this report test CORA-33 will be discussed. It was designed to address the BWR accident scenario which occurs under "dry" core severe accident conditions.

Probabilistic risk assessment studies have shown that BWR postulated accident sequence scenarios leading to core damage always involve a means for failure of function of the vessel injection systems. The station blackout accident sequence has consistently been identified as the leading contributor to the calculated core damage frequency, as the majority of the reactor vessel injection systems are dependent upon the availability of alternative electrical power.

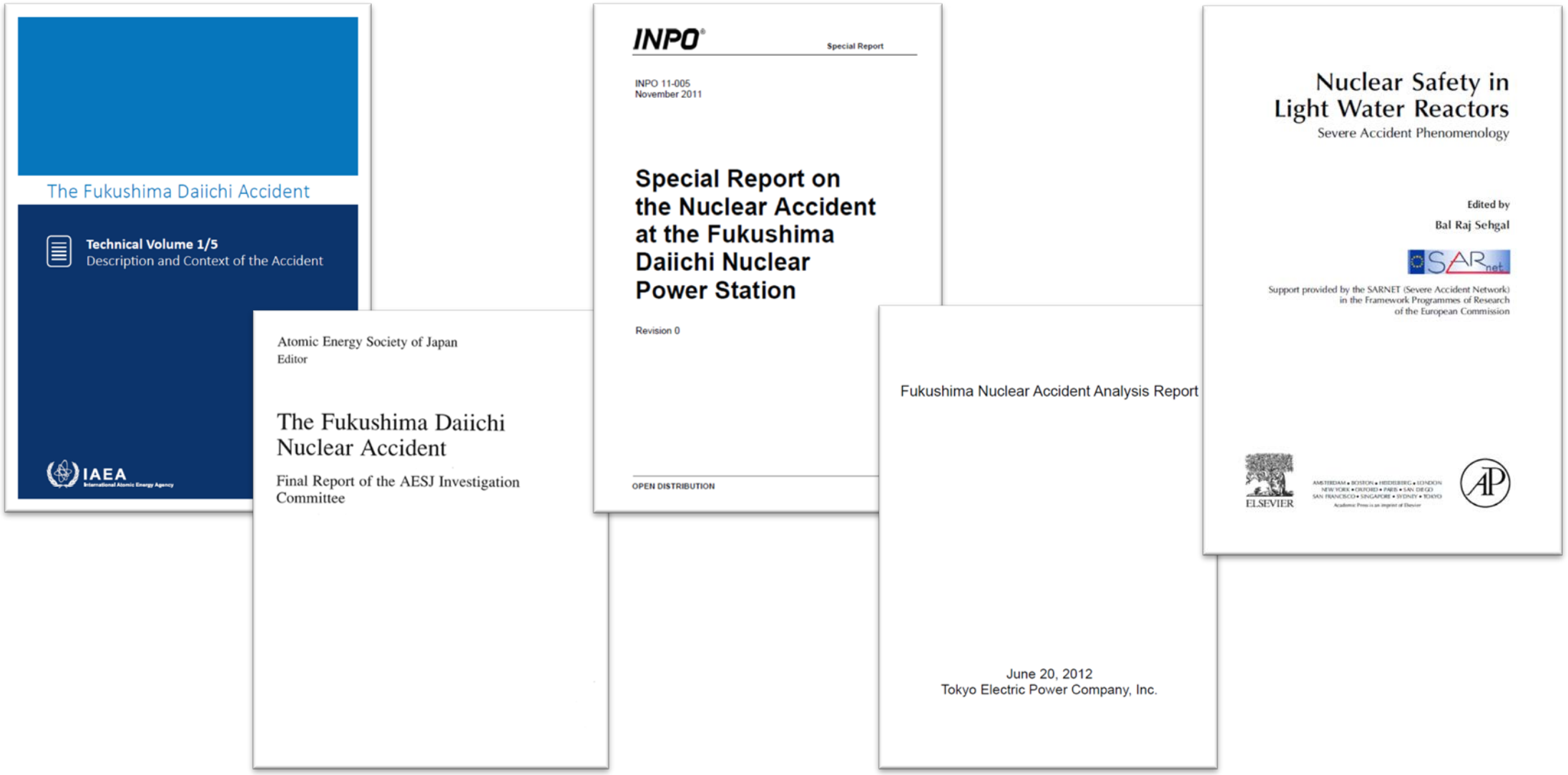
If the loss of all AC power is combined with the failure of station diesels or gas turbines the scenario is termed a Short-Term Station Blackout (STSB). In the STSB scenario, partial uncovering of the core will occur. However it is assumed that the operators can follow the Emergency Procedure Guidelines, according to which the "steam cooling" manoeuvre should be initiated. The purpose of this manoeuvre is to delay fuel heatup by cooling the uncovered upper regions of the core by a rapid flow of steam, induced by depressurisation.

Since the source of the steam is the remaining inventory of water in the reactor vessel, the steam cooling manoeuvre provides only a temporary delay (20 to 30 minutes) in core heatup and concludes with a vessel water level below the core plate. The characteristics of this sequence are: no injection, vessel depressurized, boil off with flashing during depressurisation and steam starved core degradation. This sequence is therefore termed a "dry" core degradation scenario because core degradation occurs with a stagnant, steam starved core atmosphere.

The "station blackout", "loss-of-coolant", "depressurization" and "dry core degradation" under "steam-starved core environment" conditions are the key phenomena to expect in a case of a nuclear accident in BWRs

Accident at the Fukushima-1 nuclear power station (1F)

11-3-2011 14:46 →



Current status BWR related tests* (incl. PWR with B_4C)

Heating rate → Atmosphere↓	0.3 K/s, low (3rd day decay heat + cooling or boil-away)	0.6 K/s, intermediate (2nd day decay heat + cooling)	1 K/s, high (decay heat 1st day w/o cooling time after SCRAM)
Model tests in Ar	(!) No Info, but predictable melt formation	(!) Not enough Info, but predictable melt attack of Zr components like CRFCBF-01 (JAEA)	**XR2-1 test (SNL),** CRFCBF-02 (JAEA), severe melt attack of Zr components (!) (not enough BWR information)
Steam starvation (always not enough even at 800-900 °C) < 0.02 g/(s*m*rod) for our facility and our assembly	(!) No Info Necessary for steam-starved degradation understanding 1F Unit 2	(!) No Info	Absorber melt, severe melt attack of Zr components CRFCBF-04 (JAEA) (!) (not enough BWR information)
Intermediate steam (enough at 800-900 °C but not enough at elevated T) 0.02<g/(s*m*rod)<0.05	(!) Only one test no preoxidation **CORA-33 (KfK)**	Intermediate escalation Example is QUENCH-07 or -09 (KIT) and Phebus FPT-3 (CEA) prototypic for PWRs. (!) (no prototypic tests for BWRs)	Absorber melt CRFCBF-03 (JAEA) (!) (not enough BWR information)
Steam rich (always enough) > 0.05 g/(s*m*rod)	(!) Only one test no preoxidation **CORA-31 (KfK)**	QUENCH tests for EU PWRs, CODEX-B_4C (KFKI) and CORA-W2 for VVER-400 with B_4C (!) (no prototypic tests for BWRs) QUENCH-20 (BWR) is planned	**CORA-16,-17,-18 (no preoxidation) (KfK), CORA-28 (with preoxidation) (FZKA), DF-4 (SNL)**

*More details in the paper "*Phenomenology of BWR fuel assembly degradation" M. Kurata, M. Barrachin, T. Haste, M. Steinbrück // Journal of Nuclear Materials, 500 (2018) 119-140*



Part 2
Motivation for new test

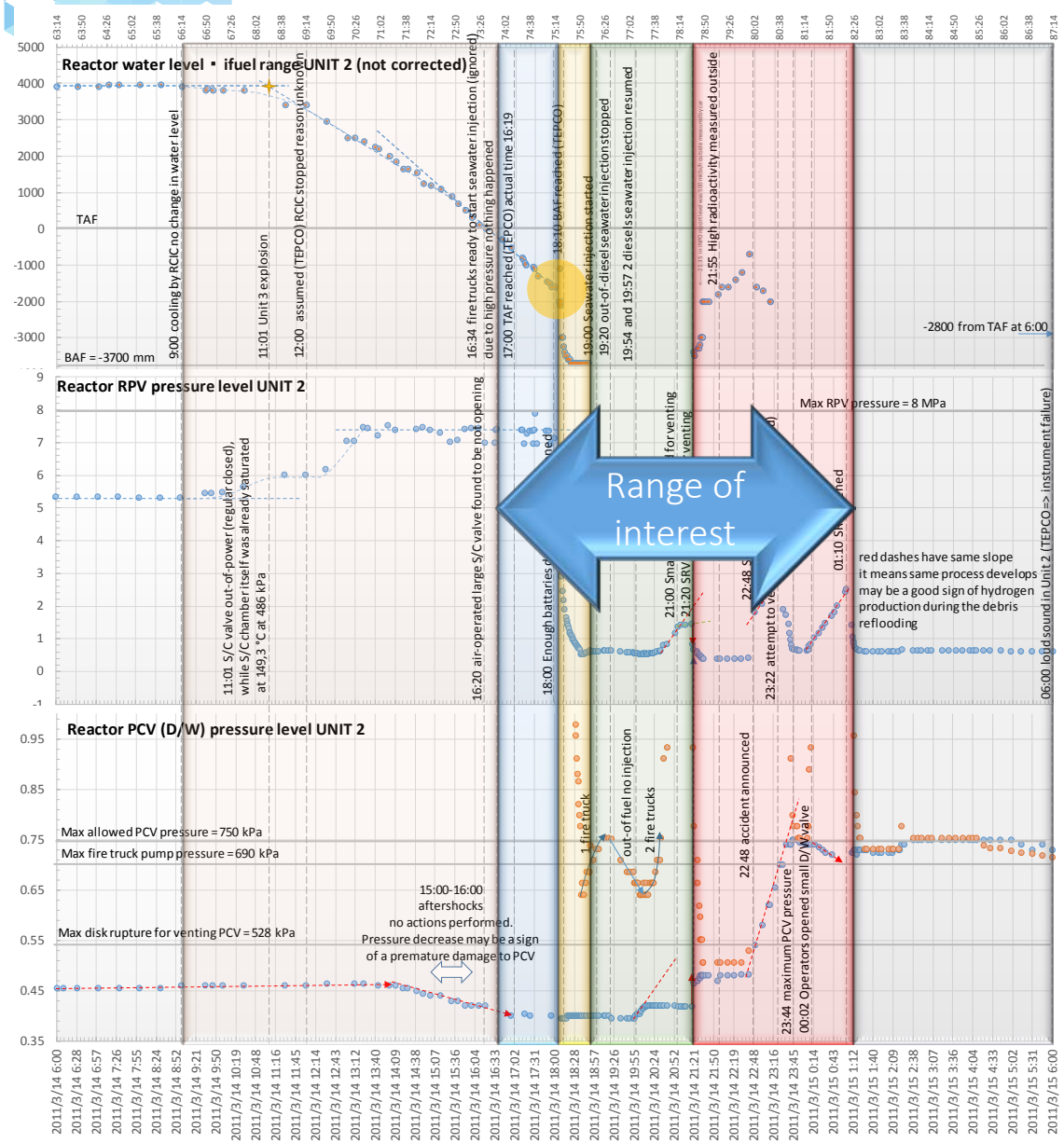
JAEA-CLADS Test technology development group

Accident features comparison at 1F

Unit 1 (1st day) ->	Unit 3 (2nd day) ->	Unit 2 (3rd day)
• BWR3 (smaller) reactor/containment volume • Full Station Black-Out (SBO) situation • Loss of cooling at the beginning by manual shut-down of IC just before tsunami arrival • Water level and pressure measurements uncertain • Probably steam rich atmosphere during water boil-out • No gas leakage from PCV assumed (explosion not due to leakage, but after a successful venting)	• BWR4 (bigger than Unit 1) reactor size • AC power -> lost • DC Power -> available • RCIC started after tsunami • Loss of cooling on the 2nd day • Pressure data available and poorly explainable • Water level decreased very fast but not completely • Further water level was at TAF -2 m • Because of that probably intermediate steam atmosphere • Considerable gas leakage from PCV assumed • Explosion some time after reaching max PCV pressure and venting	• BWR4 bigger containment than Unit 1 but still much lower than any PWR • Full SBO situation • RCIC ran before tsunami and worked automatically • Loss-of-cooling on the 3rd day after RCIC stopped (reason unknown), probably explosion at Unit 3 • Pressure decrease data available and explainable together with depressurization valves operation data published in official reports • Water level decreased very fast (≈ 40 minutes from TAF to BAF) leaves less possibility for steam rich conditions • Further water level behavior during accident is uncertain (lower than BAF for a long time) • Probably steam poor (or even starvation) environment during at least 2 hours 33 minutes • PCV leakage can be assumed but not clear (no PCV pressure decrease during accident) High-pressure scenario • No explosion (but still can be the possibility of the internal explosion like TMI-2 case)

THE MOST INTERESTING

Deep analysis of 1F Unit 2 accident



Phase duration

Phase duration	
7 h : 30 min	Slow water level decrease due to the cooling function degradation
1 h : 40 min	Water level reached TAF. Slow fuel temperature increase and low-T oxidation in steam-rich environment were possible
Point of no return	
1 h : 00 min	Depressurization, fast loss-of-coolant. Slight temperature decrease by “flashing”. Then again increase during oxidation in steam-rich environment
2 h : 20 min	Complete loss-of-coolant in the depressurized reactor. No further oxidation but melting and relocation was possible in steam-poor (starvation) environment
4 h : 00 min	Re-oxidation of high-T fuel rests and melt in steam or in water
> 5 h	Late phase of the accident MCCI, debris cooling (not in the focus of this study)

Our experimental capabilities

Real accident timing（graph based estimation）

1 h : 40 min	1 h : 00 min	2 h : 20 min	4 h : 00 min

Depressurization, fast loss-of-coolant. Slight temperature decrease by "flashing". Then again increased during oxidation in steam-rich environment

Suggested timing of our experiment

3 h	1 h	1 h	30 min
Pre-oxidation	**Transient**	**Starvation**	**Re-oxidation**

Our timing suggestion is representative for performing early phase fuel degradation experiment

Our plan to contribute to the BWR SA knowledge

Heating rate → Atmosphere↓	0.3 K/s, low (3rd day decay heat + cooling or boil-away)	0.6 K/s, intermediate (2nd day decay heat + cooling)	1 K/s, high (decay heat 1st day w/o cooling time after SCRAM)
Model tests in Ar	(!) No Info, b… melt formation	…melt attack of Zr components like CRFCBF-01 (JAEA)	XR2-1 test (SNL), CRFCBF-02 … melt attack of Zr … (!) (nc… …ation)
Steam starvation (always not enough even at 800-900 °C) < 0.02 g/(s*m*rod) for our facility and our assembly	1F Unit 2 Starvation phase !=BWR Key issue=! Will be investigated in CLADS-MADE-01	(!) No Info	Ab… …elt a… …s (!) (nc… …ation)
Intermediate steam (enough at 800-900 °C but not enough at elevated T) 0.02<g/(s*m*rod)<0.05	(!) Only one test	1F Unit 3 (with cooling and lower decay heat) !=BWR Key issue=! Will be investigated in CLADS-MADE-02	(!) (nc… …ation)
Steam rich (always enough) > 0.05 g/(s*m*rod)		QUENCH tests for EU PWRs, CODEX-B_4C (KFKI) and CORA-W2 for VVER-400 with B_4C (!) (no prototypic tests for BWRs)	prec… …A-28 (with preoxidation) (FZKA).

Oxidized samples' behaviour needs to be investigated here

Additional info on control blade degradation under specific starvation conditions needed

Especially for 1F Unit 1 prototypic BWR blade fast degradation study is still needed

Only one BWR test for this area is definitely not enough, that is why possibilities for future tests are huge

Good PWRs and not enough BWRs investigated area

*More details in the paper "*Phenomenology of BWR fuel assembly degradation" M. Kurata, M. Barrachin, T. Haste, M. Steinbrück // Journal of Nuclear Materials, 500 (2018) 119-140*



Part 3
Mock-up Assembly DEgradation test (CLADS-MADE-01)

JAEA-CLADS Test technology development group

Large-scale Equipment for Investigation of Severe Accidents in Nuclear reactors (LEISAN)

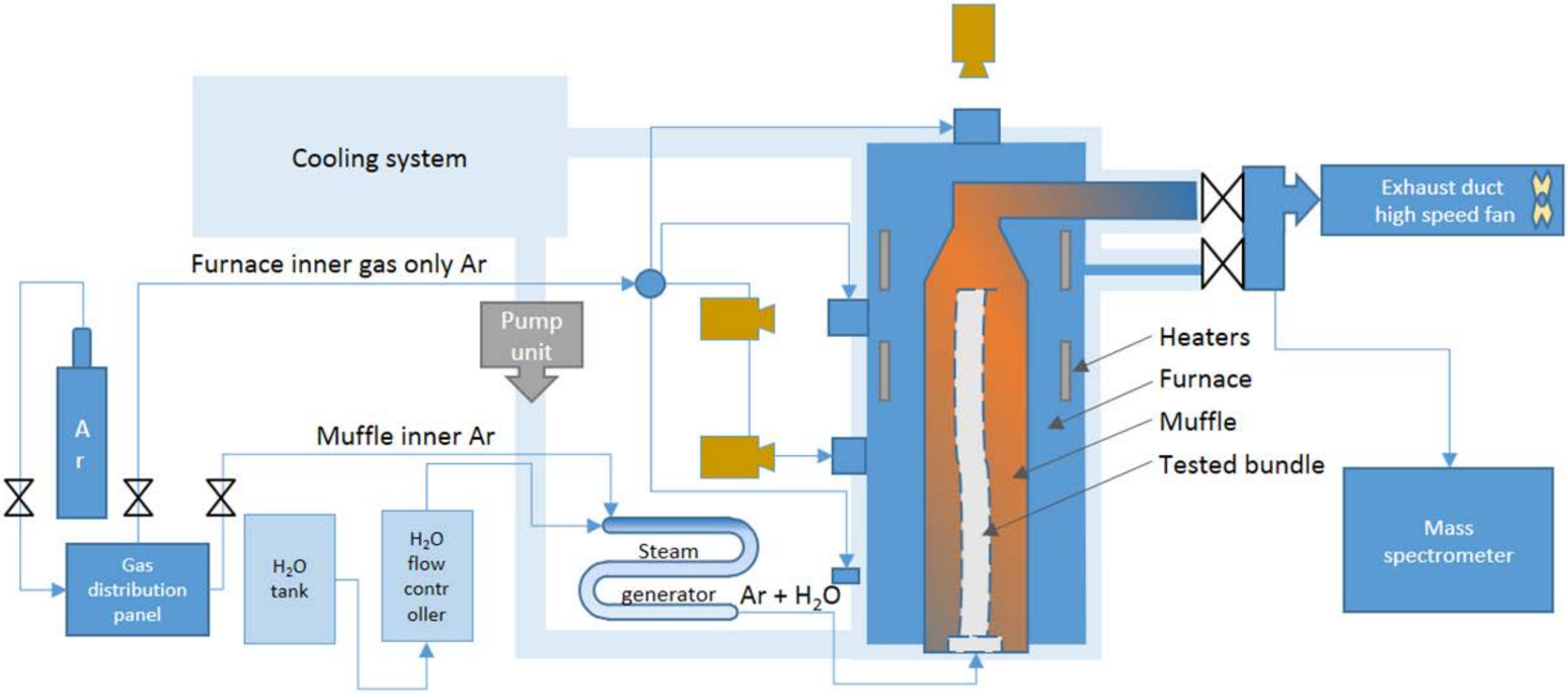






Specification	
Max assembly size for steam oxidation (limited by muffle)	20 ×20×120 cm
Max sample size for Ar environment (limited by furnace inner dimensions)	45×40 ×159 cm
Max temperature	2073 K / 1800 ℃
Atmosphere	Steam + Ar, pure Ar
Steam flow rate	0 – 50 g/min
Ar pre-heating temperature	Max. 300 ℃
Heating control / Heating rate	PID-controller / up to 1 K/s
Form of samples	Customized assemblies
Test materials	Nonradioactive

Large-scale facility flow diagram



Test schedule (tentative)

- FY2017 – CLADS-MADE-01 Fuel assembly degradation in steam-starved environment with smooth gradient simulating 1F Unit 2 accident conditions (successfully carried out)

- FY2018 – CLADS-MADE-02 Fuel assembly degradation test in steam-rich conditions with sharp gradient simulating 1F Unit 3 accident conditions

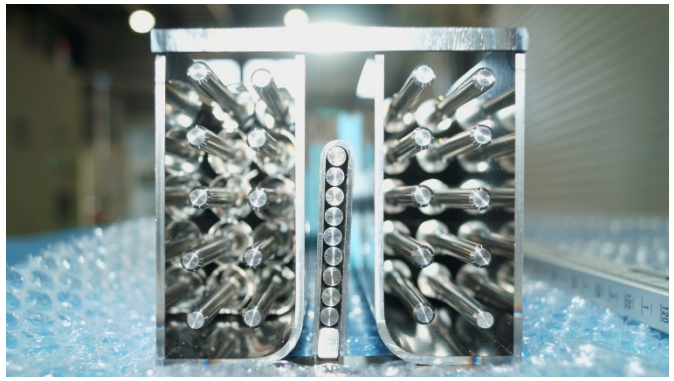
- FY2019 – BWR Lower head failure test possibly with international collaboration

Mock-up of BWR fuel assembly before test

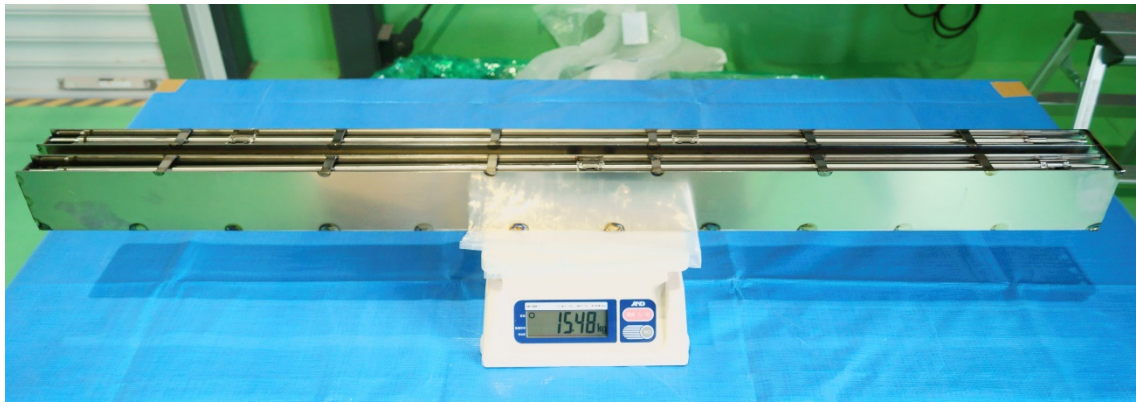


Assembly front and back

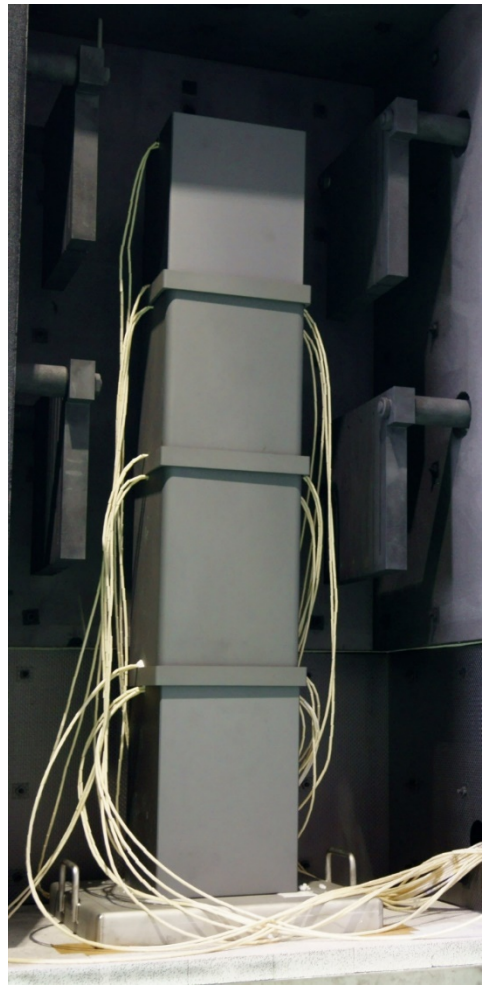
Assembly top



Overall weight 15.48 kg
(Zr : SS : B_4C ≈ 7 : 3 : 0.2)*

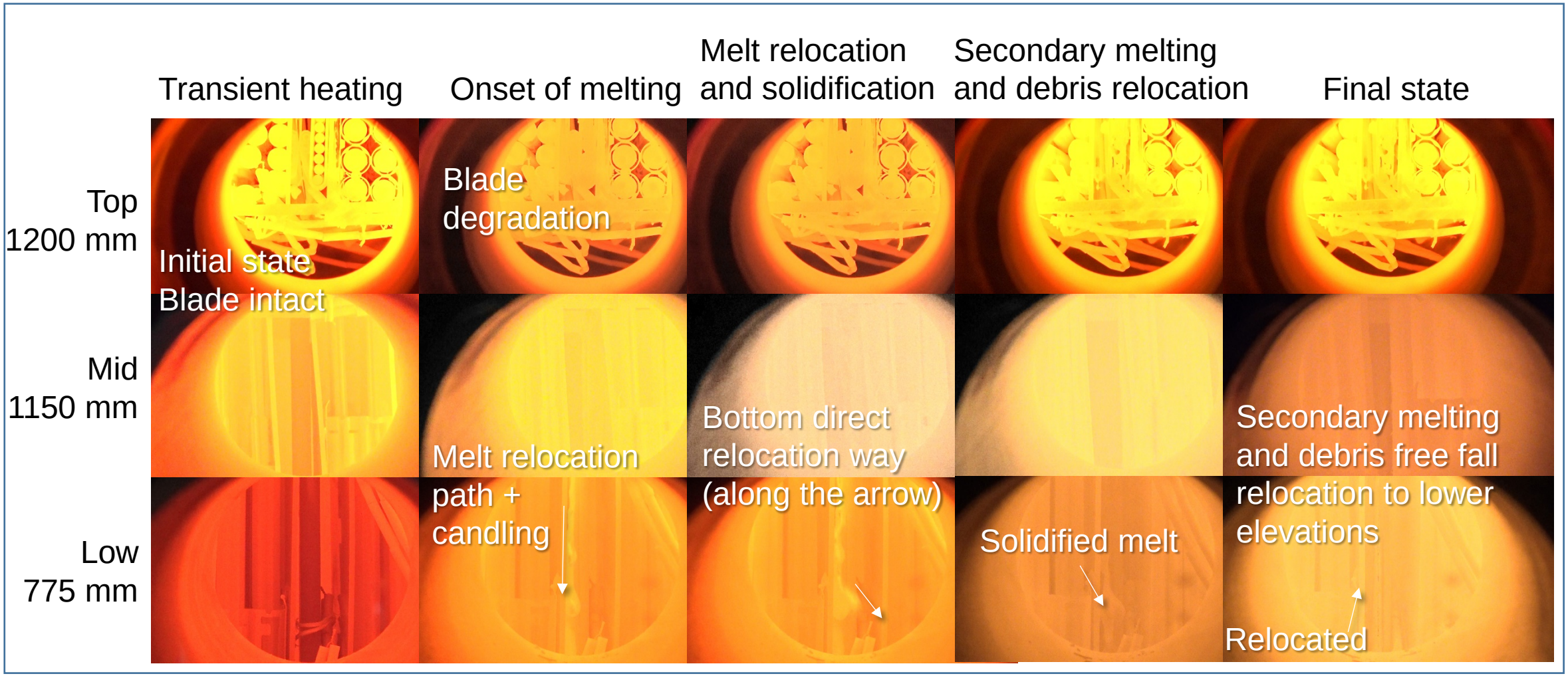


In the protective muffle
SiC coated carbon



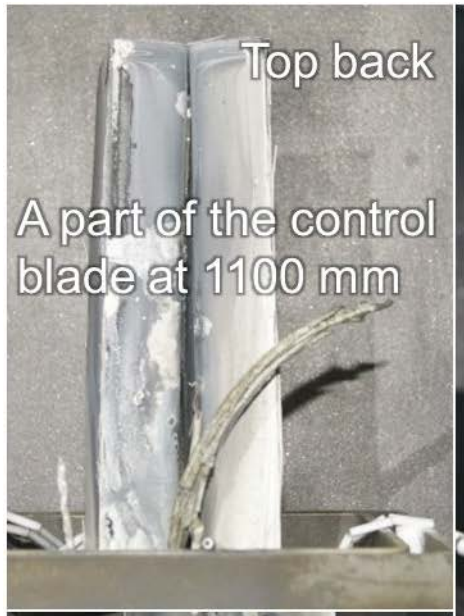
*close to 1F Unit 2 (44.8 : 17.7 : 0.82) / 4.1 = (10.9 : 4.3 : 0.2)

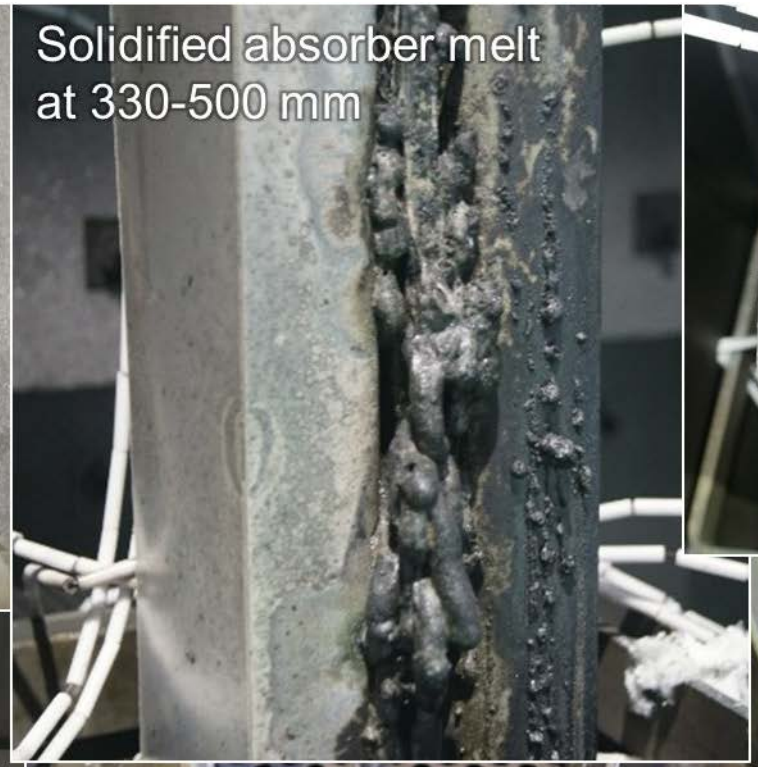
Mock-up of BWR fuel assembly during test



Mock-up of BWR fuel assembly after test







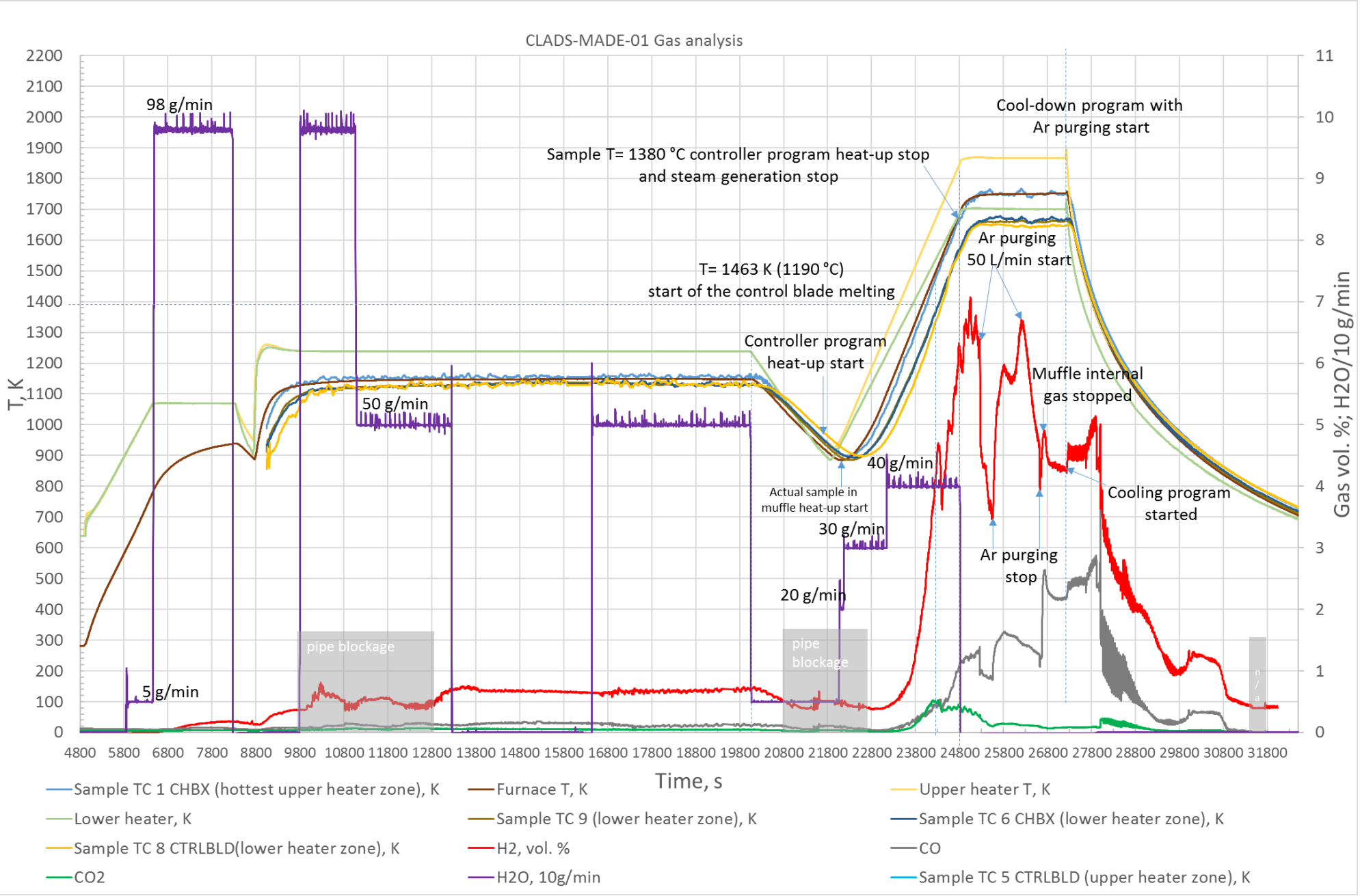




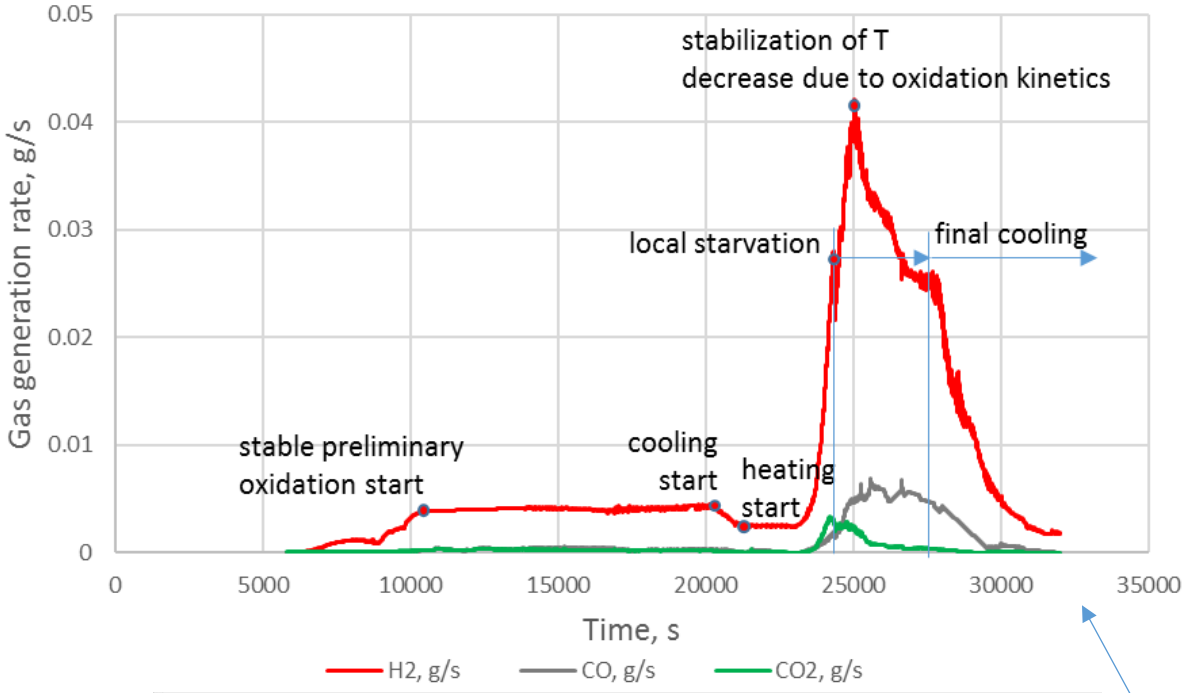


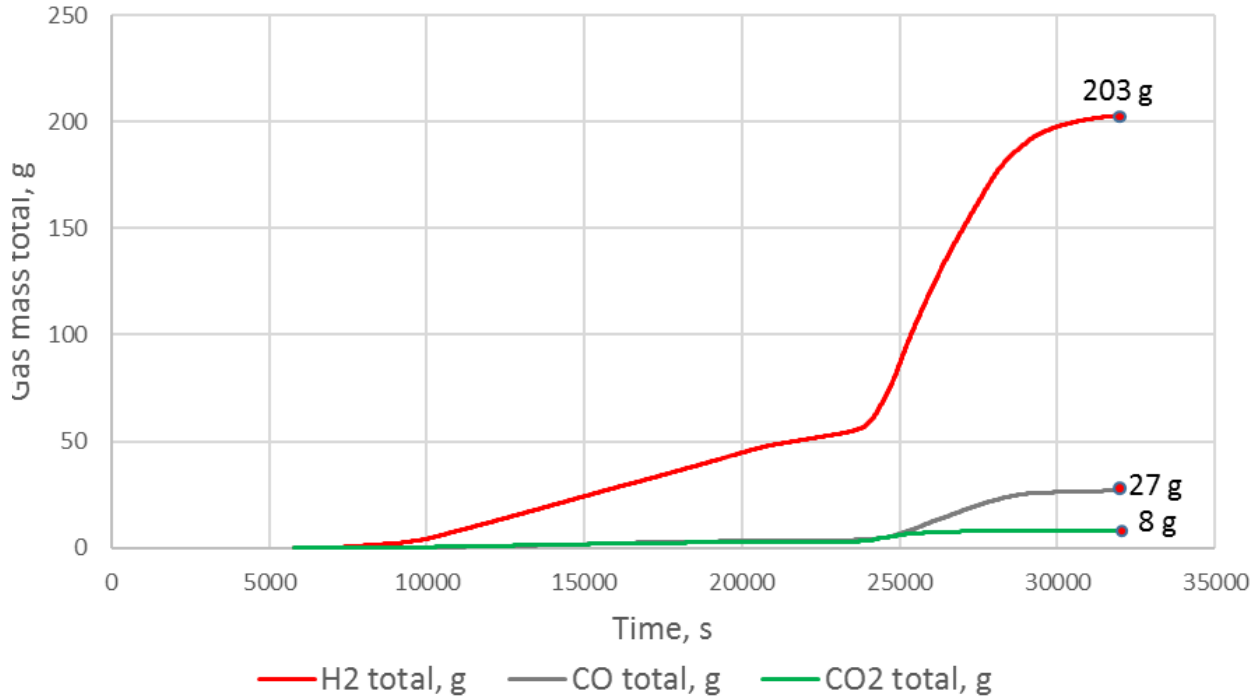


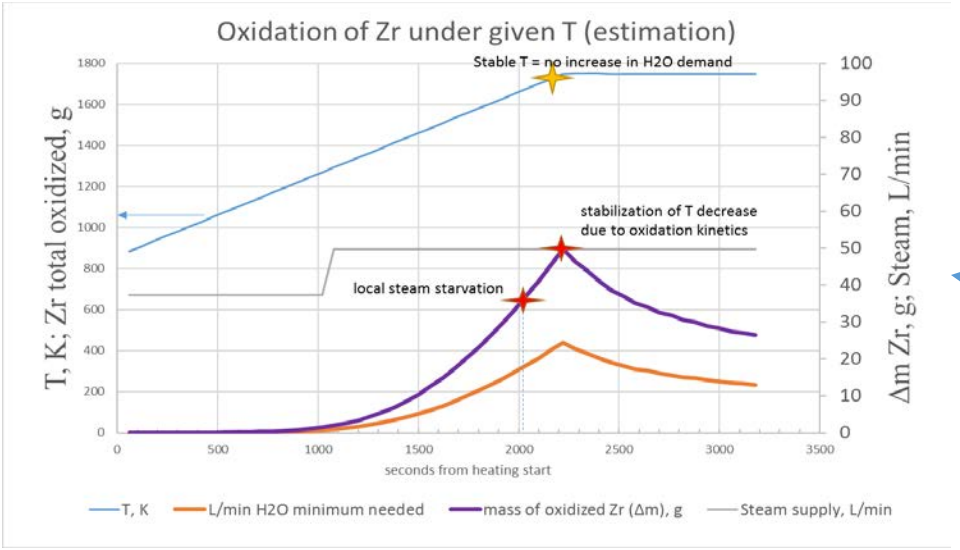
CLADS-MADE-01 test parameters' trends



CLADS-MADE-01 test parameters' trends

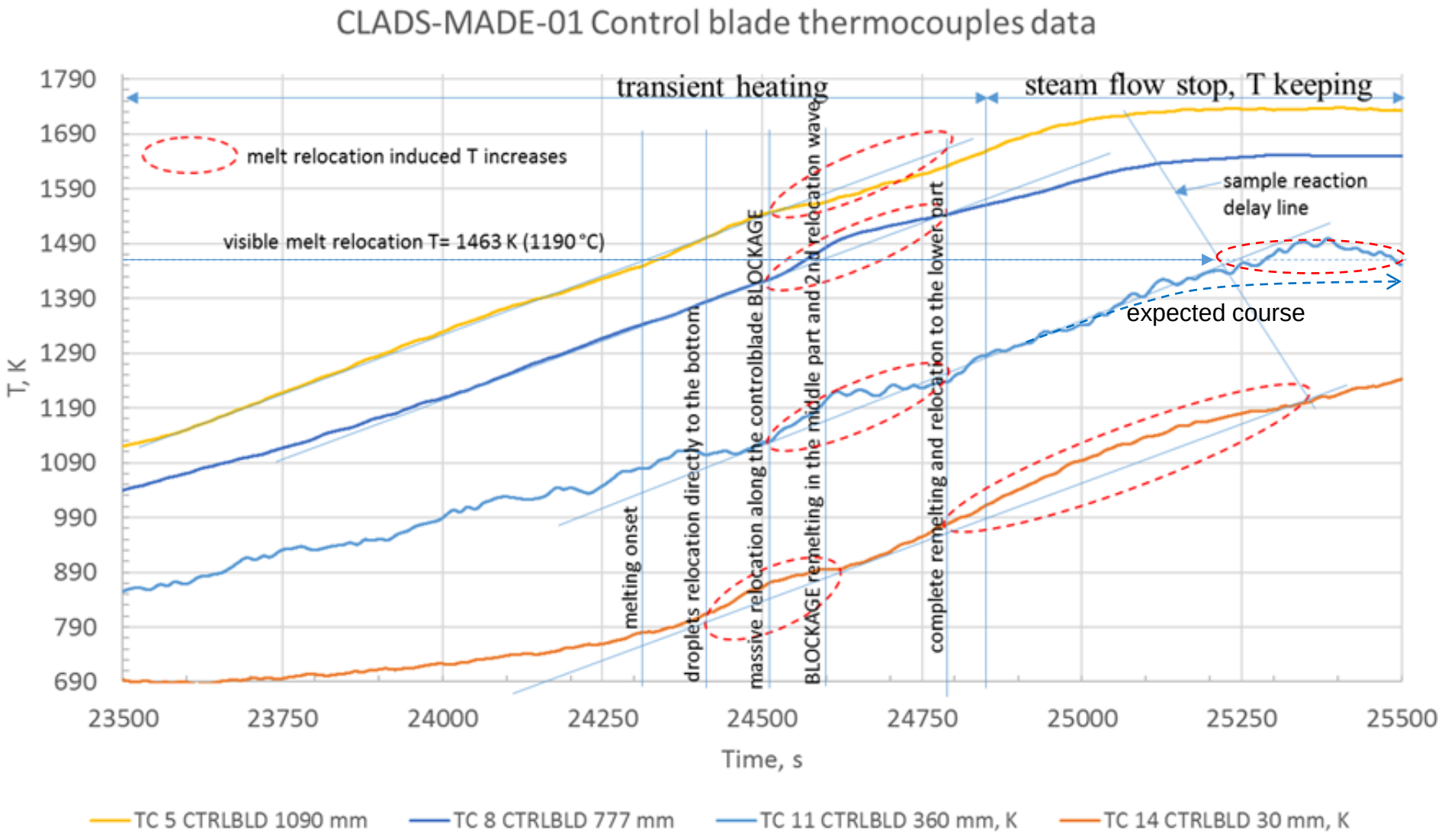




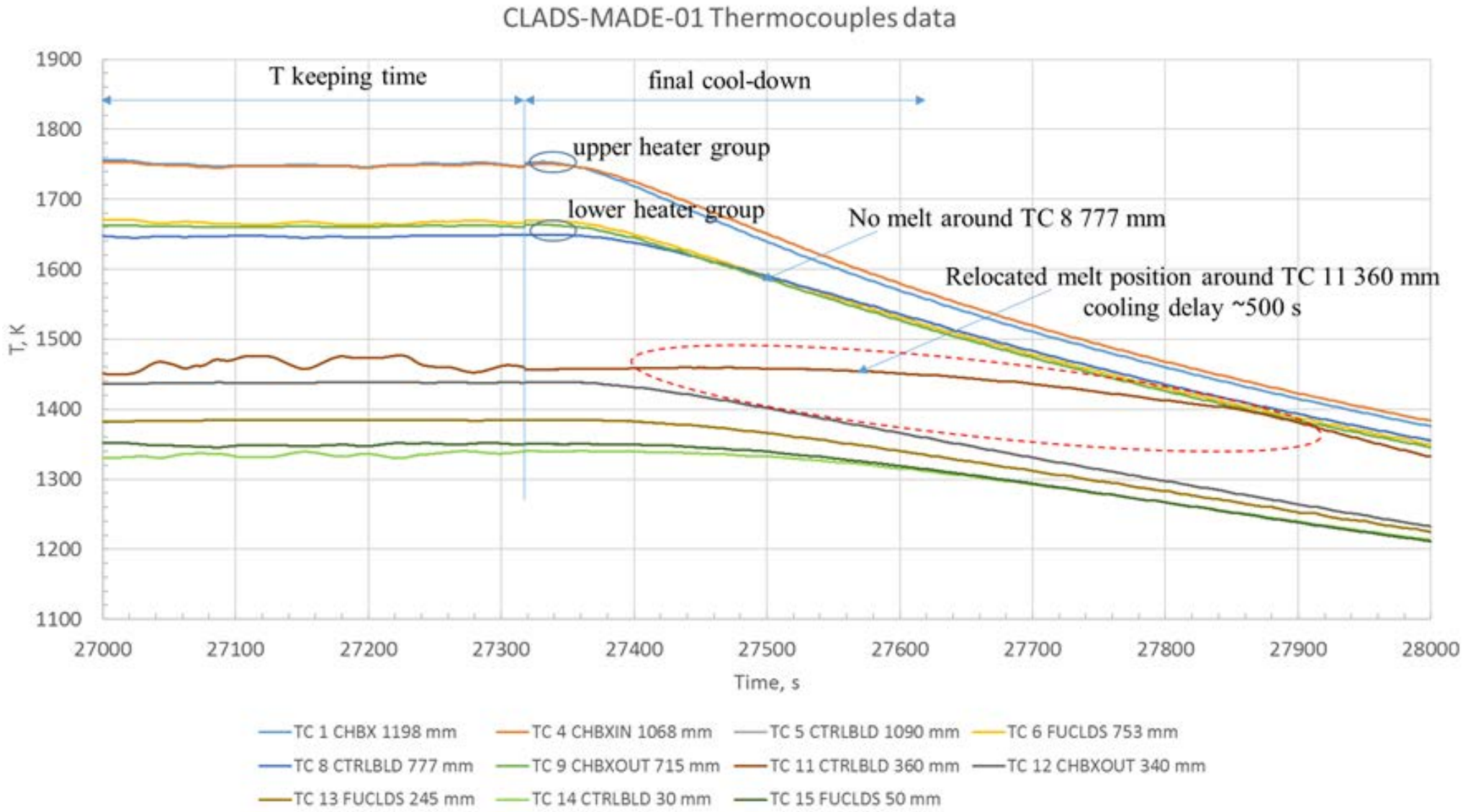


Experimental behaviour is the same as calculated using Leistikow-Schanz oxidation kinetics

CLADS-MADE-01 test melt relocation analysis



CLADS-MADE-01 blockage cooling delay





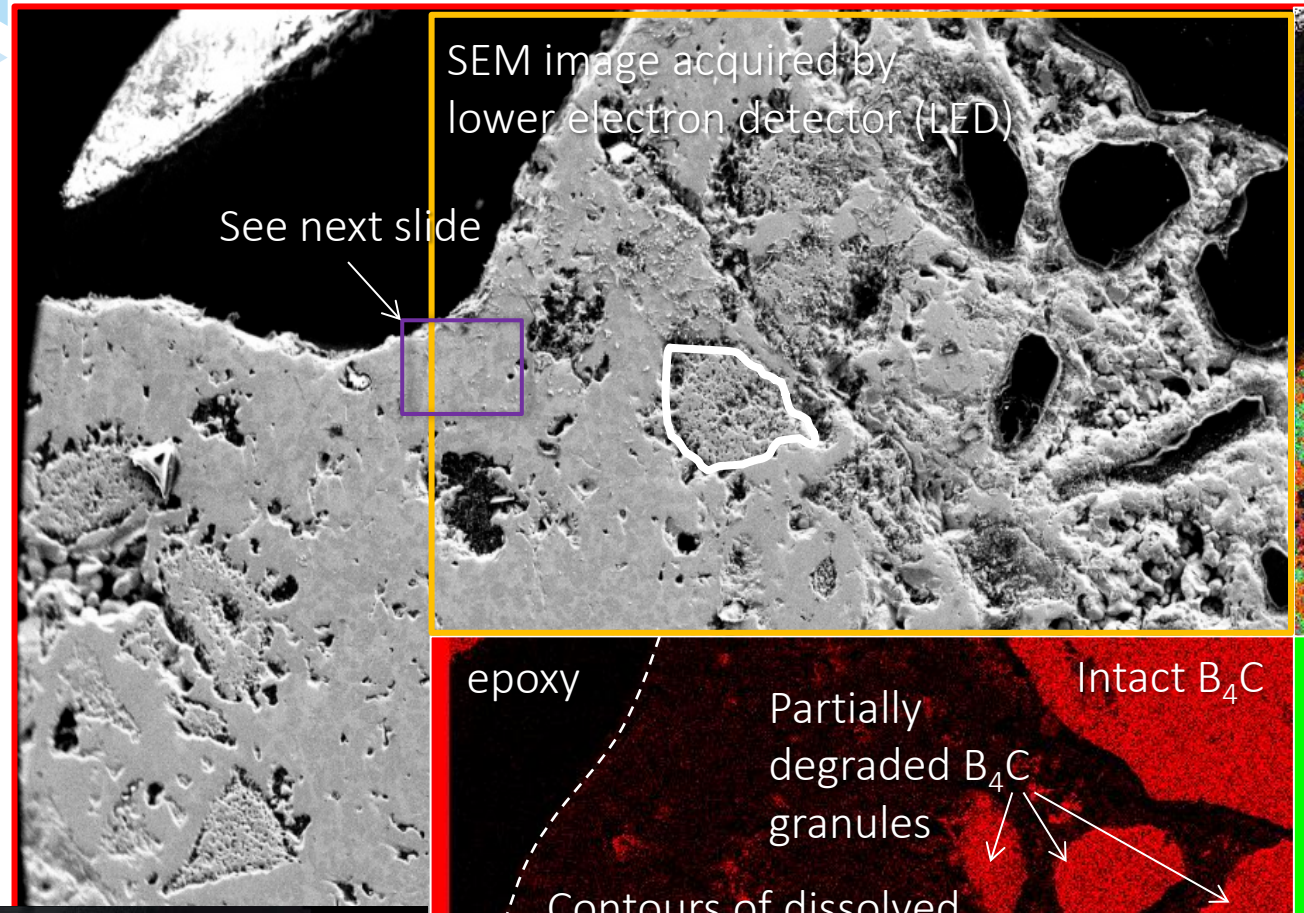
Part 4
Underlying mechanisms interpretation

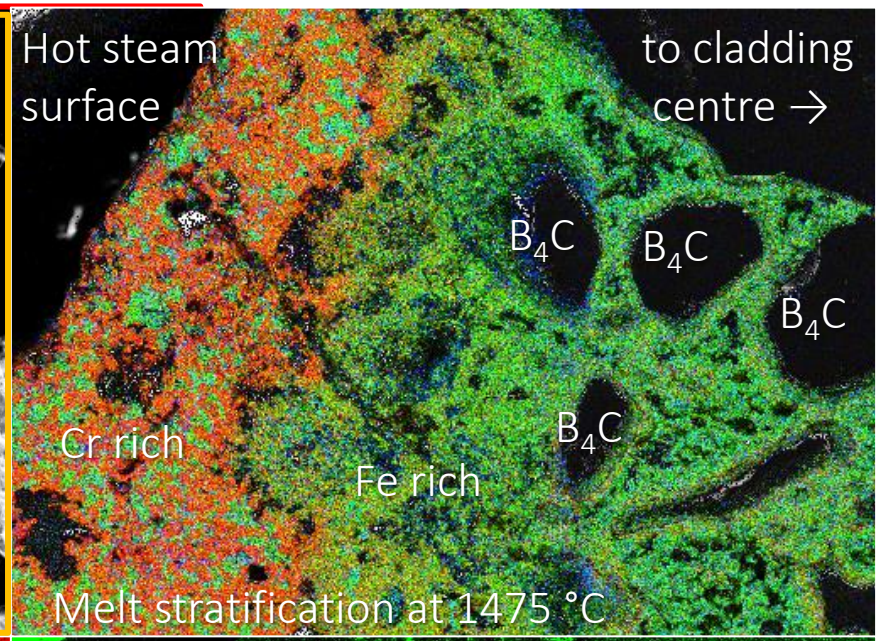
JAEA-CLADS Test technology development group

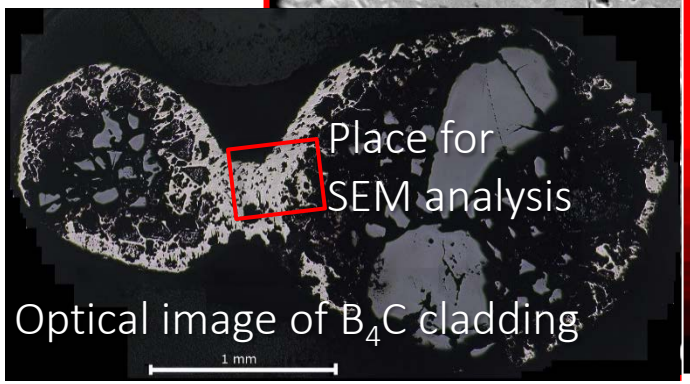
Degraded control blade cladding analysis

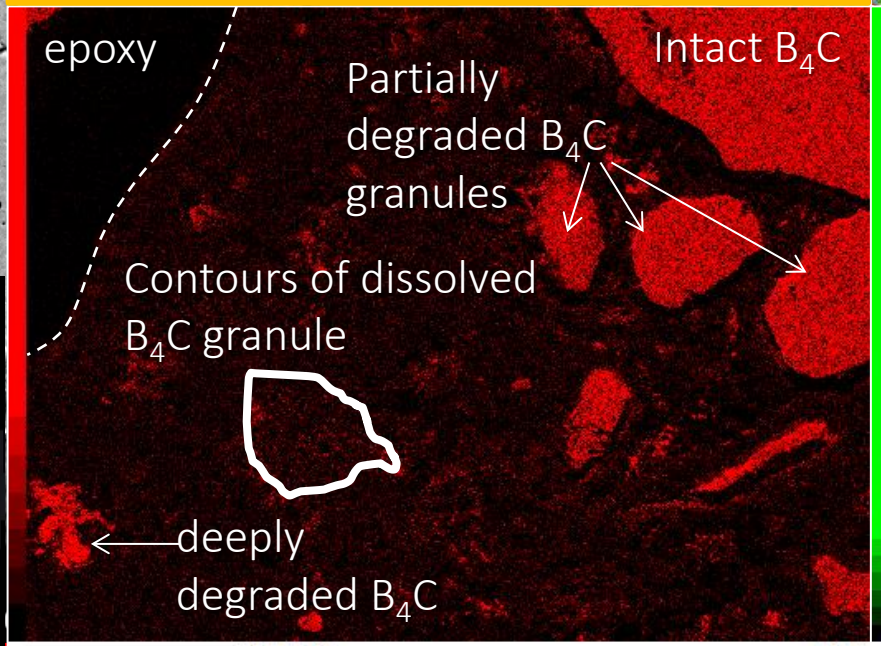
B4C behaviour In accordance with CORA results published in FZKA 7447.

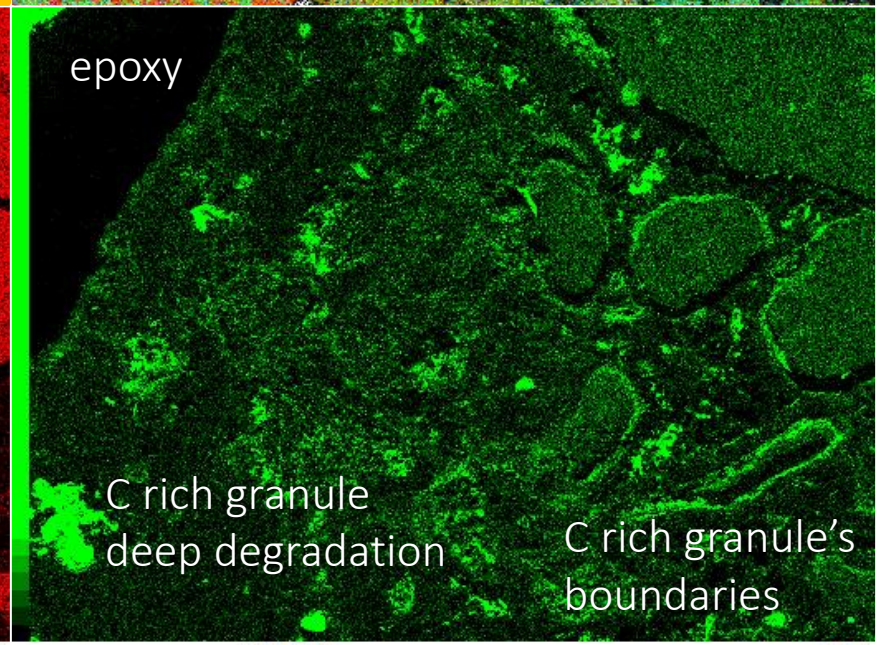
Cr-rich surface layer is a “new” finding



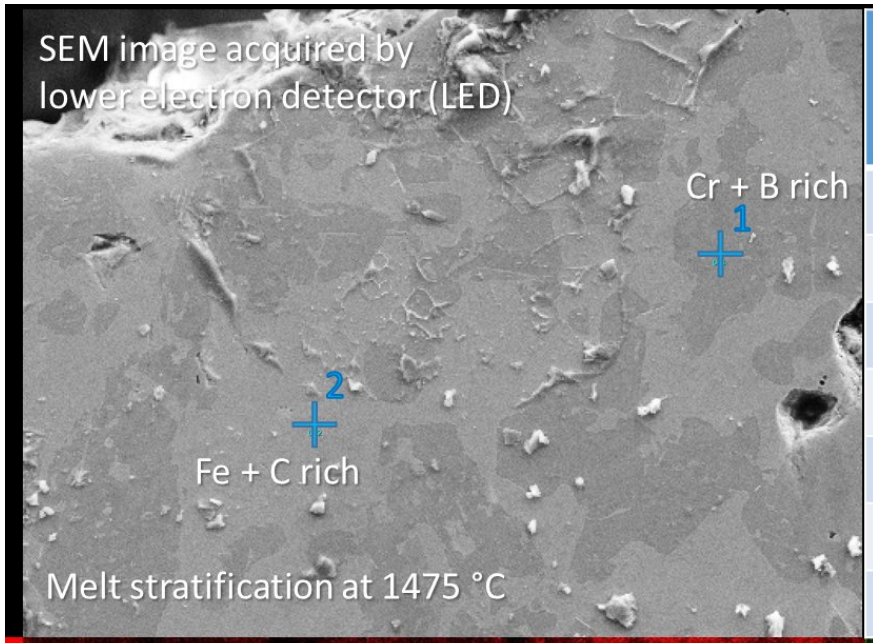




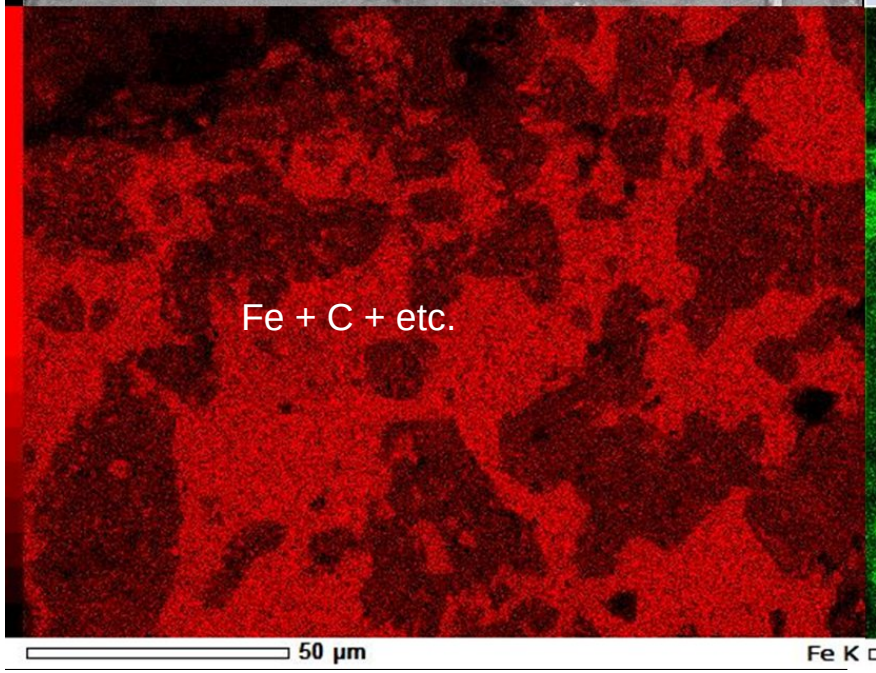


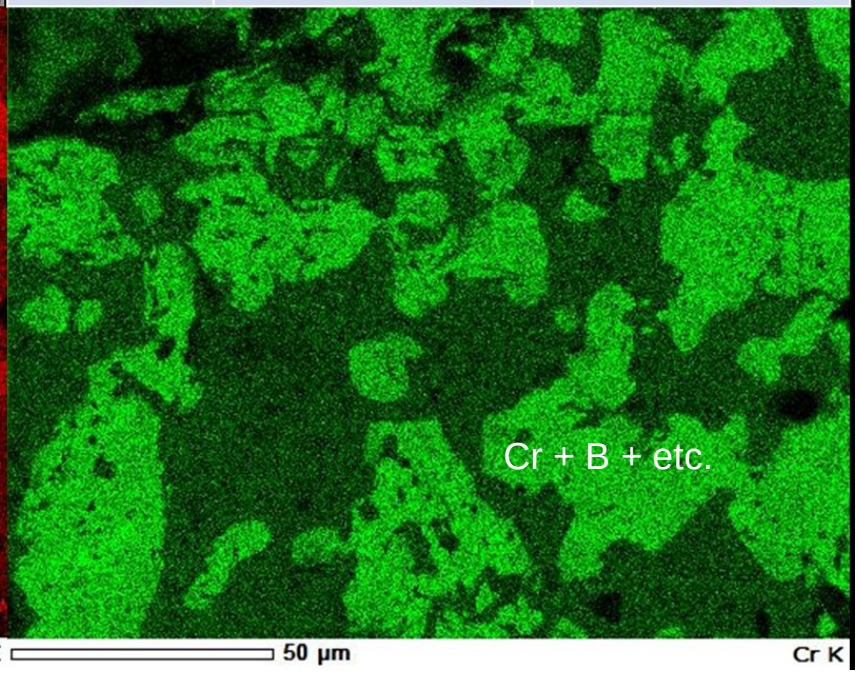


Degraded control blade cladding analysis (continued)



Element	1 (Cr + B rich), mass % (atom %)	2 (Fe + C rich), mass % (atom %)
B	15.5 (41.5)	6 (18.6)
C	6.9 (16.5)	10.8 (29.8)
O	0.5 (0.9)	1.1 (2.2)
Cr	47.9 (26.6)	13 (8.4)
Fe	25.5 (13.2)	59.9 (35.9)
Ni	1.3 (0.6)	8.8 (5)
Mo	2.5 (0.8)	0.4 (0.2)





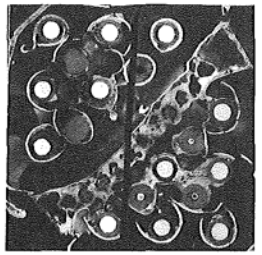
Control blade cladding analysis (history)



426 mm 1830°C

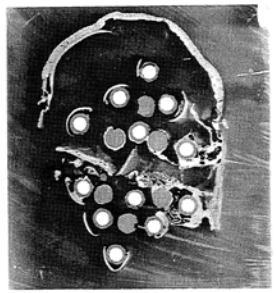


284 mm 1660°C

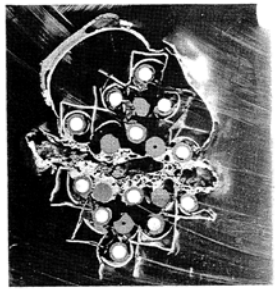


269 mm 1720°C

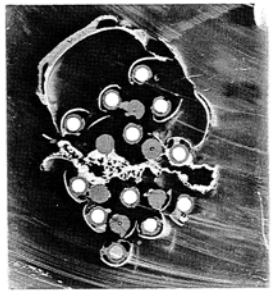
KfK 5383
CORA-31



597mm

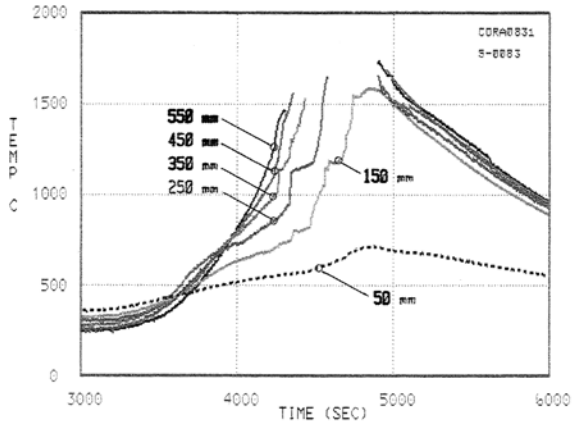


512mm



497mm

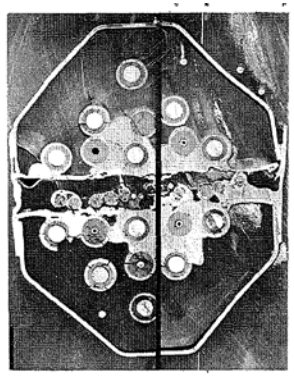
FZKA 7447
CORA-16



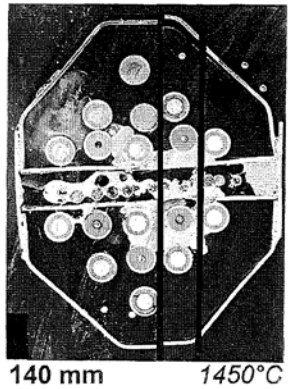
FZKA 7447
CORA-16

1200 °C is the very beginning of control blade degradation sequence.

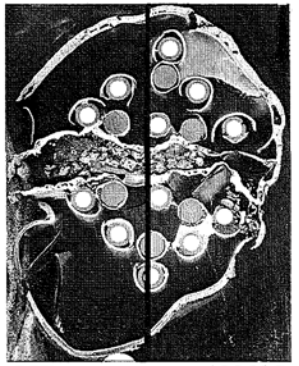
The end was not emphasized?



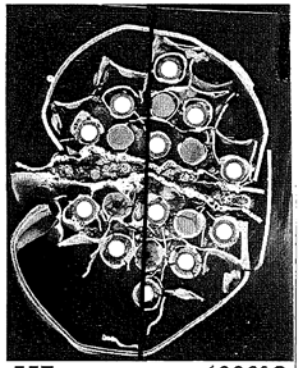
155 mm 1450°C



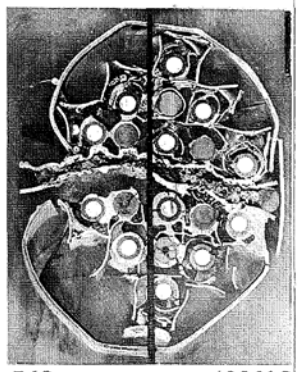
140 mm 1450°C



657 mm 1890°C



557 mm 1930°C



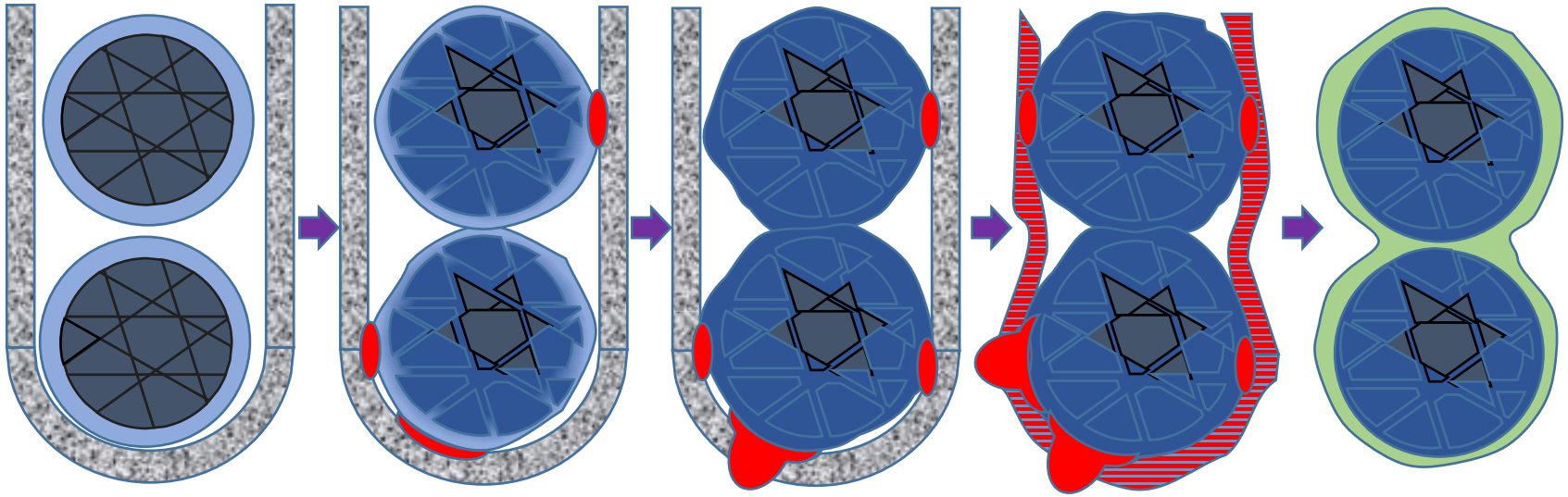
542 mm 1930°C

FZKA 5571
CORA-28

Illustration of a control blade melting and destruction

Assumed mechanism directly observed on video during our test and by post-test analysis and by previous data

Intact B_4C granules
316L
316L melt
304L
Dissolved B_4C contours
Melt B_4C+304L
Melt B_4C+304L+316L
Cr rich layer



Initial state

Dissolution of the absorber blade claddings due to full contact with B_4C + local attack of sheath

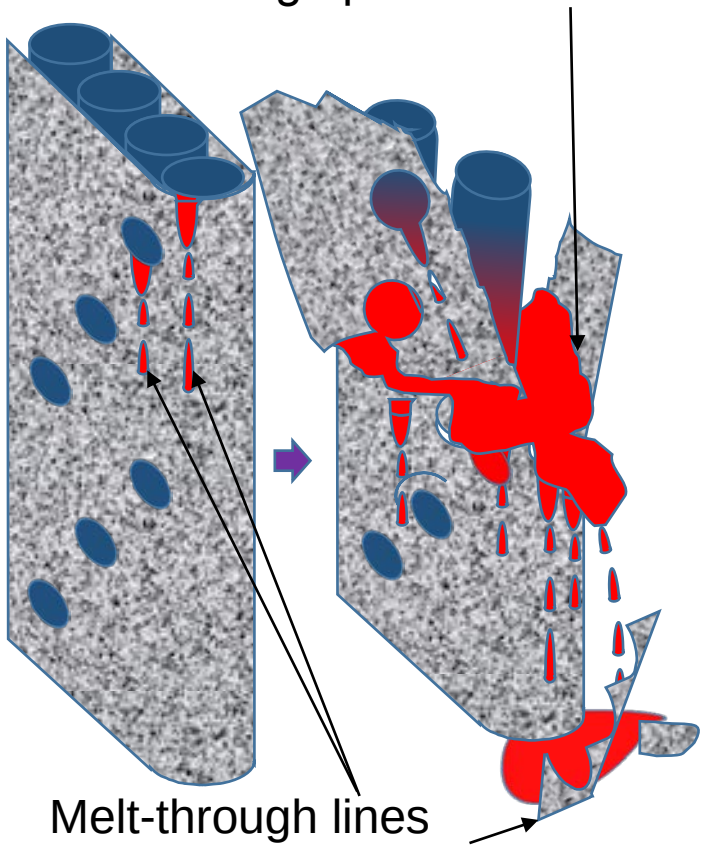
Local sheath melt-through

Fe-containing melt active relocation

Cr shielding of clads with B_4C + further B enrichment of Fe and Cr

3D view

T melt onset =
T eutectic point =
T blockage point ≈ 1174 °C



Melt-through lines

Strongly oxidised parts

<1174 °C → ≈1190 °C → ≈1200 °C → 1220…1400°C → 1400 °C → ?

? Absorber clads' remnants were observed at ≈ 1750 °C (CORA-31,-16,-18) and 1930 °C CORA-28 BWR tests



Part 5
Conclusions

JAEA-CLADS Test technology development group

Conclusions

- CLADS-MADE-01 test for Fukushima-1 Unit 2 accident steam-starved scenario has been successfully performed;
- In situ video allowed thorough analysis of melt relocation features: onset, progress, candling, blockage formation and its subsequent melting were directly observed using video cameras;
- Boron carbide (B_4C) containing absorber blade was severely degraded by melting, but most of it surprisingly remained at its position. The remnants of the control blade with intact B_4C granules survived in the upper part at 1475 °C for 45 minutes, being protected by Cr + B enriched high melting point surface layer;
- By isolation of B_4C clads by using high-melting point materials (for example ceramics) we could shift relocation of neutron absorber material to late phase of an accident;
- Melt relocation (mostly Fe+B) created a blockage between oxidised channel boxes under suitable temperature conditions (lower than 1174 °C (1447 K));
- Blockage causes a big delay in the final cooling of a surrounding area especially in the large-scale reactor;
- Preliminarily oxidised channel boxes (≈ 45 µm) were intact after they survived during nearly 45 minutes proving high resistance to the melt attack even under steam-starved conditions (post-test detailed investigations are underway);
- During melt relocation no significant oxidation of melt happened as it relocated fast to the cooler region and solidified there;
- No temperature escalation related to that or any other phenomena was observed, though small temperature increase due to relocation of the molten material from warmer to a bit colder region was good detectable;
- Metallic part of the absorber melt blockage can be melted again, when temperature increases above the eutectic point 1174 °C (1447 K); In this case of already oxidised surface layer will relocate directly to the bottom as debris. The process can happen many times during corium movement downwards if the metal (not oxidised) is available;
- Following this mechanism the RPV lower head at the end can be full of metallic debris and heated up they can attack the welding joints of Control rod guide tubes, which can lead to failure of RPV by previously not investigated mechanism. The work in this direction should be continued.

Acknowledgement

This study is performed in the framework of "Advanced Multi-scale Modelling and Experimental Tests on Fuel Degradation in Severe Accident Conditions" supported by Ministry of Economy, Trade and Industry, Japan.

The authors would like to thank Dr. H.V. Pham, Mrs. A. Sudo, Mr. T. Sato, Mr. J. Imoto, Mr. I. Kudo, Mr. K. Tanizawa helping us during different stages of the test.

Thank you for your attention

The talk was given by:

Dr. Anton Pshenichnikov

Special topic researcher,

Japan Atomic Energy Agency (JAEA)

Collaborative laboratories for Advanced Decommissioning Science (CLADS)

Fuel Debris Characterization & Core Status Evaluation Division

Simulation Test Technology Development Group

E-mail: pshenichnikov.anton@jaea.go.jp

Collaborative Laboratories for Advanced Decommissioning Science

In situ video data during test



CLADS-MADE-01 has been performed on 22nd of March 2018, Tomioka, Fukushima, Japan, International Collaborative Decommissioning Research Centre, JAEA-CLADS,

Dr. Anton P. Pshenichnikov, Dr. Saishun Yamazaki, Dr. Yuji Nagae, Dr. Masaki Kurata

Comparative analysis of simulation results for the bundle tests QUENCH-07 and QUENCH-09 conducted with the Severe Accident Analysis Code ASTEC V2.1

24th International QUENCH Workshop, November 2018, Karlsruhe

Jan Mathis Peschel, Florian Gremme, Marco K. Koch

Plant Simulation and Safety Group (PSS),
Ruhr-Universität Bochum (RUB)

Jan.Peschel@pss.rub.de, gremme@pss.lee.rub.de, koch@pss.lee.rub.de
ORCID-ID: 0000-0002-6529-2492 / 0000-0002-3395-8237 / 0000-0001-7260-5250

One of the working packages of the research project “External Validation and Analysis of Selected Models of the Accident Analysis Codes ASTEC, ATHLET and ATHLET-CD” are simulations of core degradation phenomena related to the absorber material B_4C. These are performed with the integral code ASTEC V2.1, that is developed by IRSN. The bundle tests investigated in this work, QUENCH-07 and QUENCH-09, are both part of the QUENCH testing series, which is being performed by KIT since 1997. The two tests had the aim to analyse the impact of a B_4C absorber rod failure on the generation of H_2, CO, CO_2 and CH_4.

As QUENCH-09 was a reference test for QUENCH-07, the test conducts show similarities. From the beginning of the tests a mixture of overheated steam and argon flows through the bundle, which consists of 20 heated fuel rod simulators and one central unheated B_4C absorber rod simulator. After a heat-up phase the bundle is stabilized on a constant level of approximately 1,723 K where the pre-oxidation processes begin. The main differences between the two tests can be found in the last two phases. In the transient phase, where the power input is increased comparatively fast, QUENCH-09 additionally has a steam starvation phase where the input of overheated steam is decreased from 3.4 g/s to 0.4 g/s. Afterwards the quenching process is initiated by switching the superheated steam flow to a saturated steam flow. The other main difference concerns the coolant flow rate (15 g/s for QUENCH-07 and 49 g/s for QUENCH-09) of the two tests.

Objective for the analysis of the simulation results is to validate the code capabilities to simulate the relevant phenomena in particular related to B_4C during the investigated QUENCH tests. While the resulting temperature evolutions are in good accordance with the test results, the calculated H_2 generation is either under- or overestimated. This applies especially to the simulations conducted for QUENCH-09 due to the higher flooding rate and thus the higher amount of H_2 that is generated. Although the oxidation mechanisms implemented for B_4C are already very comprehensive the current interaction with stainless steel is not completely comprehensible yet.

Supported by:

Federal Ministry for Economic Affairs and Energy

on the basis of a decision by the German Bundestag

This work was funded by the German Federal Ministry of Economic Affairs and Energy under grant number 1501522 on the basis of a decision by the German Bundestag.

The simulations were performed with the code version ASTEC V2.1, developed by IRSN.


TOSHIBA



RUB

RUHR-UNIVERSITÄT BOCHUM

Comparative analysis of simulation results for the bundle tests QUENCH-07 and QUENCH-09 conducted with the Severe Accident Analysis Code ASTEC V2.1

Jan Mathis Peschel, Florian Gremme, Marco K. Koch

24th International QUENCH Workshop, Karlsruhe

Wednesday, 14th November 2018

PSS Plant Simulation and Safety
Prof. Dr.-Ing. Marco K. Koch

Content

- Introduction
- Experimental Setup
- Modelling approach
- Simulation Results
- Conclusion

Introduction

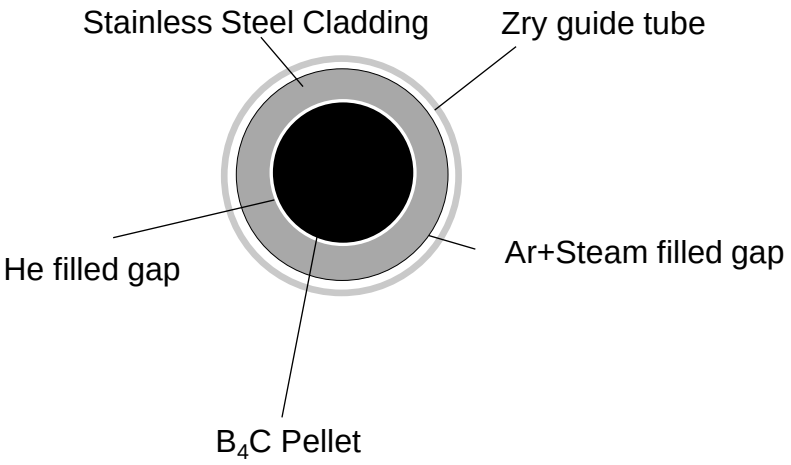
The QUENCH testing programme

Test	Quench medium & flooding rate	Temp. At onset of flooding	Max. ZrO_2 layer thickness	Remarks, objectives	Date of test conduct
06	Water 42 g/s	≈ 2,060 K	630 µm	OECD-ISP 45; blind test predictions by different computer codes.	13.12.2000
07	Steam 15 g/s	≈ 2,100 K	Completely oxidized	COLOSS Project; impact of B_4C absorber rod failure on H_2, CO, CO_2 and CH_4 generation.	25.07.2001
08	Steam 15 g/s	≈ 2,100 K	Completely oxidized	As QUENCH-07, but without B_4C absorber rod.	24.07.2003
09	Steam 49 g/s	≈ 2,090 K	Completely oxidized	As QUENCH-07, but with steam starvation.	03.07.2002

Description of experiments

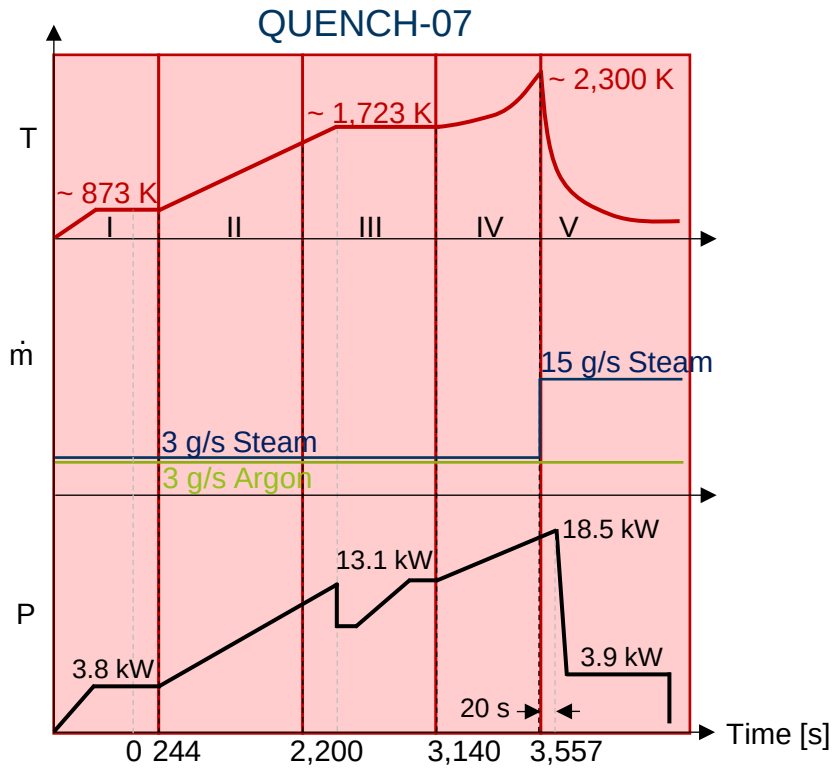
Experimental Facility

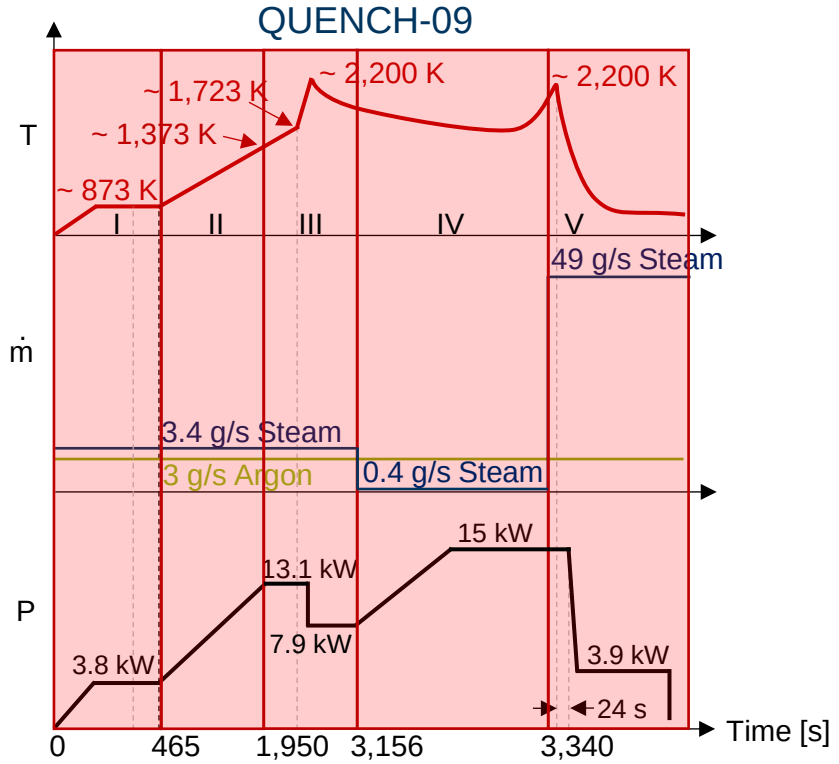
- Cooling jacket
- Insulation fiber
- Shroud
- 20 heated fuel rod simulators
- Four corner rods
- One unheated central absorber rod simulator
  - B_4C pellet stack
  - Stainless steel cladding
  - Zircalloy guide tube



Description of experiments

Comparison of Test Conducts



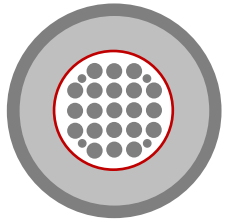


[illegible] changes

Modelling approach

- ASTEC input deck based on an existing setup for QUENCH-03 and QUENCH-11
  - Outer circuit resistance evaluated by testing
  - No perforation of the Zry guide tube modelled
    → Third Channel added
  - Differences between suggested input regarding starting and boundary conditions
    → Different runs realized

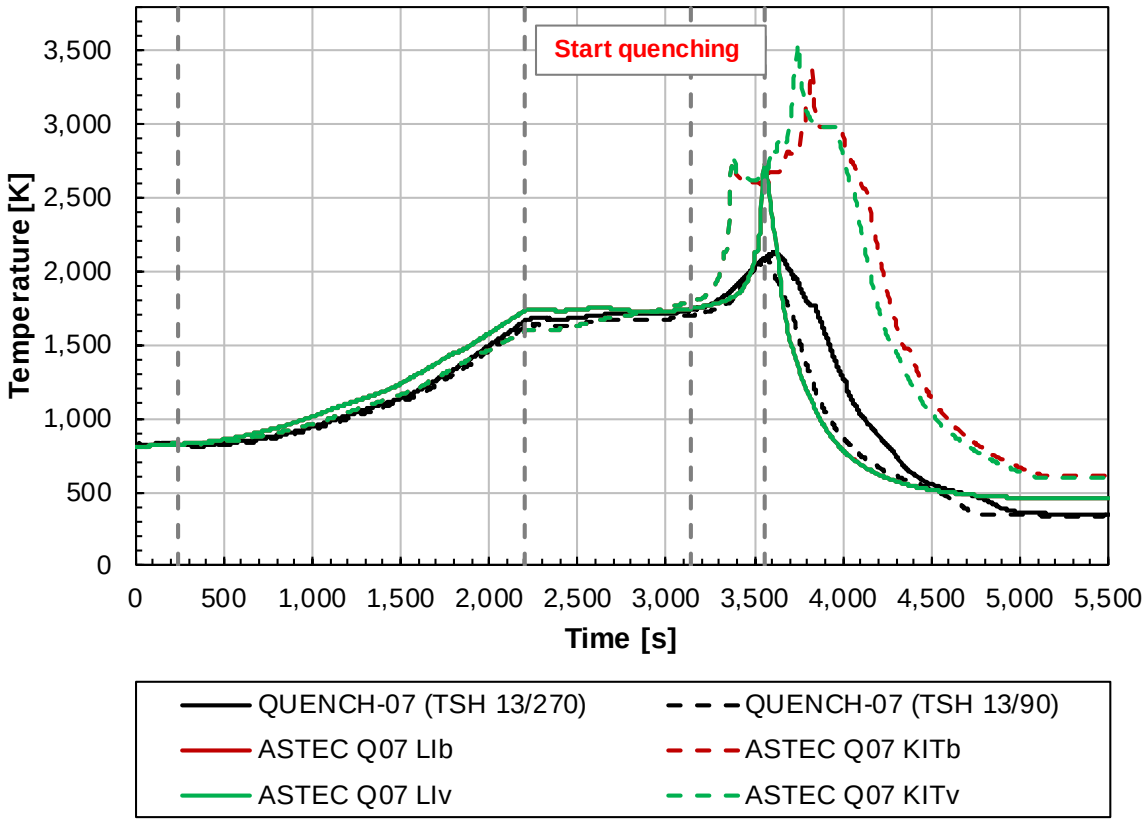
Run	Starting parameters	Correlation method B_4C Oxidation
LIb	L. Laborde / F. Igier	BESTFIT
LIv	L. Laborde / F. Igier	VERDI
KITb	KIT	BESTFIT
KITv	KIT	VERDI

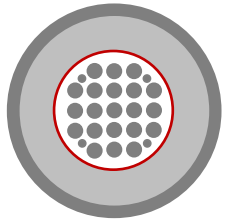


Simulation Results

QUENCH-07 – Shroud Temperature (950 mm)

- Within the first three phases all simulations are in good accordance with the experimental results
- With the beginning of the transient phase KITb and KITv overestimate the test results again
- LIb and LIv also overestimate the temperature escalation before the cooldown is initiated

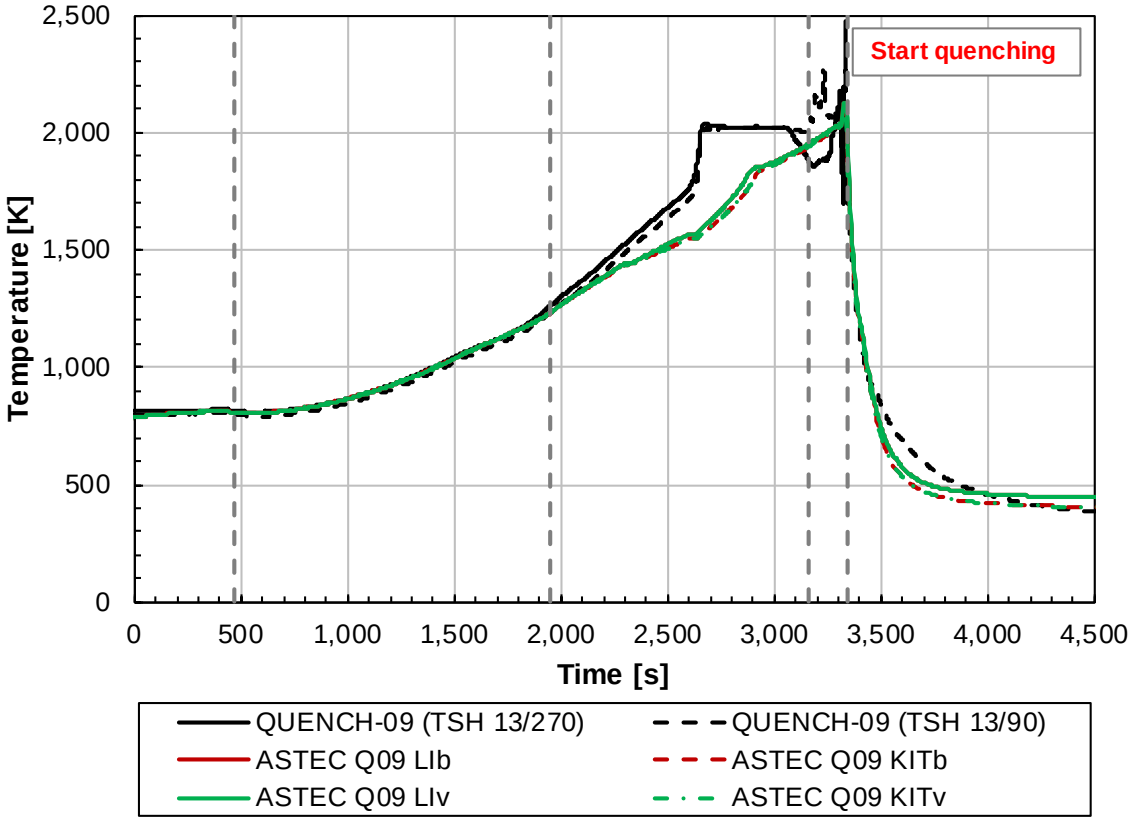




Simulation Results

QUENCH-09 – Shroud Temperature (950 mm)

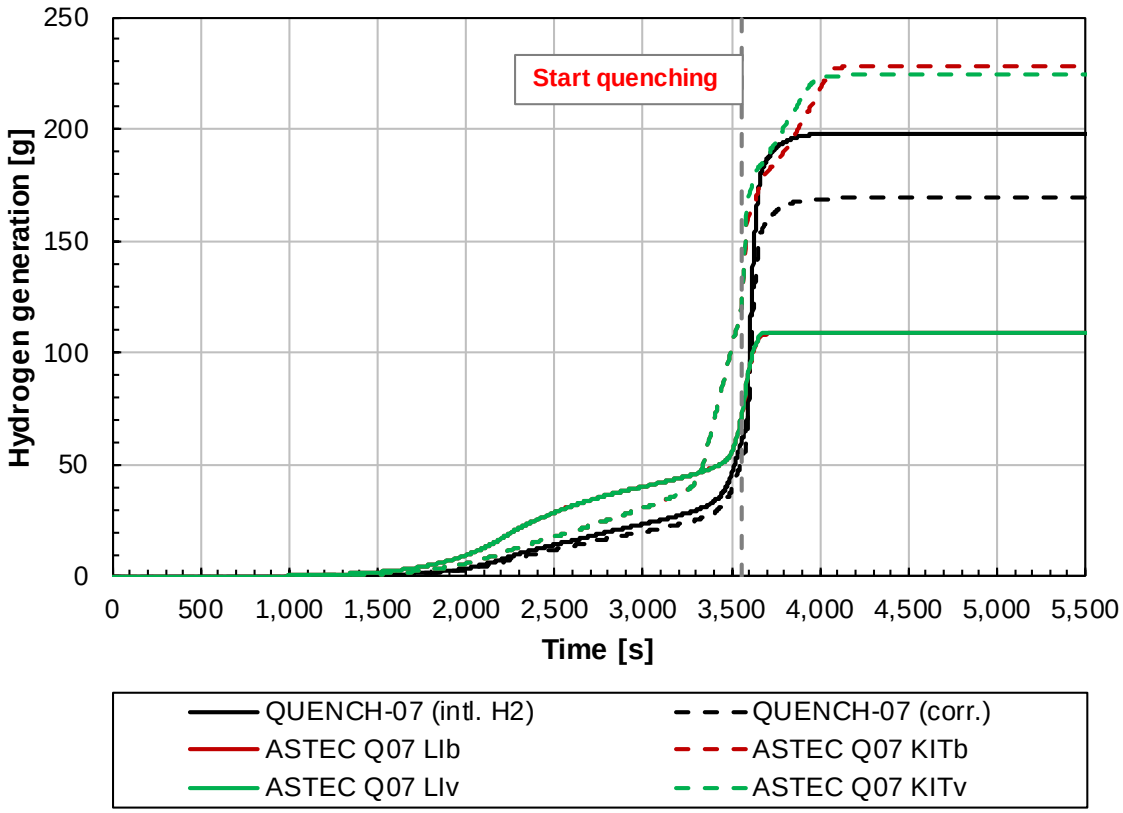
- Simulation results in good accordance until pre-oxidation phase is initiated
- No temperature escalation visible after bundle heatup
- All simulation runs in very good accordance during the cooldown phase



Simulation Results

QUENCH-07 – Total hydrogen generation

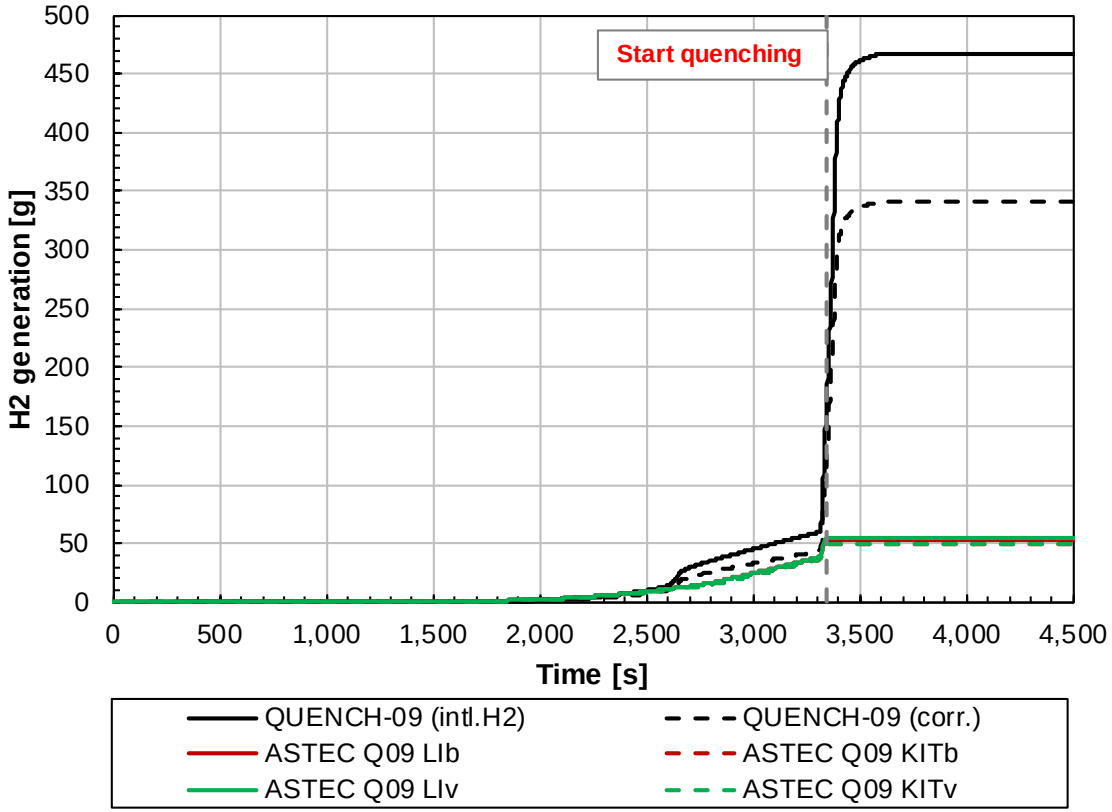
- Hydrogen generation extremely underestimated in Run LIb and LIv
- KITb and KITv slightly overestimate the total results although the temperature escalation was very extreme
- Influence of oxidation correlation method only visible for KITb and KITv
- Corrected H_2 generation closer to LIb and LIv



Simulation Results

QUENCH-09 – Total hydrogen generation

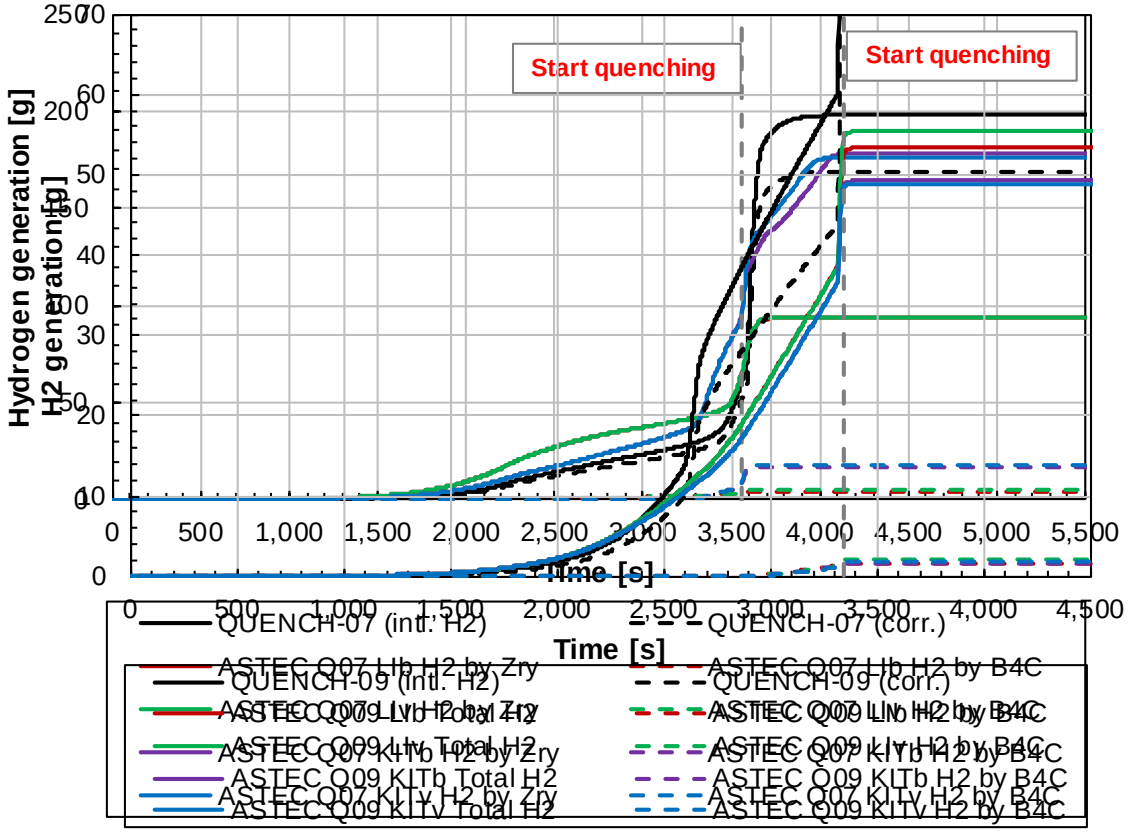
- All four runs underestimate the experimental results extremely
- Differences regarding selected B_4C oxidation correlation method only slightly visible



Simulation Results

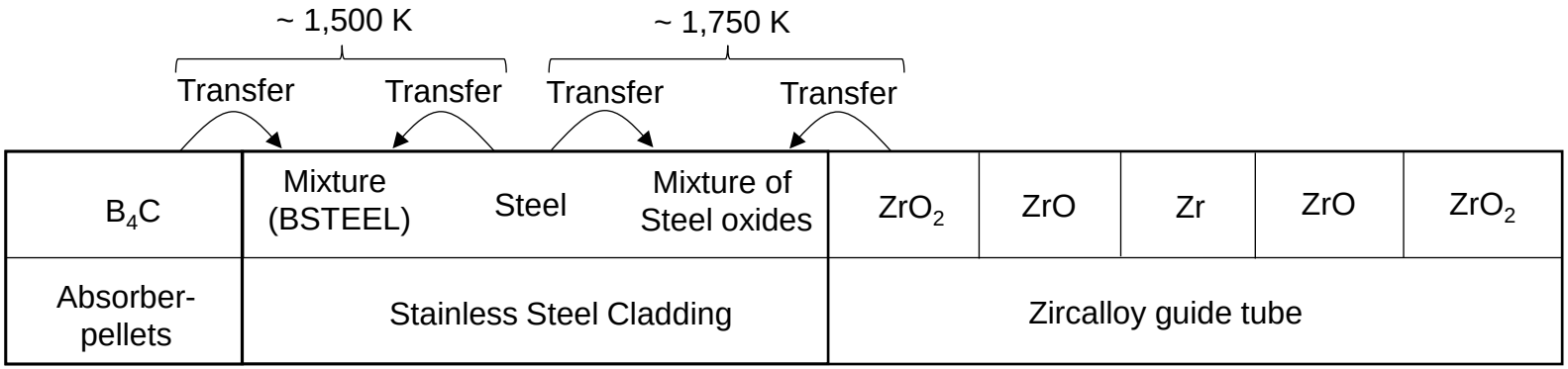
QUENCH-07 – Hydrogen generation by sources

- Hydrogen generation mainly caused by Zry oxidation mechanisms
- B_4C oxidation processes only have a small impact on total hydrogen generation
- Q09: Only slight differences for the four simulations; B_4C with small impact



Simulation Results

Oxidation/Interaction behaviour of B_4C absorber rod in ASTEC



- New mixture material called BSTEEL added to cladding component, without transferring B_4C to it

  → To consider B_4C oxidation it remains in place without relocation due to eutectic liquefaction

- Impact of B_4C underestimated

Conclusion

- The code provides good modelling options to represent QUENCH-07 and QUENCH-09
- Temperature profile as referencing parameter to the bundle test in good accordance to experimental results in ASTEC Runs LIb and LIv
- Hydrogen generation overestimated (QUENCH-07 LIb and LIV, QUENCH-09) or underestimated (QUENCH-09)
- Results for B_4C oxidation mechanisms comprehensive
  - Influence of selected oxidation correlation method for B_4C only visible for QUENCH-09
- B_4C - Stainless Steel interaction mechanisms not completely comprehensible
- Impact of B_4C underestimated

Acknowledgements

The used code system **ASTEC V2.1** is developed by IRSN.

These works were funded by the German Federal Ministry of Economic Affairs and Energy under grant number **1501522** on the basis of a decision by the German Bundestag. Responsibility for the content lies with the authors.



Thank you for your attention

Uncertainty and Sensitivity Analysis by means of ASTEC/URANIE Platform of the QUENCH-08 Experiment

F. Gabrielli, V.H. Sánchez-Espinoza

Karlsruhe Institute of Technology (KIT), Hermann-von-Helmholtz-Platz 1,

D-76344 Eggenstein-Leopoldshafen, Germany

fabrizio.gabrielli@kit.edu, victor.sanchez@kit.edu

Abstract

The Integrated Safety Assessment Methodology (ISAM) is nowadays employed for current and future nuclear systems to enhance their safety compared with the former concepts. The Defense-in-Depth concept is applied to assess a robust architecture to prevent severe accident (SA) conditions and to demonstrate that their consequences do not violate safety criteria. Efforts are therefore worldwide underway to improve the performance of the current integral codes for SA analyses of Light Water Reactors (LWRs).

In this framework, the use of Uncertainty & Sensitivity (U&S) tools for validating the complex physical models employed in the modern system codes plays an important role. Such a need becomes fundamental when SA analyses are considered, because of the large uncertainties associated to the physical models employed to simulate these scenarios.

At the Karlsruhe Institute of Technology (KIT) analytical investigations of SAs have been carrying out since many years. In this frame, we widely employ the Accident Source Term Evaluation Code (ASTEC), developed by IRSN, which is continuously improved to analyze the complete SA scenario from the initiating event until radioactive release from the containment in Gen. II and Gen. III water-cooled reactors. At the same time, U&S tool are employed at KIT to evaluate the performance of the safety codes we use.

Having this in mind, an ASTEC/URANIE platform has been assessed at KIT based on C++ and Python scripts with two main goals: 1) improve and validating the physical models employed in ASTEC for the analysis of SA scenarios, and 2) evaluating the performance of URANIE when applied to ASTEC.

In this work, the ASTEC/URANIE platform is to employed to perform the sensitivity analysis of the ASTEC results for the H2 production and temperature distributions for the QUENCH-08 experiment. For our evaluation, the probability Distribution Functions (PDF) describing the uncertainties associated to more than 20 input parameters (geometrical modelling, heat-transfer models, clad integrity criteria, oxidation models for solid and molten materials) have been propagated.

The results ASTEC results for the Best-Estimate cases show an excellent agreement with the experimental data. The sensitivity analysis show that the H2 production is mainly affected by the uncertainties on the definition of the scenario, on the geometrical model have significant effects, and on the radiative heat transfer model. Further, the sensitivity to the models for relocation and oxidation of molten material are not negligible. Such an observation provides important hints with respect to future analyses of the performance of the ASTEC physical models to SA scenarios. In this sense, the current work provides a solid basis of understanding of the performance of the ASTEC/URANIE platform.


TOSHIBA

Uncertainty and Sensitivity Analysis by means of ASTEC/URANIE Platform of the QUENCH-08 Experiment

F. Gabrielli, V. Sanchez

Institute for Neutron Physics and Reactor Technology (INR)
Reactor Physics and Dynamic Group (RPD)



Outline

- Motivation
- The ASTEC/URANIE Platform
- The ASTEC Model of the QUENCH-08 Experiment
- Input Parameters for the ASTEC/URANIE Analysis
- Results
  - Hydrogen production
  - Clad and Shroud Temperature
- Conclusions

Motivation

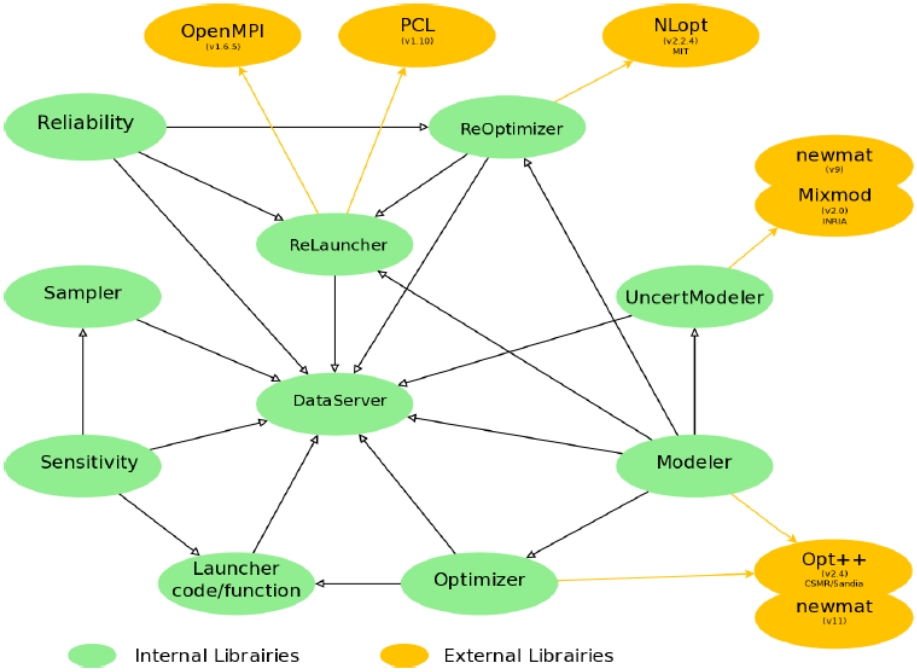
- The improvement of the performance of the BE system codes for analyzing operational and SA scenarios is a continuous on-going process.
- The use of Uncertainty & Sensitivity (U&S) tools for validating the complex physical models employed in such a codes plays an important role.
- ..which becomes **fundamental when SA analyses are considered**, because of the large uncertainties associated to the physical models employed, e.g., the MELCOR, MAAP, ASTEC Xwalk studies on 1F1[*,**].
- **An ASTEC/URANIE Platform has been assessed at KIT in order to:**
  - **Improve and validate the physical models employed in ASTEC for the analysis of SA scenarios;**
  - **Evaluate the performance of URANIE when applied to ASTEC.**
- **Having this in mind, the ASTEC/URANIE analyses of the H2 production for the QUENCH experiments represents a solid basis of understanding.**

*Andrews, N, Belon, S, et al., Preliminary Results of ASTEC-MELCOR Crosswalk, 2016, https://www.osti.gov/servlets/purl/1380096.
**David L. Luxat, et al., MAAP-MELCOR Crosswalk Phase 1 Study, NURETH-16, Chicago, IL, August 30-September 4, 2015.

The URANIE tool

- URANIE allows performing studies on uncertainty propagation and sensitivity analysis based on stochastic sampling.
- Since it is based on ROOT, many features are available (C++ interpreter, Python interface, access to SQL databases, advanced visualization).

- The PDFs of the variables of the problem are stored in the **DataServer**.
- The **Launcher** library applies a an analytical function or an external simulation code (ASTEC) to the DataServer data.
- The results of the sensitivity analysis (**Sensitivity library**) are sampled by the **Sampler** library.

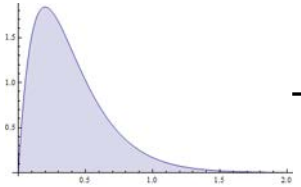


F. Gaudier, URANIE : The CEA/DEN Uncertainty and Sensitivity platform, Procedia Social and Behavioral Sciences 2 (2010) 7660–7661.

The ASTEC/URANIE Platform @KIT

- An interface based on C++ and Python scripts has been assessed to integrate the ASTEC (v2.1.1.3) results within the URANIE (v3.9.0) framework.

PDFs of the n input ASTEC parameters



Ref. ASTEC input

URANIE *DataServer*

Sampled input parameters

N ASTEC input deck

N ASTEC runs *Launcher*

N ASTEC Outputs

Export data to sampling

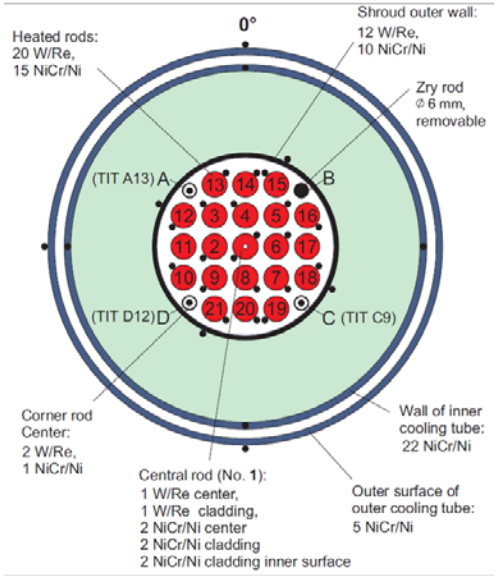
URANIE *U&S analysis*

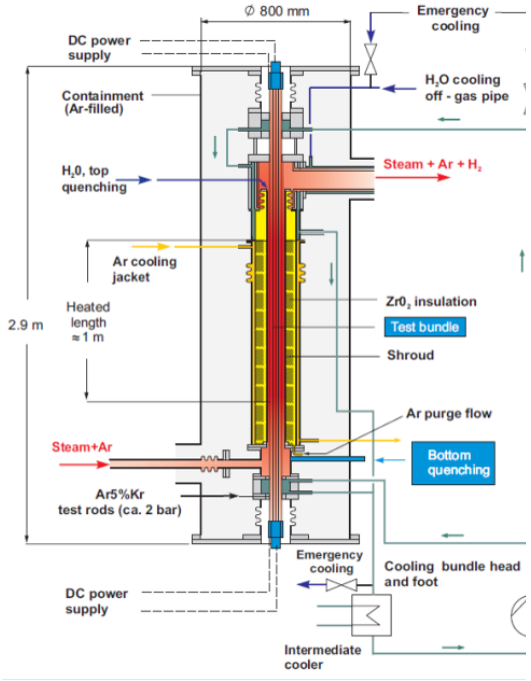
Post-Processing

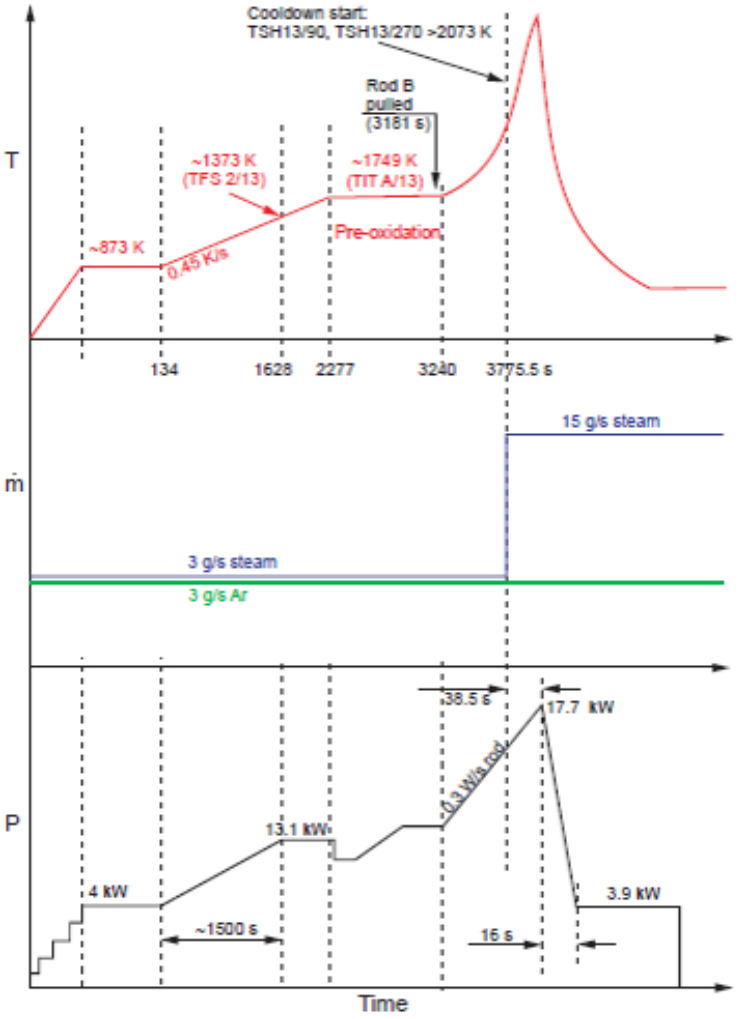
- **For each time step:**
  - **Min, max, mean, and st. dev of the output parameter**
  - **Sensitivity coefficients**

The QUENCH-08 Experiment

- **The Q-08 test aims analyzing the effect of the injection of a low mass flow rate (steam) on H2 production** → it represents the dispersed flow region located above the Transition Boiling Region.

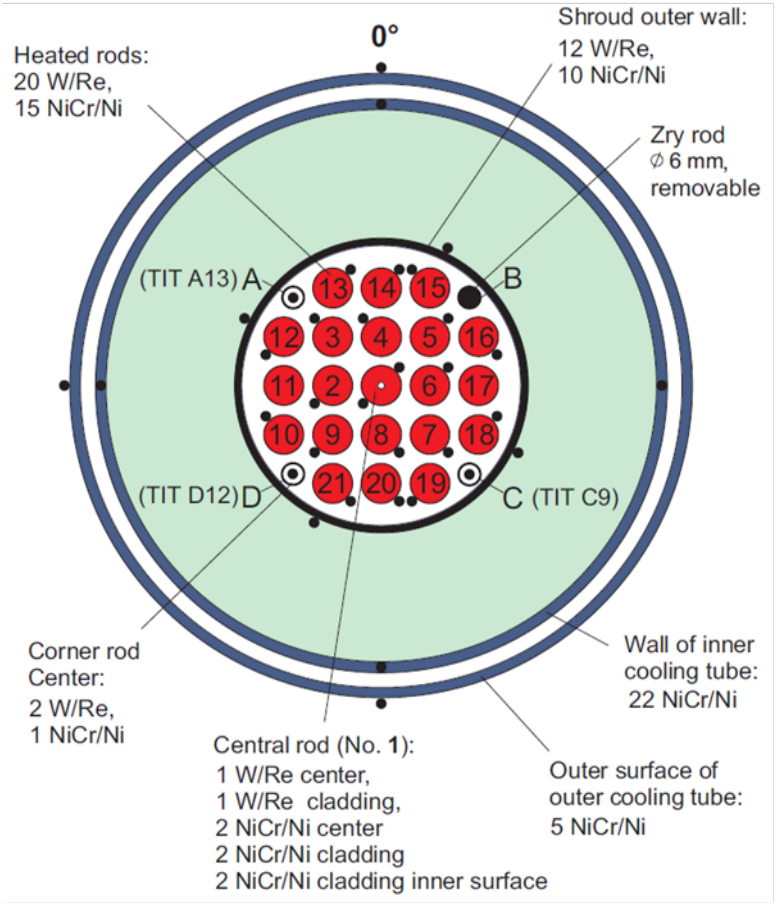


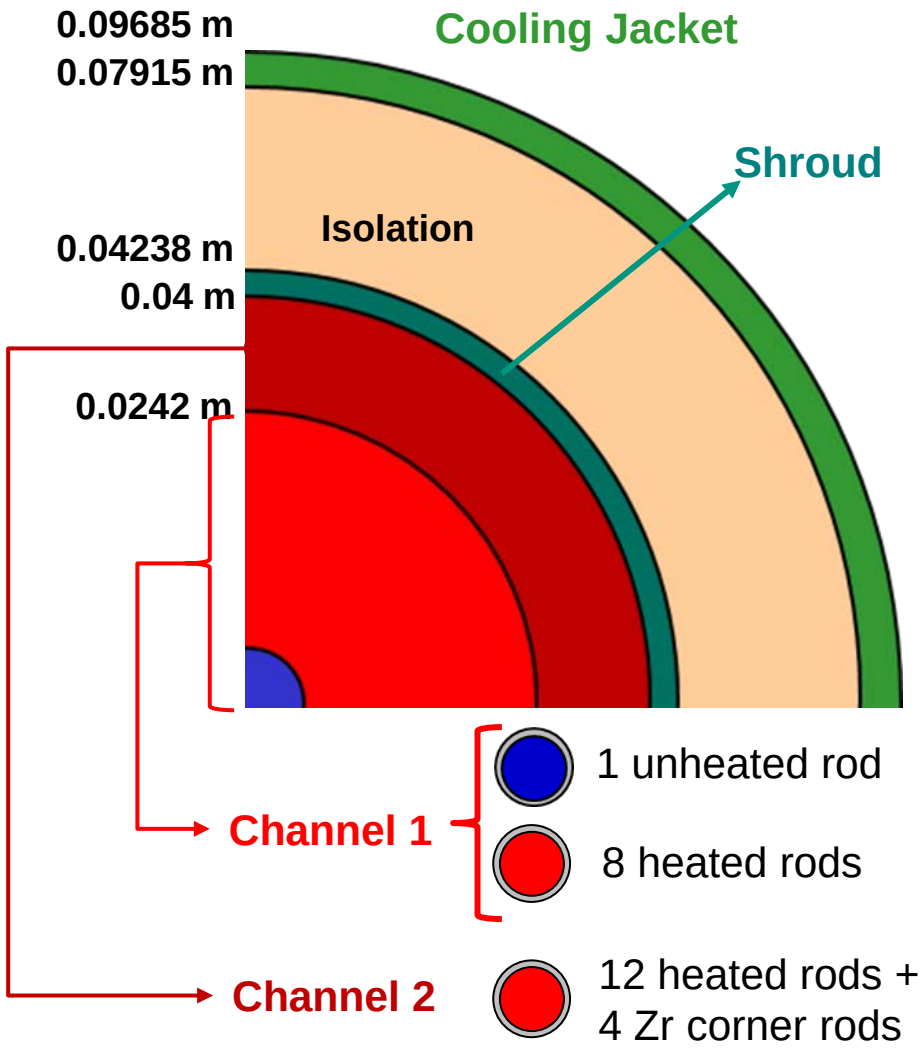




- 21 Zr-4 Fuel Rod Simulators (FRS) (20 heated+1 unheated) **with identical radial dimensions as PWR fuel-element cladding** (pin pitch=1.43 cm).

The ASTECv2.1.1.3 Model





- **The same material compositions as in the experiment have been employed in the ASTEC model.**

I. Gómez García-Toraño, Further development of Severe Accident Management Strategies for a German PWR Konvoi Plant based on the European Severe Accident Code ASTEC, PhD, KIT, 2017.

The Assumptions on the ASTECv2.1.1.3 Model

- **The W heater is in contact with the fuel pellets** to avoid the consideration of radiation from heater with unknown surface properties.

- **The corner rods stay during the whole transient** → not possible to remove physical elements from ICARE during the calculation.

- **The conductive heat exchange between the shroud and the cooling jacket has been defined through the argon gap** (1024-1300 mm) → the shroud/cooling jacket direct radiative exchange cannot be directly calculated by ASTEC.

- **The gap is therefore assumed to be a solid argon cell**, whose thermal resistance is updated at each time step.

Physical Models Employed

- **Heat transfer**
  - **Conduction** within each element and between the different elements in contact.
  - **Convection** between each element facing the channel.
  - **Radiation** among FRS claddings, corner rods and the shroud.

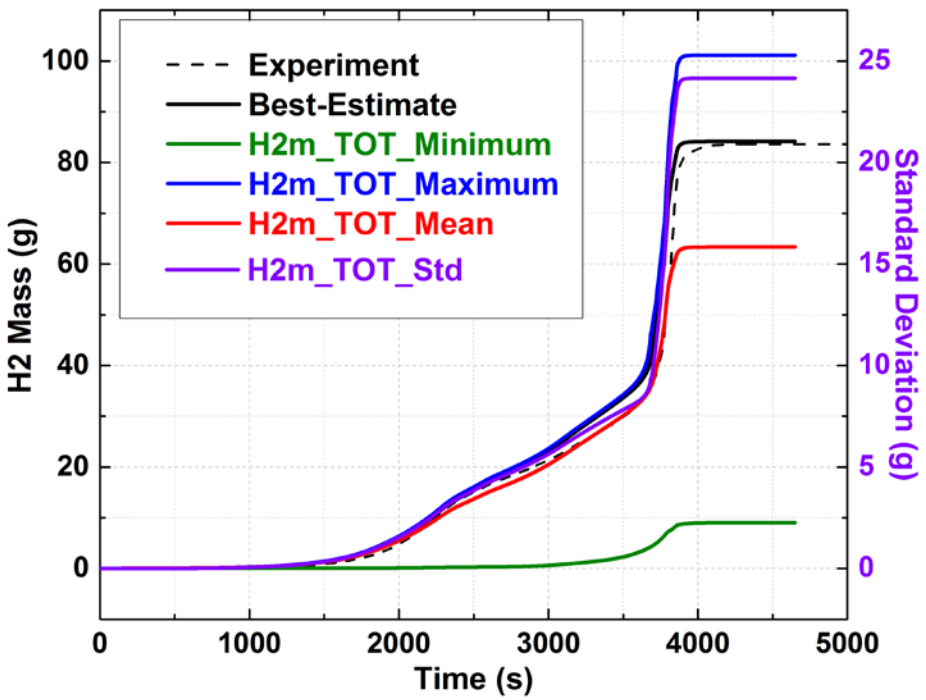
- **Chemical interactions**
  - Oxidation of Zry-4.
  - The shroud and corner rods can also oxidize.

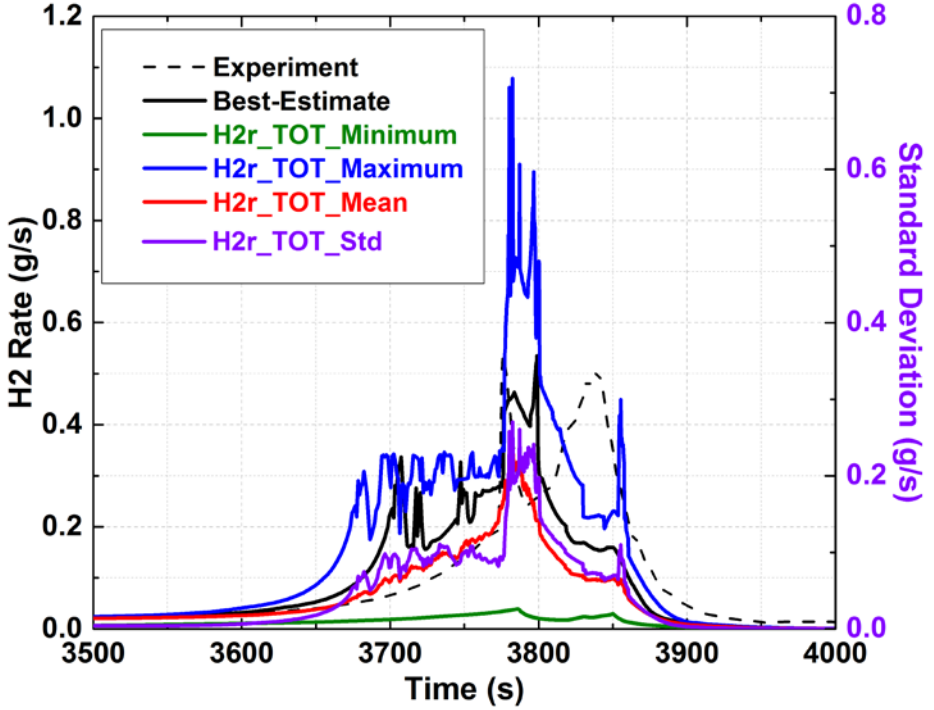
- **Mechanical processes**:
  - **Cladding, corner rod, and shroud failure** if its temperature is greater than 2300 K and their ZrO2 thickness is lower than 300 µm.
  - **Relocation of molten material** along the rods and molten material oxidation.

Input Parameters for ASTEC/URANIE

- **The sensitivity analysis of the ASTEC results for the H2 production and temperature distributions has been performed by propagating the uncertainties associated to the:**
- **Geometry model**
  - Shroud internal diameter and thickness, Insulator thickness
- **Scenario**
  - Ar and Steam mass flow rate, outlet P
- **Integrity Criteria of the clad**
  - ZrO2 thickness and T
- **Radiative exchanges in a bundle (RADB)**
  - Rod and Shroud anisotropic factors
- **Solid/magma and fluid Convective Heat Transfer (CONV)**
- **Relocation of molten material (MOVEMAG)**
- **Oxidation of molten material (UZOXMAG)**
- **Uniform and normal PDFs have been assessed for each parameter, the default values being employed as basis.**

Hydrogen Mass



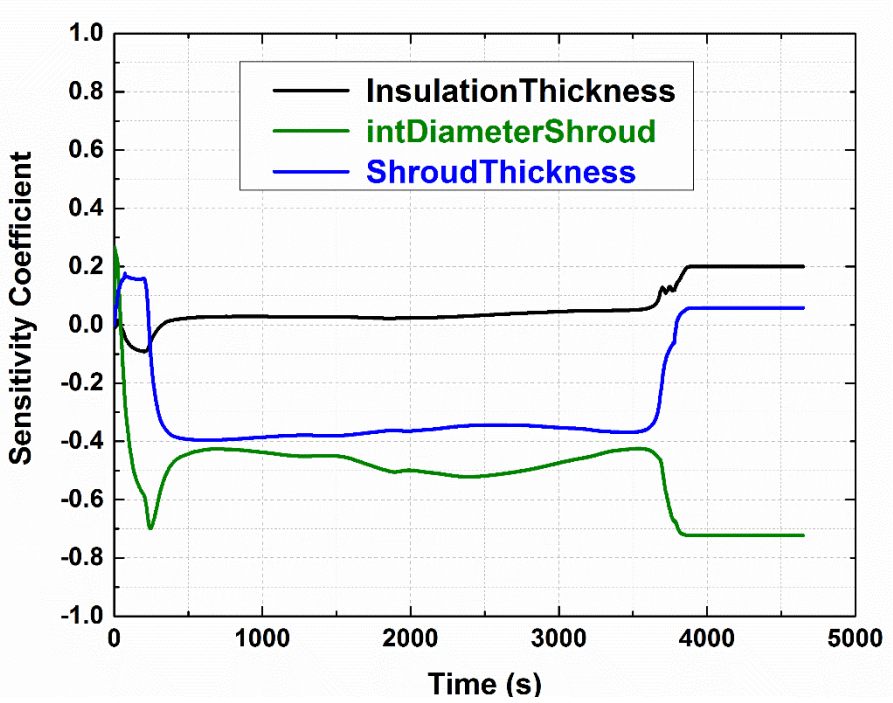


- **The BE results show an excellent agreement with experiment.**
- **On the other side, the U&S analysis show a quite large spread.**
- As expected, large variations occur in correspondance of the steam injection.

H2 Mass: Sensitivity Results (1/3)

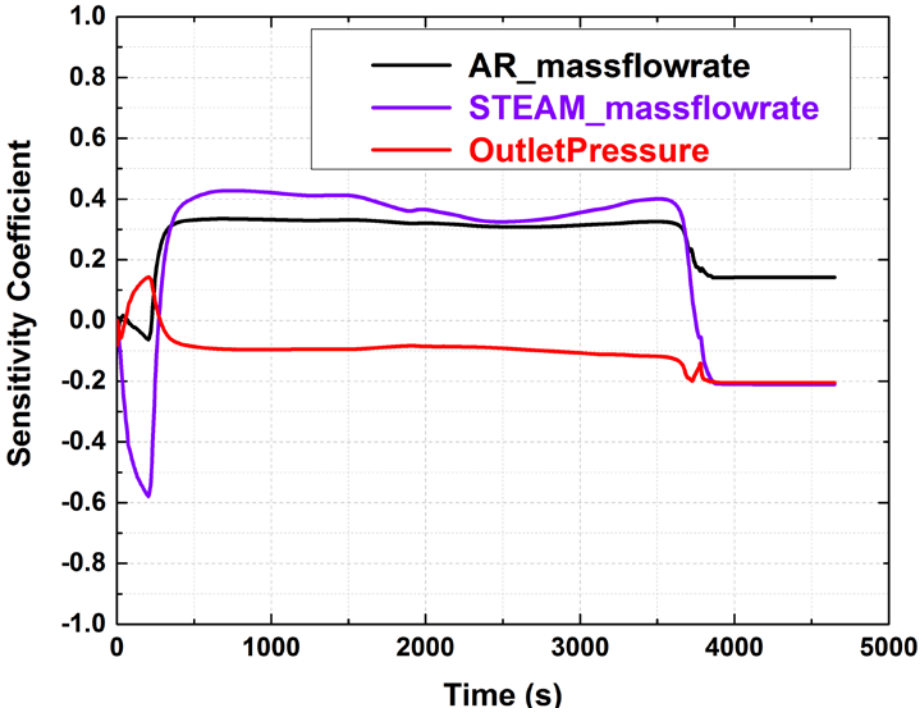
Geometry

Parameter variation +/- 1%



Scenario

Parameter variation +/- 5%

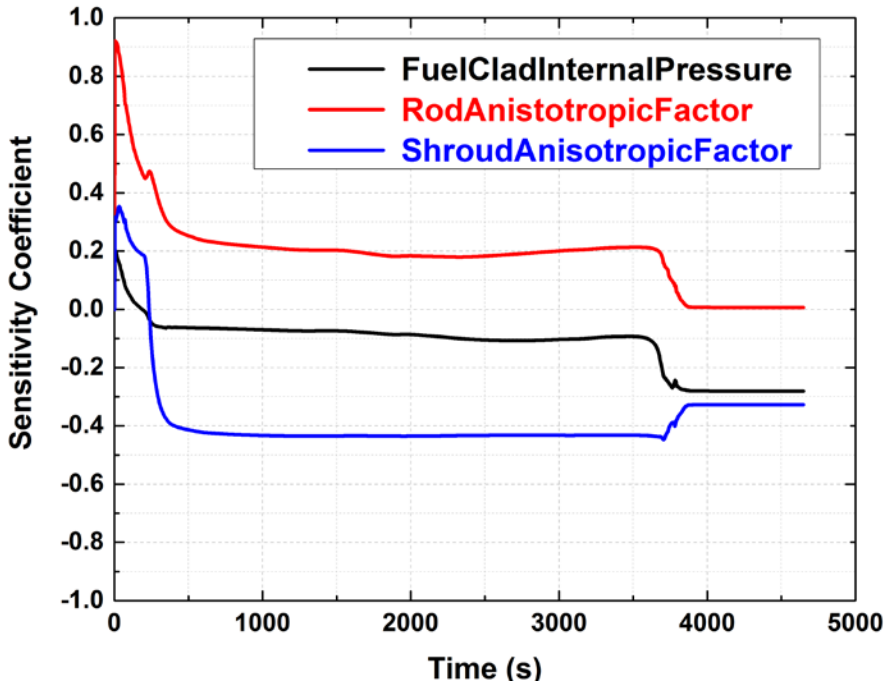


- **The uncertainty associated to the internal diameter of the shroud is significant.**
- **Similarly, sensitivities to the scenario may not be neglected.**

H2 Mass: Sensitivity Results (2/3)

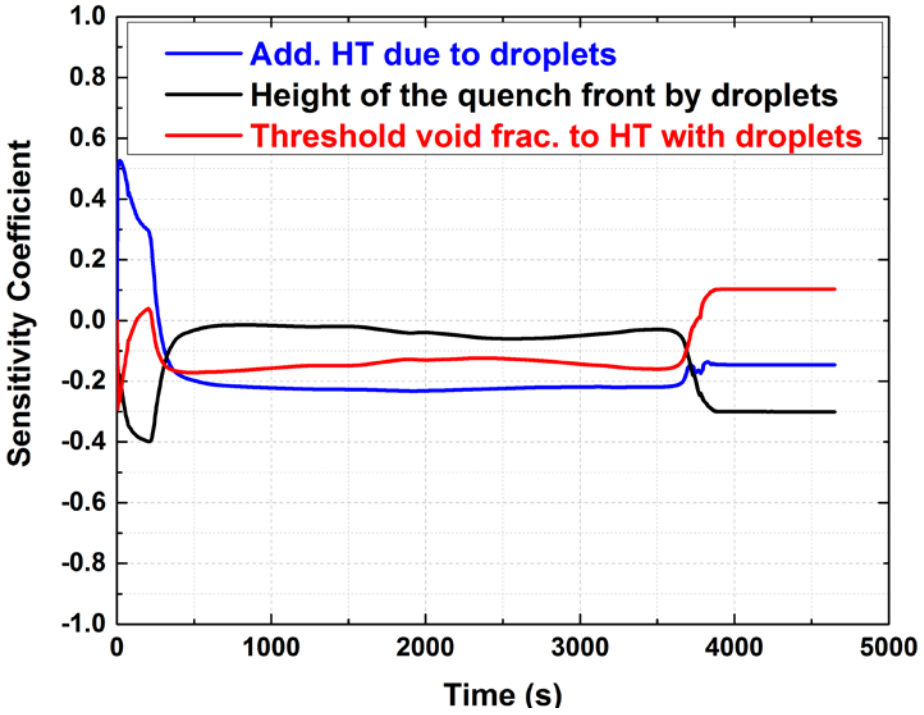
Radiative Exchange

Parameter variation +/- 50%



Convective HT

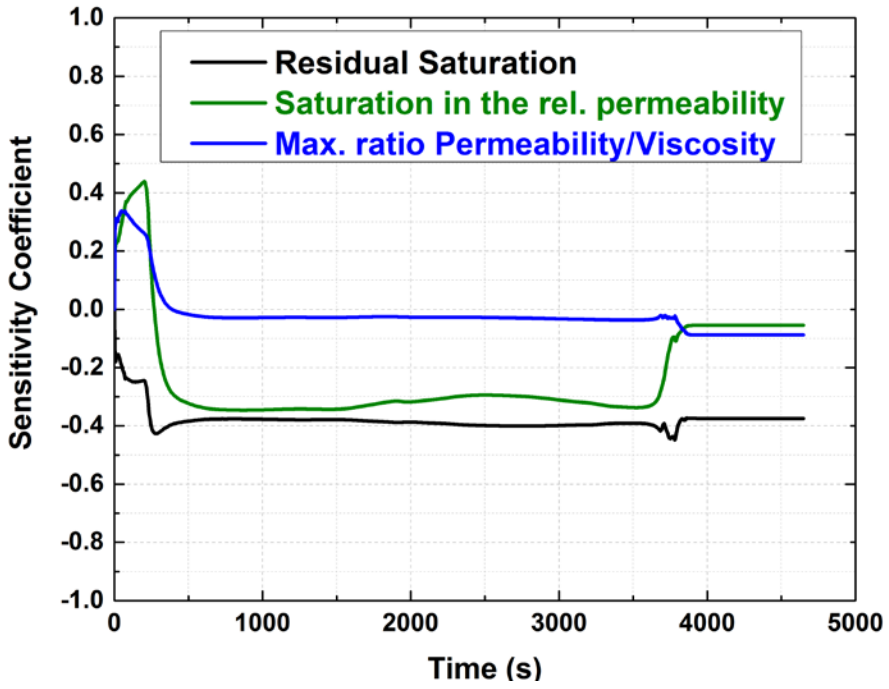
Parameter variation +/- 5%



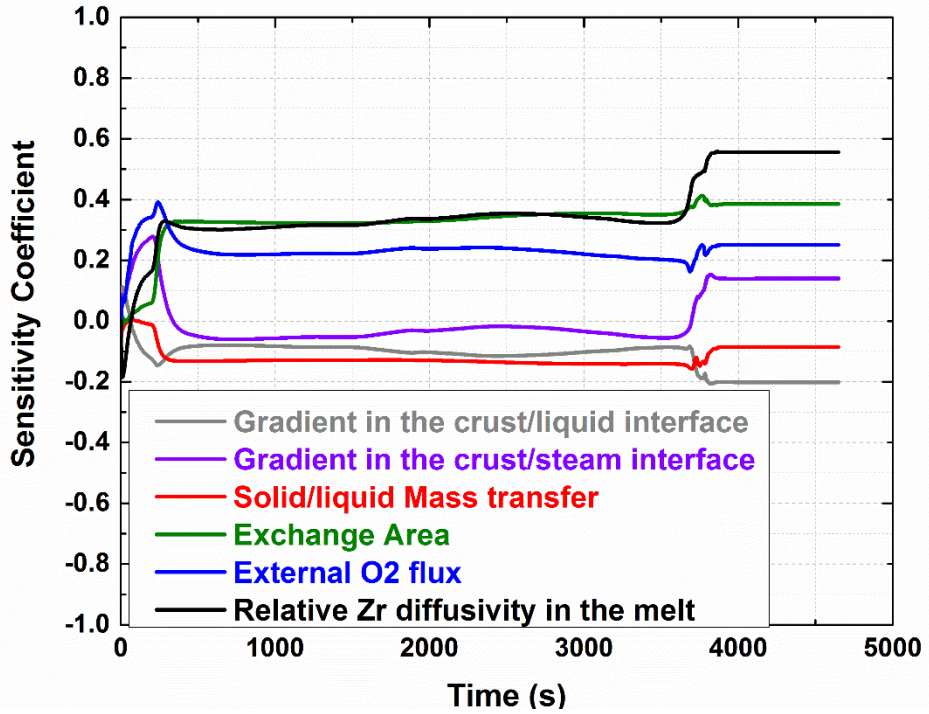
- **Significant effect due to the radiative exchange.**
- **Small or negligible sensitivity to the convective HT model.**

H2 Mass: Sensitivity Results (3/3)

Relocation of molten material
Parameter variation +/- 10%

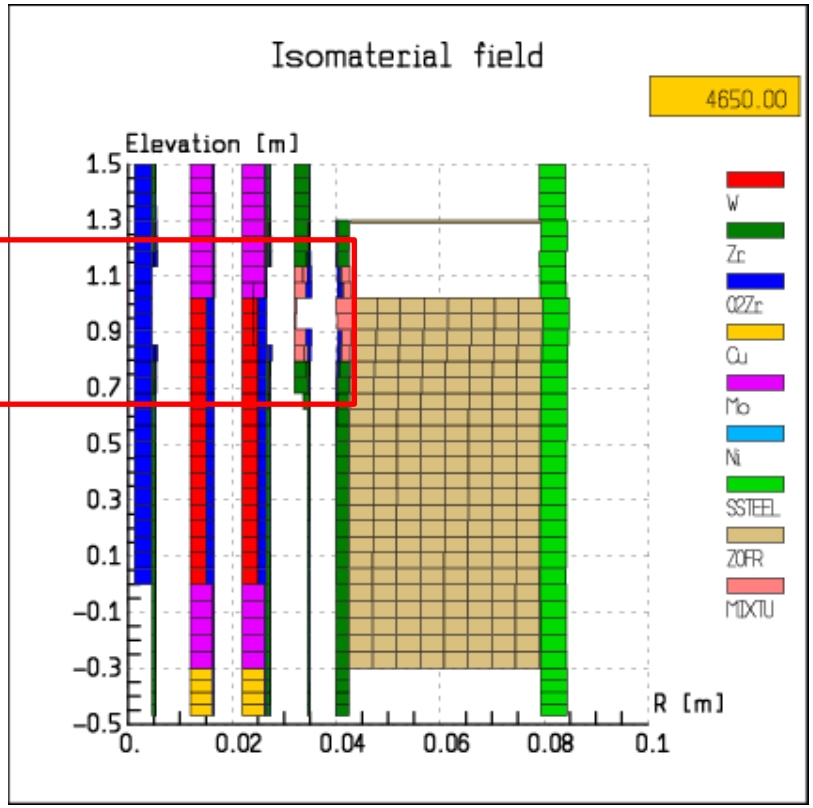


Oxidation of molten material
Parameter variation +/- 10%



- **Small or negligible sensitivity to the molten material relocation.**
- **Sensitivity of the oxidation of molten material drops up in correspondence of the clad dissolution.**

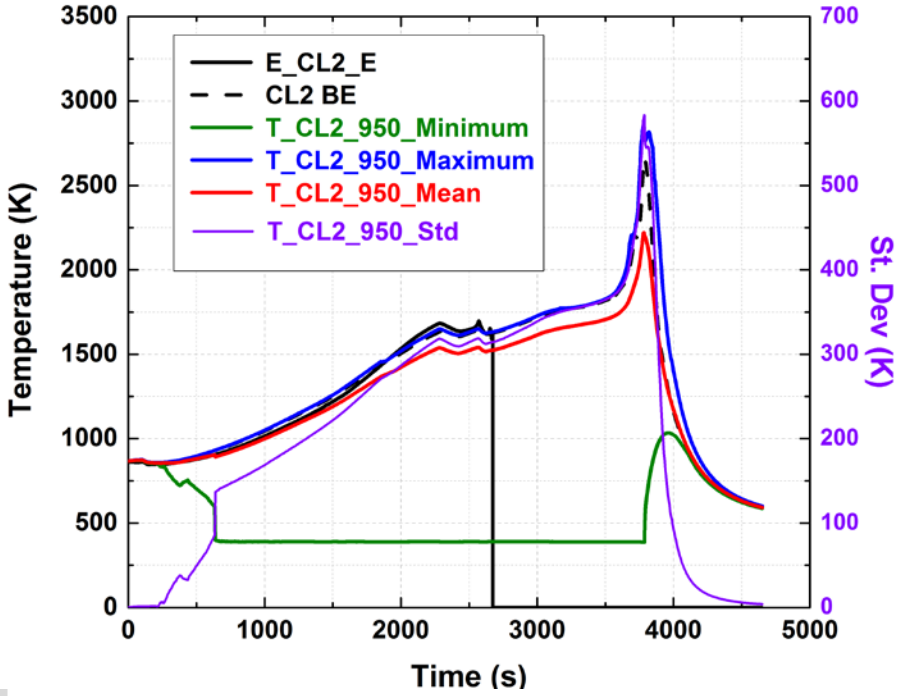
Sensitivity to the Oxidation of Molten Material

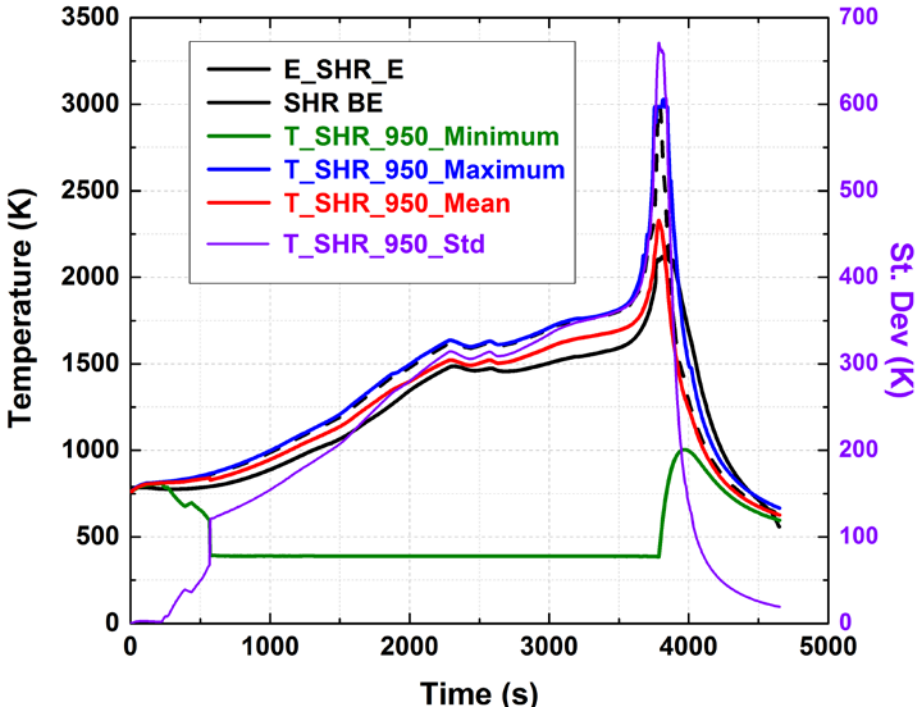


- The results are consistent with the BE evaluations.
- The ASTEC simulations predict the shroud and clad dissolution at 900-1100 mm height.
- Such an effect has been observed in the post-analysis of the test*.

*Stuckert, J., et al., 2005, Experimental and Computational Results of the QUENCH-08 Experiment (Reference to QUENCH-07). Report FZKA 6970.

Clad and Shroud Temperatures @950 mm Height



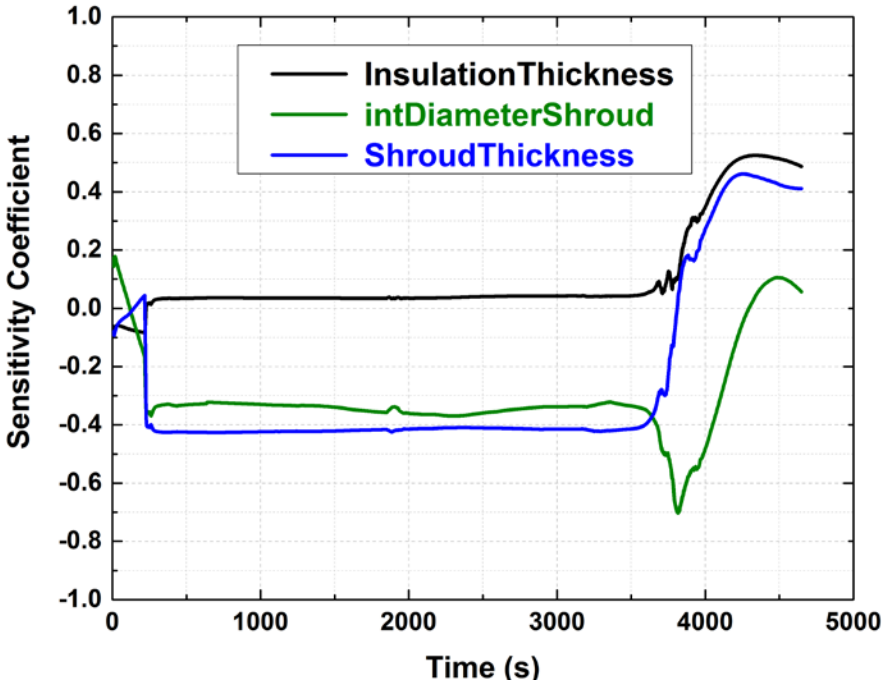


- **The clad and shroud temperature show a large spread of the results.**
- **The mean value is in good agreement with experiment, despite the standard deviation ranges between 300 K and 600 K.**

Clad T: Sensitivity Results (1/3)

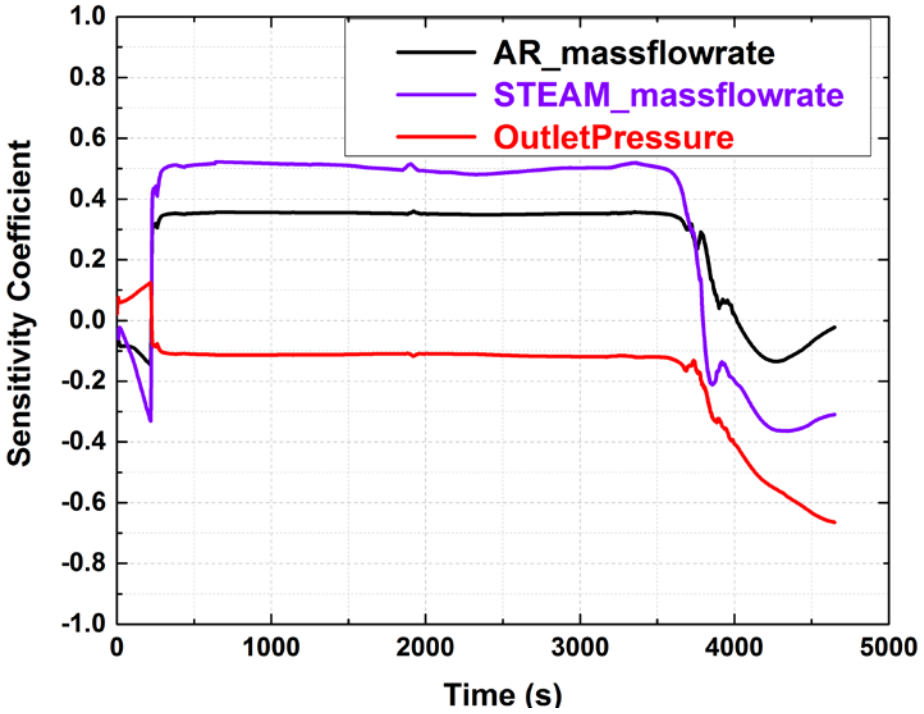
Geometry

Parameter variation +/- 1%



Scenario

Parameter variation +/- 5%

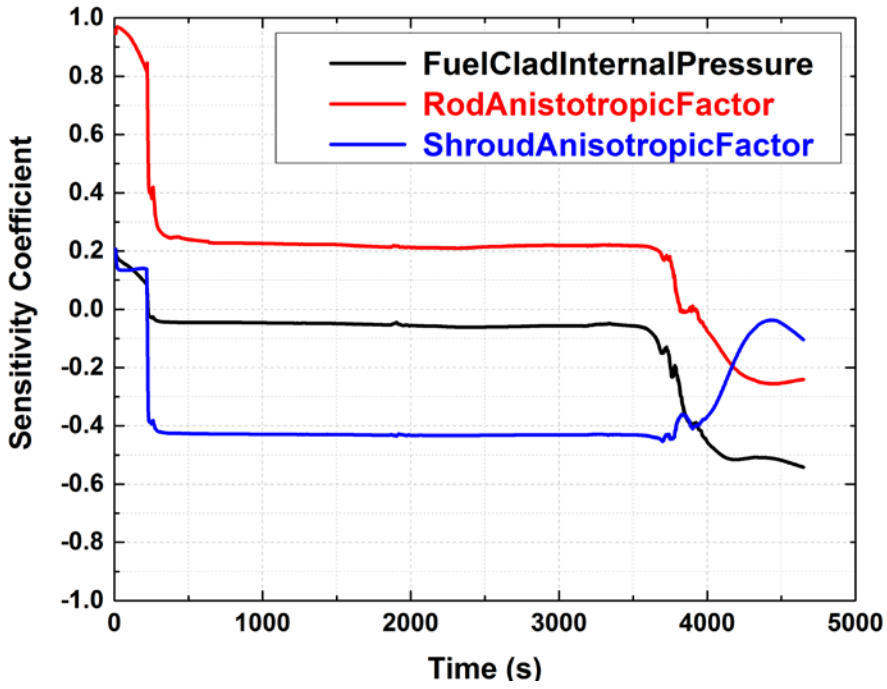


- **Sensitivities significantly drop after the steam injection.**
- **Sensitivities to the scenario may not be neglected.**

Clad T: Sensitivity Results (2/3)

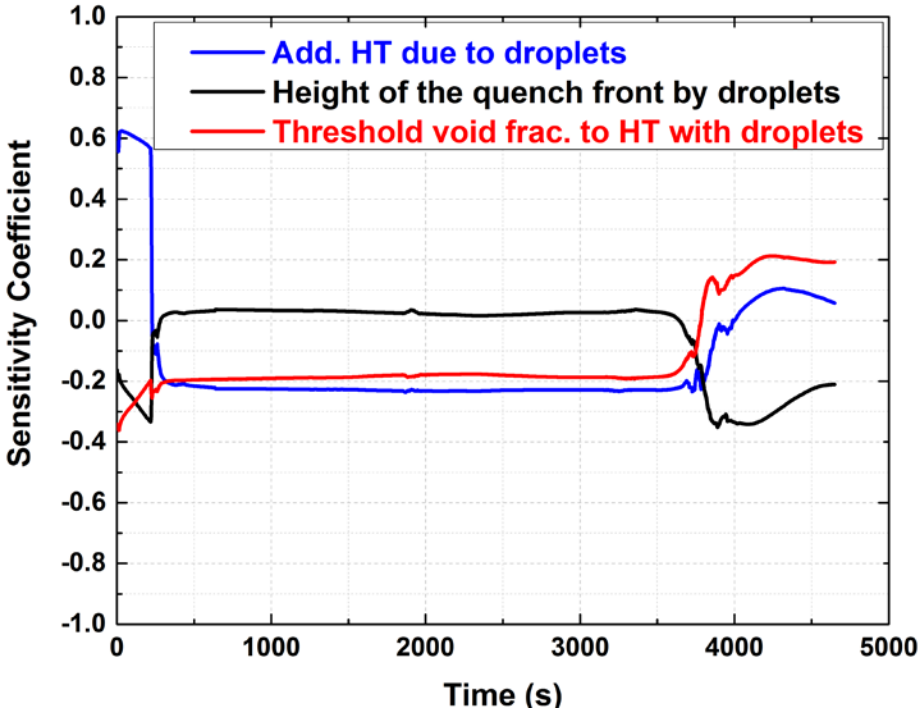
Radiative Exchange

Parameter variation +/- 50%



Convective HT

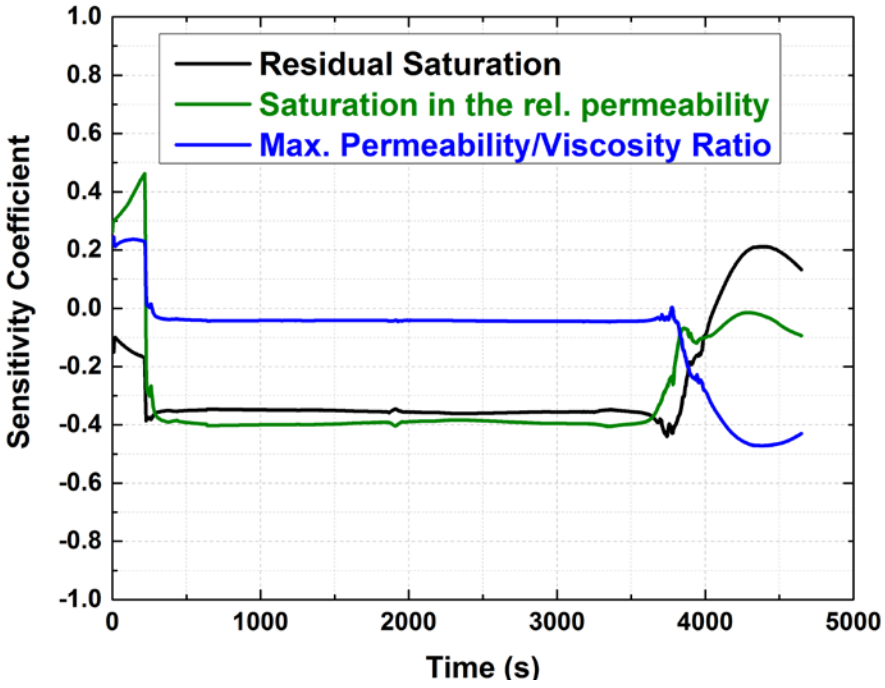
Parameter variation +/- 5%



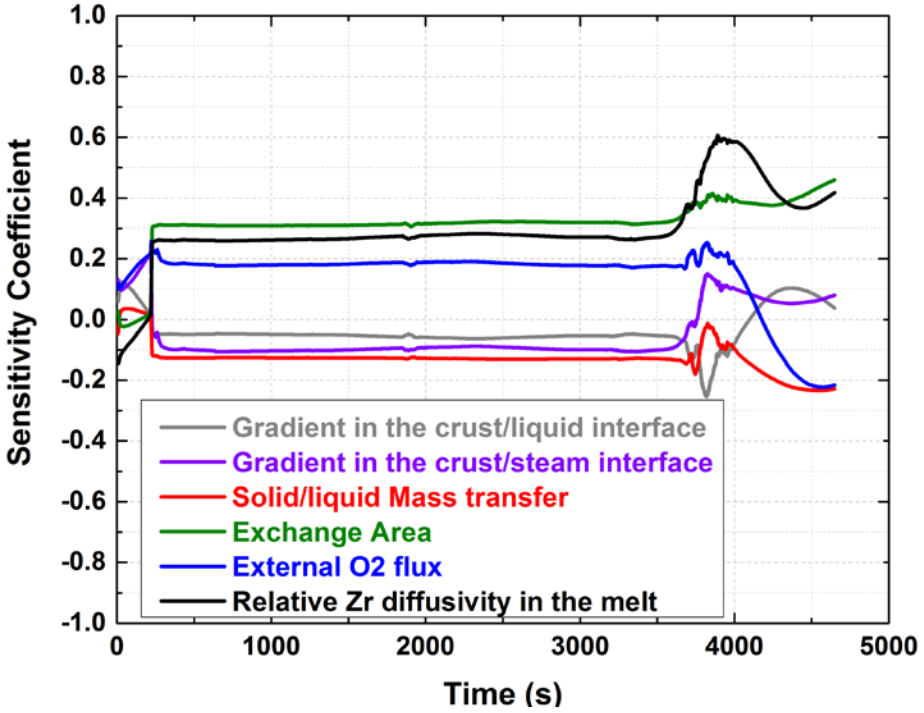
- As expected, significant effect due to the radiative exchange.
- Small or negligible sensitivity to the convective HT model.

Clad T: Sensitivity Results (3/3)

Relocation of molten material
Parameter variation +/- 10%



Oxidation of molten material
Parameter variation +/- 10%



- **Small or negligible sensitivity to the molten material relocation.**
- **Sensitivity of Zr diffusivity and exchange area with coolant are significant.**

Conclusion

- **The ASTEC/URANIE platform has been assessed at KIT with the final goal to be employed to the analysis of SA scenarios.**
- The application of ASTEC/URANIE to the QUECH-08 experiment with respect to the H2 production shows that:
  - The BE results very well agree with the reference results;
  - The propagation of small uncertainty (+/- 1%) on the definition of the scenario and on the geometrical model have significant effects;
  - Similarly, as expected, concerning the radiative heat transfer model.
- **The sensitivity on H2 production to the ASTEC models related to the relocation and oxidation of molten material are not negligible.**
- **Such an observation provides important hints with respect to future analyses of the performance of the ASTEC physical models to SA scenarios.**

24th International QUENCH Workshop
Karlsruhe Institute of Technology, Campus North, H.-von-Helmholtz-Platz 1, 76344 Egg.-Leopoldshafen, Germany
13-15 November 2018

Validation of ASTEC2.1 using QUENCH-12 for VVER-reactors

Ahmet Kağan Mercan[1], Victor Hugo Sánchez-Espinoza[1], Fabrizio Gabrielli[1]
Karlsruhe Institute of Technology (KIT), Hermann-von-Helmholtz-Platz 1,
D-76344 Eggenstein-Leopoldshafen, Germany
ahmet.mercan@partner.kit.edu, victor.sanchez@kit.edu, fabrizio.gabrielli@kit.edu

Abstract

Severe accident codes such as ASTEC, MELCOR, MAAP, ATHLET-CD, etc. are widely used to study the behavior of nuclear power plant under hypothetical severe accident sequences. At KIT, both experimental and numerical investigations are carried out to understand the behavior of fuel rods under severe accident conditions as well as to predict the amount of hydrogen released into the containment and the radiological source term.

In the frame of a doctoral thesis devoted to severe accident investigations of VVER-reactors with the goal of the quantification of the radiological source term for a subsequent JRODOS-simulation, the first step is to perform ASTEC-2.1-validation using the KIT QUENCH-12 test, where a representative VVER-fuel rod simulator was used. The main goal of the QUENCH-12 test was to evaluate the hydrogen generation resulting from the injection of cold water into an overheated and oxidized VVER-bundle. The focus of the investigations is the high-temperature oxidation, the melt formation and its relocation as well as its behavior under the quenching conditions. In this test, the bundle is heated-up with steam and argon mixture for a certain period of time and then it is quenched with cold water. The test section is equipped with thermocouples located at different axial and radial positions as well as with a mass spectrometer to measure both the temperature and the hydrogen generation.

For the post-test simulation of this test, an ASTEC-model of the QUENCH-facility and test section was developed considering the material and geometrical peculiarities of the VVER fuel rods. The boundary conditions for the pre-and quench-phase simulation were provided by the QUENCH-team. An exhaustive comparison of the predicted key-parameters and the measured ones is underway to assess the ASTEC-prediction capability. Based on the current evaluation of the simulations, it can be stated that the amount of hydrogen predicted by ASTEC2.1 is close to the experimental values. This paper will discuss a. o. the test conduction, the modelling issues and finally the obtained results of the code-to-data comparison. After the successful validation of ASTEC2.1, a plant model for a VVER of Generation III will be developed in order to analyze selected SA-sequences for the source term quantification as needed by JRODOS.

Keywords: QUENCH-12, ASTEC2.1, VVER, Validation


TOSHIBA
KIT

Validation of ASTEC2.1 using VVER QUENCH-12 Experiment

24th International QUENCH Workshop
13-15 November 2018

A. K. Mercan
ASTEC-Team at KIT

Institute for Neutron Physics and Reactor Technology (INR)
Reactor Physics and Dynamic Group (RPD)



Content

- Motivation
- QUENCH-12 VVER test:
  - Description
  - Test conduction
- **ASTEC model**
- Simulations and discussion of results
- Conclusions
- Outlook

Motivation

- Fukushima accidents shown needs for further improve severe accident codes such as ASTEC, MELCOR, ATHLET-CD

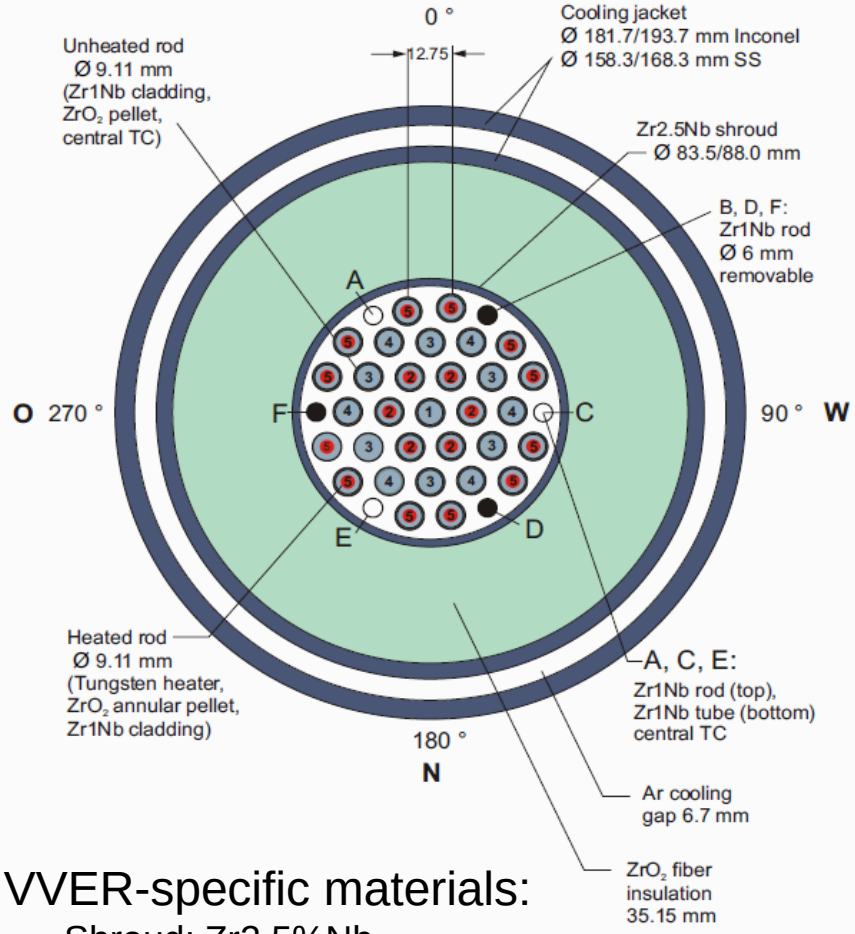
- Assess prediction capability of ASTEC related with the in-vessel severe accident phenomena of VVER reactors.
  - Oxidation and hydrogen generation
  - Molten material formation and relocation

- Applied validated ASTEC version to analyse severe accident sequences of VVER reactors for accident management (SAM).

QUENCH-12 Test Description

QUENCH-12: Test Section

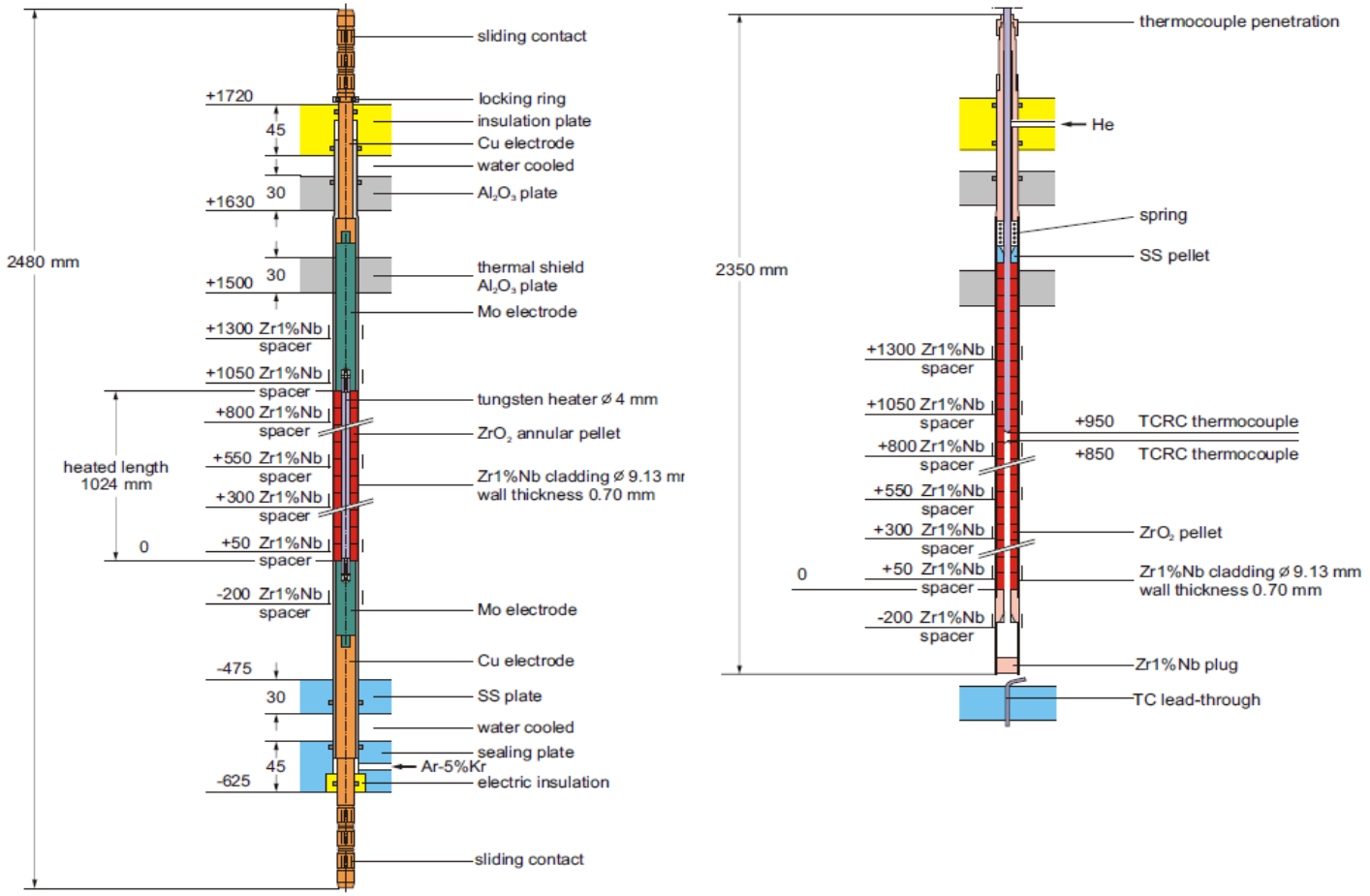
- QUENCH-12 includes 31 rods and 6 corner rods.
- 18 of these rods are heated with tungsten heaters. 13 rods are unheated.
- Pitch distance is 12.75 mm.
- Rods are hexagonal and lattice is triangular.
- Heating is performed by 4 mm diameter tungsten heaters which are installed in rod center. Heated length is 1024 mm.
- Heaters covered with annular ZrO2 pellets which bore size 4.15 mm. Unheated ones covered with annular ZrO2 pellets which bore size 2.5 mm.
- Cladding is those used in VVER reactor (Zr-%1Nb, 9,13 mm outside diameter, 0.7 mm thickness)
- Six Zr-1%Nb corner rods were installed in the bundle.
- Shroud is made of Zr-2.5%Nb.
- 7 spacer grids are located in experiment in different elevation. These are also made of Zr1%Nb.



VVER-specific materials:

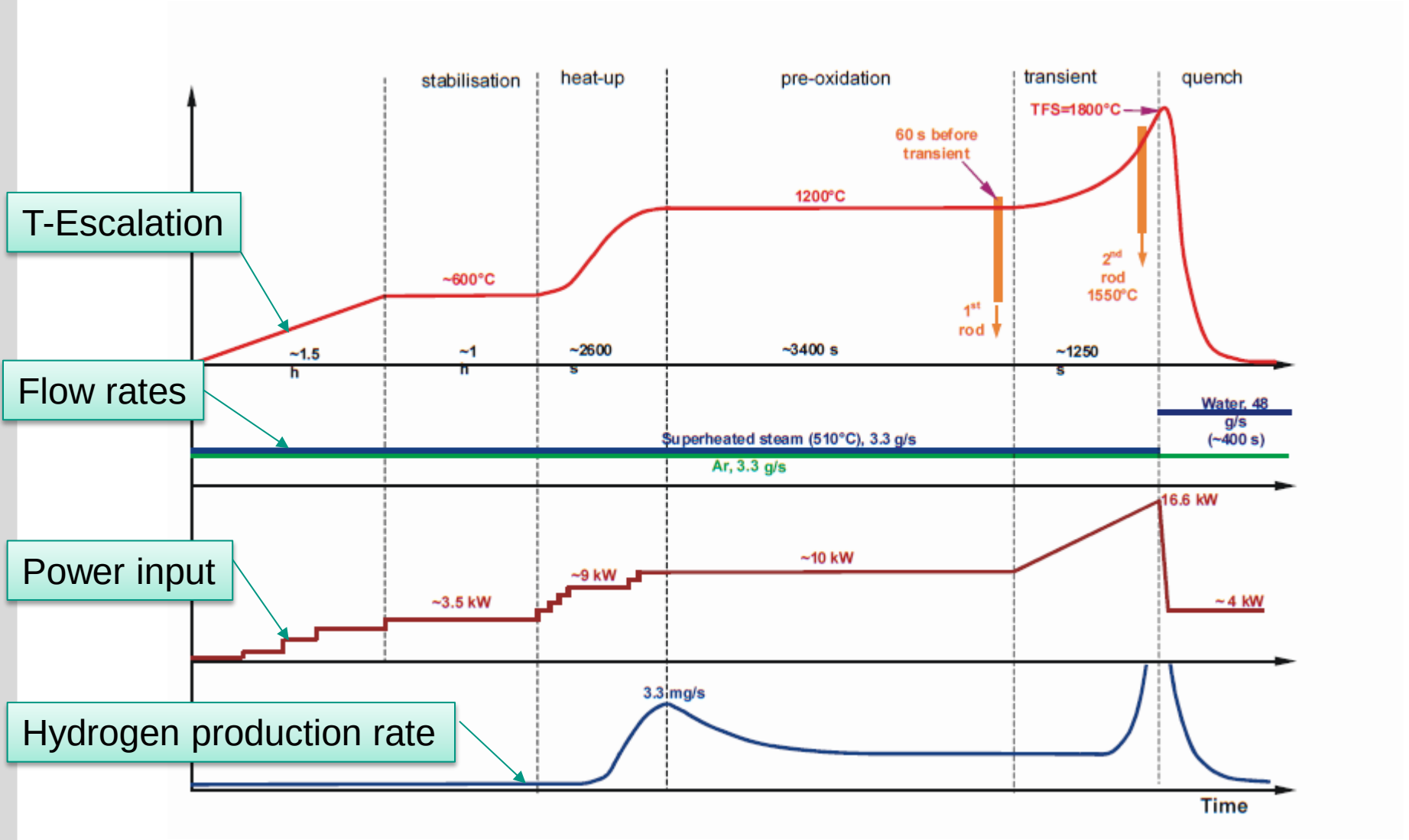
- Shroud: Zr2.5%Nb
- Cladding: Zr1%Nb
- Corner rods: Zr1%Nb
- Spacer grids: Zr1%Nb

QUENCH-12: Heated and unheated rods



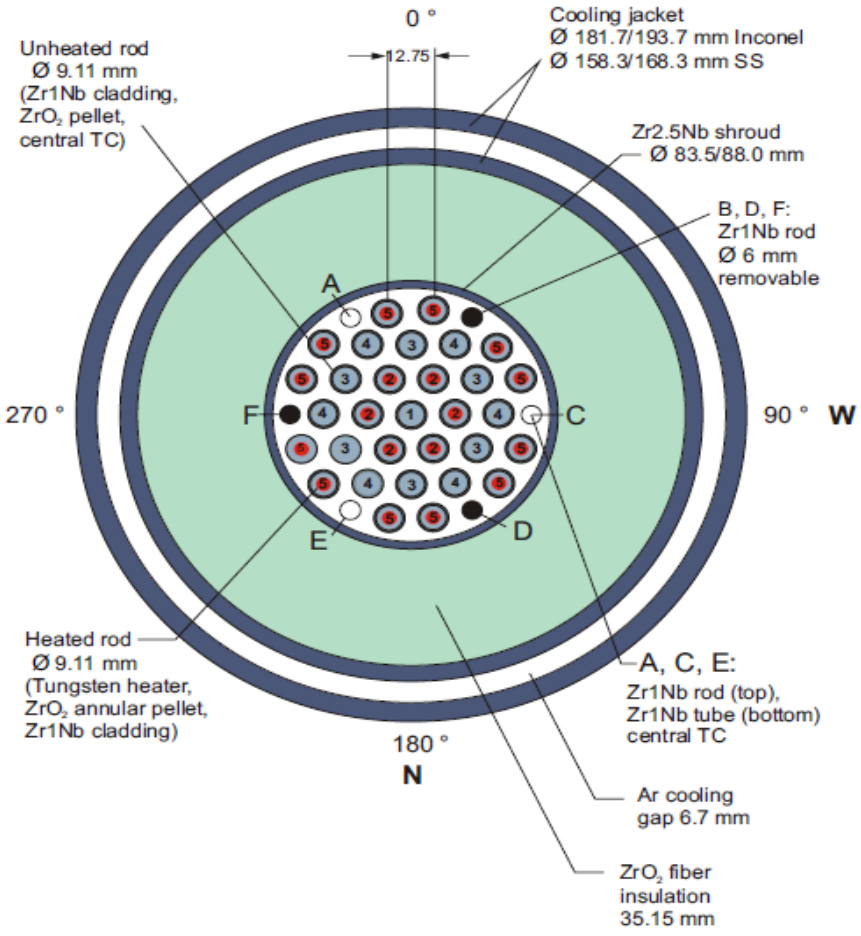
QUENCH-12 Heated and unheated rods

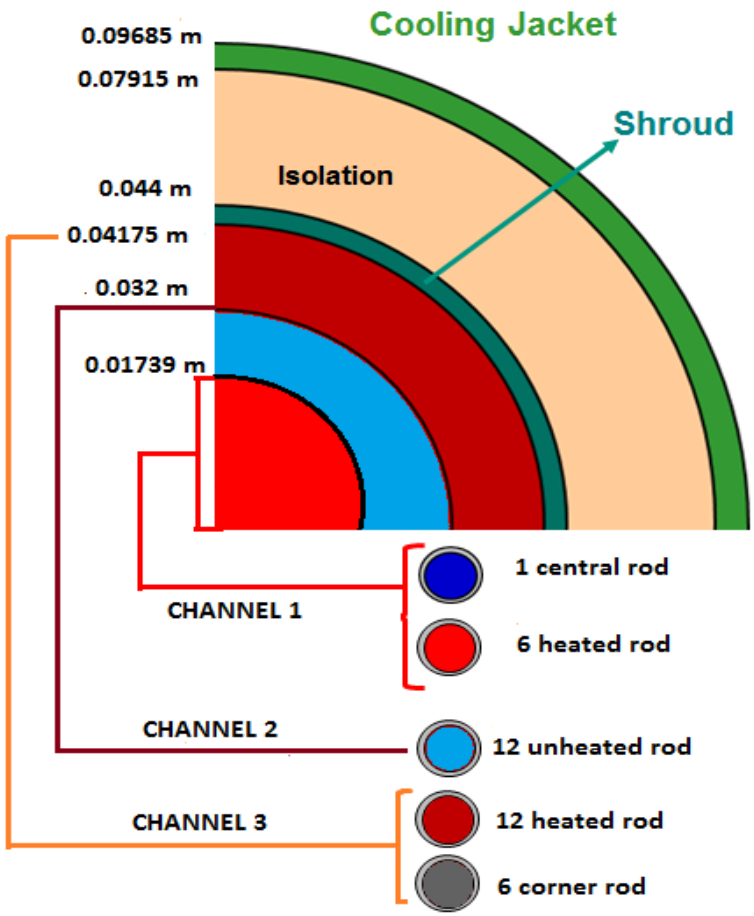
QUENCH-12 Boundary Conditions



ASTEC Model of QUENCH-12

QUENCH-12: ASTEC Modelling



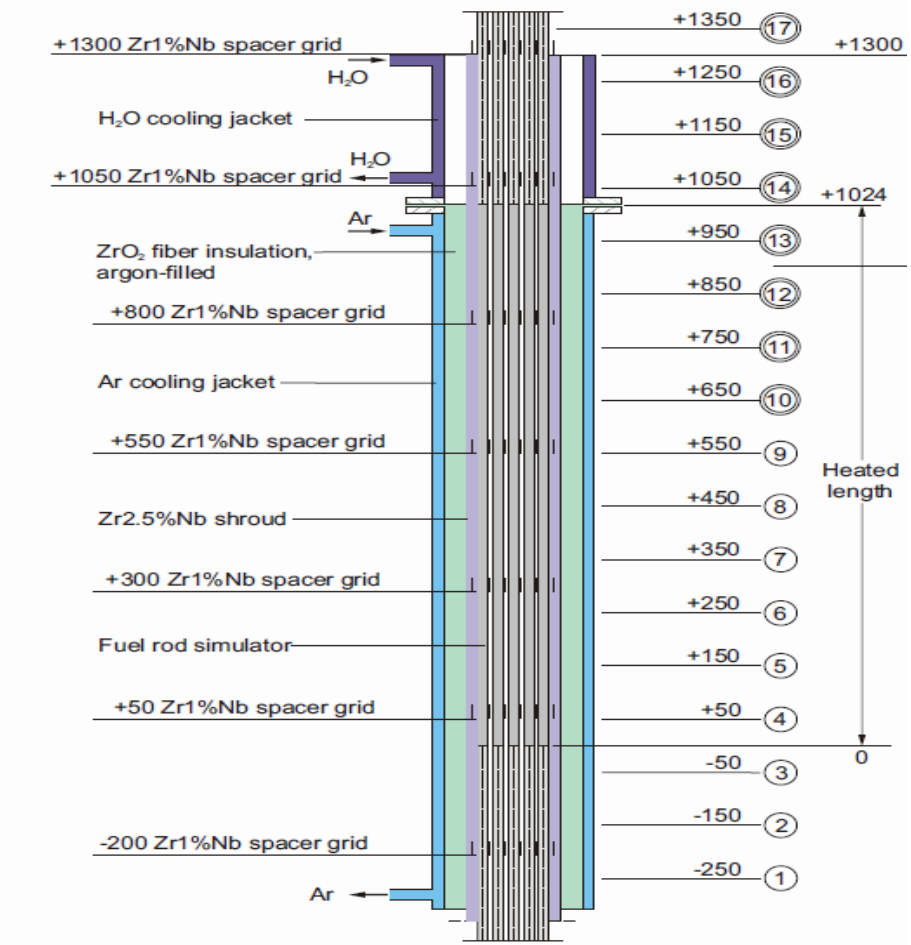


Test Section → **ASTEC Model**

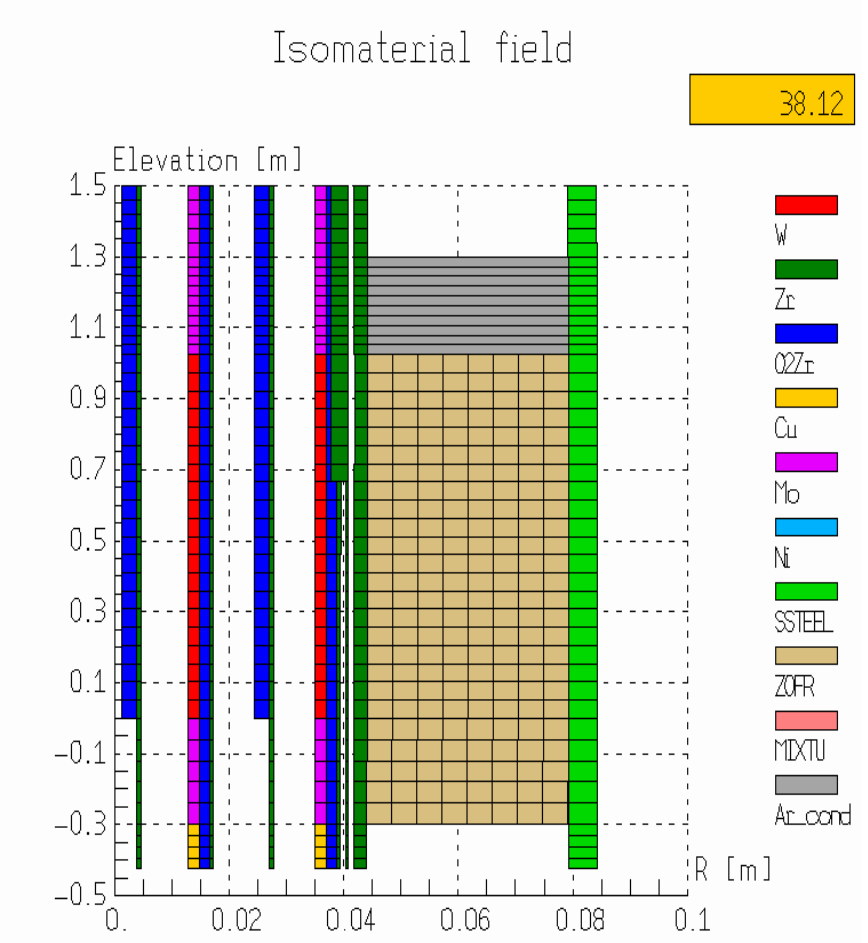
QUENCH-12: ASTEC Modelling

- Three fluid channels
  - 1. CHAN: Radius 17.39 mm
    - one central unheated rod
    - 6 heated rod
  - 2. CHAN: Radius 32 mm
    - 12 unheated rod. Radius is 32 m
  - 3. CHAN Radius 41.75 mm
    - 12 heated fuel rod
    - 6 corner rod
- Rest of system consists on shroud, ZrO2 insulation, inner cooling jacket and argon cooling.. They are put according to experimental data
- 7 Zr spacer grids used in system. Their elevations are -200 mm, 50 mm, 300 mm, 550 mm, 800 mm, 1050 mm and 1300 mm.
- Heated region divide 10 meshes.(10.24 mm/mesh)

ASTEC Model: Radial and axial Nodalization



QUENCH-12: Vertical Cut of Test Section



ASTEC: Representation of test section

QUENCH-12: Boundary conditions

- Boundary conditions:
  - Heat profile obtained from experimental data .
  - Resistance is calculated from experimental data.
  - There is 3.3 g/s argon flow and 3.3 g/s steam flow in system
  - Quench water activates after 7270 s in experiment. Flow rate is 48 g/s
  - Cooling jacket temperature is put for boundry temperature.
  - Initial temperatures of clad structures are taken from experiment.

ASTEC-Model: Activated Models

- **Heat transfer definitions**
  - Radiation among clads, corner rods, and the shroud. Axial location of each rod entered.

- **Chemical interactions**
  - Cladding oxidation: Best-Fit model
  - Corner rods oxidation: Best-Fit model
  - Shroud oxidation: Best-Fit model

- **Mechanical processes**:
  - Cladding / corner rod / shroud failure condition:
    - temperature >2300 K and ZrO2 thickness <300 µm.
  - Relocation of molten material and molten material oxidation.
    - Melting of clads, insulations, shroud and grids.
    - Start molten material relocation criteria (Candling model): ??

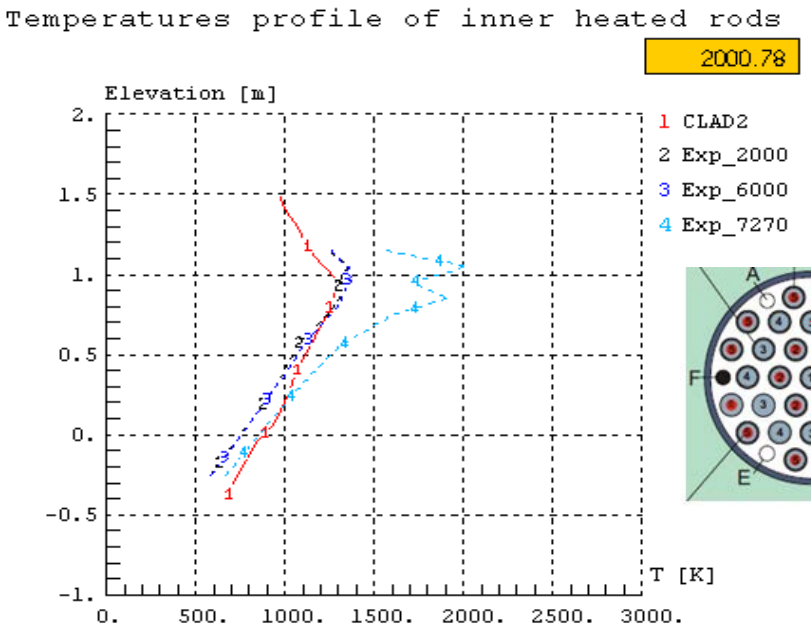
  - Re-flooding model: DRACCAR.

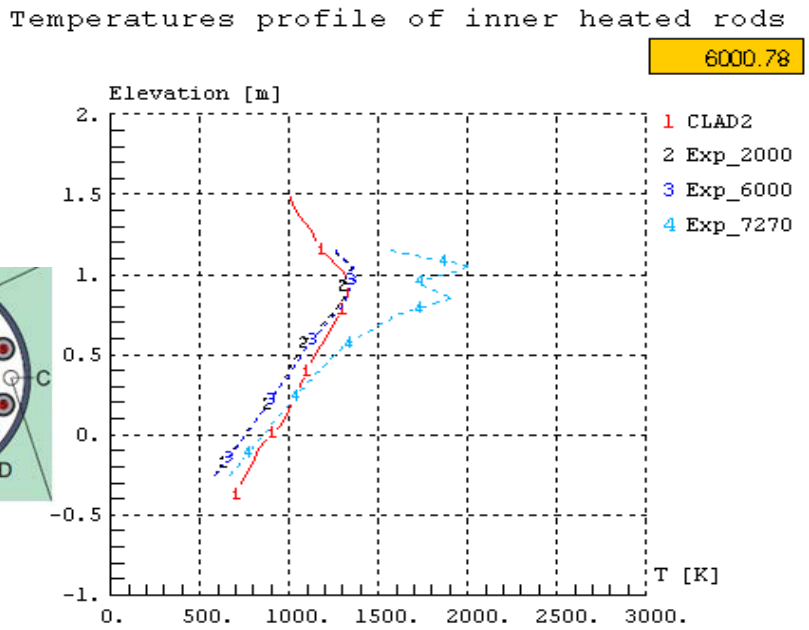
ASTEC Model: Assumptions

- The corner rods stay during the whole transient (rod D at the end of pre-oxidation, rod F during the transient phase and rod B after the test.) → not possible to remove physical elements during the calculation.
- Heat exchange between the shroud and the cooling jacket between 1024-1300 mm has been defined through the argon gap.
- Electrical heaters assumed not melting.
- ASTEC do not accept flow entry below zero levels, quench and pre-injection water enter system at level zero m. (-0.25 m in experiment)
- Zircaloy used instead of ZrNbx for cladding, spacer grids, shroud and magma sections. (because of lack of information in databank of ASTEC).
- Steam entrainment into the fiber or the argon gap after shroud failure has not been modelled.

QUENCH-12- Simulations and Discussion of Results

Phase xx: Comparison of Axial Temperature

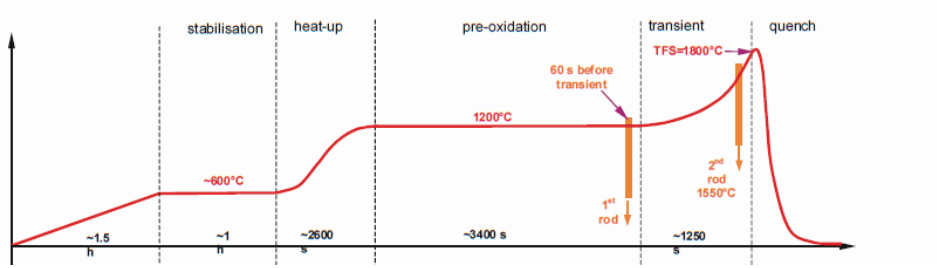




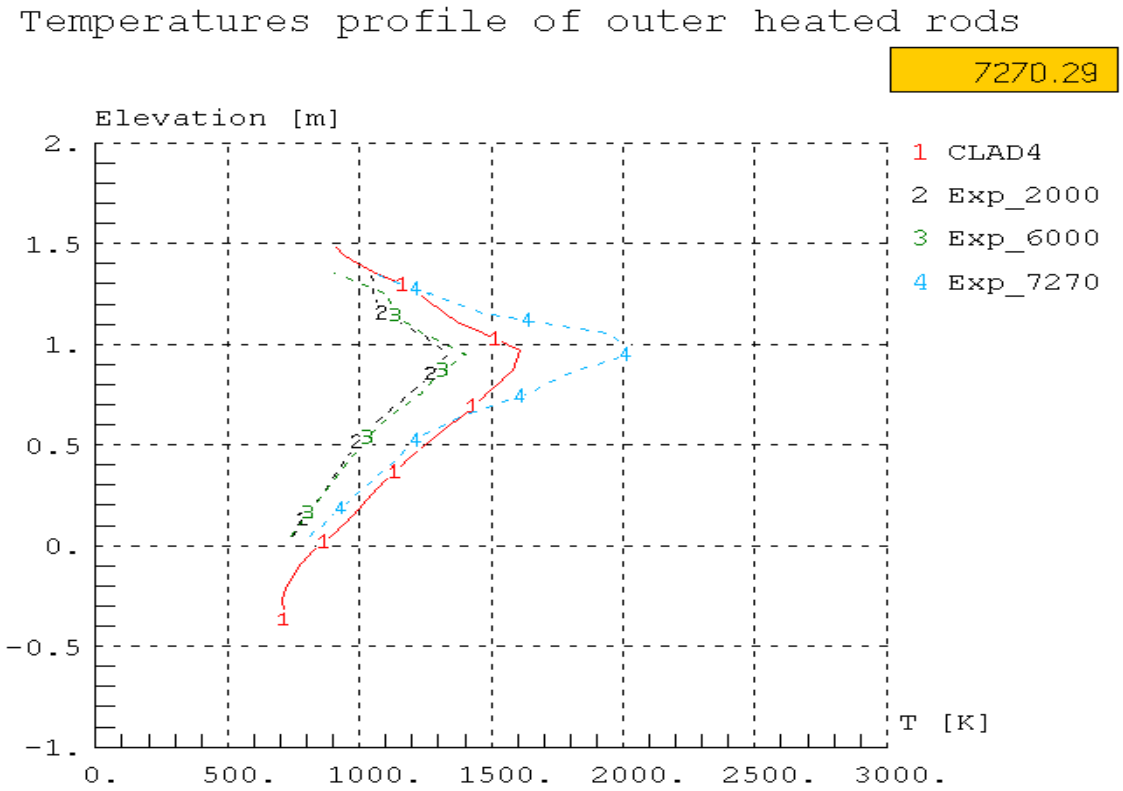
Time: 2000 s
Data vs ASTEC-predictions

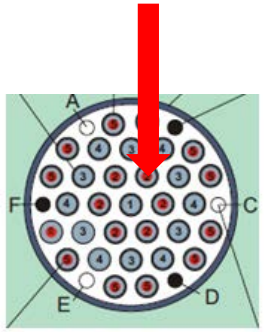
Time: 6000 s
Data vs ASTEC-predictions

Conclusion:
Temperature at higher levels of inner heated rods (CLAD2) at 2000s and 6000s is consistent. However temperatures are higher in lower section.

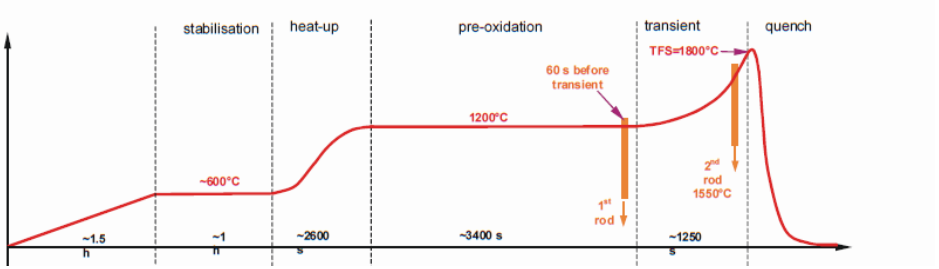


QUENCH-12- Current Simulations (2/12)



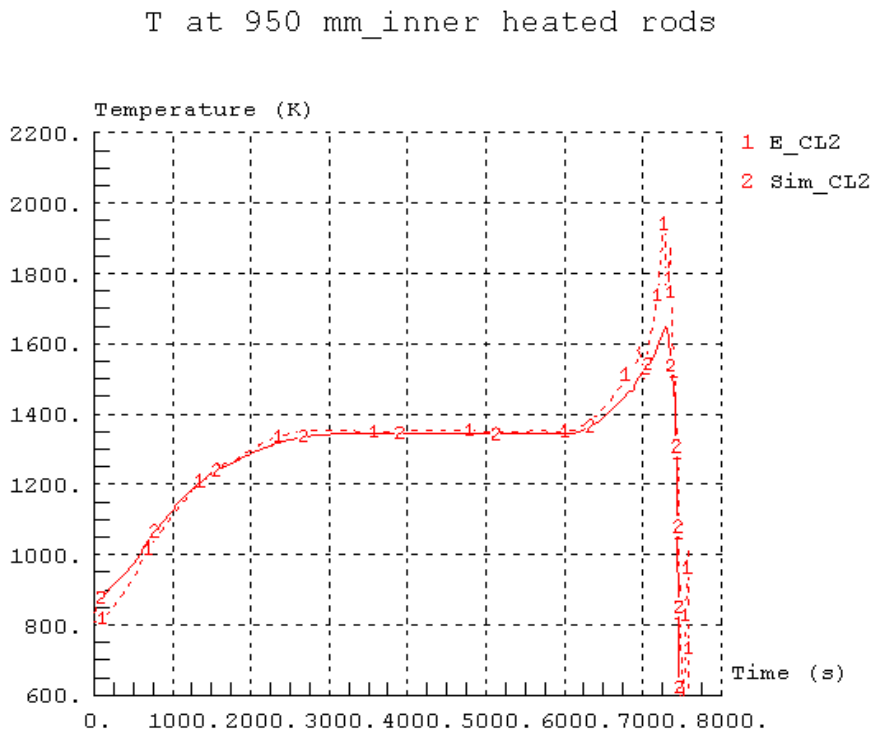


Time: 7270
Data vs. ASTEC prediction

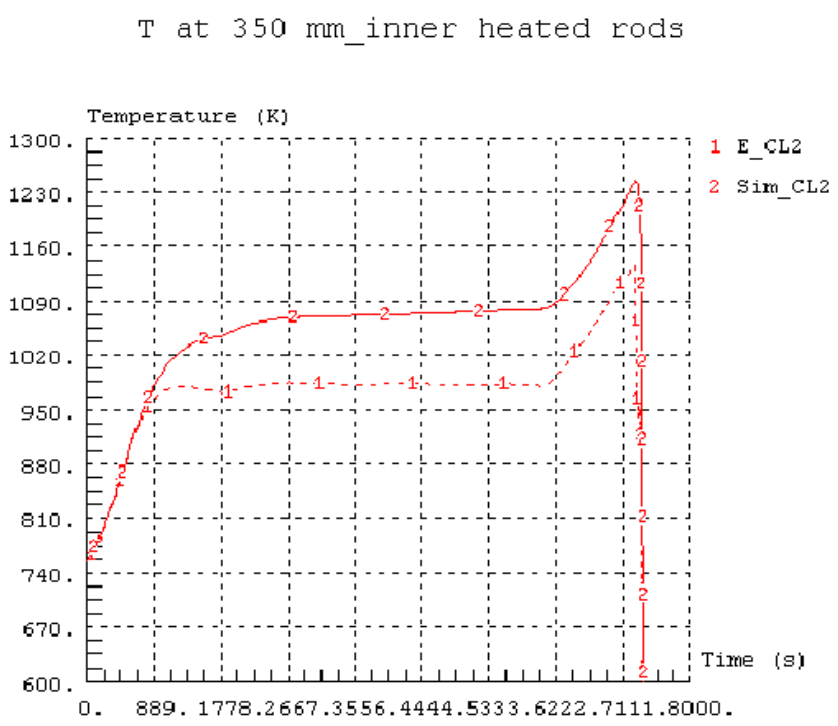


Conclusion:Temperature distribution before quench shows that model calculated temperatures
at middle section lower.

QUENCH-12- Current Simulations (3/12)

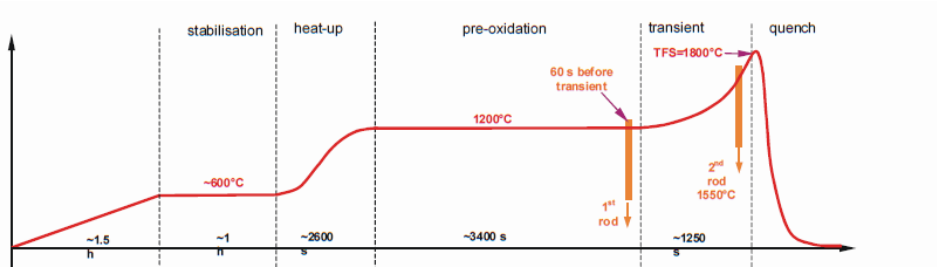


Temperature vs Time at 950 mm

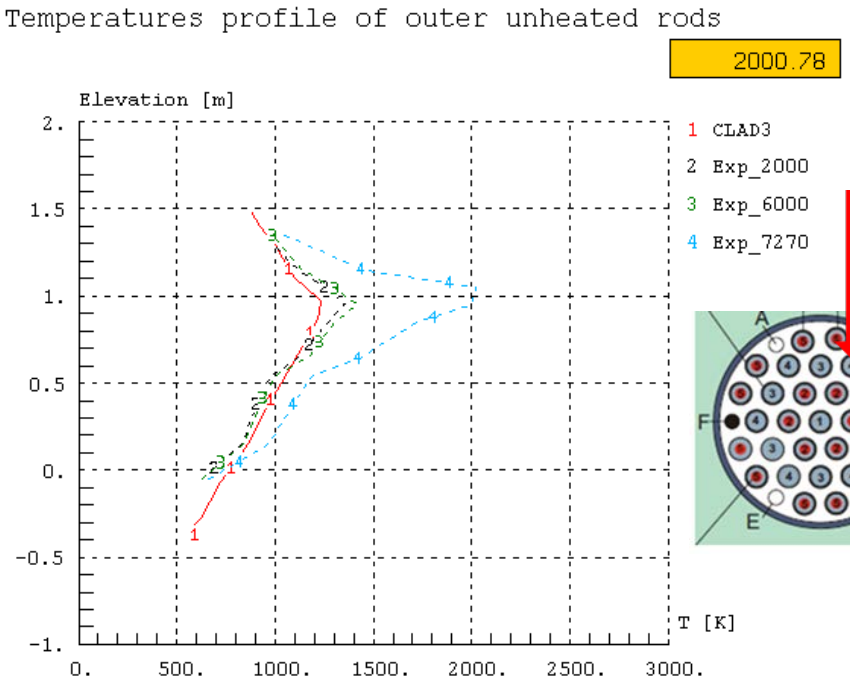


Temperature vs Time at 350 mm

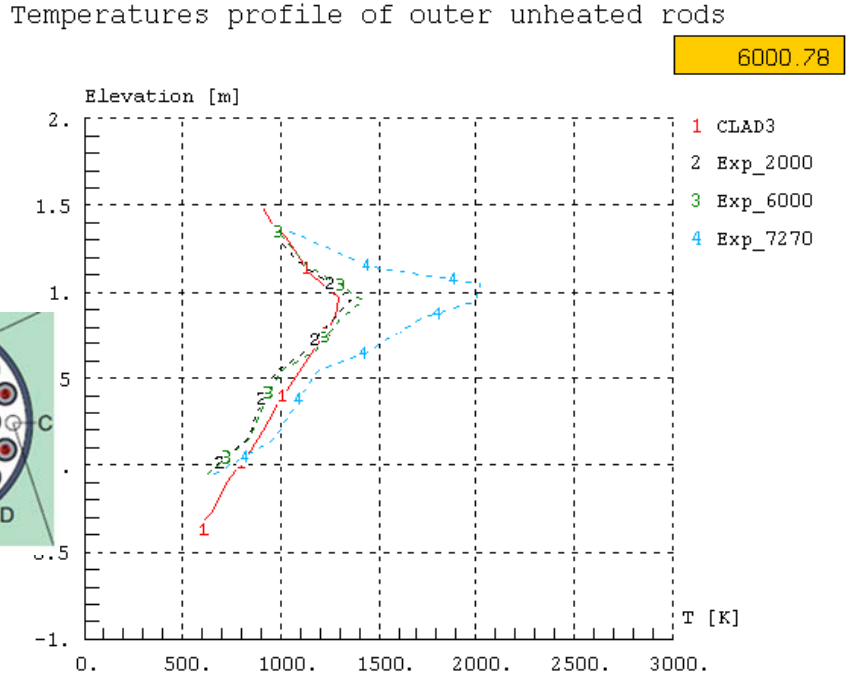
Conclusion: Temperature for inner heated rods calculated accurately at 950 mm until quench
but temperatures are over-estimated at lower regions.
However temperature
difference is smaller than 100 K



QUENCH-12- Current Simulations (4/12)

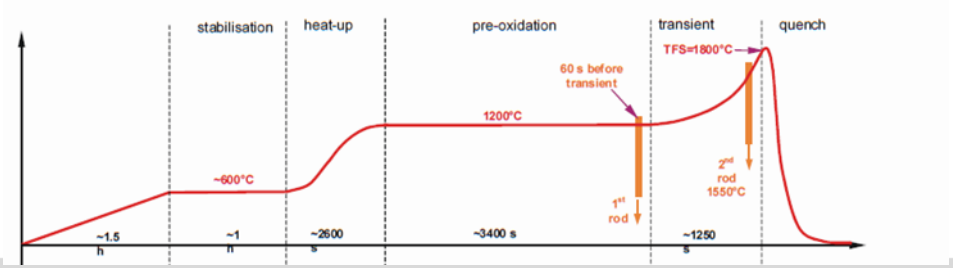


Time: 2000 s
Data vs ASTEC-predictions

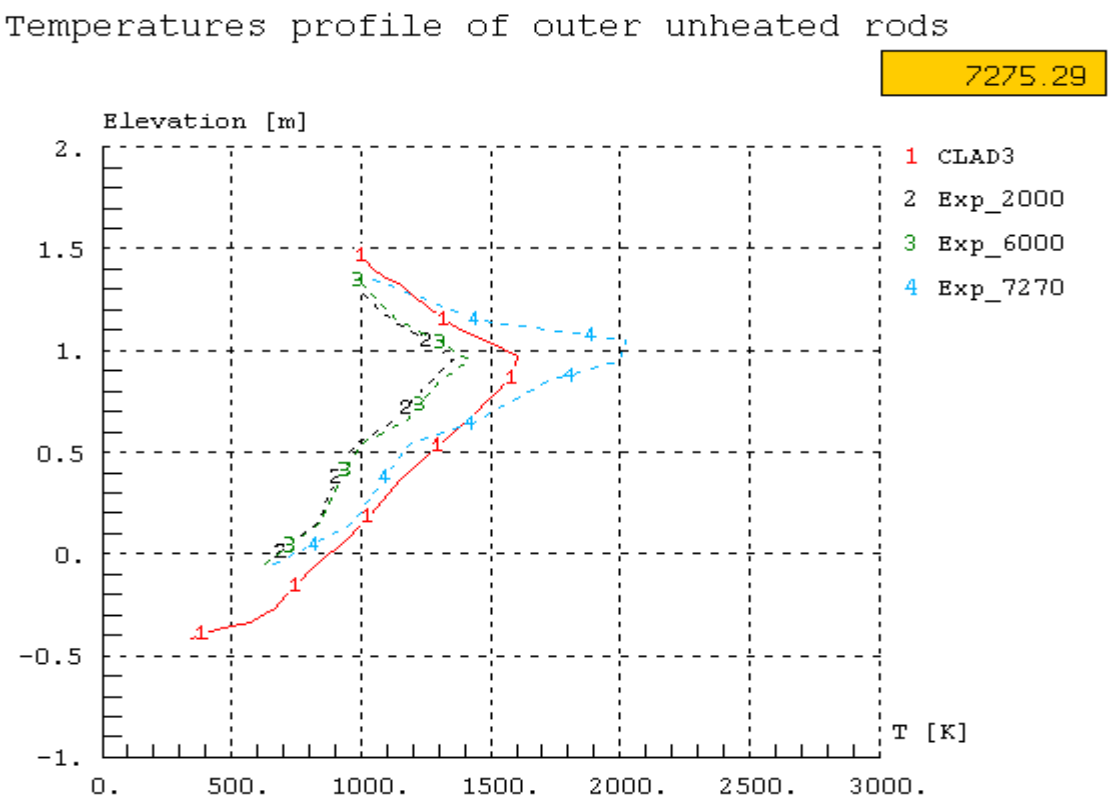


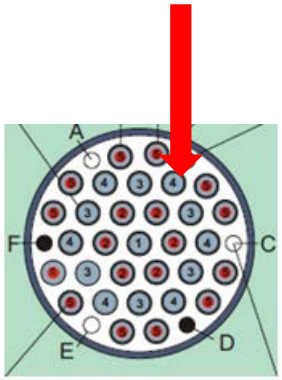
Time: 6000 s
Data vs ASTEC-predictions

Conclusion:Similarly temperature at higher levels of outer unheated rods (CLAD3) at 2000s and 6000s calculated higher temperatures at lower section

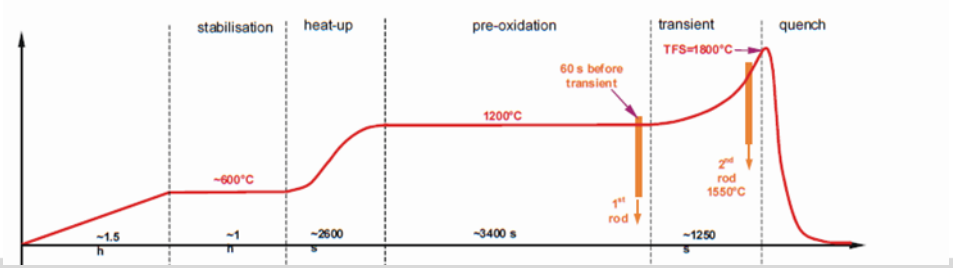


QUENCH-12- Current Simulations (5/12)



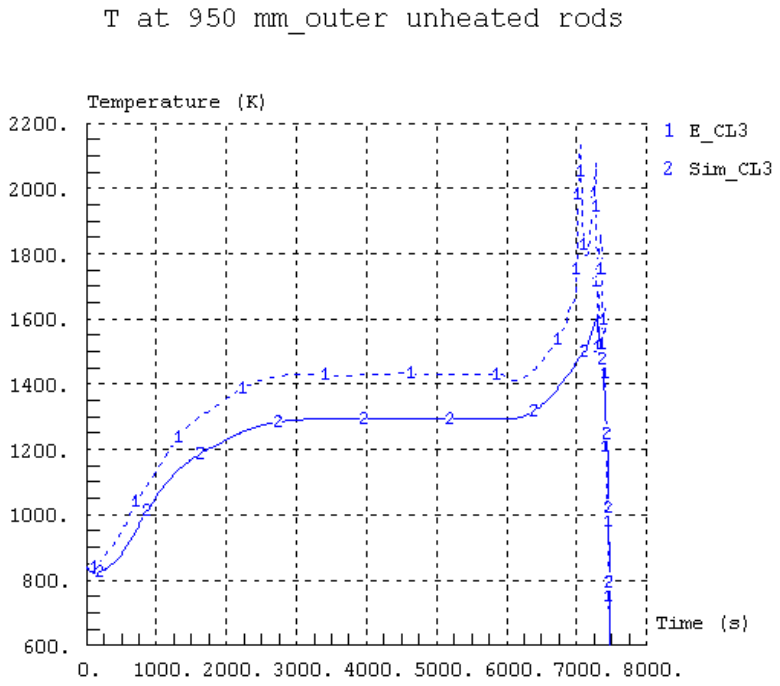


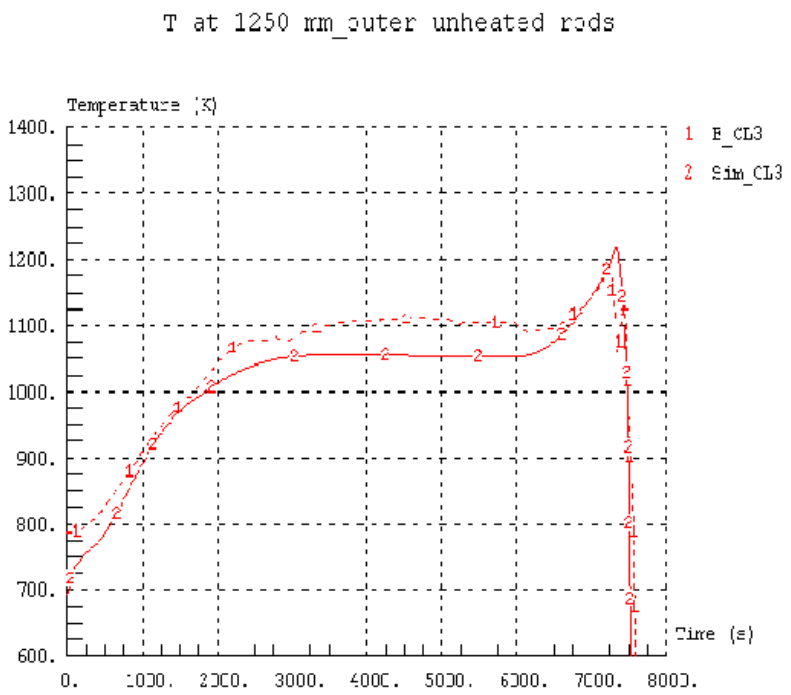
Time: 7270
Data vs. ASTEC prediction



Conclusion: Temperature distribution before quench calculated for outer unheated rods lower estimated due to model.

QUENCH-12- Current Simulations (6/12)

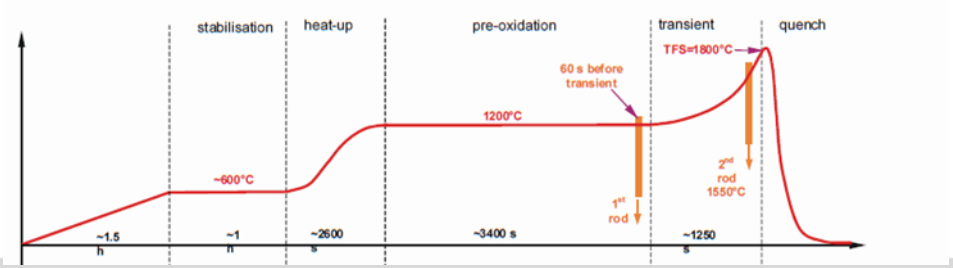




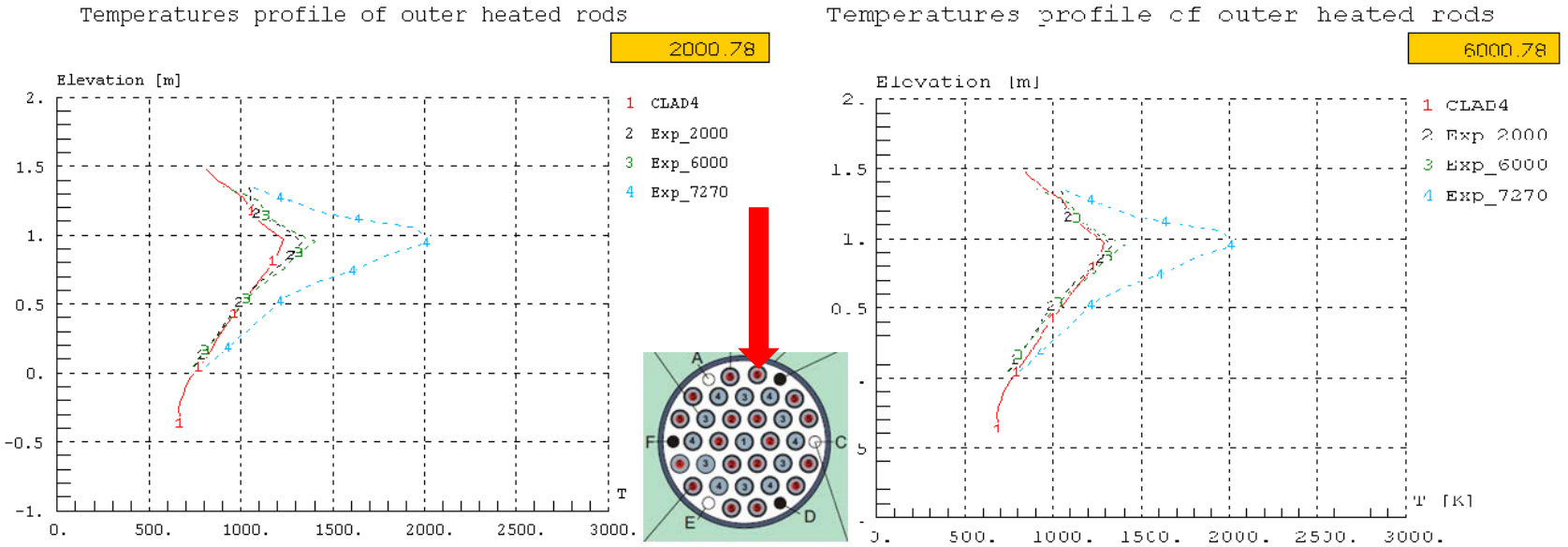
Temperature vs Time at 950 mm

Temperature vs Time at 1250 mm

Conclusion:Temperature for outer heated rods calculated in similar trend but for both elevations which will result as lower hydrogen generation



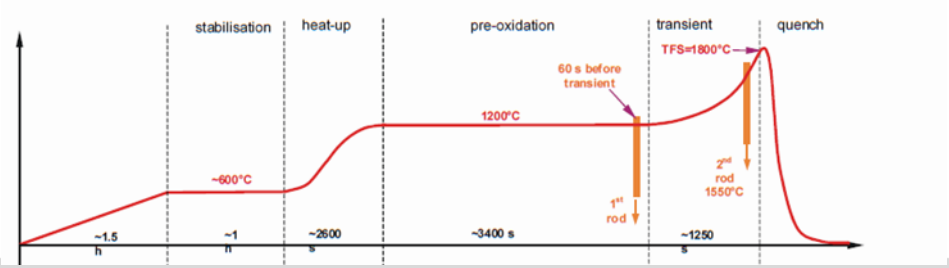
QUENCH-12- Current Simulations (7/12)



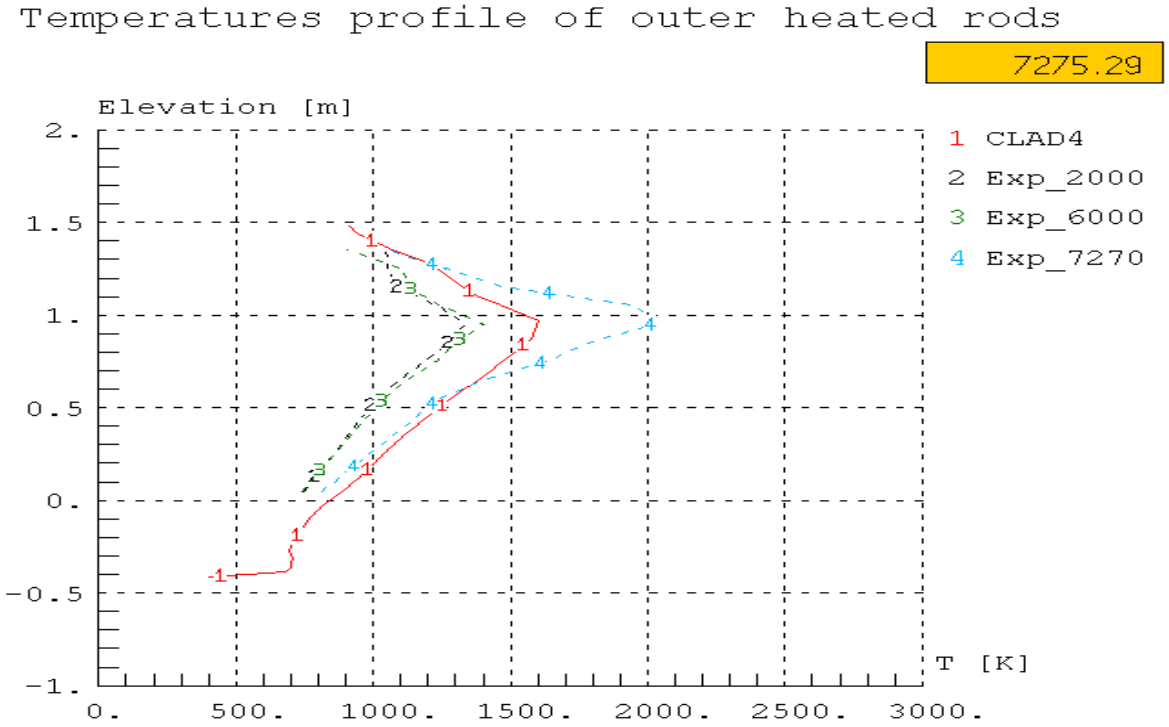
Time: 2000 s
Data vs ASTEC-predictions

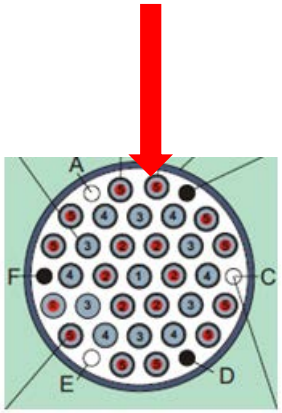
Time: 6000 s
Data vs ASTEC-predictions

Conclusion: Temperature distribution for outer heated rods at 2000s and 6000 s is similar with experiment results.



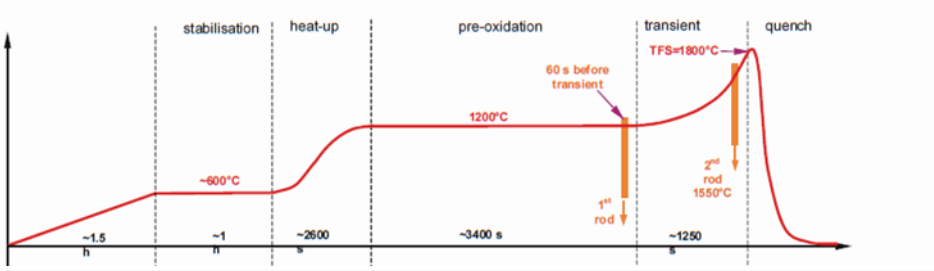
QUENCH-12- Current Simulations (8/12)



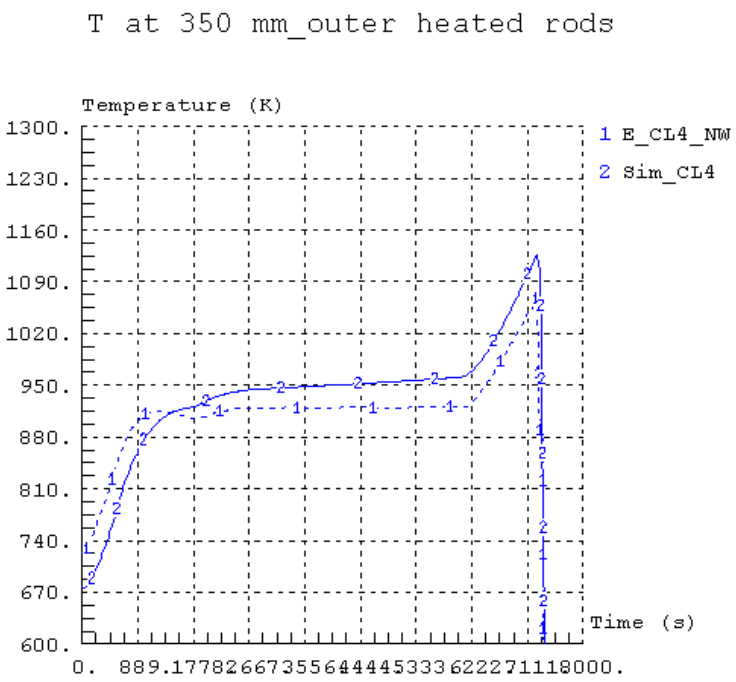


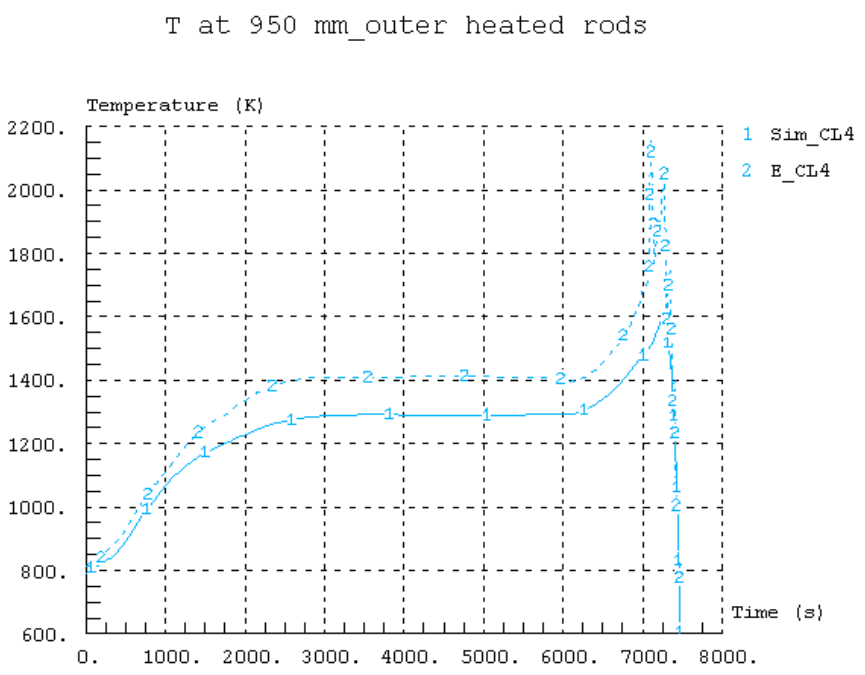
Time: 7270
Data vs. ASTEC prediction

Conclusion:Similarly, developed model calculated temperatures before quench lower than experiment.



QUENCH-12- Current Simulations (9/12)

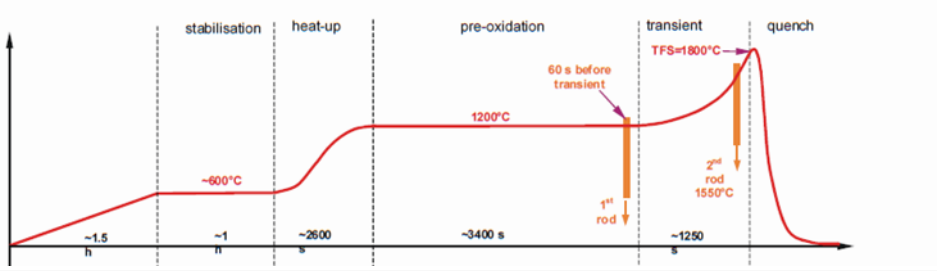




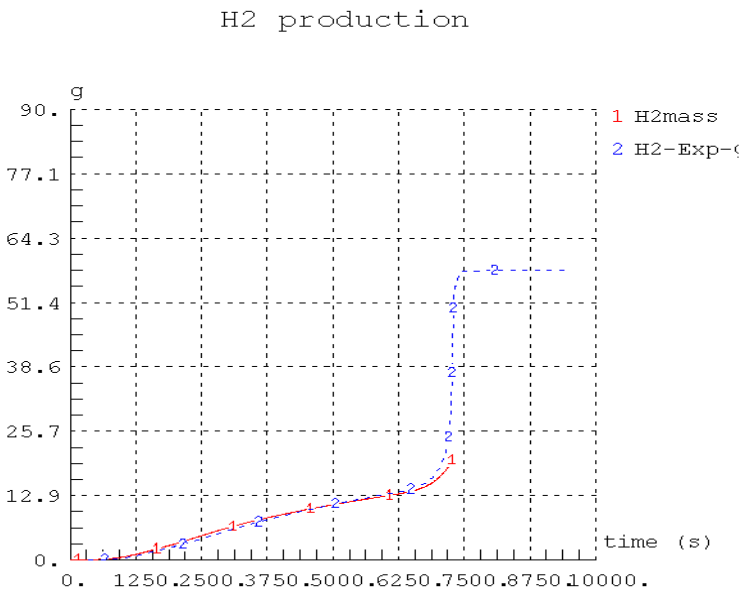
Temperature vs Time at 350 mm

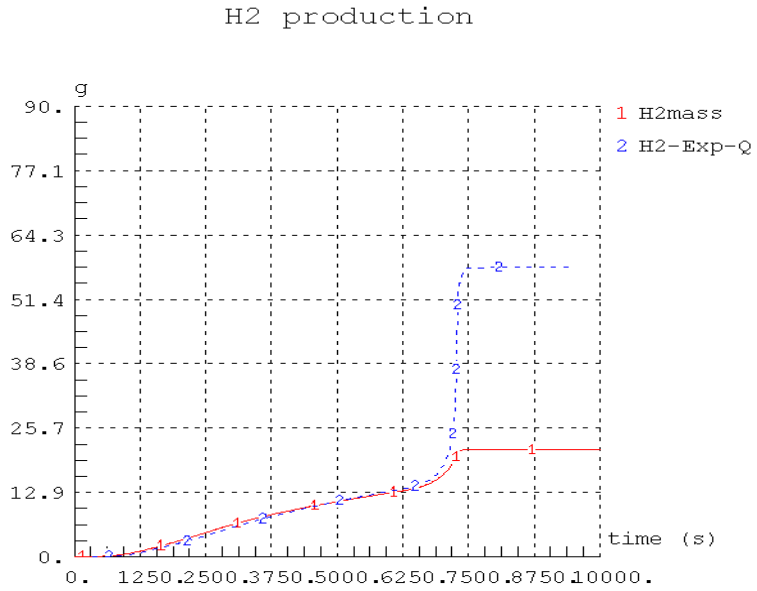
Temperature vs Time at 950 mm

Conclusion: Model calculated higher temperatures at lower elevations and higher temperatures
at middle section.



QUENCH-12- Current Simulations (10/12)

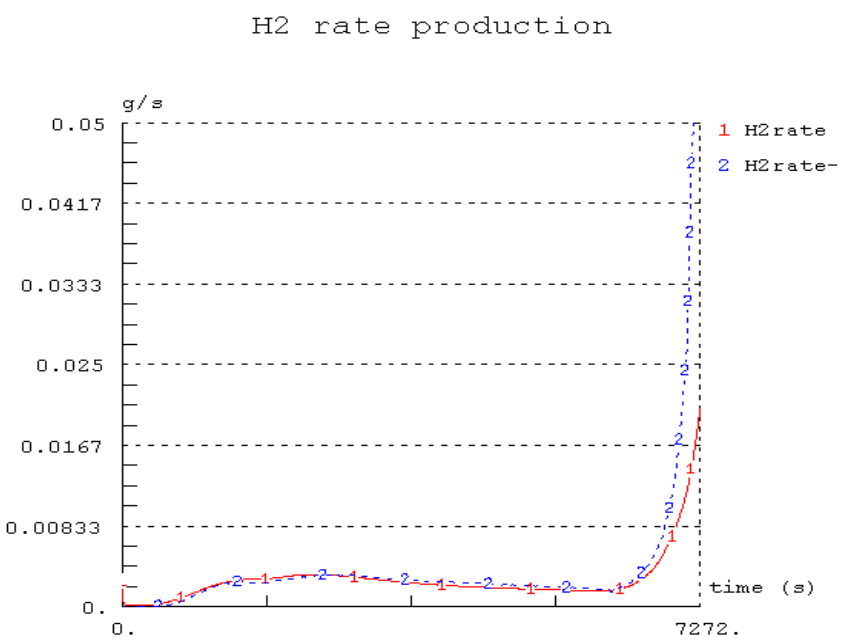


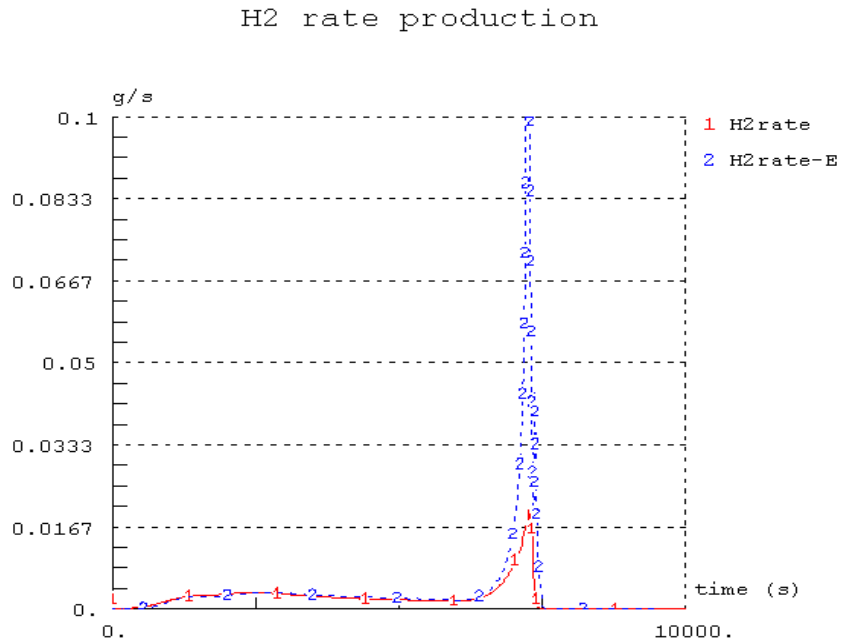


Hydrogen production until quench **Hydrogen production end of calculation**

Initial results showed that developed model calculate hydrogen generation accurately until quench phase. However model can not calculate peaking in generation.

QUENCH-12- Current Simulations (11/12)



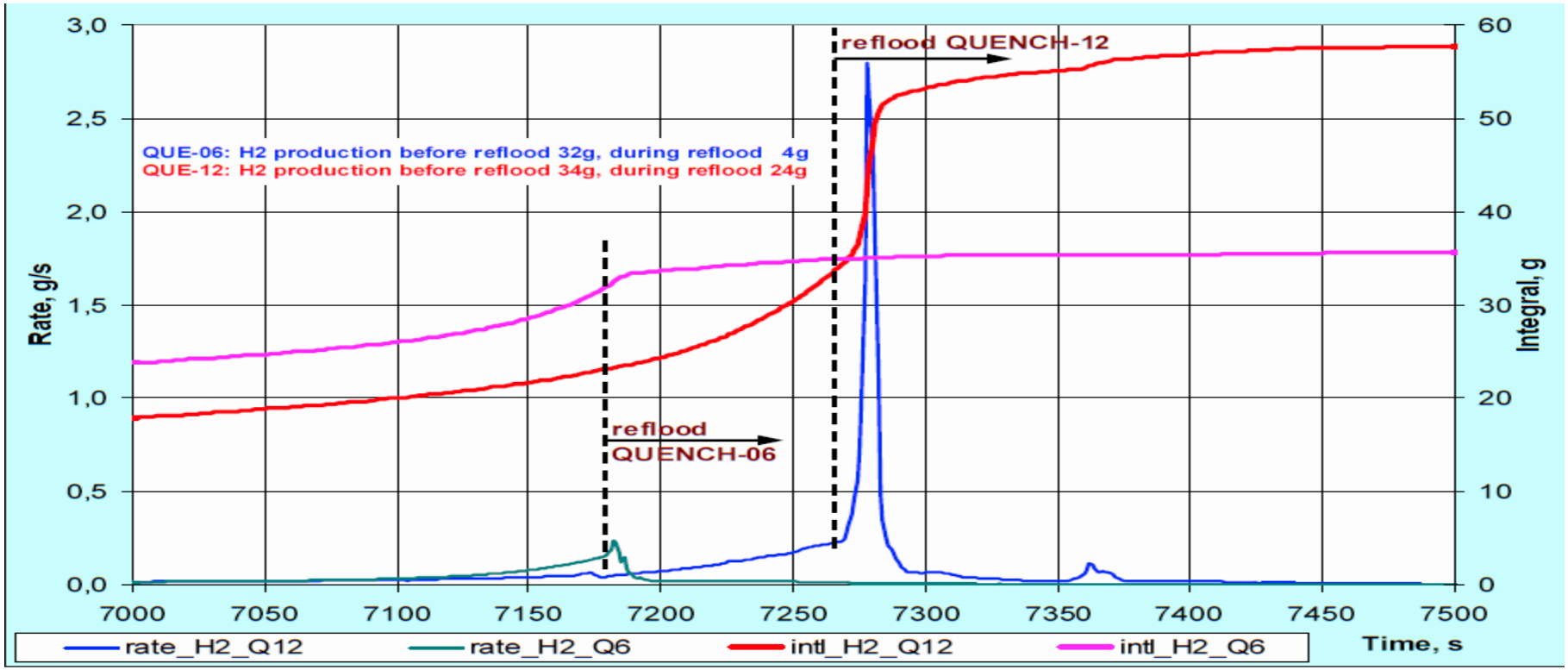


Hydrogen production rate until quench

Hydrogen production rate end of calculation

In initial results, model calculated hydrogen generation rate similar trend with experimental results until pre quench phase. Hence peaking temperatures are not observed in clads, hydrogen generation rate calculated highly low than experiment.

QUENCH-12- Current Simulations (12/12)



QUENCH-06 and QUENCH-12 Experiment Comparison

- Quench-6 is an experiment to investigate hydrogen production for PWR. Same power profile and same conditions with Quench-12.
- If the model works with the condition for Zr-4 as we developed because of the lack of data of E110 and E250, code calculates similar trend with Quench-6 model, even though core parameters, quench flow and time of quench is different.

Conclusions and Outlook

Conclusions and Outlook

- Post-test simulation of QUENCH-12 done with ASTECV2.1.1.3
  - Comparison of predicted fuel rods temperatures and measured ones for the pre-quench phase are under predicted. This can be result of not using VVER clad material models.
  - Predicted temperature trends for QUENCH Phase qualitatively follows or not follows the measured evolutions
  - Total predict hydrogen production is similar for pre-quench phase and lower for quench phase than the experiment.
  - Reasons for deviations to be investigated in the near future.

- Outlook
  - Review material and geometry of QUENCH-12
  - Review of physical models activated
  - Use the latest ASTEC versions V2.1.1.3

Numerical simulation of QUENCH-15 experiment with SOCRAT/V1 code

Dolganov K.S., Kiselev A.E., Philippov M.F., Tomashchik D.Y.

Abstract

At present, IAEA is implementing the ACTOF project with the aim to investigate the properties of nuclear fuel that would be resistant to severe accidents.

Within the framework of this project, IBRAE as a participant organization is responsible for numerical simulations of the integral experiment with reflooding of the overheated bundle with FeCrAl alloy as cladding material. For analytical studies, SOCRAT/V1 code is used.

With respect to the experimental facility configuration, the scenario and the initial, boundary conditions, the counterpart of FeCrAl bundle experiment is QUENCH-15 bundle test with Zr alloy(ZIRLO™) cladding material which is currently used in certain NPPs with PWR. In this connection, the simulation of QUENCH-15 test is considered as a necessary step that is required to develop and verify the QUENCH model which will be further used for the simulation of the FeCrAl bundle test. Comparison of the calculated and measured data for these two testsallows assessing the effect of the FeCrAl cladding on the bundle oxidation and core reflood.

This presentation provides the results of QUENCH-15 test modeling with SOCRAT/V1 code. In accordance to state-of-the-art recommendations and best practices, the test simulation are supplemented by uncertainty and sensitivity analysis.


TOSHIBA
11

РОССИЙСКАЯ АКАДЕМИЯ НАУК
Институт проблем безопасного развития атомной энергетики

RUSSIAN ACADEMY OF SCIENCES
Nuclear Safety Institute (IBRAE)



Numerical simulation of QUENCH-15 experiment with SOCRAT/V1 code

Philippov M.F., Dolganov K.S., Kiselev A.E., Tomashchik D.Y.

philippov@ibrae.ac.ru

+7(495)955 22 85

Motivation

- Numerical simulation of QUENCH-15 experiment is a one of preparatory stages of the IAEA ACTOF Project, performing with an aim to development a new type of nuclear fuel with a modern, nuclear grade FeCrAl alloy cladding.
- The test features: ZIRLO cladding, a great duration of pre-oxidation stage and weak escalation of hydrogen release

- The aim of QUENCH-15 modeling by integral SOCRAT code:
  - ✓ development and validation of QUENCH-15 facility model, that will be used for experiment with FeCrAl cladding simulation;
  - ✓ Validation of SOCRAT/V1.

SOCRAT/V1 modules used for simulation

SVECHA – core degradation

PROF - Model of oxidation and eutectic interaction processes in zirconium elements of the core elements (T<2105 K);

LIQF - Model of oxidation and interaction processes in fuel-zirconium system in the core elements (T>2105 K);

CROX - Model of mechanical destruction of fuel cladding, double oxidation;

DROG- Model of drip and stream relocation of liquid melt.

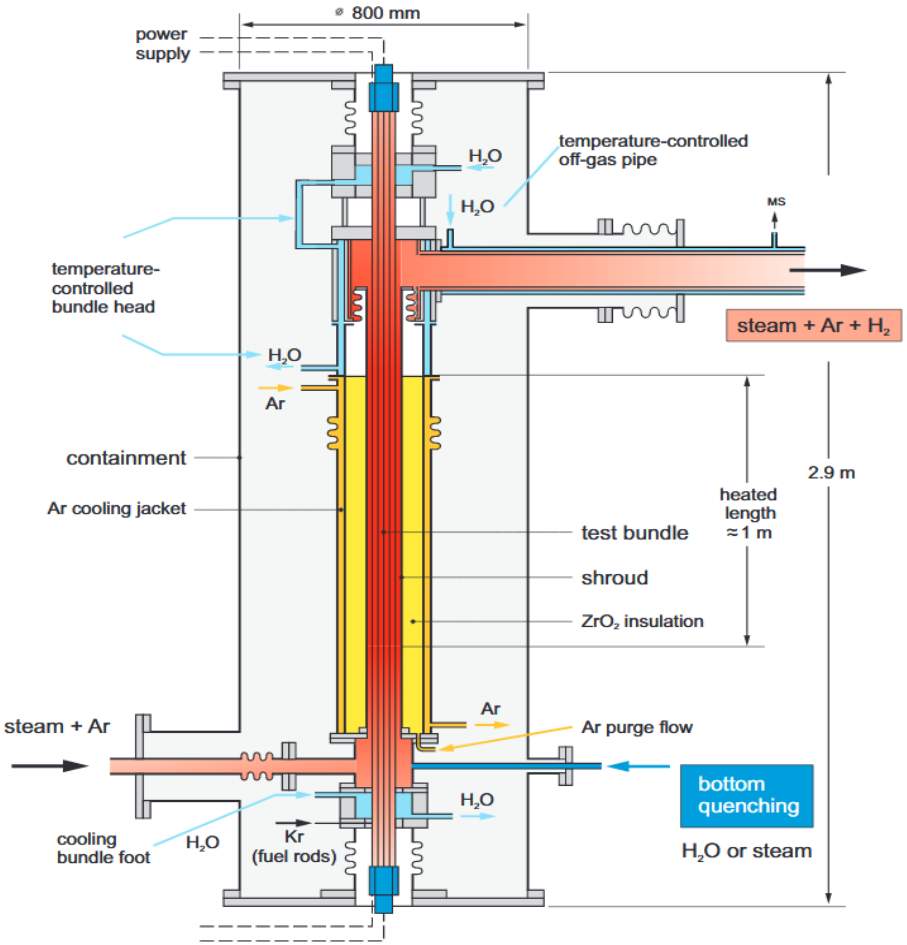
RATEG – primary and secondary thermal hydraulics, heat transfer in solid bodies

RADIATION – radiation heat exchange between elements

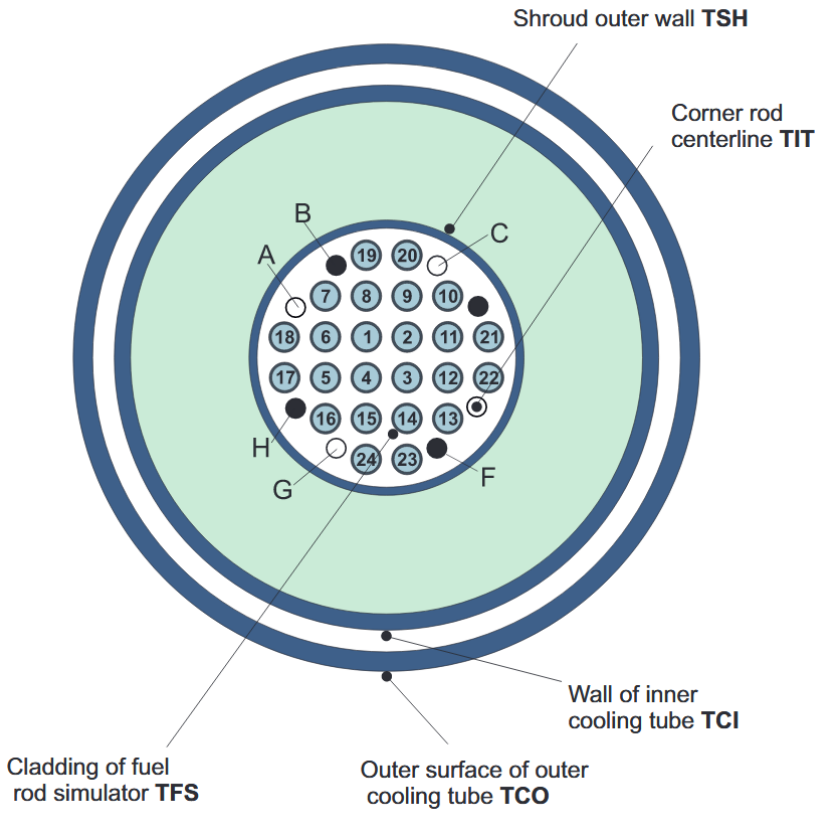
+ **material properties database**

QUENCH-15 facility

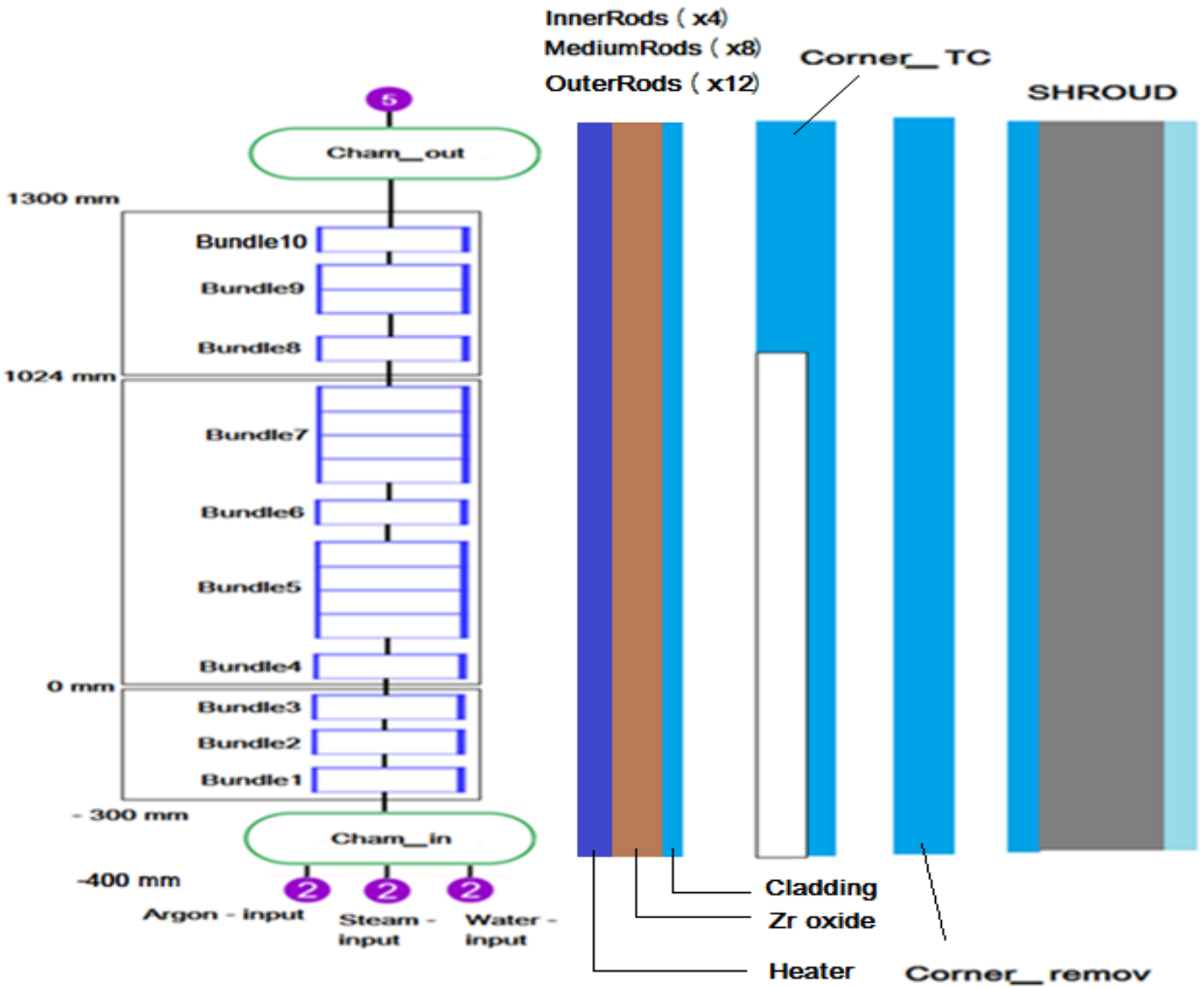
QUENCH-15 test section



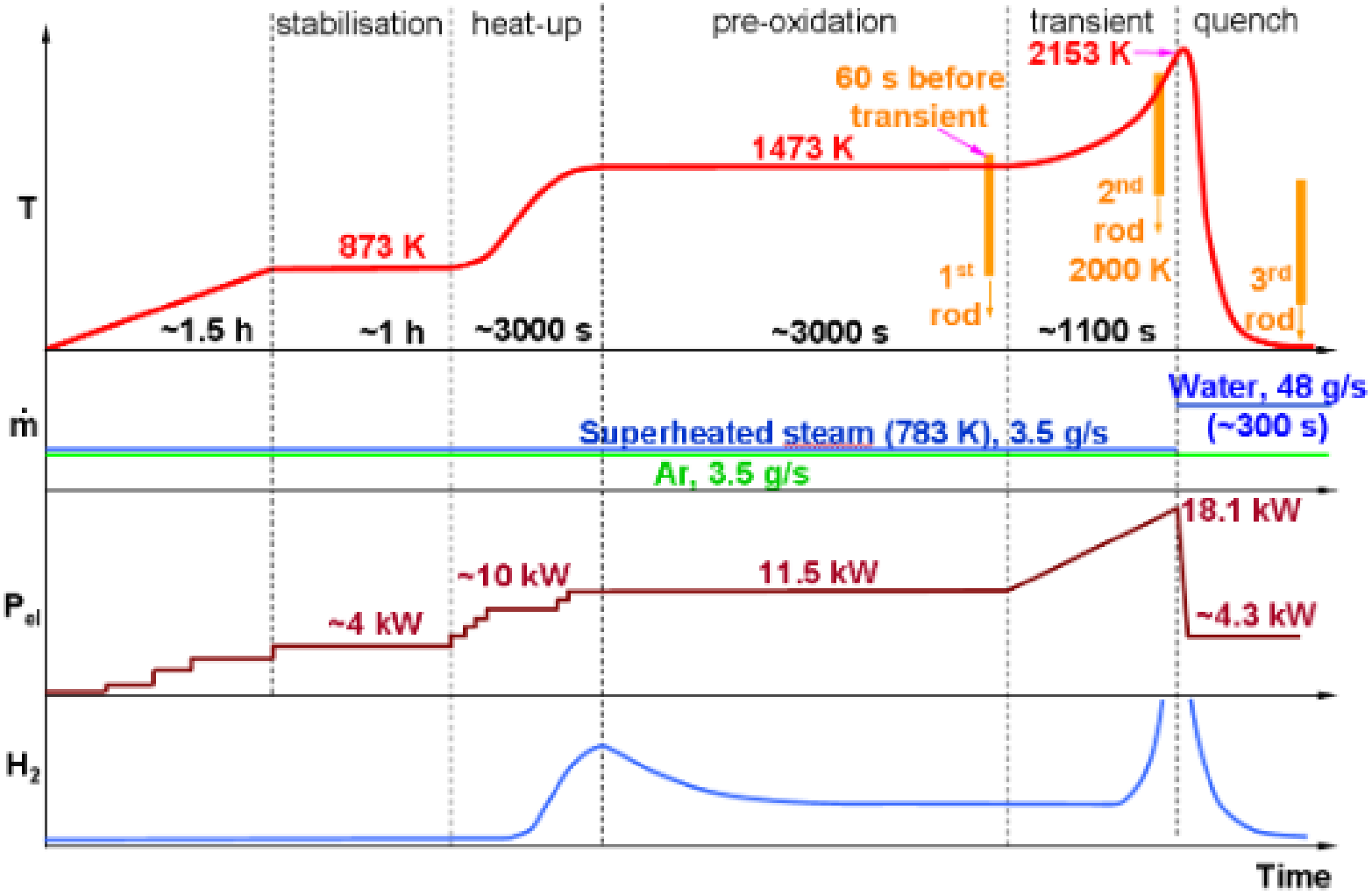
Fuel rod simulator bundle



QUENCH-15 facility model

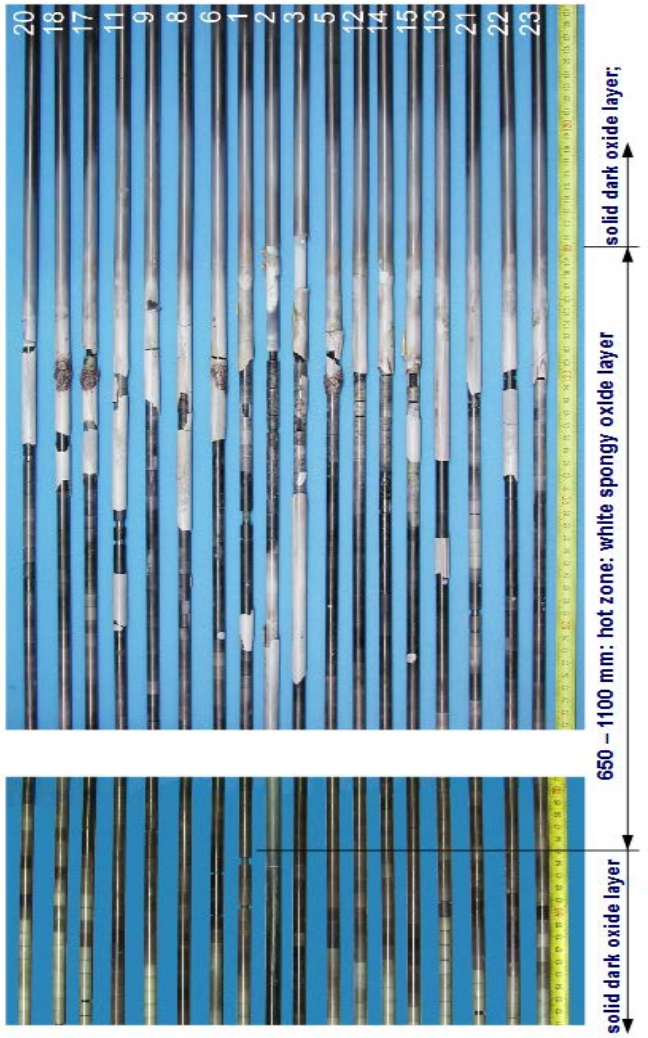


Experiment scenario and boundary conditions



Main results

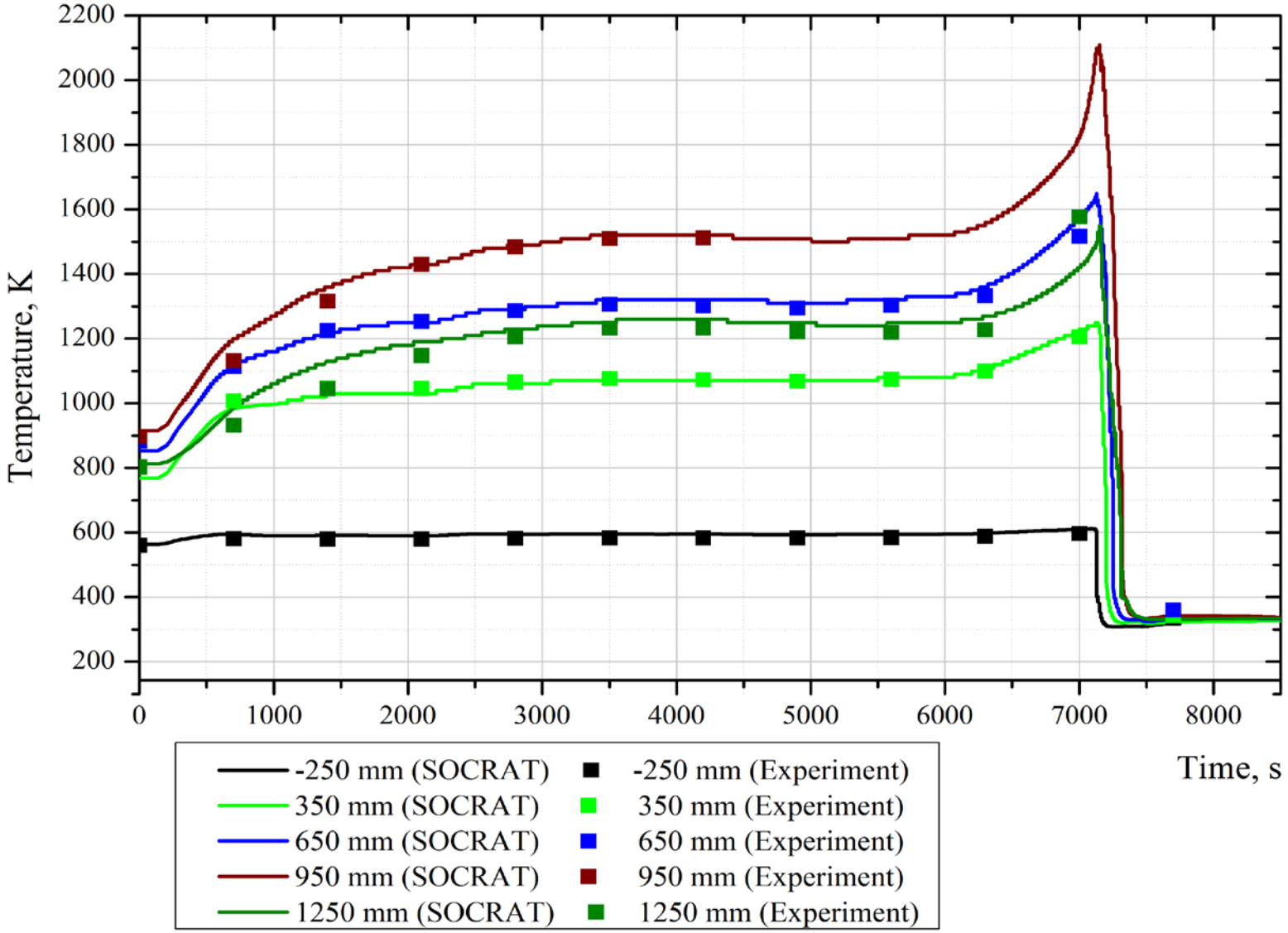
Post-test view



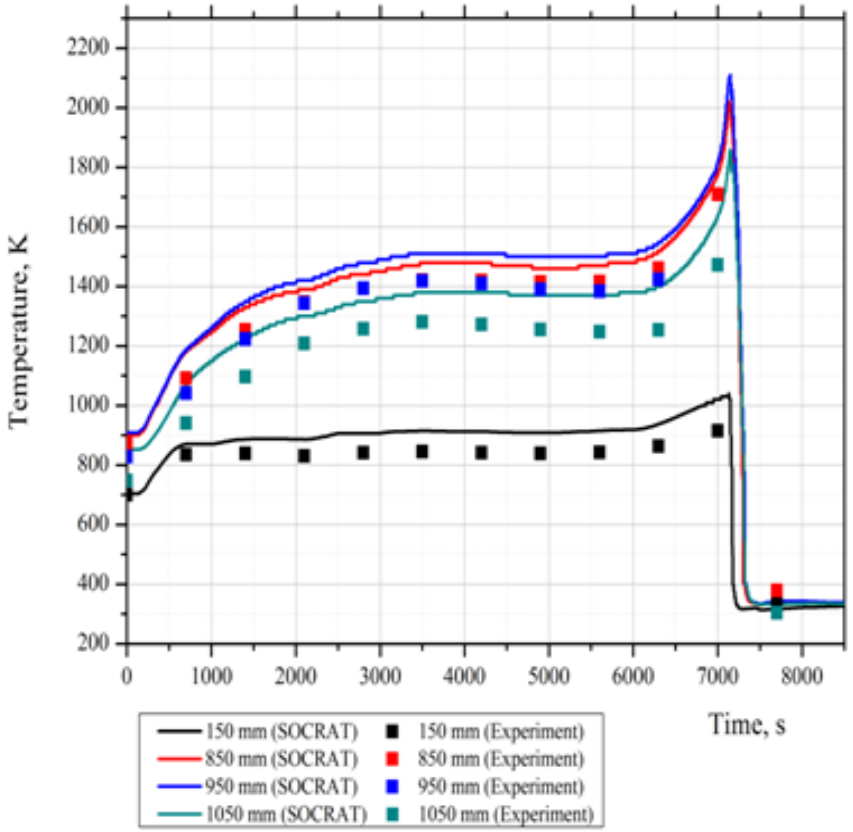
Calculation

- Calculation time dependences of surfaces temperature and hydrogen mass show a good agreement with experimental data;
- Fuel simulators claddings rupturing was observed at 900 mm (at 870 and 970 mm in simulation);
- there was no blockade formation and massive melt relocation.

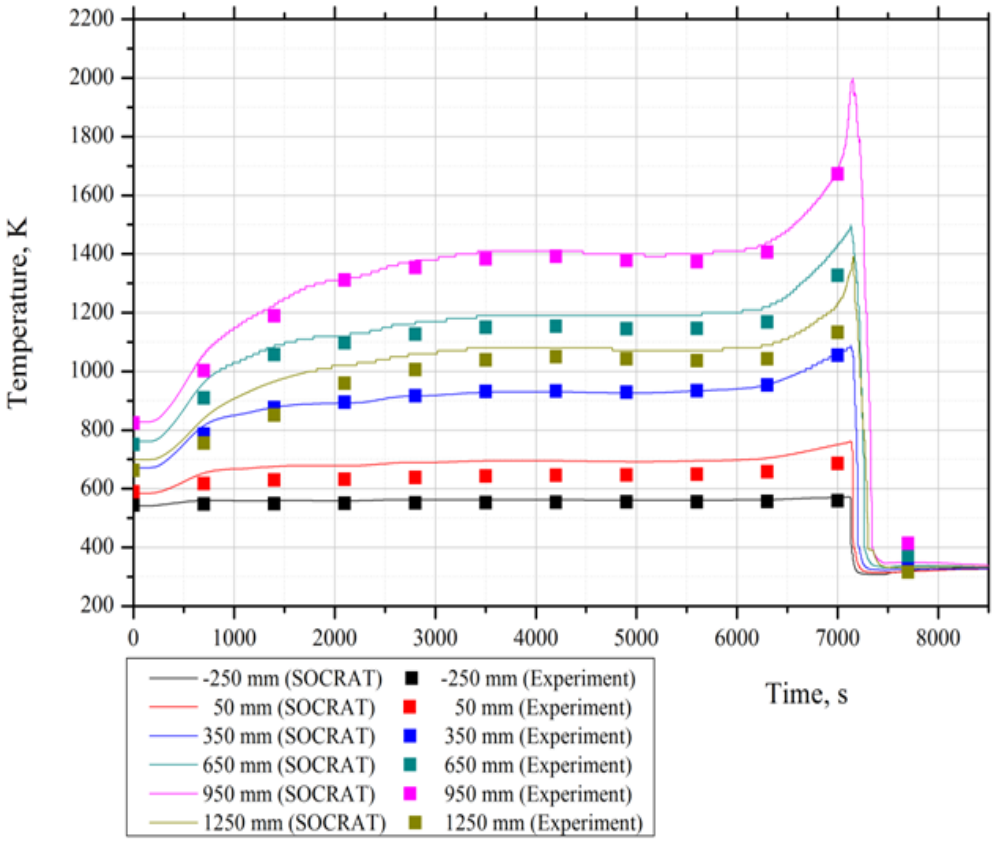
Cladding temperature of inner rods



Cladding temperatures of outer rods and shroud

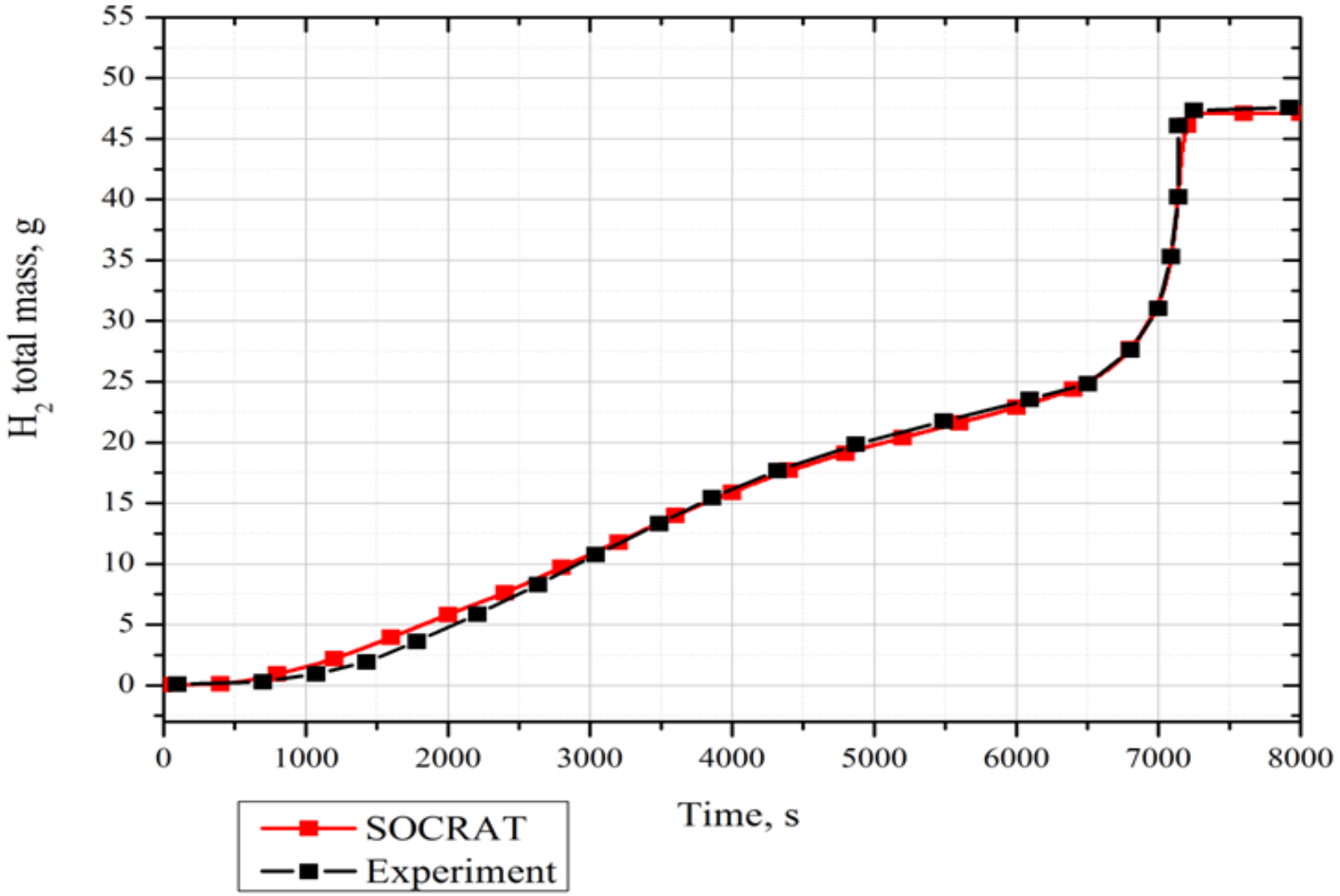


Cladding temperatures of outer rods



Cladding temperatures of shroud

Hydrogen release



Conclusion

- As a result of the work, a model of QUENCH-15 test section was created and validated, which can later be used to simulate a similar experiment with FeCrAl cladding;

- SOCRAT code adequately reproduces the cladding temperatures evolutions, hydrogen production.

Authors would like to thank the IAEA for providing financial support for participating in 24d Workshop.

Status of RELAP/SCDAPSIM/MOD3.X Reassessment Activities –Integrated Uncertainty Analysis of CORA PWR Experiment –CORA-13

Asmaa Salem
University of Alexandria
Chris Allison, Judy Hohorst, Marina Perez-Ferragut
Innovative Systems Software

RELAP/SCDAPSIM, designed to predict the behavior of reactor systems during normal and accident conditions, is being developed by Innovative Systems Software (ISS) as part of the international SCDAP Development and Training Program (STDP). The RELAP/SCDAPSIM/MOD3.X series, with best estimate models and correlations for LWRs/HPWRs, includes MOD 3.4, MOD3.5, and MOD3.6. MOD3.4 has models and correlations most like those contained in the US NRC SCDAP/RELAP5 code released in the early 1990s. It is the version most commonly used by the general RELAP/SCDAPSIM user community. MOD3.5 and MOD3.6 are experimental versions developed to support specific RELAP/SCDAPSIM users' design and analysis activities. MOD 3.5 has advanced best estimate fuel and severe accident behavior models that are important in the design and analysis of experiments, the analysis of LWRs under Fukushima-like conditions, and LWR spent fuel storage facilities. MOD3.6 includes the MOD3.5 improvements plus PHWR specific models and correlations developed for CANDU and Atucha-2 channel type reactor designs. Although the accuracy of the MOD3.x models and correlations has been routinely assessed since the early 1980s, a systematic reassessment of MOD3.x is being performed using selected integral experiments performed as part of the LOFT-FP, PBF-SFD, FLHT, PHEBUS-FPT, CORA, QUENCH, and PARAMETER programs. The purpose of this reassessment is to establish the uncertainties in the calculated behavior for representative LWRs and accident conditions.

The systematic publication of the results of these reassessment activities for the MOD3.x series in the open literature started in 2016 and thus far have included PHEBUS FPT3, PBF SFD ST and 1-4, LOFT L2-5, and Quench 06.

The presentation for Quench 2018 describes the results of the analysis of CORA-13, focused on the influence of important modeling options for bundle heat up and quench phases. The calculations were run using RELAP/SCDAPSIM/MOD3.4. The integrated uncertainty analysis was performed with MOD3.4 with the IUA, "Integrated Uncertainty Analysis", option introduced into RELAP/SCDAPSIM/MOD3.4 in the summer of 2017. This presentation looks at the influences of estimated uncertainties in thermal hydraulic boundary conditions include (a) total bundle electrical power, (b) radial heat losses through changes in the thermal conductivity of porous zirconia used in the shroud, (c) inlet steam temperatures and flow rates, (d) the influence of the injection water by the quench tank was also considered.



SDTP

Development of best estimate methods for reactor and advanced fluid systems safety analysis and training

CORA-13 – RELAP/SCDAPSIM/MOD3.4
Uncertainty analysis of CORA PWR experiments using RELAP/SCDAPSIM

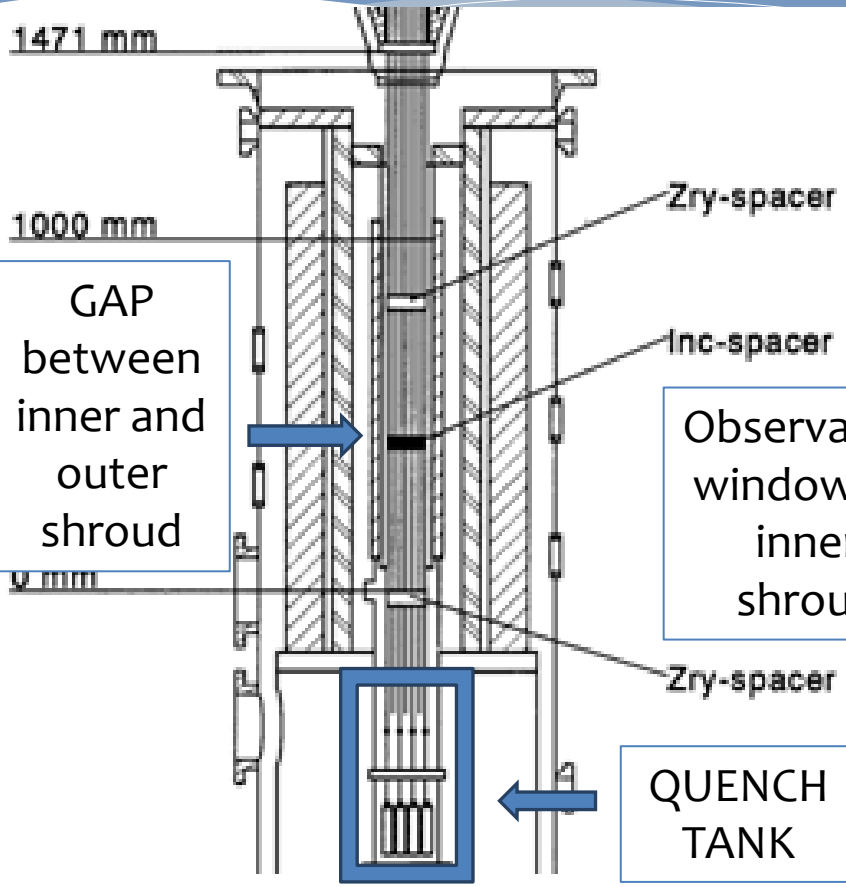
Analysis and Presentation
Asmaa Salem
University of Alexandria

Contributions by
Chris Allison and Judith Hohorst – ISS
Dr. S. Hagen – KIT (retired)

Outline

- **Objective** – CORA-13 uncertainty analysis focused on influence of important modeling options for bundle heat up and quench phases
  - User guidance for modeling of CORA experiments using MOD3.4
  - Updating of model parameter defaults for electrically heated experiments
- **Sensitivity analysis results using MOD3.4**
  - Influence of selected modeling options
  - Selection of base case for integrated uncertainty analysis
- **Conclusions**
- **Additional slides**
  - Test conditions and MOD3.4 nodalization
  - Integrated uncertainty analysis for base case

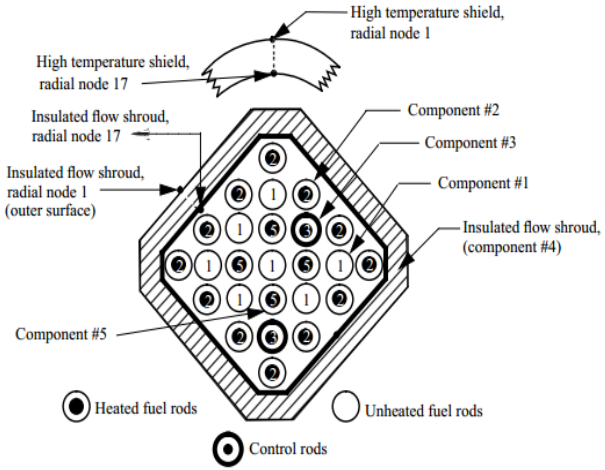
CORA facility has more complicated thermal boundary conditions than that of Quench facility



GAP between inner and outer shroud

Observation windows in inner shroud

QUENCH TANK

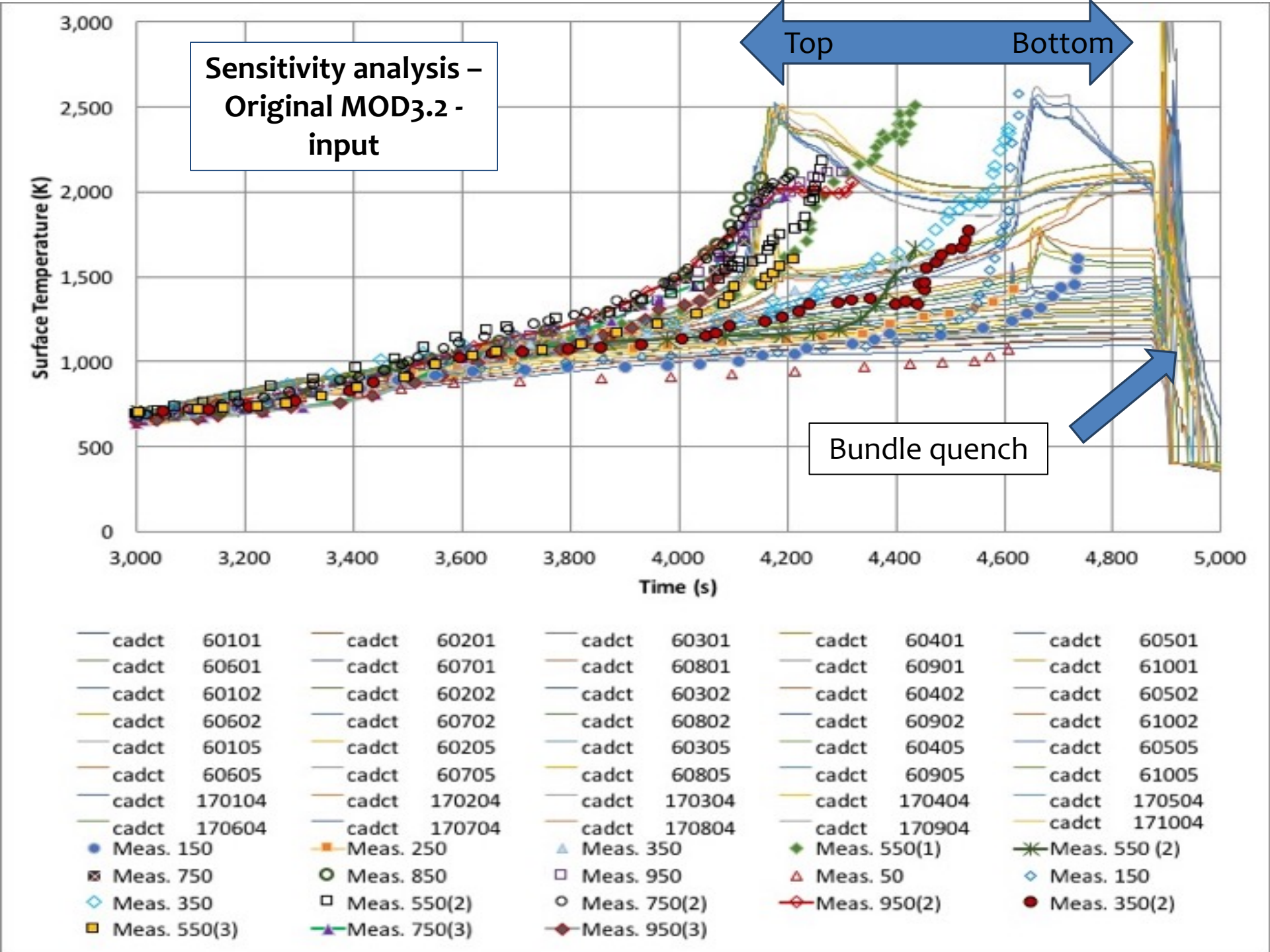


See extra slides for test conditions and nodalization

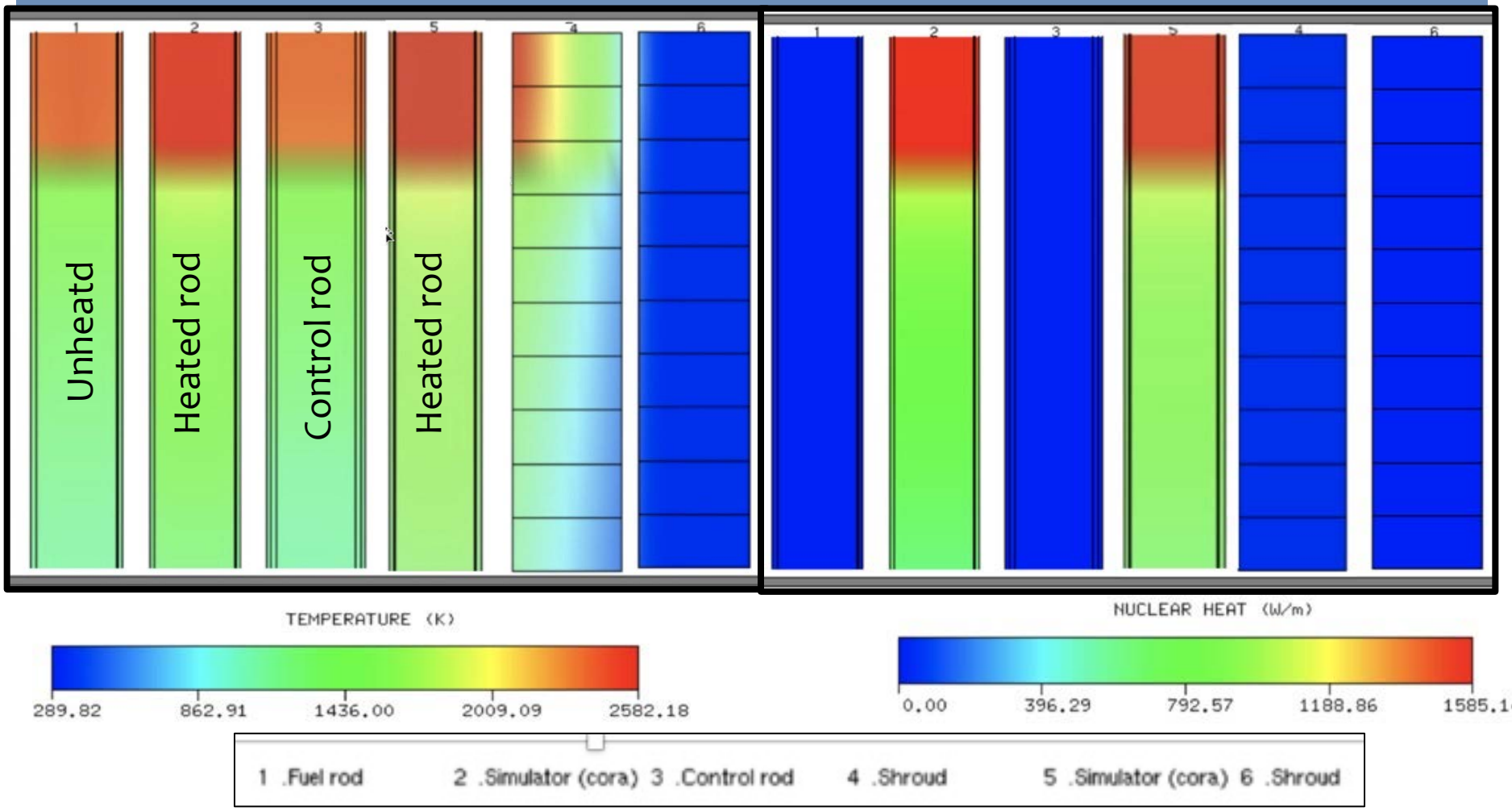
Original MOD3.2 input model resulted in ballooning and rupture of heated rods with double sided oxidation in ballooned region

* Original MOD3.2 input model did not adequately define conditions for internal gas pressure
  * CORA-13 published report did not describe upper plenum region
* Increasing plenum volumes and reducing fill pressures, increasing (default) cladding strain limits for double-sided oxidation **(limited impact)**
* Turning off ballooning models **(Notable impact)**

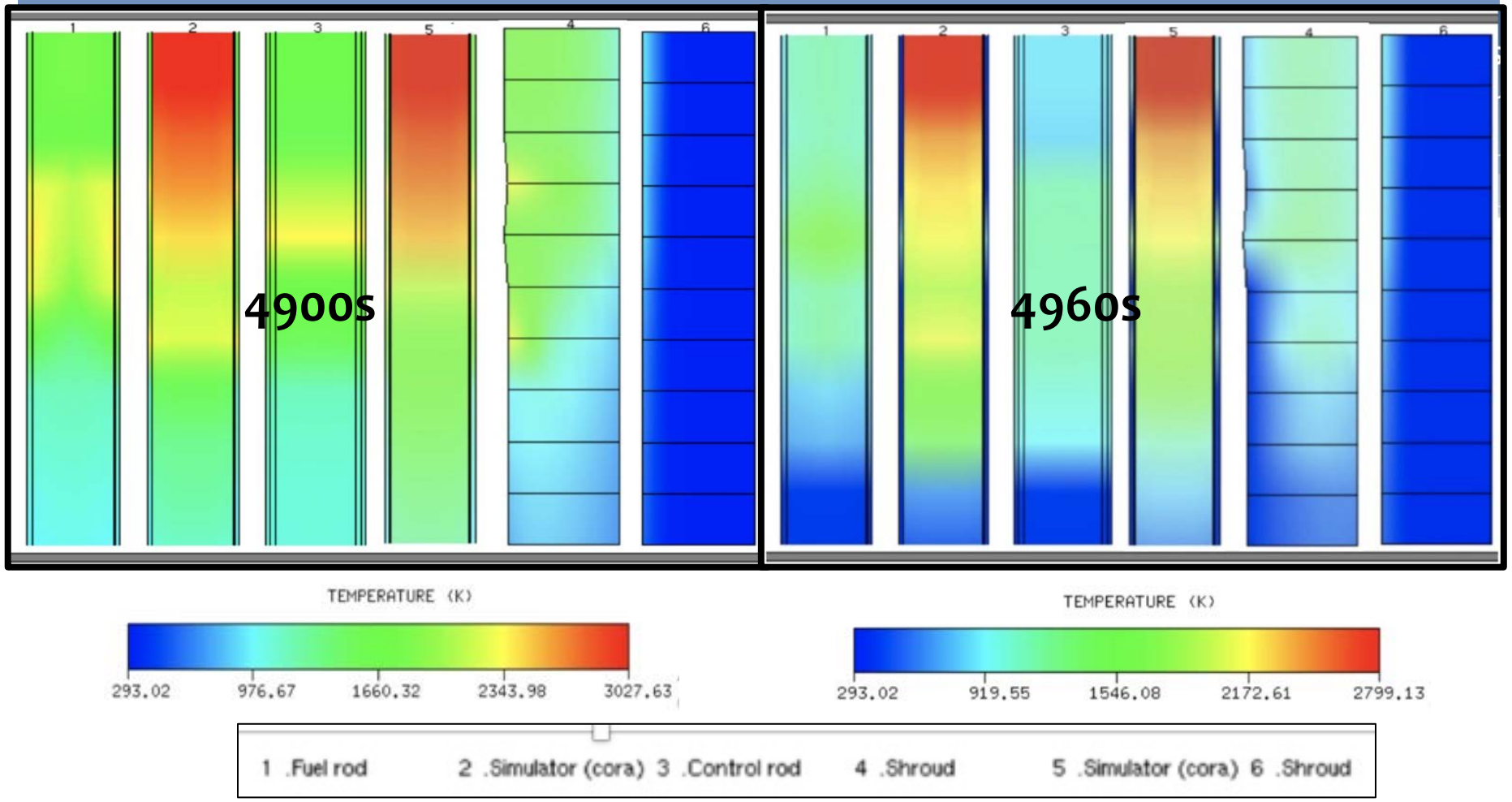
Sensitivity analysis

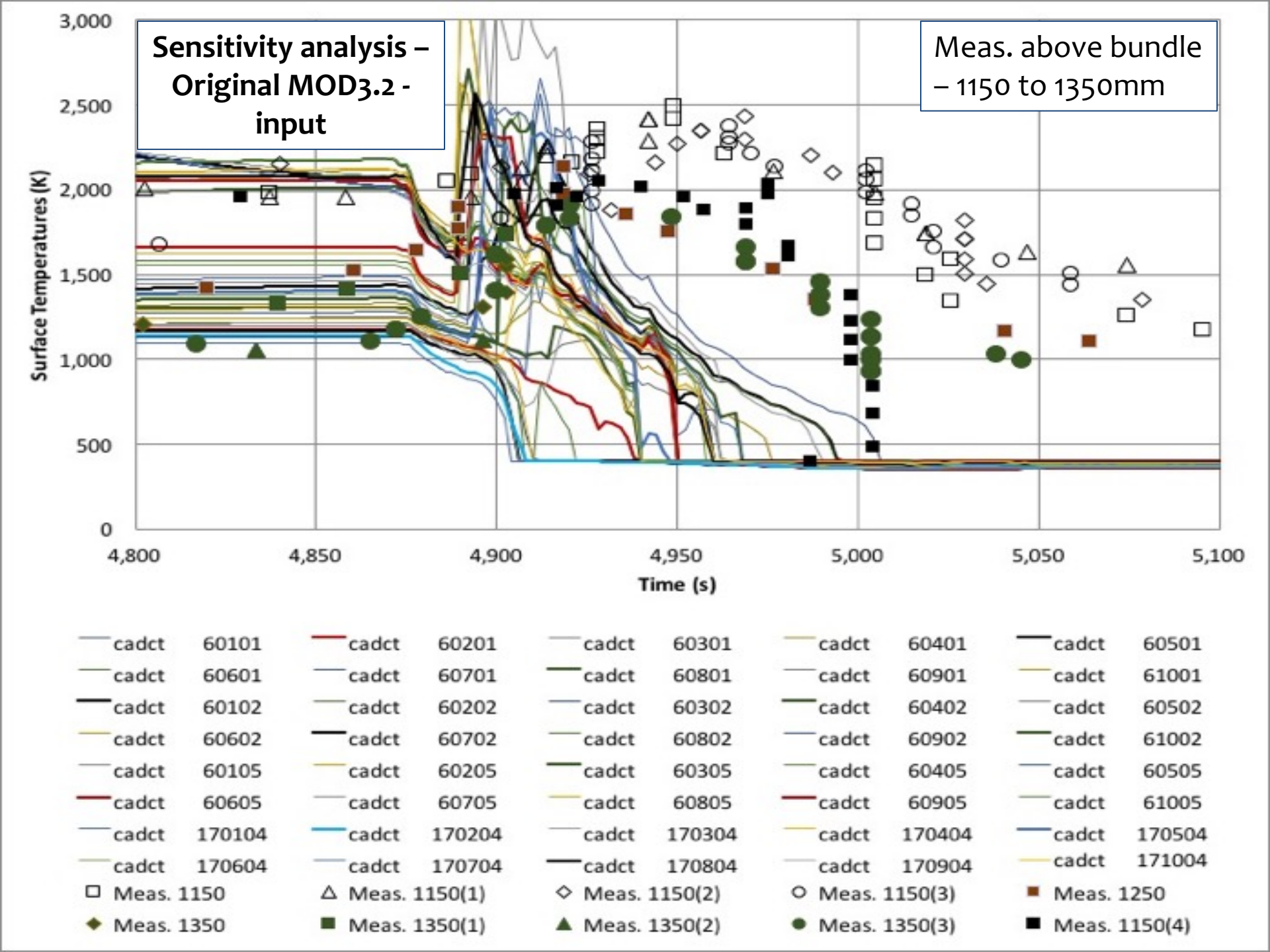

Sensitivity analysis – Original MOD3.2 - input
Top
Bottom
Bundle quench
Surface Temperature (K)
Time (s)
3,000
2,500
2,000
1,500
1,000
500
0
3,000
3,200
3,400
3,600
3,800
4,000
4,200
4,400
4,600
4,800
5,000
cadct 60101
cadct 60201
cadct 60301
cadct 60401
cadct 60501
cadct 60601
cadct 60701
cadct 60801
cadct 60901
cadct 61001
cadct 60102
cadct 60202
cadct 60302
cadct 60402
cadct 60502
cadct 60602
cadct 60702
cadct 60802
cadct 60902
cadct 61002
cadct 60105
cadct 60205
cadct 60305
cadct 60405
cadct 60505
cadct 60605
cadct 60705
cadct 60805
cadct 60905
cadct 61005
cadct 170104
cadct 170204
cadct 170304
cadct 170404
cadct 170504
cadct 170604
cadct 170704
cadct 170804
cadct 170904
cadct 171004
Meas. 150
Meas. 250
Meas. 350
Meas. 550(1)
Meas. 550 (2)
Meas. 750
Meas. 850
Meas. 950
Meas. 50
Meas. 150
Meas. 350
Meas. 550(2)
Meas. 750(2)
Meas. 950(2)
Meas. 350(2)
Meas. 550(3)
Meas. 750(3)
Meas. 950(3)

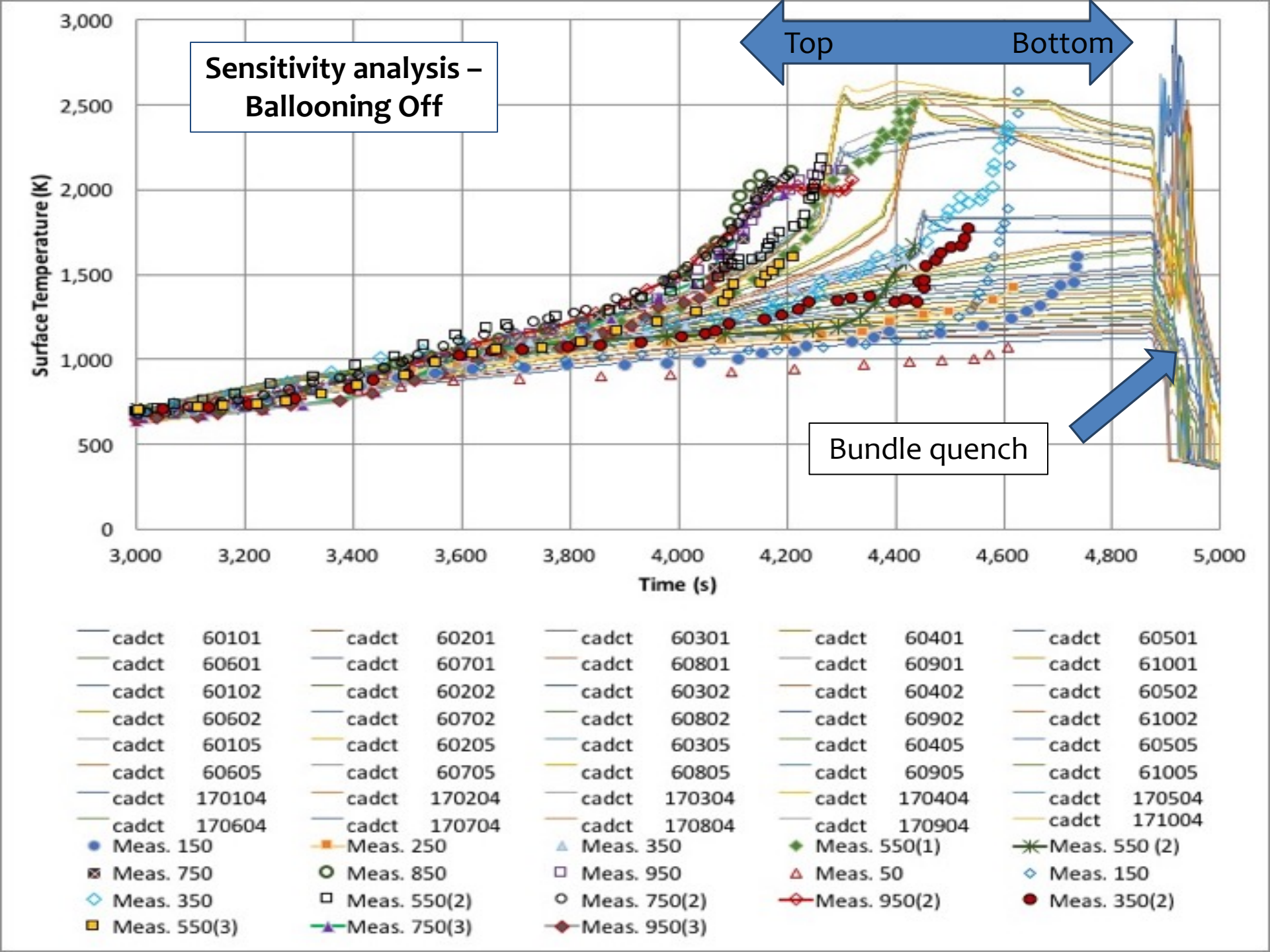
Ballooning with double sided oxidation increased electrical heating at top of bundle - MOD3.2 input



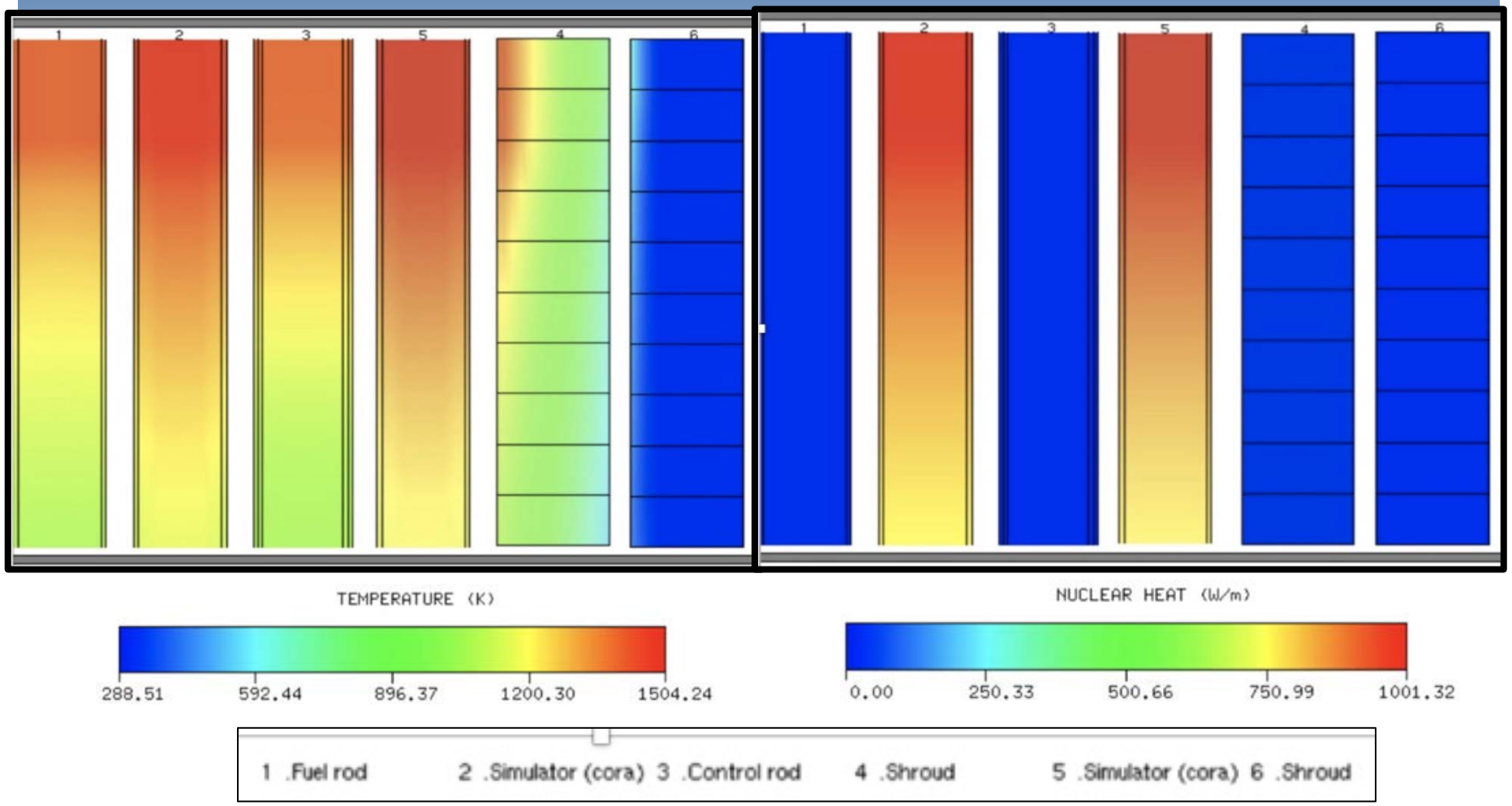
Ballooning with increased gap resistance increased heated rod temperatures during heatup **and quench**



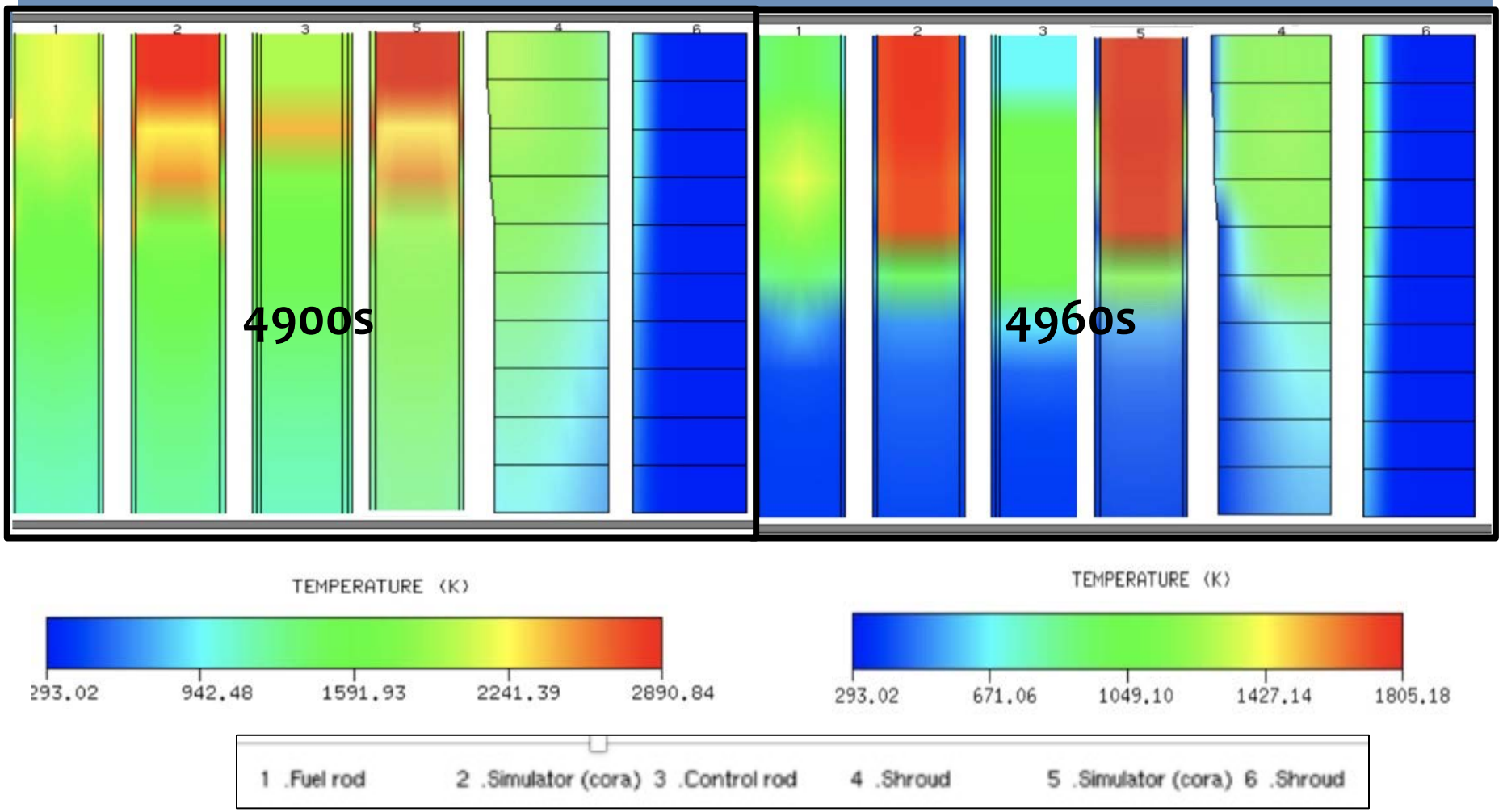

Sensitivity analysis – Original MOD3.2 - input
Meas. above bundle – 1150 to 1350mm
Surface Temperatures (K)
3,000
2,500
2,000
1,500
1,000
500
0
4,800
4,850
4,900
4,950
5,000
5,050
5,100
Time (s)
cadct 60101
cadct 60201
cadct 60301
cadct 60401
cadct 60501
cadct 60601
cadct 60701
cadct 60801
cadct 60901
cadct 61001
cadct 60102
cadct 60202
cadct 60302
cadct 60402
cadct 60502
cadct 60602
cadct 60702
cadct 60802
cadct 60902
cadct 61002
cadct 60105
cadct 60205
cadct 60305
cadct 60405
cadct 60505
cadct 60605
cadct 60705
cadct 60805
cadct 60905
cadct 61005
cadct 170104
cadct 170204
cadct 170304
cadct 170404
cadct 170504
cadct 170604
cadct 170704
cadct 170804
cadct 170904
cadct 171004
Meas. 1150
Meas. 1150(1)
Meas. 1150(2)
Meas. 1150(3)
Meas. 1250
Meas. 1350
Meas. 1350(1)
Meas. 1350(2)
Meas. 1350(3)
Meas. 1150(4)

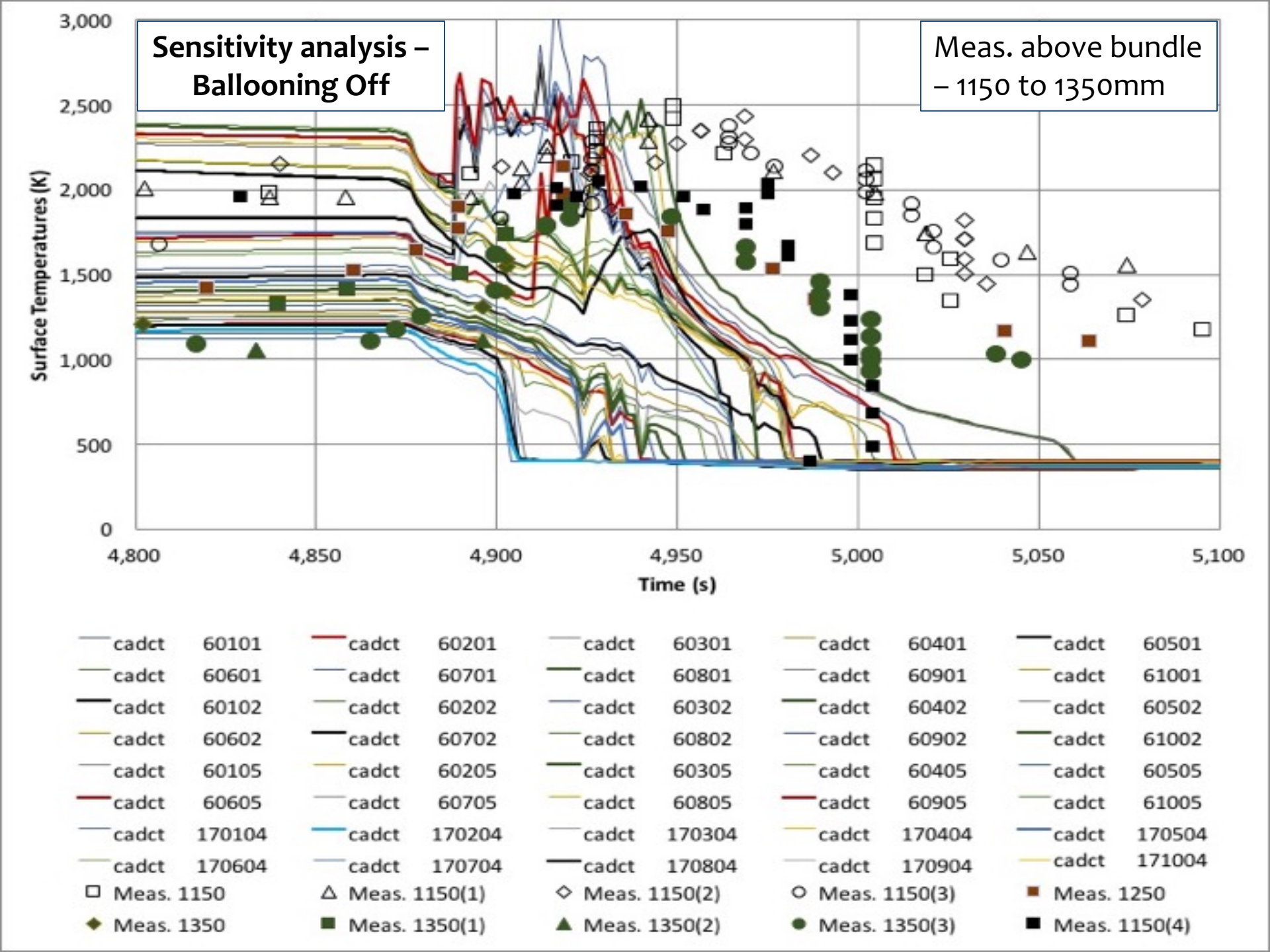

Sensitivity analysis – Ballooning Off
Top
Bottom
Bundle quench
Surface Temperature (K)
3,000
2,500
2,000
1,500
1,000
500
0
3,000
3,200
3,400
3,600
3,800
4,000
4,200
4,400
4,600
4,800
5,000
Time (s)
cadct 60101
cadct 60201
cadct 60301
cadct 60401
cadct 60501
cadct 60601
cadct 60701
cadct 60801
cadct 60901
cadct 61001
cadct 60102
cadct 60202
cadct 60302
cadct 60402
cadct 60502
cadct 60602
cadct 60702
cadct 60802
cadct 60902
cadct 61002
cadct 60105
cadct 60205
cadct 60305
cadct 60405
cadct 60505
cadct 60605
cadct 60705
cadct 60805
cadct 60905
cadct 61005
cadct 170104
cadct 170204
cadct 170304
cadct 170404
cadct 170504
cadct 170604
cadct 170704
cadct 170804
cadct 170904
cadct 171004
Meas. 150
Meas. 250
Meas. 350
Meas. 550(1)
Meas. 550 (2)
Meas. 750
Meas. 850
Meas. 950
Meas. 50
Meas. 150
Meas. 350
Meas. 550(2)
Meas. 750(2)
Meas. 950(2)
Meas. 350(2)
Meas. 550(3)
Meas. 750(3)
Meas. 950(3)

Turning off ballooning decreased oxidation and electrical heating at top of bundle



No ballooning decreased peak heated rod temperatures during heatup and quench




Sensitivity analysis – Ballooning Off
Meas. above bundle – 1150 to 1350mm
Surface Temperatures (K)
3,000
2,500
2,000
1,500
1,000
500
0
4,800
4,850
4,900
4,950
5,000
5,050
5,100
Time (s)
cadct 60101
cadct 60201
cadct 60301
cadct 60401
cadct 60501
cadct 60601
cadct 60701
cadct 60801
cadct 60901
cadct 61001
cadct 60102
cadct 60202
cadct 60302
cadct 60402
cadct 60502
cadct 60602
cadct 60702
cadct 60802
cadct 60902
cadct 61002
cadct 60105
cadct 60205
cadct 60305
cadct 60405
cadct 60505
cadct 60605
cadct 60705
cadct 60805
cadct 60905
cadct 61005
cadct 170104
cadct 170204
cadct 170304
cadct 170404
cadct 170504
cadct 170604
cadct 170704
cadct 170804
cadct 170904
cadct 171004
Meas. 1150
Meas. 1150(1)
Meas. 1150(2)
Meas. 1150(3)
Meas. 1250
Meas. 1350
Meas. 1350(1)
Meas. 1350(2)
Meas. 1350(3)
Meas. 1150(4)

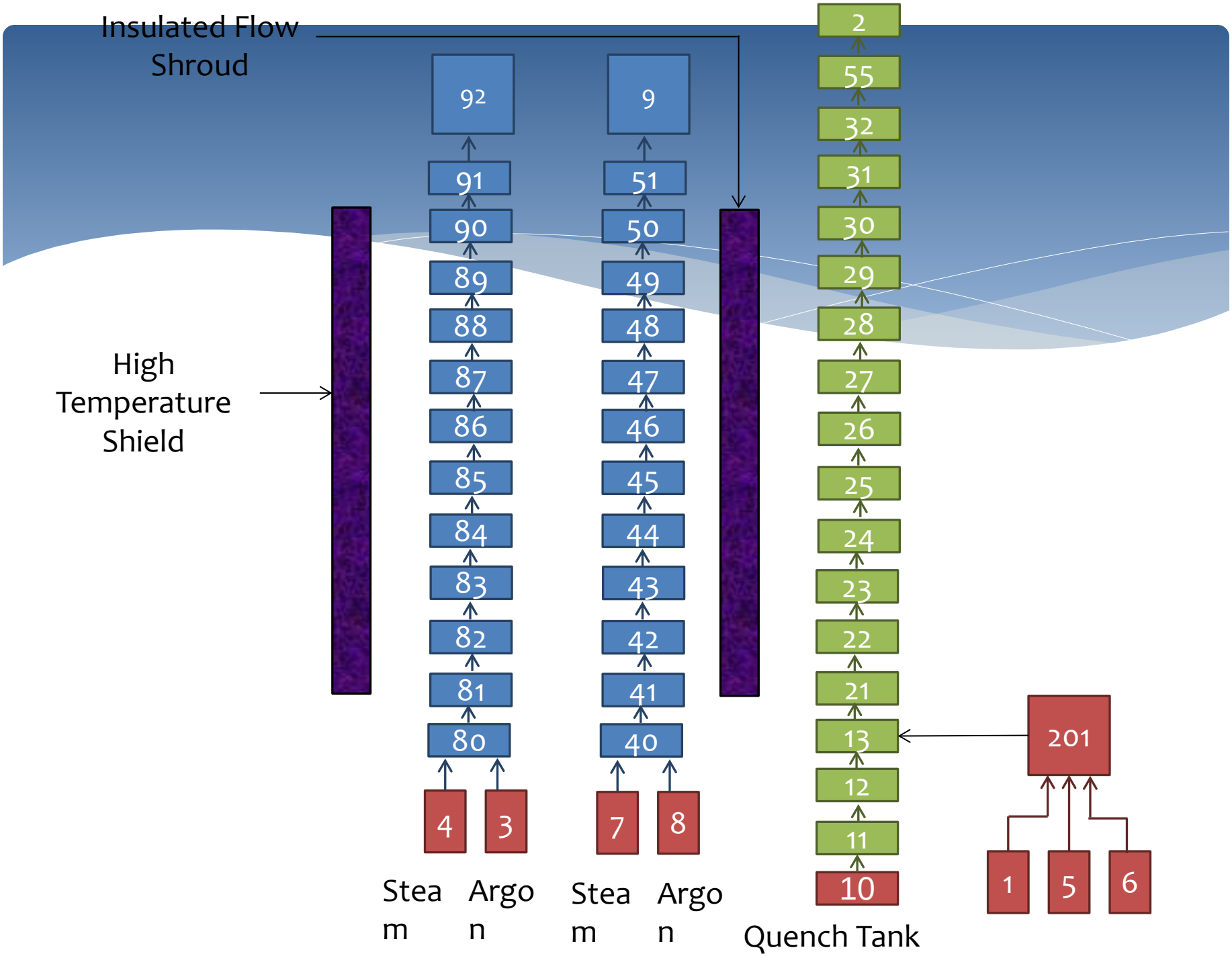
Conclusions

- **Cladding deformation with resulting changes in double sided oxidation and changes in gap conductance has significant impact on peak cladding temperatures during heatup and quenching**
  - Influence increased by increasing electrical power with temperature
  - Comparison of calculated and measured temperatures inconclusive in assessing predicted impact of ballooning on peak bundle powers and temperatures, **however,**
- CORA design parameters would indicate that **ballooning should be deactivated as default for CORA PWR experimental analysis**
  - Non-ballooning case used for integrated uncertainty analysis

Additional slides

CORA-13 uncertainty analysis using RELAP/SCDAPSIM/MOD3.4 with IUA (integrated uncertainty analysis)

* RELAP/SCDAPSIM/MOD3.X(IUA) allows user to easily compute ranking statistics and uncertainty distributions using base input model
  * User defines parameters to include plus uncertainty distributions for defined parameters
    * Input parameters
    * Source code parameters
  * New "setup" option builds input models and uncertainty files for uncertainty analysis
  * New "post processing" option computes uncertainty distributions and ranking statistics for user selected quantities


Insulated Flow Shroud
High Temperature Shield
92
91
90
89
88
87
86
85
84
83
82
81
80
9
51
50
49
48
47
46
45
44
43
42
41
40
2
55
32
31
30
29
28
27
26
25
24
23
22
21
13
12
11
10
201
4
3
7
8
1
5
6
Steam
Argon
Steam
Argon
Quench Tank

CORA-13 uncertainty analysis using RELAP/SCDAPSIM/MOD3.4 with IUA (integrated uncertainty analysis)

* RELAP/SCDAPSIM/MOD3.X(IUA) allows user to easily compute ranking statistics and uncertainty

User defines parameters to include plus uncertainty distributions for defined parameters

Input parameters

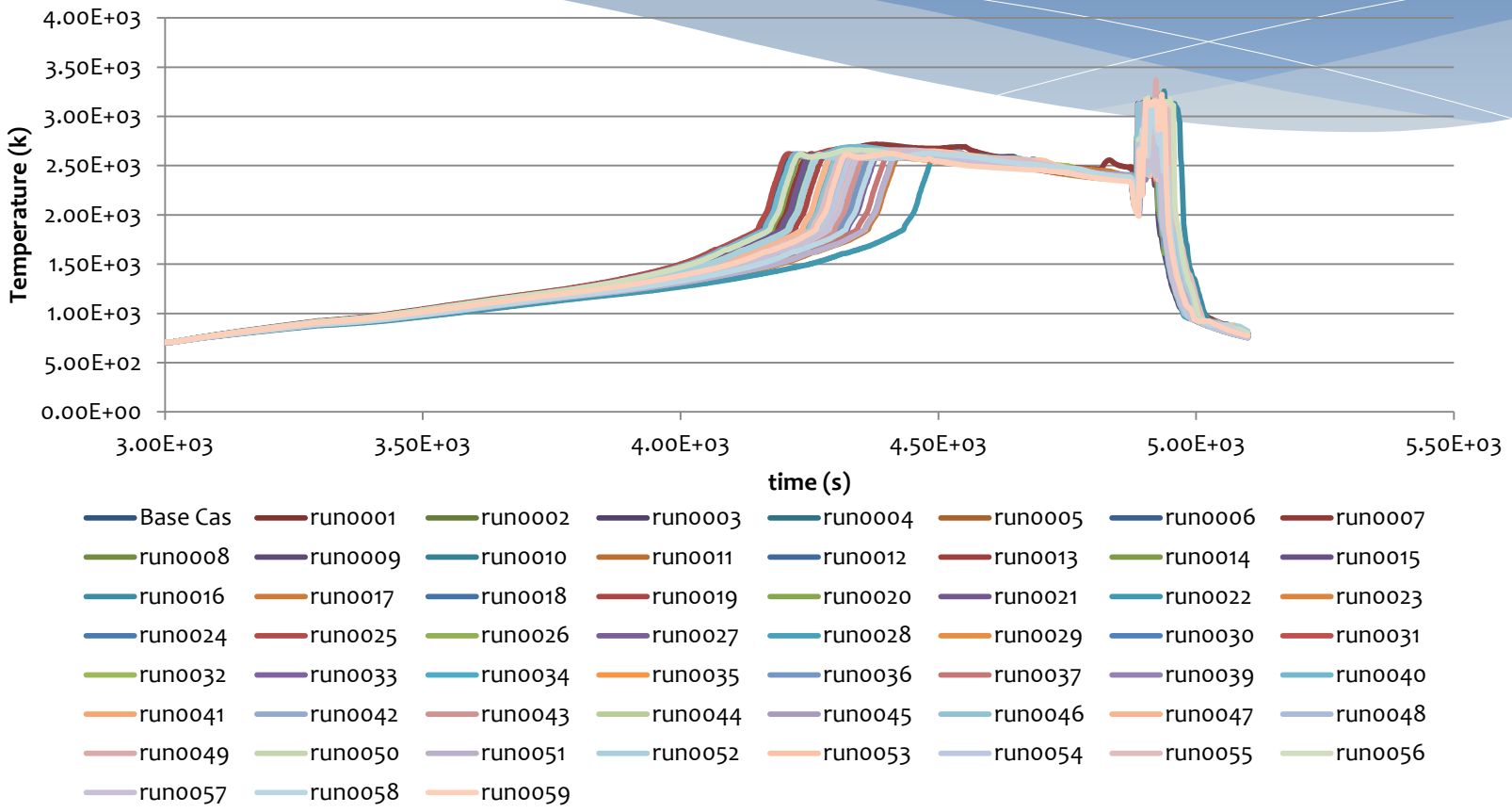
Source code parameters

computes uncertainty distributions and ranking statistics for user selected quantities

CORA-13 Example

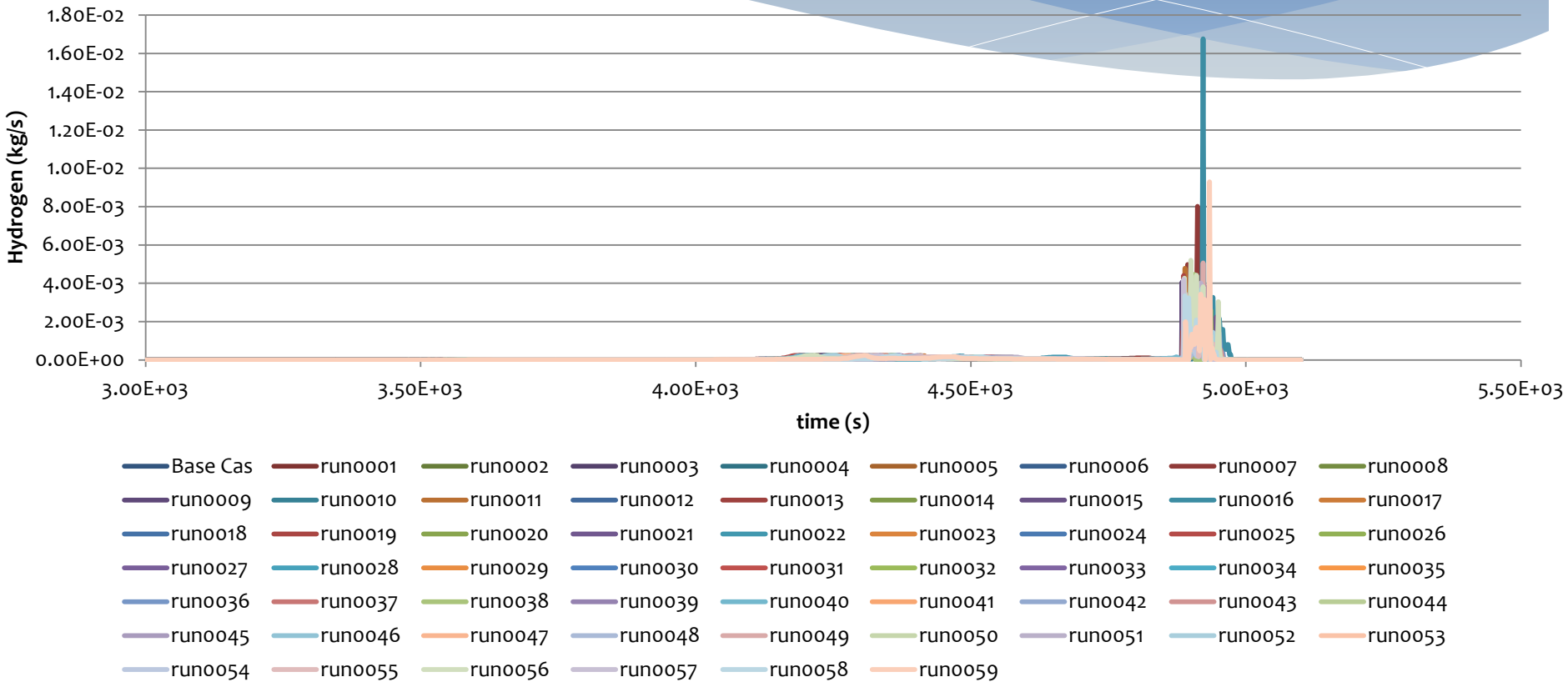
* Shroud Zirconia therm. cond.
* Electrical power
* Mass flow rate
* Steam inlet flow rate
* Steam inlet temperature
* Flow rate of quench tank

Peak bundle temperature



Uncertainty analysis

Total hydrogen production



Uncertainty analysis

Analysis of CORA BWR experiments using RELAP/SCDAPSIM/MOD3.4 – CORA-28 Pre-oxidation phase sensitivity studies

Rawan Mustafa – Jordan Atomic Energy Commission
Chris Allison– Innovative Systems Software

The reassessment of the CORA BWR experiments using RELAP/SCDAPSIM is an important component of our (Innovative Systems Software's) ongoing Fukushima Daiichi assessment activities. These experiments (a) accurately reflect the design of a BWR fuel assembly with associated channel box/ control blade and (b) cover a range of thermal hydraulic conditions most like those expected among the three units. Several, although not all, of these experiments have been previously analyzed using both SCDAP/RELAP5 (in the 1980s) and by RELAP/SCDAPSIM over the past 10-15 years. The calculated results, were in general, in reasonably good agreement with the experimental results with notable sources of uncertainty associated with the modeling of the electrically heat fuel rod simulators, shroud thermal properties and associated radial heat losses, and unique thermal hydraulic design of the CORA facility. However, no studies have been performed on the preparation phase prior to the test phase previously.

This presentation provides a sensitivity study of German Pre-Oxidation phase of CORA 28 electrically heated experiment, looking at both the influence of uncertainties in experimental conditions and important models/correlations in order to establish most proper initial conditions for the main test phase using RELAP/SCDAPSIM/MOD3.4.

The presentation included comparisons between calculated and measured bundle temperatures for the Pre-oxidation phase of CORA-28 experiment.



SDTP

Development of best estimate methods for reactor and advanced fluid systems safety analysis and training

Analysis of CORA BWR experiments using RELAP/SCDAPSIM/MOD3.4 – CORA-28 Pre-oxidation phase sensitivity studies

Analysis and contributions by

Rawan Mustafa – Jordan Atomic Energy Agency

Dr. S. Hagen – KIT

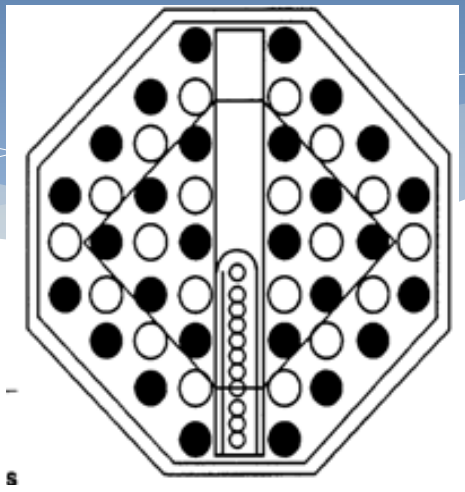
Dr. Chris Allison - ISS

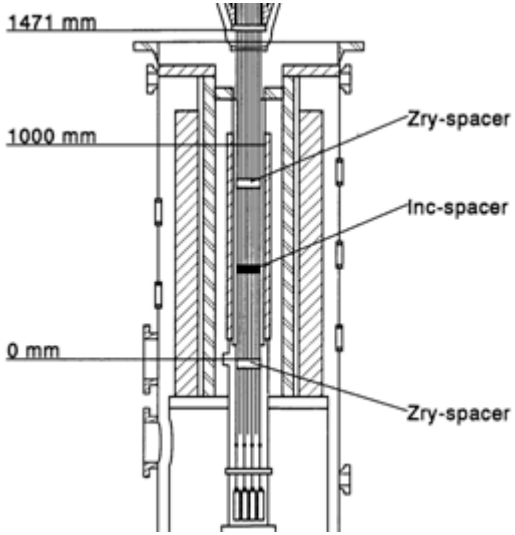
Outline

* **Representative BWR assembly experiments in CORA facility – CORA 16/17/18/28/30/31/33**
  * Recently "published" and on-going uncertainty analysis focused on influence of uncertainties in thermal hydraulic boundary conditions
* **CORA-28 – Influence of pre-oxidation**
  * Sensitivity studies on thermal hydraulic boundary conditions and modeling options during pre-oxidation phase
  * **Uncertainties in initial conditions** for transient analysis
* **Conclusions**

Representative BWR assembly experiments in CORA facility – CORA 16/17/18/28/30/31/33

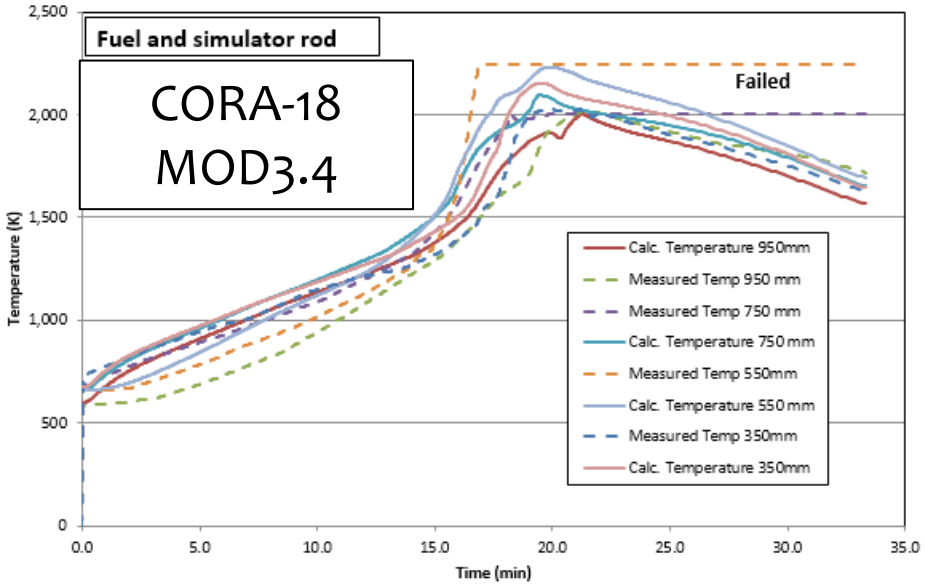
Experiment	Conditions
CORA 16	Reference experiment
CORA 17	Water addition
CORA 18	Large bundle – influence of size
CORA 28	Influence of pre-oxidation
CORA 31	Influence of slow initial heatup (0.3 K/s)
CORA 33	Influence of steam starvation



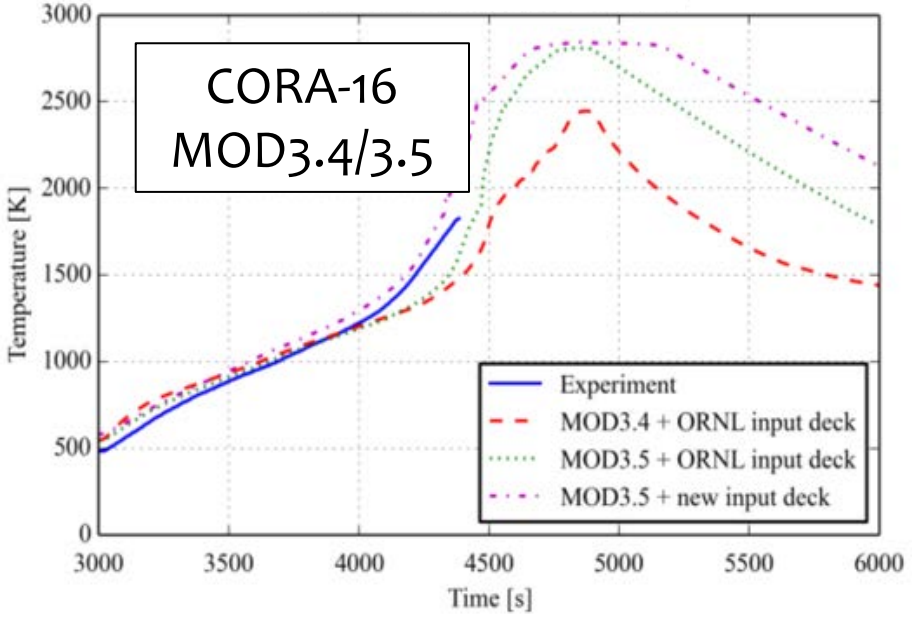


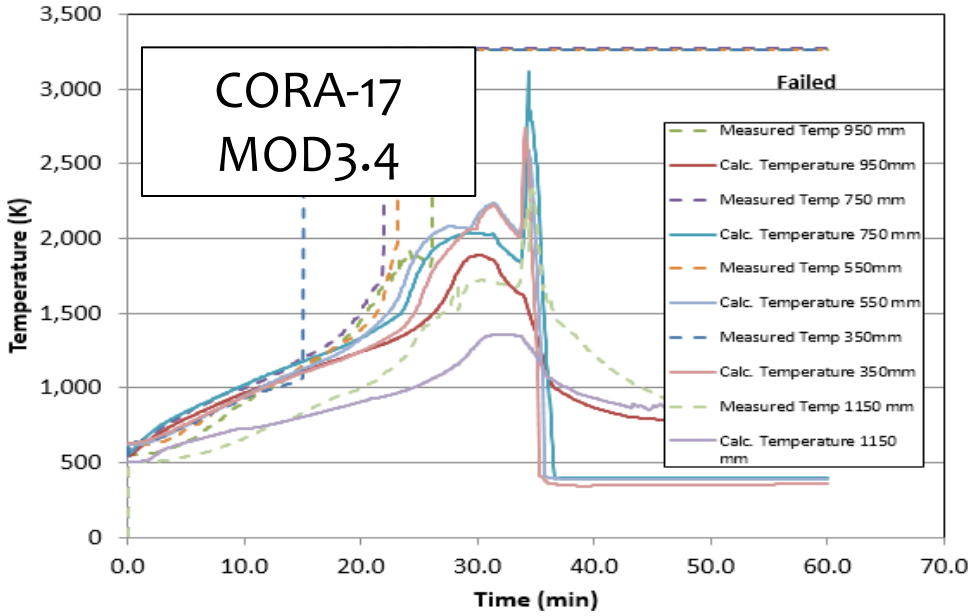
Recently "published" and on-going uncertainty analysis focused on influence of uncertainties in thermal hydraulic boundary conditions

* Input models follow recommended guidelines for nodalization and modeling parameters for CORA facility so have little impact on results
* **Dominant contributors to uncertainties**
  * **Bundle temperatures** - Shroud thermal properties (radial heat losses), axial power distribution (due to temperature dependency of resistance), flow bypass between inner and outer shroud, observation windows in inner shroud
  * **Hydrogen generation rates** - Time delays and variations in hydrogen measurements, steam generation from lower quench tank in CORA facility

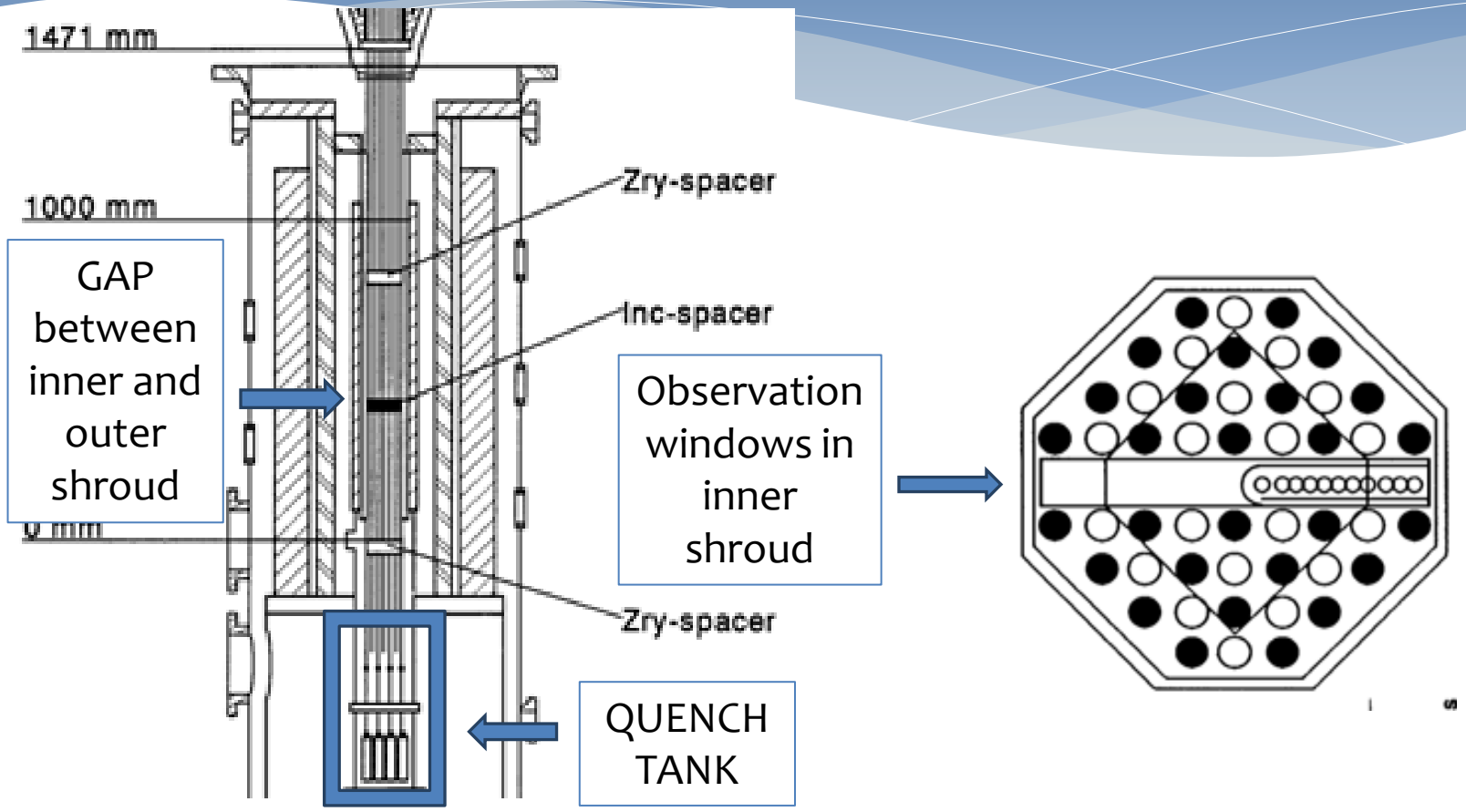


Analysis and contributions by
Hiroshi Madokoro – University of Tokyo
Rawan Mustafa – Jordan Atomic Energy Agency
Heriberto Sanchez - University of Mexico





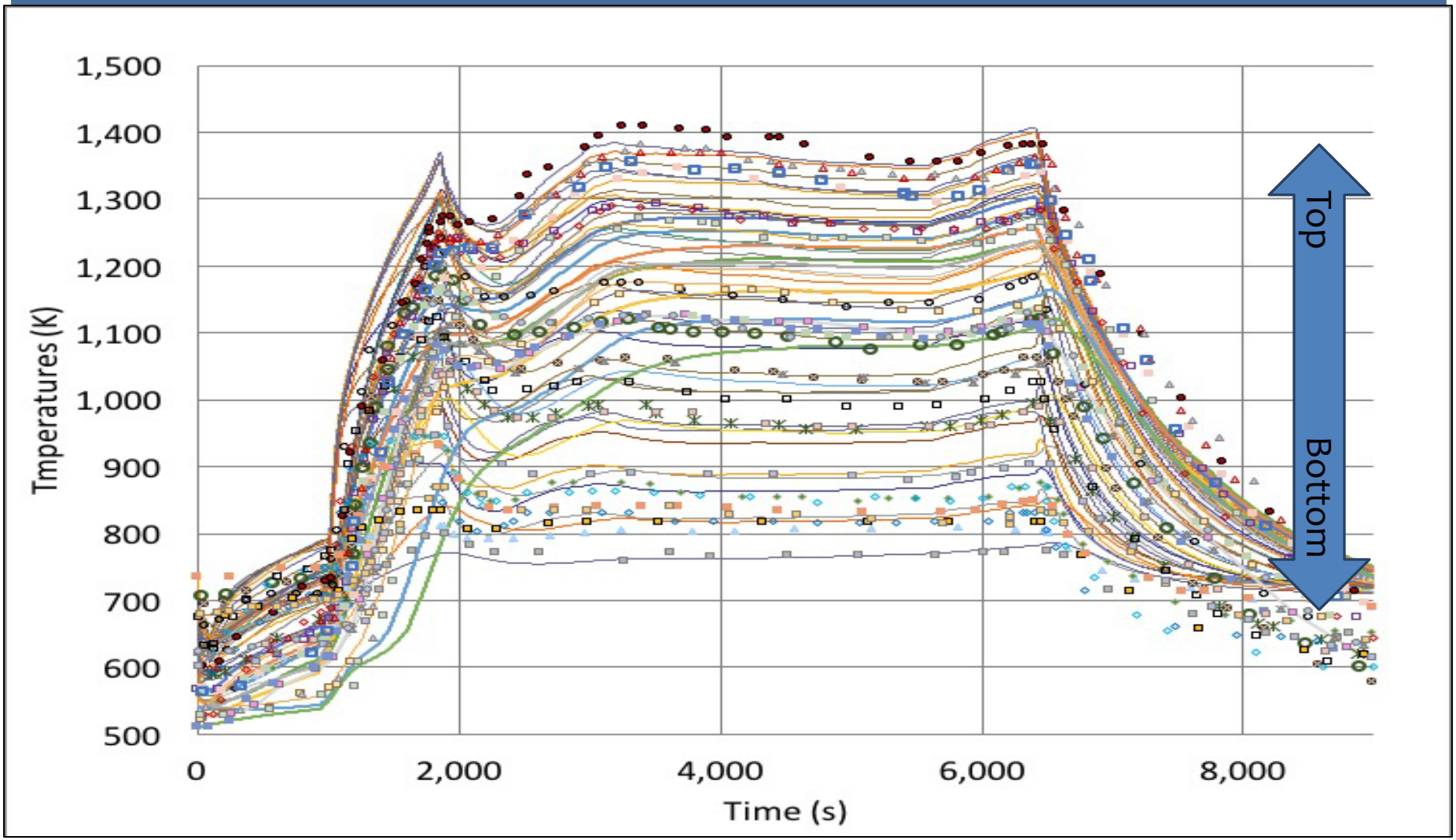
CORA facility had more complicated thermal boundary conditions than that of Quench facility



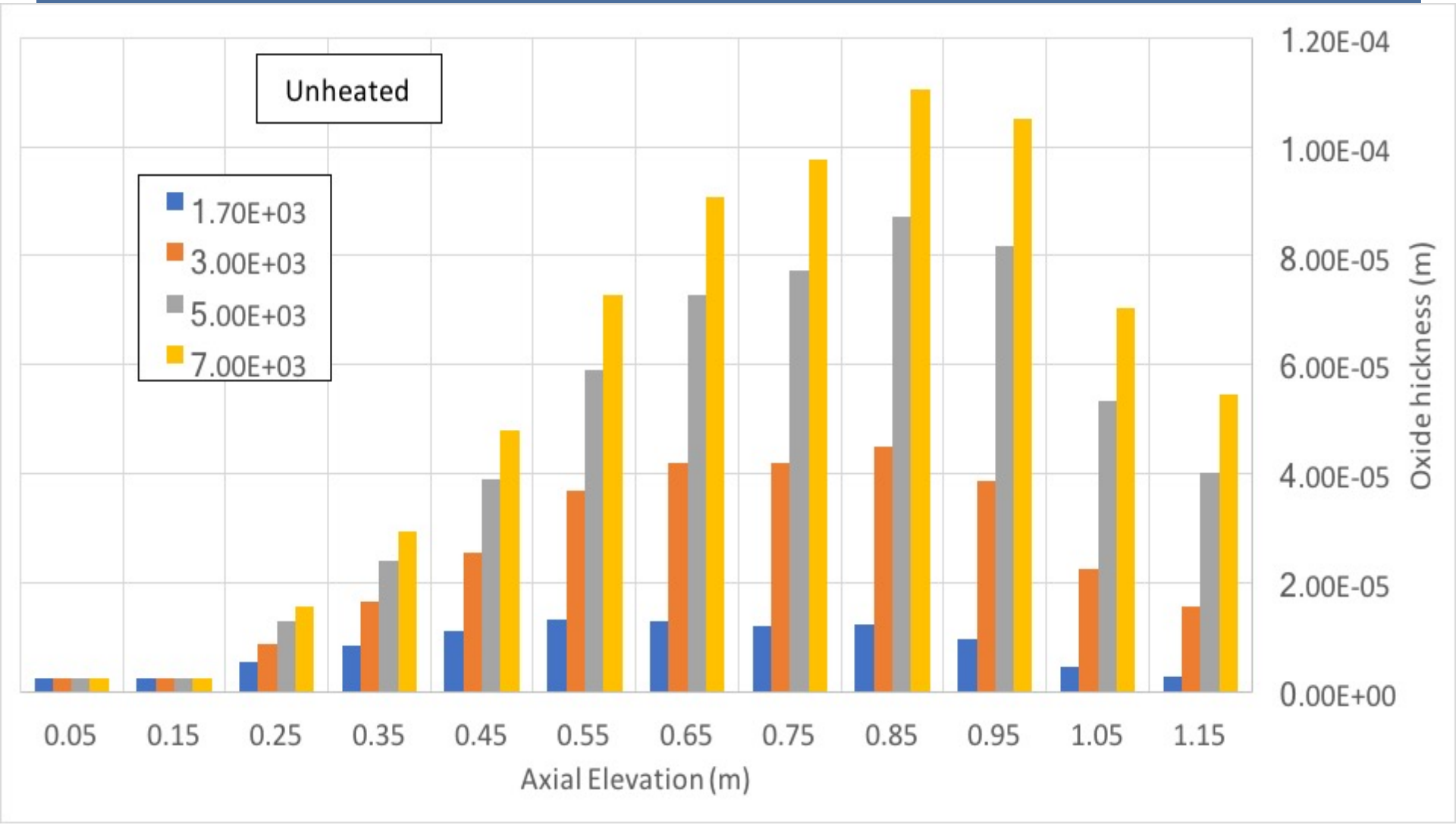
Base CORA-28 input was adjusted to match pre-oxidation phase measured temperatures

- Adjustments were
  - Ballooning was deactivated to insure original cladding and gap dimensions were not changed during pre-oxidation phase
  - Maximum power was adjusted to match calculated and measured bundle temperatures during pre-oxidation phase
  - Length of phase was adjusted to match measured oxide thickness in sample rods prior to beginning of transient
- Sensitivity studies were performed to estimate influence of changes
  - Peak power was adjusted to show influence on peak temperatures

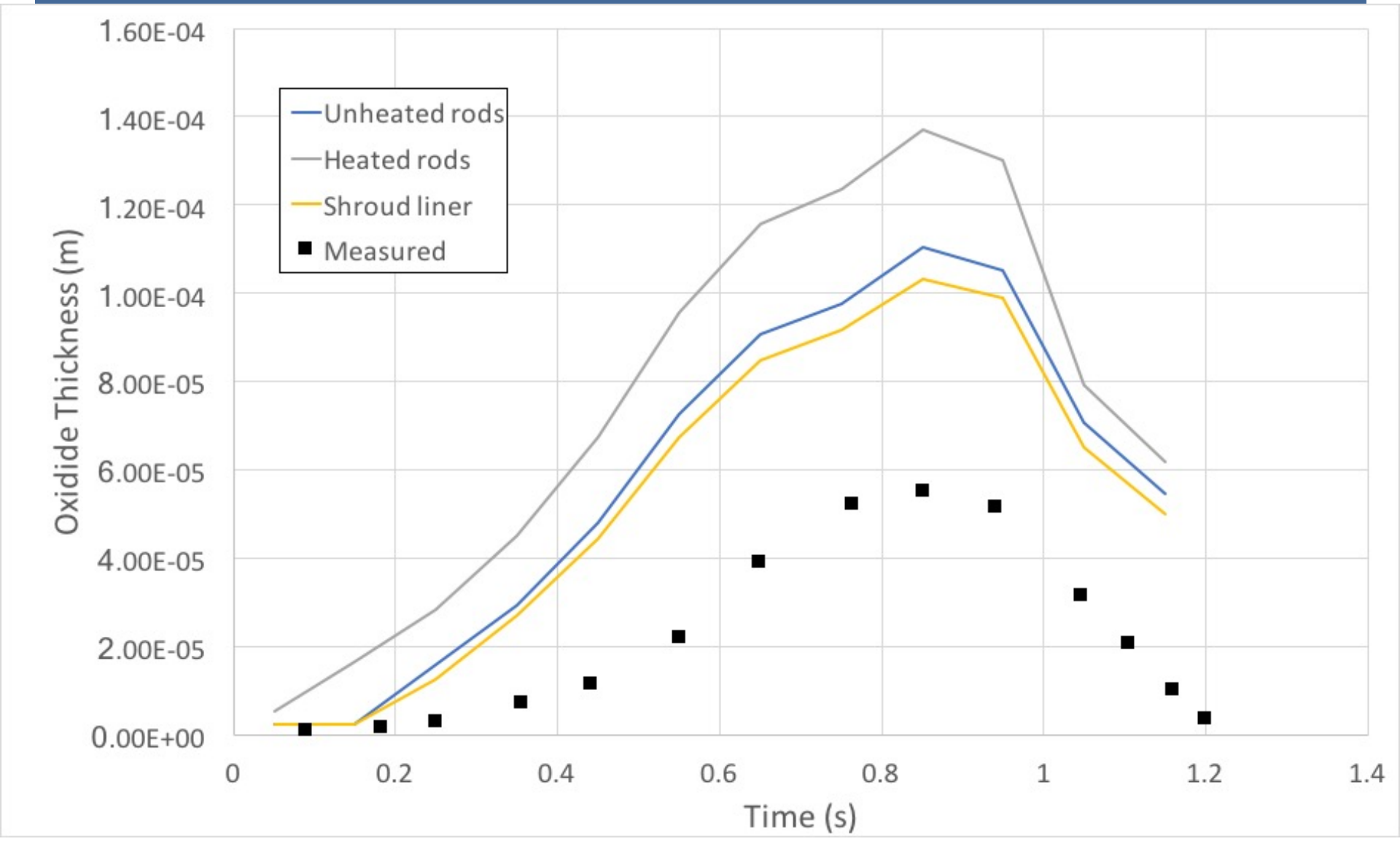
Bundle measured and calculated temperatures – Base case



Unheated Rods Oxide Thicknesses– Base case



Comparison of Calculated and Measured Oxide Thicknesses– Base case



Conclusions – Uncertainties in Pre-Oxidation End State?

- **Bundle temperatures are well represented (most important)**
- **Oxide thicknesses (apparently) overpredicted**
  - Cathcart-Pawel oxidation kinetics not accurate (not likely)
  - Temperatures of structure used to defined oxide thicknesses (possible)
    - Sensitivity analysis would indicate that temperatures would have to be 200-300 K lower that heated rods
  - Our misinterpretation of measured oxide thicknesses (?)
- **Initiation conditions for transient and integrated uncertainty analysis will use calculated bundle temperatures and oxide thicknesses**
  - Variation in oxide thicknesses will be addressed through integrated uncertainty analysis as perturbed parameter to include possibility of lower values

RELAP5 MOD3.4 with IUA modeling of LOFT L3-7 experiment

Barbara Kędzierska[1,*], Chris M. Allison[2], Judith K. Hohorst[2]

[1] Warsaw University of Technology, Poland
[2] Innovative Systems Software, Idaho, USA

* Corresponding author: kedzierska_barbara@wp.pl

RELAP/SCDAPSIM, a detailed system thermohydraulic code with best estimate severe accident models and correlations, is being developed by Innovative Systems Software with support from an international group of users, universities and research organizations that are part of the SCDAP Development and Training Program (SDTP). MOD3.4 is the most widely used version of the code, whereas MOD3.5 and MOD3.6 are advanced experimental production versions from RELAP/SCDAPSIM/MOD3.X series.

Integrated Uncertainty Analysis (IUA) was introduced into MOD3.4 and MOD3.5 and has been distributed since the summer 2017 for use. IUA allows the user to implement a list of chosen modeled parameters with their uncertainty distributions in base assessment input model. Uncertainty distributions of source code models, initial and boundary conditions values, as well as the material properties can be computed and ranking statistics for these parameters can be obtained.

As a part of the systematic code reassessment program, several CORA, PHEBUS, QUENCH and LOFT experiments have been reanalyzed. This presentation concerns the LOFT L3-7 experiment, performed in the LOFT complete reactor system at the Idaho National Laboratory as part of the NRC safety research program. LOFT L3-7 was a 2.5-cm (10-in.) cold-leg noncommunicative-break LOCA.

The LOFT L3-7 experiment was previously analyzed in 1980's and 90's as part of the SCDAP/RELAP5/MOD3.3, MOD3.2 and previous releases (NRC approved) assessment. Experimental results and data from NRC reports have been used as benchmark data for MOD3.4 with IUA verification.

The uncertainty analysis covers initial conditions, fuel properties (conductivity, heat capacity and fuel pin geometry) and operator action accuracy. The presentation includes comparison of lowest- and highest-estimate rankings to the base case and measured values until 1000 seconds (as in the NRC full reports). For the chosen transients the whole array of ranking curves is shown. The sequence of events with the time of occurrence according to MOD3.4 with IUA and MOD2 is provided.


14.11.2018

RELAP5 MOD3.4 with IUA modeling of LOFT L3-7 experiment

Barbara Kędzierska

QUENCH Workshop, 13-15.11.2018

Question:

Does RELAP5 MOD3.4 with IUA give better estimation of measured parameters than older versions? How big are the discrepancies from uncertainties range?

Outline:

1) LOFT facility

2) L3-7 experiment

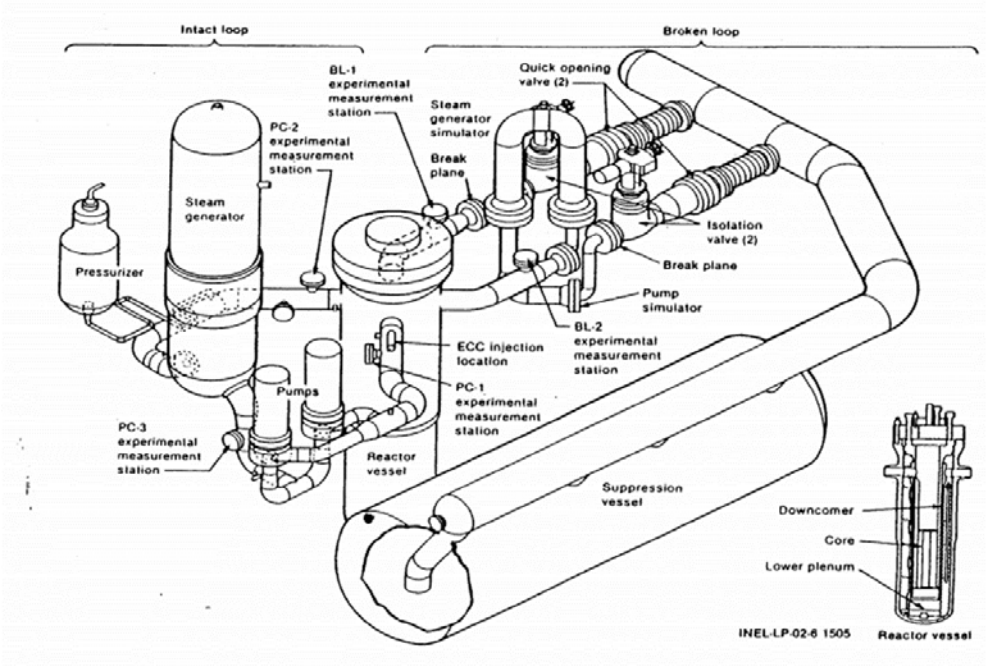
3) Experiment modeling

4) Results and conclusions

LOFT facility

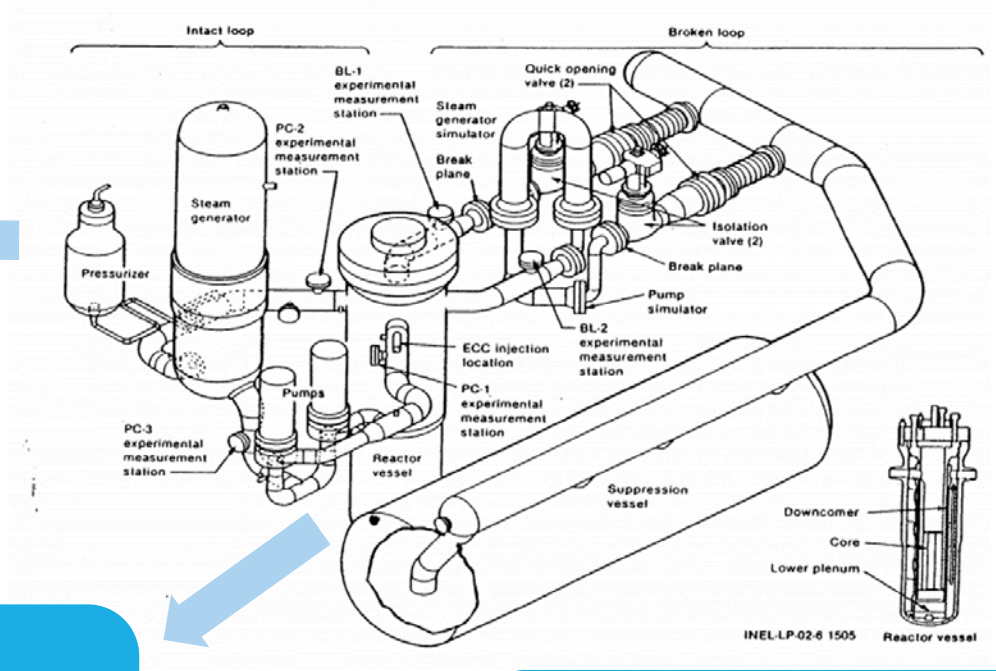
- Operated from 1976 to 1985,
- Over 40 tests conducted – mostly large- and small break LOCA
- 50 MWt, volumetrically scaled 1000-MW-PWR
- The system consists of:
  - Reactor vessel with nuclear core
  - An intact loop
  - A broken loop

  } Primary coolant system
  - The blow down suppression system
  - The emergency core coolant system (two LPIS, two HPIS pumps, two accumulators)
  - Secondary coolant system



LOFT facility

Intact loop:
- steam generator
- pressurizer
- coolant pumps
- hot and cold leg piping



Broken loop:
- steam generator and pump simulators
- hot and cold leg piping
- Two quick opening valves to provide the break flow

Core:
- 1,68m – long, 0,61m – diameter
- 9 fuel assemblies, containing 1300 fuel rods
- Fueled by real fuel

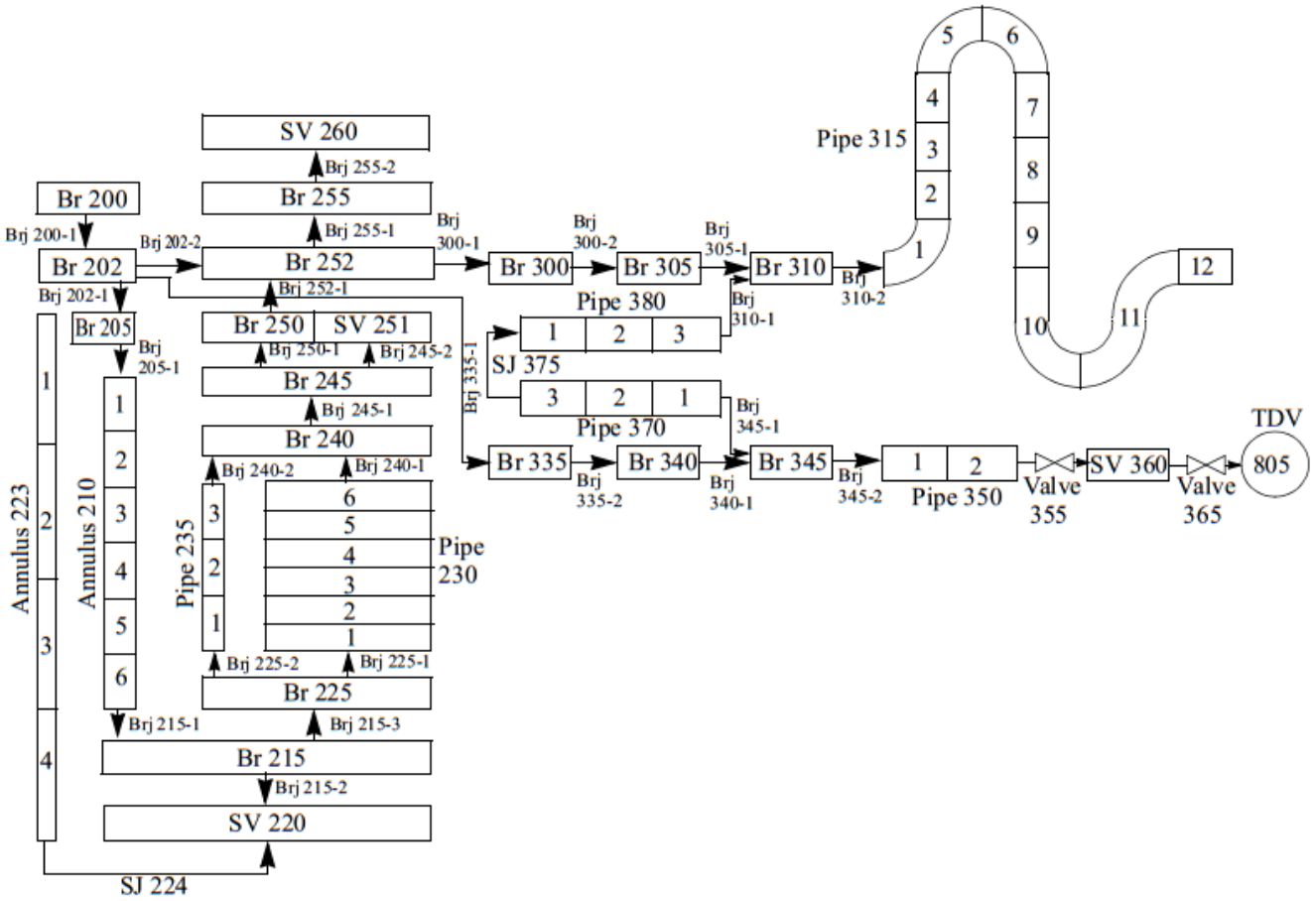
Safety systems:
- High Pressure Injection System (HPIS)
- Accumulators
- Low Pressure Injection System (LPIS)

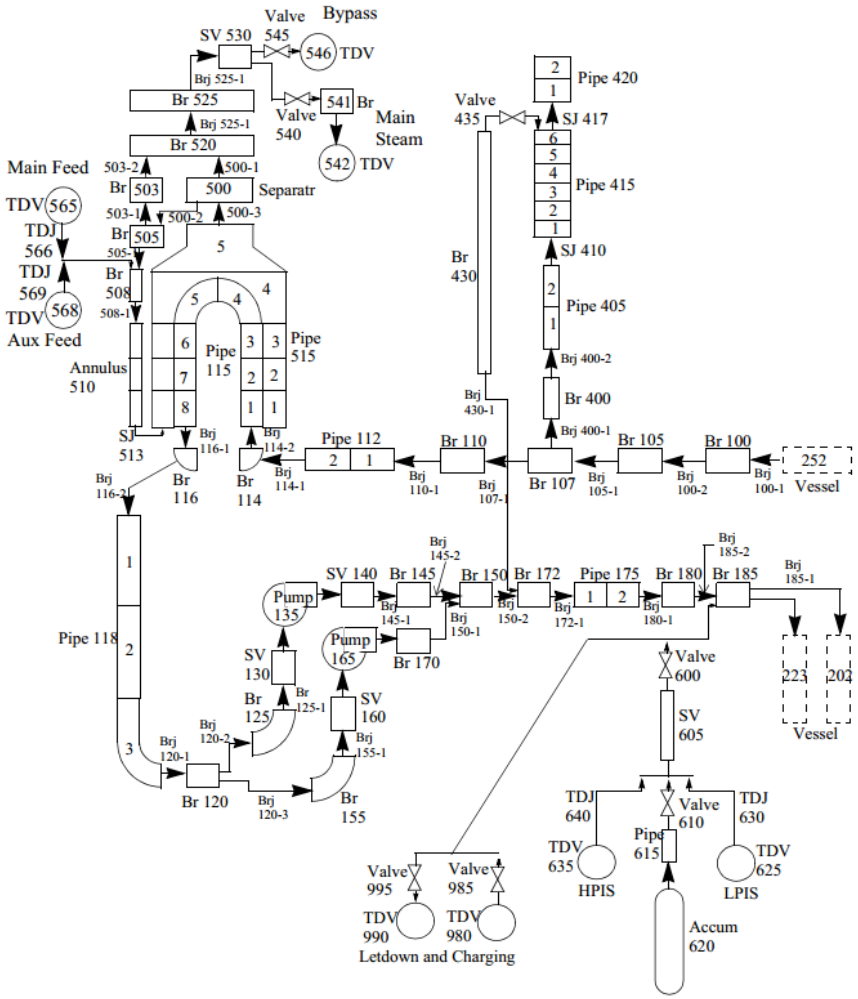
LOFT L3-7 Experiment

- SBLOCA – relevant break diameter is less than 10 in.
- Break belongs to the lower end of the SBLOCA range if the diameter is less than 1 inch – leakage from a valve or joint.
- 4-mm-break in the broken loop - 2,54-cm (1-inch)-break in the full scale PWR reactor.
- Low pressure signal was the driving force of the experiment, flow is injected through the cold leg into the vessel.

Measurement instrumentation:

- fluid pressure
- fluid temperature
- liquid and vapor velocity
- mixture density
- thermocouples in 196 core locations for rod cladding and suport tubes temperature measurements





Nodalization diagrams

The system was divided into 130 volumes and 137 heat structures. They were connected by 136 junctions. The break happens on the quick-opening valve 365 connecting the whole system with the time-dependent volume 805.

A simplified core design was used – no SCDAP components, they were replaced by heat structures.

Uncertainties – initial conditions

Parameter	Uncertainty distribution
PCS intact loop cold leg structures temp.	ND (1.0, 2.60e-3)
PCS intact loop hot leg structures temp.	ND (1.0, 2.60e-5)
PCS hot leg pressure	ND (1.0, 1.04e-4)
PCS intact loop mass flow rate	ND (1.0, 2.60e-3)
PCS broken loop cold leg temp.	ND (1.0, 2.60e-3)
PCS broken loop hot leg temp.	ND (1.0, 2.60e-3)
Piping temperature	ND (1.0, 2.60e-5)
Accumulator pressure	ND (1.0, 2.60e-3)
Accumulator temp.	ND (1.0, 2.60e-5)
Pressurizer initial pressure	ND (1.0, 2.60e-5)

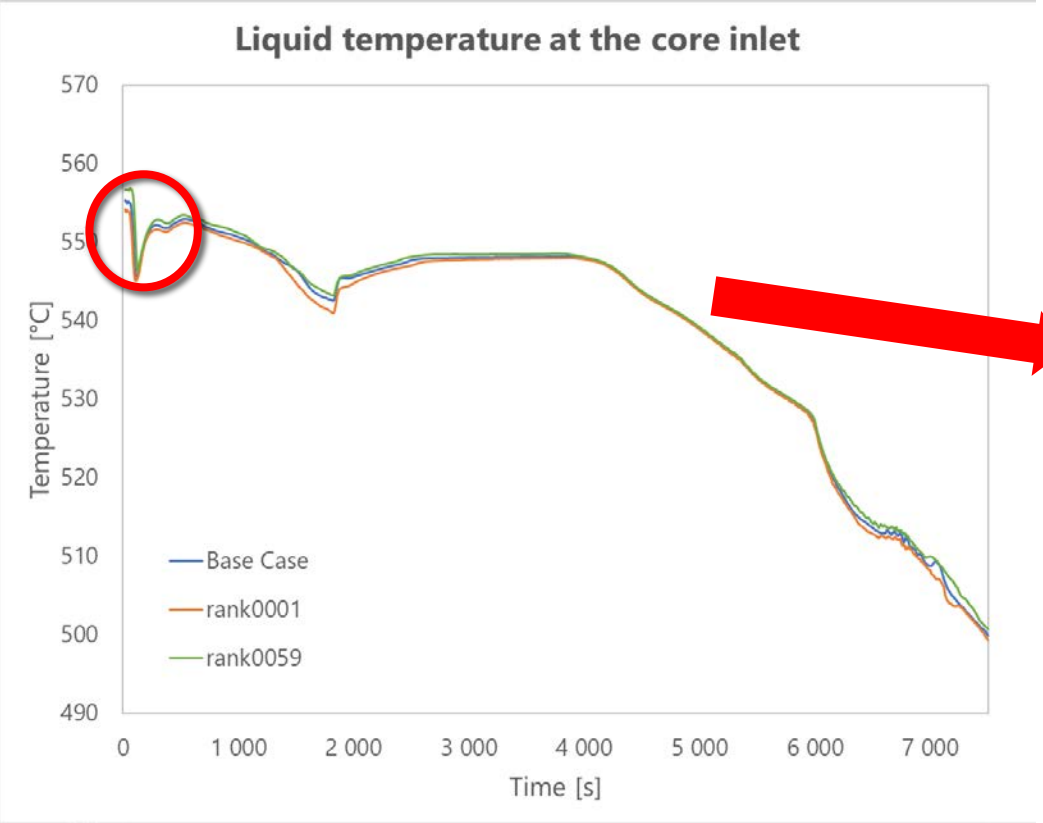
Uncertainties – other parameters

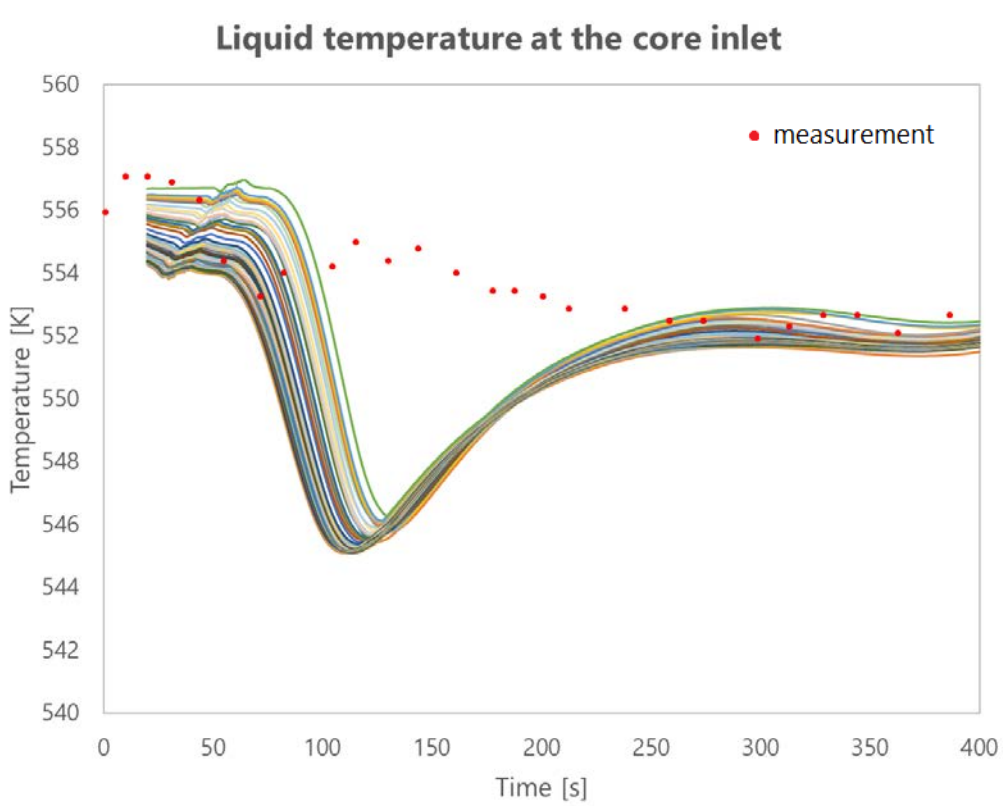
Parameter	Uncertainty distribution
Initial total reactor power	ND (1.0, 1.04e-4)
Time during transient initiation	ND (1.0, 2.60e-3)
HPIS initiation pressure	ND (1.0, 2.60e-3)
Axial peaking factor	ND (1.0, 6.51e-4)
Power during transient	ND (1.0, 1.04e-4)
Fuel conductivity	ND (1.0, 2.60e-3)
Fuel volumetric heat capacity	ND (1.0, 1.04e-4)
Fuel pin geometry (junction flow area)	ND (1.0, 6.51e-4)

Uncertainties – transient events

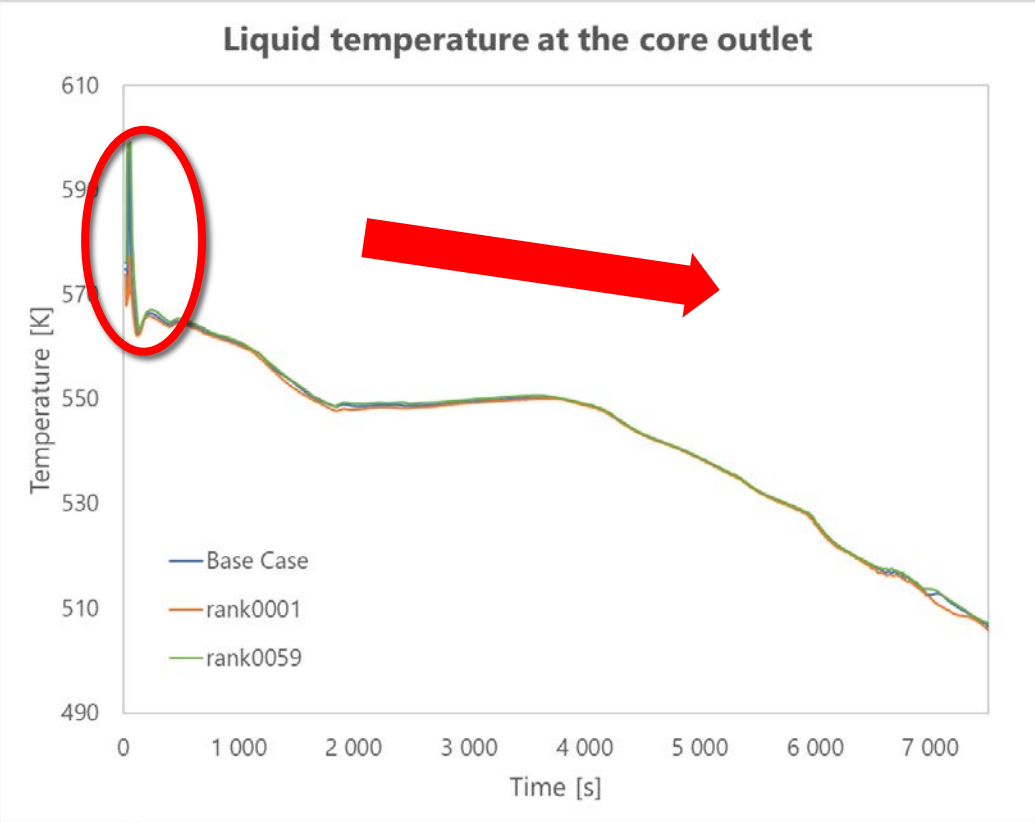
Parameter	Uncertainty [s]
SCS auxiliary feed terminated	1800 ± 5
SCS steam bleed initiated	3603 ± 1
HPIS flow reinstated	5974.2 ± 0.1
Break isolation	7302.0 ± 0.1

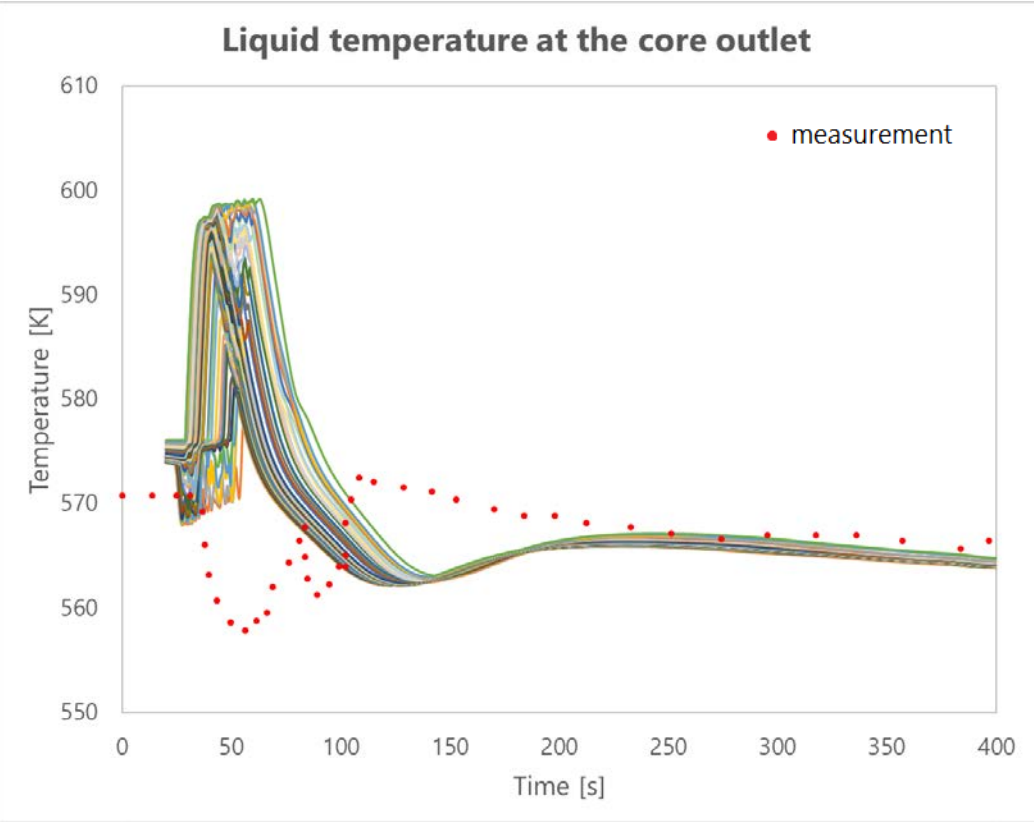
Results - temperatures



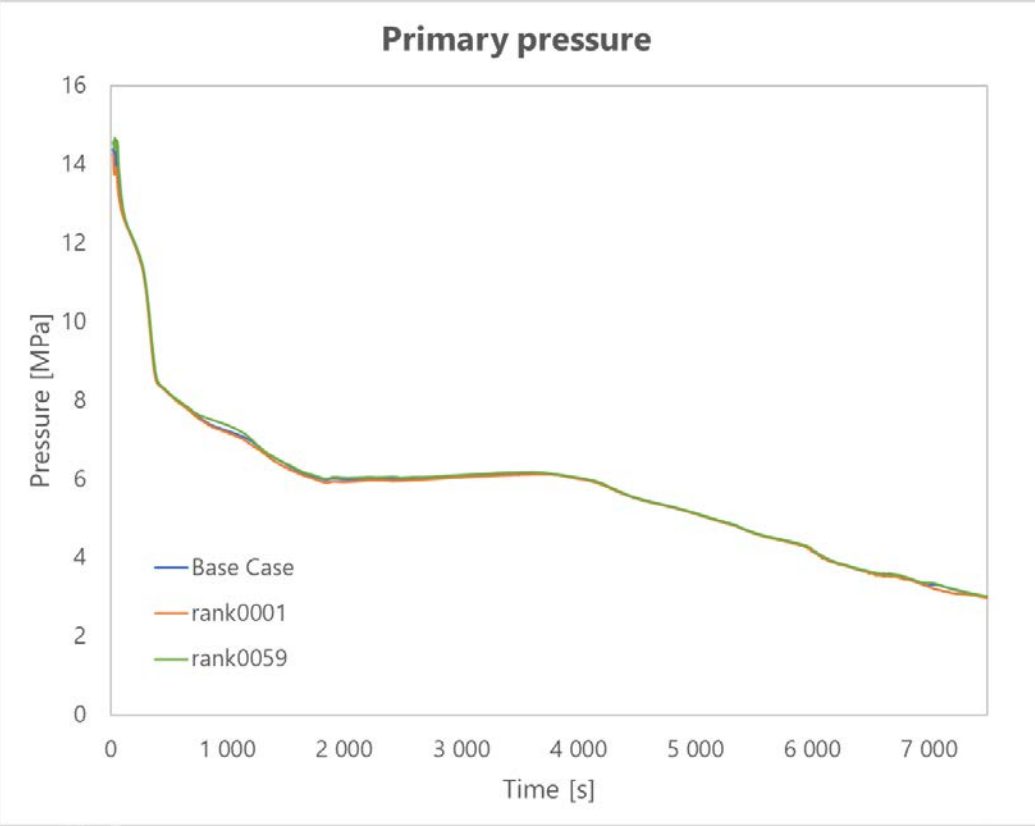


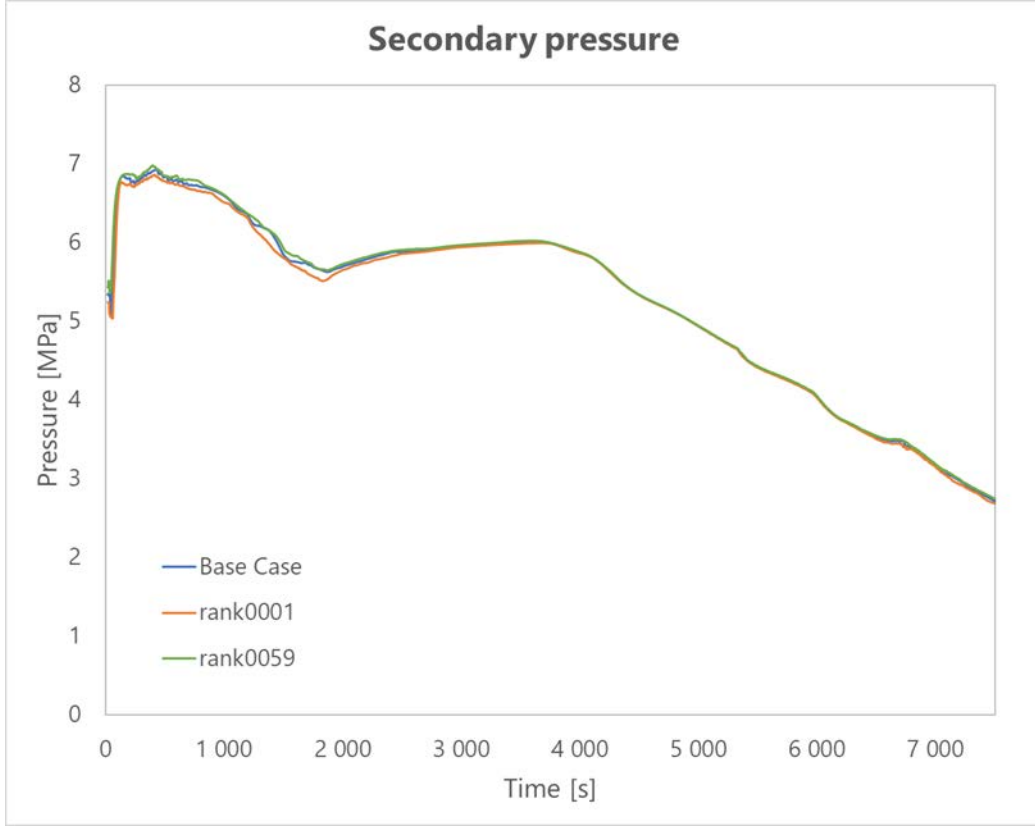
Results - temperatures



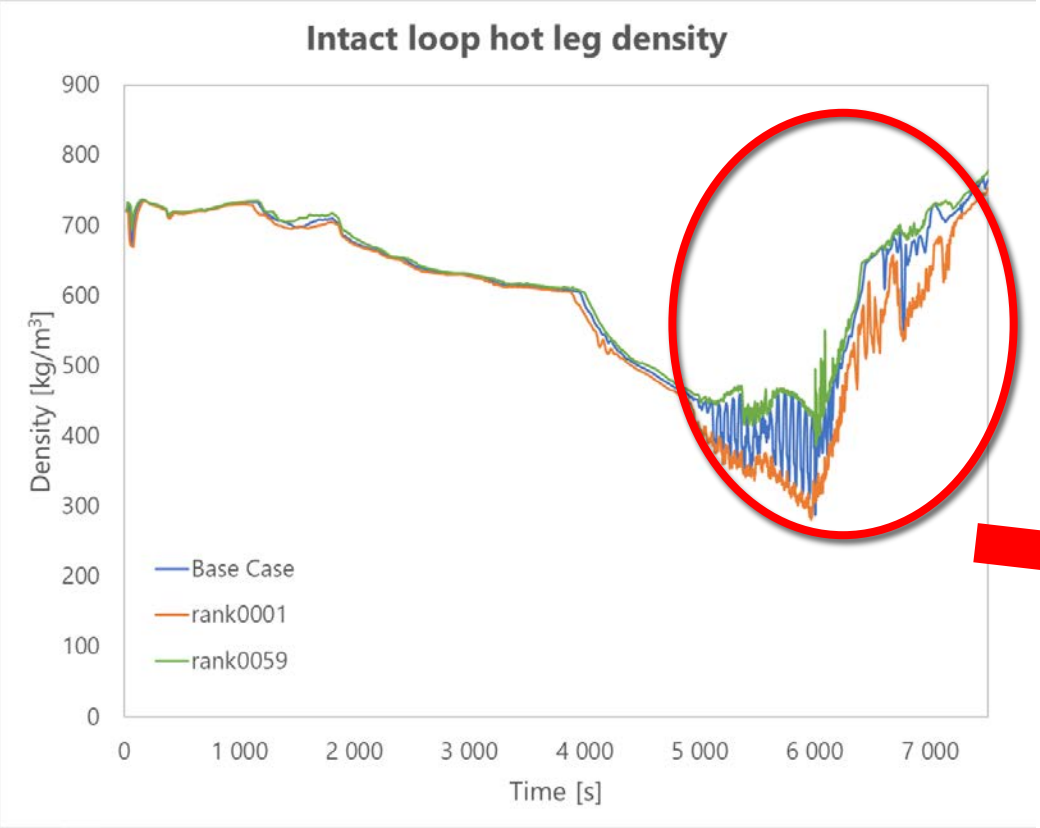


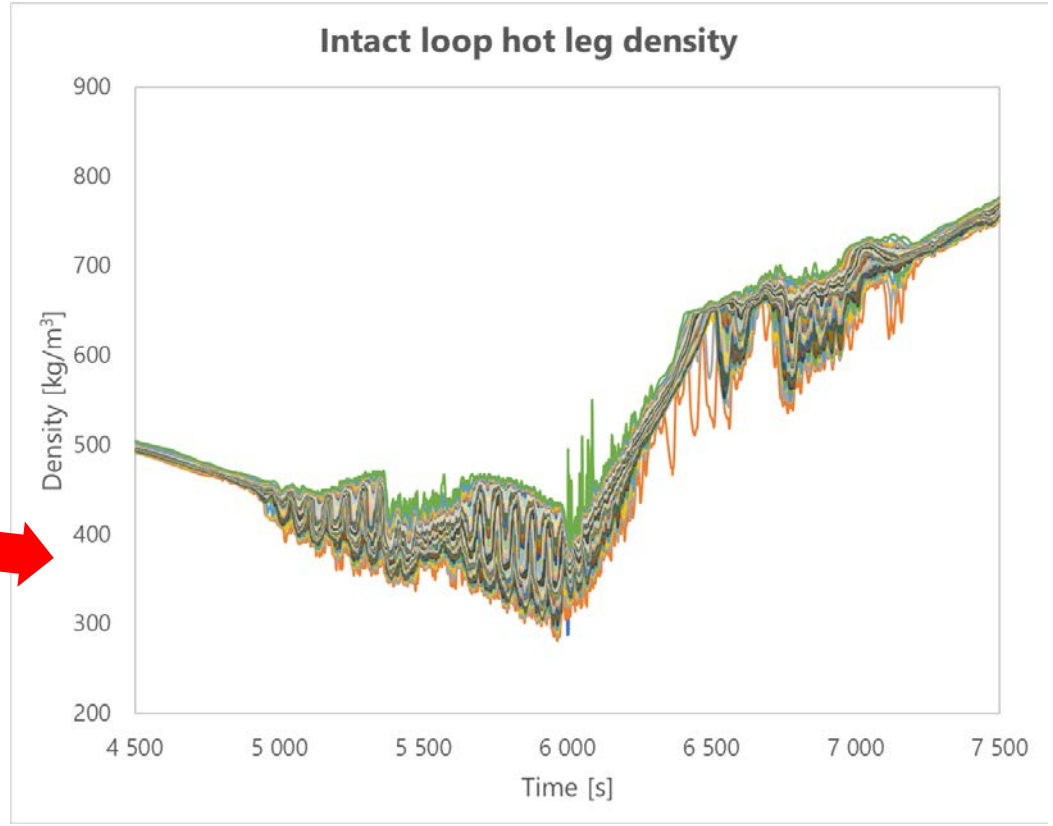
Results - pressures



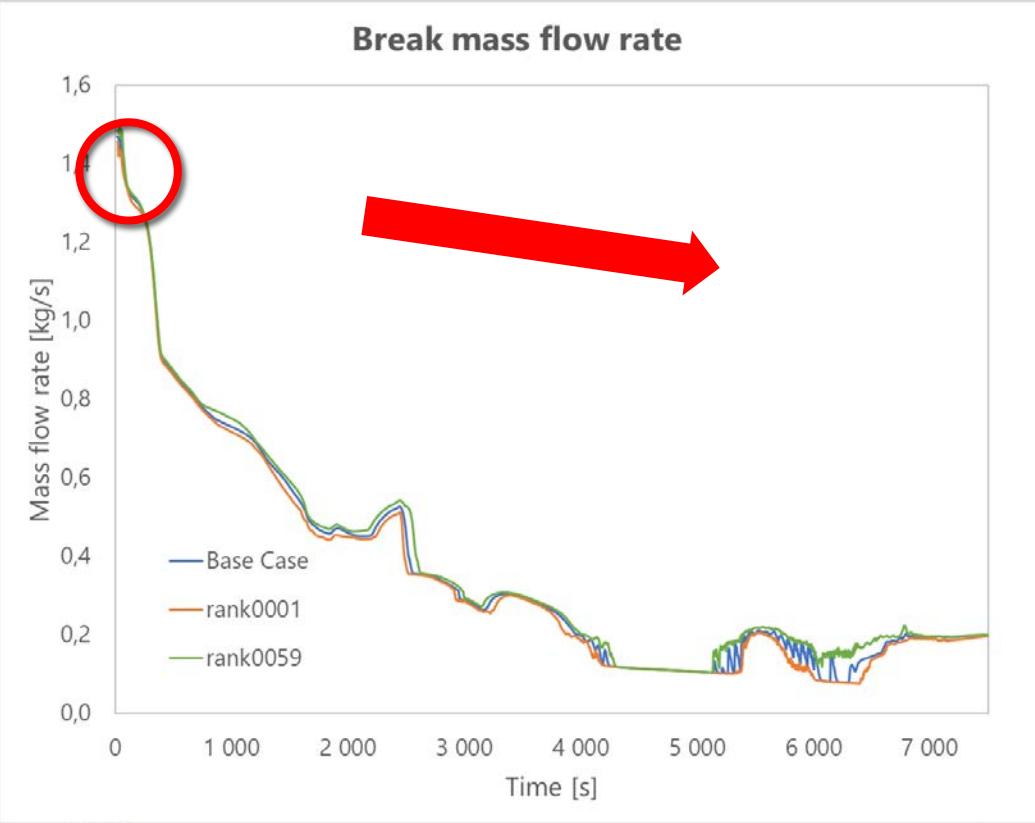


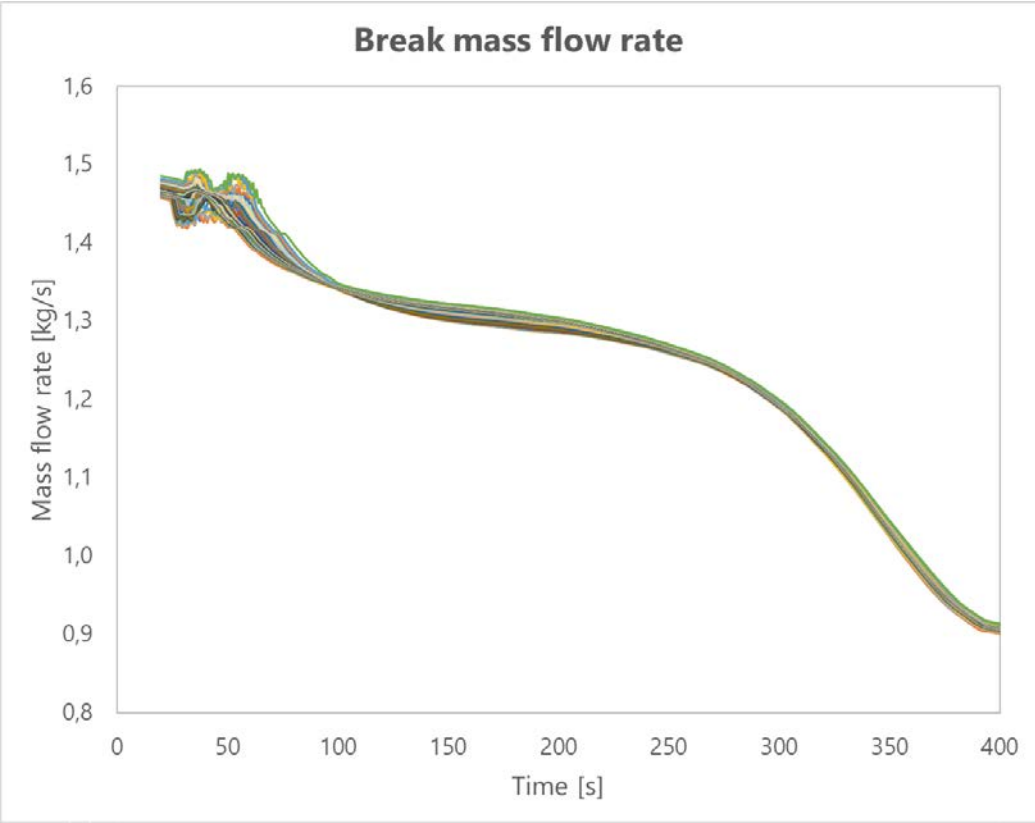
Results – intact loop hot leg density



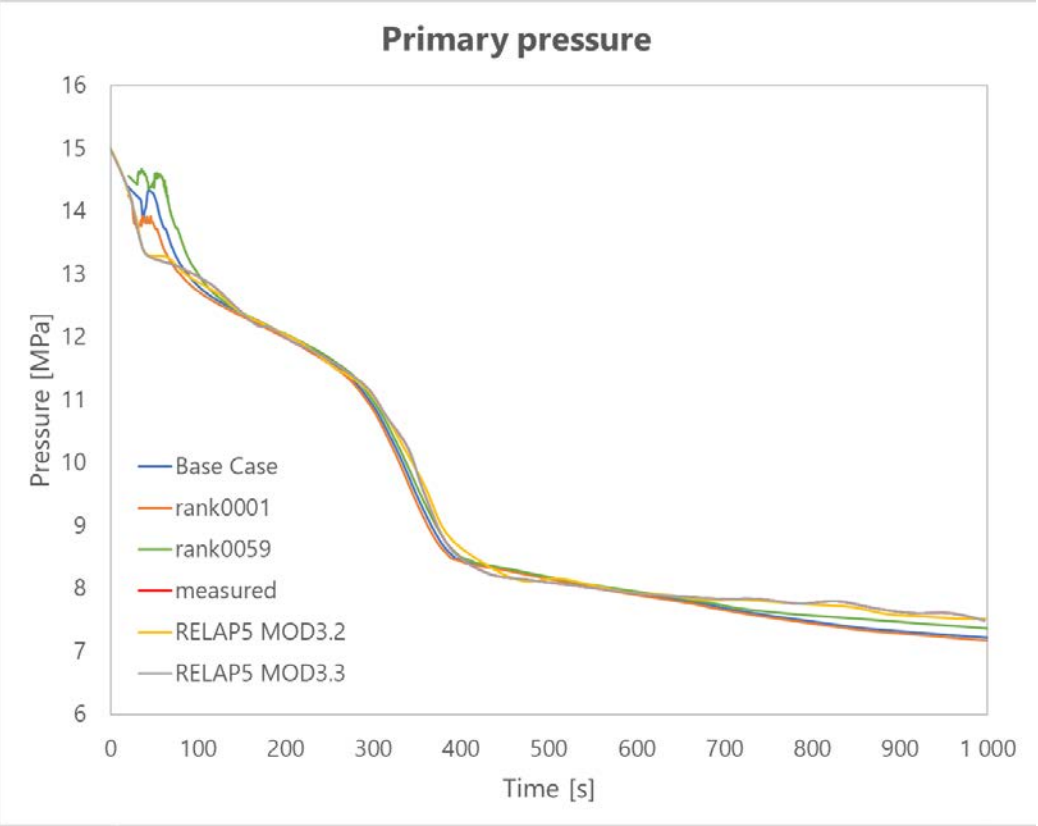


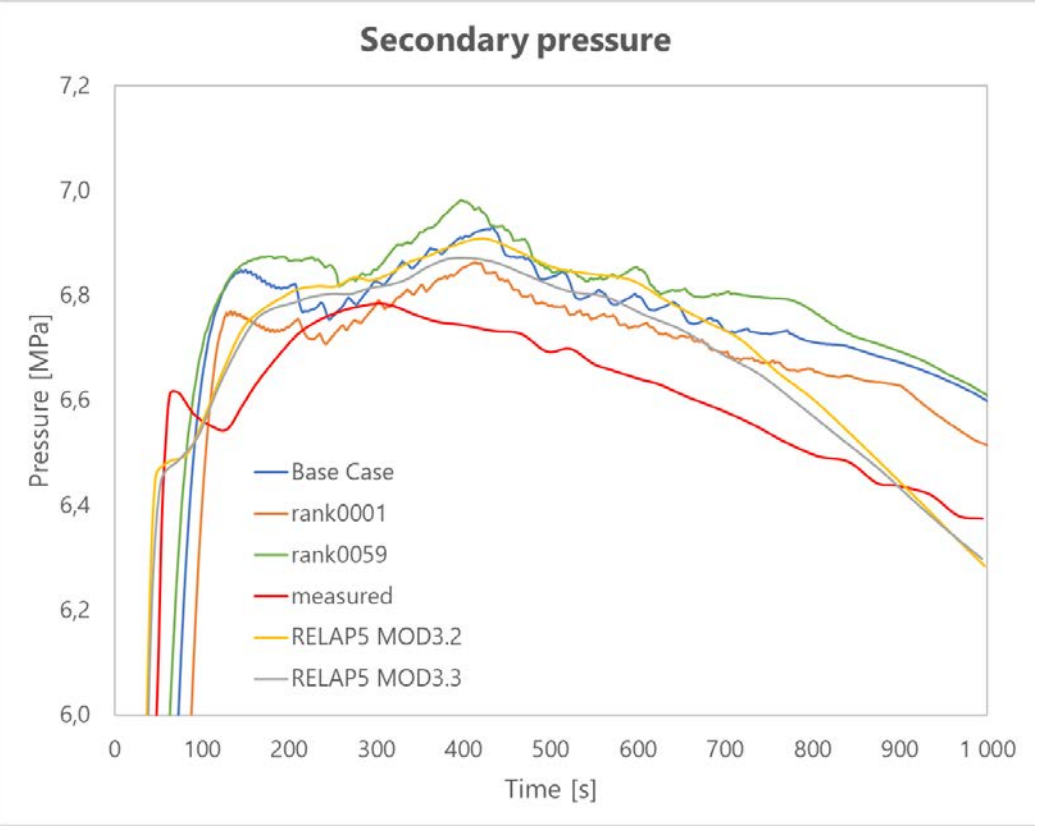
Results – break flow rate



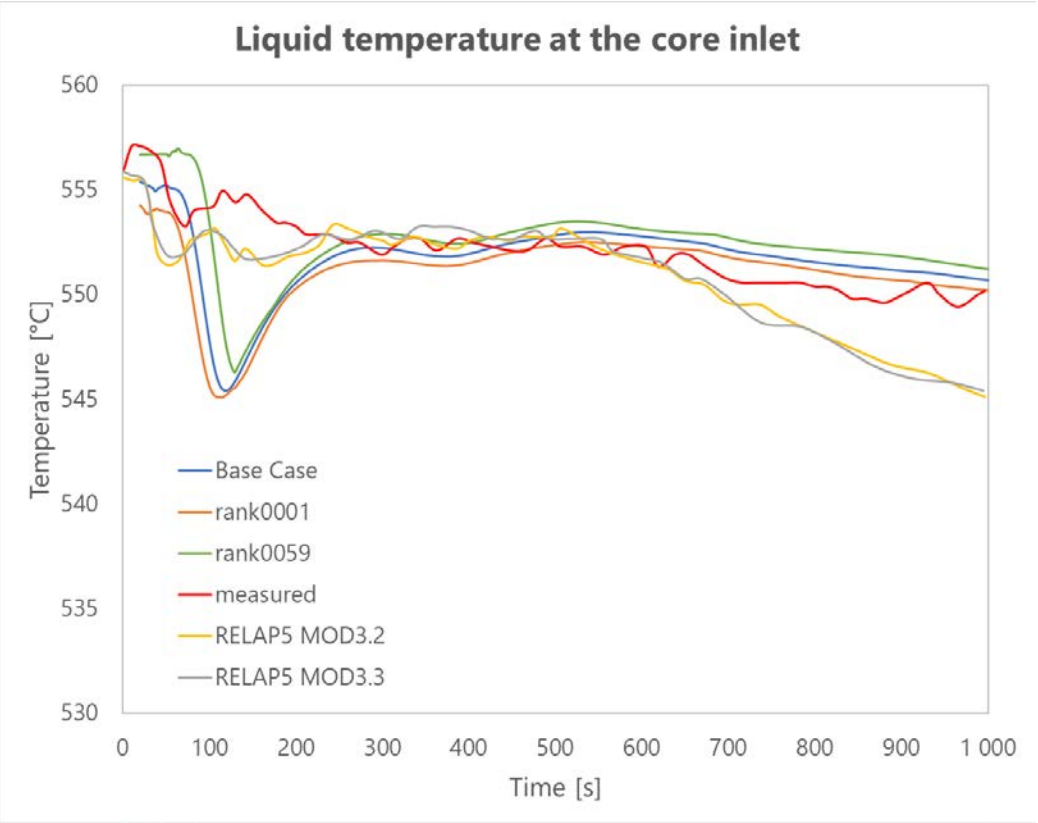


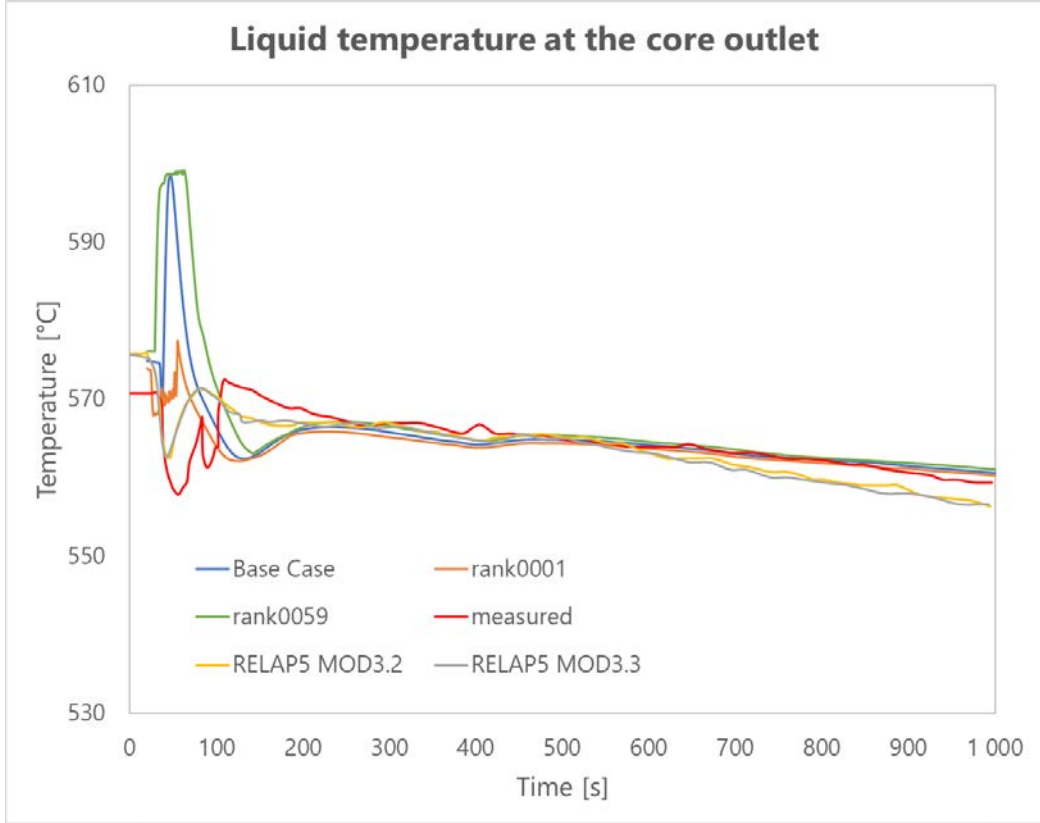
Results verification



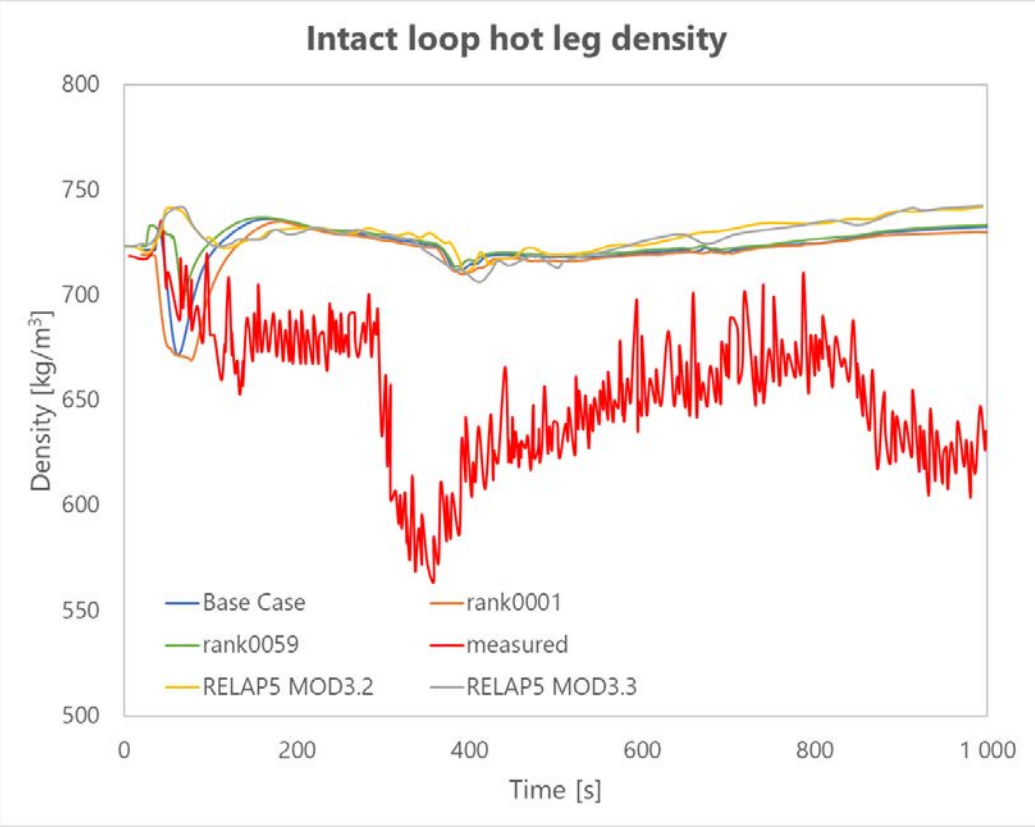


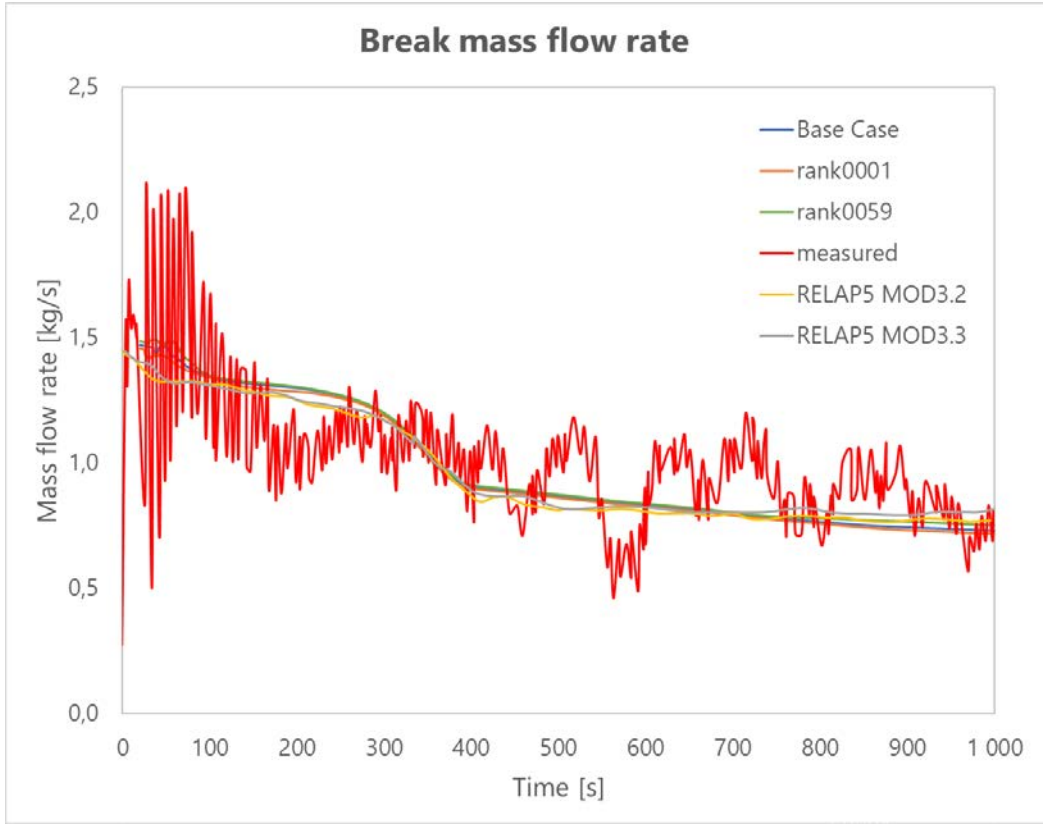
Results verification





Results verification





Conclusions

- RELAP5 MOD3.4 gives adequate represetnation of temperature of liquid flowing in and out of the core. During most of the transient duration, measured values are close (1-3 K) or within uncertainties range. Greater errors appear during the first phase of the experiment: at the core inlet absolute error does not exceed 10 K and at the core outlet the code overpredicts the temperature by max. 40 K.
- Calculations of primary pressure are nearly perfect, again, with slight overprediction after HPIS injection initiation. Secondary pressure varies with time shift to the measured values.
- Significant uncertainty appears in case of density calculations after saturation temperature is reached. Verification of the results is difficult, however, due to high measurement noise.
- MOD3.4, using Ransom-Trapp model, gives prediction of break mass flow rate by few percent different to NRC MOD3.2 and 3.3 (Henry-Fauske model). High noise makes models assessment impossible.
- Further research on this experiment may include uncertainty input improvement, as well as other available models testing. Also, code assessment by LOFT LP-FP-2 experiment modeling is ongoing.

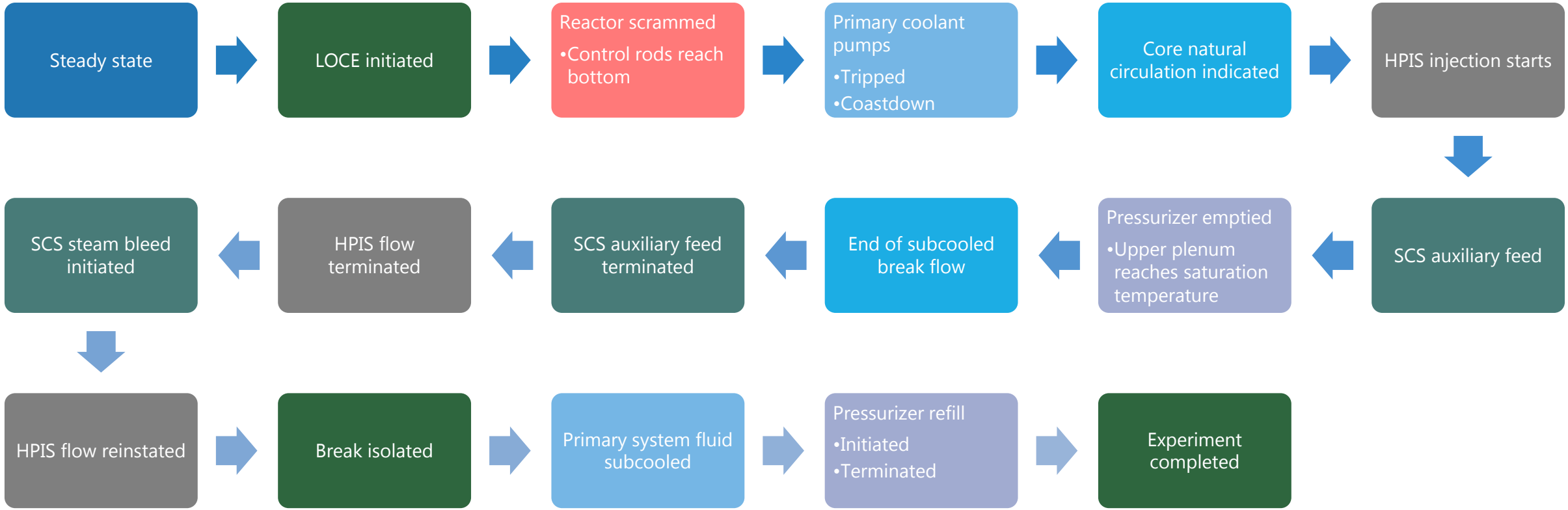
Thank you for your attention!

Questions?

kedzierska_barbara@wp.pl

Support slides

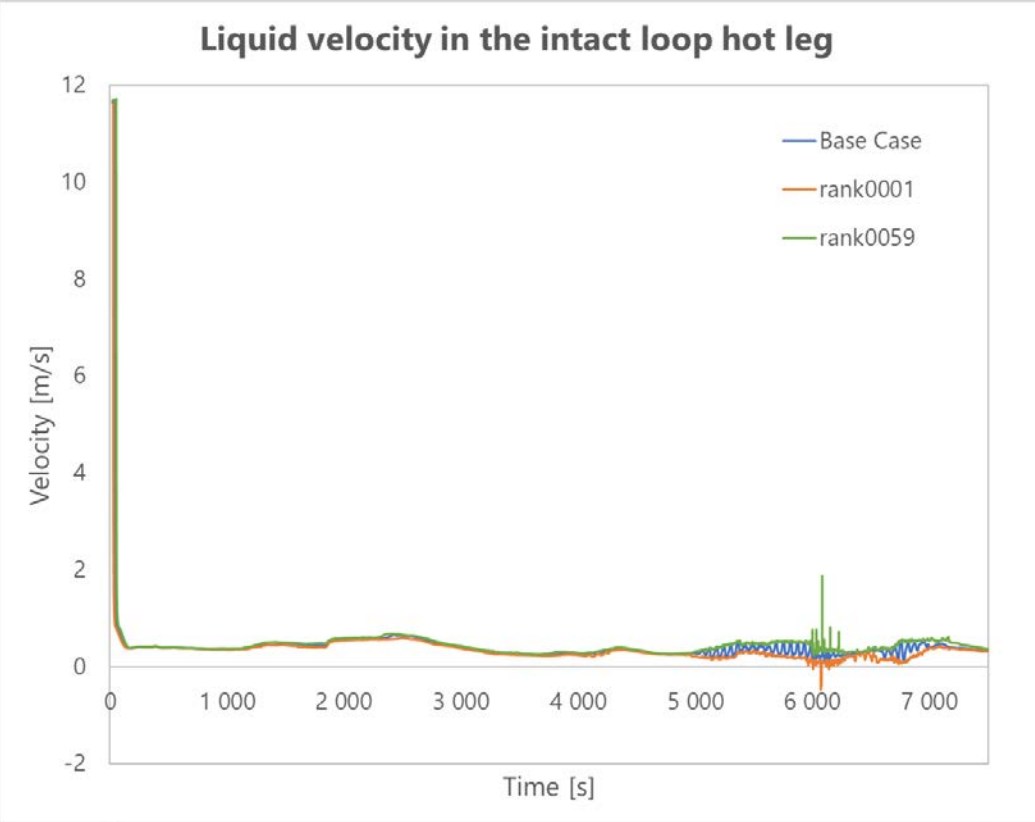
LOFT L3-7 Events

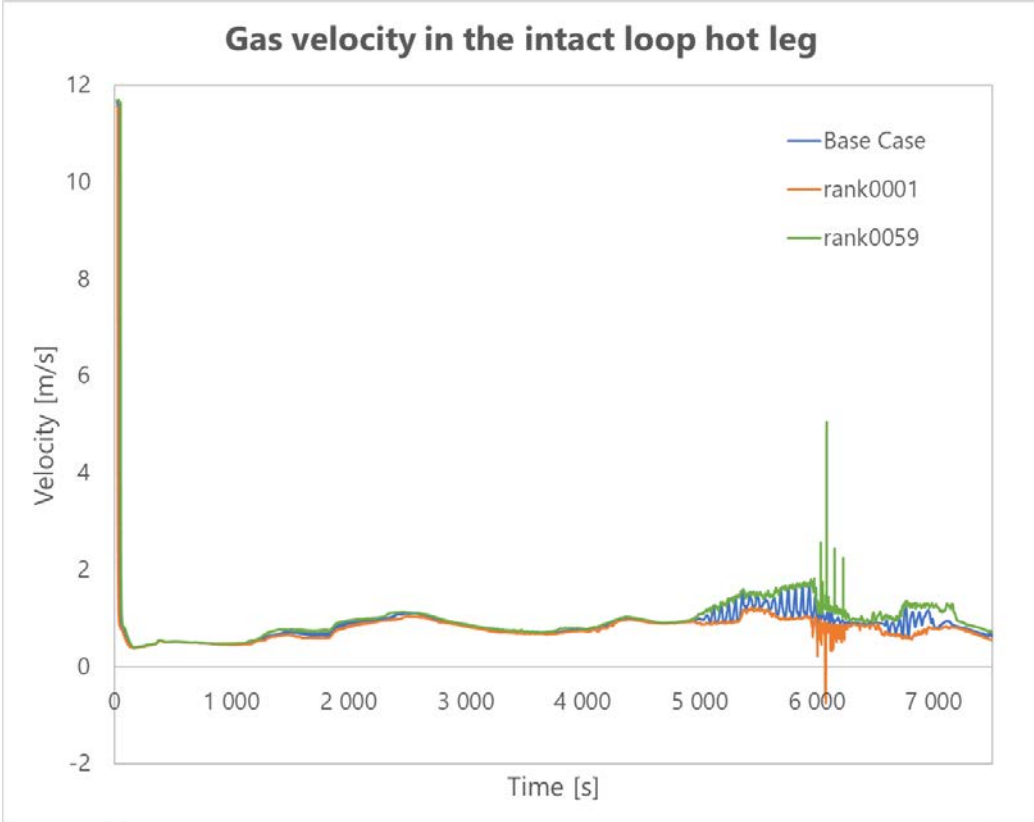


Times of main events

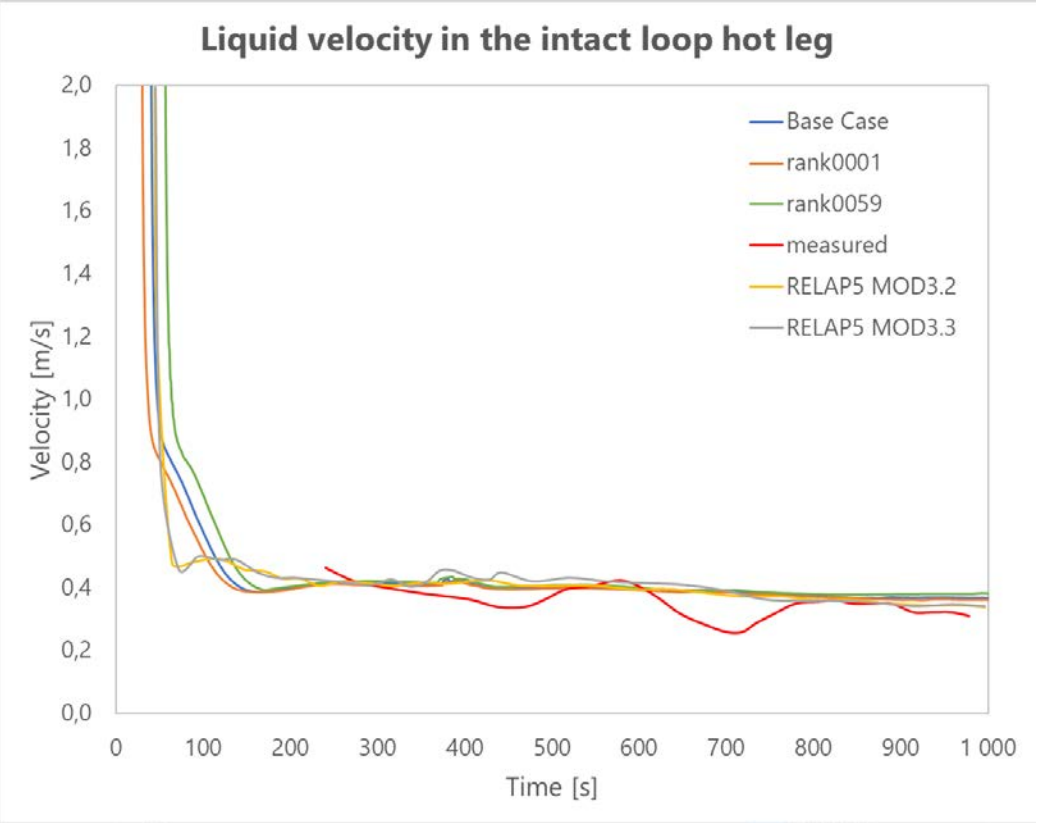
Event	Time [s]				
	Measured	Calculated (MOD2)	Calculated (MOD3.4 with IUA)		
			Rank0001	Base case	Rank0059
Transient initiated – break opens	0	0	-0.1	0	0.1
Reactor scram signal	36	-	24	28	35
Primary coolant pumps tripped	39	34	24	28	35
HPIS injection started	66	71	52	62	75
Secondary system auxiliary feed initiated	75	100	71	83	98
Pressurizer emptied	264	182	222	248	264
Secondary system auxiliary feed terminated	1800	-	1797	1889	1976
HPIS flow terminated	1805	1820	1776	1800	1851
HPIS flow reinstated	5974	5974	5943	5974	6023
Accumulator injection initiated	6028	5581	5308	5407	5539
Break isolated	7302	-	7217	7302	7389

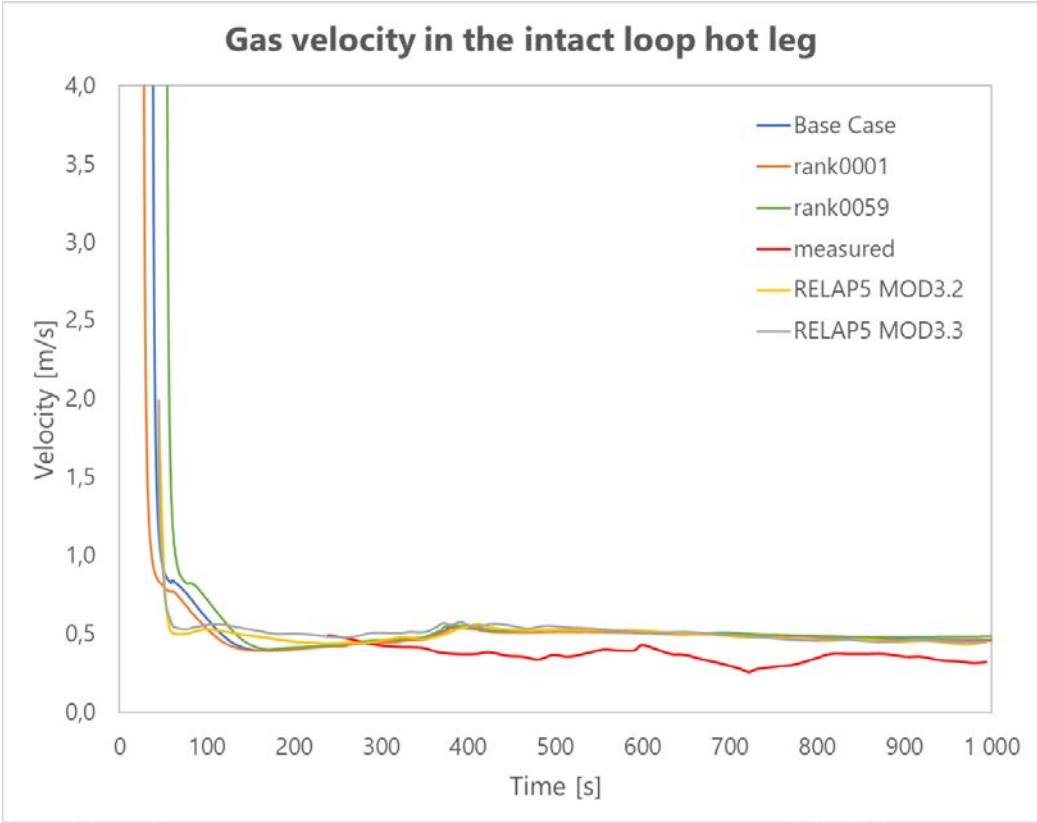
Results –intact loop hot leg velocities



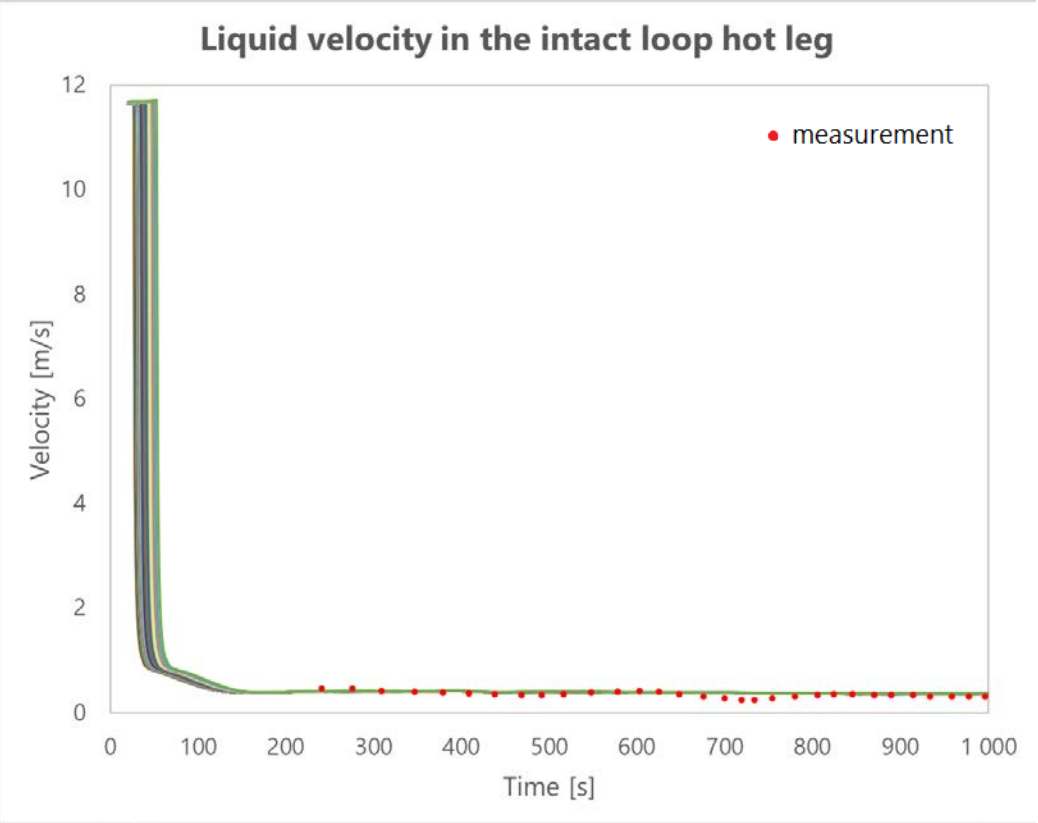


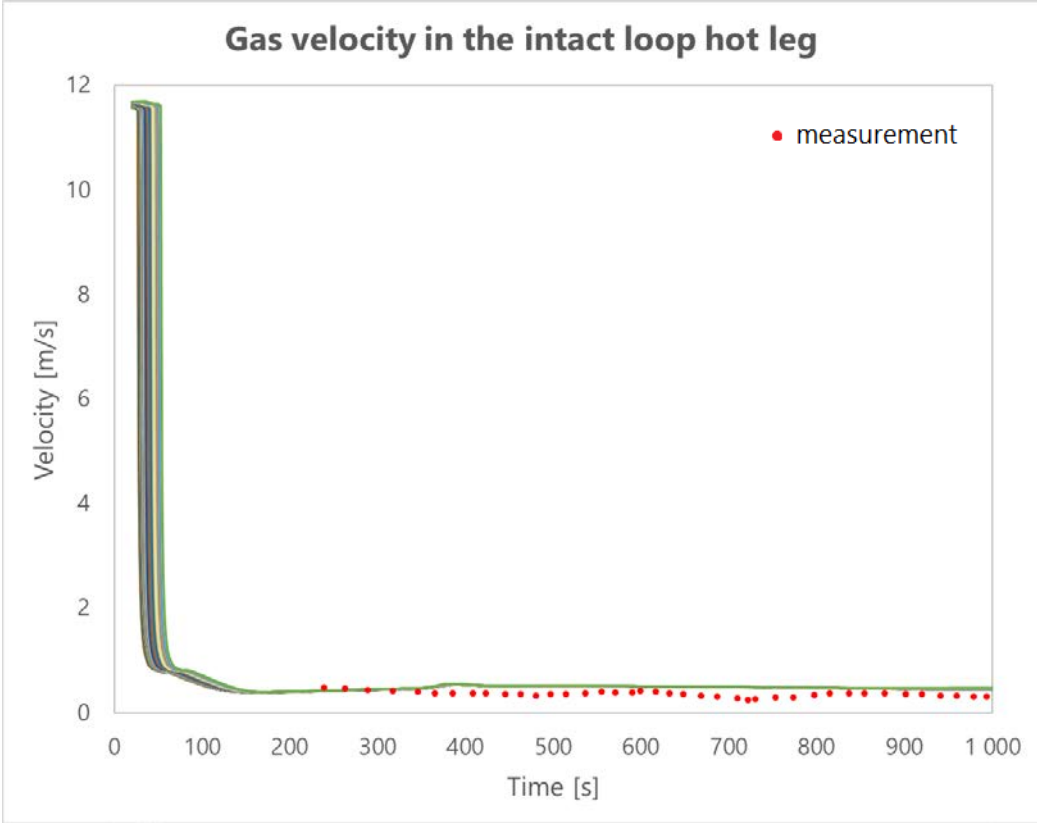
Validation –intact loop hot leg velocities



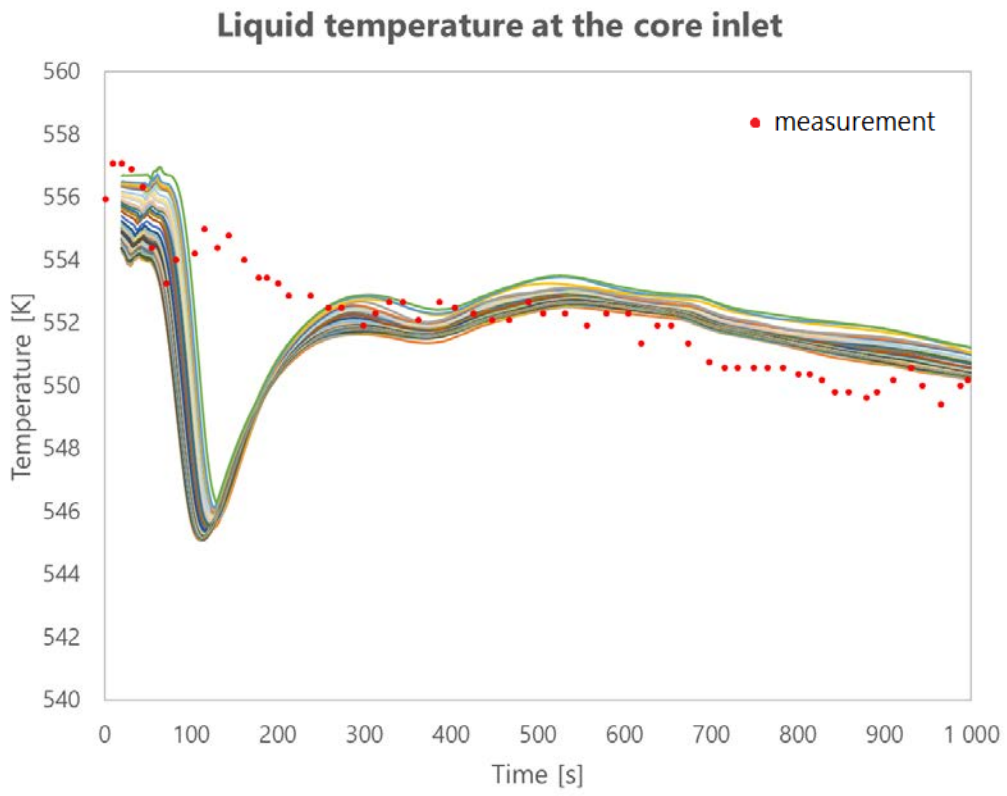


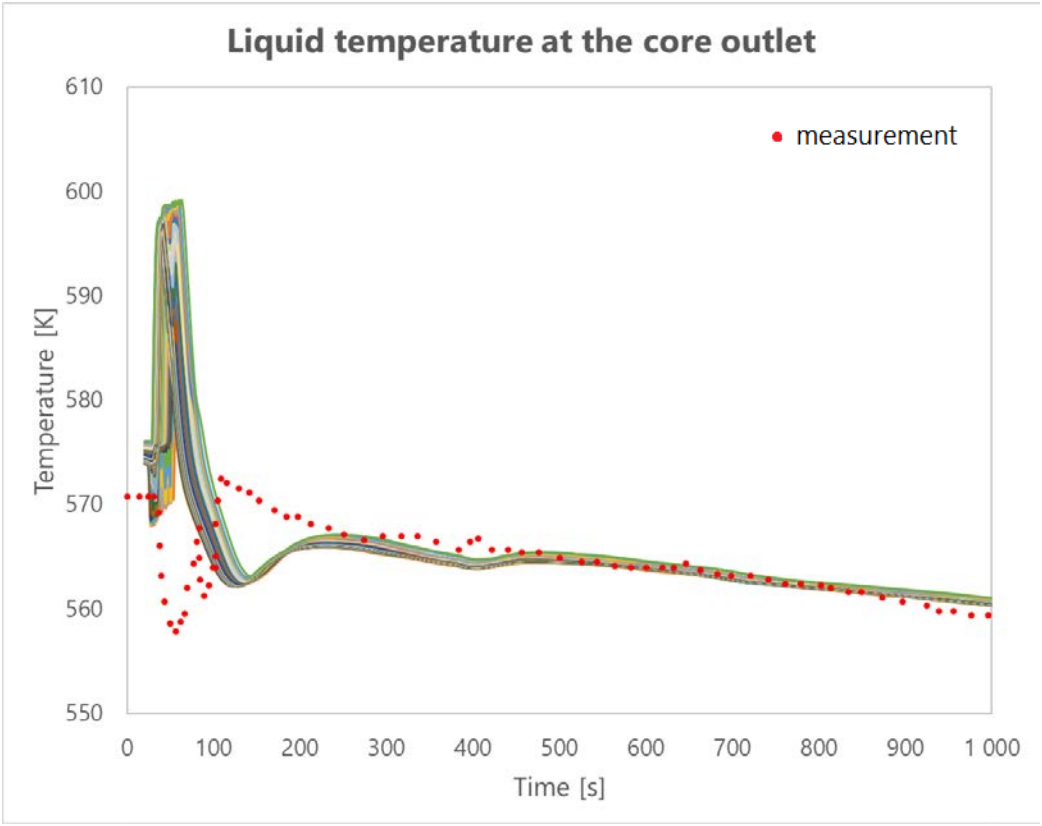
Results


Liquid velocity in the intact loop hot leg
measurement
Velocity [m/s]
Time [s]
0
2
4
6
8
10
12
0
100
200
300
400
500
600
700
800
900
1 000

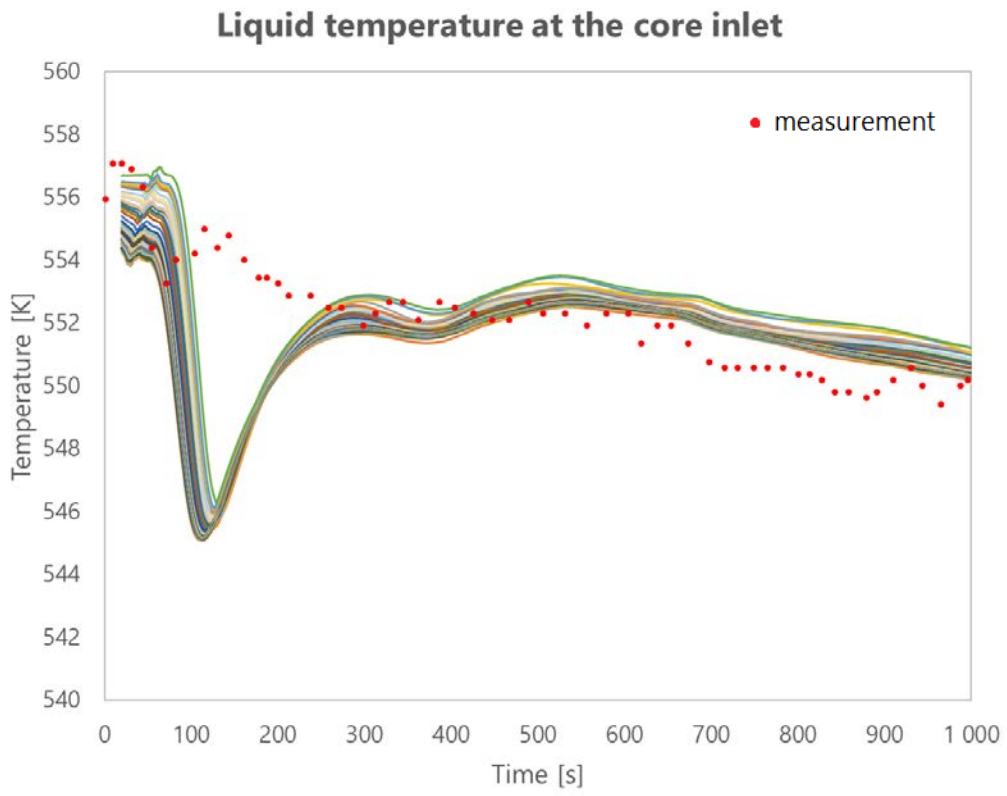

Gas velocity in the intact loop hot leg
measurement
Velocity [m/s]
Time [s]
0
2
4
6
8
10
12
0
100
200
300
400
500
600
700
800
900
1 000

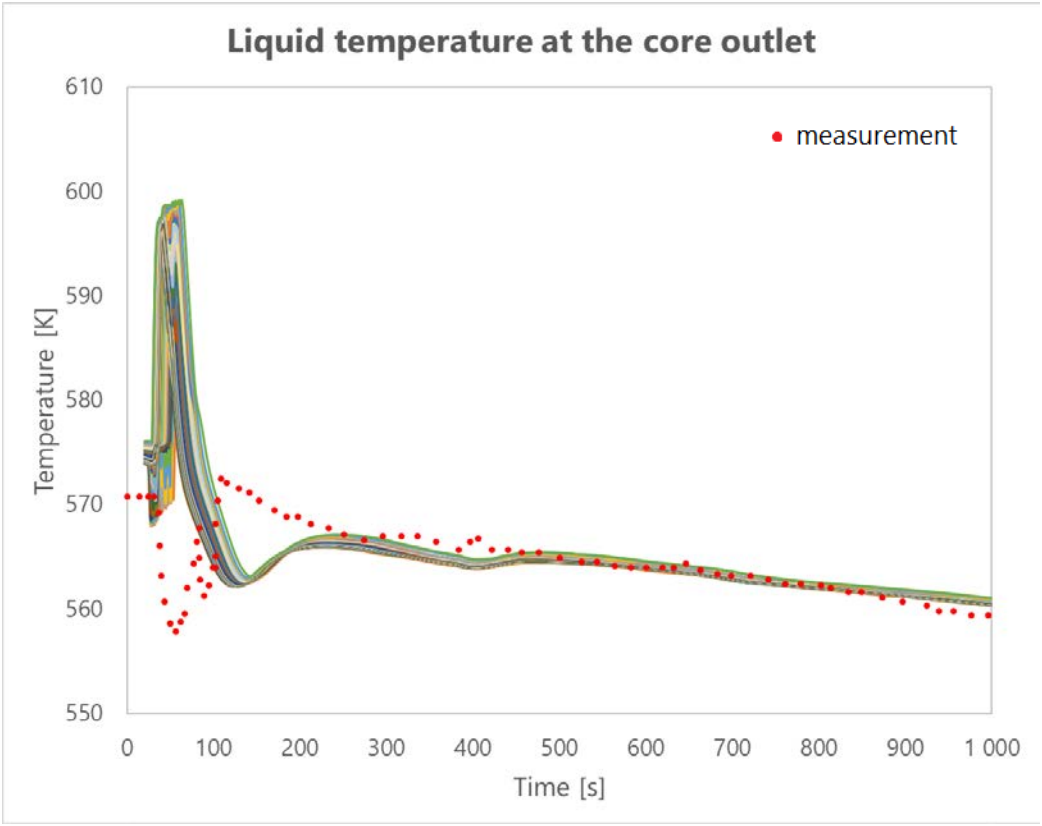
Results


Liquid temperature at the core inlet
measurement
Temperature [K]
560
558
556
554
552
550
548
546
544
542
540
0
100
200
300
400
500
600
700
800
900
1 000
Time [s]

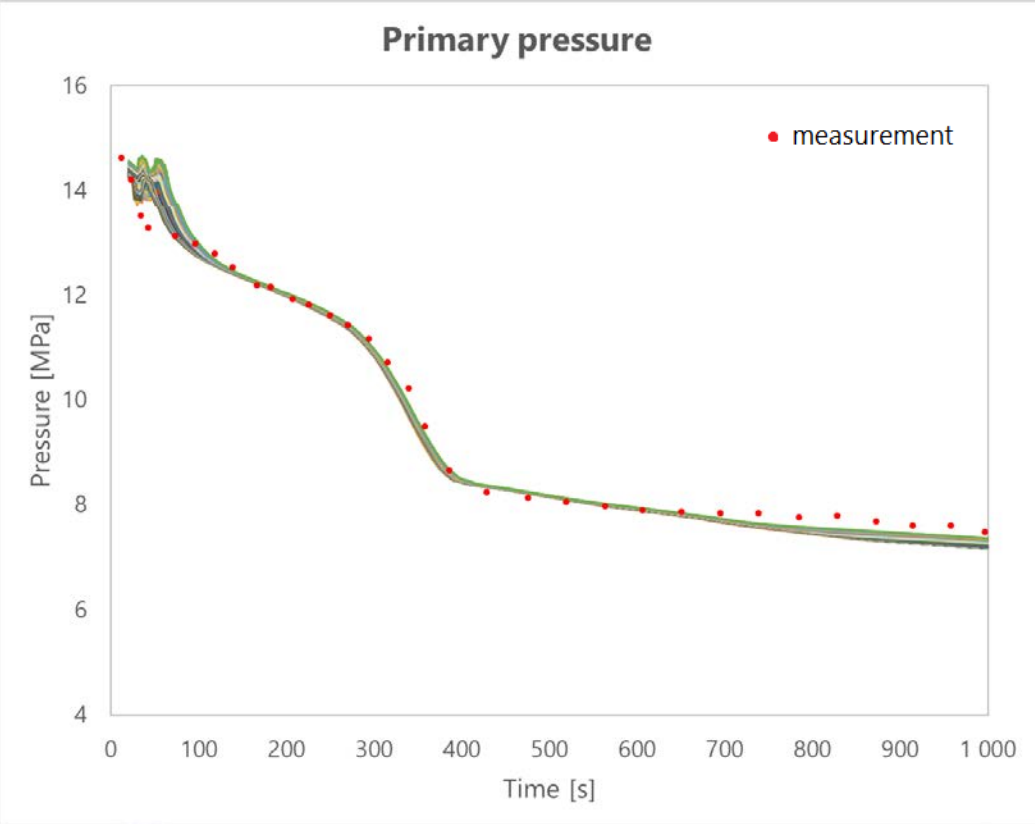

Liquid temperature at the core outlet
measurement
Temperature [K]
610
600
590
580
570
560
550
0
100
200
300
400
500
600
700
800
900
1 000
Time [s]

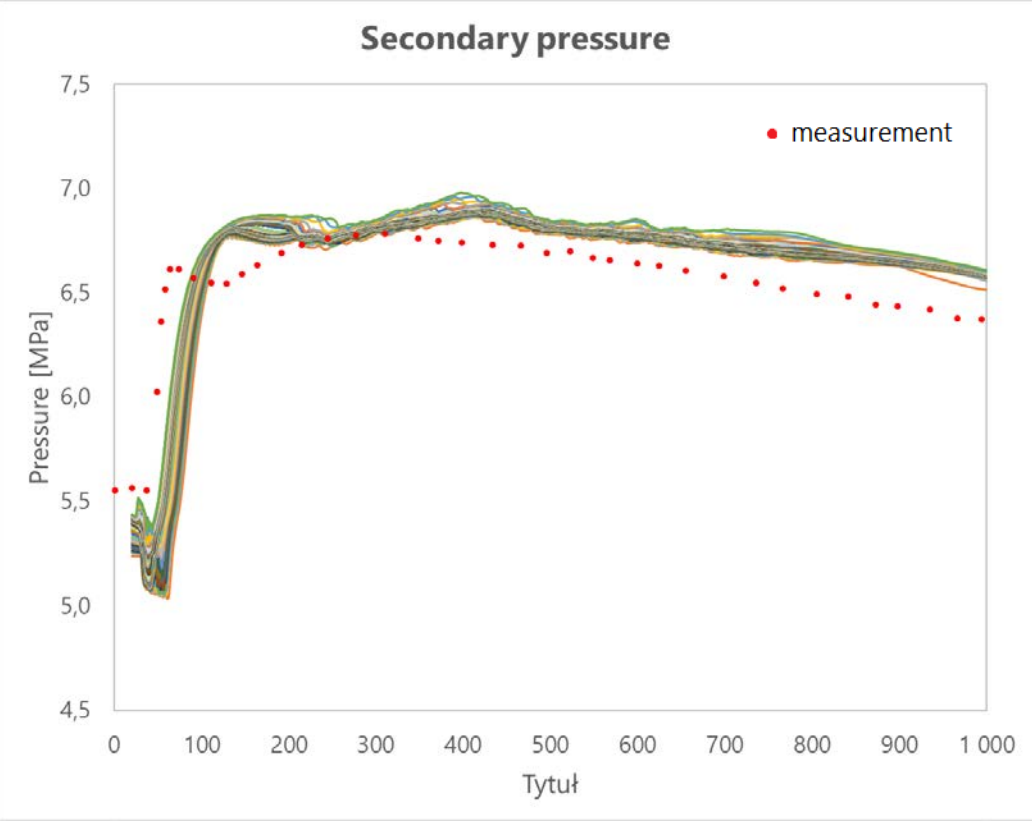
Results


Liquid temperature at the core inlet
measurement
Temperature [K]
560
558
556
554
552
550
548
546
544
542
540
0
100
200
300
400
500
600
700
800
900
1 000
Time [s]

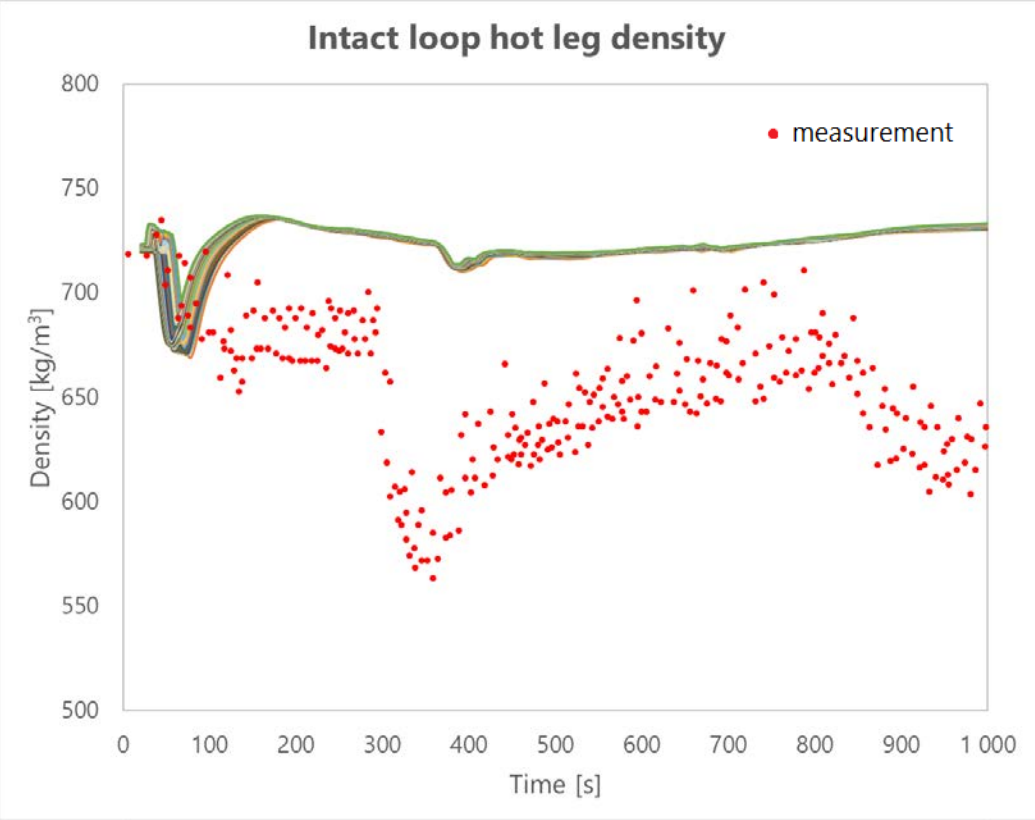

Liquid temperature at the core outlet
measurement
Temperature [K]
610
600
590
580
570
560
550
0
100
200
300
400
500
600
700
800
900
1 000
Time [s]

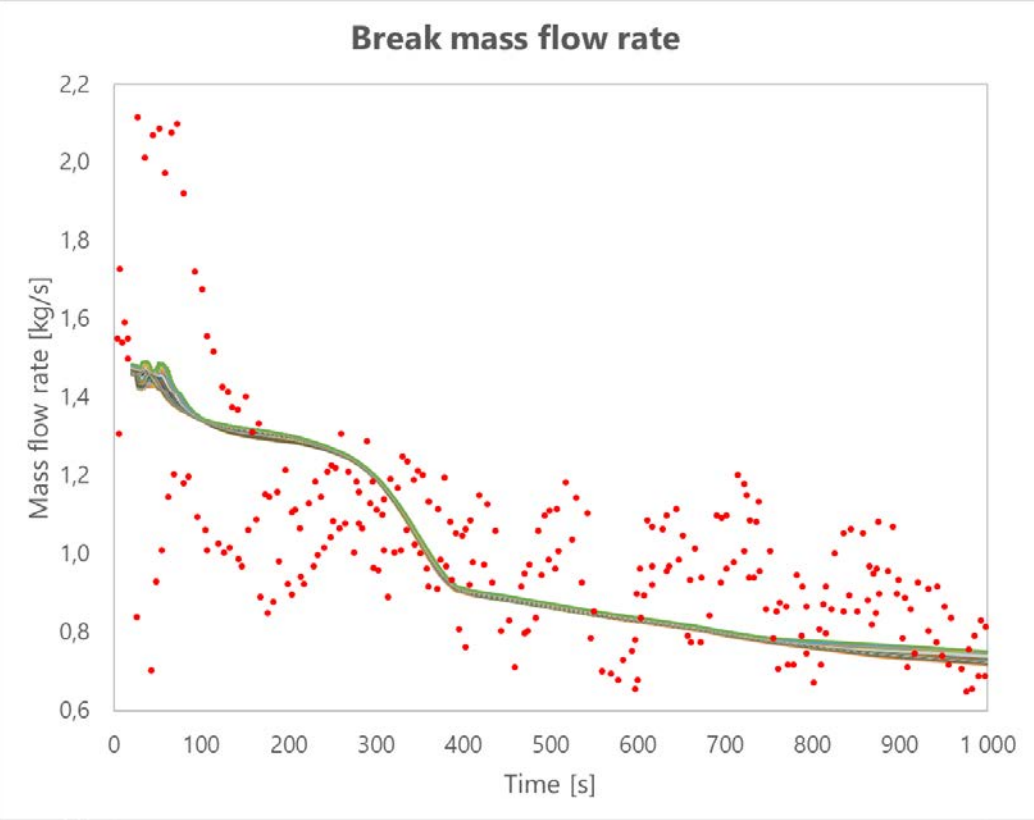
Results


Primary pressure
measurement
Pressure [MPa]
16
14
12
10
8
6
4
0
100
200
300
400
500
600
700
800
900
1 000
Time [s]


Secondary pressure
measurement
Pressure [MPa]
7,5
7,0
6,5
6,0
5,5
5,0
4,5
0
100
200
300
400
500
600
700
800
900
1 000
Tytuł

Results


Intact loop hot leg density
measurement
Density [kg/m³]
800
750
700
650
600
550
500
0
100
200
300
400
500
600
700
800
900
1 000
Time [s]


Break mass flow rate
Mass flow rate [kg/s]
2,2
2,0
1,8
1,6
1,4
1,2
1,0
0,8
0,6
0
100
200
300
400
500
600
700
800
900
1 000
Time [s]

PSI-KIT Nitriding Model with Validation Calculations

B. Jäckel, L. Fernandez-Moguel, T. Lind, S. Park, M, Steinbrück

ABSTRACT

Two full scale experiments conducted in 2011 and 2012 at the Sandia National Laboratories during the Sandia Fuel Project (SFP), three QUENCH bundle tests at KIT as well as many separate effect tests in various labs have shown that nitrogen plays an active role in the degradation process of the Zr-based fuel cladding materials. Cladding oxidation in the presence of nitrogen may lead to accelerated loss of the only barrier for the fission product release in case of a spent fuel storage accident. To account for the effect of nitrogen in the cladding degradation, PSI together with KIT has conducted an experimental programme during the years 2014 and 2015.

More than 70 separate effect tests were conducted by a PhD student of PSI at KIT. The results of the tests provide a data base sufficient for the development of a nitriding and re-oxidation model to describe the accelerated degradation of Zr-based cladding materials under air ingress conditions in the temperature range 900-1200°C. The samples were analyzed not only for the mass gain during exposure to subsequently oxygen, nitrogen, and again oxygen, but also for the composition after the tests using a combined metallographic and image analysis. The conceptual model for nitriding includes formation of ZrO_2 and oxygen stabilized α-Zirconium (α-Zr(O)) during pre-oxidation in oxygen, the effect of breakaway oxidation, fast nitriding and slow nitriding during the exposure to nitrogen, and the fast re-oxidation of ZrN and remaining metal.

A standalone computer code to describe the nitriding reactions was developed based on the separate effect tests conducted at KIT. In the presentation, the model concept and the first calculations are shown for all phases of pre-oxidation, nitriding and re-oxidation. The model includes the nitriding process under starvation of oxygen and steam and the strongly accelerated process of re-oxidation when oxygen or steam is recovered as observed in several separate effect tests and also integral experiments. The model distinguishes between two regimes, the breakaway regime at temperatures below 1050°C and the non-breakaway regime above 1050°C. In the high temperature regime the acceleration of the oxidation is based on the morphology change due to the nitriding reaction (porous structure of ZrO_2 formed by re-oxidation of ZrN).



PAUL SCHERRER INSTITUT

PSI



B. Jäckel, L. Fernandez-Moguel, T. Lind, S. Park, M. Steinbrück

PSI-KIT Nitriding Model with Validation Calculations

24th QUENCH Workshop, November 13-15, 2018

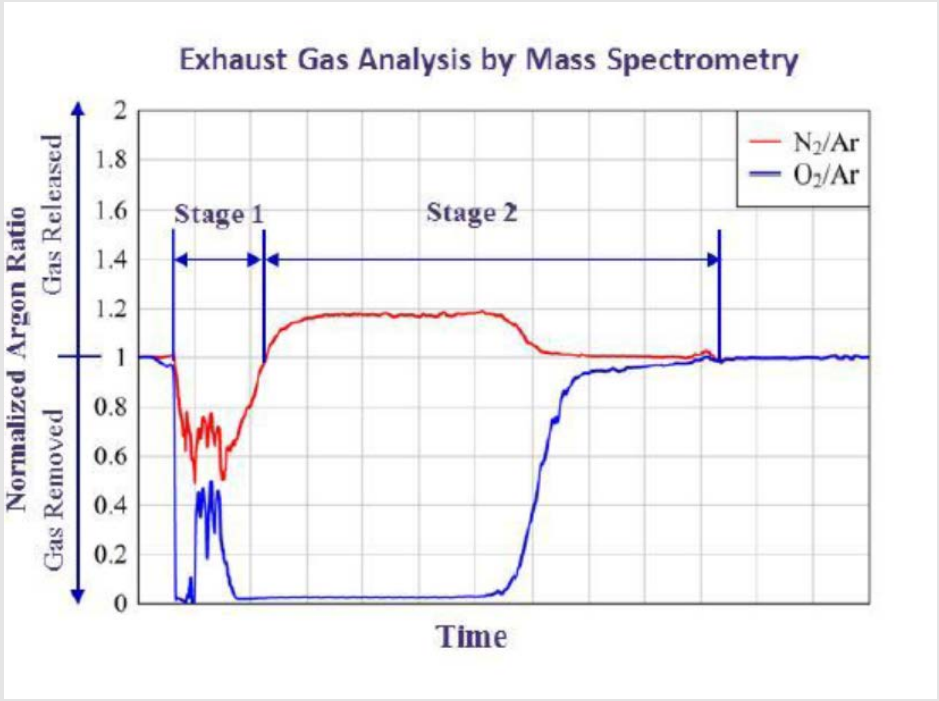
PAUL SCHERRER INSTITUT

Content

1. Motivation
2. Model Scheme
   1. Pre-oxidation
   2. Diffusion
   3. Nitriding
   4. Re-oxidation
3. Separate-effect tests
4. Sandia Fuel Experiment Phase II
5. Outlook

Sandia Fuel Project phase II (2011)



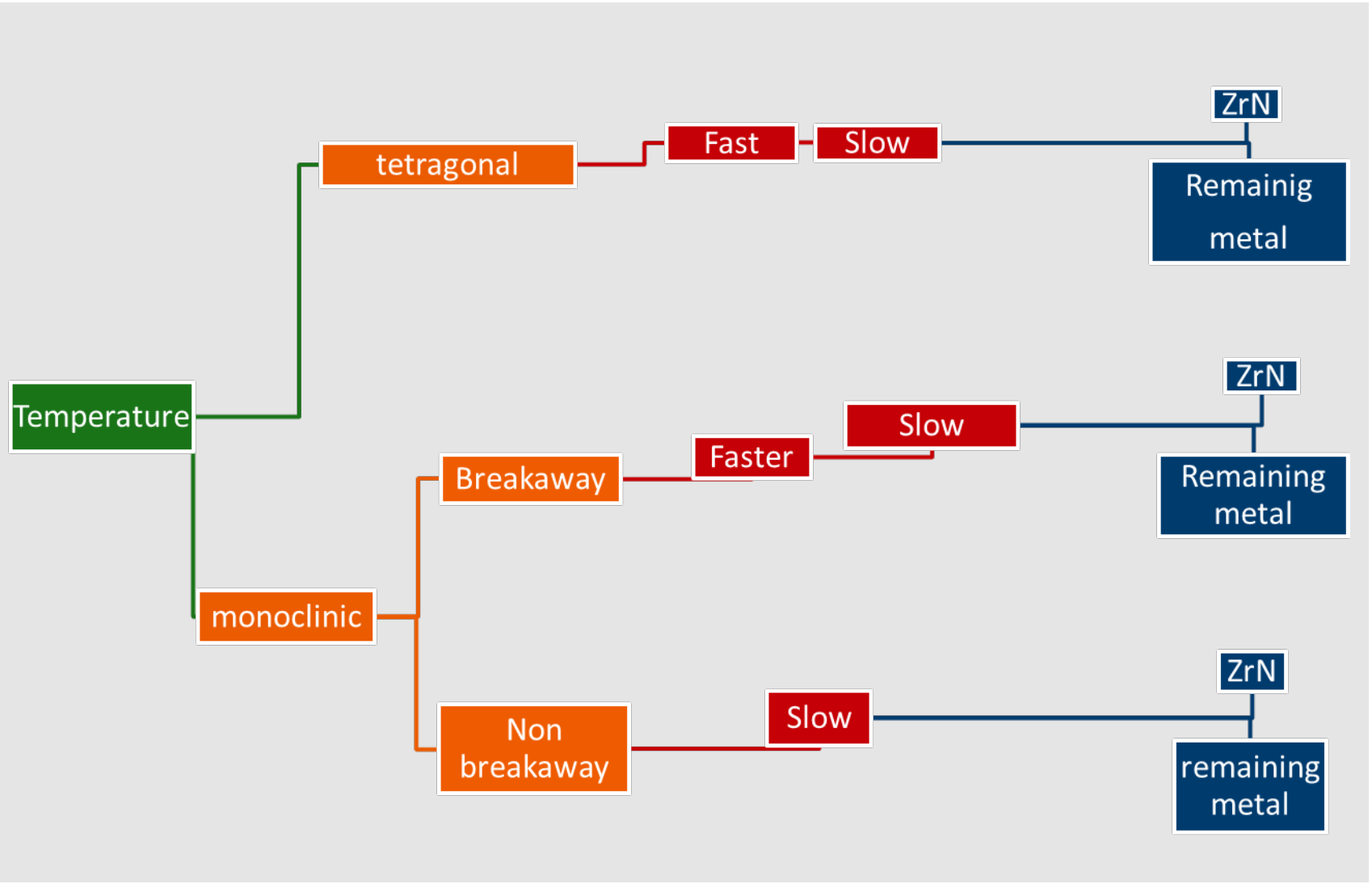


PAUL SCHERRER INSTITUT

Content

1. Motivation
2. Model Scheme
   1. Pre-oxidation
   2. Diffusion
   3. Nitriding
   4. Re-oxidation
3. Separate-effect tests
4. Sandia Fuel Experiment Phase II
5. Outlook

Model Scheme



Pre-oxidation

Standard oxidation correlations are used to calculate oxidation by steam, air and oxygen.

Below 1050°C PSI-breakaway model is used.

Above 1050°C PSI-breakaway model is used only for air.

Additional to earlier model α-Zr(O) is calculated using the Leistikow correlation.

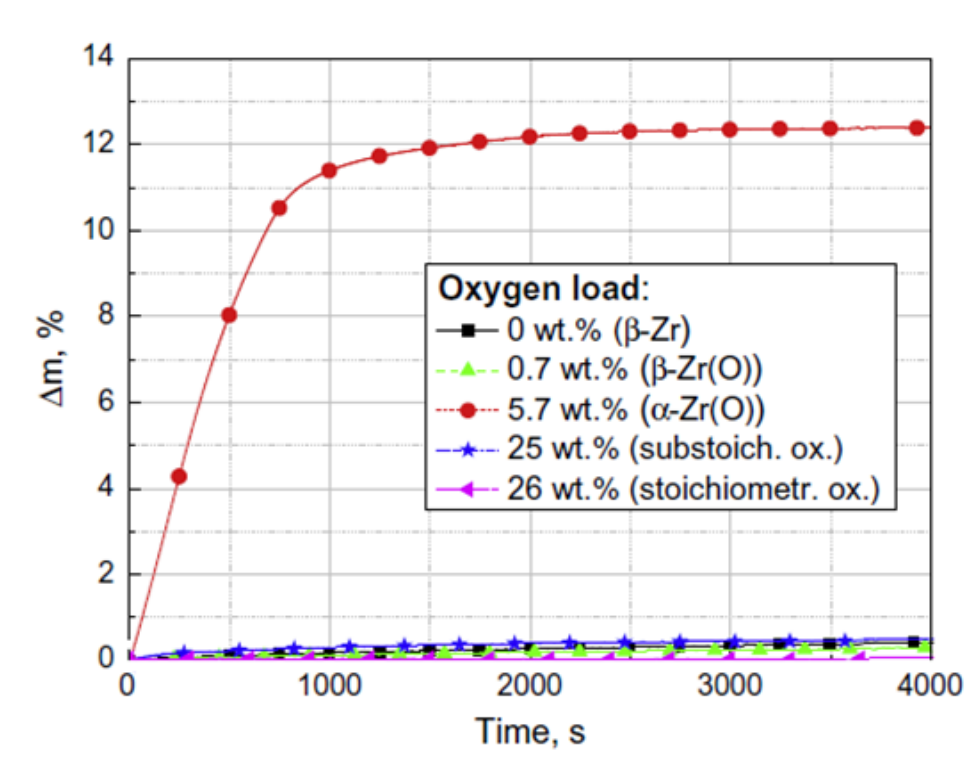
(during partial oxygen and steam starvation production of α-Zr(O) is enhanced)

Diffusion

Under complete starvation of steam and oxygen and without presence of nitrogen the oxygen bound in the ZrO_2 layer starts to diffuse into the zirconium metal, building oxygen stabilized alpha zirconium α-Zr(O).

The same correlation from Leistikow as mentioned before is used to calculate the growth of the alpha layer and the reduction of the oxide layer by diffusion. (No weight gain)

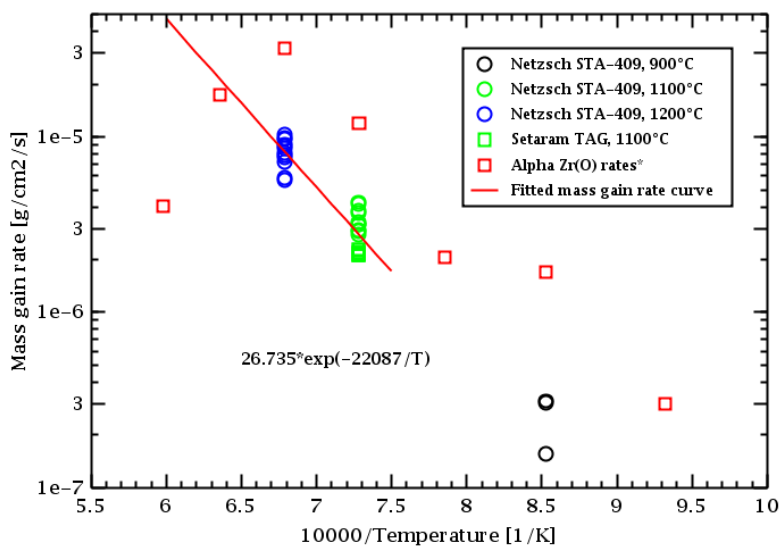
Nitriding

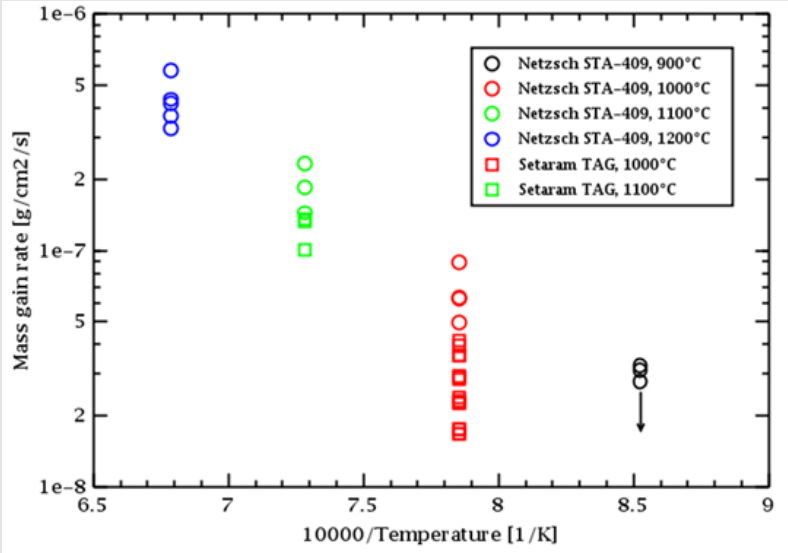


M. Steinbrück, Journal of Nuclear Materials 447 (2014) 46-55

The preferred phase for the nitriding reaction is α-Zr(O) as can be seen from investigations at KIT at 1200°C.

Nitriding





*** M. Steinbrück, Journal of Nuclear Materials 447 (2014) 46-55**

The nitriding correlations in Arrhenius plots are used as constant values for the temperatures. The nitriding reaction is not parabolic (or protective) as the oxidation reaction. The data are calculated from SETs conducted at KIT.

Re-oxidation

The re-oxidation starts fast with the oxidation of the ZrN and slows down when ZrN is completely oxidized and the remaining α-Zr(O) and metal will be oxidized

In both temperature regimes the re-oxidation of zirconium metal reaches reaction rates which are known from 'breakaway' experiments (at high temperature only with air)

The post breakaway reaction rates at high temperatures are due to the change in the morphology only

Content

1. Motivation

2. Model Scheme
   1. Pre-oxidation
   2. Diffusion
   3. Nitriding
   4. Re-oxidation

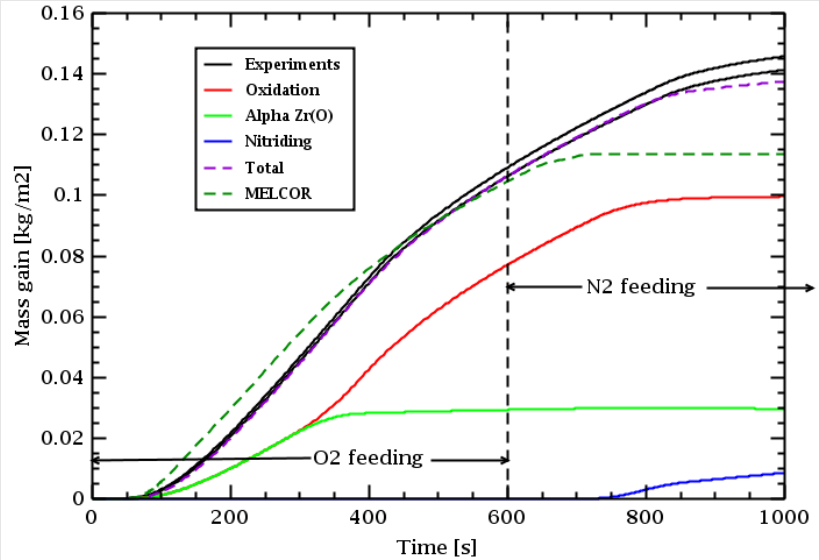
3. Separate-effect tests

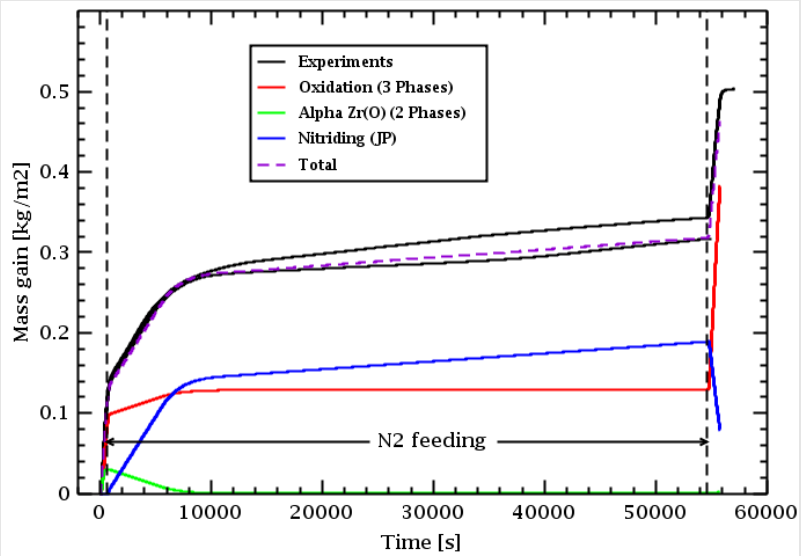
4. Sandia Fuel Experiment Phase II

5. Outlook

Separate-effect tests (PO + N + RO)

1100°C, 10 min O_2, 15 h N_2, 20 min O_2

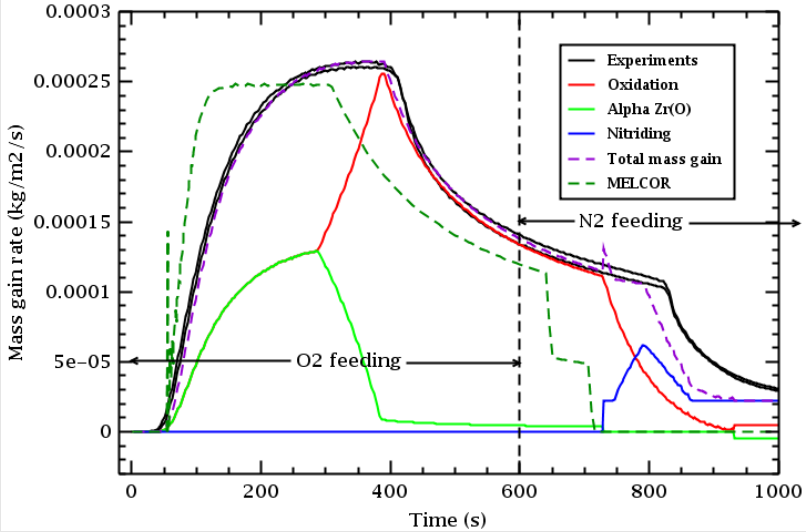


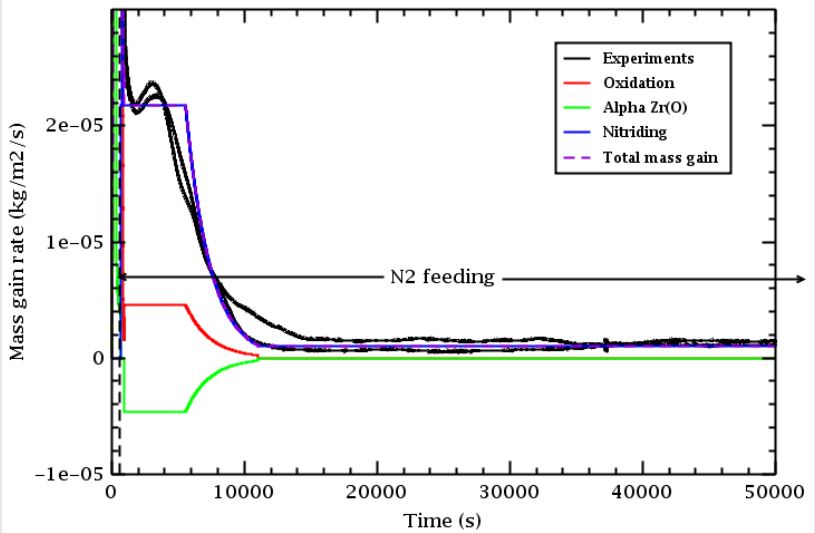


For the mass gain calculation a MELCOR model was constructed for comparison. The pre-oxidation shows good estimation between standalone code, MELCOR and the experimental measurements.

Separate-effect tests (Pre-oxidation and nitriding)

1100°C, 10 min O_2, 15 h N_2, 20 min O_2

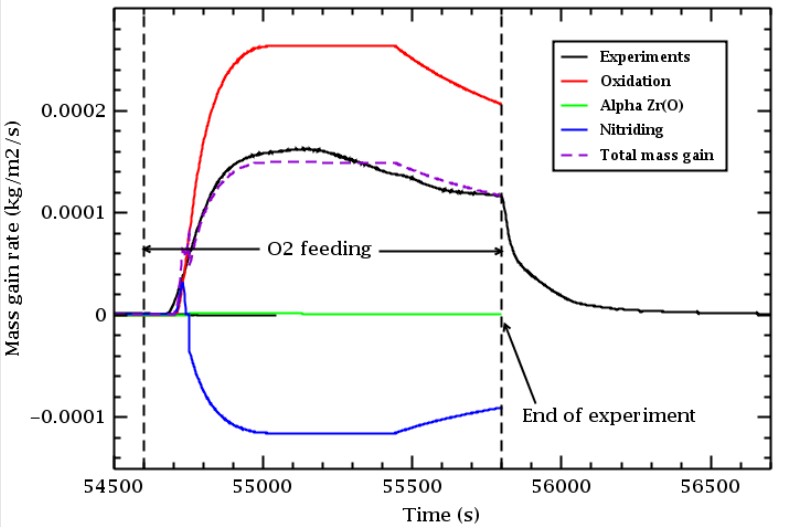




The mass gain rates show a bit more in detail the different species. Under starvation of oxygen the production of α-Zr(O) is enhanced. The nitriding process starts with the fast nitriding rate and slows down after the α-Zr(O) reaches a cutoff thickness.

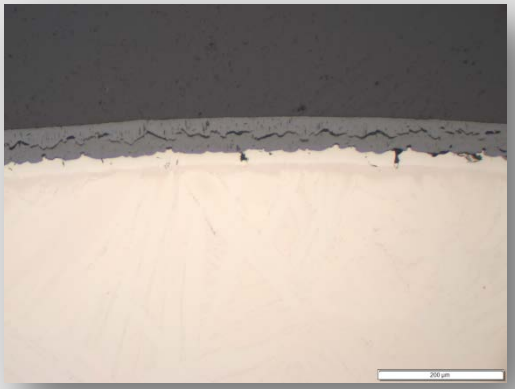
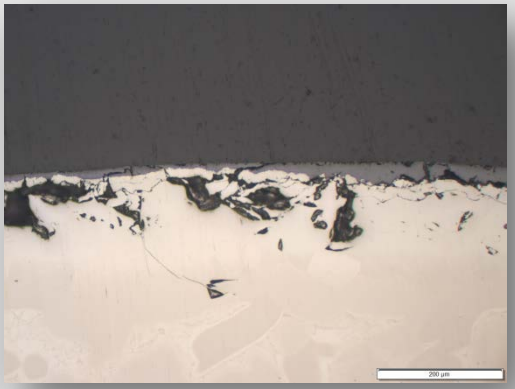
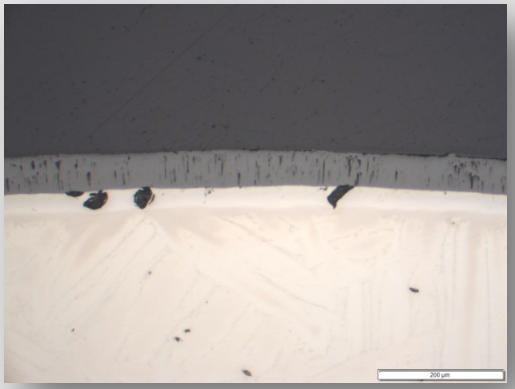
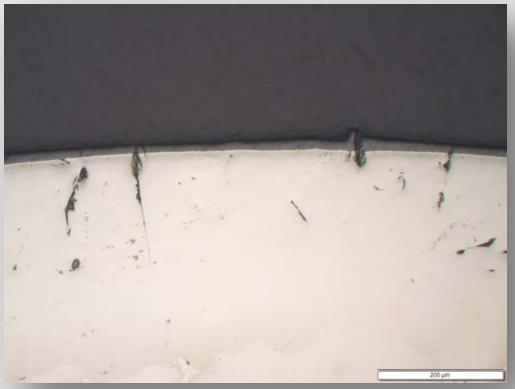
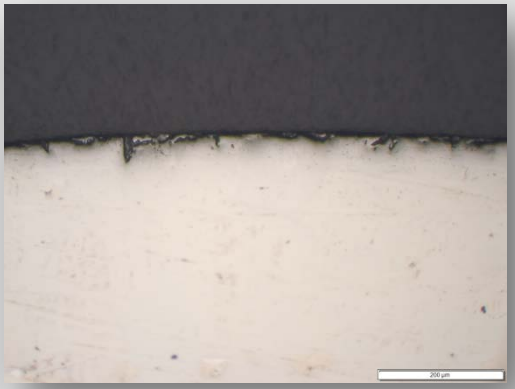
Separate-effect tests (Re-oxidation)

1100°C, 10 min O_2, 15 h N_2, 20 min O_2



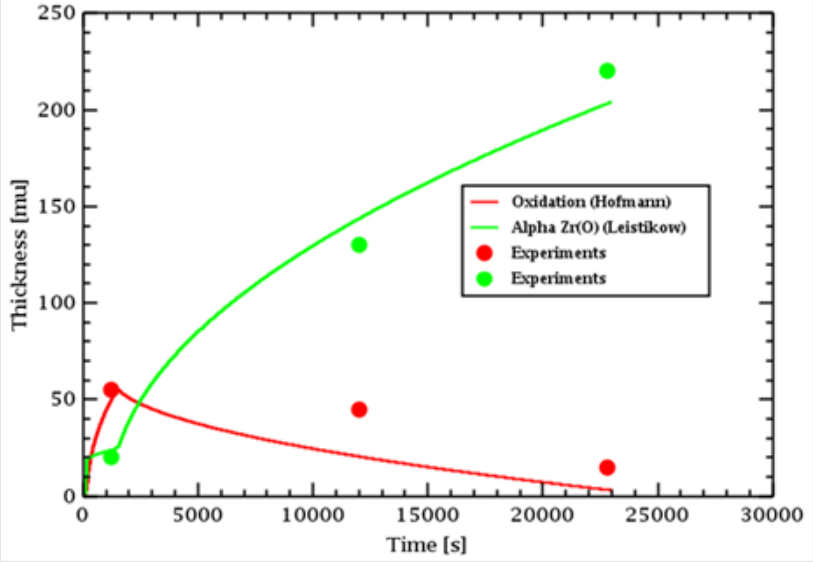
The re-oxidation of the nitrited sample shows a good estimation with the experiment and is running under starvation of oxygen at the beginning. After ZrN is reaching the cutoff thickness of 20 µm the reaction rate slows down until it reaches the rate of metal oxidation.

Separate-effect tests (Diffusion)

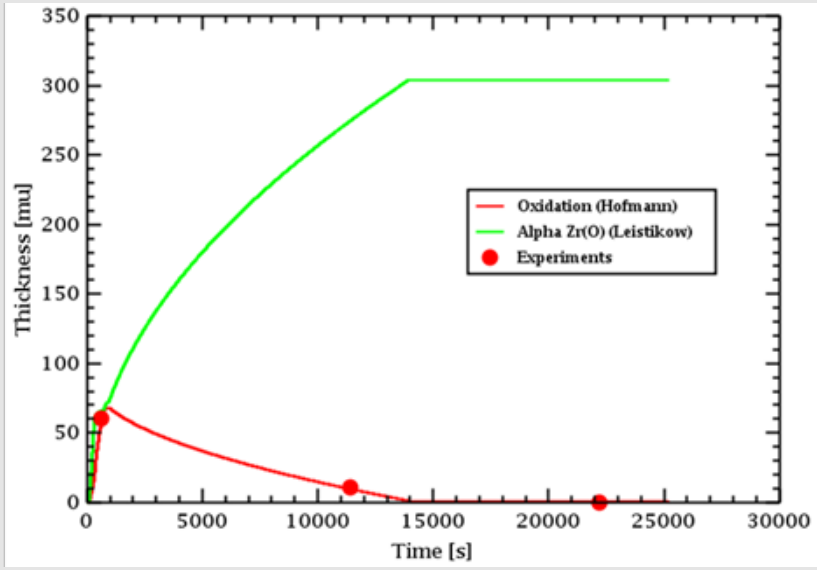
	Pre-oxidation	3 h	6 h
1000°C			
1100°C			

Separate-effect tests (Diffusion)

1000°C



1100°C



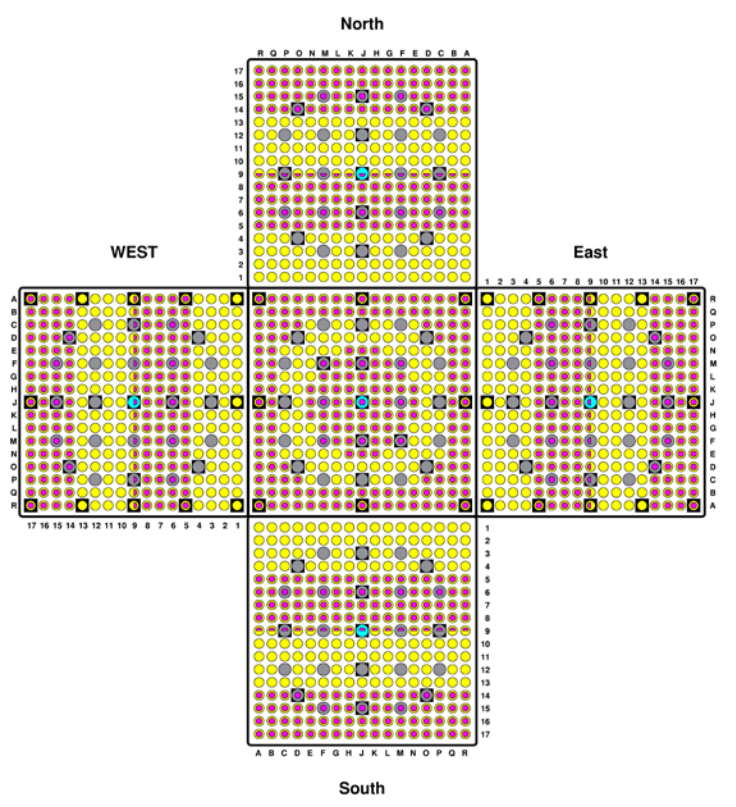
The diffusion model was tested with SETs at 1000°C and 1100°C. After producing a ZrO_2 layer of about 50 µm the samples were heated under argon flow for 3 and 6 hours. The optical post test observations (dots) and the calculation of the standalone code are in good agreement.

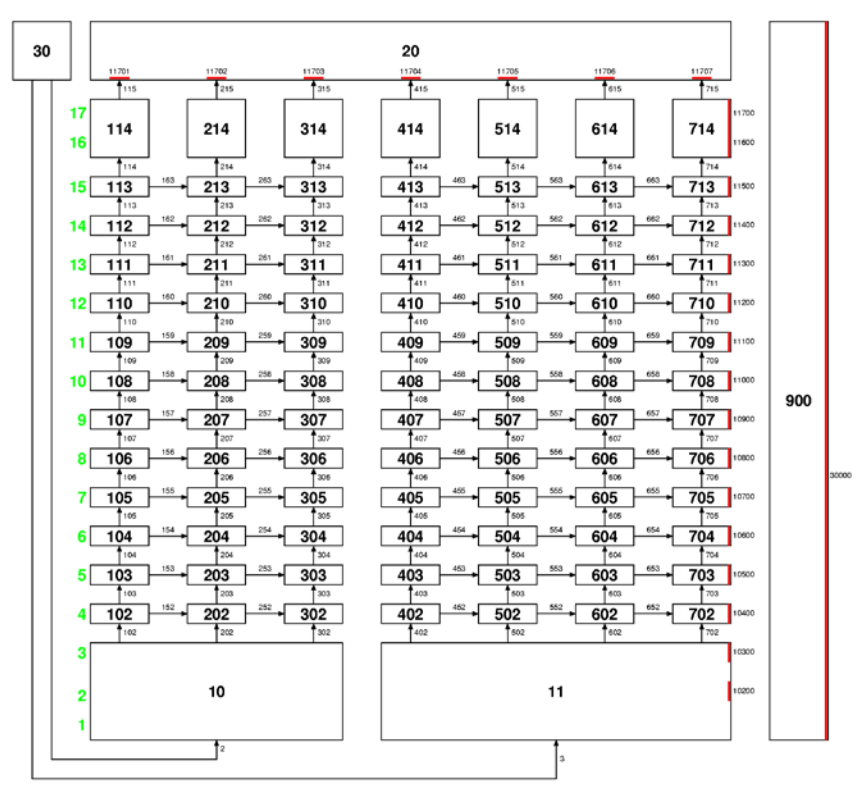
PAUL SCHERRER INSTITUT

Content

1. **Motivation**
2. **Model Scheme**
   1. Pre-oxidation
   2. Diffusion
   3. Nitriding
   4. Re-oxidation
3. **Separate-effect tests**
4. **Sandia Fuel Experiment Phase II**
5. **Outlook**

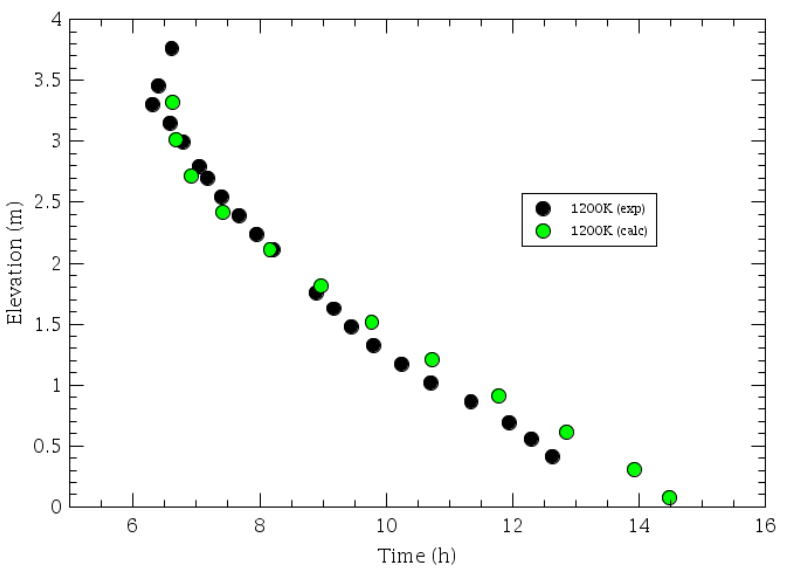
Sandia Fuel Experiment Phase II

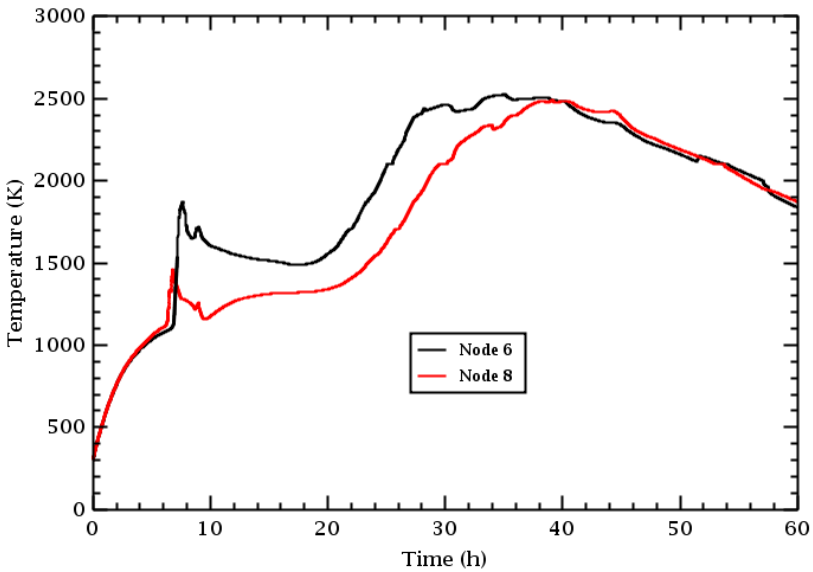




MELCOR nodalization of SFP phase II experiment with 7 rings and 17 axial nodes. 12 nodes (4 – 15) represents the electrically heated (active) zone.

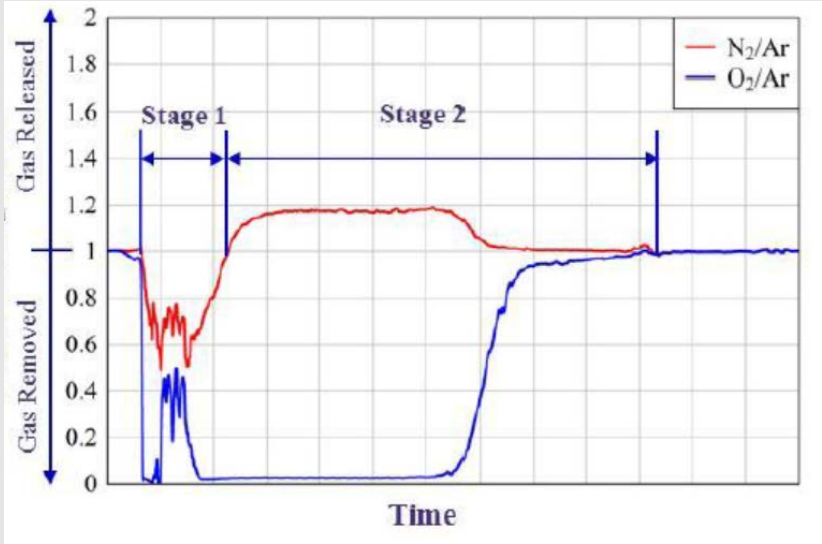
Sandia Fuel Experiment Phase II



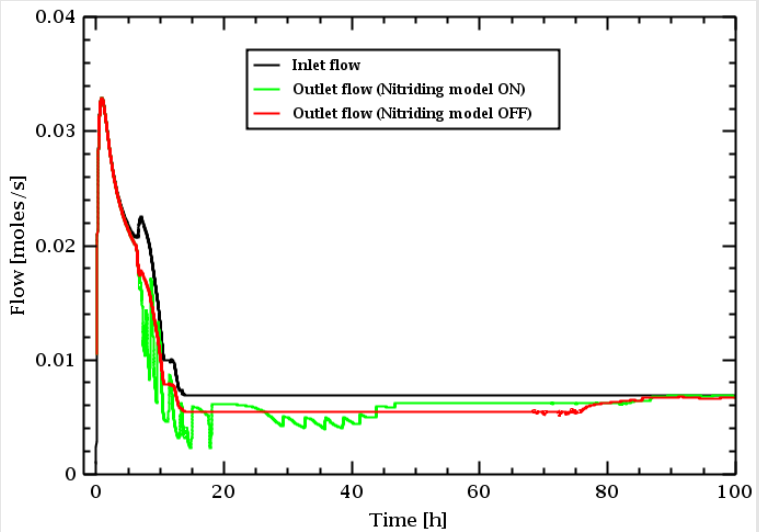


The MELCOR calculation showed a good estimation with measured data, but could not explain the fact, that oxygen was measured at the outlet of the bundle. The calculated temperature profiles could not be compared with experimental data after ignition happened at the position of the TC's, because they failed when the zirconium fire passed. Until failure the temperatures showed a good estimation between experiment and data.

Sandia Fuel Experiment Phase II



Each vertical line is about 10 hours

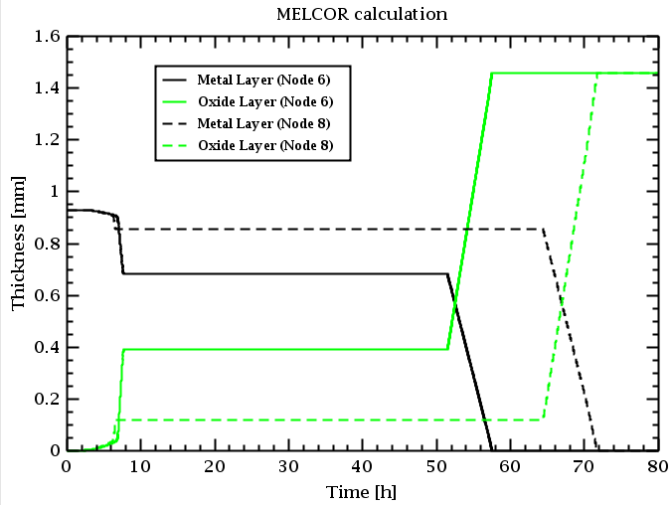


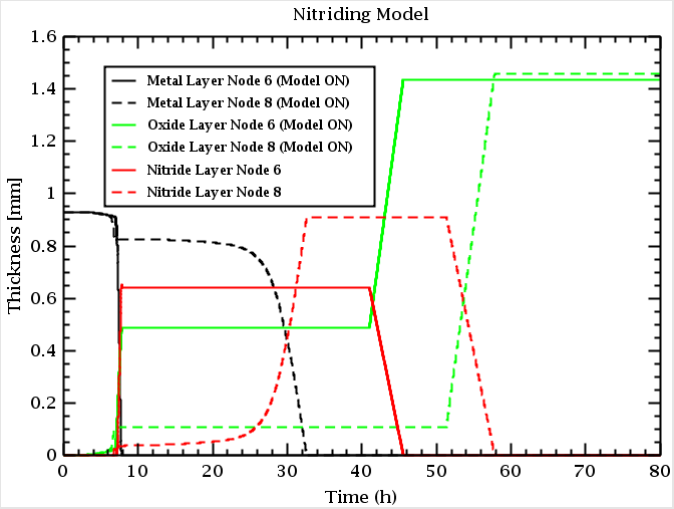
The new nitriding model shows an almost complete consumption of the air flowing into the bundle from below at about 15 hours. This means that the convectional heat loss is much smaller as calculated by MELCOR.

Sandia Fuel Experiment Phase II

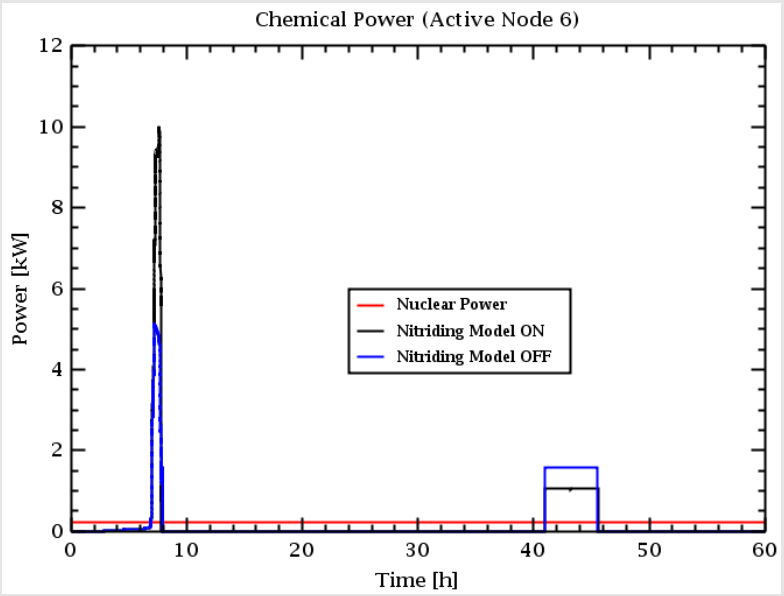
The metal thickness calculated with MELCOR compares with the metal thickness calculated with the standalone code without using the nitriding option.
Loss of metal is between 50 and 60 hours for active node 6.

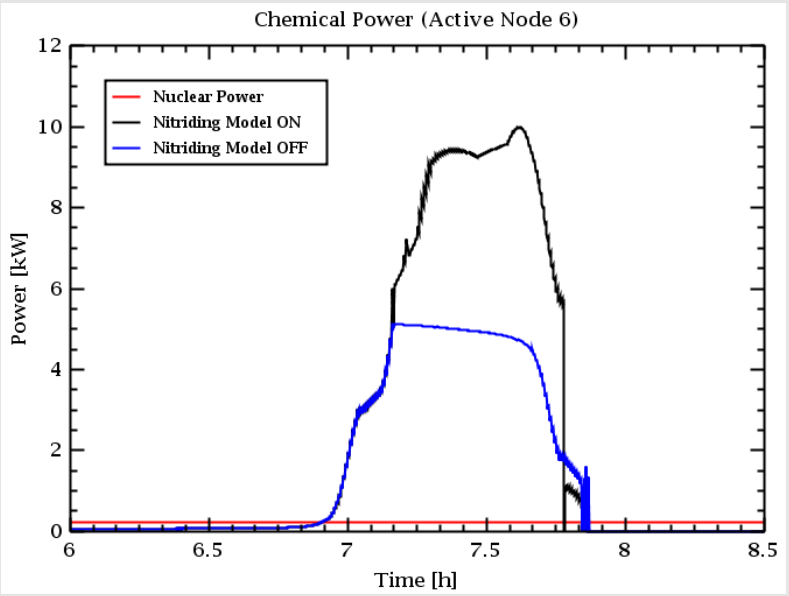
The nitriding model results in a complete loss of the remaining metal at 8 hours due to the production of ZrN in active node 6. After recovery of the oxygen the nitride is then oxidized. In active node 8 there is a delay of the nitriding because of the low temperatures calculated by MELCOR.





Sandia Fuel Experiment Phase II





The chemical power produced due to the nitriding process increases the power released to the bundle during downward propagation of the zirconium fire and leads therefore in the later stage of the experiment to a lower chemical power production during the oxidation of ZrN.

Content

1. Motivation
2. Model Scheme
    1. Pre-oxidation
    2. Diffusion
    3. Nitriding
    4. Re-oxidation
3. Separate-effect tests
4. Sandia Fuel Experiment Phase II
5. Outlook

Outlook

- **The standalone code will be used to calculate the QUENCH 16 experiment to check if the nitriding reaction is able to explain the enormous hydrogen production during the quenching process.**
- **Fine tuning of the temperature dependent reaction rate functions has to be done especially for the temperature range below 1050°C. The mechanical breakaway effect complicates the picture of the nitriding process.**
- **The new model will be prepared and described for the implementation in the severe accident codes SCDAP/Sim and MELCOR.**


Questions?

Behavior of nitrogen with oxidized zirconium – Findings and Remaining Questions

Sanggil Park

ACT Co., Ltd. / Handong Global University / Lee & Ko

It has been known that the nitrogen reacts with oxidized zirconium when the oxygen is sufficiently consumed. The nitrogen actively reacts with the oxygen stabilized alpha zirconium and the sub-stoichiometric oxide. In this paper, we provide the results of Zircaloy-4 air oxidation tests and discussed the nitriding behavior. The nitride formation was observed from the 800°C with a very small amount at the oxide-metal interface. According to the temperature range, the nitride was formed at different locations. For the temperature range of 800-1000°C, the nitride formation was at the oxide-metal interface and its amount was increased by the temperature and air oxidation duration. At the 1100-1400°C, the nitride was found all over the oxide scale. From 1100 to 1200°C, the nitride contents were increased by temperature and air oxidation duration, but they were decreased from 1300 to 1400°C. For higher temperature of 1500-1600°C, almost no nitride was seen by the optical microscopies of the post-test samples. Based on the findings of nitride formation behavior, the nitriding seems to be very active in the temperature range where the tetragonal zirconium oxide is stable. Further investigation is ongoing to reach a better understanding of nitriding behavior in the air oxidation of zirconium cladding.



Lee & Ko 법무법인 광장

Behavior of Nitrogen with Oxidized Zirconium

Findings and Remaining Questions

2018.11.14

Lee & Ko (Formerly PSI)
Sanggil Park

PAUL SCHERRER INSTITUT PSI

KIT Karlsruher Institut für Technologie

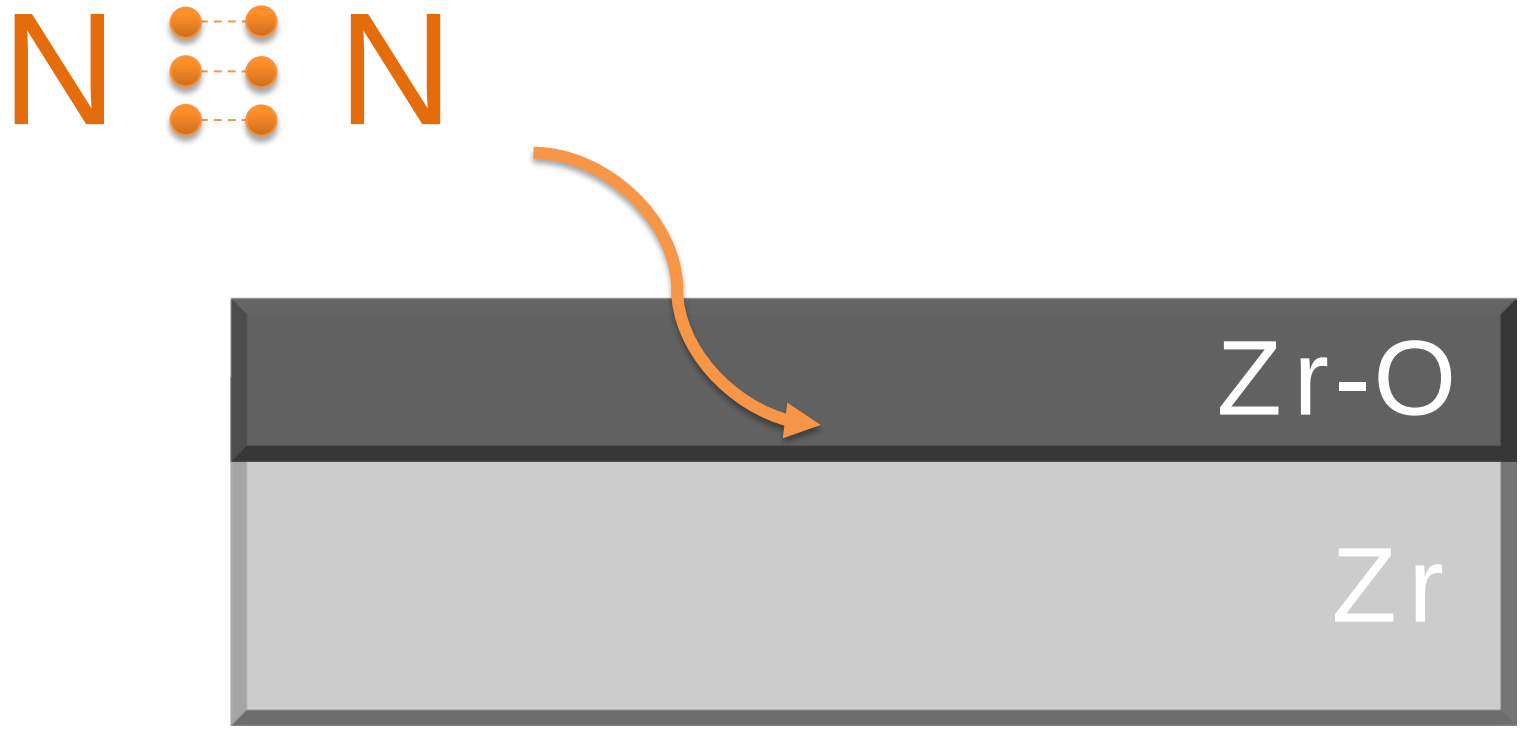
Activity of Nitrogen in the Zr-O system



Contents

1. Active Regime
2. Inactive Regime
3. Findings
4. Remaining Questions

Nitrogen Incorporation into the Zr-O system



Nitriding Conditions & Behaviors

Number of Considerations



Atmospheric Condition

Reaction with Zirconium



Bonding

Dissociation First

Dissociation Energy

497 kJ/mol

945 kJ/mol

Reaction

Formation Second

Gibbs Energy of Formation

ΔG_{ZrO_2} = -896 kJ/mol

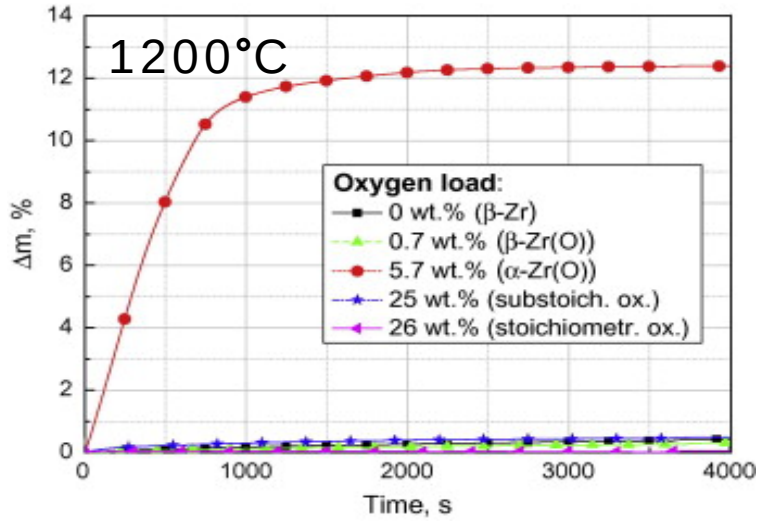
ΔG_{ZrN} = -264 kJ/mol

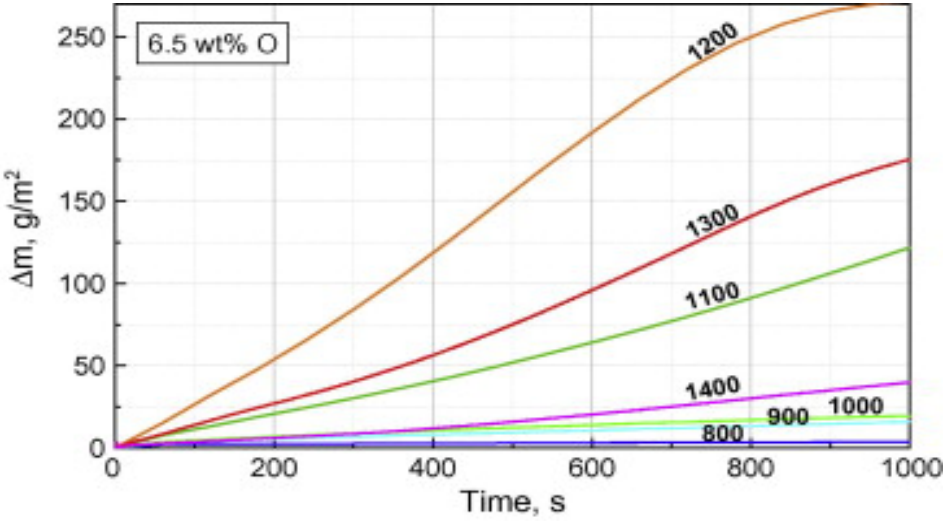
Oxygen Consumption First

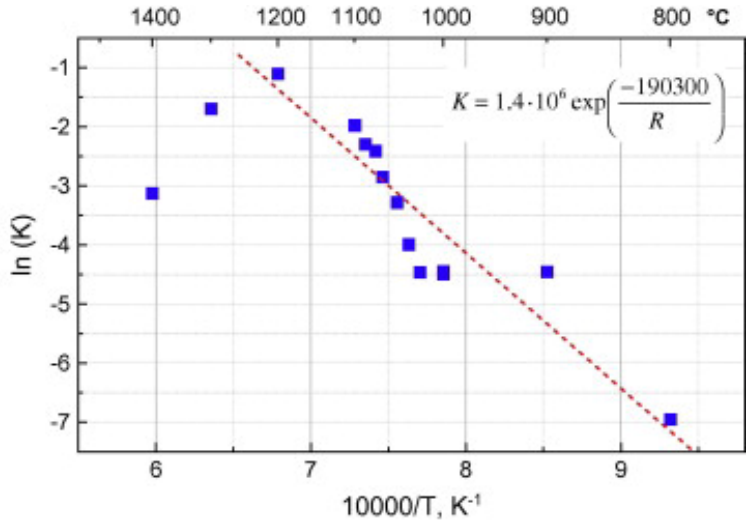
Nitrogen Reaction Later

Phase Preference

Nitrogen with α-Zr(O)





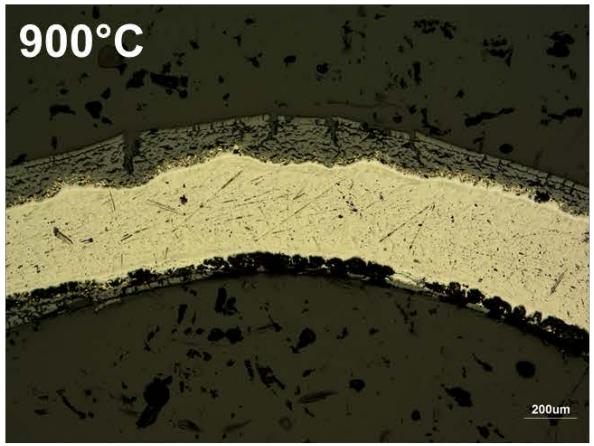


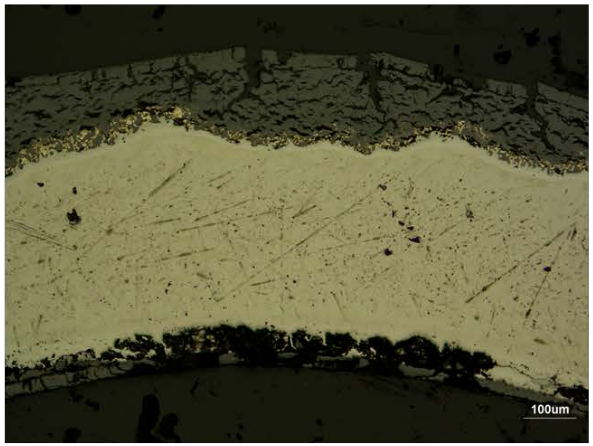
Main Results

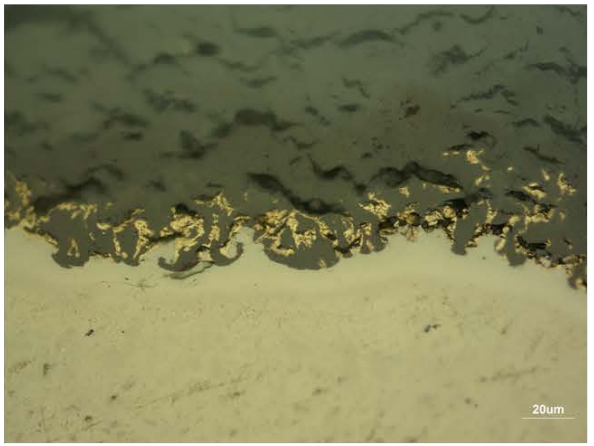
- N_2 reacts favorably with α-Zr(O)
- (800-1000) Moderate Reaction
- (1050-1200) Very Active Reaction
- (1300-1400) Less Active Reaction

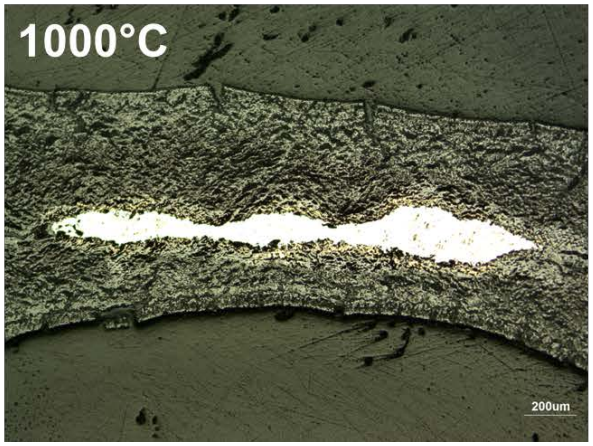
Temperature

Moderate Temperature Regime: 900 ~ 1000° C

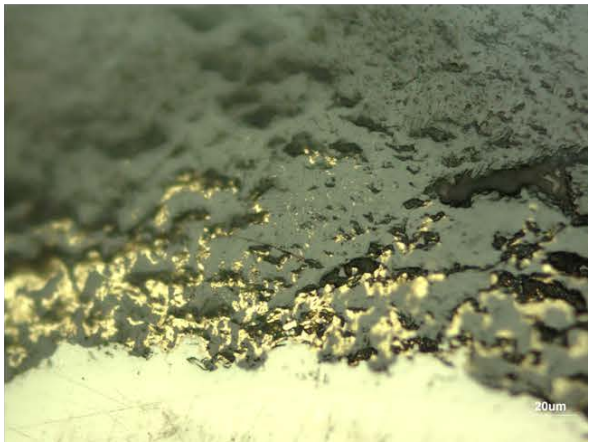












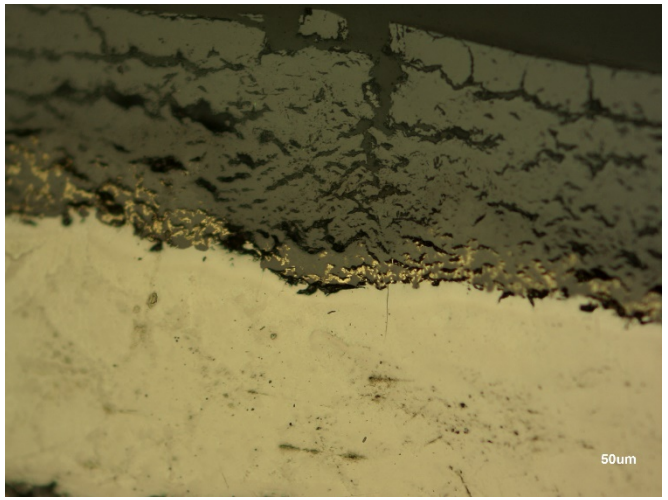
Temperature

Moderate Temperature Regime: 900 ~ 1000° C



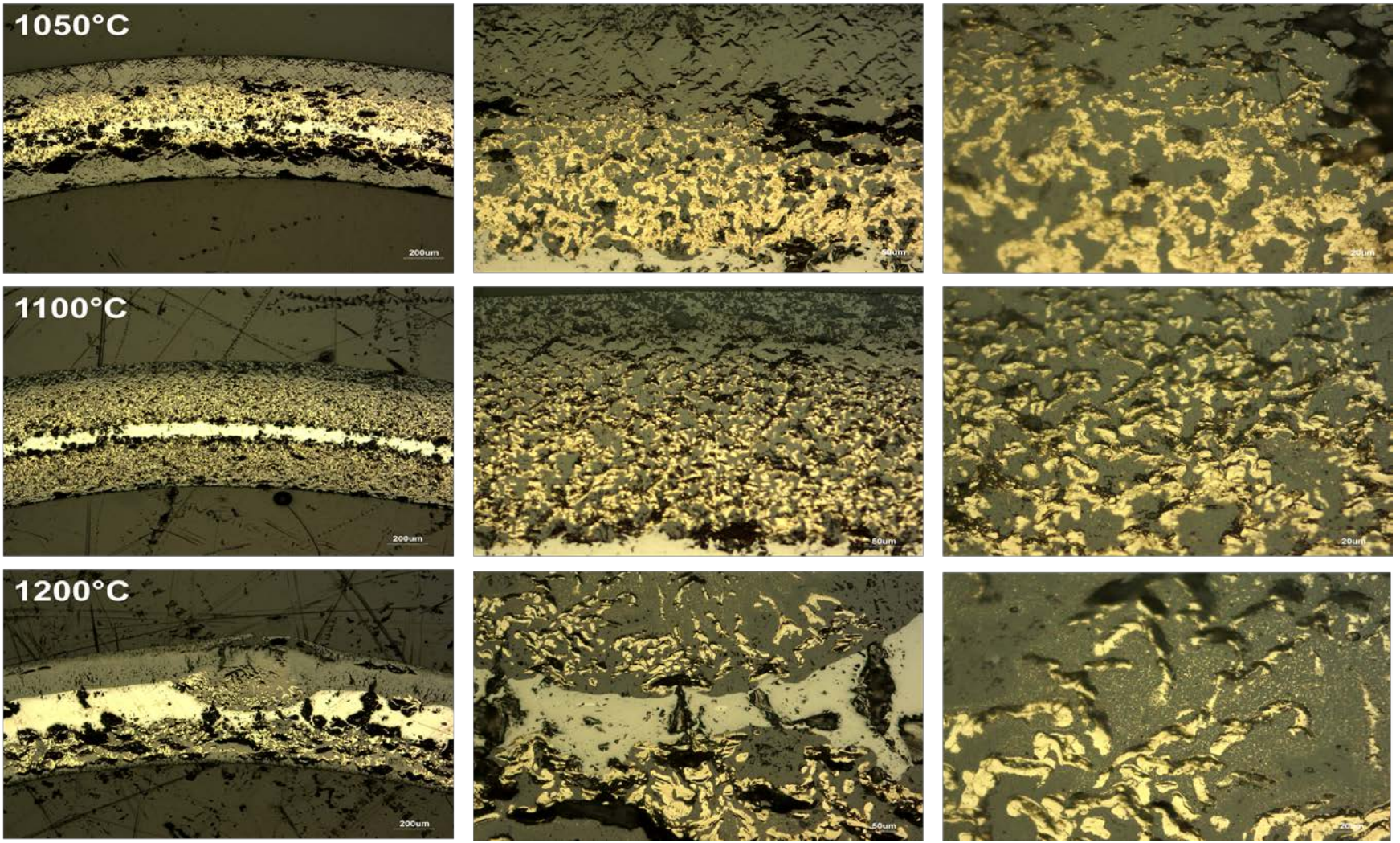


Interfacial Nitride



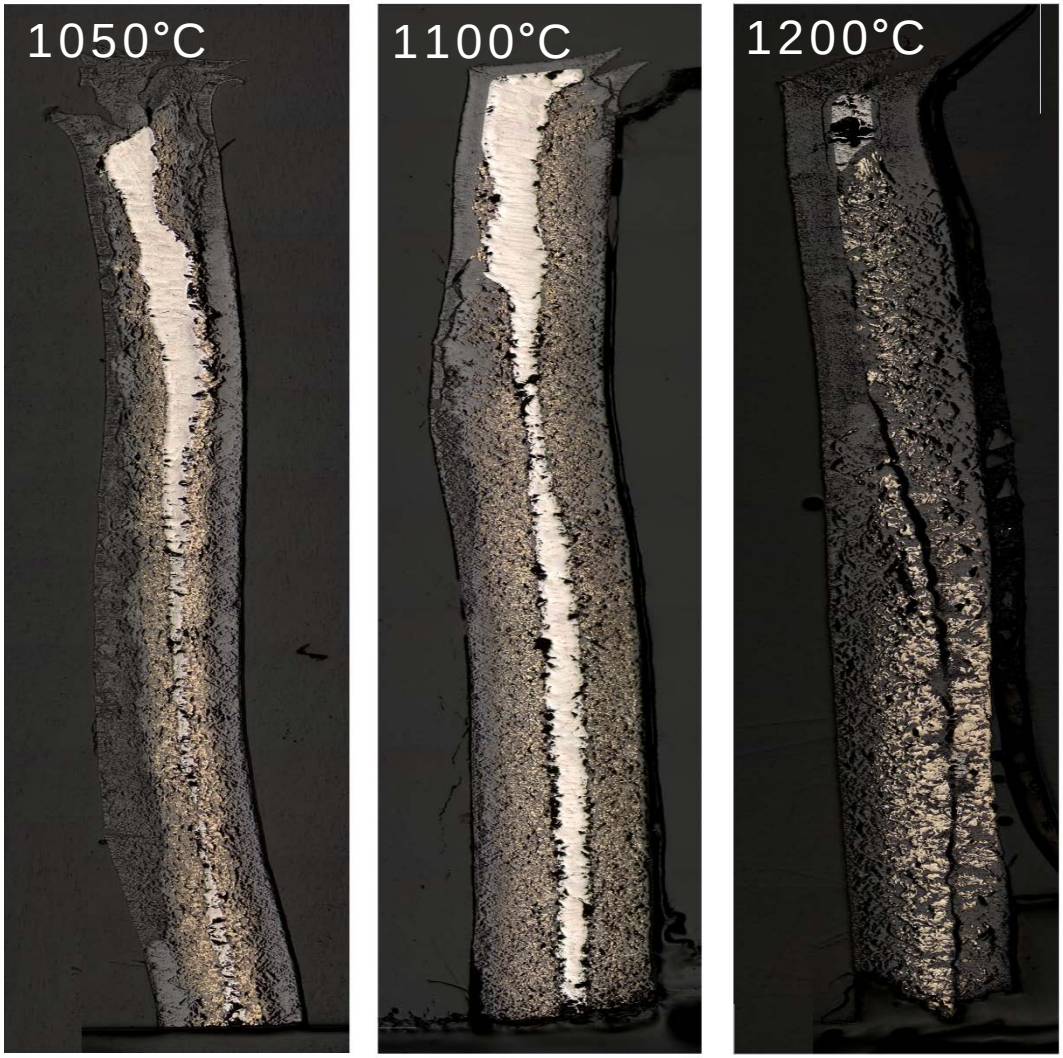
Temperature

More Active Temperature Regime: 1050 ~ 1400° C

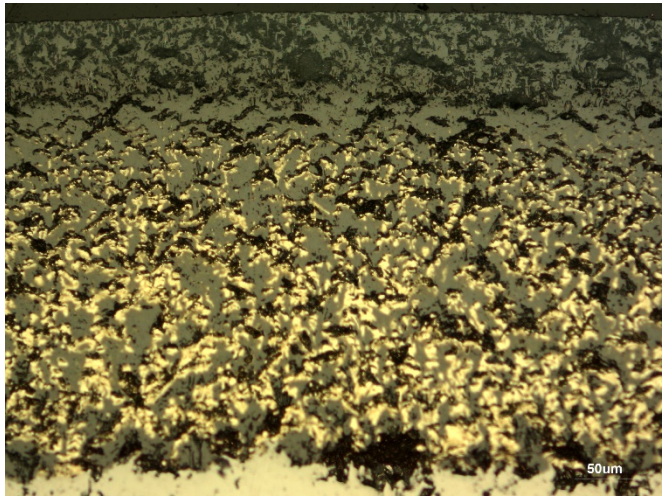


Temperature

More Active Temperature Regime: 1050 ~ 1200° C

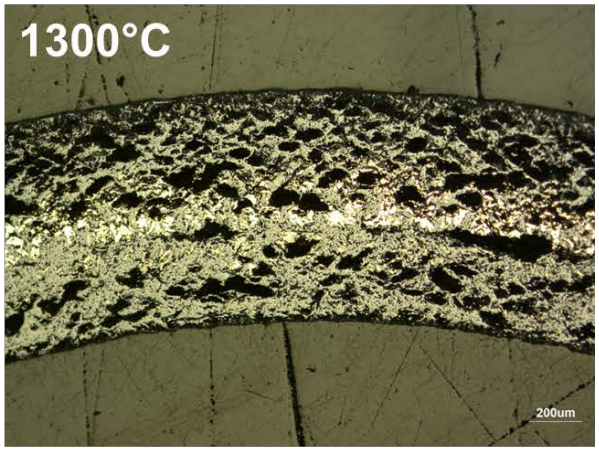


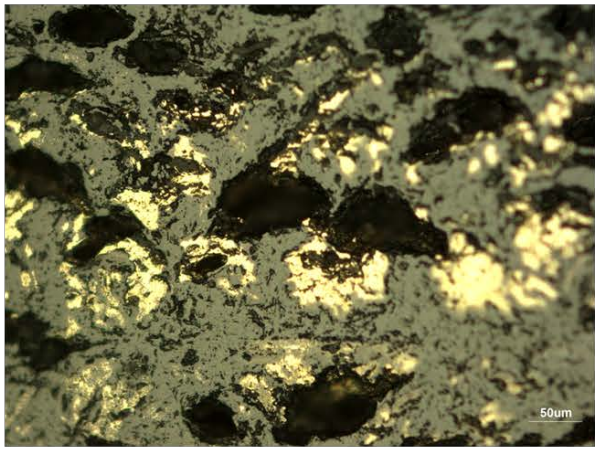
Widespread Nitride

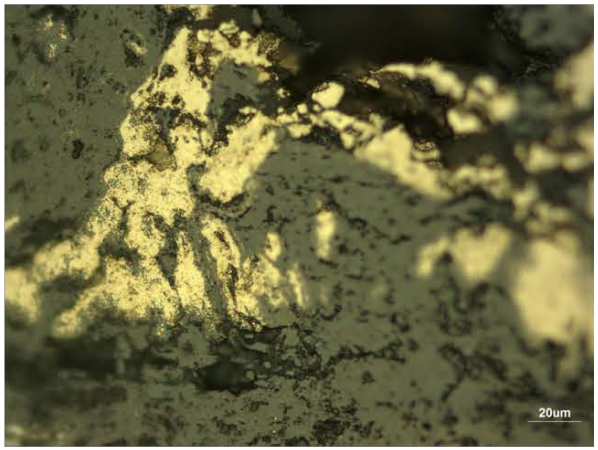


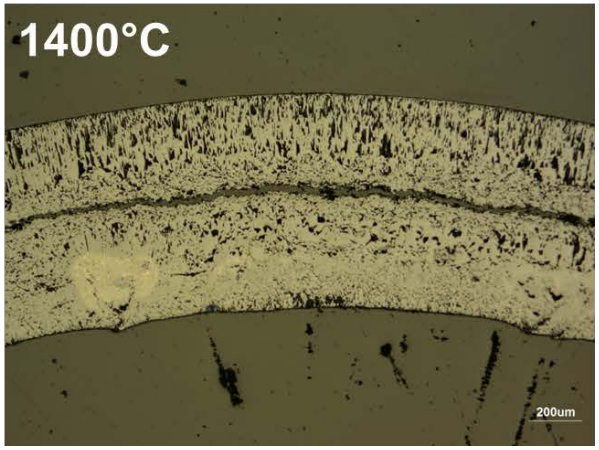
Temperature

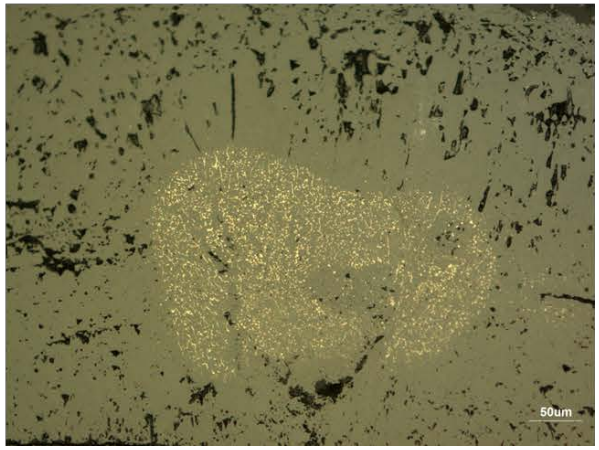
Less Active Temperature Regime: 1300 ~ 1400° C

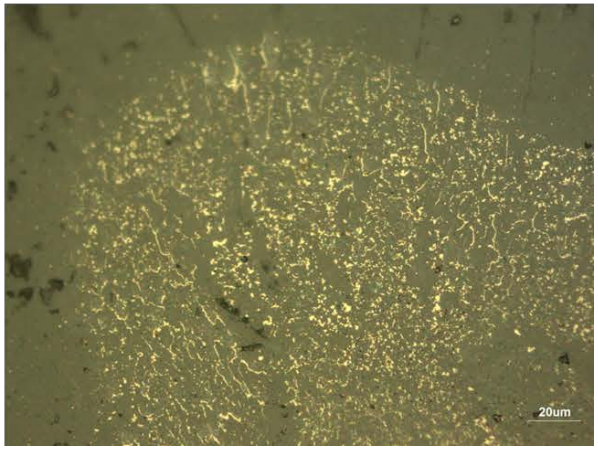












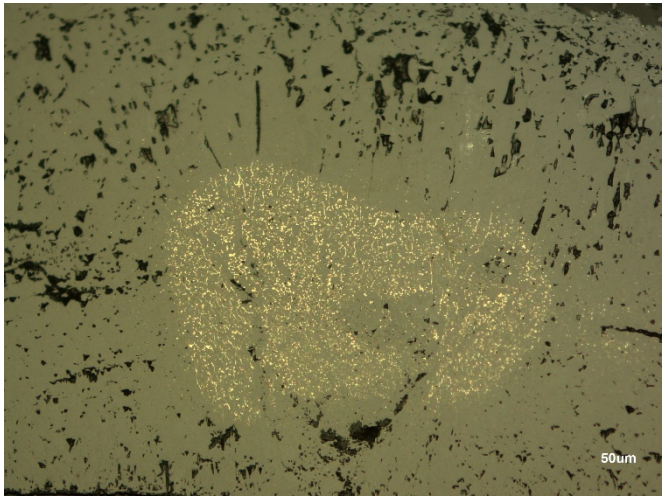
Temperature

Less Active Temperature Regime: 1300 ~ 1400° C



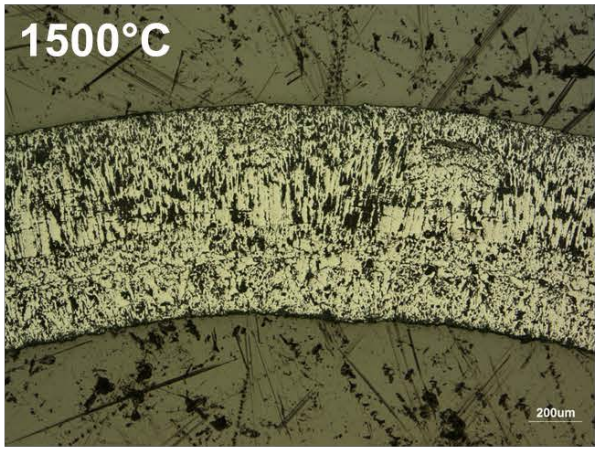


Hidden Nitride

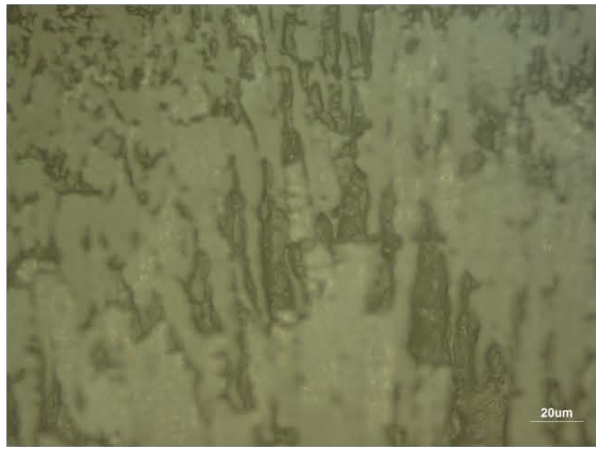


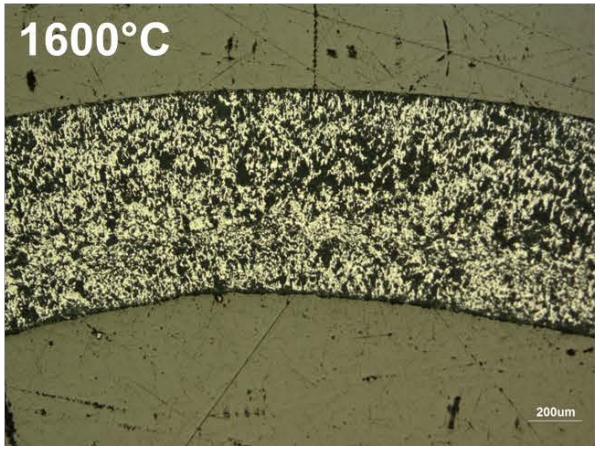
Temperature

Inactive Temperature Regime: 1500 ~ 1600° C









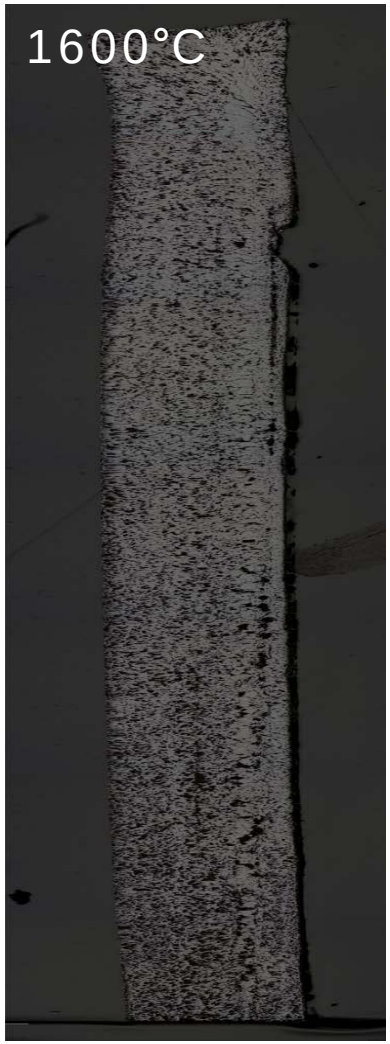




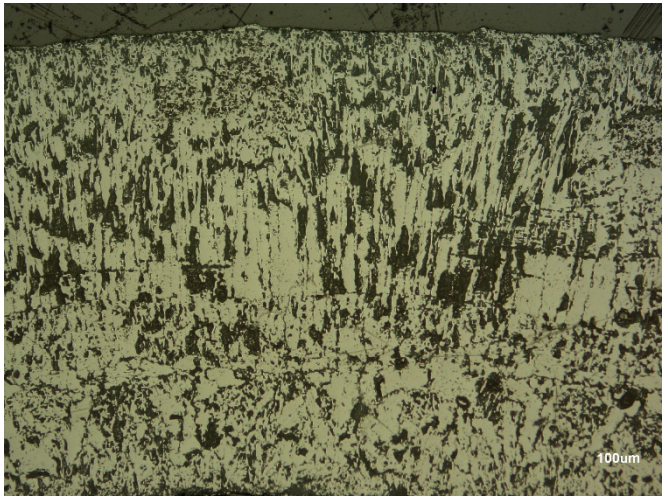
Temperature

Inactive Temperature Regime: 1300 ~ 1600° C

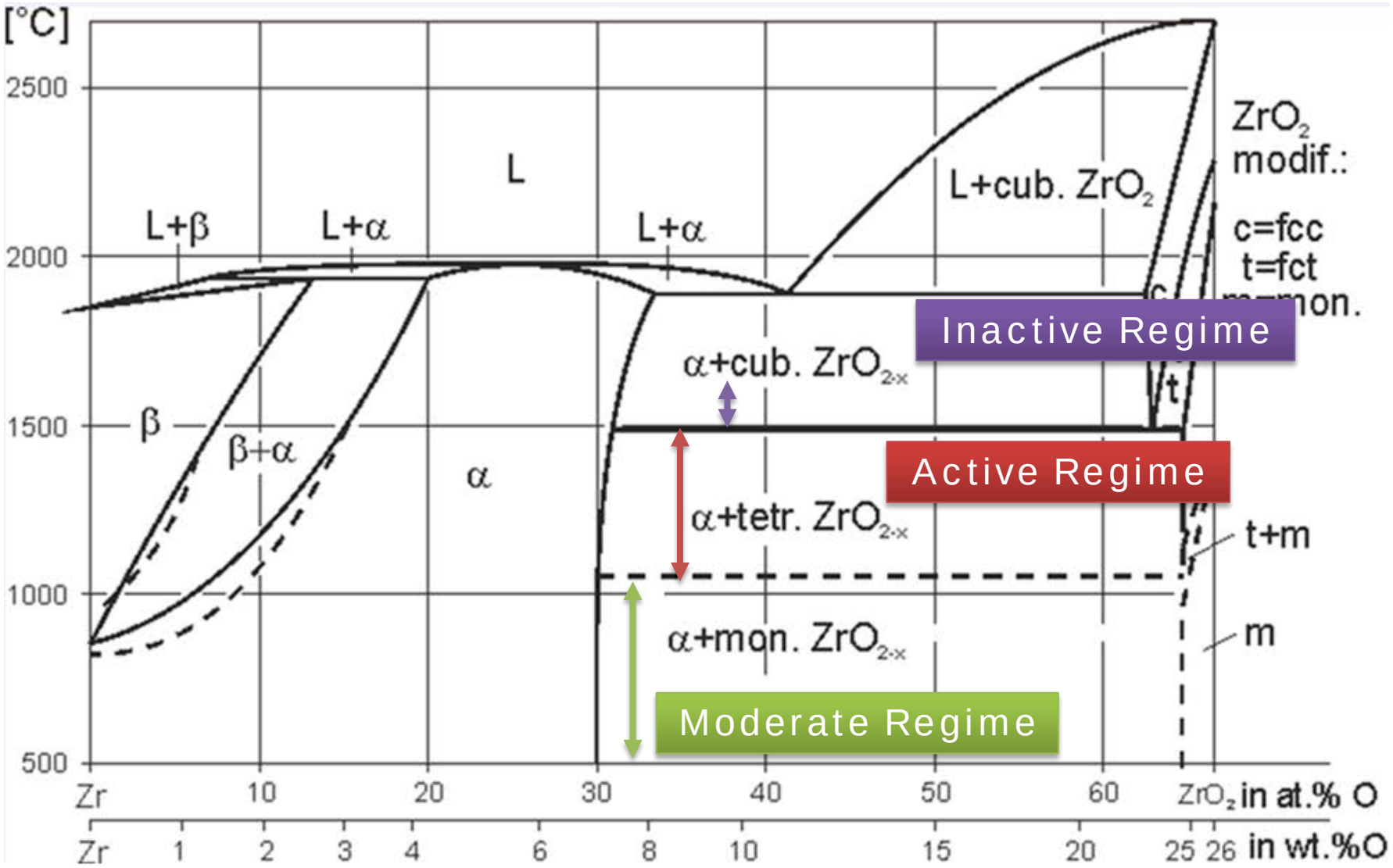




No Nitride



Findings

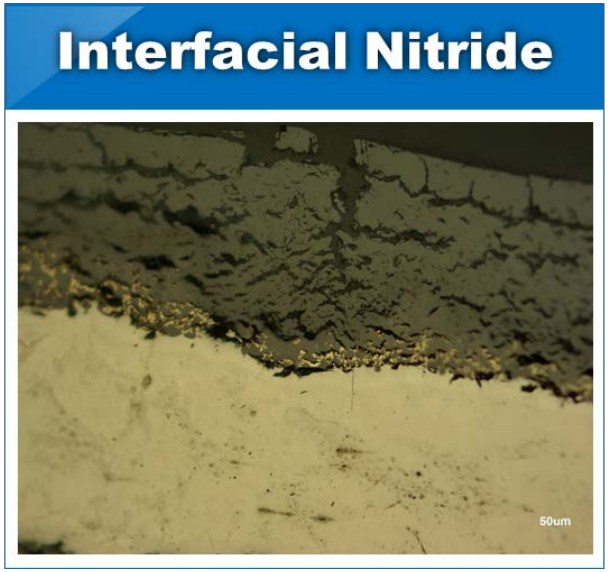

[°C]
2500
2000
1500
1000
500
L
L+β
L+α
L+α
L+cub. ZrO2
ZrO2 modif.:
c=fcc
t=fct
mon.
Inactive Regime
α+cub. ZrO2-x
β
β+α
α
Active Regime
α+tetr. ZrO2-x
t+m
α+mon. ZrO2-x
m
Moderate Regime
Zr
10
20
30
40
50
60
ZrO2 in at.% O
Zr
1
2
3
4
6
8
10
15
20
25
26
in wt.%O

Remaining Questions

Nitrogen with α-Zr(O) and/or t-ZrO_{2-x} ??

The oxide scale is developed mainly by m-ZrO_2, but **a small quantity t-ZrO_2 is formed close to the metal/oxide interface as a very thin layer**. The tetragonal phase is preferentially located near the interface by some of the following reasons.

1. High compressive stress
2. Low grain size
3. The presence of defects; hypostoichiometry.



Effect of flow rate on zirconium breakaway timing under oxygen atmosphere at 1000℃

Gippeum Kim[a)*], Sanggil Park[b)], Jaeyoung Lee[a)]

a) School of Control and Mechanical Engineering, Handong Global Univ., Pohang, 37554, Korea

ACT Co. Ltd., Tecnho 9 Ro, Yuseong-gu, Daejeon, 34027, Korea

[*]Corresponding author: joy-kim@naver.com

Abstract: In this study, it is mainly studied about flow rate effect on zirconium(Zr) breakaway(BA) phenomena because there are a few report about it even if it might influence on zirconium oxidation and BA phenomena by followed reasons: a) Diffusivity of reactive gas(oxygen, air, vapor, and mixtures), b) Residential time of reactive gas on zirconium cladding, c) Zirconia(ZrO_2) development process. So, series of isothermal test with Zry-4 were conducted under various oxygen(O_2) flow rate at 1000℃. The oxygen flow rate is varied from 20 to 200ml/min and argon(Ar) is used as a carrier gas. (The ratio of oxygen and argon is 2:1)

The results of BA timing show two different tendencies. First, under oxygen flow rate 140ml/min, BA is occurred at very similar time. Second, however, after 160ml/min, it is observed dramatically delayed BA time. In order to understand those, qualitative analysis is conducted with initial temperature overshoot data, which is resulted from heat of reaction between Zr and O_2: $Zr+O_2 \rightarrow ZrO_2+Q$.

By this analysis, we can identify there are temperature overshoot above 1050℃ from 160ml/min, which is known as zirconia phase transformation limitation temperature from monoclinic zirconia(mono-ZrO_2) to tetragonal zirconia-(tetr-ZrO_2). The tetr-ZrO_2 is also known as having a better stress relieving capacity compared to mono-ZrO_2.

As a result, we assume that the zirconia phase, which is developed during initial temperature overshoot period, might influence on BA delayed.


TOSHIBA

Effect of flow rate on zirconium breakaway timing under oxygen atmosphere at 1000℃

G. Kim(HGU)
S. Park (HGU/ACT), J. Lee (HGU)
14 November 2018

Outline

1. Motivation
2. Experiment
   2.1. Experiment detail
   2.2. Experiment results
3. Questions
4. Analysis and Discussion
5. Conclusions

1. Motivation

- It is hard to find reports about showing zirconium oxidation and BA phenomena **in terms of reactive gases flow rate.**

- The flow rate of reactive gases might effect on **diffusivity of reactive gas, residential time of it on zirconium cladding and oxide development(ZrO_2).**

- To understand flow rate effect on zirconium BA phenomena, series of isothermal test were conducted with various O_2 flow rate at 1000℃.

a) **b)**



Figure1.
Example of BA phenomena
a) Mass gain curve b) Optical picture (Zry4 under air atmosphere at 800℃ at KIT)

Experiment

2.1. Experiment Detail

- Isothermal test at 1000℃
- Setaram Setsys TGA
- Zry-4 cladding was used.

(OD: 9.5mm ID: 8.25mm L: 10mm)

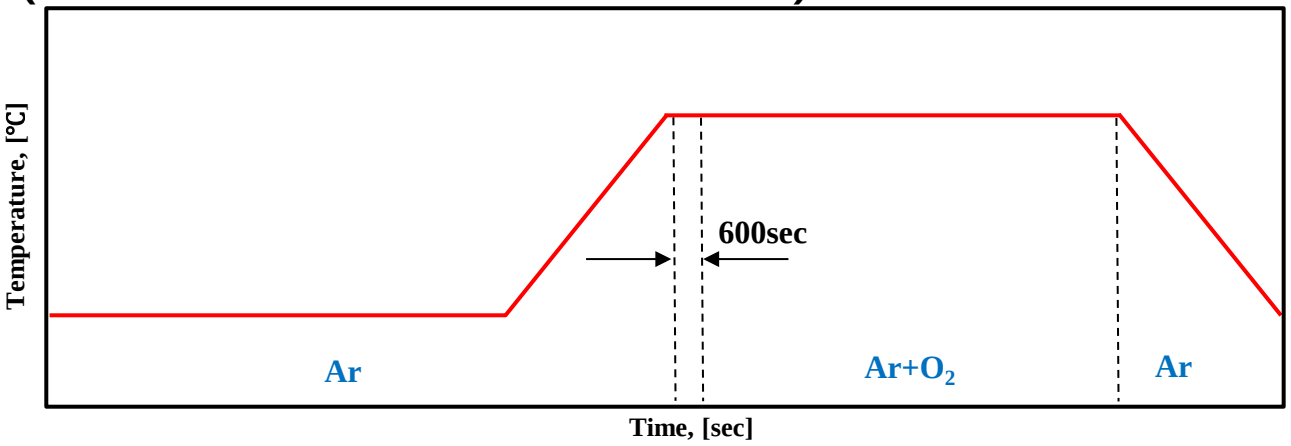


Figure2.
Isothermal test procedures at 1000℃

Test Matrix	Temperature [℃]	Test time(Ar+O_2) [hour]	Argon [ml/min]	O_2 [ml/min]
Zry4_1000C_20	1000	2	10	20
Zry4_1000C_40	1000	2	20	40
Zry4_1000C_60	1000	2	30	60
Zry4_1000C_80	1000	2	40	80
Zry4_1000C_100	1000	2	50	100
Zry4_1000C_120	1000	2	60	120
Zry4_1000C_140	1000	2	70	140
Zry4_1000C_160	1000	2	80	160
Zry4_1000C_180	1000	2 and 4	90	180
Zry4_1000C_200	1000	2 and 4	100	200

Table1. Experiment matrix detail

2.2. Experiment Results (1/3)

- Mass gain graph(%) under oxygen atmosphere at 1000℃

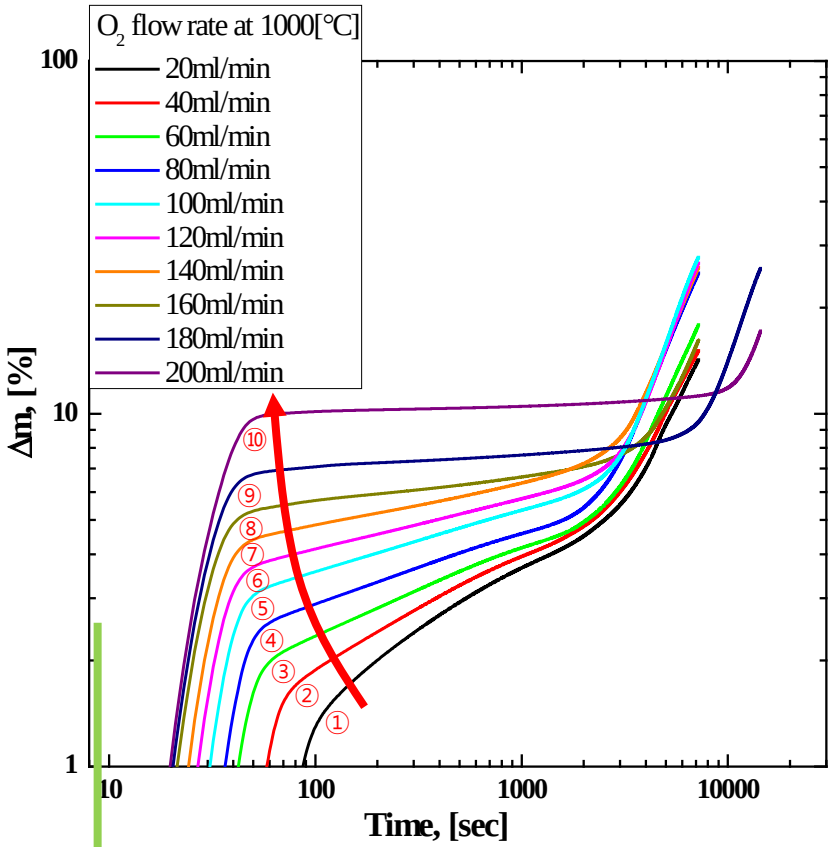


Figure3. Oxidation mass gain(%) curve with different O_2 flow rate at 1000℃ (log-log scale)

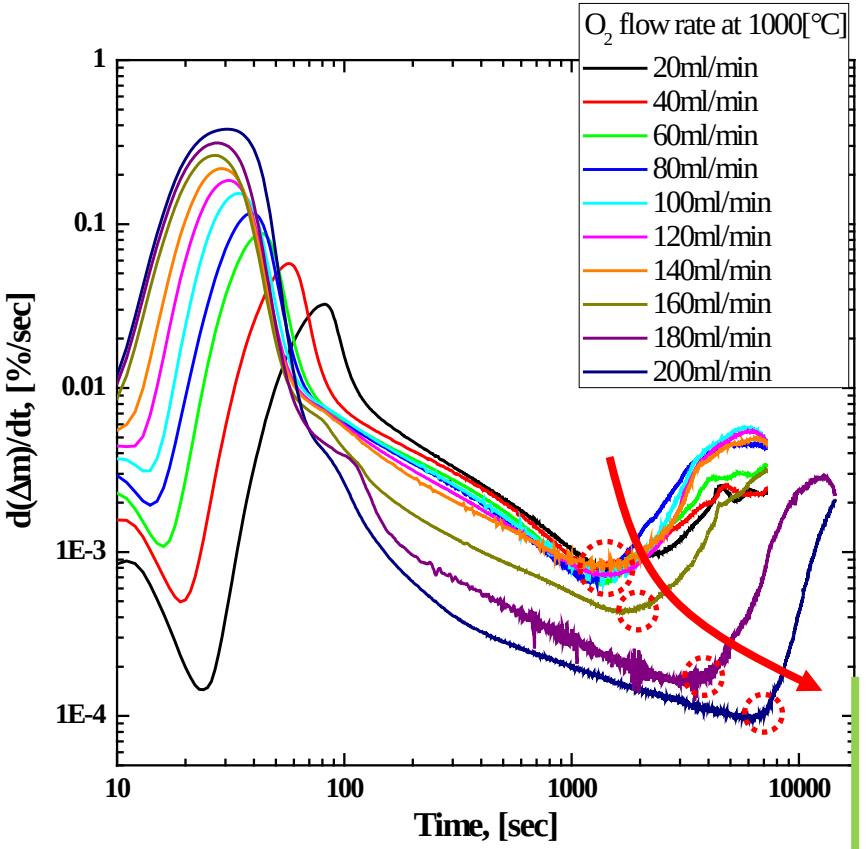


Figure4. Derivative oxidation mass gain curve with different O_2 flow rate at 1000℃ (log-log scale)

Magnitude of initial mass gain is increased by flow rate increment.

Breakaway time is delayed after flow rate beyond 160[ml/min].

2.2. Experiment Results (2/3)

- Breakaway(BA) time versus O_2 flow rate

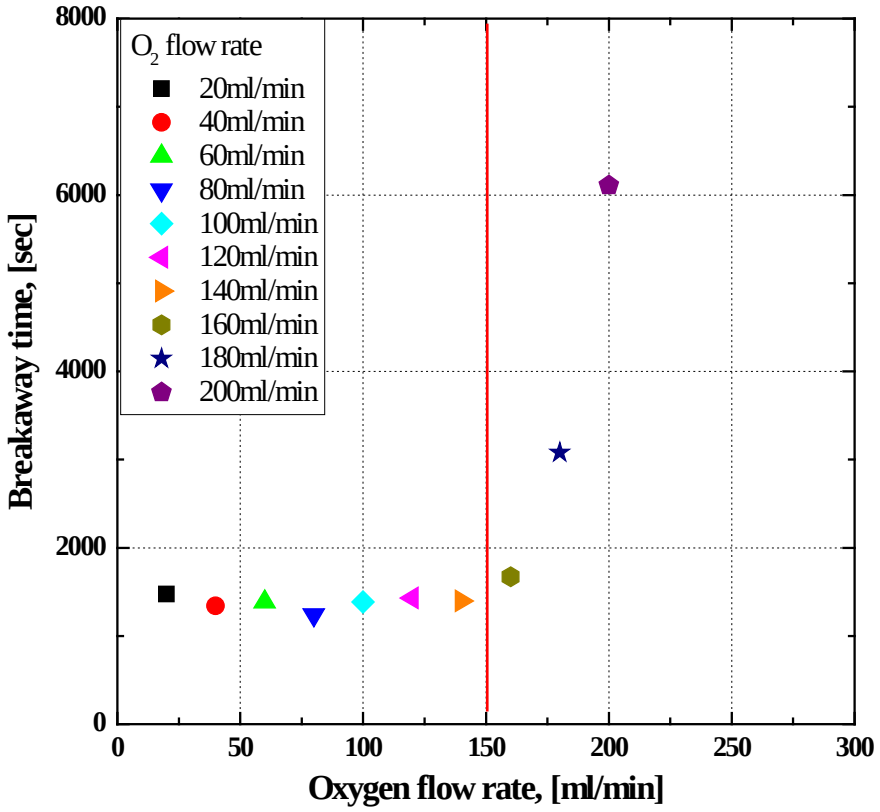


Figure5. Results of BA time with different O_2 flow rate at 1000℃

Flow Rate [ml/min]	BA time [sec]
200	6109 (102min)
180	3079 (51min)
160	1672 (28min)
140	1395 (23min)
120	1430 (24min)
100	1386 (23min)
80	1242 (21min)
60	1387 (23min)
40	1341 (22min)
20	1473 (25min)

BA times are delayed after 160ml/min, but before that point, it shows similar BA time.

2.2. Experiment Results (3/3)

- Oxide thickness(μm) at each BA time
- $\triangle\delta = (\triangle m/S)/\rho_{ZrO2}$ (assumption that ρ_{ZrO2} is mono-ZrO_2)

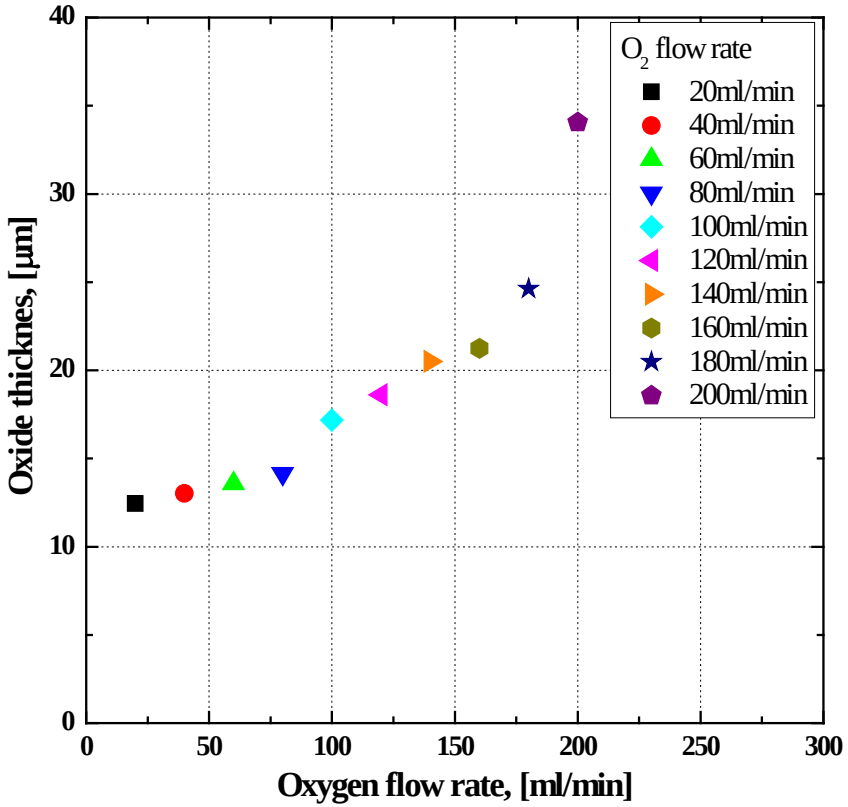


Figure6. Results of oxide thickness at each BA time with different O_2 flow rate at 1000℃

Flow Rate [ml/min]	Oxide thickness at BA [μm]
200	34.05
180	24.62
160	21.24
140	20.50
120	18.61
100	17.18
80	14.15
60	13.57
40	13.02
20	12.44

Figure6 shows that **oxide thickness at BA time is increased** by flow rate increment.

It is increased almost linearly, but excepting 200ml/min case.

3. Questions

Q1. Why are results of **magnitude of initial mass gain and the time** different with O_2 flow rate?

Q2. **Can BA be affected by flow rate?**

Q3. Why are results of **oxide thickness at each BA time** changed?

Q4. Why is **BA time delayed** dramatically after 160ml/min flow rate?

➔ Among the questions, **qualitative analysis for Q4** was conducted.

Analysis and Discussion

4. Analysis and Discussion (1/2)

- **Initial peak temperature by heat of reaction interaction between Zr and O_2**
- **$Zr+O_2 \rightarrow ZrO_2+Q$**

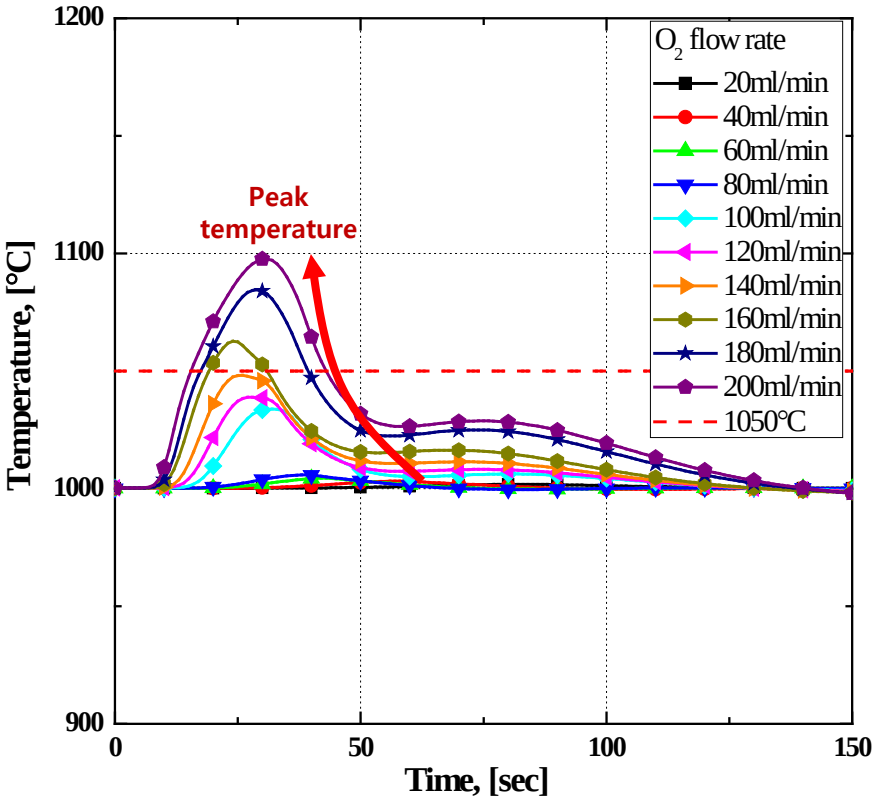


Figure7. Results of initial peak temperature with different O_2 flow rate at 1000℃

Flow Rate [ml/min]	Peak Temp [℃]
200	1097.70
180	1084.47
160	1062.71
140	1048.33
120	1038.88
100	1033.81
80	1005.81
60	1004.44
40	1003.17
20	1001.86

The peak temperatures are increased by O_2 flow rate increment.

Especially, **beyond flow rate 160ml/min, the peak temperatures are exceed 1050℃**, which is known as zirconia phase transformation limitation.

→

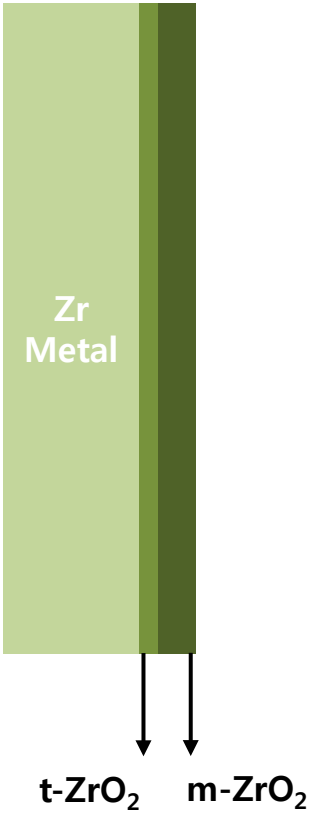
mon. ZrO_{2-x} < 1050℃

tetr. ZrO_{2-x} > 1050℃

4. Analysis and Discussion (2/2)

- Description of flow rate effect on oxide grow mechanism (Hypothesis)

a) O_2 flow rate under 140ml/min(20~140ml/min)



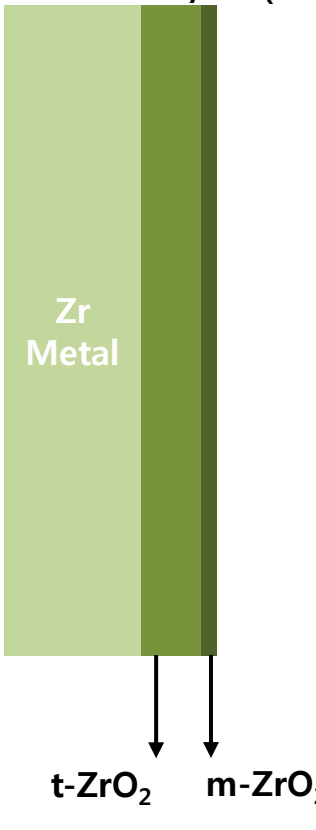
1) Under O_2 flow rate 140ml/min, the peak temperatures are not exceed 1050℃.

2) Therefore, the zirconium oxide is mainly developed with m-ZrO_2 formation.

3) Between Zr and m-ZrO_2 layer, if the condition where t-ZrO_2 can be built are satisfied, t-ZrO_2 can be made at that interface.

4) The BA can be occurred and understood with following typical assumptions:
(a) Critical oxide thickness
(b) Phase transformation (t-ZrO_2 → m-ZrO_2)

b) O_2 flow rate beyond 160ml/min(160~200ml/min)



1) Beyond O_2 flow rate 160ml/min, the peak temperatures are exceed 1050℃.

2) Thus, **t-ZrO2 zirconium oxide is mainly developed in the very begining.** (Hypothesis)

3) Because mainly formed oxide is t-ZrO_2, which is known as relatively less diffusion barrier compared to m-ZrO_2, so **it allows high initial mass gain**.

4) This formation also promotes relatively high stress releasing capacity compared to m-ZrO_2, thus, **it can lead delay of BA time.**

Figure8. Schematic diagram of zirconium oxide development mechanism
a) 20~140[ml/min] b) 160~200[ml/min]

5. Conclusions

- To understand of flow rate effect on BA time, series of experiments are conducted under O_2 atmosphere at 1000℃.

- The BA times are similar until flow rate 140ml/min(20~140ml/min), however, it is delayed beyond 160ml/min flow rate(160~200ml/min).

- Also, oxide thickness at each BA time is increased by O_2 flow rate increment.

- The delayed BA time is explained by magnitude of initial peak temperature, which might effect on oxide development in the very beginning: m-ZrO2, t-ZrO2.

- Further studies are needed to identify oxide formation developed in the very beginning.

Thank you for attention!

joy-kim@naver.com

Appendix



Figure9. Setaram Setsys TGA



- Material: Zry-4
- Length: 10[mm]
- Outer diameter: 9.5[mm]
- Inner diameter: 8.25[mm]

Figure10. Zry-4 cladding tube specification

Pavel Vrbka

High Temperature Oxidation of Sponge-based E110 Cladding Alloy in Air

The work is focused on separate-effect testing of sponge-based E110 alloy during high temperature oxidation in air. A dependence of weight gain on exposure time and other post-experimental evaluation as length growth, cross-section metallography, microhardness, ring compression test were investigated at temperature range 700–1200 °C. As-received as well as pre-oxidized samples in various conditions were oxidized to examination of influence of behavior on default state. A comparison between sponge-based and electrolytic E110 were performed at 800 °C and 1100 °C. Based on experimental measurements, correlations for the oxidation kinetics of sponge-based E110 alloy were determined in pre-breakaway and post-breakaway region. Gained results were compared with other alloys tested during other experiments.



High Temperature Oxidation of Sponge-based E110 Cladding Alloy in Air



UJP PRAHA



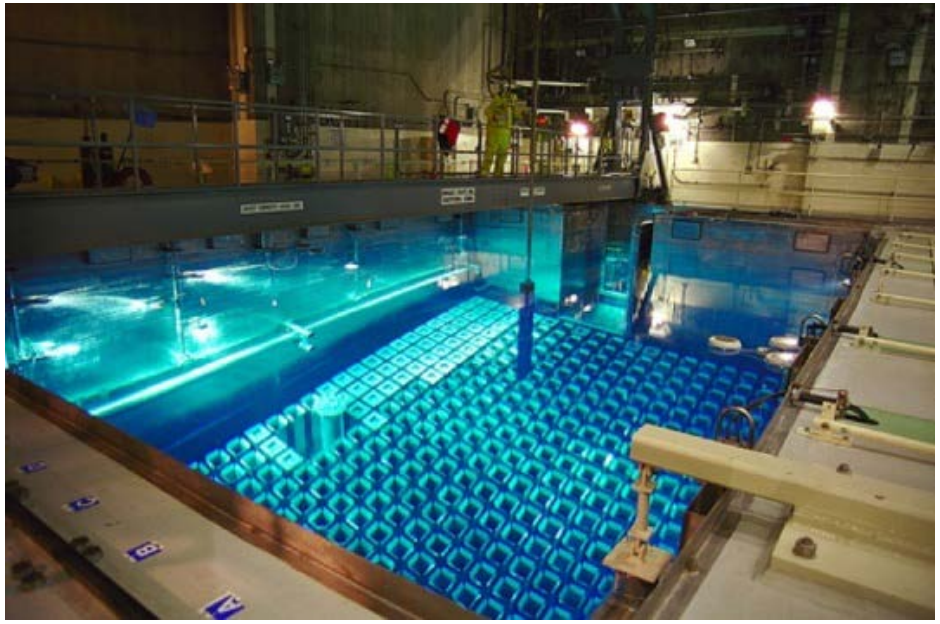
P. Vrbka, J. Krejčí, J. Kabátová, J. Kočí, F. Manoch, V. Vrtílková

Presentation for 24th QUENCH Workshop 2018

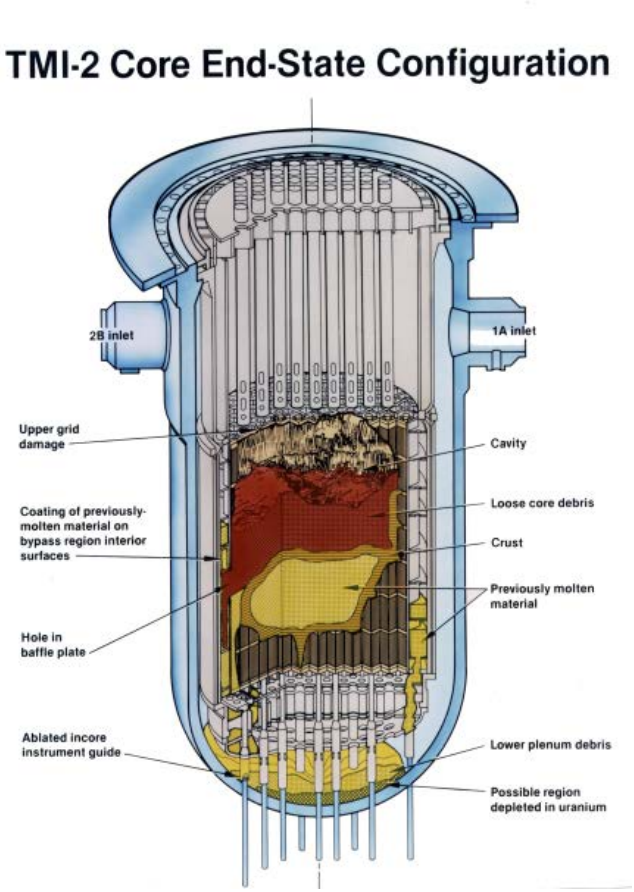
13 – 15th November 2018

SCENARIOS FOR HIGH TEMPERATURE (HT) AIR OXIDATION:

- Loss of cooling accident in spent fuel pool
- Air ingress during reactor vessel failure
- Loss of integrity of spent fuel transportation cask



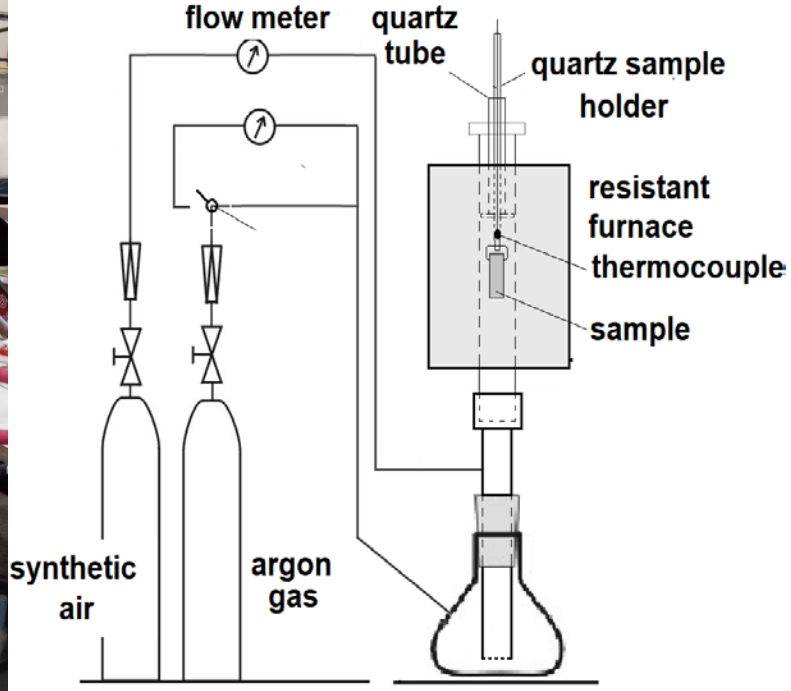




EXPERIMENTAL SETTINGS

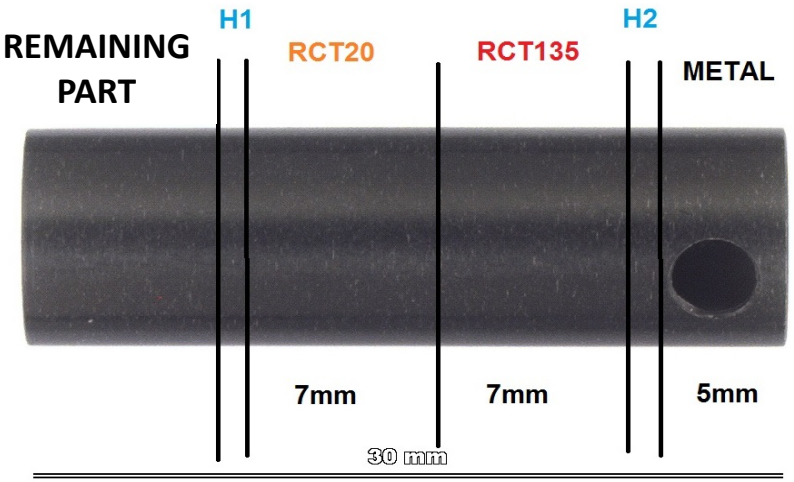




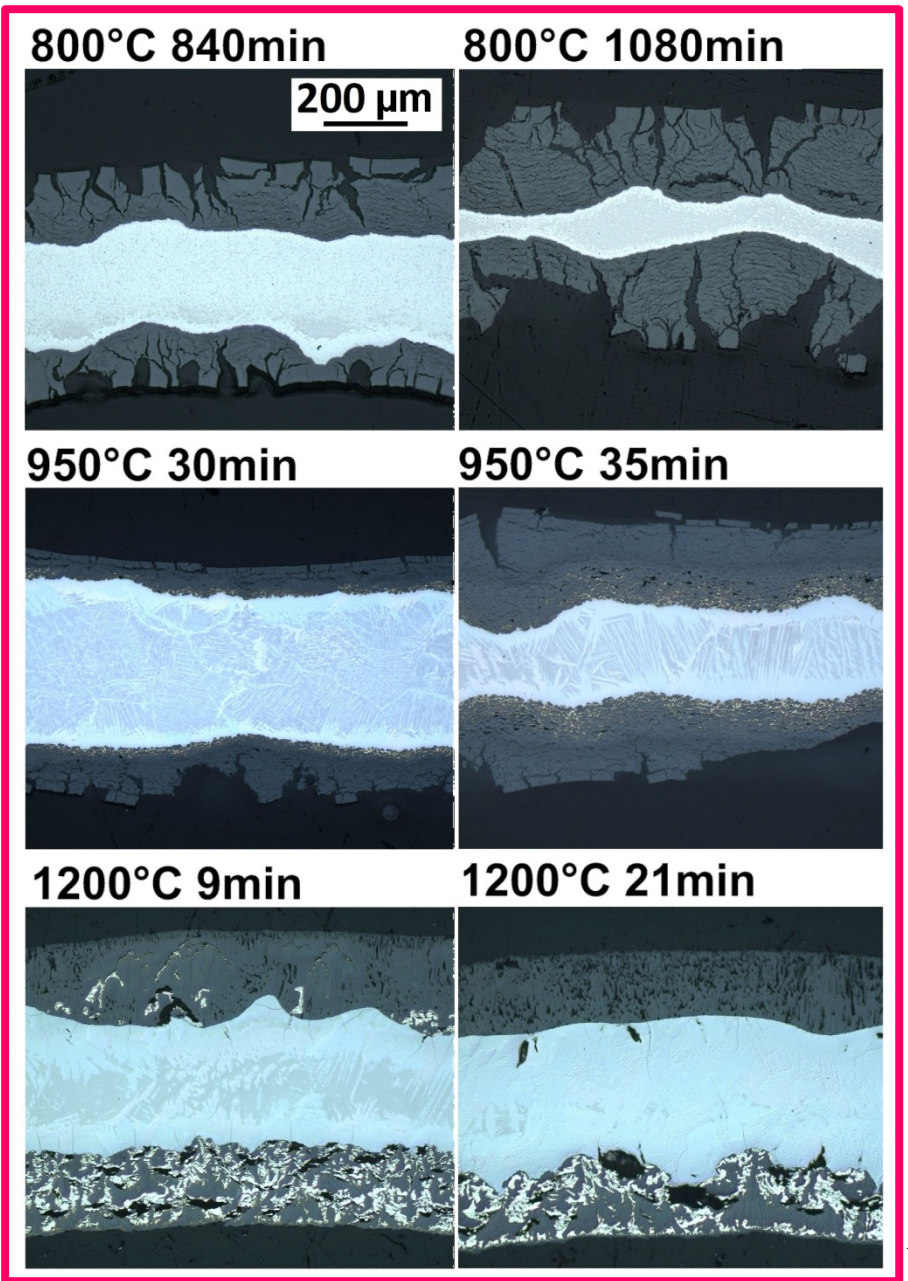


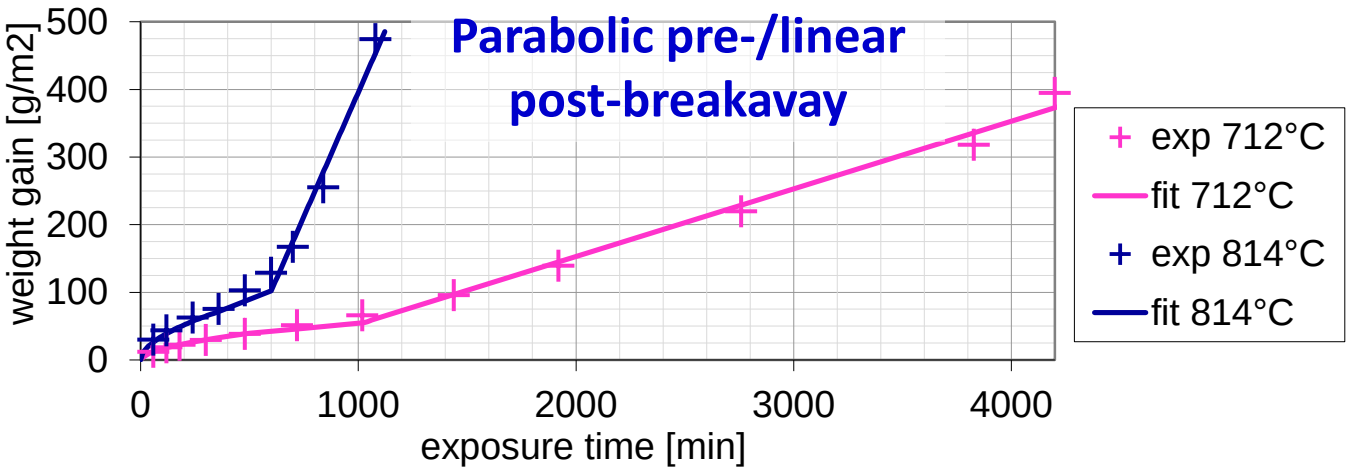
- **Flow Rate**: 18 l/h air + 6 l/h argon, double-side oxidation
- **Specimens**: Ø 9.1×7.93 mm, length 30 mm
- **Pre-oxidation**:
  - **In-autoclave**: steam 425 °C/10.7 MPa for 42 days (**5 µm**) and 105 days (**9.2 µm**)
  - **In HT furnace**: steam (800, 1000, 1200) °C/0.1 MPa at **10-130 µm**

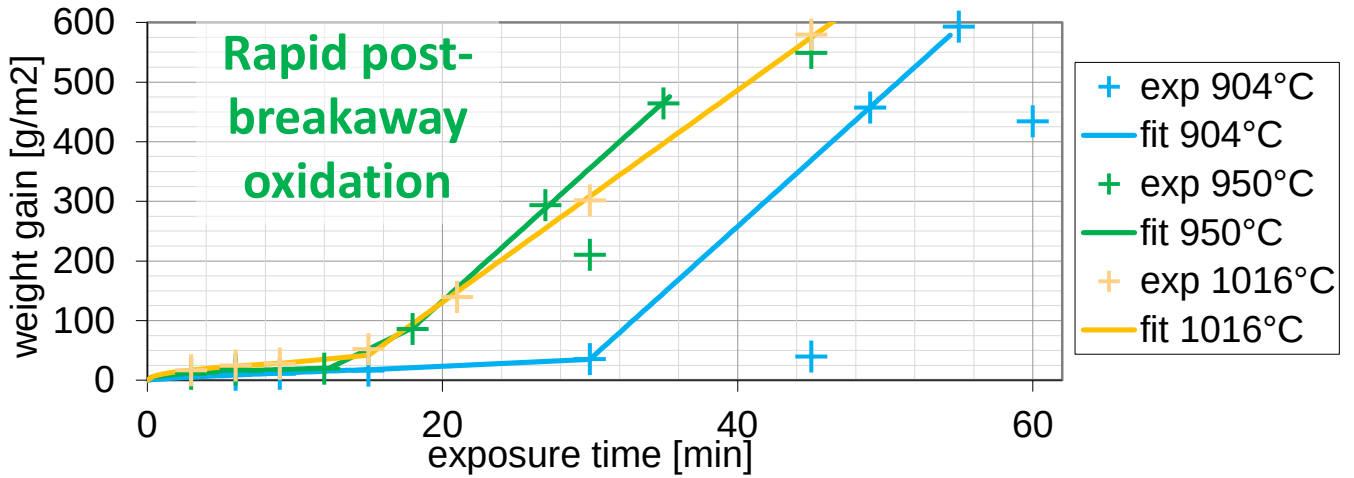
- Post-experimental examination:
  - Weight Gain
  - Visual Inspection
  - Microstructure
  - Microhardness
  - Hydrogen Content
  - Ring Compression Test (20 °C)

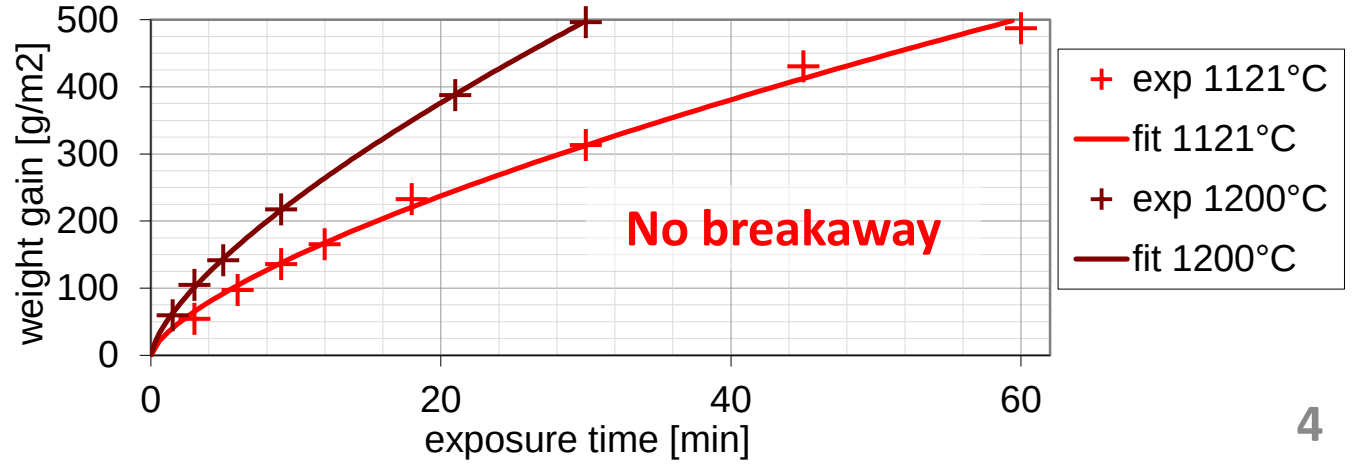


AS-RECEIVED E110 RESULTS



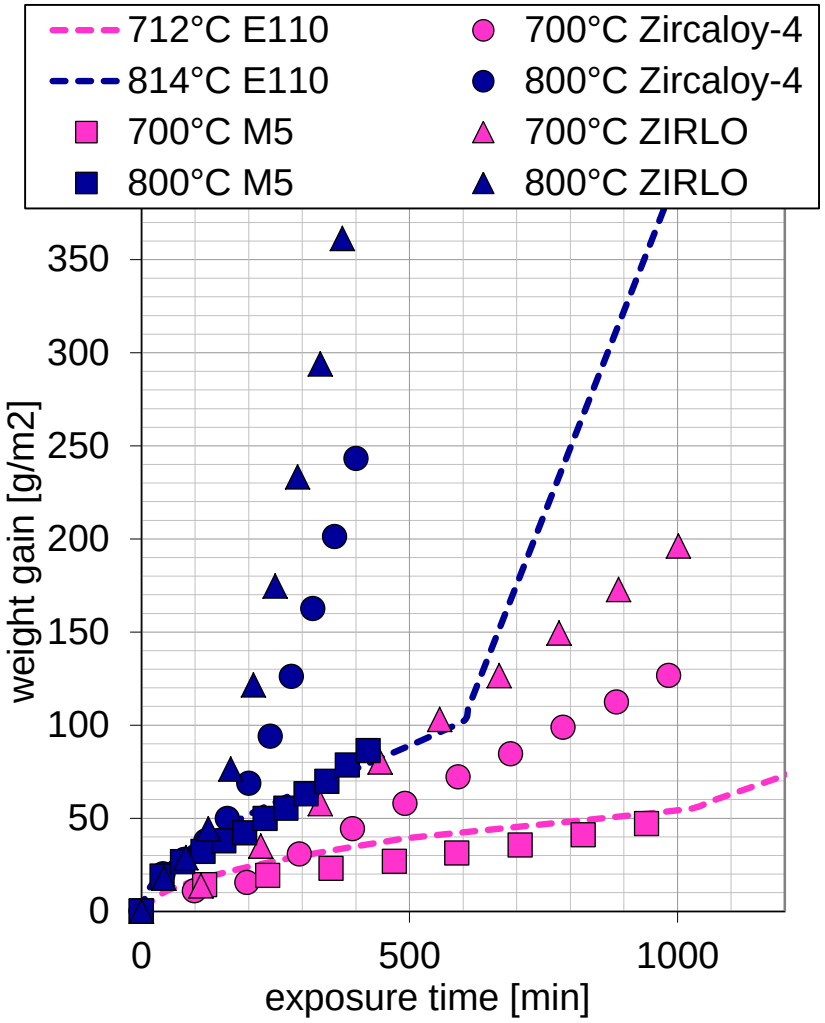


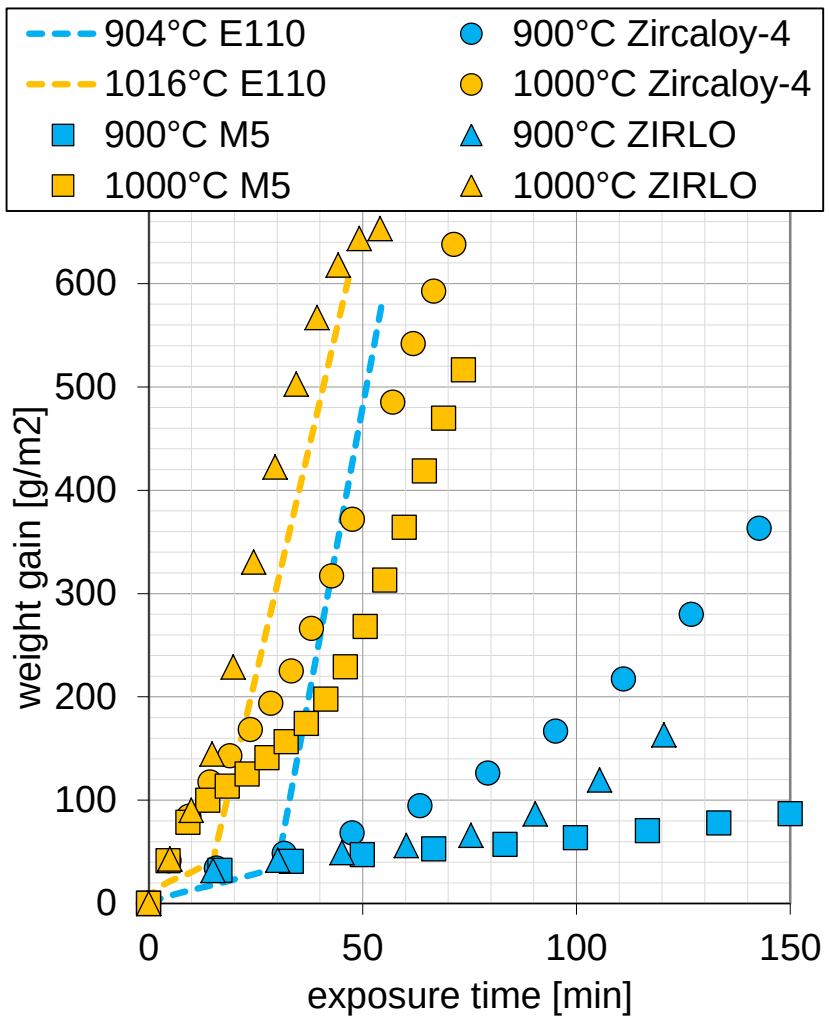


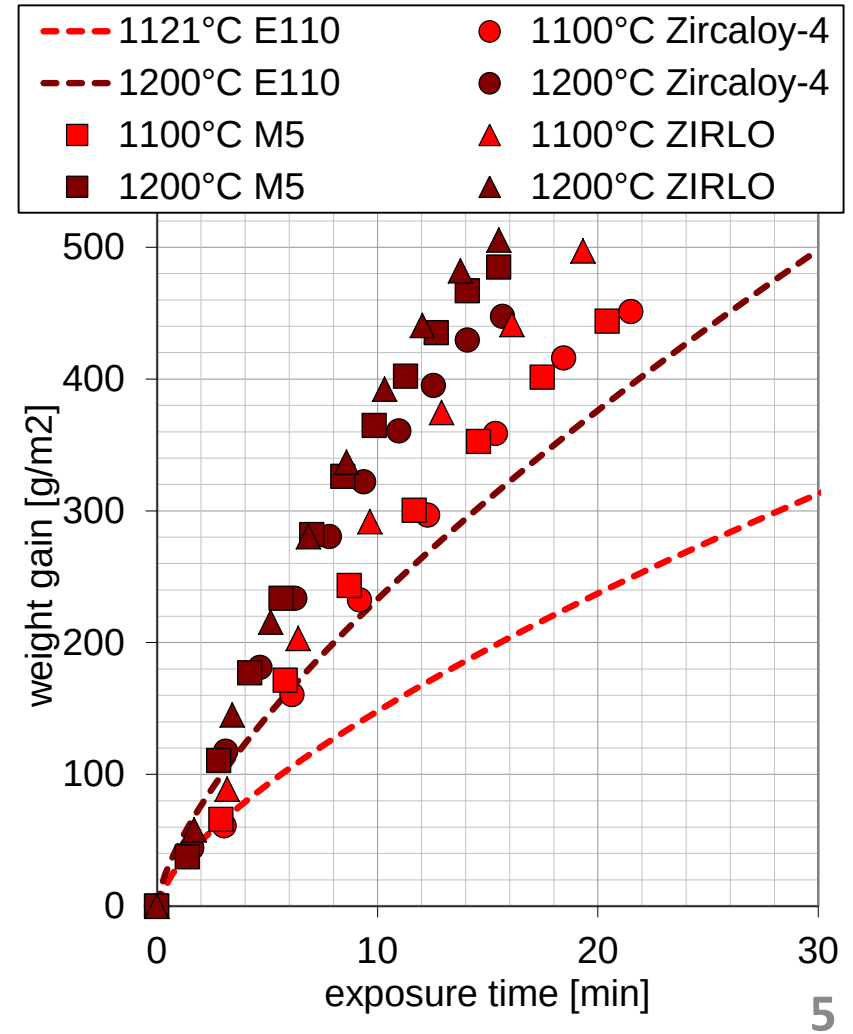


AS-RECEIVED E110 – COMPARATION WITH KIT

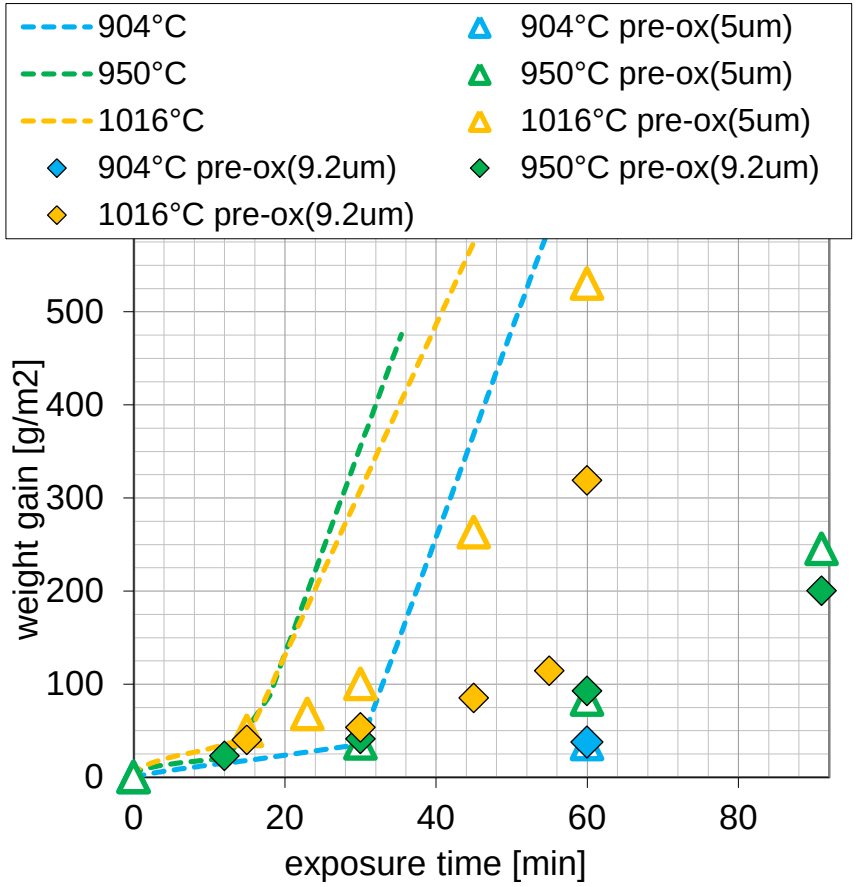
- **700, 800 °C**: similar to M5
- **900, 1000 °C**: higher weight gain in post-breakaway area

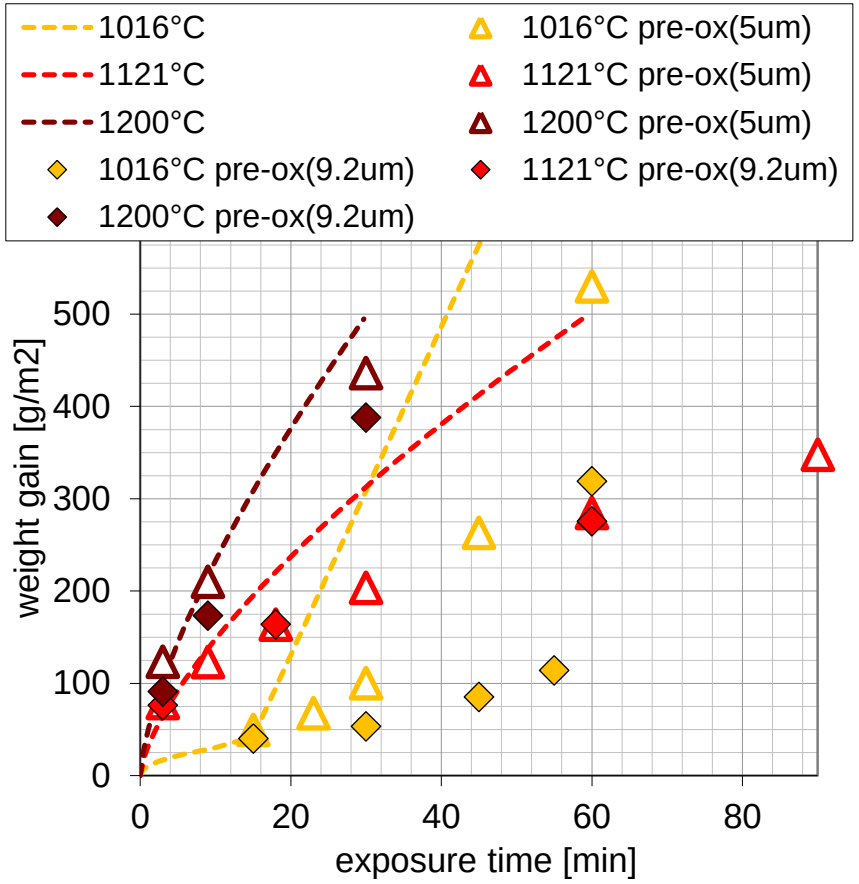






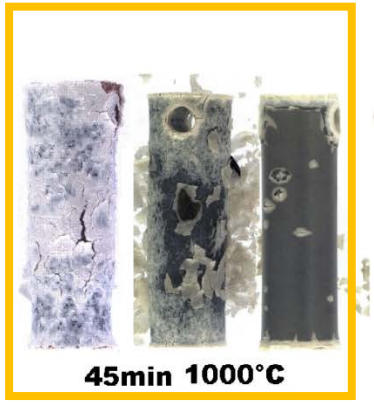
IN-AUTOCLAVE PRE-OXIDIZED E110 RESULTS





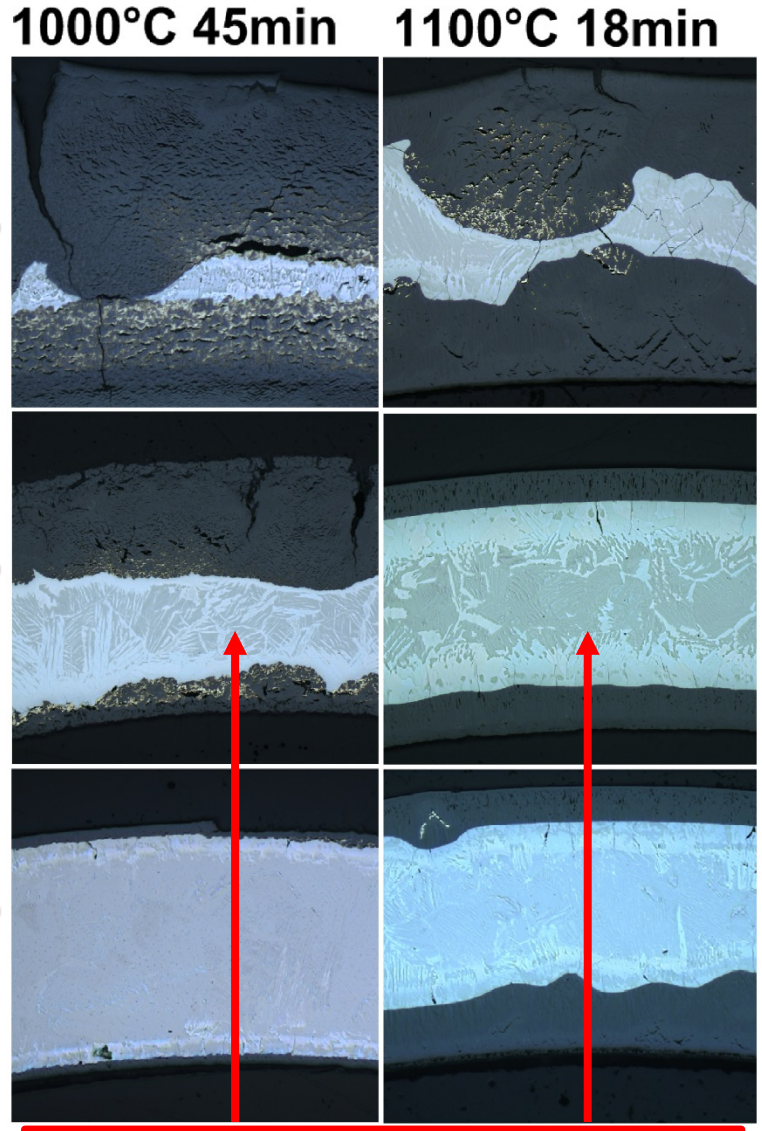








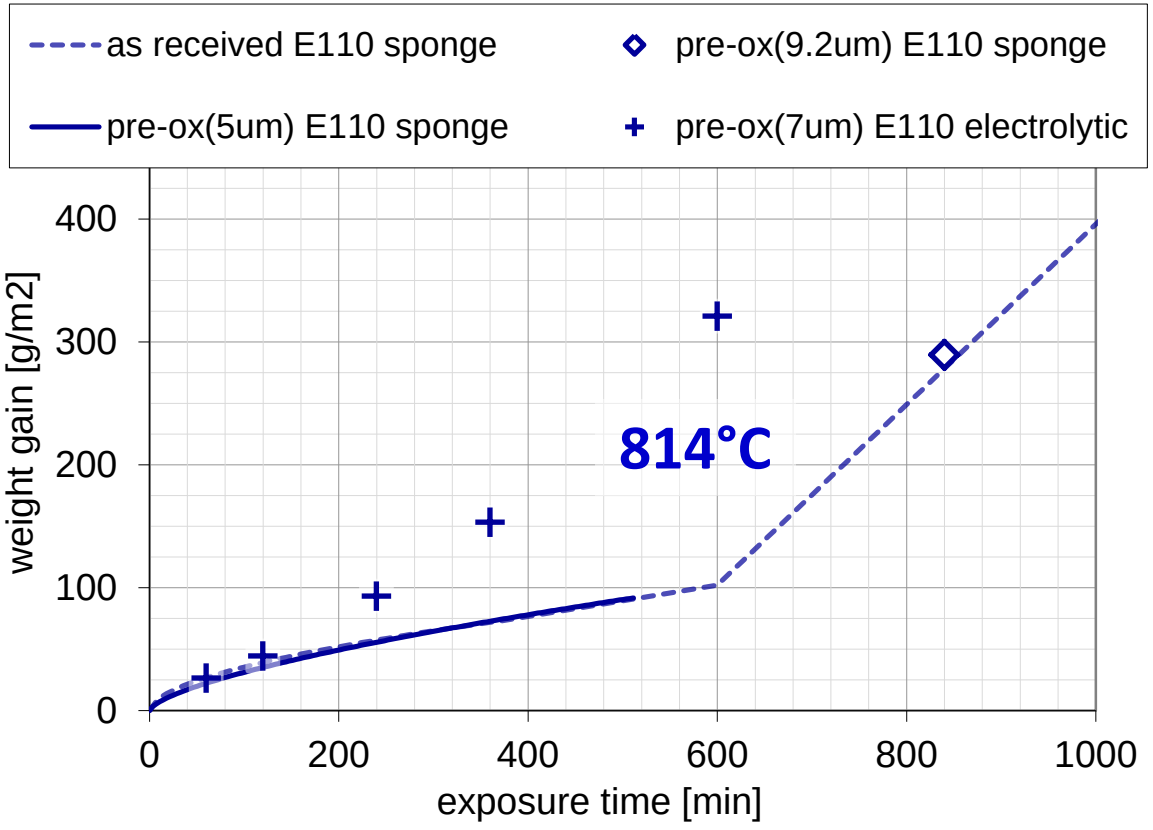


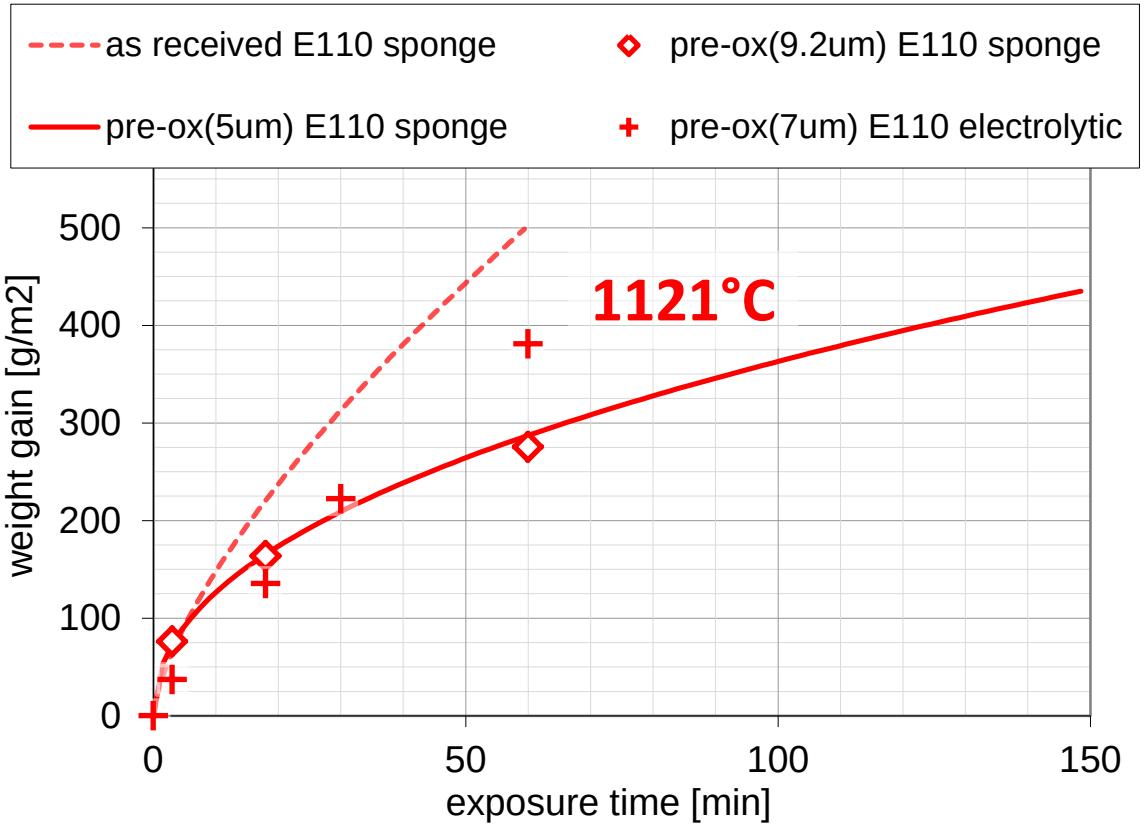


Less nitrides x more α-Zr(O)

IN-AUTOCLAVE PRE-OXIDIZED E110 – SPONGE X ELECTROLYTIC

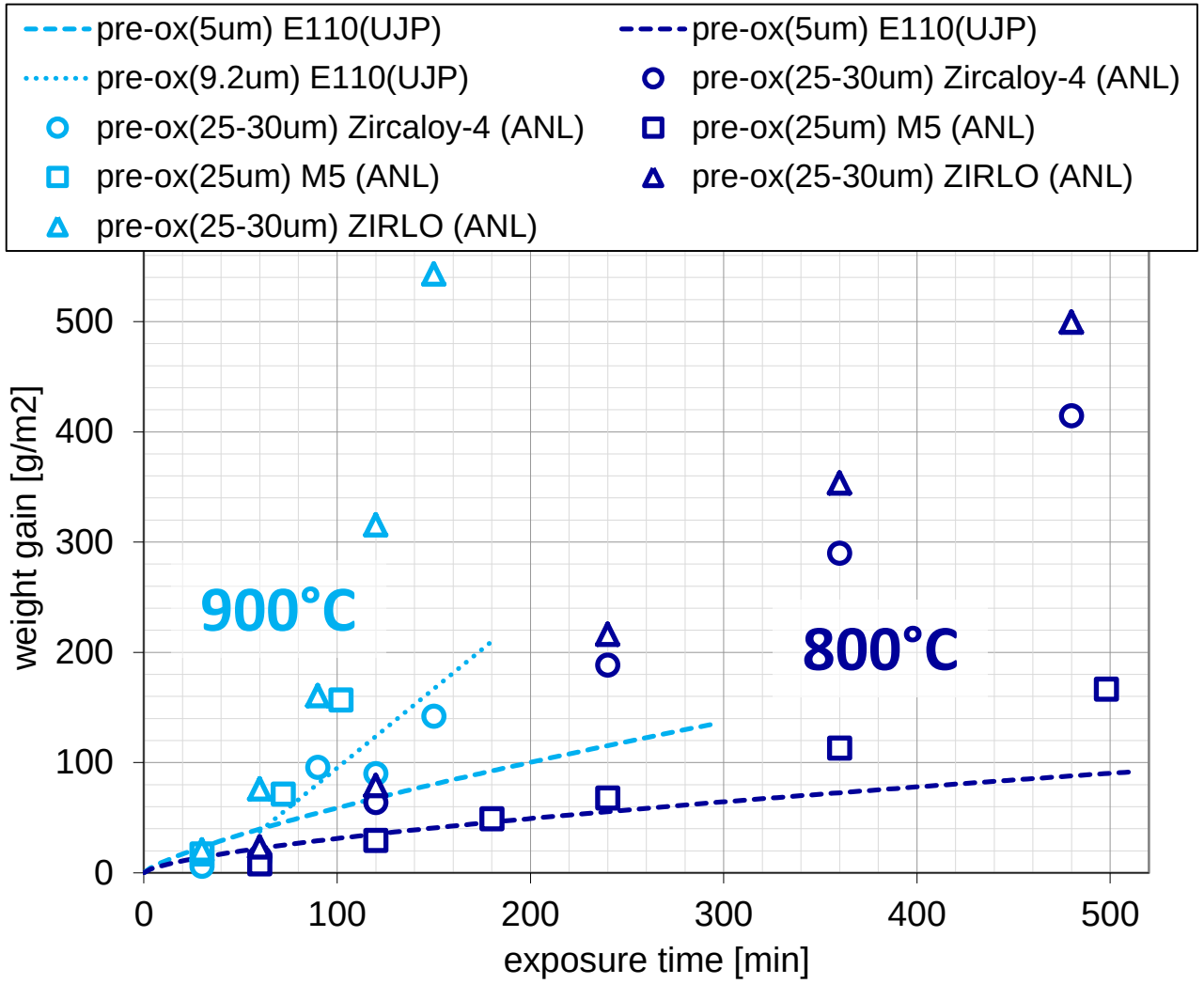
- **800 °C:** higher WG of electrolytic E110
- **1100 °C:** lower WG of electrolytic E110 up to 30 min

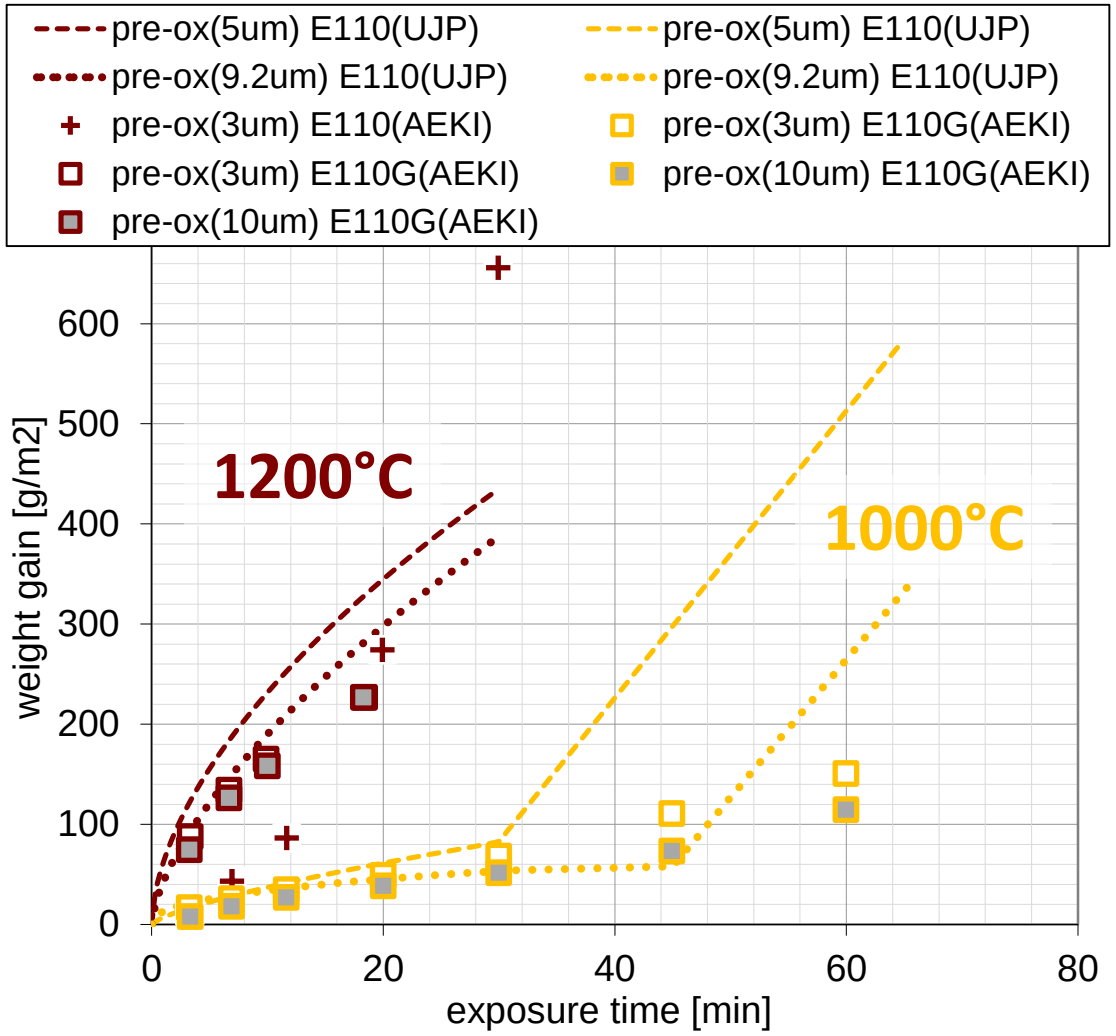




IN-AUTOCLAVE PRE-OXIDIZED E110 – COMPARISON WITH ANL, AEKI

- AEKI: E110G (sponge) x E110 (electrolytic)

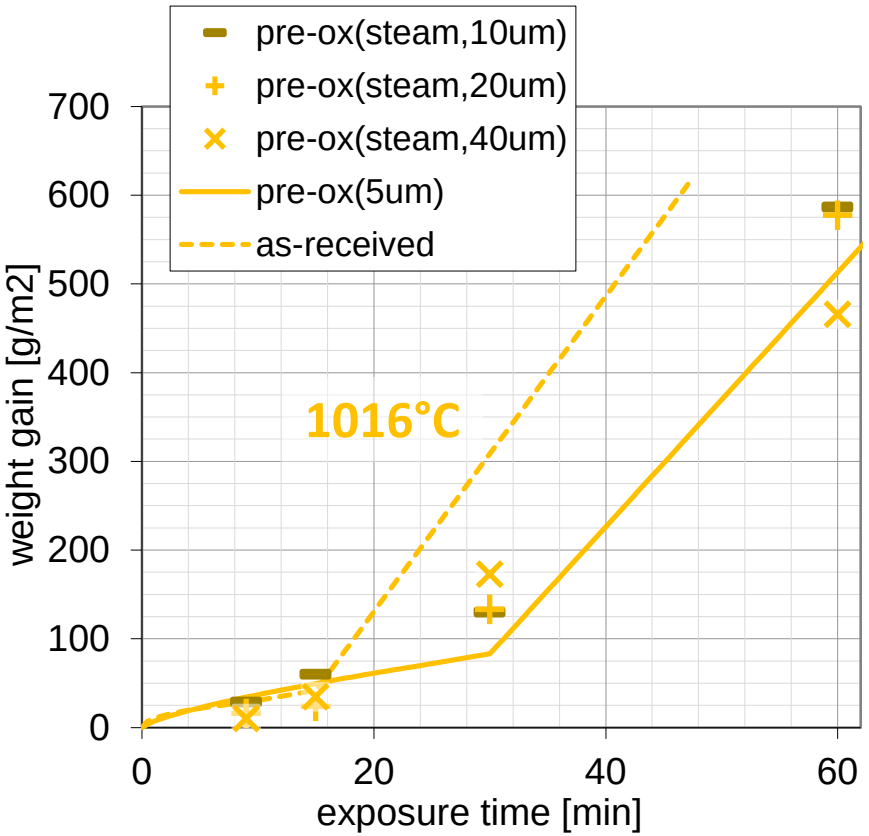


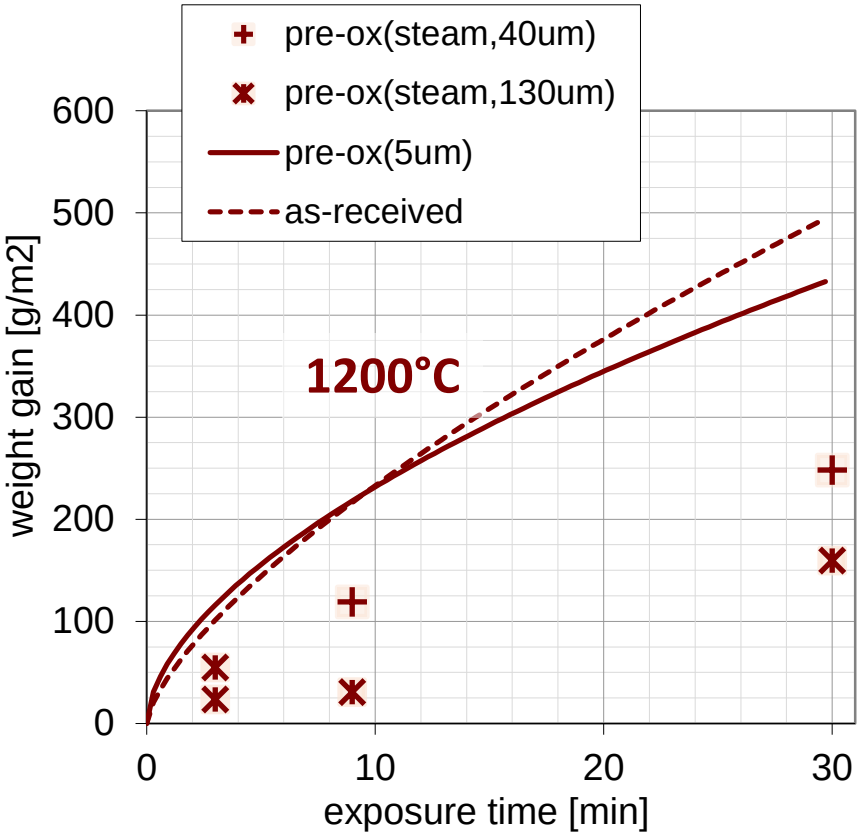


HIGH-TEMPERATURE PRE-OXIDIZED E110 RESULTS

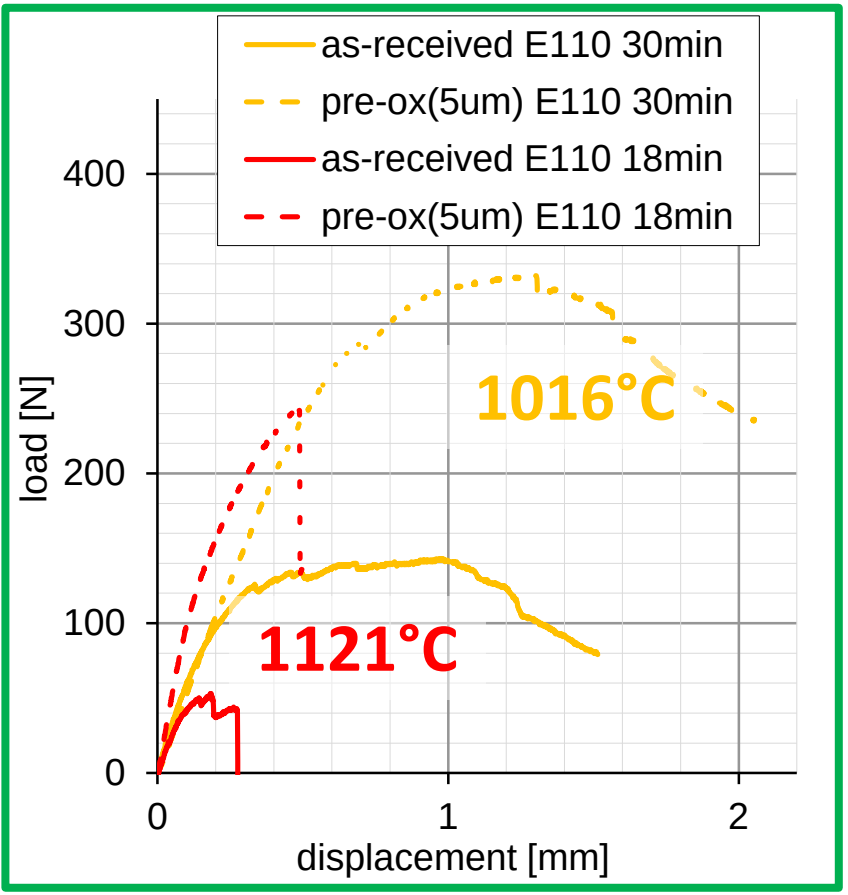


- **814 °C:** No differences
- **1016 °C:** Slightly higher WG than in-autoclave pre-oxidized E110
  - Beam-shaped stoichiometric oxide
- **1200 °C:** Lower WG than in-autoclave pre-oxidized E110
  - No global oxidation starvation, deep axial cracks



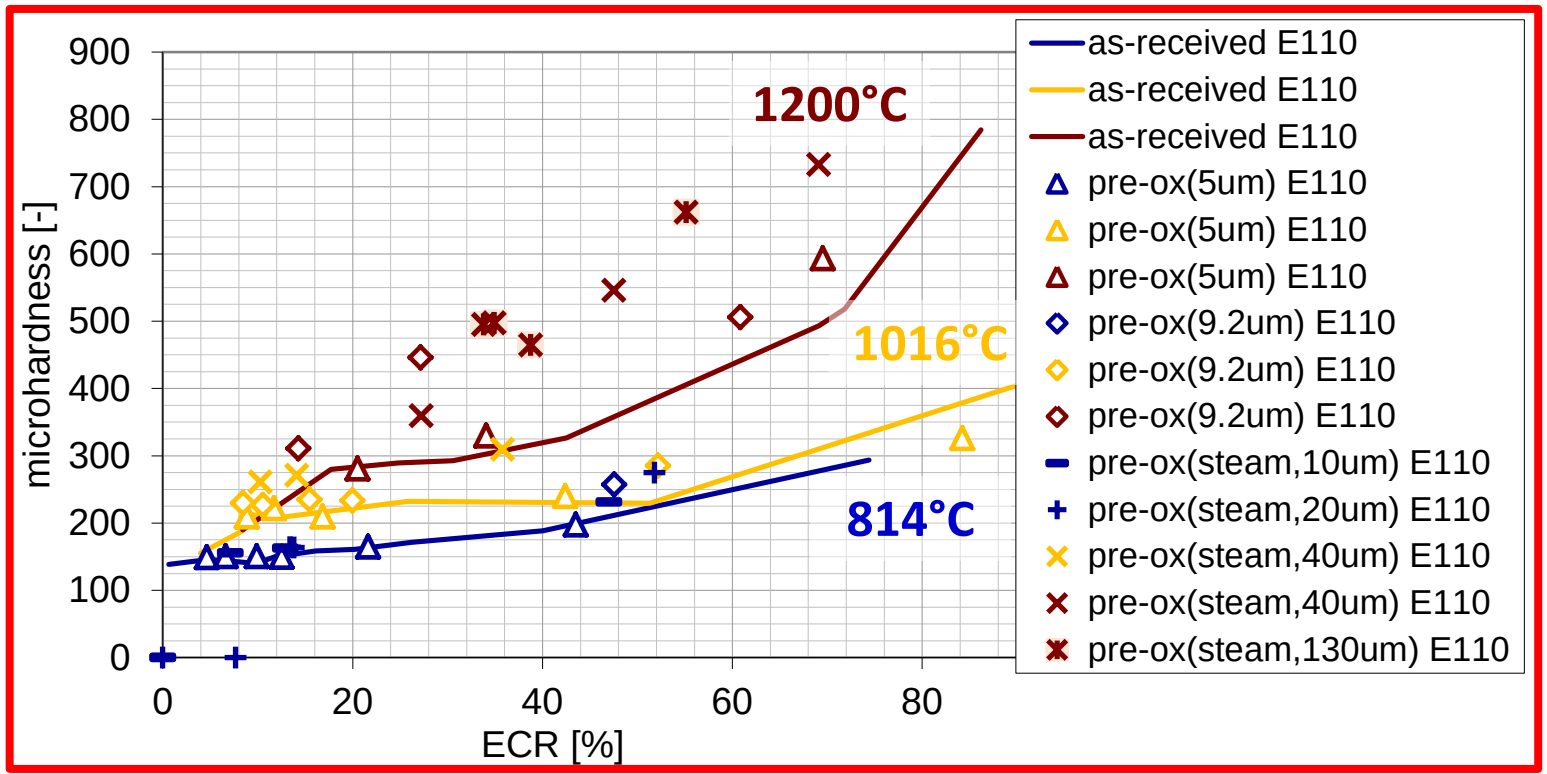


MECHANICAL PROPERTIES



Exposure time [min]	energy [N.m]	
	as-recieved	pre-ox(5um)
15	0.37	0.66
23	0.25	0.62
30	0.12	0.31
3	0.406	0.311
9	0.128	0.148
18	0.053	0.078
30	0.006	0.016

- **RCT:**
  - In-autoclave pre-oxidation → higher maximal load and energy
  - HT pre-oxidation at 1200 °C – prompt cracking during RCT
- **Microhardness:**
  - higher temperature → sharper microhardness increase with ECR
  - pre-oxidation → higher microhardness (800°C no difference)
  - HT pre-oxidation → the highest values due to higher oxygen content



CONCLUSION

- **Air vs. steam** during severe accidents: worse heat transfer, higher reaction heat, nitrogen attack
- Rapid oxidation increase observed at 900–1000 °C
  - Above 1100 °C no breakaway, global oxidation starvation
  - Mechanical properties influenced by microstructure
- Protective effect of pre-oxidation confirmed
  - Higher microhardness of pre-oxidized samples
  - **In-autoclave pre-oxidation**: higher absorbed energy and maximal load
  - **HT vs. in-autoclave pre-oxidation**: lower weight gain only at 1200 °C (**x** lower ductility!)
- Lower oxidation of sponge E110 than electrolytic one
- The lowest weight gain of E110 among comparated alloys except of 900–1000 °C
  - Similar to M5 alloy at 700 °C, 800 °C

Thanks for your attention





UJP PRAHA

REFERENCES

[1] NATESAN, K.; SOPPET, W.K. *Air Oxidation Kinetics for Zr-Based Alloys*. NUREG/CR-6846 ANL-03/32 [online]. 2004. 108 s. [cit. 2017-03-27]. Dostupné z: https://www.nrc.gov/docs/ML0419/ML041900069.html

[2] NEGYESI, Martin a AMAYA, Masaki. Oxidation kinetics of Zry-4 fuel cladding in mixed steam–air atmospheres at temperatures of 1273–1473 K. *Journal of Nuclear Science and Technology* [online]. 2017, **54**(10), 1143-1155 [cit. 2018-05-18]. DOI: 10.1080/00223131.2017.1344583. ISSN 0022-3131.

[3] PEREZ-FERÓ, E., NOVOTNÝ, T. a HORVÁTH, M. *Recent studies on the air oxidation of pre-oxidised E110G and E110 alloys*. Presentation presented at: [Seminar on Cladding Oxidation by Air Under Severe Accident Conditions in a Nuclear Reactor; 2016 Jun 14-15; Budapest; Hungary].

[4] STEINBRÜCK, Martin. Prototypical experiments relating to air oxidation of Zircaloy-4 at high temperatures. *Journal of Nuclear Materials* [online]. 2009, **392**(3), 531-544 [cit. 2018-05-18]. DOI: 10.1016/j.jnucmat.2009.04.018. ISSN 00223115.

[5] STEINBRÜCK, Martin, STEGMAIER, U. a ZIEGLER, T. *Prototypical Experiments on Air Oxidation of Zircaloy-4 at High Temperatures* [online]. Karlsruhe, 2007 [cit. 2018-02-16]. Dostupné z: https://publikationen.bibliothek.kit.edu/270067262.

[6] STEMPNIEWICZ, M.M. *Air oxidation of Zircaloy, Part 1 – Review of correlations. Nuclear Engineering and Design* [online]. 2016, 301, 402-411 [cit. 2017-03-21]. DOI: 10.1016/j.nucengdes.2016.02.042. ISSN 00295493.

[7] STUCKERT, J., HÓZER, Z., KISELEV, A. a STEINBRÜCK, M. Cladding oxidation during air ingress. Part I: Experiments on air ingress. *Annals of Nuclear Energy* [online]. 2016, **93**, 4-17 [cit. 2018-05-18]. DOI: 10.1016/j.anucene.2015.12.034. ISSN 03064549.

Recent activities for analyses of PWR cladding during LOCA quench condition

Hsingtzu Wu

This talk is divided into two parts. The first is about the work done at Japan Atomic Energy Agency (JAEA). Accident Tolerant Fuel (ATF) has attracted much attention after the Fukushima accident, and most of the research focuses on the reduction of cladding corrosion and less hydrogen generation. However, no one has taken thermal properties of ATF into consideration to the best of the author’s knowledge. A series of experiments has been conducted by the author and staff at JAEA to evaluate the effect of the thermal capacity inside cladding on fuel behavior during a LOCA quench condition. It was found that low thermal capacity resulted in tougher cladding during quench, which suggested that decreasing thermal capacity of ATF may be desirable. This series of equipments also implied that that during a LOCA quench condition, the oxygen stabilized zirconium alpha layer may fracture first, then the zirconia layer, and finally the prior beta layer. In addition, a computation using RANNS code suggested the off-center pellets might have a significant impact on fracture stress during quench. The second part of the talk introduces an exciting research plan in the department of a Nuclear Engineering and Technology at Huazhong University of Science and Technology.


TOSHIBA

Resent Activities for Analyses of PWR Cladding During LOCA Conditions

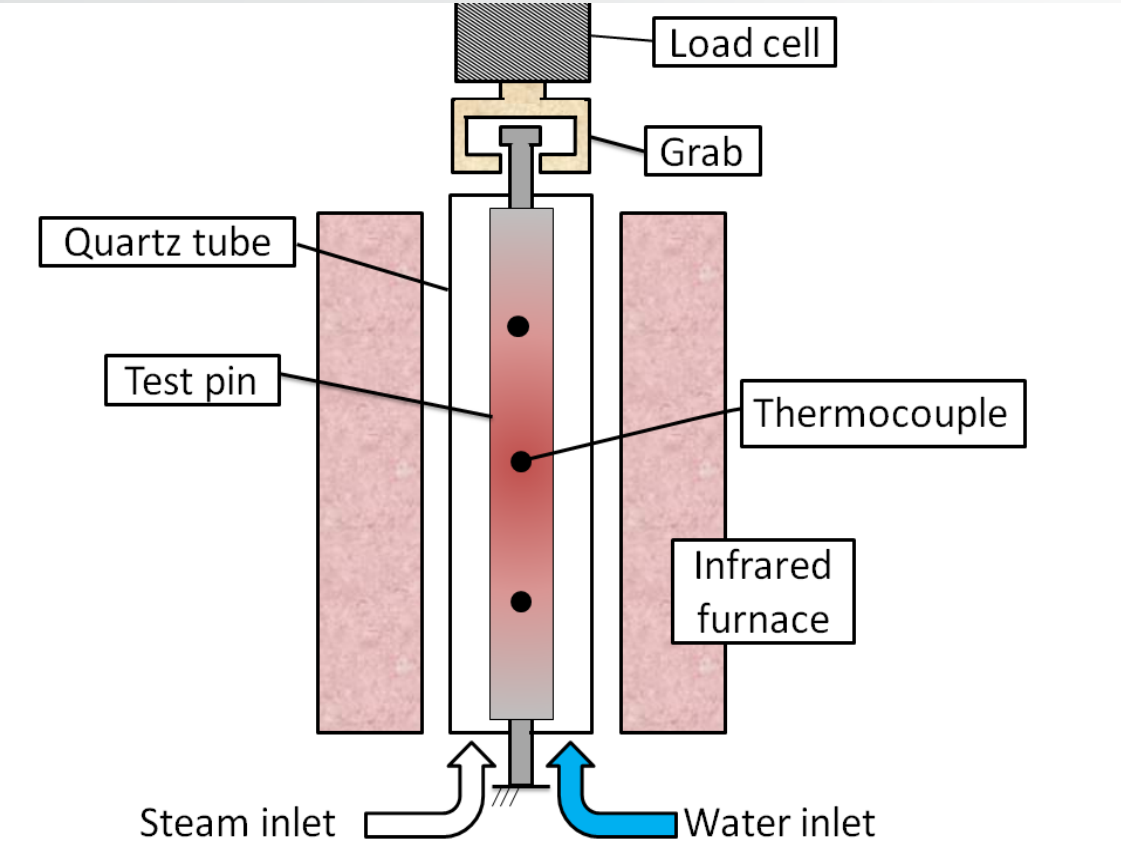
WU Hsingtzu

Associate researcher

Department of Nuclear Engineering and Technology

Huazhong University of Science and technology, Wuhan, China

LOCA quench experimental setup



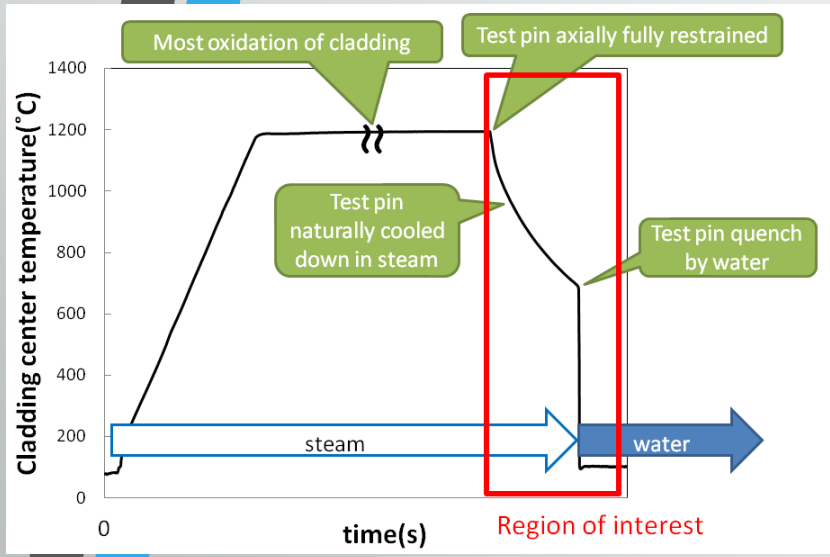
Experimental Specifications:

Cladding type: Zircaloy-4
Pellet type: Al_2O_3
Length of cladding: 19.0 cm
Rod fill pressure: 0.1 MPa
Oxidation temperature: 1200 ˚C
Quench onset temperature: 700 ˚C
Fully restrained
One-sided oxidation



Apparatus of the experiment

The experimental results showed that the fracture load in case 2 was larger by about 1000 N



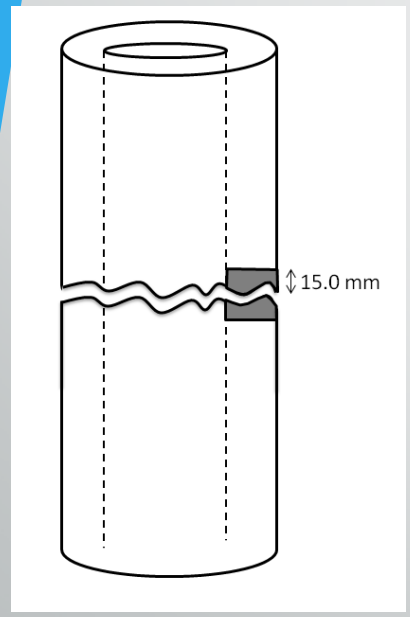
Case 1: high heat capacity inside cladding
Case 2: low heat capacity inside cladding

Experimental data				
BJ-ECR	25%			
Case number	1	1	2	2
Pellets inside cladding	Yes	Yes	No	No
Average oxidation temperature* (˚C)	1198.4	1198.6	1199.2	1197.9
Oxidation time*(s)	1875.7	1881.0	1872.5	1872.5
Quench temperature* (˚C)	699.2	694.5	681.1	693.1
Fracture time (TAQ**) (s)	7.8	4.0	55.5	50.9
Fracture temperature* (˚C)	116.6	110.7	71.1	52.6
Fracture load (N)	1996.0	2128.0	3100.0	3146.0

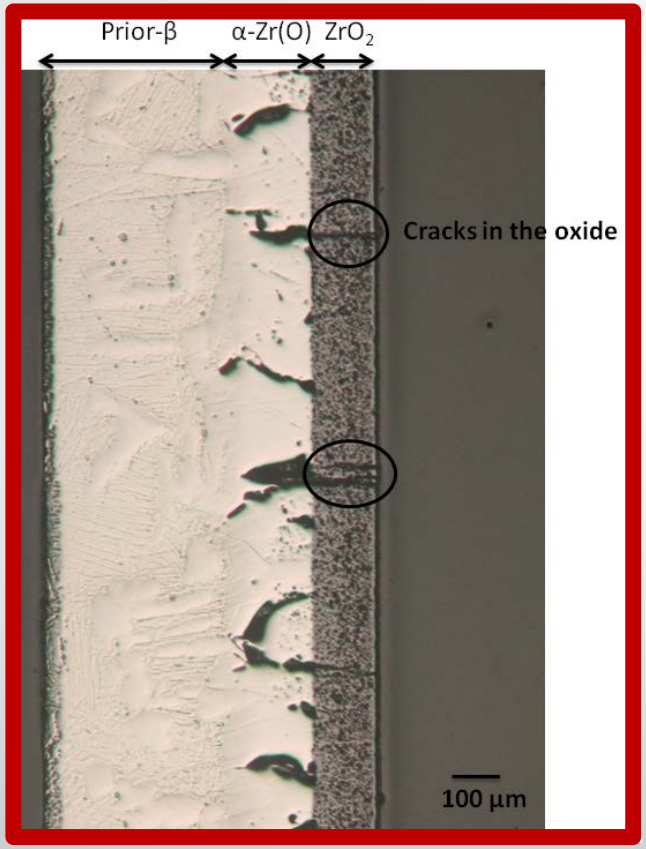
*the control temperature
**time after quench

Hsingtzu Wu, Yutaka Udagawa, Takafumi Narukawa, and Masaki Amaya, "Crack formation in cladding under LOCA quench conditions, Nuclear Engineering and Design, Vol. 303, July 2016, Pages 25-30.

Fracture sequence：α-Zr(O) → ZrO_2 → Prior-β



Case 1: high heat capacity inside cladding



Case 2: low heat capacity inside cladding

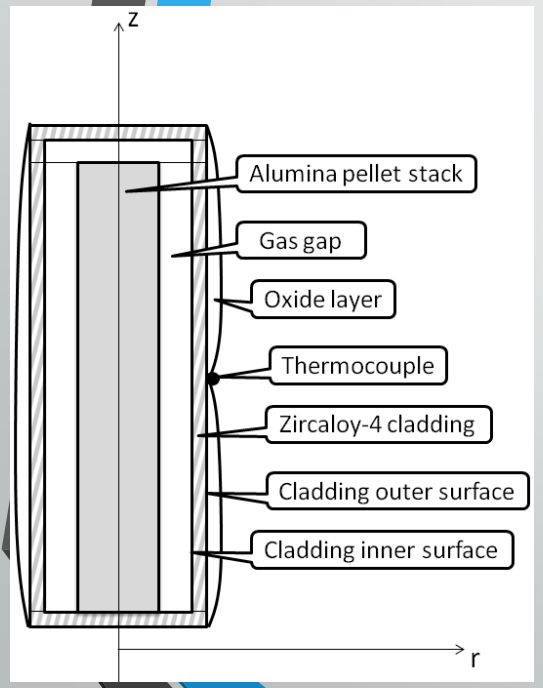


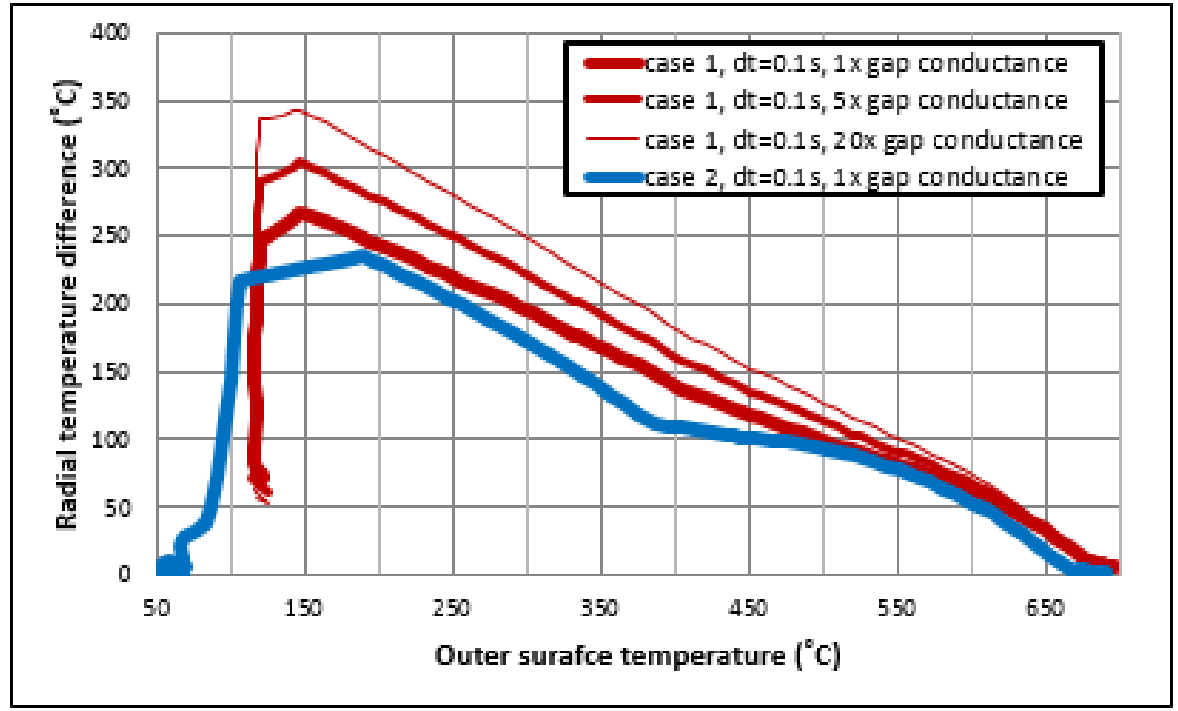
The crack formation is caused by the maximum thermal stress in cladding, which is related to the maximum radial temperature difference.

Hsingtzu Wu, Yutaka Udagawa, Takafumi Narukawa, and Masaki Amaya, "Crack formation in cladding under LOCA quench conditions, Nuclear Engineering and Design, Vol. 303, July 2016, Pages 25-30.

RANNS analysis suggests factors affecting radial temperature difference

Sketch of RANNS model





Case 1: high heat capacity inside cladding
Case 2: low heat capacity inside cladding

RANNS suggests that

1. the maximum radial temperature difference increases with the heat capacity inside cladding

2. the radial temperature difference increases considerably with off-center pellets, which might also affect crack formation.

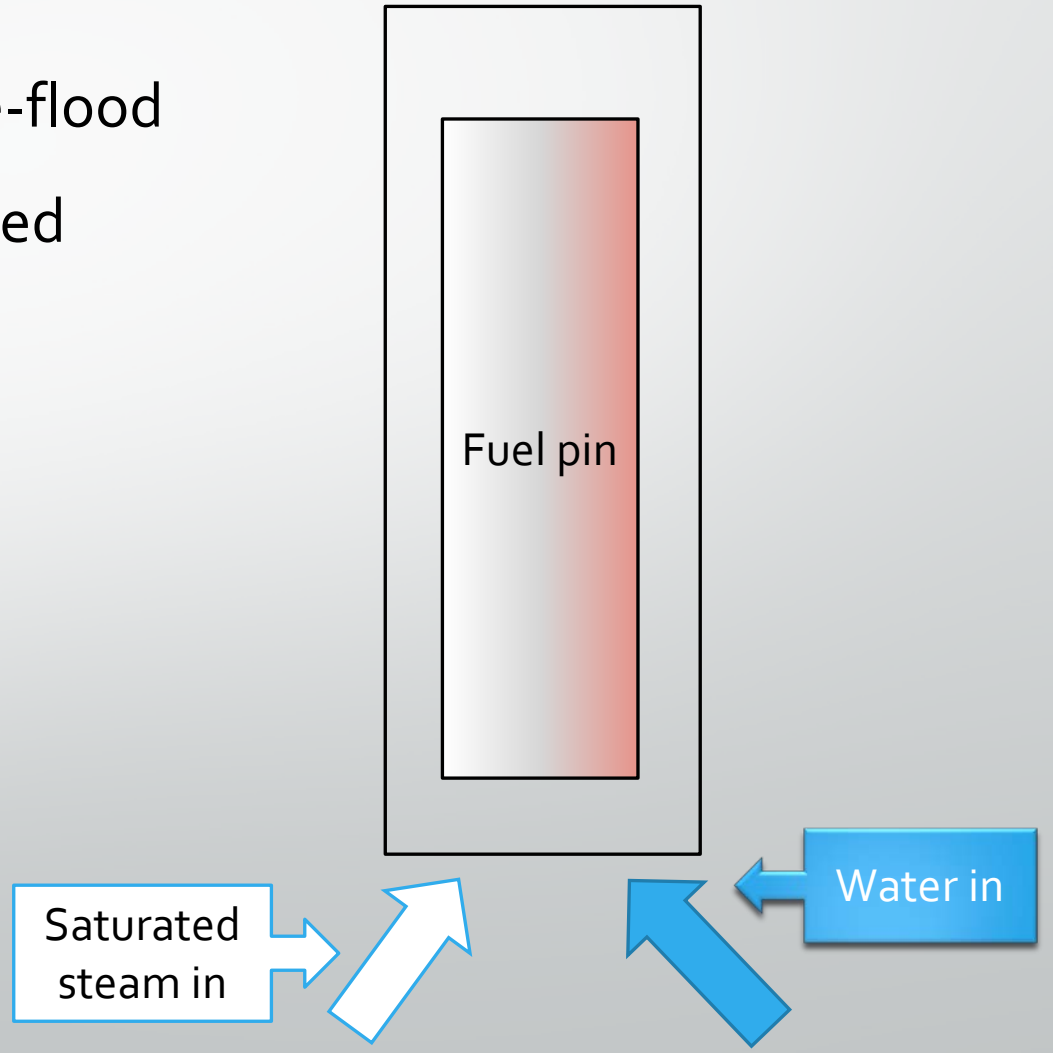
Hsingtzu Wu, Yutaka Udagawa, Takafumi Narukawa, and Masaki Amaya, "Crack formation in cladding under LOCA quench conditions, Nuclear Engineering and Design, Vol. 303, July 2016, Pages 25-30.

Possible new LOCA test equipment at HUST

- Advice seeking
- Purposes of the new LOCA test equipment:
  - Better understand behavior of fuel cladding during LOCA
  - Update database of some mechanical properties for more accurate computation
  - Support new design of nuclear fuel

Features of new LOCA test equipment

- Fuel pellet skipped
- Continuous heating during quench and re-flood
- Measurement of temperature with infrared sensor instead of using thermocouples
- Heating controlled by
  - Cladding surface temperature or
  - Heat flux from the heating pin
- Filming of the whole process in detail

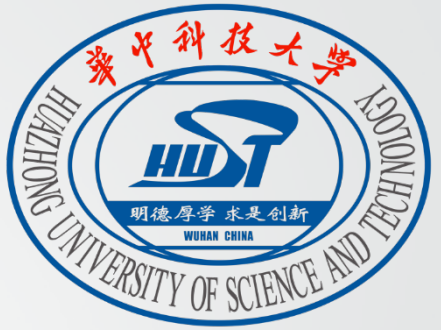


Experiments to be conducted

- Measurement (update the database, the latest is MATPRO, 1979)
  - Oxidization of cladding
  - Thermal expansion due to phase transformation
  - Creep rate
  - Fatigue
- Comparison with the past experimental data
  - Different oxidation temperatures
  - Different thickness of ZrO_2
  - Different quench temperatures
- Effect of non-uniform heating during quench and re-flood
- Effect of tempering
- Effect of varying amount of coating on toughness of cladding

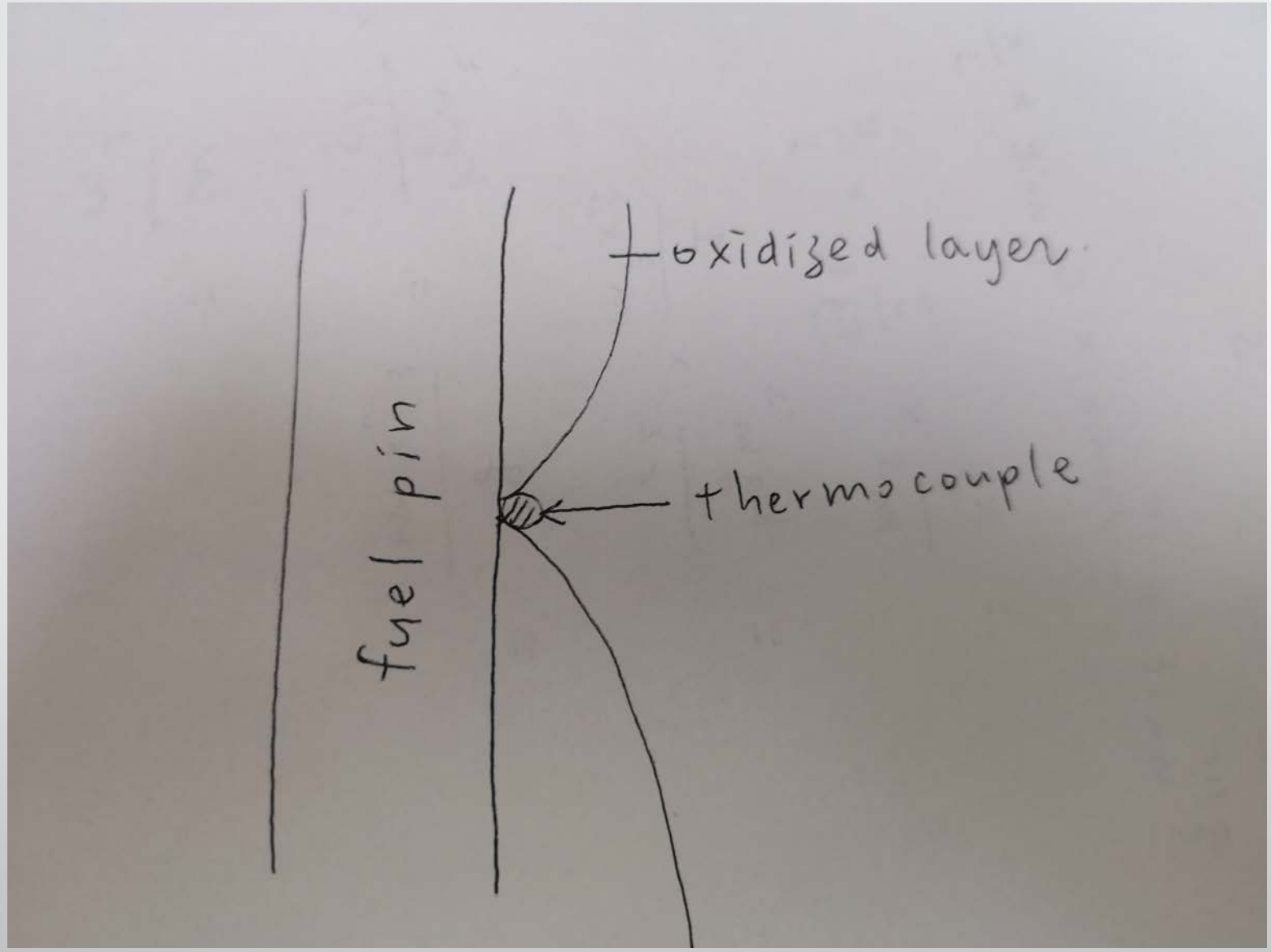
Nuclear power is expanding in China

- Therefore lots of work on nuclear safety
- Nuclear engineering at HUST is expanding, too
  - Welcome international collaboration
  - Welcome scholars' visiting
  - Hiring faculty members and postdocs
  - Lots of opportunities



Thanks for your attention ☺

Questions or comments?


oxidized layer
thermocouple
fuel pin

Summary Report of 24th-QUENCH Workshop

Junhui DIAO, Xiaojun HE, Qian XU, Songtao JI

Nuclear Safety and Fuel Performance Research Lab,
China Institute of Atomic Energy

For developing higher performance fuel rods, the cladding behavior under LOCA condition, one of the main content of the fuel safety characteristics R&D project, has been studying in China Institute of Atomic Energy since 2013. CIAE research team is interested in two main items concerned with LOCA test: one is for new cladding materials; the other is for new structure fuel rods. The study for the former item has been lunching based on the requirements of 10 CFR50.46 ©, meanwhile, the rod failure process test plan has been establishing for the second item. The study will get the necessary data for checking if the new cladding materials and the new structure fuel rods' design criteria meet the current LOCA design requirements.

Test facilities, such as high temperature oxidation test loop, single rod behavior test instrument, have been established in CIAE. The calibration test, using Zr-4 alloy claddings, has been done for testing the facilities' ability, mainly includes, high-temperature oxidation test and relative material characteristic examination, the single rod ballooning and burst test, and the small bundle test.

Until now, necessary test abilities and test samples have been carefully prepared by CIAE. All tests will be done in the following two years. The test for annular fuel rod, with inner and outer cladding, is regarded as a new technical challenge in the LOCA research field.



This Document and the information it contains are proprietary to CIAE. No parts of this documents or the information it contains may be reported, stored in a retrieval system, or transmitted to third parties in any form or by any means, electronic, mechanical, photocopying, recording or otherwise, without the prior written of the CIAE Management Board.

Overview of R&D Progress on Cladding Behavior under LOCA condition in CIAE

Diao Junhui, He Xiao-jun, Xu Qian, Ji Song-tao

Nuclear Safety and Fuel Performance Research Lab.
China Institute of Atomic Energy



Outline

- **Motivation and projects introduction**
- **The status up to now**
  - Test facilities setup
  - Calibration experiments with Zr-4
  - Single rods behavior test
  - 3X3 bundles behavior test
  - Modeling and code development
- **Future works in 2019 & 2020**
  - Test plan and technical challenge
  - Test facilities updating
  - Draft schedule for study

Motivation for LOCA Tests in CIAE

➢ In the past (before ~ 2000)

- FA mainly depends on import: France, Canada, Russia, U.S.A
- No strong needs to do the experiments (calculation + single-function verification experiments)
- In the earlier of1990s, there was a LOCA test lunched in CIAE for Qinshan-I NPP (Mr. Huang Yucai, etc)

➢ from ~2000 to current

- China determined to develop its FAs (*with independent intellectual property rights*)
- ***CIAE get the support from State Funds, to do the safety test for fuel rods***
- Study of cladding's behavior under LOCA condition is one of the most important task.

Background of the Projects

➢ For new cladding (structure unchanged / material changed):

- Get the design criteria, based on the 10CFR50.46（C）requirements
- ***New Zircaloy Cladding Safety Characteristics Study In LOCA condition*** (2013-2017, State Funds);
- ***Zircaloy Cladding Performance Study for CAP-1400 LTA*** (2017-2020, State Funds);
- Technical Service Projects from NPIC and CGN (from 2010)

➢ For new design fuel rods (structure changed / material unchanged):

- Check current design criteria's applicability , Clarity the rod failure process, Optimize the fuel rods' design.
- ***Annular Fuel Assembly Research & Manufacture for PWR*** (2016-2020, CNNC)
- ***Key Technology Study for Annular Fuel Assembly*** (2017- 2020, CAEA)

For New Claddings

- **The samples mainly comes from NPIC (National Power Investment Corp.)**
- **SAZ-6, SAZ-4, compare to the M5, ZIRLO, and Zr-4**

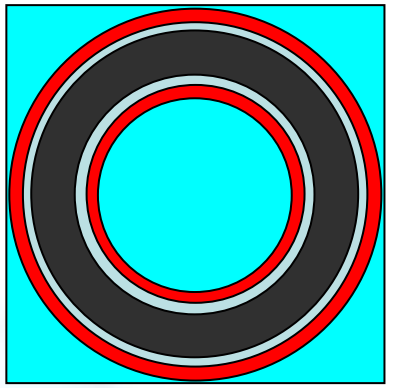
10CFR50.46（C）requirements

- **PCT**
- **Brittle**
- **Breakaway oxidation**
- **Maximum hydrogen generation**
- **Long-term cooling**

- *Cladding failure process study*
- *Safety criteria study*
- *Transient performance code development*
- Breakaway oxidation study
- Long-term cooling study
- Ductility study with quenching
- Ductility study during the ballooning process
- Long term internal-pressure creep study
- Rupture study with axial-loading (with quenching)

For New Design (Annular fuel)

- Annular fuel: double cladding (Zr-4), annular pellet (UO_2) with two coolant channels. LOCA test is necessary for getting the license.



Cross section of annular fuel rod

- Inner cladding behavior:

  The failure way: collapse, different with current cladding

  Inner surface oxidation: could it introduced new criteria**?**

- outer cladding behavior:

  Failure way: Balloon and burst, similar to current cladding;

  Could the geometry parameter affect the current design criteria**?**

- Single rod behavior:

  Could annular fuel keep the integrity under current LOCA condition?

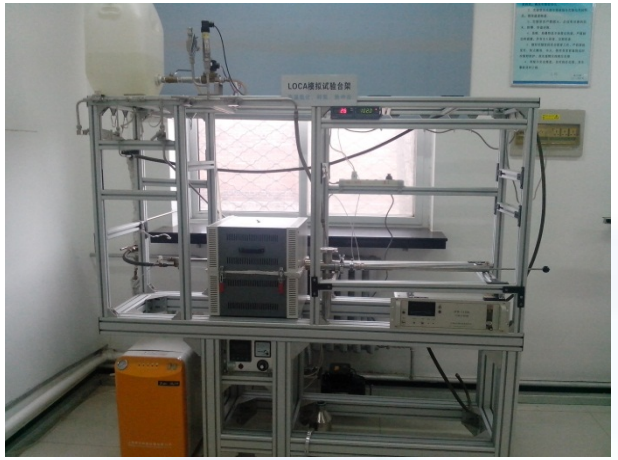
  Which cladding will be failure firstly, and corresponding effects on long-term cooling ability…..

  Optimize the thickness of inner/outer cladding, delay the failure time, get more response time for ECCS



Annular rod samples

Test Facilities Setup



High-temperature oxidation test loop



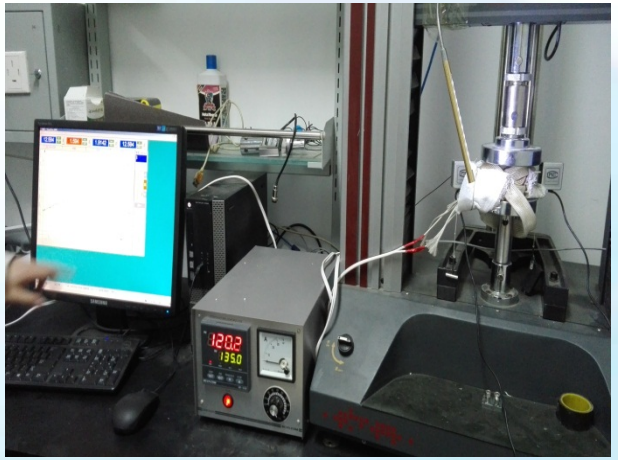
Thermal Gravimetric Analyzer



breakaway oxidation test loop



Reflood T-H test loop (8X8 fuel length bundle)



Ring-compression Installation



LOCA test loop



Pre-Hydrogen Installation

Calibration Test

Compare to NRC-RG 1.223 & ANL's test condition

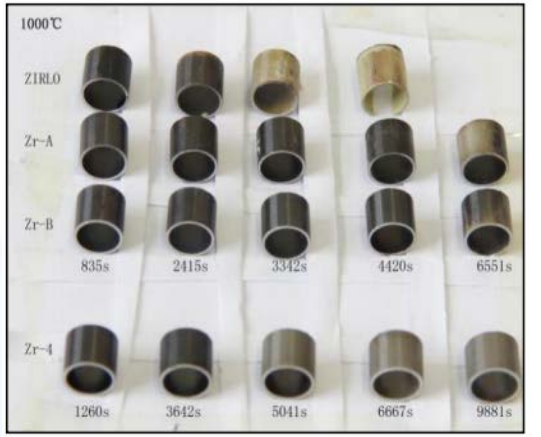
	NRC-RG 1.223	ANL	Test in CIAE
Sample length （double side）	≥25mm	30mm	30mm
Sample length for Ring compression	8mm	8mm	8mm
Ring compression temperature	135℃	135℃	135℃
Ring compression velocity	2mm/min	2mm/min	2mm/min
Flow rate of the steam	0.048~1.8 g/cm^2.min	~0.32 g/cm^2.min	~0.25 g/cm^2.min
Heating rate	300~1000℃，>20℃/s （<35s），1000~1200℃，>2℃/s（<100s）	300~1200℃，~90s	300~1200℃，~30s
Cooling Rate to 800℃	1200~800℃，>2℃/s（<200s）	~13℃/s（30s）	~13℃/s（30s）

- Cladding samples: ZIRLO, SAZ-4, SAZ-6, Zr-4, M5

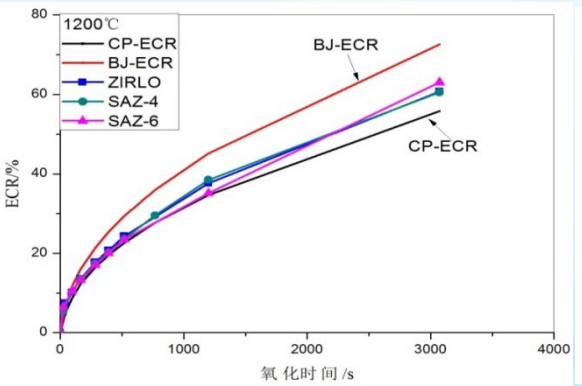
Oxidation weight test

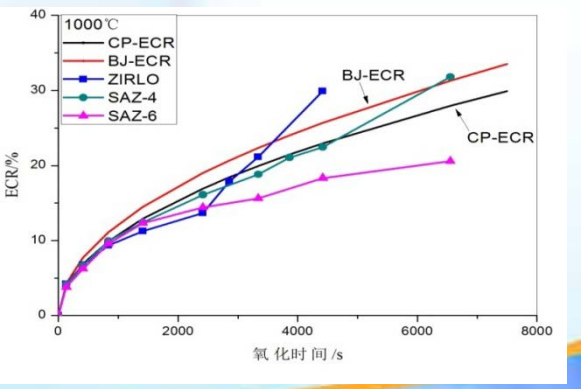


a 1200℃



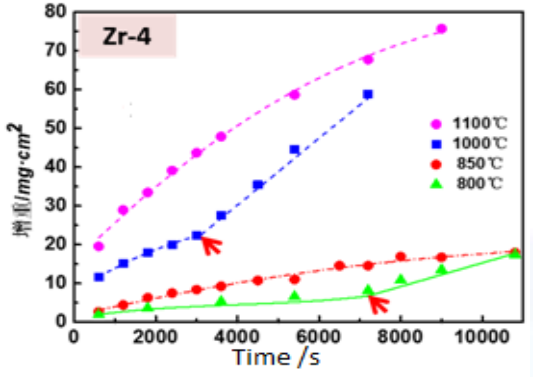
b 1000℃



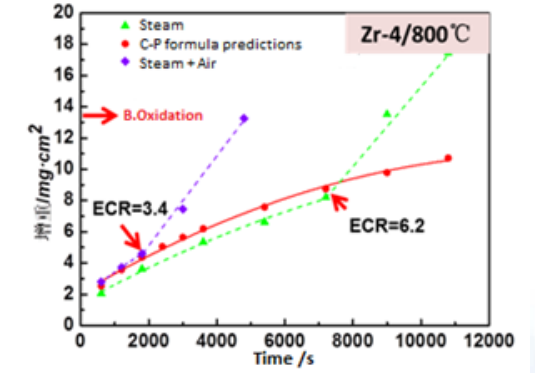


Oxidation weight for 3 materials

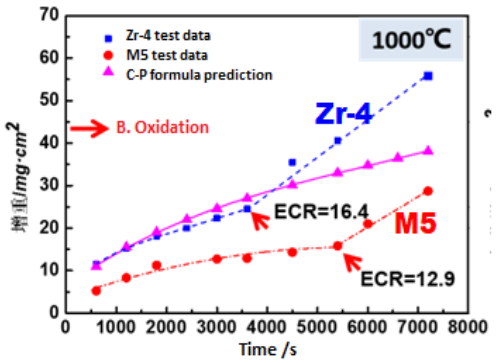
➢ Oxidation test of Zr-4 Cladding



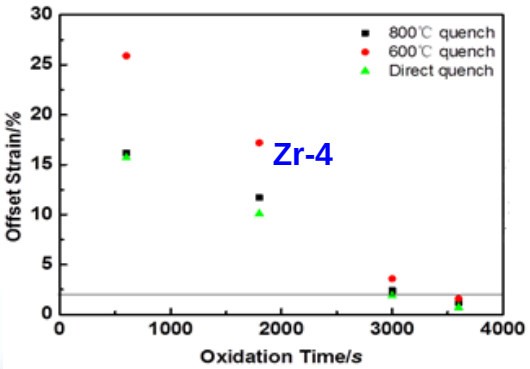
Temperature effects



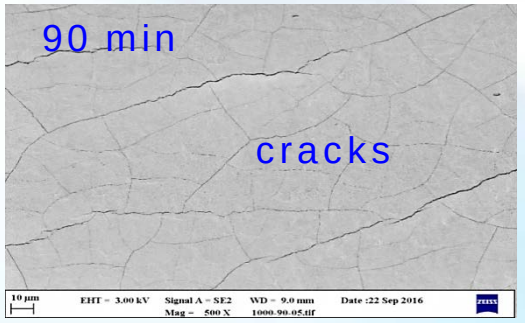
Environment effects



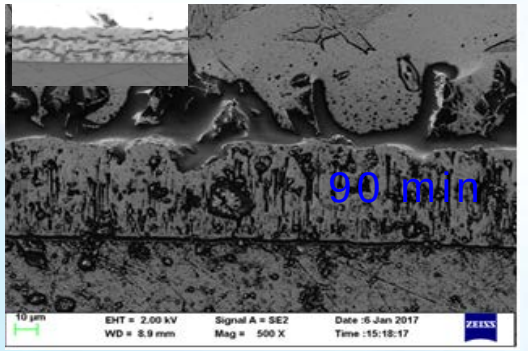
Material comparison



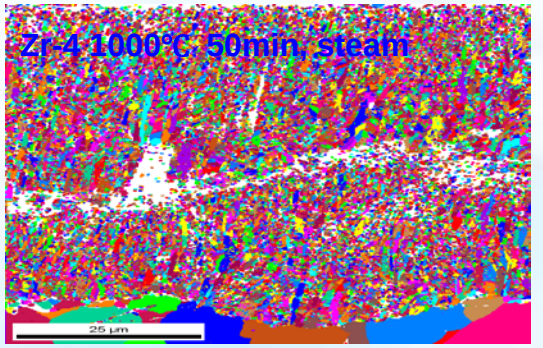
Quench Temperature effects on Ductility



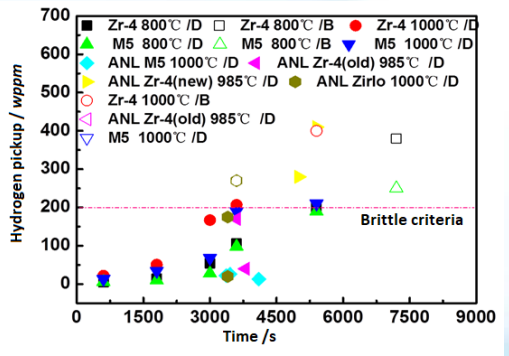
Microstructure of oxide film surface



Microstructure of oxide film cross-section (500X)

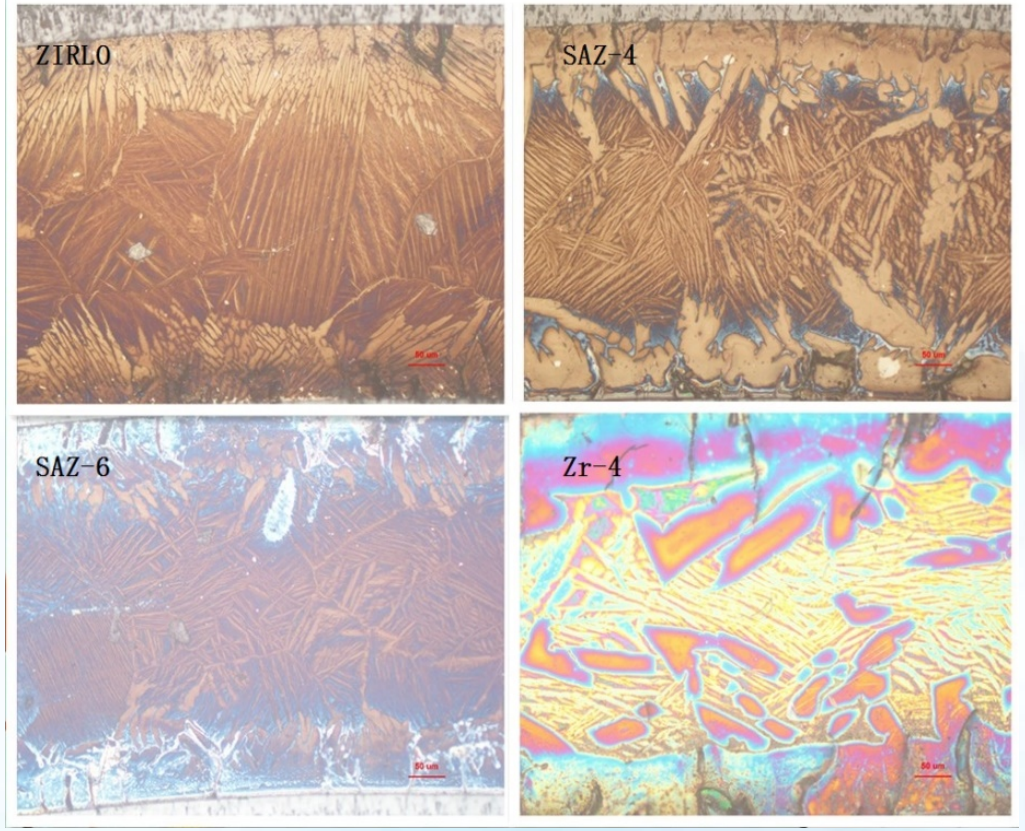


Grain distribution in oxide film (EBSD)



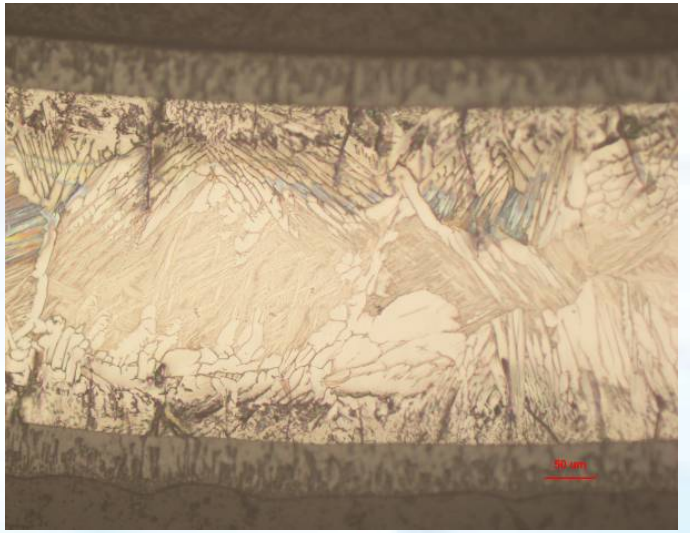
Brittle criteria checking

1200℃，CP-ECR=16.5%



Metallographic phase of the different materials after oxidation

1204℃，CP-ECR=15%，ZIRLO



100ppmH



400ppmH

Metallographic phase of the ZIRLO with different Hydrogen content

➢ Single Rod Behavior under LOCA condition

- 12 samples: 4 different cladding materials
- Pre-pressure: 3.2-6.4 MPa;
- Heating rate: 4.2-9.6℃/s



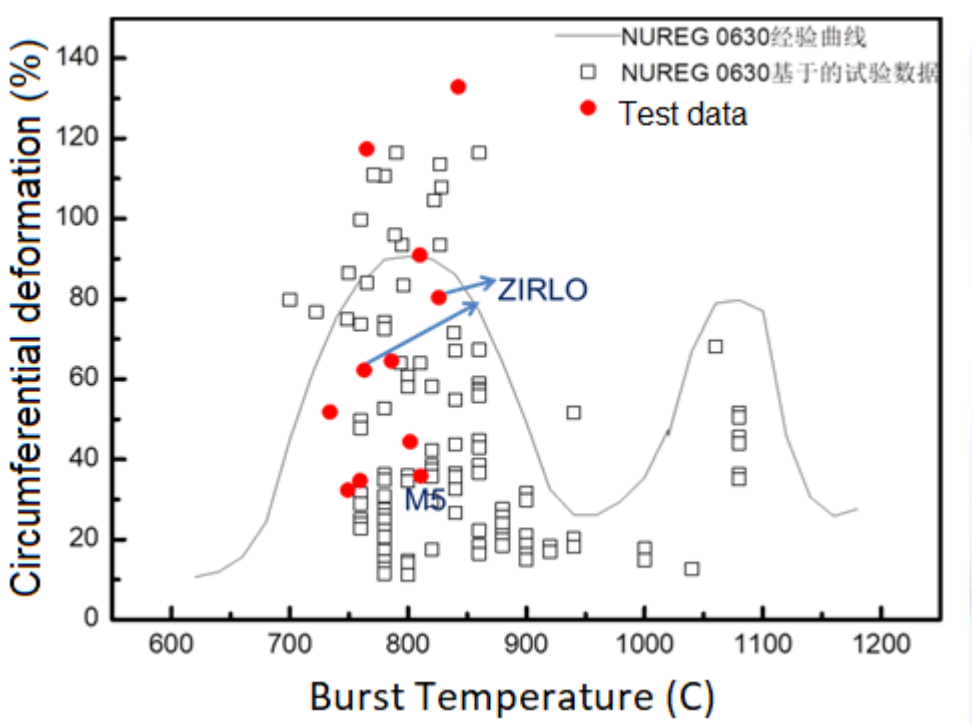
Main Results(1):

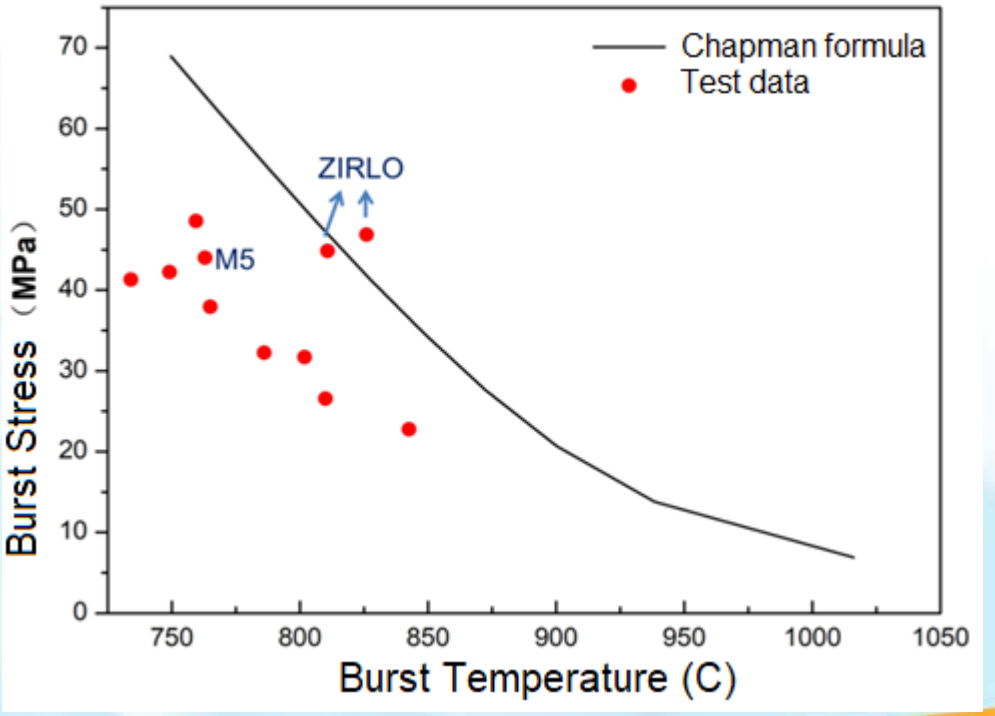
- The shape of the rupture: small size (needle type) and big size. no relation to the pressure and heating rate, but the small size rupture always appeared near the thermal-couple's position: welding affects the local strength?
- The position of the rapture: all appeared near the steam out-let part, but, the exact position could not be well predicted.



Main Results(2):

- Circumferential deformation: 20-130% (Normal), due to thickness, temperature non-uniform distribution in axial and circumferential direction.
- Burst T-S curve: Chapman Formula prediction has a good agreement with ZIRLO cladding.





➢ Small bundles(3x3-2) LOCA behavior

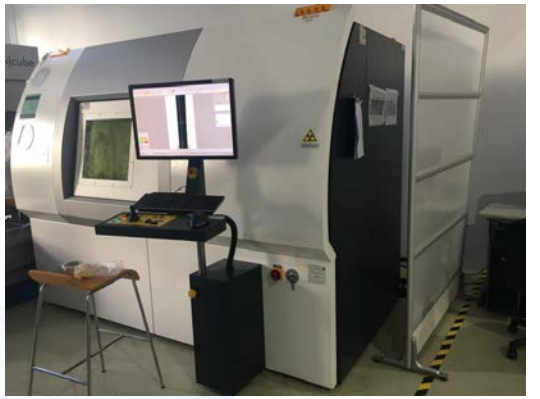


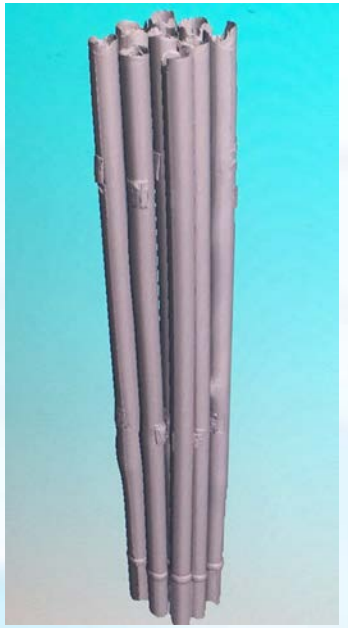


Bundles pictures after LOCA test

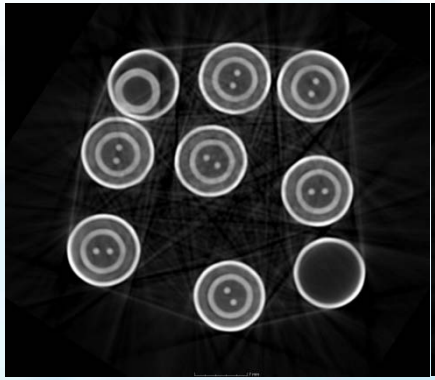
➢ Blockage rate measurement

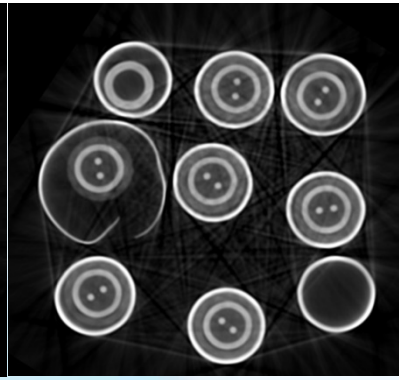
- neutron radiography in CARR
- **X-ray CT**





3D Pictures from CT



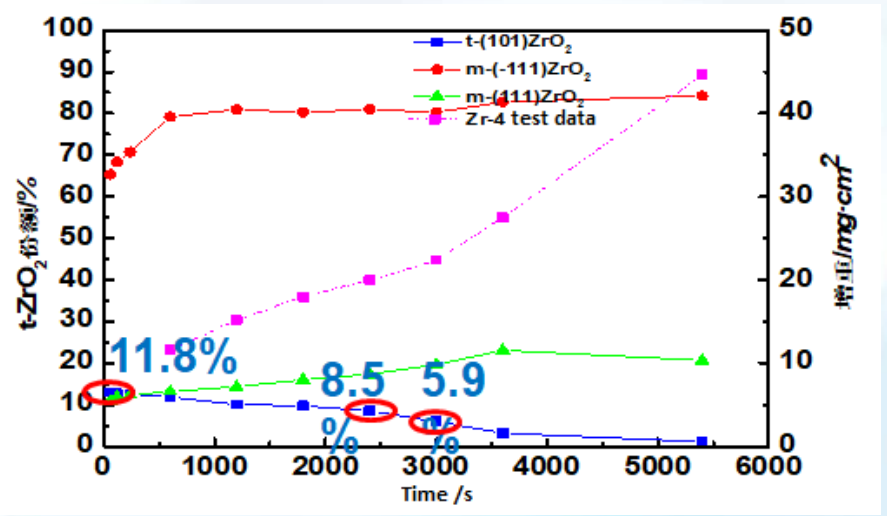


Cross section Pictures from CT

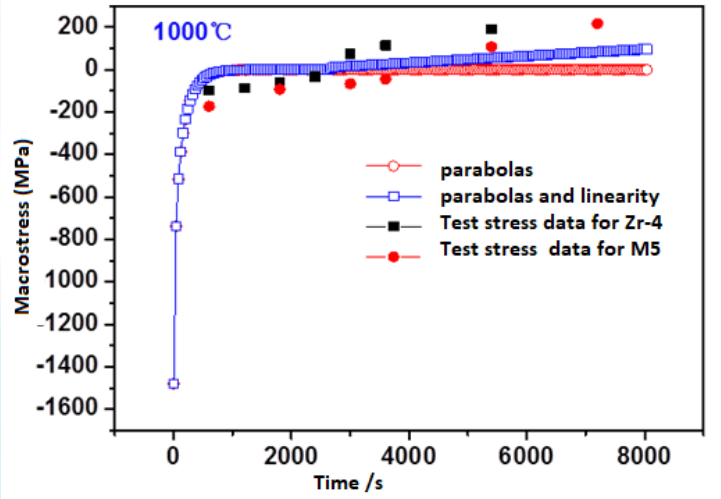
- Average blockage rate: 20.49%;
- Max blockage rate: 37.91%;

➢ Modeling and code developments

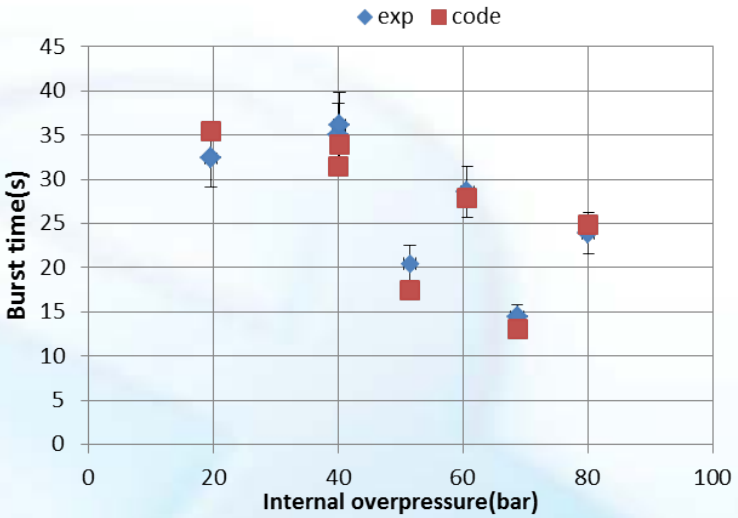
- Crystal structure in Oxide film analysis model: predict the portions of t-ZrO_2 and m-Zr-O_2
- Oxide film stress analysis model: predict the onset of breakaway oxidation, determine the stress value at certain oxide film thickness
- 3-D Ballooning model: predict the balloon and burst process, coupled with FTPAC code, DAKOTA (uncertainty analysis)



Predictions of the model

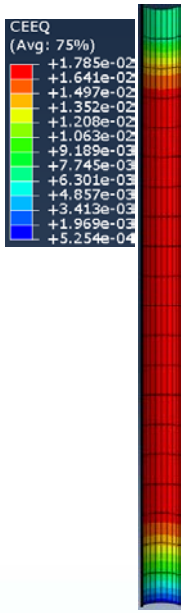


Prediction Vs. Test Dada



Prediction Vs. Test Dada

IAEA FUMAC, SCIP-3, OECD-NEA PCMI benchmark



Test Plan and technical challenge

➢ **For SAZ-4, SAZ-6 and outer cladding of annular fuel rod: Check if its characteristics meet the current LOCA criteria**

- For item1-4:

  Follow the standard procedure, with enough samples.

  Compare to the Zr-4 and ZIRLO data

- For item 5:

  Uniform heating Burst test :

  One heating rate, 11 pressure points (1-14 Mpa) , 3 samples for points

  Burst test with axial-loading:

  4 heating rate, 11 pressure points (1-14 Mpa), 3 samples for points

  mass flow rate, cooling rate, axial-loading

  Test condition:

  Cladding temperature:~1200 ℃; Heating rate : 2.8~28℃/s;

  During the 700-1200 ℃, circumferential T difference: ~30 ℃; Steam environments

➢ For inner cladding of the annular rod:

- Collapse Test

  Four heating rate, 11 pressure points (1-14 Mpa) , 3 samples for points

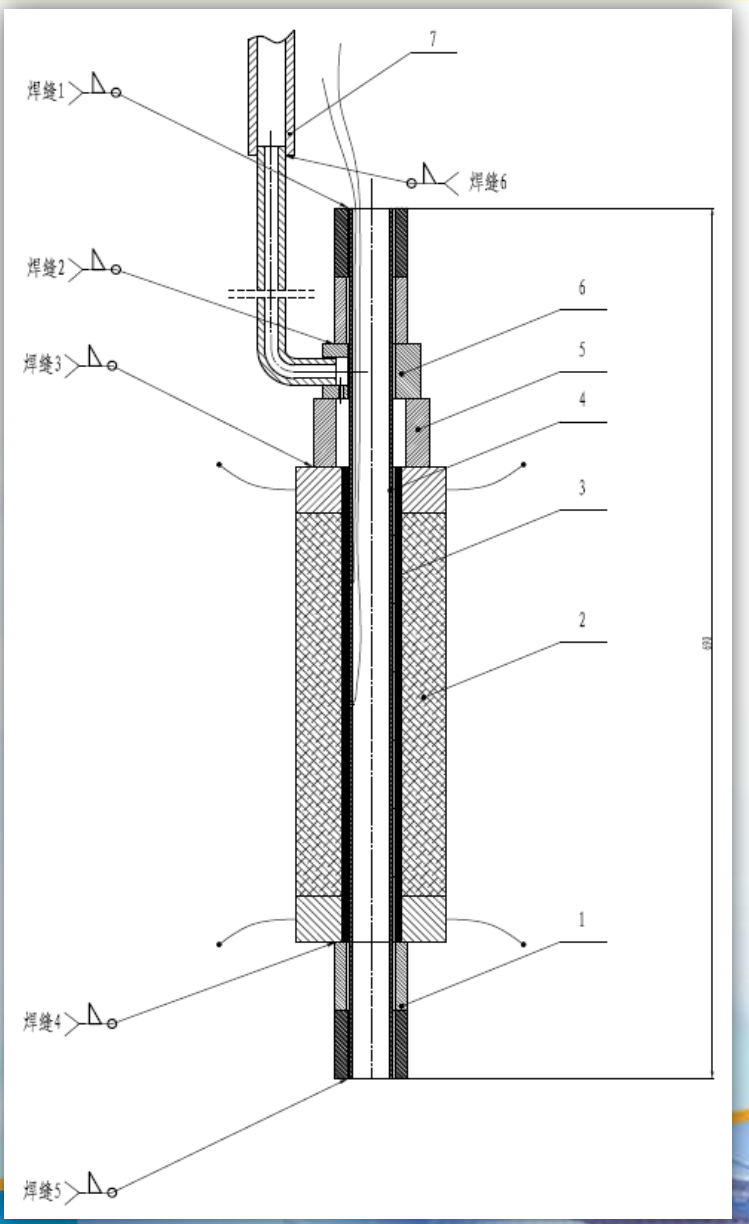
  Deformation analysis after collapse.

  Test condition:

  Cladding temperature:~1200 ℃; Heating rate : 2.8~28℃/s;

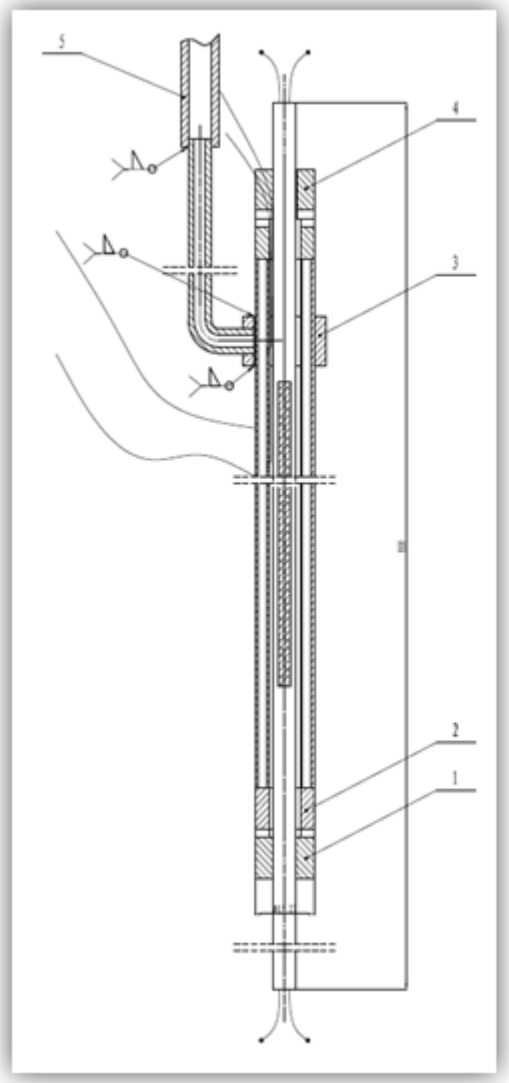
  Steam environments

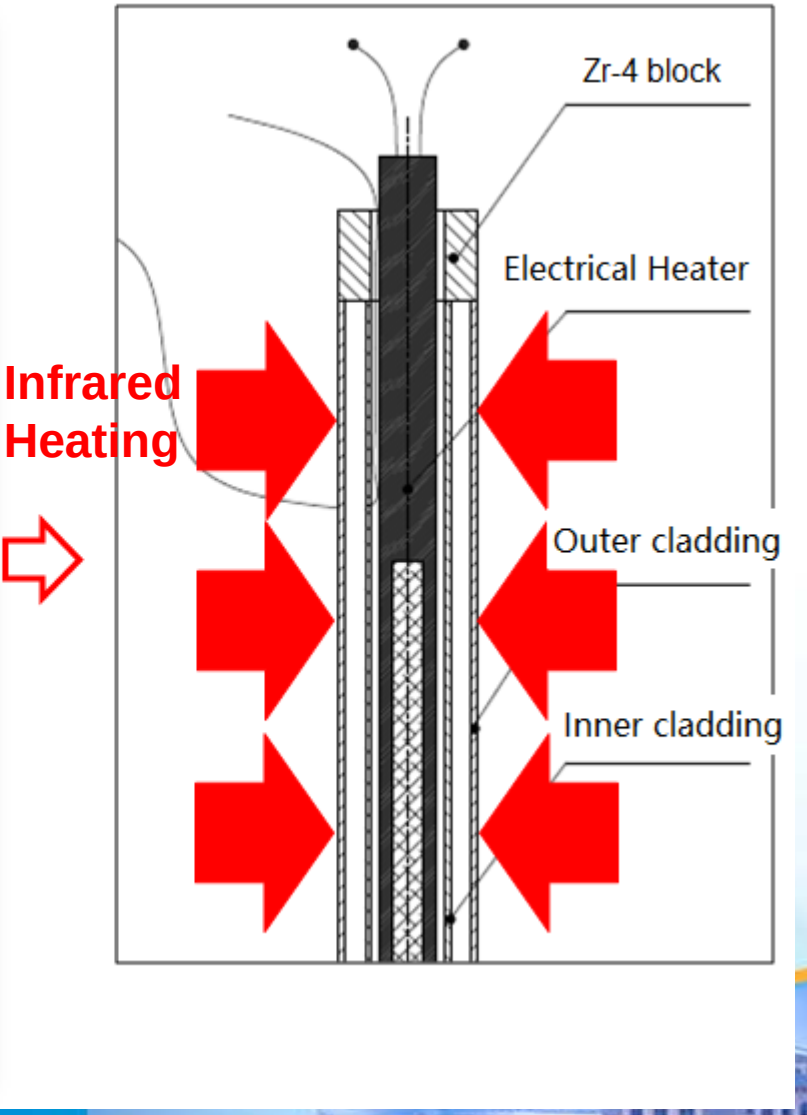
  Key technology: temperature detection of inner surface



➢ For single annular fuel rod LOCA test

- It is should be finally determined according to the separate LOCA test results (inner cladding and outer cladding)
- Make a comparison to the solid fuel rod's results
- the test plan is already made by CIAE engineers, big technical challenges.





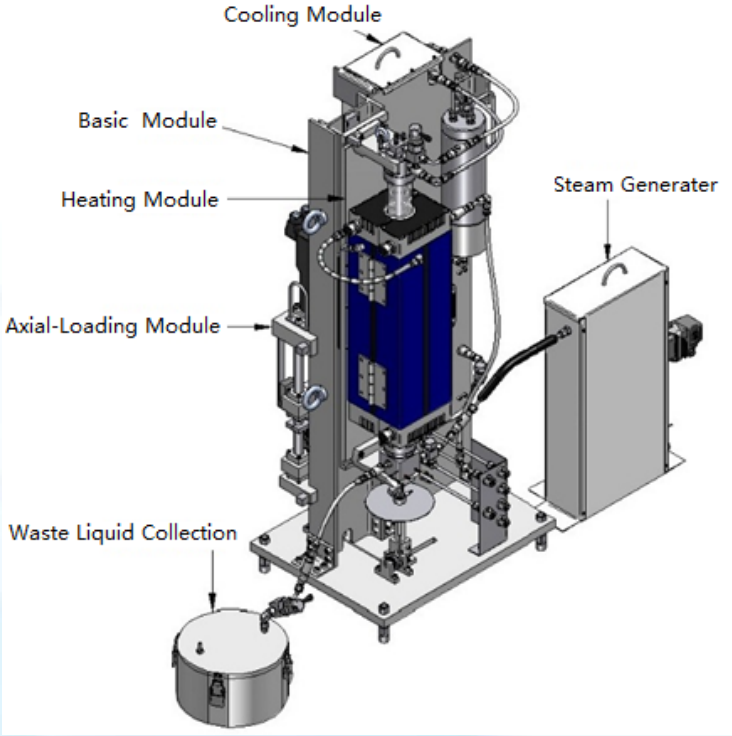
Future Work (- 2020)

➢ Upgrade the test abilities

- the H-T oxidation test loop: plastic deformation test;
- a new LOCA test loop: full length single rod balloon and burst test/ bundle test
- the test installation for single rod:
  - direct and indirect heating ability
  - with axial-loading
  - with temperature measurement (contact and non-contact)
- Breakaway oxidation test loop (based on TGA)

➢ Test schedule

- Test facilities upgrading: ～ 2019.06
- annular fuel rod test: ～ 2020.06
- SAZ series cladding test: ～ 2020.12



Test installation for single rod

Thanks for your attention

More Detail:

Cladding material test : Ms. Xu Qian, magic-xu@hotmail.com

Rod and bundle's behavior test : Mr. Diao Jun-hui, 44984442@qq.com

Code development : Mr. Han Zhi-jie, mr_hanzhijie@163.com

Project manager : Mr. He Xiao-jun, ciae.hexiaojun@gmail.com

The CODEX-AIT-3 integral air ingress experiment

Róbert Farkas, Imre Nagy, Nóra Vér, Péter Szabó, Zoltán Hózer
Hungarian Academy of Sciences Centre for Energy Research (MTA EK), Budapest

During severe accidents with air ingress conditions complex phenomena take place in the fuel bundle. Several integral experiments were performed in the past in CODEX, QUENCH and PARAMETER facilities to address different scenarios.

In the framework of the EU SAFEST Project a new air ingress test was proposed for the CODEX facility. The reference scenario was a reactor accident with melt through of the bottom head and penetration of air+steam mixture from the reactor cavity into the reactor vessel. It was intended to simulate the high temperature interactions of peripheral fuel assemblies in air+steam atmosphere. Limited air and steam flowrates were intentionally selected in order to simulate high temperature chemical interactions. Slow cool-down was proposed to provide information on bundle state before quench.

The preparation of the experiment included significant extension of CODEX capabilities. The electrically heated 7-rod bundle had double heaters inside of the pellets and the central rod could be pressurized. Additional external heating was built on the surface of the test section. Mass spectrometer was included to measure outlet gas composition. In order to provide low gas and steam flowrate for starvation conditions special flow controllers and pumps were applied.

The CODEX-AIT-3 experiment was successfully performed in June 2018. Cladding burst took place at maximum measured temperature of 840 °C due to fast pressurization of the central rod and the opening allowed the coolant to enter the rod and start chemical reactions on both sides of the cladding. Pre-oxidation was carried out in high flowrate steam and the estimated oxide scale thickness in the hottest section of the bundle reached 100 μm. The duration of air ingress phase was about 45 minutes and the maximum cladding temperature was slightly above 1600 °C. The outlet gas composition showed that during the air ingress phase oxygen and steam starvation conditions were established. The partial consumption of nitrogen indicated the formation of nitrides. Cool-down of the bundle was performed in argon in order to avoid interactions that might have taken place during water quench.


TOSHIBA

CENTRE FOR ENERGY RESEARCH HUNGARIAN ACADEMY OF SCIENCES

THE CODEX-AIT-3 INTEGRAL AIR INGRESS EXPERIMENT

N. Vér, I. Nagy, R. Farkas, M. Horváth, Z. Hózer, P. Szabó

24th International QUENCH Workshop

INTRODUCTION

- First call "Rules of access to SAFEST facilities" in 2014

- " First User Selection Panel Meeting ", Marseille, 27th March 2015

  An air ingress scenario proposed by KIT was accepted for the CODEX facility

- " Cladding Oxidation by Air Under Severe Accident Conditions in a Nuclear Reactor ", Budapest, 14-15 June 2016

  The main aspects and conditions of CODEX test was decided by KIT, GRS, PSI, IRSN, EDF, IBRAE, UJP PRAHA, HGU, KAERI, NUBIKI and MTA EK

- Pre-test calculations performed by GRS, IBRAE, NUBIKI and PSI

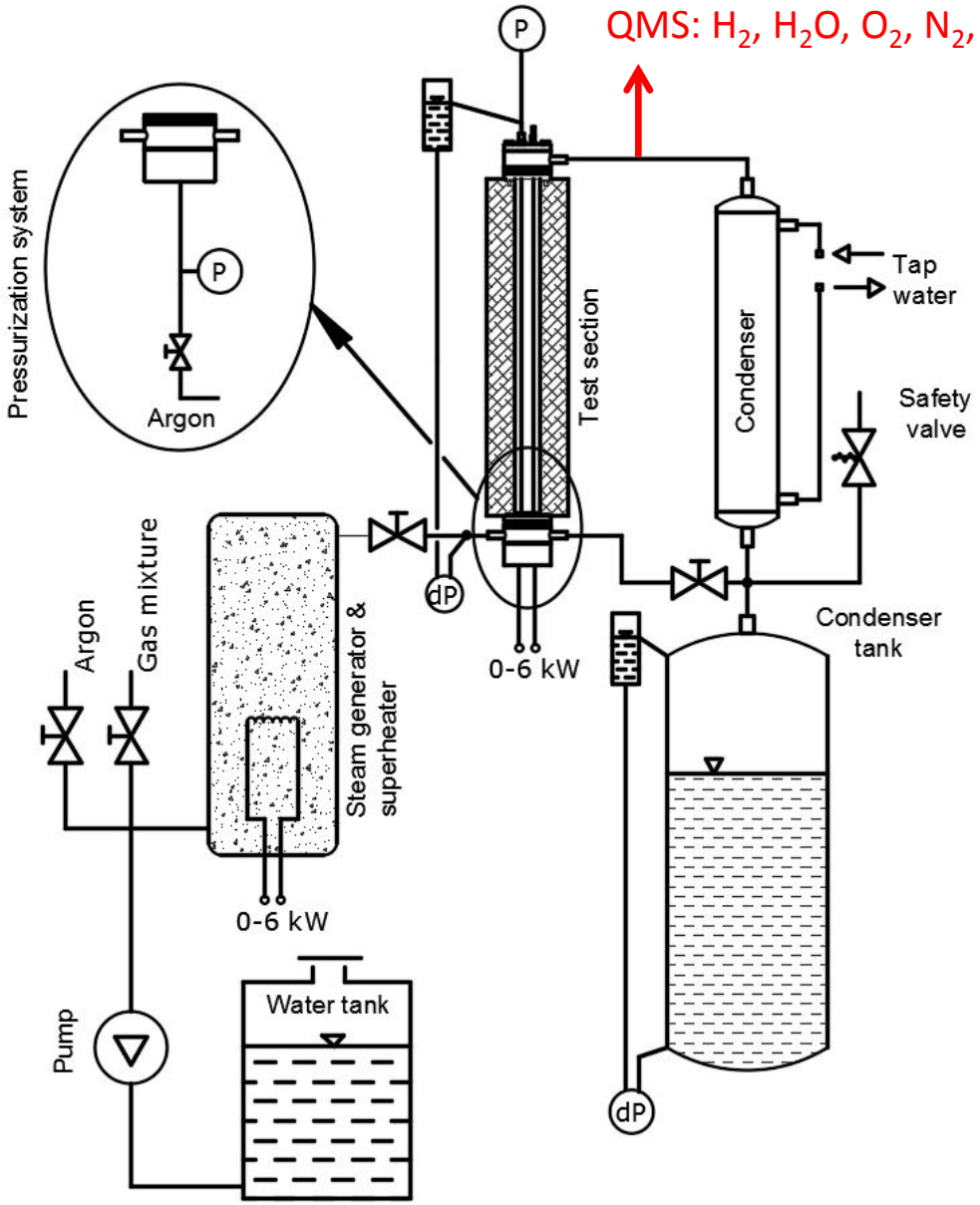
  The test conditions of the CODEX-AIT-3 test were specified in August 2017

OBJECTIVE

- Reference scenario: a reactor accident with melt through of the bottom head and penetration of air+steam mixture from the reactor cavity into the reactor vessel
- The CODEX-AIT-3 test will simulate the high temperature interactions of peripheral fuel assemblies in air+steam atmosphere
- Steam and oxygen starvation in the bundle will be established
- Slow cool-down will be applied to provide information on bundle state before quench.

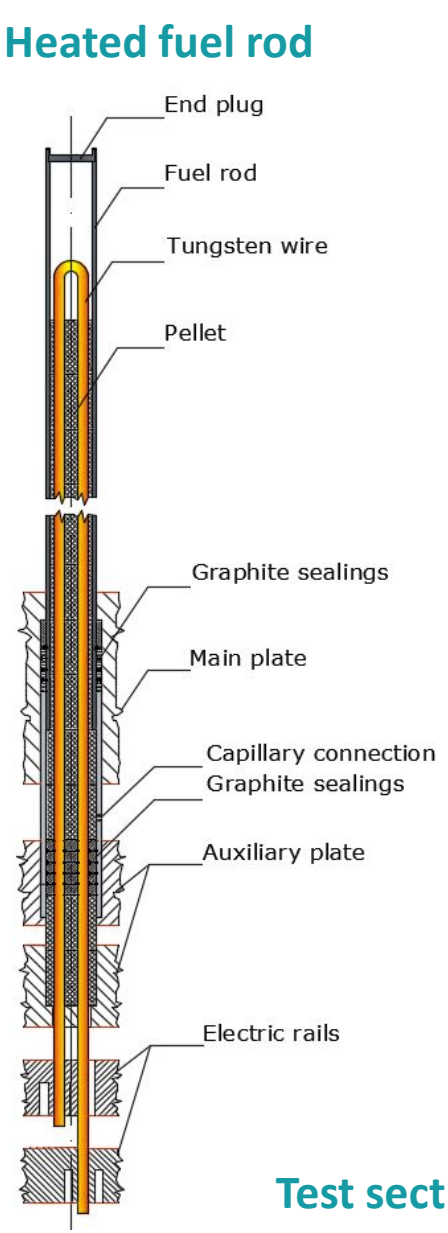
CODEX FACILITY

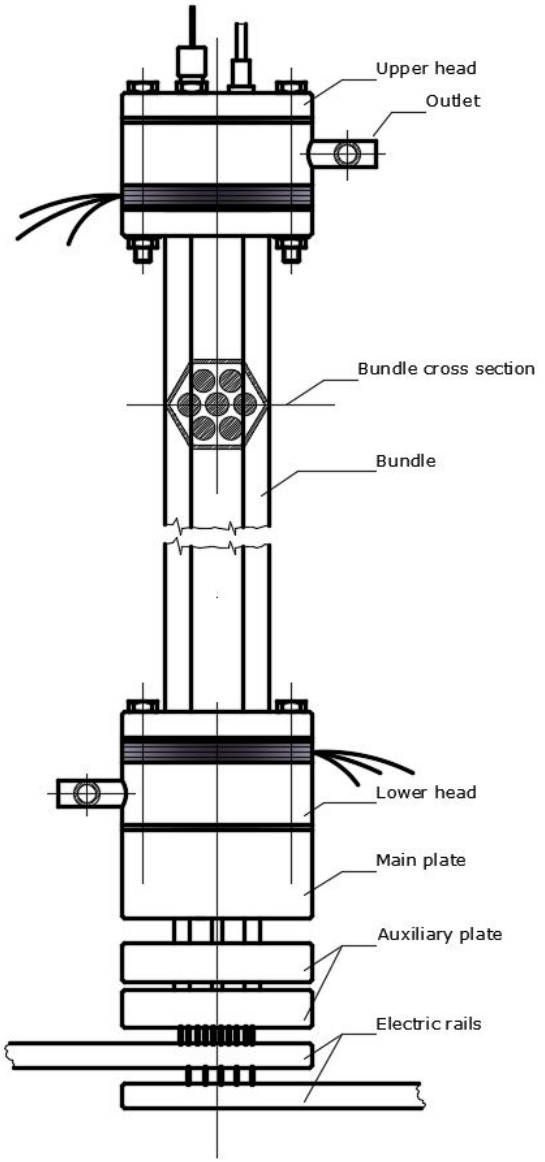
1. Water tank & gas inlet
2. Steam generator & superheater
3. Test section
4. Condenser
5. Condenser tank
6. Pressurisation system



BUNDLE DESING

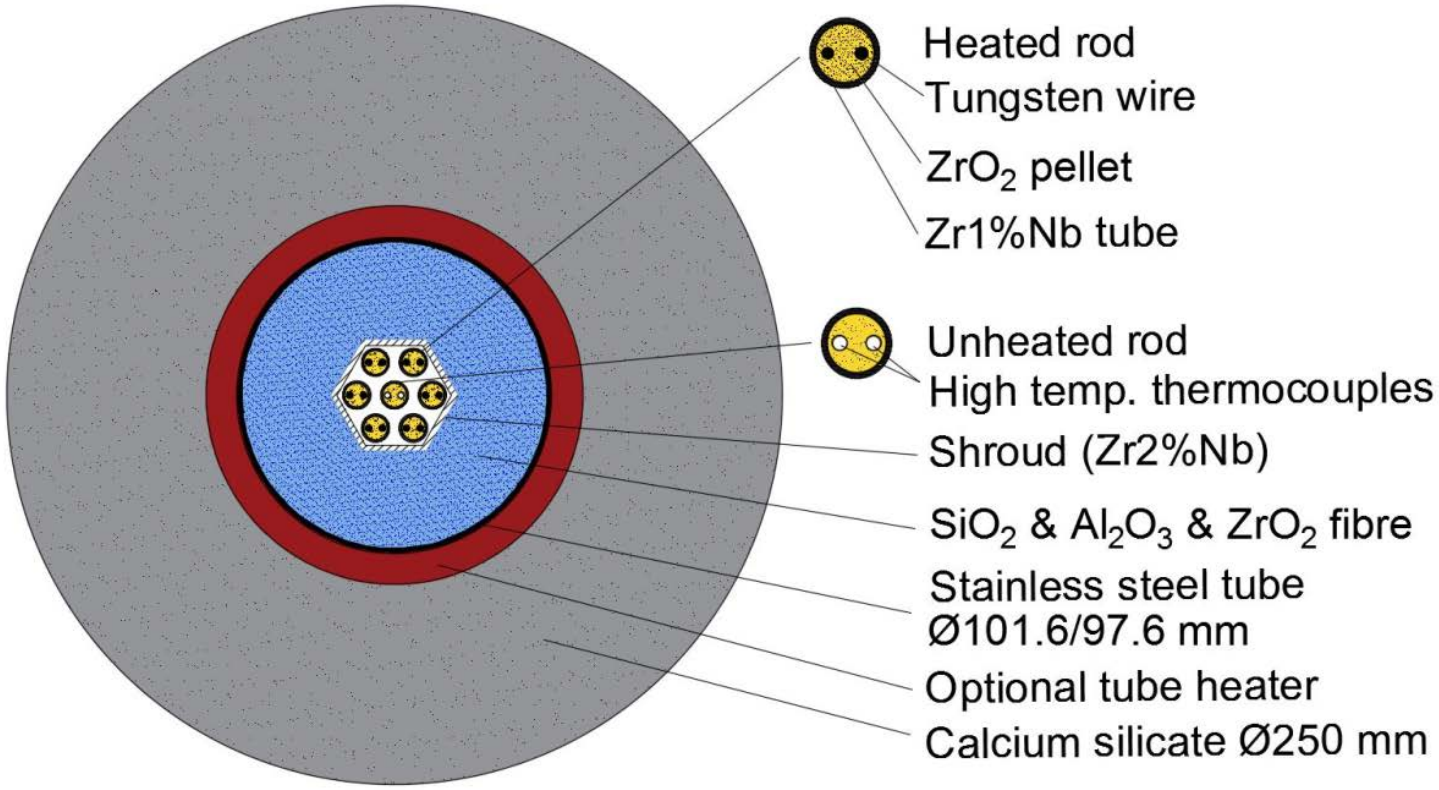
- VVER bundle type:
  hexagonal arrangement of 7 rods
- Height of rods: 1000 mm
  - 6 rods (periphery)
    electrically heated - no pressurized
  - 1 rod (in the center)
    unheated - pressurized
- Cladding material: E110G alloy
- ZrO_2 ceramic pellets
- Tungsten heaters (990 mm)
- 3 spacer grids (Zr1%Nb alloy)
- Hexagonal shroud (Zr2.5%Nb alloy)





Test section with seven-rod bundle

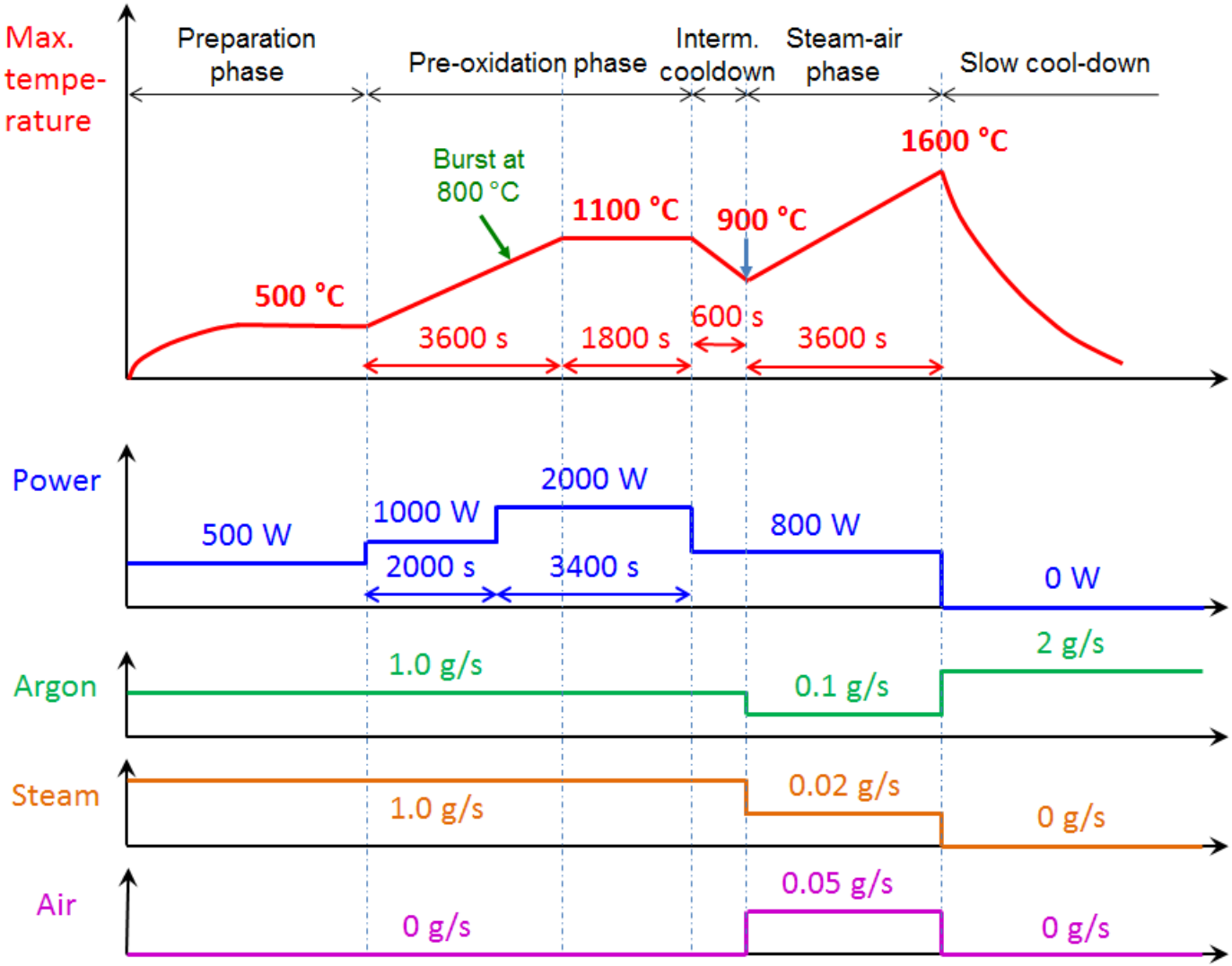
CROSS SECTION OF THE TEST SECTION WITH THERMAL INSULATIONS



MEASUREMENT OF PARAMETERS

Parameter	Device	Placement
Temperature	K-type, W5% Re/W26% Re in Zr shield tube	Rod surfaces and inner side
	K-type	Others (coolant , off-gas, stainless steel tube, …)
Argon/air flowrate	Calibrated flowmeter	Gas supply system
Steam flowrate	Calibrated pump	Pump
Gas composition	Mass spectrometer	Gas outlet
Power	DC power units	Rail of electric connections
System pressure	P transducer, 6 bar/4-20 mA	Test section upper head
Fuel rod pressure	P transducer, 100 bar/4-20 mA	Pressurization system
Water level	DP transducer device	Condenser tank

SPECIFIED SCENARIO



Targets in the pre-test calculations:

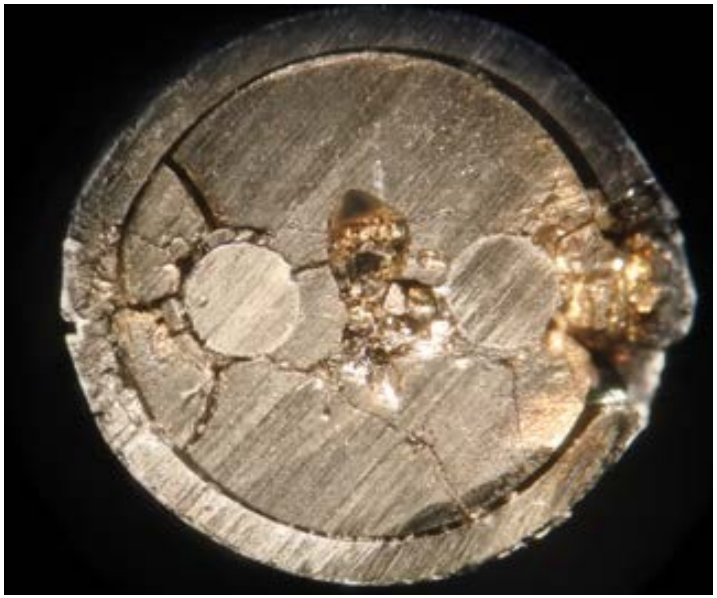
Pre-oxidation phase:

- T_{max} = 1100 °C
- Max. oxide scale ~ 100 µm

Air ingress phase:

- steam and oxygen starvation
- t ~ 1 hour
- T_{max} = 1600 °C

SINGLE ROD TESTS



Cross section of degraded bottom part of the single rod

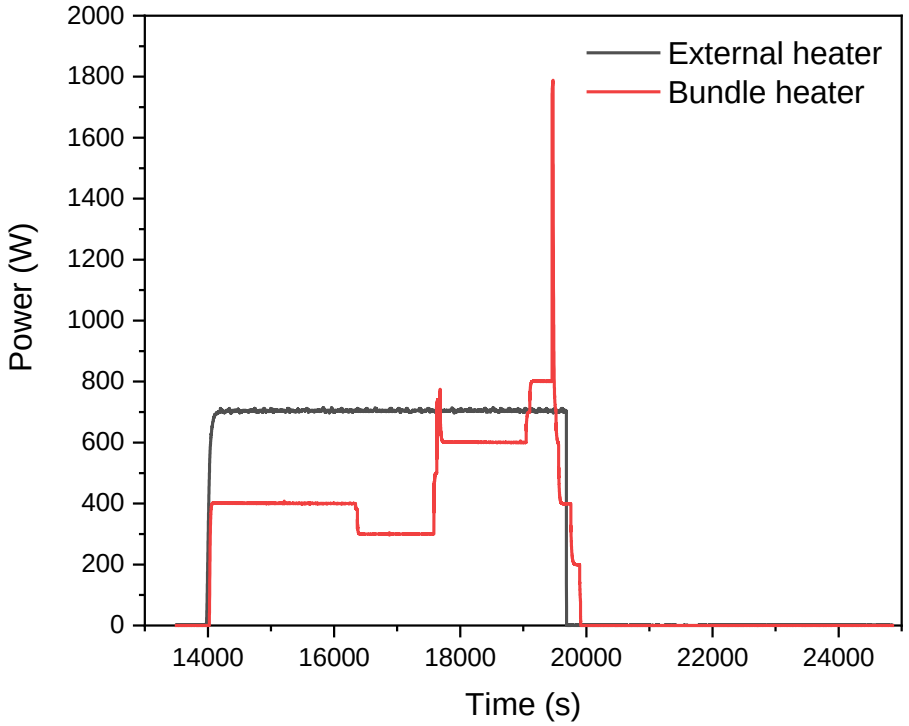
Single rod test No. 1.

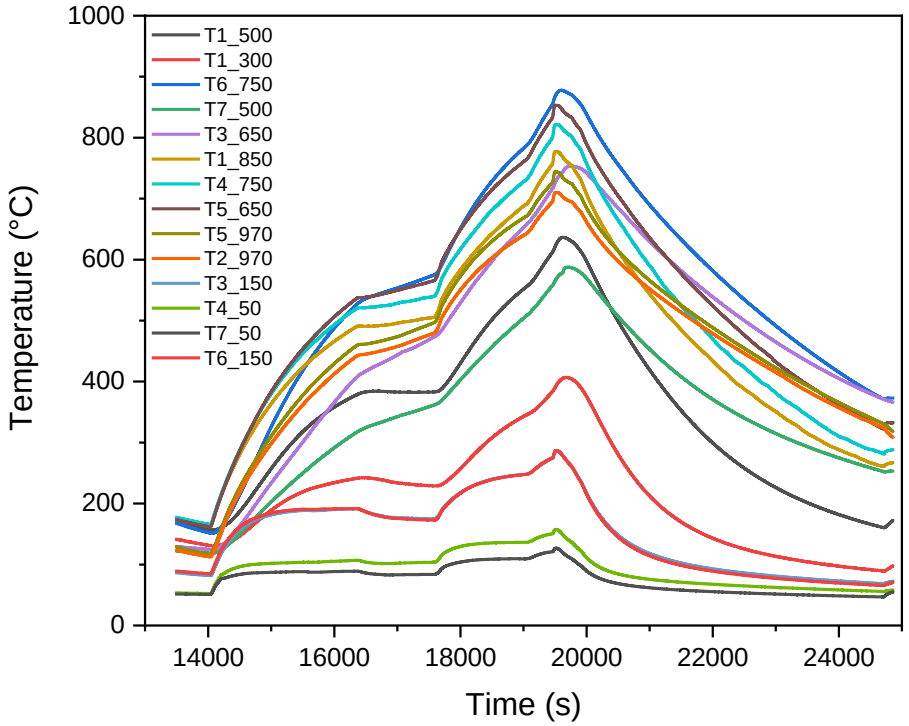
- successful heating test: T > 1000 °C, t ~ 1 hour
- strong degradation in the lower part of the rod → eutectic interactions between the non-oxidized cladding surface and the K type thermocouple?

Single rod test No. 2.

- with insulated thermocouple
- again strong degradation in the lower part of the rod → high voltage (30 V) AC power could result in partial shortcut in the lower section of the rod and it could lead to degradations
- solution → use of DC power

COMMISSIONING TEST No. 1.

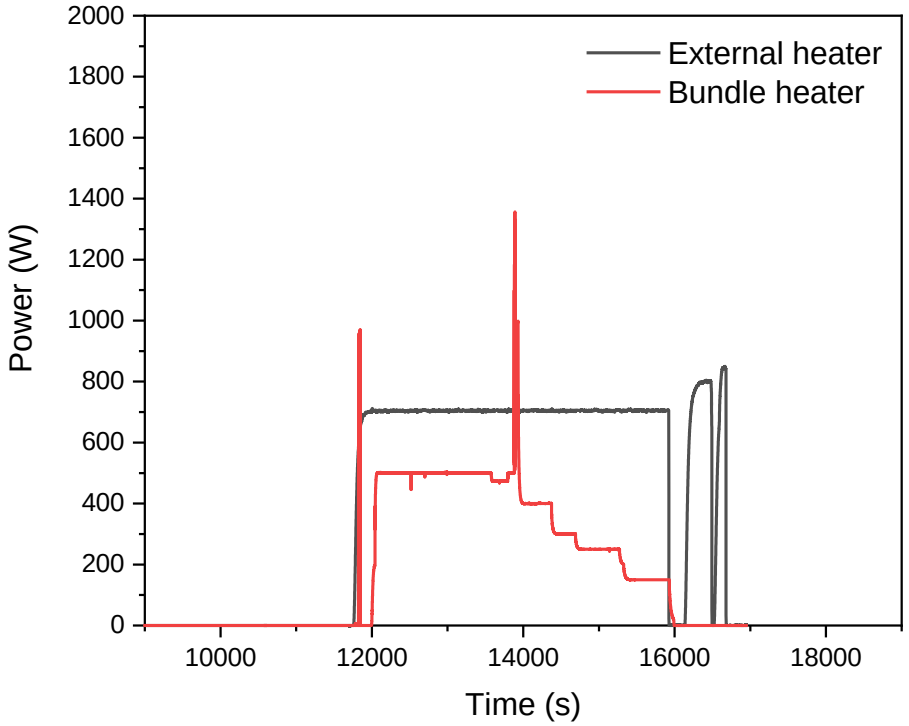


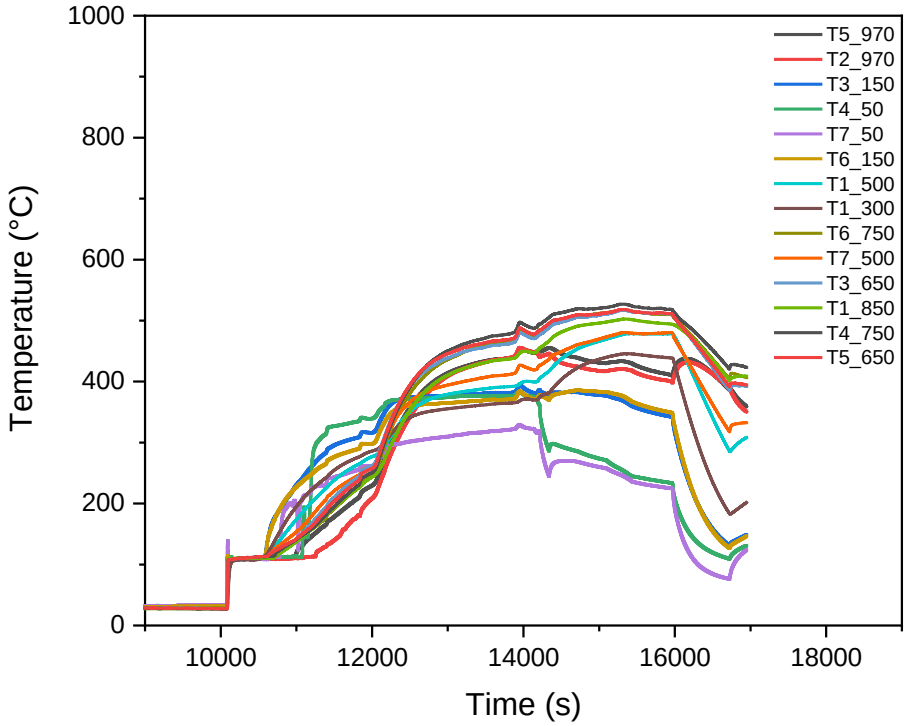


in argon atmosphere
max. power for the rods: 1800 W
max. power for the external heaters: 700 W

t ~ 6000 s
$T_{max.\ rod}$ ~ 900 °C at 750 mm
$T_{max.\ shroud}$ ~ 800 °C at 750 mm

COMMISSIONING TEST No. 2.

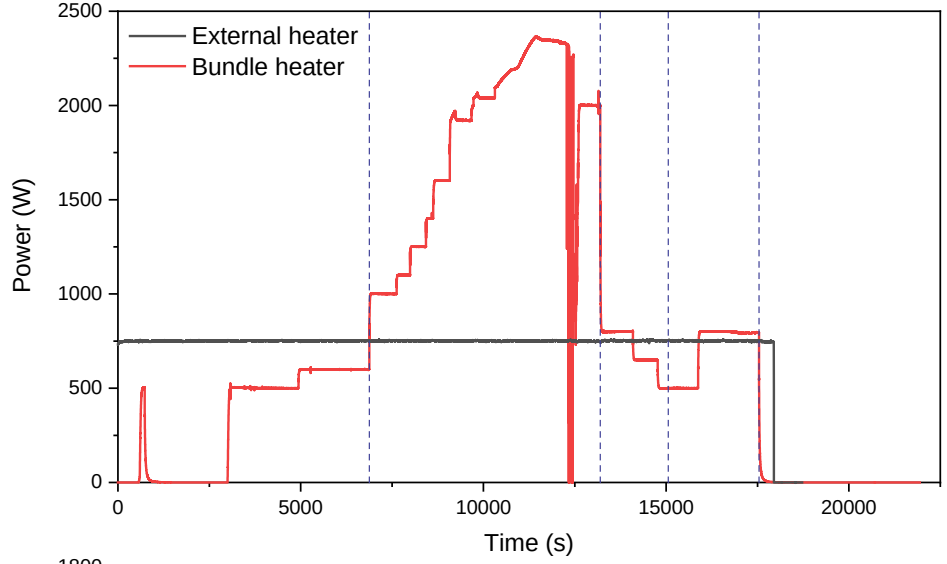


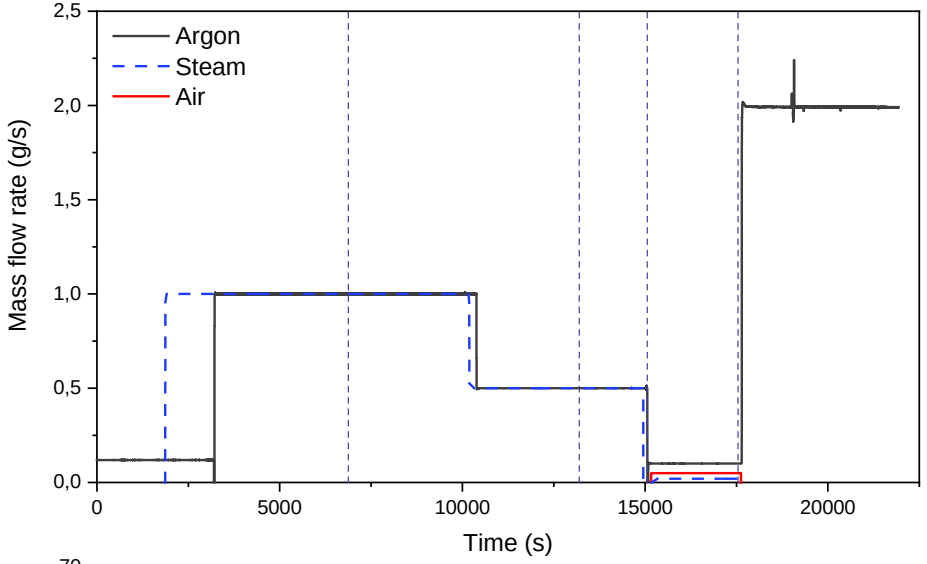


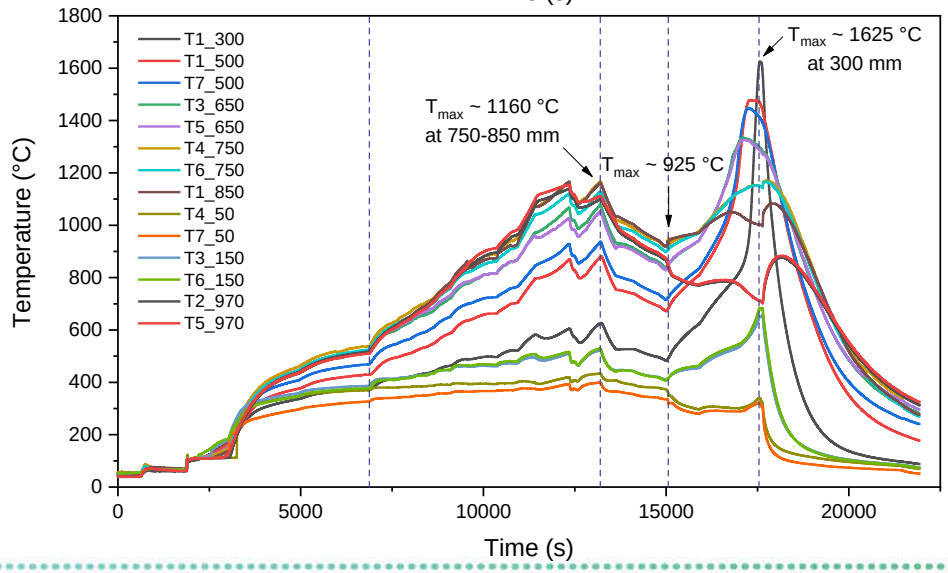
in argon atmosphere
max. power for the rods: 1350 W
max. power for the external heaters: 700 W

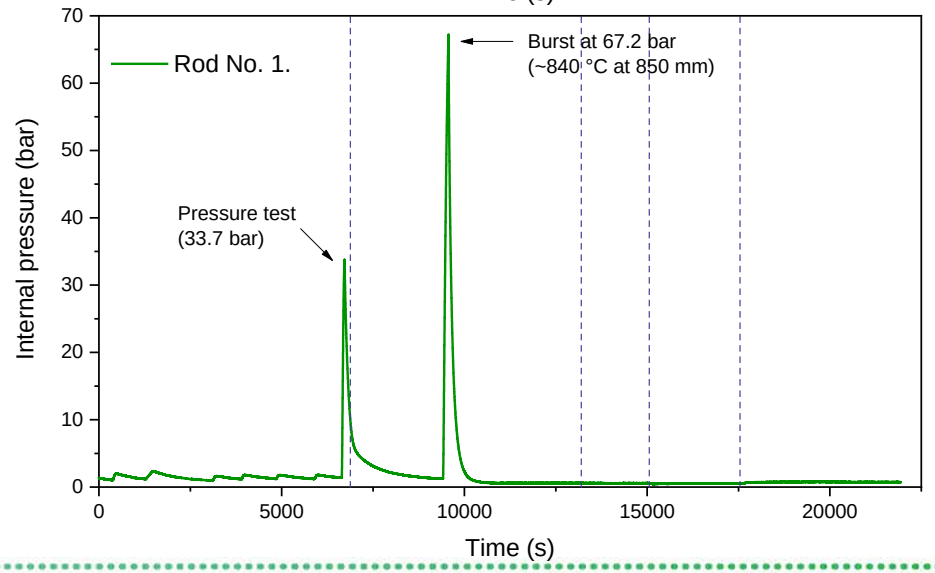
t ~ 5000 s
$T_{max.\ rod}$ ~ 500 °C at 750 mm
$T_{max.\ shroud}$ ~ 450 °C at 750 mm

CODEX-AIT-3 EXPERIMENT

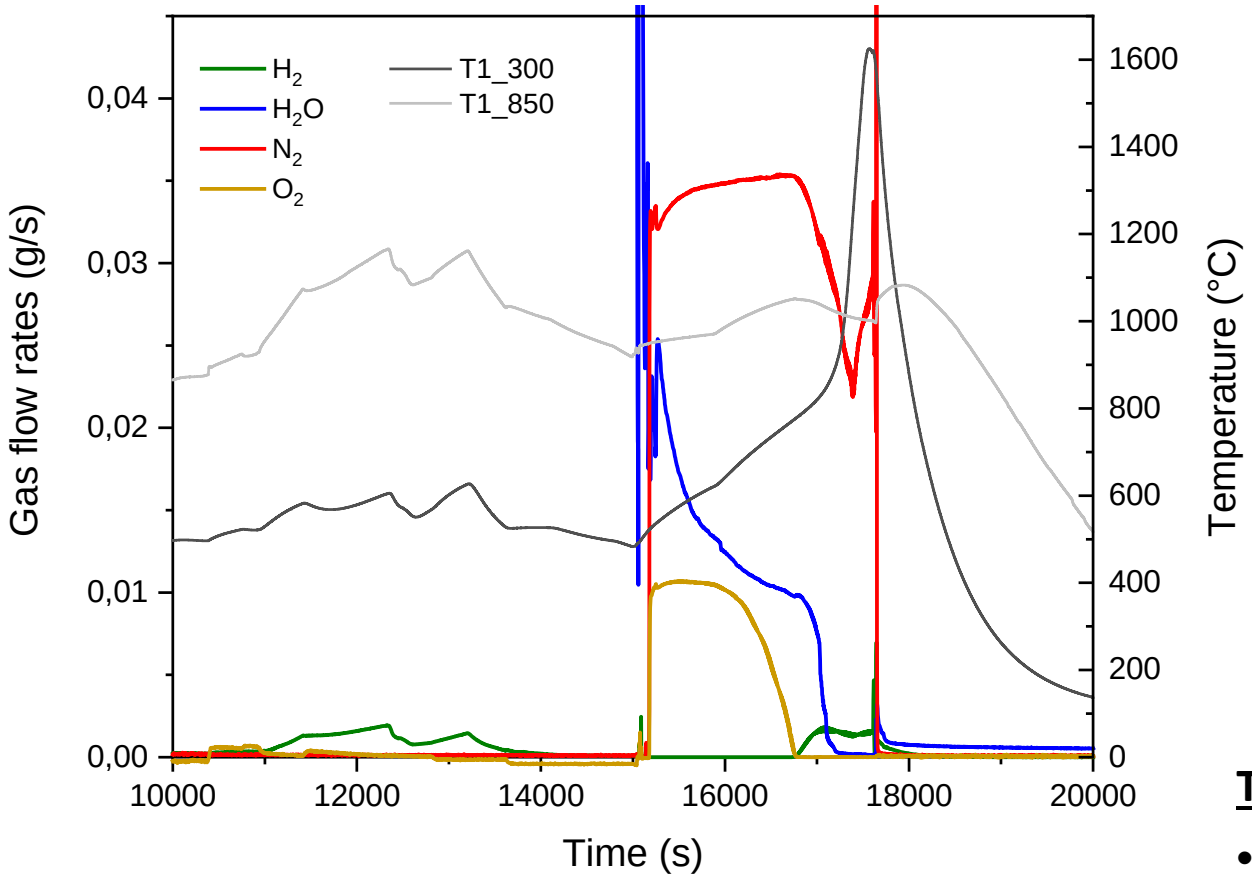








CODEX-AIT-3 EXPERIMENT

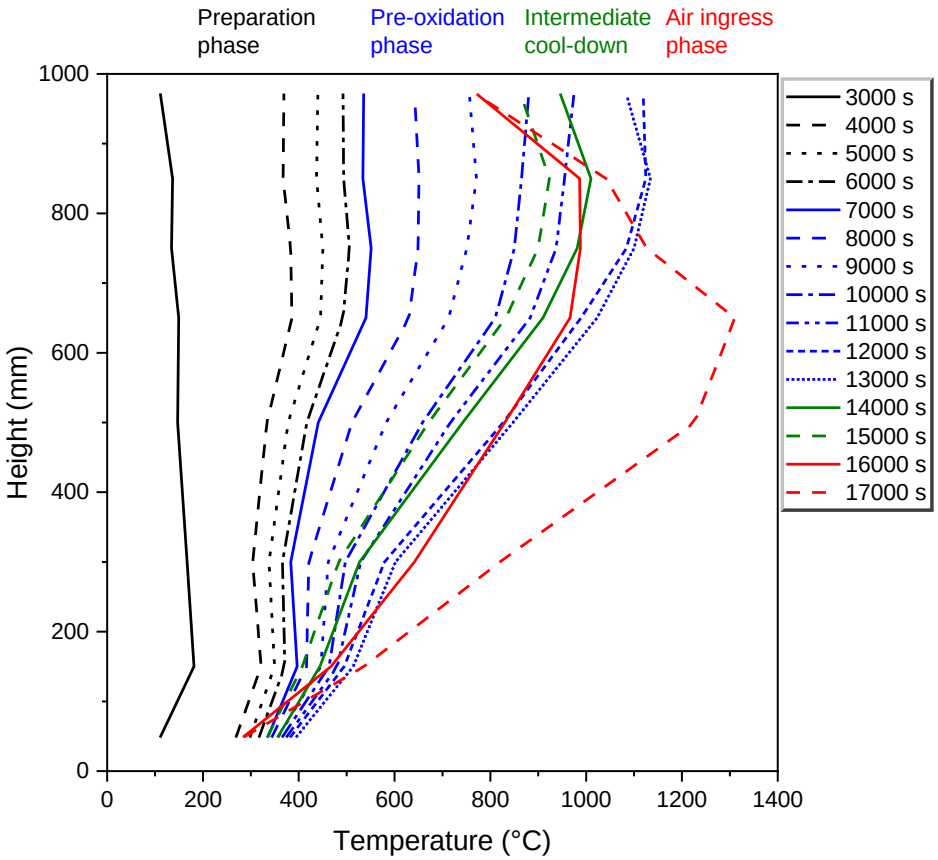


Total H_2 generation:

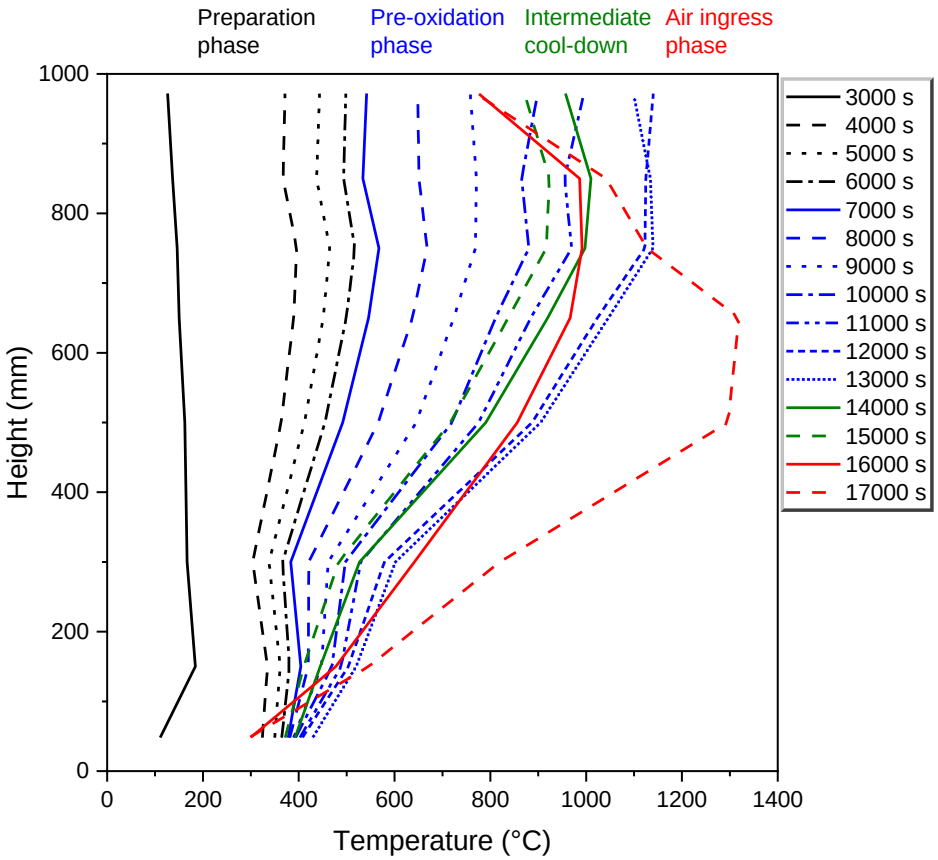
- end of pre-oxidation: ~ 3.8 g
- end of air ingress: ~ 5.2 g

CODEX-AIT-3 EXPERIMENT

minimum local temperatures



maximum local temperatures



SUMMARY

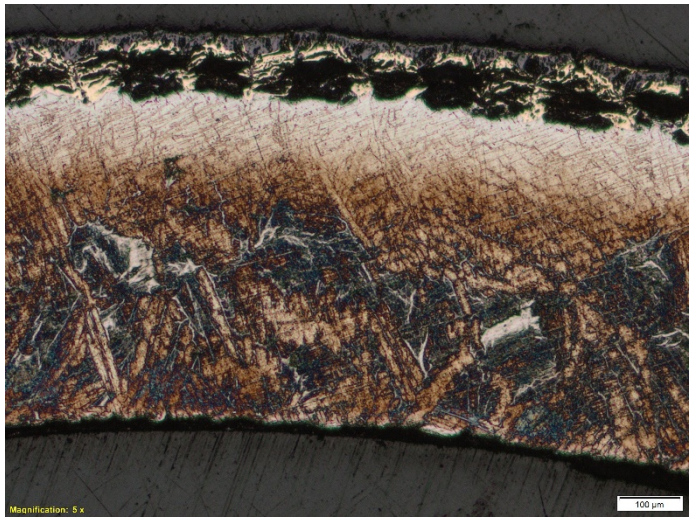
- The CODEX-AIT-3 test (Air Ingress Test) was successfully performed on the 13th June 2018 in the framework of the EU SAFEST project.
- The experiment was carried out with temperature conditions which were close to the specified ones by pre-test calculations.
- Cladding burst took place at 840 °C due to pressurization of the central rod. The opening allowed the coolant to enter the rod and start chemical reactions on both sides of the cladding.
- Pre-oxidation was carried out in high flowrate steam with maximum temperature above 1100 °C. The estimated oxide scale thickness in the hottest section of the bundle reached 100 µm.
- With intermediate cool-down phase the temperatures were reduced below 925 °C.

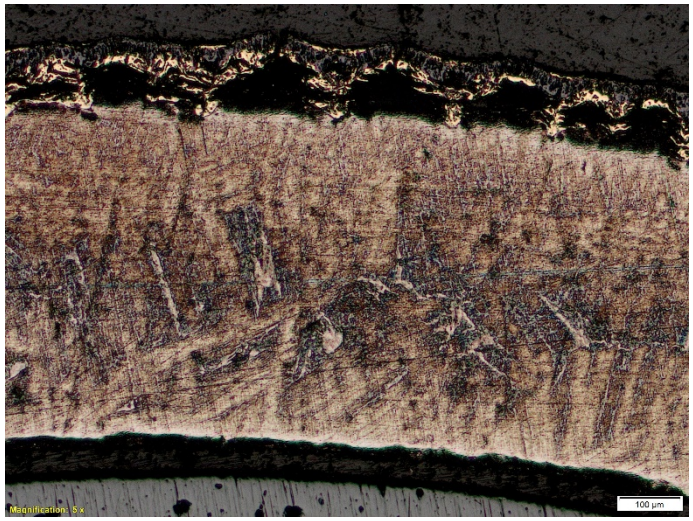
SUMMARY

- The duration of air ingress phase was 1 hour and the maximum cladding temperature was slightly above 1600 °C.
- The outlet gas composition showed that during the air ingress phase steam and oxygen starvation conditions were established. The partial consumption of nitrogen indicated the formation of nitrides, too.
- The temperature profile significantly changed during the air ingress phase: the maximum temperature moved from the upper section to the middle of bundle due to the intense chemical interactions in the less oxidised central part.
- Cool-down of the bundle was performed in argon in order to provide information on bundle state before quench.

FURTHER ACTIONS AND SCHEDULE

- Post-test examination of the bundle is ongoing





Cross section of burst central rod No. 1. at 750 mm

- CODEX-AIT-3 Experimental Data Report with the experimental database will be released by end of November 2018



Thank you for your attention!

mtaEK CENTRE FOR ENERGY RESEARCH
HUNGARIAN ACADEMY OF SCIENCES

An overview of high-temperature oxidation behavior of various ATF cladding candidates in steam

Chongchong Tang, Vincent Faraus, Martin Steinbrueck, Mirco Grosse

Institute for Applied Materials (IAM-AWP), Karlsruhe Institute of Technology (KIT), Germany

Email: chongchong.tang@kit.edu

The Fukushima accidents emphasized the necessary to develop advanced accident tolerant fuel (ATF) cladding for enhancing the safety margins and increasing the coping time for severe accident management of water-cooled reactors. Currently, mainly three strategies are being developed worldwide, i.e. coated state-of-the-art Zr alloy claddings, new metallic claddings (like FeCrAl alloys) and ceramic matrix composites cladding (SiC_f/SiC). The oxidation behavior and failure mechanisms of these new materials in high-temperature steam needs to be evaluated.

In this presentation, I will focus on newly developed potential ATF candidates involved in two projects, i.e. EC project IL TROVATORE and IAEA CRP project ACTOF, which are tested in Quench group in Karlsruhe Institute of Technology (KIT). In case of the bulk materials, oxides reveal low volatilization rates in high-temperature steam (may be a concern for thin films application). Ti_2AlC, Cr_2AlC and $(TiNb)_2AlC$ MAX Phases are alumina formers with excellent oxidation resistance, while Ti_3SiC_2 and $(Zr_{0,5}Ti_{0,5})_2(Al_{0,5}Si_{0,5})C$ reveal high oxidation rates. A critical content of Cr and Al and reactive elements (Y) doped is needed to establish a protective, adherent Al_2O_3 scale on FeCrAl alloys. SiCf/SiC possesses excellent performance up to at least 1700°C by forming a protective silica layer. Martensitic steel (Fe18Cr7Ni) shows bad performance with non-protective Fe-based scale.

With respect to the coated Zr alloys, it was found that a critical thickness of the coatings is needed for HT protection in steam. Lower toughness/adherence of ceramic-based coatings (Cr_2AlC) was observed compared to metallic coatings (Cr and CrSiZr). During heating and oxidation, significant diffusion of coating elements, especially light elements (Si and Al), into the substrate was confirmed. The influence of the interdiffusion on the mechanical properties of the substrate and of the eutectic reaction between the coatings and the substrate on the failure modes of the coated claddings need further investigations.

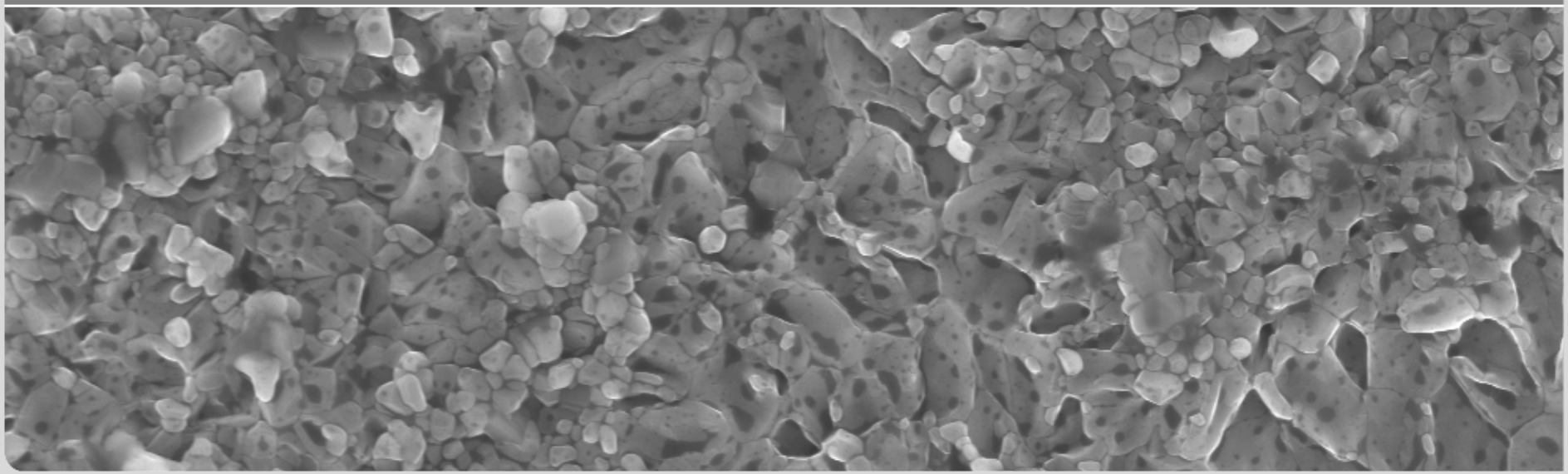

hnologie
TOSHIBA

An overview of high-temperature oxidation behavior of various ATF cladding candidates in steam

Chongchong Tang, Vincent Faraus, Martin Steinbrueck, Mirco Grosse

Institute for Applied Materials (IAM-AWP), Karlsruhe Institute of Technology (KIT), Germany

Institute for Applied Materials IAM-AWP

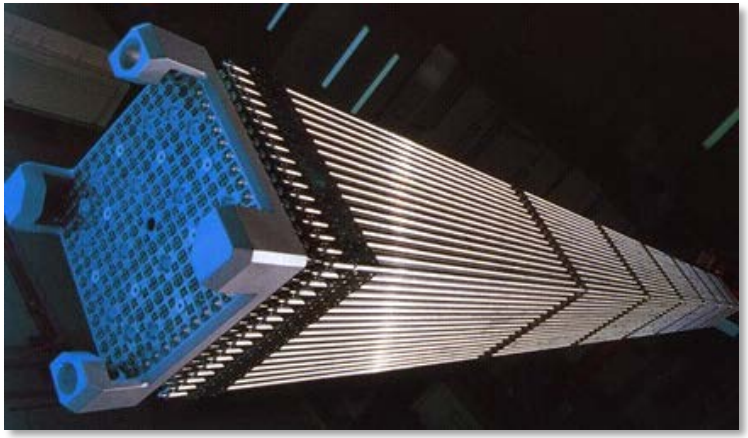


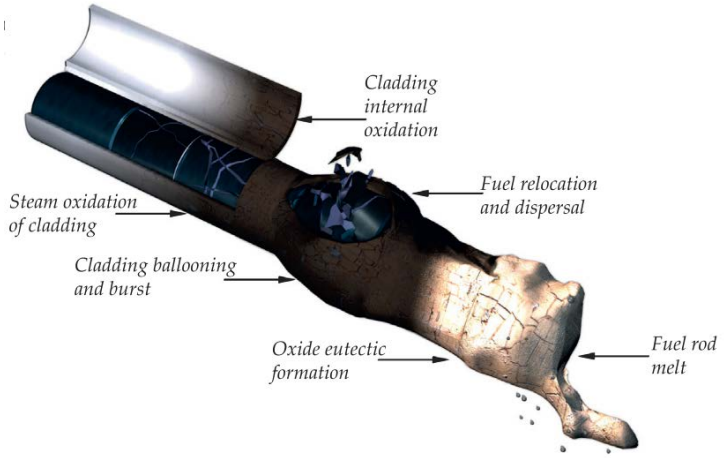
Outline

- Introduction
- Experiment arrangements
- Results and analyses
  - EC project IL TROVATORE
  - IAEA CRP project ACTOF
- Conclusions

Introduction

- Zirconium-based alloy fuel claddings
  - Hydrogen absorption
  - Ballooning and burst (~700°C)
  - Rapid exothermic oxidation (~1200°C)
  - Significant hydrogen release
  - Hydrogen explosion + radioactive products release





Evolution of Zr fuel cladding under severe accident

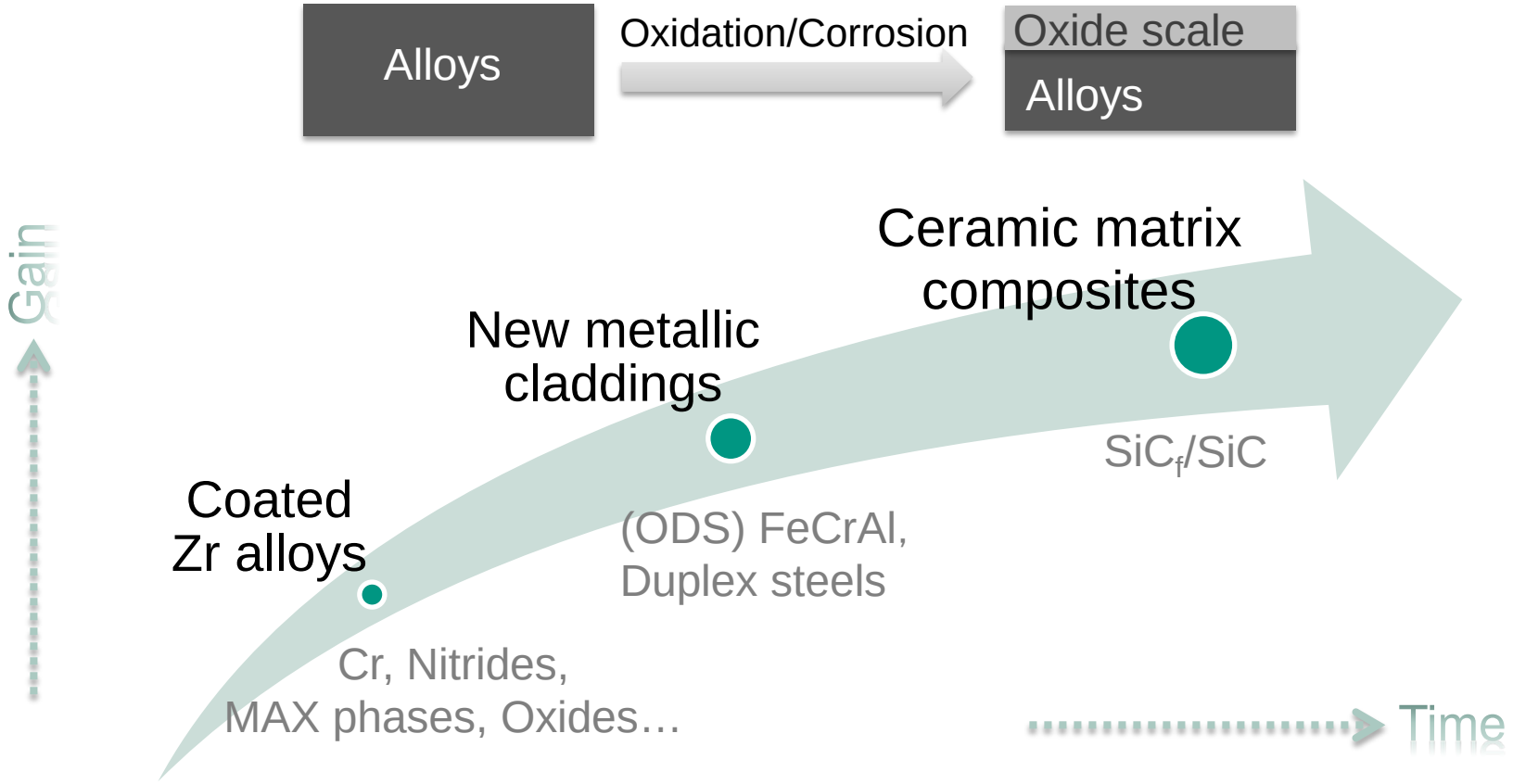


Fukushima, 2011
Light water reactor

Zinkle et.al, JNM, 448 (2014) 374–379.

Introduction

- **Accident tolerant fuels(ATF)** cladding
  - Reduced release of hydrogen and heat of cladding-steam oxidation
  - Increased coping time for severe accident management



Experiment arrangements

- Test conditions

  20 g/h H_2O + 20 l/h Ar, heating/cooling: 10K/min in Ar

- Samples
  - EC project IL TROVATORE
    - Zircaloy-4, Oxides, MAX phases, SiC_f/SiC, Fe-based alloys
    - 1200°C, 1h (GO/NO-GO test)
  - IAEA project ACTOF
    - Zircaloy-4, M-steel, Cr coated-, Cr_2AlC coated-, SiCrZr coated- Zr alloys
    - 1100°C-1h, 1200°C-30min, 1300°C-5min (Round Robin test)
- Characterization
  - Macroscopic comparisons & Mass changes
  - H_2 release (Mass spectrometry, total oxygen consumption)
  - XRD analysis & Surface/Cross section observation using SEM

Results I

EC project IL TROVATORE

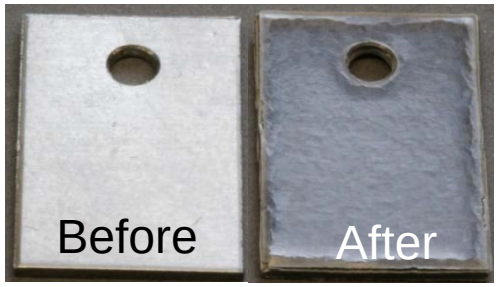
Zircaloy-4, Oxides, MAX phases,

SiC_f/SiC, Fe-based alloys

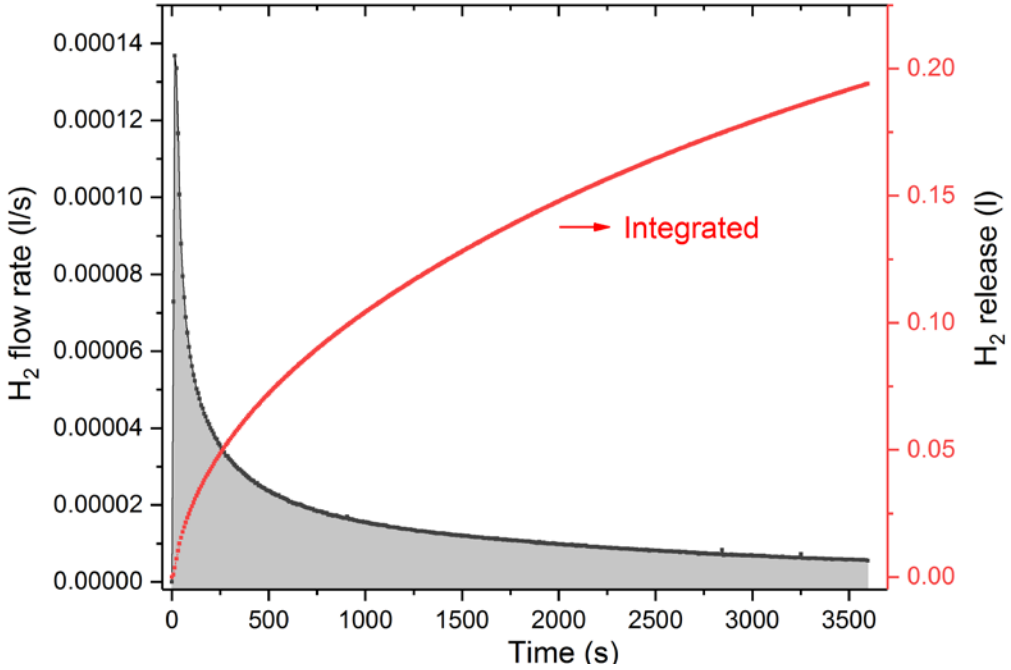
1200°C, 1h (GO/NO-GO test)

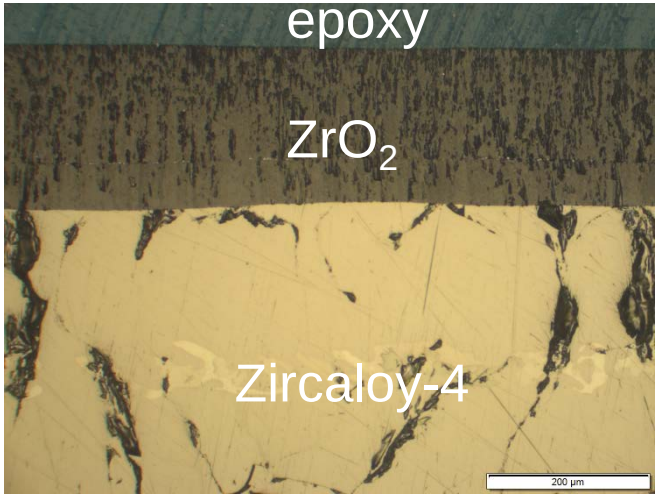
EC project IL TROVATORE

- I. Zircaloy-4



Sample	Relative mass gain (%)	Surface mass gain (g/m^2)	H_2 release (g/m^2)
REF: Zircaloy-4	22.81	431.52	54.78





- 220µm-thick oxide layer

EC project IL TROVATORE

- II. Oxides

Sample	Area (cm^2)	Mass change (g)	Relative mass change (%)	Surface mass change (g/m^2)
Al_2O_3 SM8	5.407	-0.0005	-0.021	-0.92±0.18
La-doped Al_2O_3	4.957	-0.0002	-0.011	-0.40±0.20
Y-doped Al_2O_3	4.918	-0.0001	-0.005	-0.20±0.20
CEZ12 ZrO_2 ($12\%CeO_2$)	4.23	0.001	0.035	2.36±0.26
TZ8Y ZrO_2 ($8\%Y_2O_3$)	4.23	0.002	0.077	4.73±0.29
Cr_2O_3	4.032	-0.0023	-0.096	-5.70±0.18
TiO_2	3.276	-0.002	-0.139	-6.10±0.21
Y_2SiO_5	4.055	-0.002	-0.101	-4.93±0.19
$Y_2Si_2O_7$	3.575	-0.0003	-0.019	-0.84±0.27

- Mass loss: alumina (with and without doping), chromia, titanium dioxide and yttrium silicates (volatilization).
- Mass gain: zirconia (oxygen vacancies).

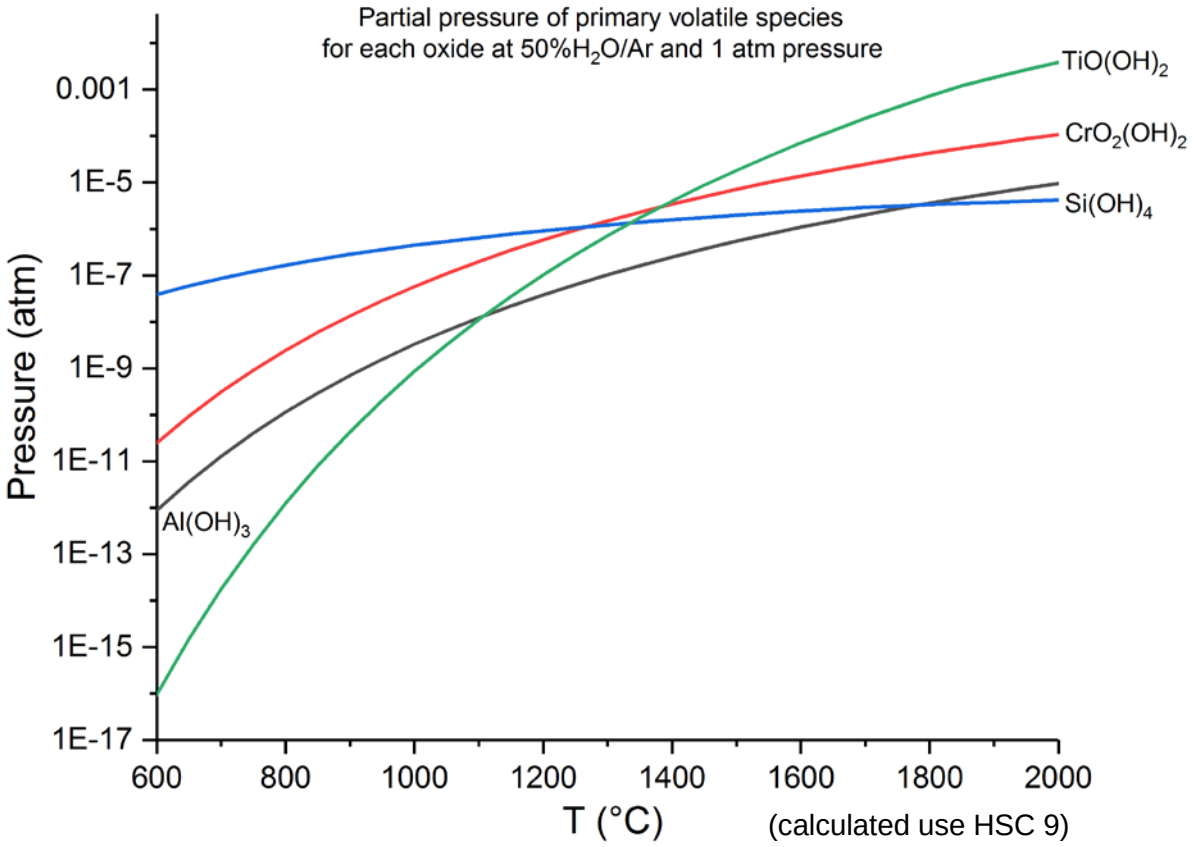
EC project IL TROVATORE

II. Oxides

Volatilization rate measured:

$TiO_2 > Cr_2O_3 > Y_2SiO_5 > Al_2O_3$

(TiO_2 : ~1.4 um degradation calculated)



$TiO_2 + H_2O(g) = TiO(OH)_2$

$Cr_2O_3 + 5H_2O(g) = 2CrO_2(OH)_2(g) + 3H_2(g)$

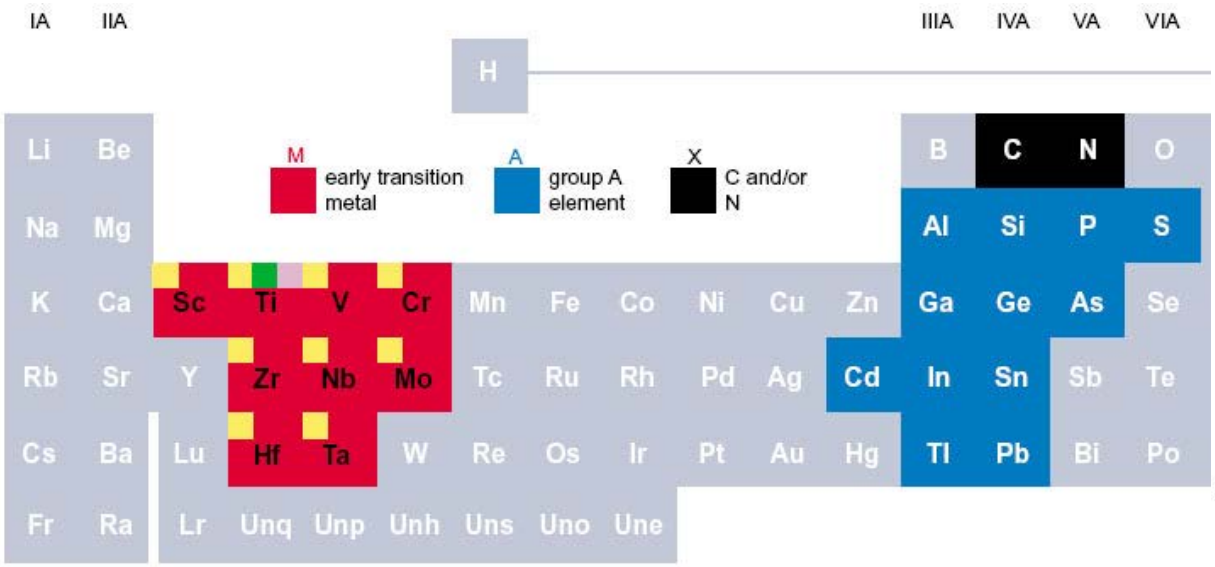
$SiO_2 + 2H_2O(g) = Si(OH)_4(g)$

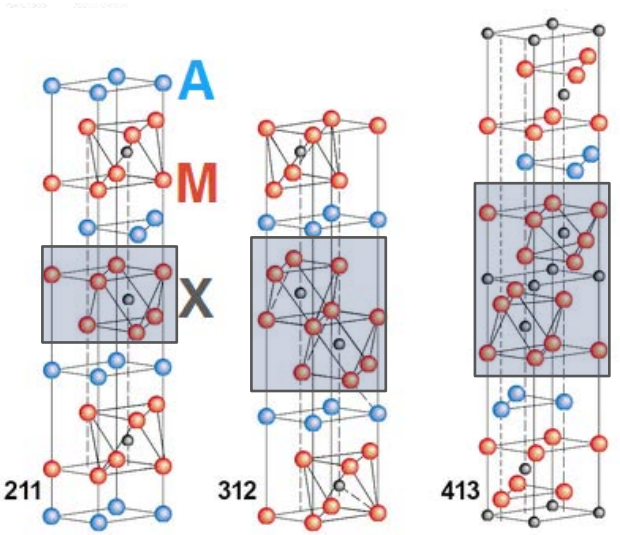
$Al_2O_3 + 3H_2O(g) = 2Al(OH)_3(g)$

EC project IL TROVATORE

III. MAX Phases

- MAX phases: ternary carbide and nitride compounds described by the general formula $M_{n+1}AX_n$, where n typical is 1, 2, 3
- Nanolaminated crystal structure: M_6X octahedral interleaved with A layers





Unique combination of physical, chemical, mechanical properties of both metals and ceramics

Nanolaminated crystal structure

M-X: strong covalent-ionic bonds

M-A: weak metallic bonds

 M.W. Barsoum, MAX phases: properties of machinable ternary carbides and nitrides, John Wiley & Sons, 2013.

EC project IL TROVATORE

III. MAX Phases

Sample	Surface mass gain (g/m²)	Oxide thickness (µm)	H_2 release (g/m²)
Ti_2AlC "Poitiers"	3.4±0.2	<2	2.6
Ti_2AlC "Maxthal 211"	8.2±0.4	<4	4.3
Ti_3SiC_2 "Leuven"	38.0±0.6	36	14.7
Pre-oxidized Ti_3SiC_2	44.2±0.7	90	12.5
Ti_3SiC_2 "Maxthal 312"	70.3±1.7	70	21.8
Cr_2AlC "Poitiers"	2.8±0.3	<2	4.1
Cr_2AlC "Leuven"	126.3±3.0	<2	25.4
$(Ti_{0.5}Nb_{0.5})_2AlC$	4.0±0.5	2 to 4	4.6
$(Zr_{0,5}Ti_{0,5})_2(Al_{0,5}Si_{0,5})C$	532.2±6.8	>1500	124.3

$(Zr_{0,5}Ti_{0,5})_2(Al_{0,5}Si_{0,5})C$

Ti_3SiC_2

$(Ti_{0.5}Nb_{0.5})_2AlC$ Cr_2AlC

Ti_2AlC

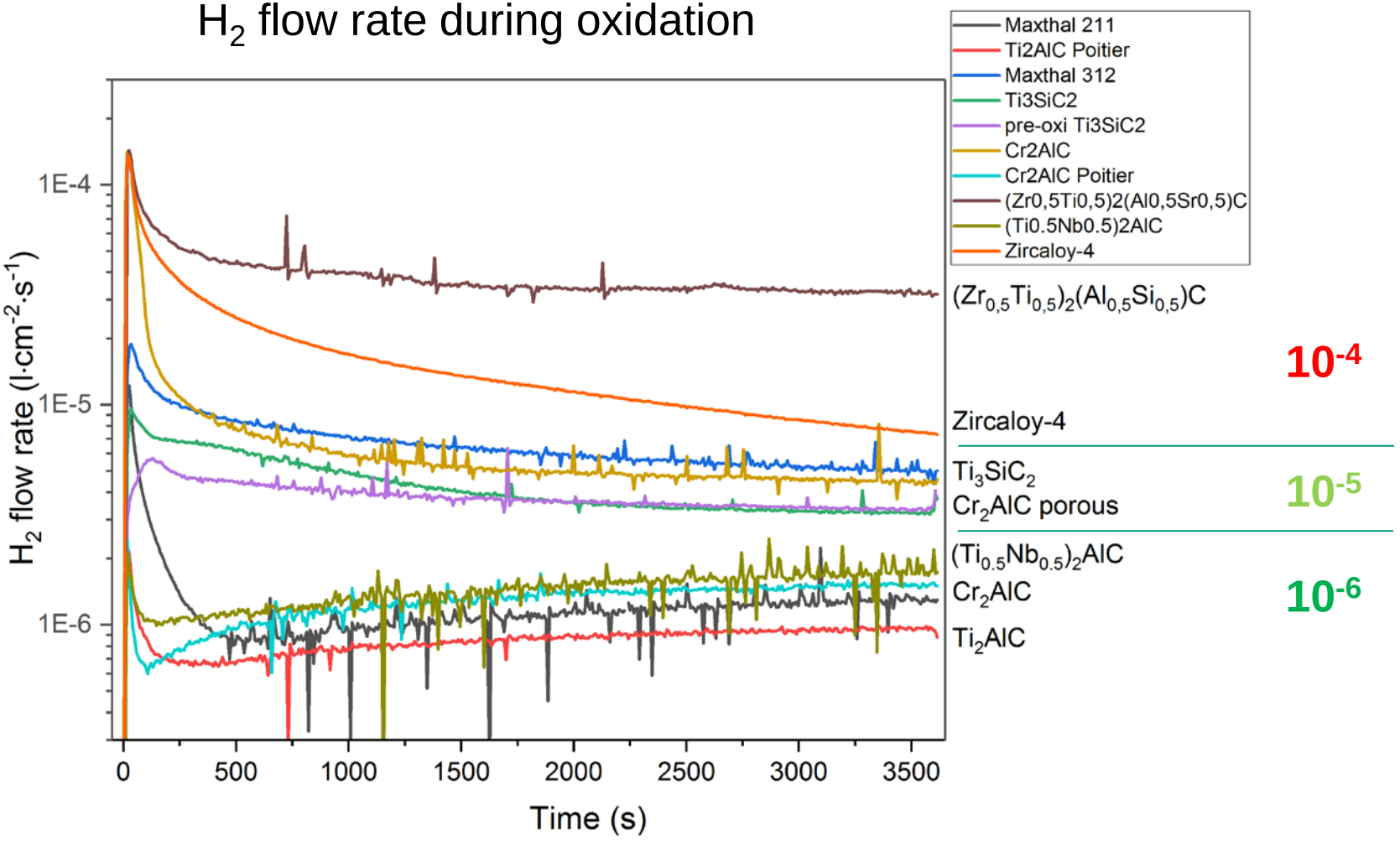
Oxidation performance

Purity & Porosity

EC project IL TROVATORE

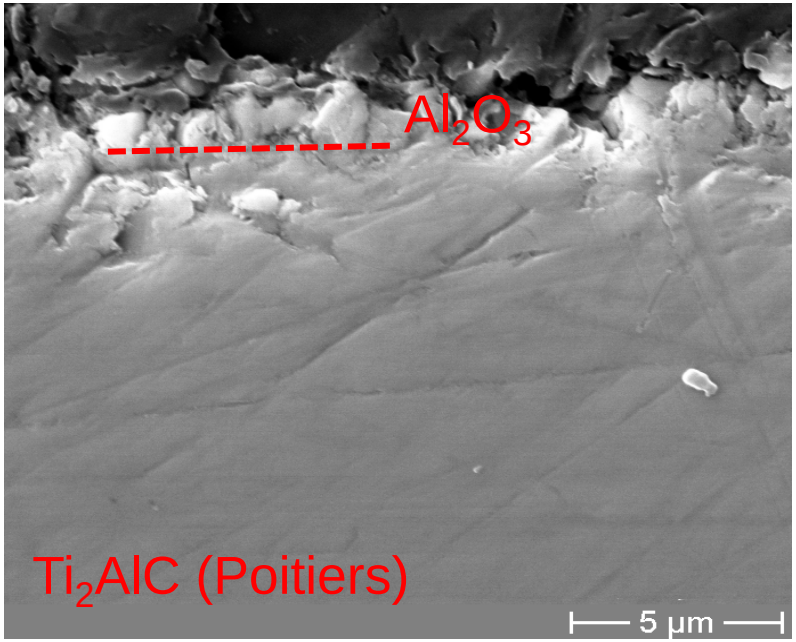
III. MAX Phases

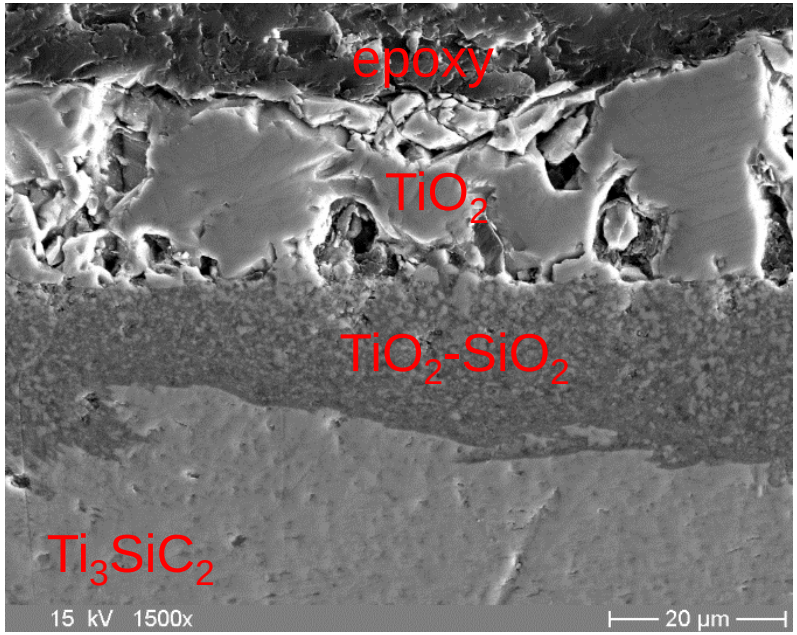
H_2 flow rate during oxidation



EC project IL TROVATORE

- III. MAX Phases

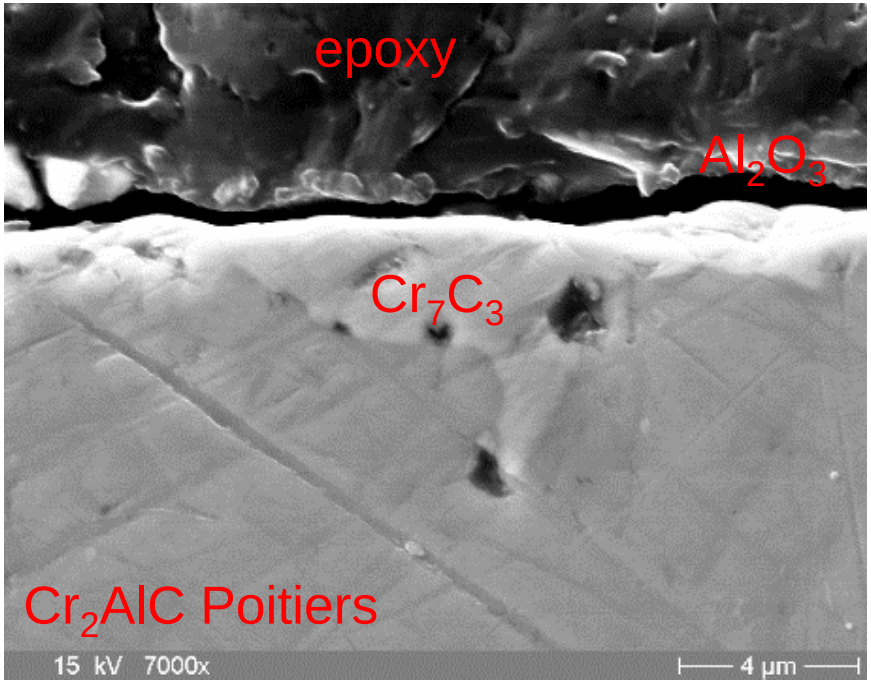


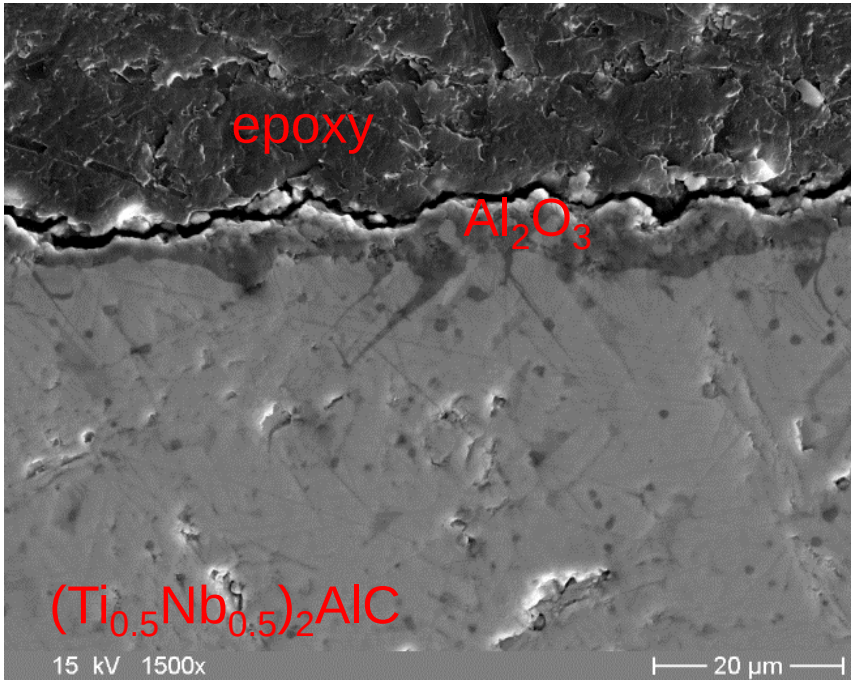


- A thin, dense Al_2O_3 layer grew on Ti_2AlC samples.
- All three Ti_3SiC_2 samples formed an oxide scale with two sublayers: outer TiO_2 layer and inner TiO_2+SiO_2 layer.
- Impurities (binary carbides and intermetallics) increase the oxidation rate.

EC project IL TROVATORE

- III. MAX Phases



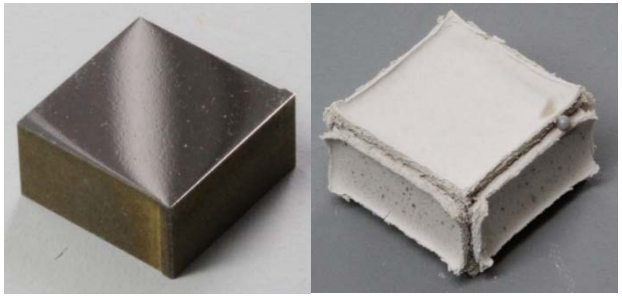


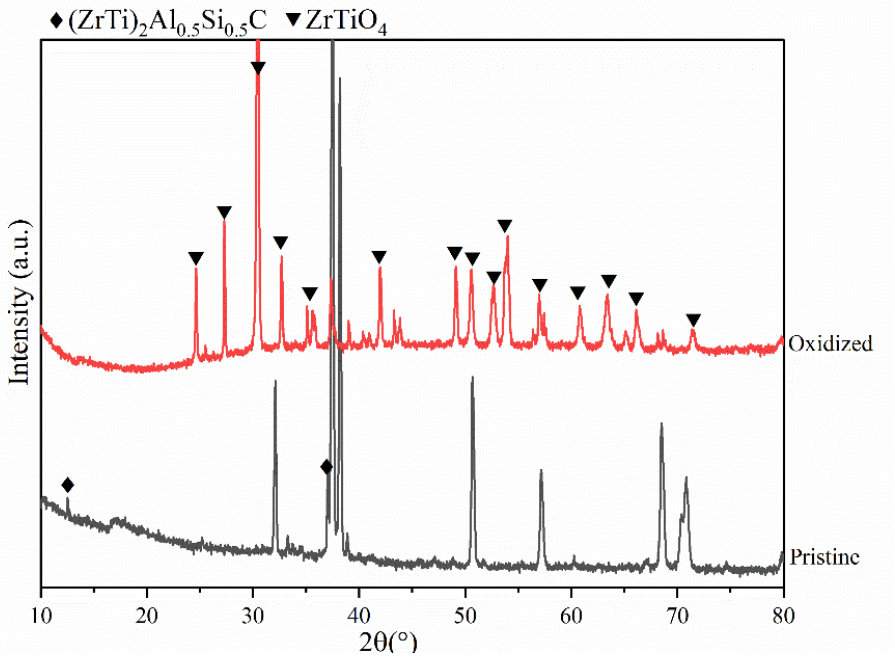
- A protective Al_2O_3 layer appeared with a continuous Cr_7C_3 layer beneath of Cr_2AlC, partial spallation of oxide was observed.
- A thin, protective, adherent Al_2O_3 layer established on $(Ti_{0.5}Nb_{0.5})_2AlC$.

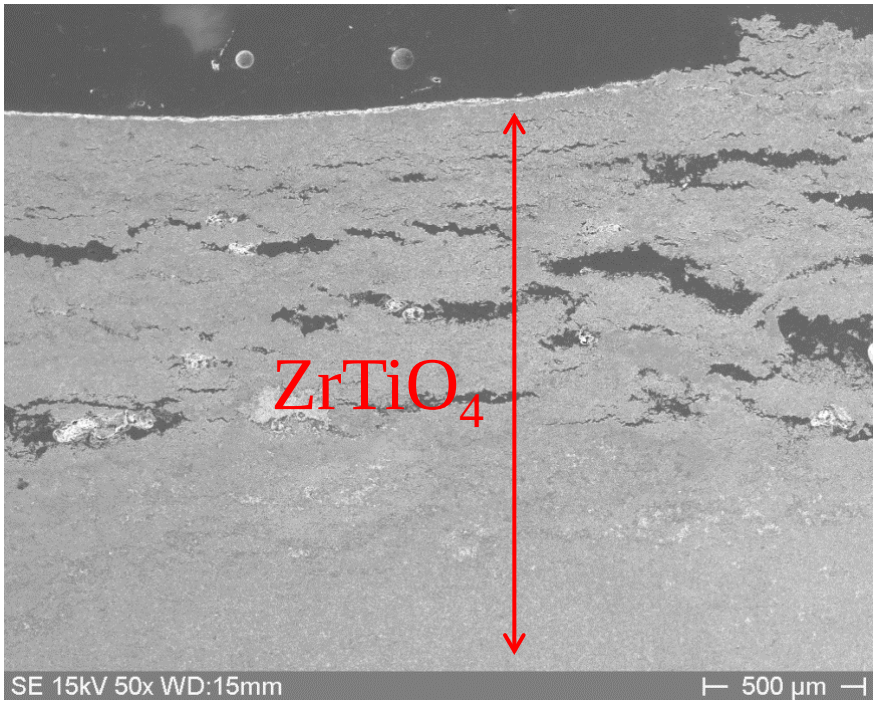
EC project IL TROVATORE

- III. MAX Phases

- $(Zr_{0,5}Ti_{0,5})_2(Al_{0,5}Si_{0,5})C$







- Completely oxidized
- Non-protective $ZrTiO_4$ layer

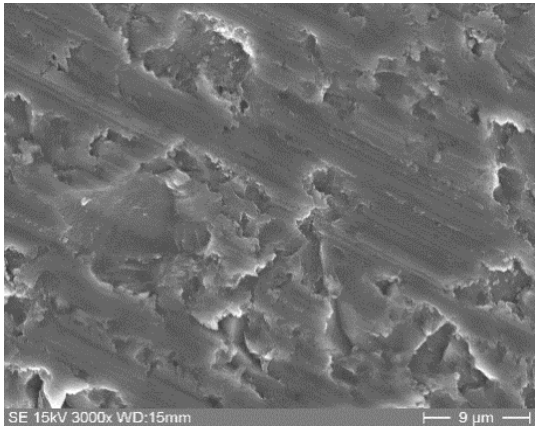
EC project IL TROVATORE

- IV. SiC_f/SiC

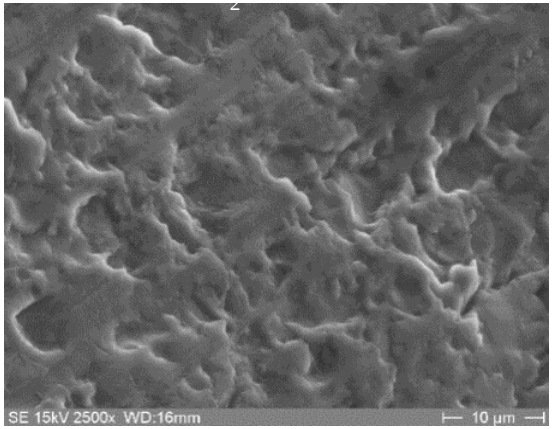




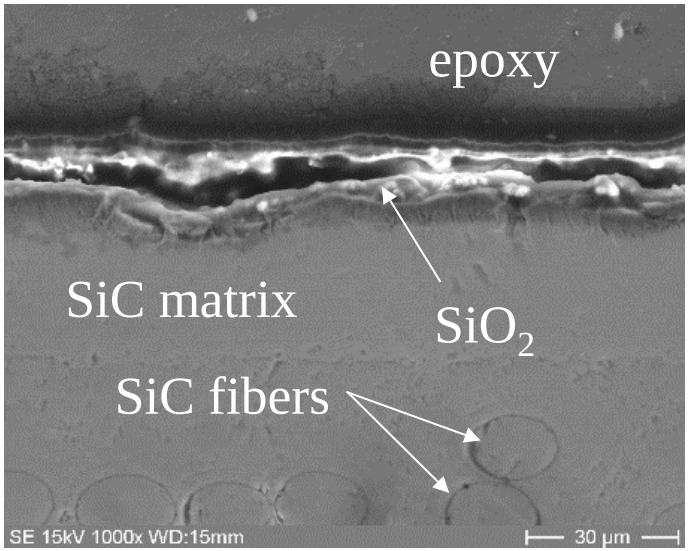
Sample	Surface mass gain (g/m²)	Oxide thickness (µm)	H_2 release (g/m²)
SiC_f/SiC	0.17±0.17	<1	2.6



Before



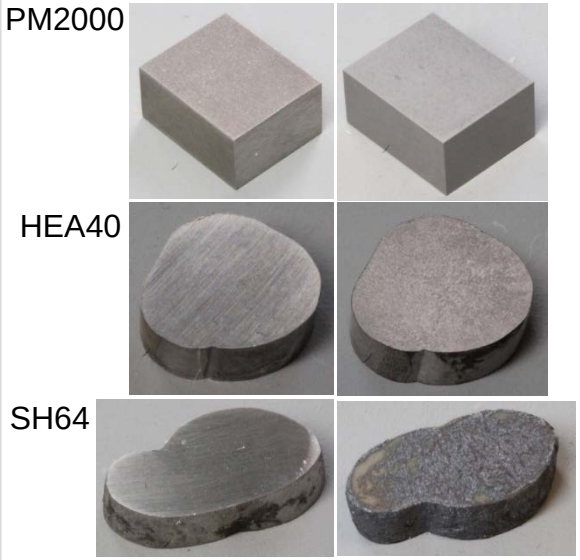
After



- Thin protective SiO_2 scale

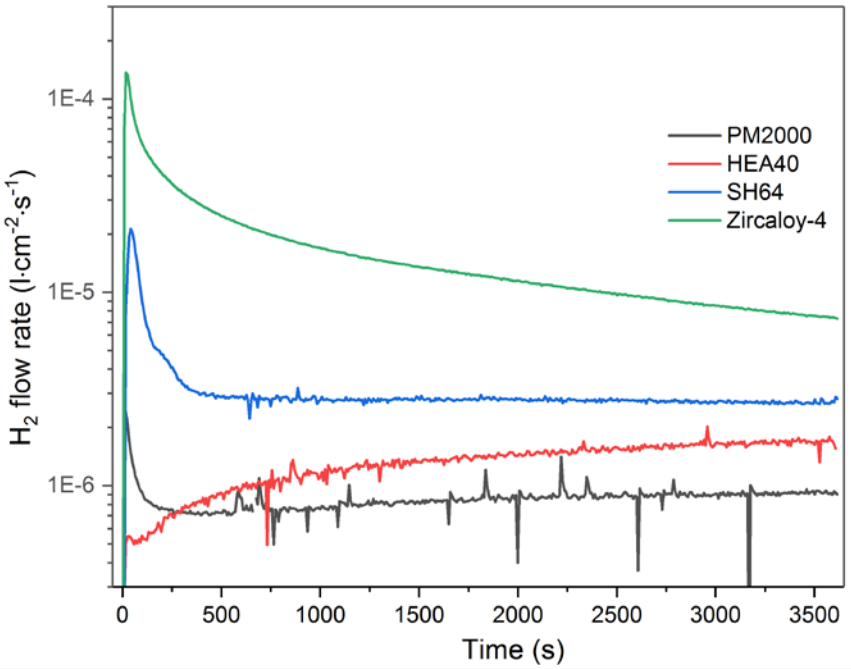
EC project IL TROVATORE

V. Fe-based Alloys



Sample	Surface mass gain (g/m²)	Oxide thickness (μm)	H_2 release (g/m²)
PM2000 $Al_{5.5}Cr_{19}Ti_{0.5}(Y_2O_3)_{0.5}Fe_{base}$	1.67±0.18	~3	0.28
HEA40 $Al_{4.5}Cr_{22.5}Ni_{37}Fe_{35.88}$	2.37±0.38	~3	0.44
SH64 $Al_4Cr_{16}Ni_{24}Nb_{1.5}Y_{0.5}Fe_{base}$	34.84±0.91	20	10.4

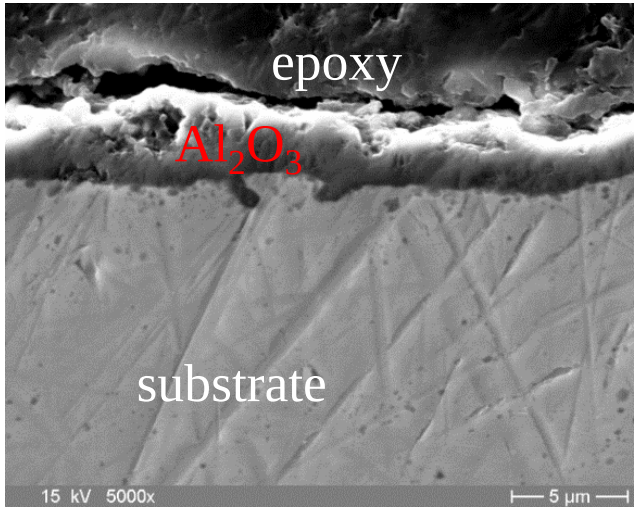
- Al_2O_3 scale for PM2000 and HEA40
- $FeCr_2O_4$ scale on SH64



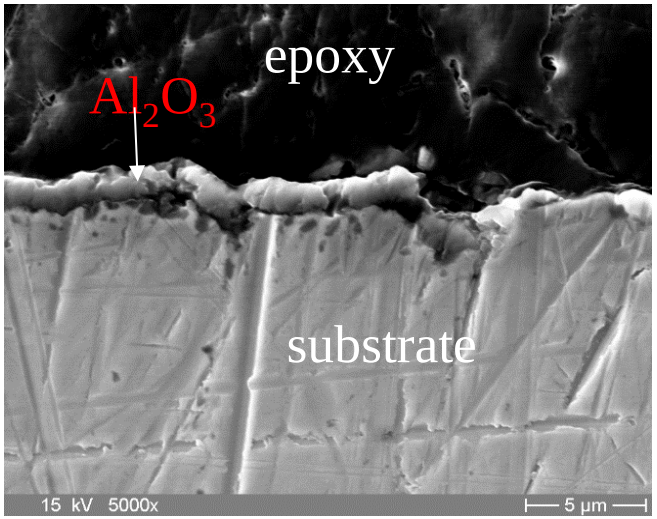
EC project IL TROVATORE

V. Fe-based Alloys

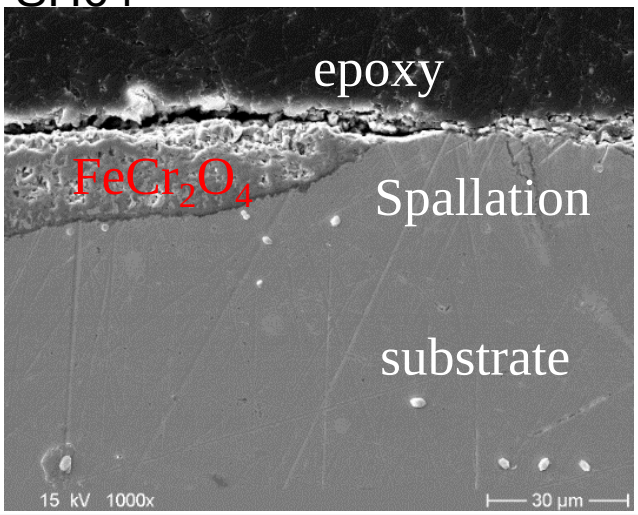
PM2000



HEA40

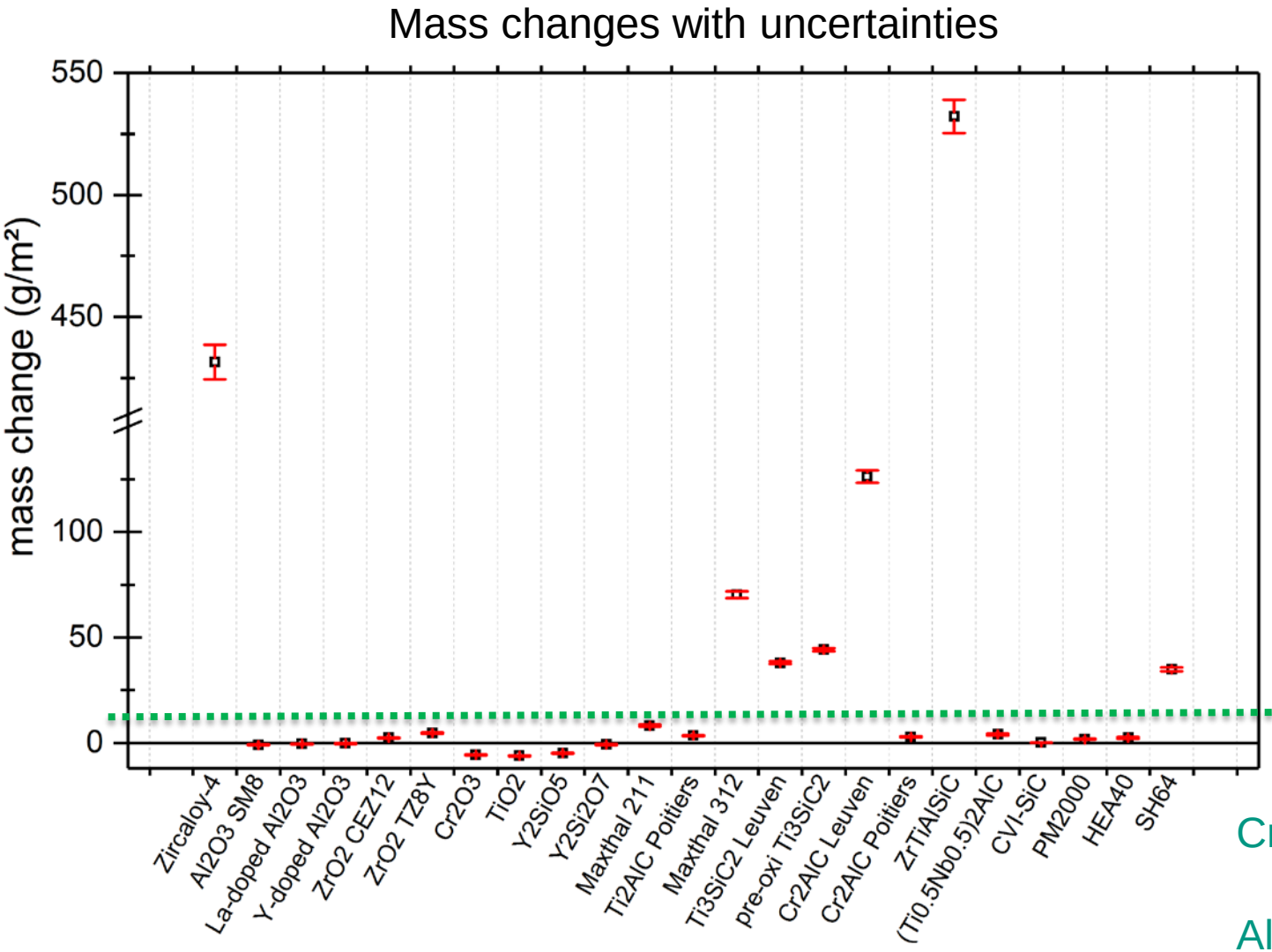


SH64



- A protective and dense Al_2O_3 layer covers PM2000 and HEA40
- Scale spallation was observed on HEA40
- $FeCr_2O_4$ scale and large nodules on SH64, with spallation

EC project IL TROVATORE



$(ZrTi)_2(Al_{0,5}Si_{0,5})C$

Porous Cr_2AlC

Ti_3SiC_2

SH64

(Al4Cr16Ni24Nb1.5Y0.5Febase)

Oxides, Ti_2AlC, Cr_2AlC, $(TiNb)_2AlC$, SiC, Al_2O_3-forming alloys

Results II

IAEA project ACTOF

Zircaloy-4, M-steel, Cr coated-, Cr_2AlC coated-,
SiCrZr coated- Zr alloys

1100°C-1h, 1200°C-30min, 1300°C-5min

(Round Robin test)

IAEA project ACTOF



Ref. Zircaloy-4

(15x10x0.65, 320 mm^2)



Martensitic-Steel
(Fe18Cr7Ni)

(20x5x1.5, 280 mm^2)



Cr(25um)
coated Zry2

(20x20x1, 880 mm^2)



Cr/Cr_2AlC/Cr(6um)
coated Zry4

Cr(1.5um)/ Cr_2AlC (4.5um)/ Cr (0.5 um)

(15x10x0.65, 320 mm^2)



$Si_{24}Cr_{36}Zr_{40}$ (wt.%, 2.5 um)
coated Zry2

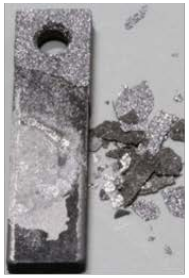
(20x20x1, 880 mm^2)

IAEA project ACTOF

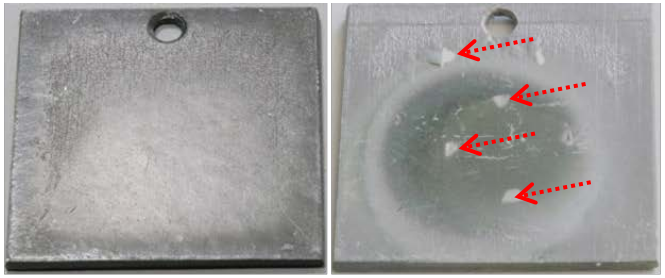
- 1100°C-1h



Ref. Zircaloy-4



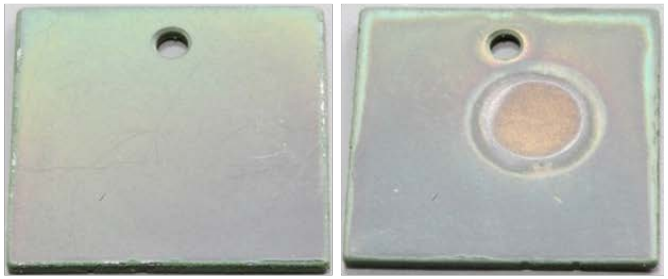
M-Steel



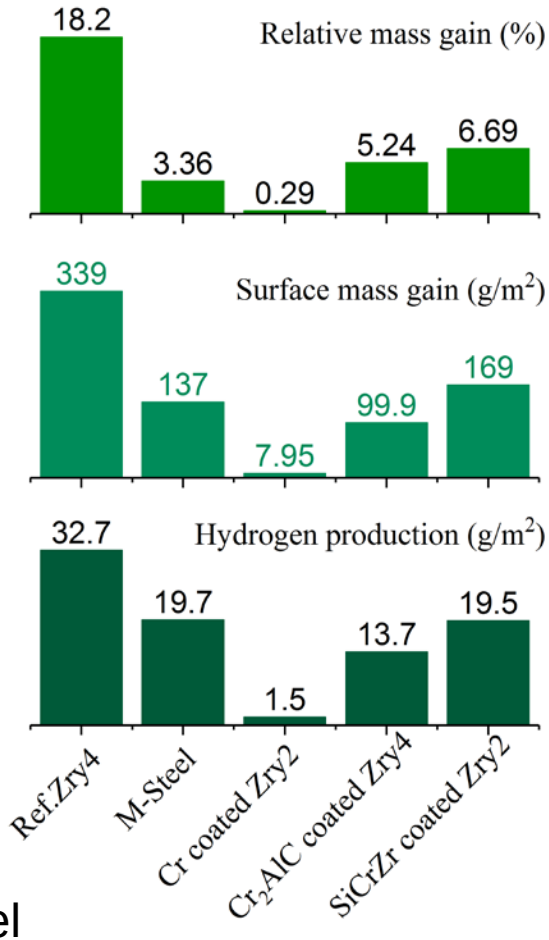
Cr(25um) coated Zry2



Cr/Cr_2AlC/Cr(6um) coated Zry4



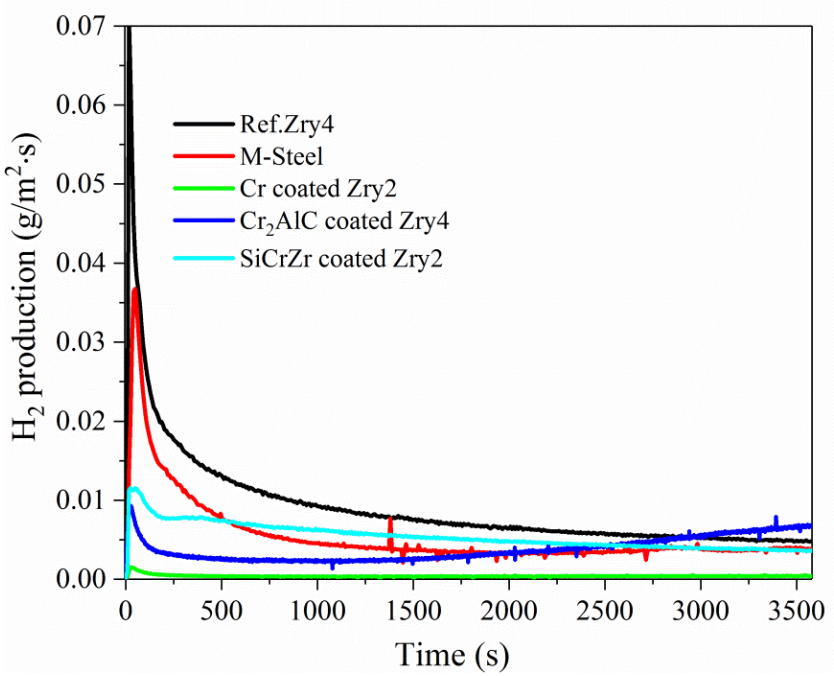
$Si_{24}Cr_{36}Zr_{40}$ (wt.%, 2.5 um) coated Zry2

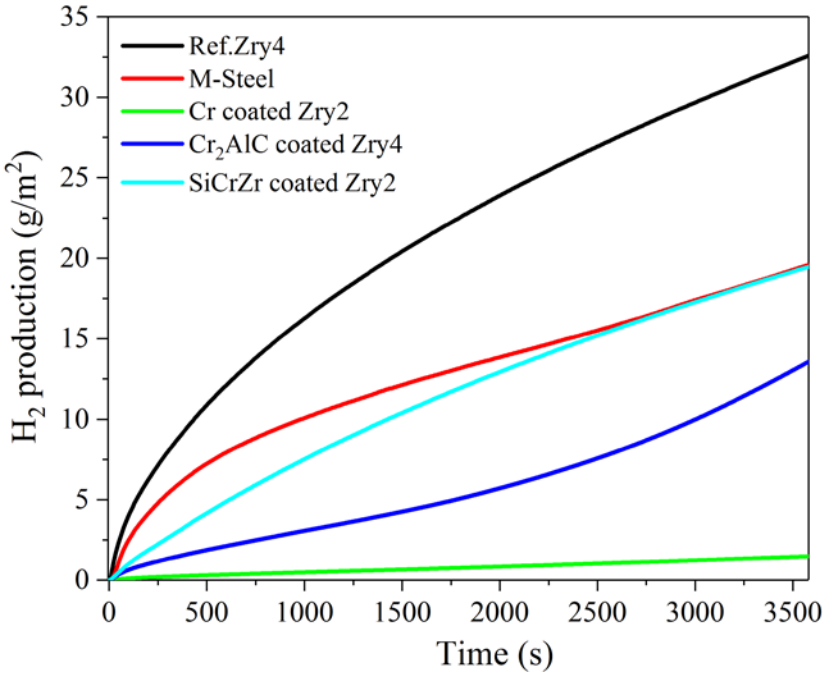


- Fast oxidation rate and low scale adherence of M-steel
- Higher adherence of metallic coatings than ceramic coatings

IAEA project ACTOF

- 1100°C-1h

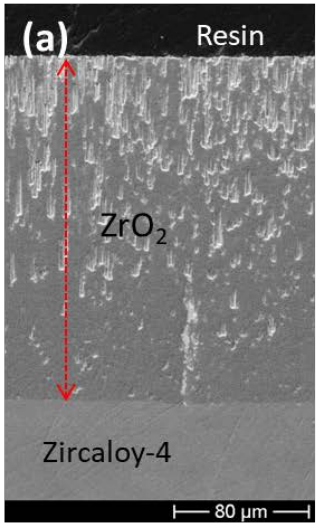




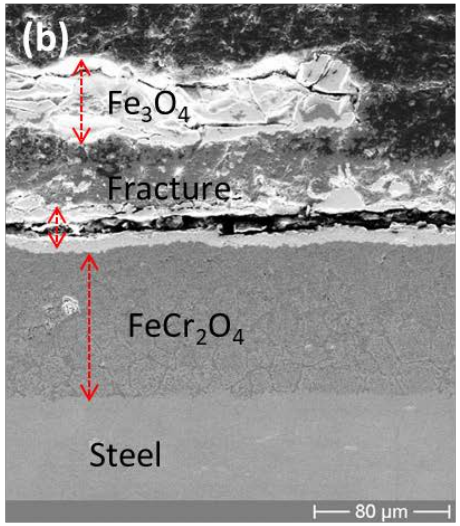
- The oxidation kinetics all roughly follow a parabolic law

IAEA project ACTOF

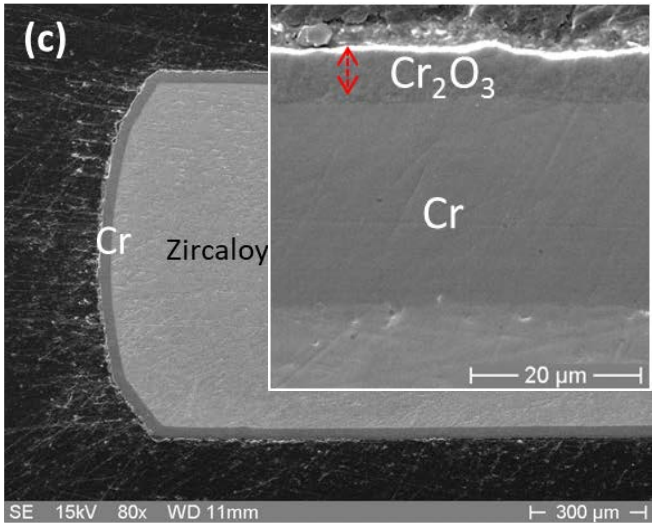
- 1100°C-1h



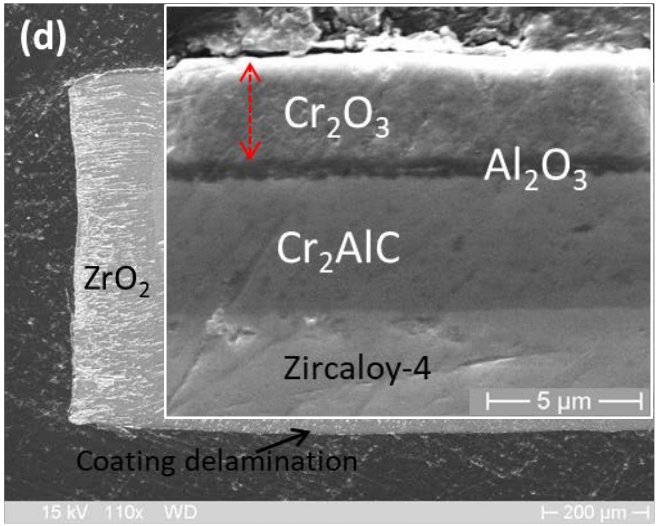
190 um ZrO_2



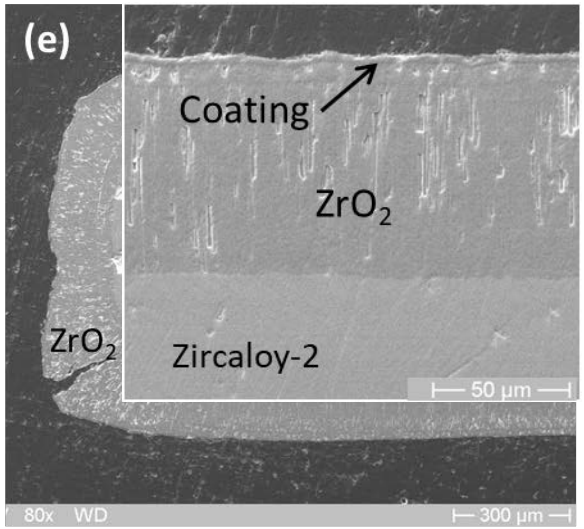
~95 um Fe_3O_4+ 90 um $FeCr_2O_4$



~5.5 um Cr_2O_3 (22 um Cr unoxidized)



~2.5 um Cr_2O_3 + 0.5 um Al_2O_3 (coating attached area)



73 um ZrO_2 (coating completely oxidized)

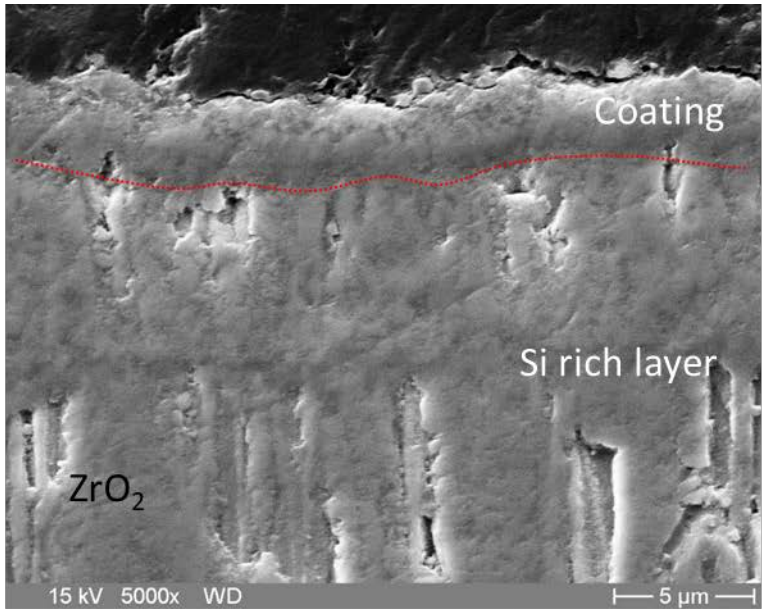
- Completely covered of Cr and CrSiZr coated
- Edges uncoated for Cr_2AlC coated

(a) ref. Zircaloy-4
(b) M-steel
(c) Cr coated Zry2
(d) Cr_2AlC coated Zry4
(e) CrSiZr coated Zry2

IAEA project ACTOF

1100°C-1h

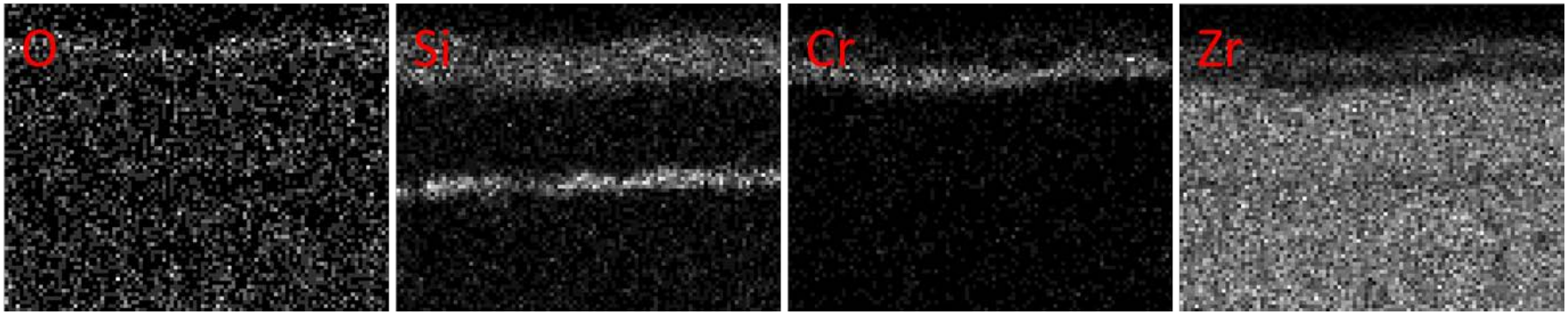
$Si_{24}Cr_{36}Zr_{40}$ (wt.%, 2.5 um) coated Zry2



SiO_2 and ZrO_2 layer

SiO_2 and Cr_2O_3 layer

Eutectic reaction
Si-Zr: 1365°C
Cr-Zr: 1335°C



IAEA project ACTOF

- 1200°C-30 min



Ref. Zircaloy-4



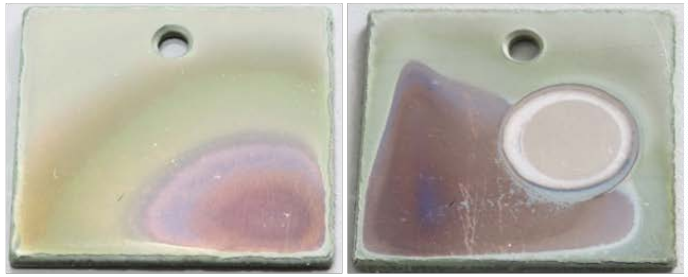
M-Steel



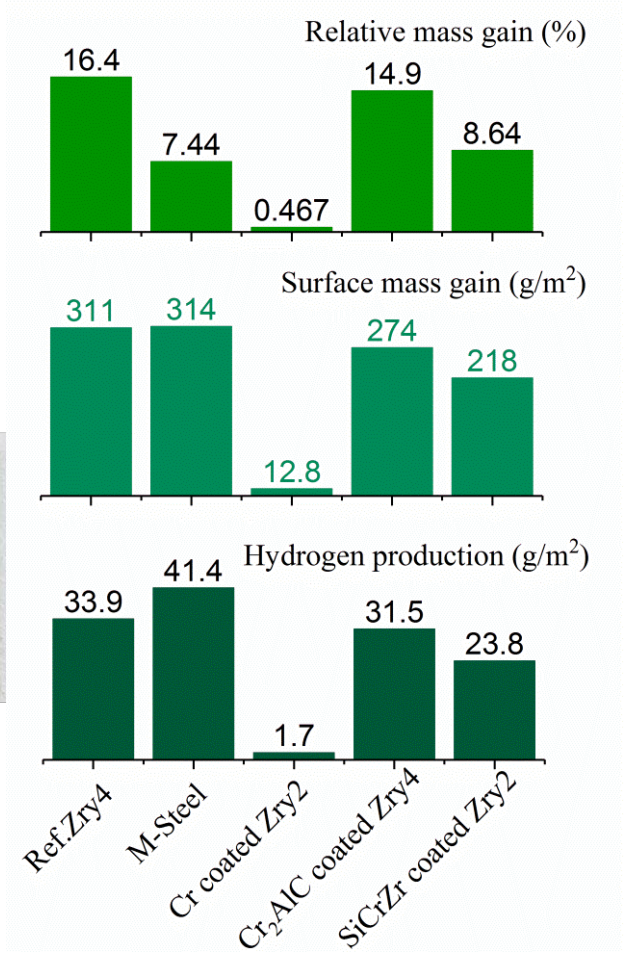
Cr(25um) coated Zry2



Cr/Cr_2AlC/Cr(6um) coated Zry4

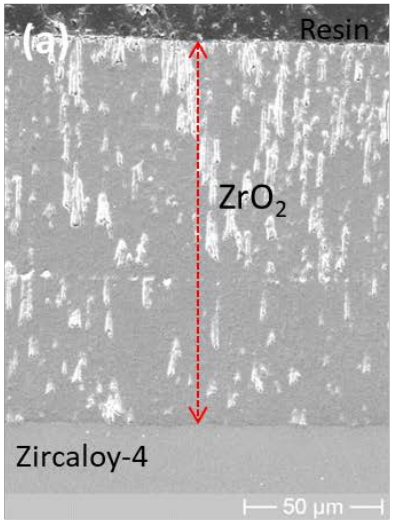


$Si_{24}Cr_{36}Zr_{40}$ (wt.%, 2.5 um) coated Zry2

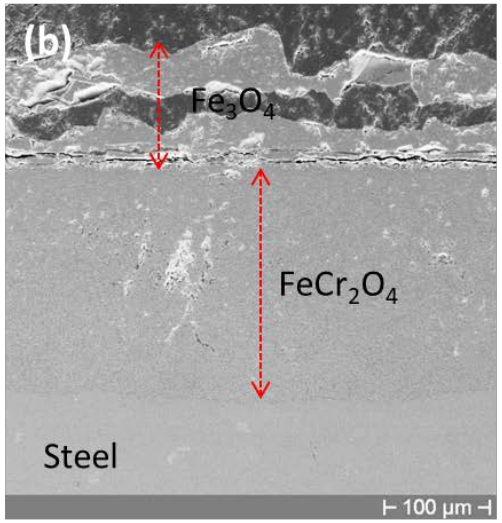


IAEA project ACTOF

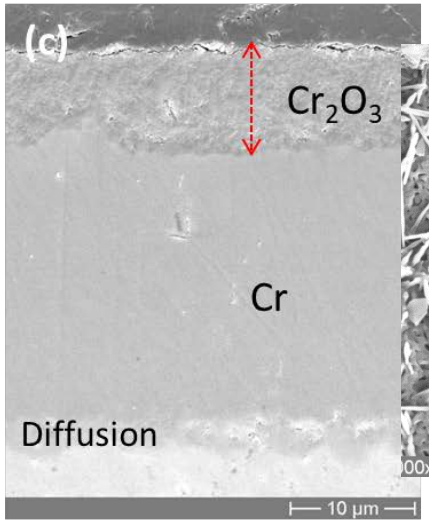
- 1200°C-30 min



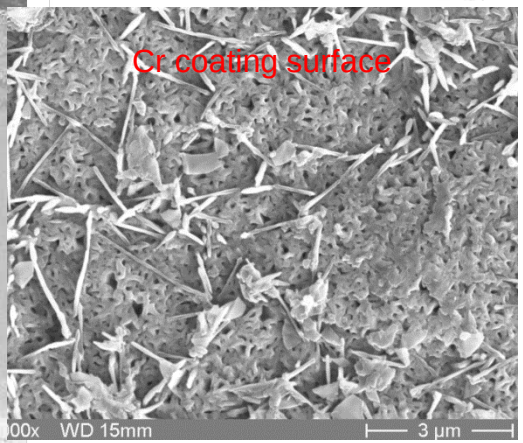
130 um ZrO_2



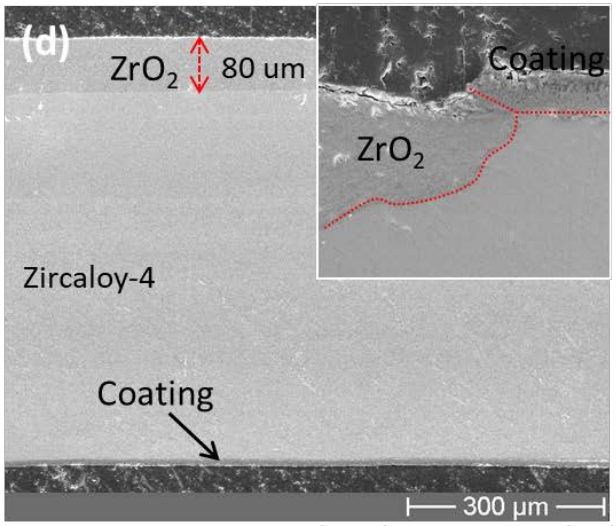
~80 um Fe_3O_4+ 220 um $FeCr_2O_4$



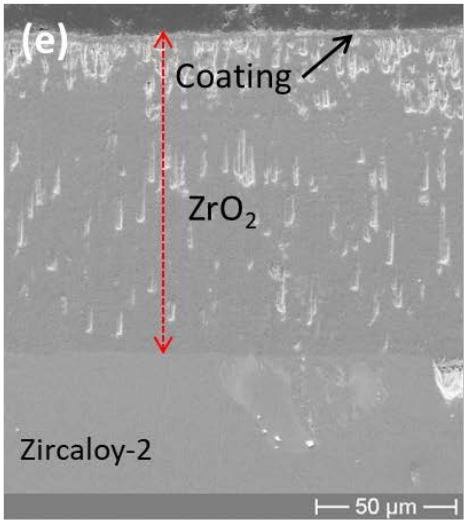
~7.3 um Cr_2O_3 (20 um Cr unoxidized)



Whiskers+ fine voids



~2.5 um Cr_2O_3 + 0.6 um Al_2O_3 (coating attached area)



110 um ZrO_2 (coating completely oxidized)

(a) ref. Zircaloy-4
(b) M-steel
(c) Cr coated Zry2
(d) Cr_2AlC coated Zry4
(e) CrSiZr coated Zry2

IAEA project ACTOF

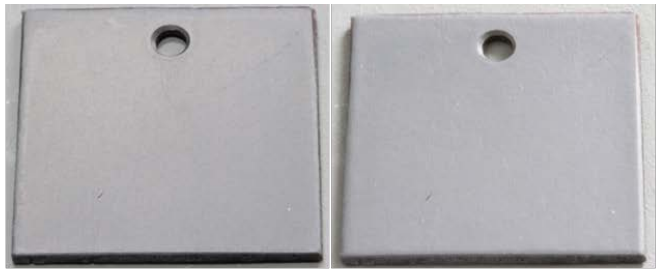
1300°C-5 min



Ref. Zircaloy-4



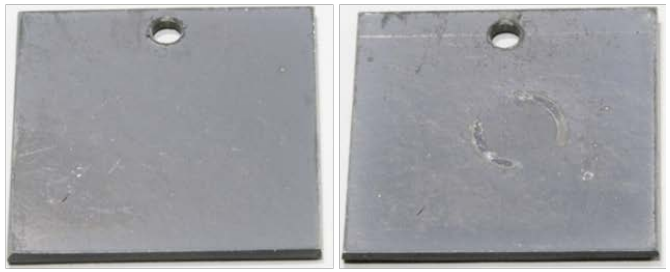
M-Steel



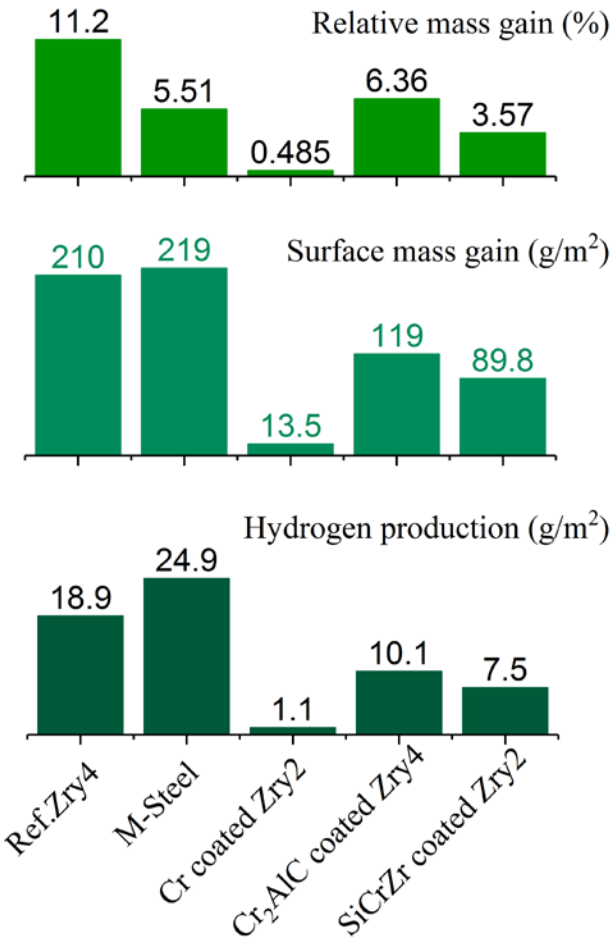
Cr(25um) coated Zry2



Cr/Cr_2AlC/Cr(6um) coated Zry4

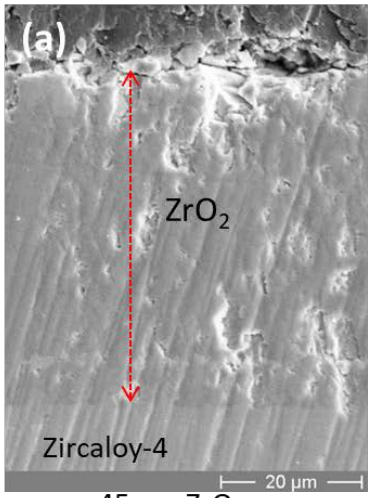


$Si_{24}Cr_{36}Zr_{40}$ (wt.%, 2.5 um) coated Zry2

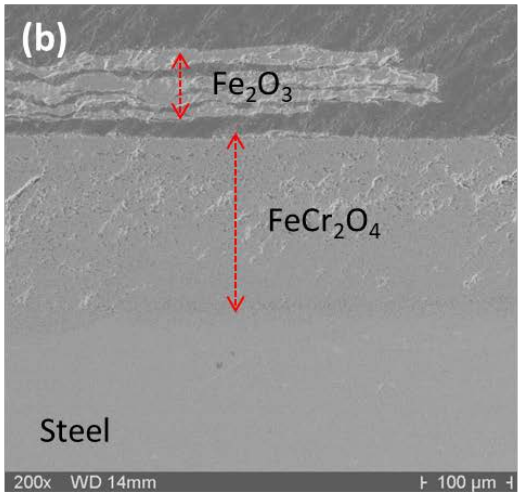


IAEA project ACTOF

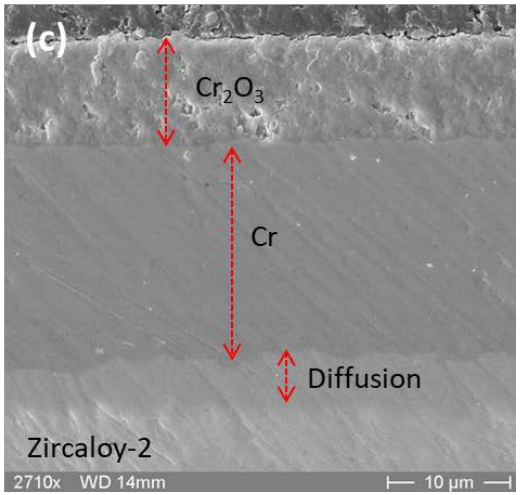
- 1300°C-5 min



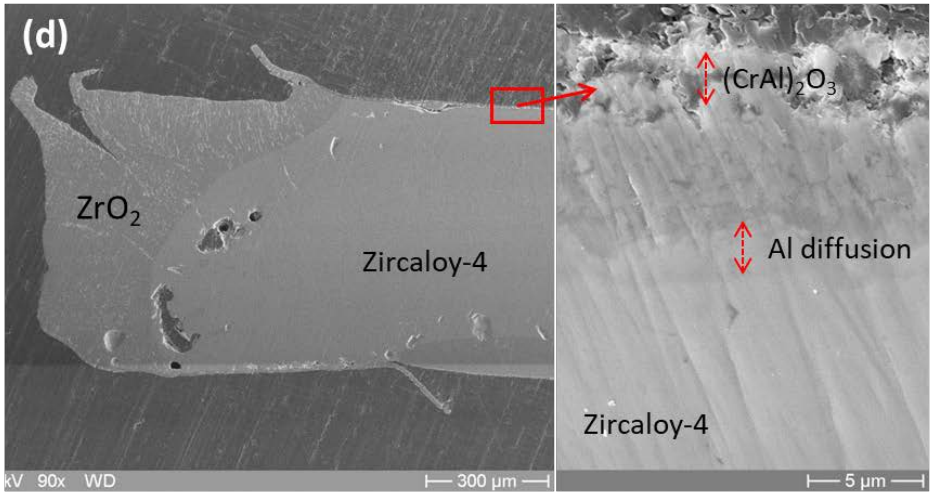
45 um ZrO_2



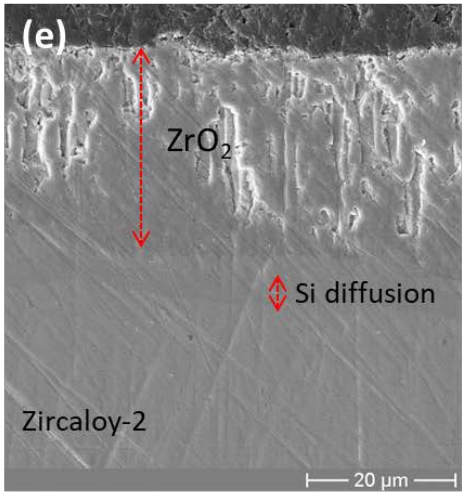
~85 um Fe_2O_3+ 170 um $FeCr_2O_4$



~8 um Cr_2O_3 (16 um Cr unoxidized)



~ 1.5 um $(CrAl)_2O_3$ layer (coating attached area)



23 um ZrO_2

- Remarkably improved oxidation rate and inward diffusion rate of Cr coating
- Cr/Cr_2AlC multilayer structure seems destroyed during heat-up period due to pronounced interdiffusion

(a) ref. Zircaloy-4
(b) M-steel
(c) Cr coated Zry2
(d) Cr_2AlC coated Zry4
(e) CrSiZr coated Zry2

Conclusions

Bulk materials

- **Oxides**: low volatilization rates in HT steam (concern for thin films)
- **MAX Phases**: Ti_2AlC, Cr_2AlC and $(TiNb)_2AlC$ are alumina formers with excellent oxidation resistance, Ti_3SiC_2 and $(Zr_{0,5}Ti_{0,5})_2(Al_{0,5}Si_{0,5})C$ reveal high oxidation rates
- **FeCrAl alloys:** a critical content of Cr and Al and reactive elements (Y) doped to establish a protective, adherent Al_2O_3 scale
- **SiC_f/SiC**: a protective silica layer with excellent performance
- **Martensitic steel (Fe18Cr7Ni):** bad performance with non-protective Fe-based scale

Coated Zr alloy cladding

- A critical thickness of the coatings is needed for HT protection in steam
- Lower toughness/adherence of ceramic based coatings (Cr_2AlC) compared to metallic coatings (Cr and CrSiZr)
- Significant diffusion of coating elements, especially light elements (Si and Al), into the substrate
- Fast oxidation rate of Cr coatings at temperatures >1200°C
- Oxidation behavior and failure mechanisms beyond eutectic temperature need further investigations

IAM

Karlsruhe Institute of Technology

Many thanks to:

High-temperature chemistry group, Thin film group

EC project IL TROVATORE, IAEA CRP project ACTOF

Thanks for your attention !

J.C. Brachet et al.

Overview of recent CEA-Framatome-EDF results obtained on Cr-coated M5 cladding tested upon LOCA conditions

One-sided steam oxidation tests have been conducted at various temperatures between 1000 and 1500°C on several facilities on 12-15µm thick Cr-coated M5 claddings. Microstructural observations and micro-chemical analysis have been performed after oxidation and quenching. Some post-quenching ring compression tests have been also carried out to assess the residual strength/ductility of the Cr-coated materials oxidized at High Temperature (HT). It was confirmed that in the 1000-1300°C oxidation temperature range, the oxidation resistance of the coated materials was enhanced, with a significant additional “coping period” at HT before the material became macroscopically brittle during and/or after quenching. The study was then extended to steam oxidation temperatures higher than 1300°C (Design Extension Conditions). Those tests have confirmed that a eutectic reaction occurred between the zirconium based substrate and the residual metallic Cr coating above 1300°C. For the DEC-type conditions applied, the tested Cr-coated clad segments did not fail upon the final water quenching while some uncoated reference segments did.

Furthermore, first results of amorphous/nanocrystalline CrC coating deposited by DLI-MOCVD inside fuel cladding were presented.


eDF
French alternative energies and atom
Saclay center | F91191 Gif-sur-Yvett
T. +33 (0)1 69 08 51 66 | F. +33 (0)1
Nuclear Energy Division
Nuclear Materials Department
Section for Applied Metallurgy R
jean-christophe.brache
KIT

Overview of recent CEA-Framatome-EDF results obtained on Cr-coated M5 cladding tested upon LOCA conditions (*)

(*) most of the results presented here are based on presentations done at the last "Topfuel 2018" meeting, Praha, Czech Republic, (Sept. 2018)

24th. International QUENCH Workshop
Karlsruhe Institute of Technology, Germany

JC. Brachet et al., CEA Saclay

(13-15 November 2018)

FROM RESEARCH TO INDUSTRY

cea den

framatome

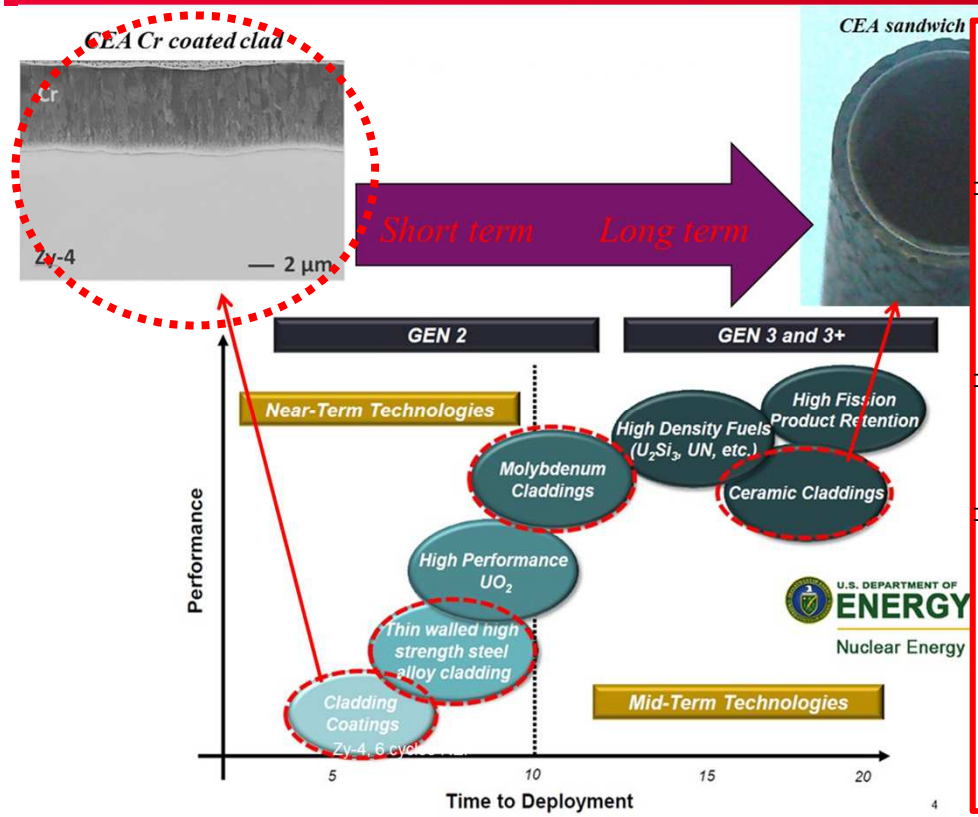
eDF

French alternative energies and atomic energy commission
Saclay center | F91191 Gif-sur-Yvette Cedex
T. +33 (0)1 69 08 51 66 | F. +33 (0)1 69 08 82 52

Nuclear Energy Division
Nuclear Materials Department
Section for Applied Metallurgy Research

jean-christophe.brachet@cea.fr

COATED NUCLEAR FUEL CLADDINGS STUDIED AND DEVELOPED SINCE 2013 WITH FRAMATOME AND EDF AS A SHORT-TERM (EVOLUTIONARY) ENHANCED-ATF CLAD CONCEPT



Specific objectives of coated clads **upon LOCA (and beyond) conditions**:

⇒ **additional copying time before loss of clad integrity** (*i.e., strength upon final quenching and post-quenching ductility/toughness*)

⇒ **decrease the gazeous hydrogen production kinetics** (explosion risk)

⇒ **minimize the heat produced by the HT oxidation of Zr**, thus **decreasing Peak Clad Temperature** (PCT) and **limit the risk of temperature escalation occurence for T > 1200°C** (Design Extension Conditions, DEC)

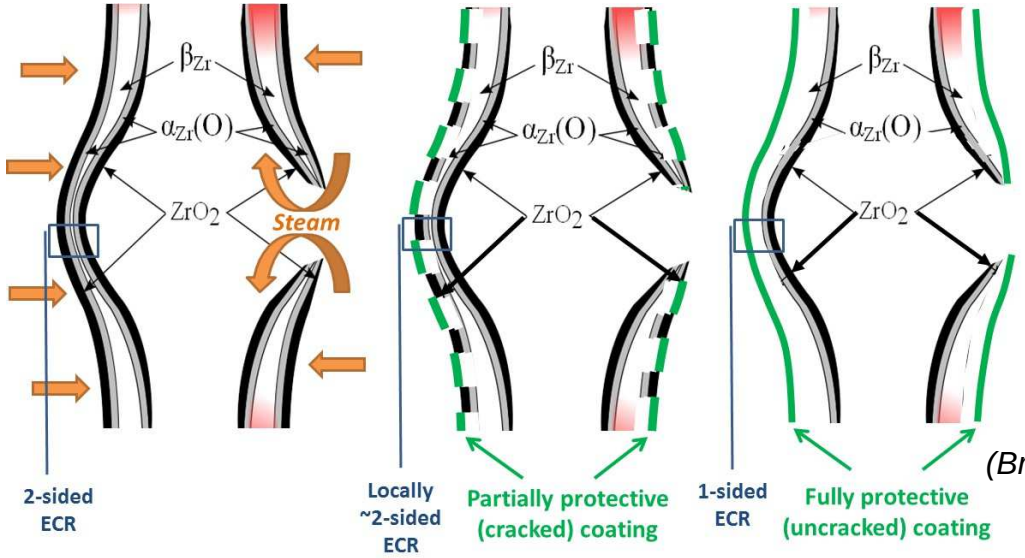
Upon nominal (in-service) conditions:

- **Faster/easier « licensing »** thanks to the preservation of the reference Zr clad properties;
- **Preserve or enhance** the clad behavior (**corrosion, wear resistance**...);
- **Negligible or very limited neutron penalty** for thin enough coatings.

24th. Quench workshop, KIT, Nov. 2018, "Recent results on LOCA behavior of Cr-coated M5" (CEA/Framatome/EDF)

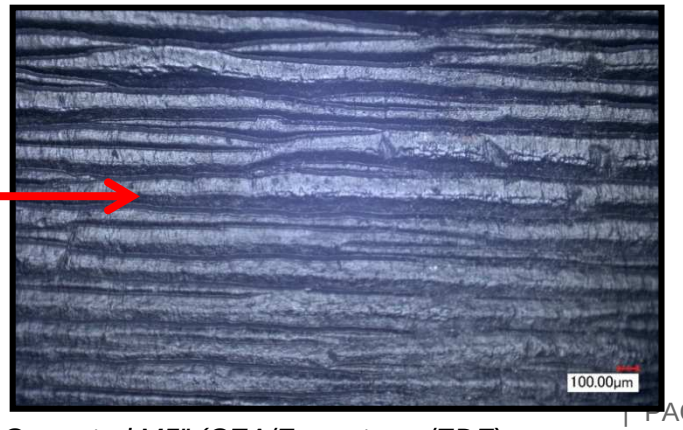
WHY CHOOSING METALLIC (CHROMIUM) COATING?

One fundamental reason for choosing a metallic coating (such as Cr), instead of ceramic ones, is its capacity (ductility) to sustain significant clad deformation without extended damage/cracking **upon LOCA at HT => clad ballooning** (due to internal pressure) **=> $\varepsilon_{\theta\theta}$ up to a few tenths of %**

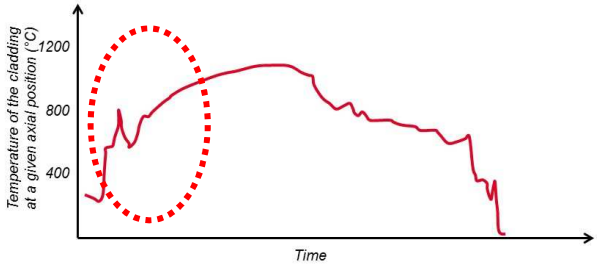


(Brachet, Le Saux, 2017)





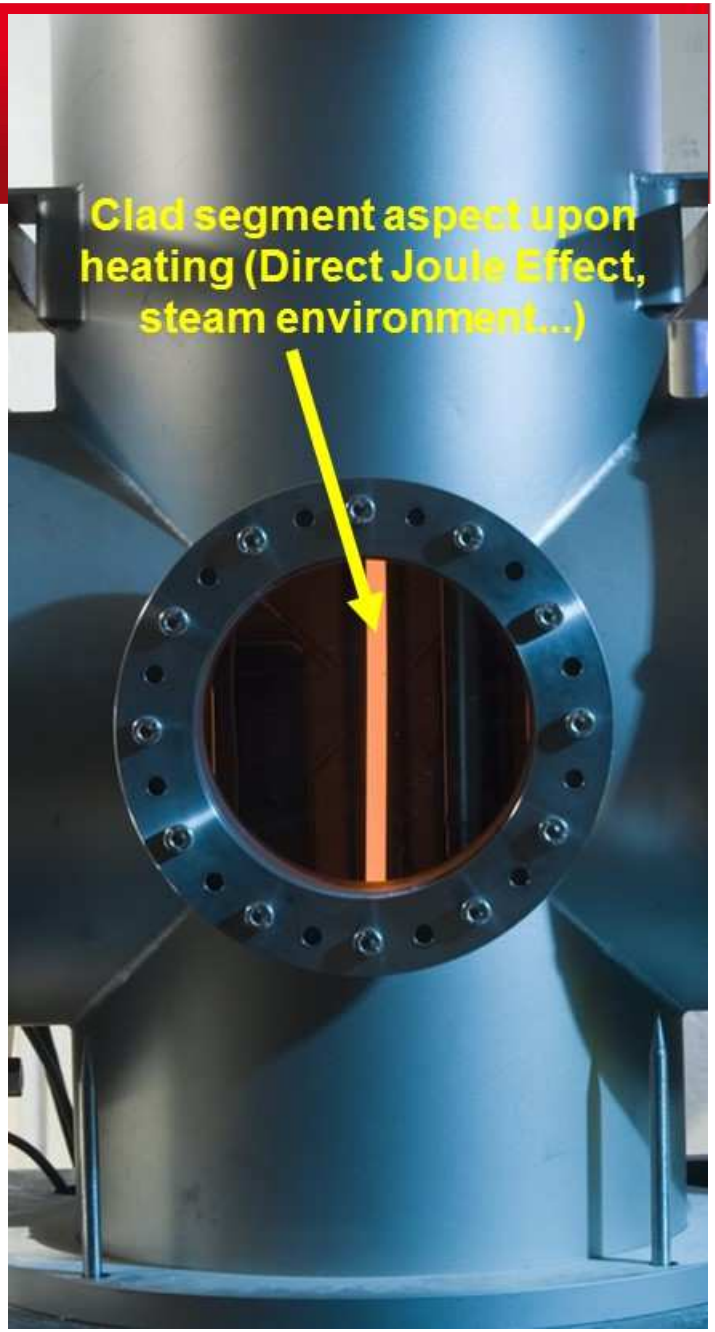
LOCA BEHAVIOR: (1) CREEP-BALLOONING & BURST
"EDGAR" CREEP/RAMP TESTS



"EDGAR facility developed at the end of the eighties at CEA to be able to perform single-rod internal pressure tests upon any kind of LOCA transients
=> More than 2000 tests performed so far

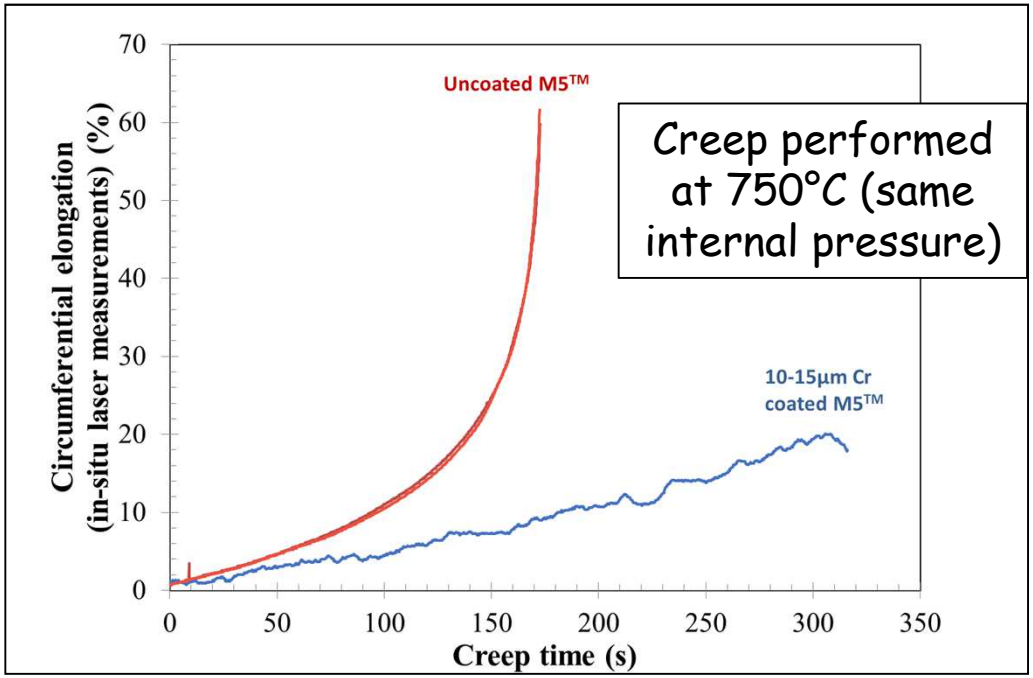
Conditions applied on Cr-coated M5 50 cm long clad segments: - Heating rates = **0.1 to 25°C/s**
- Internal pressure range = **10-100 bars**
- Atmosphere: **steam**

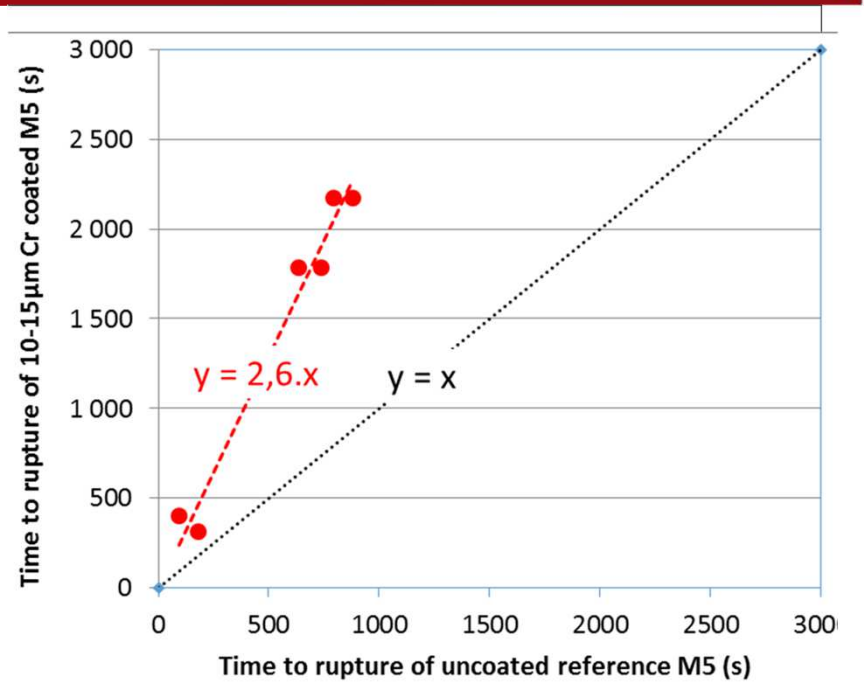
In-situ measurements: **internal pressure**, **clad deformation** (non-contact laser), **clad temperature** (pyrometry).

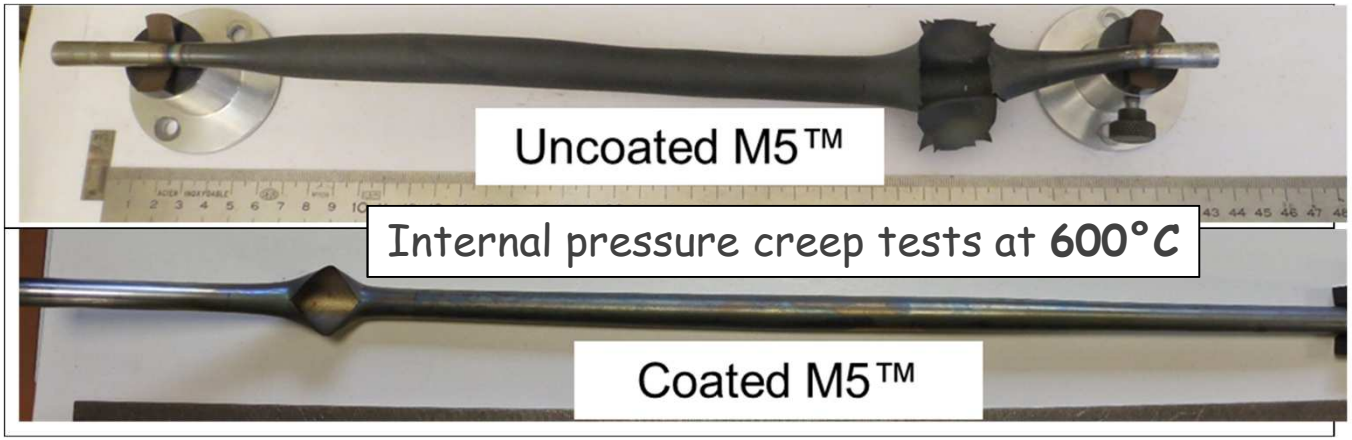


Ref.: T. Forgeron, et al., ASTM STP 1354, (2000), pp. 256-278

ILLUSTRATION OF SOME RESULTS OBTAINED FROM PREVIOUS "EDGAR" ISOTHERMAL CREEP TESTS



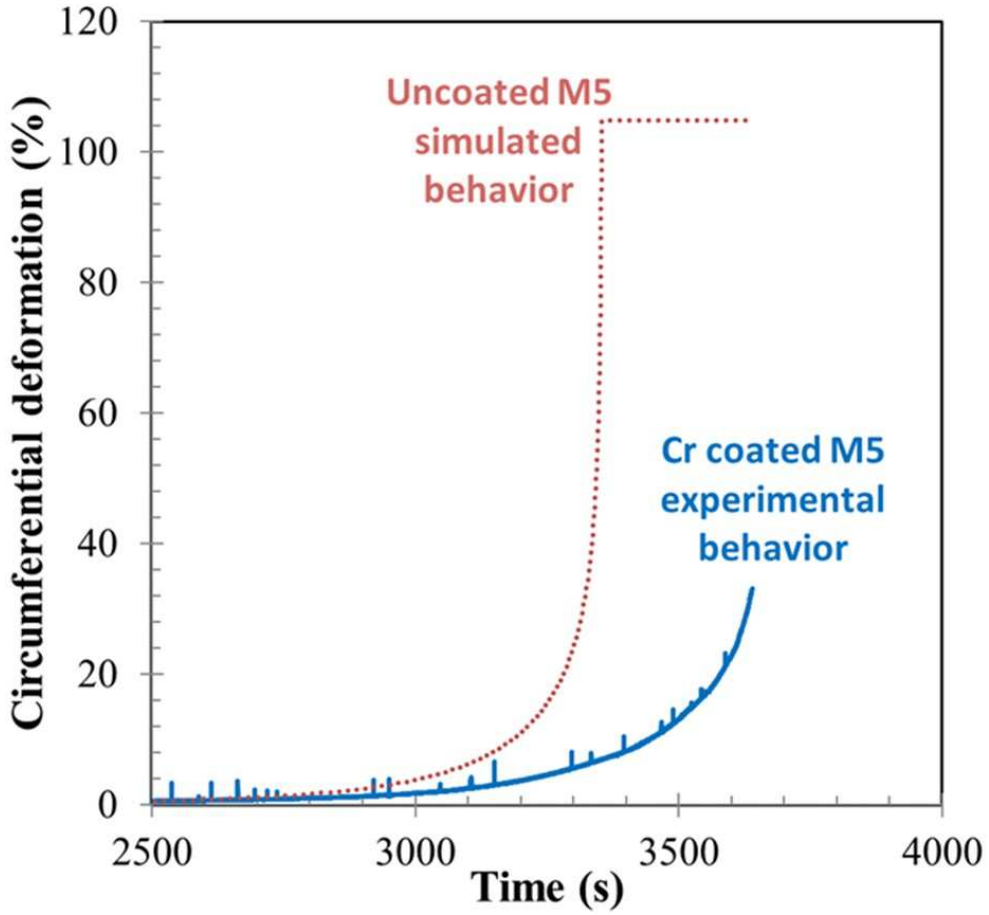




24th. Quench workshop, KIT, Nov. 2018, "Recent results on LOCA behavior of Cr-coated M5" (CEA/Framatome/EDF)

ILLUSTRATION OF SOME OF THE THERMAL RAMP TESTS RESULTS OBTAINED RECENTLY ON 10-15µm THICK Cr-COATED M5 1/3

Experimental times to rupture of the Cr-coated-M5 are generally higher than the experimental or simulated uncoated ones



24th. Quench workshop, KIT, Nov. 2018, "Recent results on LOCA behavior of Cr-coated M5" (CEA/Framatome/EDF)

THERMAL RAMP TEST RESULTS 2/3

Ex.: 2 tests performed upon dynamic conditions:
same heating rate & same low internal pressure applied
=> rupture occurs within the β_{Zr} temperature range (>1000°C)

Uncoated reference M5 - rupture occurs **between 1030°C and 1090°C**:

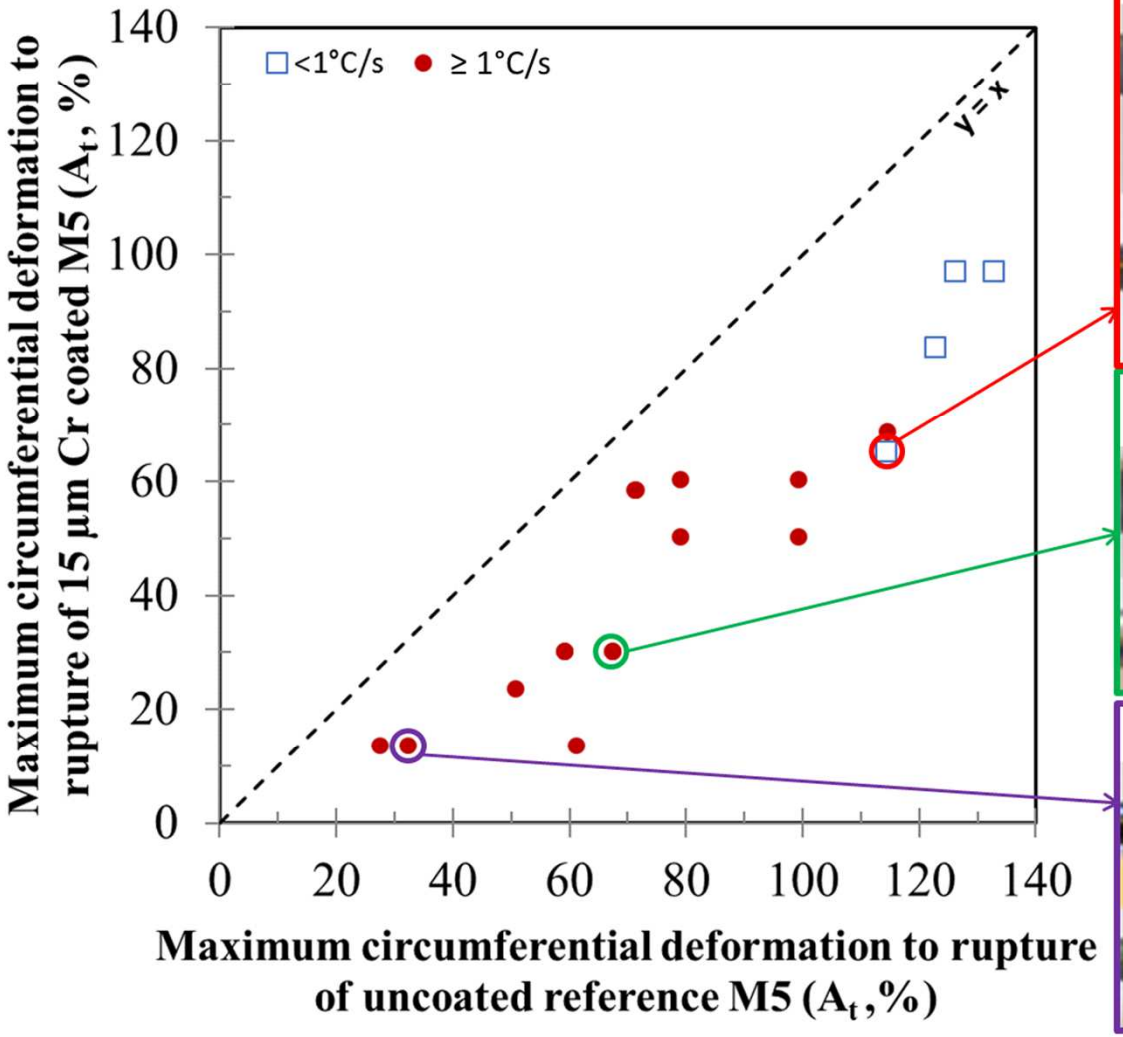


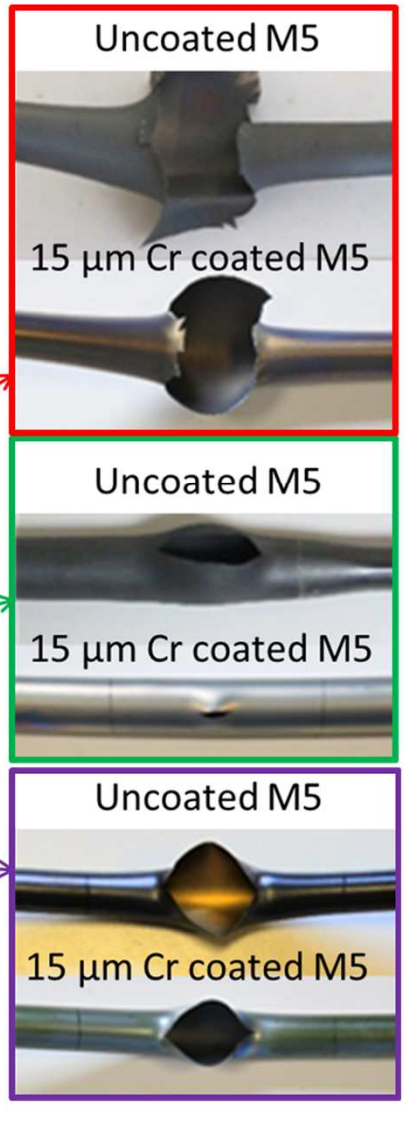
12-15 µm Cr-coated M5 - **no burst occurrence until**, at least, **1130°C (and negligible oxidation)**:

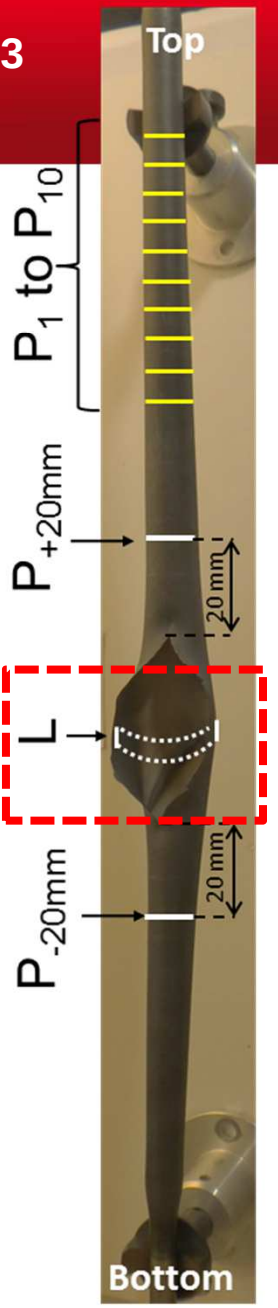


=> Confirm the **HT strengthening effect of the Cr coating** on the actual creep properties of Cr-coated claddings **upon dynamic ramp tests**

THERMAL RAMP TEST RESULTS 3/3



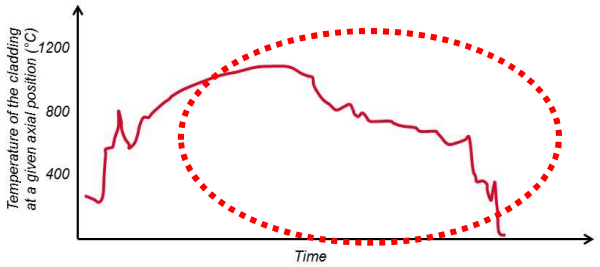




24th. Quench workshop, KIT, Nov. 2018, "Recent results on LOCA behavior of Cr-coated M5" (CEA/Framatome/EDF)

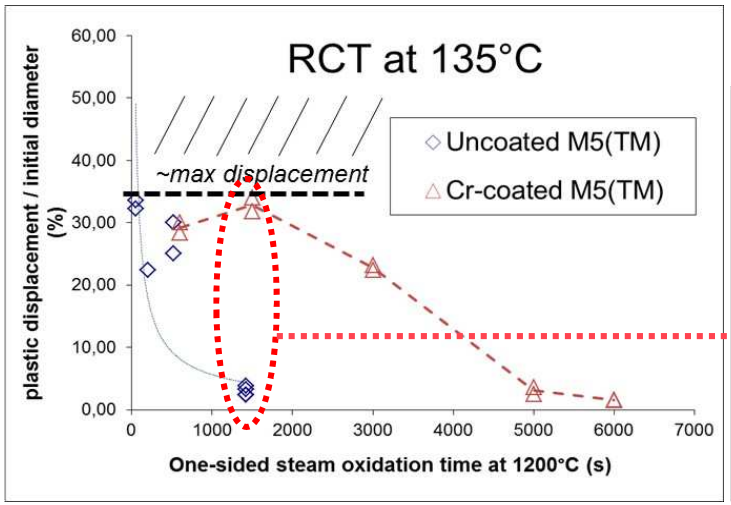
LOCA BEHAVIOR: (2) HT SEAM OXIDATION – PREVIOUS RESULTS

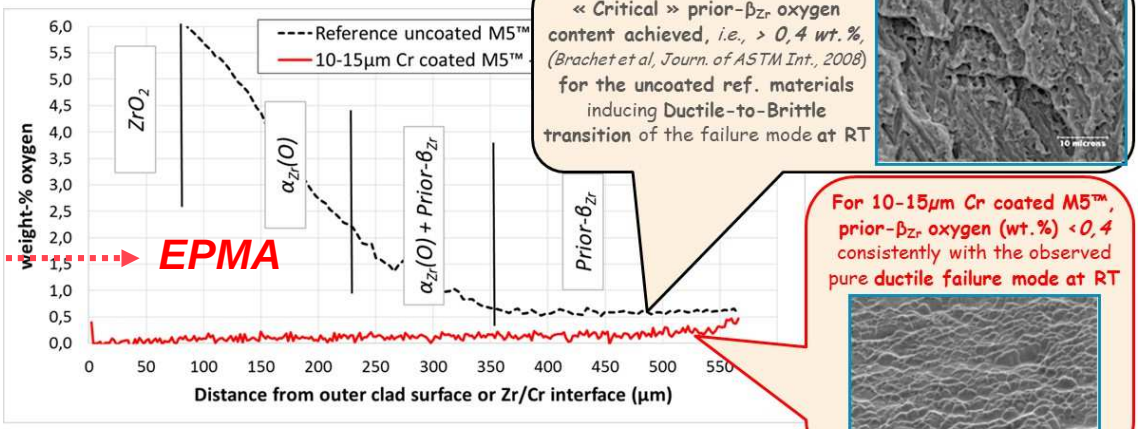
=> RESISTANCE TO QUENCHING & POST-QUENCHING (PQ) MECHANICAL PROPERTIES



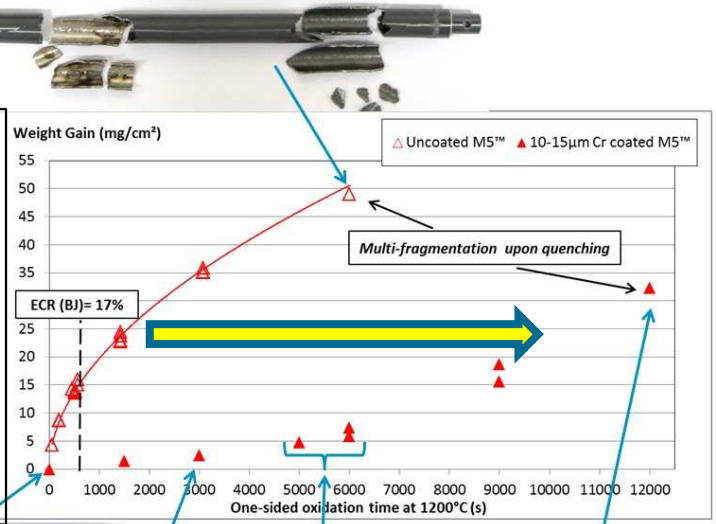
=> For the Cr-coated M5™: significant **increase of critical oxidation time** to achieve **macroscopic PQ brittle behavior** at 135°C

=> For the Cr coated M5™: **significant delay** of the **oxidation time inducing fragmentation** upon final quenching from 1200°C, *due to* ***much slower HT steam oxidation kinetics***

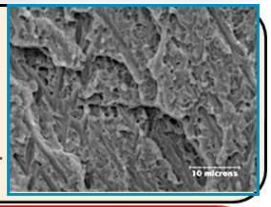




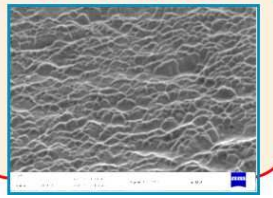
EPMA



« Critical » prior-β_{Zr} oxygen content achieved, *i.e., > 0,4 wt.%*, *(Brachet et al, Journ. of ASTM Int., 2008)* for the uncoated ref. materials inducing Ductile-to-Brittle transition of the failure mode at RT

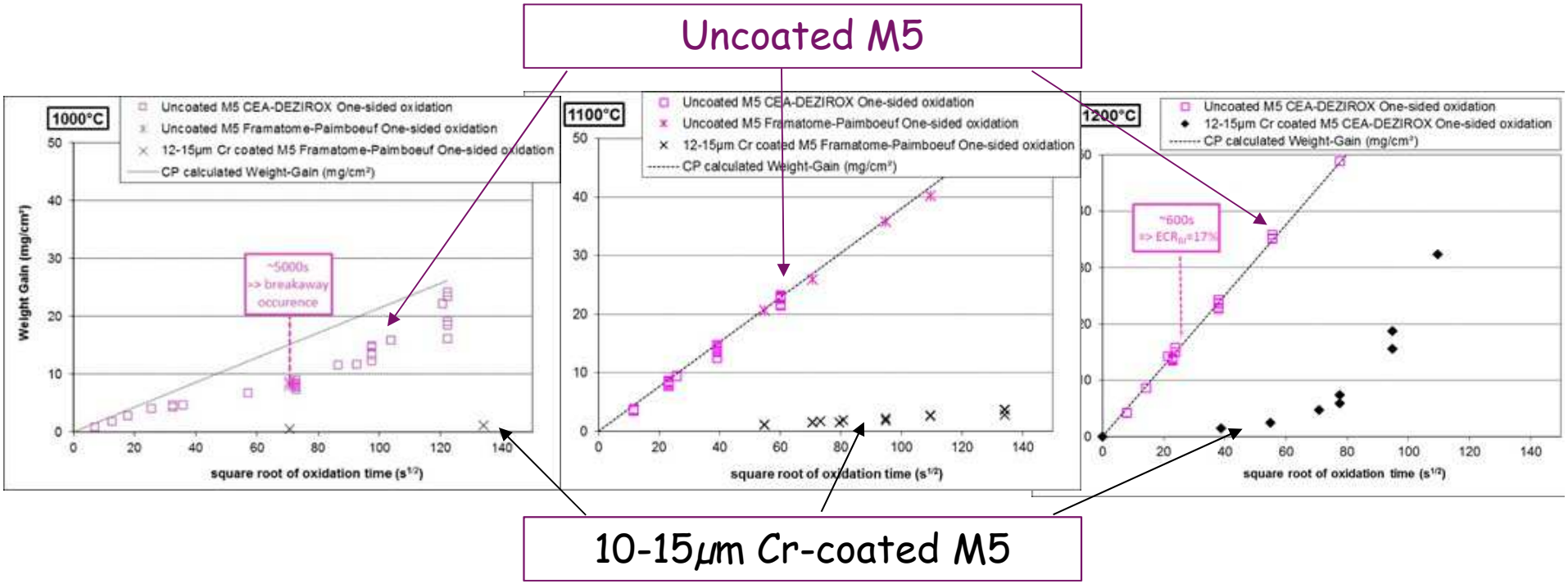


For 10-15µm Cr coated M5™, prior-β_{Zr} oxygen (wt.%) *< 0,4* consistently with the observed pure ductile failure mode at RT



RECENT ONE-SIDED STEAM OXIDATION TESTS UPON LOCA CONDITIONS (1000-1200°C)

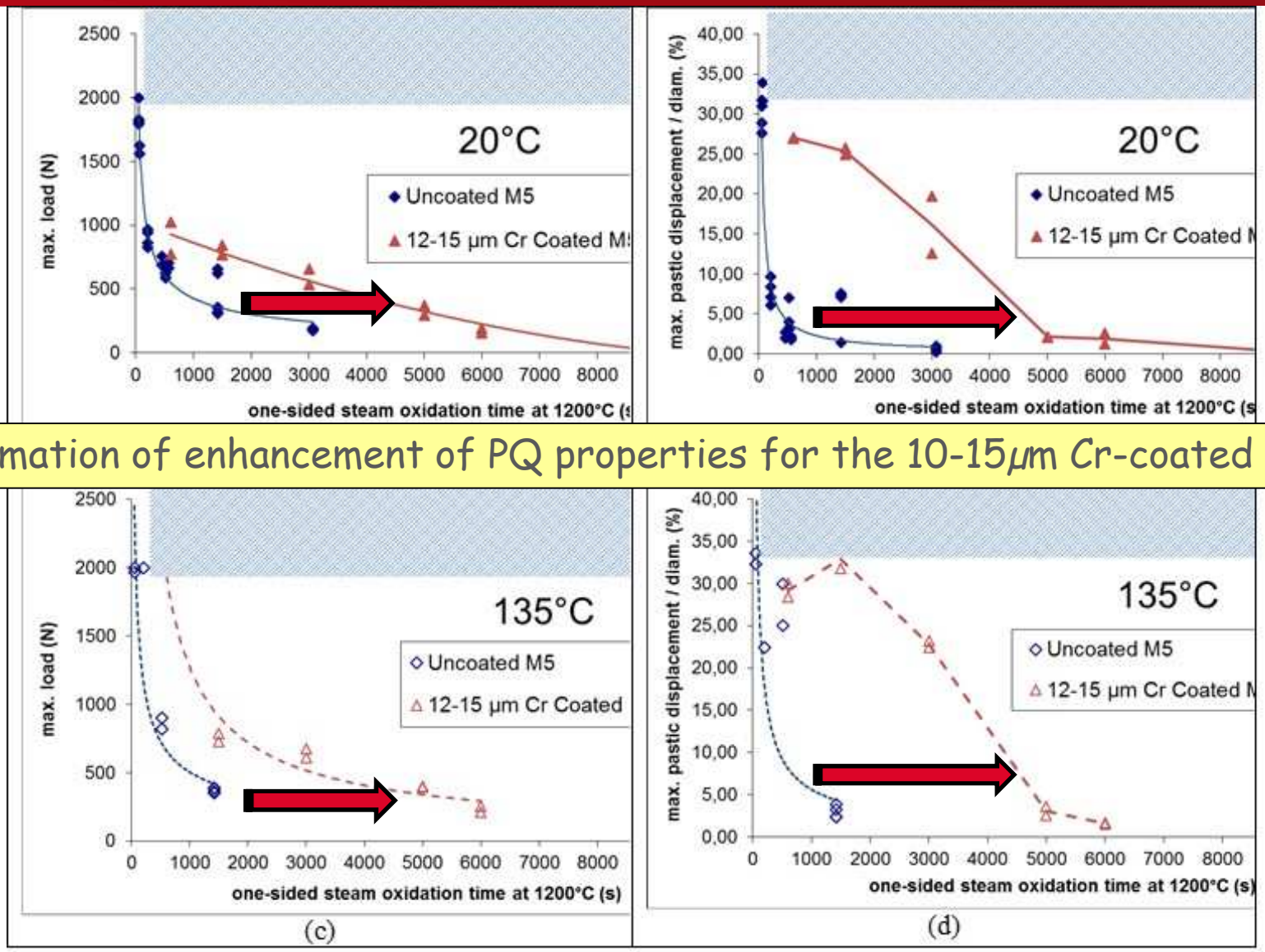
Benchmark tests performed both at CEA and at Framatome-Paimboeuf



(1) Tests performed on two different HT oxidation facilities are consistent;

(2) Very limited oxidation of 10-15µm Cr-coated M5 after several hours (at least up to 5h) after steam oxidation at 1000-1100°C.

ONE-SIDED STEAM OXIDATION UPON LOCA CONDITIONS
PQ RING COMPRESSION TESTS (RCT):

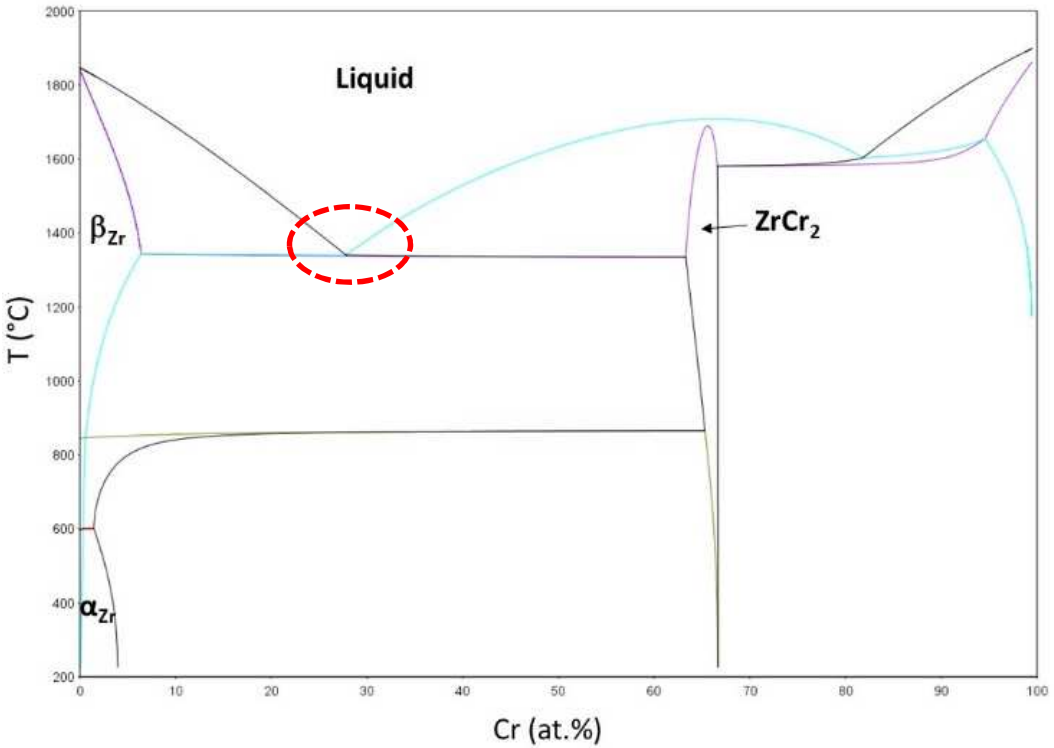


Confirmation of enhancement of PQ properties for the 10-15µm Cr-coated M5

DESIGN EXTENSION CONDITIONS (DEC) HT STEAM OXIDATION BETWEEN 1300°C AND 1500°C => *Zr-Cr EUTECTIC REACTION ISSUE*

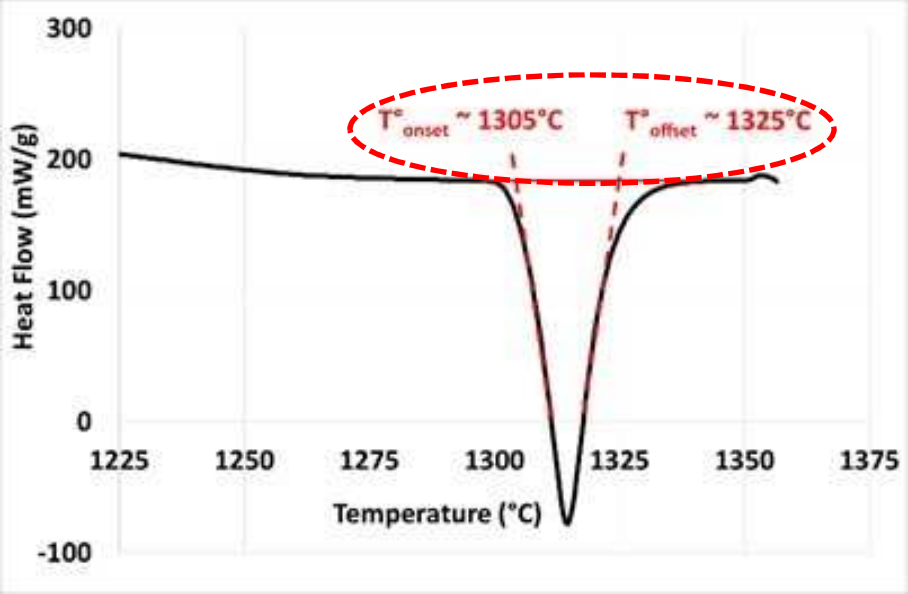
One Cr-coated Zr clad issue:
potential occurrence of Zr-Cr eutectic reaction and its potential (unknown?) effects on the Cr-coated clad behavior at T>1300°C:
i.e., potential oxidation escalation, very rapid loss of integrity / failure, potential (fast) reaction with other structural components of the nuclear fuel sub-assembly… ???

=> To address this issue, HT oxidation tests recently performed ***up to 1500°C***

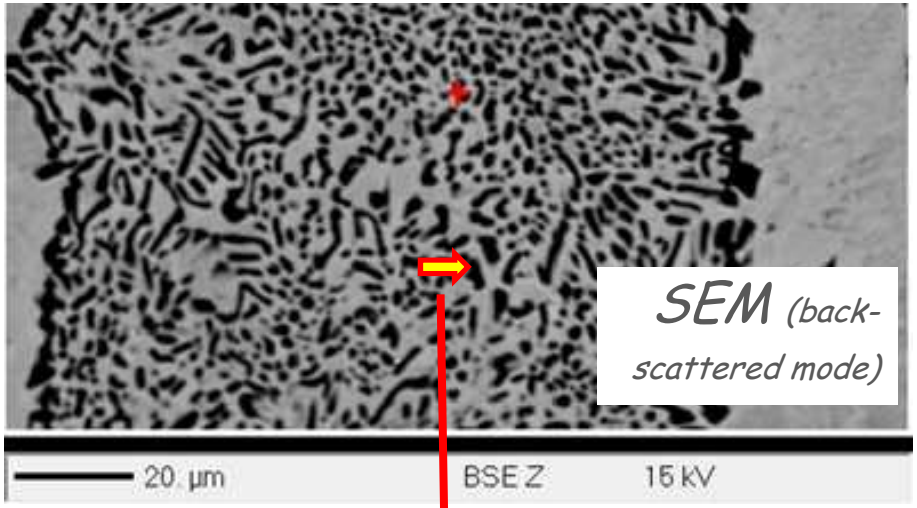


Calculated **pseudo-binary M5-Cr phase diagram** (using Thermocalc® + CEA thermodynamic database for zirconium alloys called « Zircobase », *(Dupin et al. – JNM, 1999; P. Lafaye, PhD, 2017)*

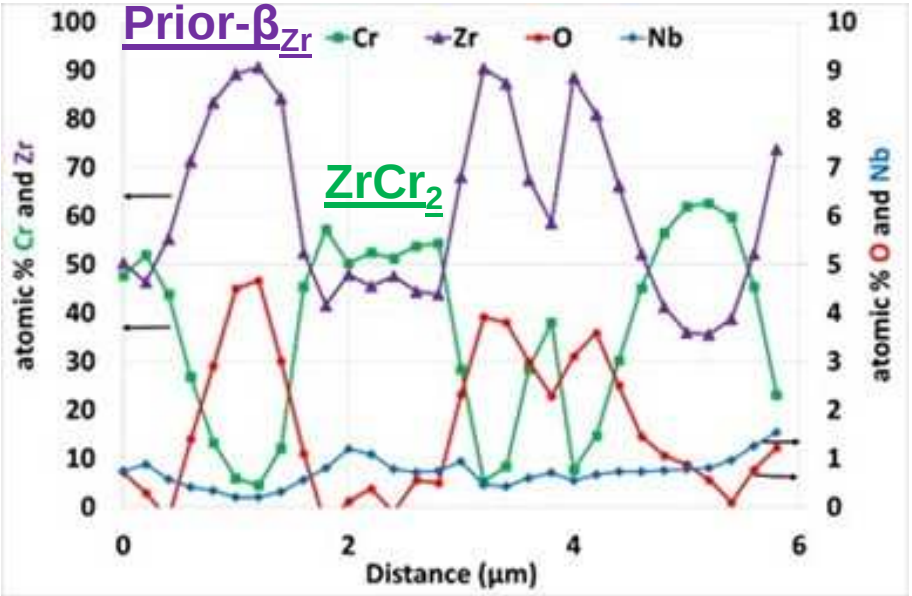
CALORIMETRIC TESTS UP TO 1400°C (~EQUILIBRIUM CONDITIONS, NEUTRAL ENVIRONMENT)



Calorimetric (DSC) experiments
(quasi-equilibrium conditions, heating/cooling at 10°C/min)

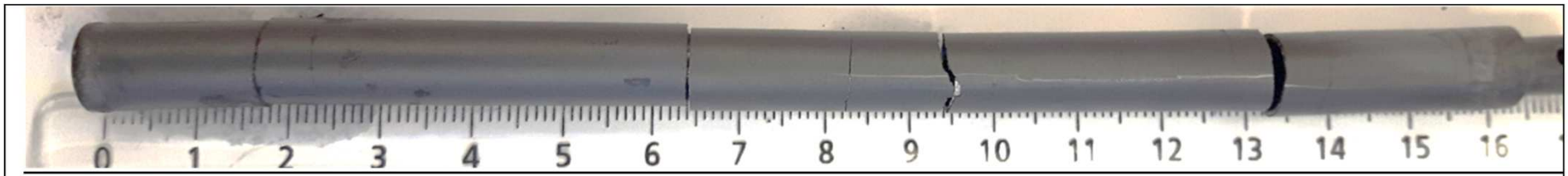


EPMA:

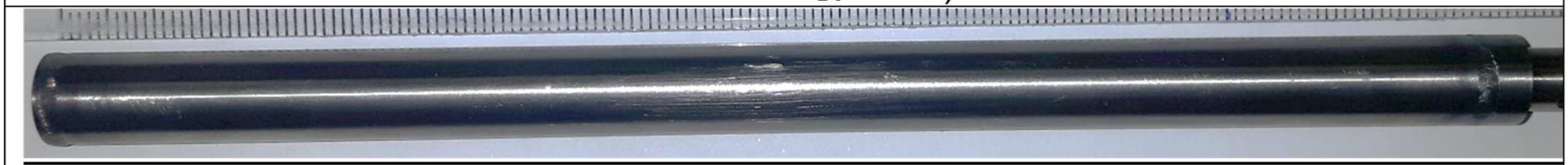


OXIDATION AT 1300°C

Steam oxidation **at 1300°C - 600s - just below the eutectic point**:



(a) Uncoated M5 (overshoot ~50°C, measured weight gain = 31.1 mg/cm², ECR_{BJ}=29%)



(b) 12-15µm Cr coated M5 (no temperature overshoot, weight gain = 2.4 mg/cm²)

24th. Quench workshop, KIT, Nov. 2018, "Recent results on LOCA behavior of Cr-coated M5" (CEA/Framatome/EDF)

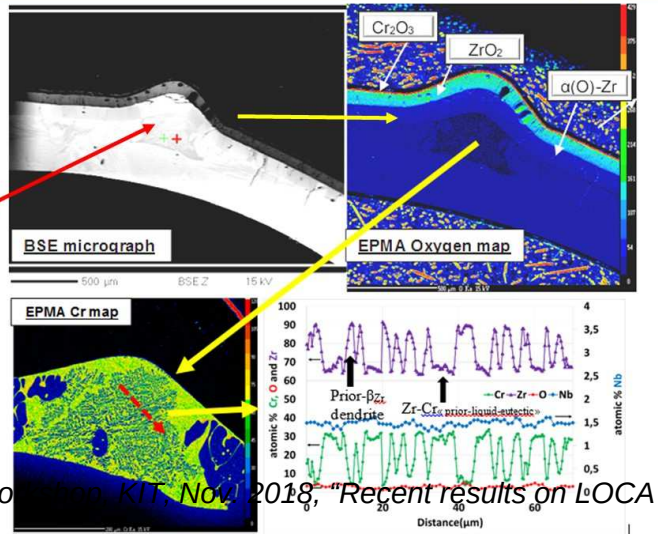
T > 1300°C, *Zr-Cr EUTECTIC ISSUE*
=> TESTS PERFORMED UP TO 1500°C

Cr-coated or not?	T(°C) of steam introduction upon heating at 1°C/s	Temperature range achieved (°C)	Oxidation time (s)	Measured Weight Gain (mg/cm²)	Baker-Just-ECR (%)	Failed or not upon quenching?
No	600°C	1300-1320	600	24.8	29.0	No
Yes		1300-1320	600	2.8-2.9 (**)	-	No
No		1400-1420	100	20	23.4	No
Yes		1400-1450	100	19.0	-	No
No		1500-1530	50	28.7	31.7	Yes or No
Yes		1500-1550	50	Not measured	-	No
No	1300°C	1300-1350	600	31.1	29.0	Yes
Yes		1300-1310	600	2.4	-	No
No		1400-1450	100	25.8	24.8	Yes
Yes		1400-1450	100	19.6	-	No

One-sided steam oxidation **at T> 1300°C, above the eutectic point:**

Cr-coated M5 : "crocodile skin" morphology with continuous blisters forming an external protruding pattern





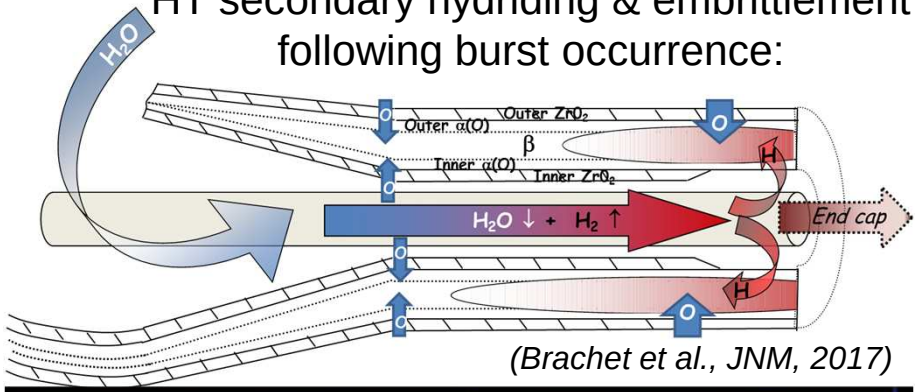
Reassuring results: **no temperature escalation / limited temperature overshoot** & **Cr-coated M5** clad segments tested **kept their integrity upon the final water quenching** (even if eutectic reaction has occurred), **while some uncoated reference claddings did not**

24th. Quench workshop, KIT, Nov. 2018, "Recent results on LOCA behavior of Cr-coated M5" (CEA/Framatome/EDF)

PROSPECTIVE CEA STUDIES FOR INNER SIDE COATING (INTERNAL) PROTECTION

Inner coating should be a **potential mitigation solution vs. inner oxidation and associated massive secondary hydriding** (*both for nominal / leaking fuel rod and accidental / LOCA situations)*

HT secondary hydriding & embrittlement following burst occurrence:

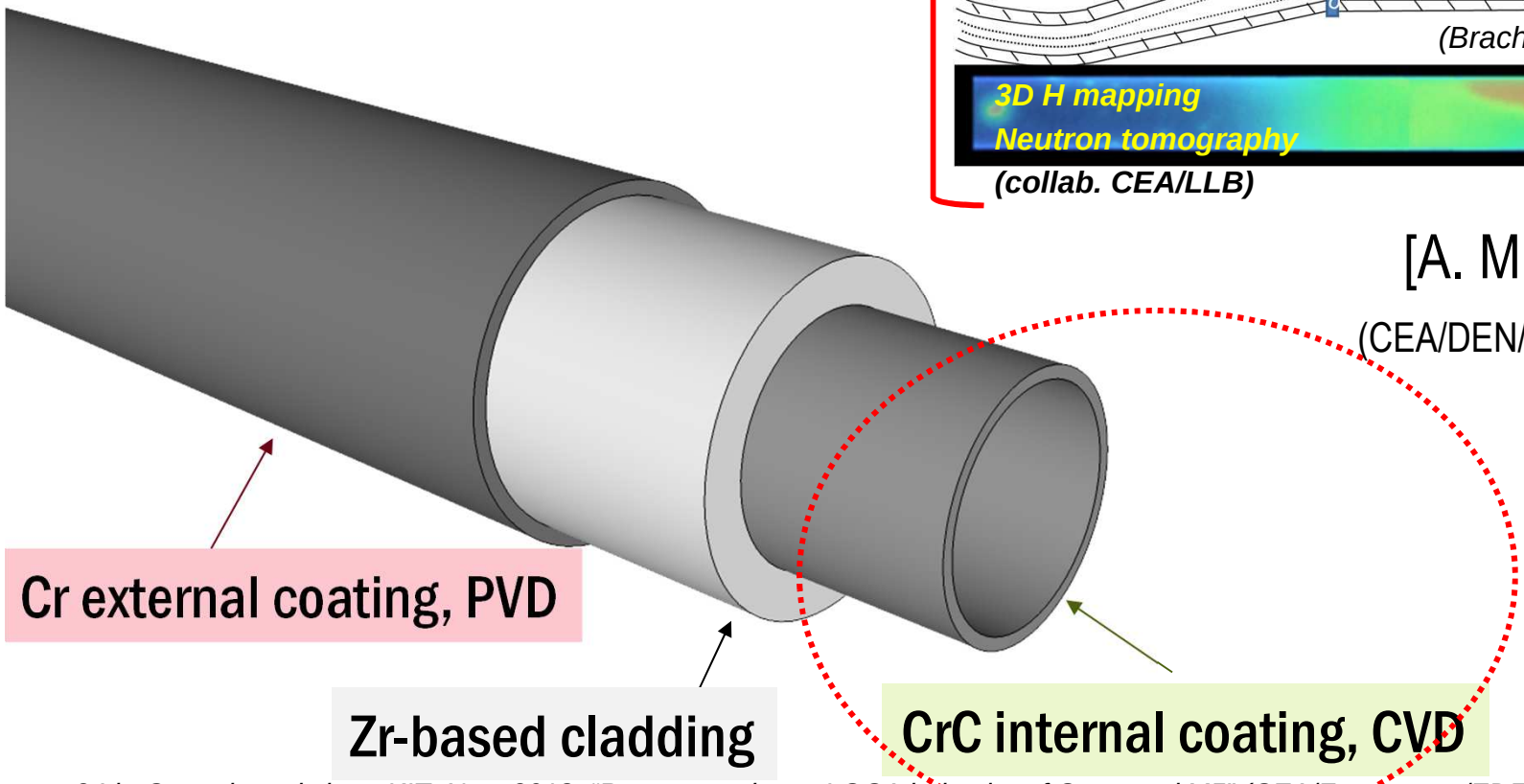


(Brachet et al., JNM, 2017)



(collab. CEA/LLB)

[A. Michau et al., (CEA/DEN/DPC/SEARS/LISL)]



24th. Quench workshop, KIT, Nov. 2018, "Recent results on LOCA behavior of Cr-coated M5" (CEA/Framatome/EDF)

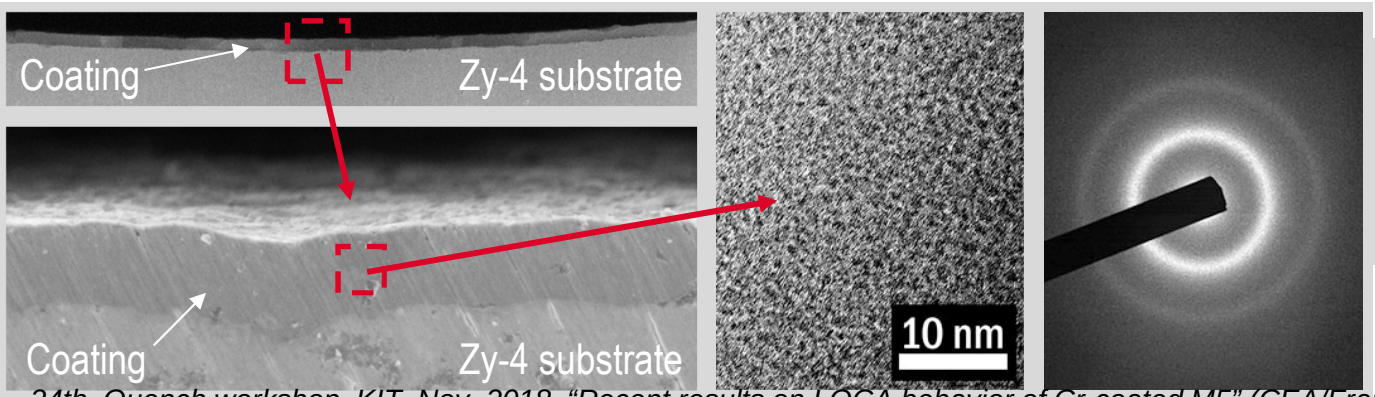
INTERNAL COATING
Selection of the deposition process

Requirements

Homogeneous, dense and adherent coating	Preservation of Zr metallurgical state	Complex geometry (Ø, L)
Direct Liquid Injection Tailored generation of concentrated reactive vapor (Q_i, C_i)	**MetalOrganic** Low temperature deposition (T) with careful choice of chemical system	**Chemical Vapor Deposition** Low pressure process (P, t_i, v_i)

DLI-MOCVD

(CEA et al. Patents, 2017)



Amorphous/Nanocrystalline CrC coating deposited by DLI-MOCVD inside fuel cladding

[A. Michau et al., SCT 332 (2017) 96]

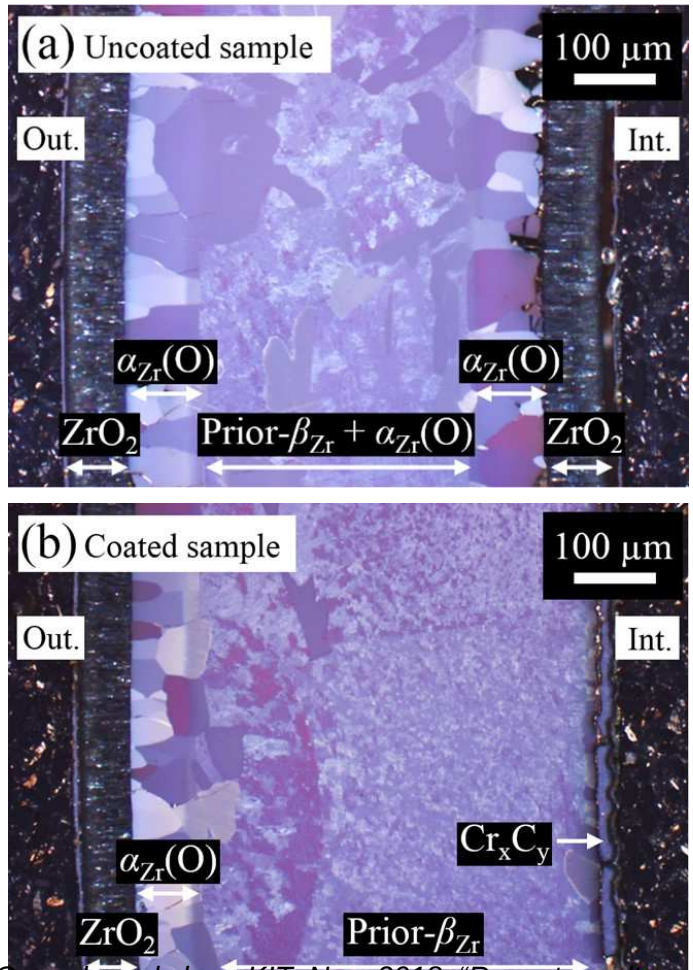
INTERNAL COATING - HT STEAM OXIDATION (LOCA)

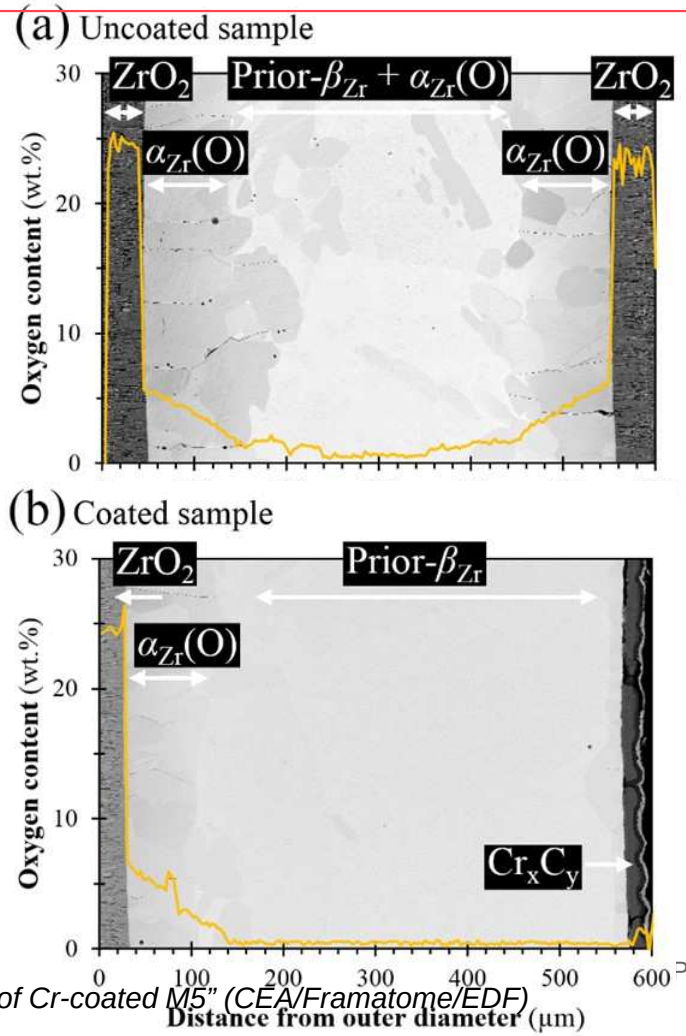
PRELIMINARY RESULTS OBTAINED ON INNER CrC COATED ZIRCALOY-4 CLAD SEGMENT

Encouraging results obtained after one-sided steam oxidation for **600s at 1200°C**

(*corresponding to ECR_{BJ}~17%, i.e., historical LOCA regulatory limit*)

=> **full protection of the inner surface from oxygen ingress** into the Zirc-4 substrate



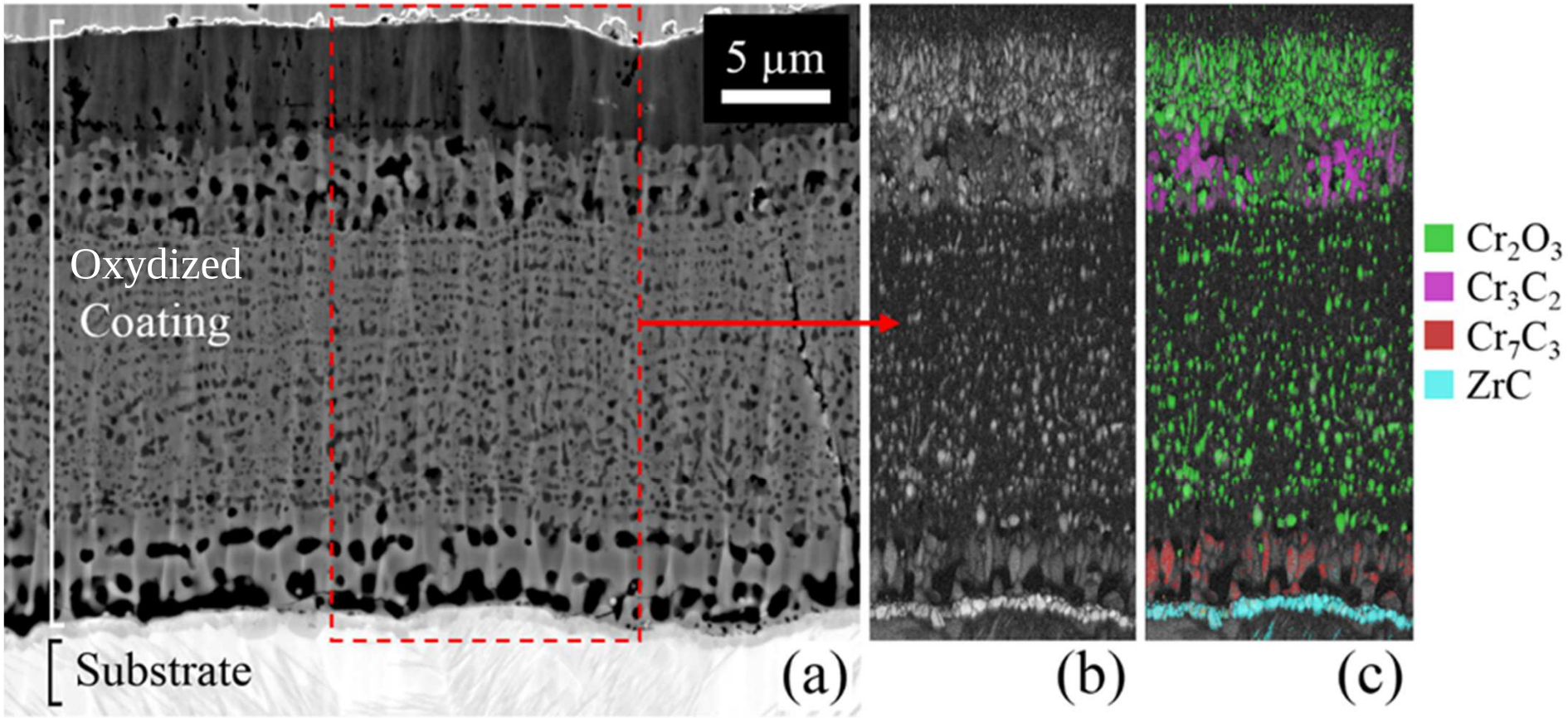


INTERNAL COATING - HT STEAM OXIDATION (LOCA)

PRELIMINARY RESULTS OBTAINED ON INNER CrC COATED ZIRCALOY-4 CLAD SEGMENT

FEG-SEM examination & EBSD analysis – CrC inner coated Zircaloy-4

after one-sided steam oxidation for 600s at 1200°C and direct water quenching



24th. Quench workshop, KIT, Nov. 2018, "Recent results on LOCA behavior of Cr-coated M5" (CEA/Framatome/EDF)

SUMMARY AND CONCLUSIONS (1/3) - BEHAVIOR OF Cr-COATED M5 UPON INTERNAL PRESSURE THERMAL RAMP (EDGAR) TESTS -

New "EDGAR" thermal ramp tests (0,1 – 25°C/s) under internal pressure (**10-100 bars**) carried out on **10-15µm thick Cr-coated M5**:

- **Higher rupture temperatures** (HT Cr-coating strengthening effect);
- **Significantly lower balloon and burst opening sizes** *=> lower nuclear fuel subassembly flow blockage, lower probability of fuel relocation/dispersal;*
- **Very good Cr-coating adherence and no/limited Cr-coating cracking**, even at the vicinity of the burst where high circumferential clad deformation is achieved *=> Cr-coating should keep most of its HT resistance efficiency after ballooning & burst (likely not the case for ceramic coatings)*

SUMMARY AND CONCLUSIONS (2/3)

BEHAVIOR OF Cr-COATED M5 UPON 1000-1200°C STEAM OXIDATION

For DBA-LOCA oxidation temperatures (1000-1200°C):

- HT oxidation tests Performed both at CEA and Framatome on two different HT oxidation facilities are **consistent**;
- At 1000-1100°C, **very limited oxidation** up to several hours (at least 5 h);
- **Significant enhancement** of the quenching resistance and **PQ mechanical properties** (residual strength & ductility)

HT steam oxidation results (1200°C, 600s) obtained on **inner** amorphous-nanocrystallized **CrC-coated Zircaloy-4** claddings, deposited by a new ("DLI-MOCVD") process, are **encouraging**

FROM RESEARCH TO INDUSTRY cea den

SUMMARY AND CONCLUSIONS (3/3) - BEHAVIOR OF Cr-COATED M5 UPON 1300-1500°C STEAM OXIDATION - DEC

- Consistently with thermodynamic predictions, DSC experiments have confirmed the **Zr-Cr eutectic reaction occurrence between 1305 & 1325°C;**
- **Reassuring results** showing **no temperature escalation / limited temperature overshoot** when compared to the overshoot associated with the exothermic HT oxidation taking place on uncoated reference M5 tested in the same conditions;
- For the conditions tested, the **Cr-coated M5 clad segments tested kept their integrity upon the final water quenching** (even if eutectic reaction has occurred), **while some uncoated reference claddings tested in the same conditions did not**;
- From metallurgical examinations performed and thermodynamic considerations, it was possible to derive a **phenomenological (metallurgical) mechanism for describing the eutectic formation and re-solidification sequences**;
- One important observation was that the local **oxidation kinetics was outstandingly the same at the liquid eutectic protruding blisters and at the neighboring Cr-depleted clad surface zones**
- Additionally, the outer ZrO_2 scale that rapidly grows may have also some beneficial effects, by acting as a **confinement barrier** and **avoiding (likely) potential chemical interactions with some other components of the nuclear fuel sub-assembly**

FROM RESEARCH TO INDUSTRY

cea den

THANK YOU FOR YOUR ATTENTION

Some CEA references on Cr-coated Zr based nuclear fuel claddings:

[1] I. Idarraga et al., "Assessment at CEA of coated nuclear fuel cladding for LWRs with increased margins in LOCA and beyond conditions", in proceedings of TopFuel 2013, Charlotte, USA, (Sept. 15-19, 2013)

[2] J.C. Brachet et al., "On-going studies at CEA on Cr-coated zirconium based nuclear fuel claddings for enhanced tolerant LWRs fuel", proceedings of TopFuel 2015, Zurich, Switzerland (Sept. 13-19, 2015)

[3] J.C. Brachet et al., "Behavior under LOCA conditions of Enhanced Accident Tolerant Chromium Coated Zircaloy-4 Cladding", proceedings of TopFuel 2016, Boise, IDAHO, USA, (Sept. 11-16, 2016)

[4] J.C. Brachet et al., "Behavior of Cr-coated M5™ claddings under LOCA conditions", Proceedings of 2017 Water Reactor Fuel Performance Meeting, (Sept. 10-14, 2017), Jeju Island, Korea

[5] A. Michau, et al., "High-temperature oxidation resistance of chromium-based coatings deposited by DLI-MOCVD process for enhanced protection of the inner surface of long tubes", Surf. & Coat. Tech. (2018)

[6] J.C. Brachet, et al., « Behavior of Cr-coated M5 claddings during and after high temperature steam oxidation from 800°C up to 1500°C (LOss-of-Coolant Accident & Design Extension Conditions)", Proceedings of WRFPM/TOPFUEL 2018, (30 Sept. – 04 Oct. 2018), Prague, Czech Republic

[7] M. Dumerval, et al., « Behavior of Chromium Coated M5 Claddings upon thermal ramp tests under internal pressure (LOss-of-Coolant Accident Conditions)", Proceedings of WRFPM/TOPFUEL 2018, (30 Sept. – 04 Oct. 2018), Prague, Czech Republic

[8] J. Ribis, et al., "Atomic-scale interface structure of a Cr-coated Zirc-4 », Journ. of Mat. Sci., (2018)

[9] A. Wu, et al., "HRTEM and chemical study of an ion-irradiated chromium/zircaloy-4 Interface", Journal of Nuclear Materials 504 (2018) 289-299

FROM RESEARCH TO INDUSTRY

cea den

BACK SLIDES…

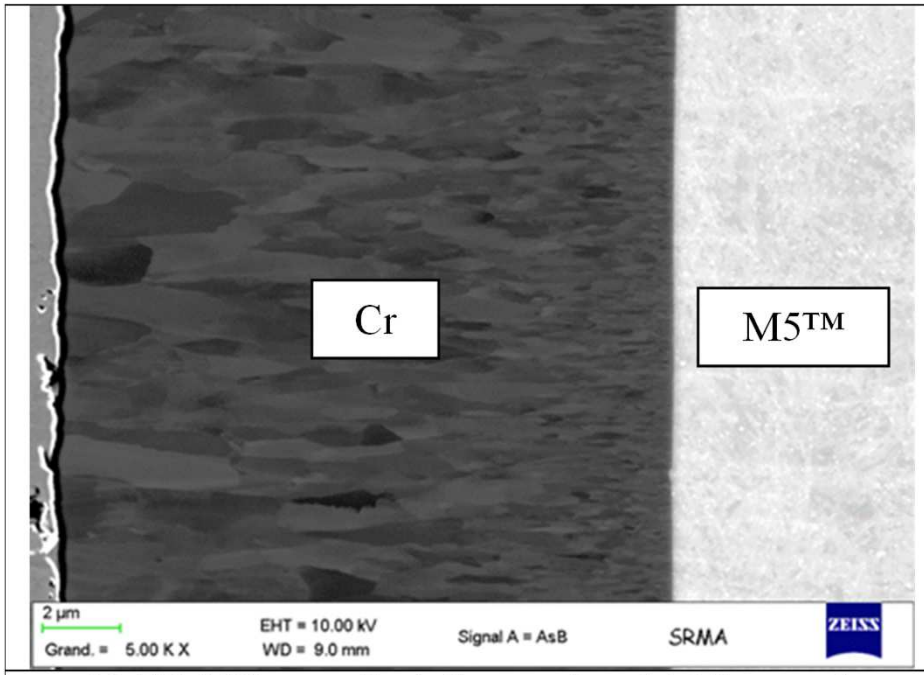
AS-RECEIVED 10-15µm Cr COATED M5™

Special PVD deposition process (*CEA patent*) on **50cm long M5™ clad segments**

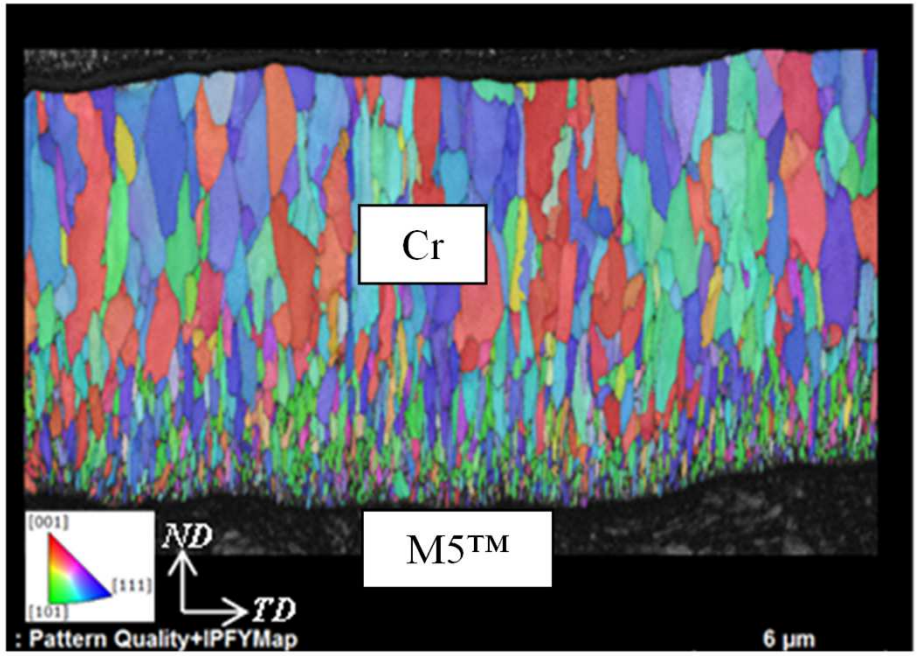
=> **Dense and very homogenous coating** obtained

⇒ **Very good bonding** on the M5™ substrate

⇒ **No modification of the as-received metallurgical conditions/properties** of the M5™

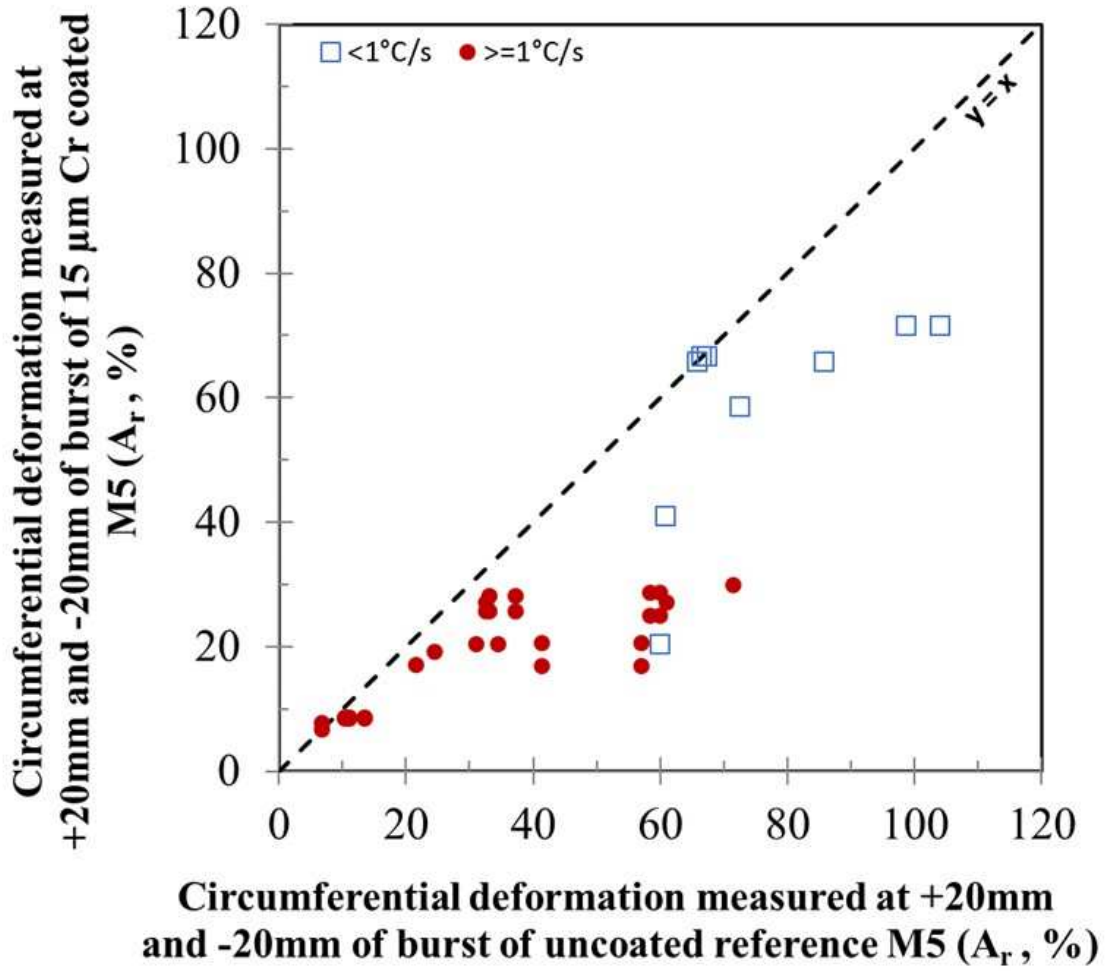


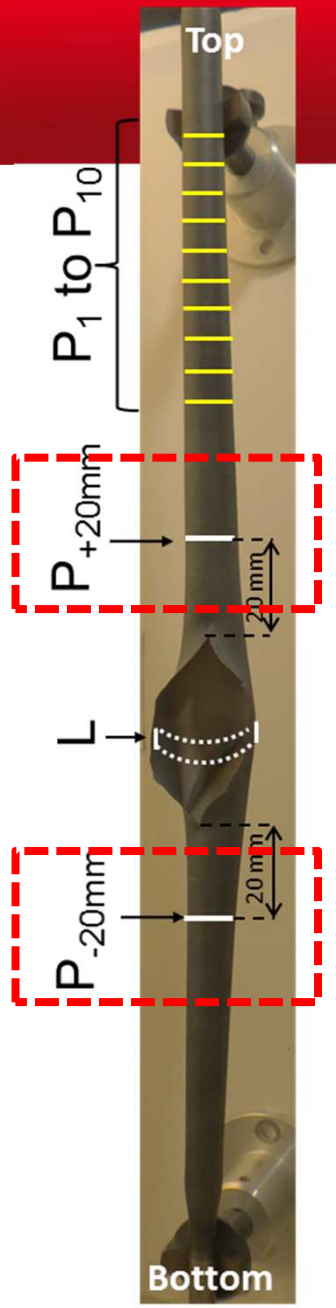
(a) SEM (Electron Back-Scattered mode) Micrograph



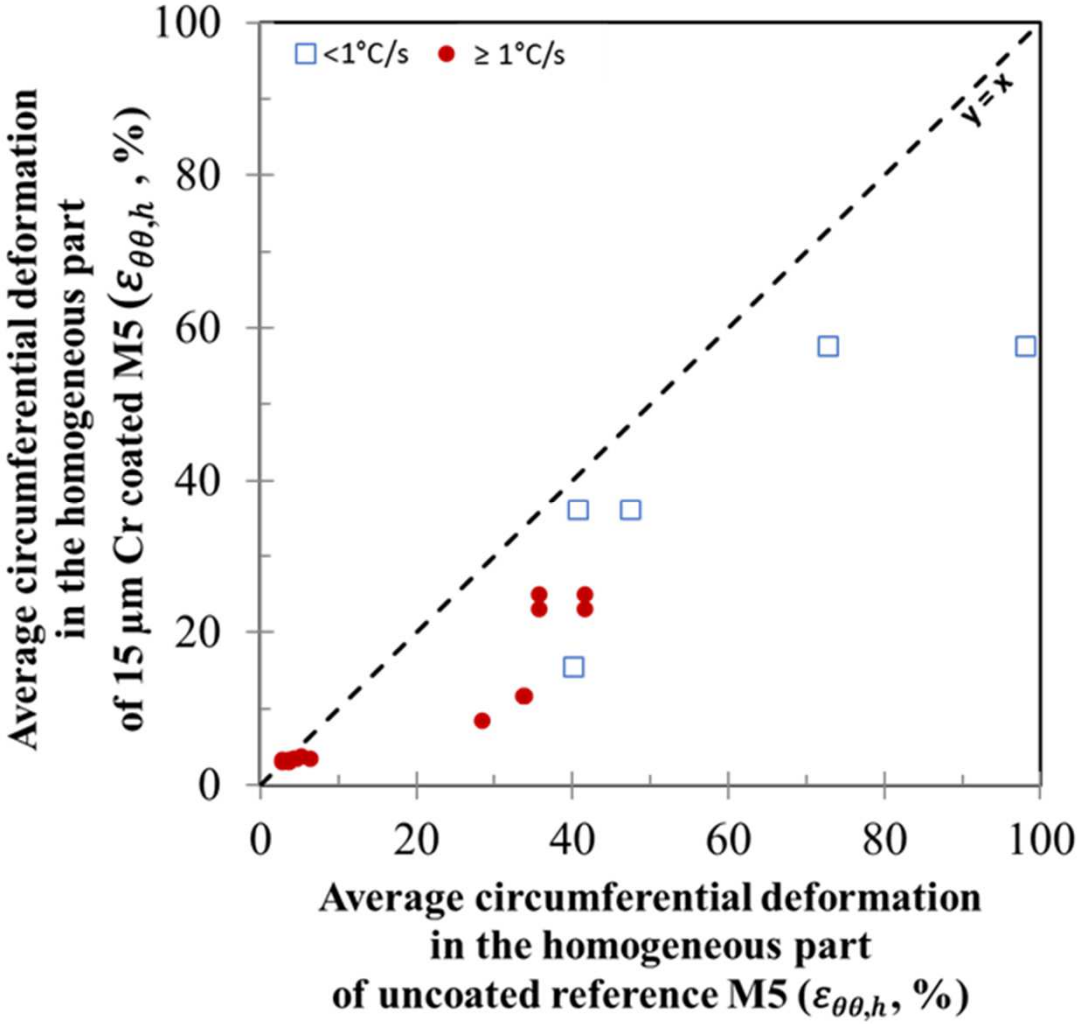
(b) SEM-EBSD orientation map

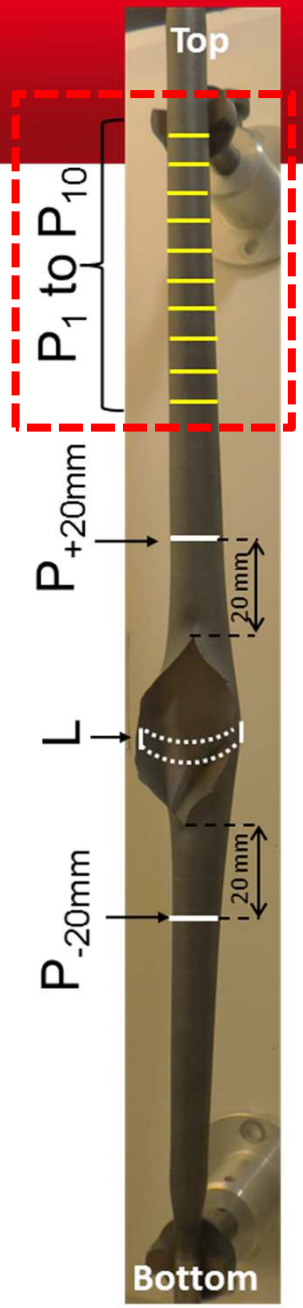
Typical microstructure of a 10-15µm Cr thick chromium coating on a M5™ clad substrate





24th. Quench workshop, KIT, Nov. 2018, "Recent results on LOCA behavior of Cr-coated M5" (CEA/Framatome/EDF)





24th. Quench workshop, KIT, Nov. 2018, "Recent results on LOCA behavior of Cr-coated M5" (CEA/Framatome/EDF)

Jakub Krejci, UJP

Experimental Behavior of Cr-coated Cladding Materials

ABSTRACT: Development of nuclear fuels with enhanced accident tolerance is one of the main current objectives of researchers around the world. The contribution focuses on Cr-coated cladding concept developed in cooperation of UJP Praha a.s. and CTU in Prague. Presented results show highly protective behavior of thin Cr-layers against high temperature steam oxidation and improved mechanical ductility of samples after transients. A more complex approach to simulate LOCA transient is applied in presented study. A set of experiments was performed to understand with the behavior of Cr-coated claddings during the whole phenomena. The presented results show the influence of coatings on high-temperature creep, ballooning size, time to burst, cracking of coating, high temperature oxidation through cracked and intact coating. Secondary oxidation and hydriding from inner uncoated surface after cladding failure is discussed as well. Microhardness and microstructure analysis of the material after testing revealed local cladding damage. The mechanical properties of cladding after LOCA can locally deteriorate due to cracks in coating, but the influence on the bulk mechanical behavior of the whole fuel cladding needs to be further investigated.


TOSHIBA

UJP PRAHA

Czech Technical University in Prague

Experimental Behaviour of Cr-coated claddings

J. Krejčí[1,2], J. Kabátová[1], F. Manoch[1], V. Rozkošný[1], J. Kočí[1], A. Chalupová[1,2], M.Ševeček[2], L. Cvrček[2]

[1] UJP, [2] CTU



24rd International QUENCH Workshop

Karlsruhe Institute of Technology, Germany

November 13-15, 2018

Presentation outlines

UJP PRAHA

- UJP activities in ATF area
- Material and deposition
- LOCA accident
- Experimental methodology
- Ballooning + burst
- Oxidation after cladding failure
- Conclusions/Discussion

UJP activities in ATF area

UJP PRAHA

- Experimental research of fuel cladding tubes has been carried in UJP PRAHA since 1971
- UJP role is to provide independent research for our customers (e.g. Czech NPPs operator ČEZ,…)
- Cr-based coatings research
  - Started in the end of 2016 - cooperation with CTU in Prague
  - Current cooperation: CTU (coating deposition, EDS, WDS, EBSD), NTC UWB (XRD), Research Centre Řež (EDS, WDS, neutron irradiation), UCT (EIS), Czech Academy of Sciences (proton irradiation, AFM),…
  - Experiments in UJP:
  - long term corrosion autoclave experiments (Cr-coating in 360°C WWER chemistry: 320 days +)
  - high temperature steam oxidation (Cr, CrN, Cr+CrN coatings 1000-1450°C)
  - high temperature air oxidation (Cr-coating)
  - **burst-tests** (**Cr**, CrN, Cr+CrN coatings)
- Projects connected with ATF
  - Cr-based coatings (ČEZ a.s.)
  - Cr-coating, max-phase coating, ZrSi-coating, AISI 348 (round robin test: IAEA CRP T12030)

Material and deposition

- Material:
  - E110 cladding tubes: ∅ 9.1 × 7.9 mm
  - Specimen length 10 cm
- PVD deposition (CTU):
  - Magnetron sputtering
  - Hauzer Flexicoat 850
  - Coating from outer side of speciemens only
  - Cr-coating (30mic)



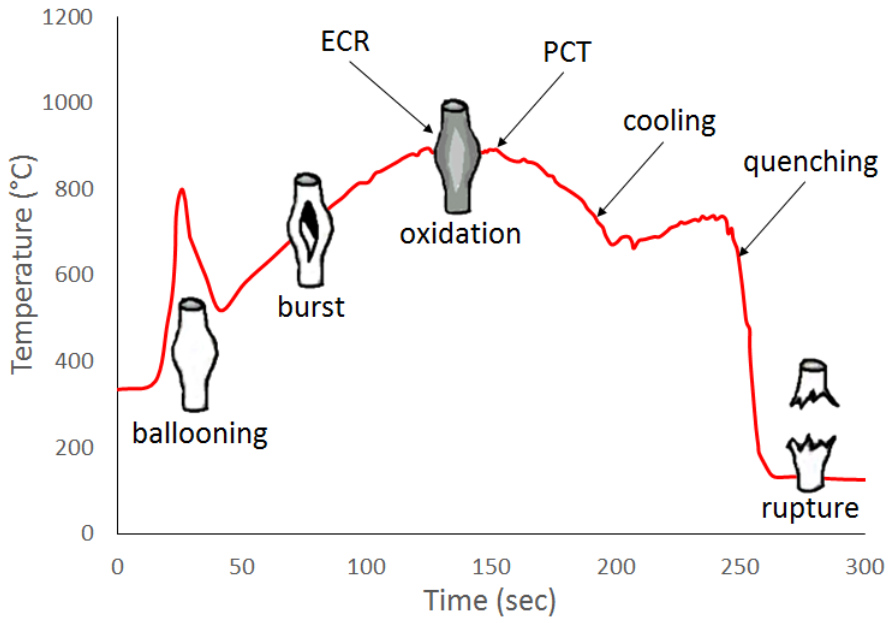
LOCA accident

- <u>Phenomena during LOCA:</u>

- ballooning, burst
- high temperature oxidation + secondary hydridation
- cooling, quenching
- mechanical properties after transient

- <u>QUESTIONS - Influence of Cr-coating on:</u>

- Ballooning (size/cross-section blockage)?
- Coating failure/cracking during ballooning?
- Time to burst?
- High temperature oxidation through cracks?
- High temperature oxidation from inner side?
- Hydrogen absoption during oxidation?
- Mechanical properties after LOCA?



Experimental methodology & facilities

A) burst-test facility

- resistance furnace up to 1100°C
- Ar or steam environment
- 10 cm specimen inner pressure: Ar up to 16 MPa



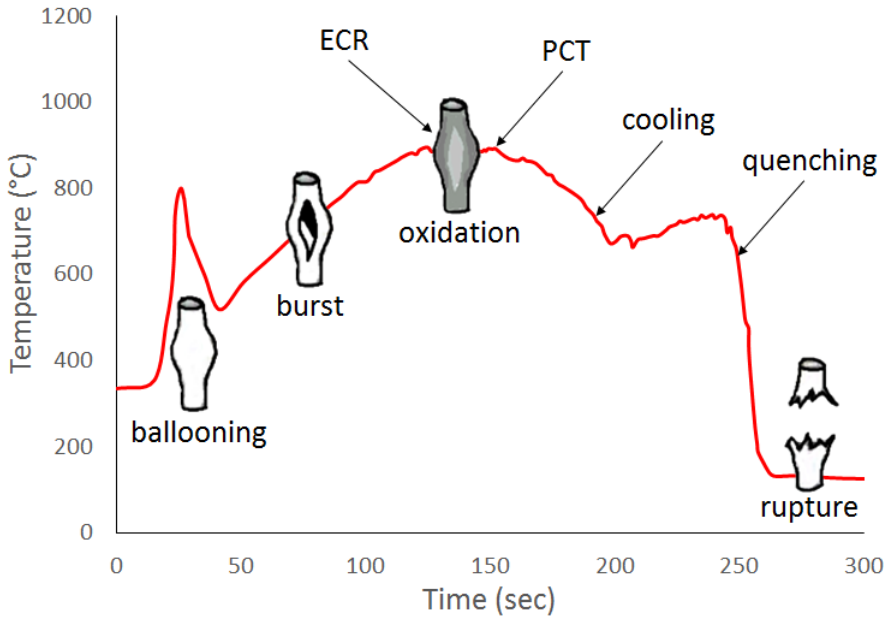
B) high temperature oxdidation furnace

- steam oxidation up to 1300°C



Experimental methodology & facilities

- Experiment 1:
  - Burst-tests in argon 600-800°C (burst fac.)
- Experiment 2:
  - Burst-test in steam (900°C) + steam oxidation after burst (900°C/10min) + quench (burst fac.)
- Experiment 3:
  1) Burst-tests in argon at 600°C (burst fac.)
  2) Specimen cutted
  3) High temperature steam oxidation 1200°C/4.5min + quenching (steam oxidation furnace)



burst-test facility

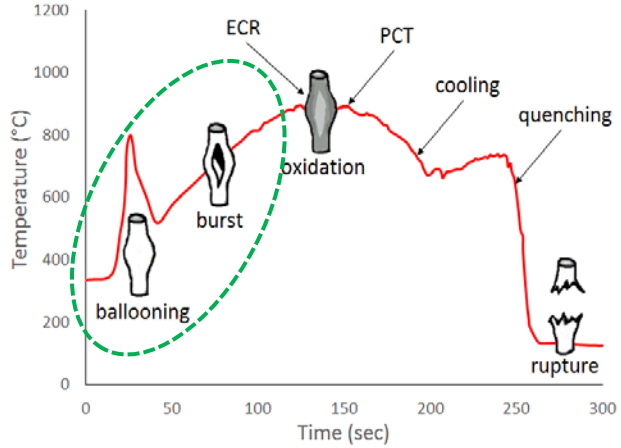


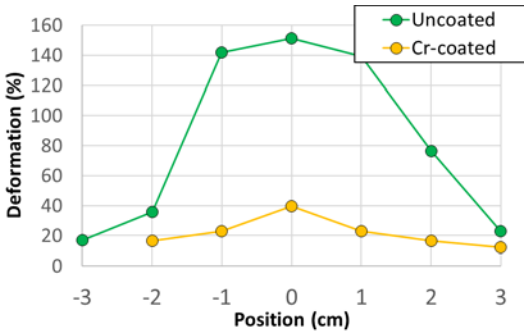
HT ox. furnace

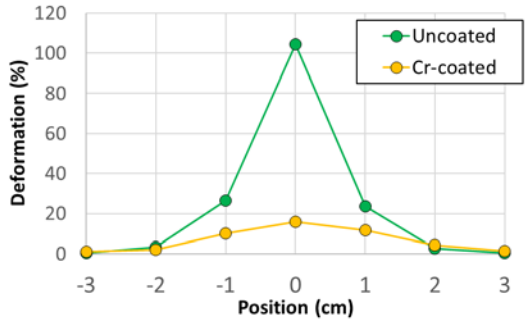


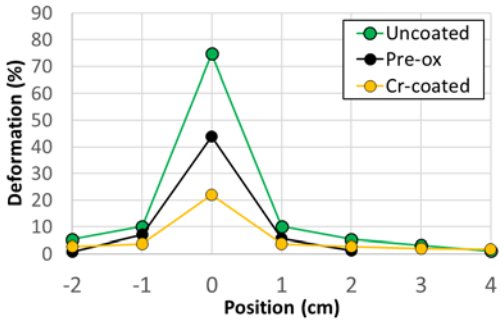
Ballooning and burst

- Experiments 600°C, 800°C, 900°C (in steam)
  - Pressurized samples inserted into pre-heated furnace (temp. ramp)
- Table summary: Cr-coated specimens
  - Burst-time delayed during experiment
  - Significant reduction of ballooning





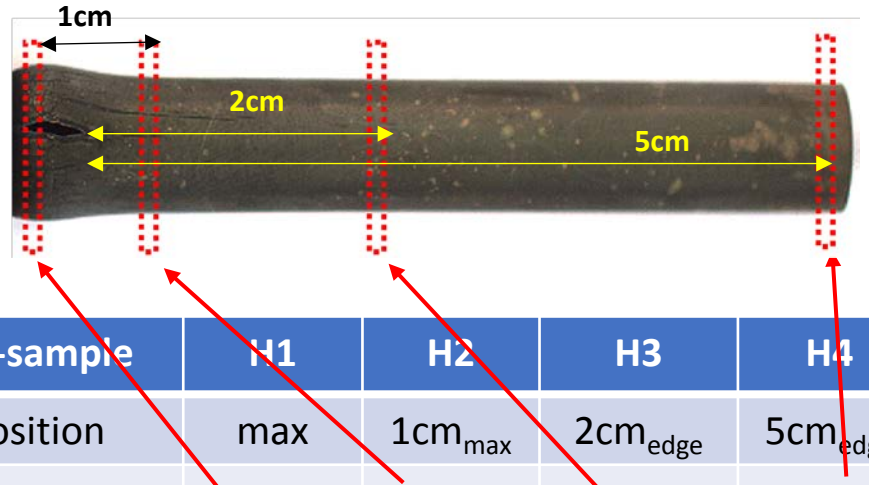




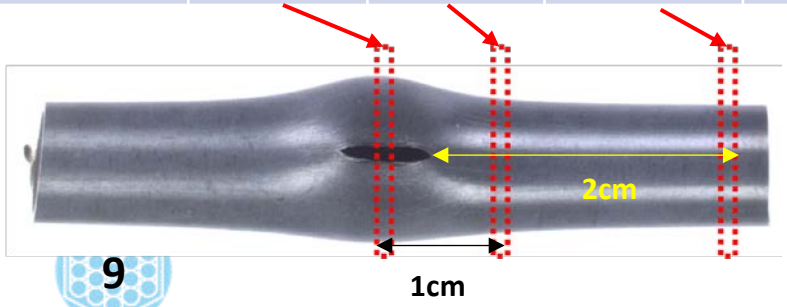
Experiment	600°C/12MPa*/Argon		800°C/6MPa/Argon		900°C/6MPa/Steam		
Sample	Cr-coated	Uncoated	Cr-coated	Uncoated	Cr-coated	Uncoated	Pre-ox 8µm
Time to burst	?	420 sec	232 sec	114 sec	175 sec	102 sec	76 sec
Temp at burst	600 °C	600 °C	796 °C	822.9 °C	915 °C	845 °C	869 °C
Strain in max.	40 %	151 %	16 %	104 %	20 %	69 %	39 %
Eq. Strain (2cm)	17 %	56 %	2.4 %	2.5 %	2.1 %	5.4%	4.4 %

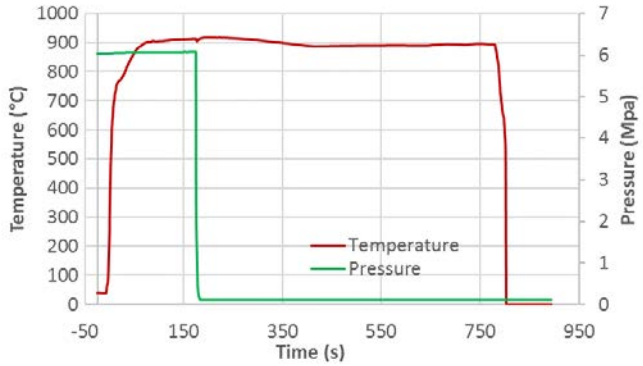
Oxidation after cladding failure: H-content

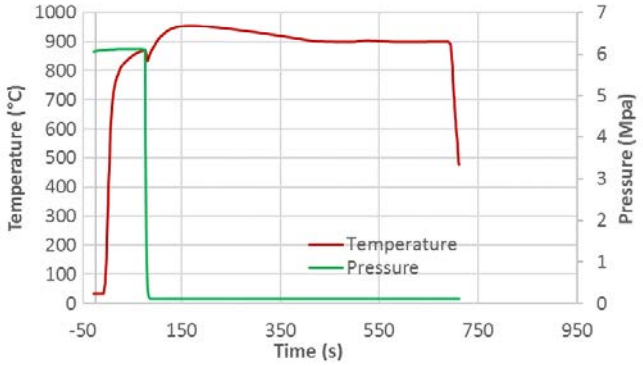
- Burst + 10min steam oxidation at 900°C
- Cr-coated & double side pre-ox. (8mic and 180 ppm)

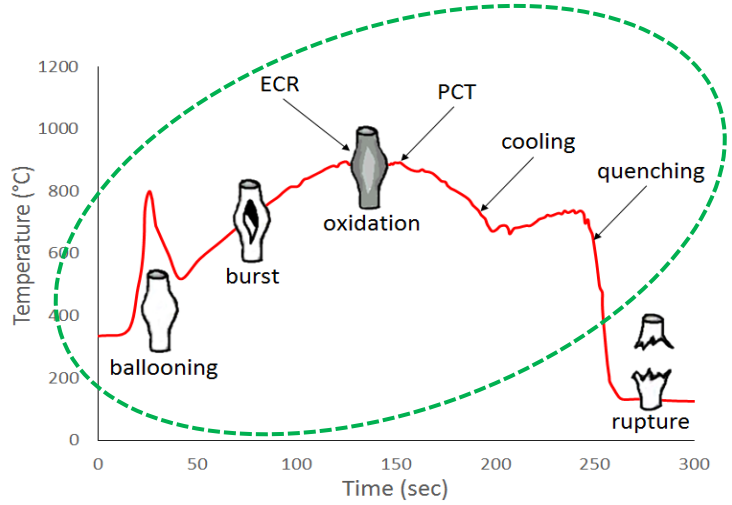


H-sample	H1	H2	H3	H4
Position	max	$1cm_{max}$	$2cm_{edge}$	$5cm_{edge}$
Cr-coated	128	364	314	21
Pre-oxided	229(49)	248(68)	343(163)	x









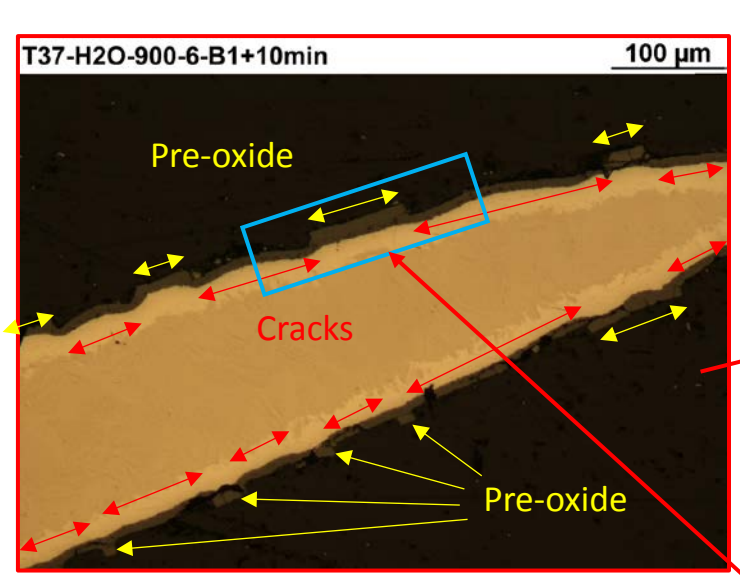
- Cracks in ballooned area were observed
- Hydrogen absorption
  - Pre-ox: protected by inner pre-oxide layer (cracks only – outer & inner side)
  - Cr-coated: through cracks in coating + **<u>secondary hydriding</u>**

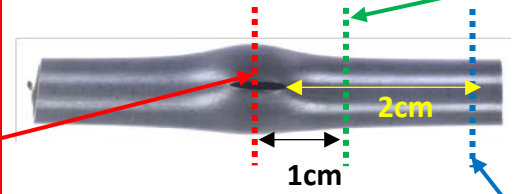
=> Higher for Cr-coated

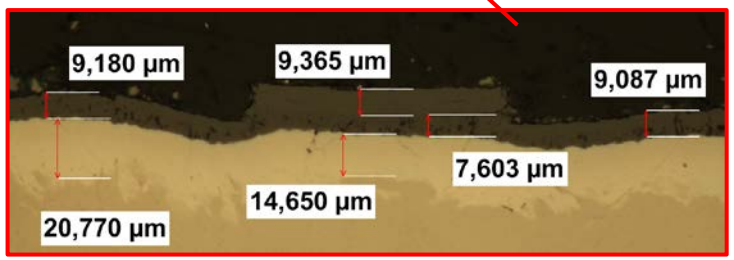
Pre-oxided: 900°C/6MPa/Steam + 10min: ballooning & oxidation

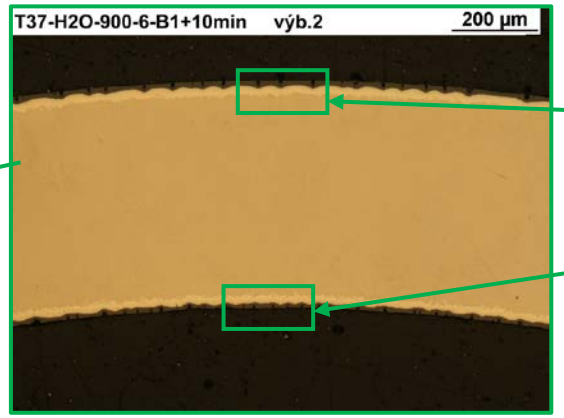
UJP PRAHA

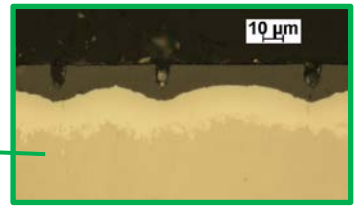
- Size of cracks coresponds to size of deformation: the bigest cracks close to burst-opening
- Majority of new oxide layer was formated through craks
- Inner ZrO_2 thickness is connected to distance from burst-opening (2cm only pre-ox)

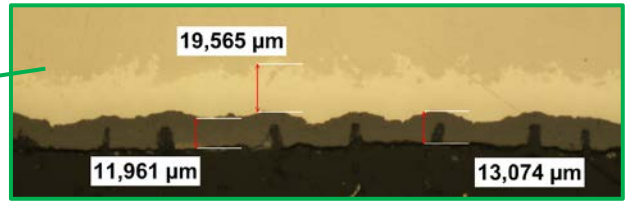


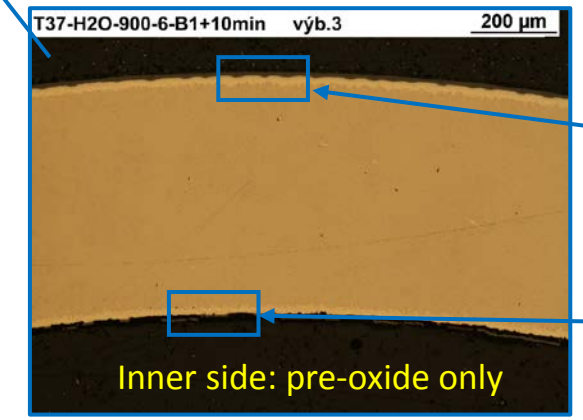


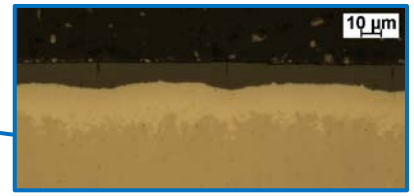


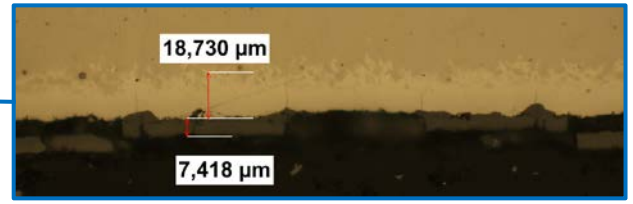








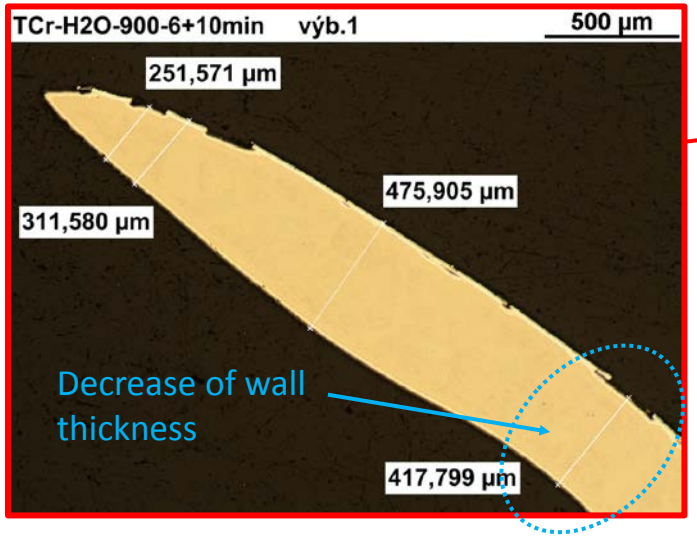




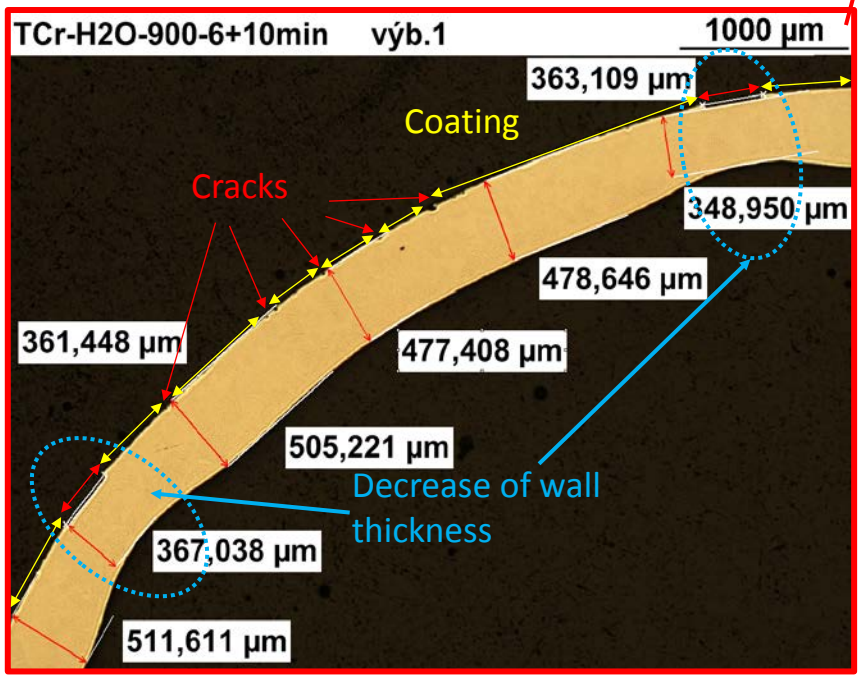
Cr-coated: 900°C/6MPa/Steam + 10min: ballooning

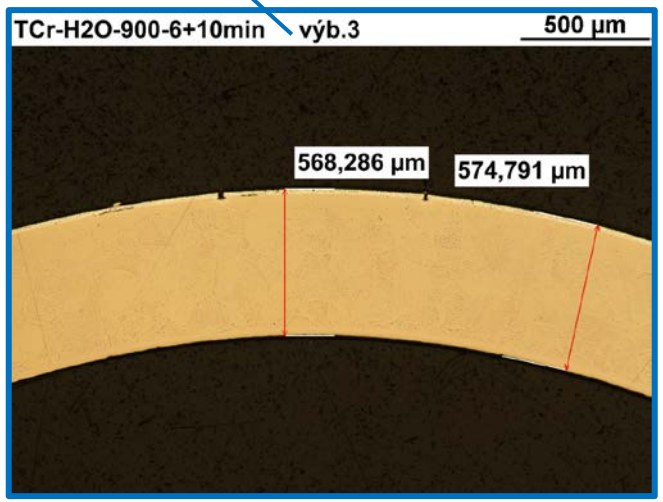
- Creep durring balloning: amount and size of cracks correspond to deformation
  - Cr-coating: thickness decreasses from original 30 mic to 18 mic
  - Under cracks coating significantly thinner

=> Cr-coating decreasses creep rate, after craks appearence is creep rate localy increased



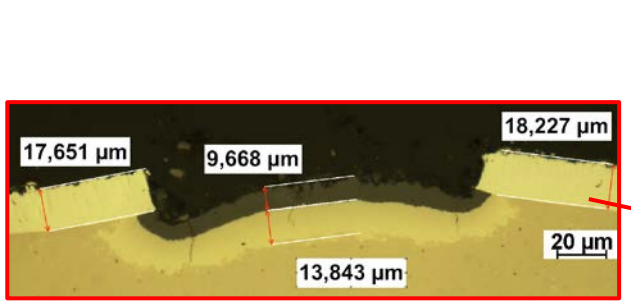


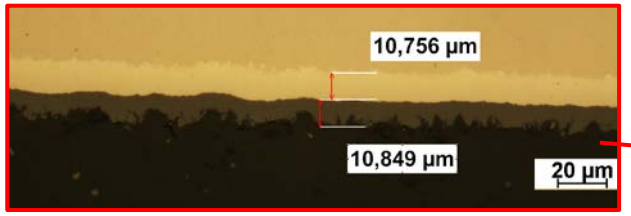


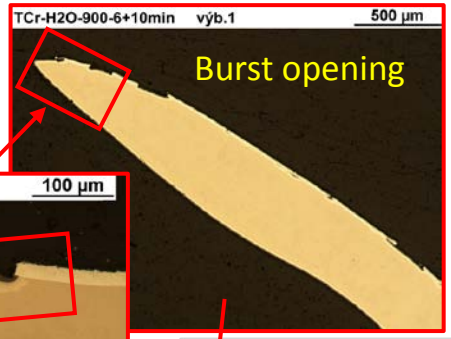


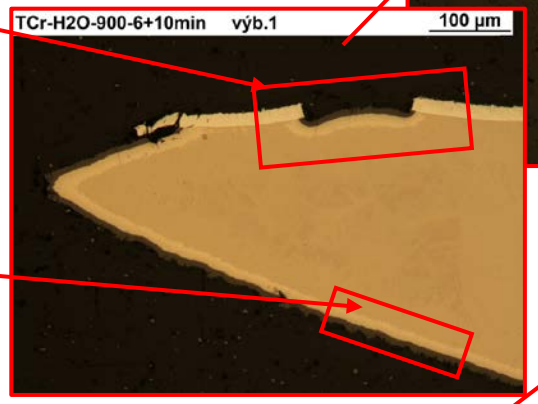
Cr-coated: 900°C/6MPa/Steam + 10min: oxidation

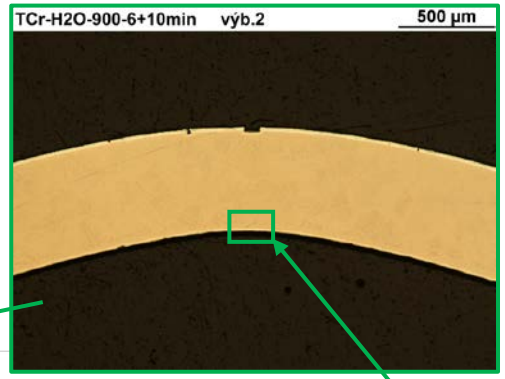
- Thinner Cr-coating is still protective against steam oxidation and it is not spalling
- In cracked areas ZrO_2 and alfa-Zr(O) formation
- Inner oxid layer thickness decreasses with distance from burst-opening: from 10 mic (Burst opening area) to no ZrO_2 (2cm)



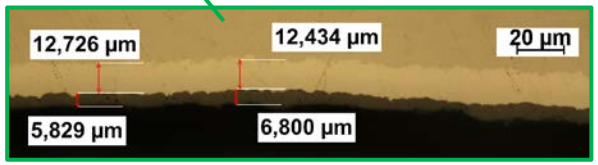




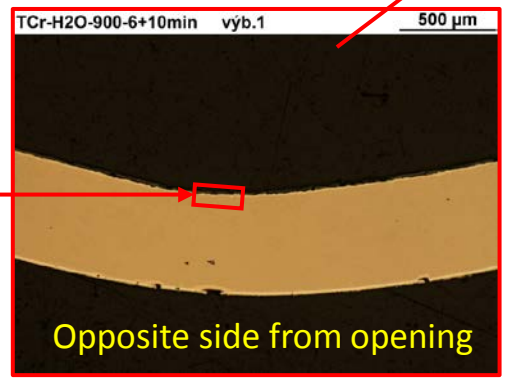


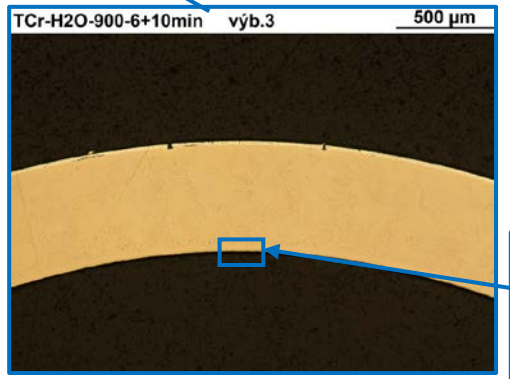












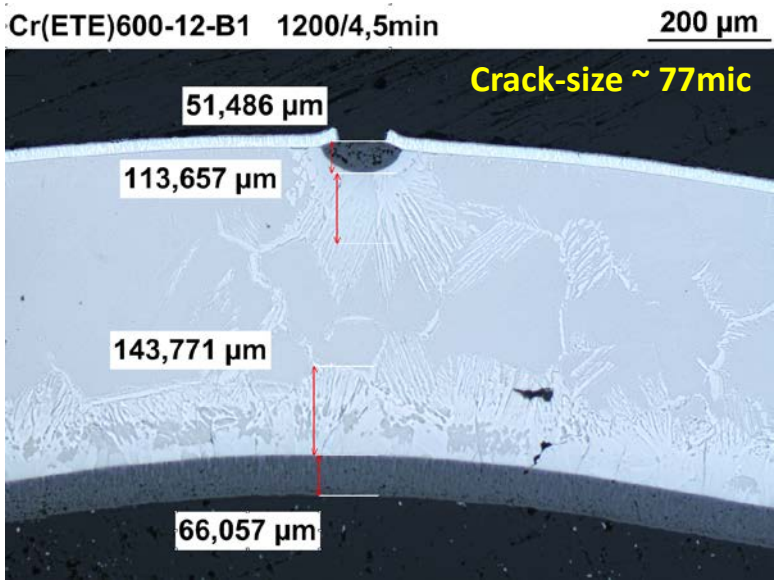


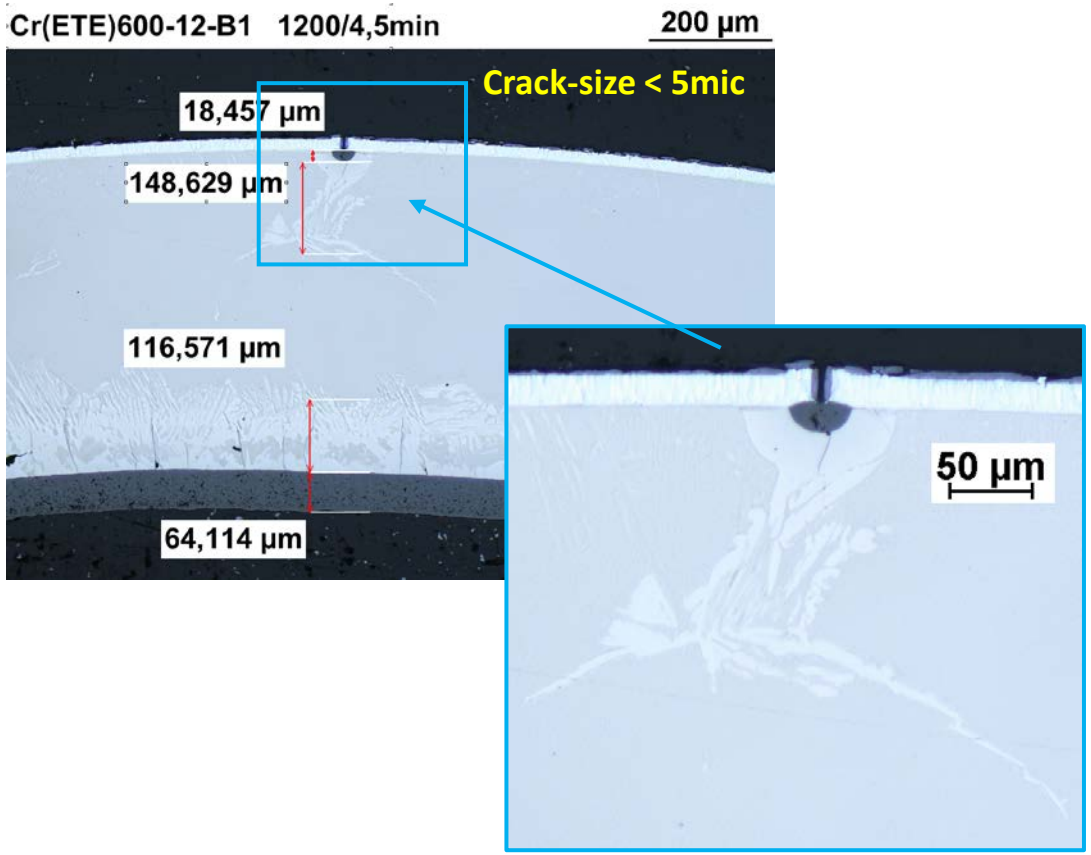
Double-side oxidation 1200°C/4.5min on ballooned spec.

- Scenario: burst+ballooning at low temp., then increasing temp. + oxidation
- Outer side: Cr-coating after ballooning, inner side no coating
- Oxidized part
- Oxidation through all cracks (including very small)
- Smaller cracks => lower level of oxidation
- Comparison:
  - Thinner oxid-layer through cracks then for uncoated
  - alfa-Zr(O) on grain boundaries

  – local thickness similar for: big/small cracks and uncoated

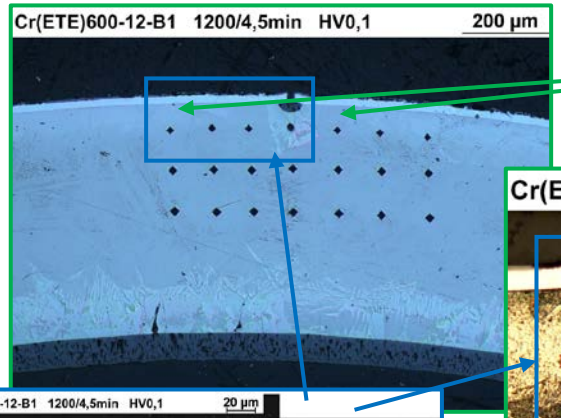




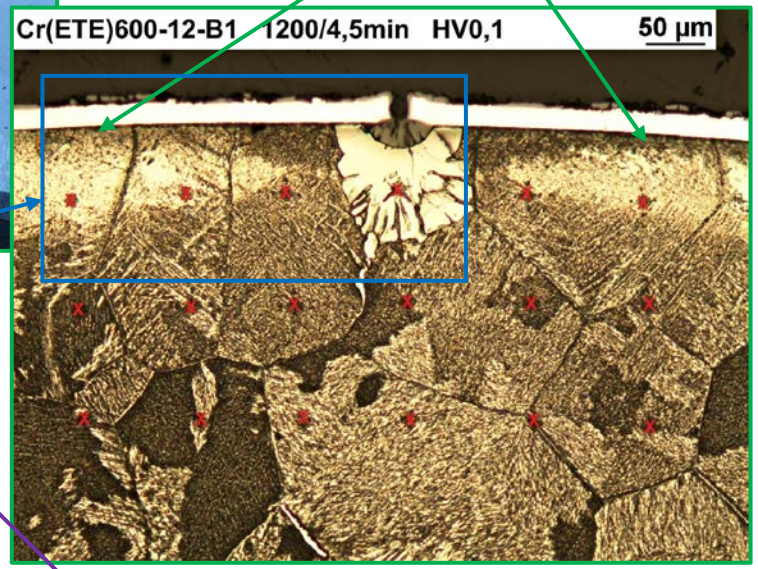


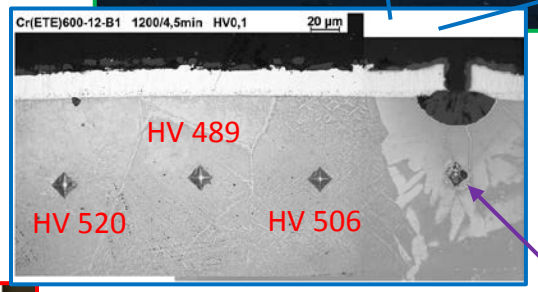
Microhardness after oxidation 1200°C/4.5min

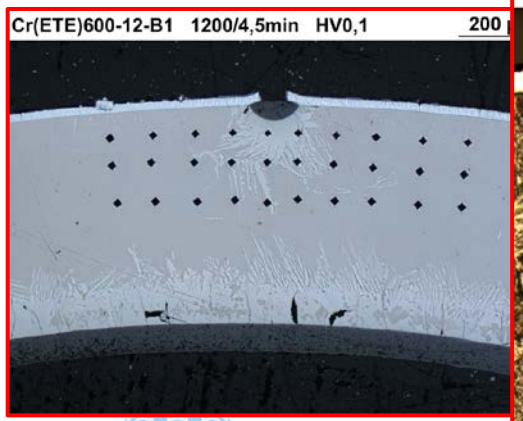
- Vickers indentation, 100 g (HV0.1) in 3 rows
- Big crack (63 mic)
  - α-Zr(O) area in first two rows
- Small crack (12 mic)
  - Influence of Cr-diffusion under coating
- Microhardness in the middle-wall row:
  - Uncoated: only oxidation: HV0.1 ~ 350-360
  - Big crack: HV0.1 ~ 406, Small crack: HV0.1 ~ 366
  - Non-uniform HV distribution depends on crack-size
  - Higher temp., influence of Cr dissolution (↑O in β)???

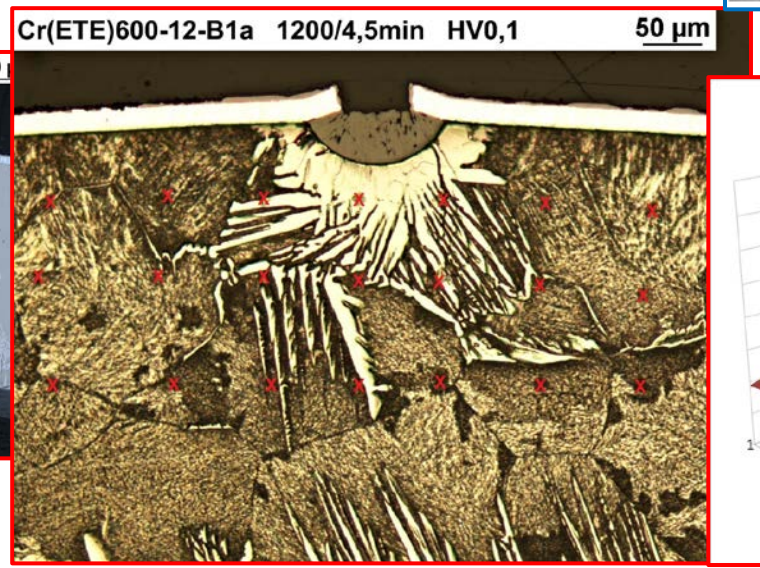


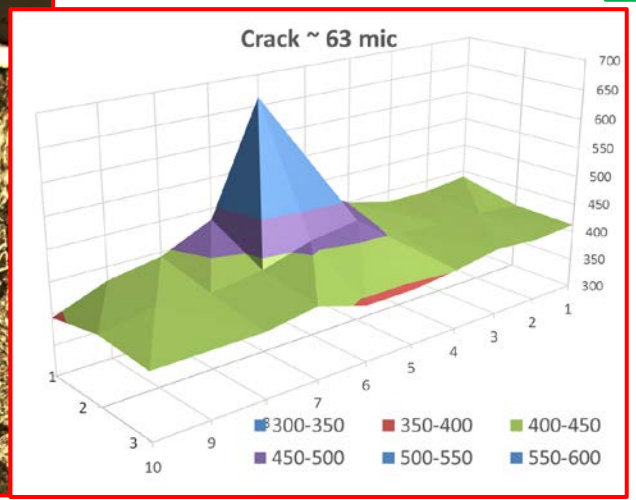
Cr-enriched area

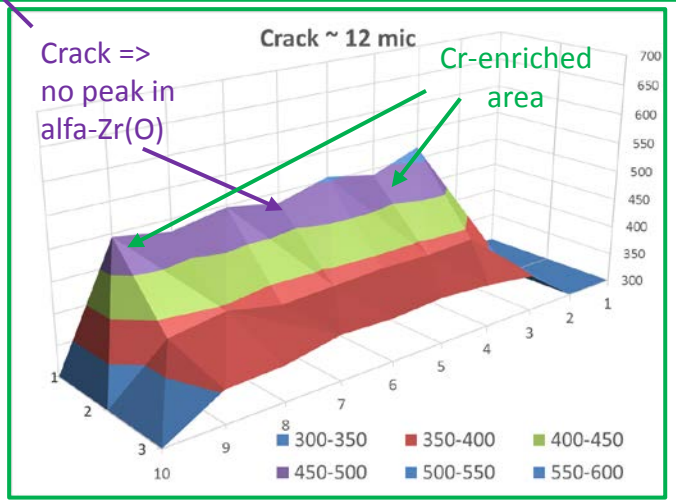












Conclusions/Discussion 1

- <u>QUESTIONS - Influence of Cr-coating on:</u>
- Ballooning (size/cross-section blockage)?
  - Significant reduction of ballooning for Cr-coated specimens

  => Lower level of blockage or fuel relocation in ballooned region can be expected
- Time to burst?
  - Increasing time to burst
- Coating failure/cracking during ballooning?
  - Cr-coating is not spalling
  - After reaching some level of deformation Cr-coating craks
  - Deformation in cracked area is faster => cladding is localy thinner
- High temperature oxidation through cracks?
  - Parts of Cr-coating without cracks not lose protective behavior
  - Through all cracks was oxidation observed
  - Level of oxidation depend on crack-size => non-uniform level of oxidation
  - Lower oxid layer thickness then Cr-coated samples, alfa-Zr(O) area similar

Conclusions/Discussion 2

- High temperature oxidation from inner side?
  - In balloned region was observed
- Hydrogen absoption during oxidation?
  - Through inner unprotected side after cladding failure
  - Through cracks
- Mechanical properties after LOCA?
  - For uncoated claddings:
    - RCT of specimens after LOCA transient (Zr-alloys uniform, no problems with local oxidation)
  - (Cr)-coated cladding
    - Cladding supported with (Cr)-coating
    - Specimen localy oxidized through cracks
    - Interaction coating/substrate: influence of Cr-diffusion => higher oxygen dissolution into beta-Zr
    - Significantly different oxidation of outer (coated) and inner uncoated side

  $\Rightarrow$ Much more complicated situation then for uncoated Zr-alloys

  $\Rightarrow$ **How to prove post-quench ductility for coated samples???**

Thank you for your attention

Acknowledgements

The authors thanks to whole UJP-zirconium department (J. Šustr, D. Rada, V. Vrtílková) for sample preparation, running experiments, and post-experimental evaluation.

Financial support of this research through ČEZ a.s. company is gratefully acknowledged.

Also, this work was supported by the Ministry of Education, Youth and Sport of the Czech Republic, programme NPU1, project No LO1207,

Grant Agency of the Czech Technical University in Prague, grant No. SGS16/252/OHK4/3T/14,

Grants no. „TA02011025, program ALFA – TAČR“, „TH02020477, program EPSILON – TAČR“, „TH02020691, program EPSILON – TAČR“, CZ.2.16/3.1.00/21563.

Zirconium alloy coatings with Si based compounds – INCT experiments

Sartowska Bożena [1] *, Starosta Wojciech [1], Lech Waliś [1], Jerzy Smolik [2], Andrzej Krześniak [1]

[1] Institute of Nuclear Chemistry and Technology, Warsaw, Poland
[2] Institute for Sustainable Technologies, Radom, Poland

ABSTRACT

Zirconium alloys have very good water corrosion and radiation resistance at normal working conditions of nuclear reactors. Due to these properties it is commonly used as cladding material for fuel elements. However, in the case of LOCA conditions, the extremely fast oxidation of zirconium at steam atmosphere or and air/steam mixture results in intense hydrogen generation.

Advanced materials that are intended to be more tolerant of severe accident conditions with the safe operation under normal conditions are looking for. The concept of Accident Tolerant Fuels (ATF) and Accident Tolerant Materials (ATM) has been developed for this purpose. There are two main ideas for the increasing of claddings' corrosion resistance: (ii) developing of new materials for claddings production (SiC, FeCrAl), (ii) modification of the surface layer of claddings (protective layer on the base of silicon, MAX, FeCrAl, Cr).

Works carried out in INCT are connected with the subject: Silicide/silicate coatings on zirconium alloys for improving the high temperature corrosion resistance. Works are aimed to develop the silicon-based coatings on zirconium alloys claddings and evaluation of their properties at accident scenario as well as in the reactor normal working conditions. The examined materials were Zry-2 coated with $ZrSi_2$-Cr using PVD method. Oxidation tests with autoclave PARR 4653 were performed in 360°C/195 bar/21, 42, 63 days.

The results of experiments concerning coatings characterization and autoclave oxidation tests results are presented in this work.

Acknowledgements
This work has been partially supported under IAEA Research Contract No. 19026/R0 and by Polish Ministry of Science and Higher Education under decisions 3689/IAEA/2017/0


KIT
Bozena Sarbinska

ZIRCONIUM ALLOY COATINGS WITH Si BASED COMPOUNDS

INCT EXPERIMENTS

Sartowska Bożena *, Starosta Wojciech, Lech Waliś, Andrzej Krześniak
Institute of Nuclear Chemistry and Technology, Warsaw, Poland

Jerzy Smolik,
Institute for Sustainable Technologies, Radom, Poland

Jan Mizeracki
Unipress, Warsaw, Poland

WHAT WE KNOW



- Severe accidents such as those at three Mile Island and Fukushima Daiichi have shown that under such extreme conditions, nuclear fuel will fail and the high temperature reaction between zirconium alloys and water will lead to generation of hydrogen with the potential for explosions, damaging the plant further.

  - There have been many improvements to the original design and materials used, However , the basic concept of uranium oxide feel pellets clad with zirconium alloy tubing has reminded the fuel of choice for the vast majority of commercial nuclear power plants

- Development of the solution to minimize the risk related to the design and unforseable situations is urgently needed

- The concept of Accident Tolerant Fuels **(ATF)** and Accident Tolerant Materials **(ATM)** - it means materials with increased accident tolerance - has been developed recently for this purpose

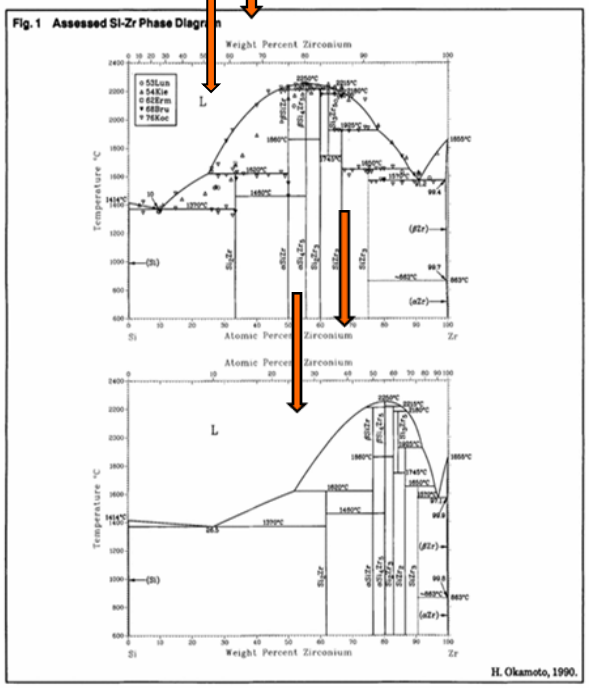
WHY SILICON BASE COATINGS

- The **zirconium silicide** or **zirconium silicate** coatings are known for good resistance in high temperature conditions and are applied as environmental barrier coatings for high-temperature gas-turbine components

- **Silicon based coatings** may provide a more protective barrier than the native ZrO_2 films formed on alloy cladding during routine nuclear plant operations and may provide an protective barrier during high-temperature accident scenarios

- Both, Zr and Si form their respective oxides at high temperatures and surface layers of ZrO_2 or SiO_2 or even **$ZrSiO_4$** may be formed depending on the stoichiometry

- **Chromium** shows good properties influences positive for materials/alloys corrosion processes in water; it plays protective role



514 Bulletin of Alloy Phase Diagrams Vol. 11 No. 5 1990

Phase diagram for zirconium-silicon systems: of intermetallic compounds - different Zr/Si ratios and stability regions
For example:
ZrSi2 is stable up to 1620°C
ZrSi is stable up to 2210°C

INCT PROPOSAL
Silicide/silicate coatings on zirconium alloys for improving the high temperature corrosion resistance

⌘ **The aim:**

to develop the silicon-based coatings on zirconium alloys claddings and evaluation of their properties at accident scenario as well as in the reactor normal working conditions

⌘ **The main topics:**

- dvelopment of deposition methods of silicide or/and silicate coatings on zirconium alloys surface
- determination of corrosion properties of deposited layer in water, steam and air atmospheres at high temperatures.

Characterisations

1. Surface morphology: OM, SEMs including HR SEMs
2. Elemental analysis: EDS with Quantax 400 (Bruker, Germany)
3. Phase analysis: X-ray diffractometer D8 Advanced (Bruker, Germany) with geometries Θ-2Θ, ω=5o, ω=10o

4. Oxidation tests

- in the autoclave (360°C, 196 bar, water simulating water used in reactor)

- 1100oC in air and quenching in water

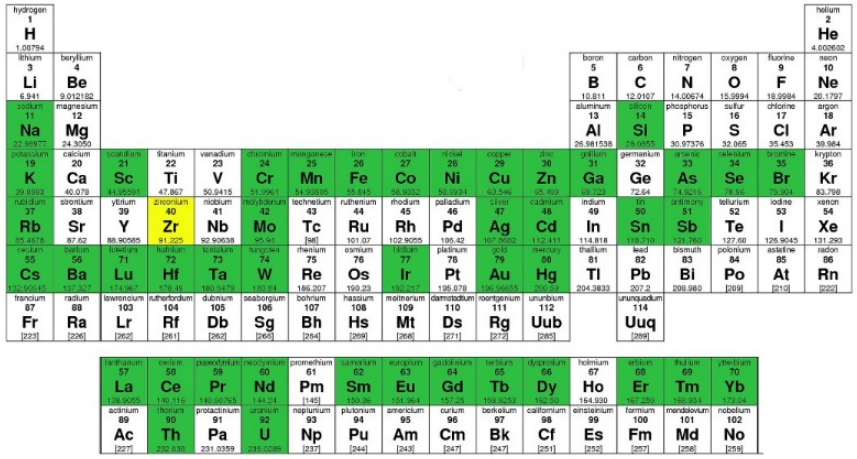
S**ilicide** - any compounds containing silicon bonded to a more electropositive element. S**ilicate** is a compound containing an anionic silicone compound, the great majority of the silicates are oxides

MATERIAL FOR INVESTIGATIONS – Zry-2

Producer info

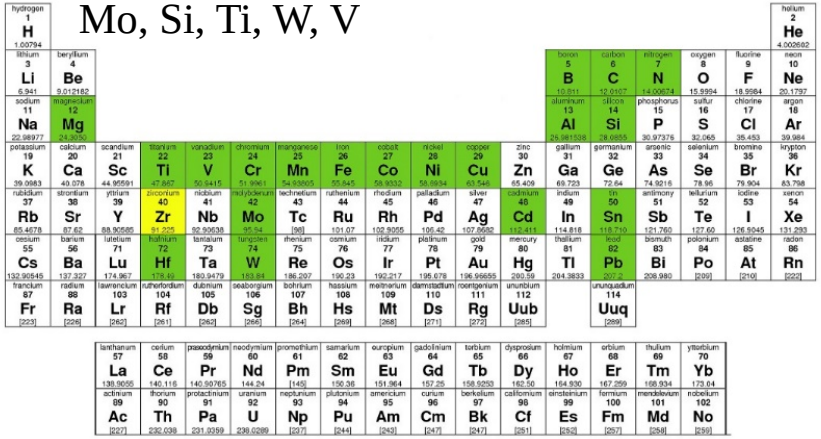
ELEMENT	CONCENTRATION
	wt.%
Sn	1.3 - 1.6
Fe	0.07 - 0.20
Cr	0.05 - 0.16
Ni	0.03 -0.08

INAA analysis



Impurities (ppm)

Al, B, Cd, C, Co, Hf, Pb, Mg, Mn, Mo, Si, Ti, W, V



PHYSICAL VAPOUR DEPOSITION - PVD

The multisource plasma magnetron sputtering system with 3 magnetron plasma sources



It allows to deposit materials from separate targets and to obtain multielemental coatings from targets



Used separate targets:

- composite $ZrSi_2$
- chromium

Both sides covered

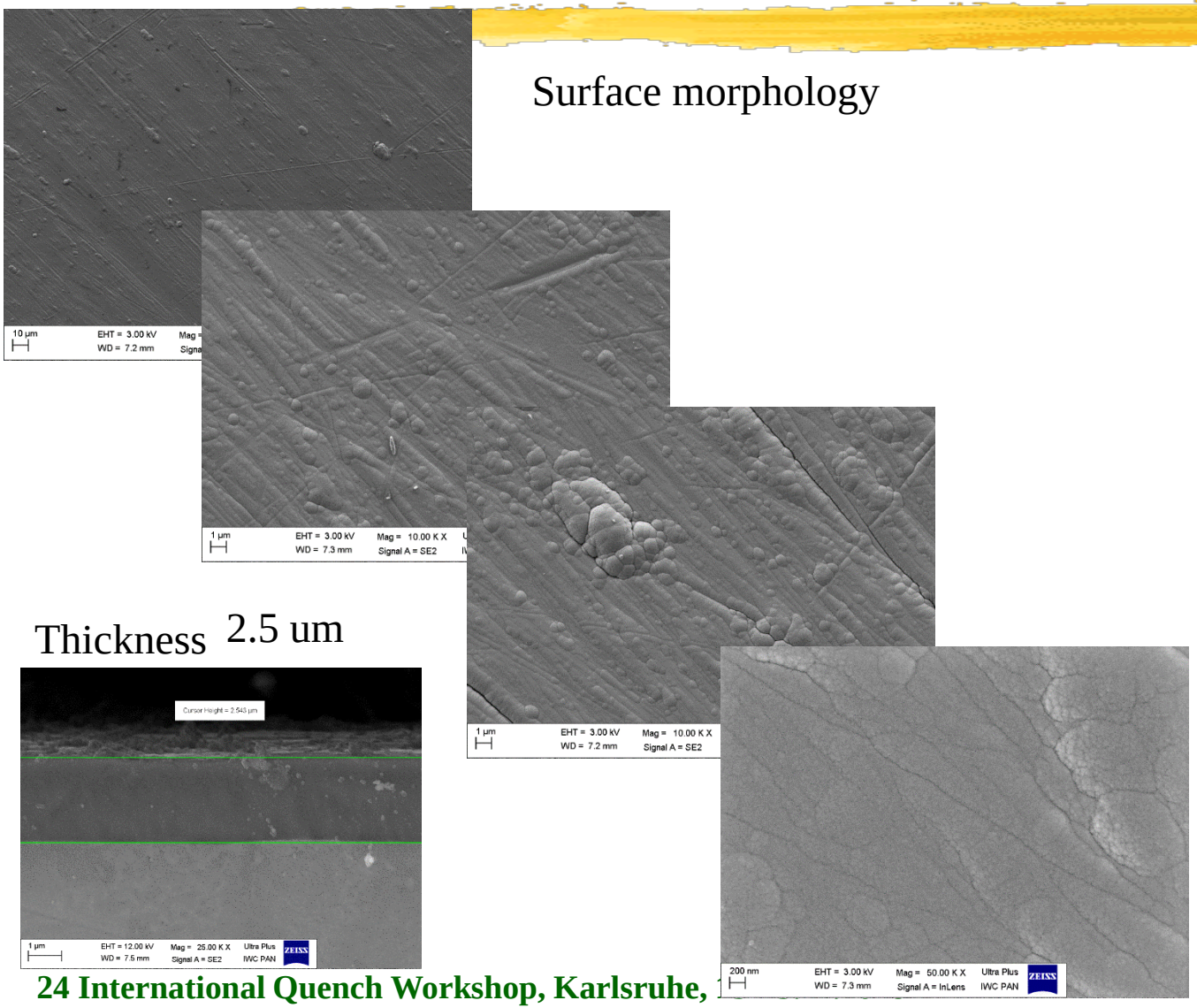
	Si	Cr	Zr
at.%	43,30	34,80	21,90
wt.%	24,20	36,00	39,80

Radom1 2059.spx

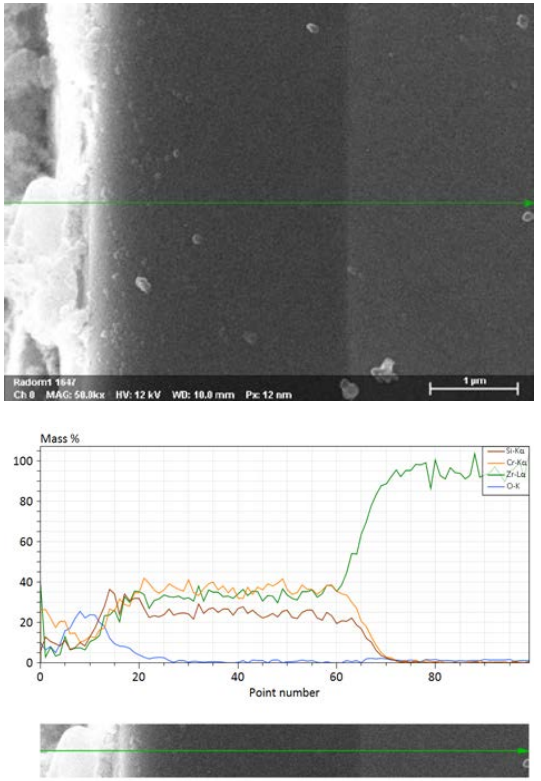
Element	At. No.	Netto	Mass [%]	Mass Norm. [%]	Atom [%]
Carbon	6	4370	0.00	0.00	0.00
Silicon	14	64462	24.28	26.19	45.31
Chromium	24	22614	35.48	38.26	35.76
Zirconium	40	49691	32.96	35.55	18.93
		Sum	**92.72**	**100.00**	**100.00**

OBTAINED COATINGS

Surface morphology



Elemental composition



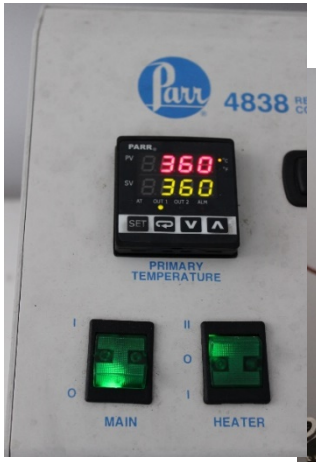
Thickness 2.5 um

AUTOCLAVE OXIDATION TESTS

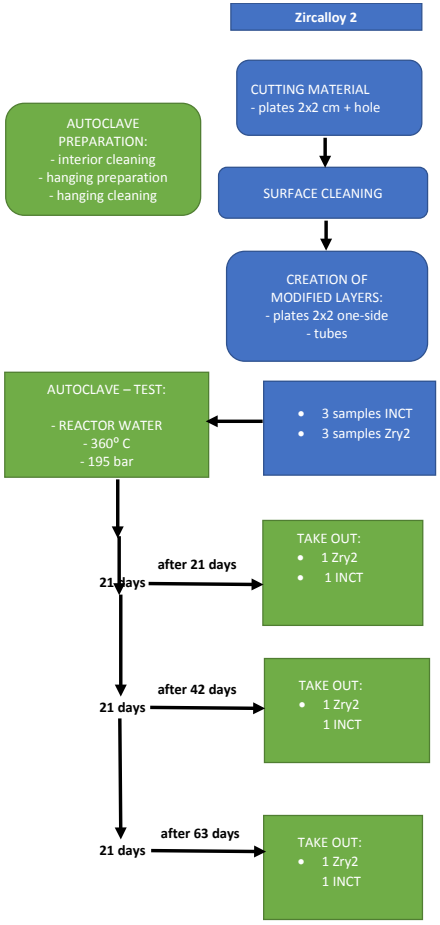




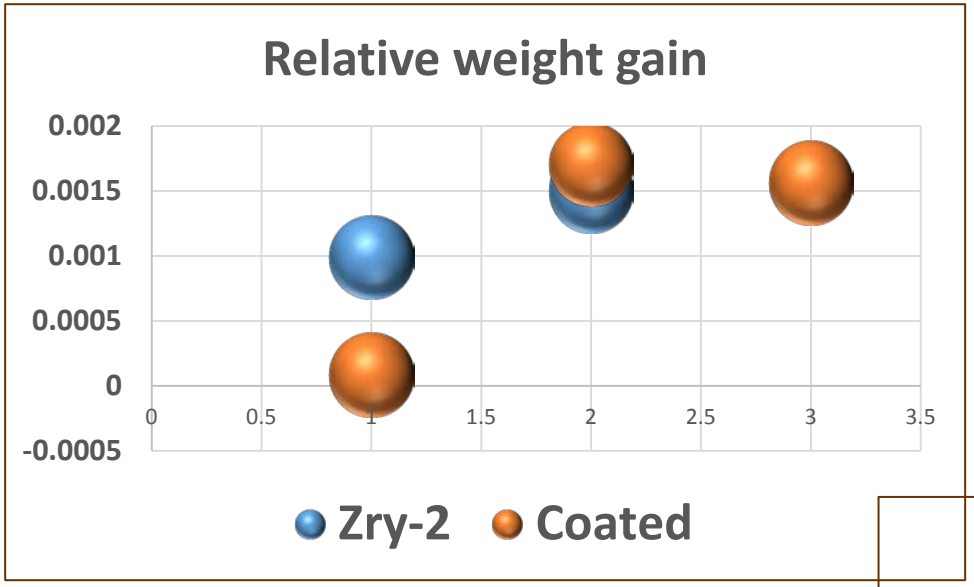


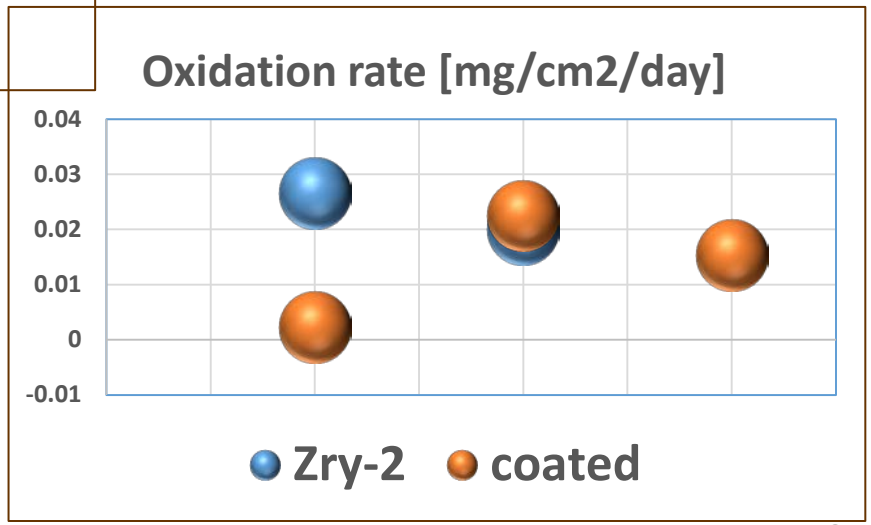






OXIDATION - WEIGHT GAIN

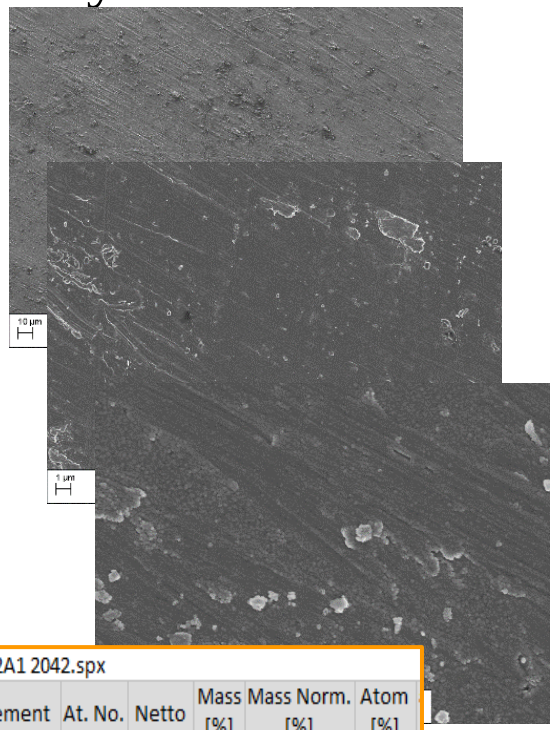




Without results for Zry-2 A3

OXIDATION Zry-2 - SURFACE

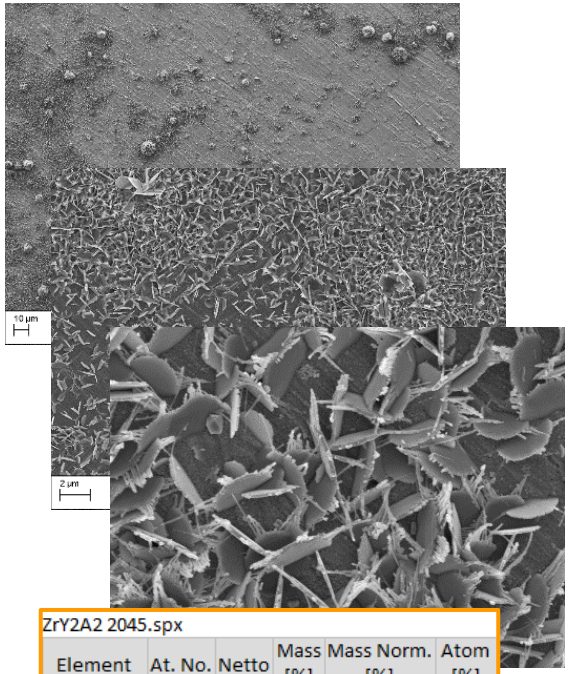
Zry2A1



ZrY2A1 2042.spx

Element	At. No.	Netto	Mass [%]	Mass Norm. [%]	Atom [%]
Carbon	6	4498	0.00	0.00	0.00
Oxygen	8	18027	20.51	21.76	54.55
Zirconium	40	218673	69.64	73.88	32.48
Tin	50	1698	0.90	0.95	0.32
Boron	5	1239	3.21	3.41	12.64
		Sum	**94.26**	**100.00**	**100.00**

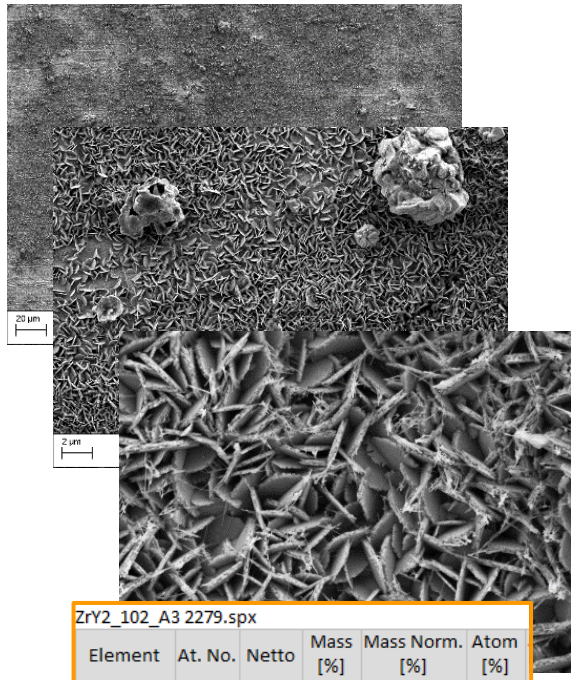
Zry2A2



ZrY2A2 2045.spx

Element	At. No.	Netto	Mass [%]	Mass Norm. [%]	Atom [%]
Carbon	6	4558	0.00	0.00	0.00
Oxygen	8	66754	36.81	38.81	70.68
Aluminium	13	5154	1.19	1.25	1.35
Chromium	24	53954	29.88	31.50	17.65
Iron	26	4560	3.85	4.06	2.12
Copper	29	812	1.47	1.55	0.71
Zirconium	40	64368	21.20	22.35	7.14
Calcium	20	1483	0.46	0.48	0.35
		Sum	**94.85**	**100.00**	**100.00**

Zry2A3

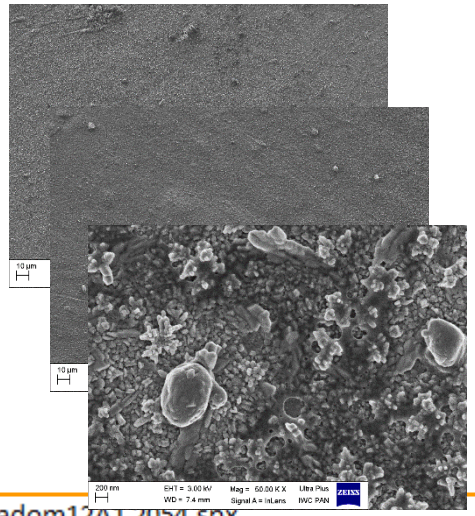


ZrY2_102_A3 2279.spx

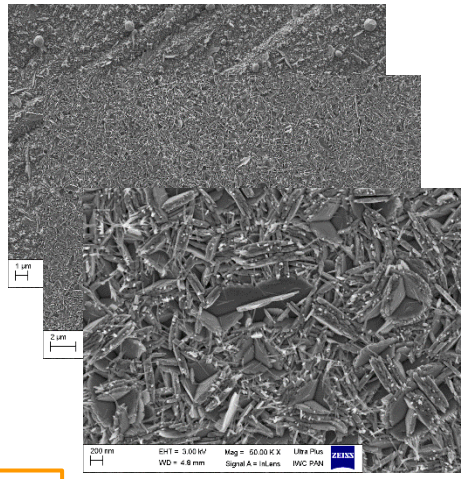
Element	At. No.	Netto	Mass [%]	Mass Norm. [%]	Atom [%]
Carbon	6	3431	5.88	5.77	13.62
Oxygen	8	47422	36.00	35.32	62.57
Aluminium	13	2363	0.54	0.53	0.56
Chromium	24	30338	17.91	17.57	9.58
Iron	26	4311	3.69	3.62	1.84
Copper	29	1338	2.41	2.37	1.06
Zirconium	40	103074	35.01	34.35	10.67
Tin	50	1044	0.48	0.47	0.11
		Sum	**101.93**	**100.00**	**100.00**

OXIDATION Zry-2 COATED - SURFACE

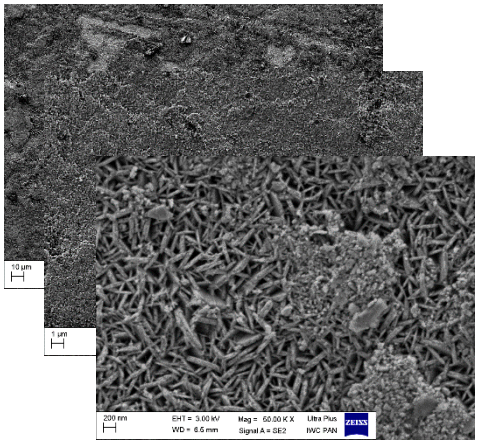
12A1



13A2



11A3



Radom12A1 2054.spx

Element	At. No.	Netto	Mass [%]	Mass Norm. [%]	Atom [%]
Carbon	6	7522	0.00	0.00	0.00
Oxygen	8	27925	21.69	24.02	52.48
Silicon	14	38554	8.07	8.94	11.13
Calcium	20	3353	1.17	1.30	1.13
Chromium	24	43119	26.28	29.11	19.57
Iron	26	4069	3.80	4.21	2.64
Copper	29	908	1.64	1.81	1.00
Zirconium	40	74769	27.32	30.25	11.59
Aluminium	13	1359	0.32	0.35	0.46
		Sum	**90.30**	**100.00**	**100.00**

Radom13A2 2049.spx

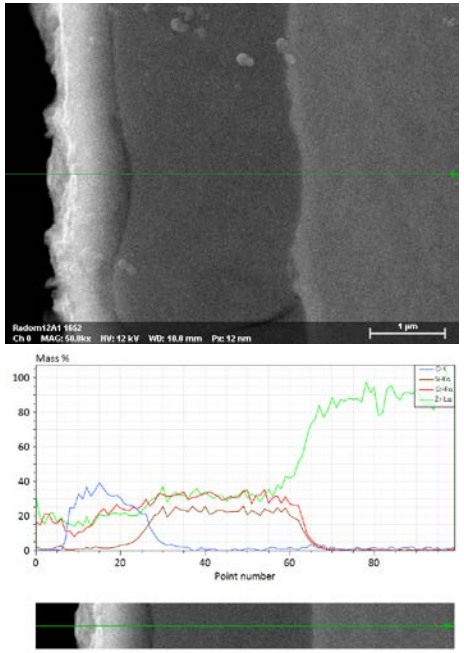
Element	At. No.	Netto	Mass [%]	Mass Norm. [%]	Atom [%]
Carbon	6	3356	0.00	0.00	0.00
Oxygen	8	65102	31.56	35.89	65.42
Aluminium	13	4950	1.23	1.40	1.51
Silicon	14	2739	0.60	0.69	0.71
Calcium	20	2404	0.81	0.92	0.67
Chromium	24	67464	40.60	46.17	25.90
Iron	26	4376	4.16	4.73	2.47
Zirconium	40	23885	8.60	9.78	3.12
Copper	29	191	0.36	0.41	0.19
		Sum	**87.93**	**100.00**	**100.00**

Radom 13_A3 2282.spx

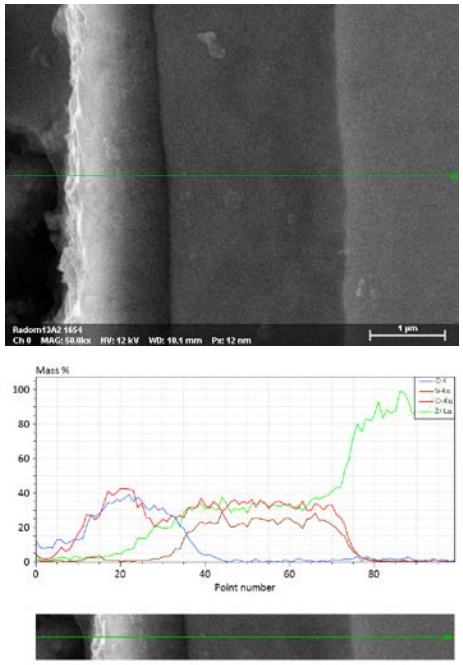
Element	At. No.	Netto	Mass [%]	Mass Norm. [%]	Atom [%]
Carbon	6	2434	4.55	4.68	11.55
Oxygen	8	38559	31.59	32.55	60.27
Aluminium	13	2097	0.51	0.53	0.58
Chromium	24	38259	25.28	26.06	14.84
Iron	26	2501	2.42	2.50	1.32
Zirconium	40	86008	31.82	32.79	10.65
Calcium	20	1315	0.48	0.49	0.36
Silicon	14	1790	0.39	0.41	0.43
		Sum	**97.04**	**100.00**	**100.00**

OXIDATION Zry-2 COATED - SURFACE

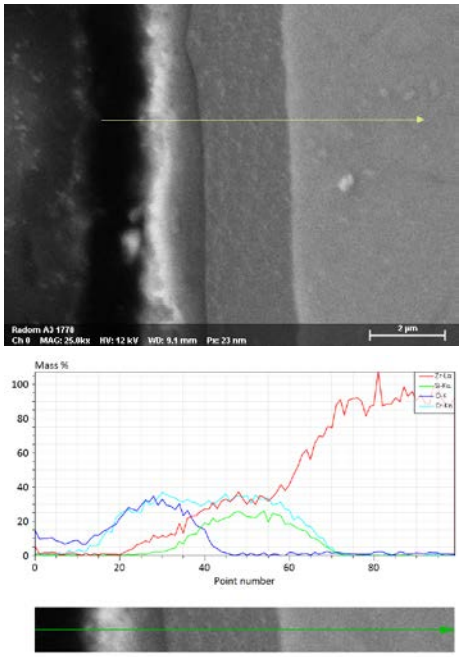
12 A1

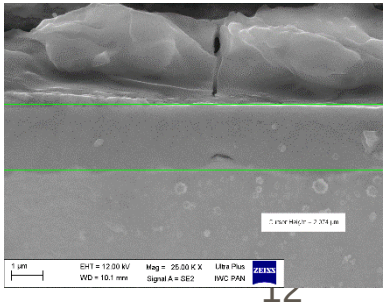


13 A2



11A3





Thickness oxide layer [um]:
Coated A1: 0.5166 // A2: 1.090 // A3: 0.914
Zry-2: A1: 1.488 // A2: 2.074 // A3: 2.016

OXIDATION – PHASE ANALYSIS

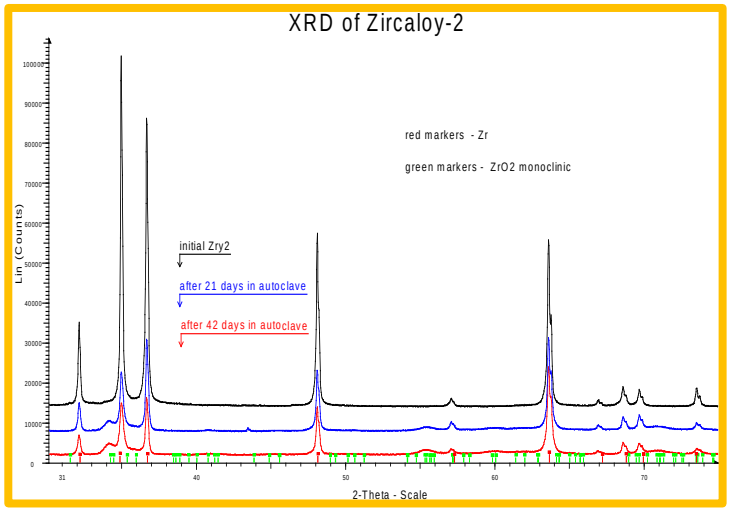
red marks – Zr

green marks – monoclinic ZrO_2

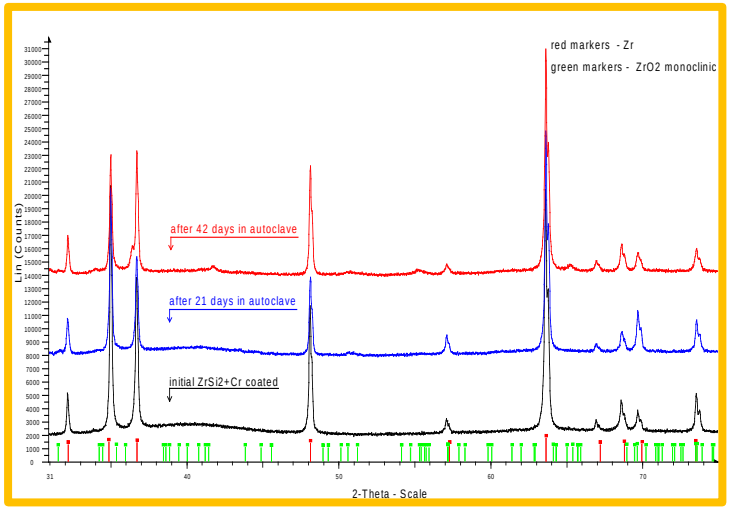
black line – initial

blue line – 21 days in autoclave

red line – 42 days in autoclave



XRD of Zircaloy-2 after autoclave tests



XRD spectra of Zry2 coated with $ZrSI_2$ - Cr layer after autoclave test

Presence of Zr was confirmed

Zr oxidation proces was confirmed

Dispersive phase was formed during the autoclave tests

Results summary

1. Zirconium coatings with compounds on the base of silicon was obtained using PVD method using two sepatare targets: $ZrSi_2$ and Cr

2. Surface layers with 2.5um thickness and presence of Zr, Si, Cr were obtained

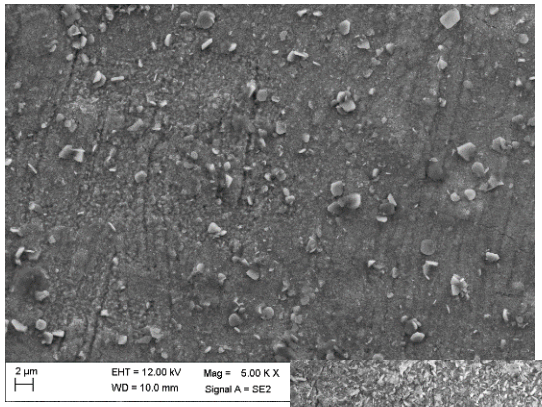
3. Autoclave oxidation tests 21/42/63 days showed
- surface without cracks, crevices were observed
- presence of oxide layer with ZrO_2 above the coatings
- presence of Cr and O in the oxide surface layer what confirmed diffusion of Cr to the surface

4. Proposed coatings played the protective role during autoclave tests in water 360°C/195 bar/21//42//63 days

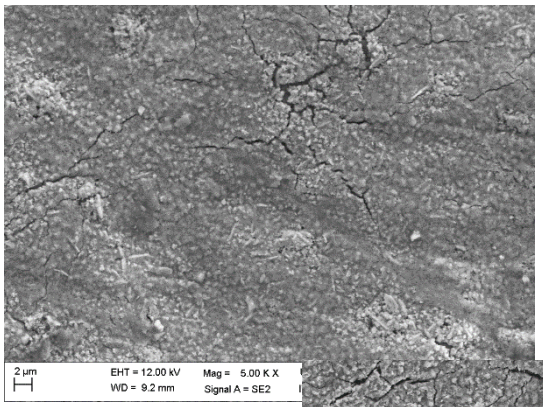
HIGH TEMPERATURE OXIDATION TEST

Samples of initial Zry-2 and after autoclave tests were oxidized:
1100°C/1 h/air and quenched in water

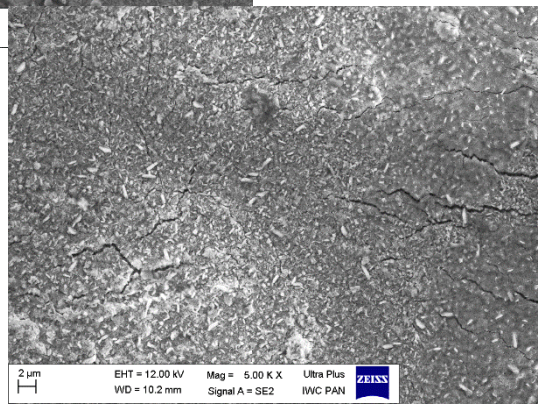
A0



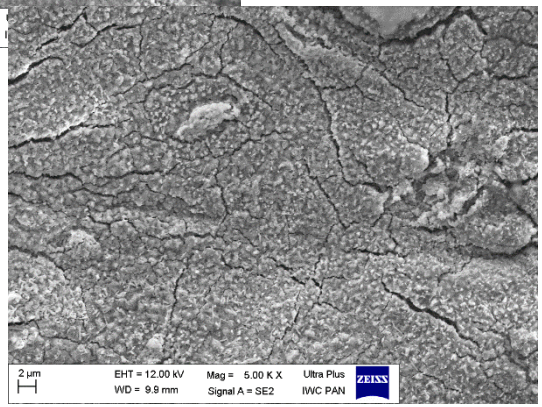
A1



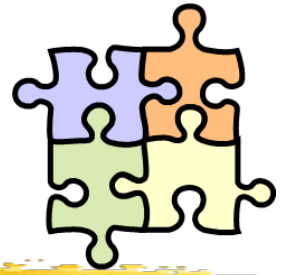
A2



A3



CONCLUSIONS



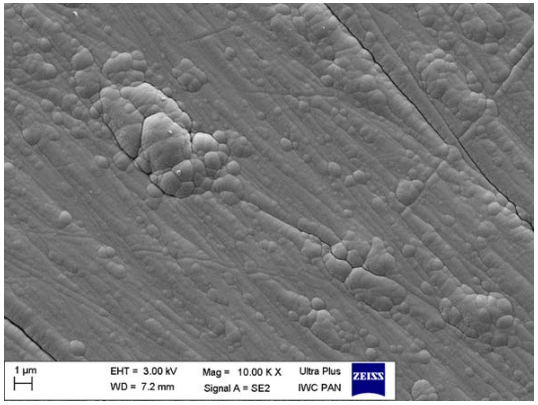
1. **Proposed new material : ZrSi2-Cr for Zry2 coating can be considered as protective layer for Zry-2 normal work in PWR conditions**

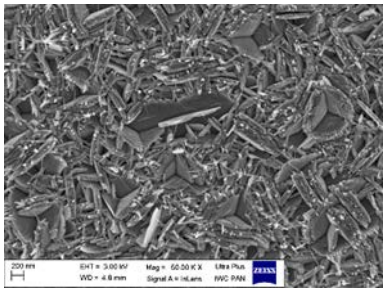
2. **Protective mechanism is assumed to two facts:**
- **chromium diffusion to the surafce**
- **presence of high temperature stable Si compounds**

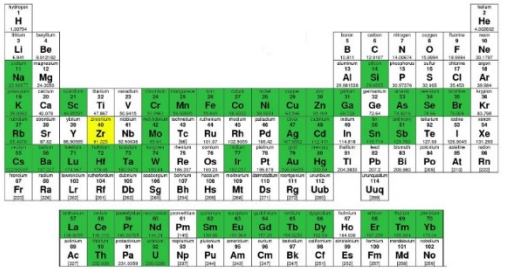
3. Plans for future:
- **longer autoclave experiments**
- **high temperature oxidation tests**

ACCIDENT TOLERANT MATERIALS – IDEAS and RESEARCH DIRECTIONS

Thank you for your attention







Acknowledgements
This work has been partially supported under IAEA Research Contract No. 19026/R0
and
by Polish Ministry of Science and Higher Education under decision 3525/IAEA/2016/0 and 3689/IAEA/2017/0.

IAEA International Atomic Energy Agency

Ministerstwo Nauki i Szkolnictwa Wyższego

Silicon concentration changes in Zry-2 coated with Zr-Si and $ZrSi_2$-Cr during the autoclave oxidation tests

Andrzej Krześniak[1], *Bożena Sartowska*[1], *Wojciech Starosta*[1], *Lech Waliś*[1], *Jerzy Smolik*[2], *Magdalena Miłkowska*[1]

[1]*Institute of Nuclear Chemistry and Technology, Warsaw (Poland)*
[2]*Institute for Sustainable Technologies, Radom (Poland)*

Severe accidents in nuclear power plants connected with LOCA (Loss Of Coolant Accidents) lead to a brand new branch of studies - Material engineering focused on finding new materials which will have better physical properties than actual constructive materials used in NPPs and therefore will better serve during such accidents. So far, studies have been conducted on two fields – finding a new material (for example new alloys) and finding a new coating material, which would prevent coated alloy from fast degradation (mainly by oxidation). Latter option has been widely examined and resulted in developed and formed various coatings. One of them is the group of the silicon-based coatings.

The mentioned problem with coatings containing silicon is that after oxidation processes in high temperatures the amount of silicon can be different than before experiments. This problem has been described in literature, where some authors suggested various reactions at the material-coating interface which may result in silicon escape.

Experiments conducted in Institute of Nuclear Chemistry and Technology (INCT) in Warsaw were focused on examination of Zircalloy materials with coatings based on silicon in PWR working conditions. The examined materials were: Zry-2 coated with Zr-Si using sol-gel method and Zry-2 coated with $ZrSi_2$-Cr using PVD method. Oxidation tests with autoclave PARR 4653 were performed in 360°C/195 bar. The silicon concentration was considered and obtained results are presented in this work.

Acknowledgements
This work has been partially supported under IAEA Research Contract No. 19026/R0 and by Polish Ministry of Science and Higher Education under decisions 3689/IAEA/2017/0


TOSHIBA

Silicon concentration changes in Zry-2 coated with Zr-Si and $ZrSi_2$-Cr during the autoclave oxidation tests

Andrzej Krześniak[1], Bożena Sartowska[1], Wojciech Starosta[1], Lech Waliś[1], Jerzy Smolik[2], Magdalena Miłkowska[1]

[1]Institute of Nuclear Chemistry and Technology, Warsaw (Poland)

[2]Institute for Sustainable Technologies, Radom (Poland)

QUENCH – 24th QUENCH Workshop, 13-15.11.2018 Karlsruhe

LOCA accidents

- Severe accidents in nuclear power plants connected with LOCA (Loss Of Coolant Accidents) lead to a brand new branch of studies – Material engineering focused on finding new materials which will have better physical properties than actual constructive materials used in NPPs and therefore will better serve during such accidents
- So far, studies have been conducted on two fields:
  finding a new material (e.g. new alloy) and
  finding a new coating material, which would prevent coated alloy from fast degradation



Fire at the Fukushima nuclear power plant in 2011 [1]

Primary idea: Si-based coatings

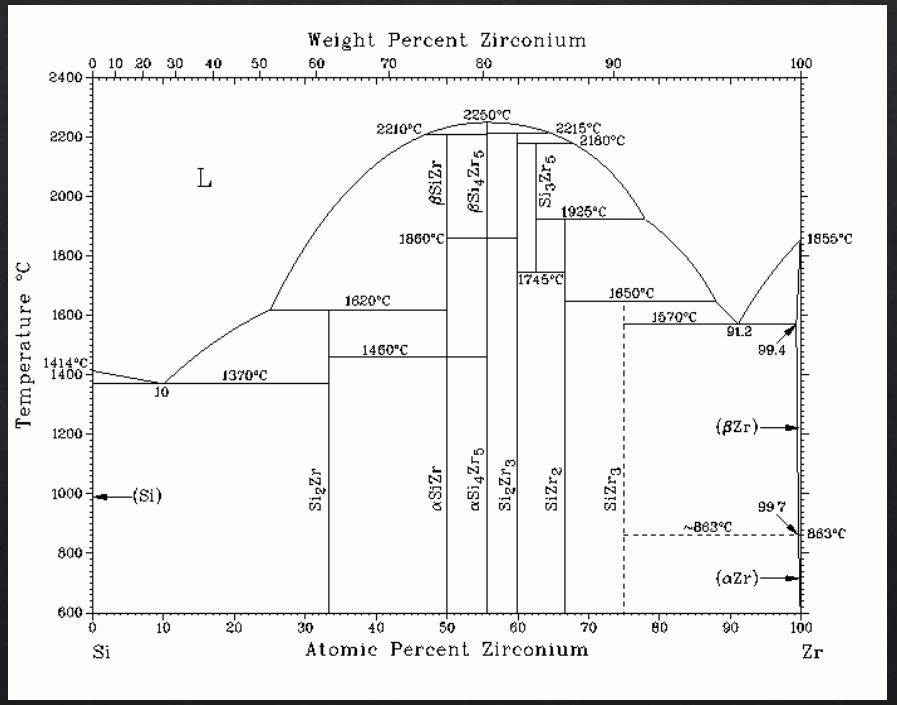
- Latter option has been widely examined and resulted in various coatings. One of them is a group of silicon-based coating.
- Zr-Si coating is expected to bond strongly to Zircalloy substrate.
  Intermetallic compound phases of Zr-Si have high melting points and oxidation of zirconium silicide produces highly corrosion resistant $ZrSiO_4$ and SiO_2 which possessing self-healing qualities. [2]

- Reactions:

  Liquid + $\beta SiZr \leftrightarrow \underline{Si_2Zr}$ $\underline{1620^0C}$

  Liquid + $\beta Si_4Zr_5 \leftrightarrow \underline{\beta SiZr}$ $\underline{2210^0C}$

  Liquid + $\beta Si_3Zr_5 \leftrightarrow \underline{SiZr_2}$ $\underline{1925^0C}$



Si-Zr Phase Equilibrium Diagram [3]

Problems with Si-based coatings

- One of the problems with coatings containing silicon is that after oxidation tests in high temperatures the concentration of silicon is smaller than before experiments.
- This problem has been described in literature, where some authors suggested different reactions at the material-coating interface which may result in silicon escape.



Nuclear fuel assembly [4]

„Silicon loss” – the background

- Primary reaction in high-temperature steam that has been proposed by H.Yeom et al.[5.] is the reaction of $ZrSi_2$ with water vapour at 400°C:

$$(1.)\ ZrSi_2 + 6H_2O \rightarrow ZrO_2 + 2SiO_2 + 6H_2$$

Both ZrO_2 and SiO_2 form a dense layer with good adhesion to substrate, which may be used as a protective layer.

On the other hand, at the same time as the silicon dioxide layer builds up, it volatilizes in the following reactions (mainly 2. - depending on the conditions) [6]:

$$(2.)\ SiO_{2(S)} + 2H_2O_{(G)} \rightarrow Si(OH)_{4(G)}$$

$$(3.)\ SiO_{2(S)} + H_2O_{(G)} \rightarrow SiO(OH)_{2(G)}$$

$$(4.)\ SiO_{2(S)} + 1/2H_2O_{(G)} \rightarrow SiO(OH)_{(G)} + 1/4O_{2(G)}$$

„Silicon loss” – the background

- T. Nakagiril and K. Kurokawa [7] proposed, that at high water vapour partial pressure silica can also volatilize into $Si_2O(OH)_6$ according to reaction:

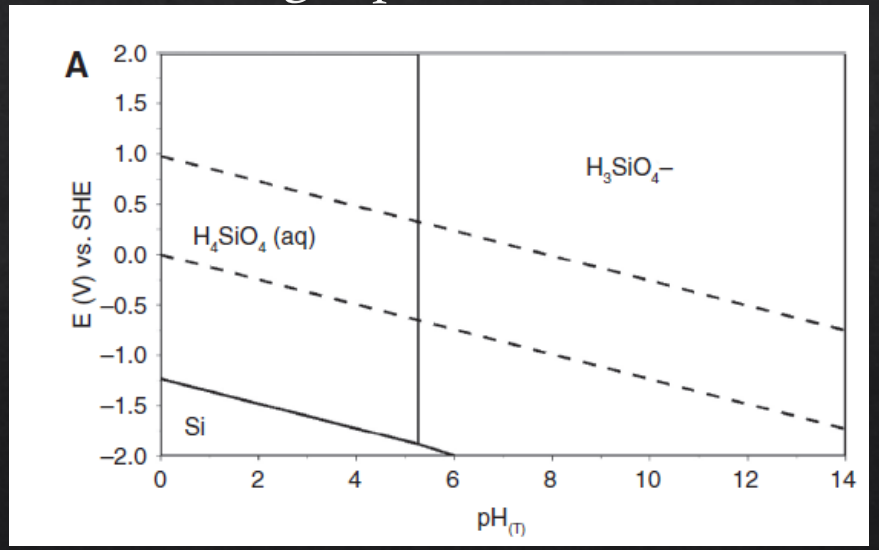
$$(5.)\ 2SiO_{2(S)} + 3H_2O_{(G)} \rightarrow Si_2O(OH)_{6(G)}$$

- At low oxygen partial pressure in water the formation of SiO is preferred over SiO_2 and the first oxide does not form a protective layer [8]:

$$(6.)\ Si + 1/2O_{2(G)} \rightarrow SiO_{(G)}$$

„Silicon loss" – the background

- The main process responsible for silicon loss during normal operation of PWR in high-temperature water is the hydrothermal corrosion. Water used as a coolant in PWR reactors under high pressure has a high temperature and it is in a subcritical state. Thus it is a highly reactive agent. [9]
- Below, a Pourbaix diagram for Si at 350°C, 25 MPa and 10^{-6}mol/kg is presented:
- The conditions for the aqueous solution in PWR are -0,5 V_{SHE} and pH=7,0. In such conditions some soluble aqueous ions are formed.



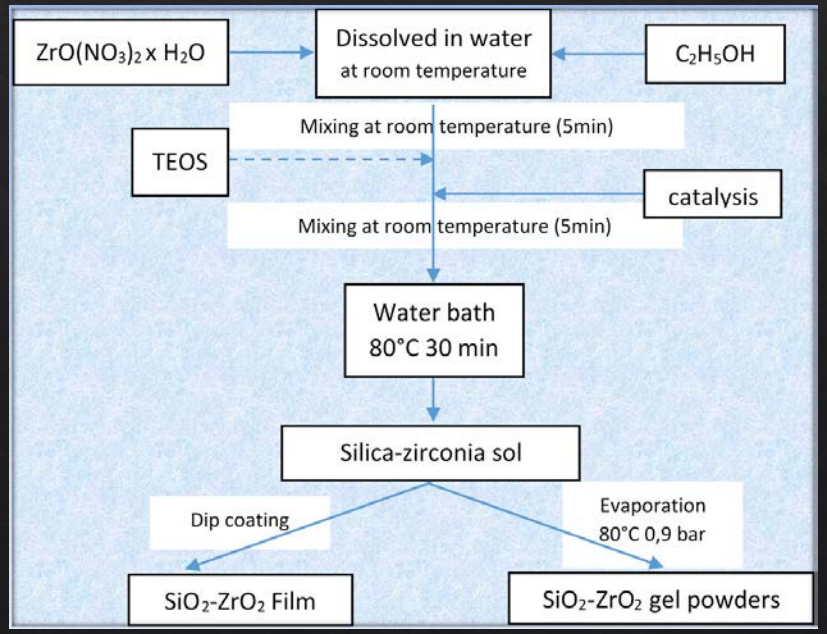
Pourbaix diagram for Si at 350°C, 25 MPa and 10^{-6}mol/kg (SHE – standard hydrogen electrode) [10]

Experimental part – samples preparation

- Material for testing: Zircalloy-2 (Zr-1.5%Sn-0.15%Fe-0.1%Cr-0.05%Ni)
- 1. Sol-gel method - a method for producing solid materials from small molecules, which is used for the fabrication of metal oxides, especially the oxides of silicon (Si). The process involves conversion of monomers into a colloidal solution (sol) that acts as the precursor for an integrated network (or gel) of either discrete particles or network polymers.

  → Zr-Si coating
- 2. PVD method – is based on the deposition on the substrate of atoms ejected from the target by the action of energetic argon ion beam bombardment In our case a plasma magnetron sputtering with 2 targets ($ZrSi_2$ and Cr) has been used.

  → $ZrSi_2$-Cr coating



General flow-chart for the preparation of silica-zirconia films and powders

Experiments settings

- 1. Autoclave Parr 4653 water, 360°C, 195 bar, 7 days

  → Zr-Si coating

- 2. Autoclave Parr 4653 water, 360°C, 195 bar, 21/42/63 days

  → $ZrSi_2$-Cr coating

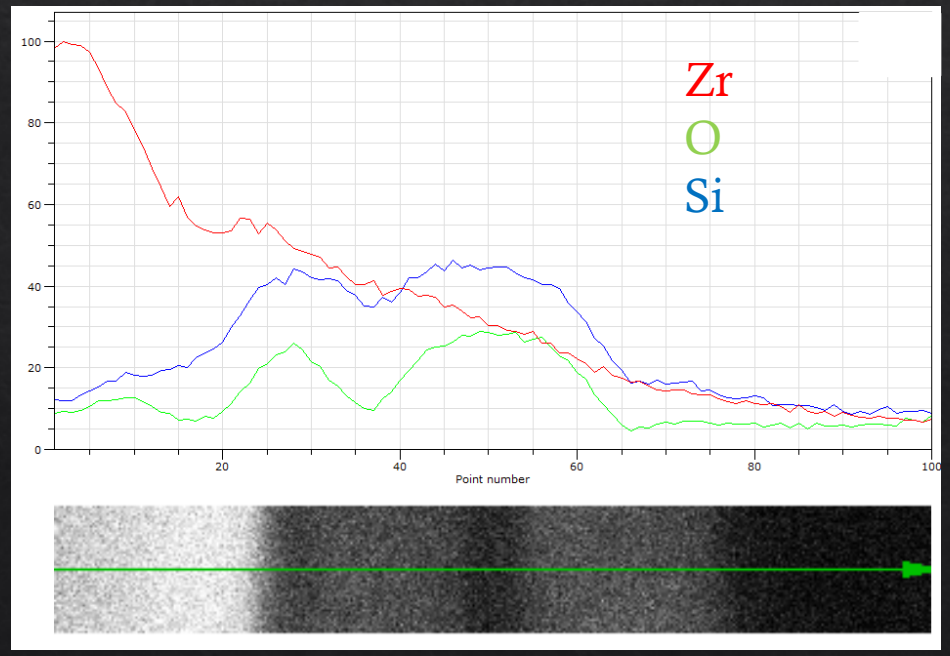


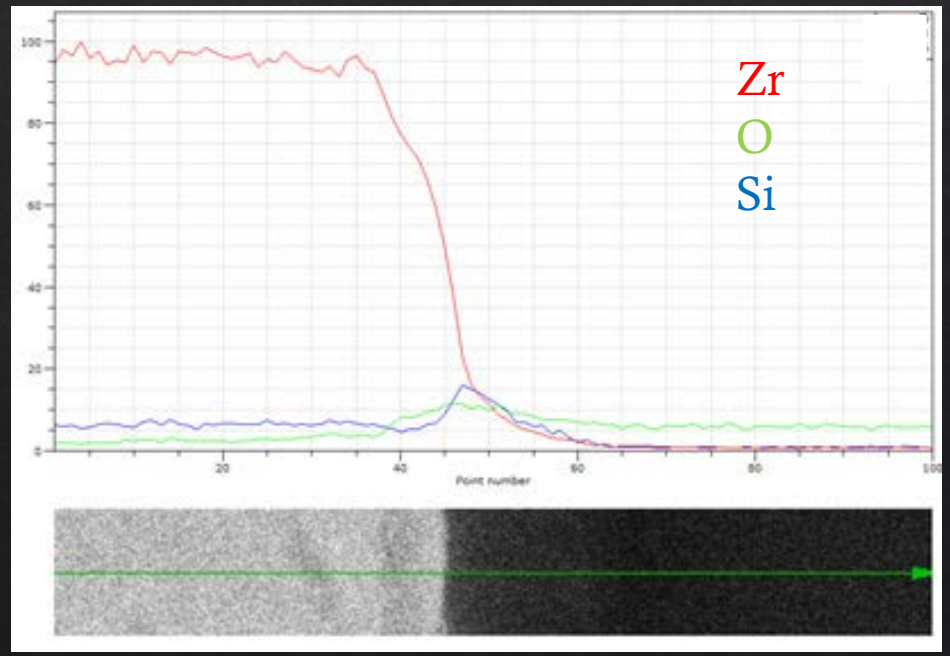




Zr-Si coating - results

- Cross section and EDS analyses of the Zr-Si film before (on the left) and after (on the right) autoclave test:





$ZrSi_2$-Cr coating - homogeneity testing

- Samples made by PVD method were first carefully examined to prove, that the deposited layer is homogenous. Thus, a point EDX analysis has been done (results in wt.%):

O 1,08 Si 24,24 Zr 35,62 Cr 39,05	O 1,09 Si 24,25 Zr 35,47 Cr 39,19	O 1,16 Si 24,27 Zr 35,23 Cr 39,34
O 0,99 Si 24,32 Zr 35,72 Cr 38,96	O 1,27 Si 24,20 Zr 35,35 Cr 39,18	O 1,01 Si 24,26 Zr 35,31 Cr 39,41
O 1,27 Si 24,31 Zr 35,51 Cr 39,59	O 1,12 Si 24,22 Zr 36,14 Cr 40,13	O 1,38 Si 24,07 Zr 35,57 Cr 38,97

- Results above clearly show, that the coating has been deposited homogeneously and further examination can be done without choosing certain place on the surface.

$ZrSi_2$-Cr coating - results

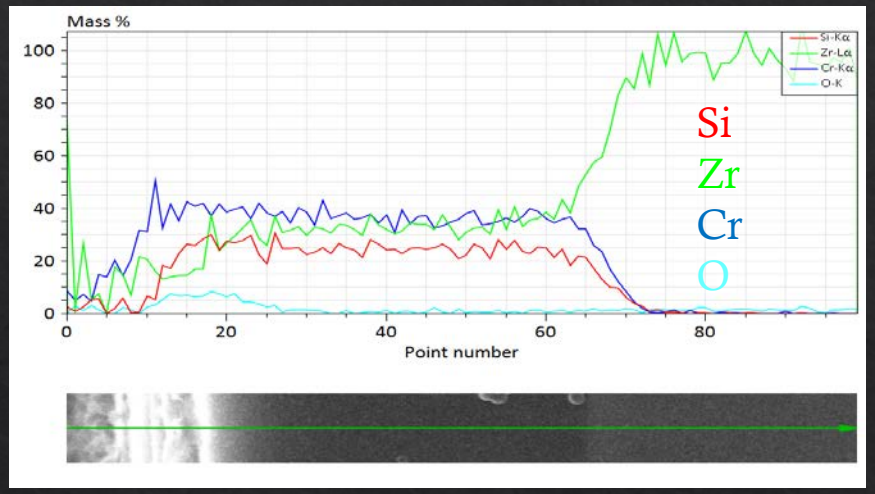
- EDS analysis from surface layer has been done before autoclave test, after 21, 42 and 63 days in autoclave:

	0d wt.%	0d at.%	21d wt.%	21d at.%	42d wt.%	42d at.%	63d wt.%	63d at.%
Zr	35,45	18,68	30,59	11,69	9,69	3,09	18,25	6,18
Si	24,26	41,52	9,09	11,28	0,71	0,73	0,58	0,64
Cr	39,07	36,12	28,88	19,36	46,29	25,88	34,46	20,47
O	1,23	3,68	24,21	52,72	36,15	65,67	31,31	60,43
rest	-	-	7,20	4,95	7,16	4,63	15,40	12,28

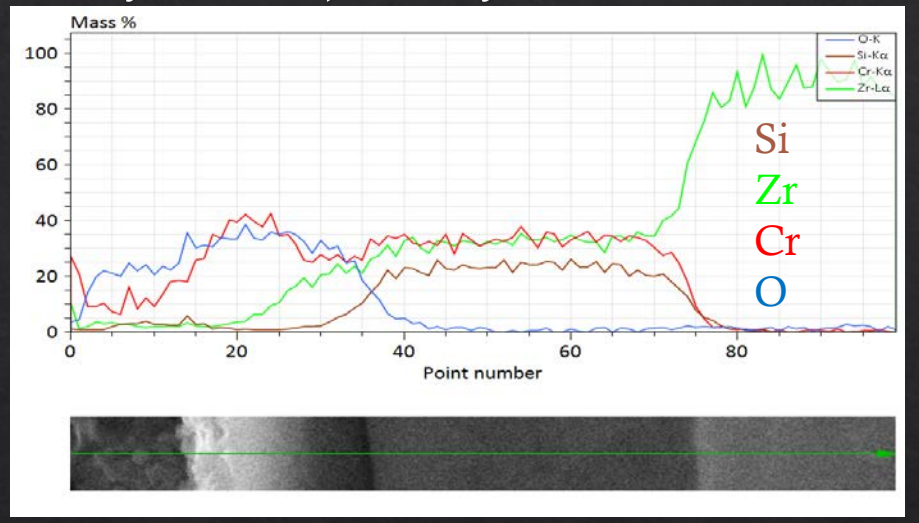
- Rest – Fe, Cu, Al, Ca

$ZrSi_2$-Cr coating – cross section

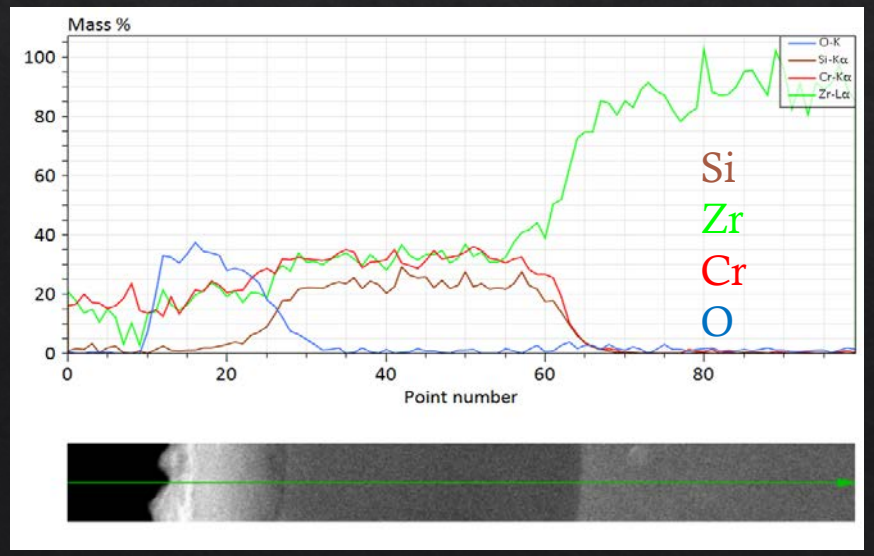
- Cross sections A) at the start, after B) 21 days, C) 42 days and D) 63 days in autoclave:



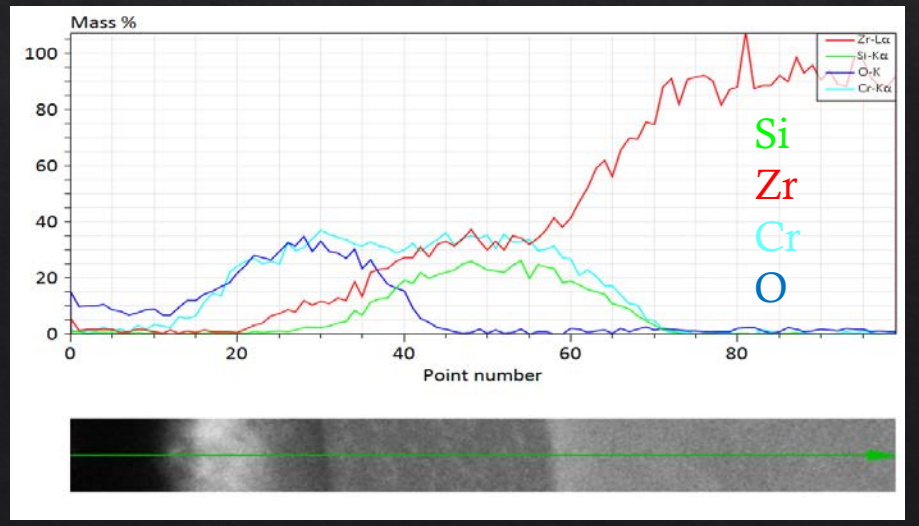
A



C



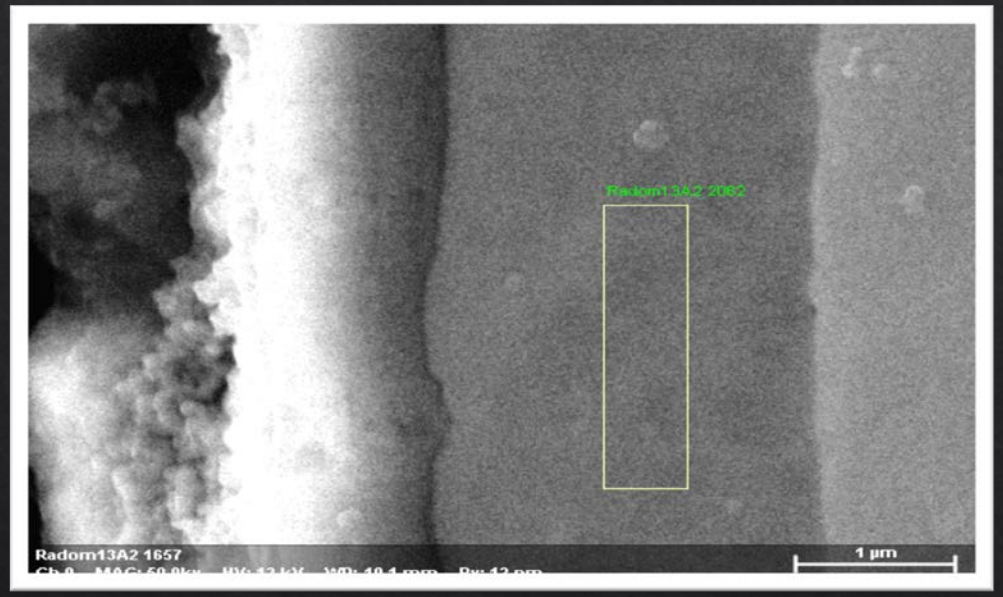
B



D

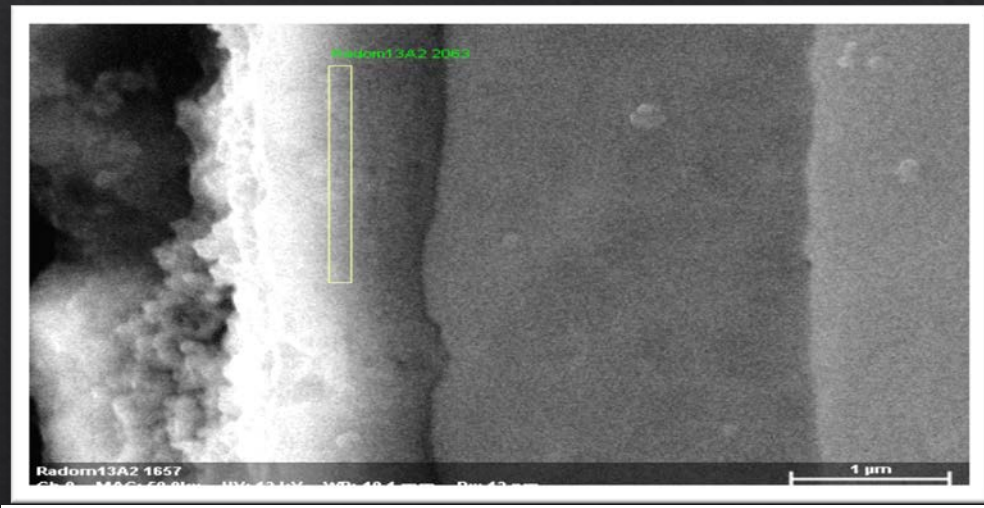
$ZrSi_2$-Cr coating – layers analysis

- Elemental analysis of coating (on the left) and oxide layers (on the right) after 42 days:



Radom13A2 2062.spx

Element	At. No.	Netto	Mass [%]	Mass Norm. [%]	Atom [%]	abs. error [%] (1 sigma)	rel. error [%] (1 sigma)
Silicon	14	76132	23.20	25.87	44.31	0.98	4.22
Chromium	24	24136	33.46	37.32	34.53	1.12	3.36
Zirconium	40	59484	32.38	36.11	19.04	1.23	3.81
Oxygen	8	621	0.63	0.71	2.12	0.19	30.00
		Sum	**89.68**	**100.00**	**100.00**		



Radom13A2 2063.spx

Element	At. No.	Netto	Mass [%]	Mass Norm. [%]	Atom [%]	abs. error [%] (1 sigma)	rel. error [%] (1 sigma)
Carbon	6	10385	0.00	0.00	0.00	0.00	10.00
Oxygen	8	60844	36.98	41.11	70.93	4.32	11.69
Aluminium	13	3404	0.94	1.04	1.06	0.07	7.84
Silicon	14	3124	0.95	1.05	1.04	0.07	7.40
Calcium	20	1765	1.14	1.27	0.87	0.07	6.39
Chromium	24	23811	33.43	37.16	19.73	1.12	3.36
Iron	26	1597	3.78	4.20	2.08	0.20	5.27
Zirconium	40	26395	12.74	14.16	4.29	0.51	3.98
		Sum	**89.96**	**100.00**	**100.00**		

Conclusions:

- 1. Silicon concentration in Zr-Si coating made by sol-gel method in surface layer was much lower after the experiments, which is in a good compliance with literature. In this case no passivation layer is formed.
- 2. Cross sections of $ZrSi_2$-Cr coating and EDS analysis suggest, that a dense layer of a

  non-stoichiometric metal oxides are formed at the coating, which can be a protective layer for the coating. Si concentration inside the coating remains at the same level (ca. 20 wt.%).
- 3. The main reason for „silicon loss" in the first experiment was the hydrothermal corrosion. During this process soluble aqueous ions of Si are formed.

Futher research on the topic of Si-based coatings and „silicon loss" will be carried out in next year…

References:

1. http://www.cleanwater.news/2017-10-12-radioactive-material-from-fukushima-discovered-in-the-sand-and-groundwater-beneath-the-beach-releasing-cesium-into-the-ocean.html
2. Development of Self-Healing Zirconium-Silicide Coatings for Improved Performance Zirconium-Alloy Fuel Cladding DE-NE0008300 Final Report
3. T. B. Massalski, Binary Alloy Phase Diagrams, Vol. 1, 1990, ASM International, 3382-3385
4. https://www.technologyreview.com/s/601121/this-new-fuel-could-make-nuclear-power-safer-and-cheaper/
5. H. Yeom et al., Journal of Nuclear Materials 499 (2018) 256-267
6. Accident tolerant fuel concepts for light water reactors : proceedings of a Technical Meeting held at Oak Ridge National Laboratories, United States of America, 13-16 October 2014 / International Atomic Energy Agency.
7. T. Nakagiri1, K. Kurokawa, Evaporation Behavior of SiO2 in N2-O2-H2O Atmospheres, Materials Transactions, Vol. 45, No. 2 (2004) pp. 334-337
8. M. Mitoraj-Królikowska, E. Godlewska. (2018) Silicide coatings on Ti-6Al-1Mn (at.%) alloy and their oxidation resistance. Surface and Coatings Technology 334, 491-499
9. C. C. Tang et al., Protective coatings on zirconium-based alloys as accident-tolerant fuel (ATF) claddings, Corros. Rev., 35(3), 141-165, 2017
10. M. D. Allendorf et al., Theoretical study of the thermochemistry of molecules in the Si-O-H system, J. Phys. Chem. 1995; 99: 15285–15293.

Thank you for your attention!



Acknowledgements

This work has been partially supported under IAEA Research Contract No. 19026/R0

and by Polish Ministry of Science and Higher Education under decisions 3689/IAEA/2017/0

HIGH TEMPERATURE INTERACTION OF SiC AND Zry-4

M. Grosse, T. van Duijnhoven, C. Tang, S. Ahmed, U. Gerhards, I. Markel
Karlsruhe Institute of Technology; P.O.Box 3640; D-76021 Karlsruhe; Germany

Stacked couples of silicon carbide and Zircaloy-4 discs were annealed for 1 h in nominal inert atmosphere (6N Ar) at temperatures of 1200, 1400, 1500, 1550, 1575 and 1600°C. Strong interactions between silicon carbide and Zircaloy-4 occurred at temperatures of 1500°C and above. The width of the influenced zone exceeds 1 mm at 1550°C. A pronounced layer structure was found consisting of Zr-Si intermetallic compounds with different stoichiometry, the Zr-Sn intermetallic phases Zr_2Sn and Zr_3Sn as well as sub-stoichiometric ZrC_{1-x} but also tin rich compounds. The six different layers formed at temperatures of 1500°C and above contain these phases in diverse concentrations. At temperatures of 1575 and 1600°C, the discs welded together. This paper gives a detailed description of the results of the post-annealing examinations and an analysis of the interaction between the two materials. The analysis is supported by phase field calculation using the CALPHAD software packages.

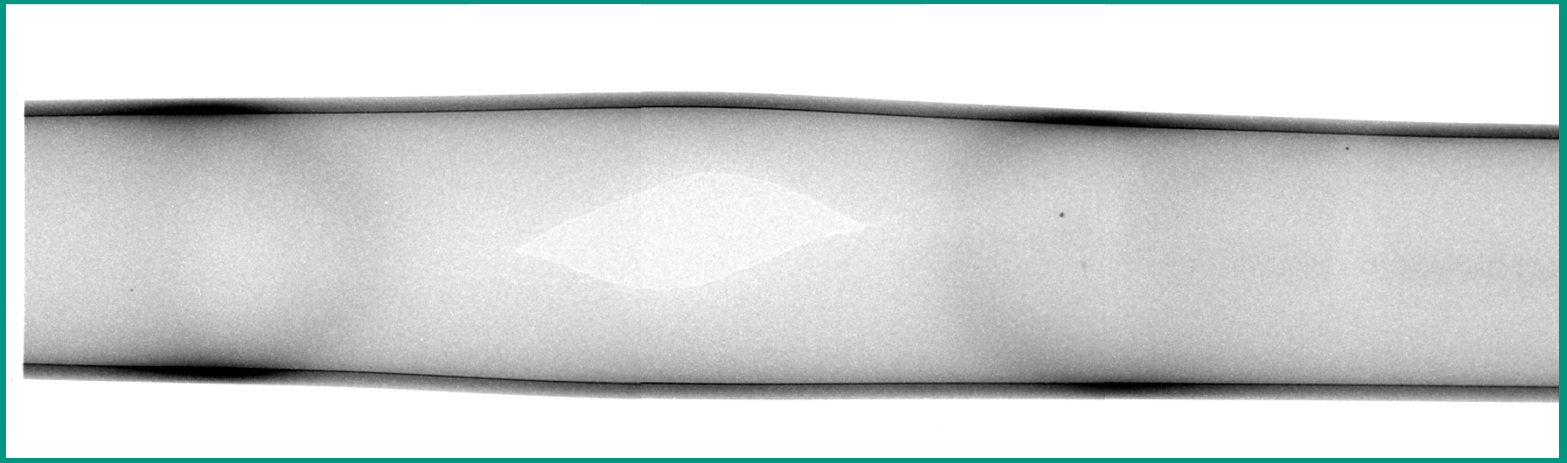

TOSHIBA

Karlsruhe Institute of Technology

High Temperature Interaction of SiC with Zircaloy-4

KIT / Institute for Applied Materials / Program NUSAFE

T. van Dujinhoven, M. Grosse



Co authors

- Chongchong Tang, XRD investigations
- Sarfraz Ahmed, annealing tests
- Uta Gerhards, WDX investigations
- Ingo Markel, CALPHAD calculations

The presentation was already given at ICAPP2018

Motivation for investigation of SiC – Zry-4 interaction

What happens when SiC comes in contact with Zircaloy-4 at high temperatures?

This can happens because:

- SiC is discussed as coating on zirconium alloys to improve its high temperature oxidation behaviour,
- Zr is discussed as coating on SiC to improve its hydrothermal corrosion behaviour,
- Lead test rods or assemblies with SiC claddings will be tested in reactors with zirconium alloy claddings and spacers.

Annealing tests

Quick tests to check the compatibility of SiC and Zry-4:

Zry-4 disks were stacked on mono-block SiC discs and annealed for 1 h at temperatures between 1200 and 1600°C in flowing argon atmosphere.



Mass changes and macroscopic appearances

Temp, °C	Δm_{SiC}, mg	Δm_{Zry-4}, mg	SiC	Zry-4	
RT	0	0			
1200	0	1.2			small interaction at interface
1400	-0.3	0.8			small interaction at interface
1500	-5.5	14.0			strong interaction at interface
1550	-91.0	63.5			strong interaction at interface

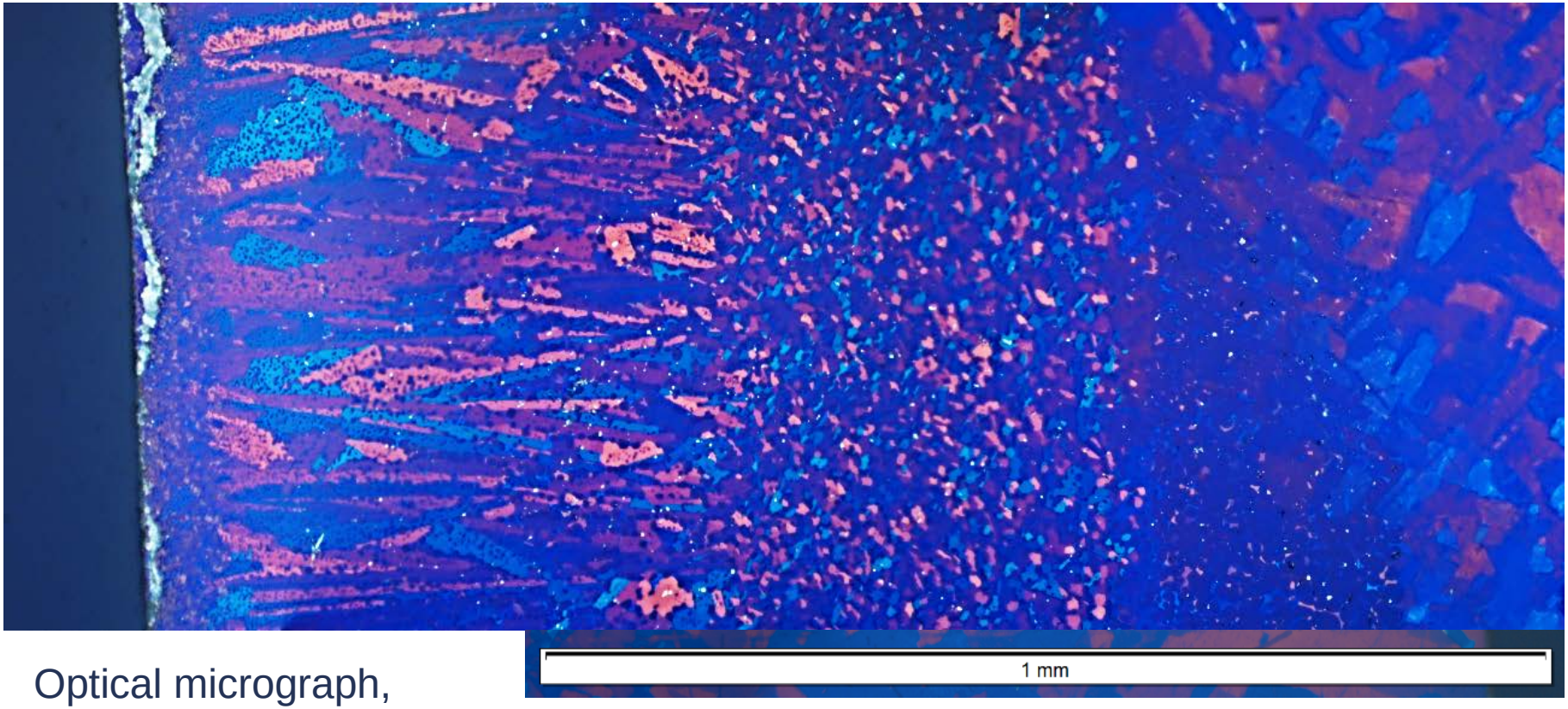
Mass changes and macroscopic appearances

continued

Temp, °C	Δm_{SiC}, mg	Δm_{Zry-4}, mg	SiC	Zry-4	
1575	-	-			welding
1600	-	-			welding

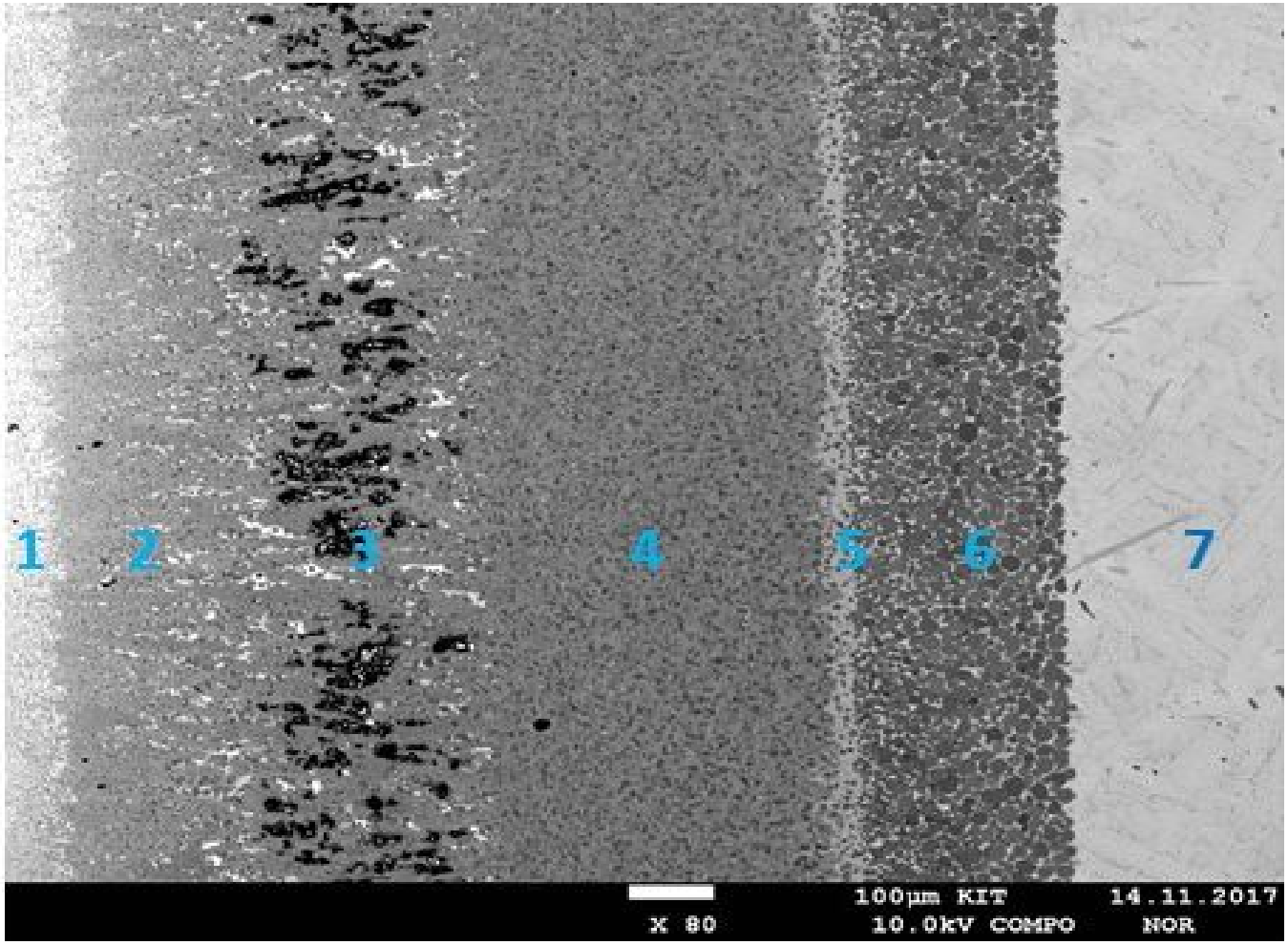
Microstructure

No changes in the SiC microstructure are visible, but at Zry-4 a wide range with new structure can be seen.



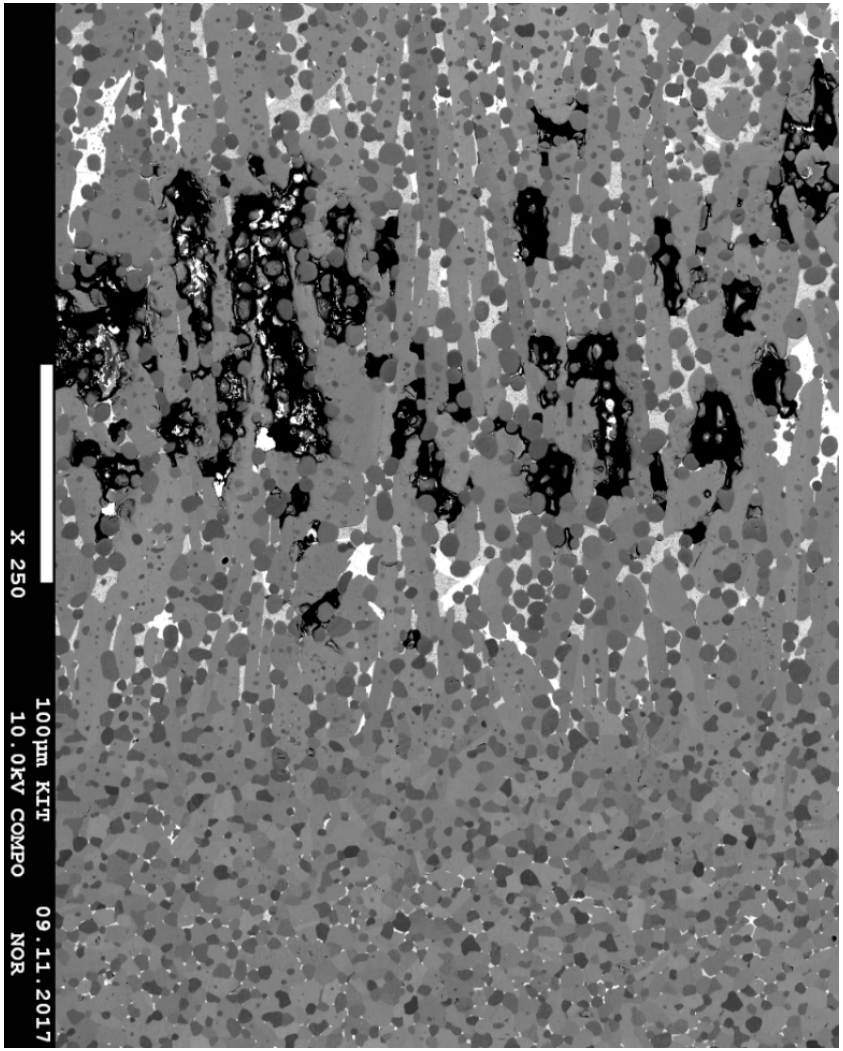
Optical micrograph,
using polarized light, of the Zry-4 disc after sandwich annealing at 1550°C

Microstructure



SEM BE micrograph of the Zry-4 disc after sandwich annealing at 1550°C

Detailed microstructure



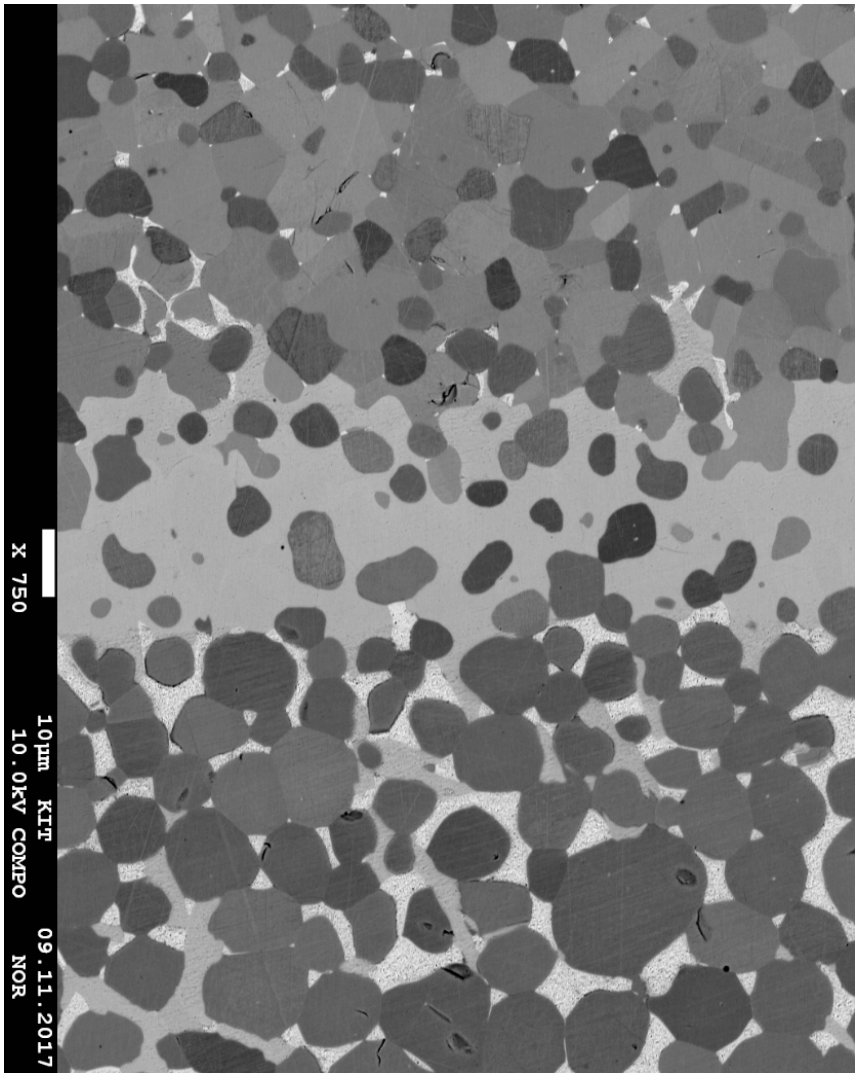
Layer 1: Zr_2Sn, Zr_2Si

Layer 2: Zr_2Si, ZrC_{1-x} and
Zr with very fine ZrC_{1-x}

Layer 3: Zr_2Sn, ZrC_{1-x}
Zr with very fine ZrC_{1-x}
large elongated pores

Layer 4: ZrC_{1-x}, Zr_2Si

Detailed microstructure

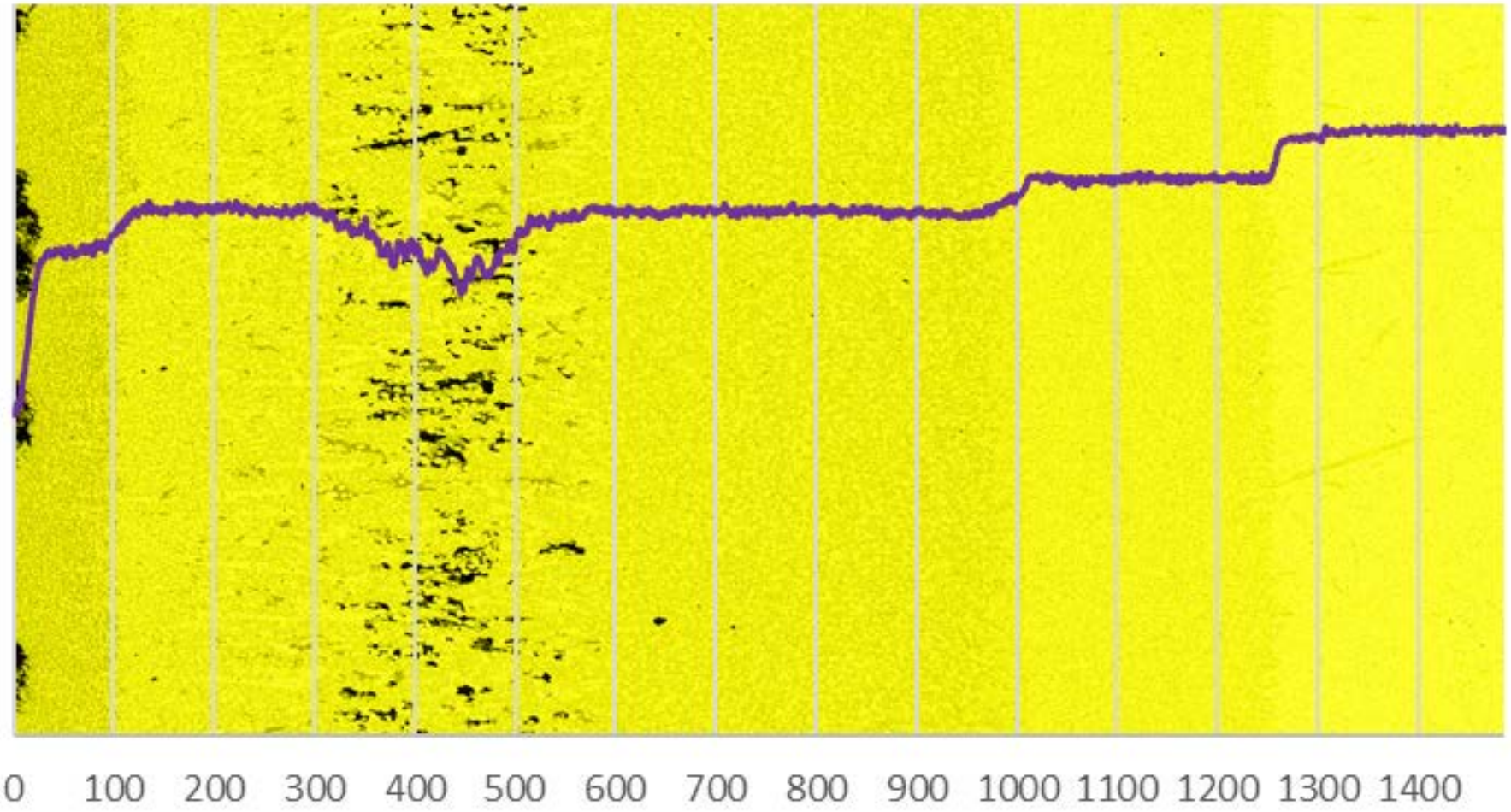


Layer 4: ZrC_{1-x}, Zr_2Si

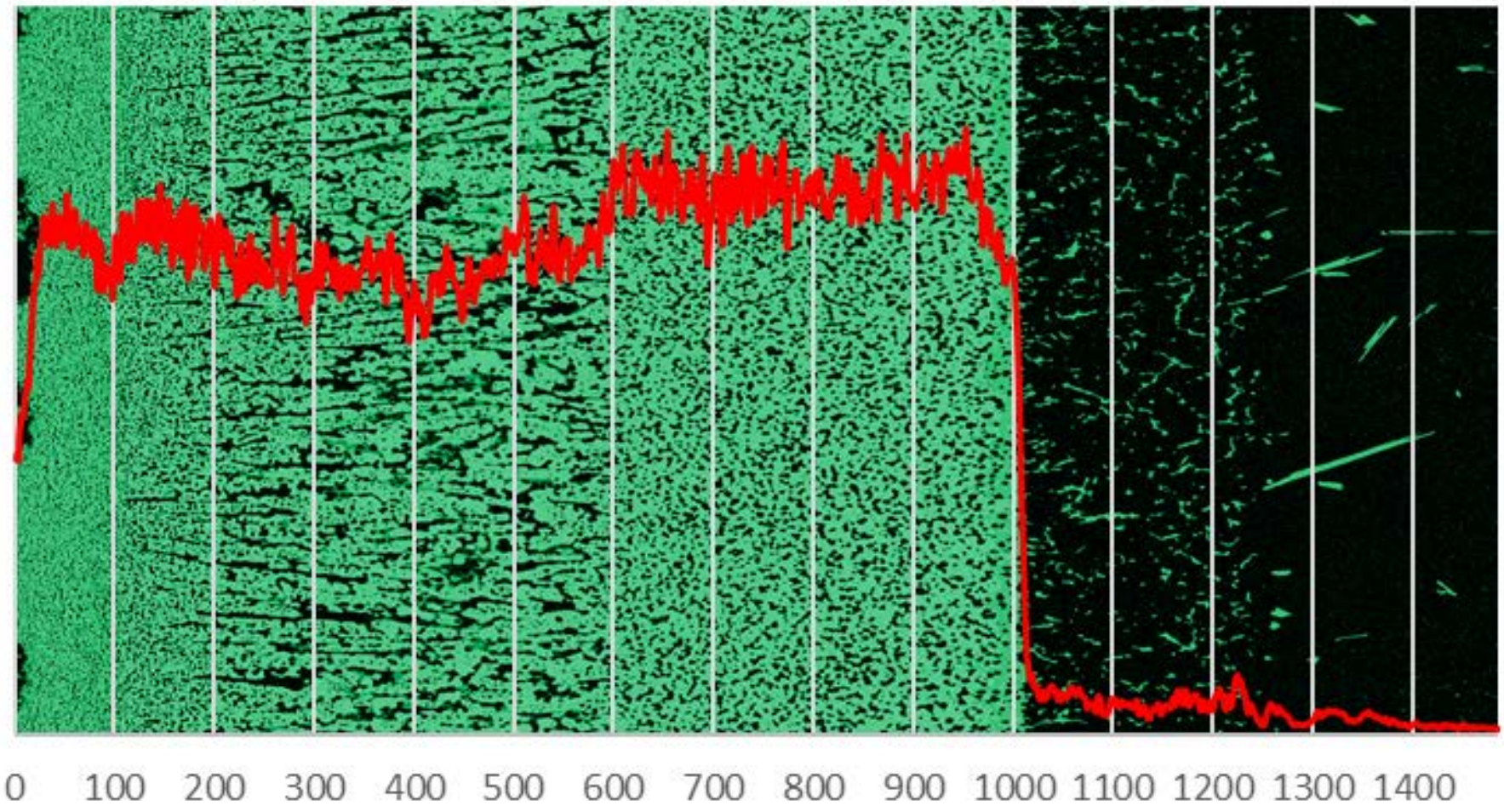
Layer 5: Zr_3Si matrix with ZrC_{1-x} and Zr_2Si grains

Layer 6: Zr matrix with fine ZrC_{1-x} precipitates and ZrC_{1-x} and Zr_3Si grains

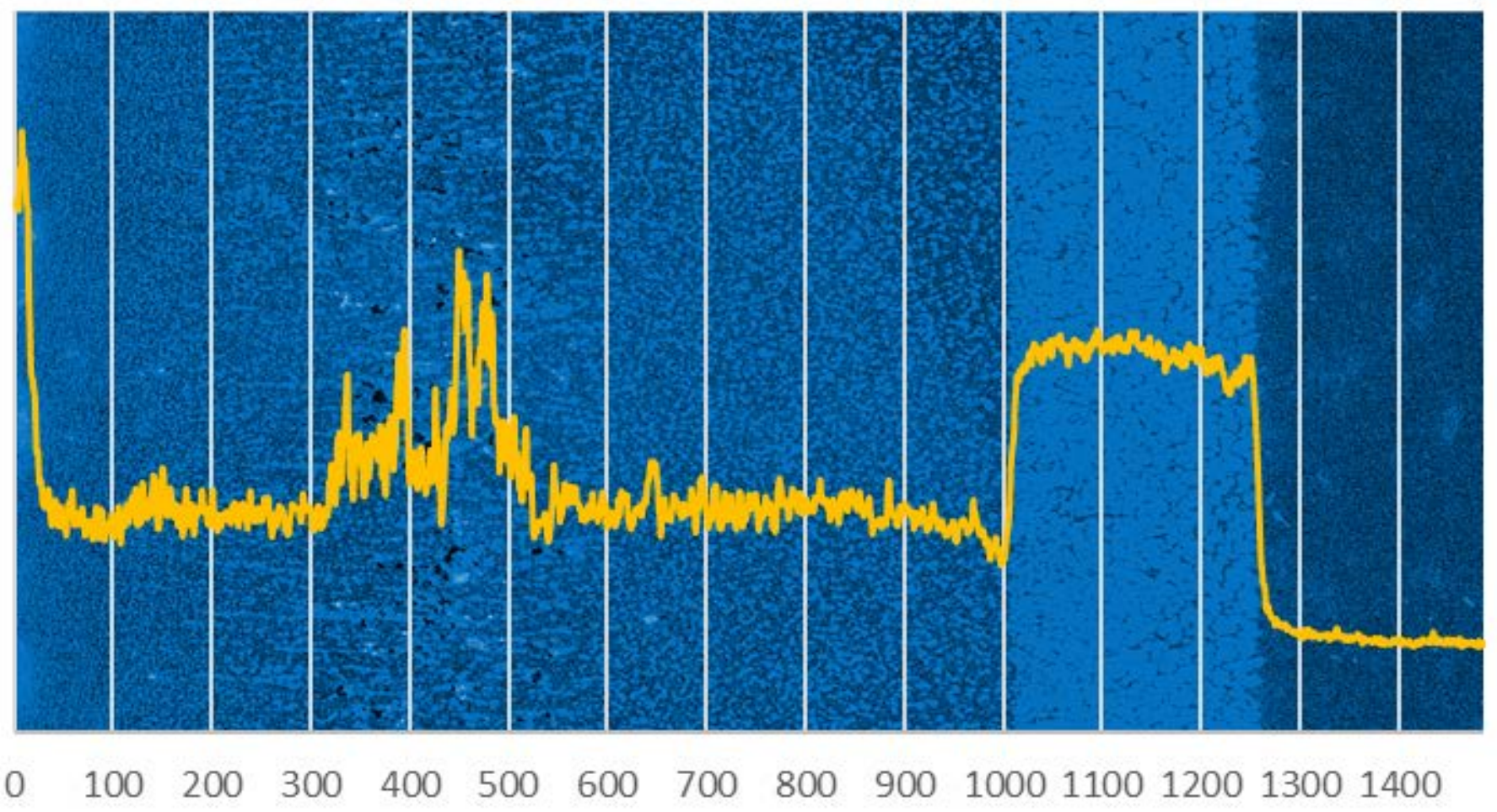
Element distribution Zr



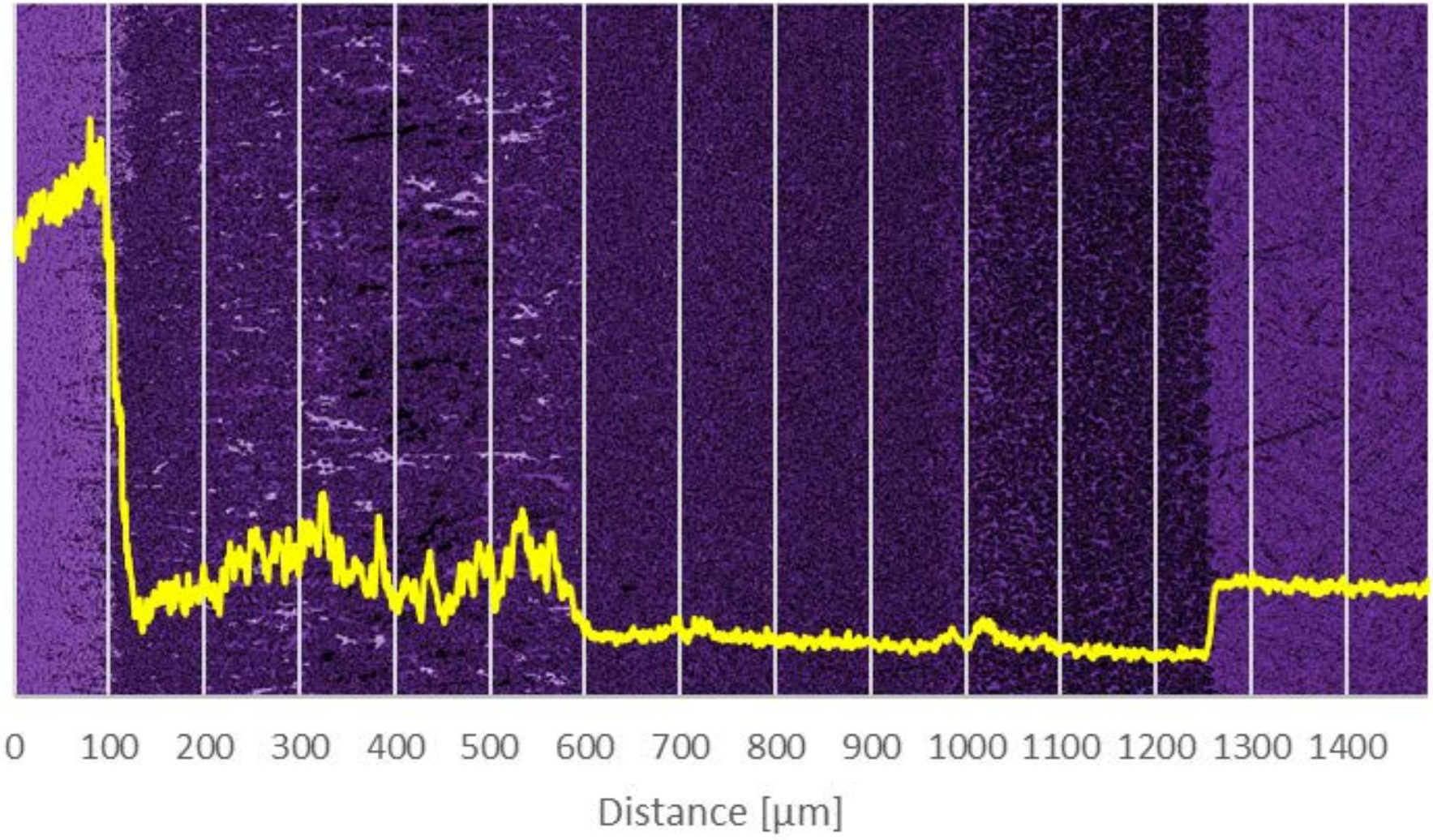
Element distribution Si



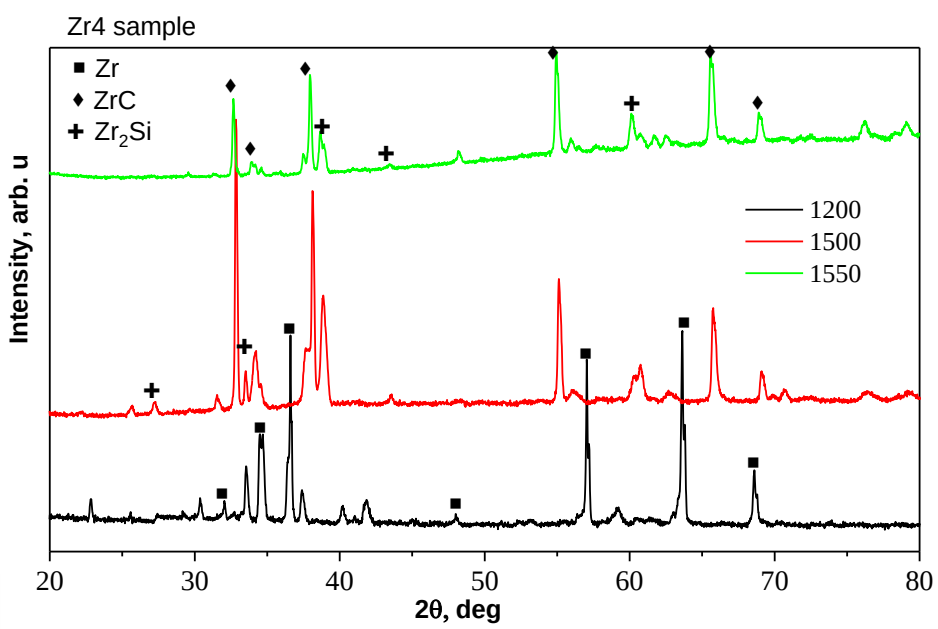
Element distribution C

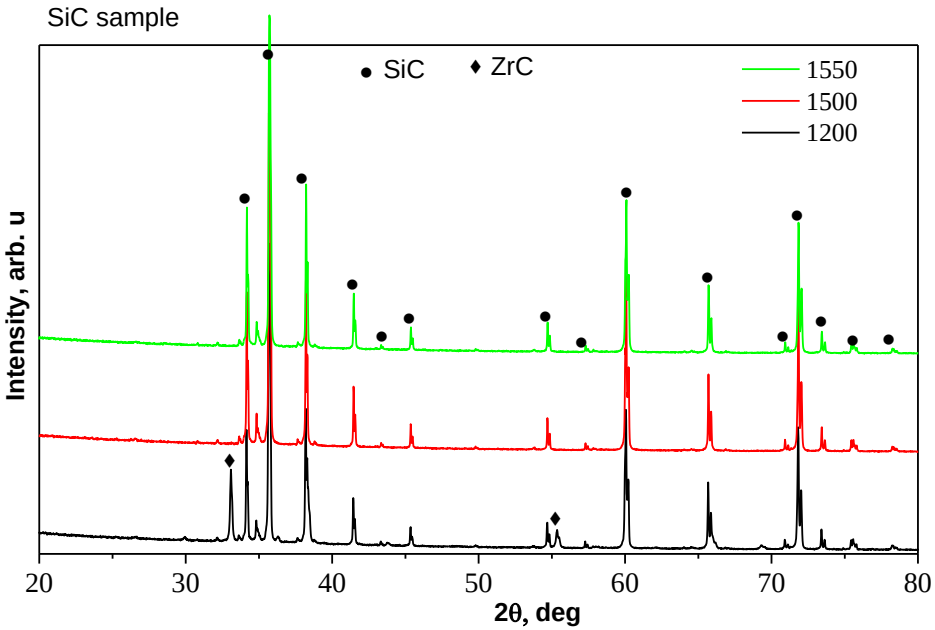


Element distribution Sn



XRD measurements at the interfaces





	Zry-4	**SiC**
1200°C	Zry-4	SiC + ZrC
1500°C	ZrC + Zr_2Si	SiC
1550°C	ZrC + Zr_2Si	SiC

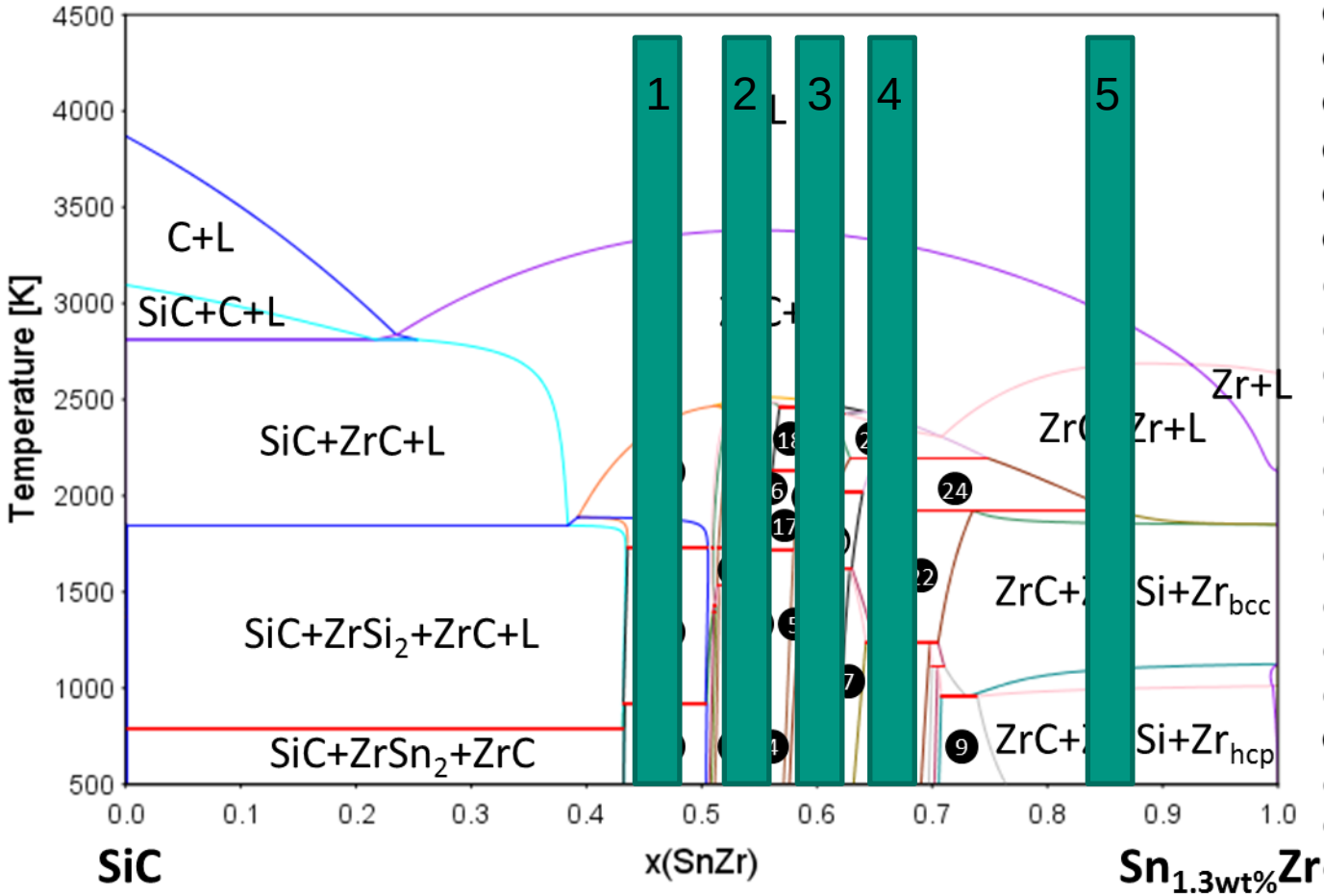
Discussion

- Reaction between Zry-4 and SiC:

$$(2a + 3b + (a+b)/1-x)\ \mathbf{Zr} + \mathbf{SiC} = a\ \mathbf{Zr_2Si} + b\ \mathbf{Zr_3Si} + (a+b)\ \mathbf{ZrC_{1-x}}$$

- C diffuses faster than Si in Zr.
- Si pushes the C further into the Zry-4.
- Sn diffuses to the surface.

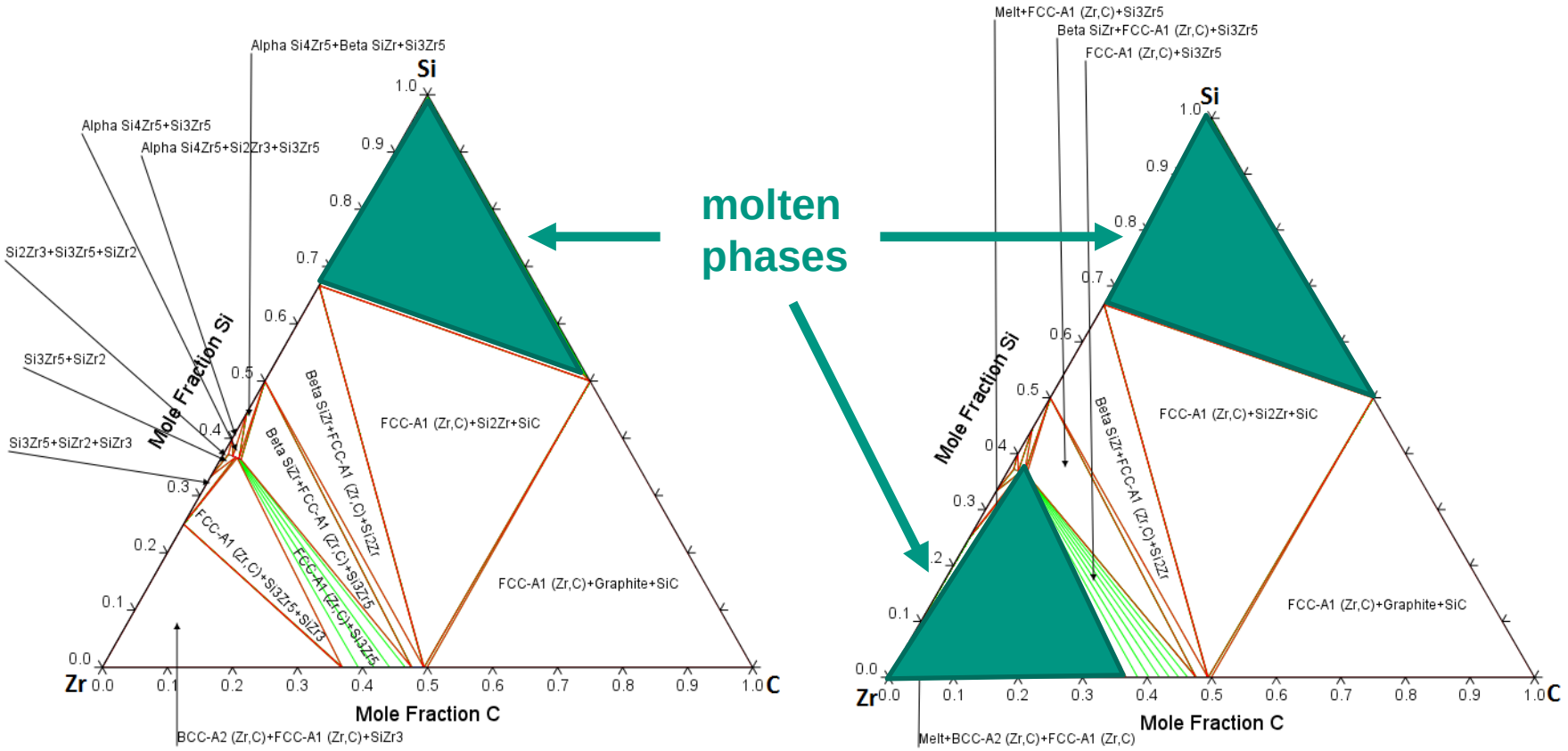
Discussion



1. $ZrSn_2$+ $ZrSi_2$+ZrC+αZrSi
2. ZrC+Zr_5Sn_3+αZrSi+αZr_5Si_4
3. ZrC+Zr_5Sn_3+αZr_5Si_4
4. ZrC+Zr_3Si_2+Zr_5Sn_3+αZr_5Si_4
5. ZrC+Zr_3Si_2+Zr_5Sn_3
6. ZrC+Zr_2Si+Zr_3Si_2+Zr_5Sn_3
7. ZrC+Zr_2Si+Zr_5Sn_3
8. ZrC+Zr_2Si+Zr_3Si+Zr_5Sn_3
9. Zr_3Si+ZrC+Zr_3Sn+Zr_{hcp}
10. L+$ZrSi_2$+ZrC+αZrSi
11. L+$ZrSi_2$+ZrC+βZrSi
12. L+ZrC+βZrSi
13. Zr_{bcc}+ZrC+ αZr_5Si_4 +αZrSi
14. Zr_{bcc}+ZrC+ αZr_5Si_4 +βZrSi
15. Zr_{bcc}+ZrC+ βZr_5Si_4 +βZrSi
16. Zr_{bcc}+ZrC
17. Zr_{bcc}+ZrC+αZr_5Si_4+Zr_3Si_2
18. Zr_{bcc}+ZrC+βZr_5Si_4+Zr_3Si_2
19. Zr_{bcc}+ZrC+Zr_3Si_2
20. Zr_{bcc}+ZrC+Zr_3Si_2+Zr_2Si
21. Zr_{bcc}+ZrC+Zr_2Si
22. Zr_{bcc}+ZrC+Zr_3Si+Zr_2Si
23. L+Zr_{bcc}+ZrC+Zr_5Si_3
24. Zr_{bcc}+ZrC+L+Zr_2Si

Discussion

- Molten phases are formed 1400°C (Si rich) and above. At T > 1570°C (Si – Zr eutectic) the Zry-4 and SiC weld togeter.



Ternary phase diagram of the system Zr, Si and C at 1550 and 1575°C.

Conclusions

- Strong and fast interaction between Zry-4 and SiC occurs at temperatures of 1550°C and above.
- Melts are formed at T > 1400°C but only the Zr rich melt at T > 1570°C results in welding.
- Zry-4 and SiC are welded above the Zr – Si eutectic temperature of 1570°C.

Open questions:

- Kinetics?
- What happens if Zry-4 comes in contact with other silicide compounds (e.g. U_3Si)?
- Can we use the reactions for joining of SiC? (This will be investigated in IL TROVATORE)

The authors thanks the KIT technicians U. Stegmaier and P. Severloh for their support in the sample preparation and SEM and optical metallography investigations.

Thank you for your attention.

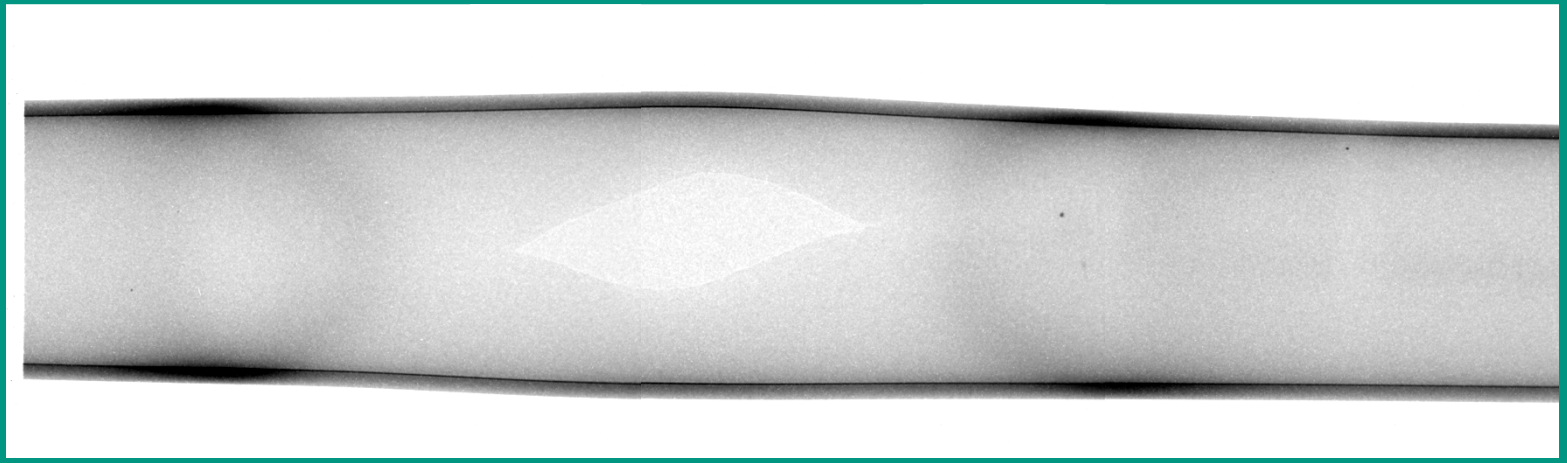
What are your questions?

Karlsruhe Institute of Technology

High Temperature Interaction of SiC with Zircaloy-4

KIT / Institute for Applied Materials / Program NUSAFE

M. Grosse, T. van Dujinhoven



Participants 24th International QUENCH Workshop
13 - 15 November 2018

Family Name	First Name	Institution	Country	e-mail
Algama	Don	US-NRC	USA	don.algama@nrc.gov
Allison	Chris	Innovative Systems Software	United States	iss@srv.net
Austregesilo	Henrique	GRS	Germany	henrique.austregesilo@grs.de
Bals	Christine	GRS	Germany	Christine.Bals@grs.de
Birchley	Jonathan	Independant	England	birchley@hotmail.com
Bottomley	David	JAEA-CLADS	Japan	dboksb3@gmail.com
Brachet	Jean-Christophe	CEA, Université Paris-Saclay	France	jean-christophe.brachet@cea.fr
Fargette	Andre	FRAMATOME	France	andre.fargette@areva.com
Gabrielli	Fabrizio	KIT	Germany	fabrizio.gabrielli@kit.edu
Gremme	Florian	RUB	Germany	florian.gremme@pss.rub.de
Große	Mirco	KIT	Germany	Mirco.Grosse@KIT.edu
Hagen	Siegfried	retired	Germany	siegfried.hagen@bitpri.de
Haste	Timothy	IRSN	France	tim.haste@irsn.fr
He	Xiaojun	China Institute of Atomic Energy	P.R.China	ciae.hexiaojun@gmail.com
Hollands	Thorsten	GRS	Germany	thorsten.hollands@grs.de
Howell	Jutta	KIT	Germany	jutta.howell@kit.edu
Jäckel	Bernd	PSI Switzerland	Switzerland	bernd.jaeckel@psi.ch
Kaliatka	Tadas	Lithuanian Energy Institute	Lithuania	tadas.kaliatka@lei.lt
Kedzierska	Barbara	ISS / Warsaw Univ. of Technology	United States	kedzierska_barbara@wp.pl
Kim	Seok	KAERI	Korea, Republic of	seokim@kaeri.re.kr
Kim	Won Ku	Khunghee University	South korea	mono0224@naver.com
Kim	Gippeum	Handong Global University	South Korea	wkzwkyb2@naver.com
Krejci	Jakub	UJP PRAHA a.s.	Czech Republic	krejci@ujp.cz
Krześniak	Andrzej	Institute of Nuclear Chemistry and Technology	Poland	a.krzesniak@ichtj.waw.pl
Laier	Jutta	KIT	germany	jutta.laier@kit.edu
Le Belguet	Alix	EDF R&D	France	alix.le-belguet@edf.fr
Lee	Jaebong	KAERI	Rep. of Korea	jaebonglee@kaeri.re.kr
Li	L ei	China Nuclear Power Technology Research CO. LTD.	China	li_lei2@cgnpc.com.cn
Lind	Terttaliisa	PSI Switzerland	Switzerland	terttaliisa.lind@psi.ch
Madokoro	Hiroshi	KIT	Germany	hiroshi.madokoro@kit.edu
Matocha	Vitezslav	UJV Rez	Czech Republic	vitezslav.matocha@ujv.cz
Mercan	Ahmet Kagan	KIT	Germany	ahmet.mercan@partner.kit.edu
Moch	Jürgen Alexander	KIT	Germany	juergen.moch@kit.edu
Muscher	Heinrich	KIT	Germany	heinrich.muscher@kit.edu
Mustafa	Rawan	Jordan Atomic Energy Commission	United States	rawanmstf2008@yahoo.com
Ott	Larry	ORNL	USA	LJOtt13@gmail.com
Park	Sanggil	ACT Co., Ltd./Handong Global Univ/Lee & Ko	South Korea	sanggil.park@leeko.com
Peschel	Jan Mathis	RUB	Germany	jan.peschel@pss.rub.de
Philippov	Mikhail	IBRAE	Russia	philippov@ibrae.ac.ru

Participants 24th International QUENCH Workshop
13 - 15 November 2018

Pshenichnikov	Anton	JAEA-CLADS	Japan	pshenichnikov.anton@jaea.go.jp
Raqué	Manuel	Eidgenössisches Nuklearsicherheitsinspektorat (ENSI)	Schweiz	manuel.raque@ensi.ch
Salem	Asmaa	Alexandria University	Egypt	asmaa.nuc55@gmail.com
Sanchez	Victor	KIT	Germany	victor.sanchez@kit.edu
Sartowska	Bożena	Institute of Nuclear Chemistry and Technology	Poland	b.sartowska@ichtj.waw.pl
Schubert	Arndt	JRC Karlsruhe	Germany	Arndt.Schubert@ec.europa.eu
Shisheng	Wang	KIT	Germany	Shisheng.Wang@KIT.edu
Stegmaier	Ulrike	KIT	Germany	ulrike.stegmaier@kit.edu
Steinbrück	Martin	KIT	Germany	martin.steinbrueck@kit.edu
Stuckert	Juri	KIT	Germany	juri.stuckert@kit.edu
Tang	Chongchong	KIT	Germany	chongchong.tang@kit.edu
Tiborcz	Livia	GRS	Germany	livia.tiborcz@grs.de
Van Uffelen	Paul	JRC Karlsruhe	Germany	paul.van-uffelen@ec.europa.eu
Vasiliev	Alexander	IBRAE	Russia	vasil@ibrae.ac.ru
Ver	Nora	Hungarian Academy of Sciences	Hungary	nora.ver@energia.mta.hu
Veshchunov	Mikhail	IAEA	Austria	m.veshchunov@iaea.org
Vrbka	Pavel	CTU Prague	CZ	pavel.vr@seznam.cz
Wang	Guoqiang	Westinghouse Electric Company LLC	USA	wangg@westinghouse.com
Wolff	Marc	Eidgenössisches Nuklearsicherheitsinspektorat ENSI	Switzerland	marc.wolff@ensi.ch
Wu	Hsingtzu	Huazhong University of Science and Technology	China	wu.hsingtzu@pm.me
Yamashita	Shinichiro	JAEA	Japan	yamashita.shinichiro@jaea.go.jp


KIT


VAIO















































